The Electronic States of the BH and CH Radicals

By Jiro HIGUCHI

(Received June 25, 1952)

Introduction

On the electronic states of the BH and CH radicals the electronic terms observed are $^1\Sigma^+$, $^1\Pi$, $^3\Sigma$, $^3\Pi$ and $^2\Pi$, $^2\Delta$, $^2\Sigma^-$, $^1\Sigma^+$,(1) respectively, and their electronic structures were determined by Stehn(2) and King(3) using the semi-empirical approximation. But in their calculations the electronic configurations of the boron and carbon atom were assumed to be only the $(2s)^2(2p)$ and $(2s)^2(2p)^2$ ones, respectively, and the values used for the energy integrals were empirically evaluated from the experimental data. Recently, in the work on the CH_2 radical by Niira and Oohata,(4) the electronic energies of the CH radical were calculated using the method of atomic orbital, considering both the $(2s)^2(2p)^2$ and $(2s)(2p)^3$ electronic configurations of the carbon atom, assuming all atomic orbitals to be orthogonal to each other. The lowest state was found to be the $^4\Sigma^-$. In this paper the electronic energies have been calculated using the method of the atomic orbital. The overlap integrals and all the permutations have been explicitly included for the $2s$ and $2p$ electrons, but no $1s$ electron integrals for the boron atom and the carbon atom have been considered. The electronic configurations of the boron atom are assumed to be both the $(2s)^2(2p)$ and $(2s)(2p)^2$, and of the carbon atom both the $(2s)^2(2p)^2$ and $(2s)(2p)^3$, have been taken into account.

The Basic Wave Functions for the CH Radical

If the calculation of the CH radical is treated as a five electron problem excluding the $1s$ electrons and assuming the $(2s)^2(2p)^2$ and $(2s)(2p)^3$ configurations for the carbon atom, there are eight possible kinds of the electronic orbital wave functions for the entire radical, which are given by the products of atomic orbitals:

$$\left.\begin{aligned}
\Phi_1 &\equiv (2s)(2s)(2p\sigma)(2p\sigma)(H)\\
\Phi_2 &\equiv (2s)(2s)(2p\pi_+)(2p\pi_-)(H)\\
\Phi_3 &\equiv (2s)(2s)(2p\sigma)(2p\pi_\pm)(H)\\
\Phi_4 &\equiv (2s)(2s)(2p\pi_\pm)(2p\pi_\pm)(H)
\end{aligned}\right\} \quad (1)$$

in the s^2p^2 configuration, and

$$\left.\begin{aligned}
\Psi_1 &\equiv (2s)(2p\sigma)(2p\pi_+)(2p\pi_-)(H)\\
\Psi_2 &\equiv (2s)(2p\sigma)(2p\sigma)(2p\pi_\pm)(H)\\
\Psi_3 &\equiv (2s)(2p\pi_\pm)(2p\pi_\pm)(2p\pi_\mp)(H)\\
\Psi_4 &\equiv (2s)(2p\sigma)(2p\pi_\pm)(2p\pi_\pm)(H)
\end{aligned}\right\} \quad (2)$$

in the sp^3 configuration for the carbon atom, where $(2s)$, $(2p\sigma)$ and $(2p\pi_\pm)$ are the $2s$, $2p\sigma$ and $2p\pi_\pm$ atomic orbitals of the carbon atom, respectively, and (H) is the $1s$ orbital of the hydrogen atom.

Since the spatial symmetry of the CH radical belongs to the symmetry group $C_{\infty v}$, and the electronic terms with different multiplicity or symmetry do not interact, the basic wave functions for this radical, which are constructed from (1) and (2) to fit the Pauli principle, can be classified by the irreducible representations of $C_{\infty v}$ (Σ^+, Σ^-, Π and Δ), and they are as follows:

	$^2\Sigma^+$	$^2\Sigma^-$	$^2\Pi$	$^2\Delta$	$^4\Sigma^+$	$^4\Sigma^-$	$^4\Pi$	$^4\Delta$	$^6\Sigma^-$
Φ_1	1	0	0	0	0	0	0	0	0
Φ_2	1	1	0	0	0	1	0	0	0
Φ_3	0	0	2	0	0	0	1	0	0
Φ_4	0	0	0	1	0	0	0	0	0
Ψ_1	2	3	0	0	1	3	0	0	1
Ψ_2	0	0	2	0	0	0	1	0	0
Ψ_3	0	0	2	0	0	0	1	0	0
Ψ_4	0	0	0	2	0	0	0	1	0
Sum	4	4	6	3	1	4	3	1	1

(3)

In this table, it is shown that, for instance, there are three basic wave functions arising from the Φ_2, each belonging to the type of $^2\Sigma^+$, $^2\Sigma^-$ and $^4\Sigma^-$. Thus there are, in all, four basic wave functions belonging to the type of $^2\Sigma^+$, and four, six and three for the types of $^2\Sigma^-$, $^2\Pi$ and $^2\Delta$, respectively, and so on.

(1) H. Sponer, "Molekülspektren 1, Tabellen", Julius Springer, Berlin, 1935, P. 24.
(2) J. R. Stehn, *J. Chem. Phys.*, **5**, 186 (1937).
(3) G. W. King, *J. Chem. Phys.*, **6**, 378 (1938).
(4) K. Niira and K. Oohata, *J. Phys. Soc. Japan*, **7**, 61 (1952).

The Secular Equations

Using these antisymmetrized basic wave functions, which are linearly independent from each other, a secular equation is obtained for each symmetry type. Since the 1*s* electrons of the carbon atom have been considered to locate in the nucleus, the total Hamiltonian of this system should be given by

$$\boldsymbol{H}=-1/2\sum_{i=1}^{5}\Delta_i+4/R_{CH}-\sum_{i=1}^{5}4/r_{Ci}-\sum_{i=1}^{5}1/r_{Hi}+\sum_{\substack{i,j=1\\(i\neq j)}}^{5}1/r_{ij}. \tag{4}$$

Approximately the perturbing term in the present calculation is taken as,

$$\boldsymbol{H}'=4/R_{CH}-4/r_{C5}-\sum_{i=1}^{4}1/r_{Hi}+\sum_{\substack{i,j=1\\(i\neq j)}}^{5}1/r_{ij} \tag{4'}$$

where R_{CH} is the nuclear distance between the carbon and the hydrogen atom. r_{Ci} and r_{Hi} are the distances between the carbon and hydrogen atoms and the i-th electron, and r_{ij} is the distance between the i-th and j-th electrons. In (4′) electrons 1 to 4 are the 2*s* or 2*p* orbitals of the carbon atom and electron 5 is the 1*s* orbital of the hydrogen atom.

Then the secular equations can be set up for the type $^4\Sigma^-$; for instance, it can be written as

$$\text{det.}\mid H_{ij}-\Delta_{ij}W\mid=0, \tag{5}$$

where

$$H_{11}=\mathfrak{M}^{\Phi_2}-\mathfrak{N}_{ss}^{\Phi_2}-6F_2-2J_{sp}-2N_{\pi\pi}+6F_2S^2{}_{sh}+4L_{s\pi\pi h}S_{sh}$$

$$H_{22}=\mathfrak{M}^{\Psi_1}+\frac{1}{4}\mathfrak{N}_{ss}^{\Psi_1}+\frac{1}{4}\mathfrak{N}_{\sigma\sigma}^{\Psi_1}-12F_2-3J_{sp}+\frac{1}{2}N_{\pi\pi}-3F_2S_{sh}{}^2-\frac{3}{2}F_2S_{\sigma h}{}^2-\frac{1}{2}(L_{s\tau\sigma h}S_{sh}+L_{\sigma ssh}S_{\sigma h}-K_{s\sigma}S_{sh}S_{\sigma h})-L_{s\pi\pi h}S_{sh}-L_{\sigma\pi\pi h}S_{\sigma h}-\frac{1}{2}J_{sp}S_{\sigma h}{}^2$$

$$H_{33}=\mathfrak{M}^{\Psi_1}-\frac{3}{4}\mathfrak{N}_{ss}^{\Psi_1}-\frac{3}{4}\mathfrak{N}_{\sigma\sigma}^{\Psi_1}-6F_2-J_{sp}-\frac{3}{2}N_{\pi\pi}+3F_2S_{sh}{}^2+\frac{9}{2}F_2S_{\sigma h}{}^2+\frac{3}{2}(L_{s\sigma\sigma h}S_{sh}+L_{\sigma ssh}S_{\sigma h}-K_{s\tau}S_{sh}S_{\sigma h})+L_{s\pi\pi h}S_{sh}+L_{\sigma\pi\pi h}S_{\sigma h}-\frac{1}{2}J_{sp}S_{\sigma h}{}^2$$

$$H_{44}=\mathfrak{M}^{\Psi_1}-\frac{1}{2}\mathfrak{N}_{ss}^{\Psi_1}-\frac{1}{2}\mathfrak{N}_{\sigma\sigma}^{\Psi_1}-9F_2-2N_{\pi\pi}+3F_2S_{sh}{}^2+3F_2S_{\sigma h}{}^2-(L_{\sigma\sigma sh}S_{sh}+L_{\sigma ssh}S_{\sigma h}-K_{s\sigma}S_{sh}S_{\sigma h})+2L_{s\pi\pi h}S_{sh}+2L_{\sigma\pi\pi h}S_{\sigma h}$$

$$H_{12}=\frac{\sqrt{5}}{2}(2L_{\sigma ssh}S_{sh}-K_{s\sigma}S_{sh}{}^2)-\frac{\sqrt{5}}{2}\mathfrak{N}_{s\sigma}^{\Phi_2\Psi_1}+3\sqrt{5}F_2S_{sh}S_{\sigma h}+\sqrt{5}L_{\sigma\pi\pi h}S_{sh}+\sqrt{5}J_{sp}S_{sh}S_{\sigma h}$$

$$H_{13}=-\frac{1}{2}(2L_{\sigma ssh}S_{sh}-K_{s\tau}S_{sh}{}^2)+\frac{1}{2}\mathfrak{N}_{s\sigma}^{\dagger_2\Psi_1}-3F_2S_{sh}S_{\sigma h}-2L_{s\pi\pi h}S_{\sigma h}-L_{\sigma\pi\pi h}S_{sh}+J_{sp}S_{sh}S_{\sigma h}$$

$$H_{14}=\sqrt{2}\,\mathfrak{M}_{s\sigma}-\frac{1}{\sqrt{2}}(2L_{\sigma ssh}S_{sh}-K_{s\sigma}S_{sh}{}^2)-\frac{1}{\sqrt{2}}\mathfrak{N}_{s\sigma}^{\Phi_2\Psi_1}+3\sqrt{2}F_2S_{sh}S_{\sigma h}+\sqrt{2}L_{s\tau\pi h}S_{\sigma h}+\sqrt{2}L_{\sigma\pi\pi h}S_{sh}$$

$$H_{23}=-\frac{\sqrt{5}}{4}\mathfrak{N}_{ss}^{\Psi_1}-\frac{\sqrt{5}}{4}\mathfrak{N}_{\sigma\sigma}^{\Psi_1}+\frac{\sqrt{5}}{2}N_{\pi\pi}+3\sqrt{5}F_2S_{sh}{}^2+3\frac{\sqrt{5}}{2}F_2S_{\sigma h}{}^2+\frac{\sqrt{5}}{2}J_{sp}S_{\sigma h}{}^2+\frac{\sqrt{5}}{2}(L_{s\sigma\sigma h}S_{sh}+L_{\sigma ssh}S_{\sigma h}-K_{s\sigma}S_{sh}S_{\sigma h})$$

$$H_{24}=\frac{\sqrt{5}}{2\sqrt{2}}\mathfrak{N}_{ss}^{\Psi_1}-\frac{\sqrt{5}}{2\sqrt{2}}\mathfrak{N}_{\sigma\sigma}^{\Psi_1}-6\sqrt{\frac{5}{2}}F_2S_{sh}{}^2+3\sqrt{\frac{5}{2}}F_2S_{\sigma h}{}^2+\sqrt{\frac{5}{2}}J_{sp}S_{\sigma h}{}^2-\sqrt{\frac{5}{2}}L_{s\pi\pi h}S_{sh}+\sqrt{\frac{5}{2}}L_{\sigma\pi\pi h}S_{\sigma h}$$

$$H_{34}=-\frac{1}{2\sqrt{2}}\mathfrak{N}_{ss}^{\Psi_1}+\frac{1}{2\sqrt{2}}\mathfrak{N}_{\sigma\sigma}^{\Psi_1}+3\sqrt{2}F_2-\sqrt{2}J_{sp}-3\frac{1}{\sqrt{2}}F_2S_{\sigma h}{}^2+\frac{1}{\sqrt{2}}J_{sp}S_{\sigma h}{}^2+\frac{3}{\sqrt{2}}L_{s\pi\pi h}S_{sh}-\frac{3}{\sqrt{2}}L_{\sigma\pi\pi h}S_{\sigma h}$$

$$\Delta_{11}=1-S_{sh}{}^2$$

$$\Delta_{22}=1+\frac{1}{4}S_{sh}{}^2+\frac{1}{4}S_{\sigma h}{}^2$$

$$\Delta_{33}=1-\frac{3}{4}S_{sh}{}^2-\frac{3}{4}S_{\sigma h}{}^2$$

$$\Delta_{44}=1-\frac{1}{2}S_{sh}{}^2-\frac{1}{2}S_{\sigma h}{}^2$$

$$\Delta_{12}=-\frac{\sqrt{3}}{2}S_{sh}S_{\sigma h}$$

$$\Delta_{13}=\frac{1}{2}S_{sh}S_{\sigma h}$$

$$\Delta_{14}=-\frac{1}{\sqrt{2}}S_{sh}S_{\sigma h}$$

$$\Delta_{23}=-\frac{\sqrt{5}}{4}S_{sh}^2-\frac{\sqrt{5}}{4}S_{\sigma h}^2$$

$$\Delta_{24}=\frac{\sqrt{5}}{2\sqrt{2}}S_{sh}^2-\frac{\sqrt{5}}{2\sqrt{2}}S_{\sigma h}^2$$

$$\Delta_{34}=-\frac{1}{2\sqrt{2}}S_{sh}^2+\frac{1}{2\sqrt{2}}S_{\sigma h}^2$$

Here

$$\left.\begin{aligned}\mathfrak{M}^{\chi}_{\alpha\alpha}&=\int\bar{\chi}\boldsymbol{H}'\chi d\tau\\ \mathfrak{N}^{\chi}_{\alpha\alpha}&=\int P_{\alpha H}\bar{\chi}\boldsymbol{H}'\chi d\tau\end{aligned}\right\}$$

where $P_{\alpha H}$ shows a permutation between the α and H electrons. All the other two-center energy integrals are defined in the table by Kotani and Amemiya[5], and their values used in this calculation are deduced from the same table, the value of δ being chosen as 1.59 (in the atomic unit) for the carbon atom. The internuclear distance between the carbon atom and the hydrogen atom is taken to be 1.12 A., which is the equilibrium distance in the $^2\Pi$ state. The values of energy integrals are as follows:

S_{sh}	= 0.5598	L_{ssssh}	=7.754 e. v.
$S_{\sigma h}$	= 0.4679	$L_{ss\sigma sh}$	=6.076 〃
M_{ss}	=11.174 e. v.	$L_{ss\sigma\sigma h}$	=1.313 〃
$M_{s\sigma}$	= 3.085 〃	$L_{s\sigma\sigma h}$	=2.335 〃
$M_{\sigma\sigma}$	=12.205 〃	$L_{\sigma s\sigma h}$	=8.036 〃
$M_{\pi\pi}$	=10.658 〃	$L_{\sigma\sigma\sigma h}$	=6.664 〃
N_{ss}	= 4.637 〃	$L_{\pi s\pi h}$	=7.613 〃
$N_{s\sigma}$	= 4.376 〃	$L_{\pi\pi sh}$	=1.354 〃
$N_{\sigma\sigma}$	= 4.742 〃	$L_{\pi\sigma\pi h}$	=5.782 〃
$N_{\pi\pi}$	= 0.664 〃	$L_{\pi\pi\sigma h}$	=0.273 〃

J_{sh}	= 9.750 e. v.
$J_{\sigma h}$	= 7.045 〃
J_{hs}	=10.618 〃
$J_{h\sigma}$	=12.687 〃
K_{ss}	=12.362 〃
$K_{s\sigma}$	= 4.656 〃
$K_{\sigma\sigma}$	=14.672 〃
$K_{\pi\pi}$	=11.199 〃
K_{hh}	=12.268 〃

The values of the one-center energy integrals are deduced from those which are calculated from the Hartree field of carbon atom by Ufford[6]. Accordingly, the energy difference between the states $^3D^0$ and ^3P of the carbon atom is given by

$$W_c(^3D^0)-W_c(^3P)=7.813 \text{ e. v.}$$

which is slightly smaller than the observed value[7] (7.94 e. v.).

The Electronic Energies of the CH Radical

Using these values, the electronic energies W can be computed from the secular equation (5). The resulting energy levels are shown in the middle of Fig. 1, and the energy levels which are obtained from the $(2s)^2(2p)^2$ or $(2s)(2p)^3$ only are shown in the left and the right of Fig. 1., respectively. The electronic energies in this calculation are compared with the values by Niira and Oohata which are calculated assuming all the atomic orbitals to be orthogonal to each other, and with the observed values, in Table 1.

Table 1

The Comparison between the Calculated and the Observed Values of the CH Radical

	Calc. (e. v.) (This work)	Calc.[4](e. v.) (Niira-Oohata)	Exp.[1](e. v.)
$^2\Sigma^+$	+0.83	+0.31	(+0.47)
$^2\Sigma^-$	+0.14	−0.18	(−0.28)
$^2\Delta$	−0.61	−1.14	(−0.60)
$^2\Pi$	−2.87	−2.95	−3.47
$^4\Sigma^-$	−3.60	−3.00	—
$^2\Sigma^+\rightarrow{}^2\Pi$	3.70	3.26	3.94
$^2\Sigma^-\rightarrow{}^2\Pi$	3.01	2.77	3.19
$^2\Delta\rightarrow{}^2\Pi$	2.26	1.81	2.87

The Electronic Energies of the BH Radical

The electronic energies of the BH radical are calculated in a similar manner as in the CH radical, and the resulting energy levels and their comparison with the observed values are shown in Fig. 2 and Table 2. In this

Table 2

The Comparison between the Calculated and the Observed Values of the BH Radical

	Calc. (e. v.)	Exp. (e. v.)
$^1\Pi\rightarrow{}^1\Sigma^+$	2.53	2.86[1]
$^3\Sigma\rightarrow{}^3\Pi$	3.08	3.36[8]
$D(^1\Sigma^+)$	4.07	<3.49

(5) M. Kotani and A. Amemiya, *Proc. Phys. Math. Soc. Japan*, **22** Extra No. 1 (1940).

(6) C. W. Ufford, *Phys. Rev.*, **53**, 568, (1938).

(7) B. Edlen, *Z. f. Phys.* **84**, 746, (1933).

(8) G. M. Almy and R. B. Horsfall, *Phys. Rev.*, **51**, 491 (1937).

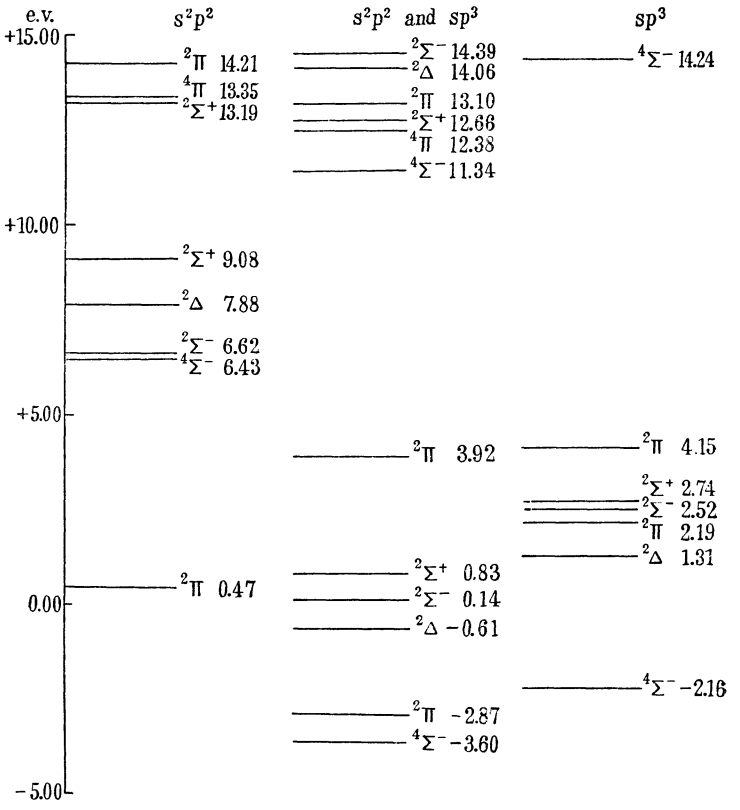

Fig. 1.—The electronic energies of the CH radical.
The origin of the energy is chosen to be $C(^3P)+H(^2S)$.

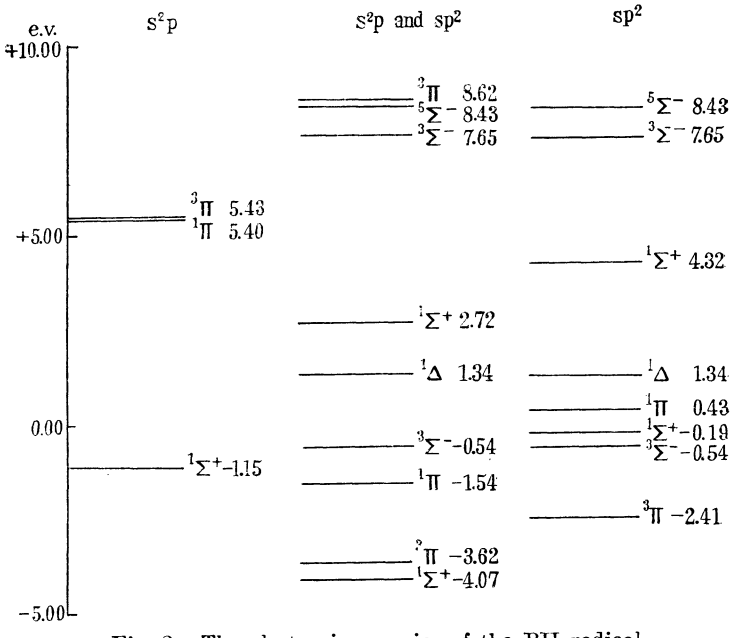

Fig. 2.—The electronic energies of the BH radical.
The origin of the energy is chosen to be $B(^2P^0)H(^2S)$.

case the values of the one-center energy integrals are calculated from the functions used in the two-center integrals. The energy difference between the states ^2D and $^2P^0$ of the boron atom is deduced from the spectroscopic data:

$$W_B(^2D) - W_A(^2P^0) = 5.932 \text{ e. v.}$$

and the value of δ is chosen as 1.26 for the boron atom. The internuclear distance between the boron atom and the hydrogen atom is taken as 1.226A. which is the equilibrium distance of the $^1\Sigma^+$ state.

Discussion

These energies obtained in the present calculation can explain satisfactorily the observed values, a consequence of the fact that the electronic configurations of the boron atom have been assumed to be both the $(2s)^2(2p)$ and $(2s)(2p)^2$, and of the carbon atom both the $(2s)^2(2p)^2$ and $(2s)(2p)^3$. Since the overlap integrals and the higher order permutations have been considered, the resulting values become more close to the observed ones than in the case of neglecting the overlap integrals. The lowest state of the CH radical in this calculation is $^4\Sigma^-$, which is not actually observed, but the result is the same as those in the molecular orbital approximation by Mulliken[9] and in the atomic orbital by Niira and Oohata[4]. This result is of some interest in comparison with the calculation by Niira and Oohata[4] in which the lowest state of the CH_2 radical is found to be $^3B_1$.

But in the present calculation the electronic configuration of the carbon atom is assumed to be both the $(2s)^2(2p)^2$ and $(2s)(2p)^3$ only and the others are not included. Even if the $(2p)^4$ configuration is added to those, the lowest state of the CH radical is $^4\Sigma^-$ as it is. This is explained as follows: If the $(2p)^4$ electronic configuration for the carbon atom is taken, there are four possible kinds of electronic orbital wave functions for the entire radical, which are given by the products of the atomic orbitals:

$$\left.\begin{aligned}
\chi_1 &\equiv (2p\sigma)(2p\sigma)(2p\pi_+)(2p\pi_-)(H)\\
\chi_2 &\equiv (2p\pi_+)(2p\pi_+)(2p\pi_-)(2p\pi_-)(H)\\
\chi_3 &\equiv (2p\sigma)(2p\pi_\pm)(2p\pi_\pm)(2p\pi_\mp)(H)\\
\chi_4 &\equiv (2p\sigma)(2p\sigma)(2p\pi_\pm)(2p\pi_\pm)(H)
\end{aligned}\right\} \quad (6)$$

These wave functions are classified into the symmetry types as

	$^2\Sigma^+$	$^2\Sigma^-$	$^2\Pi$	$^2\Delta$	$^4\Sigma^+$	$^4\Sigma^-$	$^4\Pi$	$^4\Delta$	$^6\Sigma^-$
χ_1	1	1	0	0	0	1	0	0	0
χ_2	1	0	0	0	0	0	0	0	0
χ_3	0	0	2	0	0	0	1	0	0
χ_4	0	0	0	1	0	0	0	0	0
Sum	2	1	2	1	0	1	1	0	0

(7)

Thus including the $(2p)^4$ configuration the numbers of the basic wave functions belonging to the types $^2\Pi$ and $^4\Sigma^-$ increase by two and one, respectively. In the $^4\Sigma^-$, the χ_1 corresponds to the Φ_2 with the replacement of $(2s)$ by $(2p\sigma)$, and so considerably interacts with the Ψ_1 like the Φ_2. Consequently the electronic energy is well stabilized. But in the $^2\Pi$, the χ_3 corresponds to the Ψ_3 with replacement $(2s)$ by $(2p\sigma)$ and then scarcely interacts to the Φ_3 and Ψ_2 like the Ψ_3. (The dissociation energy obtained for the Φ_3 and Ψ_2 is 2.82 e. v., while including the Ψ_3 2.87 e. v. These results show that the energy is stabilized by 0.05 e. v. only.) Thus in the lowest energy of the $^2\Pi$ the Φ_3 and Ψ_2 affect it far more strongly than the Ψ_3 and χ_3; therefore even if the χ_3 is included, it may be improbable that the lowest state of $^2\Pi$ becomes more stable than the $^4\Sigma^-$.

Recently interesting discussions[10]~[14] have been offered as to the dissociation energy and the ground state of the CH radical. In the discussions Glockler has suggested from the regularities of bond energies found in various hydrides, that the dissociaiton energy of the radical 3.47 e. v. (80 kcal.), estimated by Herzberg[15] assuming $^2\Pi$ as the ground state and usually accepted, is too low and that a somewhat larger value of 4.0 e. v. (92.3 kcal.) should be taken.

The results of this work that the ground state is not $^2\Pi$ but $^4\Sigma^-$ and the former lies 0.73 e. v. higher than the latter seem to explain quantitatively Glockler's results: for, if this conclusion is correct, the dissociation energy (for the ground state $^4\Sigma^-$) becomes 0.73 e. v. larger than that for $^2\Pi$ (3.47 e. v.), namely 4.20 e. v., which is in close agreement with Glockler's estimation.

No 1s electron integrals of the boron and the carbon atoms have been considered and also the ionic states of the radicals and the

(9) R. S. Mulliken, *Rev. Mod. Phys.*, **4**, 1 (1932).

(10) G. Glockler, *Disc. Farad. Soc.*, No. **10**, 26 (1951).
(11) A. G. Gaydon, ibid., P. 108.
(12) C. A. McDowell and J. W. Warren, ibid., p. 53.
(13) G. Porter, ibid., p. 115.
(14) R. G. W. Norrish, G. Porter and B. A. Thrush, *Nature* **169**, 582 (1952).
(15) G. Herzberg, "Molecular Spectra and Molecular Structure, I. Spectra of Diatomic Molecules," 2nd ed. D. Van Nostrand Co. Inc., New York, 1950.

other excited states of the atoms of the radicals are not included. In the excited states of the radicals the effects of these states seem to be fairly large, and so strictly speaking it may be desirable to carry out a calculation including those states.

As the nuclear distances in the present calculation are taken to be the observed values for the ground states, but these are not always equal to the values for the excited states. Accordingly, the electronic energies of these radicals should be calculated changing the nuclear distances.

Summary

The energy levels of the CH and the BH radicals have been calculated by the method of atomic orbitals, taking both s^2p^2 and sp^3 configurations together for the carbon atom and s^2p and sp^2 for the boron atom and including the overlap integrals and the higher order permutations. The values obtained are in excellent agreement with observations.

Acknowledgements are made to Assistant Professors S. Shida and I. Tanaka and Mr. Y. Mori of this Laboratory, and Assistant Professor K. Niira and Mr. K. Oohata of the Laboratory of Physics for their kind discussions and suggestions. The author also expresses his sincere thanks to Dr. G. Glockler (Office of Ordnance Research, Durham), Dr. G. Porter (University of Cambridge, Cambridge) and Dr. A. G. Gaydon (Imperial College, London) for their kind and valuable discussions.

Laboratory of Physical Chemistry,
Tokyo Institute of Technology, Tokyo

Note on Polymer-mixed Solvents System. III. Selective Adsorption

By Toru KAWAI

(Received June 13, 1952)

A recent paper by Ewart, Roe, Debye, and McCartney (E. R. D. M.)[1] on the light scattering of polymer dissolved in binary mixtures suggests that this method should yield interesting information regarding the interaction of polymer not only with good solvents but with non-solvents. As was shown by the authors mentioned above, the addition of a third component to a polymer-solvent mixture should cause a change in light scattering due to preferential adsorption of one or other of the solvent components by the polymer. Result obtained by them may be written

$$\lim_{c\to 0}(\tau/c)=M\times(32\,\pi^3n^2/3\lambda^4N_0)(\partial n/\partial c + \alpha\,\partial n/\partial\varphi)^2, \qquad (1)$$

where τ=turbidity, c=concentration of polymer, M=molecular weight of polymer, n=refractive index, λ=wave-length of exciting radiation, N_0=Avogadro's number, φ=volume fraction of solvent in a solvent-diluent mixture exclusive of the volume occupied by the polymer, and $\alpha=-\partial\varphi/\partial c$.

The significance of this factor α can bn understood as a measure of the change ie composition of the solvent-diluent mixture (surrounding the polymer) due to selective adsorption. Thus, if the solvent component adsorbed has a higher refractive index than the diluent ($\partial n/\partial\varphi>0$), the ratio of polymer concentration to turbidity in the limit of zero concentration, $(c/\tau)_0$, should decrease. The contrary would be true if the refractive indices were in the reverse order.

On the other hand, a comprehensive theory of composition fluctuations in multi-component systems has been developed independently by Kirkwood and Goldberg,[2] and Stockmayer.[3] In their discussions, the deviation

(1) R. H. Ewart, C. P. Roe, P. Debye and J. R. McCartney, *J. Chem. Phys.*, **14**, 687 (1946).

(2) J. G. Kirkwood and E. J. Goldberg, *J. Chem. Phys.*, **18**, 54 (1950).

(3) W. H. Stockmayer, *J. Chem. Phys.*, **18**, 58 (1950).

of the value of M calculated from the limiting value, $(\tau/c)_0$, from the true molecular weight was interpreted as showing that the thermodynamic interaction between a polymer and a diluent may cause the former to induce composition fluctuations with respect to the latter of the same order of magnitude as composition fluctuations with respect to the polymer species itself. Therefore, the approximate treatment of E. R. D. M., in which such deviation was discussed under the consideration of selective adsorption of one of the solvent components by polymer, should be regarded as a supplementing one on some molecular assumption rather than the basis for an exact analysis of turbidity data. However, such an approximate treatment may give some interesting information concerning selective adsorption in the actual polymer-mixed solvents systems. It will be shown in the present paper that the magnitude of selective adsorption can be well interpreted quantitatively by the interaction parameters characterizing the polymer-mixed solvents system, which were introduced in the free energy expression presented in the previous paper.[4] This will enable us to estimate the magnitude of selective adsorption in any system if the values of the interaction parameter are known. (The various methods by which the interaction parameters can be calculated were already presented in the previous paper.[5]) Here it is also shown that these parameters can be computed from turbidity data by considering the dependence on polymer concentration.

The Significance of the Factor α

The theoretical treatments of light scattering in multi-component systems permit us to express the results of light scattering measurements in the language of thermodynamics. According to Stockmayer,[3] turbidity τ is adequately represented by an equation of the form

$$\tau = HV\sum_i\sum_j \psi_i\psi_j A_{ij}/\,|\,a_{ij}\,| \qquad (2)$$

where $H = 32\pi^3 n^2 k T/3\lambda^4$, $\psi_i = (\partial n/\partial m_i)_{T,P,m}$ (n is the refractive index, and the quantities m_i of the component i in volume V may be measured by any desired units, the definitions of their chemical potentials μ_i varying accordingly), $a_{ij} = (\partial\mu_i/\partial m_j)_{T,P,m}$, $|\,a_{ij}\,|$ represents the determinant of all the a_{ij}, and A_{ij} is the co-factor. From Eq. (2) the difference $\Delta\tau$, between the turbidity of the polymer 3-solvents 1 and 2 system[6] and that of the solvents mixed in the same proportion in the absence of polymer, may be written

$$\Delta\tau/HV = \frac{\psi_3^2 a_{22} - 2\psi_2\psi_3 a_{23} + \psi_2^2 a_{33}}{a_{33}a_{22} - a_{23}^2} - \frac{\psi_2^2}{a_{22}^0}$$
$$= \frac{[\psi_3 - (a_{23}/a_{22})\psi_2]^2}{a_{33} - a_{23}^2/a_{22}} + \psi_2^2\left(\frac{1}{a_{22}} - \frac{1}{a_{22}^0}\right), \qquad (3)$$

where the superscript zero denotes a solution containing no polymer. Obviously from the discussion in the last section on the dependency of the a's on polymer concentration, $(\Delta\tau/HC)_0$ at infinite dilution, may be given by

$$(\Delta\tau/HC)_0 = M[\psi_3 - (a_{23}/a_{22})\psi_2]^2. \qquad (4)$$

Eq. (4) agrees with the result of E. R. D. M (Eq. (1)). The correspondence is better seen when the equality

$$a_{23}/a_{22} = \frac{(\partial\mu_2/\partial m_3)_{T,P,m_2}}{(\partial\mu_2/\partial m_2)_{T,P,m_3}} = -(\partial m_2/\partial m_3)_{T,P,\mu_2} \qquad (5)$$

is examined. It is clear that the ratio a_{23}/a_{22} is the analogue of the factor α. Thus, we can assume the factor α as a measure of the magnitude of selective adsorption, because the significance of the factor can be interpreted through the thermodynamic description of light scattering in the multi-component system.

Theoretical Treatment of Selective Adsorption

In the previous paper[4] a general free energy expression covering much of the experimental data has been derived for the polymer-mixed solvents system, removing the Scott's assumptions,[7] which are not always applicable to the actual cases. The partial molal free energy of components may be written[8]

$$\Delta\bar{F}_1 = RT[(V_1/V_3)\{\ln v_1 + (1-1/x)v_3 + \mu_s v_3^2\} + (V_1/RT)\{A_{12}v_2^2 + A_{13}v_3^2 + (A_{12}+A_{13}-A_{23})v_2v_3\}] \qquad (6a)$$

$$\Delta\bar{F}_2 = RT[(V_2/V_3)\{\ln v_2 + (1-1/x)v_3 + \mu_s v_3^2\} + (V_2/RT)\{A_{12}v_1^2 + A_{23}v_3^2 + (A_{12}+A_{23}-A_{13})v_1v_3\}]. \qquad (6b)$$

(4) T. Kawai, This Bulletin, **25**, 336 (1952).
(5) T. Kawai, This Bulletin, **25**, 341 (1952).

(6) Here we adopt the same notation of components 1, 2, 3 as employed in the previous papers (reference 4 and 5) instead of that of Stockmayer.
(7) R. L. Scott, *J. Chem. Phys.*, **17**, 268 (1949).
(8) See Eq. (19a, b) in reference 4. As discussed there, the volume of polymer submolecule is larger than molecular volumes of both solvent and diluent in the actual systems.

The notation of these equations is similar to that was employed in the previous paper.[4]

Generally, when two phases co-exist in equilibrium,

$$\Delta\bar{F}_1' = \Delta\bar{F}_1'' \tag{7a}$$
$$\Delta\bar{F}_2' = \Delta\bar{F}_2'' \tag{7b}$$
$$\Delta\bar{F}_3' = \Delta\bar{F}_3'' \tag{7c}$$

must be fulfilled in a three component system. (Here we distinguish the two phases by primes and double primes.) Combining Eqs. (7a) and (7b)[9] through respective substitution from Eqs. (6a) and (6b), there is obtained

$$\ln(v_1'/v_2') - \ln(v_1''/v_2'') = (V_3/RT)[\{A_{12}v_2''^2 - A_{13}v_1''^2 + (A_{13}-A_{23})v_3''^2 + (A_{12}+A_{13} - A_{23})v_2''v_3'' - (A_{12}+A_{23}-A_{13})v_1''v_3''\} - \{A_{12}v_2'^2 - A_{13}v_1'^2 + (A_{13}-A_{23})v_3'^2 + (A_{12} + A_{13}-A_{23})v_2'v_3' - (A_{12}+A_{23}-A_{13})v_1'v_3'\}]. \tag{8}$$

If we write $v_2'/v_1' = \theta'$, $v_2''/v_1'' = \theta''$, $v_1 = v_0/(1+\theta)$, and $v_2 = \theta v_0/(1+\theta)$, Eq. (8) may be converted to the form

$$\ln(\theta''/\theta') = (V_3/RT)\left[(v_0''-v_0')\left\{-\left(\frac{1-\theta'}{1+\theta'}\right)A_{12} - A_{13}+A_{23}\right\} - v_0''\left\{\left(\frac{1-\theta''}{1+\theta''}\right) - \left(\frac{1-\theta'}{1+\theta'}\right)\right\}A_{12}\right]. \tag{9}$$

Here we rewrite $\theta' = \theta$, and $\theta'' = \theta + \Delta\theta$. Then, expanding the terms $\ln(\theta''/\theta')$ and $\left\{\left(\frac{1-\theta''}{1+\theta''}\right) - \left(\frac{1-\theta'}{1+\theta'}\right)\right\}$ in series of $\Delta\theta/\theta$, and neglecting terms after the first two, it follows that

$$\Delta\theta/\theta \fallingdotseq (V_3/RT)\left[-\Delta v_3\left\{-\left(\frac{1-\theta}{1+\theta}\right)A_{12} - A_{13} + A_{23}\right\} + \{2(1-v_3'')\Delta\theta/(1+\theta)^2\} \times A_{12}\right] \tag{10}$$

$$\{1/\theta - [2(1-v_3'')/(1+\theta)^2] \times A_{12}V_3/RT\}\Delta\theta \fallingdotseq -(V_3/RT)\Delta v_3\left\{-\left(\frac{1-\theta}{1+\theta}\right)A_{12} - A_{13} + A_{23}\right\} \tag{11}$$

where $\Delta v_3 = v_3'' - v_3' = v_0' - v_0''$.

Now, let us turn our attention to a polymer molecule in the solvent and consider the influence of its environments on it. It may be assumed that each molecule is distributed within an effective volume such as is often considered in the treatments of high polymer solutions especially for coiled molecules.[10] The relations concerning the partition of the two solvents inside and outside of this effective volume pervaded by a polymer molecule will be obtained from the condition of the equilibrium between the above region and its environments. Approximately Eq. (10) may be applicable to this equilibrium, although, strictly speaking, the partial molal entropy in the region assumed could not be expressed by the entropy terms in Eqs. (6a, b).

Since the values of $A_{12}V_3/RT$ are supposed to be comparatively small in usual cases,[11] the term $\{2(1-v_3'')/(1+\theta)^2\} \times A_{12}V_3/RT$ in Eq. (11) can be neglected as compared with $1/\theta$, if θ were sufficiently small. (We assumed here liquid 1 is a principal solvent, and liquid 2 a diluent.) Thus, Eq. (11) becomes

$$-\Delta\theta/\theta \fallingdotseq (V_3/RT)\Delta v_3\left\{-\left(\frac{1-\theta}{1+\theta}\right)A_{12} - A_{13} + A_{23}\right\}. \tag{12}$$

Since $\Delta\theta/\theta$ is assumed to be a measure of the magnitude of selective adsorption and the A's are the interaction parameters characterizing the polymer-mixed solvents system, Eq. (12) enables us to estimate roughly the magnitude of selective adsorption in any system.

It was shown in the previous paper[5] that the medium containing non-solvent to some extent sometimes behaves as a better solvent than the pure solvent itself, and that the solvent power of the mixture shows a maximum at the solvent-precipitant composition which fulfils the condition;

$$(V_0/RT)\left\{-\left(\frac{1-\theta}{1+\theta}\right)A_{12} + A_{23} - A_{13}\right\} = 0. \tag{13}[12]$$

Thus, we can draw an interesting conclusion from Eqs. (12) and (13) as follows. Namely, when the solvent has a strong solvent power and the diluent has a strong precipitating power, a polymer molecule exhibits a conspicuous preference for the solvent molecules in its statistical environment. In this case, of course, the solvent ability of the mixture decreases uniformly with increasing θ as was

(9) Eq. (7a) $\times V_3/V_1$ − Eq. (7b) $\times V_3/V_2$

(10) For example, see T. Kawai, This Bulletin, **24**, 70 (1951).

(11) Although the exact values of V_3 cannot be deduced, the A_{12} values calculated from vapor pressure data in various two liquids systems show that the values of $A_{12}V_3/RT$ are anticipated in the range from 0.5 to 2.0.

(12) See Eq. (7) in reference (5). V_0 is a mean value of the volumes of the solvent and the diluent.

discussed in the previous paper[5](when $A_{23}-A_{13} > A_{12}$, the solutions of Eq. (13) cannot afford any physical meaning). When the solvent abilities of the two liquids do not differ very much from each other, selective adsorption is not notable. However, the contribution of the parameter A_{12} must be considered. When the $(A_{23}-A_{13})$ value becomes comparable to the A_{12} value, the magnitude of selective adsorption depends considerably on the solvent-diluent composition as seen in Eq. (12). Actually, this can be true only when the $(A_{23}-A_{13})$ values are tolerably small since the values of A_{12} are comparatively small. If $A_{23}-A_{13}<A_{12}$, an inversion in the sign of $\Delta\theta/\theta$ in Eq. (12) occurs with increasing θ, i. e., the diluent is rather preferentially adsorbed by the polymer until $\theta=\theta_c$, at which Eq. (13) is satisfied, and hereafter the solvent is adsorbed much more than the diluent as in usual cases. This corresponds to the fact that the solvent ability of the medium is improved in the first stage of addition of the diluent, and, after a certain solvent-diluent composition is reached, it decreases as the content of the diluent increases. As was discussed in the previous paper,[5] it appears also from experiments that this phenomenon occurs sometimes in polymer-mixed solvents systems. The turbidity data presented by Blaker and Badger[13] for nitrocellulose-two liquids systems can well be interpreted from the above reasoning. Quantitative discussion is impossible because the above treatment can not be applied to non-flexible chains such as nitrocellulose. However, considering that the energy term in the free energy expression gives predominant contribution to the result obtained in the above approximate treatment, it may be clear that we can roughly estimate the magnitude of selective adsorption even in such a case. The experiments of Blaker and Badger can be understood from the above procedure as follows; the diluent is positively adsorbed by the polymer in the solvent-diluent composition range used $(\theta<\theta_c)$. As Blaker and Badger pointed out, rather strong interaction between nitrocellulose and non-solvents is not surprising from many experimental facts.[13]

Comparison with Experimental Data

The factor α is not a characteristic constant of any one system, because it does not appear to behave in the same way for different systems. The value of α varies with the volume occupied by the polymer in the solvent (accordingly with molecular weight and concentration of the polymer etc.) and solvent-diluent composition. If we adopt the assumption of E. R. D. M. concerning the physical size of the effectively pervaded volume of a polymer molecule in the solvent, the factor α may be written as

$$\alpha=-\frac{\partial\varphi}{\partial c}=\left(\frac{v}{m}-\bar{v}\right)(\varphi_1''-\varphi_1') \qquad (14)$$

where v is the volume effectively occupied by a polymer molecule, m its mass, $\bar{v}$ the partial specific volume of the polymer and $(\varphi_1''-\varphi_1')$ is the difference in the volume fractions of solvent between in the effectively pervaded volume and in its environment.[14] The value of v/m can be calculated from the intrinsic viscosity of the solution by employing the relation $[\eta]=2.5\,v/m$ (with concentration measured in grams per cc.). Since $\Delta\theta/\theta$ in Eq. (12) can easily be computed from the $(\varphi_1''-\varphi_1')$ value thus obtained, we can examine the validity of Eq. (12) comparing with turbidity data. (Since $\Delta v_3\doteqdot v_3''$ in the present situation, Δv_3 can be estimated from the relation $[\mu]=2.5/v_3''\rho$, where ρ is the density of the polymer.) For this purpose the light scattering data of E. R. D. M. on solution of polystyrene in benzene-methanol mixture is cited. As will be discussed in the next section, the interaction parameters μ_{13}, μ_{23}, and μ_{12} have been employed instead of A_{13}, A_{23}, and A_{12} respectively $(\mu_{13}=(V_0/RT)A_{13}$, $\mu_{23}=(V_0/RT)A_{23}$, $\mu_{12}=(V_0/RT)A_{12})$[15], and these parameters have been calculated from the dependency of turbidity on polymer concentration. Thus Eq. (12) may be rewritten as

$$-\Delta\theta/\theta \doteqdot (V_3/V_0)\left\{-\left(\frac{1-\theta}{1+\theta}\right)\mu_{12}+\mu_{23}-\mu_{13}\right\}\Delta v_3. \qquad (15)$$

In Table 1 the numerical calculation of Eq. (15) for this system is illustrated. The V_3/V_0 values calculated by Eq. (15) show a satisfactory constancy for different compositions of the solvent-diluent mixtures as was shown in the last column in Table 1. In spite of the approximation supposed here, the result is rather surprising.

Owing to the scantiness of available data, we cannot show that the theory presented here gives a satisfactory explanation of the

(13) R. H. Blaker and R. H. Badger, *J. Am. Chem. Soc.*, **72**, 3129 (1950).

(14) Considering that the $(\varphi_1''-\varphi_1')$ values depend on the solvent-diluent composition, we assume $\Delta\theta/\theta$ as a measure characteristic to the system with regard *to* the magnitude of selective adsorption.

(15) V_0 is a certain mean value of the molal volumes of solvent and diluent as employed in reference (4).

Table 1

Numerical Calculation of Eq. (15) for Polystyrene-benzene-methanol System

$\mu_{13}=0.45$, $\mu_{23}=3.20$, $\mu_{12}=2.67$

φ_1'	$\varphi_1''-\varphi_1'$	$-\Delta\theta/\theta$	$-\left(\frac{1-\theta}{1+\theta}\right)\mu_{12}+\mu_{23}-\mu_{13}$	$[\mu]$	Δv_3	V_3/V_0
1	0	0	0.45	131.5	0	
0.925	0.25	0.0359	0.48	122.0	0.0224	3.96
0.90	0.51	0.0563	0.61	118.7	0.0208	4.75
0.875	0.79	0.0679	0.75	110.6	0.0194	4.53
0.85	1.00	0.0775	0.88	102.6	0.0189	3.93

experiments in many other systems. The interaction parameters for polystyrene-butanone-isopropanol system are calculated as $\mu_{12}=0.168$, $\mu_{13}=0.487$, and $\mu_{23}=0.711$ from the turbidity data in the same paper. ($\mu_{13}=0.471$ from the osmotic pressure data of Doty, Brownstein and Schlener[16]) In this system $\alpha\,\partial n/\partial\varphi$ is negligible compared with $\partial n/\partial c$, and the limiting value of τ/HC at infinite dilution gives polymeric molecular weights in agreement with those found in pure solvents. Since this condition is fulfilled if either α or $\partial n/\partial c$ is sufficiently small and $\partial n/\partial c$ is extremely small in this case ($\partial n/\partial c=0.0004$), the value of α cannot be deduced from the turbidity data. It is supposed, however, from the μ's that α is probably very small in this system. Since the interaction parameters can be estimated from various other measurements of the colligative properties of polymer solutions as discussed in the previous paper, we can anticipate the magnitude of selective adsorption in any system.

Calculation of the Interaction Parameters

The theories of light scattering in multicomponent systems presented by the above mentioned authors provide a complete description of turbidity in the language of thermodynamics, although the significance of the interaction parameters employed individually by them is a little different in each case. If the relations between the parameters employed in our treatment and those of the others are given, we can compute the parameters in Eq. (15) from turbidity data.

The statistical treatment of general multicomponent systems by McMillan and Mayer[17] permits us to express the activity coefficient γ_s of component as

$$\ln\gamma_s=-\frac{1}{c_s}\sum_{\nu n}n_s B^*_{\nu n}\left(\frac{\Delta\alpha}{\gamma}\right)^{\nu}\pi(c_r)^{n_r} \qquad (16)$$

from Eq. (82b) in their paper (the notation is entirely the same with what employed by them), which may be written for the present system[18]

$$\ln\gamma_1=2B^*_{20}C_1+B^*_{11}C_2+B^*_{12}C_2^2+2B^*_{21}C_1C_2+\cdots \qquad (17a)$$

$$\ln\gamma_2=2B^*_{02}C_2+B^*_{11}C_1+B^*_{21}C_2^2+2B^*_{12}C_1C_2+\cdots, \qquad (17b)$$

where the irreducible integral, B^*_{ij}, shows that the integral for i molecules of component 1 (diluent) and j molecules of component 2 (polymer).[18] Now, according to the notation employed by Kirkwood and Goldberg, the activity coefficient either of the solvent additive 1 or of the polymer 2 is represented by the form

$$\ln\gamma_i=\sum_{k=1}^{2}A_{ik}C_k+\sum_{j,k=1}^{2}B_{ijk}C_jC_k. \qquad (18)$$

Comparing Eq. (18) with Eqs. (17a, b), it is clear that the interaction parameters of Kirkwood and Goldberg correspond to the above irreducible integral B^*_{ij}.

On the other hand, the parameter β of Stockmayer may be written from Eq. (18)

$$\beta_{12}=d\ln\gamma_1/dm_2=A_{12}M_2+2B_{122}M_2^2m_2+2B_{112}M_1M_2m_1+\cdots \qquad (19a)$$

$$\beta_{21}=d\ln\gamma_2/dm_1=A_{21}M_1+2B_{211}M_1^2m_1+2B_{212}M_1M_2m_2+\cdots, \qquad (19b)$$

where M_i is molecular weight of component i. (the quantities m_i have been expressed in molalities.)

Obviously from the definition of β,

$$\beta_{12}=\beta_{21}. \qquad (20)$$

(16) P. Doty, M. Brownstein and w. Schlener, *J. Phys. Chem.*, **53**, 213 (1949).

(17) W. G. McMillan and J. E. Mayer, *J. Chem. Phys.*, **13**, 276 (1945).

(18) For convenience, the notation of components 1, and 2 employed by Kirkwood and Goldberg was used throughout in this section.

So, the following relations exist between the parameters of Kirkwood and Goldgerg;

$$A_{12}/A_{21}=B_{112}/B_{211}=B_{122}/B_{212}=M_1/M_2. \quad (21)$$

And

$$\beta_{11}=A_{11}M_1+2B_{112}M_1M_2m_2+\cdots \quad (22a)$$

$$\beta_{22}=A_{22}M_2+2B_{212}M_1M_2m_1+\cdots \quad (22b)$$

Similarly, the expressions for the a's in Eqs. (2)~(5) are easily obtained, but are not presented here.

Although the interaction parameters μ_{12}, μ_{13}, and μ_{23} in Eq. (15), which have been used throughout in our preceding papers, can strictly be related to those of the above mentioned authors, the following approximate method offers a convenient means for calculation of the parameters μ_{12}, μ_{13}, and μ_{23}. To indicate clearly the dependency of turbidity on polymer concentration, Eq. (3) may be rewritten (from Eq. (3, 5) in reference 3)

$$HVm_2/\Delta\tau RT=\{1/[\psi_2-(m_1\beta_{12}\psi_1)/(1+\beta_{11}m_1)]^2\}\{1+[\beta_{22}-(m_1\beta_{12}^2)/(1+\beta_{11}m_1)]m_2+\cdots\}. \quad (23)^{(18)}$$

On the other hand, Scatchard[19] showed that the osmotic pressure P in two diffusible components-one non-diffusible solute systems may be expressed by the equation

$$P=AM_2(m_2+BM_2m_2^2+\cdots) \quad (24)$$

where $2BM_2=\beta_{22}-(m_1\beta_{12}^2)/(1+\beta_{11}m_1)$. (See Eq. (35) in reference 19) It is easily seen from Eq. (23) and (24) that we can calculate the second virial coefficient in the osmotic pressure expression by power series expansion in polymer concentrations from the light scattering data in polymer-mixed solvent systems. The method of estimating the parameters μ_{12}, μ_{13} and μ_{23} from the second virial coefficient in the osmotic pressure expression for various solvent-diluent compositions, is already represented in the previous paper.[5]

The writer wishes to thank his director, K. Makishima, for constant encouragement and many helpful suggestions. This report was presented at the Fifth Meeting of the Chem. Soc. Japan, at Tokyo University, April, 1952.

Laboratory of Textile Chemistry,
Tokyo Institute of Technology, Tokyo

(19) G. Scatchard, *J. Am. Chem. Soc.*, **68**, 2315 (1946).

Electrolytic Reduction of Aromatic Carboxylic Acids. II. Electrolytic Reduction of Cinnamic Acid[1]

By Shin-ichi ONO and Tadao HAYASHI

(Received May 9, 1952)

Introduction

It was reported in the previous paper[2] that the electrolytic reduction of benzoic acid at a lead cathode in acid solution gave benzyl alcohol and the reduction was favored under high pressure. Structually, cinnamic acid resembles benzoic acid, with the only exception that the latter has no α,β-unsaturated double bond between phenyl- and carboxyl-groups. It is probable, therefore, that cinnamic acid is reducible to γ-phenylpropyl alcohol under suitable conditions, as in the case of benzoic acid.

Already, Inoue[3a] reported that the electrolytic reduction of cinnamic acid at a lead cathode in alcoholic sulfuric acid solution gave the γ-phenylpropyl alcohol in 38% yield. But, later, Wilson[3b] explained that the γ-phenylpropyl alcohol and glycol which Inoue had claimed to isolate by the reduction of cinnamic acid were essentially ethyl β-phenylpropionate and diethyl β,γ-diphenyladipate respectively.

In this paper, it is intended to discuss the

(1) This paper was presented at the Annual Meeting of the Chem. Soc. Japan, held at Tokyo, April, 1951.

(2) S. Ono and T. Yamauchi, This Bulletin, **25**, 404 (1952)

(3) a) H. Inoue, *J. Chem. Soc. Ind. Japan*, **24**, 916 (1921).
b) C. L. Wilson and K. B. Wilson, *Trans. Electrochem. Soc.*, **84**, 153 (1943); C. L. Wilson, ibid., **92**, 369 (1947).

reduction mechanism of cinnamic acid, the change in products resulting from a change in experimental conditions, and moreover, to develop the influence of external pressure in the course of the electrolytic reduction.

Experimental

(1) **Materials.**—Cinnamic acid was prepared by the usual method in this laboratory. It had a m. p. of 132-133°C. Solvents used in these experiments were ethyl-, methyl- and iso-amyl-alcohols.

Cathodes used were as follows;

a) Lead cathode: commercial products (99.9% purity), a sheet or tube type (100 cm.^{2}), it was oxidized before use.

b) Mercury cathode: purified by washing with nitric acid and distillation in a vaccum, cathode area (16 cm.^{2}).

c) Zinc amalgum cathode: prepared by the electrolytic method.[4] cathode area (16 cm.^{2}).

d) Platinized-platinum cathode: cylindrical platinum plate (100 cm.^{2}) was platinized by the electrolysis of platinic chloride solution.

(2) **Reduction Method.**—The usual diaphragm type of the electrolytic cell was used. A porous cup (17 cm.×4.6 cm.) was placed in the cell as a cathode compartment and the cell was immersed in a water-bath to maintain the desired temperature. The reduction was carried out in the same manner as described in the previous paper.[2] Usually twice the theoretical amount of current was passed.

(3) **Isolation and Estimation of Products.**—(a) **Reduction at a Pb-, Hg-, and Hg-Zn-Cathodes.**—When the reduction was completed, the catholyte was decanted into a beaker, cooled and any precipitates which remained were filtered off. Then it was extracted with ether and washed with water.

After evaporation of ether, the remaining viscous liquid was steam-distilled.

(i) Distillate from steam-distillation was extracted with ether, and dried with anhydrous sodium sulfate. Evaporation of ether gave a liquid, which was distilled under diminished pressure. The fraction coming over at 106-112°/10 mm.Hg was collected. Redistillation gave a liquid, b. p. 110-112°/10 mm.Hg, D_4^{25} 1.0101, n_D^{25} 1.4920, identified as an ethyl β-phenylpropionate. (Found: C, 74.23; H, 7.8. Calculated for $C_{11}H_{14}O_2$: C, 74.16; H, 7.86). Saponification with 20% alcoholic potassium hydroxide solution gave a β-phenyl-propionic acid, m. p. 48-49°C.

(ii) Residual solution from steam-distillation was neutralized with potassium hydroxide solution, then extracted with a large volume of ether. Evaporation of ether gave a light yellow oily liquid from which a fine precipitate (m. p. 112-113°C.) was separated by standing overnight. Recrystallization from ethyl alcohol gave a colorless prism, m. p. 116-116.5°C. It was identified as a meso-diethyl diphenyladipate. (Found: C, 73.38; H, 7.04. Calculated for $C_{22}H_{26}O_4$: C, 74.55; H, 7.39).

The remaining oily liquid was treated with excess potassium hydroxide solution and cooled. Acidification with conc. hydrochloric acid produced a semi-solid materials which was treated with ether. The bulk of meso-diphenyladipic acid, (m. p. 260-265°C.), remained undissolved by ether. Evaporation of ether left a highly viscous liquid, from which insoluble diphenyladipic acid (m. p. 165-170°C.), was separated by treating with hot benzene.

(b) **Reduction at a Pt-Pt Cathode.**—After completing the reduction, the catholyte was diluted with water to some extent, then extracted with ether. The ether extracts were collected, washed with water and dried over anhydrous sodium sulfate. After evaporation of ether, the remaining liquid was distilled under diminished pressure. The fractions obtained were characterized. The reduction of cinnamic acid gave a cyclohexylpropionic acid, b. p. 143-145°/11 mm. Hg., m. p. 16°C., D_4^{20} 0.9966, n_D^{20} 1.4658. (Found: C, 70.03; H, 9.68. Calculated for $C_9H_{16}O_2$: C, 69.3; H, 10.25)

(4) **Constants of Products.**—The following products were obtained in the present experiments.

(i) , β-Phenylpropionic acid, m. p. 48-49°C., recrystallized from ligroin.

Ethyl ester, b. p. 110-112°/10 mm.Hg, D_4^{25} 1.0101, n_D^{25} 1.4920

Methyl ester, b. p. 126-128°/25 mm.Hg, D_4^{25} 1.0420, n_D^{25} 1.5102

iso-Amyl ester, b. p. 136-138°/7 mm.Hg, n_D^{25} 1.4840

(ii) β,γ-Diphenyladipic acid

a) Meso acid, m. p. 260-265°C, recrystallized from EtOH.

Diethyl ester, m. p. 116-116,5°C.

Dimethyl ester, m. p. 175-176°C.

Di-iso-amyl ester, m. p. 120-121°C.

b) Racemic acid, m. p. 170-175°C.

(iii) Cyclohexylpropionic acid, m. p. 16°C, b. p. 143-145°/11 mm.Hg D_4^{20} 0.9966, n_D^{20} 1.4658.

Ethyl ester, b. p. 91-94°/8 mm.Hg, D_4^{20} 0.9674, n_D^{20} 1.4488.

Results and Discussions

(1) **Effect of Cathodes.**—The reduction at a Pb cathode gave β-phenylpropionic acid (I) in 45-70%, β,γ-diphenyladipic acid (II) in 10-20% and polymeric material (III) (so-called benzene soluble factor), but Hg cathode gave only 6-10% of (I), the remaining 90% consisting of approximately equal amounts of (II) and (III). Hg-Zn cathode also gave the similar results obtained from a Hg cathode in a weak acid solution, but gave less β,γ-

(4) Sakurai, This Bulletin, **7**, 155 (1932).

diphenyladipic acid and (III) in a strong acid solution.

On the other hand, Pt-Pt cathode gave no bimolecular compounds, whereas it gave rise to cyclohexyl compounds as well as β-phenylpropionic acid. It was also determined that the reduction of unsaturated ethylenic double bond took place first and then that of benzene ring in the case of Pt-Pt cathode.

When cinnamic acid (0.05 mol.) was reduced for 6.0 amp. hrs., the main product was β-phenylpropionic acid, but the prolongation of the reduction for 15.0 amp. hrs., gave the cyclohexylpropionic acid. This fact shows that the reduction process at a Pt-Pt cathode contrast sharply with that pursued at a Pb or a Hg cathode. In any case, the carboxyl group in cinnamic acid was observed to be quite resistant to the electrolytic reduction, that is, no γ-phenylpropyl alcohol was produced.

Table 1 gives the yield of products obtained from the different type of cathodes.

The characteristic properties of the Pt-Pt cathode had been discussed in an other paper.(5)

Table 1

Effect of Cathodes

Catholyte; Cinnamic acid 14, 8 g., EtOH 60 ml., Sulfuric acid 40 ml., Quantity of Current; 12 amp. hrs., Temp. 25-35°C.

Run No.	Cathode	H_2SO_4 (%)	C. D. (amp./dm²)	Products. A (%)	B (%)	C (%)
1	Pb	75	3.0	70	10	
2	〃	28	3.0	45	18	
3	Hg-Zn	75	10.0	40	24	
4	〃	28	10.0	15	40	
5	Hg	75	10.0	10	24	
6	〃	28	10.0	5.7	44	
7	Pt-Pt	75	5.0		—	75
8	〃	28	5.0		—	70

Run Nos. 7 and 8; Cinnamic acid, 7.4 g., Q. of Current, 15.0 amp. hrs.

Product; A: β-Phenylpropionic acid.
B: β,γ-Diphenyladipic acid.
C: Cyclohexylpropionic acid.

Note: In the forthcoming Tables, the yield of benzene soluble factor was omitted, owing to the difficulty of separating a pure form from benzene solution in which usually small amounts of β-phenylpropionic acid and β,γ-diphenyladipic acid were included.

(2) **Effect of High Pressure.**—The special study was undertaken to develop the effect of high pressure of hydrogen in the course of electrolytic reduction. Examination of these results (Table 2 and 3), shows that the reduction of cinnamic acid under high pressure of hydrogen at a Pb, Hg, or a Hg-Zn cathode, and also at a Pt-Pt cathode, gave quite the same products as in the case of the ordinary state.

It was observed that the formation of β,γ-diphenyladipic acid was favored at high pressures, especially in the case of Pb cathode. However, an increase in the hydrogen pressure has no clear effect on the products, and moreover, at a Hg cathode, there are no remarkable changes in the yield of products.

In the case of Pt-Pt cathode, an increase in the yield of cyclohexyl compounds is not proportional to the hydrogen pressure.

So far as the hydrogen overvoltage is concerned, there would be no definite conclusion in regard to the high pressure.(6) Therefore, the influence of hydrogen overvoltage may be omitted in this stage. It is a new attempt to study the influence of high pressure in the course of electrolytic reduction of organic compounds. And the electrode reaction is not well settled for the time being; therefore, no conclusion comes from these results on this matter.

(3) **Effect of Temperature.**—In the present experiments, using either Pb, Hg, or Hg-Zn cathode, cinnamic acid gave bimolecular compounds, as well as β-phenylpropionic acid. Wilson[3b] suggested that the bimolecular compounds were produced by the dimerization of free radicals, $Ph\dot{C}HCH_2COOH$, from cinnamic acid.

In connection with the acid concentration, the temperature was observed to affect the formation of bimolecular compounds.

The results are shown in the Table 4.

(4) **Reduction Mechanism.**—As for the formation of γ-phenylpropyl alcohol, cinnamic acid has a conjugated system between the phenyl and carboxyl groups, if it were probable, the reduction would proceed in the formation of β-phenylpropion aldehyde or cinnamyl aldehyde and further γ-phenylpropyl alcohol. But it must be pointed out that the carbon-double bond is more active for the electrolytic reduction, as is seen in the case of α,β-unsaturated ketones.(7)

(5) S. Ono, T. Hayashi and J. Nakaya, Presented at the Symposium on Electro-organic Chemistry of the American Electrochem. Soc., held at Detroit, Oct., 1951.

(6) J. O'm Bockris, *Chem. Rev.*, **43**, 538 (1948).

(7) Pasternack R. and V. Halban H., *Helv. chim. Acta.*, **31**, 753 (1948).

Table 2

Effect of Hydrogen Pressure (a) Reduction at a Pb, Hg-Zn or Hg Cathode.
Catholyte; the same as in Table 1

Run No.	Cathode	H_2SO_4 (%)	Temp. (°C)	C. D. (amp./dm.^{2})	Press. (atm.)	Products A (%)	Products B (%)
1	Pb	75	50—55	10.0	—	79	6
2	〃	〃	〃	〃	25	64	14
3	〃	40	30—35	3.0	—	60	17
4	〃	〃	〃	〃	35	50	22
5	〃	〃	〃	〃	40	52	20
6	〃	〃	40—45	10.0	40	40	20
7	〃	28	25—35	3.0	—	42	20
8	〃	〃	〃	〃	25	37	28
9	〃	〃	〃	〃	45	32	36
10	〃	〃	40—45	10.0	20	32	35
11	Hg-Zn	75	40—45	10.0	—	53	18
12	〃	〃	〃	〃	20	47	22
13	〃	40	40—45	〃	—	50	22
14	〃	〃	〃	〃	20	46	28
15	Hg	75	25—30	10.0	—	12	24
16	〃	〃	〃	〃	20	12	25
17	〃	〃	〃	〃	40	11	25
18	〃	28	〃	〃	—	5.7	44
19	〃	〃	〃	〃	30	6	44

Table 3

Effect of Hydrogen Pressure (b)
Reduction at a Pt-Pt cathode

Catholyte; Cinnamic acid 7.4 g., EtOH 60 ml., Sulfuric acid 20 ml., Quantity of Current; 15 amp. hrs., Cathode (100 cm.^{2})

Run No.	H_2SO_4 (%)	Temp. (°C)	C. D. (amp./dm.^{2})	Press. (atm.)	Product. C. (%)
1	75	25—35	5.0	—	75
2	〃	〃	〃	30	76
3	40	40—45	5.0	35	75
4	〃	〃	〃	45	71
5	28	25—35	3.0	—	60
6	〃	〃	〃	20	63
7	〃	〃	〃	30	69
8	〃	〃	5.0	45	73
9	〃	〃	〃	50	73

C; Cyclohexylpropionic acid.

Table 4

Effect of Temperature
Catholyte; the same as in Table 1

Run No.	Cathode	H_2SO_4 (%)	Temp. (°C)	C. D. (amp./dm.^{2})	Products A (%)	Products B (%)
1	Pb	75	25—35	3.0	70	10
2	〃	〃	55—60	3.0	75	8
3	〃	〃	〃	10.0	79	6
4	〃	40	25—35	3.0	60	17
5	〃	〃	55—60	3.0	70	15
6	〃	〃	25—35	10.0	62	15
7	〃	28	25—35	3.0	42	18
8	〃	〃	55—60	3.0	50	15
9	Hg-Zn	75	20—25	10.0	40	25
10	〃	〃	40—45	10.0	55	12
11	Hg	40	25—30	10.0	10	38
12	〃	〃	55—60	10.0	15	35

Assuming that the reduction would take place by the following process, (shown in Fig. 1)

After coordination of proton at an alpha carbon atom, forming the free radicals and further β-phenylpropionic acid, or bimolecular compounds, there would be no conjugation between carboxyl and phenyl groups; that is, under these conditions, the electronic interaction between them no longer exists.

Therefore, the carboxyl group in cinnamic acid would not be reduced to the corresponding aldehyde or alcohol.

It is of interest to see the fact that the reduction of cinnamic acid at a Pt-Pt cathode gave cyclohexyl compounds.

Judging from the fact that (1) both α,β-unsaturated double bond and benzene ring

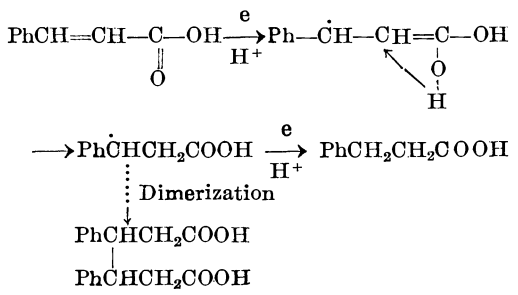

Fig. 1.—Reduction mechanism of cinnamic acid at Pb, Hg or Hg-Zn cathode.

were hydrogenated and (2) no bimolecular compounds were obtained in the case of Pt-Pt cathode, it is likely that the reduction at a Pt-Pt cathode consists mainly in the catalytic mechanism similar to the catalytic hydrogenation.

Summary

The electrolytic reduction of cinnamic acid at a Pb, a Hg, a Hg-Zn or a Pt-Pt cathode in acid solution was studied.

It was found that the formation of bimolecular compounds depended on the nature of cathode materials and the condition of the reduction. It was confirmed that the γ-phenylpropyl alcohol could not be produced by the electrolytic reduction of cinnamic acid. It was found that the reduction of cinnamic acid at a Pt-Pt cathode gave cyclohexyl propionic acid.

The effect of high pressure of hydrogen in the course of reduction was discussed.

The authors express their sincere thanks to Dr. C. L. Wilson for his kind advice and encouragement.

Department of Chemistry, Faculty of Engineering, Naniwa University, Osaka

Absorption Spectra of Coordination Compounds. V. The Hyperchromic Series of Ligands

By Shoichiro YAMADA and Ryutaro TSUCHIDA

(Received May 14, 1952)

Introduction

Although an extensive literature is available about the nature of absorption bands of metallic complexes and as to the relations among the wave-lengths of their absorption maxima, investigations on the effects of substitution of ligands on the intensity of absorption have seldom been carried out.[1][2] One of the present authors has reported that the magnitude of extinction coefficients of a "specific absorption band" is approximately proportional to the number of the ligands concerned in the complex.[3] Mathieu[4] has found that extinction coefficients for an absorption band of a cobaltic complex increase as molecules of ammonia are substituted by heavier ligands such as ethylenediamine and propylenediamine, the effect being attributed mainly to the change of mass. Sueda[5] attempted to express intensities of absorption bands of several complexes by the addition of component absorptions, each of which was assigned over the regions of an absorption band for a pair of respective ligands in *trans*-positions.

The present paper deals with the effect of substitution of ligands on the maximal extinction coefficients of coordination compounds.

Hyperchromic Series of Ligands

If one ligand in a complex is substituted for by another, the absorption bands of the complex are subjected to a hypsochromic or bathochromic effect respectively according as the immigrant ligand precedes or stands behind the emigrant in the spectrochemical

(1) R. Tsuchida and M. Kobayashi, *J. Chem. Soc. Japan*, **59**, 591 (1938).
(2) R. Tsuchida and H. Kuroya, ibid., **59**, 1142 (1938).
(3) R. Tsuchida and M. Kobayashi, This Bulletin, **13**, 476 (1938).
(4) J. P. Mathieu, *Bull. Soc. Chim. France*, **3**, 463 (1936).
(5) H. Sueda, *J. Chem. Soc. Japan*, **57**, 406, 542 (1936); ibid., **59**, 47 (1938).

series.[6] At the same time the bands suffer a hyperchromic or hypochromic change according to the nature of the ligands concerned. Thus NO_2 is more hyperchromic than NH_3 and the latter in its turn is hyperchromic to H_2O, as is shown in Table 1.

Table 1

Comparison of Hyperchromic Effects of Ligands for the First Absorption Band

NO_2 and NH_3

Compound	ν 10^{13}/sec.	log ε	Ref.
$[Co(NH_3)_6]Cl_3$	63.6	1.66	(7)
$[Co(NH_3)_5NO_2]Cl_2$	65.8	1.95	(7)
$[Co(NH_3)_4(NO_2)_2^{(1)}_{(2)}]Cl$	65.5	1.99	(7)
$[Co(NH_3)_3(NO_2)_3]$	68.7	2.21	(7)
$[Co(NH_3)_2(NO_2)_4]NH_4$	69.0	2.56	(7)

NH_3 and H_2O

$[Co(NH_3)_6]Cl_3$	63.6	1.66	(7)
$[Co(NH_3)_5H_2O]Cl_3$	61.6	1.62	(7)
$[Co(NH_3)_4(H_2O)_2]Cl_3$	60.0	1.40	(7)

The extinction coefficients of nitroammine complexes increase with the number of NO_2-ions in coordination.

Further examples of substitution are shown in Table 2, in which oxalate ion (ox) is the most hyperchromic and NH_3 the most hypochromic, ethylenediamine (en) being intermediate.

Table 2

Comparison of Hyperchromic Effects of Ligands for the First and the Second Absorption Bands

en and NH_3

Compound	1st Band ν 10^{13}/sec.	1st Band log ε	2nd Band ν	2nd Band log ε	Ref.
$[Co(NH_3)_6]Cl_3$	63.6	1.66	88.8	1.57	(7)
$[Co(NH_3)_2en_2]Cl_3$	64.8	1.72	89.2	1.62	(9)
$[Co\ en_3]Br_3$	65.2	1.88	89.2	1.81	(9)

ox and en

$[Co\ en_3]Br_3$	65.2	1.88	89.2	1.81	(9)
$[Co\ en_2ox]Br$	60.0	1.96	84.2	2.10	(9)
$[Co\ ox_3]K_3$	49.6	2.09	71.0	2.19	(9)

From the above considerations, it is expected that there should be a series concerning the hyperchromic effects of ligands. On the basis of experimental data with pentammine cobaltic complexes (Table 3) was obtained the following series as the descending order of the hyperchromic effect of ligands on the first absorption band[7]:

$$NCS^- \ CrO_4^= \ SO_3^= \ NO_2^- \ CO_3^= \ C_2O_4^= \ en$$
$$OH^- \ NO_3^- \ SO_4^= \ Br^- \ NH_3 \ Cl^- \ H_2O$$

Table 3

Hyperchromic Series with Pentammine Complexes for the First Absorption Band

Ligand	Compound	ν 10^{13}/sec.	log ε	Ref.
NCS^-	$[Co(NH_3)_5NCS]Cl_2$	60.2	2.16	(6), (7)
$CrO_4^=$	$[Co(NH_3)_5CrO_4]NO_3$	55.6	2.16	(6), (7)
$SO_3^=$	$[Co(NH_3)_5SO_3]Cl$	63.6	2.15	(8)
NO_2^-	$[Co(NH_3)_5NO_2]Cl_2$	65.8	1.95	(6), (7)
$CO_3^=$	$[Co(NH_3)_5CO_3]NO_3$	59.0	1.90	(6), (7)
$ox^=$	$[Co(NH_3)_5ox]Br$	59.2	1.87	(6), (7)
OH^-	$[Co(NH_3)_5OH](NO_3)_2$	59.8	1.82	(6), (7)
NO_3^-	$[Co(NH_3)_5NO_3](NO_3)_2$	60.0	1.74	(6), (7)
$SO_4^=$	$[Co(NH_3)_5SO_4]I$	60.0	1.70	(6), (7)
Br^-	$[Co(NH_3)_5Br]Br_2$	55.4	1.68	(6), (7)
NH_3	$[Co(NH_3)_5NH_3]Cl_3$	63.6	1.66	(6), (7)
Cl^-	$[Co(NH_3)_5Cl]Cl_2$	57.5	1.64	(6), (7)
H_2O	$[Co(NH_3)_5H_2O]Cl_3$	61.6	1.62	(6), (7)

It is seen that the above series hold also for the tetrammine series (Table 4), and for complexes containing only one kind of ligand (Table 5).

Table 4

Hyperchromic Series with Cobaltic Tetrammine Complexes

Ligand	Compound	1st Band ν 10^{13}/sec.	1st Band log ε	2nd Band ν 10^{13}/sec.	2nd Band log ε	Ref.
NO_2^-	$[Co(NH_3)_4(NO_2)_2]Cl$					
	trans.	67.9	2.32			(7)
	cis.	65.5	1.99			(7)
$CO_3^=$	$[Co(NH_3)_4CO_3]Cl$	57.2	2.02	82.6	2.03	(7)
$C_2O_4^=$	$[Co(NH_3)_4ox]Cl$	58.8	1.78	84.0	1.88	(7)
NH_3	$[Co(NH_3)_4(NH_3)_2]Cl_3$	63.6	1.66	88.8	1.57	(7)
H_2O	$[Co(NH_3)_4(H_2O)_2]Cl_3$	60.0	1.40	84.0	1.48	(7)

Table 5

Hyperchromic Series with Cobaltic Hexa-coordinated Complexes

Ligand	Compound	1st Band ν 10^{13}/sec.	1st Band log ε	2nd Band ν 10^{13}/sec.	2nd Band log ε	Ref.
$ox^=$	$[Co\ ox_3]K_3$	49.6	2.09	71.0	2.19	(7)
en	$[Co\ en_3]Br_3$	65.2	1.88	89.2	1.81	(10)
NH_3	$[Co(NH_3)_6]Cl_3$	63.6	1.66	88.8	1.57	(7)

(6) R. Tsuchida, *J. Chem. Soc. Japan*, **59**, 586, 731, 819 (1938).

(7) R. Tsuchida, This Bulletin, **13**, 388, 436 (1938), etc.

The above series, which has been deduced for simpler cases, would be considered to hold for more general cases unless mutual relations among ligands are highly complicated. The series holds also for chromic complexes, so far without the slightest alteration, though experimental data are less numerous (Table 6 and 7) in comparison with cobaltic complexes.

Table 6

Comparison of Hyperchromic Effects of Ligands for Chromic Complexes

NCS and NH_3

Compound	1st Band ν 10^{13}/sec.	1st Band log ε	2nd Band ν 10^{13}/sec.	2nd Band log ε	Ref.
$[Cr(NH_3)_6]Cl_3$	65.0	1.48	86.0	1.44	(7)
$[Cr(NH_3)_5NCS](NCS)_2$	61.6	1.82	(83)	1.67	(7)
$[Cr(NH_3)_2(NCS)_4]NH_4$	57.5	1.95	(75)	1.75	(7)
$[Cr(NCS)_6]K_3$	53.1	2.08	70.8	2.00	(7)
ox and H_2O					
$[Cr(H_2O)_6]Cl_3$	52.5	1.02	73.6	1.20	(7)
$[Cr(H_2O)_2ox_2]K$ *cis.*	53.1	1.80	72.3	1.83	(10)
$[Cr(H_2O)_2ox_2]K$ *trans.*	53.1	1.71	71.4	1.63	(10)
$[Cr\ ox_3]K_3$	52.6	1.87	71.4	1.91	(10)

Table 7

Hyperchromic Series with Chromic Complexes

Ligand	Compound	1st Band ν 10^{13}/sec.	1st Band log ε	2nd Band ν 10^{13}/sec.	2nd Band log ε	Ref.
NCS^-	$[Cr(NCS)_6]K_3$	53.1	2.08	70.8	2.00	(7)
$ox^=$	$[Cr\ ox_3]K_3$	52.6	1.87	71.4	1.91	(11)
en	$[Cr\ en_3]Cl_3$	65.9	1.84	85.7	1.72	(11)
NH_3	$[Cr(NH_3)_6]Cl_3$	65.0	1.48	86.0	1.44	(7)
H_2O	$[Cr(H_2O)_6]Cl_3$	52.2	1.02	73.6	1.20	(7)

Relation between ν_{max} and ε_{max}

It is of interest to compare the hyperchromic and the spectrochemical series.

The hyperchromic series:

$$NCS^-\ CrO_4^=\ SO_3^=\ NO_2^-\ CO_3^=\ C_2O_4^=\ en$$
$$OH^-\ NO_3^-\ SO_4^=\ Br^-\ NH_3Cl^-\ H_2O$$

The spectrochemical series[6],[12]:

$$CN^-\ NO_2^-\ SO_3^=\ en\ NH_3ONO^-\ H_2O\ NCS^-$$
$$SO_4^=\ NO_3^-\ OH^-\ C_2O_4^=\ CO_3^=\ Cl^-\ CrO_4^=\ Br^-$$

It appears to be difficult at first sight to find any relation between the series, for ligands preceding in one of the series do not always take precedence in the other. For examples, NCS^- at the head of the hyperchromic series stands in the middle part of the spectrochemical series and $CrO_4^=$, one of the most hyperchromic ligands, is nearly at the tail end of the latter series, while NO_2^- is situated among the highest positions in both the series.

One of the principal factors which determine the nature of absorption of a complex is the kind of atom coordinated directly to the central ion. From this viewpoint the ligands are classified into the following groups: viz. (A) those coordinated with an atom of inert-gas structure, such as Cl^-, NH_3, OH_2 and their derivatives including oxygen-acid anions, (B) those coordinated with an atom of incomplete-shell structure, such as NO_2^-, and (C) those coordinated with an atom having one or more π-electrons, such as NCS^-, CN^-, N_3^-, NC_5H_5, NO, CO, etc. Among the similar ligands of the group A, there exists a regularity with respect to the hyperchromic and the hypsochromic property. For example, in Fig. 1 are plotted ε_{max}'s against ν_{max}'s of the first bands of pentammine-cobaltic complexes containing various oxygen-acid anions. It is seen in the figure that an approximately linear relation holds between ν_{max} and ε_{max}.

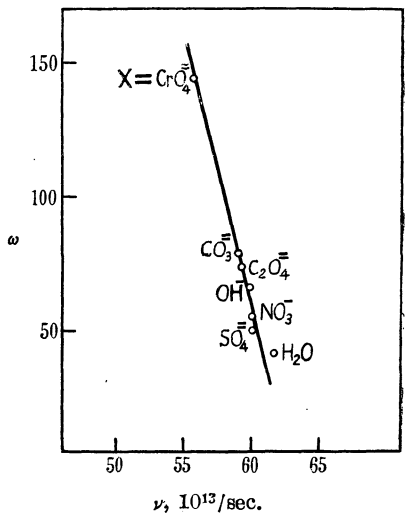

Fig. 1.—ν versus ε for the first band of pentammine cobaltic complexes containing various oxygen-acid anions, $[Co(NH_3)_5X]^{(3-n)+}$.

A similar relation exists between ν_{max} and ε_{max} of the first band of halogenopentammine

(8) A. v. Kiss and D. v. Czegledy, *Z. Anorg. Chem.*, **235**, 407 (1938).
(9) R. Tsuchida and H. Kuroya, This Bulletin, **15**, 427 (1940).
(10) K. Sone, *J. Chem. Soc. Japan*, **71**, 270 (1950).
(11) A. Mead, *Trans. Faraday Soc.*, **30**, 1052 (1934).
(12) Y. Shimura, This Bulletin, **25**, 49 (1952).

Table 8

Compound	1st Band ν 10^{13}/sec.	1st Band log ε	2nd Band ν 10^{13}/sec.	2nd Band log ε	3rd Band ν 10^{13}/sec.	3rd Band log ε
$K_3[Fe(CN)_6]$	72.5	2.97	100.0	3.29	115.5	3.24
$K_3[Cr(CN)_6]$	78.9	1.81	96.6	1.66	114.7	3.87
$K_3[Co(CN)_6]$	(72.0)	(−0.28)	97.2	2.37	117.0	2.08

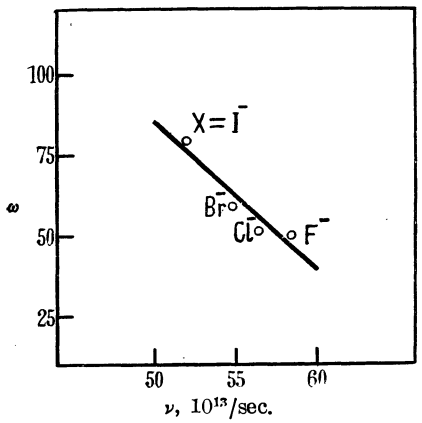

Fig. 2.—ν versus ε for the first band of halogeno-pentammine cobaltic complexes, $[Co(NH_3)_5X]^{2+}$.

cobaltic complexes, as is shown in Fig. 2[13].

For similar ligands of the group A, therefore, the order in the hyperchromic series is completely reverse to that in the spectrochemical series, showing that the stronger the coordinate linkage the less the chances of transitions of d-electrons.

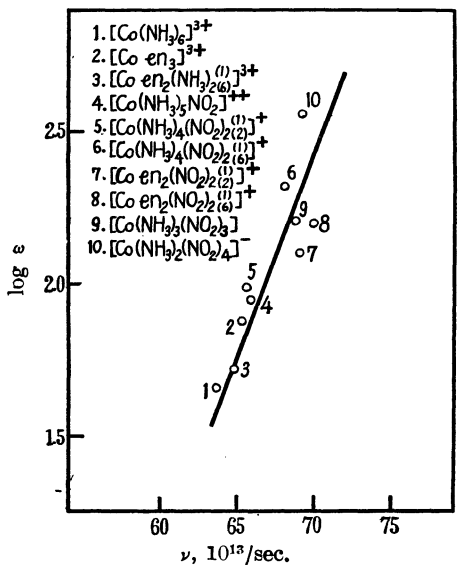

Fig. 3.—ν versus log ε for the first band of nitroammine cobaltic complexes.

In Fig. 3 are plotted log ε_{max}'s against the corresponding ν_{max}'s of the first bands of complexes containing NO_2^- of the group B.

It is found that there exists a quite different relation from that for the ligands of group A. Namely, NO_2^- stands almost at the head of both the hyperchromic and the hypsochromic series, making a remarkable contrast to the ligands of group A, among which the more hyperchromic are the more bathochromic.

This difference between the groups A and B suggests that the modes of coordination of the ligands are quite different from each other. The incomplete shell of the nitrogen atom in NO_2^- favours the transitions of d-electrons, which reinforce the coordinate linkage, resulting in the strong absorption and the stable coordination.

The absorption of complexes containing ligands of the group C seems rather complicated. The high extinction coefficients of rhodanato-complexes may be explained as due to the interaction of the π-electron of the ligand with d-electrons of the central cation, which facilitates transitions of the latter electrons. To this category belongs CN^-, which is usually hypsochromic and hyperchromic. For examples, the first bands of $K_3[Fe(CN)_6]$ and $K_3[Cr(CN)_6]$ are fairly strong as is shown in Table 8.[14]

But CN^- is sometimes hypsochromic and hypochromic, e.g., the first band of $K_3[Co(CN)_6]$ is extremely weak.[14] This fact may be understood as due to a sort of anti-parallel bonding between the d- and π-electron, which suppresses transitions of the d-electron. As an evidence for such a bonding, may be cited the planar configuration of [Au(dipyridyl)$(CN)_2]^-$ and [Au(phenarthrolin)$(CN)_2]^-$, in spite of the pseudo-inert-gas structure of the central ion.

The position of CN^- in the hyperchromic series, therefore, varies according to the nature of the central ion in such a way that it is hypochromic or hyperchromic according as the central ion has the same number of

(13) Experimental data are taken from the work by M. Linhard and M. Weigel, *Z. Anorg. Chem.*, **266**, 4 (1951).

(14) H. Kuroya and R. Tsuchida, *J. Chem. Soc. Japan*, **61**, 597 (1940).

d-electrons as the number of the ligands or not.

The Hyperchromic Effects of Ligands in Geometrical Isomers

It has been recognized by investigations on chemical behaviour and absorption spectra of complexes that there is greater interaction between negative ligands coordinated in *trans*-positions to each other than between those in *cis*-positions. Thus Shibata[15] has explained the third absorption bands of nitroammine cobaltic complexes by his *trans*-dinitro-hypothesis. And extending the Shibata hypothesis, one of the present authors[16] explained the third bands of many other complexes as due to a pair or pairs of negative ligands in *trans*-positions to each other. Basolo[17] reported that complexes with a pair of negative ligands in *cis*-positions also showed the third bands, which, however, were always located in regions of shorter wave-lengths than those of the *trans*-isomers. Recently, Shimura[12] has found on investigating wave-lengths of absorption maxima of the first bands of geometrical isomers that a pair of ligands in *trans*-positions has a greater effect on the first band than a pair in *cis*-positions, whether it is bathochromic or hypsochromic. The trans-effect has been recognized also on reactions of complex compounds. Thus Chernyaev[18] reported that ligands trans to negative groups are more mobile than those opposite to neutral groups, and the idea of the trans-effect has been extended in explanation of reactions of coordination compounds.[19] All these results imply that there should be a larger pairing interaction between ligands, especially anions, in *trans*-positions than between those in *cis*-positions. Experimental results with tetrammine cobaltic complexes are shown in Table 9.

From the experimental data the following rule may be induced: of geometrical isomers of a hexa-coordinated complex containing ligands of two kinds, in which a pair of ligands of one kind has larger hyperchromic and trans-pairing effects than the remaining four of the other kind, the *trans*-isomer has larger ε_{max} than the *cis*-isomer.

Thus, since NO_2 stands much higher in the hyperchromic series than en or NH_3, the *trans*-isomers of dinitro-complexes have larger extinction coefficients than the corresponding *cis*-isomers. The same is true for dirhodanato- and disulphono-complexes, which contain respectively NCS^- and $SO_3^=$, the most hyperchromic ligands. On the contrary, in regard to geometrical isomers of tetrammine-cobaltic complexes which coordinate H_2O or Cl^-, the least hyperchromic ligands, the *trans*-isomers have smaller extinction coefficients than the corresponding *cis*-isomers.

Table 9

Comparison between *cis*- and *trans*-Isomers

Compound		1st Band ν (10^{13}/sec.)	1st Band log ε	Ref.
[Co $en_2(NCS)_2$]Cl	*trans*-	59.0	2.42	(21)
	cis-	59.3	2.40	(21)
[Co$(NH_3)_4(SO_3)_2$]Na	*trans*-	66.6	2.32	(12)
	cis-	65.9	2.26	(12)
[Co$(NH_3)_4(NO_2)_2$]Cl	*trans*-	67.9	2.32	(7)
	cis-	65.5	1.99	(7)
[Co $en_2(NO_2)_2$]NO_3	*trans*-	69.9	2.20	(10)
	cis-	69.0	2.10	(10)
[Co en_2Cl_2]Cl	*trans*-	48.0	1.54	(20)
	cis-	56.6	1.88	(20)
[Co $en_2(H_2O)_2$]Br_3	*trans*-	60.4	1.65	(20)
	cis-	60.6	1.85	(20)

(15) Y. Shibata, *J. Chem. Soc. Japan*, **36**, 1243 (1915).
(16) R. Tsuchida, This Bulletin, **13**, 436 (1938).
(17) F. Basolo, *J. Am. Chem. Soc.*, **70**, 2643 (1948); **72**, 4393 (1950).
(18) I. I. Chernyaev, *Ann. Inst. Platine*, **4**, 243 (1926).
(19) H. D. K. Drew, et al, *J. Chem. Soc.*, 1004 (1932); D. I. Ribchikov, *Compt. rend. U. R. S. S.*, **28**, 231 (1940); J. C. Bailar and D. F. Peppard, *J. Am. Chem. Soc.*, **70**, 2634 (1948), etc.
(20) F. Basolo, *J. Am. Chem. Soc.*, **72**, 4393 (1950); data in methanolwater solvent.
(21) Y. Shimura, *J. Am. Chem. Soc.*, **73**, 5079 (1951).

Summary

The relation between the kind of ligands and extinction coefficients of the first absorption bands of cobaltic complexes has been discussed. The order of ligands as to the magnitude of the effect which they exert on extinction coefficients of the first bands has been determined empirically, thus

$$NCS^- \; CrO_4^= \; SO_3^= \; NO_2^- \; CO_3^= \; C_2O_4^= \; en$$
$$OH^- \; NO_3^- \; SO_4^= \; Br^- \; NH_3Cl^- \; H_2O.$$

For pentammine cobaltic complexes with the sixth ligands, each of which is coordinated with an oxygen atom, a linear relation has been found to hold between ν_{max}'s and ε_{max}'s of the first bands. For complexes of the type $[CoA_4X_2]$, the *trans*-isomer has larger ε_{max} if X has more hyperchromic and trans-pairing effects than A. This investigation was supported by a grant from the Ministry of Education.

Department of Chemistry, Faculty of Science, Osaka University, Osaka

Mechanical Properties of Concentrated Hydrogels of Agar-agar. II. Creep under Constant Load in Compression

By Hiroshi FUJITA, Kazuhiko NINOMIYA and Terutaka HOMMA

(Received April 30, 1952)

Introduction

Although there exists some information on the elastic properties of hydrogels of agar-agar, papers dealing with their viscoelastic behavior are still very meager in the literature in colloid chemistry or in rheology. Considering that agar-agar is a prototype of gel-forming natural substances but also a kind of polyelectrolytes, however, the investigation of the viscoelastic behavior of its gels seems to be an interesting problem. As is well known, creep under constant load is one of the most commonly observed and measured of the phenomena pertaining to viscoelastic behavior of materials. For these reasons, an investigation of the creep under compressive load was carried out for concentrated agar-agar gels in various environmental conditions and is reported in this paper.

Experimental

All agar-agar samples used in this work were taken from the same stock of a grade of powdered agar-agar as that which was prepared in a previous investigation[1] of this series. The process of making the test piece which was shaped cylindrically and whose dimensions were about 3 cm. both in height and in diameter was identical with that employed in I. All tests were commenced after the 90 min. chilling of the sol; this value is also the same as that adopted in I. The apparatus which was constructed in I for the measurement of the compression stress-strain curves was usable as an autographic machine for measuring creep under constant compressive load by making a slight modification as follows. This modification was simply attained by fixing the movable end of the chains (see Figure 1 in I) at a desired height. Then a constant compressive load could be applied on a given test piece over any desired operating interval of time, and thus our apparatus proved to be usable as an autographic creepmeter.[2] The apparatus was equipped in an air thermostat which was regulated to about ±0.25°C. Humidity in the thermostat was maintained at an almost saturated state, and in addition, liquid paraffin was amply applied on the whole surface of the specimen. In this way, evaporation of the solvent from the gel was almost completely checked during the course of a creep test. The interval of time of measurement in each creep run was exclusively limited to 100 min.

There are probably a considerable number of factors which may have influence upon creep behavior in a gel-system. But, in this work, only the effects of temperature, concentration and load were considered. In order to study the effects of these factors, experimental measurements were carried out according to the following plan.

First, the effect of applied load was studied at a temperature 23°C. and a concentration 4 g./100 cc. by varying stress from 0 to 5×10^4 dyn./cm^2., where the stress was defined as applied load per unit original unstrained cross section of each test piece. Because the stress thus defined was not kept constant but continuously decreased with increasing deformation resulting from creep, our creep tests were not true creep tests. However, considering that the resultant maximum strains within the interval of time of measurement herein adopted were as small as less than, at most, 10 percent, it might be assumed that, to a first approximation, our creep tests were enough to elucidate the true creep behavior of the material in question.

The effect of temperature was studied at a concentration 4 g./100 cc. in the temperature range from 5° to 40°C., at each temperature the stress being varied from 0 to 4×10^4 dyn./cm^2.

The effect of concentration was studied at a temperature 23°C. in the concentration range from 2 g. to 4 g./100 cc., at each concentration the stress being varied in the same range as in the above.

Results and Discussion

General Remarks.—The general trend of the creep curves obtained is illustrated in Figure 1, where the experimental conditions are indicated in the legend. This shape of creep curve is one of the most commonly observed in many materials.[3] It was found

(1) H. Fujita, K. Ninomiya and T. Homma, This Bulletin, **25**, 374 (1952).

(2) Details of the present apparatus will be described in a separate paper by K. Ninomiya.

(3) W. J. Lyons, *J. Appl. Phys.*, **17**, 472 (1946); in particular, pp. 472-474.

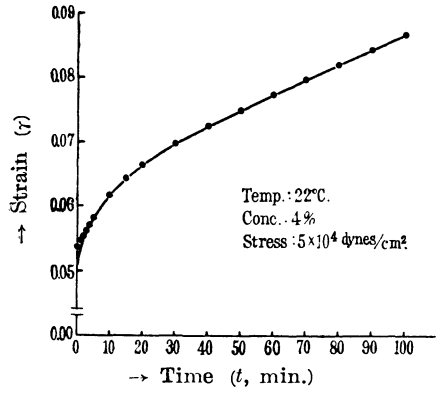

Fig. 1.—A fitting of Eq. (1) to an experimental creep curve; ● represents a ca'culated value, and — the observed curve.

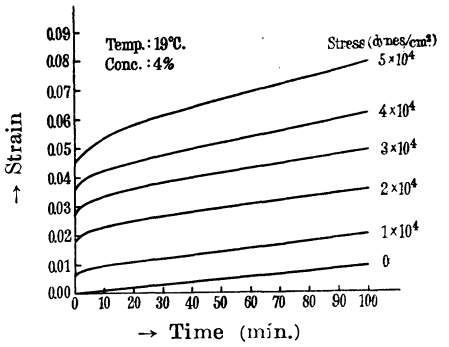

Fig. 2.—Effect of stress upon the shape of creep curve.

that this shape of curve was well fitted by a well-known creep equation of the form:

$$\gamma(t)=\gamma(0)+A(1-e^{-t/\tau})+\lambda t, \qquad (1)$$

where $\gamma(t)$ is the strain at time t, $\gamma(0)$ is the initial strain, λ is the constant creep rate in the viscous flow region, A is the final, maximum strain due to retarded elasticity of the material (retarded elastic strain was defined as transient creep minus viscous flow), and τ is the retardation time. Dependencies of $\gamma(0)$ on various environmental factors such as temperature, concentration, stress, and gelation time were studied in a previous paper I. Consequently, our present investigation concerning creep behavior of concentrated agar-agar gels was reduced to determining parameters λ, A and τ as functions of such environmental factors as mentioned above.

An example showing the conformity of Eq. (1) with an observed curve is given also in Figure 1, where the circles indicate the calculated values from Eq. (1). Such a degree of agreement between Eq. (1) and the observed curve as seen here was found to hold for all data obtained in the present work.

As is seen in Figure 1, or will be seen in Figure 2, relative length of the transient creep region is generally so much shorter than that of the viscous flow region that it may be considered that the general trend of the creep behavior in concentrated agar-agar gels herein concerned is primarily determined by the behavior of the constant rate term λt in Eq. (1). For this reason, in what follows, we shall be interested mainly in examining the effects of environmental factors on the value of λ.

Effect of Stress.—Figure 2 shows how creep curves for a concentrated agar-agar gel differ for different stress magnitudes. We can see from this figure a number of interesting things. Of special interest is a clear evidence showing that even at zero stress state there occurred definitely a creep process which was closely linear over the range of observation time indicated. Such an apparent creep at zero stress state was always observed in this work irrespective of temperature and concentration. This fact seems to indicate that all test specimens employed were not at true thermodynamic equilibria within the interval of the present observations, though thermal equilibrium had previously been established before the beginning of the observations. In connection with this phenomenon, we must describe a characteristic fact observed simultaneously during the course of this apparent creep. This was a continuous, though small in amount, expulsion of the solvent from the test piece. It took place at a very slow rate as the specimen was deformed. It was observed clearly even in the absence of any external force. The solvent expulsion in the case of non-external force necessarily resulted in spontaneous and isotropic contraction of the specimen gel; this is nothing but the phenomenon usually called syneresis. The spontaneous contraction of a gel block should look to an observer as if creep (compressive) is occurring in it. Thus, the apparent creep observed in the present work at zero stress state is interpreted as arising from the volume contraction due to syneresis. Ferry[4] has stated that the progressive closer binding, or coming-together, of the network strands in a gel results in syneresis of the gel. It is, however, beyond the present authors' scope to discuss in what way this Ferry's idea can be formulated as a quantitative theory for describing the contractility of gel-systems.

(4) J. D. Ferry, "Advances in Protein Chemistry," IV, Academic Press Inc., Publishers, New York, 1948, pp. 1-78; in particular, Chapt. III.

Now, we shall proceed to examine the effect of stress quantitatively. From Figure 2 and other similar data obtained, λ is plotted against stress S as shown in Figure 3, from which the plotted curves are seen to be well fitted by an equation of the form:

$$\lambda=\lambda_0+\frac{S}{\eta}, \qquad (2)$$

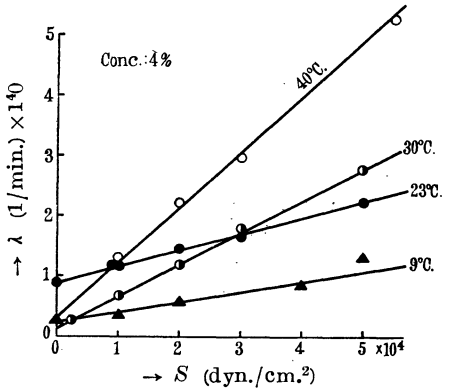

Fig. 3.—Effect of temperature upon the viscous flow behavior.

where λ_0 is the creep rate observed at zero stress condition, that is, the rate of the apparent creep discussed above, and η is a parameter having the dimension of viscosity. The linearity between λ and S as seen here implies that the viscous flow of the material exhibits a so-called Newtonian behavior[5] so far as the environmental conditions indicated are concerned.

Effect of Temperature.—Figure 3 also shows how the λ_0 value and the viscosity η are affected by temperature θ. We see that (1) the value of λ_0 is changed with temperature just as it reaches a maximum near about 20°C.; and (2) the value of η is decreased with increasing temperature, as should be expected. To make it clear, the logarithm of η is plotted against the reciprocal of the absolute temperature $T(=273+\theta)$ as shown in Figure 4. It is seen that the temperature dependency of the viscosity does not follow the well-known Andrade equation with a constant activation energy. However, by replacing the experimental curve by a straight line as indicated in the figure, the corresponding apparent activation energy U is estimated approximately at

$$U\fallingdotseq 12 \text{ kcal./mol.}$$

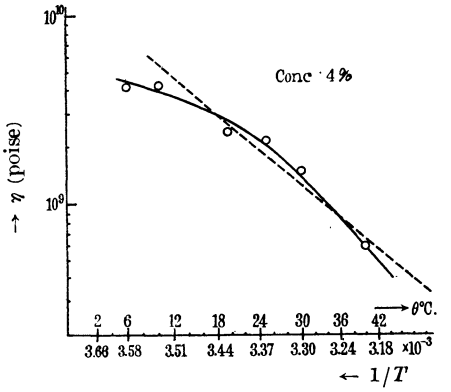

Fig. 4.—Temperature dependency of viscosity η.

This value of the energy of activation for viscous flow may suggest that the strength of flow units involved in concentrated agar-agar gels is of a secondary nature as should be expected from the current view of the molecular structure of polymer gels. The deviation of the experimental curve from the Andrade relation may partly be ascribed to the change in the effective number of cross-linkages in the gel network with change in temperature.

Effect of Concentration.—The effect of concentration on λ vs. S plot is shown in Figure 5, where all data presented were obtained at a constant temperature 23°C. We see

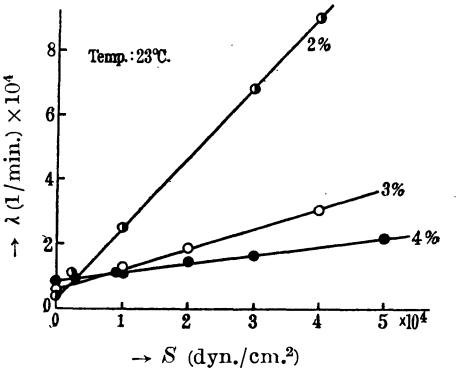

Fig. 5.—Effect of concentration upon the viscous flow behavior.

that (1) the concentration effect on λ_0 is not appreciable, though detailed information on it is not ensured due to the paucity and inaccuracy of the data; and (2) the concentration dependency of η is, on the contrary, rather remarkable, and, so far as the plotted data are concerned, it is represented approximately by

$$\eta=kC^3,$$

(5) H. Leadermen, *J. Colloid Sci.*, **4**, 193 (1949).

where C is the concentration of agar-agar in the gel and k is a proportionality constant.

Remarks on the Behavior in the Transient Creep Region. — Finally, short discussions will be made for the behavior of the transient creep region. As is understood from Eq. (1), this behavior can be characterised by two parameters τ and A. Figure 6 shows the effect of stress on the retardation time τ at several temperatures and a constant concentration 4 g./100 cc. Because of the marked scattering of the experimental points it is difficult

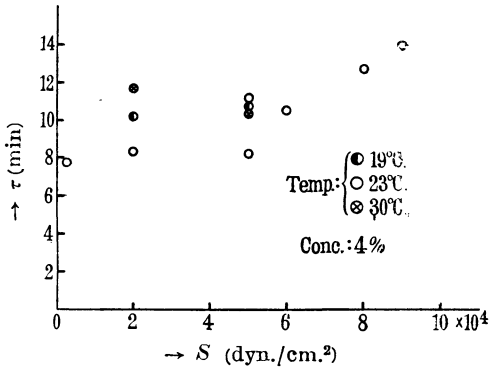

Fig. 6.—Effect of stress upon retardation time τ.

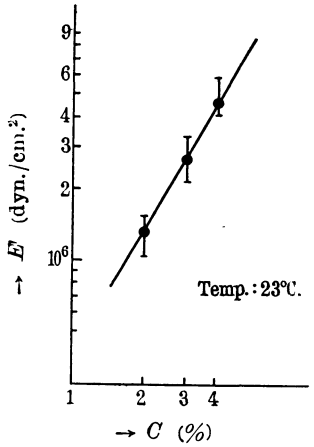

Fig. 7.—Modulus of elasticity E' for the retarded mechanical element.

to draw the definite conclusions on both the stress and temperature effect on the retardation time. We must restrict ourselves to pointing out that the value of τ appears to be little influenced by either stress or temperature. In Figure 7, instead of A, the modulus of retarded elasticity E' defined by S/A is plotted against concentration C.

Summary

In this report, we have presented the results of an experimental investigation carried out of the creep under constant compressive load for concentrated hydrogels of agar-agar.

The apparatus which was designed in a previous paper I of this series for the measurement of the compression stress-strain curve was modified to suit the measurement of the creep under constant compressive load. The shape of the creep curves obtained was found to be well fitted by Eq. (1). The influences of temperature, concentration and applied stress on the creep rate in the viscous flow region were investigated separately. One of the interesting facts found was a clear evidence showing that even at zero stress condition there occurred a definite creep process which was closely followed by a straight line within the interval of time of observation employed. It seemed likely that this phenomenon should be associated primarily with the molecular structural feature of the agar-agar gel network which leads the gel to syneresis.

It was found for all the data obtained that the relation between λ and S followed Eq. (2) within the limits of experimental error, where λ is the creep rate in the viscous flow region and S is the magnitude of stress applied. This equation involves two parameters λ_0 and η, where λ_0 stands for the value of λ in the absence of external stress, and η is the Newtonian viscosity corresponding to the region in which a linear viscous flow appears. The influences of various environmental parameters on these two quantities were investigated, obtaining the results as shown in Figures 3, 4 and 5.

We wish to express our gratitude to Mr. T. Nakagawa, the Department of Chemistry, Tokyo University and to Mr. N. Hirai, the Department of Chemistry, Okayama University for their kind advice and interest in this work.

Applied Physics Laboratory, Department of Fisheries, Faculty of Agriculture, Kyoto University, Maizuru

Mechanical Properties of Concentrated Hydrogels of Agar-agar. III. Relaxation of Stress in Compression

By Hiroshi FUJITA and Kazuhiko NINOMIYA

(Received June 23, 1952)

Introduction

In recent years, a number of papers have been published on the relaxation of stress in high polymers, reflecting its fundamental importance in rheological investigation of these substances. However, papers are still rather rare in the literature dealing with relaxation experiments on gel-systems. Some examples of the latter are the recent studies of Ferry and his co-workers on several important protein gels.[1] For agar-agar gel with which we have been concerned in this series of rheological studies, no information of stress-relaxation appears to have yet been reported, so far as the authors are aware. For this reason, we have carried out an experimental study of the relaxation of stress in agar-agar gel held at constant compression, and the results obtained are reported in this paper.

A cylindrical test piece was kept at constant compression between two parallel plates under relaxing stresses, and the process of decay of stress was followed autographically by means of a relaxometer which was constructed based on the principle of the chainomatic balance. Measurements were conducted at different temperatures from 9° to 70°C., and at different fairly small strains. Because of the complexity of the phenomenon, experiments were restricted only to a single agar-agar concentration of 4 g./100 cc.. However, it is hoped that we may have an opportunity in a forthcoming paper of this series to present data on the concentration effect along with data on other subjects left untouched in the present work.

Experimental

The agar-agar samples and the procedure of preparing the specimen gels used in the present work were, in all respects, identical with those which have been used in Part I[2] of this series; the specimen gel was shaped in a cylindrical column whose height and diameter were both about 3 cm. An autographic relaxometer was designed employing the principle of the chainomatic balance used by Dart and Guth[3] for the study of compression stress-relaxation in natural cork. A schematic diagram of the relaxometer is shown in Figure 1. To save space, the description of the mechanism and the procedures for

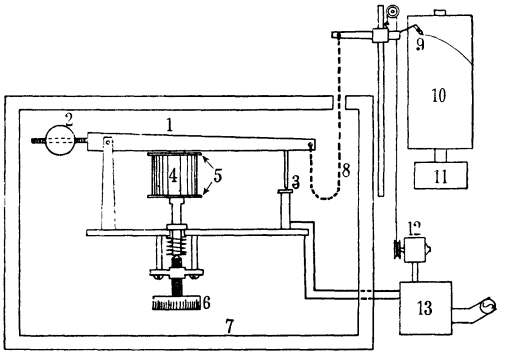

Fig. 1.—Schematic diagram of the relaxometer; 1: balance arm. 2: balancer. 3: point of contact. 4: test piece. 5: metal plates for compression. 6: screw gauge. 7: air oven. 8: chain. 9: recording pen. 10: rotating drum. 11: driving clock. 12: driving motor. 13: relay.

practical use of this apparatus is omitted here; it will be published in a separate paper by one of the present authors.[4] The relaxometer was installed in an air oven made of wood and glass lined with thick layers of asbestos and cardboard cartons. Temperature control was attained by means of a bimetallic thermoregulator which was accurate to about ±0.25°C.. Humidity was maintained at an almost saturated state to prevent drying of the specimen gel as much as possible. In addition, with the same object, liquid paraffin was sufficiently applied on the surface of the specimen exposed to air. With these treatments, drying of the specimen was almost checked up to about 60°C., so that at temperatures below 60°C., it might be regarded that actual temperatures of the specimen during the course of a

(1) M. Miller, J. D. Ferry, F. W. Schremp and J. E. Eldridge, *J. Phys. and Colloid Chem.*, **55**, 1387 (1951).
(2) H. Fujita, K. Ninomiya and T. Homma, This Bulletin, **25**, 374 (1952).
(3) S. L. Dart, and E. Guth, *J. Appl. Phys.*, **17**, 314 (1946).
(4) K. Ninomiya, *J. Chem. Soc. Japan*, in preparation.

relaxation test were substantially equal to the temperatures of air in the oven. However, at temperatures higher than about 60°C., it was concluded, as a consequence of evaporation of the solvent from the specimen, that the gel reached thermal equilibria at temperatures somewhat lower than those of its surrounding air; and difference of these two temperatures was found to become more and more marked with the increase of the air oven temperature. In view of this finding, a preliminary experiment was carried out to determine this temperature difference as a function of the given temperature of the air oven. With the result thus obtained, when the relaxation test was made at temperatures higher than 60°C., we estimated the actual gel temperature from the experimentally given temperature of the air oven.

Compressions adopted in the present work were from 0.6 to 8.6% at lower temperatures, and from 0.6 to 3.6% at higher temperatures. Within these limits of compression, the resultant stresses were varied almost linearly with strains. In dealing with experimental data on viscoelasticity in the light of the current theories for the mechanical behavior of high polymers, it is important to bear in mind that those theories are applicable only for materials, the elastic behavior of which follows closely the so-called Hooke's law.

Results and Discussion

Type of Stress-Relaxation Curves Obtained.—A typical example of relaxation data obtained is shown in Figure 2, which shows

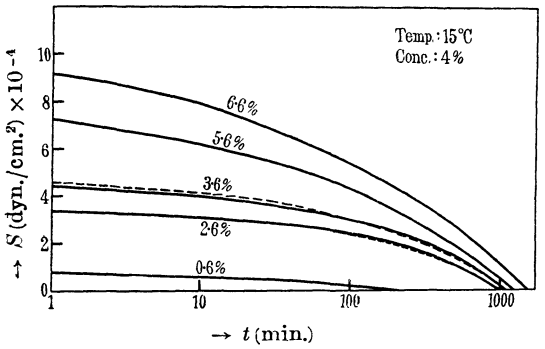

Fig. 2.—Experimental stress relaxation curves.

relaxation curves for different compressions at a constant temperature of 15°C. The fairly rapid decay of stress at this room temperature is a clear evidence of the lack of the primary network structure in agar-agar gels. This is in agreement with the current view for the structure of the majority of polymer gels that it consists of a three-dimensional network cross-linked with bonds of a secondary nature. The shape of the relaxation curves is apparently similar to that which would be observed in a viscoelastic body obeying a single Maxwell equation. However, as will be seen later on, a single Maxwell equation is not sufficient to describe these plotted curves but at least two Maxwell equations are required. It is important to note a characteristic behavior of our relaxation curves in the neighborhood of the zero stress base. In usual polymer solids which lack the primary network structure (e. g., polyisobutylene[5]), it is known that stress at constant deformation is relaxed to zero after an infinitely or sufficiently long run for all values of given deformation. Contrary to this, our relaxation curves for concentrated agar-agar gel are apparently lowered to zero after running certain finite intervals of time, which are apparently seen to be largely dependent on the given strain magnitudes. According to the data obtained at temperatures different from 15°C., the value of time interval at which stress is relaxed to zero is also a function of temperature. The reason why our relaxation curves for agar-agar gel are so markedly different in the manner of decaying to zero stress from those of other polymer solids has yet not been fully elucidated, but, as will be shown in a later part of this paper, there is a fairly reliable reason to believe that this is essentially due to the effect of syneresis which is characteristic of the majority of gel-systems.

In Figure 2, results of duplicate experiments are also indicated with dotted lines for two strains of 2.6 and 3.6%. Stress magnitude is seen not always to be reproducible in these duplicate experiments. However, allowing for the sample variance, which is usually encountered in this kind of experiments dealing with natural substances, and for difficulty of precise determination of strain magnitude, the agreements of stress magnitude attained in these duplicate experiments must be regarded as rather satisfactory.

Analysis of Data.—In Part II[6] of this series of papers, we have known as a result of the measurements of compression creep that agar-agar gel has a general tendency as a consequence of syneresis to contract spontaneously at a certain definite rate of deformation, which is dependent on the conditions of the particular experiment. Therefore, it is reasonable to suppose that when a cylindrical column of agar-agar gel is made to deform between two parallel plates under compressive load, the observed rate of decrease in the column height with time is the sum of the following two

(5) R. D. Andrews, N. Hofman-Bang and A. V. Tobolsky, *J. Polymer Sci.*, **3**, 669 (1948).

(6) H. Fujita, K. Ninomiya and T. Homma, This Bulletin, **26**, 20 (1953).

rates of deformation, one of which is that due to molecular structural flows caused only by the action of the external load, and another of which is that due to the spontaneous contraction of the cylinder as a whole.

To formulate this consideration, we shall assume that the relaxation mechanisms contained in an agar-agar gel whole solid can be represented by two Maxwell mechanical elements connected in parallel. Since, in this mechanical model, the individual relaxation elements are equally subjected to compression resulting from the self-contraction, the rate of change in strain with time, $d\gamma/dt$, for each element is written as:

$$\frac{d\gamma}{dt}=\frac{1}{E_1}\frac{dS_1}{dt}+\frac{S_1}{\eta_1}+f, \qquad (1)$$

$$\frac{d\gamma}{dt}=\frac{1}{E_2}\frac{dS_2}{dt}+\frac{S_2}{\eta_2}+f, \qquad (2)$$

and for the total stress S, we have

$$S=S_1+S_2, \qquad (3)$$

where f stands for the rate of deformation resulting from the self-contraction, and S_i, E_i, and η_i denote the partial stress, the elastic constant of the spring, and the viscosity of the dash-pot, of the ith element, respectively ($i=1, 2$).

To solve the above set of equations for any given condition of stress or strain, it is necessary to know the mathematical expression for f corresponding to that condition. However, unfortunately, we have hardly had information available on this point. It has been revealed in Part II that when the external stress is absent, and moreover, when the environmental conditions are kept constant, f takes a constant value for a long period of time. If, as has been stated by Ferry,[7] syneresis in gel-systems is produced as a result of the progressively closer binding of the network strands, the rate of change in volume with time thereby resulting would be much less modified even if the material is subject to external stress. If this view be true, it may be assumed as a first approximation that the value of f remains unchanged even under stressed condition so far as the stress magnitude is sufficiently small as was the case with the present relaxation tests. This assumption is the same as saying that the f value is constant over a long interval of time at any stress condition. We shall here presume this assumption to be justifiable and denote the constant value to be assigned to f by C.

Introducing the condition that $f=C$ into Eqs. (1) and (2), and solving the resultant set of equations for S with the condition of relaxation experiment at constant strain, we obtain the following solution:

$$S=\gamma_0(E_1e^{-t/\tau_1}+E_2e^{-t/\tau_2}) -C\{\eta_1(1-e^{-t/\tau_1})+\eta_2(1-e^{-t/\tau_2})\}, \qquad (4)$$

where γ_0 is the strain at which the specimen is held fixed, and τ_i is the Maxwellian relaxation time of the ith element as defined by the so-called Maxwell relation:

$$\tau_i=\frac{\eta_i}{E_i}. \qquad (5)$$

Our main object in what follows is to determine the numerical values of parameter, E_i and τ_i, as functions of temperature by fitting Eq. (4) to experimental data. For this purpose the following procedure of fitting is employed:

Firstly, from the relaxation data for different strains at constant temperature, we construct a system of plots between S and γ_0 with t as parameter. According to Eq. (4), if the parameter, E_i and τ_i, are constants characteristics of the material concerned, the plots thus obtained should be linear and their inclinations to the γ_0 axis should give the values of the quantity Q defined by

$$Q=E_1e^{-t/\tau_1}+E_2e^{-t/\tau_2}. \qquad (6)$$

It was found for all the relaxation data

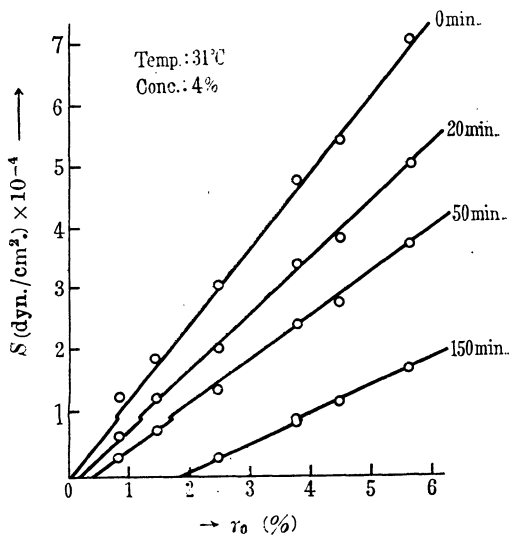

Fig. 3.—An example of the S vs. γ_0 plot.

(7) J. D. Ferry: "Advances in Protein Chemistry", IV, Academic Press, Inc., Publishers, New York, 1948, Chapt. I, pp. 1-78.

obtained that this linearity between S and γ_0 was approximately realized; a typical illustration of this is given in Figure 3, where to avoid confusion of the diagram only several representative lines are plotted. That the straight lines drawn visually to give the best fit to the experimental points do not pass through the origin of coordinates is apparently to be ascribed to the contribution from the term involving C. It is now possible to evaluate Q as a function of time t. A typical graph of this function in the form of $\log Q$ plotted against the linear time t is shown in Figure 4. Seeing this graph, one can at once

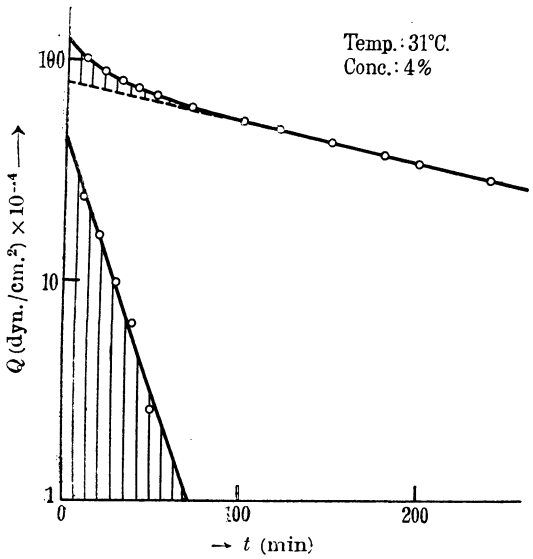

Fig. 4.—An example of the log Q vs. t plot.

expect that the plotted curve may nicely be fitted by an expression of the form of Eq. (6).* This prediction was satisfactorily confirmed for all temperatures studied except for the two cases mentioned below, and thus we could determine the required values of E_i and τ_i ($i=1,2$) with sufficient accuracy. The two exceptional cases were the temperatures as low as 9° and 15°C., at which Eq. (6) proved somewhat insufficient to represent the plots precisely at small values of t. Thus, in these cases, it had to be modified as:

$$Q=E_1e^{-t/\tau_2}+E_2e^{-t/\tau_2}+E_3e^{-t/\tau_3}.$$

Accurate determination of the numerical values of the newly introduced parameters, E_3 and τ_3, was, however, rather prohibitive, so we had to be content with obtaining their rough values.

In this way, the results tabulated in Table 1 have been determined, in which the figures enclosed by brackets are somewhat doubtful. E represents the sum of E_i's, so that it is nothing but the overall modulus of elasticity in compression of the agar-agar gel investigated. In passing, it is of interest to note that the above method of analysis has an advantage in that, on its application, no allowance needs to be made for actual value of C.

Table 1

Temperature (°C.)	Elastic constants (dyn./cm.²) $\times 10^{-5}$				Relaxation times (min.)	
	E_1	E_2	E_3	$E=\Sigma E_i$	τ_1	τ_2
9.0	(7.5)	(4.1)	(1.4)	(13.0)	(700)	(32)
15.0	8.0	4.7	1.1	13.8	625	43
21.0	8.9	3.9	(1.0)	(13.8)	380	32
26.0	8.8	3.9	—	12.7	314	30
31.0	7.9	4.3	—	12.2	246	19
37.0	7.6	2.4	(0.5)	(10.5)	(191)	15
49.0	6.8	3.1	—	9.9	90	9
56.0	4.0	2.2	—	6.2	52	6
64.0	2.4	0.5	—	2.9	30	3
70.0	2.0	—	—	2.0	16	—

We shall next consider the temperature dependencies of the relaxation times, τ_1 and τ_2, in the light of the Arrhenius equation of the form:

$$\tau=A\exp(U/RT),$$

where τ is the relaxation time, A is the so-called "frequency factor," U is the activation energy for stress-relaxation, and R and T are the gas constant and absolute temperature, respectively. For this purpose, we plot the logarithms of τ_1 and τ_2 against $1/T$, the resultant plots being shown in Figure 5. It is seen that both relaxation times, though they differ markedly in numerical values, vary with temperature following an almost similar process. Up to about 40°C., the plots are regarded as linear and approximately parallel each other, indicating that in this temperature region, the activation energies U_1 and U_2

* Assuming preferentially $\tau_1>\tau_2$, Eq. (6) indicates that for large values of time the logarithm of Q, when plotted against t, provides a straight line whose inclination is τ_1 and whose interception on the ln Q-axis is ln E_1. A good illustration of this relation is given in Figure 4. If this relation proves to hold, Eq. (6) further predicts that the logarithm of $Q-E_1e^{-t/\tau_1}$ should also become linear with t and that the straight line obtained allows to evaluate the values of τ_2 and E_2 respectively from its inclination and its intercepti on the ordinate axis. A fairly good establishment of the latter straight line is also illustrated in the lower portion of Figure 4 (the shadowed triangle).

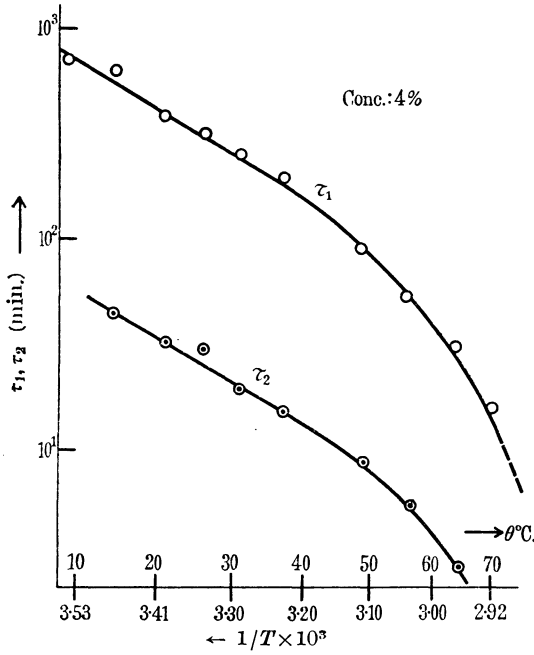

Fig. 5.—Relaxation times, τ_1 and τ_2, as functions of temperature.

corresponding to these two elements are constant and take nearly equal values, the average of which is estimated at 9 kcal./mole. This value of the energy of activation for relaxation is in good harmony with the view that polymer gels usually consist of a three-dimensional network structure whose strands are cross-linked at points of contact of a secondary strength. Above 40°C., the plotted lines have curvatures, being deviated more and more from linearity and appearing to fall rapidly in the neighborhood of 90°C. This result is that which should be expected a priori, because agar-agar gels usually have their melting points in the vicinity of 90°C. It would be reasonable to suppose that the increasing deviations of the plotted curves from linearity are chiefly associated with the decrease in the frequency factor (or probably, the increase in entropy for relaxation) accompanying the increase in temperature.

We are not yet in a position to have molecular theoretical interpretation of mechanical model constants obtained above for agar-agar gel. However, it may be of some interest to infer, referring to Ferry's view,[8] that τ_1, the longer relaxation time, corresponds to slippage at points of contact of the network strands, and τ_2, the shorter relaxation time, to rotation of the individual strands over the potential barrier into the next position of minimum energy.

Solving Eqs. (1), (2) and (3) under the conditions that $S=\text{constant}\equiv S_0$ and $f=C$, we obtain the creep equation in the form:

$$\gamma=\frac{S_0}{E_1+E_2}+B\left(1-e^{-\frac{1+\frac{E_2\tau_2}{E_1\tau_1}}{1+\frac{E_2}{E_1}}\frac{t}{\tau_2}}\right)+\left(\frac{S_0}{\eta_1+\eta_2}+C\right)t \tag{7}$$

where B is an indeterminable constant. This equation is exactly the same in form as the empirical creep equation presented in Part II of this series of papers, in which the term $\eta_1+\eta_2$ in the above equation has been represented by a symbol η. In that study, the values of η were evaluated at different temperatures by fitting that empirical creep equation to data of compression creep tests therein conducted. On the other hand, individual values of η_i can readily be calculated from the results listed in Table 1 by use of the Maxwell relation (5). Thus, it is now possible to examine if the values of η from the creep measurement can be reproduced as the sum of the individual viscosity values η_i from the present relaxation test. In Fig. 6, the result of this examination is indicated in the form of $\log\eta$ plotted against $1/T$, from which we see that all plotted points approximately fall on a single curve. This agreement

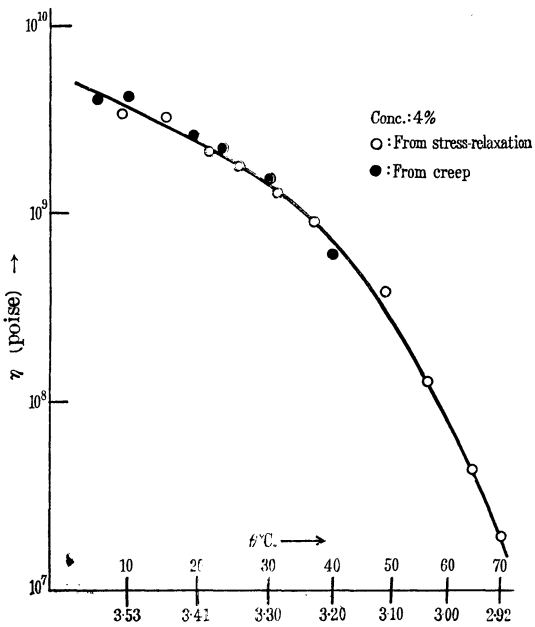

Fig. 6.—Overall viscosity as a function of temperature.

(8) J. D. Ferry, W. M. Sawyer and J. N. Ashworth, *J. Polymer Sci.*, **2**, 593 (1947); especially, p. 611.

between the viscosity values from different sources of data suggests that our mechanical model set forth above is sound as a consistent basis for describing the static viscoelastic behavior of concentrated agar-agar gels.

In the foregoing lines we have remarked that relaxation curves of agar-agar gel in compression fall across zero stress after running a certain finite interval of time, differing from those in other polymers which lack the primary network structure. This behavior can now be interpreted adequately in the light of Eq. (4). It proves readily that the right-hand side of Eq. (4) vanishes at a certain positive value of t if C is positive, and that it vanishes only at infinitity if C is identically zero. This result implies that when and only when self-contraction of the material is operative, stress at constant compression should be relaxed completely after a finite interval of time has elapsed, just as has been demonstrated in the present relaxation study on agar-agar gels.

Summary

As the third report of the series of papers concerning the viscoelastic behavior of concentrated hydrogels of agar-agar, the results of an experimental investigation of the relaxation of stress in an agar-agar gel of a concentration 4 g./100 cc. have been presented, which are summarized as follows:

(1) The general type of the relaxation curves obtained may be seen in Figure 2, in which particular attention must be drawn to the behavior that the plotted curves fall across the zero stress base after running certain finite intervals of time. An adequate interpretation of this has been presented in the last section of the text.

(2) As was illustrated in the second paper of this series, an agar-agar gel block decreases spontaneously and gradually its volume under the experimental conditions adopted in this series of experiments. Taking into account he spontaneous volume contraction, a system of equations for representing the viscoelastic deformation of an agar-agar gel column subject to compressive load has been presented, in which as a mechanical model of the material two Maxwell relaxation elements connected in parallel have been assumed.

(3) All the data of relaxation obtained have been considered in the light of this set of equations. In this way, the numerical results listed in Table 1 have been obtained.

(4) The activation energy for relaxation has been calculated for each individual mechanical element by the use of the Arrhenius equation. It has been found that the activation energies so calculated are constant below about 40°C. for both elements, amounting to nearly equal values, the average of which is estimated at about 9 kcal./mole. Above 40°C., for both relaxation elements, deviations from the Arrhenius equation appeared, which are gradually marked with increase in temperature. We have ascribed these deviations to the decrease in the frequency factor in the Arrhenius equation.

(5) Finally, the set of equations presented above has been solved for the case of compression creep under constant load, resulting in a creep equation coinciding exactly in form with the empirical creep equation derived in the previous paper II of this series. In addition to this formal agreement of the present theoretical and the previous empirical creep equations, quantitative agreement of them has been demonstrated by showing that the viscosity values from the previous creep test can be well reproduced by the sum of the individual viscosity values obtained from the present relaxation test.

The authors wish to express their hearty thanks to Mr. T. Nakagawa of Tokyo University for his continued interest and encouragement to the present work.

Applied Physics Laboratory, Department of Fisheries, Faculty of Agriculture, Kyoto University, Maizuru

Physicochemical Properties of the Surface of Aqueous Solutions. IV. Classification of Mechanical Behavior of Several Aqueous Surfaces*

By Hideo KIMIZUKA

(Received June 2, 1952)

In the preceding paper[1] the mechanical behavior of the surface of aqueous solutions was measured and discussed by means of the mechanical models. Further studies on the mechanical behavior of surfaces of aqueous solutions of various substances have been continued from the similar point of view.

Experimental

Measurements of surface rigidity and surface viscosity coefficient were carried out using the same apparatus as described previously.[1] Of the samples used, saponin, crystal violet, polyvinyl alcohol and horse serum albumin were those used in the preceding experiment.[1] Gum arabic, peptone, egg albumin and sodium stearate were commercially pure and were used without further purification. In this experiment, the mechanical behavior of the surface of the solution was studied as a function of concentration. Solutions were prepared using freshly distilled water. The time of aging prior to the measurement was kept to one hour* and the experiments were carried out at room temperature.

Result

The concentration dependence of viscoelastic constants for each system observed was shown in Figures from 2 to 9. In these figures, the ordinates represent G,G' and η which correspond to the elasticity and viscosity constants of a three-parameter model respectively shown in Fig. 1 and the abscissa, the logarithm of concentration, C. The portions of dotted line in $\eta\sim\log C$ curves represent the region of non-Newtonian flow. Here, non-Newtonian flow observed did not always obey the empirical relation,

$$\log\frac{d\theta}{dt}=A-B\theta$$

which was obeyed in the case of the measurement reported in the preceding paper.[1] The temperature range of the experiment was also

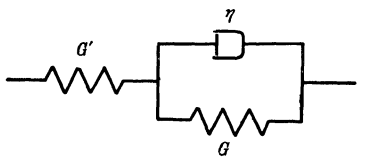

Fig. 1.

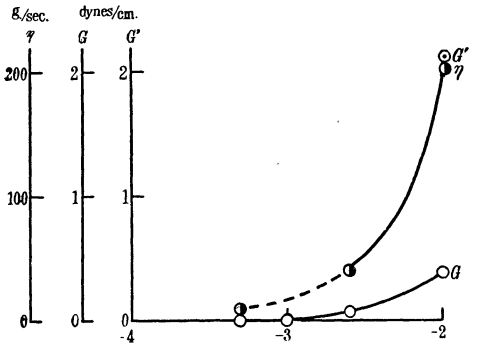

Fig. 2.—Crystal violet solution. 18.5~20.5°C.

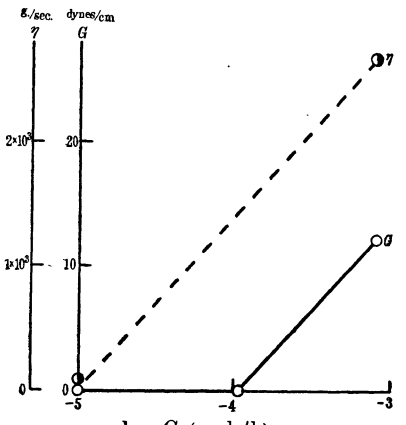

Fig. 3.—Sodium stearate solution. 10.5~11.5°C.

* This work was reported at the meeting for general discussion of colloid chemistry held on Nov. 10, 1951, in Tokyo, under the auspices of the Chemical Society of Japan.

(1) T. Sasaki and H. Kimizuka, This Bulletin, **25**, 318 (1952).

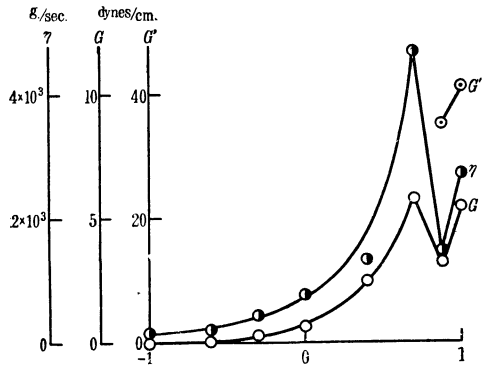

Fig. 4.—Saponin solution. 18.0~20.0°C.

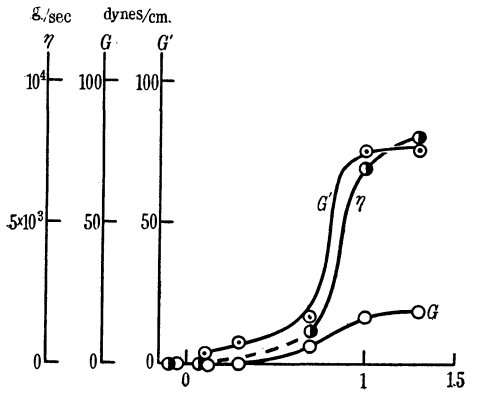

Fig. 5.—Gum arabic solution. 18.0~20.0°C.

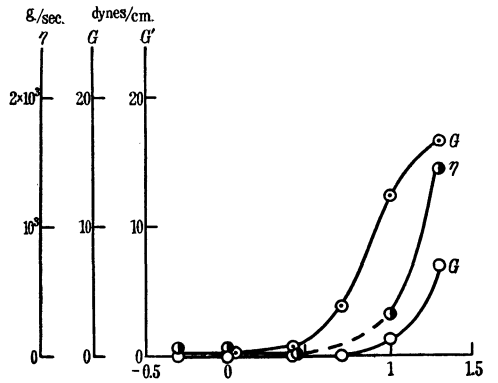

Fig. 6.—Peptone solution. 23.0~25.0°C.

indicated in each figure. The time effect on the mechanical behavior of the surface was also studied, of which an example was shown in Table 1. In Table 2, observed values of the relaxation time, η/G', and the retardation time, η/G, were summarized where T denoted the time scale.

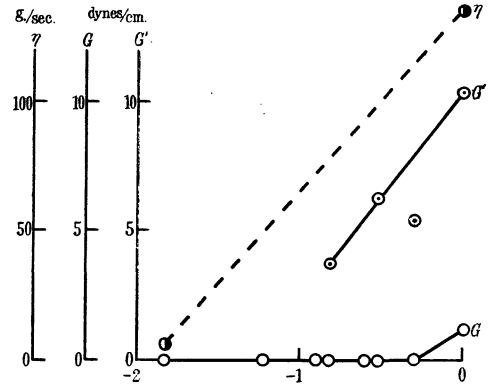

Fig. 7.—Horse serum albumin solution. 23.0~25.0°C.

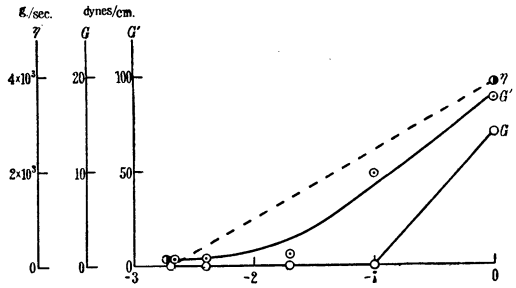

Fig. 8.—Egg albumin solution. 19.5~20.5°C.

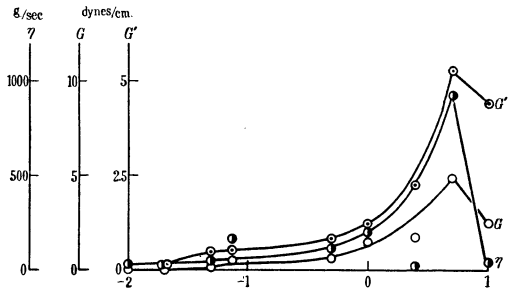

Fig. 9.—Polyvinyl alcohol solution. 18.0~20.0°C

Table 1

Effect of the Time of Aging on the Mechanical Behavior of the Surface of Polyvinyl Alcohol Solution (1.25×10^{-3} g./l.)

Time of Aging of Surface (hrs.)	G' (dyn./cm.)	G (dyn./cm.)	η (g./l.)
1		0.00	~0.00
2		0.00	0.03
3	5.11×10^{-4}	0.00	1.62
10	3.30×10^{-2}	1.23×10^{-2}	0.42

Table 2

Comparison between the Time Scale and Retardation Time or Relaxation Time

Model	η/G' (sec.)	η/G (sec.)
Three-parameter model	5.0—810$\sim T$	3.6—535$\sim T$
Maxwell model with non-Newtonian flow	$\sim$	$>$
Maxwell model	0.8—7.8$\sim$	$\gg$
Voigt model	$\ll$	60—1440$\sim$
Non-Newtonian flow	$\ll$	$>$
Non-Newtonian flow	$<$	$\gg$
Newtonian flow	$\ll$	$\gg$

Discussion

As seen in the results shown in the Figures from 2 to 9, a type of mechanical model for a given solution generally changed with the increase in concentration, presumably due to the change in the mechanical structure of the surface layer. This change ocurred in the following two ways in the present experiment.

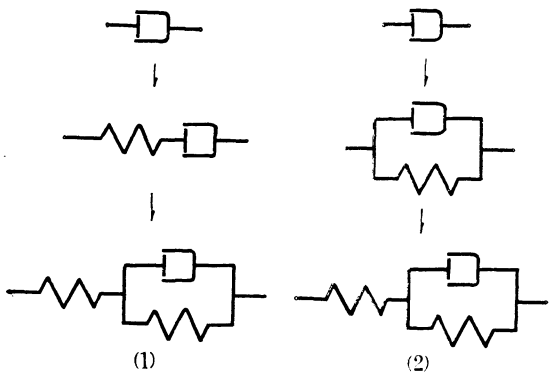

Fig. 10.—Mode of transformation in mechanical behavior of surface.

Surfaces of solutions of high polymers, such as egg albumin, horse serum albumin, peptone, gum arabic and polyvinyl alcohol changed according to the mode 1,* while those of sodium stearate, crystal violet and saponin, the mode 2. Among the substances of the mode 2, sodium stearate did not exhibit the mechanical behavior of three-parameter model under the condition of one hour aging. Prolonged aging, however, made it to be realised, as in the case of fifty hour's aging of 1 g./l. solution where $G'=7.03$ dyn./cm. $G=0.45$ dyn./cm. and $\eta=188$ g./sec. The author should like to take the opinion that this difference in the mode of change in a mechanical model is likely to come not from the difference in molecular structure of corresponding substances, but from that in the structure of higher order, for instance, whether it is a high polymeror a micelle. This requires further confirmation since it is not clear at present.

As seen in Table 1, a change in the time of aging without changing concentration caused such a change in mechanical model as that produced by the change in concentration with constant aging. From this, we can presume that the solute is gradually accumlating at the surface of the solution in the course of time and that the mode of change in a mechanical model with concentration generally does not change with the time of aging.

Table 2 shows the relaxation and retardation times observed which are of course the same order of magnitude to the time scale of the present experiment, in agreement with the requirement of the theory of viscoelasticity.(2) This table also shows the correspondence between the mode of change with concentration in the mechanical model and the process in which relaxation time and retardation time, starting from a much smaller or larger value for the viscous flow, approach the order of the magnitude of the time scale of the experiment.

Summary

1. Mechanical behaviors of surfaces of aqueous solutions were studied, and were explained by the three-parameter model with various relaxation times and retardation times.

2. The mode of change of mechanical models with the increase in concentration of the solution were classified into two groups; a change from the dashpot through the Voigt model to the three-parameter model, and a change from the dashpot through the Maxwell model to the three-parameter model. Saponin, crystal violet and sodium stearate belonged to the former, and egg albumin, horse serum albumin, peptone, gum arabic and polyvinyl alcohol, to the latter. It was presumed that this difference was due to the difference in the state of aggregation of their molecule.

* Inokuchi, however, reported somewhat different results on the monolayer of egg albumin and horse serum albumin, in which the Maxwell model was not observed (The annual meeting of the Chemical Society of Japan, Tokyo, on April, 1952.).

(2) T. Alfrey Jr., "Mechanical Behavior of High Polymers", Interscience Publisher, Inc., New York, 1948, p. 116.

In conclusion, the author wishes to express his sincere thanks to Prof. T. Sasaki for his guidance and encouragement given to the author during this experiment. A part of the cost of this research has been defrayed from the Scientific Research Expenditure of the Ministry of Education given to the professor.

Department of Chemistry, Faculty of Science, Kyûsyû University, Fukuoka

Physicochemical Properties of the Surface of Aqueous Solutions. V. Mechanical Properties of the Surface of Dye Solution

By Hideo KIMIZUKA

(Received June 9, 1952)

Some dyes are known to be remarkably surface active and their surface physicochemical properties have been studied in connection with the adsorption,[1] film strength,[2][3] foam[4][5] etc. Especially in our laboratory, the interaction between stearic acid and some dyes was investigated using wetting,[6] monolayer[7] and built-up film techniques.[8] In connection with these experiments, the present author has also studied the mechanical properties of the surface of dye solution.

Experimental

The experiment was carried out by the same concentric ring apparatus as described previously.[9] Dyes used in this experiment were conventionally classified according to their molecular structure into three groups, namely those of cationic, anionic and amphoteric ones. As anionic dyes, phloxine and scarlet red; as cationic dyes, crystal violet and night blue; as amphoteric dyes, methyl orange and congo red were chosen. Of the dyes used, crystal violet, methyl orange and congo red were specially purified by salting out or recrystllization[10] and the mechanical behavior of each was compared with that of crude ones, but they could not be distinguished from each other. So the rest of the dyes were used without special purifications. Each of these dyes was dissolved in water to the concentration of 10^{-2} mol./l. and was aged for about ten days before use. Just before the measurements, the solution was diluted to 10^{-4} mol./l. except for crystal violet, which was made to 10^{-3} mol./l. The hydrogen ion concentration of dye solution was varied from 1 to 13 in pH using hydrochloric acid and ammonium hydroxide. Here the use of ordinary buffer salt was avoided because of its disturbing effect upon the properties to be measured. The experiments were carried out at room temperature (10~13°C) and the time of aging prior to the measurement was kept to thirty minutes.

Result

As to the rheological property measured, the surfaces of solutions of scarlet red and methyl orange could not be distinguished from the surface of distilled water throughout the whole range of pH and up to the concentration of 0.1 mol./l. in the present experiment, while the formation of a coherent adsorbed layer was perceptible and sometimes remarkable in the solution of the rest of the dyes. The results

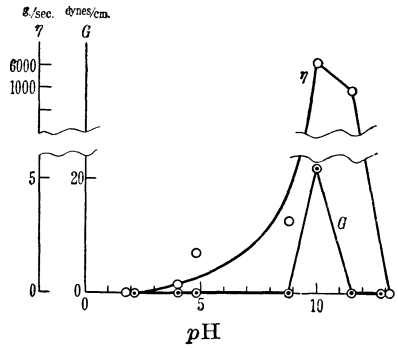

Fig. 1.—Crystal violet solution. 10^{-3}mol./l.

(1) K. S. G. Doss, *Kolloid-Z.*, **84**, 138 (1938); **86**, 205 (1939); **87**, 272 (1939), etc.
(2) W. Ramsden, *Z. physik. Chem.*, **47**, 336 (1904); O. Rhode, *Ann. Physik*, **19**, 936 (1906); Wo. Ostwald und M. Meiszner, *Kolloid-Beih.*, **26**, 1 (1928), etc
(3) A. Buzágh und J. Szonyi, *Kolloid-Z.*, **113**, 146 (1949).
(4) M. Nakagaki, This Bulletin, **22**, 201 (1949); **23**, 48, 105 (1950).
(5) T. Sasaki and H. Kimizuka, This Bulletin, **24**, 230 (1951).
(6) A. Inaba, to be published.
(7) R. Matuura, This Bulletin, **24**, 282 (1951).
(8) M. Muramatsu, to be published in a near future.
(9) T. Sasaki and H. Kimizuka, This Bulletin, **25**, 318 (1952).
(10) C. Robinson and H. A. T. Mills, *Proc. Roy. Soc.*, **A 131**, 576 (1931).

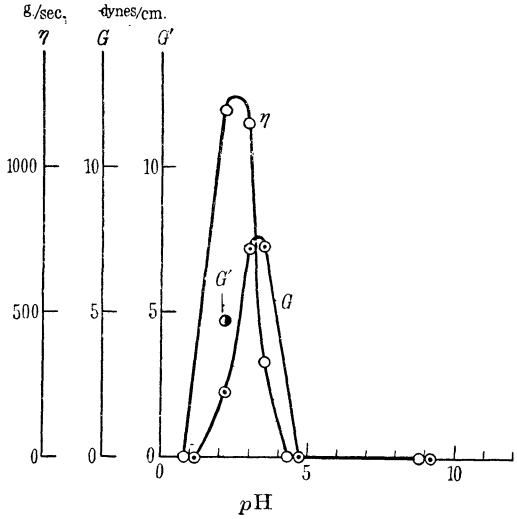

Fig. 2.—Congo red solution. 10^{-4} mol./l.

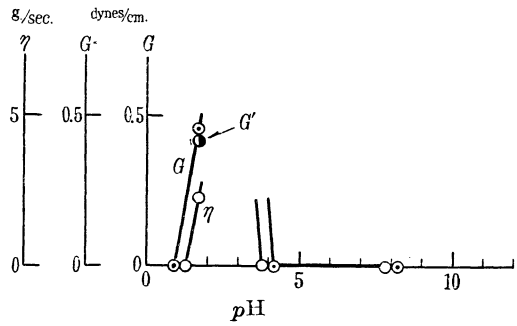

Fig. 3.—Phloxine solution. 10^{-4}mol./l.

obtained for the surfaces of solutions of crystal violet, congo red and phloxine were shown in Figs. 1, 2 and 3 respectively. The result with night blue was not shown which was essentially the same in its nature with crystal violet. In these figures, the ordinates represent instantaneous elasticity, G', retarded elasticity, G, and viscosity coefficient, η, corresponding to those of the three-parameter model,[9] the abscissa, pH. As seen in these figures, the surfaces showed the transformation of a mechanical model as well as sharp maxima in the value of surface rigidity and surface viscosity when pH of the solution was changed, keeping concentration constant.

Discussion

In our laboratory, Matuura[7] observed a remarkable expansion of the monolayer of stearic acid on the aqueous substrate containing dye at certain range of pH, and accounted for its mechanism by the interaction between the dyes and stearic acid. Inaba[6] confirmed this view by the experiment on wettability and Muramatsu,[8] by the study of built-up film. The present experiment also shows that the solution of dyes forms a coherent adsorbed layer in certain range of pH, where a remarkable effect on stearic acid was reported by the above authors. It may be emphasized from the above facts that the formation of a coherent adsorbed layer at surface together with the interaction between dyes and stearic acid result in the characteristic behavior of the monolayer.

Recently, Buzagh[3] made the measurement of strength of an adsorbed layer with respect to a change in pH and pointed out that anionic dyes formed a coherent adsorbed layer in an acid region, cationic, in an alkaline region and amphoteric, in neutral condition; but unfortunately he did not study the mechanical behavior of the film precisely. The result obtained in the present experiment shows that the mode of transformation of mechanical model exhibited by the dye solution belongs to that of micellar solution reported in the preceding paper[11] which again confirms the view presented there that the difference in mechanical behavior is due to a difference in higher order structure rather than a molecular one. Further, Buzagh[3] studied an effect of electrolyte on the surface of dye solution and emphasized that the formation of a coherent film is governed by the same factors determining other aggregation phenomena. This is in agreement with the behavior observed with the solution of congo red, crystal violet and night blue at appropriate range of pH.

In the case of scarlet red and methyl orange, the failure in the formation of a coherent adsorbed layer may be due to the weak attractive force between molecules in the surface layer because of its strongly ionizable $-SO_3Na$ group and therefore strongly hydrophilic character. The formation of a coherent adsorbed layer might be expected here if the solution is rendered much more acidic than in this experiment.

In the preceding paper,[5] the close correlation between surface viscosity and foam stability of solutions were reported, in which the neutral solution of congo red, fuchsine, auramine, crysoidine and malachite green were reported to form no coherent adsorbed layer. In the case of congo red solution, however, a change in pH of solution enables the formation of stable foam[4] as well as the coherent adsorbed layer which was overlooked in the preceding report.

Summary

The rheological property of the surface of dye solution with a change in pH under constant concentration was studied. Solutions of crystal violet, night blue, congo red and phloxine form the coherent adsorbed layer, while those of scarlet red and methyl orange, do not. The differences between them was considered to be due to the difference in the

(11) H. Kimizuka, This Bulletin, **26**, 30 (1953).

intensity of the interaction between molecules in the adsorbed layer. The surfaces of solutions of crystal violet, night blue, congo red and phloxine show the transformation of a mechanical model as well as sharp maxima in the value of surface rigidity and surface viscosity coefficient with a change in pH.

The author wishes to express his hearty thanks to Prof. T. Sasaki for his kind guidance in the course of this study and to acknowledge the contribution of Dr. M. Nakagaki for the discussion of the result. A part of the expense of this research has been defrayed from the Scientific Research Expenditure of the Ministry of Education given to the Professor.

Department of Chemistry, Faculty of Science,
Kyūsyū University, Fukuoka

Theory of Monolayer. II. Vibration of Molecule in the Monolayer Normal to the Surface.

By Hiroshi HOTTA

(Received June 9, 1952)

The author assumed in the previous paper[1] the equality of the vibrational term of the partition function of the molecule normal to the surface in both gaseous and liquid states of the monolayer. In the present paper, we shall criticise this propriety as a problem of the dynamics of material points and derive the relation between frequency and intermolecular distance or potential energy.

This vibration should be, of course, independent of the surface area per molecule in the region, where the mutual interaction between the surface molecules is negligible. Therefore, we now consider the system with mutual interaction. As a model of such a system we imagine a molecule vibrating normal to the surface, which is connected with n surrounding fixed molecules by springs, the strength of which is equal to the mutual potential energy, u, as shown in Fig. 1. The mass of the molecule is m.

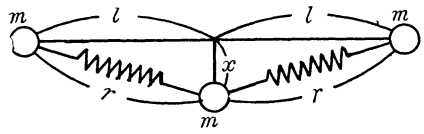

Fig. 1.

The mutual potential energy between any pair of the vibrating molecule and the surrounding one, U, is generally expressed in the form

$$U=nu=\frac{a}{r^6}-\frac{b}{r^k}, \qquad (1)$$

and

$$r^2=l^2+x^2, \qquad (2)$$

where r is the distance between two neighboring molecules, l the distance between them at equilibrium position, x the displacement normal to the surface, k the constant which is generally taken within a range of $12\geqq k\geqq 9$. The obtained value from the experimental data, as found in the previous paper,[1] was not u but U. Hence, the force normal to the surface, F, is as usual

$$F=-\frac{dU}{dr}\frac{dr}{dx}=\left(\frac{6a}{r^7}-\frac{kb}{r^{k+1}}\right)\frac{x}{r} \qquad (3)$$

from (1) and (2). Since the equation of motion is

$$m\frac{d^2x}{dt^2}+F=0, \qquad (4)$$

which may be rewritten as

$$m\frac{d^2x}{dt^2}+y^2x=0, \qquad (5)$$

inserting (3) into (4) and comparing this with (5),

$$y^2=\frac{6a}{(l^2+x^2)^4}-\frac{kb}{(l^2+x^2)^{\frac{k}{2}+1}}$$

$$=\left(\frac{6a}{l^8}-\frac{kb}{l^{k+2}}\right)+\left[\frac{k\left(\frac{k}{2}+1\right)b}{l^{k+4}}-\frac{24a}{l^{10}}\right]x^2+\cdots\cdots. \qquad (6)$$

First Approximation

If we neglect the second term in (6), viz., $l\gg x$,

(1) H. Hotta, This Bulletin, **25**, 398 (1952).

according to well-known treatment, the frequency ν is expressed by

$$\nu=\frac{1}{2\pi}\sqrt{\frac{1}{m}\left(\frac{6a}{l^6}-\frac{kb}{l^{k+2}}\right)}$$
$$=\frac{1}{2\pi l^4}\sqrt{\frac{a}{m}\left(6-k\cdot\frac{b}{a}\cdot\frac{1}{l^{k-6}}\right)}. \quad (7)$$

If we define

$$U^c=\frac{a}{l^6}, \quad (8)$$

the equation (7) is rewriteen as

$$\nu=\frac{1}{2\pi l}\sqrt{\frac{6U^c}{m}}. \quad (9)$$

On the other hand, if we define

$$U^c=\frac{a}{l^6}-\frac{b}{l^k}, \quad (10)$$

the equation (7) is rewritten as

$$\nu=\frac{1}{2\pi l}\sqrt{\frac{6U^c}{m}\left(1-\frac{k-6}{k}\cdot\frac{b}{a}\cdot\frac{1}{l^k}\cdot\frac{1}{U^c}\right)}. \quad (11)$$

Since the mutual potential energy in the liquid expanded film near the vaporization point may be approximately expressed in the form (8) as shown in the previous paper,[1] the equations (7) and (9) are rewritten as the limiting form

$$\nu^c=\frac{1}{2\pi l^4}\sqrt{\frac{6a}{m}} \quad (12)$$
$$=\frac{1}{2\pi l}\sqrt{\frac{6U^c}{m}}, \quad (13)$$

where ν^c is the frequency corresponding to (8). It is shown by (12) that ν^c is inversely proportional to the fourth power of the intermolecular distance or the square of the surface area per molecule.

If we insert the value of U^c of myristic acid at 14°C. obtained in the previous paper[1] into (13), the frequency normal to the surface under the condition metioned above becomes

$$\nu^c=1.2\times10^{11}\ \text{sec.}^{-1} \quad (14)$$

On the other hand, if the frequency of the vibration on the surface, ν^S, can be defined, according to the harmonic oscillator model,[2] by

$$\nu^S=\sqrt{\frac{kT}{2\pi mA_f}}, \quad (15)$$

where A_f is the molecular free surface as defined by equation (18) in the previous paper.[1] By inserting the numerical value corresponding to (14) into (15), we obtain

$$\nu^S=1.6\times10^{11}\ \text{sec.}^{-1}. \quad (16)$$

Next, since the vibration in the gaseous film may be the thermal agitation, the corresponding frequency, ν^G, is given, according to the cage model,[3] by

$$\nu^G=\frac{1}{4r^G}\sqrt{\frac{2kT}{\pi m}}, \quad (17)$$

which is one-third of the three-dimensional frequency, where r^G is the radius of a cage. Therefore, we obtain also

$$\nu^G=\frac{2\times10^{11}}{r^G}\ \text{sec.}^{-1} \quad (18)$$

by inserting the numerical value to (17), where r^G is in the A. unit. If we suppose that the maximum displacement of the centre of a surface molecule in the gaseous film, viz., r^G, may be at the most a few Angstroms, the ratio of ν^L to ν^G in the equation (9) in the previous paper should be nearly equal to unity, and the contribution to the heat of surface vaporization negligible.

These three frequencies are nearly equal. This shows that the effect of the mutual potential energy to the vibration should be negligible at the surface vaporization point. And these orders of magnitude of the frequencies may be plausible, compared with the experimental results in the other branches of science, e. g., rheology and microwave, etc.[4]

Since we must consider the repulsion term as in (10) in the more compact film, the frequency must be given by (11). If we define

$$z=\frac{b}{l^k}\cdot\frac{1}{U^c}, \quad (19)$$

which means the fraction of the repulsion term, then the equation (11) is transformed into the form

$$\nu^c=\frac{1}{2\pi l}\sqrt{\frac{6U^c}{m}\left(1-\frac{k-6}{6}z\right)}, \quad (20)$$

where ν^c is the frequency corresponding to (10). Müller[5] has calculated the van der Waals potential and the lattice energy of an n-hydrocarbon molecule in a paraffin crystal. Since z is supposed to be at the most one- or two-tenths even in the liquid condensed film from his estimation, if we neglect the effect of the head group, the contribution of the term $(k-6)z/6$ to the frequency

(2) Fowler and Guggenheim, "Statistical Thermodynamics," 1939, p. 325.

(3) Ibid., p. 530.

(4) M. Toda, "Ekitai-Kozo-ron" (The theory of liquid structure) (in Japanese). Chap. VIII; C. V. Raman and C. S. Venkateswaran, *Nature*, **143**, 798 (1939); C. P. Smyth et al., *J. Am. Chem. Soc.*, **70**, 4102 (1948); ibid., **72**, 3447 (1950).

(5) A. Müller, *Proc. Roy. Soc.*, **A 154**, 628 (1936)

may be small, when k is within the range of $12 \geqq k \geqq 9$. Therefore, the equations (13) and (20) are generalized in the form,

$$\nu = \frac{1}{2\pi l}\sqrt{\frac{6U}{m}} \tag{21}$$

within the error mentioned above.

But, since the steric hindrance should be considered in the compact film, the model at the beginning must be modified suitably.

Second Approximation

When the equation of motion is expressed as

$$m\frac{d^2x}{dt^2} + y^2x + \beta x^3 = 0, \tag{22}$$

the corresponding frequency is approximately

$$\nu \fallingdotseq \frac{1}{2\pi}\sqrt{\frac{1}{m}\left(y^2 + \frac{3}{4}\beta C^2\right)}, \tag{23}$$

where C is the amplitude.[6] Therefore, when we consider the second term in (6), the frequency becomes

$$\nu = \frac{1}{2\pi l}\times \sqrt{\frac{1}{m}\left[\left(\frac{6a}{l^6} - \frac{kb}{l^k}\right) - \frac{3}{4}\left(\frac{C}{l}\right)^2\left(\frac{24a}{l^6} - \frac{k\left(\frac{k}{2}+1\right)b}{l^k}\right)\right]}$$

$$= \frac{1}{2\pi l}\times \sqrt{\frac{6U}{m}\left[\left(1 - \frac{k-6}{6}z\right) - 3\left(\frac{C}{l}\right)^2\left(1 - \frac{k\left(\frac{k}{2}+1\right)-24}{24}z\right)\right]} \tag{24}$$

using (1) and (19). When the amplitude is small against intermolecular distance, *viz.*, $l \gg C$, the equation (24) becomes similar to (7).

Summary

The author has assumed in the previous paper that the vibrational term of the partition function of the molecule normal to the surface is equal in both gaseous and liquid films. This assumption was verified at the surface vaporization point in the present paper with the dynamics of material points. The derived relation between frequency and intermolecular distance or potential energy is (12) or (13).

In conclusion, the author wishes to express his sincere thanks to Prof. T. Isemura for his kind advice and encouragement.

Institute of Scientific and Industrial Research, Osaka University, Osaka

(6) T. Tsuboi, "Shindo-ron" (Theory of Vibration) (in Japanese), p. 255.

4, 4′-Dimethoxy-α, α′-dihalogeno-stilbenes: Estrogenic Halogen Derivatives of the Stilbestrol Series

By Michinori ŌKI

(Received July 23, 1952)

It has been postulated by the author and Y. Urushibara[1] that the development of a strong estrogenic activity requires not only the presence of two active hydrogen atoms or any groups capable of producing such in vivo at the optimum distance from each other[2] but also an optimum thickness of the molecule. Diethylstilbestrol acquires its favorable molecular thickness through the steric effect of the two ethyl groups at the α, α′-positions which force the benzene rings to rotate to a moderate extent. The substitution of lower or higher alkyl groups for the ethyl groups reduces the estrogenic activity and, as far as the molecular thickness is concerned, it is attributed to the deviation of the rotation of the benzene rings and consequently the molecular thickness from the optimum. The rotation of the benzene rings and its extent were deduced from the absorption spectra on

(1) M. Ōki and Y. Urushibara, This Bulletin, **25**, 109 (1952).
(2) F. W. Schueler, *Science*, **103**, 221 (1946)

the assumption that the deterioration in the light absorption is associated with the loss in conjugation caused by the rotation of the benzene rings from the coplanar structure, although nothing can be said as to the direction of the rotation.[3]

It has been proved that the groups carrying or producing the active hydrogen atoms need not be the hydroxyl or the alkoxy groups. Namely, thio-analogs of diethylstilbestrol dimethyl ether, $CH_3SC_6H_4C(C_2H_5)=C(C_2H_5)-C_6H_4SCH_3$ and $CH_3OC_6H_4C(C_2H_5)=C(C_2H_5)-C_6H_4SCH_3$, were found potent estrogens as reported by the author.[4] On the other hand, no fundamental change in the physiological properties is caused by the replacement of the ethyl groups of diethylstilbestrol by other groups capable of exerting a similar steric effect. Thus, 1,2-bis-(*p*-methoxyphenyl)-1,2-bis-(methylthio)-ethylene, $CH_3OC_6H_4C(SCH_3)=C(SCH_3)C_6H_4OCH_3$, has been found a strong estrogen as reported from this laboratory.[5]

In this paper the author presents the results of the studies on 4,4'-dimethoxy-α,α'-dihalogeno-stilbenes. Dodds et al.[6] prepared already the dichloro-compound and found 1,000 international units per gram. The present author prepared the same substance by a different method and synthesized other symmetrical and unsymmetrical dihalogeno-compounds. The methods of preparation of these substances are described in the Experimental Part. The absorption data and the estrogenic activity are shown in Table 1. In Table 2 the absorption data of dialkylstilbestrols and some reference substances are given for comparison.

Although the bromine atom possesses a van der Waals radius comparable with that of the methyl group, the absorption spectrum of the dibromo-compound (II) appears to show that the steric effect on the rotation of the benzene rings is smaller than that of the methyl group, provided that the bathochromic effect of the halogen atoms is such as shown by the absorption spectra of *p*-cresol methyl ether (X) and of *p*-methoxy-benzyl chloride (XI). And, on the same assumption, it can be said that in the diiodo-compound (III) the steric effect is greater than in the dipropyl compound (IX). The spectra of the unsymmetrical dihalogeno-compounds (IV and V) show two maxima attributable to two halves of their molecules. If it can be assumed that each half has a structure with a benzene ring which rotates in the same manner as it does in the symmetrical compound corresponding to the double of it, then it can be concluded that the hypsochromic effect of the unsymmetry is slight in the bromo-iodo-compound (V), while it is greater in the chloro-iodo-compound (IV).

The physiological activity was examined by the vaginal smear test with ovariectomized mice, substances in oil solution being subcutaneously injected in two portions. Among the symmetrical dihalogeno-compounds the dichloro-compound (I) showed the greatest activity, although only slightly more active than the dibromo-compound (II). If it is taken as significant, then it is deduced that there is another favorable thickness, to which the dichloro-compound is nearer than the dibromo-compound. H. Suzuki[7] estimated the angle of the rotation of the benzene rings in α,α'-dimethylstilbene as 60 or 56°. As the same rotation angle should be valid for the 4,4'-dimethoxy-α, α'-dimethylstilbene (VII), the angle of the rotation of the benzene rings in the dibromo-compound (II) must be smaller than this value and still smaller in the dichloro-compound (I), while naturally greater in diethylstilbestrol (VIII), but the angle peculiar to diethylstilbestrol is far surpassed in the diiodo-compound (III).

By the molecular thickness the author means the molecular dimension in the direction perpendicular to the plane of the central ethylene grouping, and, as far as the domains of the benzene rings are concerned, the thickness is complementary with the width. If the thickness and the width are interchangeable for the purpose

Table 1

Absorption Data and Estrogenic Activity of 4,4'-Dimethoxy-α,α'-dihalogeno-stilbenes, $CH_3OC_6H_4CX=CX'C_6H_4OCH_3$

	X	X'	$\lambda_{max.}$ ($m\mu$)	$\varepsilon_{max.}$ $\times10^{-4}$	Minimum active dose in mice
(I)	Cl	Cl	282	2.87	200γ(6.5×10⁻⁷mol.)
(II)	Br	Br	263	2.53	300γ(7.5 〃)
(III)	I	I	235	2.24	inactive at 800γ(16 〃)
(IV)	Cl	I	227, 267	1.22, 1.27	100γ(2.5 〃)
(V)	Br	I	234, 261	1.72, 1.58	>600γ(13 〃)

Table 2

$CH_3OC_6H_4CR=CRC_6H_4OCH_3$ [1]		$\lambda_{max.}$ ($m\mu$)	$\varepsilon_{max.}$ $\times10^{-4}$
(VI)	R=H	230, 305, 326	1.27, 3.47, 3.37
(VII)	$R=CH_3$	247	2.85
(VIII)	$R=C_2H_5$	236	2.20
(IX)	$R=C_3H_7$	235	1.81
(X)	*p*-Cresol methyl ether	224, 277, 286	0.66, 0.14, 0.13
(XI)	*p*-Methoxy-benzyl chloride	227, 272	1.17, 0.25

(3) Cf. G. A. Jeffrey, H. P. Koch, and S. C. Nyburg, *J. Chem. Soc.* **1948**, 1118; C. H. Carlisle and D. Crowfoot, ibid., **1941**, 6.

(4) M. Ōki, This Bulletin, **25**, 112 (1952).

(5) Y. Urushibara, M. Ōki and R. Ikeda, ibid., **25**, 66 (1952).

(6) E. C. Dodds, L. Golberg, E. I. Grünfeld, W. Lawson, C. M. Saffer, Jr. and R. Robinson, *Proc. Roy. Soc.*, B **132**, 83 (1944).

(7) H. Suzuki, This Bulletin, **25**, 145 (1952).

of attaining the optimum molecular shape, then there can be two favorable structures, unless the angle of the rotation is 45°. Then it comes out that none of the symmetrical dihalogeno-compounds correspond to the favorable structure of diethylstilbestrol but the dichloro-compound (I) is near to the other favorable structure which does not exist in the dialkylstilbestrols.

The chloro-iodo-compound (IV), being the most active of the present series, reminds the author of methyl-propyl-stilbestrol, which is as active as diethylstilbestrol. As it is probable that the steric effect of the chlorine atom is smaller than that of the methyl group while the iodine atom exerts a greater effect than the propyl group, as mentioned above, then, regarding the molecular thickness, the chloro-iodo-compound is more unbalanced than the methyl-propyl-stilbestrol; but their potency may probably be explained on the same grounds,

The direction of the rotation of the benzene rings being left in ambiguity, it is impossible to visualize a definite figure of the molecular structure. Moreover, the animal test may not offer a reliable basis for a quantitative discussion, and no information is available as to the physiological effect of the halogen atoms themselves. Hence, the considerations presented in this paper cannot claim more than only a reserved significance.

Experimental Part

4, 4'-Dimethoxy-α, α'-dichlorostilbene (I).—To a suspension of 472 mg. of 4,4'-dimethoxytolane, prepared by the oxidation of anisil dihydrazone with yellow mercuric oxide,[5] in acetic acid (5 c.c.), 5 c.c. of an acetic acid solution containing 142 mg. of chlorine was gradually added with good cooling and shaking. The reaction mixture was left to stand for 2 hours at room temperature and then the crystals were collected and recrystallized from alcohol containing a little acetone. The mother liquor from the reaction mixture gave a more crop. Yield, 347 mg. Colorless prisms melting at 163–164°. Found: Cl, 23.08; Calculated for $C_{16}H_{14}O_2Cl_2$: Cl, 22,94%. Dodds et al. [6] give m.p. 170°.

4, 4'-Dimethoxy-α, α'-dibromostilbene (II).—This substance was already prepared by H. Wiechell[9] who gave m.p. 197°. The present author prepared this compound by adding an equivalent amount (320 mg.) of bromine to a suspension of 4, 4'-dimethoxytolane (472 mg.) in acetic acid. Recrystallization of the product from acetone or ethyl acetate gave colorless prisms melting at 198°. Yield, 552 mg. Found: Br, 40.32; Calculated for $C_{16}H_{14}O_2Br_2$: Br, 40.08%.

4, 4'-Dimethoxy-α, α'-diiodostilbene (III).—To a suspension of 472 mg. of 4, 4'-dimethoxytolane in 5 c.c. of acetic acid, 15 c.c. of an acetic acid solution containing 508 mg. of iodine was added and the reaction mixture was left to stand for 72 hours at room temperature, when the brown color of iodine almost disappeared. The crystalline deposits were collected and carefully recrystallized from acetic acid. The substance was obtained in colorless prisms hardly soluble in most organic solvents and decomposing at 173° with evolution of iodine vapor. Yield, 847 mg. Found: I, 52.04; Calculated for $C_{16}H_{14}O_2I_2$: I, 51.58%.

4, 4'-Dimethoxy-α-chloro-α'-iodostilbene (IV)—Prepared from 472 mg. of 4, 4'-dimethoxytolane and 325 mg. of iodine monochloride in freshly distilled acetic acid in the same way as the dichloro-compound. Recrystallization of the product from acetone gave colorless prisms melting at 176–177°. Yield, 615 mg. Found: Cl, 9.16; I, 31.84; Calculated for $C_{16}H_{14}O_2ClI$: Cl, 8.85; I, 31.68%.

4, 4'-Dimethoxy-α-bromo-α'-iodostilbene (V).—Prepared from 4, 4'-dimethoxytolane and equivalent iodine monobromide in an analogous way. Recrystallization of the product from a large quantity of ethyl acetate gave colorless prisms melting at 207° with decomposition. 472 mg. of 4, 4'-dimethoxystilbene gave 708 mg. of the product. Found: Br, 18.03; I, 28.68; Calculated for $C_{16}H_{14}O_2BrI$: Br, 17.73; I, 28.29%.

Ultraviolet absorption spectra.—They were recorded with a Beckman Model DU photoelectric quartz spectrophotometer. Substances were dissolved in 95% ethanol. The concentrations are given in Table 3. The thickness of the solutions was 5 mm.

Table 3

Substances	Concentration
p-Methoxy-benzyl chloride	7.03×10^{-5}mol./l.
I	2.33 〃
II	4.10 〃
III	4.29 〃
IV	3.03 〃
V	2.12 〃

The author wishes to thank Professor Y. Urushibara for his kind guidance and thanks are also due to Mr. F. Ueno, Teikoku Hormone Manufacturing Co., Ltd., Kawasaki, for bioassays and to the Ministry of Education for the Grant in Aid for Fundamental Scientific Research.

Department of Chemistry, Faculty of Science, Tokyo University, Tokyo

(8) W. Schlenk and E. Bergmann, *Ann.*, **463**, 82 (1928).
(9) H. Wiechell, *Ann.*, **279**, 339 (1894).

Electron Microscopic Observation of Carbon Brushes. I.

By Tokiti NODA, Hiroshi TOMITA and Kenichi MIYATA

(Received June 16, 1952)

It was found in the previous paper concerning the X-ray examination of several commercial carbon brushes that the degrees of graphitization, i. e. the completeness of crystallization and the crystal size and form of graphite crystallites of brushes could be distinguished from each other by the X-ray method.(1) The electron microscopic examination of carbon brushes has been made in the present study to observe the microstructure of brushes, such as the mode of aggregation, the form and size of carbon particles.

Carbon brushes observed were the laboratory products of known composition and treatments.

Experimental

Samples:

Experimental carbon brushes of Nippon Carbon Co.:

Raw materials and intermediate product:

A: Carbon black (Nippon Oil Co.), Ash 0.11%, Density 1.730.

B: Pitch coke (Great Lake), Ash 0.8%, Density 2.080.

C: [(A 50%, B 50%): Tar=10:6] graphitized at 2500°C.,

Carbon brush blocks:

D: [Powder of C):(Tar 30%, Pitch 70%)=100:45] graphitized at 2500°C.,

E: [(B graphitized at 2500°C. 50%, Domestic coal tar pitch coke (ash 1.0%, density 1.800) graphitized at 2500°C. 50%):(Tar 30%, Pitch 70%)=100:45] graphitized at 2500°C.,

F: [(Coal tar pitch coke graphitized at 2500°C.):(Tar 30%, Pitch 70%)=100:45] graphitized at 2500°C.,

G: [(B graphitized at 2500°C.):(Tar 30%, Pitch 70%)=100:45] graphitized at 2500°C.,

H: [(A 30%, B 70%):Tar=10:6 graphitized at 2500°C.):(Tar 30%, Pitch 70%)=100:45] graphitized at 2500°C.,

I: [(A 50%, B 50%):(Tar 80%, Pitch 20%)=100:45] graphitized at 2500°C.,

J: [(A 50%, B 50%):(Tar 50%, Pitch 50%)=100:45] graphitized at 2500°C.,

K: Carbon brush block showing glancing specks.

Raw materials, intermediate product and some of the brush blocks were powdered and dispersed in a dilute aqueous solution of alcohol by super-sonic vibration. Surface replicas of carbon brushes were prepared to observe the microstructure of brushes. The block of the carbon brush sample was flattened by rubbing on a ground glass plate, with a little amount of No. 800 Alundum and water. Carbon fragments which adhered on the surface of the block were rubbed away by a piece of wet cotton. Ten % solution of polyvinyl alcohol or nitrocellolose was placed on the surface. A film which formed on the surface was stripped, so as to remove carbon fragments attached to the surface of the block. It was necessary to repeat the procedure two or three times in order to obtain a clear replica with only a small amount of adhered carbon particles. Positive aluminum replicas of the cleaned surface were prepared by the well-known methyl metacrylate-aluminum method. The thickness of aluminum replica film of about 25~30 mμ was suitable to observe carbon brush surfaces.

Results:

A: The particle size of A was 0.1~0.05 μ or smaller (Fig. 1.).

B: The powdered B consisted of irregular flakes (Fig. 2.).

C: C consisted of two different parts, i. e. parts of aggregates of minute carbon particles of approximately the same size as A and parts of pitch coke origin resembling B (Fig. 3.). The appearance of minute carbon particles of the former parts was slightly altered from the original black. They must be single crystals of graphite as were observed in the graphitized carbon blacks. The hexagonal face angle could not be seen, as the particles were too small to resolve the angle with our instrument.

D: The observation of surface replicas of D showed that the parts of pitch coke origin were aggregates of flat and irregular crystals and the parts of carbon black origin had small projects of approximately the same size as the original black (Fig. 4. and 5.).

E: Flat and irregular crystal surface of the size 0.5~0.6 μ predominated and crystal surfaces of several microns were observed in some parts of the replicas of E. Thin irregular crystals of graphite were found attached on the replica (Fig. 6.). The layer structure of graphite crystal can be seen on the large crystal surface shown in Fig. 7. A sectional view of layers of graphite crystals were reproduced in the replica and are seen near the large crystal surface on the figure. Smaller crystal surfaces are seen in other parts of the replica. Minute particles of ca. 0.01 μ

(1) T. Noda and S. Sato, This Bulletin **25**, 195 (1952).

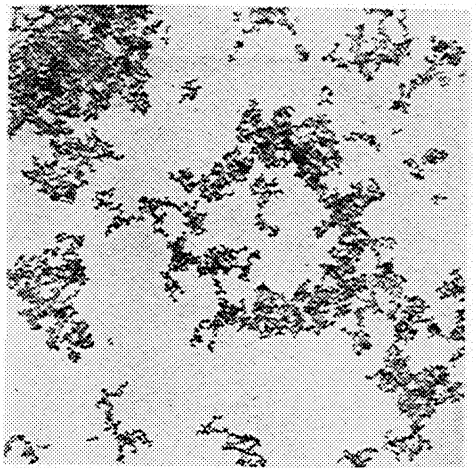

Fig. 1.—A (Nippon Oil Co. black). ×10,000

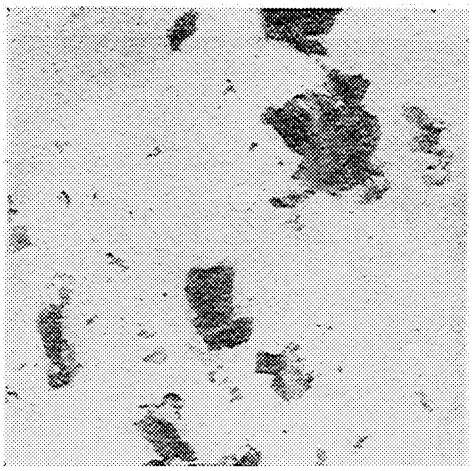

Fig. 2.—B (Great Lake pitch coke). ×10,000

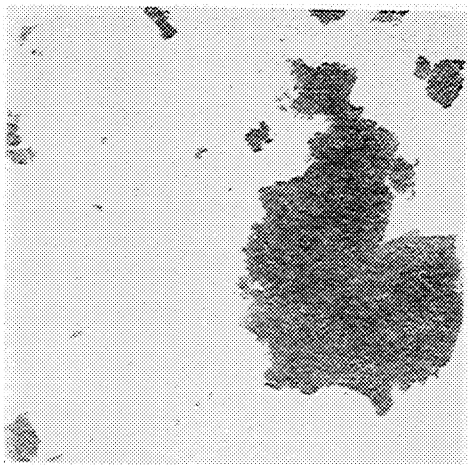

Fig. 3.—C. ×10,000

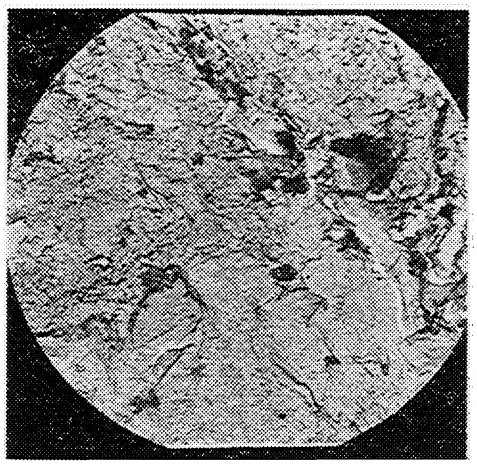

Fig. 4.—D. ×4,200

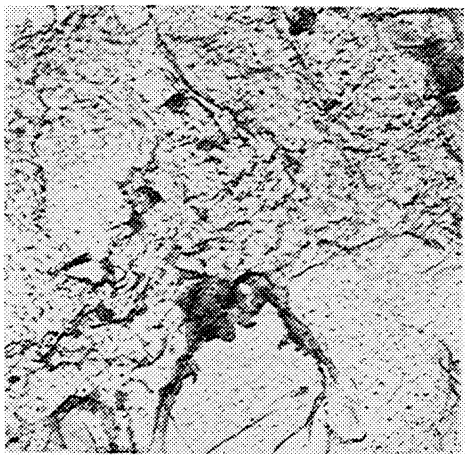

Fig. 5.—D. A part of Fig. 4. ×10,000

Fig. 6.—E. ×4,200

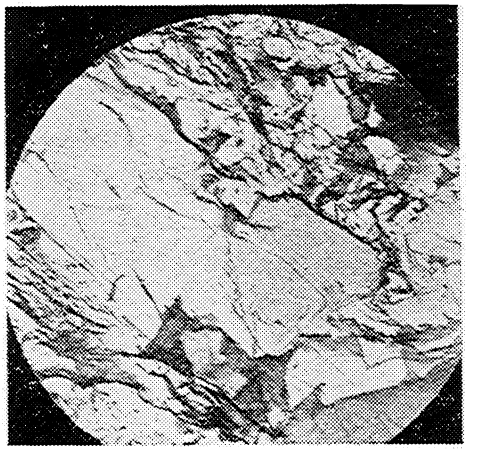

Fig. 7.—E. ×4,200

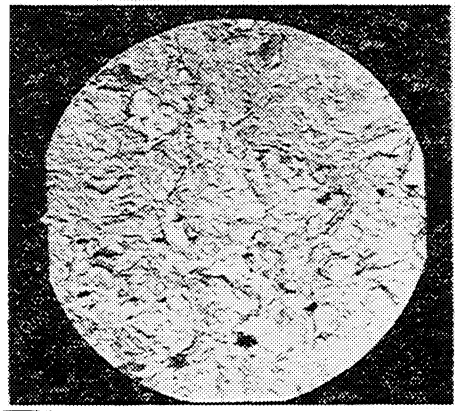

Fig. 8.—F. ×2,000

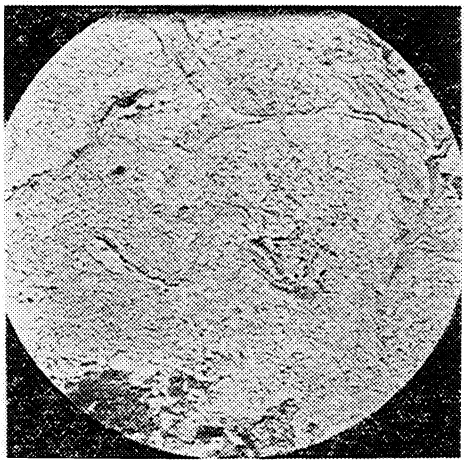

Fig. 9.—I. ×4,200

Fig. 10.—I. ×4,200

were found besides flaky graphite crystals in the directly observed powdered specimens of E.

F: Main parts of crystals of F were more irregular and smaller than those of E (Fig. 8.).

G: Well developed crystal surfaces were seen in larger parts of G.

H: The parts of carbon black origin and of pitch coke origin were clearly seen from an electron micrograph of the powdered specimens of H. The appearance of the powders was the same as those of C. Particles of approximately the same size as the original carbon black A linked together to aggregates.

I: A part of carbon black origiin of I is shown in Fig. 9. Boundaries of particles of aggregated carbon blacks are seen. A part of pitch coke origin is shown besides a part of carbon black origin in Fig. 10.

J: The appearance of J was the same as I.

K: Well developed crystal surfaces as F were seen in replicas of K.

Summary and Discussion

Pitch coke type brushes were found to consist of graphite crystallites having irregular forms and flat surfaces. Sizes of the graphite crystallites were very variable. Well graphitized crystals have relatively flat and smooth surfaces. Less graphitized crystals have rough surfaces. Well-developed flat crystals were split into thin flakes and attached on replica films. Parts of small and badly developed crystallites were seen side by side with the well-developed ones.

Carbon black type brushes were found to contain aggregated parts of minute carbon particles and parts of pitch coke origin. The size of the minute particles was approximately the same as that of the original carbon black particles. The minute particles were seen as minute projections or pits on replicas, while they were observed as being linked together to aggregates in directly observed specimens.

The authors wish to express their hearty thanks to Prof. Yoneichiro Sakaki of Nagoya University for his kind advice for the manipulation of electron microscope. This research was supported by the Grant in Aid for Developemental Scientific Research of the Ministry of Education and was made under authority of Comittee No. 117 (Carbon Materials for Electrical Machines) of the Japan Society for the Promotion of Scientific Research.

Department of Applied Chemistry, Faculty of Engineering, Nagoya University, Nagoya.

Wettability of Solid Surface. VI. The Effects of Metallic Cations on Stearic Acid Built-up Film

By Ayako INABA

(Received July 19, 1952)

Introduction

Formerly, Sasaki and Mitsui[1] reported the nature of wettability of stearic acid built-up film in relation to the number of layers and the condition of building up. The present author has also studied the wettability of stearic acid surface and has been confronted with the necessity of the more precise information on this problem.

It was shown in the fifth report[2] of this series that metallic cations were divided into three types, according to their effects on the wettability of stearic acid surface solidified in air, namely (I) wetting ion I (Na, K, Rb, etc.), producing surface dissociation of stearic acid, (II) wetting ion II (Al, Th, Fe, Cu, etc.), forming hydrated metal stearate of a complex structure, and (III) non-wetting ion (Ba, Sr, Ca, etc.), forming simple stoichiometric compound of principal valency. Here the difference between (II) and (III) is the most interesting problem. Matuura and Sasaki[3] of our laboratory reported the similar difference in the interaction of metallic ions~stearic acid monolayer, from the study of the pressure~area curve and film elasticity. Muramatsu and

(1) S. Mitsui and T. Sasaki, *Survey of the Recent Colloid Chemistry*, **1**, 196 (1948).
(2) A. Inaba, This Bulletin, **25**, 174 (1952).
(3) T. Sasaki and R. Matuura, This Bulletin, **24**, 274, 278 (1951).

Sasaki[4] also arrived at the same conclusion in their investigation of built-up film. The purpose of this work is to show the effect of metallic cations for the wettability of stearic acid built-up film.

Experimental

Material.—Materials used were stearic acid, barium chloride, aluminum sulfate, mercuric chloride, calcium nitrate, sodium hydroxide, and hydrochloric acid. These were purified by the usual methods which were described in a former report.[2]

Measurement.—The monolayer of stearic acid was built up on a glass rod under the pressure of oleic acid, excepting the case of B-layer technique, from the surface of aqueous substrate containing various metallic ions of 10^{-3} or 10^{-4} mol. The *p*H of the substrate was controlled in the range of 4.2~12.0 by adding 0.5N sodium hydroxide or 0.6N hydrochloric acid. The glass rod had been successively cleansed with chromic acid mixture, potassium hydroxide~alcohol mixture and distilled water, and dried in the current of dry air. The built-up film thus obtained was used for the wettability experiment. Du Noüy's apparatus was used to measure the degree of wettability.[5]

Results

a. Wettability and the Time of Drying.—Wettability of stearic acid film built up from the surface of tap water decreased with the time of drying after it was deposited from water surface and came to a certain limiting value after 1.5 hour as shown in Table 1. Therefore in the following experiment, observation was made at least 1.5 hour after the film was built up, unless mentioned otherwise.

Table 1

Time Effect of Drying on the Wettability of Films Built Up from Tap Water (*p*H 6.8)

Time of drying after built up (hr.)	9-*Y* layers		19-*Y* layers	
	θ_a	θ_r	θ_a	θ_r
0	90°	23°	117°	64°
0.5	109	37	108	64
1.5	112	60	114	70
24.0	112	57	113	70

b. Wettability and the Number of Layers.—Wettability of stearic acid film built up from the surface of tap water and substrate containing calcium ion (called Ca-substrate hereafter) was shown in Table 2. The contact angle, especially the receding contact angle of the film increased with increasing number of layers, approaching a certain value. It was noticed that the difference between advancing and receding contact angles was larger in the case of built-up film than in the case of the stearic acid solidified in air. (In the latter case, $\theta_a=110°$, $\theta_r=103°$.) This large hysteresis of wetting of the built-up film may come from an extremely systematic molecular arrangement in the film and the marked difference in the nature on both sides of the outermost monolayer resulting from it. The hysteresis was larger for the film which had a smaller number of layers. In the case of tap water as a substrate, θ_a was large and almost constant, independent of the number of layers, while the Ca- or Ba-substrate film did not give such a large θ_a value for the film which had a small number of layers. The phenomena may be attributed to the trace impurities like ferric or cupric ion in tap water.

Table 2

Wettability and the Number of Layers of Mixed Ca-stearate *Y*-film Built Up on Glass

Number of layers	Substrate, tap water, *p*H 6.8		Substrate, $Ca(NO_3)_2$ 10^{-4} mol. *p*H 6.8*	
	θ_a	θ_r	θ_a	θ_r
1	107°	20°	46°	15°
3	116	23	47	21
5	113	53	55	14
7	117	53	32	15
9	112	60	38	10
11	113	60	108	66
13			38	12
15			116	82
17			103	7
19	115	65	115	65
29	114	70	112	88
39			113	50

* Similar results were obtained in the case of $Ca(NO_3)_2$ 10^{-4} mol. (*p*H 8.6) and $BaCl_2$ 2×10^{-4} mol. solutions as substrate.

c. Wettability and the Type of Built-Up Film.—*X*-film could not be deposited directly on the glass surface and could only be deposited on 9 or 11 *Y*-layers. Therefore, comparison was made between *X*-film and *Y*-film both built up on the basis of 15 *Y*-layers. The results are shown in Table 3.

It is said that *X*-film has a larger receding contact angle than that of *Y*-film.[1],[6] This statement is true for the comparison of *Y*-film

(4) M. Muramatsu and T. Sasaki, This Bulletin, **25**, 21, 25 (1952).

(5) A. Inaba, *Memoirs of the Faculty of Science, Kyushu Univ., Ser. C*, **I**, 1 (1948).

from solution of *p*H 6~7 and *X*-film, which can only be obtained from solution of *p*H>9 as shown in Table 3. But we should rather insist upon the importance of *p*H. Namely, *Y*-film from low *p*H substrate showed smaller θ_r than that of *X*-film from high *p*H substrate. Further, as is shown in Table 3, *Y*-film deposited from alkaline solution showed the same value of contact angle with that of the *X*-film occasionally deposited under the same conditions. It is interesting to note that there was no difference in contact angle between the odd and even number of *X*-layers, contrary to the expectation that odd layers and even layers might show different contact angles because of their different molecular arrangement in the outermost two layers.[7] Importance of *p*H can readily be recognized when we consider the fact that calcium or barium content in the stearic acid monolayer which appreciably affects the wettability of stearic acid surface[2] is chiefly determined by *p*H.[8]

Table 3

Wettability of *Y*-film and *X*-film of Ba- or Ca-stearate

Substrate, $BaCl_2$ 2×10^{-4} mol., *p*H 6.8 (*Y*-film), *p*H 9.8 (*X*-film), 10°C

	θ_a	θ_r
15*Y*	46°	8°
15*Y*+1*X*	117	81
17*Y*	107	25
15*Y*+2*X*	114	86
15*Y*+3*X*	112	89
19*Y*	115	82
15*Y*+4*X*	117	91

Substrate, $Ca(NO_3)_2$ 10^{-4} mol., *p*H 6.8 (*Y*-film), *p*H 9.6 (*Y'*- and *X*-films), 10°C

	θ_a	θ_r
15*Y*	114°	71°
15*Y*+1*X*	118	72
15*Y*+2*X*	118	80
15*Y*+3*X*	116	79
15*Y*+4*X*	113	90
15*Y*+2*Y'*	117	75
15*Y*+4*Y'*	112	77
15*Y*+10*Y'*	114	78
15*Y*+20*Y'*	114	84
15*Y*+28*Y'*	115	80
15*Y*+30*Y'*	116	82

d. Wettability and the Nature of Substrate Cations.—Stearic acid films were built up from redistilled water (*p*H 4.2~4.5), 10^{-4} mol. Al-substrate (*p*H 5.0), 10^{-3} mol. Ba-substrate (*p*H 10.5), and 10^{-3} mol. Hg-substrate (*p*H 8.8), on 29 *Y*-layers of barium stearate which was built up from Ba-substrate of *p*H 7.0. These *p*H values bracketed are those of optimum conditions for the interaction between stearic acid monolayer and metallic cations specified.[2],[3],[4] The author selected barium and aluminum, because they were typical of the group (II) and (III) mentioned above. Mercuric ion was selected for the sake of its exceptional behavior, that it formed a non-wettable product with solidified stearic acid in spite of its co-ordination tendency,[2] and elasticity of mercuric stearate monolayer.[3] Ions classified in group (I) are known to form no condensed monolayer with stearic acid and we were able to obtain no built-up film of first group metal stearate. A monolayer of stearic acid itself could not be built up directly on glass, but could be built up on the basis of barium stearate built-up film as *Y*-layer. Monolayer of barium stearate was built up as *Y*-layer and aluminum stearate as *B*-layer. The monolayer of aluminum stearate on water showed remarkable elasticity[3] and could not be built up under the piston pressure of oleic acid. Therefore it was built up with the aid of a drop of benzene solution of stearic acid placed near the glass rod as practised by Muramatsu.[4] The monolayer of mercuric stearate was not so elastic at first that it could be built up as *Y*-layer or sometimes as *X*-layer by oleic acid as a piston oil; however, the monolayer soon became elastic and it could not be built up as *Y*-layer or *X*-layer. It could be built up as *A*- or *B*-layer with the pressure of benzene solution of stearic acid placed near the rod. The built-up films thus obtained were hydrophobic, but their wettability was affected by dipping in water of *p*H about 6. The relation between wettability and dipping time are shown in Figs. 1a~4a. After withdrawing, the films were kept over $CaCl_2$ for about twenty hours and then dipped again in the water. The results of the second dipping are shown in Figs. 2b~ 4b.

e. Wettability and After Treatment of Stearic Acid Built-up Film with Various Metallic Cations.—Stearic acid films built up from distilled water (*p*H 4.2~4.5) were treated with 10^{-3} mol. barium salt solution (*p*H 11), 10^{-4} mol. aluminum salt solution (*p*H 5.0), and 10^{-3} mol. mercuric salt solution (*p*H 8.8), and the wettability of the treated surface against the same solutions were observed. The results are shown in Figs. 5a~7a. After treating, the films were kept in a desiccator containing $CaCl_2$ for about twenty hours and

(6) J. J. Bikerman, *Proc. Roy. Soc.* (*London*), **A 170**, 130 (1939).
(7) E. F. Porter and J. Wyman Jr., *J. Am. Chem. Soc.*, **58**, 1083 (1938).
(8) I. Langmuir and V. J. Schaefer, *J. Am. Chem. Soc.*, **58**, 284 (1936).

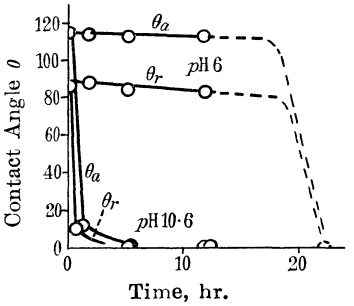

Fig. 1a.—Wettability of 29 *Y* mixed Ba-St+ 10 *Y* H-St, being treated with water of *p*H 6 and 10.6.

again they were dipped into the water. The results of the second dipping are shown in Figs. 5b~7b.

Discussion

The built-up film of stearic acid was hydrophobic even after immersion for ten hours (Fig. 1a). The fact is the same with the case of stearic acid solidified in air.[2] However, the former was detached or dissolved from the glass surface after prolonged dipping. The dissolution phenomenon was remarkable in the alkaline region as shown in Fig. 1a, which

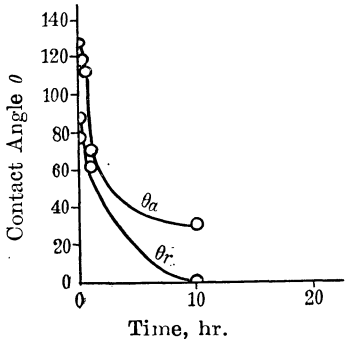

Fig. 2a.—Wettability of 29 *Y* mixed Ba-St+ 10X Ba-St being treated with water of *p*H 6.

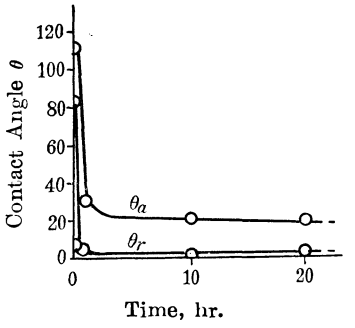

Fig. 2b.—Retreatment after drying of sample of 2a with water of *p*H 6.

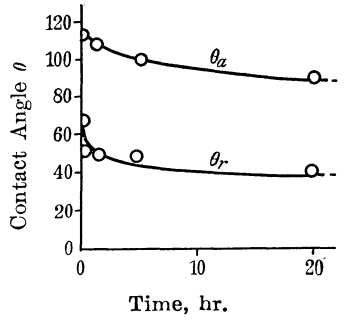

Fig. 3a.—Wettability of 29 *Y* mixed Ba-St+ 1 *B* Al-St, being treated with water of *p*H 6.

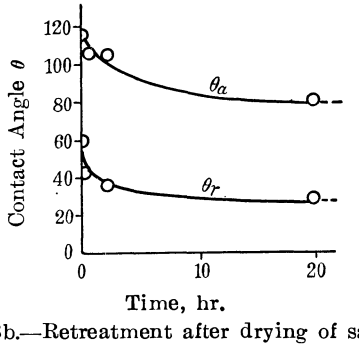

Fig. 3b.—Retreatment after drying of sample of 3a with water of *p*H 6.

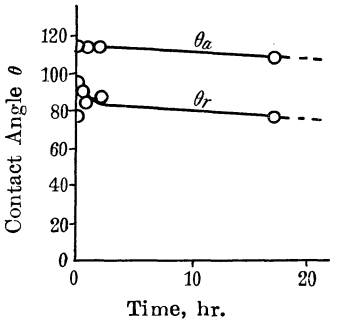

Fig. 4a.—Wettability of 29 *Y* mixed Ba-St+ 1 *B* Hg-St, being treated with water of *p*H 6.

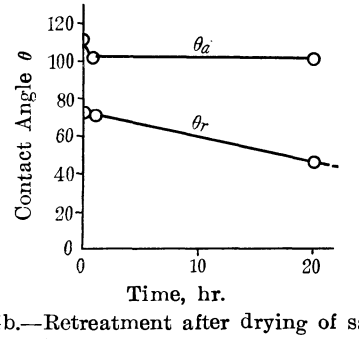

Fig. 4b.—Retreatment after drying of sample of 4a with water of *p*H 6.

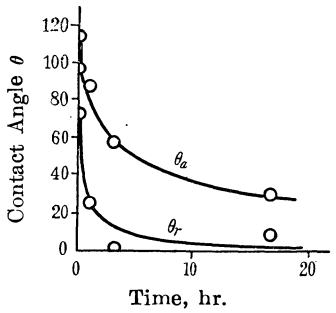

Fig. 5a.—Wettability of 29 Y mixed Ba-St+ 10 Y H-St towards 10^{-3} mol. Ba^{++} (pH 10.5).

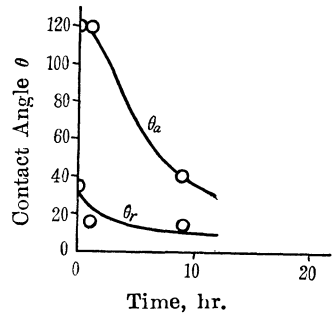

Fig. 5b.—Retreatment after drying of sample of 5a with water (pH 6).

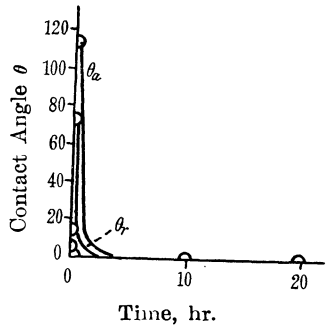

Fig. 6a.—Wettability of 29 Y mixed Ba-St+ 10 Y H-St towards 10^{-4} mol. Al^{+++} (pH 5).

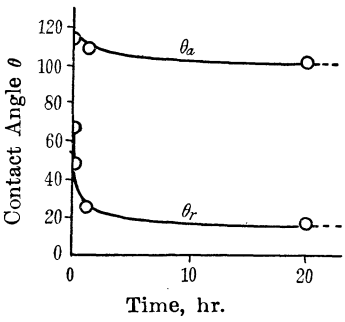

Fig. 6b.—Retreatment after drying of sample of 6a with water (pH 6).

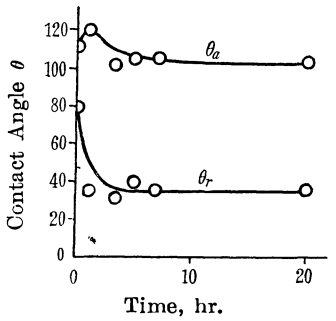

Fig. 7a.—Wettability of 29 Y mixed Ba-St+ 10 Y H-St towards 10^{-3} mol. Hg^{++} (pH 8.8).

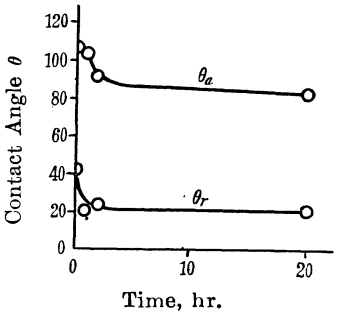

Fig. 7b.—Retreatment after drying of sample of 7a with water (pH 6).

was similar to the case of bulk surface previously reported.[2] A remarkably large wetting hysteresis hereby encountered may possibly be attributed to the considerable difference in the wetting properties on both sides of the outermost oriented monolayer.

In the case of barium stearate built-up film (ion of the type III), there was not such a detachment and the film became hydrophilic. This may be attributed to the orientation of barium stearate molecules in the surface, which may be not so hydrophilic and soluble as free acid, perhaps due to a weaker dissociation of barium bond. The surface of stearic acid built-up film treated with barium salt solution is also considered to be in a similar state as that of barium stearate built-up film. Here, however, the easiness of orientation should be assumed. The results shown in Figs. 2a, 2b, 5a, and 5b can be explained similarly.

B-layer of aluminum stearate (ion of the type II) was hydrophobic (Fig. 3a). Its θ_a value was large, showing a little decrease after prolonged treatment with water, while θ_r was rather small and practically constant after an initial rapid decrease by treatment with water. Moreover, only one B-layer of aluminum stearate on bare glass showed similar

properties. B-layer of aluminum stearate is considered to have a complex structure as described in the fifth report.[2]

Wolstenholme and Schulman[9] obtained the results that a monolayer of myristic acid was in an expanded state on the distilled water containing no metallic ion except for sodium, while it condensed and exhibited high rigidity on the solution containing aluminum, cobaltous, ferric ions etc. They explained their results under the assumption that basic metal ion forms a large network structure in the range of pH proper to that ion. Their explanation is similar to ours in that metallic ion and stearic acid combine in a complex manner and that the extended network is produced. But we are rather inclined to the non-stoichiometric composition between metal and stearic acid while they assumed the stoichiometric one. Moreover we pointed out the distinct difference in nature between the ions of (II) and (III) as far as the wettability was concerned,[2] while they arranged them in the order of ease of hydroxide formation.

Anyway, in aluminum stearate B-layer, the network structure of aluminum stearate may prevent the overturning of molecules. Therefore hydrocarbon groups remain to be exposed in the outermost surface of the film, giving a large and unaffected value of θ_a.

In the case of the treatment of stearic acid built-up film with aluminum solution, a loose hydrophilic network may be formed in the outermost surface of the built-up film, making the surface extremely hydrophilic. Therefore both θ_a and θ_r may be small (Fig. 6a). When it is, however, withdrawn from the solution, it may happen that stearate radicals loosely interlocked in the surface, overturn themselves, directing carboxyl groups inside, and then the network forms again firmly as the time elapses. Now the surface may be considered to have similar structure with that of aluminum stearate B-layer. In fact, the results of the present experiment can be accounted for by these considerations (Fig. 6b). Relating to the results of aluminum salt~stearic acid system, an interesting phenomena was also observed for the interaction of octadecyl amine and sodium alginate. In this case, amine monolayer on alginate solution was so rigid that it was difficult to build up amine film even as B-layer. On the other hand, the film of free amine built up at pH 7.5 was remarkably hydrophobic even after prolonged contact with water, but it became hydrophilic by treating it with sodium alginate solution, which finally dissolved amine into the solution. Similar experiments were conducted by Muramatsu and Sasaki.[10]

B-layer of mercuric stearate behaved similarly as that of aluminum stearate. However, treatment of stearic acid built-up film with mercuric salt solution was different from the corresponding case for aluminum. They rather had resemblance in behavior to B-layer of mercuric stearate treated with water. This may be explained as follows. The network formation in this case is delayed and the overturning of the mercuric stearate molecules precedes already in the solution. Mercuric stearate molecules thus overturned gradually interlock and give a surface just like B-layer of aluminum stearate. Thus it can be reasonably understood that the film behaves similarly to barium initially but is essentially different from it as shown in Fig. 7a and 7b. The film also showed larger resistance against the treatment with an aluminum salt solution like aluminum stearate than the barium stearate film.

It is noticed that the treatment of solidified stearic acid surface with metallic salt solutions reported in the preceding paper,[2] gave a little different results from those of the stearic acid built-up film. The difference may be attributed to the difference in molecular arrangement between the two cases.

Summary

1. Wettability of mixed built-up film of stearic acid and barium or calcium stearate decreased with the number of layers, the advancing contact angle tending to the value of about 115°. The difference between θ_a and θ_r of built-up film was larger than that of solidified surface.

2. X-film and Y-film of barium or calcium stearate prepared occasionally at almost the same condition showed the same wettability. Increase of barium or calcium content in the film was considered to result in the wettability decrease.

3. Of the three types of metallic ion classified according to the influence on wettability of stearic acid, the following two were studied precisely.

(a) Ions of the type III, forming relatively simple stoichiometric compound with stearic acid, the stearates being able to overturn themselves easily in the surface, and the

(9) G. A. Wolstenholme and J. H. Schulman, *Trans. Faraday Soc.*, **46**, 475 (1950).

(10) M. Muramatsu and T. Sasaki, to be published in a near future.

wettability changing with the condition. (Ba, Ca)

(b) Ions of the type II, forming a network of a complex structure with stearic acid, which overturn themselves with difficulty in the surface and their wettability does not change with the condition.

II—1. Ions, rapidly forming network and render the surface hydrophilic tempolarily. (Al, Cu)

II—2. Ions, slowly forming network and rendering the surface hydrophobic (Hg).

The author wishes to express her thanks to Prof. T. Sasaki for his valuable suggestion, Mr. M. Muramatsu for his kind advice, and also to Miss. S. Miyazaki for her assistance throughout this work. The author thanks the Ministry of Education for the grant given to Prof. Sasaki, which enabled this work.

Department of Chemistry, Faculty of Science, Kyushu University, Fukuoka

The Effect of the Substituents (Alkyl-groups) on the Thermal Dissociation of Carbaminic Acid Esters

By Teruaki MUKAIYAMA, Shinichi MOTOKI and Yasushi HAMADA

(Received June 4, 1952)

Introduction

The kinetics of the thermal dissociation of urea[1],[2] and carbaminic acid ester[3] in fatty acid have already been reported. On heating, these compounds dissociate, respectively, to isocyanate and amine, and to isocyanate and alcohol.

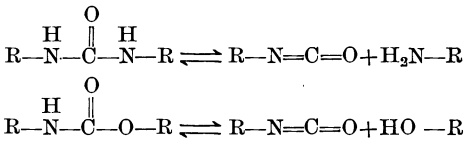

When the ester is heated in fatty acid, the dissociated isocyanate reacts with the solvent acid and forms carbaminic acid-fatty acid-anhydride, which easily decomposes to acylated amine and carbon dioxide.

In the previous reports, it has been shown that the dissociation process is the rate-determining step and the rate can be measured by determining the amount of carbon dioxide evolved during the reaction.

In the present work, the effects of substituents (alkyl-groups) on the thermal dissociation of

(1) T. Hoshino, T. Mukaiyama and H. Hoshino, *J. Am. Chem. Soc.*, **74**, 3097 (1952).
(2) T. Hoshino, T. Mukaiyama and H. Hoshino, This Bulletin, **25**, 392 (1952).
(3) T. Hoshino, T. Mukaiyama and H. Hoshino, ibid. **25**, 396 (1952).

carbaminic acid esters were studied.

The dissociation of the esters may be considered to proceed by a intramolecular proton transfer. On the consideration, when the rates of dissociation of phenyl-carbaminic acid alkylesters (ϕ—N(H)—C(=O)—OR) are measured, the relative rates denote the ability of —OR groups as proton acceptors and when that of alkylcarbaminic acid phenylester (R—N(H)—C(=O)—O—ϕ) are measured, the relative rates denote the ability of R—N(H)—C(=O)— groups as proton donors.

The addition reactions of alcohols to isocyanate, the reversal of the dissociation reaction, have been investigated kinetically.[4],[5],[6],[7]

$$\phi\text{—N=C=O} + \text{R—O H} \longrightarrow \phi\text{—N(H)—C(=O)—O—R}$$

The rates of the reaction have the following order.

$$\text{R= Me} > \text{Et} > \text{isoPr} \gg \textit{tert}\text{-Bu}$$

In the reaction of alkyl-groups, the rate depends on whether the reactant is a primary, secondary, or tertiary alkyl-group. On the experimental facts, the rates of the thermal dissociation of phenylcarbaminic acid-methylester, -isopropylester and -*tert* butylester were determined. The rates showed the following order.

$$\textit{tert}\ \text{Bu} \gg \text{isoPr} \geq \text{Me}$$

The rates of the thermal dissociation of acetyl-, methyl- and isopropylcarbaminic acid phenylester were determined and they showed the following order.

$$\text{Acetyl} \gg \text{isoPr} > \text{Me}$$

Several fatty acids were used as the solvent and the effect of the solvent on the dissociation of ester were studied.

Experimental Part

A 35 ml. long-necked, round-bottomed flask was connected to a gas buret by means of a capillary tube. Halfway along the capillary tube, a 10 ml. bulb was inserted and this was maintained at 0° to condense the reaction product less volatile than carbon dioxide. Prior to the experiment, carbon dioxide gas was passed through the acid contained in the flask for thirty minutes. By the treatment, carbon dioxide evolved during the reaction can be measured thoroughly. However, there was found a minor difference depending upon whether carbon dioxide was previously absorbed in the solvent acid or not. Then a sealed ampoule containing a sample was inserted and the ampoule was broken for the reaction. The reaction vessel was maintained at a desired, constant temperature by immersion into the vapors above a suitable boiling liquid contained in a three-necked flask equipped with condenser and thermometer; the reaction vessel was inserted in the centre neck of the flask. Vapors of the following liquids were used as heating agent: water, xylene, anisole, cyclohexanole and aniline. During the course of an experiment the temperature remained satisfactorily constant.

Phenylcarbaminic acid methylester,[8] m. p. 47°, recrystallized from petroleum ether.

Phenylcarbaminic acid isopropylester,[9] m. p. 86°, recrystallized from 50% ethanol-water solution.

Phenylcarbaminic acid *tert* butylester,[10] m. p. 136°, recrystallized from 50% ethanol-water solution.

Methylcarbaminic acid phenylester was prepared from methylisocyanate and phenol according to the procedure similar ot that described by R. Leuckart.[11] Recrystallized from petroleum ether, m. p. 83°.

Anal. Calcd for $C_8H_9N_1O_2$: N, 9.27
Found N, 8.91%

Isopropylcarbaminic acid phenylester was prepared from isopropylisocyanate and phenol by the same method as described in methylcarbaminic acid phenylester, recrystallized from petroleum ether, m. p. 85°.

Anal. Calcd for $C_{10}H_{13}N_1O_2$: N, 7.82
Found N, 7.77%

Acetylcarbaminic acid phenylester,[12] m. p. 117°, recrystallized from 50% ethanol-water solution.

Monochloroacetic acid, isovaleric acid and propionic acid were distilled twice. Caproic acid and α-chloro isocaproic acid were purified by vacuum distillation.

The ratio of ester to fatty acid was 1 mole: 100 moles.

The rate constants were computed by the same

(4) Tenney L. Davis and James McC. Farnum, *J. Am. Chem. Soc.*, **56**, 883 (1934).
(5) Baker and Holdsworth, *J. Chem. Soc.*, **1947**, 713.
(6) John W. Baker and J. Gaunt, *J. Chem. Soc.*, **1949** 9, 19, 24, 27.
(7) Elizabeth Dyer, Hugh A. Taylor, Shirley J. Mason and Jan Samson, *J. Am. Chem. Soc.*, **71**. 4106 (1949).
(8) A. W. Hofmann, *A.*, **74**, 17; *Ber.*, **3**, 651.
(9) Franz Gumpert, *J. Pr.*, **32**, 279. (1885).
(10) E. Knoevenagel, A., 297, 148. (1897).
(11) R. Leuckart, *J. Pr.*, **41**, 318 (1889).
(12) Otto C. Billeter, *Ber.*, **36**, 3216 (1903).

method as described in the previous report.[2] For example, the experiment gave the following result, calculated with the value of $t=7$ min.

Table 1

Thermal Dissociation of Phenylcarbaminic Acid *t*-Butylester in Caproic Acid at 180.5°

Time (min.)	CO_2 evolved (cc.)	Time (min.)	CO_2 evolved (cc.)	ΔY
2.5	13.3	9.5	53.9	40.6
3.0	17.9	10.0	55.4	37.5
3.5	22.5	10.5	57.2	34.7
4.0	26.7	11.0	59.0	32.3
4.5	29.3	11.5	60.6	31.3
5.0	32.5	12.0	62.0	29.5
5.5	36.0	12.5	63.2	27.2
6.0	38.4	13.0	64.4	26.0
6.5	41.0	13.5	65.3	24.3
7.0	43.3	14.0	66.2	22.9
7.5	45.9	14.5	66.9	21.0
8.0	48.2	15.0	67.6	19.4
8.5	50.4	15.5	68.5	18.1
9.0	52.2	16.0	69.0	16.8

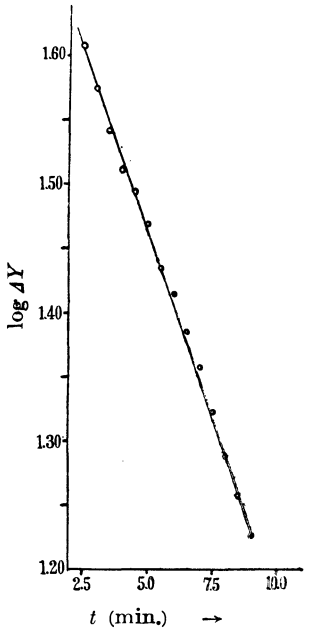

Fig. 1.—Thermal dissociation of phenylcarbaminic acid *t*-butylester in caproic acid at 180.5°. The plot of log Y against t.

First-order kinetics with respect to ester were observed. The results of the rate studied are summarized in Table 2 and 3.

Discussion

On the experimental results, it can be concluded that carbaminic acid esters dissociate to isocyanate and alcohol by the proton transfer. Whether it proceeds by a tautomerization as described in the previous report or by a catalytic action of the solvent acid, the transition state can be considered as the state (a). The (a) shows a loose state of bond between oxygen and carbon according to the transferring proton from nitrogen, forming a new bond with oxygen.

Table 2

The Rate Constants of the Thermal Dissociation of Phenylcarbaminic Acid Alkylesters in Fatty Acids

Ester	Rate const. ($min.^{-1}$)	Temp. (C°)	Solvent
-*tert*-butyl	1.35×10^{-1}	180.5	caproic acid
	2.60×10^{-1}	138.7	α-chloroisocaproic acid
	1.93×10^{-1}	99.9	monochloroacetic acid
-isopropyl	2.48×10^{-2}	181.0	caproic acid
	4.88×10^{-3}	159.1	α-chloroisocaproic acid
	5.87×10^{-2}	181.0	monochloroacetic acid
-methyl	1.84×10^{-2}	181.0	caproic acid
	6.90×10^{-3}	159.0	α-chloroisocaproic acid
	3.22×10^{-2}	181.4	monochloroacetic acid

Table 3

The Rate Constants of the Thermal Dissociation of Alkylcarbaminic Acid Phenylester in Fatty Acids

Ester	Rate const. ($min.^{-1}$)	Temp. (C°)	Solvent
acetyl-	1.25×10^{-1}	137.6	caproic acid
	1.51×10^{-1}	138.9	propionic acid
	1.46×10^{-1}	139.1	isovaleric acid
isopropyl-	2.58×10^{-2}	153.7	caproic acid
	2.18×10^{-2}	153.7	α-chloroisocaproic acid
	9.20×10^{-3}	138.7	propionic acid
	3.05×10^{-2}	153.7	isovaleric acid
methyl-	4.74×10^{-3}	153.7	α-chloroisocaproic acid
	6.17×10^{-3}	153.7	caproic acid
	2.86×10^{-3}	138.3	propionic acid
	6.96×10^{-3}	153.4	isovaleric acid

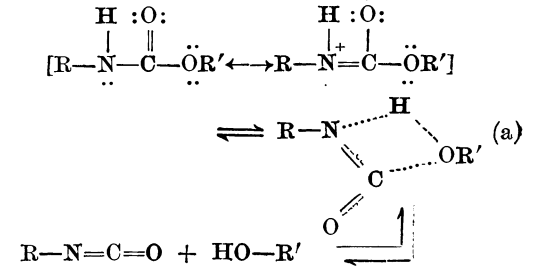

In case of phenylcarbaminic acid alkylesters, the relative rates are shown in the table 4.

Table 4

Relative Rates of the Thermal Dissociation of Phenylcarbaminic Acid Alkylester in Fatty Acids

Solvent	Ester		
	-methyl	-isopropyl	*tert*-butyl
Caproic acid (at 181°)	1	1.3	7.3
α-Chloroisocaproic acid (at 159°)	1	0.7	very large
Monochloroacetic acid (at 181°)	1	1.8	very large

These results will be explained by using the terms chemical driving force and chemical inertia introduced by Evans and Polanyi.[13] The energy of formation of the new molecule is to a certain extent utilized in disrupting the old one. In the case of phenylcarbaminic acid alkylesters, the chemical driving force necessary for the rupture of the ester linkage may be attributed to the formation of the alcohol. The chemical driving force of esters may be orderized as follows.

$$tert\text{-Bu} > \text{isoPr} > \text{Me}$$

By chemical inertia is meant the work that must be done to produce reaction. In this case, it is contributed to the work in breaking the C—O linkage and to that in overcoming the interference action against the transferring proton from nitrogen to oxygen. In these esters, there are few differences in the former effect and the chemical inertia will be controlled by the latter effect. By the inductive effect of the alkyl- groups, it will be orderized as follows:

$$\text{Me} > \text{isoPr} > tert\text{-Bu}$$

The difference between the chemical inertia and the chemical driving force is the necessary patentialenergy of activation. By the consideration, it will be concluded that the activation energy of esters will be in the following order.

$$\text{Me} > \text{isoPr} > tert\text{-Bu}$$

The tendency agrees with the relative rates of the dissociation of esters determined experimentally.

As the rate of reaction is dependent on the entropy of activation and the activation energy, the entropy term must be involved. The potential energy term, however, will be dominative in the thermal dissociation of phenylcarbaminic acid alkylesters.

In case of alkylcarbaminic acid phenylesters, the relative rates are shown in Table 5.

Table 5

Relative Rates of the Thermal Dissociation of Alkylcarbaminic Acid Phenylester in Fatty Acids

Solvent	Ester		
	methyl-	isopropyl-	acetyl-
Caproic acid (at 153°)	1	4.1	very large
Propionic acid (at 138°)	1	3.2	52.8
α-Chloroisocaproic acid (at 153°)	1	4.8	
Isovaleric acid (at 153°)	1	4.3	very large

By the same consideration as in the case of phenylcarbaminic acid alkylesters, the inductive effect of alkyl-group leads to the conclusion that transferring the proton from the nitrogen will be made more easily in methylcarbaminic acid phenylester than in isopropylcarbaminic acid phenylester, which shows that the former ester dissociates more easily than the latter one. The experimental results show, however, that isopropylcarbaminic acid phenylester dissociates faster than methylcarbaminic acid phenylester does. In the isopropylcarbaminic acid phenylester the consideration of the molecular models suggests that the isopropyl-group attached to nitrogen becomes closer to the hydrogen attached to the same nitrogen than the methyl-group in the methylcarbaminic acid phenylester. And according to the steric hindrance, the two hydrogen atoms repel each other. Therefore, the hydrogen attached to nitrogen becomes more active. In this case, the rate seems to be attributed to the steric effect of the substituent group and this will mean that the entropy term may be dominative in the rate factors.

Acetylcarbaminic acid phenylester

$$CH_3-\overset{\overset{O}{\|}}{C}-\overset{\overset{H}{|}}{N}-\overset{\overset{O}{\|}}{C}-O\phi$$

dissociates faster than isopropylcarbaminic acid phenylester does. In the former ester, by the resonance effect of the carbonylgroups of the R—C=O and COOφ, the intervening nitrogen aquires a positive potential. Therefore, the proton attached to nitrogen has more tendency to transfer. The phenomenon will make the reaction proceed quickly.

The thermal dissociation of carbaminic acid

(13) Reviewed by Evans and Polanyi, *Trans. Farad. Soc.*, **34**, 11 (1938).

esters depends on the nature of the solvent acid. In the esters, as shown in the urea linkage, a qualitative relationship was found between the rate constant and the dielectric constant of the solvent acid.

Summary

The rate constants of the thermal dissociation of carbaminic acid esters in fatty acids were determined. In the case of phenylcarbaminic acid alkylestees, the rates showed the following order. *tert*-Bu≫isoPr≧Me
The relative rates may be considered to denote the ability of —OR groups as proton acceptors and the results of the experiment can be explained by the inductive effect of the substituted alkyl-groups.

In the case of alkylcarbaminic acid phenylesters, the rates showed the following order. Acetyl≫isoPr>Me
The relative rates may be considered to denote the ability of R—N(H)—C(=O)— groups as proton donors. In acetylcarbaminic acid phenylester, because of the resonance effect of the R—C(=O)— and COOR groups, the intervening nitrogen aquires a positive potential. The phenomenon will make the hydrogen attached to nitrogen have more tendency to transfer, hence the reaction. That isopropylcarbaminic acid phenylester dissociates faster than methylcarbaminic acid phenylester will be explained by the steric effect of alkyl-groups.

The rates of the thermal dissociation of esters depend on the nature of the solvent acids.

The authors are indebted to Prof. Toshio Hoshino for suggesting this problem and giving valuable advice during the course of the work.

Laboratory of Organic Chemistry,
Tokyo Institute of Technology, Tokyo

Walden Inversion of Amino Acids. VII. The Formation of N-*p*-Toluenesulfonylproline from N^{δ}-*p*-Toluenesulfonylornithine[1]

By Nobuo IZUMIYA

(Received June 16, 1952)

Formation of proline by the reaction of ammonia on δ-nitroguanidylamino-α-bromovaleric acid prepared by the action of nitrosyl bromide on nitroarginine was distinctly shown on a paper chromatogram.[2] The author has assumed for explanation of the phenomenon that the formation of N-nitroguanidylproline had occurred after the splitting-off of hydrogen bromide from α-bromine atom and δ-imino hydrogen atom, and the subsequent hydrolysis of the N-nitroguanidyl group took place. By the amination of δ-benzoylamino-α-bromovaleric acid, only N^{δ}-benzoylornithine was obtained, and there was no formation of N-benzoylproline.[3] Therefore, it may be concluded that the degree of formation of a pyrolidinyl ring depends upon the degree to which the functional group combined with the δ-amino group activates the δ-imino hydrogen atom.

It is well known that the toluenesulfonyl group activates the imino hydrogen atom belonging to the same group on a compound which has the toluenesulfonylamino group. In the present paper, the formation of N-*p*-toluenesulfonylproline was practically occurred in the case of the reaction of ammonia and methylamine on [L]-δ-*p*-toluenesulfonylamino-α-bromovaleric acid, and the configurations of resulting N-*p*-toluenesulfonylprolines were studied comparing with the specific rotation of N-*p*-toluenesulfonyl-L-proline. The reactions were carried out as follows:

(1) The present paper was read at the 5th Annual Meeting of the Chemical Society of Japan, April 4, 1952, Tokyo.

(2) N. Izumiya, unpublished.

(3) N. Izumiya, *J. Chem. Soc. Japan, Pure Chem. Sect.*, **72**, 149 (1951).

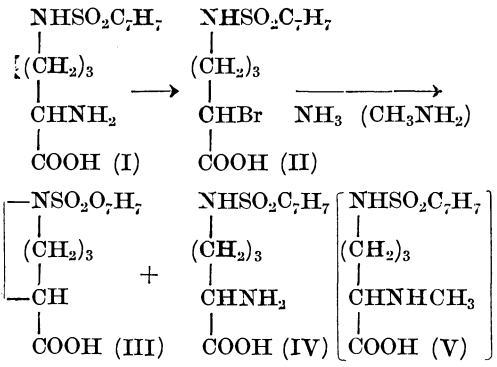

By the amination at 0° of [L]-δ-*p*-toluenesulfonylamino-α-bromovaleric acid (II), N-*p*-toluenesulfonylproline (m. p. 129—132°, D:DL=11:89) was obtained in a good yield and N^{δ}-*p*-toluenesulfonylornithine (IV) was detected by paper chromatography. The amination of (II) at 100°, gave the compound (III) (m. p. 130—133°, pure DL-form) in a good yield, and the compound (IV) in a small quantity. The methylamination at 0° as well as 100° gave the compound (III) (oily state, D:DL=27—31:73—69), and N^{δ}-*p*-toluenesulfonyl-N^{α}-methylornithine (V) which was detectable only by paper chromatography. In order to confirm the configurational ratios of the compounds (III), these were hydrolysed with hydrobromic acid, prolines isolated through rhodanilate, and their specific rotations measured.

Kapfhammer and Eck[4] reported the synthesis of N-*p*-toluenesulfonyl-L-proline (VI) melting at 130—133°, and that it was easily crystallized, while McChesney,[5] however, reported that the substance (VI) could not be crystallized. The specific rotation of (VI) was not given by either of them. In order to find the specific rotation of it, the present author synthesized (VI) in the usual way, and it was not easily crystallizable. After various trials, however, (VI) melting at 41—43° was crystallized, while N-*p*-toluenesulfonyl-DL-proline was easily obtained crystalline and melted at 134°. Hence, Kapfhammer and Eck must have synthesized N-*p*-toluenesulfonyl-DL-proline instead of N-*p*-toluenesulfonyl-L-proline.

The author had supposed that there was some difference in the mechanism of reaction between amination or methylamination on δ-*p*-toluenesulfonylamino-α-bromovaleric acid (II) and that on δ-benzoylamino-α-bromovaleric acid (VII). So that, the splitting-off velocity of bromine ion was measured under various conditions, but no difference in the velocity was observed between (II) and (VII).

(4) J. Kapfhammer and E. Eck, *Z. physiol. Chem.*, **170**, 294 (1927).
(5) E. W. McChesney, *J. Am. Chem. Soc.*, **59**, 1116 (1937).

Experimental

N-*p*-Toluenesulfonyl-DL-proline.—DL-Proline[6] (0.01 mol.), *p*-toluenesulfonyl chloride (0.014 mol.) and 2N-sodium hydroxide (0.03 mol.) were made to react in the usual way.[7] The solution was acidified with hydrochloric acid, and the oily substance formed was crystallized immediately (m. p. 130—133°). This was recrystallized twice from 40% alcohol. m. p. 134°, rhombic plates. Found: N, 5.10%; neut. equiv., 273. Calcd. for $C_{12}H_{15}O_4NS$: N, 5.19%; neut. equiv., 270.3.

N-*p*-Toluenesulfonyl-L-proline.—L-Proline (0.01 mol), having $[\alpha]_D^{19}=-84.6°$ (c=2.55, water), *p*-toluenesulfonyl chloride (0.01 mol., recrystallized twice from acetone-water) and 2N-sodium hydroxide (0.02 mol.) were made to react. The oil produced by the addition of hydrochloric acid was extracted with chloroform. The chloroform solution was washed with water, and reextracted with aqueous sodium bicarbonate. It was acidified with hydrochloric acid, and the resulting oil was allowed to stand in an ice box for 1 to 2 days, and crystallized in needles (m. p. 39—42°). The extraction with chloroform and sodium bicarbonate and the addition of hydrochloric acid were repeated. m. p. 41—43° (reported m. p. 130—133°,[4] oily state[5]), $[\alpha]_D^{19}=-158.5°$ (c=2.21, 2 equivs. of NaOH) and $[\alpha]_D^{19}=-92.5°$ (c=1.78, alcohol). Found: N, 5.14%; neut. equiv., 276. Calcd: N, 5.19%; neut. equiv., 270.3.

N^{δ}-*p*-Toluenesulfonyl-L-ornithine(I).—This was prepared by applying Kurtz's procedure[8] from L-ornithine monohydrochloride. m. p. 236—238° (decomp.) (reported m. p. 210—215°[9]), $[\alpha]_D^{20}=+14.9°$ (c=2.23, 2 equivs. of HCl) and $[\alpha]_D^{20}=+23.4°$ (c=1.85, 3N-HCl). The regenerate copper complex melted at 240—242° with decomposition. Found: N, 8.71%. Calcd. for $(C_{12}H_{17}N_2O_4S)_2Cu$: N, 8.83%.

[L]-δ-*p*-Toluenesulfonylamino-α-bromovaleric acid (II).—(I) (0.01 mol) and potassium bromide (0.035 mol) were dissolved in 2.5N-sulfuric acid (0.052 mol). To the mixture was added sodium nitrite (0.016 mol) in portions during 1 hour with stirring at ice cooling, and the stirring was continued thereafter for 2 hours at room temperature. The resulting pale yellow oil was washed with water by decantation until bromine ion became undetectable. It was then dried in a vacuum desiccator. The yield was 95%. $[\alpha]_D^{15}=-35.2°$ (c=3.05, alcohol). Found: N, 4.14%. Calcd. for $C_{12}H_{16}NO_4SBr$: N, 4.00%. Though the dried substance and the alcoholic solution were allowed to stand at room temperature (10—20°) for 2 weeks, there was no change in their specific rotation.

Amination of (II) at 100°.—(II) (3.50 g.) was

(6) D. Hamer and J. P. Greenstein, *J. Biol. Chem.*, **193**, 81 (1951).
(7) E. Fischer and W. Lipschitz, *Ber.*, **48**, 360 (1915).
(8) A. C. Kurtz, *J. Biol. Chem.*, **180**, 1253 (1949).
(9) H. N. Christensen, *J. Biol. Chem.*, **160**, 75 (1945).

dissolved in 30 cc. of 28% ammonia and heated in a sealed tube at 100° for 20 minutes. The solution was evaporated to dryness under reduced pressure, and the residue was collected by the aid of water, washing it several times with water (the filtrate and washings were to be used in the next step). It crystallized out in small rectangular plates from hydrochloric acid and ammonia, and there was obtained 0.17 g. (yield 6%). This was N^{δ}-*p*-toluenesulfonyl-DL-ornithine, and had m. p. 229-232° (decomp.) and no rotation. Found: N, 9.85%. Calcd. for $C_{12}H_{18}N_2O_4S$: N, 9.79%. Its copper complex had m. p. 244—246° (decomp.). Found: N, 8.68%. Calcd.: N, 8.83%. The filtrate and washings combined were acidified with hydrochloric acid, and the oil formed solidified immediately. This was recrystallized once from 40% alcohol, and obtained 1.95 g. (yield 72%). This was N-*p*-toluenesulfonyl-DL-proline (III), and had m. p. 131—133° and no rotation. Found: neut. equiv., 277. Calcd.: neut. equiv., 270.3. (III) (0.01 mol) was refluxed with 48% hydrobromic acid (30 cc.) for 2 hours. The solution was evaporated under reduced pressure, and the concentration was repeated with the addition of water. The residue was dissolved in water (30 cc.). To the solution was added ammonium rhodanilate (0.008 mol) dissolved in methylalcohol (55 cc.). DL-Proline rhodanilate was obtained 72% yield, and had m. p. 130—133°. DL-Proline was isolated from rhodanilate by Bergmann's method,[10] and had m. p. 202—204° (decomp.) (reported m. p. 203—204°[11]).

Amination of (II) at 0°.—(II) was dissolved in ammonia in the manner described above and kept at 0° for 10 days. N-*p*-Toluenesulfonylproline (III) was obtained in 69% yield, having m. p. 129—132° and $[\alpha]_D^{10} = +17.4°$ (c=2.12, 2 equivs. of NaOH). Found: neut. equiv., 279. Calcd.: neut. equiv., 270.3. It was shown that (III) are composed of approximately 11% D-form and 89% DL-form. In another experiment, (III) had $[\alpha]_D^{10} = +15.5°$ (c=1.98, 2 equivs. of NaOH). From the filtrate of the compound (III), N^{δ}-*p*-toluenesulfonylornithine was detected by a paper chromatography, though its isolation was unsaccessful. Proline was isolated from (III) ($[\alpha]_D^{10} = +17.4°$) in the manner described above, and had $[\alpha]_D^{10} = +8.4°$ (c=1.88, water).

Methylamination of (II) at 100°.—(II) (0.01 mol) was dissolved in 35 cc. of aqueous methylamine (33%) and heated at 100° for 10 minutes. The solution was concentrated under reduced pressure, and the residue was dissolved in water, and acidified with hydrochloric acid. The oily N-*p*-toluenesulfonylproline (III) formed could not be solidified even when it had been allowed to stand in an ice-box for several weeks. This was washed with water by decantation, and dried in a vacuum desiccator. The yield was 77%. It had $[\alpha]_D^{10} = +42.6°$ (c=2.02, 2 equivs. of NaOH), showing it to be a mixture of 27% D-form and 73% DL-form. Found: neut. equiv., 283. Calcd.: neut. equiv., 270.8. Proline isolated had $[\alpha]_D^{10} = +21.6°$ (c=1.85, water). N^{δ}-*p*-Toluenesulfonyl-N^{α}-methylornithine (V) has never been synthesized, so that its *Rf* value on paper chromatogram is unknown. The mother liquid obtained by decantation was tested by paper chromatography, and it showed only one spot of ninhydrine reaction. The *Rf* values of this spot and N^{δ}-*p*-toluenesulfonylornithine in various solvents were compared with *Rf* values of N^{δ}-benzoylornithine and N^{δ}-benzoyl-N^{α}-methylornithine. From the observed regularity, the substance showing a spot of ninhydrine reaction was considered to be the compound (V) which could not be isolated. *Rf* values are shown in Table 1. The composition of each solvent was the same as in Part VI of this Series.[12]

Table 1

Rf values

Amino acid	Solvent: Phenol	Collidine + Lutidine	Acetic Acid + Butanol
N^{δ}-*p*-T. S.-L-ornithine	0.91	0.72	0.71
N^{δ}-*p*-T. S.-N^{α}-methylornithine	0.97	0.77	0.74
N^{δ}-Benz.-L-ornithine	0.94	0.63	0.69
N^{δ}-Benz.-DL-N^{α}-methylornithine	0.98	0.67	0.72

Methylamination of (II) at 0°.—(II) was kept at 0° for 4 days. The oily N-*p*-toluenesulfonylproline had $[\alpha]_D^{10} = +48.3°$ (c=2.08, 2 equivs. of NaOH), showing it to be a mixture of 31% D-form and 69% DL-form. The yield was 81%. Found: neut. equiv., 285. Calcd.: neut. equiv., 270.3. Proline isolated had $[\alpha]_D^{10} = +24.7°$ (c=1.91, water).

Splitting-off Velocity of Bromine Ion from

Table 1

Splitting-off % of Br Ion at 0°

Hours	Compound (II) NH_3	Compound (II) CH_3NH_2	Compound (VII) NH_3	Compound (VII) CH_3NH_2
1		37.0		36.8
2	2.2	50.5	2.3	51.1
4		70.1		71.2
10	11.1	91.5	11.7	90.9
20	23.1	98.3	23.3	98.6
40	45.0	98.6	46.1	98.7
100	77.9		78.8	
200	95.6		95.5	
300	98.5		99.1	

(10) M. Bergmann, *J. Biol. Chem.*, **110**, 471 (1935).
(11) N. F. Albertson and J. L. Fillman, *J. Am. Chem. Soc.*, **71**, 2818 (1949).
(12) N. Izumiya and A. Nagamatsu, This Bulletin, **25**, 265 (1952).

Table 2

Splitting-off % of Br Ion at 100°

Minutes	Compound (II)		Compound (VII)	
	NH_3	CH_3NH_2	NH_3	CH_3NH_2
0.25		78.0		81.4
0.5	60.5	93.3	64.0	91.8
1	81.6	99.1	80.9	100.0
2	92.8	100.1	93.2	99.8
4	98.6	99.9	98.9	100.2
6	99.5		99.7	
10	100.2		99.9	

α-Bromo Acids.—[L]-δ-*p*-Toluenesulfonylamino-α-bromovaleric acid (II) and [L]-δ-benzoylamino-α-bromovaleric acid (VII)[3] were used as α-bromo acids. 0.001 mol. of (II) or (VII) was dissolved in 2.72 cc. of 28% ammonia (0.04 mol.) or in 3.77 cc. of 33% methylamine (0.04 mol.). At adequate intervals at 0° or 100°, to 0.2 cc. of the reaction mixture was added 2 cc. of 0.05 N-silver nitrate (its solvent was 7 N-nitric acid), and 1 cc. of the filtrate was titrated with 0.05 N-thiocyanate solution. The results are shown in Tables 1 and 2.

Summary

(i) Kapfhammer and Eck's report touching the synthesis of N-*p*-toluenesulfonyl-L-proline was corrected.

(ii) N-*p*-Toluenesulfonylproline was resulted by the amination and methylamination of [L]-δ-*p*-toluenesulfonylamino-α-bromovaleric acid. In this case, racemization took place in consequence of amination at 100°, and partial Walden inversions were caused by amination at 0° and methylamination at 0° and 100°.

This work was carried out partly with a grant from the Scientific Research Funds of the Ministry of Education. The author wishes to thank Prof. Dr. R. Hirohata for his guidance in carrying out this work, and also Mr. S. Saeki for his microanalysis of the substances.

Department of Medical Chemistry, Faculty of Medicine, Kyushu University, Fukuoka

On the Mechanism of the Reduction Process of the Hydrogen Ion at the Dropping Mercury Electrode. III. Experimental Part —The Half-wave Potential, Log-plot Analysis and the Reversibility of the Wave

By Reita TAMAMUSHI[1]

(Received June 17, 1952)

While the properties of the limiting current of the hydrogen wave have been discussed in Part II of the present study,[2] the experimental results and the discussion on the half-wave potential of the hydrogen wave, the reversibility of the reduction process of the hydrogen ion and the other properties of the wave are presented in this paper.

Experiments

Apparatus.—Most of the measurements concerning the electrode potential were carried out by the manually operated polarograph,[2] with which the electrode potential of the dropping mercury electrode (D.M.E.) referred to a certain reference electrode can be directly measured without any correction of the iR-drop.

To study the reversibility of the electrode reaction by Kalousek's methods,[3] a photo-recording polarograph with the special circuit for this method was used. By this apparatus all methods presented by Kalousek can be carried out with a simple operation, the details of which are omitted in the present paper.

The assembly of the electrode and the polarographic cell and the materials used were quite the same as described in Part II of the present study.[2]

The system of the dil. HCl in 0.1 N KCl solution was used throughout the following experiments, because, as shown in Part II, we can obtain a typical polarogram of the hydrogen ion in this system.

(1) Present address: Chemistry Department, Faculty of Science, Ochanomizu Women's University, Tokyo.
(2) R. Tamamushi, This Bulletin **25**, 293 (1952).
(3) M. Kalousek, *Collection Czechoslov. Chem. Communs.*, **13**, 105 (1948).

Experimental Results

On the Half-wave Potential and the Log-plot

The Log-plot Analysis of the Reduction Wave—The log-plot, i. e. the relation between $\log I/(I_1-I)$ and the electrode potential, V, is widely used to analyse the form of the current-voltage curve, where I is the current flowing at V and I_1 the limiting current. In the reduction wave of the hydrogen ion in 0.1 N KCl solution, this relation is not linear and an apparent deviation from a straight line appeared at the more negative potential region than the half-wave poteneial as shown in Fig. 1. It must be noted that this deviation

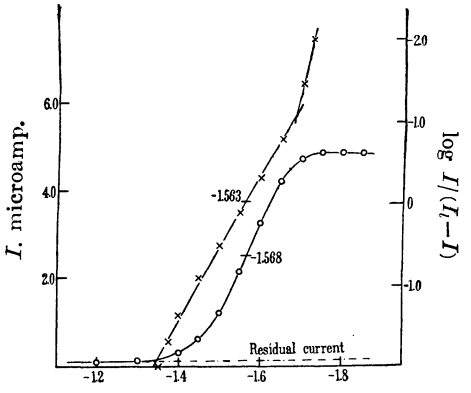

V, volt *vs.* NCE.

Fig. 1.—Polarogram of the hydrogen ion of dil. HCl in 0.1 N KCl solution and the log-plot analysis of the wave. $[C_{H^+}]^\circ = 0.78$ millimole/l.

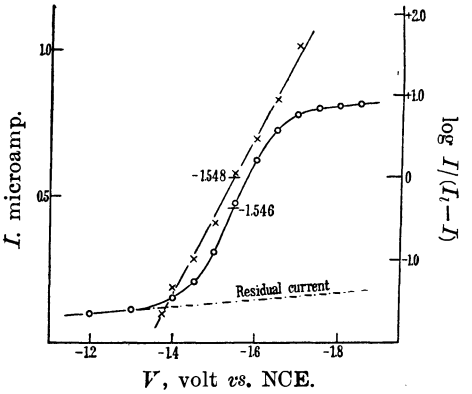

V, volt *vs.* NCE.

Fig. 2.—Polarogram of the hydrogen ion of dil. HCl in 0.1 N KCl solution and the log-plot analysis of the wave. $[C_{H^+}]^\circ = 0.137$ millimole/l.

is not clear when the concentration of the hydrogen ion is less than about 0.5 millimole/l. (Fig. 2). At present, it is not clear whether this tendency in the log-plot of the lower concentration of the hydrogen ion is an essential phenomenon or only due to the inaccuracy of the measurement.

The Relation between the Half-wave Potential and the Concentration of the Hydrogen Ion.—It was found out by the experiment carried out in 0.1 N KCl-dil. HCl system that the half-wave potential, $V_{1/2}$, of the hydrogen wave changes with the change of the concentration of the hydrogen ion in the bulk of the solution, $[C_{H_+}]^\circ$, or I_1 over the concentration range of 0.039 to 1.95 millimole/l. As $[C_{H_+}]^\circ$ or I_1 became larger, $V_{1/2}$ shifted to be more negative. The experimental results are shown in Table 1 and Fig. 3. From these data we can obtain the following

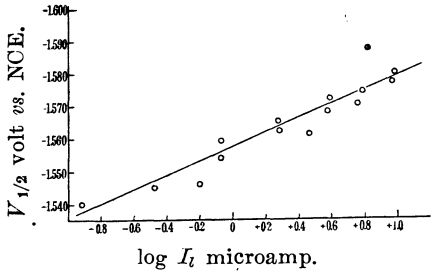

log I_l microamp.

Fig. 3.—The relation between $V_{1/2}$ and log I_l.

relation between $V_{1/2}$ and I_1 by the least square method:

$$V_{1/2} = -1.687 - 0.022 \log I_1 \qquad (1)$$

in which I_1 is represented in amp. and $V_{1/2}$ in volt.

The Effect of the Temperature on $V_{1/2}$.—The value of $V_{1/2}$ became more positive as the temperature, τ, of the cell-solution rose over the temperature range of 0 to 50° as shown in Table 2 and Fig. 4. From these data the absolute temperature coefficient of

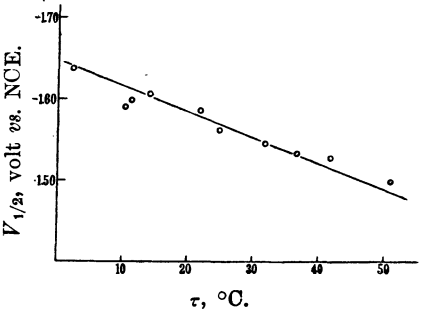

τ, °C.

Fig. 4.—The effect of temperature on $V_{1/2}$. $[C_{H^+}]^\circ = 0.78$ millimole/l.

$V_{1/2}$, $\Delta V_{1/2}/\Delta T$, was obtained to be about 0.003 volt per degree.

The Application of the Kalousek's Methods

In order to examine the reversibility of the electrode process of the hydrogen ion discharge at the D.M.E., the Kalousek's methods—K-I, K-II and K-III—were applied to the solution of 0.52 millimole/l. HCl in 0.1 N KCl solution, the results of which are illustrated in Figs. 5, 6, 7 and 8. The polarograms of the reduction of Pb^{2+} ion in the medinm of KOH solution are also presented in these figures as the typical examples of the application of the Kalousek's methods to a reversible electrode reaction.

It is said that no oxidation current due to the oxidation process of the reduction product of the hydrogen ion at the D.M.E. ever appears in any cases. On the other hand, the apparent oxidation currents appear in the case of the reduction of Pb^{2+} ion in KOH solution.

Discussion

It is shown in Figs. 5~8 that no oxidation current appeared when the Kalousek's methods were applied to the reduction process of the hydrogen ion at the D.M.E. These results exclude the possibility of the existence of any electrochemically active hydrogen species at the surface of the electrode. If the reduction product can be easily oxidized at the potential region of the reduction wave and does not escape from the electrode surface instantaneously, the oxidation current should appear as in the case of Pb^{2+} ion, when the Kalousek's methods are applied. Under this circumstance, it is impossible to assume the reduction mechanism in which the redox process between H^+ and H is kept in a rapid equilibrium and the recombination process is the slowest step. It seems possible to conclude that probably the current-voltage curve of the hydrogen ion obtained in 0.1 N KCl solution at the D.M.E. is a kind of the activation-controlled type.

This conclusion is also confirmed by the relatively large temperature coefficient of the half-wave potential, namely about 0.003 volt per degree, because the temperature coefficient of $V_{1/2}$ expected from the diffusion-controlled type is much smaller than the value mentioned above.(4)

In this paper, the activation-controlled type means the process in which the rate constant of the forward reaction of the redox process is much smaller than that of the diffusion process at the potential region, where the forward rate is nearly equal to the reverse one, and the reverse rate of the redox reaction is negligibly small at the electrode potential where the reduction wave appears. On the other hand, we define the process as the diffusion-controlled type when the rate constant

Fig. 5.—Polarograms of Pb^{2+} ion and H^+ ion: a, Pb^{2+} ion in KOH solution; b, 0.52 millimole HCl—0.1 N KCl.

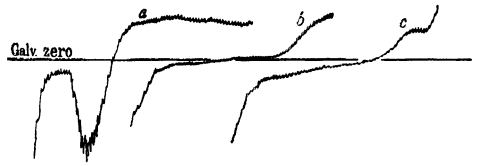

Fig. 6.—Application of the Kalousek's method K-I: a, Pb^{2+} ion in KOH solution, ΔV = 300 mV.; b, 0.52 millimole HCl—0.1 N KCl, ΔV = 100 mV.; c, the same solution as b, ΔV = 300 mV.

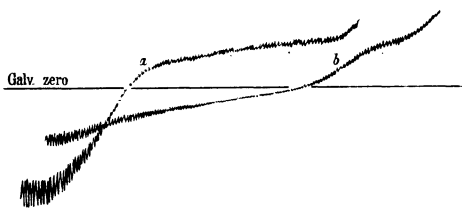

Fig. 7.—Application of the Kalousek's method K-II: a, Pb^{2+} ion in KOH solution, $V_{aux.}$ = −0.8 volt; b, 0.52 millimole HCl—0.1 N KCl, $V_{aux.}$ = −1.9 volts.

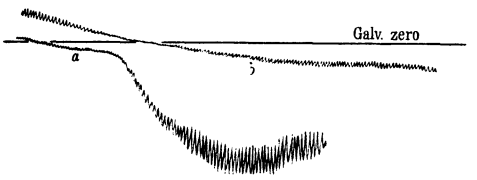

Fig. 8.—Application of the Kalousek's method K-III: a, Pb^{2+} ion in KOH solution, $V_{aux.}$ = 0; b, 0.52 millimole HCl—0.1 N KCl, $V_{aux.}$ = −0.6 volt.

(4) I. M. Kolthoff and J. J. Lingane, "Polarography", Interscience Pub. Inc., New York, N. Y., 1946, p. 153.

of the forward or the reverse reaction of the redox process is much larger than that of the diffusion at the electrode potential where the forward rate is nearly equal to the reverse one. As for the details about these points, the previous papers should be referred.(5)

Now, let us consider the relation between the half-wave potential and the limiting current of the hydrogen ion. It was found out that $V_{1/2}$ tends to be more negative as the limiting current increases as shown by Eq. (1). This result does not agree with those of the previous authors, i.e., J. Tomes(6) reported that the half-wave potential of the hydrogen ion of the diluted solution of HCl in 1 N LiCl or $CaCl_2$ solution becomes to be more positive with the increase of the diffusion current, I_d, according to the relation $\Delta V_{1/2}/\Delta \log I_d = 0.028$ volt, and, quite recently, it was mentioned by J. Kůta(7) that the half-wave potential of the hydrogen ion in the system, HCl or H_2SO_4 in 0.1 N solution of the supporting electrolyte (KCl, KBr, K_2SO_4 and $BaCl_2$), is independent of the concentration of the acid.

Furthermore, as for the log-plot of the current-voltage curve Kůta stated that this relation is a straight line whose tangent is nearly equal to $2RT/F$, while the present author observed the apparent deviation from a straight line, as shown in Fig. 1 over a certain range of the concentration of the hydrogen ion. It must be noted that, although the results on the relation between $V_{1/2}$ and I_d obtained by J. Tomes and by the present author are in considerable contradiction, the same deviation in the log-plot analysis as mentioned above was also observed by Tomes, because he found experimentally the following relation:

$$(V_{1/4}-V_{1/2})-(V_{1/2}-V_{3/4})=+0.006 \text{ volt}$$

in which $V_{1/4}$ and $V_{3/4}$ represent the electrode potentials where $I=1/4\ I_d$ and $I=3/4\ I_d$, respectively. J. Kůta attributed this discrepancy between his results and those of J. Tomes to the possibility of the existence of the maximum of the second kind in 1 N solution of the supporting electrolyte. At any rate, further investigations on the current-voltage curve of the hydrogen ion in the solution of various supporting electrolytes are necessary to make clear these points.

When we consider the results mentioned above, it seems possible to assume the following probable mechanism for the deposition process of the hydrogen ion of the dil. HCl in 0.1 N KCl solution, at the D.M.E.:

$$H^+(\text{surface}) \rightleftharpoons H^+(\text{adsorbed}), \text{ adsorption}$$
$$H^+(\text{adsorbed}) \rightleftharpoons H(\text{surface}), \text{ oxidation-reduction}$$

This means that only the hydrogen ion adsorbed on the electrode surface can be neutralized at the electrode and that the produced hydrogen atom will disappear from the electrode surface by a certain process, e.g., the recombination process giving the hydrogen molecule. It is assumed that there exists an adsorption equilibrium of the Freundlich adsorption isotherm type between H^+ (surface) and H^+ (adsorbed) and that the reduction-oxidation process proceeds under the condition of the activation-controlled type. As in the preceding paper (Part I),(8) let us call this mechanism the "slow discharge mechanism of the adsorbed hydrogen ion." If we consider that the whole process is kept in a dynamic equilibrium, the equations for the current-voltage curve and for the half-wave potential can be represented as follows, according to the derivation carried out in Part I:

$$V = const. - \frac{RT}{\alpha' F}\log\frac{I}{I_l - I} + \frac{RT}{\alpha' F}(\nu-1) \times \log(I_l - I) \quad (2)$$

$$const. = \frac{RT}{\alpha' F}\left(-\frac{\Delta F_1}{RT} + \log\gamma + \log s + \log\frac{kT}{h} + \log F - \nu\log(FK'_{H^+})\right) \quad (2')$$

$$I_1 = FK'_{H^+}[A_{H^+}]^\circ = FK_{H^+}[C_{H^+}]^\circ \quad (3)$$

and

$$V_{1/2} = \text{const}'. + \frac{RT}{\alpha' F}(\nu-1)\log I_l \quad (4)$$

$$const'. = \frac{RT}{\alpha' F}\left(-\frac{\Delta F_1}{RT} + \log\gamma + \log s + \log\frac{kT}{h} + \log F - \nu\log(FK'_{H^+}) - (\nu-1)\log 2\right) \quad (4')$$

in which K_{H^+} and K'_{H^+} are the constants concerning the diffusion process of the hydrogen ion, $[A_{H^+}]^\circ$ the activity of the hydrogen ion in the bulk of the solution, F the Faraday constant, and s a proportional constant which

(5) N. Tanaka and R. Tamamushi, This Bulletin, **22**, 187 (1949); R. Tamamushi and N. Tanaka, ibid., **22**, 227 (1949).

(6) J. Tomes, *Collection Czechoslov. Chem. Communs.*, **9**, 150 (1937).

(7) J. Kůta, *Proc. I. International Polarographic Congress in Prague, Part* I, p. 852 (1951).

(8) R. Tamamushi, This Bulletin, **25**, 287 (1952).

can be represented as follows as an approximation[9]:

$$s \cong q \cdot \mu \cdot 10^{-3} \qquad (5)$$

μ: the thickness of the reaction layer at the electrode surface in cm.
q: the surface area of the dropping mercury electrode in cm^2.

α' is also a proportional constant concerning the distribution of the electrode potential at the vicinity of the electrode surface. The terms ν and γ are constants in the equation for the adsorption equilibrium between H^+ and H_a^+,

$$[A_{Ha}^+] = \gamma [A_H^+]^\nu \exp\left(-\frac{V_a F}{RT}\right)$$

where $[A_{Ha}^+]$ and $[A_H^+]$ mean the equilibrium activities of the hydrogen ion adsorbed on the electrode and at the electrode surface (solution side), respectively, and V_a is the electrical potential difference between the adsorbed state and the solution side.

As ν is generally less than unity, it is quite obvious from Eq. (4) that the half-wave potential shifts to more negative potential as the limiting current increases and this is in accordance with the experimental results obtained by the present author. Moreover, the same tendency in the log-plot analysis of the current-voltage curve, which showed a deviation from a straight line, can be expected from Eq. (2).

The values of the constants, α' and ν, can be obtained from the experimental data on the current-voltage curve by the following method: Eq. (2) is rewritten as follows:

$$-V = a_0 + a_1 A + a_2 B \qquad (6)$$

$$A \equiv \frac{RT}{F}\log\frac{I}{I_l - I}, \quad B \equiv \frac{RT}{F}\log(I_l - I)$$

$$a_1 \equiv \frac{1}{\alpha'}, \quad a_2 \equiv \frac{1-\nu}{\alpha'}, \quad a_0 \equiv const.$$

The values of a_1 and a_2 are obtained by the application of the least square method. It is natural that these values change with the change of the unit of the current as well as the change of the value of the reference electrode to which the electrode potential is referred, if the least square method is applied to Eq. (6). To avoid this effect due to the change of the unit, the least square method was applied to the following equation instead of Eq. (6):

$$\Delta V_i = a_1 \Delta A_i + a_2 \Delta B_i \qquad (7)$$
$$\Delta V_i = -V_{i+1} - (-V_i)$$
$$\Delta A_i = A_{i+1} - A_i$$
$$\Delta B_i = B_{i+1} - B_i$$

From the normal equations of Eq. (7), the next relations are derived:

$$a_1 \sum_i (\Delta A_i)^2 + a_2 \sum_i (\Delta A_i \Delta B_i) - \sum_i (\Delta V_i \Delta A_i) = 0$$
$$a_1 \sum_i (\Delta A_i \Delta B_i) + a_2 \sum_i (\Delta B_i)^2 - \sum_i (\Delta V_i \Delta B_i) = 0$$

from which we can easily calculate α' and ν.

Let us consider the meaning of the constant term, a_0, in Eq. (6) more closely. As shown in Eq. (2'), this constant term involves the free energy of activation of the forward process of the redox reaction, ΔF_1, and the constant γ of the equation of the adsorption equilibrium. According to the theoretical derivation of the Freundlich adsorption isotherm,[10] γ and ν can be represented as follows:

$$\gamma = \exp\left(\frac{f'(T)}{RT} + \frac{1}{i} - 1\right) \qquad (8)$$

$$\nu = \frac{1}{i} \qquad (9)$$

where i is a constant in the equation of state for the adsorbed layer, namely, $FA = iRT$, in which F is the surface pressure and A the surface area. $f'(T)$ is a function of the temperature and can be considered to be equal to the free energy of adsorption, $-\Delta F_a$ (Fig. 1 in Part I). If we ignore the term $\frac{1}{i} - 1$ against $f'(T)/RT$, Eq. (8) is reduced to

$$\gamma = \exp(-\Delta F_a / RT) \qquad (8')$$

From Eps. (2') and (8') the following equation for the constant, a_0, is obtained:

$$a_0 = -\frac{\vec{\Delta F}}{\alpha' F} - \frac{\nu RT}{\alpha' F}\log(FK'_H) + \frac{RT}{\alpha' F}\log F + \frac{RT}{\alpha' F}\log s + \frac{RT}{\alpha' F}\log\frac{kT}{h} \qquad (10)$$

$$\vec{\Delta F} = \Delta F_1 + \Delta F_a$$

where $\vec{\Delta F}$ is the difference of the free energy

(9) R. Brdicka and K. Wiesner, *Collection Czechoslov. Chem. Communs.*, **12**, 138 (1947).

(10) B. Tamamushi, This Bulletin, **9**, 363 (1934).

between the activated state of the redox process, $H^+(adsorbed) \rightleftarrows H(surface)$, and the solution side, S, in Fig. 1 of Part I, and can be considered as the free energy of activation of the overall discharge process of the hydrogen ion, $H^+(solution) \rightarrow H(surface)$. If we assume that FK'_{H^+} is nearly equal to FK_{H^+}, the terms α', ν and FK'_{H^+} in Eq. (10) can be obtained from the experimental data. The constant, s, which is represented by Eq. (5), is also calculated from the experimental results by using the following expression for the mean surface area of the dropping mercury electrode:

$$q=\frac{3}{5}\times 0.85\times m^{2/3}t^{2/3} \quad (\text{cm.}^2) \qquad (11)$$

in which m is the weight of mercury in gram flowing from the capillary per second and t the drop-time of one drop in second. In the present calculation the thickness of the reaction layer at the electrode surface, μ, is assumed to be approximately equal to 10^{-7} cm. according to R. Brdicka.[9] When we use these values and $kT/h=6\times 10^{12}$, $\vec{\Delta F}$ can be calculated from the constant, a_0, obtained from Eq. (6). In this case, the current is expressed in amperes and the value of the electrode potential referred to a normal calomel electrode is employed.

The numerical values of α', ν and $\vec{\Delta F}$ obtained from each current-voltage curve are shown in Tables 1 and 2. The values of α' are in the range of 0.4 to 0.6, however, those of ν diverge over the range of 0.4 to 1.0. When we consider that ν is the exponent in the equation for the adsorption equilibrium and may be influenced by a slight change of the condition of the electrode surface and the solution, these diverging values of ν seem to be rather reasonable. The fairly good constancy of the values of $\vec{\Delta F}$, which were obtained under the various conditions, can be considered as one of the experimental results which prove the correctness of the present discussion on the discharge process of the hydrogen ion.

The value of $\vec{\Delta F}$ can be also determined by the relation between $V_{1/2}$ and $\log I_l$ according to Eqs. (4) and (4'). If we assume the value of either one of α' and ν, the other is automatically determined, because the relation, $(\nu-1)/\alpha'$, can be obtained from Eq. (4). According to Eq. (1) we get the following relation between α' and ν:

$$\frac{\nu-1}{\alpha'}=-0.37$$

If we assume that α' is nearly equal to 0.5, the value of $\vec{\Delta F}$ is calculated to be equal to about 29.8 kcal./mol. by this method, which is in good agreement with the values mentioned in Tables 1 and 2.

Table 1

The Effect of the Concentration of the Hydrogen Ion on the Reduction Wave

$[C_{H^+}]^\circ$, millimole/l.	I_l, microamp.	$V_{1/2}$, volt *vs.* NCE.	α'	ν	$\vec{\Delta F}$, cal.
0.039	0.136	−1.540			
0.078	0.390	1.545			
0.137	0.738	1.546	0.59		32.0
0.195	1.04	1.559	0.66		34.9
〃	1.22	1.553	0.49		28.7
〃	1.07	1.555	0.52		29.6
0.390	2.31	1.562	0.46	0.58	29.4
〃	2.32	1.565	0.42	0.39	29.1
0.585	3.60	1.561	0.53	0.74	31.5
0.780	4.79	1.572	0.51	0.69	30.6
〃	4.66	1.568	0.58	0.76	33.0
〃	4.76	1.568	0.48	0.47	30.8
0.975	6.03	1.574	0.45	0.59	29.6
1.37	8.24	1.587	0.46	0.52	29.6
〃	8.10	1.570	0.44	0.56	28.7
1.95	11.4	1.577	0.50	0.49	31.1
〃	11.8	1.581	0.42	0.63	29.8

Table 2

The Effect of Temperature on the Reduction Wave of the Hydrogen Ion

Temp. τ, °C.	I_l, microamp.	$V_{1/2}$, volt. *vs.* NCE	α'	ν	$\vec{\Delta F}$, cal.
$[C_{H^+}]^\circ=0.78$ millimole/l.					
2.2	3.50	−1.636	0.56	0.76	32.3
10.2	4.18	1.589	0.50	0.64	31.1
11.2	4.24	1.598	0.57	0.68	32.7
14.0	4.37	1.605	0.48	0.71	29.8
21.7	4.83	1.585	0.58	1.0	32.0
24.7	5.05	1.561	0.53	1.0	30.1
31.7	5.33	1.544	0.53	0.73	31.5
36.5	5.43	1.533	0.58	1.0	32.0
41.7	5.64	1.527	0.46	0.49	30.3
50.9	5.84	1.498	0.54	0.68	32.3
$[C_{H^+}]^\circ=1.95$ millimole/l.					
1.5	8.56	1.638	0.46	0.67	28.9
20.5	11.2	1.591	0.49	0.75	29.8
27.8	12.0	1.567	0.47	0.52	30.1
36.5	12.3 (?)	1.550 (?)	0.45 (?)	0.61 (?)	29.1 (?)
45.2	13.4 (?)	1.530 (?)	0.64 (?)	0.77 (?)	35.3 (?)

At the end of this discussion a brief consideration about the effect of the height of the mercury reservior, p, on the half-wave potential, $V_{1/2}$, is set down. In 1937, J. Novak[11]

(11) J. Novak, *Collection Czechoslov. Chem. Communs.*, **9**, 207 (1937).

reported that the double increase of p causes a shift of $V_{1/2}$ to a more negative potential by 13 millivolts, while quite recently J. Kůta[7] found that this shift is equal to 18 millivolts. This change of $V_{1/2}$ with the change of p can be expected from Eqs. (4) and (4'). In these equations the terms, $\log I_l$ and $\log(FK'_H{}^+)$, which are approximately equal to $\log(FK_H{}^+)$, are the functions of p. The term, $\log s$, is independent of p, because it is proportional to $m^{2/3}t^{2/3}$ which is independent of p. As pointed out in Part II of this work,[2] the limiting current of the hydrogen ion in the present case is equal to the diffusion current, I_d, and, according to the Ilkovic equation, it is represented by the relation:

$$I_d = FK_H{}^+[C_H{}^+]^\circ = Kp^{1/2}[C_H{}^+]^\circ \qquad (12)$$

where K means a constant independent of p. If the revised Ilkovic equation[12] is used instead of the Ilkovic equation, an additive constant term independeut of p appears in Eq. (12), but we can ignore this constant term as an approximation in the present discussion. By means of these relations, the following relation between $V_{1/2}$ and p can be derived:

$$V_{1/2} \doteqdot \text{const.}(p) - \frac{RT}{2\alpha' F}\log p \qquad (13)$$

in which const.(p) is a constant independent of p. As α' is generally equal to 0.4—0.6, it is said from Eq. (13) that $V_{1/2}$ shifts to more negative potential by about 18 millivolts with the double increase of p in accordance with Kůta's experemental results. In this discussion it is assumed that α' and ν are independent of p.

As described above it is obvious that all the result on the current-voltage curve of the hydrogen ion, which was obtained in the present experiment, can be satisfactorily interpreted by assuming the neutralization of the adsorbed hydrogen ion under the condition of the activation-controlled process. Under these circumstances it can be concluded that the discharge process of the hydrogen ion of the dilute hydrochloric acid in 0.1 N KCl solution may proceed according to the "slow discharge mechanism of the adsorbed hydrogen ion."

(12) J. J. Lingane and B. A. Loveridge, *J. Am. Chem. Soc.*, **72**, 438 (1950); H. Strehlov and M. v. Stackelberg, *Z. Elektrochem.*, **54**, 51 (1950); T. Kambara, M. Suzuki and I. Tachi, This Bulletin, **23**, 219 (1950); T. Kambara and I. Tachi, ibid., **23**, 225 (1950).

Summary

Various properties of the current-voltage curve of the reduction wave of the hydrogen ion were studied in the system of the dil. HCl in 0.1 N KCl solution.

It was found out that the log-plot of the reduction wave is not linear and that the half-wave potential shifts to be more negative with the increase of the limiting current.

The temperature coefficient of the half-wave potential was obtained to be about 3 millivolts per degree over the temperature range of 0 to 50°. This value of the temperature coefficient is much larger than the value which is expected when the reduction process of the hydrogen ion proceeds under the condition of the diffusion-controlled type.

The Kalousek's methods were applied to the hydrogen wave in order to test the reversibility of the reduction process and it was shown that this process is one of the irreversible type.

These experimental results were satisfactorily explained by assuming the reduction process of the hydrogen ion as follows: First, the hydrogen ion is adsorbed on the surface of the D. M. E., and, next, the adsorbed hydrogen ion is neutralized to the hydrogen atom under the condition of the activation-controlled process. In this case it was assumed that the equilibrium state represented by the Freundlich adsorption isotherm exists between the hydrogen ion in the neighborhood of the electrode surface and the adsorbed hydrogen ion in the adsorbed layer.

The value of the free energy of activation of the overall discharge process of the hydrogen ion was calculated.

The author expresses his best thanks to Prof. San-ichiro Mizushima and Assist. Prof. Nobuyuki Tanaka for their great encouragement and valuable suggestions in this study. The expense of this research has been defrayed from the Scientific Research Encouragement Grant from the Ministry of Education.

Institute of Science and Technology,
Tokyo University, Tokyo

Studies on the Heat of Solution. I. Heats of Solution of Crystalline Pentaerythritol and Mesoerythritol

By Syûzô SEKI and Keisuke SUZUKI

(Received August 4, 1952)

Introduction

The measurement of heat of solution of crystalline materials is one of the useful methods for the determination of heat of formation of solid solution as well as of molecular compound, energy content of meta-stable modifications, energy of lattice imperfections, etc. Since we have hitherto investigated the interaction energies of different kinds of molecules constituting crystalline molecular compounds by the method of vapor pressure measurement[1] and also the interaction of water and other materials by differential thermal analysis and other methods[2], we have undertaken to study the heat of solution of crystalline materials in these connections.

As is well known, among the substances interacting with water, a group of alcohols exhibits strong hydrogen bond with water. Although the measurements of the heat of solution as well as the heat of dilution of the univalent alcohols, and some saccharides have been made, accurate determinations for polyvalent alcohols are very scanty. Now that the crystal structure as well as the thermal properties of pentaerythritol[3][4] and mesoerythritol[5] have been studied in considerable detail in our laboratory, we measured the heats of solution of these materials as the first step to the investigation on the heat of solution of crystals.

Experimental

(i) Apparatus and procedure: The calorimeter used is illustrated in Fig. 1. The calorimeter vessel consists of a silvered Dewar vessel (A) with a capacity of ca. 700 cc., containing the calorimeter heater (B), the glass stirrer (C), the dissolving device (D) for specimen under investigation and the junction points (E) of copper-constantan multiple thermocouple measuring the temperature variation of the calorimeter with reference to the average temperature of the inner water jacket (X). The Dewar vessel was mounted in a water-tight submarine jacket (F) which is made of 1 mm. thick copper sheet plated with chromium and polished on the surface. The air gap between the calorimeter vessel and the wall

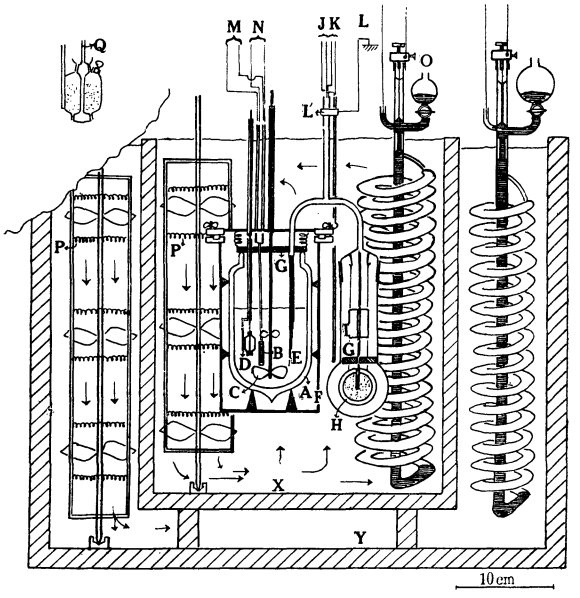

Fig. 1.

G: cork plate
I: lead block to avoid thermal leakage
J: main thermel measuring the temperature difference between calorimeter and fluctuation damper
K: thermocouple measuring the temperature difference between fluctuation damper and inner water jacket
L: earth to avoid leakage current
M: to voltmeter
N: to ammeter and battery
P: nichrome heater and stirrer

(1) I. Nitta, S. Seki, H. Chihara and K. Suzuki, *Sci. Paper Osaka Univ.*, No. 29 (1951); I. Nitta, S. Seki and H. Chihara, *J. Chem. Soc. Japan*, **70**, 387 (1949).

(2) I. Nitta and S. Seki, *J. Chem. Soc. Japan* **69**, 87 (1948); H. Chihara and S. Seki, This Bulletin, **26**, 88.

(3) I. Nitta and T. Watanabé, *Nature*, **140**, 365 (1937); I. Nitta and T. Watanabé, *Sci. Paper Inst. Phys. Chem. Research*, **34**, 1669 (1938); See also F. J. Llewellyn, F. G. Cox and T. H. Goodwin, *J. Chem. Soc.*, 883 (1937).

(4) a) I. Nitta, S. Seki and K. Suzuki, This Bulletin. **24**, 63 (1951); b) I. Nitta, S. Seki and M. Momotani, *Proc. Japan Acad.*, **26**, No. 9, 26 (1950); c) I. Nitta, S. Seki, M. Momotani, K. Suzuki and S. Nakagawa, ibid, No. 10, 11 (1950); d) I. Nitta, T. Watanabe, S. Seki and M. Momotani, ibid. No. 10, 19 (1950).

(5) I. Nitta, T. Watanabé and Y. Tomomatsu (unpublished).

of the submarine jacket was about 1.5 cm. The heat conductivity constant between the calorimeter and the outer part was found to be 0.8 cal./min. deg.

The temperature fluctuation of the outer water jacket (Y) (ca. 40 litres) was controlled within the accuracy of ±0.002°C., while the inner water jacket within ±0.0003°C. A sensitive toluene-mercury regulator (O), efficient stirring device (P) (the circulation of whole water is accomplished in the period of 5~8 sec.), and a special electrical circuit for protection of oxidation of the mercury surface of the regulator were employed.

The temperature variation of the calorimeter was measured by means of twelve-junctions copper-constantan thermocouple, each junction of which was insulated with polystyrene and covered with thin glass capillary tubes separately. The standard reference junction points were introduced in the Swietoslawsky-type fluctuation damper[6] (H) made of copper sphere covered with a layer of paraffin (ca. 4 mm.) and a thin alminium foil, and the damper was immersed in the inner water jacket. With these constructions the temperature fluctuation of the standard reference junction was minimized to ±0.0001°C. The e. m. f. of the thermo-couple was measured by means of the "P-7 Type Low-voltage Potentiometer" (0.01μV.) of Yokogawa Electric Work in combination with the "RC Type Reflection Galvanometer" (0.2 μV./mm.) of Shimadzu Co. as null indicator. Special precautions were taken to exclude "vagabond e. m. f." caused in the circuit[7]. Thus we could measure the temperature variation of 0.0001°C.

The water equivalent of the calorimeter was determined by electric energy. The heater for this purpose is made of constantan wire (ca. 10 ohm) wound on thin mica strips and insulated with a thin layer of polystyrene. The ampere and the voltage drop were measured by precision type ammeter and voltmeter. The source of constant current is a heavy duty lead storage battery (120 A. H.), which is controlled to a steady state by discharge into the ballast resistor of approximately the same resistance as the heater for a period of an hour or more before use.

The stirrer was operated with steady speed D. C. motor. The stirring velocity was regulated at about 170 r. p. m. and the heat produced by stirring at this velocity was about 0.23 cal./min. The dissolving device made of hard glass has a capacity 5~10 cc. To dissolve the powdered specimen, the glass rod (Q) is pushed downward. The endothermic heat effect due to this operation, which may be ascribed to evaporation of water into the air bubbles escaping from the glass bulb, is found to be only about 0.3 cal. even for the largest vessel.

In every run, before the measurements, the calorimeter was immersed in the thermostat for about 3~5 hours after the temperature of thermostat reached the stationary value. For the determination of the heat quantity from the temperature-time curve, the correction of heat exchange between the calorimeter and the water jacket was made by use of Newton's heat flow equation, and the other corrections mentioned above were also taken into consideration.

In order to test the usefulness of the calorimeter, the heat of solution of NaCl was determined (see Table 1). The result obtained coincides within the accuracy of 0.7% with the most reliable values at the same conditions recommended by Bichowsky and Rossini.[8]

Table 1

t°C.	Substance	N	ΔH_{soln} (this research) kcal./mol.	ΔH_{soln} (others) kcal./mol.
18	NaCl	400	1.218	1.225±0.005
18	Pentaerythritol	4300	4.77	
		2200	4.78	
		1100	4.79	6.3[9]
		620	4.83	
18	Mesoerythritol	4600	5.24	5.54[10]

(ii) Materials;

(a) NaCl: The product of "for analysis" of Takeda Co. was desiccated by heating for about five hours under high vacuum (10^{-4} mm. Hg or less) at about 150°C.

(b) Pentaerythritol: The product of Shionogi Co. was recrystallized from aqueous solution four times and then subjected twice to fractional sublimation at about 180°C. under high vacuum (m. p. 264°C.).

(c) Mesoerythritol: The product of Kahlbaum Co. was purified by fractional sublimation under high vacuum at about 110°C. (m. p. 120.3°C.). The crystal exists in two modifications, stable and metastable, at room temperature. The present specimen is of stable form.

(iii) Experimental Results: The results obtained are all given in Table 1 together with some other reference data. In this table N in the third column is the mole number of water to dissolve one mole of solute and the sign of enthalpy is taken positive for endothermic process. Comparing our values with the data in the fifth column, obtained at higher concentrations by other investigators, it is evident that the heats of dilution for both substances are a little exothermic. It is also observed that the heat of solution of pentaerythritol becomes almost constant when the degree of dilution exceeds N=1000.

(6) W. Swietoslawsky, "Microcalorimetry", Reinhold Publishing Co., 1946.

(7) "Temperature, its Measurement and Control in Science and Industry", Reinhold Publishing Co., 1944, p. 265.

(8) F. R. Bichowsky and F. D. Rossini, "The Thermochemistry of the Chemical Substances", Reinhold Publishing Co., 1936.

(9) From temperature dependence of solubility (22~58°C, N=47~22) Cooke, *Paint. Manif.*, **18**, 125 (1948).

(10) M. Berthelot, *Ann. Chim. et Phys.* **26**, 201 (1892) (24°C, N=300).

Table 2

Substances	$-\Delta H^{\infty}_{soln}$ (or ΔH^{∞}_{mix})	ΔH_{subl} (or ΔH_{vap})	$-\Delta H^{\infty}_{hyd}$ (obs)	$-\Delta H^{\infty}_{hyd}$ calc. from (2) & (3)	$-\Delta H^{\infty}_{hyd}$ calc. from (5) & (6)
Ethylene Glycol	(1.7)	(14.9)	16.6	20.9	18.5
Glycerol	(1.5)	(20.0)	21.5	30.6	25.9
Mesoerythritol	−5.2	32.3 (22.3)	27.1	41.4	34.5
Pentaerythritol	−4.8	31.4 (19.2)	26.6	40.3	33.6

Discussion of Results

As mentioned above, the heats of dilution of both substances are exothermic. Recently, Lange and his coworkers[11] measured the heats of dilution of univalent alcohols, and saccharides, and found that they are exothermic similarly to what we found in the present experiment. They explained this exothermic effect to be ascribed to the dissociation of the associated solute molecules. Even though we have not obtained the data of heats of dilution accurately enough to permit us to draw a definite conclusion on the mechanisms of the dissociation of hydrogen bond of polyalcohols investigated, it seems very plausible to assume that the exothermic heats of dilution of the present materials would also be due to the dissociation of the dimer or higher associates.

Now, we should like to discuss further the hydration state of the polyalcohols. As is well known, the heat of hydration is given by the following relation:

$$\Delta H^{\infty}_{hyd} = \Delta H^{\infty}_{soln} - \Delta H_{subl}, \qquad (1)$$

where ΔH^{∞}_{hyd} indicates the heat of hydration at infinite dilution, ΔH_{subl} the heat of sublimation and ΔH^{∞}_{soln} the heat of solution of crystal to form infinitely dilute aqueous solution. If the substance to be dissolved is liquid, the heat of vaporization and heat of mixing take the places of heats of sublimation and of solution, respectively. In Table 2 we give ΔH^{∞}_{soln} (or ΔH^{∞}_{mix}), ΔH_{subl} (or ΔH_{vap}) and $-\Delta H^{\infty}_{hyd}$ of the substances investigated and of other related ones. The heats of solution listed in Table 1 may be regarded approximately as ΔH^{∞}_{soln} on account of the independence on the concentration as shown in the column 4. As to the heats of sublimation we have already reported.[5a)(5c)] The heats of mixing at infinite dilution of ethylene glycol[12] and glycerol[13] are estimated from the extrapolation of the data at higher concentrations to the infinite dilution. For the heat of vaporization of ethylene glycol, the data by Louguinine[14] at 90°C was adopted. For glycerol there is reported the temperature variation of vapor pressures by Stedman.[15] The calculated heat of vaporization from them (21.17 kcal./mole at 75°C), however, seems to be not so trustworthy on accont of the unreasonably large value in comparison with that of pentaerythritol (19.2 kcal./mole) and of mesoerythritol (22.3 kcal./mole), having four hydroxyl groups, and of abnormally high dependence of the heat of vaporization on the temperature. So, we estimated 20 kcal./mole for the heat of vaporization of glycerol (See Table 2).

According to Butler,[16] the heats of hydration of univalent alcohols may be calculated by the following semi-empirical equations (2) and (3),

$$\Delta H^{\infty}_{hyd} = \left\{ \frac{n}{2}\gamma_{W\text{-}W} - n_{W\text{-}CH}\gamma_{W\text{-}CH} - n_{W\text{-}OH}\gamma_{W\text{-}OH} \right\}, \qquad (2)$$

$$n = n_{W\text{-}CH} + n_{W\text{-}OH}, \qquad (3)$$

where n is the total number of water molecules hydrated to the solute molecule in question, $n_{W\text{-}CH}$ and $n_{W\text{-}OH}$ the number of hydrated water molecules for CH and OH groups respectively; $\gamma_{W\text{-}W}$ is the energy required to separate a single pair of water molecules, and $\gamma_{W\text{-}CH}$, $\gamma_{W\text{-}OH}$ the energies of interaction between a hydrated water and a CH or OH group, respectively. Putting somewhat artificial assumptions of

$$\gamma_{W\text{-}W} = 5.25,\ \gamma_{W\text{-}CH_3} = 3.4,\ \gamma_{W\text{-}CH_2} = 3.4,$$
$$\gamma_{W\text{-}CH} = 3.4 \text{ and } \gamma_{W\text{-}OH} = 5.6, \qquad (4)$$

for the interaction energies (in kcal./mole), and $n_{CH_3}=3$, $n_{CH_2}=2$, $n_{CH}=1$ and $n_{OH}=3$ for the number of hydrated water molecules, Butler found that the calculated ΔH^{∞}_{hyd} values from the above equations are in good agreement with the observed values for normal univalent alcohols, and also that they are always larger by 0.8 kcal. per one branching than the observed data for branched alcohols. We have tentatively calculated the heats of hydration of polyvalent alcohols with application of these values and found indeed large positive deviations as shown in the fifth column in Table 2.

(11) E. Lange and H. G. Marlcgraf, *Z. Electrochem.*, **54**, 73 (1950).

(12) a) International Critical Table. (average value of following two: Berthelot, (1882); de Forcrande, (1890).); b) F. Schwers, *Z. phys. Chem.*, **75**, 366 (1911).

(13) a) I. C. T. average value of Berthelot (1873, 1976), de Forcrande (1887, 1888), Gerlach (1884) and Kolossowsky (1913); b) Katz. *Proc. Amsterd. Acad.*, **13** 970 (1911) R. Fricke and J. Lücke, *Z. Electrochem.*, **35**, 636 (1929).

(14) W. Louguinine, *Ann. chim. et phys.* **26** 239 (1902); W. Hieber and A. Waeruer, *Z. Electrochem.*, **40**, 252 (1934).

(15) D. F. Stedman, *Trans. Faraday Soc.*, **24**, 296 (1929).

(16) J. A. V. Butler, *Trans. Faraday Soc.*, **32**, 229 (1936).

Table 3

Substances	Molecular Volume	n	n'	θ'	θ'/θ_0	$q=\theta'/\theta$
Ethylene Glycol	55.6[a]	10	8.18	9.8	1.67	0.83
Glycerol	72.8[a]	14	10.08	13.1	2.28	0.73
Mesoerythritol	92.0[b]	18	12.22	16.9	2.90	0.71
Pentaerythritol	110.0[c]	20	14.22	16.2	2.77	0.69

a: Taken from reference[18].

b: We estimated the density of liquid from that of solid, assuming volume change on fusion is 10%.

c: As the present material belongs to the so-called plastic crystal (see reference[21]), we estimated the density of liquid from those of the two modification of solid, and heats of fusion and transition[4], using following relation:

$$\frac{\Delta V(\text{fusion})}{\Delta V(\text{transition})}=\frac{\Delta H(\text{fusion})}{\Delta H(\text{transition})}$$

To elucidate the nature of this deviation we have attempted to calculate $\Delta H^{\infty}_{\text{hyd}}$ of the polyvalent alcohols employing the experimental values of $\Delta H^{\infty}_{\text{hyd}}$ of a series of univalent alcohols and an other equation of some different meanings from that of Butler, instead of adopting somewhat artificial choice of n and γ values given above.

Supposing that the hydrated water molecules are not permanently fixed to the solute molecules owing to the thermal agitation, then the number n may be considered to have only a statistical meaning.[17] Accordingly this number may not necessarily be an integer as Butler has assumed. To create a cavity to hold a solute molecule in the liquid, the number of hydrogen bonds to be broken (n') will be 4, 6, 8, 10 and 12, if the volume of a cavity is 1, 2, 3, 4 and 5 integral multiples of that of a water molecule. It is possible, then, to determine the number n' from the ratio of the molecular volume of solute to that of water, using interpolation of above-mentioned relations between n' and molecular volume ratio. The numbers n' obtained in this way are given in Tables 3 and 4. (n' differs from n, and the relations to the heats of hydration of univalent alcohols are given in Fig. 2.) Then, inserting equation (3) into (2) and taking into account the effect of branching, we have

$$\begin{aligned}\Delta H^{\infty}_{\text{hyd}} &= n'\left\{\frac{1}{2}\gamma_{\text{W-W}}-\gamma_{\text{CH-W}}\right\}\\ &\quad -n_{\text{W-OH}}\{\gamma_{\text{W-OH}}-\gamma_{\text{W-CH}}\}\\ &\quad +\{\text{effect of branching}\}\\ &=n'\varphi-\theta+\delta \qquad (5)\end{aligned}$$

In this equation integral number n in (2) is replaced by n', and θ is proportional to the number of OH groups in the solute molecule if the intramolecular interaction between OH groups is negligibly small.

Table 4

Substances	n[16]	n'[18]	$-\Delta H^{\infty}_{\text{hyd}}$ (obs.)
Methyl Alcohol	6	6.50	11.24
Ethyl 〃	8	8.46	12.88
Propyl- 〃	10	10.28	14.42
Butyl- 〃	12	12.14	15.94
Amyl- 〃	14	14.06	17.50
Iso propyl- 〃	10	10.46	13.45
Iso butyl- 〃	12	12.24	15.24
sec-Butyl- 〃	12	12.18	15.06
tert-Butyl- 〃	12	12.42	14.44
tert-Amyl- 〃	14	14.06	15.69

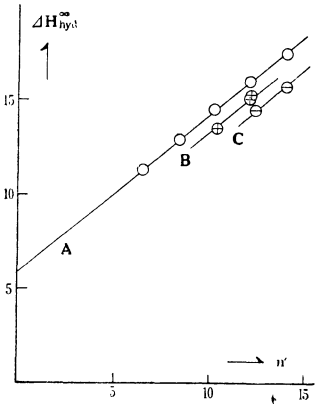

Fig. 2.

A: normal alcohols
B: one branched alcohols
C: two branched alcohols

As shown in Fig. 2 experimental data of normal, one-branched, two-branched univalent alcohols lie on three different straight lines. Thus, from these lines and equation (5), we obtain the following relations:

$$\varphi_0=-0.834,\ \theta_0=5.82 \text{ and } \delta_0=0.80/\text{branch.} \qquad (6)$$

(suffix $_0$ means the value of univalent alcohol)

(17) J. Morgan and B. E. Warren, *J. Chem. Phys.*, **6** 666 (1941); J. A. Pople, *Proc. Roy. Soc.*, A **205**, 163 (1951).

(18) J. Timmermans, "Physico-chemical Constants of Pure Organic Compounds", Elsevier Publishing Co., 1950.

The reason for the appearance of the correction factor δ may be explained by the following; (i) as was pointed out by the present authors,[4a] the polarizabilities of the carbon atoms in branched hydrocarbons are somewhat smaller than that of the normal one, so the contributions of the dispersion and induction interaction energies become smaller; ii) in branched hydrocarbons the interatomic distances between hydrated water molecules and the inner carbon atoms are larger than that of the normal one, hence, the contribution to the interaction energy of these atoms becomes smaller.

Inserting n' values derived from the molecular volume of solute in liquid state into equation (5) under the assumption that the intramolecular interaction of OH groups is negligible and putting in the numerical values of equation (6), we obtain the heats of hydration of polyvalent alcohols given in the last column in Table 2. There remain still some deviations from the experimental values, although they are diminished considerably in comparison with the results obtained by the method of Butler. Certainly, the origin of these deviations is to be attributed to the intramolecular interaction of OH groups which gives rise to decrease of the number of hydration water molecules. The similar fact has been recently observed by Shimura.[19] He measured the electrostriction of water caused by dissolving various sorts of amino acids and found that, in comparison with the δ- or γ-amino acid the electrostriction caused by NH_3^+ group of α-amino acid is decreased. As a measure of decrement of intermolecular hydrogen bond forming powers of OH groups in the polyvalent alcohols, we have tentatively calculated the factor $q=\theta'/\theta$. Here θ' is given by use of equation (5) from the observed heat of hydration of polyvalent alcohol and the values of φ and δ of the univalent alcohols. The results are given in the last column of Table 3 which indicate evidently the intermolecular interactions decrease (intramolecular interaction increases) from ethylene glycol to pentaerythritol. As to the former, it has been found recently[20] that from the study of infra-red spectroscopy intramolecular hydrogen bond of this molecule in solution state is not so strong as expected before. On the other hand, the possibility of more frequent formation of the intramolecular hydrogen bond may be enhanced by the internal rotation about C-C single bond in the case of more complex polyvalent alcohols. This may, in part at least, explain the decreasing tendency of q-values given in Table 3.

Summary

(i) The heats of solution of pentaerythritol and mesoerythritol have been measured at 18°C and found to be both of endothermic. (4.77 kcal./mole and 5.24 kcal./mole).

(ii) The heats of dilution of both substances are of exothermic.

(iii) From the heats of sublimation and of solution, the heats of hydration were determined (26.6 kcal./mole for pentaerythritol and 27.1 kcal./mole for mesoerythritol).

(iv) It was found that the intramolecular hydrogen bonds cause considerable deviations from the improved Butler rule on the heats of hydration of alcohols.

In conclusion the authors wish to express their sincere thanks to Professor Nitta for his kind guidance throughout this work. The cost of this investigation was defrayed from the funds of Taniguchi Kôgyô Shôreikai as well as from the Scientific Research Expenditure Grant from the Ministry of Education to which the authors' thanks are due.

Department of Chemistry, Faculty of Science, Osaka University, Osaka

(19) K. Shimura, *J. Agr. Chem. Soc. Japan*, **23** 31, 48 (1949); **24** 412 (1951).

20) R. Mecke, *Z. Electrochem.*, **52**, 269 (1948).
(21) S. Seki, *J. Chem. Phys.*, **18**, 397 (1950).

Spectrophotometric Determination of Camphor-aldehydes. I.

By Yoshikazu SAHASHI, Jinkichi UENO and Minoru MORI

(Received July 20, 1952)

Introduction

In 1934, the senior author and his co-workers[1] reported the results of their studies on the chemical synthesis of hydroxycamphors and their carbonyl derivatives. Afterwards, much progress in physiological and clinical aspects was made, thanks to the efforts of numerous investigators. In connection with the chemical and biological determination of their unstable camphor-aldehydes in O_2 atomosphere, many procedures have also been carried out by several authors, but twenty years have passed since that time, while no reliable reports have appeared about the physicochemical estimation of these camphor-aldehydes except those by ordinary iodometry, bisulfite-CrO_3 titration method etc. On the other hand, studies on elctrophotometric assay of various compounds have been markedly improved, and it is especially well known that Roe[2],[3] and coworkers succeeded during 1942-4 in colorimetrically determining dehydro-ascorbic acid with 2,4-dinitrophenylhydrazine (DNP). Therefore, the authors have recently attempted to prepare pure 2,4-dinitrophenylhydrazones of β-oxocamphor and π-oxocamphor, in order to undertake spectrophotometric estimation of camphor-aldehydes with the standard crystals of their 2,4-dinitrophenylhydrazones. Experiments are outlined as follows:

1) The absorption spectra of β-oxocamphor-2,4-dinitrophenylhydrazone and π-oxocamphor-2,4-dinitrophenylhydrazone were exactly determined in isopropylalcohol solution by a Beckman spectrophotometer to give absorption maxima, $E^{1\%}_{1\,cm}356\ m\mu=658$ and $E^{1\%}_{1\,cm}354\ m\mu=678$, respectively.

2) The E value of camphor-aldehyde-hydrazone in the solution to be tested was measured electrophotometrically, and the real amount of the camphor-aldehydes contained was calculated from the above standard E value.

(1) Y. Sahashi and co-workers, *Scient. Pap. Inst. Phys. Chem. Res.* **25**, 47 (1934).
(2) Roe, Kuether, *J. Biol. Chem.*, **147**, 399 (1943).
(3) A. Fujita, *Vitamins*, **4**, 53 (1951).

β(10) Apocamphor-1-aldehyde

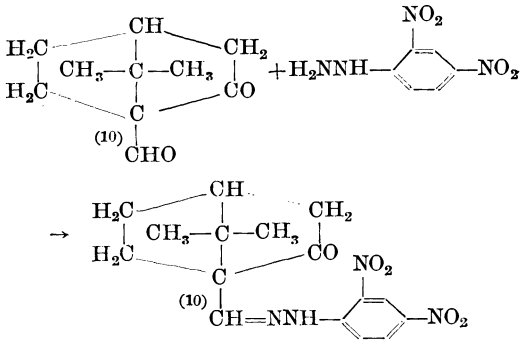

π(8 or 9) Apocamphor-7-aldehyde

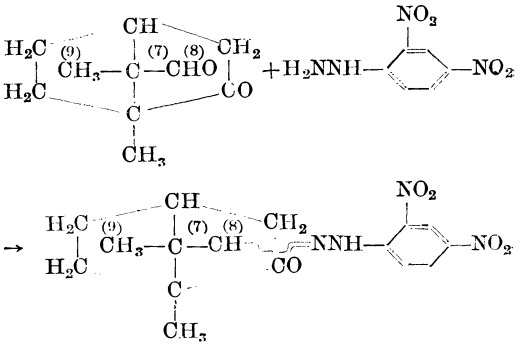

Experimental

(1) Preparation of Camphor-aldehyde-2,4-dinitrophenylhydrazones.—β (10) Apocamphor-1-aldehyde-2,4-dinitrophenylhydrazone: Freshly prepared crystals of β(10) apocamphor-1-aldehyde (β-oxocamphor) from β-(10) hydroxycamphor by means of chromic acid oxidation and sodium bisulfite purification were dissolved in alcohol and treated by hot saturated 5N HCl solution of 2,4-dinitrophenylhydrazine. After a few minutes heating, the hydrazone separated out as an insoluble amorphous precipitate which when recrystallized from hot alcohol formed yellow needle crystals, yield almost quantitative; m. p. 212°C. (uncorr.)

Found: C, 54.61, 54.67; H, 5.75, 4.90; N, 16.12, 16.34, Calcd. for $C_{16}H_{18}O_5N_4$: C, 55.46; H, 5.24; N, 16.18%

π(8 or 9) Apocamphor-7-aldehyde-2,4-dinitrophenylhydrazone: Crystals of π(8 or 9) apocamphor-7-aldehyde (π-oxocamphor), freshly prepared

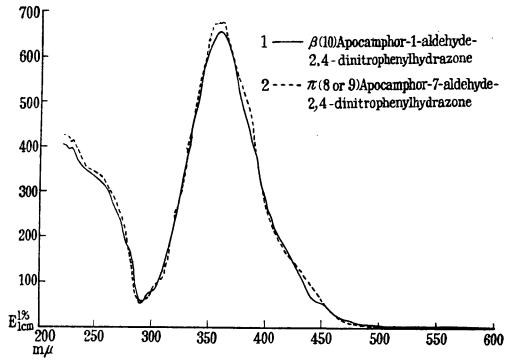

Fig. 1.—Absorption spectra of camphor-aldehyde-2, 4-dinitrophenylhydrazone in isopropylalcohol.

from π-bromocamphor according to Sahashi's method, were dissolved in alcohol and treated with hot saturated 5N HCl solution of 2, 4-dinitrophenylhydrazine by the same process mentioned above. The amorphous precipitate thus obtained was recrystallized from hot alcohol, yielding yellow needle crystals in a quantitative amount; m. p. 202°C. (uncorr.)

Found: C, 55.29, 55.49; H, 4.82, 5.09; N, 16.04, 16.01, Calcd. for $C_{16}H_{16}O_5N_4$: C, 55.46; H, 5.24; N, 16.18%

(2) Spectrography of Camphor-aldehyde-2, 4-dinitrophenylhydrazones. — 100 γ of camphor-aldehyde-2, 4-dinitrophenylhydrazone to be tested were dissolved in 10 cc. of isopropyl alcohol. The standard absorption of the above compounds were measured by a Beckman spectrophotometer with the following results.

	β(10) Apocamphor-1-aldehyde-2, 4-dinitrophenyl-hydrazone	π(8 or 9) Apocamphor-7-aldehyde-2, 4-dinitro-phenylhydrazone
Absorption-maxima	$E^{1\%}_{1\,cm}$	$E^{1\%}_{1\,cm}$
	356 mμ=658	354 mμ=678

(3) Analytical procedure.—DNP Reagent: 5g. 2, 4-dinitrophenylhydrazine (DNP) were dissolved in 200 cc. hot 5N HCl solution and filtered after cooling.

Procedure: A) 1 cc. of aq. β(10) oxocamphor solution was refluxed for about a minute with 10 cc. of the DNP reagent and allowed to cool. After 30 minutes the yellow precipitate was filtered, washed with water and dissolved in 100 cc. isopropyl alcohol. The solution thus obtained was diluted up to 10 γ/cc. (2000 cc.) The extinction was then measured by a Beckman spectrophotometer.

B) 1 cc. of aq. π (8 or 9) oxocamphor solution was heated for about a minute with 10 cc. of DNP reagent and treated as mentioned above. The separating hydrazone was dissolved in 100 cc. of isopropyl alcohol and diluted up to 10 γ/cc. (1000 cc.) The Beckman photometric observation was then carried out in the ordinary way.

Calculation: β(10) oxocamphor: Found, $E^{1\%}_{1\,cm}356\ m\mu=528$

$$\text{Hence,}\quad 10\gamma\times\frac{528}{658}\times 2000=16.04\ \text{mg.}$$

$$16.04\times\frac{166}{346}=7.69\ \text{mg./cc.}$$

π(8 or 9) oxocamphor: Found, $E^{1\%}_{1\,cm}354\ m\mu=488$

$$\text{Hence,}\quad 10\gamma\times\frac{488}{678}\times 1000=7.19\ \text{mg.}$$

$$7.19\times\frac{166}{346}=3.44\ \text{mg./cc.}$$

C) Cases where the solution to be tested contains other emulsifying organic agents such as Tween, Span etc., it is best to carry out the separation of camphor-aldehydes by the process of steam distillation, and DNP reagent must be added to the distillate.

Summary

1) 2, 4-dinitrophenylhydrazones of β(10) apocamphor-1-aldehyde and π(8 or 9) apocamphor-7-aldehyde were prepared and their absorption spectra were exactly determined.

2) From the standard *E* values, the amount of the above compounds in an unknown solution can be calculated from the estimation by a Beckman spectrophotometer.

The authors wish to express their sincere thanks to Dr. M. Yoshida for Beckman-photometry.

Laboratory of Biochemistry, Faculty of Agriculture, University of Tokyo and Institute of Pharmaceutical Resources, Tokyo

Peculiarity of Dichroism of Aromatic Molecular Compounds. II. The Dichroisms of *s*-Trinitrobenzene—Anthracene and 4, 4′-Dinitrodiphenyl—Diphenyl

By Kazuo NAKAMOTO

(Received June 27, 1952)

Introduction

An earlier paper of this series[1] is concerned with dichroism of typical molecular compounds and the general rule regarding the dichroism of the first band principally due to the π-electrons of the benzene rings. That is, the absorption by the light with the electric vectors vibrating perpendicular to the molecular planes of both the components is always bathochromic and hyperchromic to the absorption by the light with those vibrating parallel to those planes. So, in the present investigation, measurements of dichroisms of molecular compounds, *s*-trinitrobenzene—anthracene and 4,4′-dinitrodiphenyl — diphenyl have been made in visible and ultraviolet regions, and their results have been discussed applying the general rule stated above.

Experimental

Materials.—(1) *s*-Trinitrobenzene—Anthracene —Fine orange acicular crystals are produced by mixing the methanol solutions of both the components in the molar ratio of 1:1, and allowing the solution to evaporate at room temperature. M. p. 164°. Monoclinic system. Straight extinction. This substance shows dichroism; orange, when viewed with linearly polarized light whose electric vector vibrates parallel to the *c*-axis (needle axis) and light yellow, when observed with those vibrating parallel to the *b*-axis.

(2) (4, 4′ - Dinitrodiphenyl)$_3$ — Diphenyl — Pale yellow acicular crystals are prepared by mixing the hot acetone solutions of both the components in the molar ratio of about 3:1 and allowing the solution to cool gradually. Monoclinic system. A striking characteristic of this crystal is that it has no clear melting point, owing to continuous decomposition with the elevation of temperature.[2] Straight extinction. Dichroism can not be observed with the naked eye.

Measurements.—Dichroisms of the crystals have been quantitatively measured by the microscopic method with microcrystals, as described in the former paper.[3]

Results and Discussion

(1) *s*-Trinitrobenzene—Anthracene.—In 1932, Briegleb and Schachowskoy[4] studied the absorption spectrum of this molecular compound in chloroform solution and calculated the heat of dissociation from their spectroscopic data. As to the crystal structure, Hertel and Römer[5] have inferred the orientation of both the molecules from the observed values of the lattice constants alone, and no further report has been presented.

Fig. 1 records the absorption spectra by linearly polarized lights with the electric vectors vibrating parallel to the *c*- and *b*-axes, respectively. The absorption curve of pure anthracene crystal by ordinary light is also shown for comparison (Curve 4). Absorption curves of both the components (Curve 1 and 2) and the molecular compound (Curve 3)[4] in liquid state are given in Fig. 1. From the comparison of the absorption curves in crystalline state with that of the components in solution, it is evident that the bands at 500~400 mμ in crystalline state consist mainly of the

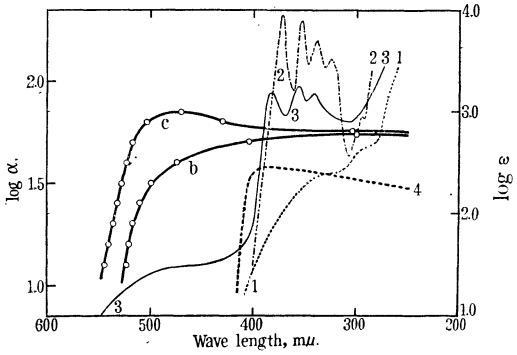

Fig. 1. — Absorption spectra of *s*-trinitrobenzene-anthracene and its components: 1, *s*-trinitrobenzene; 2, anthracene; 3, *s*-trinitrobenzene-anthracene; 4, anthracene in crystalline state (by ordinary light).

(1) K. Nakamoto, *J. Am. Chem. Soc.*, **74**, 1739 (1952).
(2) K. Suzuki, Presented before the Division of Structural Chemistry at the 4th Meeting of the Japan Chemical Society, Tokyo, April, 1951.
(3) K. Nakamoto, *J. Am. Chem. Soc.*, **74**, 390 (1952).
(4) G. Briegleb and T. Schachowskoy, *Z. physik. Chem.*, **B 19**, 255 (1932).
(5) E. Hertel and G. H. Römer, ibid., **B 11**, 77 (1931).

absorption due to the π-electron system of aromatic rings of both the molecules. It should be noted that these bands absorb the same region with the characteristic band of the molecular compound in Curve 3. As already discussed in the former work,[1] all of these absorptions at 500~400 mμ are essentially attributed to the intermolecular charge-transfer spectra resulting from an inter-benzoid overlap of the π-orbitals. Curve 3, however, does not indicate any distinct maximum since the anisotropic absorption in crystalline state is reduced by random orientation of molecules in liquid state.

As is shown in Fig. 1, the *c*-absorption is bathochromic and hyperchromic to the *b*-absorption. This result offers a further evidence to support the validity of the general rule for the dichroism of molecular compounds, if we accept the crystal structure predicted by Hertel and Römer for this compound. In other words, the *c*-absorption is bathochromic and hyperchromic to the *b*-absorption, because both the component molecules are piled up alternately along the *c*-axis making their molecular planes parallel to each other and the overlap of the π-orbitals that are thrust out perpendicularly from each molecular plane occur along the *c*-axis. We have, therefore, shown conclusively that the dichroism of this molecular compound can be interpreted by the general rule described before.

(2) **(4,4'-Dinitrodiphenyl)$_3$—Diphenyl.** — Since 1946, Saunder and his co-workers[6] have studied the crystal structure of molecular compounds of 4,4'-dinitrodiphenyl with various substituted diphenyls. According to their results, all of these compounds have a definite type of structure in which dinitrodiphenyl molecules form layers in face-centred array and lie one above another with a spacing of about 3.7 A. In a continuous arrangement of these layers, long tubular cavities are left running through the structure, and the other component molecules occupy these cavities and lie nearly normal to the planes containing dinitrodiphenyl molecules. The orientations of both the molecules in the crystal are shown graphically in Fig. 2. That is, these compounds have a peculiar structure which is quite different from that of typical molecular compounds. Moreover, based on the measurements of the closest intermolecular distance of approach, Saunder and his co-workers concluded that there is no localized bonding between the component molecules. So it is expected that the dichroism of such a compound will be considerably modified as compared with that of typical molecular compounds.

In the present paper, one of these molecular compounds, *(4,4'-dinitrodiphenyl)$_3$*—diphenyl, is selected and its dichroism has been measured in the ultraviolet region. Absorption spectra by linearly polarized lights with the electric vectors vibrating parallel to the *b*- and *c*-axes, respectively, are shown in Fig. 2, and their numerical data are given in the following table.

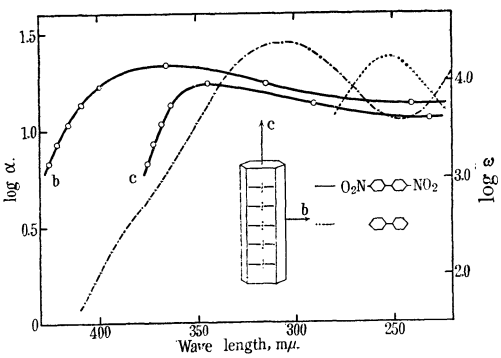

Fig. 2.—Absorption spectra of 4,4'dinitrodiphenyl-diphenyl: ——·——, 4,4'-dinitrodiphenyl; ----, diphenyl.

Table

	λmax. (mμ)	log αmax.
b-abs.	365	1.34
c-abs.	345	1.24

The spectra of both the components in alcoholic solutions are also marked in the same figure.

According to Niekerk and Saunder,[7] in the crystal of this compound, dinitrodiphenyl molecules are nearly parallel to the (001) plane, whereas diphenyl molecules are nearly normal to it and lie on the (010) plane. Comparing these results with our spectroscopic data, we may conclude that the *b*-absorption is the spectrum by the light whose electric vector vibrates parallel to the molecular plane of dinitrodiphenyl and perpendicularly to that of diphenyl. On the other hand, the *c*-absorption is the spectrum by the light whose electric vector vibrates perpendicularly to the molecular planes of dinitrodiphenyl and parallel to that of diphenyl.

So far, it is impossible to analyze these bands into the two absorptions due to dinitrodiphenyl and diphenyl, respectively. As is shown in the spectra of both the components in solution, however, dinitrodiphenyl (λmax, 308 mμ; log εmax, 4.39) is far more bathochromic to diphenyl (251 mμ; 4.26). It is reasonable to assume that this relation holds also for the spectra of both the components in crystalline state. Moreover, according to the stoichiometrical consideration of the mixing ratio in this compound, dinitrodiphenyl is expected to play a main rôle in the dichroism of the crystal. Thus, in the longer wave length region of these spectra, both the *b*- and *c*-absorptions can be assumed to consist principally of the absorption due to dinitrodiphenyl.

The fact that the *b*-absorption is bathochromic

(6) D. H. Saunder, *Proc. Roy. Soc. London*, **A 188**, 31 (1946).

(7) J. N. van Niekerk and D. H. Saunder, *Acta Cryst.*, **1**, 44 (1948).

and hyperchromic to the *c*-absorption suggests that the general rule about the dichroism of common aromatic crystals[8] holds also for the longer wave length region in these spectra. Namely, the absorption which is parallel to the molecular plane of dinitrodiphenyl is bathochromic and hyperchromic to the absorption which is perpendicular to it. Thus, the results obtained from the dichroism measurement have led us to the conclusion that there does not exist $\pi-\pi$ attraction in the direction normal to the molecular plane of dinitrodiphenyl. In other words, the foregoing consideration suggests that the dichroism of this molecular compound is explicable on the assumption that it is only a kind of mixed crystals except that it has a definite combining ratio determined solely by the geometrical consideration in crystal structure.

Summary

Measurements of the dichroisms of molecular compounds, *s*-trinitrobenzene—anthracene and 4,4′-dinitrodiphenyl—diphenyl have been made quantitatively made in the visible and ultraviolet region. It can be concluded that the crystal of the former compound has the same dichroic property as the typical molecular compound already given in the previous report. The dichroism of the latter compound suggests that there exists no special attraction in the direction normal to the molecular plane of dinitrodiphenyl.

The author wishes to express his sincere thanks to Prof. R. Tsuchida for his kind guidance and encouragement throughout this work. Appreciation is also expressed to Mr. K. Suzuki for the gifts of 4,4′-dinitrodiphenyl and diphenyl used in this research.

Department of Chemistry, Faculty of Science, Osaka University, Osaka

(8) K. Nakamoto, *J. Am. Chem. Soc.*, **74**, 392 (1952).

Spectrochemical Study of Microscopic Crystals. III. The Dichroisms of μ-Peroxo-Dicobalt Compounds

By Shoichiro YAMADA, Yoichi SHIMURA and Ryutaro TSUCHIDA

(Received July 29, 1952)

It has been known since long ago that compounds containing the atoms of the same element in different valency states often show extraordinarily deep colors. Although the phenomena have attracted the attention of many investigators, and speculative views were also proposed on the phenomena,[1],[2] no direct research, based upon the absorption spectra of those compounds in the crystalline state, has ever been reported.

This work was initiated to clarify the above phenomena with the aid of their absorption spectra and further to investigate the nature of the chemical linkages in these compounds. For this purpose decammine-μ-peroxo-dicobalt compounds were selected. These compounds, which have two metal atoms of the same element combined through a peroxy radical, present an adequate model for those more complicated compounds in which would exist the above supposed mutual interaction between two metal atoms through a negative ion.

In the present work the dichroisms of decammine-μ-peroxo-cobalt (III)-cobalt (IV) nitrate and of decammine-μ-peroxo-dicobalt (III) nitrate dihydrate have been measured, and the results obtained from the above measurements have been discussed.

Experimental

Materials. (1) **Decammine-μ-peroxo-cobalt (III)-cobalt (IV) nitrate,** $[(NH_3)_5Co\text{-}O_2\text{-}Co(NH_3)_5](NO_3)_5$.—This compound was prepared as dark green acicular crystals according to the direction of Werner and Mylius.[3] The crystals exhibit a

(1) See, for examples, E. H. Riesenfeld, "Lehrbuch der anorganischen Chemie," Rascher Verlag, Zürich, Switzerland, 1943, p. 573; H. J. Emeléus and J. S. Anderson, "Modern Aspects of Inorganic Chemistry," George Routledge and Sons, Ltd., London, England, 1940, p. 139.

(2) J. Whitney and N. Davidson, *J. Am. Chem. Soc.*, **69**, 2076 (1947); H. McConnell and N. Davidson, ibid., **72**, 3168 (1950), etc.

(3) A. Werner and A. Mylius, *Z. anorg. Chem.*, **16**, 245 (1898).

remarkable dichroism, i. e., they appear pale brownish yellow by polarized light with electric vector parallel to the direction of elongation and indigo blue by that perpendicular to the above. Acidic aqueous solutions of the compound, which appear dark blue, are comparatively stable, while neutral or alkaline solutions spontaneously decompose. The dichroism measurement of the crystal was made in the prism face.

(2) **Decammine-μ-peroxo-dicobalt (III) nitrate dihydrate,** $[(NH_3)_5Co\text{-}O_2\text{-}Co(NH_3)_5](NO_3)_4 \cdot 2H_2O$.—Dark greenish brown crystals were prepared by the method of Werner and Mylius.[3] These show a marked dichroism, i. e., brown by polarized light with electric vector parallel to the direction of elongation of the crystal, and bluish green by that perpendicular to the above. This compound is so unstable in aqueous solutions, acidic,[4] neutral or alkaline, that the absorption spectrum in solution could not be measured.

Measurements.—Quantitative dichroism measurements of the crystals were performed by the microscopic method[5] in the region covering 7500 to 2300 A. The //- or ⊥-absorption in the figures denotes, respectively, absorption with electric vector perpendicular or parallel to the direction of elongation of the crystals.[6] α represents absorption coefficient per mm. of the crystal.

The absorption spectrum of the aqueous solution, slightly acidified with dil. sulfuric acid, was determined with a Beckman model DU quartz spectrophotometer in silica cells having a 1 cm. light path. Extinction coefficients were calculated from the equation

$$\varepsilon = 1/\mathrm{cd} \cdot \log(I_0/I).$$

Measurements were made at room temperature. The complete spectrum was obtained from 8000 to 2200 A. Aqueous solutions of the complex salt were used at concentrations of 5.82×10^{-4} and 5.82×10^{-5} F.

Results and Discussion

Absorption Spectrum of the Aqueous Solution.—Results of the measurements with the aqueous solution are shown in Fig. 1 and Table 1. There have been published a few reports concerning absorption spectra of cobaltic polynuclear complexes in solutions. Shibata and Ohyagi reported the qualitative absorption curves of polynuclear

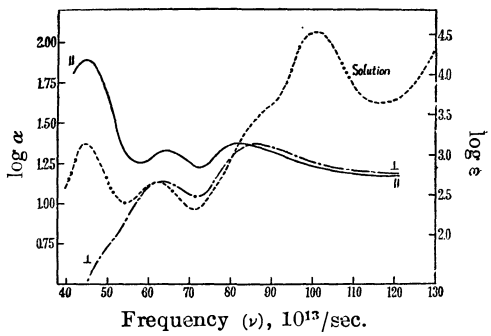

Fig. 1.—Dichroism of the crystal of $[(NH_3)_5Co\text{-}O_2\text{-}Co(NH_3)_5](NO_3)_5$ and absorption spectrum of the aqueous solution (dotted curve).

complexes in aqueous solution[7] and in phosphoric acid.[8] One of the present authors and Kuroya[9] reported absorption spectra of $[Co\{(OH)_2Co\ en_2\}_3](NO_3)_6$, $[Co\{(OH)_2Co(NH_3)_4\}_3]Cl_6$ and $[(NH_3)_4Co(OH)_2Co(NH_3)_4]Cl_4$, and found that polynuclear complexes of such a type generally display a "third band,"[10] caused by ligandolysis,[11] the dissociation of NH_3 in coordination into NH_2^- and H^+, at $\nu=100$ to 110×10^{13}/sec. and $\log\varepsilon=3$ to 4, besides two absorption bands corresponding to the first and the second absorption band.[10] Consequently, the absorption band at $\nu=101$ in the absorption spectrum of $[(NH_3)_5Co\text{-}O_2\text{-}Co(NH_3)_5](NO_3)_5$ is considered to be a "third band."

According to the previous report, monoaquo- and monohydroxy-pentammine cobaltic complexes show the first band at $\nu=$ about 60 and hexammine cobaltic salt at $\nu=64-65$. Since binuclear complexes should show the corresponding absorption band at longer wave length than related uninuclear complexes,[12] it is supposed that the absorption band at $\nu=62.6$ is the second absorption band and the band at $\nu=44.6$ corresponds to the first absorption band. Besides those absorption bands as discussed above, there can be found an inflexion at $\nu=88$. This inflexion should be attributed to the peroxy group and may well be named the "peroxy-specific band," since the solutions of binuclear complexes with a peroxy radical as a bridge[8] exhibit a similar inflexion or a separated band at $\nu=$ about 90 and $\log\varepsilon=$ about 3.

It is seen that the ε_{max} of the first absorption band is considerably larger than that of the

(4) Decomposition of the compound was observed even in phosphoric acid solution.

(5) R. Tsuchida and M. Kobayashi, "The Colours and the Structures of Metallic Compounds," Zoshindo Co., Osaka, Japan, 1944, p. 180. See also the previous reports of this series (R. Tsuchida and M. Kobayashi, This Bulletin, **13**, 619 (1938); S. Yamada and R. Tsuchida, ibid., **25**, 127 (1952)).

(6) As will be shown in the later part of the present paper, the //-or ⊥-absorption corresponds to the absorption with the electric vector vibrating parallel or perpendicular to the Co-O-O-Co direction.

(7) Y. Shibata, *J. Coll. Sci., Imp. Univ. Tokyo*, **37**, Art. 8, 19 (1916); *J. Chem. Soc. Japan*, **38**, 99 (1917).

(8) Y. Ohyagi, This Bulletin, **15**, 186 (1940).

(9) R. Tsuchida and H. Kuroya, ibid., **15**, 427 (1940).

(10) As to the first, the second and the third absorption band, see for example, R. Tsuchida, This Bulletin, **13**, 388 and 436 (1938).

(11) R. Tsuchida and M. Kobayashi, *J. Chem. Soc. Japan*, **64**, 1268 (1943); L. Tschugaev, *Z. anorg. Chem.*, **137**, 1401 (1924); G. Urbain, *Bull. soc. chim.*, **51**, 853 (1932); G. Okamoto, *J. Chem. Soc. Japan*, **57**, 1175 (1936); T. Uemura and H. Sueda, This Bulletin, **10**, 50 and 85 (1935), etc.

(12) See, for example, ref. (5), p. 159.

Table 1

Absorption Maxima of $[(NH_3)_5Co\text{-}O\text{-}O\text{-}Co(NH_3)_5](NO_3)_5$

	1st Band		2nd Band		O_2-Band		3rd Band	
Crystal	ν	$\log \alpha$	ν	$\log \alpha$	ν	$\log \alpha$		
//-abs.	45	1.88	64.6	1.32	82.6	1.38		
$\perp$-abs.			63.0	1.13	86.8	1.38		
Solution	ν	$\log \varepsilon$	ν	$\log \varepsilon$	ν	$\log \varepsilon$	ν	$\log \varepsilon$
	44.6	3.14	62.6	2.66	(88)	(3.5)	100.8	4.54

second band, which seems unusual as compared with previous data. This will be discussed in the later part of the present report along with the dichroisms of the crystals.

It is found that the compound is greatly bathochromic to the hexol and the diol complexes which contain bridging OH^- radicals. This shows that bathochromic effect of a peroxy radical is larger than that of OH^-.

The Dichroisms of the Crystals. (1) $[(NH_3)_5Co\text{-}O_2\text{-}Co(NH_3)_5](NO_3)_5$.—The dichroism of the crystal of the compound is shown in Fig. 1 and the data are tabulated in Table 1. The crystal exhibits the first, the second and the "peroxy-specific" absorption band, but lacks the third band, which is found in the absorption spectrum of the solution and observed to be considerably large as compared with the other bands. Comparing the absorption in the crystalline state with that of the aqueous solution, it is found that in the //-absorption the band at $\nu=45$ corresponds to the first band, the one at $\nu=64.6$ to the second band, and the one at $\nu=82.6$ to the peroxy-specific absorption band. Similarly, in the $\perp$-absorption the band at $\nu=63$ represents the second absorption band and the one at $\nu=86.8$ the peroxy-specific absorption band, the first band being so weak that it could be assumed that the band has no component in that direction.

The dichroic nature is found in any of the first, the second and the peroxy-specific band. Above all, exceedingly large dichroism is recognized in the first absorption band. Comparing the two characteristic directions, the Co-O-O-Co direction and that perpendicular to the above, a larger electric moment is expected in the former than in the latter. In consequence, the dichroism measurement shows that the direction, Co-O-O-Co, in the complex should be perpendicular to the direction of elongation of this crystal. The remarkable dichroism in the first band shows the far more frequent transition of d-electrons in the direction of the linkage, Co-O-O-Co, than in the direction perpendicular to the linkage. And the different features of the first and the second absorption band suggest the different origins of these bands.

(2) $[(NH_3)_5Co\text{-}O_2\text{-}Co(NH_3)_5](NO_3)_4\cdot 2H_2O$. — The dichroism of the crystal is shown Fig. 2 and Table 2. Similarly as in the cobalt (III)-cobalt (IV) complex, the crystal shows the first, the second and the peroxy-specific band, but the third band, which should be exhibited by the aqueous

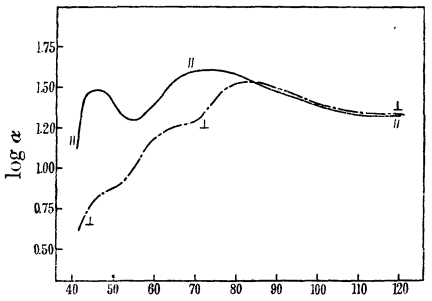

Fig. 2.—Dichroism of the crystal of $[(NH_3)_5Co\text{-}O_2\text{-}Co(NH_3)_5](NO_3)_4\cdot 2H_2O$.

solutions, was not observed. From a similar consideration as in the case of the cobalt (III)-cobalt (IV) complex, it is found that the band at $\nu=46$ in the //-absorption is the first absorption band. The broad and flat band at $\nu=60$ to 80 may be considered to be superposition of the second and the peroxy-specific band. Similarly, the band at $\nu=48$ in the $\perp$-absorption is the first absorption band, the one at $\nu=63$ the second absorption band, and the one at $\nu=83$ the peroxy-specific absorption band.

Table 2

Absorption Maxima of $[(NH_3)_5Co\text{-}O\text{-}O\text{-}Co(NH_3)_5](NO_3)_4\cdot 2H_2O$

	1st Band		2nd Band		O_2-Band	
	ν	$\log \alpha$	ν	$\log \alpha$	ν	$\log \alpha$
//-abs.	46.0	1.48	flat (superposed)			
$\perp$-abs.	(48)	0.85	(63)	(1.2)	83.0	1.53

The dichroism is observed in any of those bands. The dichroism as to the first band appears especially marked. Electric moment responsible for the first absorption band, which is supposed by the present authors to originate from transitions in an incomplete transition shell of the central cobaltic ions, would be larger in the Co-O-O-Co direction than in the direction perpendicular to the above. Therefore, it may be presumed that in the crystal the complex ions are arranged so that the Co-O-O-Co direction is almost perpendicular to the direction of elongation.

General Features of the Dichroisms.—Both the complexes in the crystalline state as well as in solution are bathochromic to the diol, the hexol

and related complexes which have two OH- radicals as bridges. This indicates that the peroxy radical usually exerts larger bathochromic effect than the hydroxy radical.

The crystals of both compounds lack the third band which should usually be observed in solution at ν=about 100 and log ε=3~4. This shows that the said band may be attributed to such a ligandolysis, as is greatly favoured by interaction of solvent molecules with ligands of the complex ions. It is possible to suppose that ammonia molecules in the complex ion, which may be rather labilized under the influence of the peroxy radical in the complex, would be much more easily dissociated when the solvent molecules approach the ions, and that the band would disappear in the crystalline state where there exists no interaction of solvent molecules.

The two complex ions, μ-peroxo-dicobalt (III) and μ-peroxo-cobalt (III)-cobalt (IV) ions, have a similar configuration having two metal atoms connected through a peroxy radical. From the results of their dichroism measurements the following rules may be obtained for the dichroism of complexes of the above type:

(1) The first absorption band. The //-absorption, the absorption with the electric vector vibrating along the Co-O-O-Co direction, is remarkably hyperchromic to the $\perp$-absorption, the absorption with the electric vector vibrating perpendicularly to the above.

(2) The second absorption band. The //-absorption is hyperchromic and hypsochromic to the $\perp$-absorption.

(3) The peroxy-specific absorption band. The //-absorption is bathochromic to the $\perp$-absorption,[13] extinction coefficients of both absorptions being almost equal.

Interaction between Central Metallic Ions through a Bridging Peroxy Group.—Examining the absorption curves as presented in this report, it is found that the first absorption band of peroxy-cobalt (III)-cobalt (IV) nitrate is different from what the so-called first band should be, since (1) the first band in aqueous solution is about three times as strong as the second absorption band, which differs from the empirically derived tendency[14] that the first band of a cobalt (III) complex in solution is almost as strong as the second band, (2) in the //-absorption of the crystal, too, the first band is about three times as strong as the second band, which represents a quite unusual case with the absorption spectra of crystals, and (3) the first band of the //-absorption is extraordinarily hyperchromic to that of the $\perp$-absorption, the latter having a negligibly small extinction coefficient.

From the above discussions, and considering the fact that the absorption with the electric vector vibrating along the Co-O-O-Co direction should be much larger than the absorption with the electric vector perpendicular to the above, it may be supposed that two cobalt atoms of different valency states exert an interaction upon each other through a peroxy-radical between them; one may think that electrons vibrate back and forth between the two cores through a peroxy-radical as a bridge, and that in the ground state two cobalt atoms may not be distinguishable.

The previous data on absorption spectra of coordination compounds indicate that, generally speaking, complexes of a metal of a higher oxidation number show their absorption bands at shorter wave length regions than the corresponding ones of the same metal of a lower oxidation number. The absorption curves of the compounds reported in the present paper are inconsistent with the above tendency derived with most compounds. Thus comparing the μ-peroxo-cobalt (III)-cobalt (IV) complex with the μ-peroxo-dicobalt (III) complex, the former is not hypsochromic but even slightly bathochromic to the latter. This discrepancy also suggests the unusualness of the former compound and the possibility of the strong interaction between the central metallic ion as described above.

In the case of the μ-peroxo-dicobalt (III) complexes, too, the difference in α of the first band between the //- and the $\perp$-direction is so large that it may be possible to expect a sort of interaction between central metallic ions through a peroxy radical in the Co-O-O-Co direction. As is clear from the above descriptions, however, the interaction seems much large in the Co (III)-O-O-Co (IV) direction than in the Co (III)-O-O-Co (III) direction. This can also be understood from electronic configurations of cobalt ions. That is, since Co (III) has a $3d^6$ configuration and Co (IV) has a $3d^5$ configuration, it is probable that the said interaction in the μ-peroxo-Co (III)-Co (IV) complex is much stronger than in the Co (III)-Co (III) complex.

The same applies for similar Fe (II)-Fe (III)-polynuclear complexes, since Fe (II) and Fe (III) are isoelectronic, respectively, with Co (III) and Co (IV). Thus, in the magnetite, Fe_3O_4, and the prussian blue, K Fe Fe $(CN)_6$, mutual interactions between Fe (II) and Fe (III) are expected through an oxygen ion or a cyanide ion, which would cause anomalies in optical and magnetic properties of those compounds.

It is also suggested that a similar explanation holds for those compounds of a similar type which contain atoms of the same element in different valency states and exhibit unusual colours, and that the interaction of the above type between metallic ions through a bridging ion or radical represents a favourable and adequate model for processes in those more complicated compounds.

(13) This tendency resembles the rule observed about the dichroism of the π band of the benzene ring (cf. R. Tsuchida, M. Kobayashi and K. Nakamoto, *J. Chem. Soc. Japan*, **70**, 12 (1949); K. Nakamoto, *J. Am. Chem. Soc.*, **74**, 390 (1952)), which may suggest that the electronic state of O-O- in those complexes is rather similar to that of the π-linkage in the benzene ring.

(14) H. Kuroya, *J. Inst. Polytech., Osaka City Univ.*, **1**, No. 1, Ser. C, 29 (1950); K. Sone, *J. Chem. Soc. Japan*, **71**, 270 (1950).

Summary

(1) The dichroisms of decammine-μ-peroxo-dicobalt (III) nitrate dihydrate, $[(NH_3)_5Co\text{-}O_2\text{-}Co(NH_3)_5](NO_3)_4 \cdot 2H_2O$, and of decammine-$\mu$-peroxocobalt (III)-cobalt (IV) nitrate, $[(NH_3)_5Co\text{-}O_2\text{-}Co(NH_3)_5](NO_3)_5$, and the absorption spectrum of the latter in aqueous solution have been quantitatively measured.

(2) The empirical rules on the dichroisms of those crystals have been obtained.

(3) The considerations on the absorption spectra of the above compounds have led to the conclusions that there exists a kind of mutual interaction between metallic ions through a bridging peroxy-radical and that the interaction between Co (III) and Co (IV) is considerably larger than that between two Co (III) atoms. The interaction of the above type is supposed to be applicable to the explanation of unusually deep colors in the crystals containing the same atoms in different oxidation states.

This work was supported in part by a grant from the Ministry of Education. Our thanks are offered to the analytical laboratory of our department for the absorption spectrum measurement of the aqueous solution.

Department of Chemistry, Faculty of Science, Osaka University, Osaka

The Effect of Methyl Substitution on the Absorption Maxima of Quinoline Derivatives

By Kazuo SHIBATA and Takashi HOMMA

(Received July 4, 1952)

In 1947, Herzfeld[1] proposed a theory dealing with the effect of various kinds of substitutions on the position of the electronic absorption maxima of conjugated systems. According to his theory, the effect of substitution by the radicals containing two $2p\pi$ electrons as in the case of -Cl, -NH_2, -OH, etc. must always be bathochromic. Along the line of his reasoning, the effect of methyl substitution must be expected also to be more or less bathochromic, since the two bonding electrons between C and H will interact with the electrons of conjugated systems. In conformity with this expectation, there are extensive data showing that the absorption bands of $2p\pi$ electron systems are shifted redward by the effect of the methyl substitution.

In the course of our systematic study on spectroscopic properties of some conjugated systems, we have found, however, that some conjugated systems having quinoline nucleus represent exceptions to the above rule. The object of this paper is to present such examples and to describe some rule governing the effect of substitution on the position of absorption maxima of these compounds.

(1) K. F. Herzfeld, *Chem. Rev.*, **41**, 233 (1947).

Experimental

The compounds investigated were methyl derivatives of quinocyanines, tetrahydro-quinolines, benztetrahydro-quinolines and their picrates. Absorption spectra were measured by photoelectric method, with an Adam Hilger monochrometer. The solvent used was ethanol, and the thickness of the cell compartment was 1 cm.

Results

The data obtained for quino-cyanines are listed in Table 1. As may be seen from this table, the substitution of methyl group in position 2 of quinoline nucleus shifts the absorption maxima redward, while the reverse is the case when the substitution is made at position 4. The absolute values of the shift caused by the substitution into position 2 are larger than those caused by the substitution in position 4.

With methyl derivatives of benztetrahydroquinoline, we obtained the results given in Table 2. Since the methyl groups in positions 5, 6, 7 and 8 will not directly interact with the conjugated system, the effect of the substitution into these positions is expected to be less than the effect of the 2-, 3- and 4-substitutions. The data obtained confirmed this expectation. It may be remarked that the absorption maxima of 2-

Table 1

Absorption Maxima of Methyl Substituted Quino-cyanines

Compounds	R	R'	λ(A.)	$\Delta\lambda$
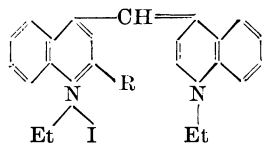	$-H$	—	5910	0
	$-CH_3$	—	5980	+70
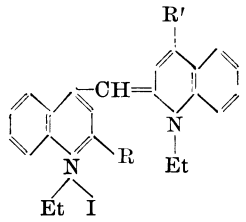	$-H$	$-H$	5580	0
	$-CH_3$	$-H$	5600	+20
	$-H$	$-CH_3$	5570	−10
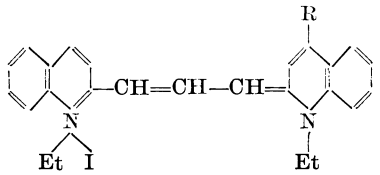	$-H$	—	6070	0
	$-CH_3$	—	6030	−40

methyl derivatives are situated at longer wavelengths than the maxima of 2,4-dimethyl derivatives.

In table 3, are shown the data obtained for the picrates of methyl substituted benztetrahydro-quinolines. These compounds have two absorption bands, of which the one situated at longer wavelength is obviously due to the picric acid which is either in combined or in free state in the solution investigated. (See Table 3) In respect to the second absorption bands, the effects of methyl substitutions in various positions were found to follow virtually the same rule as was the case with benztetrahydro-quinolines.

These findings tell us that the same rule found for the absorption maxima of quino-cyanines may be applicable to benztetrahydro-quinolines and their picrates, and it may be that this behavior of the shift of absorption band by methyl substitution is the charateristic of the conjugated system having pyridine ring as a part.

In connection with the above data, it seems worthwhile to present the data of the melting points and the solubilities (%) in water of methyl derivatives of quinoline-iodoethylate. They are listed in Table 4, which shows that a rule analogous to the above mentioned one is found also in respect to these physical quantities; namely (1) the methyl substitution into position 2 enhances the melting point but lowers the solubility of quinoline-iodoethylate, while the substitution into position 4 shows the contrary effect, and (2) the

Table 2

Methyl Derivatives of Benztetrahydro-quinoline

Positions of methyl groups.	λ(A.)	ε
2,7-	2840	18,000
2-	2800	16,000
2,4,6-	2800	13,000
2,4-	2760	14,000
none	2730	12,000
Pyridine	2550	9,000

Table 3

The Picrates of Methyl Derivatives of Benztetrahydro-quinoline

Position of Methyl Groups	First Band (A.)	Second Band (A.)	ε (Second Band)
2,7-	3630	2810	21,000
2-	3630	3810	20,000
2,4-	3620	2780	21,000
None	3640	2730	14,000
8-	3630	2690	16,000
Picric Acid	3630	—	—

Table 4

Melting Points and Solubilities of Quinoline-iodoethylates

Compounds	R	R'	m.p.(°C.)	Solubility at 25°C.(%)
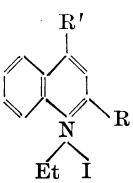	$-H$	$-CH_3$	141	19.8
	$-H$	$-H$	156—157	8.1
	$-CH_3$	$-CH_3$	222—224	1.6
	$-CH_3$	$-H$	237—238	0.6

magnitude of the former effect is larger than that of the latter effect, as will be seen from the data of 2,4-dimethyl-quinoline.

In contrast to the cases described above, the effect of methyl substitution in tetrahydro-quinoline is always bathochromic as is shown in Table 5. This may be explicable if we realize that in these compounds the pyridine moiety in quinoline nucleus is saturated and, therefore, they may be regarded as alkyl derivatives of aniline from the viewpoint of conjugated system. In these compounds, the magnitude of bathochromic shift caused by methyl substitution is most pronounced in position 6, followed by 7 and then 8. It should also be remarked that the values of molar extinction coefficient ε of these compounds decrease with the shift of absorption maxima to longer wave-lengths, a phenomenon which is in quite reverse direction to that observed in the case of benztetrahydro-quinolines.

Table 5

Methyl Derivatives of Tetrahydro-quinoline

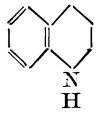

Positions of Methyl Groups.	λ(A.)	ε
2,6-	3100	1,100
2,4-	3040	1,600
2,4,6-	3030	800
2,7-	3030	1,900
2,4,7-	3000	1,300
7-	3000	1,600
8-	2990	2,000
2,4,8-	2950	2,600
2,8-	2920	3,000
Aniline	2840	—

Conclusion

The effect of methyl substitutions on the position of absorption maxima of some quinoline derivatives was investigated and it was found that there exists a certain empirical rule governing the relationship between the position of substitution and the shift of absorption band. Attention was called to the fact that in some quinoline derivatives the methyl substitution causes a hypsochromic shift of absorption band, a fact which is contrary to the expectation based on the now prevailing theory. The analysis of this phenomenon may be highly relevant from the standpoint of the theory of hyperconjugation.

The writers wish to express their earnest thanks to Prof. Eiji Ochiai and Mr. Yoshihisa Mizuno for the samples of quinoline derivatives used in the present investigation and also to Prof. Hiroshi Tamiya for his guidance and special interest in our study.

The Tokugawa Institute for Biological Research, Tokyo

An Equation of State in Analytical Form

By Tetsuya ISHIKAWA

(Received August 27, 1952)

In most of the text-books of physical chemistry which insert a table of van der Waals' constants a and b, no example of their actual evaluation is given, and students often fall into misconception that the constants are uniquely determinate from the original and its two derived equations at critical points. Concretely speaking, from these equations we obtain $b=V_c/3=RT_c/8p_c$ by substituting for V_c in the former from van der Waals' critical factor, $RT_c/p_cV_c=8/3$, and consequently $a=27p_cb^2=3p_cV_c^2=27(RT_c)^2/64p_c$, whereas for real gases, these two expressions of b give inconsistent values, $V_c/3$ being always less than $RT_c/8p_c$. The latter however has been accepted to make use of calculating molecular diameters.[1] To eliminate this inconsistency from van der Waals' equation, the following correction is needed:

$$b_{corr.}=b\left(\frac{3}{8}\frac{RT_c}{p_cV_c}\right)=\frac{V_c}{3}\left(\frac{3}{8}\frac{RT_c}{p_cV_c}\right)=\frac{RT_c}{8p_c},$$

where RT_c/p_cV_c in the correction factor is an actual critical factor, ranging from 3.23 to 3.97 for non-polar and larger slightly polar substances. Substitute $a_{corr.}$ for a corresponding to $b_{corr.}$, van der Waals' equation per mol. is

(1) e.g. Landolt-Börnstein I-1, 1950, p. 325.

Table 1

Validity of van der Waals' Equation for CO_2 at Several Isotherms ($p_c = 73.0$ atm.)

30.98°C. (critical temperature)		37.09°C.		41.95°C.		50°C.		100°C.		198°C.	
p(atm.)	f	p(atm.)	f	p(atm.)	f	p(atm.)	f	p(atm.)	f	p(atm.)	f
63.36	0.982	64.56	0.986	64.85	0.989	50	0.988	50	1.009	50	0.998
69.085	0.989	69.20	0.990	69.81	0.992	100	1.007	100	1.026	100	1.032
72.995	0.955	71.73	0.993	72.78	0.994	200	0.509	200	0.998	200	1.056
75.43	0.864	76.40	0.999	75.48	0.997	400	0.349	400	0.726	400	1.002
86.10	0.763	88.89	0.902	87.18	1.007	600	0.118	600	0.517	600	0.864
106.18	0.662	103.08	0.792	105.01	0.872	800	($V < b_{corr.}$)	800	0.337	800	0.760
138.65	0.568	136.01	0.655	134.85	0.731	1000	〃	1000	0.161	950	0.619

Table 2

Ratios of the Molecular Association Degree to the Correction Factor for Critical Factor

Liquid	V(20°C.) cc.	$b_{corr.}$ cc.	RT_c/p_cV_c	α/β(20°C.)	$A/\frac{3}{8}\frac{RT_c}{p_cV_c}$
Br_2	51.23	58.56	3.46	17.66	0.969
Hg	14.81	17.04	3.40	46.29	1.025
CCl_4	96.45	126.6	3.68	11.51	1.029
CS_2	60.28	75.13	3.49	12.84	1.068
H_2O	18.04	30.49	4.46	3.92	(negative)
$CH_3CO_2C_2H_5$	97.89	141.0	3.95	13.27	1.040
C_2H_5OH	58.35	83.90	4.08	9.65	(1.100)
$C_2H_5OC_2H_5$	103.8	131.8	3.77	8.85	0.986
C_2H_5Br	75.16	84.31	3.14	11.64	1.046
CH_3COCH_3	73.43	86.90	3.02	11.44	(1.159)
C_6H_6	88.85	119.9	3.75	11.11	1.048
C_6H_5Cl	101.8	145.4	3.76	13.07	1.077
$CHCl_3$	80.18	99.42	3.44	12.80	1.046
C_7H_{16}	146.5	205.6	3.85	10.33	1.030
cyclo-C_6H_{14}	108.2	139.8	3.63	10.17	1.027
C_6H_{14}	130.6	174.7	3.80	9.00	1.011
CH_3OH	40.46	53.09	4.75	9.92	(0.927)
C_8H_{18}	162.7	236.1	3.86	11.18	1.052
C_5H_{12}	115.2	145.9	3.76	6.61	1.008
C_3H_7OH	74.74	110.0	3.99	9.80	(1.106)
$C_6H_5CH_3$	106.4	146.4	3.71	12.41	1.054

Table 3

$(2-\varepsilon)$ Values of Ne ($t_c = -228.7$°C, $p_c = 26.9$ atm., $d_c = 0.484$ g./cc)

$b = 13.90$, $\log a = 5.147154$, $\log V_0 = 4.350791$

−213.08°C		−208.10°C		−182.60°C		−141.22°C		−103.01°C		0.00°C	
p(atm.)	$2-\varepsilon$	p(atm.)	$2-\varepsilon$	p(atm.)	$2-\varepsilon$	p(atm.)	$2-\varepsilon$	p(atm.)	$2-\varepsilon$	p(atm.)	$2-\varepsilon$
23.086	1.946	24.071	1.950	32.067	1.973	33.840	1.996	35.558	2.011	22.064	2.093
24.810	1.946	28.844	1.952	32.988	1.973	37.707	1.998	36.697	2.006	23.555	2.078
26.673	1.946	31.948	1.952	36.438	1.976	38.581	1.998	40.610	2.022	25.867	2.107
29.365	1.946	37.856	1.953	36.880	1.977	43.319	2.006	42.107	2.021	28.468	2.115
32.441	1.947	41.798	1.953	41.371	1.977	49.881	2.004	55.136	2.026	30.790	2.118
37.418	1.947	58.472	1.954	42.533	1.981	51.916	2.004	58.583	2.030	39.753	2.059
53.896	1.948	64.451	1.955	49.943	1.981	66.471	2.019	78.110	2.059	44.892	2.072
59.769	1.948	69.692	1.955	50.514	1.980	78.558	2.029		———	59.777	2.076
66.271	1.948	74.532	1.955	63.320	1.983		———	mean	2.025	66.104	2.097
72.858	1.950	76.228	1.954			mean	2.007			74.059	2.122
79.698	1.950		———	mean	1.978					79.108	2.138
	———	mean	1.953							84.662	2.118
mean	1.947										———
										mean	2.099

Table 4

$(2-\varepsilon)$ Values at Critical Points and Percentage Divergences of Approximate Formula $RT_c/p_cV_c=2/3\cdot(1+3V_c^{0.077})$ from Experimental Data

Substance	$2-\varepsilon$	Δ	Substance	$2-\varepsilon$	Δ	Substance	$2-\varepsilon$	Δ
He	1.931	+2.50	C_5H_{12}	1.924	+0.52	CH_3SH	1.922	−0.57
Ne	1.935	+2.35	i-C_5H_{12}	1.926	+1.55	C_2H_5SH	1.924	+0.85
A	1.925	+0.84	cyclo-C_6H_{14}	1.931	+3.95	CH_3SCH_3	1.920	−1.37
Kr	1.927	+1.63	C_6H_{14}	1.924	+0.53	$C_2H_5SC_2H_5$	1.933	+4.67
Xe	1.921	−0.89	C_7H_{16}	1.923	+0.28	HCO_2CH_3	1.905	−7.39
H_2	1.936	+4.31	C_8H_{18}	1.923	+0.78	$HCO_2C_2H_5$	1.913	−5.02
N_2	1.928	+1.93	Br_2	1.932	+3.51	$HCO_2C_3H_7$	1.917	−2.75
O_2	1.925	+0.83	Hg	1.915	−2.28	$CH_3CO_2CH_3$	1.909	−6.06
Cl_2	1.921	−0.79	CS_2	1.933	+4.42	$CH_3CO_2C_2H_5$	1.912	−4.82
CO	1.931	+3.01	CCl_4	1.927	+1.96	$CH_3CO_2C_3H_7$	1.914	−4.29
CO_2	1.918	−1.85	$CHCl_3$	1.940	+9.81	$CH_3CO_2CH_2CH(CH_3)_2$	1.937	+7.02
CF_2Cl_2	1.925	+0.96	CH_3OCH_3	1.918	−2.13	$C_2H_5CO_2CH_3$	1.913	−4.34
$COCl_2$	1.933	+4.31	$CH_3OC_2H_5$	1.922	−0.62	$C_2H_5CO_2C_2H_5$	1.915	−3.58
N_2O	1.908	−5.43	$C_2H_5OC_2H_5$	1.922	−0.57	$C_3H_7CO_2CH_3$	1.917	−2.82
PH_3	1.915	−3.13	$C_2H_5OC_3H_7$	1.926	+1.41	$(CH_3)_2CHCO_2CH_3$	1.912	−2.12
SO_2	1.908	−5.93	C_2H_5Cl	1.926	+1.16	$C_3H_7CO_2C_2H_5$	1.932	+4.63
$SnCl_4$	1.927	+2.06	$C_6H_5CH_3$	1.927	+1.87	$(CH_3)_2CHCO_2C_2H_5$	1.937	+7.08
CH_4	1.927	+1.64	C_6H_6	1.922	−0.49	$C_2H_5NH_2$	1.921	−0.82
C_2H_6	1.923	−0.12	C_6H_5F	1.920	−1.00	$(C_2H_5)_2NH$	1.922	−0.59
C_2H_4	1.927	+1.48	C_6H_5Cl	1.923	−0.02	$(C_2H_5)_3N$	1.934	+5.74
C_2H_2	1.915	−2.91	C_6H_5Br	1.921	−0.78	$(CH_3)_2CHCH(CH_3)_2$	1.926	+1.46
C_3H_6	1.921	−1.00	C_6H_5I	1.925	+1.01	$(CH_3)_2CHCH_2CH_2CH(CH_3)_2$	1.926	+1.57

The mean of $(2-\varepsilon)=1.923\pm0.008$, the mean of $\Delta=\pm2.6\%$.

written down:

$$p+\frac{a_{corr.}}{V^2}=\frac{RT}{V-b_{corr.}} \qquad (1).$$

The validity of equation (1) can be tested simply by calculating $f=(p+a_{corr.}/V^2)(V-b_{corr.})/RT$ at different isotherms, which must be unity, if the equation holds good. As seen from Table 1, f deviates from unity as pressure moves slightly away from the critical pressure, so that equation (1) is valid only within narrow limits of pressures, though the range becomes wider as the increase in temperature.

Moreover mere trial for the evaluation of values of $(V-b_{corr.})$ with ordinary liquids at an ordinary temperature proves that the applicability of equation (1) to liquids, should be rejected since all such values become negative (compare column 2 with column 3 in Table 2).

We have the pure thermodynamic equation

$$p+\left(\frac{\partial U}{\partial V}\right)_T=T\left(\frac{\partial p}{\partial T}\right)_V=T\frac{\alpha}{\beta} \qquad (2),$$

where α and β denote thermal expansion coefficient and isothermal compressibility.[2] If there exists an equation of state for liquids, the thermal pressure of which has the form $ART/(AV-b_{corr.})$, A being a correction factor so as to let the denominator of thermal pressure of equation (1) be positive, the equality:

$$T\frac{\alpha}{\beta}=\frac{ART}{AV-b_{corr.}} \qquad (3)$$

may be satisfied, if A is suitably chosen. Since R (82.06 cc.-atm./deg. mol.) and V (cc./mol.) are both referred to 1 mol. of gases, A may be or may not be proportional to the degree of non-polar association at T°K.

For test of this postulation, 21 kinds of liquids have been adopted from Henning's table.[3] In Table 2 are given A's divided by $3RT_c/8p_cV_c$, from which we can conclude that A is in nearly the same magnitude with $3RT_c/8p_cV_c$, for ordinary liquids except acetone, alcohols and water, or in other words, for liquids having low dielectric constants relation (3) is transformed into

$$T\frac{\alpha}{\beta}=\frac{RT}{V-b} \qquad (4).$$

In accord with the above correction for thermal pressure, an appropriate correction for cohesive pressure will be considered below.

As already known b decreases as V decreases,

(2) e.g. International Critical Tables IV, p. 19.

(3) F. Henning's "Warmetechnische Richtwerte", p. 17-19, 20-21.

and so the assumption of keeping b to be constant independent of V must yield deviation in thermal pressure, but the deviation therefrom can be attributed to a suitable correction of a in cohesive pressure.

Now assume $a^*_{corr.}$ to vary slightly with V and take the following form:

$a^*_{corr.} = aV^{\varepsilon}$,
ε = a constant independent of pressure,

then for substances having low dielectric constants it follows from (1), (3) and (4) that

$$p + \frac{a}{V^{2-\varepsilon}} = \frac{RT}{V-b}, \quad a = 3p_cV_c^2,\ b = V_c/3 \qquad (5).$$

Adopting pv- values of gases from I. C. T.[4] and Henning's table,[5] we have calculated $(2-\varepsilon)$ values for several gases. One of them is exemplified in Table 3.

As a whole, the constancy of $(2-\varepsilon)$ values is fairly good over a wide range of pressures of each isotherm, though the constant range becomes restricted as the temperature decreases. The variation of $(2-\varepsilon)$ values with temperature is similar for all the examined gases except He, their values increasing from a value less than 1.92 to a value slightly greater than 2. Inserting the mean value of $(2-\varepsilon)$ at each isotherm in equation (5), we can obtain the equation of state at respective temperature. The thus analytically determinate equation is, therefore, more reasonable and accurate than a usual equation of algebraic form: $pV = a_0 + a_1/V + a_2/V^2 + a_3/V^3 + \cdots\cdots$.

Besides the gases above examined, all gases and liquids with known critical-point data except those having high dielectric constants take a universal value, 1.923 ± 0.008, for $(2-\varepsilon)$ at critical points (see Table 4).

The following are three formulae at the critical point which can be derived from the new equation of state.

The criteria generally used to determine whether or not any equation of state holds good are RT_c/p_cV_c, T_B/T_c (T_B = Boyle point) and $T_c/p_c \cdot (dp/dT)_c$. These are of course physico-chemical constants giving the values close to 3.7, 2.6 and 7.0 respectively but none of the proposed equations gives concordant values simultaneously.

Inserting $a = 3p_cV_c^2$ and $b = V_c/3$ in equation (5) at the critical point, and rearranging them, it follows that

$$\frac{RT_c}{p_cV_c} = \frac{2}{3}(1+3V_c^{\varepsilon}) \qquad (6),$$

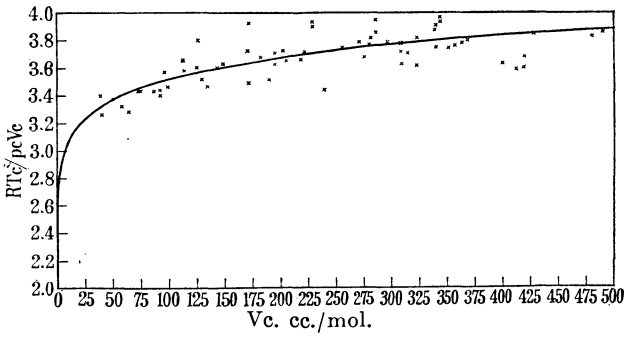

Fig. 1.—Relation between RT_c/p_cV_c and V_c for low dielectric substances.

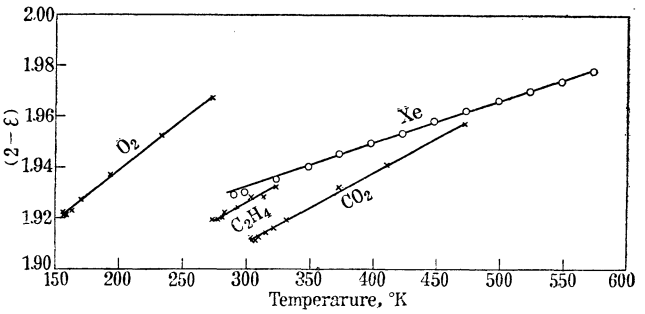

Fig. 2.—The temperature dependence of $(2-\varepsilon)$ for some gases.

here of course ε is its value at the critical point and V_c is expressed in cc.

Firstly, if we take the mean of ε from the results summarized in Table 4, relation (6) becomes

$$\frac{RT_c}{p_cV_c} = \frac{2}{3}(1+3V_c^{0.077}) \qquad (7),$$

which serves as an approximate formula. Δ's in Table 4 denote the percentage divergences from experiments and their mean value becomes ± 2.6 %. Also the relation between RT_c/p_cV_c and V_c is diagrammatically shown in Fig. 1, in which the curve is plotted by formula (7). Quite recently Himpan[6] put forward the empirical formula, $RT_c/p_cV_c = 2.92 + 1/3.\log(nM)$, where M is the molecular weight and n the degree of association, but its graphical test has shown that his formula is worse than formula (7).

Secondly, since the Boyle temperature is much higher than the critical temperature, relation $T_B = b/aR = 9p_cV_c/R$ derived from the van der Waals' equation may be allowable. Using this relation in conjunction with formula (7), there results

$$\frac{T_B}{T_c} = \frac{27}{2(1+3V_c^{0.077})} \qquad (8).$$

(4) International Critical Tables III, p. 4-19, 248-249.
(5) F. Henning, l.c., 34-40.
(6) J. Himpan, *Z. Physik*, **131**, 17 (1951).

Formula (8) gives concordant values with experiments: 2.70 (2.70), 2.60 (2.73), 2.58 (2.59), 2.57 (2.59), 2.56 (2.58) for Ne, A, N_2, CO, CH_4 respectively, the values in parentheses being the observed values.[7]

Thirdly, write equation (5) in the form

$$p=\frac{RT}{V-b}-\frac{a}{V^{2-\varepsilon}},$$

and differentiate with respect to T, remembering ε to be dependent on temperature,

$$\left(\frac{dp}{dT}\right)_V=\frac{R}{V-b}-\frac{a}{V^2}V^{\varepsilon}\log_e V\cdot\frac{d\varepsilon}{dT}.$$

Putting this in the thermodynamic relation, $(dp/dT)_c=[dp/dT)_V]_{T=T_c}$, we readily obtain

$$\frac{T_c}{p_c}\left(\frac{dp}{dT}\right)_c=\frac{3RT_c}{2p_cV_c}-3T_cV_c^{\varepsilon}\log_e V_c\cdot\left(\frac{d\varepsilon}{dT}\right)_c,$$

or replace from formula (7), it follows that

$$\frac{T_c}{p_c}\left(\frac{dp}{dT}\right)_c=1+3V_c^{0.077}-3\times 2.303T_cV_c^{0.077}\log_e V_c\left(\frac{d\varepsilon}{dT}\right)_c \qquad (9).$$

For example take CO_2 for which $T_c=304.2$°K., $V_c=44.01/0.460$ cc., $\varepsilon=0.082$ and $T_c/p_c\cdot(dp/dT)_c=7.14$[8] are given, $(d\varepsilon/dT)_c$ is evaluated to be -0.00029, or -0.00032 by the use of formula (9). These values agree well with the experimental value, $-(0.00028\pm0.0004)$, which has been obtained from the mean of $(2-\varepsilon)$ values at several isotherms: 1.912 (30.98°C., critical temperature), 1.916 (48.10°C.), 1.919 (57.75°C.), 1.935 (100°C.), 1.946 (137°C.), 1.969 (198°C.), 1.972 (258°C.).

As already stated, $3RT_c/8p_cV_c$ corresponds to the molecular association factor A at the critical point, so it follows from formula (6) that

$$A=(1+3V_c^{\varepsilon})/4$$

The numerical values of A lie from the lowest value of 1.22—1.29 for non-polar molecules such as Ne, He, A, Kr, N_2 and CO to the highest value of 1.47—1.49 for alkyl esters such as $CH_3CO_2CH_3$, $CH_3CO_2C_2H_5$ and $CH_3CO_2C_3H_7$. Although the former value, to whose class Br_2 and Hg belong, may be inconsistent with ordinary physicochemical knowledge of so-called normal liquids, yet it may be rather conceivable that non-polar association takes place at the critical point where gaseous and liquid states begin to coexist undoubtedly in a molecular aggregation different from the gaseous state, and that such association in the case of normal liquids may keep nearly constant for a wide range, from critical to ordinary temperatures.

(7) Adopted from E. A. Guggenheim's "Thermodynamics", p. 140.

(8) Adopted from S. Mizushima's "Physical Chemistry", III, p. 645.

Summary

(1) An equation of state in analytical form is proposed:

$$p+\frac{a}{V^{2-\varepsilon}}=\frac{RT}{V-b},\quad a=3p_cV_c^2,\quad b=V_c/3.$$

Values of $(2-\varepsilon)$ keep constant over a wide range of pressures of each isotherm. Taking the mean of $(2-\varepsilon)$ values at each isotherm, we obtain an equation of state which is more reasonable and accurate than the usual isothermal equation of algebraic form.

(2) Tests made with 66 kinds of substances having low dielectric constants prove that values of $(2-\varepsilon)$ at critical points are universal to give 1.923 ± 0.008.

(3) The following three formulae at the critical point are derived from the new equation in which V_c is expressed in cc./mol.

(i) $$\frac{RT_c}{p_cV_c}=\frac{2}{3}(1+3V_c^{0.077}),$$

(ii) $$\frac{T_B}{T_c}=\frac{27}{2(1+3V_c^{0.077})},$$

(iii) $$\frac{T_c}{p_c}\left(\frac{dp}{dT}\right)_c=1+3V_c^{0.077}-3\times 2.303T_cV_c^{0.077}\log V_c\cdot\left(\frac{d\varepsilon}{dT}\right)_c.$$

The first formula is concordant with $\pm2.6\%$ average divergence for 66 kinds of low dielectric substances and the two following are also equally concordant with the experimental data.

Addendum

The constancies of ε were found to be fairly good over a wide range of pressures at each isotherm. Their dependence on temperature, however, was left unsaid since there are but few favorable data from which a conclusion can be deduced.

Quite recently Beattie, Barriault and Brierley[2] reported on the compressibility measurements for gaseous xenon from the critical temperature to 300°C and over the density range of from 1 to 10 mol. per liter, and so by making use of their results we have had an opportunity to certify the linearity between ε and temperature which was already suggested in the case of CO_2.

For xenon we put $b=40.06$ cc. and $\log a=6.3993891$ calculated from their newly determined critical constants, $p_c=57.89$ atm., $d_c=8.32$ mol./liter, $T_c=16.65$°C.$+273.13$. The $(2-\varepsilon)$ values at every 50°C intervals from 25 to 275°C. are listed

(1) J. A. Beattie, R. J. Barriault, J. S. Brierley, *J. Chem. Phys.*, **19**, 1219 (1951).

Table 5

$(2-\varepsilon)$ for Xenon

mol./liter	$(2-\varepsilon)$					
	25°C.	75°C.	125°C.	175°C.	225°C.	275°C.
10.0	1.934	1.942	1.951	1.960	1.968	
9.0	1.935	1.942	1.951	1.959	1.968	1.977
8.0	1.934	1.942	1.951	1.959	1.967	1.976
7.0	1.932	1.941	1.950	1.958	1.967	1.975
6.0	1.930	1.940	1.949	1.957	1.966	1.974
5.0	1.928	1.939	1.948	1.957	1.965	1.973
4.0	1.926	1.938	1.947	1.956	1.964	1.972
3.0	1.926	1.937	1.947	1.955	1.963	1.971
2.0	1.927	1.938	1.948	1.956	1.964	1.972
1.0	1.931	1.942	1.951	1.959	1.966	1.974
Mean	1.930	1.940	1.949	1.958	1.966	1.974

Table 6

Percent Deviation from Experiments

mol./liter	$100\ (p_{calc.}-p_{obs.})/p_{obs.}$					
	25°C.	75°C.	125°C.	175°C.	225°C.	275°C.
8.0	−6.52	−1.66	−0.824	−0.396	−0.406	−0.473
7.0	−2.93	−1.35	−0.424	−0.073	−0.158	−0.164
6.0	−0.11	−0.10	−0.028	+0.163	+0.079	+0.024
5.0	+1.562	+0.525	+0.288	+0.377	+0.280	+0.213
4.0	+2.095	+0.805	+0.442	+0.493	+0.378	+0.328
3.0	+1.736	+0.724	+0.419	+0.443	+0.371	+0.321
2.0	+0.864	+0.346	+0.184	+0.259	+0.225	+0.205
1.0	−0.121	−0.162	−0.151	−0.034	−0.005	−0.011
Mean	1.99	0.709	0.345	0.258	0.228	0.217
(Beattie-Bridgeman's equation)	1.37	0.282	0.424	0.294	0.171	0.190

in, Table 5, and the percent deviations, 100 $(p_{calc.}-p_{obs.})/p_{obs.}$, from 1 to 8 mol. per liter, in Table 6. As seen from these tables, the constancies of $(2-\varepsilon)$ at respective isotherms are quite satisfactory and the average percent deviations are as small as those of the Beattie-Bridgeman equation of state (the last line in Table 6).

The variation of $(2-\varepsilon)$ with temperature is diagrammatically shown in Fig. 2, in which are also plotted those of CO_2, C_2H_4 and O_2 which were computed from the compressibility data already mentioned.

As to xenon, $(2-\varepsilon)$ is strictly a straight line over the whole range of temperatures. This relationship appears to be equally well for the other gases as judged from their graphical representations. So that we can conclude that the linearity:

$$\varepsilon=\varepsilon_c+c(T-T_c),\ \varepsilon_c,\ c=\text{consts.}$$

holds true so far as the present data are concerned. Here ε_c is not ε at the critical point but the mean at the critical isotherm.

The author is indebted to SCAP CIE at Sasebo for having made him possible by mail from Tokyo to read the Journal of Chemical Physics, October, 1951, in which Beattie, Barriault and Brierley published their compressibility measurements for xenon.

Sasebo Commercial Junior College,
Sasebo, Nagasaki

Rheology of Coal. II. Structure of Coal and Its Internal Viscosity at Audiofrequencies*

By Katsuya INOUYE

(Received July 7, 1952)

Introduction

Previous experiments on Young's moduli of coals by using a resonant frequency method[1] show that the elastic constant used as a measure of bond strength in solids describes the essential properties of coal in absolute units. A theory is proposed that coal is composed of independent molecules possessing similar crystallographic meaning and a more or less highly developed aromatic character, held together by van der Waals' forces of varying strength. These results also show that the experimental Young's moduli can be expressed by the equation,

$$E=E_0(1+K\phi) \qquad (1)$$

where, E=Young's modulus of the coal specimen, E_0=Young's modulus of "pure" coal molecules, ϕ=volume concentration of ash in the specimen, and K=a constant representing the degree of solvation. The values of E_0 and K are constants for each coal species and describe the properties of the coal. With a typical strongly-caking coal, the intermolecular forces would be expected to be small and at the same time the solvation of coal molecules by ash as skeleton should be most strong (see later). Furthermore, the physical meaning of the principal chemical theories for caking properties, i. e., the bitumen theory of F. Fischer et al.[2], or W. A. Bone and others[3] and also the gamma theory of R. V. Wheeler and his collaborators,[4] can be obtained from the Young's modulus measurements and a relationship between ash concentration and bitumen content. About the definition of caking, see Ref. 1.

If Equation 1 is valid, another linear function will exist between the internal viscosity and ϕ, because, theoretically Young's modulus and internal viscosity of solids containing "filler" show the same relationship respectively with filler volume concentration (Ref. 13 and 14). Also it may be possible to relate the phenomena of caking with viscosity measurements. With this in mind the experimental study measuring the internal viscosity at audiofrequencies by a vibration method were carried out.

Experimental

Although several experimental methods for measuring the dynamic properties of rubber-like solids[5] and tyre cord[6] have been described recently, they cannot be used with coal, because specimens of sufficient length are unobtainable and of differences in the rheological properties. Young's moduli of coal specimens can be measured with a crystal pick-up,[1] but this method is not adapted for the internal friction measurements, as the vibrational energy is characteristically dissipated by the Rochelle salt crystal. For the present purpose the author has constructed an apparatus as shown schematically in Fig. 1. The

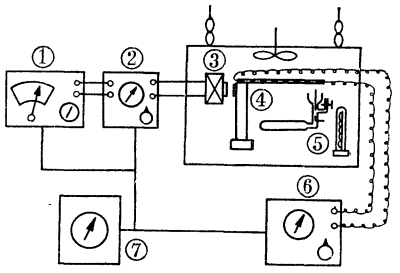

Fig. 1.—Experimental apparatus.
1. Oscillator 2. Amplifier 3. Magnet
4. Sample and Pick-up 5. Thermo-regulator
6. Amplifier 7. Voltage Stabilizer

* Presented at the Colloid Chemistry Symposium, Nov., 1950.

(1) K. Inouye, *J. Colloid Sci.*, **6**, 190, (1951).

(2) F. Fischer et al., *Brennstoff-Chem.*, **5**, 299, (1924), **6**, 33, (1925).

(3) W. A. Bone et al., *Proc. Roy. Soc. (London).* **A 105**, 608, (1924); *Trans. J. Soc. Chem. Ind.*, **44**, 291T, (1925).

(4) R. V. Wheeler et al., *Trans. J. Soc. Chem. Ind.* **103**, 1704, (1913), **109**, 707, (1916).

(5) S. D. Gehman, D. E. Woodford and R. B. Stambaugh, *Ind. Eng. Chem.* **33**, 1032, (1941); J. H. Dillon, I. B. Prettyman and G. L. Hall, *J. Appl. Phys.*, **15**, 309, (1944); A. W. Nolle, *J. Appl. Phys.*, **19**, 753, (1948); R. S. Witte, B. A. Mrowca and E. Guth. *J. Appl. Phys.*, **20**, 4881, (1949).

(6) W. J. Lyons and I. B. Prettyman, *J. Appl. Phys.*, **18**, 586, (1947).

Table 1

Descriptions of Samples

Sample	Origin	Classification	Caking Property	Volatile Matter, Mean Value (dry, ash-free basis)
American	U. S. A.	Bituminous	Strongly caking	35
Takashima	Kyushu, Japan	Bituminous	Strongly caking	38
Toro	Saghalien, U. S. S. R.	Bituminous	Weakly caking	46
Yubetsu	Hokkaido, Japan	Producer gas coal	Non-caking	64
Shosaku	China	Anthracite	Non-caking	7.7

calibrated audiofrequency oscillator sends alternating current from 50 to 10,000 c./sec. to the coil of an electromagnet through a power amplifier of 3.2 watt. Vibration of specimen with magnet and light iron plate cemented on the specimen opposite to the magnet is detected by "U-effect" of a capillary pick-up, and leads to the voltage amplifier of 55 decibels. The "U-effect" was recently discovered by S. Ueda and coworkers,[7] and is the electric voltage produced by mechanical vibration of a capillary within which are many mercury and electrolyte drops arranged alternately. The capillary pick-up used in these experiments has a length of several cm and diameter of approx. 0.4 mm., weighs about 0.1 g. including the leads and contains approx. 30 drops of mercury and 30 drops of 1N. H_2SO_4. The pick-up is cemented with bakelite cement to the top of the specimen. The specimen under examination is contained in a thermostat, regulated to 0.05°C., the thermostat being suspended by ropes and rubber cords in order to remove floor vibration.

The assembly of the supporter is important and it is found best to bury one end of the specimen in Portland cement clamping it carefully after the cement has solidified. All parts of the apparatus should be carefully shielded, the out-put of the amplifier being kept constant to avoid induction effect. The errors due to the additional mass at the top of the specimen and to the damping by air were considered to be sufficiently small to avoid consideration.

The specimens were shaped from coal blocks to the form of a rectangular bar with an accuracy of 1% in each dimension, using motor grinder and sandpaper or by grinding on a glass plate with carborundum. All specimens were cut parallel to the bedding plane.

The differential equation of the vibration of bar is assumed after K. Sezawa[8] as below,

$$\rho\frac{\delta^2 y}{\delta t^2}+E\kappa^2\frac{\delta^4 y}{\delta x^4}+\eta\kappa^2\frac{\delta^5 y}{\delta t\delta x^4}+\xi\frac{\delta y}{\delta t}=0 \qquad (2),$$

where, ρ = density of the sample, E = Young's modulus, η = coefficient of viscosity, κ = radius of gyration of cross section, and ξ = coefficient of friction by air. Resolving the above equation assuming the clamped-free bar vibration, E and η can be calculated[9] approximately as,

$$E=\frac{4\pi^2\rho n^2 l^4}{\kappa^2 m^4} \qquad (3), \text{ and}$$

$$\eta=\frac{2\lambda n\rho l^4}{\kappa^2 m^4} \qquad (4),$$

where, n = resonant frequency, l = length of the specimen, m = a factor corresponding to the mode of vibration, and λ = logarithmic decrement. If the amplitude (out-put voltage of the pick-up) is plotted as a function of the frequency, the familiar resonance curve is obtained. Taking the half value breadth of the curve as Δn, the logarithmic decrement, λ, can be easily calculated according the theory of damping vibration in the first approximation as,

$$\lambda=\frac{\pi}{\sqrt{3}}\frac{\Delta n}{n} \qquad (5).$$

From Equation 4 and 5, η can be calculated from the measurable values of n, Δn, ρ, l and the thickness of specimen. Using small specimens of coal, only the first fundamental mode of vibration can be detected, so "m" is always 1.875.

Results and Discussions

Filler Effect of Ash.—The internal viscosity values were obtained using specimens with various ash contents of five typical coals, as shown in Table 1.

The rectangular bar specimen was at first set in another apparatus for measuring the Young's modulus from the fundamental flexural resonant freqnency,[1] and then, as previously described, buried in the Portland cement, set in the thermostat of 30.0°C. and the resonance curve was measured repeatedly until constant values of n and Δn were obtained. Thus the Young's modulus calculated by Equation 3 from the clamped-free vibration was compared with the value calculated from the flexural vibration method to check the correct mode of vibration, as the flexural vibration method has better accuracy. The results for the Young's modulus are in Reference 1. As

(7) S. Ueda, F. Tsuji and M. Watanabe, *Bull. Inst. Chem. Research, Kyoto Univ., Japan*, **18**, 108, (1949), **19**, 44, (1949), **20**, 28, (1950).

(8) K. Sezawa, *Rep. Aeronautical Res. Ins. Tokyo Univ., Japan*, No. 45, (1928).

(9) K. Sezawa and K. Kubo, *J. Appl. Phys, Japan*, **1**, 1, (1932); Y. Tani, *J. Appl. Phys. Japan*, **9**, 372, (1940).

described in a later section, the damping properties of coal are markedly influenced by the resonant frequency, so η was measured at about 1400 c./sec. by adjusting the dimensions of the specimen. Some dependence of η on moisture is supposed, but on this point no information was obtained from this apparatus.

The relation between η and ϕ, calculated under the assumption that the density of ash is 2.0, and that of pure coal is 1.2, is shown in Fig. 2.

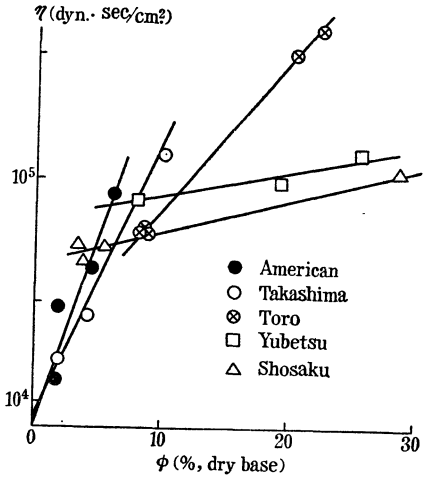

Fig. 2.—Internal viscosity and ash volume percentage.

It is noteworthy, as proposed in the introduction, that η is a linear function of ϕ,

$$\eta=\eta_0(1+K'\phi) \qquad (6),$$

where, η_0 = internal viscosity of pure coal, and K' = a factor representing the solvation of coal molecules with ash. Relation of the same form as Equation 6 has been proved theoretically on dilute suspension by A. Einstein,[10] E. Guth and R. Simha,[11] W. Kuhn[12] and others, and also on solid with filler by E. Guth and O. Gold[13] and E. Guth.[14]

Table 2

Values of η_0 and K'

Sample	η_0 dyn. sec. cm.$^{-2}$	K'	E_0 dyn. cm.$^{-2}$	K
American	1×10^3	16	1.8×10^{10}	38×10^{-2}
Takashima	3×10^3	3.5	2.0×10^{10}	20×10^{-2}
Toro	2.3×10^4	2.7×10^{-1}	3.6×10^{10}	7×10^{-2}
Yubetsu	8.4×10^4	1.0×10^{-2}	4.5×10^{10}	13×10^{-2}
Shosaku	6.8×10^4	1.3×10^{-2}	7.0×10^{10}	-2×10^{-2}

Table 2 describes two constants η_0 and K' characteristic to each coal as well as E_0 and K in Equation 1 from Reference 1. The magnitude of E_0 and η_0 and also of two "solvation factors" K and K' change in the same order, and this fact appears to support the theory and the ash skeleton models of coal structure as illustrated in Reference 1.

The caking properties of coal correspond naturally to the weakness of intermolecular forces as well as strong solvation with inorganic ash portion, namely the molecules of the caking coal become mobile at some elevated temperatures for their weak attraction and thermal stability, by the plasticizer effect of the nonsolvated molecules, in contrast to the non-caking coal molecules which decompose before such plastic condition is accomplished because of their too strong intermolecular forces.

Plasticizer Effect of Bitumen.—The bitumen is the fraction of coal molecules held together with weak van der Waals' forces so as to be extracted by benzene at 300°C. in an autoclave. The points of the chemical theories of caking properties have been that the bitumen is necessary to the caking coal[2] and that its relative relationship to residual parts is important.[3]

The author has shown[1] a relation between ϕ and bitumen content B (in %, dry, ash-free base) applicable to all bituminous coals, i. e.,

$$\phi=\frac{7.5\times10^3}{B^2} \qquad (7).$$

Substituting ϕ of Equation 6 by ϕ of Equation 7, a relation between η and B is obtained. Thus using the values of η_0 and K', η can be calculated for corresponding experimental B values. Table 3 shows calculated viscosity values compared with the measured values.

The bitumen content was determined on the same specimens previously used for measuring the internal viscosity. The specimen was powdered to pass 60 Tyler mesh sieve, dried one hour at 105°C., weighed, and five grams of the sample and 100 cc. of pure benzene were put in an autoclave. The autoclave was shaken automatically throughout the extraction, heated electrically up to 300°C. in 2.5 hours and retained at this temperature for 3 hours. The pressure was about 50 atmospheres. The extracted sample was washed with benzene in a Soxlet apparatus and then dried. The bitumen content was calculated from the difference of ash contents between the original and this extracted sample, assuming that no ash was moved into the bitumen. Fig. 3 shows the relationship between B and experimental η values.

As the relation between Young's modulus and B,[1] these results suggest the physical meaning of chemical bitumen theories, namely on one hand the plasticizer effect of bitumen molecules remarkably reduces the rheological values and on the other hand, perhaps, the importance of relative nature with residue. For instance, Toro (weakly caking) coal has lower bitumen content

(10) A. Einstein, *Ann. Phys.*, **19**, 289, (1906); **34**, 591, (1911).
(11) E. Guth and R. Simha, *Kolloid-Z.*, **74**, 147, (1936).
(12) W. Kuhn, *Kolloid-Z.*, **62**, 269, (1933); **68**, 2, (1934).
(13) E. Guth and O. Gold, *Phys. Rev.*, **53**, 322, (1938).
(14) E. Guth, *J. Appl. Phys.*, **16**, 20, (1945).

Table 3

Calculated and Experimental Viscosity

Sample	η_0 dyn. sec. cm^{-2}	K'	B, %	η_{calc}	$\eta_{exp.}$
American	1×10^3	17	36.67	9.6×10^4	9.4×10^4
			55.63	4.2×10^4	4.8×10^4
			70.00	2.7×10^4	1.9×10^4
Takashima	3×10^3	3.5	24.30	1.4×10^5	1.1×10^5
			35.72	6.5×10^4	4.5×10^4
			50.53	3.4×10^4	2.7×10^4
Toro	2.3×10^4	2.7×10^{-1}	8.77	6.3×10^5	1.5×10^5
			15.63	2.1×10^5	8.0×10^4
			21.37	1.2×10^5	7.8×10^4
			32.60	6.7×10^4	7.8×10^4

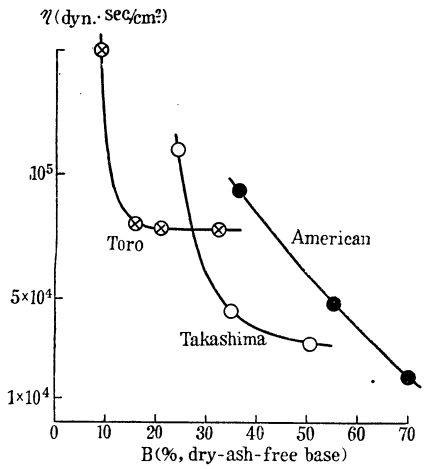

Fig. 3.—Internal viscosity and bitumen content

even in its saturation state, at higher viscosity values, in other words, the bitumen in this coal is less effective as plasticizer, and it is suggested that improvement of the relation between bitumen and residue (or, of some inner condition) is necessary, before the coal is used as better caking coal.

Dependence of Frequency and Temperature.—To elucidate the dependence of internal viscosity on frequency, three typical specimens of American strongly-caking coal, Yubetsu producer gas coal and Shosaku anthracite were selected, the dimensions of which were large enough at first for taking η values of the same specimens at various resonant frequencies by changing the dimensions occasionally. Such measurements were carried out at 30.0, 45.0, 60.0 and 70.0°C. The measurable frequency range was from ca. 400 to 950 c./sec. Detailed values are ommitted from this paper for the limitation of approved space of this Bulletin.*

At each temperature, E and η decrease with increasing frequency. At any given frequency, η of the strongly-caking coal decreases more markedly with increasing temperature, than of the producer gas coal and the anthracite. E does not decidedly change within this range of temperature.

There is at present no theoretical basis, using a relaxation distribution function, to interpret this dispersion. However, at least qualitatively, the decrease of η of the caking coal even in such low temperature range seems to be interesting as to characterize its rheological properties. Taking η values of the American coal for four different temperatures at 600 c./sec. on the graphs, an activation energy is about 1 kcal./mol., calculated by the Andrade formula,[15]

$$\eta = Ae^{U/RT} \qquad (8),$$

where, U = Activation energy of viscosity, T = Absolute temperature, R = Gas constant, and $A = a$ constant. It may be interesting to note that the activation energy of viscosity is slightly lower than the energy of thermal motion, RT, at caking temperature, say ca. 1.4 Kcal./mol. at 450°C., provided the activation energy is constant up to such high temperatures.

Although the author has to state that much theoretical and experimental work should be carried out before further detailed discussions can be done, he suggests that the caking properties are due chiefly to the remarkable decrease of friction in the viscosity element, with low activation energy, instead of thermal stability of *intra*micellar conditions, i. e., the whole system, when the temperature is elevated, fuses and swells by low viscosity of bitumen (or, more freely combined) molecules as plasticizer when the micells, in which the molecules are more strongly combined by the solvation forces with ash portion, exist presumably unchanged. This condition is expected to be accomplished more easily than when all molecules in the system have to become mobile.

The author acknowledges with sincere thanks the enthusiastic assistance of Hideo Tani, and

* The results are given in the Reports of the Fuel Research Institute, No. 66, Nov., 1952

(15) E. N. Andrade, *Nature*, **125**, 580, (1930).

Mitsuo Abiko during the investigation. He is also indebted to Dr. T. Shimmura, Dr. M. Kurokawa and Mr. A. Baba (this Institute) for their interest in this work. Thanks are expressed to Dr. H. Marsh (King's College, Univ. of Durham) for revising the manuscript.

Shigen-Gijyutsu-Shikenjo (Resources Research Institute) Saitama-Kawaguchi, Japan

Studies of Crystalline Hydrates. II. Thermal Transition and Dehydration of Ni-, Fe-, Co-, Zn-, Mn-, and Mg-sulfate Hydrates

By Hideaki CHIHARA and Syûzô SEKI

(Received June 28, 1952)

Introduction

The studies of the dehydration of crystal hydrates are of basic significance for clarifying the nature of the interaction between water and various materials on one side, and the mechanism of the typical hetero-phase reaction involving solids on another side, particularly in the cases in which atomic structures of the crystals are accurately known. Although numerous investigations have been made on the solubility of the hydrates for their successive degrees of hydration,(1) on the dissociation pressures and on the decomposition-reaction mechanisms,(2) there still remain much to be investigated from their atomistic and energetic points of view. Recently, the magnetic susceptibility measurement of hydrates containing paramagnetic ions and the nuclear magnetic resonance absorption studies of the crystal water have interested the physicists.(3) In these respects, it would be desirable to study the dehydration processes and the behavior of water molecules in hydrates in greater detail.

Although the method of the thermal analysis has been used by many investigators for the study of dehydration process, the detailed experiment in relation to the crystal structure, as far as the authors are aware, is only that of copper sulfate pentahydrate measured by Taylor and Klug.(4) We have applied the differential thermal analysis further to Ni sulfate hydrate, typical of known crystal structure, and other related hydrates under various conditions in order to elucidate their dehydration processes and also whether or not these crystals undergo transitions similar to those of $CuSO_4 \cdot 5H_2O$ which are considered to be attributed to the rotation of water molecules.

Experimental

Materials.—$NiSO_4 \cdot 7H_2O$.—The product of Kahlbaum Co. was recrystallized from an aqueous solution at about 0°C. and the excess water in the precipitate was removed by pressing it between filter paper and then dried in a desiccator containing the same hydrate partially dehydrated as a desiccating material. This procedure of drying was adopted for all of the samples mentioned below.

$ZnSO_4 \cdot 7H_2O$.—The product of Kahlbaum Co. was recrystallized from aqueous solution at about 0°C.

$MgSO_4 \cdot 7H_2O$.—The product of Merck Co. was recrystallized from aqueous solution at about 0°C.

$FeSO_4 \cdot 7H_2O$.—The product (extra pure) of Katayama Co. was recrystallized from slightly acidic solution at about 0°C.

$CoSO_4 \cdot 7H_2O$.—The product (extra pure) of Ishizu Co. was recrystallized from aqueous solution at about 0°C.

$MnSO_4 \cdot 7H_2O$.—The product (extra pure) of Ishizu Co. was recrystallized from an aqueous solution at about 0°C.

$NiSO_4 \cdot 6H_2O$.—The hexahydrate was prepared either by crystallizing from an aqueous solution

(1) N. V. Tanzov, *J. Russian Phys.-Chem. Soc.* **55**, 335 (1924); A. Chretien and R. Rohmer, *Compt. rend.* **198**, 92 (1934); H. H. Ting and W. L. McCabe, *Ind. Eng. Chem.* **26**, 1207 (1934); R. Rohmer, *Compt. rend.* **210**, 669 (1940); J. H. Krepelka and B. Rejha, *Coll. Czechoslovak. Chem. Com.* **5**. 67 (1933); F. Fraenckel. Z. *anorg. Chem.* **55**, 223 (1939).

(2) "Chemical Reactions involving Solids", Discussions of the Faraday Society, 1938; E. G. Prout and F. C. Tompkins, *Trans. Faraday Soc.* **41**, 488 (1945).

(3) J. Wheatley and D. Halliday, *Phys. Rev.* **75**, 1412 (1949); G. E. Pake, *J. Chem. Phys.* **16**, 327 (1948).

(4) T. I. Taylor and H. P. Klug. *J. Chem. Phys.* **4**, 601 (1936).

at about 40°C. or dehydrating the heptahydrate. All these samples were stored in the desiccators during various periods of time to examine the aging effect.

Apparatus and Procedures.—The apparatus used for the differential thermal analysis was the same as that previously reported,[5] so a brief comment may be given here. As shown in Fig. 1, A is a copper block with two drilled holes, in

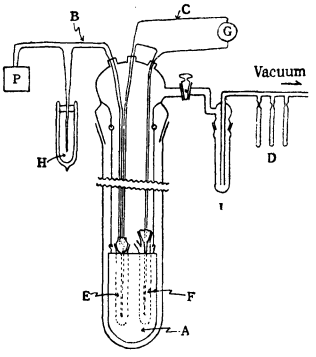

Fig. 1.—A schematic diagram of the apparatus for differential thermal analysis.
E: a reference cell containing NaCl;
F: a sample tube; G: a galvanometer;
H: the standard temperature (ice);
I: a liquid air trap; P: a potentiometer.

each of which a thinwalled glass tube is fitted: one contains NaCl as a standard material and the other the sample to be investigated. B and C are copper-constantan thermo-couples for the measurements of temperature of NaCl and of temperature difference between the sample and NaCl, respectively. In order to determine the water content of the samples, the capillary tubes D are used for collecting water vapor produced by decomposition. The water content at successive stages of dehydration is measured by the following procedure. After the completion of a stage of dehydration which is shown by the restoration of increased temperature difference to its normal steady state value, the heater is turned off and the cell system is pumped off slowly to condense the dehydrated water in a liquid air trap I. The temperature difference between the sample and NaCl is again on the increase by the self-cooling of the sample due to the evaporation of liberated water. As the amount of liberated water in the sample tube decreases, the deflection of the galvanometer for the differential thermo-couple stops increasing and then begins to decrease. As soon as this decrease turns to increase again on account of the beginning of the next step of dehydration, the pumping is stopped and dry air is introduced into the whole system to prevent further dehydration. The collected water is then led

(5) I. Nitta, S. Seki, and H. Chihara, *J. Chem. Soc. Japan, Pure Chem. Sect.* **70**, 387 (1949).

Table 1

Determination of Water Content of Nickel Sulfate Hydrates

Initial wt.	Loss of wt. at the transition or dehydration points.		
Room temp.	86°	110°	132°
0.829 g.	0.009 g.	0.115 g.	0.160 g.
	Loss of water. mole/mole of $NiSO_4$		
	≈0	2.09≈2	2.82≈3

to one of the capillary tubes D and the amount of water is weighed after the tube is fused off. As an example, data for $NiSO_4 \cdot 6H_2O$ are given in Table 1. In every run, the sample was heated at a constant rate of 0.6 to 1.5°C. per minute under atmospheric pressure, unless otherwise stated. The X-ray powder photographs were taken by copper Kα radiation. To examine the structure change at the transition temperature, a high-temperature camera was employed.

Experimental Results.—(I) **Differential thermal analysis:**

One of the typical temperature-time curves is illustrated in Fig. 2. The whole results under different conditions for various samples are given in Figs. 3 to 8 in which the positions of the vertical lines represent the dehydration or transition temperatures and their length means an approximate value of the heat effect. The diffuse band stands for a transition or a dehydration ranging over a temperature interval. The downward band is for the evolution of heat. Ordinates show the temperature scale in t°C. (Fig. 2 corresponds to Fig. 3c). Dotted vertical lines show

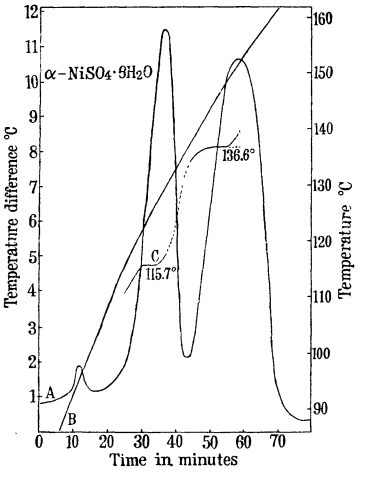

Fig. 2.—An example of differential thermal analysis.
A: Temperature difference between the sample and NaCl. (left scale)
B: Heating curve of NaCl. (right scale)
C: Heating curve of the sample which is drawn by subtracting A from B. (right scale).

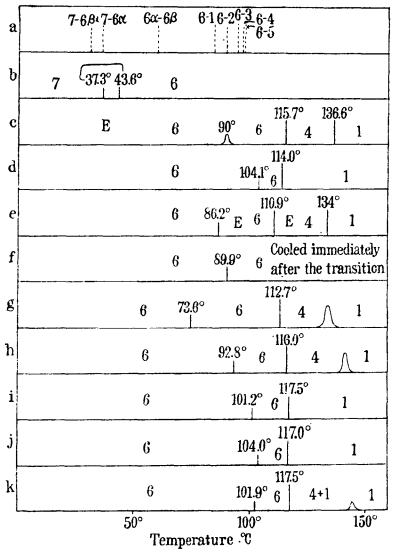

Fig. 3.—Differential thermal analyses of nickel sulfate hydrates. "E" stands for evacuation and admission of dry air. Time of storage of samples is as follows:
(b) 80 d. As to the two peaks, see in the text.
(c) 1 d. Continuation of (b).
(d, e, f) 13.5 m.
(g) Continuation of (f).
(h) 25 d. A week after grinding.
(i) 3.5 m. Immediately after grinding.
(j) 6 m. Unground sample.
(k) 6.5 m. Coarsely crushed sample.
(e, f, g, h) and (i, j, k) are two groups of specimens, each being parts of the same samples, respectively. d. = days, m. = months.

the transition or dehydration temperatures of hydrates in aqueous solutions determined from the solubility curves.[1] Fig. 3e corresponds to the experiment for determining the degrees of hydration given in Table 1.

(2) **X-ray powder photographs:**

Since the complete analysis of the crystal structure has been reported only for α-$NiSO_4 \cdot 6H_2O$ and $NiSO_4 \cdot 7H_2O$, we have applied the X-ray identification method only to these materials. The observed Debye line diagrams under various conditions are given in Fig. 9. Fig. 9e shows the reference positions calculated from the known crystal structure data of α-$NiSO_4 \cdot 6H_2O$ determined by Beevers and Lipson.[6]

Discussion of Results

(a) **Comparison of the dehydration temperatures determined from the differential thermal analysis with those from the solubility curves.**

It should be noted that the dehydration and the transition temperatures determined by these two methods have, in general, different meanings,

(6) C. A. Beevers and H. Lipson, *Z. Krist.* **83**, 123 (1932).

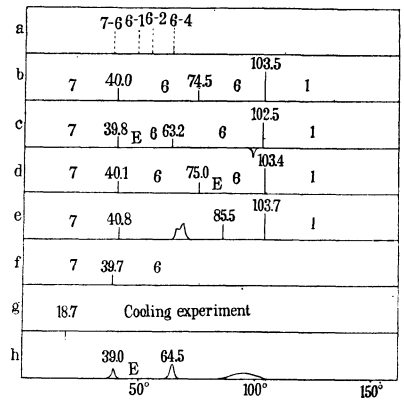

Fig. 4.—Differential thermal analysis of $ZnSO \cdot 7H_2O$.
(b) 15 m.
(c) 16.5 m. At 98°, a heat evolution is observed.
(d) 18.5 m. (e) 30.5 m. (f) 30.5 m.
(g) Continuation of (f), Cooling curve.
(h) Continuation of (g), A month after (g).

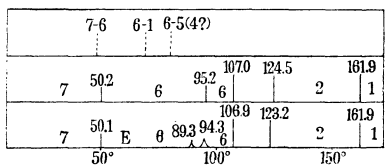

Fig. 5.—Differential thermal analysis of $MgSO_4 \cdot 7H_2O$.

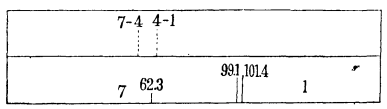

Fig. 6.—Differential thermal analysis of $FeSO_4 \cdot 7H_2O$.

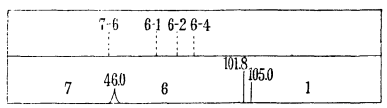

Fig. 7.—Differential thermal analysis of $CoSO_4 \cdot 7H_2O$.

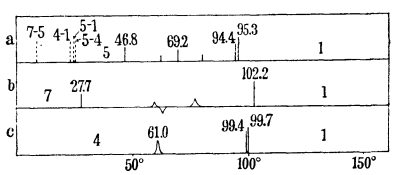

Fig. 8.—Differential thermal analysis of $MnSO_4$ hydrates.
a) Pentahydrate, b) Heptahydrate, c) Tetrahydrate.

i. e. the material subjected to the thermal analysis belongs to an open system, so that the existing phases are not absolutely in their equilibrium state, whereas in an aqueous solution the various phases in contact are in the true equilibrium state. Taking this situation into account, comparisons are now made of the transition temperatures in Figs. 3 to 8. In the case of Mn sulfate, none of the dehydration temperatures in the present study coincides with those obtained from the solubility curve, but in other hydrates the first step of dehydration (7—6) nearly agrees in both methods and this is particularly confirmed with Ni sulfate, in which case the dehydration temperature (43.6°C.) in the first run is shifted to lower temperature (37.3°C.) in the next repeated run, the second one being in perfect agreement with the dehydration temperature (heptahydrate→β-hexahydrate) in the aqueous solution (Fig. 3b). The solubility curve of hexahydrate, when temperature is raised, intersects with that of monohydrate first and then those of di-, tri-, tetra-, and penta-hydrates successively if they can exist. Hence, the lower hydrates are more stable than the higher ones in the aqueous systems (see, for instance, Fig. 3a). However, the situation is entirely different in an open system.* In raising temperature, the hexahydrates are dehydrated to form lower hydrates in just the opposite order from that in the open system. And none of the dehydration temperatures coincides in these two processes of dehydration. In aqueous solutions, the stable modification of nickel sulfate between 31.5 and 60°C. is the α-hexahydrate (6α), and it is this modification that first appears in the dehydration of the heptahydrate in the aqueous system. But in the dry system, as is shown in Fig. 3b, the transition from the heptahydrate to β-hexahydrate (6β) does take place first, which is evident by the coincidence of the dehydration temperatures in the dry and the wet systems at 37.3°C. A possible explanation of this apparent coincidence may be that a small amount of liberated liquid water causes a more or less similar situation to the wet system although the transformation to 6α from 6β is not admitted on account of the slow velocity of its nucleation. The fact that the unstable β-phase appears first is already reported by Simon and Knauer[7] and is also ascertained by our X-ray photographs. This fact, together with the phenomenon that the unstable dehydration products appear in reverse order in comparison with the result obtained from the solubility studies, may be explained by the so-called "rule of successive transformation[8]."

(b) **Dehydration stages and the phase transitions without accompanying dehydration.**

As mentioned above, prior to its first dehydration, $CuSO_4 5H_2O$ undergoes phase transitions which may be attributed to the rotation of water molecules according to Taylor and Klug.[4] As expected, similar transitions were found in the present investigation in some of the hydrates examined. The present discussion, with reference to its dehydration process, will be mainly concerned with the case of nickel sulfate which was studied in greatest detail. The β-form of hexahydrate produced by the first decomposition of heptahydrate changes spontaneously and slowly to 6α and circumstantially to tetrahydrate, so that the product initially obtained by heating heptahydrate, consisting of a mixture of 6β and heptahydrate, changes to a mixture of 6β, 6α and tetrahydrate even at a constant temperature as the decomposition proceeds. Fig. 9a corresponds to the mixture of heptahydrate and 6β containing possibly minute amount of 6α. Fig. 9c contains no heptahydrate and consists of 6β and a trace of 6α, while Fig. 9b consists mainly of 6α and a small amount of 6β. Thus, these three figures are considered to represent the main features of the successively transformed products of the heptahydrate, respectively. Although there remains a possibility that the last two figures contain traces of tetrahydrate, it was not ascertained on account of the difficulty of taking a Debye photograph of pure tetrahydrate. Further heating of the hexahydrate leads to a phase

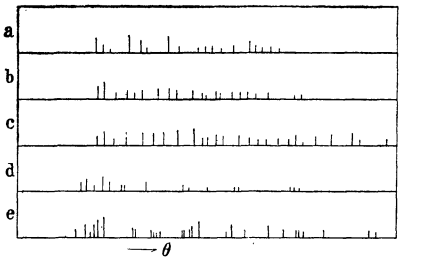

Fig. 9.—Debye photographs of nickel sulfate hydrates.

a) heptahydrate, b) α-hexahydrate,
c) β-hexahydrate (green part of the specimen formed by the dehydration of the heptahydrate),
d) γ-hexahydrate at 100°C. (Fig. 3h),
e) α-hexahydrate (Ref. 6).

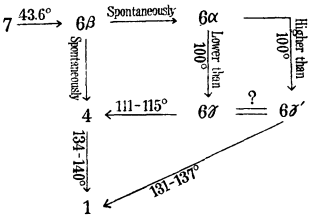

Fig. 10.—A schematic diagram correlating various modifications of nickel sulfate hydrates.

* It may be noticed that water produced in the first step of dehydration would dissolve a part of the hexahydrate, and lower hydrate than hexahydrate would be present before the second step of dehydration takes place.

(7) A. Simon and H. Knauer, *Z. anorg. allg. Chem.* **242**, 375 (1939).

(8) R. S. Bradley, *Quarterly Rev.* **5**, 323 (1951).

transition accompanying no dehydration.* This transition temperature varies very sensitively depending on the external conditions as well as on the history of the sample; that is, these temperatures range from 70.5 to 117°C. as shown in Fig. 3. Althongh a similar state of affairs is also reported in the case of $CuSO_4 \cdot 5H_2O$, detailed conditions governing it are not clearly described.[4] It is confirmed by the Debye photograph at about 100°C. that 6α changes its crystal structure at the transition point (Fig. 9 d). And it was also found that this transition is completely reversible by both the X-ray method and the differential thermal analysis (Fig. 3 f, g). It is interesting to note here that when 6α was coarsely crushed or was stored long (longer than a few months), the transition temperature is always a few degrees higher than 100°C. and on top of that the stage of tetrahydrate does not appear (see Fig. 3 d, i, j). On the other hand, the sample, finely powdered or not stored long, undergoes transition at a lower temperature and always goes through the stage of tetrahydrate (see Fig. 3 c, e, g, h). In Fig.3 k, is given the intermediate case between these two. The reason for such behavior is not yet clear, but it is very plausible to assume that a trace of tetrahydrate which may be present after grinding or short-time storing acts as a self-catalyst for the growth of the phase of tetrahydrate. Fig. 10 illustrates schematically the various phases of nickel sulfate hydrates, in which 6γ (or 6γ') denotes the phase found by the present study which is formed by the transition below (or above) 100°C. These two phases, 6γ and 6γ', may be identical with each other although there is no direct proof about it.*

In the cases of other hydrates, phase transitions without dehydration were also found at 62—85° for $ZnSO_4$, 89—95° for $MgSO_4$, and 60—85° for $MnSO_4$. In every case, these temperatures are sensitively influenced by the external conditions and the sample's history similarly to that of Ni salt. These results together with the dehydration stages are given in Figs. 4 to 8. It is of interest to note that there exists the dihydrate of magnesium sulfate which has hitherto been unknown at least in an open system. In all cases the final stages of hydration at the highest temperature examined are monohydrates.

(c) **Effect of evacuation, heat evolution, rehydration and aging effect.**

The effect of evacuation was also examined upon the dehydration and transition temperatures as well as upon the velocity of transition from an amorphous to a crystalline state. Generally, the temperature of dehydration is not so influenced by this treatment as the transition temperature. The heat evolution effect, which may be due to transformation of an amorphous, unstable, skeleton formed after dehydration to stable crystalline state, has recently been remarked by several investigators in the cases of $CuSO_4 \cdot 5H_2O$, $ZnSO_4 \cdot 7H_2O$, and $MnSO_4 \cdot 4H_2O$ by Khomyakov,[9] Mn-oxalate dihydrate by Volmer and Seydel,[10] and $ZnSO_4 \cdot 6H_2O$ and $CuSO_4 \cdot 5H_2O$ by Frost, et al.[11] Similar effects have been found in the present investigation in $ZnSO_4 \cdot 7H_2O$ at about 100°C. and in $MnSO_4 \cdot 7H_2O$ at about 65°C., the latter of which occurs even without previous evacuation (Fig. 8 b). It may be worthwhile to note that in the case of $ZnSO_4 \cdot 7H_2O$ the effect of evacuation which gives rise to evolution of heat is revealed at the temperature just below the second dehydration point after the transition (63.2°C.) is over, prior to which it has been evacuated (see Fig. 4 c).* Finally, a brief comment may be given on the experiment of rehydration for $ZnSO_4 \cdot 7H_2O$. When this substance is heated up to about 40°C. and then cooled, the evolution of heat is observed, which is attributed to the rehydration (Fig. 4 f, g). This may be explained either by the reaction

$$ZnSO_4 \cdot 6H_2O + H_2O = ZnSO_4 \cdot 7H_2O$$

or by the reaction

$$6(ZnSO_4 \cdot 6H_2O) = 5(ZnSO_4 \cdot 7H_2O) + ZnSO_4 \cdot H_2O$$

which can be predicted from the measurements of dissociation pressures.[12] The authors are for the latter interpretation since repeated heating and cooling procedure across this dehydration point results in the dehydration of more than one mole of water per mole of the heptahydrate (Fig. 4 h). The aging effect due to storing the sample for a long time is very complicated. Although, to date, no definite conclusion can be drawn about it, it may be said that the transition temperatures are much more influenced than the dehydration temperatures.

The authors wish to express their grateful thanks to professor Nitta for his encouragement and valuable suggestions during this work. The cost of this research has been defrayed from the funds of Taniguchi Kôgyô Shôreikai as well as from the Scientific Research Encouragement Grant from the Ministry of Education to which the authors' thanks are due.

Department of Chemistry, Faculty of Science, Osaka University, Osaka

* The evidence of no dehydration at the transition point is given in Table 1.

** The shift of the transition temperature of Fig. 3 j to Fig. 3 k and the simultaneous appearance of the small hump indicating the existence of the tetrahydrate may be regarded as a proof of this identity.

(9) K. C. Khomyakov, *J. Phys. Chem.* (*U. S. S. R.*) **11**, 805 (1938).

(10) M. Volmer and G. Seydel, *Z. physik. Chem.* A **179**, 153 (1936).

(11) G. B. Frost, K. A. Moon and E. H. Tompkins, *Can. J. Chem.* **29**, 604 (1951).

(12) L. C. Copeland and O. A. Short, *J. Am. Chem. Soc.* **62**, 3285 (1940); See also R. E. Barieau and W. E. Giauque, ibid. **72**, 5576 (1950).

* It is known that in the case of $ZnSO_4 \cdot 6H_2O$ the velocity of transformation from amophous to crystalline state depends on the water vapor pressure and has a maximum around pressure of 0.95 mm.Hg (Ref. 11).

Analysis of High Molecular Substances by Chromatography. I. Paper Chromatography of Polyethylene Oxide

By Sanshiro KUME, Tai YAMAMOTO, Kiyoteru OTOZAI, and Shouzow FUKUSHIMA

(Recived July 28, 1952)

Introduction

Studies of the molecular weight distribution of a variety of high polymers, which would be highly interesting, are at present impracticable because of the limitations and tediousness of conventional fractionation procedures. The recent success of paper chromatography in the separation of closely related chemical species in the fields of the organic and inorganic chemistry and the brilliant result of chromatographic "frontal analysis" of high polymers by S. Claesson,(1) together with its defects, have directed our attention to the possibility of applying paper chromatography to the analysis and fractionation of high polymers, referring to the case of partition chromatogaphy of nitrocellulose suggested by M. C. Brooks and R. M. Badger.(2)

The principal difficulties encountered in chromatography of high polymers are supposed to be: (1) difficulty in detection of the chromatograms, because polymers have in general neither color nor color reaction, (2) difficulty in the development under the condition of equilibrium of the solute between the fixed and mobile phases, because the velocity of establishing the equilibrium of high polymers is in general very slow compared with the ordinary flow rate of the developing solvent, (3) difficulty in preventing the unexpected disturbance of the solvent flow, which makes the chromatographic separation imperfect, especially in case of high polymers consisting of the continuous homologues. Overcoming these difficulties mentioned above, S. Claesson has first succeeded in the adsorption chromatography of polymers employing the frotal analysis of Tiselius. The results obtained, however have some defects related to the chromatography of adsorption type and especially to frontal analysis of homologues. That is, there is no determinate means to know whether the distribution in molecular weights is the only factor which dominates the distribution of polymer species suggested by the chromatograms obtained and the method, although very useful for analytical purposes, seems unavailable for fractionating purposes of polymers.

We have chosen polyethylene oxide of relatively low molecular weight as the first example of the hydrophilic polymers, and investigated the chromatographic separation with the use of the usual technique of paper chromatography. The difficulties and defects mentioned above have been overcome by a new technique of color development of polyethylene oxide, the selection of a suitable developing solvent, and the general features of paper chromatography.

Experiment

(A) Sample: Commercial polyethylene oxide, "carbowax 1,000", "carbowax 4,000" and "carbowax 6,000" of Carbide and Carbon Chemicals Corp. without special purification were used as the fractionated polyethylene oxide samples, which have the general properties as shown in Table 1.

Table 1

Properties of Carbowaxes

Name	Freezing Rrange (°C.)	Solubility in Water (% by weight)
Carbowax 1,000	35—40	70
〃 4,000	50—55	62
〃 6,000	58—62	50

Before the preparation of the sample solutions the crushed samples were dried for seven days ("1,000") and three days ("4,000" and "6,000") in a desiccator over calcium chloride to constant weights because they are somewhat hygroscopic.

(B) Development: With the use of micropipette 0.5 μl. of 2% aqueous solution of carbowax was put in the diameter of 3-5 mm. on filter paper strip (Toyo Roshi No. 3, for the quantitative analysis, 45 cm.×1 cm.), which beforehand has been dried for one day in a desiccator over calcium chloride in order to hold the constant amount of adsorbed water and to make the developed spot sharper. The position of the original

(1) S. Claesson, *Arkiv Kem. Mineral. Geol.*, **26** A, No. 24, 1 (1949).

(2) M. C. Brooks and R. M. Badger, *J. Am. Chem. Soc.*, **72**, 1705 (1950).

spot was 8 cm above the surface of the developing solvent when set up in the apparatus, at which the flow rate of the solvent becomes stationary. Six strips were placed in a desiccator over calcium chloride until the original spot dried up and set up in the apparatus[3] as shown in Fig. 1, which was held in the thermostatt of

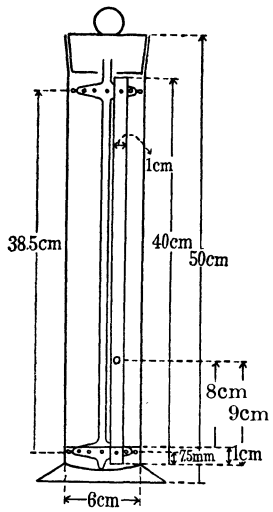

Fig. 1.—Apparatus for development.

25±0.1°C, and developed upwards with solvent for 4-6 hrs. making the distance between the solvent front and the position of the original spot 12-15 cm. The longer time interval between the putting of the sample on the paper and the development has a tendency to leave more parts of the sample of higher molecular weight at the original point.

(C) Color development: The strips developed were dried in room atmosphere, sprayed with 1/30% ethanolic solution of fluorescein, and dried

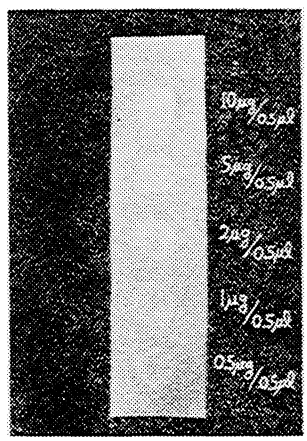

Fig. 2.—Limiting amount and concentration of detection.

naturally again. The presence of polyethylene oxide on the paper was detected as a white spot on a yellow background. The limiting amount and concentration of detection of this method were approximately 0.5 μg. polyethylene oxide per 0.5 μl water, as shown in Fig. 2. This value, however, was affected by the amount of impurity in the paper, which may cause some interference in the yellow color development of fluorescein on the paper.

Results and Discussions

The developing solvent benzene-chloroform system was at first employed, which has been investigated by G. V. Schultz et al.[4] as the solvent useful for the partition fractionation of polyethylene oxide, water being used as the parent solvent. Because of the lack of affinity with the paper, however, this solvent was not suitable for the developing solvent in paper chromatography. Among various solvents involving butanol as the principal component the butanol-ethanol-water system was found to be the most suitable for the paper chromatography of polyethylene oxide. The R_f values obtained with the use of this solvent are given in Table 2, in the case of the single samples. The symbol x corresponds to the concentration of ethanol in a mixture consisting of 100 parts of butanol, 100 parts of water and x parts of ethanol in volume. The upper

Table 2

R_f Values of Single Samples

x	$(R_f \pm \Delta R_f) \times 100$		
	Carbowax 1,000	Carbowax 4,000	Carbowax 6,000
0	22±0(22)	3±0(9)	0±0(4)
5	28±0(20)	2±0(6)	0±0(4)
10	38±0(22)	5±0(8)	0±0(4)
15	42±1(15)	7±0(10)	0±0(4)
20	50±1(16)	9±0(11)	0±0(6)
25	58±1(16)	17±0(13)	0±0(5)
30	63±2(14)	33±1(14)	6±1(10)
35	67±2(8)	46±2(8)	25±2(10)
40	76±2(10)	56±2(9)	36±2(8)
50	77±1(6)	71±2(5)	59±1(5)
60	77±1(8)	73±2(6)	66±2(6)
70	77±1(7)	76±3(5)	74±2(5)

layer was taken for developing in case the system separates into two layers at 25±0.1°C. The system consists completely of one phase for x values larger than 40. The R_f values are calculated as

$$R_f = (l_1+l_2)/2l \quad \text{(cf. Fig. 3)}$$

(3) cf. K. Otozai, *J. Japan. Chem.*, **4**, 411 (1950).

(4) G. V. Schultz and E. Nordt, *J. prakt. Chem.*, **155**, 115 (1940).

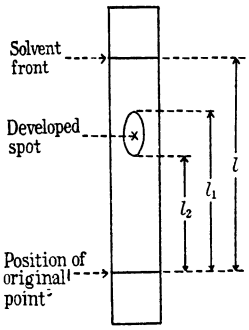

Fig. 3.

and the numerical values in brackets represent the values calculated as $(l_1-l_2)/2l$, the latter of which would correlate to the proper divergence of the spot during chromatography and the distribution of the molecular weight of polyethylene oxide used. These figures are the mean values in several experiments.

The relations between R_f values of single samples and the concentrations of ethanol in the solvent are given in Fig. 4. Furthermore the values in Fig. 4 were rearranged in Fig. 5, in which the values of the average molecular weight $\bar{M}$ of each sample were obtained by the viscosity measurement of aqueous solutions at 20±0.01°C, using the K_m constant 1.8×10^{-4} for 0.5% solution.[4]

From the form of the curves in Fig. 5 the most suitable solvent for the separation of three samples is that of $x=35$, because this solvent gives approximately linear and steep curve. A demonstration of the practical separation of the three samples by the use of this solvent is shown in Fig. 6 together with the individual developments of single samples for comparison, and R_f values obtained were shown in Table 3. which represent the good independency of each sample in paper chromatography.

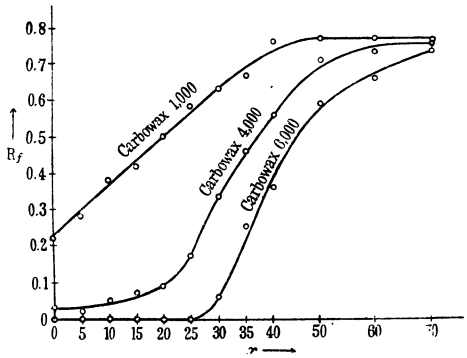

Fig. 4.—Relations between R_f and concentration of ethanol.

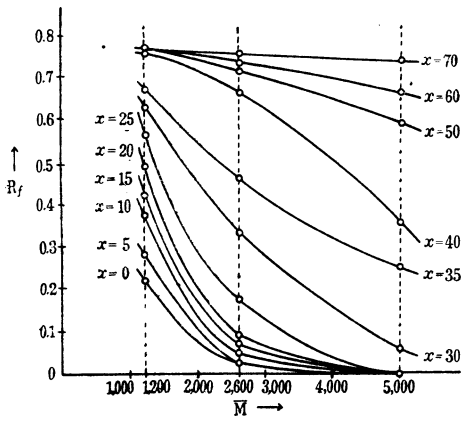

Fig. 5.—Relations between R_f and the average molecular weight.

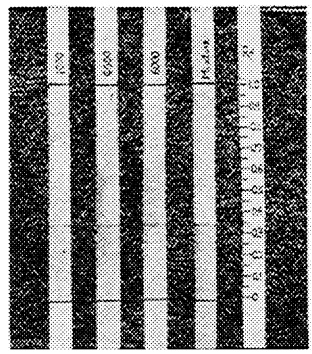

Fig. 6.—Separation of three components.

Table 3

Comparison of R_f Values of Single and Mixed Samples

$(R_f \pm \Delta R_f)\times100$

	Carbowax 1,000	Carbowax 4,000	Carbowax 6,000
Single	67±2(8)	46±2(8)	25±2(10)
Mixed	68±3(9)	45±3(7)	28±3(7)

Using the curve ($x=35$) in Fig. 5 as a working curve one can readily determine the average molecular weight of polyethylene oxide, although it is only relative, in the range of 1,000-5,000, where the molecular weight is determined only with difficulty by every known method at present. Thus employing paper chromatography a new simple relative method of determination of the average molecular weight, and a possibility of a simple method of determination of distribution function, and finally a possibility of fractionation of hydrophilic polymers have been proposed, using polyethylene oxide of molecular weight 1,000-5,000 as an illustration.

Summary

(1) It was found that polyethylene oxide on paper can readily be recognized with fluorescein as an adsorption indicator.

(2) It was found that paper chromatography can be applied also for polyethylene oxide in the range of the average molecular weight 1,000-5,000, as the first case for hydrophilic polymer, in the same manner as low molecular weight substances.

(3) It was found that paper chromatography gives a simple new relative method of determination of the average molecular weight of polyethylene oxide in the range mentioned above, where all the other conventional methods encounter serious diffiiculties.

The authors wish to express their sincere thanks to Prof. T. Titani for his encouragement of this research.

Faculty of Science, Osaka University, Osaka

On the Nature of Built-Up Film. III. Effect of Dissolved Anion on Mono- and Multilayers of Octadecylamine

By Tunetaka SASAKI and Mitsuo MURAMATSU

(Received August 14, 1952)

Introduction

In the preceding papers[1],[2] the effects of metallic ions on the built-up film of stearic acid were reported. There it was suggested that some metallic ions, e. g., copper, aluminum or thorium, are adsorbed from an aqueous solution in their characteristic *p*H range as a fairly large and complex unit. This suggestion is in agreement with the experiments of Matuura and one of the present authors,[3],[4] who have arrived at the same conclusion based upon the remarkable expansion and rigidity exhibited by the monolayer of fatty acid spread on an aqueous solution containing the ions mentioned above. A certain wetting phenomena can also be explained from the same point of view which was reported by Inaba[5] of our laboratory. Wolstenholme and Schulman[6],[7] obtained the similar experimental results and explained these phenomena from a different point of view

The fact[2] that the intensity of water-repellency of metal stearate built-up film, after the treatment with or without aqueous salt solution, is parallel to the presumed complexity or macromolecular structure of the film, seems to suggest a profound effect for the wettability of the easiness of overturning of the molecules which is hindered by two-dimensional molecular network in the film. To confirm this, we have further studied the interaction between the film of long chain amine and the organic anion of the known structure.

Experimental

Material. — Octadecylamine was prepared by reduction[8] of nitrile which was synthesized[9] from Merck's pure stearic acid and was purified by distillation in vacuo. The final product was recrystallized repeatedly from benzene. Its melting point was 83~84°C. Bigelow, Glass and Zisman[10] however obtained the free amine of melting point ranging from 51.5 to 52.5°C., and amine bicarbonate of melting point being about 80°C., while the Beilstein value of the former was reported to be 53°C. This leads us to the conclusion that we actually obtained the amine bicarbonate. In fact, the result of micro nitrogen determination of this sample agreed with theoretical value for the bicarbonate within an error (Nobs., 4.37%; Ncalc. for $C_{18}H_{37}NH_2 \cdot H_2CO_3$, 4.23 %, whilst Ncalc. for $C_{18}H_{37}NH_2$, 5.21%). The molecular area of octadecylamine in monolayer spread on water surface was calculated, taking into account of this bicarbonate formation.

Dibasic organic acids were of Takeda's or Riedel de Haën's pure grade and recrystallized

(1) M. Muramatsu and T. Sasaki, This Bulletin, **25**, 21 (1952).
(2) M. Muramatsu and T. Sasaki, This Bulletin, **25**, 25 (1952).
(3) T. Sasaki and R. Matuura, This Bulletin, **24**, 274 (1951).
(4) R. Matuura, This Bulletin, **24**, 277 (1951).
(5) A. Inaba, This Bulletin, **25**, 174 (1952).
(6) G. A. Wolstenholme and J. H. Schulman, *Trans. Faraday Soc.*, **46**, 475 (1950); **47**, 788 (1951).
(7) G. A. Wolstenholme and J. H. Schulman, *Trans. Faraday Soc.*, **46**, 498 (1950).
(8) F. Kraft, *Ber.*, **15**. 1728 (1883); N. K. Adam and J. W. W. Dyer, *J. Chem. Soc.*, **1925**, 72.
(9) H. Stephen, *J. Chem. Soc.*, **1925**, 1875.
(10) W. C. Bigelow, *E.* Glass and W. A. Zisman, *J. Colloid Sci.*, **2**, 563 (1947).

several times. A highly purified sample of sodium alginate was given by Mr. S. Miyamoto of our laboratory.

Apparatus and Method.—The surface pressure of monolayer was measured by the Wilhelmy balance modified by one of the authors of this paper.[11] The monolayers were deposited onto the metal slide by either of the two methods, namely by the ordinary Langmuir-Blodgett technique[12] and by the special method of using benzene solution of amine as a piston oil placed near the slide, the details of which were reported in the preceding paper.[2] Optical thickness of built-up films was determined by means of the interference method as used in the preceding reports.[1],[2] The experimental error associated with the apparatus was ±1.5 A. All experiments were carried out at room temperature from 7 to 14°C.

Results

Monolayers Spread on the Surface of Distilled Water.—The pressure ~ area curve of the amine monolayer spread on the surface of distilled water proved to be of a typical condensed film. The cross-sectional area of molecules at zero compression lies in the range of 21.7—25.6 A.^{2}/molecule depending upon various factors. It seems to be characteristic for this film that the reproducibility is poor presumably due to its sensitivity towards *p*H,[13] or to the presence of carbon dioxide[10] in water, and also due to the aging of the film.[14] Moreover, it was observed thet the shape of curve was profoundly affected by velocity of compression, as reported by Marsden and Schulman,[15] and Hoffman, Boyd and Ralston,[16] though the other conditions were the same. The similar result was reported in the case of the monolayer of antifoaming agent.[17]

Deposition of Multilayers from Water Surface.—By use of the Langmuir-Blodgett technique[12] attempts were made to build multilayers of free base from the surface of water, *p*H of which was adjusted to larger than 5, to prevent the formation of ammonium salt.[14] Under the pressure of tricresyl phosphate, castor oil and oleic acid as piston oils, through all *p*H region, the monolayer did not adhere to a bare surface of stainless steel slide both for down- or up-trip. On the other hand, it could be deposited onto the barium stearate base as successive Y-multilayers when the substrate *p*H was smaller than 10 and each double layer was sufficiently dry after withdrawal. Under the piston pressure of tricresyl phosphate, the films of 4—6 layers showed an optically perfect homogeneity when they were deposited from the substrate water of *p*H 5—8.6. However, in the case of the film exceeding six layers, optical contrast of the echelon became weak indicating the heterogeneity of the film, which was seen already in the first double layer when *p*H of substrate water was 8.6—10. Using castor oil or oleic acid as a piston oil, on the other hand, an optically homogeneous film could be obtained only up to 2—4 layers when it was built from substrate water of *p*H 5—6, while heterogeneous film resulted in the other range of *p*H. In the case of homogeneous film, the spacings in multilayer were found between 24.0—25.3 A. (24.5 A. for the mean value of twelve experiments) per layer irrespective of the conditions of building-up. It should be noted that remarkable fogging occurred in the built-up films of amine when more than about ten layers were deposited. Similar results were reported in the cases of the films of long chain esters[18] and phthiocerol.[19]

At *p*H>10, the films were deposited as X-layer independent of the piston pressure. The slide was withdrawn from the solution completely wetted with water but it quickly peeled back soon after.

Interaction of Amine Monolayer with Organic Anions in the Underlying Solution.—In Fig. 1 are shown the effects of some dibasic organic acids and sodium alginate dissolved in a substrate water, on the pressure~ area curve of the amine monolayer. The solutes were dissolved to 10^{-4} mol./l. for acids and 0.1% for sodium alginate, and *p*H of the substrate was kept to 4.5—5.0. The same result was also obtained when the oxalic or succinic acid was injected in water beneath the monolayer. It was seen, in general, that the monolayer expanded with increasing distance between the polar groups in each anion of the substrate. The curve of sodium alginate, in this connection, lies between succinic and

(11) T. Sasaki, *J. Chem. Soc. Japan*, **62**, 796 (1941).
(12) K. B. Blodgett and I. Langmuir, *Phys. Rev.*, **51**, 964 (1937).
(13) C. G. Lyons and E. K. Rideal, *Proc. Roy. Soc. London*, A **124**, 333 (1929).
(14) N. K. Adam, *Proc. Roy. Soc. London*, A **126**, 526 (1930).
(15) J. Marsden and J. H. Schulman, *Trans. Faraday Soc.*, **34**, 748 (1938).
(16) E. J. Hoffman, G. E. Boyd and A. W. Ralston, *J. Am. Chem. Soc.*, **64**, 498 (1942).
(17) A. L. Jacoby and C. E. Johnson, *J. Phys. Colloid Chem.*, **53**, 1417 (1949).
(18) E. Stenhagen, *Trans. Faraday Soc.*, **34**, 1328 (1938); G. Knott, J. H. Schulman and A. F. Wells, *Proc. Roy. Soc. London*, A **176**, 534 (1940).
(19) S. Ställberg and E. Stenhagen, *J. Biol. Chem.*, **143**, 171 (1942).

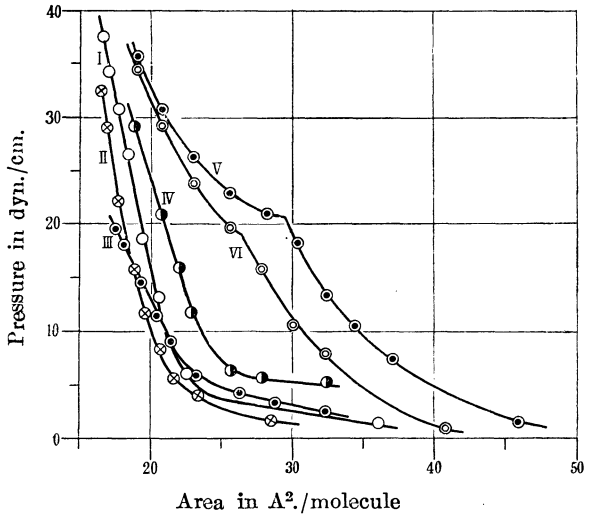

Fig. 1.—Pressure–area curve of octadecylamine monolayer spread on various substrate: I, distilled water; II, oxalic acid; III, malonic acid; VI, succinic acid; V, adipic acid; VI, Na alginate.

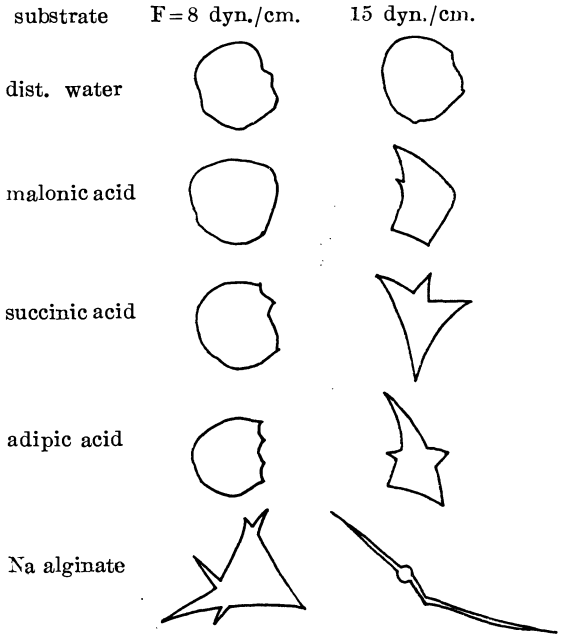

Fig. 2.—Expansion pattern of octadecylamine monolayer.

adipic acids. With respect to the mechanical properties, however, sodium alginate behaved remarkably different from the other anions. It rendered the amine monolayer highly rigid, while such an effect was not so remarkable in the case of dibasic acids. This behavior is shown in Fig. 2, in which the expansion patterns of camelia oil[4] are schematically illustrated for different solute and surface pressure.

Multilayers of Amine Built Up from the Surface of Organic Anion Solution. — The monolayer of amine formed on the surface of the solution as described above could easily be deposited onto the barium stearate echelon, excepting the case of sodium alginate, as successive Y-layers which showed an optical homogeneity up to six layers. On the other hand, X-film alone was obtained in the case of adipic acid, and this film was so patchy indicating the incomplete deposition that we could not measure its spacing. The optically perfect film was obtained by the method of deposition as described in the preceding report.[2] It was confirmed with dibasic acids except for adipic acid, that the thickness of a monolayer is unaffected by the method of deposition.

Table 1 shows the apparent spacing of these films under the piston pressure (15 dyn./cm.) of castor oil, together with

Table 1

Cross-sectional Area of Molecules and Apparent Spacing in Built-up Film

Substrate Solution	Apparent Spacing per Layer in A.	Cross-sectional Area in A.²/molecule
distilled water	24.5	20.0
$(COOH)_2$	34.7	19.1
$CH_2(COOH)_2$	32.5	19.1
$(CH_2)_2(COOH)_2$	32.6	22.1
$(CH_2)_4(COOH)_2$	20.9	31.2

the cross-sectional area of a molecule at the same pressure. All these films, especially those built up from the solutions of organic ions, proved to have an extremely hydrophobic property, as well as a strong resistance against corrosion and dissolution in contrast with the built-up film of stearic acid.[20],[1] Thus the film transferred from the aqueous oxalic acid substrate, for instance, showed no change in the film thickness as well as the water-repellent property, even when it was soaked in distilled water for a long time (44 hrs. or more). It is a very interesting fact that it became wettable towards water, when it was immersed in the sodium alginate solution. The minimum time of immersion necessary for wetting is shown in Table 2. In this table, the case of KH_2PO_4 (buffered to pH=7.2 with

(20) J. J. Bikerman, *Proc. Roy. Soc. London*, **A 170**, 130 (1939).

Table 2

Minimum Time of Immersion in Aqueous Sodium Alginate(0.1%) Required to Wet Built-Up Film Transferred from Various Aqueous Substrate

Aqueous Substrate	Time of Immersion in min.
distilled water	1-3
$(COOH)_2$	7
$CH_2(COOH)_2$	10
$(CH_2)_2(COOH)_2$	15
$(CH_2)_4(COOH)_2$	25
KH_2PO_4	∞

NaOH) was listed in addition to the cases of dibasic acids. Amine monolayer spread on this substrate was as rigid as that spread on the alginate, and it could be transferred onto the slide but was extremely heterogeneous.

Discussion

Easiness of Building-Up of Amine Film. —There are several experimental evidences that the affinity between the metal surface, e. g., platinum,[10] silver or copper surface,[7] and long chain amine when the molecules of free amine were adsorbed from non polar solvent, is as strong as that between metal and long chain acid. Then, it seems to be a contradiction that the monolayers of free base spread on water do not adhere, as was mentioned already, to the bare surface of metal. This may be explained by the stronger affinity of amine molecules towards water surface, than towards nonpolar solvent. However when the echelon of barium stearate was dipped into water carrying the monolayer, it took up the amine molecules as an A-layer, its polar group orienting towards bulk water. On withdrawal, moderately strong anchorage of amine molecules to echelon by non polar group and to the next amine layer by polar group enables the formation of AB-double layer. This interaction can reasonably by assumed from the following facts. A strong cohesion of long chain amine was predicted from the formation of islands in the monolayer[13] and from the lower value[21] of c. m. c. of long chain amine than that of the corresponding anionic soap. Also in our experiments the heterogeneity or the fogging in the film may presumably be an indication of the tendency of transformation into the three-dimensional microcrystal which may be a more stable form than the two-dimensional one. That the homogeneous thicker film could only be obtained using the lower piston pressure, and that the successive layer could be better transferred onto the echelon from the surface of aqueous substrate containing organic acid than from that without acid, may be considered to have some relation to this phenomenon.

Surface Interactions between Amine and Organic Anions. — In Fig. 1 a somewhat distinct condensation was observed for amine oxalate film* compared with the case of free base, while, for amine malonate, pressure~area curve at low pressure was nearly the same as the control test, and a remarkable expansion was seen with succinate and adipate. It is probable that the cross-sectional area of molecules in monolayer is chiefly affected by the distance between carboxyl groups in substrate anion, to which amine molecules in monolayer are considered to attach. Thus in the film of, say, amine adipate, octadecyl radicals attach separately to the carboxyl groups of adipate ion under low pressure. This idea is also supported by the decrease in apparent spacing shown in Table 1, which can be interpreted to be the increase in distance of octadecyl radicals in the film as was already pointed out[2] referring to the metal stearate. We may also find Schulman's strong polar and weak van der Waals' type interaction[22] in the behavior at a high pressure region. On the other hand condensation of amine oxalate would be accounted for by the attachment of the amine monolayer to carboxyl groups which are located closely in the acid molecules.

The effects of dissolved alginate ion upon the mono- and multilayers of amine are of very great interest. It can be pointed out from Figs. 1 and 2, and is also expected from X-ray data[23] on alginate solution, that the distance between ionic groups in the alginate ion is slightly smaller than between groups in adipate, and that a large number of polar groups in anion interact with amine molecules. This interaction renders the film highly rigid. Such a type of interaction was called multiple-point polar association by Cockbain and Schulman.[22] The remarkable rigidity due to the interaction of this type has also been shown by several investigators for amine film on

* The term "amine oxalate (malonate, succinate, and so on) film" is used hereafter as the abbreviation for the monolayer of amine spread on the surface of solution of oxalic (malonic, succinic, and so on) acid.

(21) A. W. Ralston, C. W. Hoerr and E. J. Hoffman, *J. Am. Chem. Soc.*, **64**, 97 (1942); **68**, 2460 (1946); I. M. Kolthoff and W. Stricks, *J. Phys. Colloid Chem.*, **52**, 915 (1948); M. Nakagaki, *J. Chem. Soc. Japan*, **72**, 113 (1951).

(22) E. G. Cockbain and J. H. Schulman, *Trans. Faraday Soc.*, **35**, 716 (1939).

(23) Wo. Pauli and L. Sternbach, *Kolloid-Z.*, **84**, 291 (1938).

aqueous tannin[22),(24)], silicate[6] and metaphosphate[25] and for amide film on aqueous tannin.[17]

Now we should draw attention to the fact that the interaction between monolayers of stearic acid and the polyvalent salt in the aqueous substrate closely resembles the interaction between amine monolayer and alginate in aqueous substrate, in that both can form a macromolecular complex as has been reported in the case of aluminum stearate.[26]

In this connection, the experimental data upon wettability shown in Table 2 appear to be of much value. Langmuir[27] has found the remarkable wettability of the built-up film of stearic acid and stearate when it was conditioned with the solution of various metallic ions, and explained this phenomenon by the overturning effect of molecules in the film. In the previous report[2] authors have correlated the two-dimensional network in the film with the difficulty of overturning or re-overturning which seems to be one of the chief factors for the wettability of this film. Inaba[5] also arrived at the same conclusion. The high wettability of the built-up film of amine towards a solution of sodium alginate is similar to the case of stearic acid or stearate towards metallic ion solution. The molecules of amine overturn themselves, and are fixed to the alginate ions and form a network of polyoctadecylamine alginate so that the re-overturning is not allowed and an extremely wettable surface results. In the case of amine phosphate, as shown in Table 2, a remarkable rigidity as described already also acts to hinder the overturning of amine molecules and the surface remains non-wettable. Further, we can also see in this table, though not so distinctly, that the resistance to wetting increases with increasing distance between the hydrocarbon chains attached to organic diacids. Again the authors have inclined to the opinion that the easiness of overturning when treated with alginate solution is chiefly determined by the magnitude or complexity of amine~organic acid compound formed in the film.

(24) F. Sebba and E. K. Rideal, *Trans. Faraday Soc.*, **37**, 273 (1941).
(25) I. Langmuir and V. J. Schaefer, *J. Am. Chem. Soc.*, **59**, 2400 (1937),
(26) V. R. Gray and A. E. Alexander, *J. Phys. Colloid Chem.*, **53**, 23 (1949); C. G. McGee, *J. Am. Chem. Soc.*, **71**, 278 (1949); etc.
(27) I. Langmuir, *Science*, **87**, 493 (1938).

Summary

Attempts were made to transfer the monolayers of octadecylamine on distilled water both onto the metal surface and onto the optical gauge of barium stearate. They did not adhere to the former surface, while with the latter it was shown that the homogeneous film was obtained when the substrate *p*H and the piston pressure were favorable for preventing the film from aggregating.

Effects of organic anions upon the mono- and multilayers of amine were investigated. The increase of the distance between the ionic groups of dicarboxylic acids caused the corresponding expansion and change in thickness of amine monolayer spread on the solution containing these anions. The solution of sodium alginate caused a somewhat large expansion and gave a remarkable rigidity towards the amine monolayer spread on it.

The built-up film of amine transferred from the substrate of various organic acids showed a variety of resistance for wettability when treated with aqueous sodium alginate solution. It was found that the resistance for wetting increased with the increasing complexity of the two-dimensional network formed in the film prior to the treatment. These results were discussed with regard to the easiness of overturning.

The authors wish to thank Mr. T. Tsutsumi for the micro nitrogen analysis of octadecylamine. They also wish to express their thanks to the Ministry of Education for the grant given for this research.

Department of Chemistry, Faculty of Science, Kyūshū University, Fukuoka.

The Effect of Chain Length, Salts and Alcohols on the Critical Micelle Concentration

By Kōzō SHINODA

(Received August 27, 1952)

Introduction

The effect of chain length and salts on the critical micelle concentration of colloidal electrolytes was measured by several authors,[1]~[6] and discussed by Corrin[7] and Hobbs.[8] The effect of alcohols and of alcohols and salts on the critical micelle concentration was measured by Corrin, Harkins and Herzfeld.[9][10] However, the theoretical treatment was not completely done. In the present paper, the model of large flat micelle is adopted and the following experimental facts are explained theoretically:

1) The effect of chain length on the critical micelle concentration of paraffin chain salts follows the equation.[1]~[6]

$$\log_{10} C = -K_0 m + K_1 \qquad (1.1)$$

2) The decrease of critical micelle concentration by the addition of salts follows the equation.[6]

$$\log_{10} C = -K_2 \log_{10}(C + C_s) + K_3 \qquad (1.2)$$

3) The effect of alcohol chain length on the critical micelle concentration follows the equation.[9]

$$\log_{10}(\mathrm{d}C/\mathrm{d}C_a) = K_4 m' + K_5 \qquad (1.3)$$

4) The critical micelle concentration is a linear function of the alcohol concentration.[9]

$$C' = -(\mathrm{d}C/\mathrm{d}C_a)C_a + C \qquad (1.4)$$

where C: critical micelle concentration mole per liter

C_s: concentration of added salts in equivalents of effective ion per liter.

C_a: concentration of added alcohols mole per liter.

$K_0, K_1, K_2, K_3, K_4, K_5$: constant and K_0 is nearly equal to 0.3 and K_4 is nearly equal to 0.47 according to the experimental results.

m: number of carbon atoms of the soap molecule.

m': number of carbon atoms of alcohol molecule.

$\mathrm{d}C/\mathrm{d}C_a$: rate of change of critical micelle concentration with alcohol concentration in mole units.

Basic Assumption of the Theory

1) Due to the fact that a nonpolar oil such as benzene or hexane is solubilized between the monolayers of the soap micelle increasing X-ray spacing but showing only a slight effect on the critical concentration,[11][12] we have ignored interaction of the two end discs.

2) In the light of the basic assumption of the Debye theory of the micelle, we may express the total energy change in the micelle formation in terms of the electrical energy and the cohesive energy, and the change of cohesive energy per one molecule by the formation of a micelle is assumed to be proportional to the number of carbon atoms. We express this in term of $m\omega$.

3) With respect to the value of ω, Debye[13] has adopted the heat of vaporization of the hydrocarbon, and he assumed $\omega \approx 2.0\,kT$. But Hobbs,[8] referring to the heat of vaporization, adopted $\omega = 1.0\,kT$ to explain the empirical results. Cassie and Palmer[14] assumed $\omega \approx 0.85\,kT$ or $1.2\,kT$ on the basis of adsorption data of Powney and Addison[15] at the water-xylene interface. We have calculated an approximate

(1) G. S. Hartley, *Kolloid-Z*, **88**, 22 (1939).
(2) K. Hess, W. Philippoff and H. Kiessig, *Kolloid-Z*, 88, 40 (1939).
(3) A. B. Scott and H. V. Tartar, *J. Am. Chem. Soc.*, **65**, 692 (1943).
(4) J. Stauff, *Z. Physik. Chem*, **183 A**, 55 (1938).
(5) W. D. Harkins, *J. Am. Chem. Soc.*, **69**, 1428 (1947).
(6) M. L. Corrin and W. D. Harkins, *J. Am. Chem. Soc.*, **69**, 683 (1947).
(7) M. L. Corrin, *J. Colloid Sci.*, **3**, 333 (1948).
(8) M. E. Hobbs, *J. Phys. and Colloid Chem.* **55**, 675 (1951).
(9) S. H. Herzfeld, M. L. Corrin and W. D. Harkins *J. Phys. & Coll. Chem.* **54**, 271 (1950).
(10) M. L. Corrin and W. D. Harkins, *J. Chem. Phys.* **14**, 640 (1946).
(11) E. C. Lingafelter, O. L. Wheeler and H. V. Tartar, *J. Am. Chem. Soc.*, **68**, 1940 (1946).
(12) R. W. Mattoon, R. S. Stearns and W, D. Harkins, *J, Chem. Phys.* **16**, 644 (1948).
(13) P. Debye, *J. Colloid Sci.*, **4**, 407 (1949).
(14) A. B. D. Cassie and R. C. Palmer, *Trans. Farad. Soc.*, **37**, 156 (1941).
(15) J. Powney and C. C. Addison, *Trans. Farad. Soc.* **33**, 1243 (1937).

value of ω from the fact that the solubility in water of aliphatic homologous compounds diminishes about 1/3 with the increase of one carbon atom. That is, the following equation is obtained for the homologous aliphatic compounds, since the solubility is thought to be proportional to the exponential of energy change per one molecule when it dissolves:

$$C_n/C_{n-1}\exp(-\omega/kT)=1/3 \qquad (2.1)$$

Where C_n/C_{n-1} is solubility ratio of the homologous aliphatic compounds of n carbon compound to $n-1$ carbon compound.

Calculating (2.1), we obtain

$$\omega=1.08\,kT \qquad (2.2)$$

This value will be referred to later.

The Electrical Potential at the Charged Surface of Lamellar Micelle

If long chain electrolytes are aggregated to the micelle, they will give effectively a plane charge at the micelle surface. The ordinary Debye-Hückel approximation $e\phi/kT\ll1$ can not be used, because the contribution of electrical energy is too large to assume the above condition.[8][14][16] However, for a uniformly charged plane surface the Poisson-Boltzmann equation can be integrated without making this approximation.

$$\frac{d^2\phi}{dx^2}=-\frac{4\pi}{D}\sum z_i n_i e^{-z_i\xi\phi/kT}$$

Where ϕ: electrical potential
x: the direction normal to the surface
D: the dielectric constant of the solution
Z: the valency of ion
n: number of ions per c.c. in the bulk of the solution

Giving the boundary condition and neglecting the contribution of the same ion in the bulk, Hobbs[8] obtained the equation for a uni-univalent electrolyte:

$$\phi=\frac{kT}{e}\log\left\{\frac{1000\,\pi\sigma^2}{2DRT}-\log C_t\right\} \qquad (3.1)$$

Where C_t: total concentration of gegen ion in mole per liter
σ: charge density at the micelle surface
e: electric elementary quantum

The integral work of introducing another charge of e into the surface of the micelle is given by ϕe. However, the alternative is to assume that each molecule contributes less than this because of the adsorbed gegen ions and the electrical potential due to the ion atmosphere in the solution. Accordingly, a factor K_6 should be introduced in this equation.

Then, $$(\phi-\phi')e=K_6kT\left\{\log\frac{1000\,\pi\sigma^2}{2DRT}-\log C_t\right\} \qquad (3.2)$$

Where ϕ': the electrical potential in the solution

Statistical Treatment of Critical Micelle Concentration

According to the analogy of the equilibrium condition between vapor and liquid we assumed the equilibrium condition between solute and pure liquid might be given, equating the partial potential of solute and that of liquid (micelle). The partial potential of a soap ion in the micelle is assumed to be.[17]

$$\mu^L=-\chi-kT\log(2\pi mkT)^{3/2}v/h^3-kT-kT\log j(T)+pv^L \qquad (4.1)$$

and the partial potential of a soap ion in the solution may be given by the equation

$$\mu^S=-\chi'+kT\log CNkT/1000-kT\log(2\pi m)^{3/2}(kT)^{5/2}/h^3-kT\log j'(T) \qquad (4.2)$$

Where v: free volume per one molecule
$j(T)$: partition function for the internal degrees of freedom, to be equal in the two phases
$-\chi$: uniform potential of liquid which is a smoothed value for all relative configurations of the given molecule (ion) and its neighbours, in this time χ contains electrical energy.
C: molar concentration of soap in molecular dispersion

As they are in equilibrium, equations (4.1) and (4.2) are equated, and the following equation is obtained:

$$\log C=\log 1000/Nv-(\chi-\chi')/kT-1+pv^L/kT \qquad (4.3)$$

(16) D. Edelson and R. M. Fuoss, *J. Am. Chem. Soc.*, **70**, 2832 (1948).

(17) R. H. Fowler and Guggenheim, E. A. "Statistical, Thermodynamics", Cambridge. 1939, p. 329.

Where

$\chi-\chi'$: energy difference between micellar state and solute state, and equal to the summation of cohesive energy change $m\omega$ and the electrical energy change $e(\phi-\phi')$ per one molecule.

At ordinary pressure (concentration), pv^L is negligibly small compared with kT, and might be omitted without loss of accuracy.

Then (4.3) can be written

$$\log C=\log 1000/N\upsilon-m\omega/kT+e(\phi-\phi')/kT-1 \qquad (4.4).$$

This gives critical micelle concentration in unit of mole per liter.

The effect of Salts and chain Length on the Critical Micelle Concentration

Substituting (3.2) into (4.4), we obtain

$$\log C=\log\frac{1000}{N\upsilon}+K_6\left\{\log\frac{1000\,\pi\sigma^2}{2DRT}-\log C_i\right\}-\frac{m\omega}{kT}-1 \qquad (5.1)$$

Introducing the values $\sigma=e/20.5$ A.^{2}, $D=80.8$, $T=291°$K., and $\omega=1.08\,kT$ and assuming $N\upsilon=10$ cc., equation (5.1) becomes

$$\log_{10} C=-K_6\log_{10}(C+C_S)-0.47\,m+1.565+1.686\,K_6 \qquad (5.2).$$

Where C_S: the concentration of added salts and $C+C_S$ is equal to C_i

Comparing this to the experimental equation of Corrin and Harkins[18] for Potassium Laurate:

$$\log_{10} C=-0.5696\log_{10}(C+C_S)-2.6172 \qquad (5.3).$$

We obtain

$$K_6=0.57 \qquad (5.4).$$

It is thus shown that the effect of added salts on the critical micelle concentration is given by the equation (1.2). When no salts was added we obtain from (5.2) and (5.4):

$$\log_{10} C=-0.57\log_{10} C-0.47\,m+1.565+0.96 \qquad (5.5).$$

Then $$\log_{10}C=-0.3\,m+1.61 \qquad (5.6).$$

Where m is the number of carbon atoms constituting a hydrocarbon chain, and for fatty acid soap one carbon atom which organizes carboxyl radical must be excluded. Thus the effect of chain length on the critical micelle concentration, equation (1.1), is explained. However, we must consider work of hydration to represents the experimental results for different head group.

The Effect of Alcohols on the Critical Micelle Concentration

The effect of alcohols upon the critical micelle concentration is a matter of some dispute. Herzfeld, Corrin, and Harkins measured the critical concentration of dodecylammonium chrolide in the presence of ethanol, 1-propanol, 1-buthanol, 1-hexanol, 1-heptanol, 1-decanol, 1-undecanol, 2-propanol, and trimethyl-carbinol.[9] We have measured the critical micelle concentration of potassium laurate in the presence of ethanol, 1-buthanol, isoamylalcohol, 1-hexanol, 1-octanol, 1-decanol, and 2-ethylhexanol by the dye titration method. Many other authors have measured the effect of alcohols on the critical micelle concentration.[19][20]

However, the mechanism by which long chain alcohols depress the critical concentration was unknown. It has been definitely established that the long chain alcohols penetrate into the oriented structure of the micelle.[21] An attempt is made in this paper to explain the effect of alcohols based on the concept of a decreased charge density at the micelle surface neglecting the interaction of the two end discs.

We denote the concentration of soap ion in the solution equilibrium with the soap micelle at the given temperature and pressure by $C_S°$, and the concentration of alcohol molecule in the solution equilibrium with the imaginary alcohol micelle at the given temperature and pressure by $C_A°$, and the concentrations of soap ion and alcohol in the solution equilibrium with the mixed micelle by C_S and C_A respectively. Assuming that the alcohol molecule and the soap ion in the micelle dissolve each other in the state of regular solution. We obtain:

$$C_S\fallingdotseq C_S°N_S/(N_S+N_A)\ldots.N_S/(N_S+N_A)\approx 1 \qquad (6.1).$$

(18) M. L. Corrin and W. D. Harkins, *J. Am. Chem. Soc.*, **69**, 683 (1947).

(19) G. L. Brown, P. F. Grieger and C. A. Kraus, *J. Am. Chem. Soc.*, **71**, 95 (1949).

(20) A, W. Ralston and D. N. Eggenberger, *J. Am. Chem. Soc.*, **70**, 783 (1948).

(21) W. D. Harkins, R. W. Mattoon and R. Mittelmann, *J. Chem. Phys.*, **15**, 763 (1947).

$$C_A \fallingdotseq K C_A^{\circ} N_A/(N_S+N_A) \ldots . N_A/(N_S+N_A) \ll 1 \quad (6.2).$$

Where $N_S/(N_S+N_A)$, $N_A/(N_S+N_A)$ is the molar fraction of soap and alcohol in the micelle. The molar fraction of soap is nearly equal to 1, and K is the constant. As there exists the equilibrium between the alcohol molecule in the water and that in the micelle, the concentration of alcohol equilibrium with mixed micelle is expressed as follows, using (6.2) and according to the analogy of equation (4.3):

$$C_A \propto N_A/(N_S+N_A) \exp\{-(\chi-\chi')/kT\} \quad (6.3).$$

Where $\chi-\chi'=m'\omega$: cohesive energy change per one alcohol molecule.

If we denote molar fraction of alcohol in the micelle by x, we obtain

$$x \propto C_A \exp\{m'\omega/kT\} \quad (6.4).$$

Thus the molar fraction of alcohol in the micelle increases proportionally as the bulk concentration increases. And the concentration of alcohol in the bulk equilibrium with the micelle of given molar concentration decreases about $1/3=\exp(-\omega/kT)$ with the increase of one hydrocarbon chain in the alcohol molecule. As the effect of solubilization on the alcohol concentration in the bulk must be negligibly small at the critical point, the concentration of added alcohol is equal to the concentration of alcohol in the bulk.

On the other hand the equilibrium concentration of soap ion in the bulk decreases, depending on the molar fraction of the soap ion in the micelle and on the decrease of the charge density. When the molar fraction of alcohol becomes x, the molar fraction of soap in the micelle becomes $1-x$, and the charge density decreases from σ to $(1-x)\sigma$.

Thus the critical concentration at the presence of alcohol is expressed using (6.1) and substituting $(1-x)\sigma$ into (5.1). Then we obtain:

$$(1+K_6)\log C' = (1+K_6)\log C + \log(1-x) + K_6 \log(1-x)^2 \quad (6.5).$$

Where C': critical micelle concentration of soap-alcohol mixed micelle, when the molar fraction of alcohol is x.

C: critical micelle concentration of soap micelle in the absence of alcohol

From (6.5) we deduce:

$$C'/C = (1-x)^{1+2K_6/1+K_6} \quad (6.6).$$

When $K_6=0.57$, and the molar fraction x is small compared with unity, we obtain:

$$C'/C \fallingdotseq 1-1.36x \quad (6.7).$$

Then using the equation (6.4), we obtain:

$$(C-C')/C \propto x \propto C_A \exp\{m'\omega/kT\} \quad (6.8).$$

Thus for a given alcohol we obtain the relation:

$$C' = K_7 C_A + C \quad (6.9).$$

Where K_7: always negative

This equation expresses the fact that the critical concentration is a linear function of alcohol concentration, and corresponds to (1.4).

For various alcohol we obtain:

$$\log_{10}(C-C')/C_A = 0.47\, m' + K_5 \quad (6.10).$$

This equation expresses the effect of alcohol chain length on the critical concentration, and corresponds to (1.3). And the decreasing effect by the addition of alcohol is similar with any soap.

Comparison of the Effect of Alcohols with the Experimental Results

According to the data given by Herzfeld, Corrin, and Harkins[9] for dodecylammonium-chloride at 25°C. and those given by the author for potassium laurate at 10°C the rate of change of critical concentration with alcohol concentration is constant for a given alcohol but varies with the kind of alcohol employed.

Table 1 shows the comparison with the experimental data and the calculated values, assuming the rate of change of critical concentration by hexanol is 0.213 molar concentration per mole of alcohol.

Table 1

The Rate of Change of Critical Micelle Concentration in Molar Concentration per Mole of Alcohol

Alcohol	Dodecylammonium-chloride at 25°C.	Potassium-Laurate at 10°C.	Calculated C. M. C.
Ethanol	0.00145	0.00252	0.0026
Fropanol	0.00624	—	0.0079
1-Buthanol	0.0192	0.0258	0.0237
Isoamylalcohol	—	0.070	0.071
1-Hexanol	0.213	0.23	(0.213)
1-Heptanol	0.623	—	0.639
1-Octanol	—	1.87	1.92
1-Decanol	20.2	(8.64)	17.28
1-Undecanol	44.5	—	51.8

Thus the change of the effect of alcohols on the critical concentration has explained based on the solubility ratio of alcohols.

The author thanks to Prof. H. Akamatsu for his suggestion of this problem and Dr. M. Nakagaki for the discussion of the results.

*Department of Chemistry, Faculty of Science, Tokyo University, Tokyo**

* Present address.: Department of Applied Chemistry, Faculty of Engineering, Yokohama National Univ., Yokohama.

The Absorption Spectra of Styryl Dyes

By Kazuo SHIBATA

(Received August 18, 1952)

Spectroscopic properties of polymethine dyes have been the subject of repeated investigations, especially because of the interest concerning the functional relationships between the wavelength of absorption maxima and the length of conjugated systems. It has been known that the cyanine dyes show the absorption maxima that are in approximately linear relationship to the length of conjugated systems, while in the case of polyene dyes, such as diphenyl polyenes, the squares, of the wavelengths of absorption maxima are related almost linearly to the length of conjugated systems. To account for these phenomena several theories have already been proposed, among which the one set forth by Herzfeld and Sklar[1] seems to be most coherent and cogent.

Recently we have reported that the styryl dyes, a category of polymethine dyes which is structurally different from cyanine and polyene dyes, show an intermediate spectroscopic property between those of the latter two groups.[2] It appears, therefore, worthwhile to investigate whether the theory of Herzfeld and Sklar might be extended also to the cases of this intermediate type of polyene dyes.

Experimental

The styryl dyes investigated are listed in Table 1. They were synthesized by the reaction of dimethylamino-benzaldehyde with mono- or di-methylpyridine-iodoethylates or mono- or dimethylquinoline-iodoethylates, using pyperidine as the condensation reagent.*

(1) Herzfeld and Sklar, *J. Chem. Phys.* **10**, 508, 521 (1942).

(2) K. Snibata, This Bulletin, **25**, 378 (1952).

* In the synthesis of disubstituted styryl dyes such as compound (II) in Table 1, certain amounts of monosubstituted compounds were also formed as byproducts. These byproducts were removed by the chromatographic adsorption method.

Observations of absorption spectra in a visible region were carried out by the photoelectric method, using an Adam Hilger monochrometer, the accuracy of which was about ±10 A. Throughout the experiments ethanol was used as the solvent.

Results and Discussions

The observed values of absorption maxima of the dyes are listed in the third column of Table 1. On examining the data obtained, it becomes apparent that the disubstituted compounds (II), (III) and (VI) have two absorption bands, while monosubstituted compounds (I), (IV) and(V) have only one absorption band in the visible region.

Table 1

The Absorption Maxima of Styryl Dyes

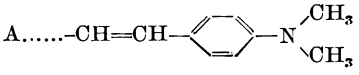

No.	Compounds	$\lambda_{obs.}$ (in A.)	$\lambda_{cal.}$ (in A.)
I	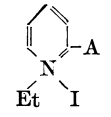	4670	4880
II	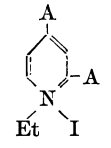	4350 5100	— —
III	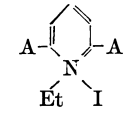	4100 4970	4160 —
IV	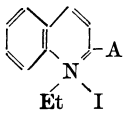	5270	—

V	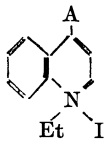	5460	5660
VI	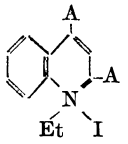	5000 5710	4620 5570

This result is of special interest from the viewpoint of the theory of Herzfeld and Sklar. According to them, the color of symmetric cyanine dyes arises from the transition between the two states caused by the resonance of two ground structures with equal energies. Let us consider trimethine dye (A) as an example of symmetric cyanine dyes. Though quite a number of resonance structures can be assumed by this substance, we may, for the present purposes, restrict our considerations to the following five structures of low energy levels.

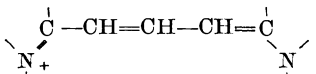
(A)

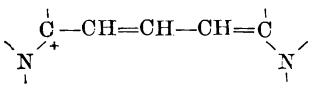
(B)

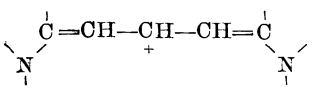
(C)

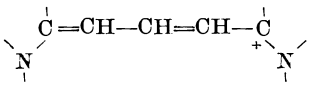
(D)

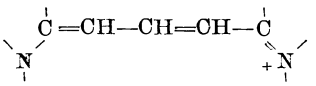
(E)

Of these resonance structures, two structures (A) and (E) have equal and lowest energies; that is, the ground level corresponding to the zero-order eigen functions is degenerate. In the first approximation by the method of valence bond eigen function, these two structures may be shown not to interact with each other directly. Their interaction results from the indirect interaction through other structures (B), (C) and (D) with higher energies; namely, (A) interacts with (B), (B) with (C),...., and (D) with (E). As a result of these interactions, the two degenerate ground levels split into two states with different energies. The situation is graphically shown in Fig. 1. The color of symmetric cyanine dyes is attributed to the transition between these split levels.

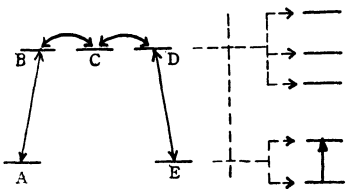

Fig. 1.

The same line of reasoning may be applied to the interpretation of the number of absorption bands of styryl dyes. For monosubstituted styryl dyes, we may consider two structures with lowest energies apart from the other levels. In contrast to the case of symmetric cyanine dyes, these two structures have slightly different energies, because the molecules are asymmetric. For example, the two resonance structures to be assumed for compound (I) will be

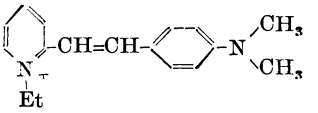
(F)

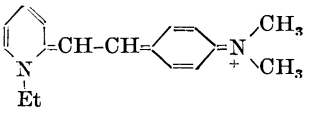
(G)

As a result of resonance, the height of energy levels will be changed, but the resulting levels of these two structures may be considered to be by far lower than those of other higher levels, since we may assume that the levels corresponding to the structure with the formal charge at the carbon atom is sufficiently higher than the levels of the structure with the charge at the nitrogen atom. The same consideration will lead to the inference that the number of levels with rather low energies must be three in disubstituted styryl dyes; for example, the structures to be assumed for compound (II) are as follows:

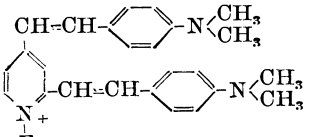
(H)

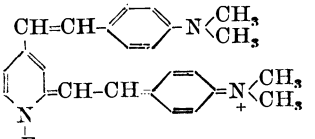
(J)

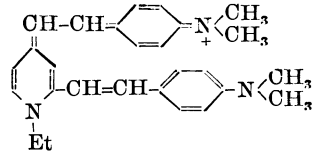

(K)

The absorption of light caused by the transitions between (F) and (G) as well as between (H), (J) and (K) may all be in the visible region. Thus, the fact that the monosubstituted dyes show one absorption band and the disubstituted dyes two in tne visible region has received a rational explanation.

On inspecting the data given in Table 1, the following facts will also be noticed.

i) The wavelengths of absorption maxima of the dyes having quinoline nucleus are always greater than those of the corresponding dyes with pyridine nucleus.

ii) The bathochromic effect of the redical A at position 4 of pyridine or quinoline nucleus is always stronger than the effect of the same radical at position 2.

In the preceding paper these relations have been explained on the basis of the "color factor", which was proposed as a convenient parameter to account for the spectral denpendency on the lengths of conjugated systems of many cyanine and polyene dyes. In the following an attempt will be made to elucidate quantitatively the spectroscopic properties of these substances from the viewpoint of the method of valence bond eigen function. It should be noted in advance that we are obliged to make a rather crude approximation because of the complex nature of the molecules of styryl dyes.

Let us consider compound (I) and assume that the energies of the eigen functions corresponding to the structures (F) and (G) are e and f, respectively. We shall neglect the interactions between many states other than (F) and (G) and assume the effective interaction energy between (F) and (G) to be α, though more precisely, these stepwise interactions must be taken into account. The height E of the levels resulting from the resonance in question can be obtained by solving the following secular determinant;

$$\begin{vmatrix} e-E & \alpha \\ \alpha & f-E \end{vmatrix} = 0 \qquad (1).$$

The same assumption will lead to the following equation* (2) for the energy of compound (III).

$$\begin{vmatrix} f-E & \alpha & 0 \\ \alpha & e-E & \alpha \\ 0 & \alpha & f-E \end{vmatrix} = 0 \qquad (2).$$

For compound (II), the interaction energy between (H) and (J) will also be α, but the interaction energy between (H) and (K), which may be denoted by β, must be assumed to be smaller than α, if we take into account the length of the conjugated double bond. Hence, the equation for the energy of the states of compound (II) will be

$$\begin{vmatrix} f-E & \alpha & 0 \\ \alpha & e-E & \beta \\ 0 & \beta & f-E \end{vmatrix} = 0 \qquad (3).$$

The solutions of equations (1), (2) and (3) are graphically shown in Fig. 2, in which dotted arrows indicate resonance.

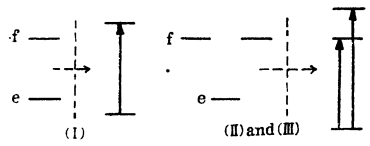

Fig. 2.

Using equations (2) and (3), the values of parameters, α, β and f-e, were calculated from the data of the two absorption bands of compound (II) and the band at the longer wavelength of compound (III). The obtained values ($\alpha = 6258\ \mathrm{cm}^{-1}$., $\beta = 5207\ \mathrm{cm}^{-1}$. and $f\text{-}e = 16228\ \mathrm{cm}^{-1}$.) were used for the calculation of the wavelength of the absorption maximum of compound (I) and that of compound (III) at a shorter wavelength.

As to compounds (IV), (V) and (VI), we assumed that the interaction energies α and β are the same as in the above cases but the energy difference f-e has a different value, which was calculated from the data of compound(IV). This value of f-e ($f\text{-}e = 14261\ \mathrm{cm}.^{-1}$) was assumed to be applicable also to compounds (V) and (VI).

The calculated value of the wavelength of absorption maximum of each compound is shown in the fourth column of Table 1. As will be seen, the coincidence between calculated and observed values is fairly good in spite of the crude approximation we have made. These results seem to substantiate the theory of Herzfeld and Sklar, showing that it may well be applied also to the cases of asymmetric conjugated systems. The results obtained give us also ground for the conclusion that the absorption bands shown by styryl dyes in a

* In this equation, the interaction between the two states, which have the positive charge at the nitrogen atom of amino group, was ignored.

visible region are due to the transition between electronic levels, and not to the transition to the split levels of one electronic level caused by the vibrational splitting.

The author wishes to express his earnest thanks to Dr. M. Katayanagi for his generous gift of the intermediate compounds for the synthesis of dyes, and to Prof. H. Tamiya for his valuable guidance and his constant interest in this study.

The Tokugawa Institute for Biological Research, Tokyo

Photoelasticity of Fe_3O_4 Film isolated from Iron Single Crystal

By Shigeto YAMAGUCHI

(Received september 3, 1952)

The test piece of iron single crystal was etched with an ethanol-bromine (10: 1 by volume) solution. The Fe_3O_4 film (thickness: about 200 A.) formed on the etched surface was isolated from the underlying substrate.[1] The isolated oxide film was placed upon a glass plate and was examined by means of polarizing microscopy. When the specimen was placed between a polarizer and an analyzer set for extinction, some light passed through it and interference effect was observed, which is shown in Fig. 1. Fig. 1 indicates that an isotropic substance Fe_3O_4 (cubic structure, spinel type) is doubly refracting, i.e., under unsymmetrical strain.

(1) S. Yamaguchi, *J. Appl. Phys.*, **22**, 680 (1951); S. Yamaguchi, T. Nakayama and T. Katsurai, *J. Electrochem. Soc.*, **95**, 21 (1949).

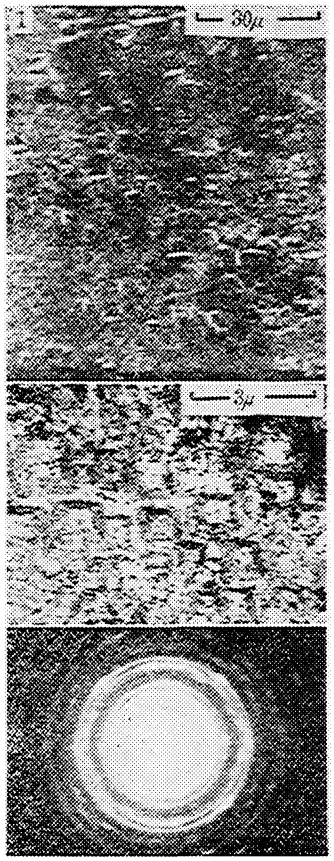

Fig. 1.—The micrograph obtained from the Fe_3O_4 film placed between a polarlizer and an analyzer set for extinction. The oxide film contains the doubly refracting domains, since the film retains unsymmetrical strain forced on it while performing a lattice fit with the underlying substrate.

Fig. 2.—Electron micrograph of the oxide film prepared in the same way as for Fig. 1.

Fig. 3.—Electron diffraction pattern obtained from the Fe_3O_4 film of Fig. 2. This pattern shows that the oxide crystallites are oriented relative to the substrate facets.

The oxide film prepared in the same way as for Fig. 1 was magnified by means of electron microscopy (vid. Fig. 2). In Fig. 2 are found the crystal forms reprinted from the etched surface by oxide replica.[2] The figures characteristic of Fig. 2 are similar to those of Fig. 1.

The oxide film of Fig. 2 gave an electron diffraction pattern of Fig. 3, which verifies the presence of regularly oriented crystallites of Fe_3O_4. This regular orientation of Fe_3O_4 crystallites suggests the lattice fit between the Fe_3O_4 crystal and the substrate crystal of iron.[2] The $Fe^{\cdots}$-$Fe^{\cdots}$ distance found in the normal Fe_3O_4 crystal is 8.37 A. (lattice constant of Fe_3O_4), and the doubled value of the distance (4.045 A.) between the nearest two atoms in the (111) planes of iron is $4.045 \times 2 = 8.09$ A. The difference between these two distances is so small (3.5 %), i. e., the strain in the oxide film caused by the underlying substrate is so slight, that the orientation and strain within the oxide film are retained even after the film is divorced from its substrate. As a matter of fact, this isolated film exhibits an anisotropic property, as is shown in the micrograph of Fig. 1, although it is difficult to determine exactly the lattice deformation of Fe_3O_4 film by measuring the diffraction pattern.[3]

The oxide film formed on a mechanically polished surface of iron and isolated from it showed no anisotropic property, distinguishable from that formed on the etched surface of single iron crystal. This oxide film gave a diffraction pattern showing the random orientation of Fe_3O_4 crystallites.

It was here demonstrated, that when a thin film of oxide of cubic structure isolated from a metal surface is doubly refracting, it is composed of oxide crystallites oriented regularly relative to the substrate facets. This photoelastic orientation is given to the oxide film by a slight shift in the lattice fit between the oxide crystal and its substrate.

Scientific Research Institute, Ltd.,
Bunkyo-ku, Tokyo

(2) S. Yamaguchi, *J. Appl. Phys.*, **22**, 1295 (1951); **23**, 445 (1952); This Bulletin, **24**, 237 (1951); *Naturwiss.*, **39**, 19 (1952); cf. *J. Appl. Phys.*, **23**, 935 (1952).

(3) cf. E. K, Halteman, *J. Appl. Phys.*, **23**, 150 (1952).

Physicochemical Studies of the Organic Dyestuffs in Relation to Photochemistry. I. Effect of Light on the Adsorption Equilibrium

By Masao KOIZUMI and Masashi IMAMURA

(Received June 20, 1952)

Introduction

Organic Dyestuffs are a very interesting group of substances from the photochemical standpoint. Of late, structures of some dyestuffs were discussed quantum-mechanically, and the theory of color hasmade much progress. However, photochemical studies are rather few; it is true that there are various kinds of investigations on the chlorophyll, which is important in assimilation, and on the photographic sensitizers, but it is desirable to investigate photochemically various other organic dyestuffs from a more general standpoint. Especially it seems necessary to study the behavior of dyestuffs in the colloidal system or the interaction between high-polymers and the dye molecules, since the dyes often play an important role in biological systems which can be considered as such complex systems.

With these ideas in mind, we have begun to study the photochemical behavior of dyestuffs, and at first have chosen the problem whether the adsorption equilibrium of dyestuff is affected by the illumination or not, when it is adsorbed on the colloidal surface from aqueous solution.

Investigations of this kind were already done by Hedvall[1], who found that when some dyestuffs are adsorbed, for example, on HgS or on ZnS from aqueous solution, illumination causes a remarkable change in the quantity of adsorption. His interest, however, was confined chiefly to the change of electronic structure of adsorbent produced by illumination. Our interest, on the contrary, is concerned with the problem whether the adsorption equilibrium is influenced by the participation of the excited dye molecules produced by illumination. As the adsorbent, therefore, the transparent substances such as silica gel or alumina were chosen. At the beginning, let us consider briefly whether there can be such possibility or not. The following two cases may be important for it.

Possibility (1). If the life of an excited molecule (or the metastable state, as the case may be) produced by illumination is much longer than the mean time of duration of the adsorbed state of a dye molecule, we may conceive two adsorption equilibria, one for the ground state and the other for the excited state. Then the adsorption potential will, in general, be different for these two states, and we can anticipate the effect of illumination in this case.

Possibility (2). This case is concerned with the dissipation of light energy absorbed by the dye molecule in the adsorbed state, and is rather independent of the life of the excited molecule. In general, the excess energy which the molecule gains by the absorption of photon dissipates as thermal energy, except when photochemical change or luminescence takes place. If the dissipation of energy happens to take place selectively toward the adsorbent-side rather than the solvent-side, the temperature of the adsorbent surface may rise locally, which will cause the decrease of the quantity of adsorption. This circumstance may, perhaps, be considered as the selective transfer of the excess energy into the bond of adsorption[2].

The First Experiment and its Results

The adsorption experiment was done in the evacuated state, with silica gel or alumina preliminary evacuated at a moderate temperature and the aqueous solution of dye also evacuated previously. In order to examine the light effect, we prepared two similar adsorption systems at one time and attached them on the disk, which was rotated in the thermostat, one system under illumination and the other in the dark, for eight hours, and

(1) Hedvall, *Z. Physik. Chem.*, **B32**, 383 (1936) etc.

(2) That such a possibility does really exist may be inferred, for example, from the fact that CO attached to the hemoglobin molecule is detached by illumination nearly quantitatively. (Cf. O. Warburg, "Naturforschung u. Medizin in Deutschland", 1939-46, Band 39, Biochemie Teil I.)

then compared the quantities of adsorption in the two systems. For this comparison, we measured with Pulfrich photometer the concentration of the dye in the solution, which was separated from silica gel after the experiment.

Dyestuffs used in this experiment were Rhodamine 6G, Rhodamine B, Flavophosphine, Trypaflavin, Acridine orange, Methylene blue, Pinacyanol iodide (all of them were adsorbed on silica gel), Erythrosine, and Uranine (for the last two, the adsorbent was alumina). For the illumination, we placed three 100 watt tungsten lamps, 20 cm. in length, parallel and 10 cm. apart from the reaction vessel. The number of photons which arrived at the reaction vessel was about $10^{15}/cm^2 \cdot sec$. The experimental results were such that we could perceive the light effect in only one case, which was Rhodamine 6G adsorbed on silica gel. Some dyes were discolored by the illumination and none of the others showed any light effect beyond the experimental error.

Some of the results for Rhodamine 6G are tabulated in Table 1.

Table 1

Temp. : 20°C.

Initial conc. (μM/l.)	Dark: Equilibrium conc. (μM/l.)	Dark: Adsorbed quantity (μM/g.)	Light: Equilibrium conc. (μM/l.)	Light: Adsorbed quantity (μM/g.)
10	1.2±0.2	0.066	1.6±0.2	0.063
	1.2±0.2	0.066	2.1±0.2	0.054
50	2.9±0.2	0.354	3.1±0.2	0.352
	2.9±0.2	0.354	3.1±0.2	0.352
100	4.0±0.2	0.720	4.8±0.2	0.710
	3.4±0.2	0.725	5.5±0.2	0.715
200	7.4±0.5	1.445	9.2±0.5	1.430
	6.3±0.5	1.452	7.4±0.5	1.445
400	15.4±0.5	2.895	20.8±0.5	2.844
	16.5±0.5	2.880	19.8±0.5	2.852
600	48.2±2	4.14	48.2±2	4.14
	49.5±2	4.13	47.7±2	4.15
800	135 ±5	4.99	138 ±5	4.97
	122 ±5	5.09	138 ±5	4.97
1000	243 ±5	5.67	240 ±5	5.70
	249 ±5	5.63	180 ±5	6.14

In Table, 1, initial conc. means the concentration of dye solution before the experiment, Equilibrium conc. is the one after the adsorption experiment. The adsorbed quantity was calculated from the above two quantities. The adsorption isotherms in the dark and the light are shown in Fig. 1. from which one can find the quantity of decrease in the adsorbed dyestuff caused by the illumination.

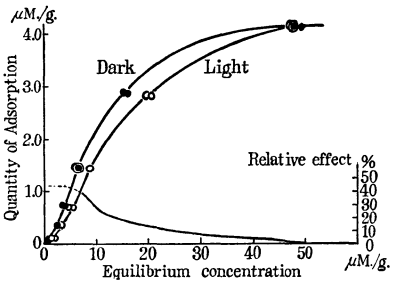

Fig. 1.—Adsorption isotherms in dark and light and the relative effect, for Rhodamine 6G.

The Second Experiment and its Results

In this experiment we used the vessel as shown in Fig. 2, in order to compare the quantity of adsorption in light and dark for the same one sample. This vessel also enabled us to study the effects of various factors for the same sample, such as light intensity, temperature, or the wave-length of light. The apparatus and the experimental procedure were as follows. The evacuated silica gel and the dye solution were placed in A. After the vessel was sealed off at B, it was shaken moderately in the thermostat and brought to the adsorption equilibrium in the specified condition, for example, light and dark, or at a certain light strength and at a certain temperature. The part A was illuminated by 100 watt tungsten lamp placed in the metal case which was attached close to this part. Glass filters were inserted between A and the light-source to test the effect of the wave-length of light. The intensity of light was varied by adjusting the voltage. The relation between voltage and light intensity through the filter (Matsuda V-G1) proved to be almost linear in the range from 20 to 90 V. With the same filter and at 20 V., the number of photons which were absorbed by the dye molecules in the vessel were about $10^{15}/cm^2$ sec.

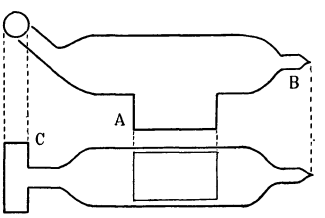

Fig. 2.—The vessel used in the Experiment II.

The determination of the dye concentration of the solution was done as follows. The solution was poured into B which acted as a

cell part for the photometric measurement. With the photomultiplier and galvanometer, the dye concentration was determined with an accuracy of about 0.05 μM/l. in favorable conditions. When one measurement was finished, part of the adsorbed dye was desorbed by warming the vessel at 40°C. for twenty to forty minutes and thus prepared for the next experiment. With such an apparatus and procedure, we performed the experiment over and over again using the same sample in different conditions.

Some of the results are tabulated in Table 2.

Table 2

Rhodamine 6G, initial concentration: 100 μM/l.

	Dark	Light		
Temperature °C.	Equilibrium concentration (μM/l.)	Equilibrium concentration (μM/l.)	Filter (Matsuda color filter)	Voltage (Volt)
25	2.4	2.55	V—G1	40
	2.35	2.6	V—G1	90
	2.4	2.6	V—G1	20
	2.4	2.35	V—R3	50
20	1.95	2.1	V—G1	90
	2.0	2.1	V—G1	50
	2.0	2.1	V—G1	20
	2.0	2.1	V—G1	15
15	1.5	1.65	V—G1	70
	1.6	1.7	V—G1	60
	1.5	1.75	V—G1	60
	1.6	1.75	V—G1	60
	—	1.8	V—G1	20
		1.8	V—G1	20
10	1.55	1.75	V—G1	60
	1.5	1.7	V—G1	60
	1.5	1.7	V—G1	60
	1.5	1.55	V—R3	50
	—	1.6	V—R3	50

From this Table it is apparent that

(1) the illumination increases the equilibrium concentration which is to be attributed to the decrease in the quantity of adsorption, although it is considerably small as compared with the results of experiment I,

(2) when the voltage of the light source is reduced below 20 V., no light effect is perceived; but in the range from 20 to 90 V., an almost constant effect, 0.2 μM/l. in equilibrium concentration is observed,

(3) the light which is not adsorbed by Rhodamine 6G cannot cause any effect, and

(4) temperature effect lies within the experimental error.

Discussion

From the above results we can definitely say that, when Rhodamine 6G is adsorbed from the aqueous solution onto silica gel, the illumination causes a decrease in adsorbability.

As for the mechanism of this phenomenon, the second possibility mentioned in "Introduction" is more favorable than the first one. Though various facts obtained by the experiment can be explained from this view point, here, we will only mention the following discussion which denies the first possibility definitely.

(1) If the first possibility is applied to this phenomenon, the number of excited molecules (or the metastable molecules) existing in the steady state must, at least, exceed the quantity of decrease in adsorption. The relation between the number of photons, q, which are absorbed per sec. (per cm^2. of the illuminated area), and the number of excited molecules, N_0, which exist in the steady state (per cm.^{2} of the illuminated area), should be represented by the equation

$$q=1/\tau\cdot N_0,$$

where τ is the mean life time of the excited molecules. As the number of photons absorbed per cm.^{2} is 10^{15} at 20 V. of the light source,

$$N_0=10^{15}\tau \qquad (1)$$

Now the difference of equilibrium concentration of dye is 0.2 μM/l. for 2 g. silica gel, the volume of the solution is 30 cc. and the illuminated area is about 15 cm.^{2} Therefore, the number of decrease in adsorbed molecules for a unit area of the illuminated surface is

$$\Delta N=0.2\times10^{-6}\times30/1000\times6\times10^{23}\times1/15\approx2\times10^{15} \qquad (2)$$

Even with an assumption that the excited molecule does not adsorb at all, the condition $N_0=\Delta N$ demands that τ should be of the order of 1 sec. The life time of the excited molecule of the fluorescent dyestuff is in general of the order of 10^{-8} sec. or less, and, in addition, there is no evidence of any metastable molecule in the solution of Rhodamine 6G, so that we may definitely conclude that the first possibility can not be realized in the case of Rhodamine 6G.

(2) If the effect is due to the second possibility, the adsorbed dye molecules which absorb photons are to desorb more easily than the ordinary ones, and the magnitude of the

effect depends upon the difference between the rate of adsorption and desorption in the illuminated system, and so we can expect an effect of some magnitude, large or small, according to the circumstances. Thus the experimental results that the decrease in the number of adsorbed molecules as large as 2×10^{15} is produced by relatively small number of photons, 10^{15} in the order, does not contradict the second possibility. But a difficulty which must be explained when we adapt the second possibility is the phenomenon of photosaturation that is reached already with absorption of ca. 10^{15} photons or more per cm.^{2} per sec. In the second mechanism, such a photo-saturation cannot simply be explained as shown by the following estimation. In the steady state, the following relation (3) must hold between the number of molecules desorbed in excess by illumination and the excess number of molecules which attack the adsorbent surface; the former will be given as κq, where q is the number of photons absorbed per sec. and κ the probability factor of desorption due to illumination, while the latter may be put as a Δn, where Δn is the excess number of dye molecules produced by illumination in the neighborhood of adsorbent, and a is the specific rate of adsorption of the dye molecule.

$$\kappa q = a\cdot\Delta n \qquad (3)$$

According to the equation (3), Δn, and hence the decrease of adsorption must increase proportionally to the increment of q. From the experimental results the number of adsorbed dye molecules per cm.^{2} of the illuminated area is 10^{17}, which is much larger than 10^{15}, the number of photons absorbed per cm^2. at 20V., and so we can not expect the photo-saturation with the light intensity of this order if all of the adsorbed dye molecules can take part in present photo-effect. In connection with this difficulty, however, it may not be useless to note the following speculation.

In the aqueous solution of Rhodamine 6G, some of the dye molecules exist in the dimerized state. When the dye is adsorbed on the high-polymer, for example polyvinylalcohol sulfonate[3], the dimer molecule adsorbs 100 times more than the monomer. If we assume that, as is very plausible, the similar situation exists in the present system, and that only the monomer adsorbed on the surface participates in the photo-effect, then the above situation might be expected when the number of monomer happens to be far less than that of photons absorbed. This speculation may be rather probable, because the monomer has a strong power of fluorescence while the dimer has none, and thus there is no doubt that the mechanism of the energy dissipation is much different for both molecular species.

We want to add some notes on the results of the first experiment. First: there exists some difference in the magnitude of the effect in experiment I and II; it can probably be attributed to the difference in experimental conditions. Second: the light effect in experiment I varies with the concentration of the solution as is shown in Fig. 1; this can be explained as due to the shielding action of the solution if we take the following two circumstances into account. In the first place, the light intensity in the first experiment is of the order that the photo-saturation commences in the second experiment. In the second place, the condition in the experiment I is such that the light must pass through a layer of solution of a moderate thickness before it reaches the adsorption surface. Thus the intensity of light which passes through the solution and arrives at the adsorbent is reduced according to Beer's law. From this point of view, we could in fact explain the results of Fig. 2 almost quantitatively.

Details of the experiments and full discussion will be published in the Journ. Inst. Polytechnics, Osaka City University. The authors would like to express their gratitude to Mr. S. Kato and Miss A. Watanabe for much help in experiments. The present investigation was supported in part by a grant from the Ministry of Education.

Institute of Polytechnics, Osaka City University, Osaka

(3) M. Koizumi and N. Mataga, to be published in the near future.

Physicochemical Studies of Organic Dyestuffs in Relation to Photochemistry. II. Influence of the Addition of K-Polyvinylsulfate upon the Absorption Spectra and Fluorescence of Rhodamine 6G in Aqueous Solution

By Masao KOIZUMI and Noboru MATAGA

(Received June 20, 1952)

Introduction

We have taken up the investigation of metachromasy, as the first step towards the study of the interaction between high polymers and organic dyes.

There are some experimental works reported on this phenomenon,[1][2][3] but the general theory which is applicable to all cases has not yet been established; the phenomenon seems in general to be very complicated and perhaps may not be explained from a single view-point. Among various ideas proposed for the mechanism, the following two seem to be most noteworthy.

(1) According to the first idea, metachromasy is considered as a result of some change in the electronic structure of dye ion which is caused by the electrostatic interaction between high-molecular-weight electrolyte and dye ion.[3]

(2) According to the second idea, it is attributed to the change of aggregation of dye ions which results from the adsorption of the latter upon high polymers.[1][2]

These two ideas do not, as we believe, contradict each other. There may exist some cases which can be comprehended simply by the first theory and others which can be explained only by the second theory. In general, however, there will be many cases which can be interpreted correctly only when both of the two theories are taken into account.

In the following discussion the above two cases will be called the ideal case (1) and case (2), respectively. For the systematic investigation of metachromasy, it is desirable, we believe, to search at first for such ideal cases which can be fully explained as case (1) or case (2). For this search, the following arguments might be of some help. If the metachromatic molecule has only one functional group and is of relatively low molecular weight, and the aqueous dye solution obeys Beer's law, then such a system may have a greater chance to be treated as the case (1). On the other hand, the case (2) may be found in those systems where the metachromatic molecule has more than two functional groups of weak nature, and the dye does not obey Beer's law.

Now the aqueous solution of Rhodamine 6 G shows, on one hand, only feeble metachromasy by the addition of K-Poly-vinylsulfate (P. V. S. K.),[3] which is rather a strong metachromatic substance, while, on the other hand, some of the Rhodamine ions are in the dimerised state in the aqueous solution, the fraction of the dimer increasing with the concentration according to the mass action law.[4] On the ground of these facts already reported by other investigators, we considered that Rhodamine 6 G-PVSK system might be treated as the case (2), and it has been confirmed to be the case by the present systematic study over a wide range of concentrations both of the dye and PVSK.

The purpose of this paper is to show how the change in the absorption spectra of the Rhodamine 6 G aqueous solution caused by the addition of PVSK can be interpreted quantitatively as the ideal case (2). In addition we will report some experimental results on the quenching of fluorescence of Rhodamine 6 G by PVSK, and will discuss them on the same ground.

Experimental

For the measurement of absorption spectra and the relative intensity of fluorescence, Beckman Spectrophotometer Model D. U. was used.

PVSK was obtained by the sulfonation of polyvinyl alcohol of which the polymerization

(1) L. Michaelis and S. Granick, *J. Am. Chem. Soc.*, **67**, 1212 (1945).
(2) L. Michaelis, *J. Phys. & Colloid* Chem., **54**, 1 (1950).
(3) Terayama, *Kagakuno Ryoiki*, **1**, 71 (1947).
(4) W. L. Levshin, *Acta Physicochim. U. R. S. S.*, **1**, 681 (1935).

degree was 1800. Two samples were prepared whose degrees of sulfonation were determined to be 61 % and 36 %.

The experimental results can be summarised as follows.

(a) The absorption spectrum of Rhodamine 6 G in aqueous solution has a peak at 526 $m\mu$ with a small shoulder at 500 $m\mu$ when dilute, while as the concentration increases, the latter grows gradually, the former reducing at the same time. This observation is the same as reported by other investigators and the peaks at 526 $m\mu$ and at 500 $m\mu$ are considered respectively to be due to the monomer (M-Band) and the dimer (D-Band).[4]

(b) The molar fluorescence intensity, F/C (where F is the intensity and C is the analytical concentration of dye in mol. mol./l.) remains constant from very dilute solution up to 5×10^{-6} mol/l., but beyond this value, it decreases monotonously with increasing concentration and approaches zero asymptotically.

(c) When PVSK is added step by step to the Rhodamine 6 G aqueous solution of a finite concentration, at first D-Band grows gradually accompanied with the reduction of M-Band, but when the quantity of the added PVSK reaches a certain critical value, then M-Band begins to grow again, though the turning point is not so sharp and varies according to the dye concentration. Some examples are shown in Fig. 1.

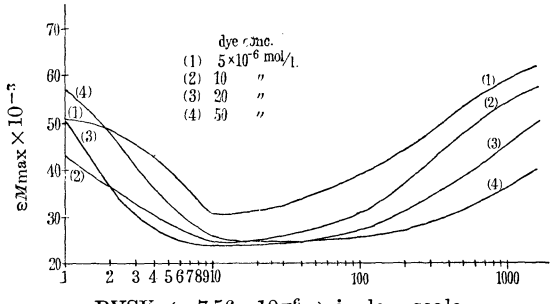

Fig. 1.—Change of molar extinction coefficient of M-band max. by P.V.S.K.

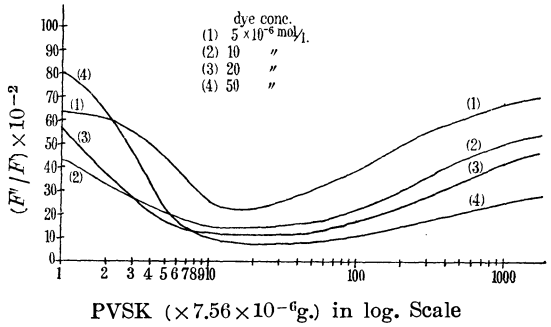

Fig. 2.—Change of relative fluorescence intensity (F'/F) by P.V.S.K.

Such behaviour is always observed in any concentration of dye between 5×10^{-6} mol./l. and 5×10^{-5} mol./l. In addition, it is to be noted that the position of M-Band does not change at all by the addition of PVSK and D-Band shows only a very feeble shift toward the shorter wave length.

(d) With the addition of PVSK the intensity of fluorescence decreases gradually at first until the concentration reaches the same critical value as the absorption, and beyond the critical concentration, the intensity gradually recovers with the further addition of PVSK. Some examples are shown in Fig. 2.

Discussion

As for the absorption spectrum of the aqueous Rhodamine 6 G solution, Levshin[4] performed a quantitative study and analysed the result on the assumption that the spectral change with concentration depends upon the monomer-dimer ratio determined by the mass action law. He also measured the intensity of fluorescence and could roughly account for the concentration quenching as a result of the dimerisation on the assumption that only monomer can fluoresce while dimer cannot.

Our results for the aqueous dye solution (with no PVSK added) are quite in accord with his.

Now when PVSK is added, such behaviour as mentioned above (cf. c and d) is observed and these results can be explained very well by the following model.

" When PVSK is added to the aqueous solution of dye, the dye ion concentrates in the neighborhood of PVSK molecule (or it may conventionally be stated, that the dye ion is adsorbed on PVSK), where the association equilibrium shifts greatly toward the dimer; but the optical properties for both monomer and dimer such as electronic states related to the light absorption, absorption coefficient and efficiency of fluorescence are supposed to be influenced scarcely at all by this adsorption ". According to this model, it goes without saying that we can explain the observed decreases both in M-Band and in fluorescence intensity when a small quantity of PVSK is added; while the phenomena of recovery both in M-Band and in fluorescence when enough PVSK is added can be interpreted as follows.

When the added quantity of PVSK reaches a certain value (which depends on the concentration of dye), the dye concentration on the surface of PVSK will begin to decrease since the amount of dye in the whole system remains constant; then the association equilibrium will become shifted back again toward the monomer and the concentration of the monomer in the whole system increases, which causes M-Band and the fluorescence intensity to recover.

Thus Rhodamine 6 G-PVSK system seems to belong to the ideal case (2) described in the introduction.

Though the above qualitative explanation is very reasonable, there might be some other ways

of explanation. For example, if the interaction between PVSK molecules, in the region of high concentration, becomes so great as to change their aggregation in some way, this change of aggregation in PVSK might cause the adsorbed dye molecule to be detached back into the solution as monomer.

In connection with such a possibility the recent report of Lovelock[5] is to be noted. He studied the fluorescence in almost the same system as ours and observed the same phenomenon of recovery; he did not however explain it clearly and attributed it rather ambiguously to the ionic effect. He seems to be of the opinion that the dye ion when attached to the high polymer loses its tendency for fluorescence. If this be true, the phenomenon of recovery must be exclusively due to the detachment of the dye ion, which will take place only when some remarkable change in the state of aggregation occurs in PVSK. This is very improbable in the case of PVSK, but, in order to confirm this more definitely, we have further examined our model more quantitatively in two ways as follows.

(1) First, on the assumption that the present system is the ideal case (2) the molar fraction of the monomeric ion in the whole system can be calculated from the following two equations ((1) and (2) respectively refer to the absorption data and fluorescence data).

$$x_M(A) = (2\varepsilon - \varepsilon_D)/(2\varepsilon_M - \varepsilon_D), \qquad (1),$$

$$x_M(F) = \frac{(F/c)(F'/F)}{(F/c)_{c\to 0}}. \qquad (2).$$

In equation (1), ε is the molar extinction coefficient at the peak of M-Band in any system, ε_M and ε_D are respectively that of monomer and dimer at the same position, which can be obtained when the concentration of dye is extrapolated to zero or infinite.

In equation (2), F is the intensity of fluorescence when the dye concentration is c and no PVSK is added, while F' is the same quantity when some PVSK is added at the same concentration of dye. The values of F'/F and $(F/c)/(F/c)_{c\to 0}$ can be obtained from the experiment and $x_M(F)$ can thus be calculated.

We have calculated $x_M(A)$ and $x_M(F)$ in the whole range of concentrations of dye and PVSK. The results can be summarised as follows.

When the concentration of dye is 5×10^{-6}mol./l., $x_M(A)$ and $x_M(F)$ coincide almost completely in the range from 7.56×10^{-6} g. to $2000\times7.56\times10^{-6}$ g. of the added PVSK, as shown in Table 1. As the dye ooncentration is increased, the ratio $x_M(A)/x_M(F)$ gradually increases to some extent*; the result suggests the existence of some other effects of the high polymer on fluorescence, which are not taken account of in our model. In spite of such a discrepancy, the values of $x_M(A)$ and $x_M(F)$ change almost in parallel over a wide range of concentrations both of the dye and PVSK.

Table 1

$x_M(A)$ and $x_M(F)$ for various quantities of added PVSK.

dye conc. (mol./l.)	conc. of PVSK (unit $=7.56\times10^{-6}$g.)	$x_M(A)$	$x_M(F)$
5×10^{-6}	0	0.95	0.87
	1	0.56	0.55
	2	0.52	0.46
	4	0.44	0.47
	10	0.24	0.21
	25	0.26	0.21
	125	0.39	0.36
	200	0.48	0.44
	1000	0.68	0.58
	1500	0.76	0.77
	2000	0.79	0.56
10×10^{-6}	0	0.94	0.79
	1	0.44	0.34
	2	0.34	0.26
	10	0.22	0.11
	25	0.17	0.12
	125	0.27	0.17
	250	0.39	0.26
	500	0.44	0.37
	1000	0.61	0.39
	1500	0.62	0.54
	2000	0.70	0.46

Those results including Table 1 are considered to support our model quite well.

(2) Next, we have tried, on the basis of our model, to derive a theoretical relation between $x_M(A)$ on one side and the change of concentrations both of dye and PVSK on the other, in order to examine more precisely whether the experimental results can be reconciled with the model.

For this purpose, we have further assumed such a simple model of adsorption as the following; the adsorption equilibria are supposed to be established separately for monomer and dimer according to the following two equations.

$$C_M' = k_M C_M, \qquad (3),$$

$$C_D' = k_D C_D. \qquad (4).$$

where C_M and C_D are, respectively, the concentrations of monomer and dimer in the solution (in mol./l.) while C_M' and C_D' are the concentrations of the two species on the surface of the adsorbent (i.e. PVSK) (in mol./cm^2.).

In addition to these two equations, the mass action law obviously holds in the solution

$$C_M^2/C_D = K, \qquad (5),$$

We put further

(5) J. E. Lovelock, *J. Chem. Soc.* **1951**, 115-20.

* Levshin (4) has observed such a discrepancy even in the simple aqueous solution of Rhodamine 6 G.

P: number of grams of PVSK
S: the area of adsorbent per 1 g. (in cm.^{2})
V: the volume of solution (in cm.^{3})
C_0: the analytical concentration of the dye (in mol./l.)

then, starting from the above three equations (3) (4) (5) we can easily derive the following equation

$$\frac{y^2}{ZK} = \frac{(1+a_M P)^2}{1+a_D P}, \tag{6}$$

where y and Z are concentrations of the monomer and dimer, respectively, in the whole system which are given by equations (7) and (8)

$$y = \frac{C_M(V+k_M SP)}{V}, \tag{7}$$

$$Z = \frac{C_0 - y}{2}, \tag{8}$$

a_M and a_D are the quantities given as follows

$$a_M = k_M S/V$$
$$a_D = k_D S/V.$$

It is remarkable that the equation (6) has the peculiar character that y^2/ZK is a universal function of the quantity of added PVSK alone, irrespective of the dye concentration. If this relation really holds between the experimentally obtained y^2/ZK values and P, we may conclude the correctness of our model with much confidence.

Now the value of y can be calculated from the relation $y = c_0 x_M(A)$* with the use of the experimentally obtained $x_M(A)$ value, and Z-value is also easily calculated by the relation (8). Thus, we have tested the applicability of the relation (6) for the experimental data. It turned out that they obey the relation (6) quite well throughout the whole range of experiment covering from 5×10^{-6} mol./l. to 5×10^{-5} mol./l. for dye concentration and from 7.56×10^{-6} g. to 15.17×10^{-3} g. for PVSK. Especially, when P is large, the theoretical requirement is satisfied almost quantitatively; in this region, the equation (6) is put approximately as follows,

$$\frac{y^2}{ZK} \approx \frac{a_M^2}{a_D} P + 2\frac{a_M}{a_D}, \tag{9}$$

and the single universal linear relation must hold between y^2/ZK and P irrespective of the dye concentration. The experimental data have proved to satisfy this condition almost completely as shown in Fig. 3.**

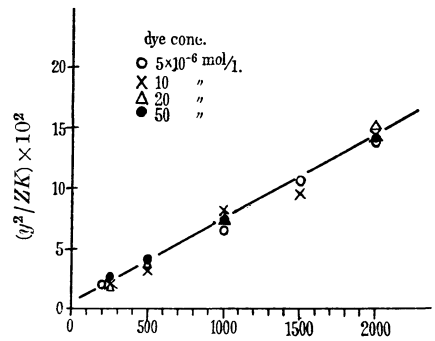

Fig. 3.—(y^2/ZK)~P diagram for various dye concentrations.

In the opposite extreme case where the quantity of PVSK is small, (6) becomes approximately as follows

$$\frac{y^2}{ZK} \approx \frac{1}{1+a_D P} \tag{10}$$

In this region, the situation is not so good; at the fixed P-value, the experimental y^2/ZK values for the different dye concentrations differ a little from one another, though, for each dye concentration, the variation of the value y^2/ZK against P conforms with the above relation. This disagreement may, however, be attributed to the inadequacy of the equations (3) and (4) in this region. For, when the dye concentration is moderate and the quantity of PVSK is very small, the adsorption is more or less in the neighbourhood of saturation, and it may be a better approximation to put

$$C_M' = 0, \quad C_D' = \text{const}$$

instead of (3) and (4). Then the equation (10) becomes

$$\frac{y^2}{ZK} = \frac{1}{1+\dfrac{C_D' SP}{C_D V}}, \tag{11}$$

which agrees with the experimental results at least qualitatively. With (9) and (10) or (9) and (11), we can estimate the value of a_M and a_D as follows

$$a_M \simeq 1.6\times10^3$$
$$a_D \simeq 1.3\times10^5.$$

Therefore

$$k_M/k_D = 1/100.$$

Thus we can conclude, on the basis of the ideal case (2), that when the dimer ion is adsorbed on PVSK about 100 times more than the monomer, the change of absorption spectrum such as experimentally observed can be explained almost quantitatively.

* For some reasons x_M (A) is more reliable than x_M (F).

** Thus, in this region are approved not only our proposition that the present system of metachromasy is the ideal case (2), but also the simplified model of adsorption (equation (3) and (4)).

Conclusion

Two ideal cases for metachromasy were proposed: (1) one in which the effect is simply due to the change of the electronic state in the dye ion as a result of the interaction between the dye ion and metachromatic molecule, (2) the other in which the effect is simply due to the change of aggregation caused by the adsorption of the dye ion on the metachromatic substance. Two such effects are considered to be superposed in a general case.

Rhodamine 6G-PVSK system can be explained almost quantitatively as a second ideal case.

The full account of the experimental data and the extensive discussion including other experimental results will be published in J. Inst. Polytech. Osaka City University.

The present research was supported in part by a grant from the Ministry of Education.

Institute of Polytechnics, Osaka City University, Osaka

The Iodine Reaction of Rare Earth Elements. II.* Colorimetric Determination of Acetate Ions by the Iodine Reaction of Rare Earth Elements

By Kenjiro KIMURA, Nagao IKEDA and Masayasu NOMURA

(Received June 28, 1952)

It has long been known that basic lanthanum acetate shows a blue color reacting with iodine[1]. Krüger and Tschirch[2] applied this color reaction to the detection of acetate or lanthanum ions and reported its relatively high sensitivity. On the other hand, the application of this reaction to the quantitative analysis has long been the problem left to be solved. However, Hutchens and Kass[3] reported in their recent publication that successful results could be obtained on the micro-determination of acetate ions by this reaction.

The present authors[4] already noticed that similar color reactions occur when the basic acetate of praseodymium, neodymium or samarium reacts with iodine under the suitable conditions. In the present paper, they confirmed the method of Hutchens and Kass, then examined the possibility for the application of the corresponding reactions of praseodymium and neodymium to the same purpose.

Experimental

Materials.—The purity of the salts of lanthanum,[5] praseodymium[6] and neodymium[7] used was examined by the X-ray spectroscopic method. These salts are sufficiently pure for the practical use.

Use of Basic Lanthanum Acetate.

1. Development of the Color.—In a 5 ml. glass-stoppered test tube, put 1 ml. of standard solution of acetate ions[8], 1 ml. of lanthanum nitrate solution[9], 1 ml. of 0.1 N ammonia[10] and 1 ml. of 0.02 N iodine-potassium iodide solution. Heat the stoppered tube in boiling water for five minutes[11]. By this procedure, the color of the

* Previous paper: Kimura and Ikeda, This Bulletin, **21**, 19 (1948).

(1) Damour, *Compt. rend.*, **43**, 976 (1856).

(2) Krüger und Tschirch, *Ber.*, **62**, 2776 (1929).

(3) Hutchens and Kass, *J. Biol. Chem.*, **177**, 571 (1949).

(4) Kimura and Ikeda, This Bulletin, **21**, 19 (1948). They also observed that basic propionate of lanthanum, praseodymium or neodymium also shows a blue color reacting with iodine.

(5) Lanthanum oxide, commercially supplied in Japan, was purified by the Prandtl's fractional precipitation method; cf. Prandtl und Losch, *Z. anorg. allgem. Chem.*, **127**, 209 (1923).

(6) Praseodymium oxide of the Auer-Gesellschaft was used.

(7) Neodymium oxide of the Auer-Gesellschaft was used.

(8) The standard solution was prepared as follows; dissolve 2.226 g. sodium acetate ($CH_3COONa \cdot 3H_2O$) in water and make the total volume 1 l. 1ml. of the solution corresponds to 1.00 mg. CH_3COOH.

(9) 1 ml. of the solution corresponds to 5.0 mg. of lanthanum.

(10) The *p*H value of mixture of 1 ml. of lanthanum nitrate solution and 1 ml. of 0.1 N ammonia is about 8.8. According to Hutchens and Kass, the *p*H value of this mixture must lie between 8.3 and 8.5.

(11) Heating time less than fifteen minutes does not affect the coloration.

solution becomes yellowish green to greenish blue according to the amounts of acetate ions present.

The absorption curve for the solution with color developed as above, measured by the Pulfrich photometer, is shown in Fig. 1. The absorption at 430 mμ[12] evidently results from the light absorption by excess iodine, and the absorption maximum at 610 mμ[13] is attributed to that by the iodine-basic lanthanum acetate compound. For the actual use, however, the authors selected the filter S66 because of its much lower absorption against excess iodine.

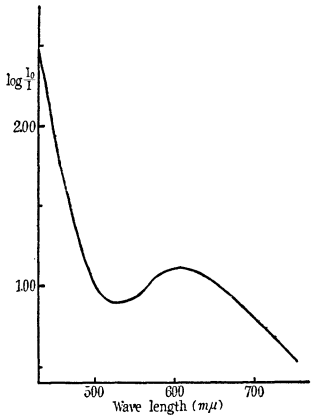

Fig. 1.—Absorption curve for the iodine-basic lanthanum acetate solution.
(0.5 mg. CH_3COOH/4 ml., Cell: 5 mm.)

The color thus obtained is very stable, and shows virtually no change even after 24 hours' standing.

2. Calibration Curve.—The solutions containing various amounts of acetate ions were treated in the way mentioned above, and the relation between the concentration of acetate ions and optical density was investigated. In Fig. 2 data obtained are presented graphically, showing the relation between optical density at 660 mμ and the amounts of acetate ions.

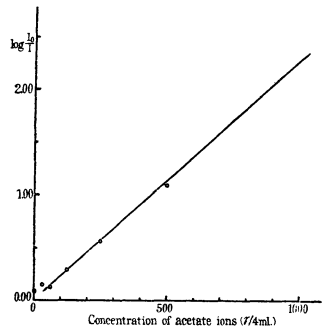

Fig. 2.—Calibration curve for basic lanthanum acetate.
(Filter: S66, Cell: 5 mm.)

As is evident from the figure, the Beer's law is adaptable in the concentration range of acetate ions between 60 γ and 500 γ (as CH_3COOH)[14] per 4 ml., i. e. the total volume of the colored solution. In this concentration range, the colored solution is clear, and the colorimetric determination of acetate ions by the Pulfrich photometer is possible.

When the concentration of acetate ions is smaller than 60 γ per 4 ml., the color caused by iodine reaction of basic lanthanum acetate is no longer observed and the resulting solution partly shows colloidal turbidity[15]. The limit of identification for acetate ions by this method is 60 γ per 1 ml. of the original sample solution.

When the concentration is greater than 500 γ per 4 ml., deviations from the Beer's law occur.

3. Effect of Other Ions Present.—As for the effect of other ions present and the method for removing the interfering ions in this procedure, it was already studied in detail by Hutchens and Kass[16], and their methods seem to be valid.

In addition, citrate ions severely interfere with this color reaction.

Use of Basic Praseodymium Acetate.

It has been believed that the color reaction between iodine and basic acetates of rare earth elements is specific to lanthanum. However, Kimura and Ikeda[17] noticed that besides the basic acetate of lanthanum, those of praseodymium, neodymium and samarium take on an intense indigo color when properly treated with iodine. It allows the prediction that in such cases the colorimetric determination of acetate ions might be possible as in the case of lanthanum.

1. Development of the Color.—Although the acetate solution was treated under the same condition as in the case of lanthanum except the use of praseodymium nitrate instead of lanthanum nitrate, no transparent colored solution suitable for the quantitative analysis could be obtained.

Since it was already pointed out in the previous paper that the amount of ammonia used always plays an important role in the iodine reaction of rare earth elements, the authors tried the experiment with various concentrations of acetate ions and ammonia. The concentration of acetate ions should be high and that of ammonia should be low for the present purpose.

1 ml. of standard solution corresponding to 5 mg. acetate[14] was treated with 1 ml. of praseodymium nitrate solution[18], 1 ml. of ammonia of various concentrations and 1 ml. of 0.02 N

(12) It corresponds to the absorption of the filter S43.
(13) It corresponds to the absorption of the filter S61.
(14) The amount of acetate ions is represented as γ or mg. CH_3COOH in this paper.
(15) In the blank test, i. e. when no acetate ion is present, the resulting solution also shows colloidal turbidity to some extent.
(16) op. cit.
(17) op. cit.
(18) 1 ml. of the solution corresponds to 11.4 mg. of praseodymium.

iodine-potassium iodide solution in a 5 ml. glass-stoppered test tube. After 15 minutes'[19] heating in boiling water, the color of the resulting solution was observed. The results are listed in Table 1. It is revealed that the use of ammonia of 0.04—0.06 N gives a transparent colored solution suitable for the colorimetric determination. The pH values in this case are much smaller than those in the case of lanthanum.

Table 1

Concentrations of Ammonia (N)	Coloration and Precipitation	pH Values of the Mixed Solution of 1 ml. of Praseodymium Nitrate and 1 ml. of Ammonia
0.02	No coloration or precipitation	—
0.03		6.0
0.04	Transparent green solution	6.3
0.045		6.5
0.05		6.6
0.06		7.0
0.07	Blue precipitation	7.4
0.08		—

2. Calibration Curve.—The solutions containing various amounts of acetate ions were treated in the way mentioned above using 0.045 N ammonia, and the relation between the concentrations of acetate ions and optical density was checked by the Pulfrich photometer. The results are illustrated graphically in Fig. 3 showing optical density at 660 mμ versus the amount of acetate ions.

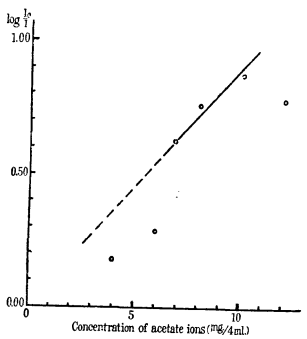

Fig. 3.—Calibration curve for basic praseodymium acetate.
(Filter: S66, Cell: 5mm.)

In the range of concentrations of 5—10 mg. acetate[14] per 4 ml., the transparent, yellowish green—bluish green solution was obtained. Beer's law is approximately adaptable in the range of 7—10 mg. per 4 ml., although the points on the graph are somewhat fluctuating. In smaller concentrations of acetate than 4 mg. per 4 ml., no coloration of the iodine reaction is observed. When it is larger than 10 mg. per 4 ml., blue precipitation occurs, and the colorimetric determination is no longer possible.

As is shown above, the sensitivity of this reaction in the case of praseodymium is much inferior to that in the case of lanthanum. Therefore, lanthanum nitrate should be used for the determination of acetate ions.

Use of Basic Neodymium Acetate.

The use of neodymium salt for the purpose of the determination of acetate ions was then investigated.

1. Development of the Color.—The mixture of 1 ml. of standard solution corresponding to 5 mg. acetate[14], 1 ml. of neodymium nitrate solution[20], 1 ml. of ammonia of various concentrations and 1 ml. of 0.02 N iodine-potassium iodide solution taken in a 5 ml. glass-stoppered test tube was heated in boiling water for ten minutes. Then, the color of the solution was observed. The results are shown in Table 2. The suitable range of concentrations of ammonia is 0.02—0.03 N, and the corresponding pH values are much smaller than those in the case of lanthanum and are almost similar to those in the case of praseodymium.

Table 2

Concentration of Ammonia (N)	Coloration and Precipitation	pH Values of the Mixed Solution of 1 ml. of Neodymium Nitrate and 1 ml. of Ammonia
0.01	No coloration or precipitation	5.7
0.02	Transparent green solution	6.0
0.03		6.4
0.04	Blue precipitation	6.8
0.05		—

2. Calibration Curve.—The solutions containing various amounts of acetate ions were treated in the way mentioned above using 0.02 N ammonia. The relation between the concentrations of

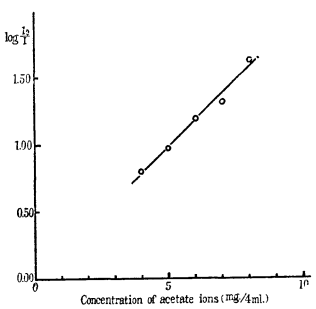

Fig. 4.—Calibration curve for basic neodymium acetate.
(Filter: S66, Cell: 5 mm.)

(19) In the case of praseodymium, fifteen minutes' heating is necessary to complete the color reaction, while five minutes' heating is sufficient in the case of lanthanum.

(20) 1 ml. of the solution corresponds to 7.0 mg. of neodymium.

Table 3

	Concentration of Ammonia used	*p*H Values of the Mixture of Nitrates and Ammonia	Concentration Range Available for the Colorimetric Determination	Limit of Identification
Lanthanum	0.1 N	8.8	60—500 γ/ml.*	60 γ/ml.*
Praseodymium	0.045 N	6.5	7—10 mg./ml.	4 mg./ml.
Neodymium	0.02 N	6.0	4— 8 mg./ml.	4 mg./ml.

* The volume is taken for the original sample solution.

acetate ions and optical density was checked by the Pulfrich photometer. Data are shown graphically in Fig. 4 representing optical density at 660 mμv ersus the amounts of acetate ions. In the concentration range of 4—8 mg.[14], Beer's law is adaptable. At smaller concentrations of acetate ions than 4 mg. per 4 ml., no coloration of the iodine reaction is observed. When it is larger than 8 mg. per 4 ml., blue precipitation occurs and the colorimetric determination is no longer possible.

The sensitivity of this reaction in the case of neodymium is much inferior to that in the case of lanthanum. It rather resembles to that in the case of preseodymium.

Conclusion

It is evident that the color reaction between iodine and the basic acetate of praseodymium or neodymium is applicable to the colorimetric determination of acetate ions as in the case of lanthanum. There are, however, partial differences between each case of them in the suitable concentration of ammonia and the sensitivity of the reaction. These are briefly tabulated in Table 3 for comparison.

The concentration of ammonia and the pH value suitable for quantitative analysis decrease in the order of lanthanum, praseodymium and neodymium, i. e., with the decrease of the basicity of the elements.

As for the sensitivity of the reaction for acetate ions, it is especially good in the case of lanthanum. In the case of praseodymium and neodymium, it resembles each other and are much inferior to that in the case of lanthanum.

Summary

The application of the color reaction between basic lanthanum acetate and iodine to the quantitative analysis has long been the problem left to be solved. Recently, hawever, Hutchens and Kass succeeded in application of this color reaction to the micro-determination of acetate ions with good results.

The present authors examined this method and confirmed that satisfactory results were obtained in its application. In addition, the authors found that the corresponding reactions for praseodymium and neodymium were applicable, too, to the same purpose, although in these cases the sensitivity was not so good as that in the case of lanthanum.

The authors wish to express their hearty thanks to Prof. Kin-ichiro Sakaguchi for his kind suggestions rendered during the course of this work.

Department of Chemistry, Faculty of Science, Tokyo University and Department of Agricultural Chemistry, Faculty of Agriculture, Tokyo University

Separation of the Components of Atmospheric Salt and their Distribution (Continued)

By Tadashiro KOYAMA and Ken SUGAWARA

(Received July 7, 1952)

Introduction

In the previous paper[1] it was shown that due to evaporation, the spray particles of the sea water in the air, separate into at least two kinds of daughter particles; the one, hygroscopic in nature and consisting mainly of sodium chloride, and the other, crystalline in nature and consisting mainly of calcium sulphate*. The latter, being more stable, continues to remain longer in the air and tends to be carried horizontally towards inland or to be raised higher vertically. Thus the distribution of several components of the atmospheric salt are so arranged that the ratios Ca/Cl, Mg/Cl and SO_4/Cl grow larger as we move towards inland or go higher from sea level.

The writers continued the study in a small island "Sugashima" (Fig. 1), located in Ise Bay, about 4 km off Toba, Mie-Prefecture, and the situation in a limited area close to the beach made it possible for them to obtain considerable new information, which will be given below.

The study was carried out as follows: Seven stations were chosen, different in height, starting from the sandy beach "Shirasaki" up to the summit of Mount Ôyama with a height of 236.6 m. At each station except Shirasaki the washings of pine needles were collected

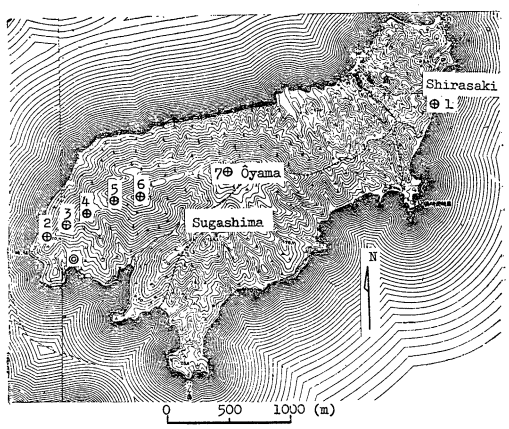

Fig. 1.

⊕···Stations where the samples were collected.
◎···Marine Biological Laboratory attached to Nagoya University.

according to the procedure which was given in the foregoing paper[1]. At Shirasaki, a bare sandy area with no pine trees, a cotton gauze, spanning a metallic frame, was fixed in the calm weather just above the sand so that it was exposed to the sea breeze. After 5 hours exposure the gauze was taken off to rinse with distilled water. In addition to the determination of Na, Mg, Ca, Cl, SO_4 of the washings of pine needles and the cotton gauze, we determined the total carbonic acid of the samples, collected on Dec. 18—19, 1949, where its ratio to chlorine was determined. Also the residual fraction of filtration of a number of the washings left on filter paper, was determined for Ca and Mg and their ratios to Cl were established. The results are given in Tables 1~4.

Results and Discussions

1. What was shown first was that the variation in the composition of the atmospheric salt was very evident already in the samples from the succeeding seven stations (See Table 1). This means that the fractional separation of the components of sea water begins to occur over the

(1) K. Sugawara, S. Oana, and Tadashiro Koyama: Separation of the Components of Atmospheric Salt and their Distribution, This Bulletin, **22**, No. 2, 47-52 (1949).

* It should be noted that a similar attempt to interpret the variation in the salt composition in rain water by the fractional segregation of the sea salt was already done by H. Matsui who assumed the segregated particles to act as condensation nuclei, thus causing the variation (*J. Meteor. Soc. Japan*, **22**, 2-12 (1944)). In the present paper, the writers deal on the one hand with the problem, and their conclusions are based upon observational and experimental firmer and more definite data, on the other hand they make it clear that the fractionation begins to occur as early as just after the spray is formed from the surface of the sea.

It should also be added that, according to the writers' view, salts are not only supplied to the rain water as condensation nuclei but a considerable amount of them is dissolved in it in its course of falling by washing after the drops are formed.

Table 1

Washings of Cotton Gauze and Pine Needles from 7 Stations, Sugashima, Different in Height and Distance from the Beach. (Nov. 13, 1948)

Ratio in Equivalent	Sea Water	Stations 1	2	3	4	5	6	7
SO_4/Cl	0.100_7	0.096_8	0.099_5	0.124_0	0.132_6	0.143_9	0.162_0	0.149_3
Na/Cl	0.860	0.829	0.819	0.848	0.860	0.845	0.845	0.853
Ca/Cl	0.037_9	0.041_2	0.061_6	0.065_5	0.071_8	0.074_6	0.105_6	0.099
Mg/Cl	0.195_1	0.198_6	0.196_9	0.198_4	0.208_4	0.223_9	0.236_6	0.224_7
Ca/SO_4	0.376_2	0.426	0.618	0.528	0.544	0.519	0.652	0.668
$\Sigma+/\Sigma-$	0.98_6	0.97_4	0.98_1	0.98_8	1.00_6	0.99_8	1.02_2	1.02_5

Table 2

The Total Carbonic Acid and its Ratio to Cl in the Washings of Pine Needles from Sugashima

	Sea Water	Stations 1	2	3	4	5	6
Cl (mg./l.)	184_{30}	215_9	725	733	$376._9$	$341._8$	561
Total carbonic acid (milli-equiv./l.)	3.63	0.56	0.35	0.61	0.38	0.47	0.93
Total carbonic acid/Cl (Ratio in equivalent) $\times 10^2$	0.69_8	0.9_2	1.7	2.9	3.6	4.9	5.9

surface of the sea as early as just after spray is formed. A fuller discussion will be given later.

2. The simultaneous determination of Cl and total carbonic acid (Table 2) shows that carbonates are important components of the atmospheric salt and their relative amount in it grows larger as we recede from the beach, a relation coming in harmony with a general trend of a relative increase of positive components, to negative ones as shown by $\Sigma+/\Sigma-$, the ratio of the sum of the equivalents of the positive components to that of those of the negative ones (Table 1). The increase of $\Sigma+/\Sigma-$ is not only evident in the case of the washings of pine needles on Sugashima, but also in sets of the comparison data of samples of rain water as well as of the pine needles between Sugashima, Nagoya and Matsumoto as given in Tables (Table 3 a, b). The relation is also true in the comparison of the ordinary rain-water, rain from thunderstorms and the rime water from Mt. Fuji (Table 3 c). The whole result tells that in addition to calcium sulphate, we must assume magnesium carbonate and particularly calcium carbonate as members of the stable segregates from the primary spray particle, which remain longer in the air and form predominant components of the atmospheric salt in the air in higher strata and over locations away from the sea beach.

The present view is supported by the determination of Mg and Ca in the residual fraction from filtration of the washings of pine needles which is assumed to consist mainly of carbonates. The result given in Table 4. suggests that actually Mg and Ca are the primary positive components of the carbonate in question and at the same time it shows that between two kinds of carbonates, calcium carbonate is more stable and its

Table 3

(a)

Ratio in Equivalent	Sea Water	Oridinary Rain Sugashima	Nagoya	Matsumoto
SO/Cl	0.1007	0.35	0.368	1.70
Na/Cl	0.860	0.85	0.882	0.91
Ca/Cl	0.0379	0.25	0.298	3.50
Mg/Cl	0.1951	0.23	0.291	0.66
Ca/SO_4	0.376	0.72	0.832	2.06
$\Sigma+/\Sigma-$	0.986	0.98	1.074	1.88

(b)

Ratio in Equivalent	Washings of Pine Needles Sugashima	Nagoya	Matsumoto
SO_4/Cl	0.17	0.72	1.82
Na/Cl	0.83	0.85	1.58
Ca/Cl	0.09	0.55	4.13
Mg/Cl	0.22	0.27	1.26
Ca/SO_4	0.53	0.76	2.27
$\Sigma+/\Sigma-$	0.97	0.97	2.47

(c)

Ratio in Equivalent	Ordinary Rain	Thunder-storm	Rime from the Summit of Mt. Fuji
SO_4/Cl	0.368	3.24	1.00
Na/Cl	0.882	2.43	1.09
Ca/Cl	0.298	2.19	1.90
Mg/Cl	0.291	0.63	0.40
Ca/SO_4	0.832	0.676	1.90
$\Sigma+/\Sigma-$	1.07_4	1.23_6	1.69

relative amount increases rapidly from the beach towards the summit of Mt. Ôyama.

Table 4

Acid Soluble Components in the Residual Fractions of the Washings of Pine Needles from Sugashima

Ratio in Equivalent $\times 10^2$	1	2	3	4	5	6
Ca/Cl	0.002	—	0.746	0.860	1.164	2.65
Mg/Cl	0.357	—	0.221	0.760	0.982	1.174

3. In the previous paper, the writers tried to picture a rough image of the processes of the fractionation of the spray of sea water which occasion the regular distribution of the components of atmospheric salt. The result, reported in the present paper, forces us to modify the picture and elaborate it in its detail to some extent. Namely in the foregoing rough picture the writers assumed that the primary particle of the spray of sea water separates into two kinds of secondary particles; the one, consisting mainly of Ca and SO_4 and more stable, remains longer in the air, and the other, consisting mainly of sodium chloride and less stable, is fated to fall down from the air earlier. The later knowledge, obtained above, affords reason to assume calcium carbonate as well as magnesium carbonate as stable segregates other than sulphates. Secondly the segregation processes must be assumed to begin to occur as early as just after the spray is formed due to wave crushing and while it is suspended in the air unstable segregates fall down back to the sea surface below, leaving a mass of particles whose composition is already quite different from that of the original sea water.

4. Further details of the segregation lie still beyond our knowledge; however, the writers may be allowed to try to draw some imaginary picture of it. Thus let us quote the old experiment by Usiglio[2] on laying down of salts from the sea water when it is fated to slow evaporation. According to him, at the first stage of concentration, i. e., till the time when 1 l. of sea water is concentrated to 533 cc., about 0.0642 g. of $CaCO_3$ is laid down and at the second stage of concentration to 112 cc., 1.466 g. of $CaSO_4 2H_2O$ with a smaller amount of $CaCO_3$ separates, leaving a brine containing certain amounts of Na, Mg, Ca, Cl and SO_4. Thus we can naturally assume a similar segregation of salts to occur on the spray in suspension, giving rise to the particles of calcium carbonate and gypsum, leaving brine particles. The particles differ in stability and the greater part of the brine particles which are the least stable, will fall down to the sea surface earlier while the particle of $CaCO_3$, probably the most stable, will remain in suspension in the largest proportion. When the composite mass of particles, thus formed, is carried up to the beach and touched by a cotton gauze or pine needles, it is quite natural to assume that a second selective adhesion occurs depending upon the different adhesivity of the individual components. Anyhow we can try to test whether it is possible to obtain the composition of the washings-samples by an appropriate combination of these three kinds of particles, i. e., (a) $CaCO_3$, (b) $CaSO_4 2H_2O$ and (c) the residual brine. For example, let us try to compose the composition of the gauze washings, given in Column 3 of Table 1, by combination of 1 part of the salt in the brine (c), x part of chalk (a) and y part of gypsum (b)*.

Each fraction from 1 l. sea water contains the following amounts of component in equivalent.

	Na	Mg	Ca	Cl	SO_4	CO_3
Fraction (a)	—	—	0.00218	—	—	0.00218
Fraction (b)	—	—	0.0065	—	0.0065	—
Fraction (c)	0.518	0.111	0.003	0.595	0.045	—

Then the amounts of the individual components in the final composite are

Na 0.518
Mg 0.111
Ca .....$0.003+0.00218x+0.0065y$
Cl 0.595
SO_4.... ....$0.045+0.0065y$

Then, in order to obtain the value of y, the following equation is set up:

$$\frac{Na}{SO_4}=\frac{Na}{Cl}\text{ obs.}\div\frac{SO_4}{Cl}\text{ obs.}$$

By introducing the values obtained above and those given in Column 3 of Table 1,

$$\frac{0.518}{0.045+0.0065y}=\frac{0.829}{0.0968}.$$

Thus $y=2.38$ and consequently the amount of SO_4 is determined as 0.0605.

Next x can be evaluated similarly by assuming an equation

$$\frac{Ca}{SO_4}=\left(\frac{0.003+0.0155+0.00218x}{0.0605}\right)=(0.426)\text{obs.}$$

Thus $x=3.33$ and consequently Ca=0.0257

Summarizing the result, we can compare the values from direct observation of the ratios of individual components of the washings of the cotton gauze to those calculated from the model process here assumed above.

(2) *Annales chim. phys.*, 3rd Ser., **27**, 92, 172 (1849).

* For convenience the amount of $CaCO_3$, laid down accompanied by gypsum, was added to fraction (a) and Br calculated as an equivalent amount of Cl.

	Sea water	Cotton Gauze Observed	Cotton Gauze Calculated
Na/Cl	0.860	0.829	0.870
Mg/Cl	0.194_4	0.198_6	0.187_6
Ca/Cl	0.037_9	0.041_2	0.043_2
SO_4/Cl	0.100_7	0.096_8	0.101_6
Ca/SO_4	0.376_2	0.42_6	0.42_6
$\Sigma+/\Sigma-$	0.97_4	0.97_4	0.99_9

The conclusion is that the combination of 3.33 parts of fraction (a), 2.38 parts of fraction (b), and 1 part of fraction (c) yields an approximate composition of the washings of the cotton gauze, showing a rough stability sequence of the three fractions which were assumed above, and at the same time it suggests that the fractionation similar to the experiment by Usiglio or something like it, actually occurs on the spray in the air close to the surface of the sea.

No doubt, the treatment above is too easy and arbitrary to explain the supposed complexity of the phenomenon in question. It was simply aimed at building up some concrete broad image along which further studies could be extended. Our knowledge, hitherto obtained, gives a concrete reason to consider magnesium carbonate as another independent fraction and fraction (c) must be divided into several subfractions. Otherwise the variability of the ratio Na/Cl can not be explained. However it will go too far, we believe, for us to discuss the matter further and to try to picture a fuller detail in the process based upon the insufficient knowledge that we now have.

Chemical Institute, Faculty of Science,
Nagoya University, Nagoya

Electrolytic Behavior of Elements of the Group VIa in the Periodic System. I. Potentiometric Studies on the Chromate, Molybdate and Tungstate Ions

By Kuan PAN and Tong Ming HSEU

(Received April 11, 1952)

Introduction

It has been known that molybdic and tungstic acids form well-defined soluble normal salts similar to those of chromates, but they do not resemble chromic acid in some electrolytic behaviors. In their abnormalities, however, molybdic and tungstic acids bear to one another remarkable similarities, such as the formation of poly-anions.

Several investigations on the formation of these poly-anions of molybdate and tungstate in aqueous solutions have been published since the beginning of the twentieth century.(1)~(8) These investigators suggested that, beside the normal ion MoO_4^{--}, various kinds of poly-anions may be formed in aqueous solution at varying dilutions and at different *p*H ranges. Thus the possible existence of $H_3Mo_6O_{21}^{3-}$, $HMo_6O_{21}^{5-}$, or $O(MoO_3)_n^{2-}$, has been proposed by estimating the ratio, Na_2O/MoO_3, from the experimental results of conductometric and potentiometric titrations of molybdate and tungstate with strong or weak acid. On account of the complexity of the relation of equilibria between these poly-anions, or due to the experimental difficulties, some of the conclusions seem to be overstrained or presumptive and further verifications seem to be left for the present investigation.

The present and subsequent papers in this

(1) H. T. S. Britton and W. Leslie, *J. Chem. Soc.*, **1927**, 147.
(2) H. T. S. Britton and M. L. German, *J. Chem. Soc.*, **1930**, 1249; **1931**, 709.
(3) R. H. Vallance and E. G. K. Pritchett, *J. Chem. Soc.*, **1931**, 1421; **1934**, 1586.
(4) G. Jander, K. F. Jahr and W. Heukeshoven, *Zeit. anorg. allgem. Chem.*, **187**, 60, 129 (1930); **194**, 383 (1930).
(5) R. A. Robinson and D. A. Sinclair, *J. Chem. Soc.*, **1934**, 642.
(6) H. Brintzinger and C. Ratanarat, *Zeit. anorg. Chem.*, **224**, 97 (1935).
(7) E. Buchholtz, *Zeit. anorg. allgem. Chem.*, **244**, 149, 168 (1940).
(8) G. Carpeni, *Bull. soc. chim. France*, **1947**, 484, 490, 492.

series have attempted to verify the existence of these poly-anions from results obtained by means of potentiometric and conductometric measurements as well as by studies of the Raman spectra or absorption spectra of these solutions. The purpose of the present paper which reports the results of potentiometric measurements is three fold: first, to obtain more accurate data on the *p*H values of the aqueous solutions of molybdates and tungstates as well as chromates by means of a glass electrode and to ascertain the existence of dimolybdate and ditungstate ions, $X_2O_7^{--}$, from the *p*H changes governing the hydrolytic process of these salts; second, to verify the dissimilarities in electrolytic behavior between chromate and molybdate or tungstate by measuring the *p*H values at varying dilutions and checking the differential quotients, $dp\mathrm{H}/d\log C$, which will also be expected from the theoretical calculation; third, to ascertain the existence of poly-anions at varying *p*H values by means of potentiometric titration of sodium molybdate or tungstate with hydrochloric acid.

Experimental

(1) **Materials.**—Conductivity water having a specific conductivity of 1.6 to 2.4×10^{-6} mho was prepared by refluxing and distilling water over potassium permanganate with sulfuric acid and then redistilling over barium hydroxide in pyrex glass apparatus.

Reagent grade hydrochloric acid was distilled twice. The constant boiling fraction was diluted to a desired concentration and used for the potentiometric titrations.

Reagent grade sodium molybdate and tungstate were recrystallized twice from the conductivity water and heated at 100°C. for two hours.

Potassium molybdate and tungstate were obtained by dissolving 1 mol. each of extra pure molybdic acid and tungstic acid, respectively, in a hot solution containing 2 mols. of potassium hydroxide. The salts separated on cooling were recrystallized, repeatedly, from the conductivity water and washed with 95% alcohol.

Sodium chromate and potassium chromate recrystallized twice from the conductivity water were used in this experiment.

The crystalline water as well as the composition of salts used in the present investigation was checked by the gravimetric method. The solutions were prepared, directly, by dissolving the salt in carbonate-free conductivity water and diluting to a desired concentration before each run.

(2) **Apparatus.**—A vacuum tube potentiometer, constructed in our laboratory, was used with a glass electrode. A vacuum tube, UX 54A,[9] made by Matsuda, Co. in Japan was used in this circuit. The characteristics of the tube are shown as follows:

filament potential	2.0 volt
plate potential	6.0 volt
screen grid potential	4.0 volt
control grid potential	4.0 volt
filament current	0.205 A.
plate current	40 μA.
screen grid current	297 μA.
control grid current	2×10^{-14} A.
mutual conductance	22 $\mu\Omega$

The working circuit is shown schematically in Fig. 1.

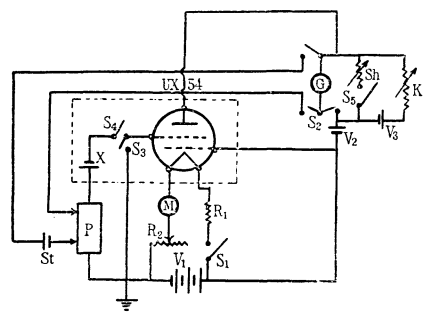

Fig. 1.—The working circuit of the vacuum tube potentiometer.

The component parts of the meter are given here for reference.

V_1:	6 volt battery
V_2:	3 volt battery
V_3:	1.5 volt battery
R_1:	10 ohm rheostat
R_2:	50 ohm rheostat
	20,000 ohm rheostat
K:	3,000, 1,500 and 200 ohms variable resistances
S_1, S_2:	switches
S_2, S_3, S_4:	three pole three throw switches
Sh:	galva shunt
G:	galvanometer
M:	milliammeter
X:	glass elec.rode cell
P:	Leeds and Northrup potentiometer
St:	standard cell

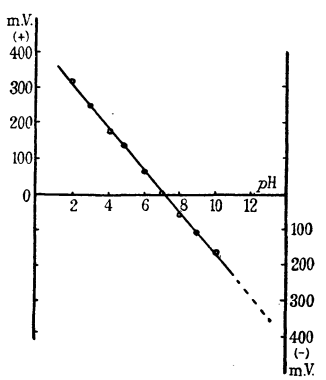

Fig. 2.—Calibration curve of the glass electrode.

(9) Yoshimura, This bulletin, **12**, 359, 443 (1937).

The glass electrode was checked frequently against the Clerk-Lubs series buffer solutions. The calibration curve plotted e. m. f. vs. the pH is indicated in Fig. 2. The quantitative relation between e. m. f., E, observed, and the pH value is formulated as

$$E=0.43-0.0001983\,T\,pH$$

Results and Discussion

(A) Hydrolyses of tungstate, molybdate and chromate.

When a salt of a weak acid dissolves in aqueous solution, the hydrolysis of anions reaches a definite equilibrium for which the generalized reaction is

$$nA^{a-}+mH_2O \rightleftarrows pB^{b-}+qOH^- \qquad (1)$$

and when we take concentration of each constituent in place of activity, in dilute solution, putting

$$[A^{a-}]=C(1-x),\ [B^{b-}]=\frac{p}{n}Cx,$$

$$\text{and } [OH^-]=\frac{q}{n}Cx,$$

where x is the degree of hydrolysis and C the concentration, the hydrolysis constant, K_h, may be given, as a first approximation, by the expression:

$$K_h=\frac{[B^{b-}]^{p/n}[OH^-]^{q/n}}{[A^{a-}]}=\frac{1}{C}\left(\frac{p}{q}\right)^{p/n}[OH^-]^{\frac{p+q}{n}}. \qquad (2)$$

Hence,

$$pOH=-\frac{n'}{p+q}\left(\log K_h-\frac{p}{n}\log\frac{p}{q}\right)-\frac{n}{p+q}\log C$$

or

$$pH=14+\frac{n}{p+q}\left(\log K_h-\frac{p}{n}\log\frac{p}{q}\right)+\frac{n}{p+q}\log C \qquad (3)$$

that is to say, a linear relationship should be held between pH and log C. Consequently, the differential quotient of the pH with respect to the logarithm of the concentration should be constant, i. e.,

$$\frac{dpH}{d\log C}=\frac{n}{p+q}. \qquad (4)$$

In a special case, $p=1$, we have

$$\frac{dpH}{d\log C}=\frac{n}{1+q} \qquad (4a)$$

or with respect to the degree of dilution, V, we obtain

$$\frac{dpH}{d\log V}=-\frac{n}{1+q} \qquad (4b)$$

as proposed by P. Souchay[10].

According to equation (3) if we assume that the hydrolytic processes of normal molybdate and tungstate in dilute solution can be formulated as

$$2XO_4^{--}+H_2O \rightleftarrows X_2O_7^{--}+2OH^- \qquad (1a)$$

and the ionic hydration as well as the other poly-anions formation can be neglected in these cases, the values of solutions may be evaluated as

$$pH=14+2/3(\log K_h+1/2\log 2)+2/3\log C \qquad (3a)$$

or

$$\frac{dpH}{d\log C}=\frac{2}{3}$$

that is to say, the slope of the curve plotted pH vs. $-\log C$ should be $-2/3$.

In the same way, in the hydrolytic process of chromate, which has been assumed to follow the reaction

$$CrO_4^{--}+H_2O \rightleftarrows HCrO_4^-+OH^- \qquad (5)$$

instead of

$$2CrO_4^{--}+H_2O \rightleftarrows Cr_2O_7^{--}+2OH^- \qquad (6),$$

the slope of the curve should be $-1/2$ instead of $-2/3$.

As shown in figure 3, in the cases of molybdate and tungstate, linear relationships exist between pH and $-\log C$ from C=0.1 to 0.001 mol. and the slope of each curve is nearly equal to $-2/3$. Agreement between the calculated and the observed values is excellent. On the other hand,

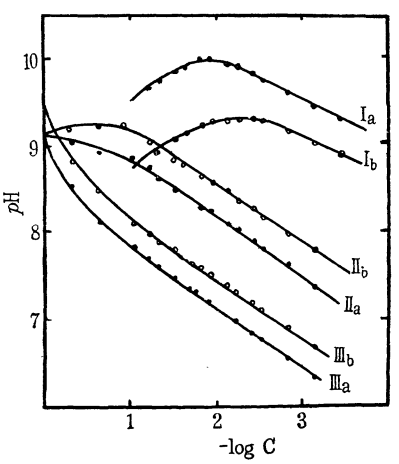

Fig. 3.—Hydrolyses of chromates, molybdates and tungstates.

I a: Sodium chromate
I b: Potassium chromate
II a: Sodium molybdate
II b: Potassium molybdate
III a: Sodium tungstate
III b: Potassium tungstate

(10) P. Souchay, *Bull. Soc. Chim. France*, **1948**, 433.

Table 1

*p*H Values of Chromates, Molybdates and Tungstates Solutions at Varying Dilutions at 30°C.

Dilution (liters/mol.)	$-\log C$	Na_2CrO_4	K_2CrO_4	Na_2MoO_4	K_2MoO_4	Na_2WO_4	K_2WO_4
10	1.00	9.49	8.72	8.88	9.18	7.84	8.10
16	1.20	9.63	8.86	8.72	9.00	7.67	7.99
20	1.30	9.71	8.90	8.58	8.98	7.60	7.91
32	1.51	9.83	9.07	8.50	8.82	7.45	7.80
40	1.60	9.89	9.12	8.45	8.77	7.39	7.71
64	1.81	9.97	9.21	8.31	8.65	7.24	7.58
80	1.90	10.00	9.26	8.26	8.59	7.18	7.52
128	2.11	9.93	9.28	8.10	8.46	7.05	7.37
160	2.20	9.90	9.30	8.04	8.38	6.97	7.33
320	2.51	9.73	9.28	7.80	8.17	6.75	7.12
640	2.81	9.59	9.16	7.60	7.98	6.53	6.90
1280	3.11	9.44	9.04	7.38	7.78	6.34	6.67
2560	3.41	9.27	8.88	—	—	—	—

in the case of chromate, the slope of the curve at lower concentrations agrees closely with $-1/2$. Although another slope having the opposite sign is also found at higher concentrations, it may probably be attributable to the effect of the secondary dissociation of bichromate ion.

The *p*H values of sodium chromate, molybdate and tungstate as well as potassium chromate, molybdate and tungstate solutions measured at varying dilutions are tabulated in Table 1. From these experimental values, we obtain a generalized empirical formula governing the *p*H values of the salt solutions with concentrations over the concentration range 0.1—0.001 mol. as follows:

$$pH = a + b \log C$$

where the constants a and b may be evaluated by the method of least squares from the experimental data. Their numerical values are summarized in Table 2.

Table 2

a and b for Chromates, Molybdates and Tungstates

Salt	a	b
Sodium Chromate	11.00	0.520
Potassium Chromate	10.50	0.485
Sodium Molybdate	9.60	0.712
Potassium Molybdate	9.85	0.675
Sodium Tungstate	8.50	0.701
Potassium Tungstate	8.80	0.683

Since the experimental results obtained by the hydrolysis of these salts are in good agreement with the theoretical values from equation (1a), the present investigation gives a confirmation for the existence of dimolybdate and ditungstate ions, $Mo_2O_7^{--}$ and $W_2O_7^{--}$ as well as bichromate ion, $HCrO_4^-$, in dilute solution, and it also gives a

Table 3

Hydrolyses of Chromates, Molybdates and Tungstates at Varying Dilutions (30°C.)

Dilution	Degree of Hydrolysis (X)						Hydrolysis Constant (K1)					
Liters/mol.	Na_2CrO_4 ($\times 10^2$)	K_2CrO_4 ($\times 10^2$)	Na_2MoO_4 ($\times 10^4$)	K_2MoO_4 ($\times 10^4$)	Na_2WO_4 ($\times 10^5$)	K_2WO_4 ($\times 10^5$)	Na_2CrO_4 ($\times 10^6$)	K_2CrO_4 ($\times 10^7$)	Na_2MoO_4 ($\times 10^{14}$)	K_2MoO_4 ($\times 10^{13}$)	Na_2WO_4 ($\times 10^{17}$)	K_2WO_4 ($\times 10^{18}$)
10	—	—	0.76	1.51	0.69	1.26	—	—	2.12	1.72	1.66	0.98
16	—	—	0.84	1.60	0.75	1.56	—	—	1.85	1.28	1.31	1.20
20	—	—	0.76	1.91	0.80	1.63	—	—	1.70	1.74	1.26	1.08
32	—	—	1.01	2.11	0.90	2.02	—	—	1.62	1.47	1.15	1.29
40	—	—	1.13	2.36	0.98	2.06	—	—	1.79	1.64	1.18	1.09
64	—	—	1.31	2.86	1.11	2.43	—	—	1.76	1.83	1.07	1.12
80	0.80	—	1.46	3.11	1.21	2.65	0.80	—	1.93	1.88	1.11	1.16
128	1.09	—	1.61	3.69	1.44	3.00	0.93	—	1.63	1.96	1.17	1.05
160	1.27	0.32	1.75	3.84	1.49	3.42	1.01	0.64	1.69	1.77	1.03	1.25
320	1.72	0.61	2.02	4.73	1.80	4.22	0.93	1.16	1.29	1.79	0.91	1.17
640	2.49	0.93	2.55	6.11	2.17	5.08	0.97	1.34	1.29	1.78	0.80	1.03
1280	3.53	1.10	3.07	7.71	2.80	5.99	0.97	0.94	1.13	1.79	0.86	0.84
2560	4.77	1.94	—	—	—	—	0.89	1.47	—	—	—	—
				Average.			0.93	1.11	1.67	1.72	1.13	1.11

confirmation for the similarity between the constitution of molybdate and tungstate as well as the dissimilarity between that of chromate and molybdate or chromate and tungstate.

Degrees of hydrolysis and the hydrolysis constants calculated from the *p*H values observed, by using equation (3a), are summarized in Table 3. Deviations at higher concentrations are not unexpected since activities have been ignored. On the one hand, from the facts that the degree of hydrolysis of molybdate is always greater than that of tungstate having the same concentration and the average value of the hydrolysis constant of the former is about a thousand times as great as the latter, as shown in Table 3, and also from the fact that *p*H values of the salt at the same dilution decrease in the order of chromate, molybdate and tungstate, as shown in figure 3, we may conclude that the strength of the acids increases with the atomic weights of these acidic metals, that is, in the order of chromic, molybdic and tungstic acids. On the other hand, by comparing the *p*H values of sodium tungstate with those of potassium tungstate, we find that potassium salt has greater *p*H values than those of the corresponding sodium salt, as in the cases of molybdates and tungstates. It may be attributable to the difference in the effect of the ionic size of the cations.

(2) Potentiometric titration of chromate, molybdate and tungstate with hydrochloric acid.

Data obtained by potentiometric titrations of normal salt solutions varying from 0.02 M to 0.1 M in molybdate ion or tungstate ion with 0.1 M hydrochloric acid at 30°C. are plotted as *p*H vs. the volume of 0.1 M hydrochloric acid added, as indicated in figure 4.

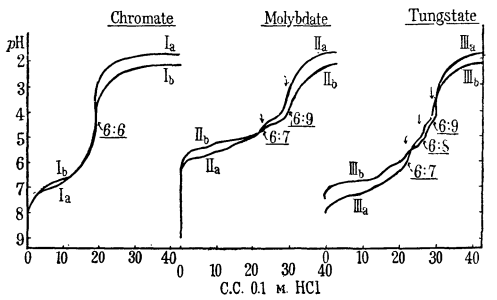

(a) (b) (c)

Fig. 4.—Potentiometric titration of sodium chromate, molybdate and tungstate with hydrochloric acid.

Ia: 0.1 M Na_2CrO_4 Ib: 0.02 M Na_2CrO_4
IIa: 0.1 M Na_2MoO_4 IIb: 0.02 M Na_2MoO_4
IIIa: 0.1 M Na_2WO_4 IIIb: 0.02 M Na_2WO_4

Data at different concentrations give exactly similar plots, and the displacements of the curves due to the dilution effects occur in each case. Curve Ia in figure 4a, curve IIa in figure 4b and curve IIIa in figure 4c indicate the titration curves of 0.1 M chromate, molybdate and tungstate with 0.1 M hydrochloric acid, while curve Ib, and curve IIb and curve IIIb in each figure indicate the titrations of 0.02 M of those salts with 0.1 M hydrochloric acid, respectively. Curves obtained for the higher concentration are steeper than those for the lower one. In figure 4b and 4c, two steep inflections occur in each curve at a XO_4^{--} to H^+ mol-ratios, 6:7 and 6:9, which have been attributed to the formation of the so-called para-molybdate and meta-molybdate ions, i. e., $HMo_6O_{21}^{5-}$ and $H_3Mo_6O_{21}^{3-}$, respectively, by Jander[4] and other authors[11][12]. The corresponding poly-anions of tungstate, para- and meta-tungstates, were observed prominently in the present investigation, though the *p*H ranges at which they are formed are different from those of molybdates. A steady inflection is revealed both in the titration curves of molybdate and tungstate, but it is not sufficiently pronounced. It is probably attributed to the existence of the poly-anion having the molar ratio, 6:4, that is, the formation of trimolybdate, $Mo_3O_{11}^{4-}$ as well as that of tritungstate, $W_3O_{11}^{4-}$, as suggested by Jander[4], but it could not be decided conclusively in this paper. Another steeper inflection at the mol-ratio, 6:8 occurs in titration curves of tungstate, IIIa and IIIb in figure 4c. It may be attributed to the existence of $H_2W_6O_{21}^{4-}$, but it is also not so pronounced as in the cases of para- and meta-tungstates. It has not been reported previously.

The equilibria between these poly-anions of tungstate, by analogy with those of molybdate may be formulated as follows:

(1) $6WO_4^{--}+4H^+=2W_3O_{11}^{4-}+2H_2O$
(2) $2W_3O_{11}^{4-}+3H^+=HW_6O_{21}^{5-}+H_2O$
or $6WO_4^{--}+7H^+=HW_6O_{21}^{5-}+3H_2O$
(3) $2HW_6O_{21}^{5-}+2H^+=2H_2W_6O_{21}^{4-}$
or $6WO_4^{--}+8H^+=H_2W_6O_{21}^{4-}+3H_2O$
(4) $HW_6O_{21}^{5-}+2H^+=H_3W_4O_{21}^{3-}$
or $6WO_4^{--}+9H^+=H_3W_6O_{21}^{3-}+3H_2O$

The mol-ratio and the *p*H ranges at which these poly-anions are formed are summarized in Table 4. Regarding to the titration curve of

Table 4
Mol-ratios and the *p*H Ranges of Poly-anions in Dilute Solutions

*p*H range	Mol-ratio Na_2MoO_4:HCl	Poly-anion
5.2	6 : 4	$Mo_3O_{11}^{4-}$
4.3—4.8	6 : 7	$HMo_6O_{21}^{5-}$
—	—	—
3.4—4.2	6 : 9	$H_3Mo_6O_{21}^{3-}$
*p*H range	Mol-ratio Na_2WO_4:HCl	Poly-anion
6.5	6 : 4	$W_3O_{11}^{4-}$
5.3—5.9	6 : 7	$HW_6O_{21}^{5-}$
4.5—4.9	6 : 8	$H_2W_6O_{21}^{4-}$
3.5—4.3	6 : 9	$H_3W_6O_{21}^{3-}$

(11) P. Souchay, *Ann. Chim.* **18** 61, 73, 169 (1934).
(12) G. Biehler, *Ann. Chim.* (12) **2**, 189 (1947).

chromate, no inflection but that at the mol-ratio, 1:1 could be found. It is attributable to the formation of bichromate ion, $HCrO_4^-$, as has been known. The further investigation on the electrolytic behaviors and the constitution of these poly-anions will be reported in the subsequent papers of this series.

Summary

(1) A vacuum tube potentiometer constructed in our laboratory has been used for the *p*H measurements with a glass electrode.

(2) A mathematical expression for the hydrolytic process has been given as a linear relation between the *p*H values and concentrations of the solutions.

(3) Hydrolyses of chromates, molybdates and tungstates in dilute solutions have been observed.

(4) The existence of dimolybdate and ditungstate ions, $Mo_2O_7^{--}$ and $W_2O_7^{--}$, as well as that of bichromate ion, $HCrO_4^-$, in dilute solutions were confirmed by measuring the *p*H values at varying dilutions.

(5) An empirical formula for expressing the relationships between the *p*H values and concentrations of the solutions was proposed for chromate, molybdate and tungstate solutions.

(6) The similarities of the electrolytic behaviors between tungstate and molybdate as well as the dissimilarities of those between chromate and molybdate or between chromate and tungstate have been ascertained by means of potentiometric studies.

(7) It has been observed by these studies that the strength of the acids increases with the atomic weights of these acidic metals.

(8) The existence of para- and meta-polyanions of tungstate as well as those of molybdate were confirmed by potentiometric titration of molybdate or tungstate with hydrochloric acid.

(9) A steady inflection at the mol-ratio, 6:4, is revealed both in molybdate and tungstate solutions, but it is not sufficiently pronounced. Another break at the mol-ratio, 6:8, was found in the titration curve of tungstate solution.

(10) No break but that at the mol-ratio, 1:1, which is attributable to the formation of bichromate ion could be found in the titration curve of chromate. It gives further confirmation of the dissimilarity between chromate and molybdate as well as tungstate.

Laboratory of Theoritical and Inorganic Chemistry, Science Department, National Taiwan University, Taipei, China

Electrolytic Behavior of Elements of the Group VIa in the Periodic System. II. Conductometric Studies on the Chromate, Molybdate and Tungstate Ions

By Kuan PAN, Sui Fong LIN and Shong Tsuo SHENG

(Received april 11, 1952)

Since the initial development of the alternating-current conductivity bridge by Kohlrausch[1], various technical advances[2] have been made in the source, in the bridge, or in the cell design and detection of the alternating-current signal. Though a properly constructed telephone receiver[3] has been used, in general, as a suitable detector for determining the setting of the alternating-current bridge, the nervous strain of listening to very weak notes is still unavoidable, especially in the case of high resistance.

As a result of advances in the field of electronics, however, the electric eye[4] and the cathode-ray oscillograph[5] have been proposed for this purpose.

(1) F. Kohlrausch, *Z. physik. Chem.*, **2**, 561 (1888).

(2) G. Jones and R. C. Josephs, *J. Am. Chem. Soc.*, **50** 1049 (1928); P. H. Dike, *Rev. Sci. Instruments*, **2**, 379 (1931); T. Shedlovsky, *J. Am. Chem. Soc.*, **52**, 1793 (1930).

(3) E. W. Washburn and K. Parker, *J. Am. Chem. Soc.*, **39**, 238 (1917).

(4) Hovorka and Mendenhall, *J. Chem. Education*, **16**, 239 (1939).

(5) Iamson, *Rev. Sci, Instruments*, **9**, 272 (1938).

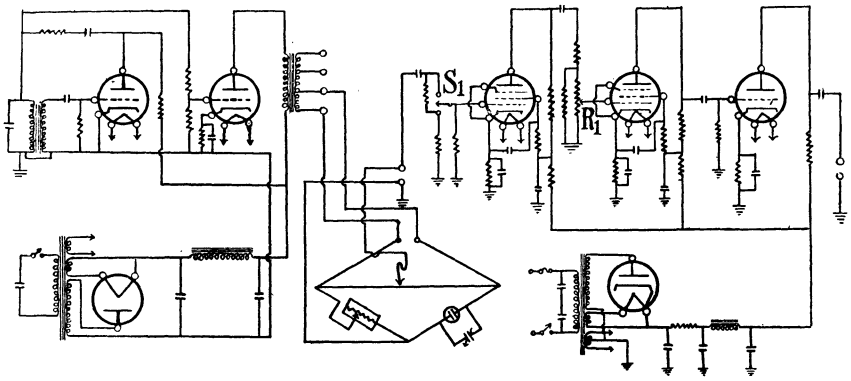

Fig. 1.

In the present investigation, measurements of the equivalent conductivities of chromate, molybdate and tungstate as well as conductometric titrations of these salts with hydrochloric acid have been carried out by using cathode-ray oscillograph as a detector for increasing the sensitiveness of the bridge setting and performing the rapid measurements.

Experimental

(1) **Materials.** — Conductivity water having a specific conductivity of 1.6 to 2.4×10^{-6} mho used in this experiment was purified by distillation according to the procedure described in the previous paper[6] of this series. The constant boiling fraction of hydrochloric acid was diluted to the desired concentration for use in the conductometric titrations.

All the salts used in the present investigation were purified by the repeated recrystallization from conductivity water as described in the previous paper[6]. After desiccating the salts in vacuo at room temperature, the crystalline water and the composition of the salts were checked by gravimetric analysis.

The solutions used for conductometric measurements were prepared, directly, by dissolving the salt in carbonate-free conductivity water and diluted to a desired concentration before each run.

(2) **Apparatus.** — Schematic diagrams of the apparatus used for the conductometric measurement in the present investigation are given in Fig. 1. A Shimazu KR-2 type Kohlrausch bridge (B), made in Japan, has been used for this purpose with 1000 cycle alternating-current supplied by an audio-frequency oscillator (A). The bridge output voltage is amplified by a three-stage variable amplifier (C), and then supplied to the vertical deflecting plate of a cathode-ray oscillograph. Dotted lines surrounding each unit of the set indicate the electrostatic shielding. Although a simple cathode-ray oscillograph was used previously by W. Juda and his co-workers[7] as a detector of the bridge setting, a Du Mont 208 type cathode-ray oscillograph has been successfully used in this experiment. When the circuit is in action, any wave pattern on the cathode-ray screen indicates the unbalanced bridge, while a single straight line indicates the balanced bridge.

An unbalance of about 0.1 ohm could be detected and the sensibility of detection could be controlled as desired by adjusting R_1 and S_1 in Fig. 1, the gain control of the cathode-ray oscillograph.

While a conductance cell of the modified Jones and Bollinger type[8] consisting of a glass vessel in which two platinum plates of 1.5 cm in diameter are fixed in parallel and platinized in ordinary manner, was used for the measurements of specific conductivity, two platinized platinum wires of 4 cm. in length and 1 mm. in diameter fused in a glass bead were used as the cell electrodes for the conductometric titration in order to attain a rapid equilibrium.

The conductance cell was immersed in a water thermostat whose temperature has been kept at 25 ± 0.05°C. for the specific conductivity measurements, and at 35 ± 0.05°C. for conductometric titration, since the room temperature was as high as 32—33°C.

Results and Discussion

(1) **Equivalent Conductivities of Sodium chromate, Molybdate and Tungstate.**—The equivalent conductivities of sodium chromate, molybdate and tungstate measured in this experiment at varying dilution are plotted against $\sqrt{10^3 C}$ or $\log V$, as shown in Fig. 2 and Fig. 3. Since the equivalent conductivities of these salts increase rapidly with the dilution, especially at extreme dilution, the limiting

(6) K. Pan and T. M. Hseu: This bulletin, **26**, 126 (1953).

(7) G. Jones, K. Myels and W. Juda, *J. Am. Chem. Soc.*, **62**, 2919 (1940).

(8) G. Jones and G. M. Bollinger, *J. Am. Chem. Soc.*, **53**, 411 (1931).

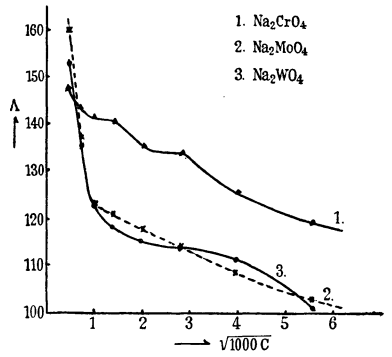

Fig. 2.—Λ and $\sqrt{1000 \times C}$.

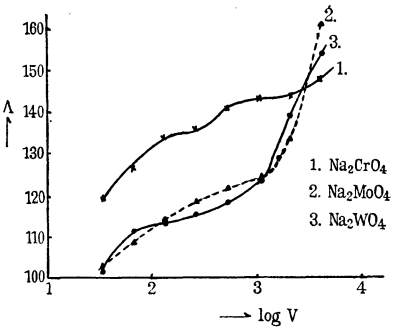

Fig. 3.—Λ and $\log V$.

value of equivalent conductivity of each salt at infinite dilution can not be estimated in the usual way. It may be attributable to the increasing degree of hydrolysis of these salts in dilute solutions and therefore, is probably due to the fact that, as the result of hydrolysis, the steady increase in the OH^- ion would lead to a rapid increase in conductivity of each salt solution, owing to the great equivalent ionic conductivity of the OH^- ion. These results are in good agreement with those obtained in the previous paper[6] which considered the hydrolytic process of molybdates and tungstates as follows:

$$2XO_4^{--} + H_2O = X_2O_7^{--} + 2OH^-$$

In this case, as degree of hydrolysis increase with the dilutions, x mol. of XO_4^{--} ion will be replaced by $x/2$ mol. of $X_2O_7^{--}$ and x mol. of OH^- ion which would lead to a rapid increase in conductivity.

Throughout the entire experimental concentration range, the equivalent conductivity of chromate is greater than those of molybdate or tungstate. It may be attributable to the different type of hydrolysis, as shown in the previous paper[6], for the chromate ion,

$$CrO_4^{--} + H_2O = HCrO_4^- + OH^-$$

The similarity between the former, i. e. molybdate and tungstate as well as the dissimilarity between the latter, i. e. chromate and molybdate or tungstate, is confirmed also in this experiment.

Table 1

Equivalent Conductivities of Sodium Chromate, Molybdate and Tungstate at Varying Dilutions at 25°C.

Dilution, V (l./equiv.)	$\log V$	$\sqrt{10^3\,C}$	Equivalent Conductivities		
			Na_2CrO_4	Na_2MoO_4	Na_2WO_4
32	1.51	5.59	119.3	102.5	101.0
64	1.81	3.95	125.6	108.4	111.1
128	2.11	2.80	133.9	113.8	113.5
256	2.41	1.98	135.4	117.9	115.2
512	2.71	1.39	140.6	121.3	117.9
1024	3.01	0.99	142.1	123.5	123.0
2048	3.31	0.70	143.2	135.5	138.9
4096	3.61	0.49	147.8	160.5	153.2
		$\Lambda_{1024} - \Lambda_{32}$	23	21	22

The differences between Λ_{1024} and Λ_{32}, $\Lambda_{1024} - \Lambda_{32}$, for sodium chromate, molybdate and tungstate solutions are found to be 23, 21 and 22, respectively, approximately equal to 2×10. The Ostwald's rule concerning the basicity and the difference, $\Lambda_{1024} - \Lambda_{32}$, for solutions of sodium salts seems to be held also in this case, though it has been mentioned that the sodium salts of the majority of inorganic acids do not follow this rule, in general. If it is not due to the accidental coincidence, it may be taken as due to the fact that molybdic or tungstic acid, or even chromic acid is a kind of weak dibasic acid similar to the weak dibasic organic acids. It is in accordance with the fact that molybdic and tungstic acids have their mean dissociation constants of the order of 10^{-5} as reported by Bhagwat and Dhar[9].

(2) **Conductometric Titration.**—Titration curves of 0.1 M and 0.02 M sodium chromate, sodium molybdate and sodium tungstate with 0.1 M HCl are shown in Fig. 4 and Fig. 5, respectively. Although one sharp break at the mol-ratio of 1:1, corresponding to the formation of bichromate ion is found in the titration curve of chromate, several kinds of breaks are found in the titration curves of molybdate and tungstate. Besides two sharp breaks at the points of XO_4^{--} to H^+ mol-ratios, 6:7 and 6:9, which have been taken

(9) W. V. Bhagwat and N. R. Dhar, *J. Indian Chem. Soc.*, **6**, 807 (1929).

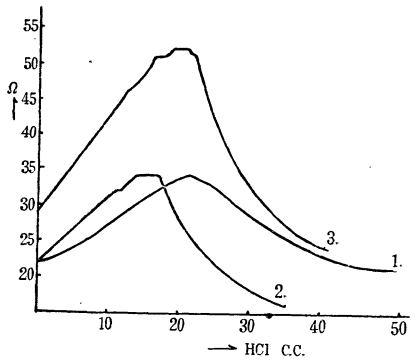

Fig. 4.—Conductometric titration of 0.1 M chromate, molybdate and tungstate with 0.1 M HCl.
1. 0.14 M Na_2CrO_4 15 cc.
2. 0.1 M Na_2MoO_4 15 cc.
3. 0.1 M Na_2WO_4 15 cc.

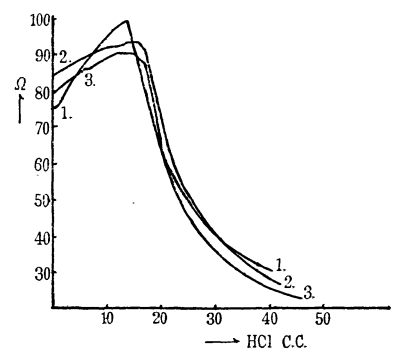

Fig. 5.—Conductometric titration of 0.02 M chromate, molybdate and tungstate with 0.1 M HCl.
1. 0.02 M Na_2CrO_4 75 cc.
2. 0.02 M Na_2MoO_4 75 cc.
3. 0.02 M Na_2WO_4 75 cc.

as the existence of para- and meta-poly-anions[10] were observed both in molybdate and tungstate, a remarkable break at the mol-ratio, 6:8, was observed in the case of tungstate. It is in good accordance with the result obtained in the previous paper[6]. Another break at 6:5.5, or 12:11, was observed prominently in the titration curves of molybdate but fairly in those of tungstate. It seems to be possibly attributable to the mixture of $[W_3O_{11}]^{4-}$ and $[HW_6O_{21}]^{5-}$, or to the formation of another kind of poly-anion.

When the sodium tungstate is allowed to stand over night before using for titration, however, a steady inflection is found at the mol-ratio, 6:4, which may be attributed to the formation of trimolybdate or tungstate as described in the previous paper[6], but we would not assert it until further confirmation could be obtained. The mol-ratios at which various kinds of recognizable breaks are revealed on the titration curves and the possible composition of the poly-anions are summerized in the Table 2.

Table 2

The Mol-ratios and Compositions of Poly-anions

Mol-ratio (calc.) $XO_4^{--}:H^+$	Poly-anion	Mol-ratio (obs.) $XO_4^{--}:H^+$		
		Na_2CrO_4	Na_2MoO_4	Na_2WO_4
6:4	$[X_3O_{11}]^{4-}$	—	6:4	6:4
6:5.5	$[HX_{12}O_{43}]^{13-}$?	—	6:5.5	6:5.5
6:6	$[HXO_4]^-$	1:1	—	—
6:7	$[HX_6O_{21}]^{5-}$	—	6:7	6:7
6:8	$[H_2X_6O_{21}]^{4-}$	—	—	6:8
6:9	$[H_3X_6O_{21}]^{3-}$	—	6:9.1	6:9

Summary

(1) Conductance measurements of sodium chromate, molybdate and tungstate solutions were carried out by using a Du Mont 208 type cathode-ray oscillograph as a detector of the Kohlrausch bridge setting.

(2) Equivalent conductivities of chromate, molybdate and tungstate at varying dilutions were measured at 25°C., but the limiting value of the equivalent conductivity of each salt at infinite dilution could not be estimated by the usual way, owing to the hydrolysis of these salts.

(3) The similarity between molybdate and tungstate as well as the dissimilarity between chromate and each of the two others were confirmed also in the present investigation.

(4) The difference $\Lambda_{1024}-\Lambda_{32}$ was found to be approximately equal to 2×10 for these sodium salts. It seems to indicate that either molybdic or tungstic or even chromic acid may be a kind of weak dibasic acid if Ostwald's rule is applicable.

(5) Besides two breaks at the XO_4^{--} to H^+ mol-ratios, 6:7 and 6:9 were found in the conductometric titration curves of molybdate and tungstate, a new sharp break at the mol-ratio 12:11 was observed prominently in the titration curves of molybdate but fairly in those of tungstate.

(6) A break at the mol-ratio, 6:8, which was reported in the previous paper, was found also in the titration curves of tungstate.

Laboratory of Theoretical and Inorganic Chemistry, Science Department, National Taiwan University, Taipei, China

(10) G. Jander, K. F. Jahr and W. Heukeshoven, *Z. anorg. allgem. Chem.*, **187** 60, 129 (1930), **194**, 383 (1930).

The New Method of Polymerization of Vinyl Compounds. I.[1] On the Polymerization of Methyl Methacrylate with Copper or Cuprous Chloride and Acids at Room Temperature

By Ryozo INOUE and Takashi YAMAUCHI

(Received June 16, 1952)

Introduction

We have discovered some new methods of polymerization of vinyl compounds, which are entirely different from the previous methods catalyzed by peroxides. Our methods are peculiar because they are able to perform polymerization very rapidly in good yield at room temperature. In this report we have treated the polymerization of methyl methacrylate with copper or cuprous chloride and acids. Copper has hitherto been considered in contradiction to our experimental results, as an anticatalyst in polymerization. For example, it has been applied as an inhibitor in the case of synthesis of methacrylate.

Experimental

In the following experiments we have applied methacrylic methyl ester as a vinyl monomer. We have, however, used aqueous solution of the ester in order to simplify experiments. As the solubility of this ester is only about 1% at room temperature, the polymerization in a considerably dilute solution is to be discussed in this report.

As an orientation, the accelerating power of the combination of the powder of metallic copper and various acids for polymerization are shown in Table 1.

The rate of polymerization, after about 1 weight % of the powder of metallic copper is thrown into the aqueous solution which contains 1% of methyl methacrylate and acid respectively is shown in the above Table. The reaction vessel was agitated vigorously at first and then allowed to stand. Generally speaking, the lower the molecular weight of organic acid is, the stronger the accelerating power for polymerization becomes, and in this case inorganic acids are not so useful. But as it will be shown later, this tendency as for the accelerating power is of course different when other kinds of metal or its lower valencial salts are used. What is important is that the polymerization is accelerated by the preceding system.

The course of the polymerization with the powder of metallic copper and formic acid is shown in Fig. 1.

(1) This paper was read in the annual meeting of the Chemical Society of Japan in April, 1952.

Table 1

The Accelerating Power of the System of the Powder of Metallic Copper and Various Acids for the Polymerization of the Methyl Methacrylate (at Room Temperature)

Formic acid	##	Lactic acid	+
Acetic acid	##	Benzoic acid	+
Propionic acid	#	Sulfuric acid	#
Butyric acid	+	Hydrochloric acid	#
Isovalerianic acid	+	Phosphoric acid	#
Oxalic acid	##		

where

means that the white precipitate (polymer) is produced within five minutes after the powder of metallic copper is thrown into the solution.

means that the white precipitate (polymer) is produced within thirty minutes after the powder of metallic copper is thrown into the solution.

\+ means that the white precipitate (polymer) is produced within several hours after the powder of metallic copper is thrown into the solution.

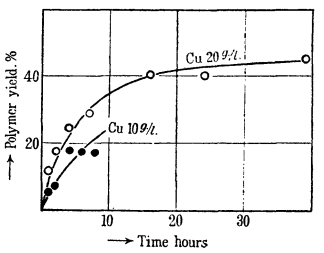

Fig. 1.

In the figure we have shown two examples with a different ammount of copper powder, i. e. 20 g./l. and 10 g./l. The solution contained 0.096 mol./l. methyl methacrylate and 0.115 mol./l. formic acid. Though an ammount of the copper powder has influence on the velocity of the polymerization, it is not easy to find any quantitative relations. It is worth notice that though the powder of metallic copper precipitates to the bottom of the vessel as a result of quiscence throughout the polymerization, separation of

polymers can be observed all over the solution (system) and that the induction period is not to be observed.

If we apply Cu_2Cl_2 instead of metallic copper, more rapid and more uniform polymerization will happen, as Cu_2Cl_2 is somewhat soluble in water. We have shown the influence of the amount of Cu_2Cl_2 and the concentration of formic acid on polymerization in Tables 2 and 3. In these experiments we have stirred the solution slowly.

Table 2

The temperature of polymerization: 40°C.
Methyl methacrylate :0.096 mol./l.
Formic acid :0.201 mol./l.

Time of polymerization (hours)	Amount of Cu_2Cl_2 (g./l.) 15 Yield (%)	$\bar{P}$	10 Yield (%)	$\bar{P}$	5 Yield (%)	$\bar{P}$
0.5	19.2	170	27.5	140	35.6	100
1.0	39.6	—	39.9	—	29.0	—
1.5	43.1	—	52.3	—	50.9	—
2.0	50.5	160	(36.7)	150	56.7	140
3.0	51.3	—	60.4	—	60.2	—
4.0	59.0	—	62.9	—	61.1	—
5.0	60.6	—	60.2	—	61.7	—
6.0	60.9	—	62.5	—		
7.0	62.7	—			64.0	—
8.0	60.9	140	55.5	140	62.9	130
24.0	62.7	140	(85.4)	130	69.6	120

Table 3

The temperature of polymerization: 40°C.
Methyl methacrylate :0.096 mol./l.
Formic acid :0.392 mol./l.

Time of polymerization (hours)	Amount of Cu_2Cl_2 (g./l.) 5 Yield (%)	$\bar{P}$	1 Yield (%)	$\bar{P}$	0.5 Yield (%)	$\bar{P}$
0.5	21.3	120	19.2	180	27.1	350
1.0	36.5	—	35.0	—	37.9	—
1.5	43.4	—	42.5	—	47.9	—
2.0	49.2	140	51.6	260	45.4	360
3.0	53.1	—	51.0	—	45.0	—
4.0	56.5	—	51.0	—		
5.0	58.8	—	50.8	—	44.7	—
6.0	58.8	—	49.8	—	44.0	—
7.0	62.3	—	49.1	—	44.6	370
8.0	54.8	140	49.0	240		
24.0	61.0	130	51.6	250	46.9	370

Though the concentration of the formic acid does not suffer a change such as can be detected by ordinary titration, the reaction mixture becomes green with the lapse of time. The polymerization stops in about two hours presumably in consequence of the exhaustion of Cu_2Cl_2; it proceeds again as shown in Fig. 2 when Cu_2Cl_2 is added anew (arrow in the Fig.).

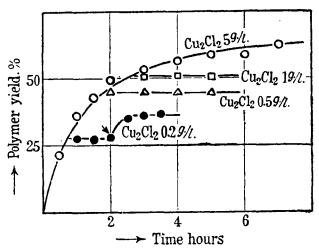

Fig. 2.

Discussion

In the reaction of the above experiments, free radical of hydrogen is produced, which can initiate the chain polymerization.

$$Cu + RCOOH \rightarrow Cu^+ + RCOO^- + H\cdot$$
$$Cu^+ + RCOOH \rightarrow Cu^{++} + RCOO^- + H\cdot$$

As H· is very unstable or reactive in comparison with benzoate radical, if the concentration of H· is somewhat high, the initiation and stabilization reaction happen at once and in an extreme case merely hydrogenation may be observed. The conditions of the above experiments allow a primary free radical to have enough time to repeat chain propagation about two hundred times before it stabilizes as the result of collision with another free radical. In other words the concentration of H· is very low in comparison with an ordinary polymerization, the catalyst of which is benzoyl peroxide. It is known that Cu or Cu_2Cl_2 is stable to acids (for example CH_3COOH and HCOOH). Therefore we may find more general combinations of acids and metals or their lower valencial salts. These kinds of metals or salts have hitherto been generally known as anti-catalysts of polymerization. The polymerization of methyl methacrylate by hydrazine and platinum[2], or formic acid and palladium[3], were reported by Paravano as experimental researches. According to the results of the present experiments, the degree of polymerization is not yet so high, but we think that this new method of polymerization is interesting both from scientific and technical points of view.

Summary

(1) It has been that the polymerization of

(2) G. Paravano, *J. Am. Chem. Soc.*, **72**, 3853 (1950).
(3) G. Paravano, ibid., **72**, 5546 (1950).

methyl methacrylate happens catalytically with Cu or Cu_2Cl_2 and acids at room temperature. Polymerization products were obtained as fine powder easily separable from the reaction mixture.

(2) It has been pointed out that the polymerization is initiated by free radicals of hydrogen.

(3) Calculating from the degree of polymerization of the produced polymers and consumed Cu_2Cl_2, the efficiency of the produced $H^{\cdot}$ for the polymerization is not so good.

Osaka Industrial Research Institute, Osaka

The Catalytic Action of Organic Peroxides on the Polymerization of Ethenoid Compounds. I. The Activity of Substituted Benzoyl Peroxides in the Polymerization of Styrene

By Matsuji TAKEBAYASHI and Tadao SHINGAKI

(Received June 26, 1952)

It is possible from a study of the catalyzed polymerization of vinyl compounds to obtain information on the activity of the radicals derived from peroxides initiating the polymerization. Cooper[1], studying the polymerization of styrene with various types of substituted benzoyl peroxide has observed that electron-attracting substituents give radicals of lower activity, while electron-repelling ones increase the activity of the radicals. However, the velocity of initiation of catalyzed polymerization is affected not only by the activity of radicals, but also by the amount of active radicals which are produced in a unit of time. Therefore the velocity of decomposition of peroxides also seems to be an important factor. Swain and his co-workers[2] have reported that electron-attracting substituents retard the reaction and electron-repelling groups accelerate in the unimolecular thermal decomposition of *m*- and *p*- substituted benzoyl peroxides, and that the data fit the Hammett equation closely. Blomquist and Buselli[3], however, have indicated that the homolytic cleavage of symmetrical benzoyl peroxides into free radicals may involve the interaction of two opposing dipoles.

The present study was initiated to see the relation between the amount and the activity of the radicals initiating the polymerization of styrene. For this purpose, symmetrical *m*- and *p*- substituted benzoyl peroxides were taken up as the catalyst.

As an empirical measure of the activities of peroxides, styrene (1/30 mol.) was polymerized with various types of substituted benzoyl peroxide (1/3000 mol.) at 60°C. for eighteen hours in the absence of air, and the effects of peroxides on the rate of polymerization have been measured. The results obtained are summarized in Table 1.

Table 1

Substituted benzoyl peroxide	Rate of polymerization (%)	K of substituted benzoic acid at 25°C. ($\times 10^{-5}$)
p,p'-Dimethoxy	99.8	3.2
m,m'-Dimethoxy	85.7	5
p,p'-Dimethyl	91.6	4.4
m,m'-Dimethyl	82.0	5.6
Unsubstituted	81.5	6.69
p,p'-Dichloro	71.9	9.3
m,m'-Dichloro	57.3	15.5
p,p'-Dicyano	28.3	23.5
m,m'-Dicyano	31.5	19.9
p,p'-Dinitro	10.1	39.6
m,m'-Dinitro	11.2	34.5
None	1.5	

This experiment shows that the activities of the substituted benzoyl peroxides on the rate of polymerization of styrene are inversely proportional to the square root of the dissociation constants K of the corresponding substituted benzoic acids, and that better linearity is found when using $\sqrt{K}$ than when using Hammett's constant σ as shown in Fig. 1.

(1) W. Cooper, *Nature*, **162**, 897 (1948).
(2) C. G. Swain, W. H. Stockmayer and J. T. Clarke, *J. Am. Chem. Soc.*, **72**, 5126 (1950).
(3) A. T. Blomquist and A. J. Buselli, *J. Am. Chem. Soc.*, **73**, 3883 (1951).

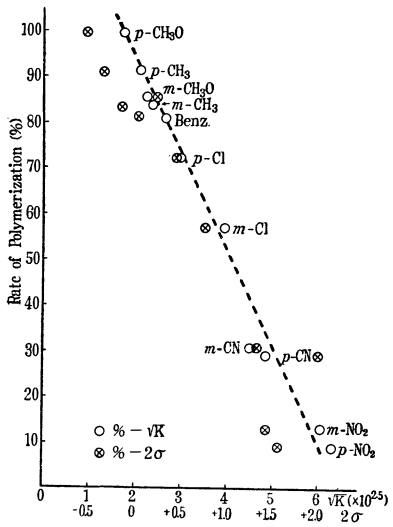

Fig. 1.

In order to elucidate the results described above, the authors observed, in the first place, the rate of decomposition of the peroxides in styrene at 60°C. for eighteen hours. The percentage of decomposition is plotted against $\sqrt{K}$ or 2σ in Fig. 2. This has been included as it shows that the rate of decomposition is inversely proportional to $\sqrt{K}$ and proportional to 2σ, and that better linearity is found with $\sqrt{K}$ than with 2σ.

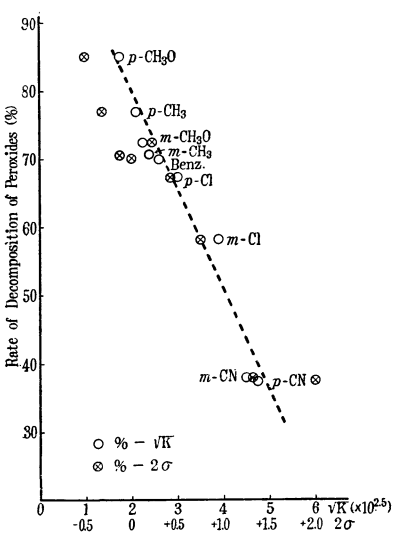

Fig. 2.

The next experimental problem was to determine the kinetic order of the thermal decomposition of the peroxides in styrene. The rate of decomposition of peroxides in solution is given generally by

$$-d[P]/dt = k_1[P] + k_i[P]^n,$$

where P expresses the concentration of the undecomposed peroxide, k_1 the rate constant of unimolecular decomposition, k_i that of induced decomposition, and n the kinetic order of induced decomposition.

The experiments with benzoyl peroxide and some substituted benzoyl peroxides (1 mol. % to styrene) were carried out at 60°C. The percentage of decomposition of peroxides was determined by the iodometric method according to the direction of Swain[2]. As for dinitrobenzoyl peroxides, the rate of decomposition was not measured exactly by this method because nitrobenzoic acids, produced during the reaction, had also an oxidizing action. The data are given in Fig. 3 and Table 2. The decomposition was observed to be of first order in all cases. Therefore, it should be possible to ignore the term for the bimolecular induced chain decomposition[4]. Then, we have

$$-d[P]/dt = k_1[P].$$

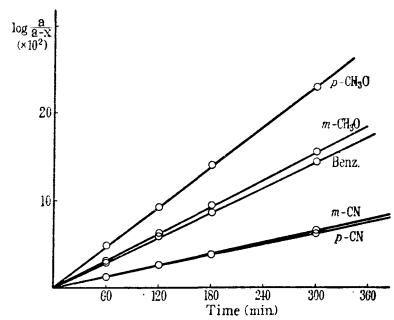

Fig. 3.

Table 2

Peroxide	$k_1 \times 10^4$, min.$^{-1}$	$\log(k/k_0)$
p,p'-Dimethoxy-benzoyl	17.7	0.206
m,m'-Dimethoxy-benzoyl	12.0	0.033
p,p'-Dimethyl-benzoyl	12.7	0.061
m,m'-Dimethyl-benzoyl	11.3	0.009
Benzoyl	11.05	0.000
p,p'-Dichloro-benzoyl	9.9	−0.047
m,m'-Dichloro-benzoyl	8.1	−0.135
p,p'-Dicyano-benzoyl	4.6	−0.380
m,m'-Dicyano-benzoyl	4.8	−0.362

Table 2 indicates also that the greater the electron-affinity of substituentsis, the more

(4) Swain has obtained a different result in the thermal decomposition of benzoyl peroxide in styrene. His rate curve for decomposition shows a marked autocatalysis, which he has supposed to be due to overheating.

rapidly the peroxides decompose in styrene. The relation between $\log(k/k_0)$ and the rate of polymerization is shown in Fig. 4, where k indicates the rate constant of substituted benzoyl peroxides, and k_0 that of unsubstituted ones. It is recognized that the rate of decomposition of peroxides is in a parallel relation with the rate of polymerization of styrene.

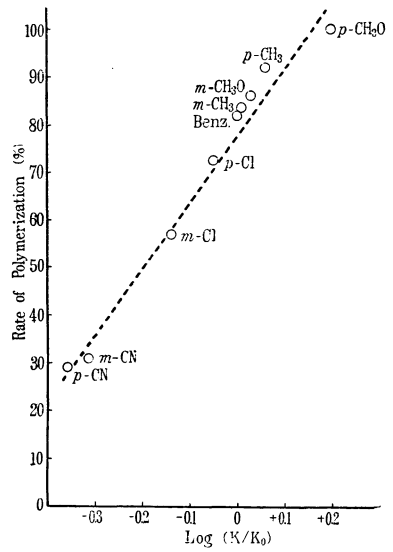

Fig. 4.

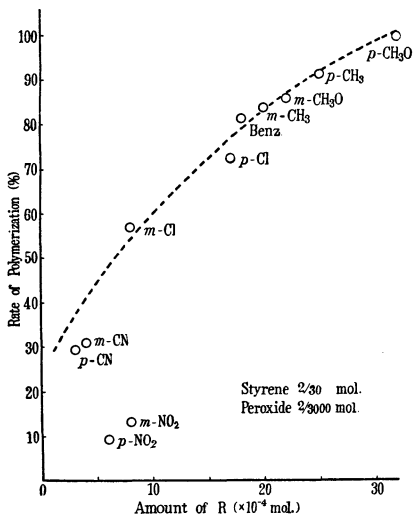

Fig. 5.

Considering that the thermal decomposition of peroxides in styrene is an unimolecular reaction, it is supposed that the radicals acting as the initiator of the polymerization are chiefly benzoate radical RCOO and aryl radical R, produced from the radical RCOO, and that the larger the amount of the radicals which are produced in unit time, the greater the rate of polymerization of styrene. The amounts of various types of the radical R were estimated from those of the carbon dioxide which was generated. Then, the above expectation seems to be satisfied about the radical, R, excepting the cases of dinitrobenzoyl peroxides, as shown in Fig. 5. Concerning this subject, furthermore, the kinetic studies on the formation of carbon dioxide are under way.

In respect to the small activity of dinitrobenzoyl peroxides, a consideration has been deduced. Assuming that the segments of the peroxides form nitrobenzene and nitrobenzoic acids during the polymerization, it might be expected that these nitro-compounds would react as inhibitors of the polymerization[5].

It is possibly owing to the inhibiting action of the nitro-compounds described above that the rate of polymerization with dinitrobenzoyl peroxides is quite small in spite of the comparatively large rate of decomposition[3].

Experimental

Materials.—The styrene employed was distilled with steam, dried over small amount of calcium chloride, and distilled under reduced pressure just before use. b. p. 63°C./55 mm. The absence of peroxides was ascertained by the test with ferrous ammonium sulfate and ammonium thiocyanate. All substituted peroxides were prepared by the reaction of a solution of an acid chloride in dry toluene with an excess of aqueous sodium peroxide according to the method of Price and Krebs[6] used for p,p'-dinitrobenzoyl peroxide. In general, the melting points or decomposition points were quite sharp after recrystallization

Table 3

Peroxide	M. p. (Dec.) (°C.)	Purity (%)
p,p'-Dimethoxy-benzoyl	128	98.5
m,m'-Dimethoxy-benzoyl	82	99.0
p,p'-Dimethyl-benzoyl	136	98.3
m,m'-Dimethyl-benzoyl	54	99.0
Benzoyl	106—107	98.2
p,p'-Dichloro-benzoyl	140	99.0
m,m'-Dichloro-benzoyl	123	98.4
p,p'-Dicyano-benzoyl	176	98.0
m,m'-Dicyano-benzoyl	163	96.7
p,p'-Dinitro-benzoyl	158	99.1
m,m'-Dinitro-benzoyl	137	98.0

(5) S. Okamura, K. Uno and K. Yamamoto, read at the fifth annual meeting of the Chemical Society of Japan, April 4, 1952; C. C. Price, "Mechanism of Reactions at Carbon-Carbon Double Bonds", New York, 1946, p. 87.

(6) C. C. Price and E. Krebs, "Organic Syntheses", **23**, 65 (1943).

from hydrocarbon solvents, and represented to a fair extent the purity of the peroxide. In Table 3 are listed the substituted benzoyl peroxides employed in this study.

Polymerization of Styrene.—The polymerization of styrene was carried out in sealed 17 cc. reaction tubes. The tubes were treated with warmed cleaning solution for several hours, left standing in a very dilute solution of sodium bisulfate for a short time, then rinsed with distilled water, and dried. A peroxide (1/3000 mol.) was mixed with 1/30 mol. of styrene in the reaction tube, the tube cooled in an ice-salt-bath, then evacuated and sealed off. The sealed tube was warmed to room temperature and then immersed in a 60±0.05°C. thermostat for eighteen hours, then removed and cooled in an ice-salt-bath. Unchanged styrene was driven off in a vacuum and the weight of polystyrene was measured. In another experiment, the reaction products were dissolved in benzene and the polymer produced was precipitated by adding methanol to the solution. The weight of polystyrene was almost equal to that of the case mentioned above.

Decomposition of Peroxides.—The apparatus is shown schematically in Fig. 6. A is the reaction tube of 22 mm. diameter and 35 cc. capacity, B the inlet tube of 7 mm. diameter for nitrogen, C the cooler with cold water, and D the soda-lime tube for the absorption of the carbon dioxide which is generated. B was connected with the source of purified nitrogen. During the reaction a soda-lime tube E was attached to D.

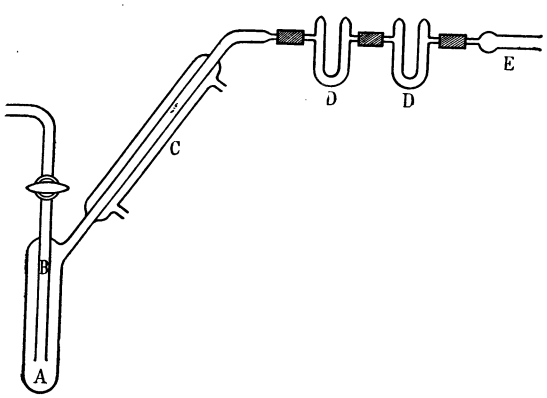

Fig. 6.

A mixture of peroxide (2/3000 mol.) and styrene (2/30 mol.) was taken in A and the tube A was cooled in an ice-salt-bath. Pure nitrogen[7] was passed through B into the whole apparatus. When the air in the apparatus was driven out, namely the weight of D had no longer increased, A was warmed to room temperature and then immersed in a 60−0.05°C. thermostat for eighteen hours. The reaction was carried out in a slow stream of nitrogen. After the required time, A was cooled, passing through nitrogen for one hour, and the weight of carbon dioxide absorbed in D was measured. In the experiments with peroxides such as benzoyl peroxide and dimethyl- and dichloro-benzoyl peroxide, the contents of A were dissolved in 30 cc. of benzene and hydrolyzed for twenty eight hours with 50 cc. of water and 4 g. of sodium hydroxide. The products were found to be chiefly the corresponding benzoic acids.

Summary

(1) The rates of polymerization of styrene with *m*- and *p*-substituted benzoyl peroxides have been found to be inversely proportional to the square root of the dissociation constants of the corresponding substituted benzoic acids.

(2) The thermal decomposition of the peroxides in styrene has been observed to be of first order in all cases.

(3) It has been found that the rate of decomposition of peroxides is in a parallel relation with the rate of polymerization of styrene.

(4) The relation between the amounts of radicals derived from the peroxides and the rates of polymerization has been studied.

(5) In respect to the small activity of dinitro-benzoyl peroxides, a tentative theory has been made.

The authors express their hearty thanks to the Ministry of Education for a grant.

Chemical Laboratory, South College, Osaka University, Osaka

(7) Purified by the method described in L. F. Fieser, "Experiments in Organic Chemistry", 2nd Ed., New York, 1941, p. 395.

Cyclopolysiloxanes from Ethyldichlorosilane

By Rokuro ŌKAWARA, Eiji ASADA and Takeo WATASE

(Received July 24, 1952)

From the hydrolysis product of ethyldichlorosilane and from its pyrolysis product, cyclic polyethylpolysiloxanes of the general formula $(C_2H_5SiHO)_n$ were obtained analogous to those reported by Sauer[1] and Brewer[2] from methyldichlorosilane.

Experimental

Starting Materials. — The ethyldichlorosilane used in our experiments was prepared by the reaction of ethyl chloride with copper-silicon and was purified by fractionation through a 75 cm. helices packed column. The fraction having the boiling point 75.5°—76°C. (760 mm.) was taken as starting material. Analysis for hydrolyzable chlorine by hydrolysis in water-methanol solution and titration of the liberated acid indicated that our sample was pure ethyldichlorosilane[3]. *Anal.* Calcd. for $C_2H_6SiCl_2$:Cl, 54.96. Found: Cl, 54.5.

Hydrolysis.—To obtain the cyclic compounds ethyldichlorosilane has been hydrolyzed in ether solution according to Sauer's direction; e. g., two moles (258 g.) of ethyldichlorosilane was added to a mixture of 0.5 liter of diethyl ether and 1 kg. of cracked ice, which was vigorously stirred, over a half-hour period, some rubbery gel being produced. To avoid the gellation, ethyldichlorosilane was diluted with the same weight of diethyl ether and this solution was added to hydrolyzing mixture. Two typical experimental results are given in Table 1.

During the addition of ethyldichlorosilane, the temperature of the hydrolyzing mixture dropped from 0° to −8°C. As soon as the addition was completed the etherlayer was separated. Then the ice-cold water (the same weight as was used in the hydrolyzing mixture) was added and vigorous stirring was continued during an additional 15 minutes. The ether layer was washed repeatedly with water until it got neutral to methylorange and dried over dehydrated sodium sulphate.

Hydrolyzates

(a) **Untreated Hydrolyzate.** — The hydrolysis products were distilled by means of a Claisen flask containing a bundle of glass wool to prevent bumping. After ether was driven off at 760mm, the distillate was collected under 20 mm. The temperature of the oil bath was gradually raised to 220°C.

The temperature ranges and the amounts of distillate collected are given in Table I. Practically no distillate was given when the residue was further heated up to 240°C.

(b) **Thermally Rearranged Hydrolyzate.** — When the untreated hydrolyzate was distilled off, transparent sticky rubbery gel remained as the residue. By means of the pyrolysis of the residue under high vacuum using a rotary pump, the liquid distillate was acquired (Table 1) and there remained a small amount of transparent thin film stuck on the upper part of the flask. It may be seen from Table 1 that the ratio of untreated hydrolyzate to thermally rearranged hydrolyzate (Exp. 1, 11.2 g.: 21.3 g., Exp. 2, 40.7 g.: 34.8 g.) was greatly influenced by the hydrolyzing condition.

Cyclopolysiloxanes from (a) and (b). — The hydrolyzate (a) and (b) were rigorously fractionated through a 40 pair packed modified Stedman

Table 1

Exp. No.	$C_2H_5SiHCl_2$ diluted with (ether)	Hydrolyzing mixture		Hydrolyzate					
				Untreated			Thermally rearranged		
				Distillate		Still	Distillate		Still
		Ice	Ether	Temp. (20 mm.)	Yield	Temp.	Temp. (high vac.)	Yield	Temp.
	g.	g.	g.	°C.	g.	°C.	°C.	g.	°C.
1	100	500	200	100—130	11.2	—180	100—130	14.2	250—310
	(100)				0	180—220	130—170	7.1	310—400
2	250	1000	400	100—110	31.7	—140	100—140	19	250—310
	(250)			110—140	9	140—220	140—180	15.8	310—400

(1) Sauer, Scheiber and Brewer, *J. Am. Chem. Soc.*, **68**, 962 (1946).

(2) Brewer, *J. Am. Chem. Soc.*, **70**, 3962 (1948).

(3) Meals, *J. Am. Chem. Soc.*, **68**, 1880 (1946).

Table 2

Hydrolyzate	Fraction No.	n_D^{20} After days 1	3	8	60	d_4^{20} After days 1	3	60
Untreated	I (a)	—	1.4139	—	1.4139	0.9834	—	0.9838
	II (a)	—	1.4176	—	1.4176	0.9922	—	0.9918
Thermally rearranged	I (b)	1.4127	—	1.4138	1.4136	—	0.9820	0.9821
	II (b)	1.4179	—	1.4176	1.4175	—	0.9920	0.9922
	III (b)	1.4201	—	1.4201	1.4198	—	1.0025	1.0022

Table 3

	Mol. Formula	Mol. Wt. calcd.	found	Mol. Refn. calcd.	found	Si-H%(c) found	C %(d) found	H %(e) found	b. p. °C (20mm.Hg.)
I	$(C_2H_5SiHO)_3$	223	223	56.70(a)	56.63(b)	1.33	32.00	8.01	106
II	$(C_2H_5SiHO)_4$	297	294	75.60	75.39	1.28	32.63	8.07	135
III	$(C_2H_5SiHO)_5$	371	362	94.50	93.68	—	32.38	7.97	165

(a) Warrick: *J. Am. Chem. Soc.*, **68**, 2455 (1946).

(b) The values d_4^{20}: 0.9836, 0.9920, 1.0023; n_D^{20}: 1.4138, 1.4176, 1.4200 (cf. Table 2) are used for the calculation of I, II, and III respectively.

(c), (d), (e): Calculated values are 1.35, 32.43, and 8.16 respectively.

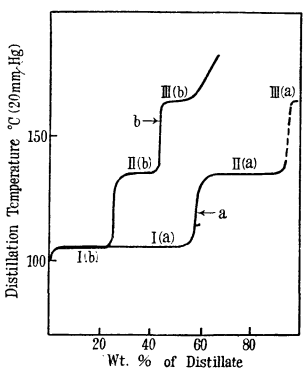

Fig. 1.—Distillation curve under 20 mm. Hg. (a) untreated hydrolyzate, (b) thermally rearranged hydrolyzate.

Distillation was performed in a course of about 7 hours.

Curve a: The fraction I(a) and II(a) were distilled out between the still-temperature of 140°—175°C. By stronger heating, between 270°—285°C the dotted curve was obtained.

Curve b: The fraction I(b) and II(b) were distilled out between the still-temperature of 170°—250°C, while III(b) was obtained between 250°—320°C.

column[4] respectively. The results are illustrated in Fig. 1.

Untreated hydrolyzate of several runs including Exp. 1 and 2 amounted to 68 g. By the rigorous fractionation, the two following fractions e. g. I(a) 40 g. and II(a) 19 g. were obtained and there remained some liquid and transparent gel. There must have occurred a partial thermal rearrangement of a lower boiling fraction to a transparent gel during a course of distillation. By stronger heating the fraction indicated by the dotted line was obtained but this fraction III(a) was not examined (Fig. 1).

Thermally rearranged hydrolyzate of several runs amounted to 97 g. By the rigorous fractionation, the three following fractions: I(b) 21 g., II(b) 14 g., and III(b) 7 g. were obtained. As shown in Fig. 1 (Curve b), above 165°C. no plateau was found. There remained some transparent rubbery gel in the still as was the case in the untreated hydrolyzate. It may be seen from these facts that a part of the lower boiling hydrolyzates polymerised to the gel.

Density and refractive index of these fractions are summarized in Table. 2.

From these data II(a) and II(b) may be regarded as the same compound. This conclusion was further supported by the molecular weight determination. The fraction I(b) which was assigned to cyclotriethyltrisiloxane by the molecular weight determination in dioxane, changed slightly its density and refractive index after a few days. But the marked changes such as Brewer[2] noted with the cyclotrimethyltrisiloxane were not found. As the molecular weight and other analytical data of this compound were the same as I(a), these may be regarded as the same compound.

The expected composition of these compounds was confirmed by determining the percentage hydrogen attached to silicon, % H(—Si), according to the equation

$$Si—H+KOH \rightarrow H_2+Si—OK$$

The samples (0.15—0.20 g.) were decomposed with 40% aqueous pottasium hydroxide solution in a Zerewitinoff apparatus. The results are given in Table 3.

Because of the identical elementary constitution of these compounds it was necessary to determine

(4) John and Rehberg, *Ind. Eng. Chem.*, **41**, 1056 (1949).

accurately their molecular weight in order to assign molecular formulas. Our determinations were made cryoscopically in dioxane with the results given in Fig. 2.

It may be seen from the figure that the association of cyclopolysiloxanes occurred in the solution. These observed values were extrapolated to zero concentration. The molecular weights thus obtained at zero concentration are listed in Table 3, together with the other analytical data.

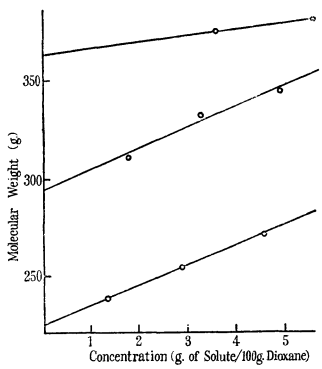

Fig. 2.—Cryoscopic molecular weight determanation in dioxane. Fisher's dioxane was distilled from sodium and the molar freezing depression constant $K=4.66$[5] was used.

(5) Landolt, Tabellen. Erg. II. b. 1468.

Since cyclic trimer was obtained in the untreated hydrolyzate, an enhanced reactivity of the siloxane linkage in these substances toward acid cleavage was not so distinct as Brewer indicated in the cyclopolymethylpolysiloxanes. This conclusion was further strengthened by the discovery that $(C_2H_5SiHO)_4$ is not readily converted in a short time into a high polymer by 20% aqueous hydrochloric acid as was the case with methyl analogue.

Summary

1. From the untreated hydrolyzate of ethyldichlorosilane, cyclic trimer $(C_2H_5SiHO)_3$ and tetramer $(C_2H_6SiHO)_4$, and from the pyrolyzed hydrolyzate cyclic trimer, tetramer and pentamer $(C_2H_5SiHO)_5$ have been acquired and characterized.

2. The reactivity of the siloxane (Si—O—Si) linkage in the $(C_2H_5SiHO)_n$ compounds toward acid cleavage appears to be not so enhanced as that exhibited by the $(CH_3SiHO)_n$ compounds.

Department of Applied Chemistry Faculty of Engineering, Osaka University, Osaka

Untersuchung über Lignin und Zellstoff. I. Eine neue Bestimmungsmethode von Ligninsulfosäure in Sulfitablauge durch Kolloidtitration

Von Ryoiti SENZYU

(Eingegangen am 22, Juni, 1952)

Einleitung

Was die Bestimmungsmethode der Ligninsulfosäure in Sulfitablauge betrifft, so sind bisher verschiedene Verfahren veröffentlicht. Alle bisherigen Methoden liegen ausnahmslos auf dem Grund, die Ligninsulfosäure mit geeignetem Fällungsmittel fällen zu lassen und danach den Niederschlag zu wägen oder den restlichen Gehalt vom Fällungsmittel nach geeigneter Methode zu bestimmen.

Die bisherigen Forscher verwendeten als Fällungsmittel die mannigfachen Amine wie β-Naphthylamin[1], Chinolin[2], Benzidin[3], Trypaflavin[4], Anilin[5], Fuchsin[6], Benzacridin[7], Dimethylaminodiphenylmethan[8], usw., aber in allen Fällen ist die mit diesem aromatischen Amin ausgefällte Ligninsulfosäure nicht die gesamte, sondern nur ein Teil davon und die Verbindung der Ligninsulfosäure mit dem aromatischen Amin weist nicht ein stöchiometrisches Verhältnis auf. Nämlich die

(1) P. Klason, *Ber.* **20**, 706 (1929).
(2) K. Freudenberg u. F. Sohns, *Ber.* **66**, 262 (1933).
(3) B. Rassow u. H. Kraft, Papier Fabr. **29**, 89 (1929).
(4) A. Noll, ibid. **36**, 41 (1938).
(5) C. Doree u. L. Hall, *J. Soc. Chem. Ind.*, **44** 270 T (1925).
(6) Hennig, Papier Fabr. **30**, 179 (1932).
(7) W. Lautsch & G. Piazolo, *Cellulosechem.*, **22**, 48 (1944).
(8) H. Erdtmann, Svensk Paperstidn, **45**, 374-80 (1942).

Menge des Niederschlags der Ligninsulfosäure ist von derselben des hinzugesetzten Amins abhängig.

Die Bestimmungsmethode, die man heutzutage verhältnissmäsig öfter gebraucht, ist diejenige nach Partansky[9], wobei man als Fällungsmittel β-Naphthylamin benutzt. Die Menge der dabei ausgefällten Ligninsulfosäure ist aber nur 80 Prozent von gesamter Ligninsulfosäure in Ablauge. Um die Menge der Gesamtligninsulfosäure zu erhalten, muss man deshalb dem Gewicht des erhaltenen Niederschlags einen Faktor multiplizieren, der sich durch geringe Verschiedenheit der Versuchsbedingungen z. B. des Waschungsgrades des Niederschlags oder der Acidität der β-Naphthylaminlösung, verändert.

Als Bestimmungsmethode der Ligninsulfosäure in Sulfitablauge ist die Partanskysche Methode deshalb wenig geeignet. In Hinsicht auf die Analyse verschiedene Bestandteile in Sulfitablauge sind bisher verschiedene Methoden vorgeschlagt worden, aber keine geeignete quantitative Bestimmungsmethode der Ligninsulfosäure ist veröffentlicht. Dass die Kontrolle des Sulfitkochprozesses heute nicht auf der wissenschaftlichen Basis stehen kann, kommt wahrscheinlich aus Mangel an der schnellen und genauen Bestimmungsmethode der Ligninsulfosäure in Ablauge. Sowohl vom rein wissenschaftlichen Bedürfnisse als auch vom technischen müssen wir nun möglichst bald eine geeignete Bestimmungsmethode der Ligninsulfosäure in Ablauge feststellen. Hierbei müssen wir den Grund, der an den bisherigen Misserfolgen geknüft ist, eingehend untersuchen.

H. Terayama[10] hat in letzter Zeit als eine Bestimmungsmethode des hochpolymeren Elektrolyten die Kolloidtitration vorgeschlagt, derren Prinzip besteht darin, dass die gegenseitig anders geladenen Kolloidteilchen sich in stöchiometrischen Verhältnisse miteinander verbinden, um sehr schwerlösliche Produkte zu bilden. Diese Kolloidtitration ist im allgemeinen zur Bestimmungsmethode der hochpolymeren Elektrolyten verwendbar. Er bediente als ein positives Kolloid das Chitosan von Polymerizationsgrad etwa 20, das durch Alkalischmelz des Chitins hergestellt wurde.

Da auch die Ligninsulfosäure in Ablauge ein negatives Kolloid ist, so muss sie sich mit positivem Kolloidteilchen fällen. Je grösser dabei das Molekulargewicht des Fällungsmittel ist, um so vollkommener ist die Fällung der Ligninsulfosäure.

Wie bereits bekannt ist, ist in Ablauge ausser hochmolekularer Ligninsulfosäure noch eine ziemliche Menge niedermolekularer Ligninsulfosäure vorhanden. Um die Ligninsulfosäure in Anlauge quantitativ fällen zu lassen, muss man deshalb möglichst hochpolymere Amin bedienen. Nach meiner Versuche ist das Terayamaschen Chitosan als Reagens für Kolloidtitration nicht die geeignet. Nach meiner Meinung beruhe dies auf seine schwache schutzkolloide Wirkung und auf seine Niedermolekularität.

Die bisherigen Forscher haben sich vergebens anstrengt, von verschiedenen aromatischen Aminen ein gutes Fällungsmittel zu entdecken. Dieser Misserfolg kommt daher, dass die bisher geprüften Amine ausnahmslos niedermolekulare Verbindungen sind. Solange man daher als Fällungsmittel für Ligninsulfosäure das niedermolekulare Amin wie aromatisches Amin wählt, wird es wie man auch sich bemüht, nicht gelingen, ein geeignetes Fällungsmittel zu entdecken.

Von diesem Gesichtpunkte aus wählte ich als Fällungsmittel ein hochpolymeres Amin Oxyäthyl-Chitosan, dessen Polymerizationsgrad etwa 600 war, und es ist mir gelungen, die Ligninsulfosaure in Ablauge bis auf β-Ligninsulfosäure quantitativ fällen zu lassen und sie schnell und genau zu bestimmen. Bei bisherigen Methoden ist die restliche Menge des aromatischen Amins, mit Ausnahme der Methode nach Noll [7], nicht schnell bestimmbar, so dass man im einzelnen das Niederschlag wägen muss. Bei Kolloidtitration ist jedoch das unverbrauchte Glykol-Chitosan (abgekürtzt G. Ch.) mit kalium Polyvinylalkohol Sulfat (abgekürtzt P. V. S.-K) titrimetrisch bestimmbar. Wenn man vorher die Menge der Ligninsulfosäure, die sich mit ein Mol. G. Ch. (auf Aminogruppe berechnet) verbindet, nämlich das Äquivalentgewicht der Ligninsulfosäure gegen Aminogruppe weiss, so kann man gleich aus Verbrauch an G. Ch. den Ligninsulfosäuregehalt in Ablauge rechnen.

Versuchsteil

a) Herstellung des Glykol-Chitosan.— Zur Herstellung des G. Ch. wurde zuerst nach Senzyu und Okimasu[11] das Chitin glykoliert und dann wurde seine Acetylgruppe entfernt. 10 g. von dem nach Rigby[12] gewonnenen, fein

(9) A. M. Partansky u. Benson, Paper Trad J. **64**, **102**, No. 7, 29 (1936).

(10) Terayama, *J. Polymer Science*, **8**, 243 (1952), "Chemical Research" **1**, (1949), **4**, (1950), (in Japanisch).

(11) R. Senzyu u. S. Okimasu, *J. Agri. Chem. Soc. Japan*, **23**, 437 (1949) (in Japanisch).

(12) Rigby, U. S. Patents 2,040,879 (1939).

gepulverten Chitin wurde durch 42%ige. Natronlauge 2 Stunden lang bei Zimmertemperatur behandelt und bis auf das vierfache Gewicht abgepresst. Das so erhaltene Alkalichitin wurde nach Thor und Henderson[13] in Kolben von 300 ccm. Inhalt mit 2.5 fachen Gewicht zerkleinertem Eis unter äuserer Kühlung gemischt, um Alkalichitin fein klar zu dispergieren.

Nachdem die Alkalikonzentration der viskosen Lösung mit 42%iger Natronlauge zu etwa 12 Prozent kontrolliert wurde, wurde 10 g. flüssiges Äthylenoxyd gegossen und gut geknetet. Der Kolben wurde mit Gummistopfel geschlossen, mit fliesendem Wasser allmählig erwarmt und dann 2 Stunden lang bei 25—30° stehen lassen. Die viskosen Lösung des glykoliertes Chitins wurde zunächst 12 Stunden lang bei etwa 60° erhitzt, um die Acetylgruppe zu entfernen. Das Produkt wurde mit dem Gemisch von Aceton und Alkohol abgeschieden. Zur Reinigung wurde mehrmals die Umfällung von wässeriger Lösung mit Alkolhol wiederholt. Der Polymerisationsgrad von dem erhaltenen G. Ch. nach Viskositätmesungen war etwa 600. Elementaranalyse;

	Gef. (%)	Ber. $(C_8H_{14}O_5NH_2)=206$ (%)
N-Gehalt (nach Kjeldahl)	6.71	6.82
NH_2-Gehalt (nach Vanslyk)	7.67	7.70

Die analytischen Date deuten darauf hin, dass das erhaltene Glykol-Chitosan dem Monoglykol-Chitosan entspricht, und dass die Entfernung der Acetylgruppe vollständig ist.

b) Herstellung des P. V. S.-K.—14 ccm Chlorsulfonsäure wurde trofenweise in dreihalsigem Rundkolben, in dem sich 60 ccm getrocknetes Pyridin befindet, unter kräftigem Rühren und kräftiger Kühlung hinzugefügt. Da der Inhalt später in weisse Masse erstarrt, so wurde der Kolben im Wasserbad erhitzt, um den Inhalt zu schmelzen. Nachdem 5 g. gut getrocknetes pulverförmiges Polyvinylalkohol allmählich hinzugegeben worden war, wurde der Kolben bei 100° 4 Stunden lang unter kräftigem Rühren erhitzt. Das dick flüssige Produkt wurde in 300 ccm. Wasser eingegossen und nach Zentrifugierung mit grosser Menge von 95% igem Alkohol versetzt, um das Pyridinsalz von Polyvinylalkoholschwefelsäure fällen zu lassen. Das Produkt wurde mit KOH in Kaliumsalz gespaltet. Zur Reinigung wurde die Umfällung mit Alkohol und Wasser wiederholt. Aus der Bestimmung des Schwefelgehalts vom Produkt ging es hervor, dass das Produkt 92.5% verestert war.

Ausführung der Bestimmung

Reagenzien. —Zum Titrieren dienen $n/100$-G. Ch.-und $n/400$-P. V. S. -K-lösung (auf NH_2- und Sulfogruppe berechnet). Löst man 0.4380 g P. V. S.-K (Schwefelgehalt 18.26%) in 1000 ccm Wasser, so erhalt man gleich $n/400$-P. V. S.-K-lösung. Zur Herstellung des $n/100$-G. Ch.-lösung löst man etwa 2.5 g. von lufttrockenen G. Ch. in 1000 ccm. Wasser, mit Essigsäure oder Salzsäure schwach säuert (pH 3-4), um die gesamte Aminogruppe in G. Ch. dissoziieren zu lassen. Die Konzentration der Aminogruppe der G. Ch.-lösung ist durch Titrieren mit $n/400$-P. V. S.-K bestimmbar. Beim Titrieren setzt man als Indikator einen Tropfen von 0.1 %iger Toluidinblaulösung zu. Solange der G. Gh. mindestens vorhanden ist, ist die Lösungsfarbe rein blau, aber sobald man die P. V. S.-K-lösung um einen Tropfen mehr als äquivalente Menge gegen G. Ch. hinzufügt, verändert sich seine Farbe rotviolet. Der Titrationsendpunkt ist innerhalb Fehlergrenz von 0.05 ccm genau bestimmbar.

Das nach Vanslyk bestimmte NH_2-Gehalt stimmt gut mit dem durch Kolloidtitration gefundenen überein. Dies deutet darauf hin, dass P. V. S.-K sich in dem klaren stöchiometrischen Verhältniss mit G. Ch. verbindet.

Methode. —Zum 5 ccm. der zwanzigfach verdünnten Ablauge setzt man je nach der Konzentration der Ligninsulfosäure 5-10 ccm. $n/100$-G. Ch.-lösung zu. Die Ligninsulfosäure fällt im Anfang flockig, aber danach wird ein Teil des Niederschlags wegen der starken schutzkolloiden Wirkung von überschussigem G. Ch. milchartig verteilt. Man verschliesst den Kolben mit Gummistopfen und schüttelt kräftig durch, um den Niederschlag der Ligninsulfosäure mit Luftblase an Oberflächen der Lösung zu bringen und damit bei Bestimmung des Endpunktes der Kolloidtitration zu erleichtern. Man gibt dann einige Tropfen von 0.1 %iger Toluidinblaulösung zu und titriert das überschussigen G. Ch., das sich mit der Ligninsulfosäure nicht verbindet, mit $n/400$-P. V. S.-K lösung zurück. Sobald die äquivalente Menge von P. V. S.-K hinzugefügt wird, wird die bisher trübende Lösung augenblicklich klar, und seine blaue Farbe verändert sich rotviolet und gleichzeitig sammelt sich der milchartig verteilte Niederschlag flockig an

(13) C. J. B. Thor und W. F. Henderson, *Amer Dyestuff Reptr.*, **29**, 461 (1940).
(14) A. Nall, Papier Fabr. **36**, 43 (1938).

Oberflächen. Der Endpunkt dieser Kolloidtitration ist auch ohne Indikator innerhalb Fehlergrenz von einem Tropfen genau bestimmbar. Der Verfasser pflegt immer ohne Indikator auszuführen. Bei der Titration der sehr verdünnten Ablauge ist es aber vorteilhafter, Indikator zu benutzen. Aus der Differenz zwischen Blindversuch und Bestimmung kann man gleich den Polyaminverbrauch der Probeablauge ermitteln.

Der Polyaminverbrauch von Sulfitablauge ist unabhängig von der Menge des zugesetzen G. Ch., was bei volumetrischer Analyse sehr wichtig ist. Durch Elementaranalyse der Verbindung der Ligninsulfosäure mit G. Ch. ist der Verhältniss von Schwefel zu Stickstoff 1:1. Diese Tatsache deutet darauf hin, dass die Verbindung der Ligninsulfosäure mit G. Ch. sauberes stöchiometrisches Verhältniss aufweist. Man kann deshalb die Menge der aus einem Mol. NH_2-Gruppe entstehenden Verbindung, nämlich das Äquivalentgewicht der Ligninsulfosäure gegen NH_2-Gruppe rechnen, indem man vom Gewicht der Verbindung der Ligninsulfosäure mit G. Ch. das bekannte Äquivalentgewicht des G. Ch. ($C_8H_{14}O_5NH_2=206$) abzieht. Die Ziffern in Tabelle 1 Spalte 5 zeigen das Äquivalentgewicht der Ligninsulfosäure.

Trotzdem die Ablague von Tabelle 1 und 2 aus zwei anderen Zellstofffabriken geschenkt sind, hat ihre Ligninsulfosäure dasselbe Äquivalentgewicht (etwa 380), das von der Kochzeit unabhängig ist.

Um die Ligninsulfosäure in Ablauge zu bestimmen, braucht man nicht den Niederschlag der Kolloidtitration im einzelnen zu wägen, weil das Äquivalentgewicht der Ligninsulfosäure im allgemeinen konstant ist. Vom dem Polyaminverbrauch einer Sulfitablauge aus kann man gleich ihren Ligninsulfosäuregehalt rechnen, wobei 1 ccm. $n/400$-G. Ch.-lösung 0.95 mg. Ligninsulfosäure entspricht. Diese Methode ist besonders darin überlegen, dass die Bestimmung auf volumetrische Weise ausserordentlich schnell ausführbar ist und derren Genauigkeit sehr gross wie später erwähnt. Deshalb ist diese Kolloidtitrationsmethode als eine Kontrollmethode des Sulfitkochprozesses zu empfangen. Bisher litten Zellstofftechniker unter Mangel an schneller Bestimmungsmethode von Ligninsulfosäure. Jedoch können sie nun mit Hilfe des G. Ch. den Verlauf des Sulfitkochprozesses mit der Zeit erkennen.

Einfluss der *p*H-Wert bei Kolloidtitration auf Polyaminverbrauch

Da die Kolloidtitration an Bestimmung von

Tabbele 1

Die Ablauge von Papierzellstoff-Fabrik

Kochzeit in Min.	Ablauge cc.	Addierte cc. $n/100$-G. Ch.-Lös.	Verbrauchte P. V. S.-K zur Zurücktitr.		Verbrauchtes G. Ch. für Fällung		Niederschlag mg./cc. Ablauge	L. S.-Gehalt mg./cc. Ablauge	Äquivalentgewicht der L. S.
			cc. $n/400$	mg.	cc. $n/100$	mg.			
460	3	23.00	11.20	9.0	20.7	42.7	132.1	80.3	388
520	3	27.60	9.50	7.7	24.6	50.9	148.0	89.4	363
570	2	25.00	10.00	8.1	22.5	46.4	140.0	85.5	380
610	2	26.00	5.70	4.6	24.6	50.6	147.6	92.4	377
640	2	30.00	9.00	7.3	27.8	57.2	163.0	105.9	383
660	2	30.00	2.80	2.3	29.3	60.4	175.3	112.6	385

Tabbele 2

Die Ablauge von Kunstseidezellstoff-Fabrik

Kochzeit in Min.	Ablauge cc.	Addierte cc. $n/100$-G. Ch.-Lös.	Verbrauchte P. V. S.-K. zur Zurücktitr.		Verbrauchtes G. Ch. für Fällung		Niederschlag mg./cc. Ablauge	L. S.-Gehalt mg./cc. Ablauge	Äquivalentgewicht der L. S.
			cc. $n/400$	mg.	cc. $n/100$	mg.			
420	1	22.00	11.50	9.3	19.13	39.4	121.1	72.4	379
450	1	24.00	10.40	8.4	21.40	44.1	134.0	81.5	381
510	1	27.00	9.35	7.55	24.66	50.8	151.5	93.2	379
570	1	27.00	7.55	6.1	25.00	51.5	155.1	97.5	390
600	1	27.00	6.50	5.30	25.38	52.3	152.9	95.4	376
690	1	27.00	3.80	3.1	26.05	53.7	155.3	98.6	378

Tabelle 3

Empfindlichkeit der Glykol-Chitosan-Reaktion

Sulfitablauge	Zu je 0.1 ccm. 0.1% iges Reagens zugesetzt Tropfen	1 Tropfen enthält Gamma Ligninsulfosäure	Ausfall der Reaktion	
			Glykol-Chitosan	Trypaflavin
10 cc. : 1000	1	32	starke Fällung	mit blossem Auge nicht mehr, mit der Lupe noch wahrnehmbare Fällung
5 cc. : 1000	1	16	starke Fällung	nicht mehr wahrnehmbar
2.5 cc. : 1000	1	8	schwache Fällung	〃
1.25 cc. : 1000	1	4	mit blossem Auge noch nehmbare Fällung	〃

dissoziierbaren Gruppen geknüpft ist, so verändert sich der Polyaminverbrauch der Ligninsulfosäure mit *p*H-Wert bei Kolloidtitration, denn es sind einige phenolische OH-Gruppe ausser Sulfogruppe in Ligninsulfosäuremolekule. Bei verschiedenen *p*H-Werten führte ich deshalb die Kolloidtitration durch. In Fig. 1 ist die Abhängigkeit des Polyaminverbrauch vom *p*H-Wert bei Titration gezeigt.

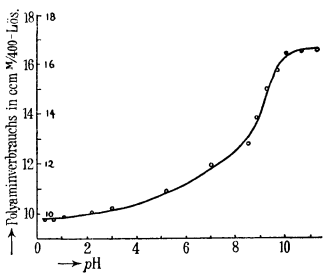

Fig. 1.—Die Abhängigkeit des Polyaminverbrauchs der Ligninsulfosäure in Sulfitablauge von *p*H-Wert bei Kolloidtitration.

Der Polyaminverbrauch nimmt plötzlich wöhrend von *p*H 8 bis 10 zu, aber bleibt ungefähr konstant unter *p*H 7. Dies deutet darauf hin, dass ausser Sulfogruppe und phenolische OH-Gruppe fast keine dissoziierbare Gruppe in Ligninsulfosäuremolekule seien. Wenn man die Titrierung im Bereich von *p*H 2-5 ausführt, so kann man die gute Reproduzierbarkeit erhalten. Der Verfasser pflegt immer in Gegenwart von etwas Essigsäure zu titrieren.

Unter *p*H 4 ist nur die Sulfogruppe und über *p*H 10 sind die gesamten dissozierbaren Gruppen titrierbar. Dass der Polyaminverbrauch bei *p*H 11 etwa 1.6 fach von demselben bei *p*H 3 ist, deutet darauf hin, dass die Ligninsufosäure in Sulfitablauge 2.8 Sulfpgruppen und 1.7 phenolische oder enolische OH-gruppen pro 840 g Lignin besitze.

Die Genauigkeit der Bestimmung

Da nach Noll[14] Trypaflavin sich von bisher aufgefundenen Fällungsmittel als das schärfste erwiesen hat, so wird es von Interese ist, die Empfindlichkeit der G. Ch.-Reaktion mit derselben der Trypaflavin-Reaktion zu vergleichen. Zu die sem Zweck wurde nach Noll je 0.03 ccm 0.15% iger G. Ch.-lösung mit je einem Tropfen extrem verdünnter Sulfitablauge versetzt. Die Ergebnisse sind aus der Tabelle 3 ersichtlich.

Noch bei einer Verdünnung von 1.25 : 1000 kann das G. Ch. die mit dem blossem Auge wahrnehmbare Fällung geben. Somit ist diese Raktion empfindlicher als die von Noll aufgefundene Fällungsreaktion mit Trypaflavin. Aus dieser Prüfung wird man ersehen, dass meine Bestimmungsmethode ausserordentlich genau ist.

Zum Schluss muss der Verfasser Herrn Prof. K. Nishida für seine freundliche Leitung sowie Herren M. Shimizu und I. Sakata, die mir arbeiten half, danken. Diese Untersuchung wurde mit Unterstützung der Takatiho Papierzellstoff-Fabrik geführt, wofür ich an dieser Stelle Dank sagen möchte.

Institut für Wissenschaft und Industrie,
Kyushu Universität

(14) A. Noll. Papier Febr., **36**, 43 (1938).

Untersuchungen über Lignin und Zellstoff. II. Eine neue Bestimmungsmethode des Lignins in Hölzern und Zellstoffen durch Kolloidtitration

Von Ryoiti SENZYU

(Eingegangen am 26, June, 1952)

Einteilung

Was die Bestimmungsmethode des Lignins in Hölzern und Zellstoffen betrifft, sind bisher verschiedene Methoden veröffentlicht, die man in zwei Gruppen d. h. die direkten und indirekten Methoden ordnen kann. Die direkten Methoden sind diejenigen, bei denen man die hochpolymeren Kohlenhydrate von Probe mittels starker Mineralsäure herauslöst und damit den Rückstand einfach als "Lignin" wägt.

Bei anderen bestimmt man mittelbar den Ligningehalt aus Methoxygehalt oder aus Verbrauch an Halogen oder Oxydationsmittel. Da jedoch die indirekten Methoden ohne Festlegung der genauen Versuchsbedingungen keine reichende Genauigkeit zu erwarten ist, so sind sie zur Bestimmung des Holzlignins heutzutage wenig gebraucht. Die heute häufigsten gebrauchten Methoden sind nämlich die direkten, bei denen man als Hydrolysemittel Schwefelsäure oder Salzsäure benutzt. Diese Methoden nahmen jedoch die zu längeren Ausführungsdauer in Anspruch. Es gibt leider noch keine Normalmethode für Ligninbestimmung.

H. Terayama[1] hat in letzter Zeit als eine neue Bestimmungsmethode der hochpolymeren Elektrolyten die Kalloidtitration vorgeschlagt. Der Verfasser[2] hat diese Kolloidtitration zur Bestimmung der Ligninsulfosäure in Sulfitablauge angewandt und die hinreichenden Resultate erhaltet, wobei er statt des Terayamaschen Chitosans das bei uns neurig hergestellten Polyamin d. h. "Oxyäthyl-Chitosan" Gebraucht, um die Endpunktbestimmung der Kolloidtitration leichter zu machen und bis auf die niedermolekularen Ligninsulfosäure quantitativ fällen zu lassen. Diese Kolloidtitration ist auch zur Bestimmung des Lignins in Hölzern und Zellstoffen ver wendbar.

Das Lignin eines verholzten Körpers verändert sich unter Einwirkung des Chlorgases in das Chlorlignin, das in verdünnten Alkali oder in 3% iger Natriumsulfitlösung leicht löslich ist. Auf diese Tatsache gründet sich die Cellulosebestimmung nach Cross und Bevan.[3]

In dem bei Gesamtcellulosebestimmung erhaltenen Waschabfall ist das gesamte Lignin der Probe als Chlorlignin (genauer gesprochen Chlorligninsulfosäure) gelöst. Wenn man das Chlorlignin in der Lösung bestimmen kann, so wird es gelingen, die Cellulose und das Lignin von Probe gleichzeitig zu ermitteln. Da die Chlorligninsulfosäure ein phenolische OH- und Sulfogruppe enthaltendes, negatives hochmolekulares Elektrolyt ist, so kann man sie mit Polyamin quantitativ fällen lassen. Indem man nach Zusatz einer bestimmter Menge der Polyaminlösung in die Lösung der Chlorligninsulfosäure das restliche Amin mit Kalium Polyvinylalkohol Sulfat zurücktriert, kann man gleich den Ligningehalt von Probe rechnen. Der Polyaminverbrauch der Chlorligninsulfosäure nimmt wegen ihrer phenolischen OH-gruppen mit dem PH-Wert bei Titration zu, um erst über *p*H 10.0 konstant zu werden. Deshalb muss man die Titrierung im Bereich über *p*H 10.0 ausführen, um immer die gute Reproduzierbarkeit zu erhalten. Aus diesem Grunde wählte ich als Fällungsmittel für Chlorligninsulfosäure N-polymethyl-Glykol-Chitosan (abgekürtzt M. G. Ch.), das noch im alkalischen Medium völlig dissoziierbar ist.

Versuchsteil

a) Herstellung des M. G. Ch.—4 g. Glykol-Chitosan wurde in 40 ccm. Wasser gelöst, mit 3.5 g. Natriumcarbonat, 15 g. Jodmethyl und 15 ccm. Methanol gut vermischt und in Druckflaschen bei 100° ein Stunde lang erhitzt. Das Produkt wurde mit Alkohol abgeschieden. Zur Reinigung wurde die Fällung von wässeriger Lösung mit Alkohol wiederholt.

(1) H. Terayama, *J. Polymer Science*, **8**, 243 (1952).
(2) R. Senzyu, *Bull. Chem. Soc. Japan*, **25**, 131 (1952).
(3) C. F. Gross and E. J. Bevan, *J. Chem. Soc. London*, **55**, 199 (1889).

Tabelle 1

1	2	3	4	5	6	7	8	9	10
Holzart	Ligningehalt nach 72% iger Schwefelsäure Methode, (%)	Menge des von 0.5 g. lufttrockener Probe extrahierten Lignins in cc. n/400 P. V. S.-K				Ligninmenge in 0.5 g. lufttrock. Probe, g.	Äquivalentgewicht des Lignins		
		erstmalige	zweitmalige	dritmalige	Gesamtsumme		Gefunden	Berechnet nach Annahme des Vorhandens von	
								6 Grup.	5 Grup.
"Akamatsu" Pinus densiflore	29.3	320	20	5	345	0.1270	147	140	168
"Masugi" Cryptomeria japonica	34.0	370	26	4	400	0.1476	147	140	168
"Buna" Fagus crenata Blume	25.9	230	14	2	246	0.1117	182	151	180
"Bambus"	26.0	220	18	2	240	0.1130	188	151	180

b) Ausführung der Bestimmung des Holzlignins

Reagenzien.—Zum Titrieren dienen n/100-M. G. Ch.-lösung und n/400-P. V. S.-K-lösung (auf Alkylamino- und Sulfogruppe berechnet).

Zur Herstellung der n/100 M. G. Ch.-lösung löst man etwa 3 g. lufttrockenen M. G. Ch. in 1000 ccm. Wasser und mit Ammoniakwasser alkalisiert. Durch Titrierung mit n/400-P. V. S.-K-lösung bestimmt man die genaue Konzentration der Alkylaminogruppe in Lösung.

Methode.—0.5 g. lufttrockenes Holzmehl, das man mit Wasser auffeuchtet, wurde in Glassfilter 15 Minuten lang Chlorgas einwirken lassen. Dabei kontroliert man die Geschwindigkeit der Durchführung von Chlorgas einige Blase pro Sekund. Nach Absaugen von haftenden Chlorgas wurde das chlorierte Holzmehl mit wenig Wasser einigemal gewaschen, um die bei Chlorierung gebildete Salzsäure zu beseitigen, und darauf 30 Minuten lang mit 10 ccm. 3% iger Natriumsulfitlösung auf Wasserbad erhitzt, womit das Chlorlignin sulfoniert wird und an Wasserlöslichkeit gewinnt. Das Holzmehl wurde dann mit heissem Wasser völlig gewaschen. Durch zweimalige Wechselwirkung von Chlorgas und Natriumsulfitlösung wurde das Lignin von Probe fast vollständig herausgelöst.

Das so erhaltene Filtrat wurde mit Ammoniak alkalisch gemacht und auf 100 ccm. aufgefüllt. Man gab in 10 ccm. davon 5 ccm. n/100-M. G. Ch.-lösung zu und titrierte das restliche Polyamin mit n/400-P. V. S.-K-lösung zurück. Bei Titrierung setzte man als Indikator einige Tropfen von 0.1% iger Toluidinblaulösung zu. Aus der Differenz zwischen Blindversuch und Bestimmung kann man den Polyaninverbrauch der Probelösung ermitteln.

Aquivalentgewicht des Lignins

Um aus dem polyaminverbrauch dieser Kolloidtitration den Ligningehalt der probe zu rechnen, muss die Polyaminverbrauch des anwesenden Lignins bekannt sein. Nimmt man an, dass die 72% ige Schwefelsäuremethode den echten Ligningehalt angete, so kann man ein Äquivalentgewicht von Lignin gegen NH_2-gruppe erhalten. (siehe Tabelle 1 Spalte 5) Vorausgesetzt, dass der Grundmolekulargewicht des Nadel- und Laubholzlignins 840(nach Brauns[4]) und 910 (nach Harris[5]) sei, so kann man als ihre Aquivalentgewicht gegen Alkylaminogruppe die Ziffern in Tabelle 1 Spalte 9 und 10 erhalten.

Wie in Tabelle ersichtlich ist es höchst wahrscheinlich, dass die Chlorligninsulfosäure des Nadelholzlignins sechs dissoziierbaren Gruppen und diejenige des Laubholzlignins fünf besitze. Nach bisherigen Untersuchungen entsteht bei Chlorierung des Lignins grosse Menge der phenolischen OH-gruppen, die gegen gebund ene Chloratome äquivalent sind. Nach Fotijew[6] kann das Chlorlignin von Nadelholz wie folgt geschrieben werden.

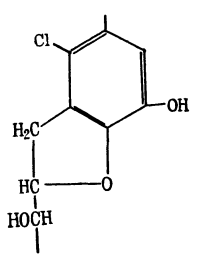

Fig. 1.—Schema des Chlorlignins.

Von dieser Tatsache aus ist es fast zweifellos, dass von sechs dissoziierbaren Guppen der Chlorligninsulfosäure des Nadelholzes fünf die phenolische OH-gruppe seien und eine die Sulfogruppe sei.

(4) F. E. Brauns, *J. Amer. Chem. Soc.*, **61**, 2120 (1939); *Paper Trad J.*, **108**, 42 (1939); Ibid **111**, No. 14, 33 (1940).
(5) E. E. Harris, *Ind. Eng. Chem.*, **32**, 1049 (1940).
(6) S. A. Fotijew, *Pulp Paper Mag. Can.*, **39**, 749 1938) (C. Z. II. 218 (1939).

Einfluss der Versuchsbedingungen auf Ergebnisse

Der Polyaminverbrauch könnte mit der Einwirkungszeit und- Temperature des Chlorgases und mit der Erhitzungszeit in 3% iger Natriumsulfitlösung verändern. Ich untersuchte daher den Einfluss dieser Versuchsbedingungen auf Polyaminverbrauch des Lignins.

a) Einfluss von Temperatur. — 0.5 g. lufttrockenes Holzmehl wurde bei verschiedenem Temperatur chloriert, und die extrahierte Chlorligninsulfosäure wurde auf die ober erwähnte Weise bestimmt. Tabelle 2 zeigt die erhaltenen Ergebnisse.

Tabelle 2

Einfluss der Chlorierungstemperatur auf Polyaminverbrauch des Lignins (Die Ziffern in Tabelle zeigen die Menge des extrahierten Lignins in ccm. n/400-P. V. S.-K-lös.)

Holzart	Temp., °C.		
	0	15	30
"Akamatsu" Pinus densiflora	350	352	347
"Sugi" Cryptomeria japonica	397	400	396
"Buna" Fagus crenata Blume	243	245	250
"Bambus"	240	238	240

Nach bisherigen Untersuchungen verändert sich das Chlorverbrauch des Holzes mit Temperatur. Wie aus Tabelle 2 ersichtlich ist jedoch das Polyaminverbrauch des Holzes von Einwirkungstemperatur des Chlorgases unabhängig. Aus dieser Tatsache geht hervor, dass die Menge der phenolischen OH-gruppe, die durch Einwirkung des Chlorgases in Ligninmolekül entsteht, von Temperatur unabhängig ist. Diese Einflusslosigkeit der Temperatur auf Polyaminverbrauch kommt wahrscheinlich auf vollkommene Chlorierung des Lignins. In diesem Punkte ist diese Methode den bisherigen Methoden überlegen, bei denen man aus Hologenverbrauch den Ligningehalt mittelbar bestimmt. Es ist sehr bemerkenswert, dass über 93% des gesamten Lignins durch nur einmalige Wechselwirkung von Chlorgas und Natriumsulfitlösung herausgelöst werden kann.

b) Einfluss der Einwirkungszeit des Chlorgases. — Wie ober erwähnt kann der grosste Teil des Lignins durch erstmalige Chlorierung und Extrahierung herausgelöst werden, deshalb kann man sagen, dass die Zeit der erstmaligen Chlorierung auf den Polyaminverbrauch entscheidend beeinflüsst. Aus diesem Grund prüfte der Verfasser nur den Einfluss der Zeit der erstmaligen Chlorierung. Das Chlorgas wurde stets bei 20° einwirken lassen.

Die Ziffern in Tabelle 3 zeigen die Menge des erstmal extraheirten Lignins in ccm. n/400-P. V. S.-K-lösung.

Tabelle 3

Einfluss der Chlorierungsdauer auf den Polyaminverbrauch des Lignins

Holzart	Dauer in Min.			
	10	15	20	45
"Akamatsu" Pinus densiflora	320	345	349	345
"Buna" Fagus crenata Blume	231	246	248	247
"Bambus"	220	240	238	238

Wenn man über 15 minuten lang des Chlorgas durchgeführt, so kann man stets die guten reproduzierbaren Resultate erhalten. Es ist gleichgültig, ob die Dauer der zweitmaligen Chlorierung lang oder kurz sei. Diese Tatsache kommt wahrschienlich daher, dass meine Methode sich nicht auf die Bestimmung des Halogenverbrauch, sondern auf diejenige der phenolischen OH-gruppe gründet.

c) Einfluss der Erhitzungszeit mit Natriumsulfit.—Das Chlorlignin wurde unter Einwirkung des Natriumsulfites in die Chlorligninsulfosäure sulfoniert und gewinnt an Wasserlöslichkeit. So wird die Erhitzungszeit mit Natriumsulfit auf Sulfonierungsgrad des Lignins einflussreich sein. Die Tabelle 4 zeigt die erhaltenen Resultate.

Tabelle 4

Einfluss der Erhitzungsdauer mit Natriumsulfit auf den Polyaminverbrauch des Lignins

Extrahierungszeit in Min.	15	25	35	45
"Sugi" (Cryptomeria japonica	355	370	368	372

Die Ziffern in Tabelle zeigen die erstmal extrahierten Ligninmenge in ccm. n/400-P. V. S.-K-lösung. Um aus dem chlorierten Holzmehl seines Chlorlignin möglichst vollständig herauszulösen, ist es nötig wie in Tabelle 4 ersichtlich, das Holzmehl 30 Minuten lang mit 3% iger Natriumsulfitlösung zu erhitzen.

Bei Bestimmung der Gesamtcellulose nach Cross und Bevan wiederholt man im allgemeinen viermal Chlorierung und Erhitzung mit Natriumsulfit. Zielt man aber nur auf Entfernung des Lignins von Probe, ist es schon genug, die Wechselwirkung von Chlorgas und Natriumsulfit zweimal zu wiederholen.

d) Einfluss *p*H. Wert bei Kolloidtitration. — Da die Kolloidtitrationsmethode an

Bestimmung von dissoziierbaren Gruppen der Chlorligninsulfosäure geknüpft ist, so sind die Ergebnisse empfindlich gegen *p*H-Wert bei Titration. Bei verschiedenen *p*H-Werten führte ich die Titration durch. In Fig. 2 ist die Abhängigkeit des Polyaminverbrauchs von dem *p*H-Wert bei Titration gezeigt.

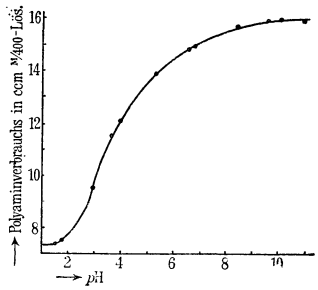

Fig. 2.—Die Abhängigkeit des Polyaminverbrauchs der in Chlorligninsulfosäure ("Sugi") von *p*H-Wert bei Kolloidtitration.

Der *p*H-Wert von Lösung wurde mit Glaselektrode bestimmt. Der Polyaminverbrauch verändert sich mit *p*H-Wert, aber bleibt konstant über *p*H 9. Wenn man die Titrierung deshalb bei über *p*H 9 ausführt, so kann man die gute Reproduzierbarkeit erhalten. Der Verfasser pflegt immer in Gegenwart von etwas Ammoniak zu titrieren.

Bestimmung der Bleichfähigkeit von Zellstoffen

Die bisherigen Methode zur Bestimmung der Bleichfähigkeit von Zellstoffen beruhen grosstenteils auf der leichten Oxydierbarkeit des Lignins oder seiner Reaktionsfähigkeit gegen Chlor. Als das hauptsächlichste Oxydationsmittel kommen Hypochlorit-, Hypobromit- und Permanganatlösung in Frage. Um befriedigende Ergebnisse zu erzielen, muss man aber in dem meisten Fallen in genauer Festlegung der Versuchsbedingungen arbeiten. Wir müssen nun daher eine Methode suchen, die keine längeren Reaktionszeit und keine genaue Einhaltung so vieler Bedingungen in Anspruch nimmt. Die Kolloidtitration erfüllt auch diese Erfordernisse.

Wie bereits bekannt ist, liegt das Lignin in Sulfitzellstoff als Ligninsulfosäure vor, die in diesem Zustande in Alkali unlösich ist. Es wird aber, wie man öfter bei Bleichen von Sulfitzellstoff erfahrt, unter Einwirkung von Chlorgas in die Chlorligninsulfosäure chloriert, die in verdünnter Natronlauge leicht lösich ist. Auch das Lignin in Kraftzellstoff kann wie bei Holz durch Wechselwirkung von Chlorgas und Natriumsulit sehr leicht herausgelöst werden. Bei Zellstoffen ist die Herauslösung des Lignins wegen ihrer günstigen physikalischen Eigenschaften sehr leichter als bei Holzmehl.

a) Ausführung der Bestimmung.—Für Probe nimmt man 2.0 trockenen Zellstoff, den man mit wasser auffeuchtet oder eine 5 g. nasse, durch Hand ausgedrückte, ungefähr 60 % Wasser enthaltende Zellstoffprobe. Die Probe wurde in Glassfilter oder in Meyerkolben etwa 2 Minuten lang mit Chlorgas einwirken lassen.

Bei Sulfitzellstoff kann man das Chlorlignin bei Zimmertemperatur nur mit verdünnter Natronlauge vollständig extrahieren, weil sein Lignin schon als Ligninsulfosäure vorliegt. Der chlorierte Sulfitzellstoff wurde nach Absaugen von haftendem Chlorgas in Meyerkolben von 200 ccm. Inhalt eingeführt, in dem sich 100 ccm. n/20-NaOH befindet. Der Kolben wurde etwa 10 Sekunden lang kräftig durchgeschüttelt, um zu zerfassern und damit die Herauslösung der Chlorligninsulfosäure zu erleichtern. Dann wurde der Zellstoff auf einer Nutsche abfiltriert. Die so erhaltenen alkalischen Filtrat wurde mit einigen Tropfen der konz. Salzsäure neutralisiert und 10 ccm. davon zur Bestimmung der Chlorligninsulfosäure benutzt, wobei n/200-M. G. Ch.- und n/400-P. V. S.-K-lösung dienten. Die Kolloidtitration wurde in Gegenwart von etwas Ammoniak ausgeführt. Je nach dem Gehalt an Chlorligninsulfosäure muss man so viel Menge Polyaminlösung zusetzen, dass mindestens das über 4 ccm. n/400 P. V. S.-K-lösung entsprechende Polyamin zurückbleibt, um die guten Reproduzierbarkeit zu erhalten.

Bei Kraftzellstoff muss man die chlorierte Probe in schwach alkalischem Medium mit 100 ccm. 3% iger Natriumsulfitlösung auf siedende Wasserbad 5 Minuten lang extrahieren. Um das Lignin von Kraftzellstoff quantitativ herauszulösen, muss man die Wechselwirkung von Chlorgas und Natriumsulfit zweimal wiederholen.

Durch erstmalige Extrahierung erhaltet man jedoch immer etwa 90% von dem Gesamtlignin. deshalb braucht man nicht die Extrahierung zweimal zu wiederholen. Indem man der erstmal extrahierte Menge des Lignins den Faktor 1.11 multipliziert, kann man gleich den Gesamtligningehalt der Probe erhalten.

Für die praktischen Bedürfnisse der Betriebskontrolle genügt es, dass man den Ligningehalt von 0.2 g. trockenem Zellstoff in ccm. n/400-Polyaminlösung angibt. Ich schlage für diese Zahl die Beseichuung "Polyaminzahl" vor. Tabelle 5 und Fig. 3 zeigen die Beziehung

Tabelle 5

Beziehung zwischen Polyaminzahl (PAZ) und Ligningehalt von Kraftzellstoff

Zellstoff Nr.	Die aus 2 g. lufttrockenem Zellstoff extrahierte Ligninmenge in ccm. n/400-P. V. S.-K				Ligningehalt nach 72%iger H_2SO_4-Methode, %	Ligninmenge in 2.0 g. lufttrock. Probe, mg.	Äquivalentgewicht von Lignin in Zellstoff	PAZ von Zellstoff
	erstmalige	zweitmalige	dritmalige.	Gesamtsumme				
1	76.0	5.0	1.9	83	2.42	42.5	205	9.5
2	101.2	8.1	2.0	111	3.35	59.5	214	12.5
3	126.9	10.8	3.1	141	4.27	74.5	212	16.2
4	135.4	9.9	3.0	148	4.42	76.6	207	17.3
5	146.4	10.9	3.1	160	4.93	85.7	214	18.5
6	201.2	13.5	3.0	217	6.28	111.0	201	25.0
7	242.8	16.6	4.0	262	7.73	134.0	204	30.6

zwischen Polyaminzahl (PAZ) und Ligningehalt des Kraftzellstoffes. Zwischen PAZ und Ligningehalt (Klason-Lignin) ist ein enger Zusammenhang vorhanden. Rechnet man wie bei Holzlignin aus Ligningehalt des Klaftzellstoffes dessen Äquivalentgewicht gegen Alkylaminogruppe, so erhalt man die Ziffern in Tabelle 5 Spalte 6.

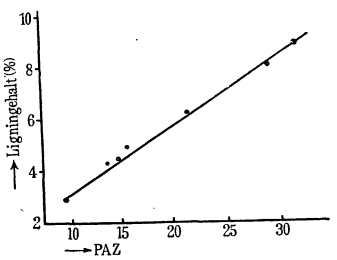

Fig. 3.—Beziehung zwischen PAZ und Ligningehalt des Kraftzellstoffes.

c) Einfluss der Veesuchsbedingungen auf Ergebnisse.—Der Verfasser untersucht zuerst die Abhängigkeit der Ergebnisse von Einwirkungszeit des Chlorgases, von der Menge und Konzentration der zur Extrahierung der Chlorligninsulfosäure gebrauchten Natronlauge und von dem *p*H-Wert bei Kolloidtitration.

Mit Ausnahme des Einfluss von *p*H-Wert sind die Ergebnisse von anderen Versuchsbedingungen unabhängig. Man erhalt denselben Wert, ganz gleich, ob die Einwirkungszeit von Chlorgas 2, 5, 10 oder 60 Minuten lang dauert. Polyaminzahl ist auch von Konzentration der Natronlauge unabhängig, die zur Extrahierung der Chlorligninsulfosäure in Sulfitzellstoff benutzt wird, wenn sie genug dick ist, um die infolge der Chlorierung gebildete Salzsäure zu neutralisieren. Der Gebrauch der zu dicken Natronlauge zur Herauslösung der Chlorligninsulfosäure ist aber nicht vorteilhaft, weil bei starker Salzlösung der Endpunkt der Kolloidtitration undeutlich wird.

Der Verfasser pflegt 100 ccm n/20 NaOH auf 2.0 g. trockenen Zellstoff zu benutzen. Die Reproduzierbarkeit der Ergebnisse ist sehr gut. Die Doppelbestimmung liegen innerhalb der Fehlergrenzen von 0.05 ccm.

Der *p*H-Wert bei Kolloidtitration hat auf Polyaminverbrauch einen grossen Einfluss, denn auch bei dem Lignin in Zellstoffen entsteht infolge der Chlorierung eine grosse Menge phenolische OH-gruppe. Bei verschiedenen *p*H-Werten führte ich die Kolloidtitration durch. In Fig. 4 und 5 ist die Abhängigkeit des Polyaminverbrauchs von dem *p*H-

Tabelle 6

Einfluss der verschiedenen Versuchsbedingungen auf Polyaminzahl

Konzent. der Natronlauge zur Extrahierung	n/10 8.20	n/20 8.20	n/40 8.00	n/60 7.98
Einwirkungsdauer von Chlorgas	2 Min. 8.18	5 Min. 8.22	10 Min. 8.00	60 Min. 8.00
Einwirkungstemp. von Chlorgas	0°C 8.20	15°C 8.20	30°C 8.20	
Häufigkeit von Extrahierung	einmal 8.18	zweimal 8.20		

Note: Die Ziffern in Tabelle zeigen die Polyamin-Zahl.

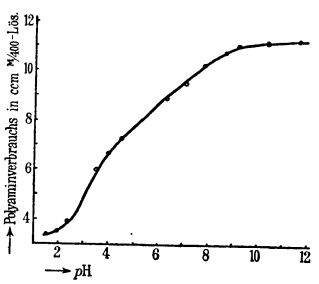

Fig. 4.—Die Abhängigkeit des Polyaminverbrauchs des Lignins in Sulfitzellstoff von dem *p*H-Wert bei Kolloidtitration.

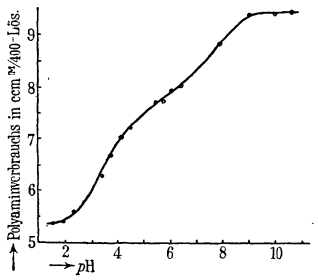

Fig. 5.—Die Abhängigkeit des Polyaminverbrauchs des Lignins in Kraftzellstoff von *p*H-Wert bei Kolloidtitration.

wert bei Titration gezeigt. Der Polyaminverbrauch nimmt zwar mit dem *p*H-Wert zu, aber bleibt konstant über *p*H 9. Wenn man die Titrierung deshalb bei über *p*H 9 ausführt, so kann man die gute Reproduzierbarkeit erhalten. Der Verfasser pflegt immer in Gegenwart von etwas Ammoniak zu titrieren.

In welchem Verhältnisse stehen nun die neu erhaltenen Wert zu den Zahlen der Oxydationsmethoden? Ich trug in dem Bild (Fig. 6) auf der Abszisse die Chlorverbrauchzahlen nach Sieber auf der Ordinat die Polyaminzahl auf.

Zwischen PAZ und Sieber-Zahl ist ein enger Zusammenhang vorhanden. Aus den Ergebnisse der neuen Methode kann man gleich den Ligningehalt des Probezellstoffes rechnen, wenn das polyaminverbrauch des anwesenden Lignins in Probezellstollen bekannt ist. Indem der Verfasser von dem Gewicht der Verbindung der Chlorligninsulfosäure mit G, Ch. oder M. G. Ch. das bekannte Gewicht des verwendeten Fällungsmittels abzieht, fand er direkt das Äquivalentgewicht des Lignins in Sulfitzellstoff. Nach seinem Versuche ist es etwa 213. Im früheren Mitteilung[7] rechnete der Verfasser aus der Polyaminzahl eines oulfitzellstoffes dessen Ligningehalt unter Annahme, dass das Lignin in Sulfitzellstoff dasselben Äquivalentgewicht (147) wie das des Lignins in Holz habe. Es ist jetzt mir deutlich worden, dass diese Annahme unrecht gewesen war. In Tabelle 7 ist der Ligningehalt der verschiedenen Sulfitzellstoffen nach verschiedenen Methoden gegenübergestellt.

Tabelle 7

Sieber-Zahl	Polyamin-zahl	Ligningehalt, % nach[8] Sieber	Ligningehalt, % berechnet aus Polyaminzahl
20.1	5.01	1.30	1.33
21.8	5.38	1.56	1.43
23.1	6.80	1.65	1.81
26.5	8.10	2.05	2.15
26.8	8.20	2.08	2.18
28.0	8.25	2.20	2.20
29.3	8.93	2.38	2.37

Wie aus Tabelle 7 ersichtlich ist, stimmt gut der aus PAZ berechnete Ligningehalt mit demjenigen nach Sieber überein.

Zum Schluss muss der Verfasser dem Herrn Prof. K. Nishida für seine freundliche Leitung, sowie Herren I. Sakata und M. Shimizu für ihren Beistand durch unermüdliche Arbeit den herzlichen Dank sprechen. Diese Arbeit wurde mit Unterstützung der Takatiho Papierzellstoff-Fabrik geführt, wofür ich an dieser Stelle Dank sagen möchte.

Institut für Wissenschaft und Industrie,
Kyushu Universität

(7) R. Senzyu, *Proc. Japan, Academy*, **28**, 304 (1952).
(8) Sieber, Schwalbe-Sieber, Die Betriebskontrolle in der Zellstoff- und Papierindustrie, S, 529 (1931).

Sterols and Other Unsaponifiable Substances in the Fats of Shell Fishes, Crustacea and Echinodermata. XI. Sterols in the Fat of Clam

By Yoshiyuki TOYAMA, Toru TAKAGI and Tatsuo TANAKA

(Received June 16, 1952)

Sterols in the fat of the clam, *Meretrix meretrix*, was studied in the 3rd report[1] of this series, and a sterol named meretristerol having m. p. 133—134.5°, and its acetate of m. p. 144—144.5° and the formula $C_{28}H_{46}O$ or $C_{29}H_{48}O$ was separated. But later in the 9th report[2] it was revealed that the meretristerol previously obtained was impure, since repeated recrystallizations of the steryl acetate gave a fraction of m. p. 149.5° which was believed to be pure meretristeryl acetate. Saponification of this acetate gave meretristerol of m. p. 144.5°. Meanwhile, Bergmann and Ottke[3] suggested that meretristerol is not a single sterol but a mixture of brassicasterol and chalinasterol.

With the purpose of obtaining pure meretristerol in a sufficient quantity to permit a further study, the sterol mixture was separated from the fat extracted from another lot of clams, and its acetate was subjected to repeated recrystallizations. There was obtained a fraction of m. p. 149°, but its melting point was raised somewhat promptly by further recrystallizations until a fraction of m. p. 173—174° was finally obtained in a very small quantity. Accordingly, it must be recognized that even the meretristerol described in the 9th report was not a pure single sterol. Also the fraction of high melting point, 173—174°, was not considered to be a single acetate from the results of the fractionation of its bromide.

The acetate mixture after removal of the high melting fraction was brominated in ether solution and the product was separated into the ether insoluble bromide (I) and the ether soluble bromide (II). The bromide I was then treated with chloroform-ethanol and ethanol, and there were obtained two fractions (Ia) and (Ib). The bromide II was treated with ethanol and a fraction melting at 120—123° was separated. Debromination of this fraction and

Table 1

	Sterol		Acetate		Benzoate		Acetate tetrabromide		Acetate dibromide	
	m. p., °C.	$[\alpha]^{\circ}_{D}$	m. p., °C.	$[\alpha]^{\circ}_{D}$	m. p., °C.	$[\alpha]^{\circ}_{D}$	m. p., °C.	$[\alpha]^{\circ}_{D}$	m. p., °C.	$[\alpha]^{\circ}_{D}$
Sterol from bromide Ia	145	−63.8	151	−60.7	158	—	202	−43.8	215—216	—
Brassicasterol[4]	146	−61.1	152	−65	163	−35[5]	205	—	236—238	—
Sterol from bromide Ib	154	−53.3	146—147	−52.1	140	−21.7	192	−42.5	213—214	—
Poriferasterol[6]	155—156	−49.7	146.5—147	−53	139.5—140.5	−21.9	192	−43.5	211—212	−31
Sterol from fraction III	136—137	−39.3	137—138	−38.2	133—135	−21.2				
Clionasterol[7]	137.5—138.5	−37	137	−41.9	134.5—135	−16.8				
Sterol from fraction IV	142	−37.6	114	—	145	−15.8				
Cholesterol	148	−38	114	−43	146	−17				

(1) Y. Toyama and M. Yajima, *J. Chem. Soc. Japan*, **64**, 878 (1943).
(2) M. Kita, I. Naka and Y. Toyama, *J. Chem. Soc. Japan, Pure Chem. Sect.*, **71**, 21 (1950).
(3) W. Bergmann and R. C. Ottke, *J. Org. Chem.*, **14**, 1085 (1949).
(4) E. Fernholz and H. E. Stavely, *J. Am. Chem. Soc.*, **61**, 142 (1939); **62**, 428 (1940).
(5) l. c., (3).
(6) F. R. Valentine, Jr. and W. Bergmann, *J. Org. Chem.*, **6**, 452 (1941); W. Bergmann and R. J. Feeney, ibid., **14**, 1078 (1949); W. Bergmann, F. H. McTigue, E. M. Low, W. M. Stokes and R. J. Feeney, ibid., **15**, 96 (1950).
(7) F. R. Valentine, Jr. and W. Bergmann, *J. Org. Chem.*, **6**, 452 (1941).

fractional crystallization of the debrominated product gave two fractions (III) and (IV). On examining each fraction, brassicasterol and poriferasterol were obtained from the bromides Ia and Ib respectively, while the fractions III and IV were found to contain clionasteryl acetate and cholesteryl acetate respectively. The properties of sterols obtained from each fraction are given in Table 1.

The occurrence of brassicasterol in the sterol components of Pelecypoda[8] had already been known, but poriferasterol had not yet been found in shell fish. Clionasterol was also found in Pelecypoda for the first time by the present study, though its occurrence in Gastropoda[9] had been known.

The acetate of m. p. 173—174° was brominated, the bromide separated into two fractions, and each fraction debrominated. The debromination products from each fraction had considerably lower melting points than the original acetate. Thus the original acetate was not regenerated by the debromination of the bromide. Accordingly the original acetate must have undergone isomerization or other changes in bromination and debromination cycle.

Experimental

Clams used in the present experiments were procured from the Shimono-isshiki Fishery Co-operation, Nagoya, in April and May, 1950. Thirty-six kg. of wet meat obtained from 150 kg. of clams was dried below 80° under vacuum, and the dried material (4.58 kg.) was reduced to powder, from which 462 g. of fat (10.1% of dried material) was extracted using trichloroethylene. Saponification of the fat and extraction of the soap solution with ether in the usual way yielded 83 g. of unsaponifiable substance (18.0% of fat), which was a mixture of crystalline solid and viscous oily liquid of dark reddish orange color.

Recrystallization of Steryl Acetate. — The unsaponifiable substance was recrystallized three times from ethanol, and there was obtained 27.1 g. of crystalline solid of m. p. 118—138°, which was acetylated by refluxing with acetic anhydride. The acetate (30.2 g.) was recrystallized five times from ethanol, once from acetone-ethanol, and twice from acetone, giving an acetate (4.5 g.) of m. p. 129—132°, $[\alpha]_D^{18}$ −40.3°, saponification value 131.1 and iodine value (pyridine sulfate dibromide method) 98.0. Further recrystallizations of this acetate were carried out as shown in Table 2.

Table 2

Recrystallized from	Acetate crystallized out		Acetate in mother liquor
	Yield, g.	m. p., °C.	m. p., °C.
Benzene-ethanol	3.0	132—135	130—132
Acetone	0.4	142—149	129—130(a)
〃	0.2	165—167	131—132
〃	0.12	173—174	155—158

(a) 2.6 g., $[\alpha]_D^{18}$ −41.5°, saponification value 128.3, iodine value 97.0. This fraction of the acetate from the mother liquor was subjected to further recrystallizations as shown below.

Benzene-ethanol	2.0	131—134	130—132
Acetone	1.2	136—141	128—132
Ether-ethanol	0.5	144—149	130—132
Acetone	0.33	145—149	132—134
〃	0.19	146—149	138—139
〃	0.16	148—149.5	142—143.5
〃	0.13	170—171	145—146
〃	0.11	173—174	145—149

Fractionation of Acetate Bromide.—Acetate contained in the mother liquors of recrystallizations was recovered, and two fractions (A) 4.9g., melting between 130° and 135°, and (B) 12 g., melting between 110° and 130°, were separated. Both fractions were brominated and bromides were fractionated in the following way. Fraction A was dissolved in 80 cc. of ether, and bromine in ether (5 g. in 20 cc.) was added dropwise under cooling at −10°. After keeping the solution at −10° for 20 hours, 1.4 g. of insoluble bromide (I) was filtered, washed twice with ether using 50 cc. each time, and then recrystallized four times from 20 cc. of chloroform-ethanol, by which there was obtained 0.12 g. of crystalline bromide (Ia). The chloroform-ethanol filtrate was added with ethanol, the precipitated bromide (0.2 g.) was filtered, and the filtrate was added with a further large quantity of ethanol, by which 0.8 g. of solid bromide (Ib) was precipitated. Fraction B yielded a very small amount of insoluble bromide by bromination in ether. The combined ether filtrate from fractions A and B was treated with sodium bisulfite solution for the removal of excess bromine, washed with water, dried over anhydrous sodium sulfate, and concentrated to a small volume by distilling ether. On adding ethanol to the concentrated ether solution, the bromide was fractionally precipitated, and there were obtained 7.4 g. of a fraction melting at 120—123° together with fractions of m. p. 175—180°, 110—114° and oily liquid.

Bromide Ia. — m. p. 202°, $[\alpha]_D^{18}$ −43.8°, Br 41.73% (calculated for $C_{30}H_{46}O_2Br_4$: Br, 42.04%). This bromide was debrominated with zinc and acetic acid. The debrominated product, after recrystallization from ethanol, had m. p. 151° and $[\alpha]_D^{18}$ −60.7°. It showed no depression of melting point when mixed with brassicasteryl acetate, m. p. 151—152°, prepared from rape oil in this laboratory. Saponification of the acetate gave

(8) l. c., (3); T. Matsumoto and Y. Toyama, *J. Chem. Soc. Japan*, **65**, 258, 310 (1914).

(9) C. A. Kind and S. C. Herman, *J. Org. Chem.*, **13**, 867 (1948).

free sterol which, after recrystallization from ethanol, had m. p. 145° and $[\alpha]^{18}_D$ −63.8°. Free sterol was added with benzoyl chloride in pyridine, kept for 24 hours at room temperature, and then water was added. The precipitated benzoate was washed with water and then recrystallized four times from acetone. It melted at 158°. A portion of the bromide Ia was partially debrominated by potassium iodide.[10] The product, dibromide, melted at 215—216° after recrystallizing several times from ethanol.

Bromide Ib.—m. p. 192° (with decomp.), $[\alpha]^{18}_D$ −42.5°, Br 41.46% (calculated for $C_{31}H_{50}O_2Br_4$: Br, 41.33%). This bromide was debrominated with zinc and acetic acid. The product, after recrystallization from ethanol, had m. p. 146—147°, $[\alpha]^{18}_D$ −52.1° and saponification value 124.7 (calculated for $C_{31}H_{50}O_2$ 123.4). Saponification of the acetate yielded free sterol which, after recrystallization from ethanol, had m. p. 154° and $[\alpha]^{18}_D$ −53.3°. Benzoylation of free sterol gave a benzoate of m. p. 140°, $[\alpha]^{18}_D$ −21.7° and saponification value 110.5 (calculated for $C_{36}H_{52}O_2$ 108.6). Dibromide obtained by partial debromination of the bromide Ib had m. p. 213—214° and Br 27.24% (calculated for $C_{31}H_{50}O_2Br_2$: Br, 26.05 %).

Sterol from Fraction III.—The ether soluble bromide of m. p. 120—123° was debrominated with potassium iodide in ethanol, whereby the debromination occurred nearly quantitatively yielding a product which had less than 0.1% of bromine. Accordingly, the bromide of m. p. 120—123° is considered to contain only a minute amount, if any, of compound having bromine in its side chain. On debromination of this bromide with zinc and acetic acid, there was obtained an acetate of m. p. 131° and $[\alpha]^{17}_D$ −38.2°. Recrystallizing twice from acetone, it had m. p. 137—138° and $[\alpha]^{17}_D$ −38.2°. The melting point was unaltered by further recrystallization. Saponification of this acetate and recrystallization of the product from acetone yielded a free sterol of m. p. 136—137° and $[\alpha]^{17}_D$ −39.3°. The benzoate prepared from this sterol had m. p. 133—135°, $[\alpha]^{17}_D$ −21.2° and saponification value 108.3 (calculated for $C_{36}H_{54}O_2$ 108.1). On solidifying the melted benzoate, it developed a blue coloration at 130—110° as is the case with clionasteryl benzoate[11].

Sterol from Fraction IV.—The acetate contained in the acetone mother liquors of recrystallizations of the acetate fraction III was saponified, the resulting free sterol was benzoylated, and the benzoate was recrystallized three times from acetone. The product had m. p. 145° and $[\alpha]^{17}_D$ −15.8°. Saponification of the benzoate yielded free sterol having m. p. 142° and $[\alpha]^{17}_D$ −37.6° after recrystallization from ethanol. The acetate prepared from this sterol had m. p. 114° after recrystallization from ethanol.

The Acetate of m. p. 173—174°.—The high melting acetate obtained by the final recrystallization recorded in Table 2 had $[\alpha]^{17}_D$ −62.5° and saponifacation value 123.9. The bromination product of this acetate was separated into two fractions, m. p. 172—174° (with decomp.) and m. p. 115—125°, by means of ethanol. The fraction of m. p. 172—174° (with decomp.) had Br 38.71%. Debromination of this fraction with zinc and acetic acid yielded a product which had m. p. 143° after three recrystallizations from ethanol. The fraction of m. p. 115—125° had Br 26.10%. Debromination of this fraction yielded a product which had m. p. 136° after two recrystallizations from ethanol.

Summary

(1) Steryl acetate obtained from clam fat was recrystallized from several different solvents, and it was found that the acetate recorded in the previous report as pure meretristeryl acetate, m. p. 149.5°, was not a pure single compound. Final recrystallization gave an acetate of m. p. 173—174°, though in a very small yield.

(2) Acetate mixture after removal of the fraction of m. p. 173—174° was fractionated by way of bromide, and it was found that brassicasterol, poriferasterol, clionasterol and cholesterol are present among the sterol components of clam fat.

(3) Bromination of the acetate of m. p. 173—174° and debromination of the bromination product yielded acetate having considerably lower melting points than the original acetate. Accordingly, there must have occurred isomerization or other changes in bromination and debromination cycle.

The expense of the present study has been defrayed from the Grant in Aid for Fundamental Scientific Research.

Department of Applied Chemistry,
Faculty of Engineering,
Nagoya University, Nagoya

(10) E. Fernholz and H. E. Stavely, *J. Am. Chem. Soc.*, **62**, 428 (1940).
(11) l. c., (7).

Rheology of Coal. III. A Structural Interpretation of Coal Oxidation from the Internal Viscosity Variations

By Katsuya INOUYE

(Received July 22, 1952)

Introduction

Many results have been reported on the phenomenon that the caking properties of coal are markedly changed by oxidation. R. V. Wheeler and others[1] have shown that even a degree of oxidation insufficient to affect the ultimate analysis reduces the caking properties profoundly. J. D. Davis and his co-workers[2] have reached the same conclusion by their own methods. In other cases, however, it is known that the caking properties can increase by mild oxidation.[3] These experimental facts, apparently contradictory, are readily understood, as H. L. Riley and his collaborators[4] have suggested, when it is accepted that the addition of oxygen to the coal molecules strengthens the intermolecular forces and results in restricting the mobility of the turbostratic system, so that excess of plasticity during carbonization, which may make the weak coke too porous, can be reduced; on the other hand, the appropriate plasticity of the caking coal at the caking temperatures is destroyed by further addition of oxygen atoms.

The author has shown from Young's modulus experiments[5] and the internal viscosity measurements[6] by vibrational methods that the caking properties of coal may be explained by these rheological factors and has proposed a theory on the structure and physical properties of coal. If the proposed theory on the difference between the structures of strongly-caking coal and weakly- or non-caking coal is valid, the corresponding variations in rheological properties should be observed experimentally by oxidation when the strongly-caking coal changes to a less-strongly caking coal. The mechanism of coal oxidation may also be discussed from the rheological standpoint. This report describes the internal viscosity variations during air-oxidation of several typical coals.

Description of Samples and Experimental Method

The coals used in this report are chosen from the same species examined in the preceding experiments, and Table 1 describes some common characteristics of the samples.

The experimental method for measuring the internal viscosity is described in the preceding paper.[6] All specimens were cut parallel to the bedding plane, in rectangular bars with accuracy of 1% in each dimension. The resonance curves between amplitude and frequency were obtained with fixed-free bar specimens at 30.0°C. and at the resonant frequency in the range of 1200~1400 c/sec. and hence the internal viscosity values were calculated according to the relations between vibrational decrement factor and viscosity,

Table 1

Description of Samples

Sample	Origin	Classification	Caking Property	Volatile Matter, Mean Value (dry, ash-free basis) in %
Takashima	Kyushu, Japan	Bituminous	Strongly-caking	38
American	U. S. A.	Bituminous	Strongly-caking	35
Toro	Saghalien, U. S. S. R.	Bituminous	Weakly-caking	46
Yubetsu	Hokkaido, Japan	Producer gas coal	Non-caking	64
Shosaku	China	Anthracite	Non-caking	7.7

(1) R. V. Wheeler and T. G. Woolhouse, *Fuel*, **11**, 44 (1932).
(2) L. D. Schmidt, J. L. Elder and J. D. Davis, *Ind. Eng. Chem.*, **32**, 548 (1940); R. E. Brewer, C. R. Holmes and J. D. Davis, *Ind. Eng. Chem.*, **32**, 930 (1940).
(3) L. D. Schmidt, J. L. Elder and J. D. Davis, *Ind. Eng. Chem.*, **28**, 1346, (1936); T. Iwasaki et al., Annual Meeting, *Chem. Soc. Japan*, 1950.
(4) H. E, Blayden, J. Gibson and H. L. Riley, *Proc. Conf. Ultra-fine Structure of Coals and Cokes, London*, **1944**, 176.
(5) K. Inouye, *J. Colloid Sci.*, **6**, 190 (1951).
(6) K. Inouye, This Bulletin, **26**, 84 (1953).

$$\eta = \frac{2\lambda n \rho l^4}{\kappa^2 m^4}, \quad (1)$$

and

$$\lambda = \frac{\pi \Delta n}{\sqrt{3}\, n}, \quad (2)$$

where, η = internal viscosity, λ = logarithmic decrement, n = resonant frequency, ρ = density of the specimen, l = length of the specimen, κ = radius of gyration of cross section, m = a factor corresponding to the mode of vibration, and Δn = the half value breadth of the resonance curve at the resonant frequency.

The measurement was carried out at first on the original (no oxidation) sample and then it was replaced into an air oven regulated at 120°C. for air-oxidation. The air was introduced from the bottom of the oven and went out of the top through a metal rack on which the specimens were set. After 30 hours' oxidation, the sample was taken out of the oven, cooled to the room temperature and fitted for vibrational measurements. The experiment was repeated after 30 more hours' oxidation (oxidized for 60 hours in total). The cement supporter had sometimes to be renewed after oxidation for the specimen separates from the supporter by heating. The change of dimensions of the specimens was considered sufficiently small, so that the dimensional factors (length and thickness) in Equations 1 and 2 were kept constant even after the oxidation. The change of weight of the specimen remained within 1%.

Changes of Caking Properties by Oxidation

The grains having diameter of approximately 0.5 cm. of each sample were prepared and oxidized in the same oven at 120°C. This diameter preferred was the mean thickness, i. e., the minimum dimension which may determine the oxidation velocity, of the specimen. Table 2 shows the changes of oxygen contents for four coals after 60 hours' oxidation. The moisture and ash contents listed are based on 76% humidity, the ultimate analysis on dry basis. The oxygen increases rather remarkably by the oxidation.

Table 3 shows the changes of the amount of extractable portion by pyridine on the existence of which the strong caking properties of the coals depend, and of the Lessing index. The pyridine extraction was carried out by the Soxlet method and the content was calculated in dry-ash-free bases, from the weight of α portion (steam distilled and dried). The Lessing caking index is a ratio of the height of carbonized sample after heating for 7 minutes at 900°C. in a silica retort to the height of 1 g. of the original coal of minus 100 Tyler mesh.

These changes seem to show that the oxidation method in this experiment can add oxygen to the coals and make the caking properties decrease. A recovery of the extraction data after 60 hours' oxidation may suggest, as explaind later, the decomposition in the coal samples.

Internal Viscosity Changes by Oxidation

As already reported in the preceding articles,[5][6] Young's modulus, E, and internal viscosity, η, of coal are respectively linear functions of ash volume concentration, ϕ,

$$\eta = \eta_0(1 + K'\phi) \quad (3)$$

Table 2

Changes of Oxygen Contents

Sample	Moisture	Ash	H	C	N	O and etc.	O and etc. (dry-ash-free)
Original Coals:							
Takashima	2.42	7.25	5.36	77.30	1.38	15.96	17.24
American	1.79	10.65	5.36	76.83	1.67	16.14	16.28
Yubetsu	4.98	11.83	5.36	67.94	1.17	25.53	29.16
Shosaku	4.50	9.29	2.31	82.27	0.91	14.51	16.07
After 60 Hours' Oxidation:							
Takashima	2.65	4.44	5.38	76.63	1.44	16.55	18.38
American	1.71	14.66	4.67	70.83	1.75	22.75	26.74
Yubetsu	3.64	17.29	5.15	63.83	1.17	29.85	36.11
Shosaku	3.79	11.05	2.33	81.18	1.08	15.41	17.41

Table 3

Changes of Properties

	Takashima			American		
	0 hour	30 hours	60 hours	0 hour	30 hours	60 hours
Extracted Portion, %, Dry-ash-free Bases	11.5	0.03	1.8	8.6	0.005	0.14
Lessing Index	3.14	1.18	1	4.99	3·84	—

and

$$E = E_0(1 + K\phi) \qquad (2)$$

where, E_0 and η_0 show the rheological values of "pure" coal molecules and K and K' represent the solvation factors of coal molecules with ash. Small E_0 and η_0 as well as large solvation factors distinguish the strongly-caking coals. The internal viscosity and ϕ relationship of the original coals is shown in Fig. 1, which also contains several data published in the preceding paper.[6] The detailed description of the curves especially minima and maxima which appeared for the caking coals will be given in the following article.* Figs. 2 and 3 show the internal viscosity values after 30 and 60 hours' oxidation. The values of η_0 and K' of the coals both before and after 30 hours' oxidation are given in Table 4.

The variations of the internal viscosity by oxidation are as follows: (1) the inclination of the linear relationship becomes flat, (2) the internal viscosity

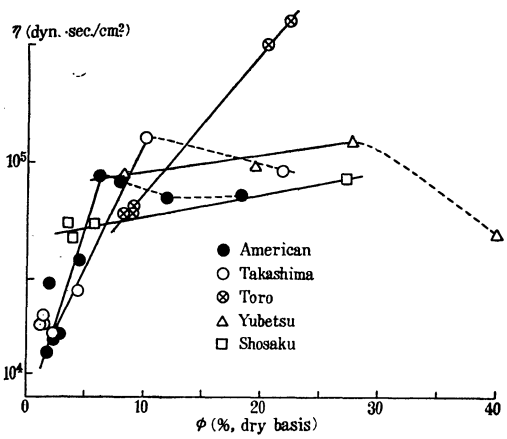

Fig. 1.—Internal Viscosity and Ash Content. Original Coals.

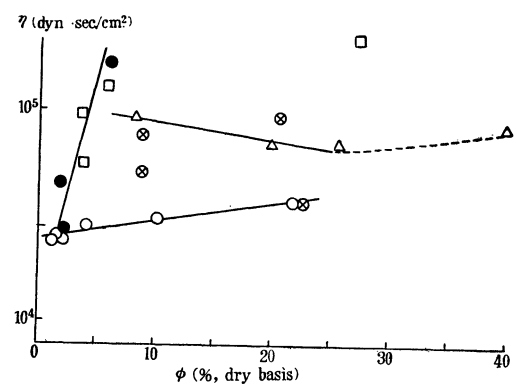

Fig. 2.—Internal Viscosity and Ash Content. Oxidized Coals for 30 hours.

* Rheology of Coal. VI. Unpublished work by K. Inouye and H. Tani.

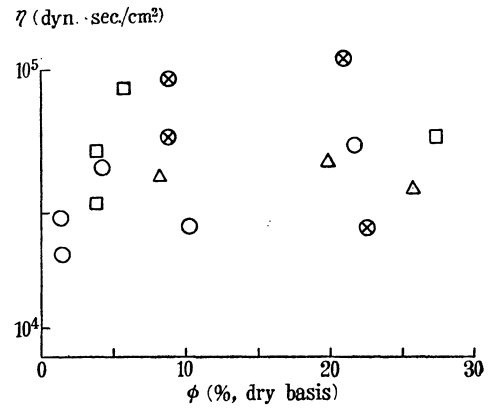

Fig. 3.—Internal Viscosity and Ash Content. Oxidized Coals for 60 hours.

Table 4

Changes of η_0 and K' by Oxidation

Sample	Duration of Oxidation: 0 hour		30 hours	
	η_0, c.g.s.	K'	η_0, c.g.s.	K'
American	1×10^{3}	16	2×10^{4}	0.95
Takashima	3×10^{3}	3.5	4.5×10^{4}	1.8×10^{-2}
Toro	2.3×10^{4}	2.7×10^{-1}	—	—
Yubetsu	8.4×10^{4}	1.0×10^{-2}	1.0×10^{5}	-6.1×10^{-3}
Shosaku	6.8×10^{4}	1.3×10^{-2}	—	—

value at $\phi = 0$ increases, and (3) further oxidation (see Fig. 3) appears to destroy the definite relationship between molecules and inorganic ash. The experimental facts suggest that the rheological conditions in strongly-caking coals change to those in weakly- or non-caking coals, i. e., the free molecules which act as a plasticizer when the coal is carbonized, obtain stronger intermolecular forces by adding the oxygen atoms, so that the micelle structure by solvation becomes indefinite.

It may be interesting to note that the changes of viscosity for Takashima coal, which showed rapid decrease of the Lessing index by oxidation, were more remarkable than in the case of American coal, although the values for the latter sample after oxidation are not many for the brittle nature of the specimens.

When the oxidized coal, originally strongly-caking, is carbonized in the coke oven, the coal cannot fuse and swell at the caking temperatures of the original coal, say at 400~500°C., because of the too strong intermolecular interactions of the matrix (bitumen) molecules of the micelle system.

Discussions

These facts may give the interpretation of the mechanism of coal oxidation, as suggested by H. L. Riley et al., that the addition of oxygen to the coal molecules causes an increase of forces between molecules and hence a decrease of the

caking properties. The experiments may also support the author's proposed theory on the mechanism of caking properties and coal structure.

Some possible causes of the experimental errors are considered.

(1) Dependence of η on the frequency. The η values are influenced by the frequency measured. The author, however, cannot state the dependence, although some results have been given in the preceding report.[7] The causes of experimental difficulty for adjusting the frequency were in the fact that the correction of the dimensions of the oxidized specimens by re-shaping was very difficult for weak mechanical property, and that there is doubt that the oxidized layers of the specimen may be removed by re-shaping. The measurements, therefore, had to be carried out at the frequency range of 1200~1400 c/sec., notwithstanding the fact that the resonance frequency of an oxidized specimen decreases in most cases.

(2) Homogeneity of oxidation. It is known that the oxidation does not proceed homogeneously when the blocks are oxidized, but the oxidized layer may be formed to prevent further oxidation. In this experiment this point is not considered and the oxidation was presumed to be homogeneous.

(3) Decomposition of coal. The decomposition of coal during oxidation was mentioned above, and the influence of decomposition upon the changes of weight, density and ash concentration of the specimen is considerable. These factors, however, were maintained constant in calculation as the weight decrease after even 60 hours' oxidation was within 1%. The most important influence of the decomposition is in the fact that the decomposition may make internal flaws by which occurence the internal viscosity values increase. The consideration of internal flaws on the rheological properties will be reported in future articles concerning the rheological studies of coke.

The autho.'s thanks are due to Hideo Tani for helpful assistance in the experiment. He is also indebted to Dr. M. Kurokawa and Mr. A. Baba (this Institute) for interest in the rheological study of coal.

Shigen-gijyutsu-shikenjo
(*Resources Research Institute*),
Saitama-Kawaguchi

(7) Reference 6 and the Report of the Fuel Research Institute, No. 66.

LETTER

On the Equilibrium between Radon and Radium and Radium B in Radioactive Mineral Waters

By Shunji UMEMOTO

(Received October 23, 1952)

From April, 1951 to March, 1952, the author measured continuously the variation of the contents of radium, radon, etc. in a spring called Hisui-no-Yu, at Misasa, Tottori, Japan; and it was found that when the amount of flow increased, the water temperature rose, the content of radon increased and the contents of radium and other common elements decreased. From these results, however, it was difficult to find any explanation for the formation and structure of this spring.(1)

Therefore, from February, 1952, the author measured continuously the radium radon, radium B and chloride content, the amount of flow and the water temperature of Hisui-no-Yu and three other springs at Misasa and the followingresults ware obtained:

(1) The radon content was higher than the valvue which would be expected from the equilibrium between radium and radon.(2)

(2) At times, the radium B content exceeded the value which would be expected from the equilibrium between radon and radium B. It is very interesting that, on some occasions, the equilibrium between such short-lived radioactive elements is not retained in mineral waters.

Further studies of this work will be made and more detailed results will be given later.

(1) S. Umemoto, *J. Chem. Soc. Japan*, **73**, 756 (1952) etc.

(2) This result was the same as that obtained already by the author and other investigators and the radium content varied with the chloride content as reported previously.

The author wishes to express his sincere thanks to Prof. K. Kimura of Tokyo Univ. for his kind guidance and encouragement.

Balneological Laboratory, Okayama University, Misasa, Tottori

Resolution of a Sterically Hindered Stilbene Derivative, 4-Amino-3′-bromo-α′-chloro-α, 2′, 4′, 6′-tetramethylstilbene

By Michinori Ōki

(Received January 30, 1953)

The author and Y. Urushibara[1] deduced the non-planar structures of α, α′-disubstituted stilbene derivatives from their ultraviolet absorption. If one of the rings is sterically hindered from rotating over the central substituted vinylene group and substituted unsymmetrically, then the stilbene derivative is expected to exist in optical enantiomorphs.

The author synthesized 4-amino-3′-bromo-α′-chloro-α, 2′, 4′, 6′-tetramethylstilbene, 4-$H_2NC_6H_4CMe=CClC_6HBrMe_3$-3′, 2′, 4′, 6′, and resolved it by means of *d*-camphorsulfonic acid. The benzoyl derivative of the resolved amine showed m. p. 159—160° and $[\alpha]_D^{20}$ +56.1°. The enantiomorph was not isolated. This is the first example of an optically active stilbene derivative containing no asymmetric carbon atom.

Experimental Part

4-Nitrobenzyl 3′-bromo-2′, 4′, 6′-trimethylphenyl ketone (I).—4-$O_2NC_6H_4CH_2COC_6HBrMe_3$-3′, 2′, 4′, 6′. Powdered anhydrous aluminum chloride (15 g.) was added gradually to a boiling solution of bromomesitylene[2] (20 g.) and *p*-nitrophenylacetyl chloride[3] (20 g.) in carbon bisulfide (150 cc.), and the mixture was heated for 30 minutes, and treated with ice and hydrochloric acid. After standing overnight the solid was recrystallized from alcohol with use of active charcoal. Nearly colorless needles melting at 121.5—123° (yield 15 g.). Found: N, 3.95. Calculated for $C_{17}H_{16}O_3NBr$: N, 3.87%.

α-(4-Nitrophenyl)ethyl 3′-bromo-2′, 4′, 6′-trimethylphenyl ketone (II).—4-$O_2NC_6H_4CHMeCOC_6HBrMe_3$-3′, 2′, 4′, 6′. I (10 g.) and a solution of metallic sodium (0.7 g.) in absolute alcohol (20 cc.) were heated to a homogeneous solution, then with addition of methyl iodide (4.3 g.) to neutral reaction, and poured into water (100 cc.). Alcohol was evaporated under diminished pressure and the remainder was shaken with ether. The ether solution was washed with aqueous sodium thiosulfate, dried, and evaporated. The residue solidified and was recrystallized from alcohol-acetone. Pale yellow leaflets melting at 125—126° (yield 8 g.). Found: N, 3.72. Calculated for $C_{18}H_{18}O_3NBr$: N, 3.72%.

4-Nitro-3′-bromo-α′-chloro-α, 2′, 4′, 6′-tetramethylstilbene (III).—4-$O_2NC_6H_4CMe=CClC_6HBrMe_3$-3′, 2′, 4′, 6′. II (12 g.) was dissolved in phosphorus oxychloride (60 cc.), phosphorus pentachloride (30 g.) was added, and the mixture was heated on a waterbath for 2 hours. The cooled reaction mixture was treated with ice water and the formed viscous substance was recrystallized from alcohol-acetone. (The mother liquor gave a hardly solidifiable mass, presumably the cis-isomeride.) One more recrystallization from acetone gave pale yellow prisms melting at 92—93° (yield 6 g.). Found: N, 3.59. Calculated for $C_{16}H_{17}O_2NClBr$: N, 3.55%.

4-Amino-3′-bromo-α′-chloro-α, 2′, 4′, 6′-tetramethylstilbene (IV).—4-$H_2NC_6H_4CMe=CClC_6HBrMe_3$-3′, 2′, 4′, 6′. III (7 g.) was heated with tin (10 g.) and alcohol (50 cc.) on a waterbath, concentrated hydrochloric acid (10 cc.) diluted with alcohol (10 cc.) was added gradually, and the mixture was heated until no violet coloration occurred on adding one drop to alcoholic potash. Alcohol was evaporated under reduced pressure, the residue was decomposed with 5% aqueous caustic soda, and the separated oil was collected. The amine, being uncrystallizable, was benzoylated for characterization. Colorless fine crystals melting at 159—160°. Found: N, 3.11. Calculated for $C_{23}H_{23}ONClBr$: N, 2.99%.

Dextro-rotatory Benzoyl Derivative from the Amine (IV).—A solution prepared by dissolving the free amine (IV) (3 g.) in an aqueous acetone solution of *d*-camphorsulfonic acid (5 g.) gave an oily deposit on cooling which solidified in a time. Recrystallization from water-acetone containing a small amount of *d*-camphorsulfonic acid to a constant melting point or rotation (three recrystallizations usually) gave colorless plates melting at 140°. Found: N, 2.42. Calculated for $C_{28}H_{35}O_4SNClBr$: N, 2.35%. $[\alpha]_D^{20}$+272.8° (0.0247 g. in 6 cc. alcoholic solution, α_D^{20}+1.14°).

The recrystallized *d*-camphorsulfonate was decomposed with 10% aqueous caustic soda. The uncrystallizable free amine was benzoylated with benzoyl chloride and pyridine, and the product was recrystallized from benzene-petroleum ether. Colorless fine crystals melting at 159—160°. Found: N, 2.96. Calculated for $C_{25}H_{23}ONClBr$: N, 2.99%. α_D^{20} of 0.0627 g. of the substance in

(1) This Bulletin, **25**, 109 (1952); Also see M. Oki, ibid., **25**, 112 (1952); **26**, 37 (1953).
(2) R. Adams and H. A. Stearns, "Organic Syntheses", Vol. XI, p. 24.
(3) E. Wedekind, *Ann.*, **378**, 289 (1911).

4 cc. alcoholic solution was found +0.88°. $[\alpha]_D^{20}$ +56.1°.

Department of Chemistry, Faculty of Science, Tokyo Metropolitan University, Meguro, Tokyo

2,4,2',4'-Tetrahydroxyazobenzene, Synthetic Estrogen of a New Type

By Yoshiyuki URUSHIBARA and Takeyoshi TAKAHASHI

(Received January 31, 1953)

The authors synthesized 2,4,2',4'-tetrahydroxyazobenzene (4,4'-azoresorcinol), 2,4-$(HO)_2C_6H_3N=NC_6H_3(OH)_2$-2',4', expecting that it might be estrogenic, because it might have a chrysene-shaped, rigid ring system by virtue of double chelation and thus its molecular shape might resemble those of potent natural and synthetic estrogens, except that it would be quite flat:

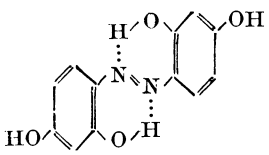

The diazo-oxide from 4-aminoresorcinol 1-benzoate, $C_6H_3(OCOC_6H_5)(OH)(NH_2)$-1,3,4, was coupled with resorcinol. 2,4,2',4'-Tetrahydroxyazobenzene 4-benzoate was obtained in yellow fine crystals melting at 235°. Saponification gave the desired tetrahydroxyazobenzene in orange-colored crystals. It did not melt at 300° but gradually turned black.

Estrogenic activity of the tetrahydroxyazobenzene was examined by the vagina smear test with ovariectomized mice, the substance in oil being injected subcutaneously in two portions. A weighed amount dissolved in acetone was mixed with camellia oil and acetone was evaporated up. The substance partly separated out in suspension. 20 γ produced full estrus in 100% animals, and 10 γ in 60%. By the same test method 1 mg. of 4,4'-dihydroxyazobenzene[1] showed full action in 80% animals, and 500 γ in 20%.

The presumed position of the coupling was *a priori* very probable, because W. Will and W. Pukall[2] obtained 2,4-dihydroxyazobenzene as the main product by coupling benzenediazonium chloride with resorcinol. H. Kauffmann and W. Kugel[3] obtained the same 2,4-dihydroxyazobenzene by coupling benzenediazonium chloride with resorcinol monobenzoate and saponifying the formed 2-benzoate. The present authors coupled the diazo-oxide from 4-aminoresorcinol 1-benzoate with resorcinol monobenzoate. The product should be 4,2'-dibenzoate of 2,4,2',4'-tetrahydroxyazobenzne by analogy. The substance obtained by saponification was the same in every respect as the tetrahydroxyazobenzene synthesized by using free resorcinol, but owing to the infusibilty of the substance it was impossible to identify both specimens by a mixed melting point.

The considerably strong action of the tetrahydroxyazobenzene provides a strong evidence for the structure consisting of the four hydroxy groups at 2,4,2',4'-positions and the formation of the chelate rings. Extra hydroxy groups introduced into natural or synthetic estrogens have hitherto always diminished activity to a great extent. The fact that the two more hydroxy groups at 2,2'-positions give the tetrahydroxyazobenzene an activity very much stronger than that of 4,4'-dihydroxyazobenzene proves that they form chelate rings with the azo nitrogen atoms and thus constitute a molecular structure, rigid and similar to those of strong natural and synthetic estrogens.

The 2,4,2',4'-tetrahydroxyazobenzene is an estrogen of a new type in that the molecular structure favorable for estrogenic activity is formed by chelation. But, as it is quite flat, such a potency as is comparable with that of diethylstilbestrol or hexestrol cannot be expected.[4]

Experimental Part

A 10% aqueous solution of sodium nitrite was added gradually to a solution of 4-aminoresorcinol 1-benzoate[5] (2 g.) in 5% hydrochloric acid (30 g.), with cooling at 0~2° and occasional test with potassium iodide-starch paper. The precipitated diazo-oxide was collected, and washed with water. Pale yellow crystals melting at 117~119° with decomposition (yield nearly theoretical). Found: N, 11.75. Calculated for C_{13}-

(1) R. Willstätter and M. Benz, *Ber.*, **39**, 3495 (1906).

(2) *Ber.*, **20**, 1121, 1145 (1887).

(3) *Ber.*, **44**, 2387 (1911).

(4) For molecular structure and estrogenic activity see: M. Oki and Y. Urushibara, This Bulletin, **25**, 109 (1952).

(5) D. H. R. Barton, W. H. Linnell and N. Senior, *J. Chem. Soc.*, **1945**, 436.

$H_8O_3N_2$: N, 11.66%.

The diazo-oxide (1.8 g.) was added gradually with stirring to a solution prepared from potassium carbonate (5 g.), resorcinol (2 g.), and water (100 cc.). After standing overnight the reaction mixture was acidified with dilute hydrochloric acid, and the precipitate was collected and recrystallized from methanol (yield 2 g.). 2, 4, 2', 4'-Tetrahydroxyazobenzene 4-benzoate thus obtained forms yellow crystals melting at 235°. Found: N, 7.95. Calculated for $C_{19}H_{14}O_5N_2$: N, 8.00%.

The above benzoate (1.5 g.) was dissolved in 15 % aqueous caustic potash, and the solution was heated for a few minutes on a waterbath, left to stand overnight, and acidified with hydrochloric acid. Repeated recrystallization of the precipitate from methanol with use of active charcoal gave 2, 4, 2', 4'-tetrahydroxyazobenzene in fine orange-colored crystals (yield 1 g.). It did not melt but turned black gradually at 265~300°. Found: N, 11.10. Calculated for $C_{12}H_{10}O_4N_2$: N, 11.38%.

Department of Chemistry, Faculty of Science, Tokyo University, Tokyo

Kinetics of the Isotopic Exchange Reaction between Carbon Monoxide and Carbon Dioxide*

By Teruo HAYAKAWA

(Received November 5, 1952)

Introduction

The kinetics of the exchange reaction between carbon monoxide and carbon dioxide have been investigated by Brandner and Urey,[1] using natural C^{13} isotope as a tracer, and by Norris and Ruben,[2] using radioactive C^{14} isotope as a tracer. The particular mechanism proposed by Brandner and Urey was based on the assumption of the presence of the activated forms of water and hydrogen (or activated hydrogen atom and hydroxyl radical) on the surface with the condition that the total amount of these molecules is constant.

The catalytic water gas reaction on the surface of a heated platinum wire in the region of 1,000°C.[3] is a famous one, and it is also generally known that water vapor and hydrogen are strongly adsorbed on quartz at these high temperatures. Nevertheless, unfortunately, the present author cannot accept their particular mechanism mentioned above for the following reasons:

(1) it seems somewhat doubtful that a considerable amount of water vapor, by which this exchange reaction was pronouncedly accelerated, was inevitably introduced and remained in the vessel,

(2) they have shown no direct evidence for the presence of the condition that the total amount of these activated molecules on the surface is constant.

On the other hand, Norris and Ruben proposed the mechanism of a bimolecular reaction between the two reactant species adsorbed on quartz. But, so far as their experimental results were concerned, it was not confirmed that the reaction is heterogeneous and catalytic.

Therefore, it seemed necessary for the present author to confirm the heterogeneity and the rate law of this exchange reaction.

Experimental

The natural C^{13} isotope, used in these experiments, was made by Prof. T. Titani[4] of Osaka University from the thermal diffusion of methane, and was fixed as silver carbonate. Carbon dioxide enriched in C^{13} was prepared from the thermal decomposition of silver carbonate and purified by several fractionations. Carbon monoxide was prepared from the decomposition of purified formic acid by heated phosphoric acid and purified by the usual method. During these purifications, water vapor was carefully prevented from entering into either of the sample gases. Argon was taken from cylinders, and was purified of oxygen and nitrogen by passage over hot copper turnings and then by calcium-arc discharges.

The reason for employing the C^{13} isotope (but not the O^{18} isotope) in these kinetic measurements has already been pointed out by Brandner and Urey.

A 55 cc. cylindrical quartz vessel (inner dia. 14 mm., length 35 cm.) was used in all runs. In testing for heterogeneity, the reaction vessel was packed with short sections of quartz tubing, whereby the surface-to-volume ratio was increased twofold approximately. The reaction vessel was connected to a glass high vacuum system through a water-cooled capillary graded seal, and closed by a capillary stopcock. Since the volume of the system was minimized by using 1.4 mm. capillary tubing throughout, the dead space between the reaction vessel and the stopcock was very small (about 0.8 cc.) compared with the volume of the reaction vessel, no correction for this was made for the results given in Table 1 and Table 2.

In these experiments the gases were premixed and introduced simultaneously into the hot quartz vessel, previously evacuated to $\approx 10^{-5}$ mm.Hg. and maintained in this vacuum during the period of 8-10 hrs. After the desired time the gases were pumped out and analysed by a mass spectrometer.

The mass spectrometer used in these experiments was of the 90° sector type, and the radius of curvature of the ion path was 13.0 cm. The details of this mass spectrometer were previously reported.[5] Though it seemed convenient to use

---

* This investigation was partly reported in the Annual Meeting of Chem. Soc. Japan (April, 1951).

(1) J. D. Brandner and H. C. Urey, *J. Chem. Phys.*, **13**, 351 (1945).

(2) T. H. Norris and S. Ruben, *J. Chem. Phys.*, **18**, 1595 (1950).

(3) C. N. Hinshelwood and C. R. Prichard, *J. Chem. Soc.*, **127**, 806 (1925).

(4) T. Titani and S. Horibe, *J. Chem. Soc. Japan*, **73**, 75 (1952).

(5) T. Hayakawa and T. Kambara, *J. Chem. Ind. Japan*, **54**, 310 (1951).

the same method with Urey and Brandner's, i. e., the direct connection of the reaction vessel to the ionization chamber of the mass spectrometer, the present author unfortunately could not use this method since the present instrument was designed for common use.

The reproducibility of this instrument for isotopic concentrations was ±0.01 (in atomic percentages); therefore, the good reproducibility was obtained in these usual runs. But, since the initial concentrations of $C^{13}O_2$ in these experiments were considerably low, the reproducibility in these several runs at the temperature of 710°C. was considerably poor. Herein, in these special runs, the average value of several measurements was adopted.

Result

The experimental results are summarized in Table 1 and Table 2, where the run numbers indicate the chronological order of the experiments.

Assuming that

(a) there is no isotope effect of C^{13}, and

(b) at equilibrium, the specific concentration of carbon dioxide (the percentage ratio, $C^{13}O_2$ to total CO_2) is equal to that of carbon monoxide,

the following first-order rate law expression[6]~[9] is easily obtained for the present exchange reaction,

$$C^{13}O_2 + C^{12}O \rightleftharpoons C^{13}O + C^{12}O_2$$

$$R = \frac{2.303\, p\mathrm{CO} \cdot p\mathrm{CO}_2}{(p\mathrm{CO}+p\mathrm{CO}_2)t} \log \frac{x_0 - x_\infty}{x - x_\infty} \qquad (1)$$

where R denotes the exchange rate, and x_0, x, x_∞, each denotes the specific concentration of carbon dioxide (the percentage ratio, $C^{13}O_2$ to total CO_2) at the time of initial, given, and equilibrium respectively.

The exchange rate, R, may also be expressed in the following form*

$$R = C \cdot f(p\mathrm{CO}_2) \cdot \varphi(p\mathrm{CO}) \qquad (2)$$

where C is a constant.

Fig. 1 gives a plot of rate *versus* carbon dioxide pressure at 900°C., at constant carbon monoxide pressure. Fig. 1 shows that the function $f(p\mathrm{CO}_2)$ is simply proportional to carbon dioxide pressure.

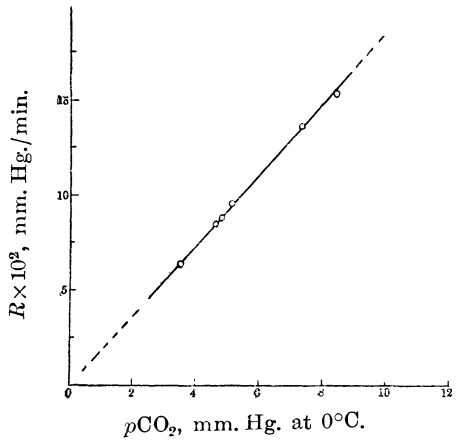

Fig. 1.—Dependence of exchange rate on carbon dioxide pressure at 900°C. $p\mathrm{CO} \approx 8.5$ mm. Hg. at 0°C.

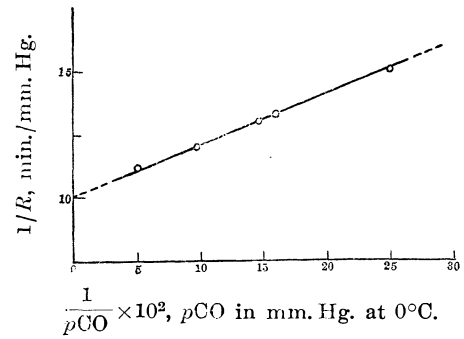

Fig. 2.—Dependence of exchange rate on carbon monoxide pressure at 900°C. $p\mathrm{CO}_2 \approx 3.9$ mm. Hg. at 0°C. $b = 0.51$.

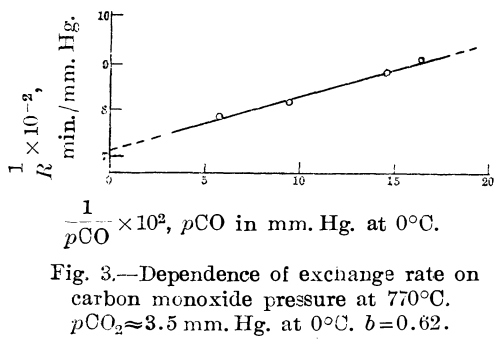

Fig. 3.—Dependence of exchange rate on carbon monoxide pressure at 770°C. $p\mathrm{CO}_2 \approx 3.5$ mm. Hg. at 0°C. $b = 0.62$.

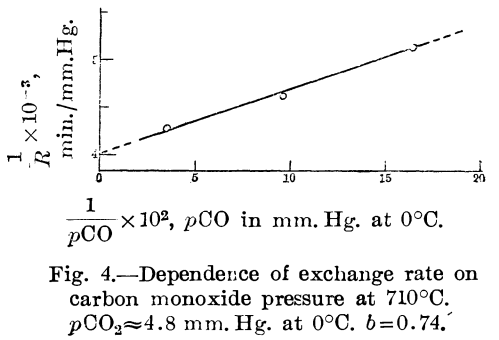

Fig. 4.—Dependence of exchange rate on carbon monoxide pressure at 710°C. $p\mathrm{CO}_2 \approx 4.8$ mm. Hg. at 0°C. $b = 0.74$.

(6) H. A. C. McKay, *Nature*, **142**, 997 (1938).
(7) R. B. Duffield and M. Calvin, *J. Am. Chem. Soc.*, **68**, 557 (1946).
(8) J. W. Weigl and M. Calvin, *J. Chem. Phys.*, **17**, 210 (1949).
(9) K. S. Pitzer, *J. Chem. Phys.*, **17**, 1341 (1949).
* See, for example: H. A. C. McKay, *Nature*, **142**, 997 (1938).

On the other hand, a log-log plot of rate *versus* carbon monoxide pressure at 900°C., carbon dioxide pressure remaining constant, gives with a poorer approximation to a straight line, a slope of 0.2. So, the present author has adopted the following expression,

$$\varphi(p\mathrm{CO}) = C' \frac{p\mathrm{CO}}{1+b\cdot p\mathrm{CO}} \qquad (3)$$

where C' is a constant, and b is a constant depending on the temperatures.

Fig. 2, Fig. 3, and Fig. 4 indicate that this expression (3) is quite satisfactory for the present results. Then, the following rate law is obtained.

$$R = k \frac{p\mathrm{CO}\cdot p\mathrm{CO}_2}{1+b\cdot p\mathrm{CO}} \qquad (4)$$

Table 1

Exchange between CO_2 and CO (no additives).

Run	Time (min.)	Pressures (mm.Hg. at 0°C.) CO	CO_2	Sp. concentrations CO_2 x_0	x	(x_∞) calcd.	CO y_0	y	k, $(k'\times 10^2)$
				Experiments at 710°±2°C.					
32	365	29.4	5.9	3.14	3.11	1.43	1.09	1.10	3.09×10^{-5}
34	420	23.5	4.7	3.14	3.10	1.43	1.09	1.11	3.63
35	510	10.3	6.0	3.12	3.08	1.82	1.08	1.09	3.01
37	720	8.4	4.9	3.12	3.07	1.82	1.08	1.10	2.64
38	810	6.1	5.9	3.13	3.08	2.10	1.09	1.16	2.96
				Experiments at 770°±2°C.					
41	54	17.6	3.5	3.14	3.10	1.43	1.09	1.10	2.10×10^{-4}
43	60	6.2	3.5	3.12	3.08	1.82	1.08	1.12	2.44
44	60	12.2	7.0	3.12	3.07	1.82	1.08	1.12	2.32
45	180	9.4	5.4	3.12	2.99	1.82	1.08	1.20	2.70
46	120	6.2	3.5	3.12	3.04	1.82	1.08	1.14	2.64
49	30	8.9	4.3	3.15	3.13	1.78	1.09	1.10	2.38
50	180	6.9	3.4	3.15	3.03	1.78	1.09	1.21	2.55
				Experiments at 900°±2°C.					
7	120	19.6	3.9	3.14	1.49	1.43	1.09	1.42	1.29×10^{-2} (2.79)
9	270	9.4	4.0	3.14	1.68	1.68	1.09	1.69	—
10	30	10.1	4.0	3.14	2.29	1.68	1.09	1.43	1.28 (2.91)
11	60	8.6	3.5	3.14	1.99	1.68	1.09	1.61	1.16 (3.05)
12	75	7.5	3.0	3.14	1.83	1.68	1.09	1.62	1.40 (3.04)
16	30	11.2	6.4	3.12	2.34	1.82	1.08	1.55	1.17 (3.06)
17	60	6.7	3.9	3.12	2.02	1.82	1.08	1.70	1.30 (3.12)
18	60	8.7	5.1	3.12	2.04	1.82	1.08	1.71	1.17 (2.96)
19	120	8.5	4.9	3.12	1.86	1.82	1.08	1.79	1.16 (2.90)
20	180	9.0	5.1	3.12	1.82	1.82	1.08	1.81	—
21	90	8.4	4.8	3.12	1.90	1.82	1.08	1.77	1.25 (3.15)
23	30	8.7	8.4	3.13	2.46	2.10	1.09	1.67	1.14 (3.50)
24	60	5.7	5.5	3.13	2.28	2.10	1.09	1.93	1.02 (2.88)
26	150	7.2	7.0	3.13	2.10	2.10	1.09	2.11	—
27	90	4.0	3.9	3.13	2.15	2.10	1.09	2.06	1.31 (3.36)
29	60	8.7	7.4	3.13	2.16	2.03	1.09	1.93	1.06 (3.56)
30	180	6.1	5.2	3.13	2.03	2.03	1.09	2.03	—
				Experiments at 900°±2°C. (Packed)					
54-P	15	6.7	4.5	3.15	2.48	1.90	1.08	1.53	2.03×10^{-2}
55-P	30	6.3	4.2	3.15	2.22	1.90	1.08	1.68	1.82
56-P	60	8.9	6.1	3.15	1.94	1.90	1.08	1.87	2.12
57-P	45	8.7	5.9	3.15	2.03	1.90	1.08	1.82	1.87
59-P	120	9.7	6.5	3.15	1.90	1.90	1.08	1.91	—

Accordingly, the equation (1) becomes

$$\frac{2.303\,p\mathrm{CO}\cdot p\mathrm{CO_2}}{(p\mathrm{CO}+p\mathrm{CO_2})\,t}\log\frac{x_0-x_\infty}{x-x_\infty}=k\frac{p\mathrm{CO}\cdot p\mathrm{CO_2}}{1+b\cdot p\mathrm{CO}} \qquad (5)$$

This equation (5) has been used to calculate the values of k given in Table 1 and Table 2. It is seen that the agreement among all the runs is fairly good.

The average k values (unpacked, non-additives) have been plotted in Fig. 5 as the logarithm of k *versus* $1/T$. The fact that the points give a reasonable approximation to a straight line suggests that there is but one exchange mechanism in this temperature range. The slope of this plot indicates an apparent activation energy of 73 kcal./mol., and this value is in good agreement with the value of 77 kcal./mol. obtained by Norris and Ruben.

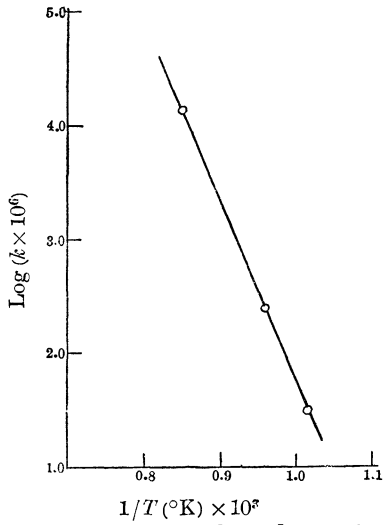

Fig. 5.—Temperature dependence of rate constant.

In order to test for heterogeneity, the reaction vessel was packed with short sections of quartz tubing, thus increasing the surface-to-volume ratio twofold approximately. From the results shown also in Table 1, it is clear that the rate of this exchange reaction is considerably increased by packing, though this increase in the rate is not correctly proportional to the surface-to-volume ratio. And this effect of packing is, as a tendency, similar to the results obtained by Brandner and Urey, but it is inconsistent with the results of Norris and Ruben.

The present results on the effect of water and argon are indicated in Table 2. As seen in Table 2, the addition of argon has no influence (rather slight retardation) on this reaction within the experimental error. On the other hand, the addition of water apparently indicates a pronounced acceleration. But as discussed below, this apparent acceleration caused by adding water is not real.

Discussion

From the facts that the reaction is considerably retarded by carbon monoxide and is

Table 2

The Influence of Argon and Water (at 900°C.)

(1) Argon addition (10 vol. %)

Run	Time (min.)	Pressures (mm.Hg. at 0°C.)			Sp. concentrations					$k\times10^2$
					CO_2			CO		
		CO	CO_2	Ar	x_0	x	(x_∞) cal.	y_0	y	
51	15	11.1	2.0	1.3	3.14	2.62	1.41	1.09	1.18	1.04
52	30	8.2	1.5	1.0	3.14	2.39	1.41	1.09	1.24	1.02
53	60	16.8	3.0	2.0	3.14	1.97	1.41	1.09	1.31	0.90

(2) Water addition ($x_0=3.14$, $y_0=1.09$.

Run	Time (min.)	Initial pressures (mm.Hg. at 0°C.)				x	Composition $(CO_2)/(CO)+(CO_2)$		$\frac{(C^{13}O_2)}{(C^{13}O_2)_0}$
		CO	CO_2	H_2O			initial (t_0),	final (t),	
62	15	8.6	3.5	1.8		1.99	0.29	0.33	0.72
63	30	10.1	4.0	2.1	(≈15%)	1.71	0.28	0.36	0.70
(10)	(30)	(10.1)	(4.0)	(0)		(2.29)			(0.74)
65	45	7.5	3.1	1.5		1.67	0.29	0.36	0.66
(12)	(75)	(7.5)	(3.0)	(0)		(1.83)			(0.58)
67	15	8.4	3.6	1.0	(≈8%)	2.21	0.30	0.34	0.80
68	30	9.8	4.3	1.2		1.98	0.30	0.35	0.73
70	15	8.6	3.5	2.4	(≈20%)	1.68	0.29	0.37	0.68
72	45	7.6	3.2	2.2		1.59	0.30	0.38	0.63

markedly accelerated by packing, it seems reasonable to consider that this exchange reaction is heterogeneous and catalytic, as it was partly suggested by Urey and Brandner. In the experiments of Norris and Ruben on this question of heterogeneity, the surface-to-volume ratio was increased sixfold by packing, but the k values obtained by them indicated almost no effect. Though they considered that their data might indicate a reaction partly homogeneous, it seems rather reasonable for the present author to consider their data indicating much lower catalytic activity of their quartz. This is partly based on the fact that their k values at 900°C. are very small compared with that of the present author's, and is also partly based on the reasons discussed later.

As generally discussed by Morita,[10] the relations expressed in equation (1) and (2) are, in themselves, well explained whenever the rate-determining process of the catalytic exchange reaction is the direct exchange between the two reactant species or the adsorption (or the desorption) of any one of the reactants. But, from the fact that the present results are well satisfied by the rate law expression (4), it seems reasonable for the present author to believe that this exchange reaction is obeyed in any one of the following mechanisms.

Mechanism (1)—

$$C^{13}O_2 \text{ (gas phase)} + C^{12}O \text{ (adsorbed)} \rightleftarrows C^{13}O \text{ (adsorbed)} + C^{12}O_2 \text{ (gas phase)}$$

$$R = k \cdot p\mathrm{CO}_2 \cdot \varphi(\mathrm{CO})$$

where $\varphi(\mathrm{CO})$ denotes the adsorbed amount of carbon monoxide.

According to this mechanism (1), the reaction is a bimolecular exchange between the strongly adsorbed carbon monoxide molecule and the carbon dioxide molecule in the gas phase. The function $\varphi(\mathrm{CO})$ may be determined from the adsorption state of carbon monoxide, and in the present experiments it must satisfy the form $c' \cdot p\mathrm{CO}/1 + b \cdot p\mathrm{CO}$.

Therefore, in order to test for this problem, it was necessary to determine the adsorption states of the two reactant species at the temperatures of these experiments, using the same quartz vessel.

The present observations using a constant volume method[11] have been plotted in Fig. 6. Each line in Fig. 6 corresponds to each separated adsorption isotherm at 900°C. Fig. 6 shows that the adsorption of carbon monoxide on this quartz surface is considerably large, especially in comparison with that of carbon dioxide, and the adsorbed amount of each reactant is simply proportional to its pressure approximately.

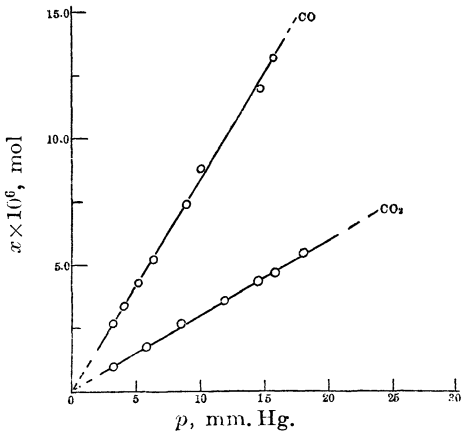

Fig. 6.—Adsorption isotherm on quartz at 900°C.

Then, according to mechanism (1), the present adsorption experiments must result in the rate law

$$R = k \cdot p\mathrm{CO} \cdot p\mathrm{CO}_2$$

However, unfortunately, thus obtained rate law is inconsistent with the results of this exchange reaction expressed in equation (4).

But, since the present observations in testing for the adsorption of carbon monoxide were obtained for the total surface of the reaction vessel and in this condition the adsorption of carbon monoxide was stronger than that of carbon dioxide at this high temperature, it seems also probable that the adsorption of carbon monoxide on the active surfaces for this reaction may be rather strong and may obey the usual Langmuir's isotherm.

$$\varphi(\mathrm{CO}) = C' \cdot p\mathrm{CO}/1 + b \cdot p\mathrm{CO}$$

Therefore, the present results of this exchange reaction are well explained by mechanism (1).

On the other hand, since it is probable to think of the present exchange reaction as an oxidation of carbon monoxide by carbon dioxide, many studies[12]~[15] of the carbon

(10) N. Morita, This Bulletin, **15**, 166 (1940); *J. Chem. Soc. Japan*, **44**, 62 (1941).

(11) See, for example: A. F. Benton and T. A. White, *J. Am. Chem. Soc.*, **52**, 2325 (1930).; W. J. C. Orr, *Proc. Roy. Soc.*, **A173**, 349 (1939).

(12) M. Bodenstein and F. Ohlmer, *Zeit. Phys. Chem.*, **53**, 165 (1905).

(13) A. F. Benton and T. L. Williams, *J. Phys. Chem.*, **30**, 1487 (1923).

(14) F. Handman, H. W. Thompson and C. N. Hinshelwood, *Proc. Roy. Soc.*, **A137**, 87 (1932).

(15) Y. Kondo and O. Toyama, *Rev. Phys. Chem, Japan*, **13**, 166 (1939).

monoxide-oxygen reaction in quartz must show certain similarities to the present one.

These studies have shown that this dry and non-explosive oxidation at the temperatures lower than 800°C. is heterogeneous and that strongly adsorbed carbon monoxide and rather weakly adsorbed oxygen interact each other.

Although the results of these studies mentioned above are inconsistent with mechanism (1), we must consider the difference between oxygen and carbon dioxide in the adsorptive properties.

Mechanism (2)—

$$C^{12}O\ (\text{adsorbed}) + C^{13}O_2\ (\text{adsorbed}) \rightleftarrows C^{12}O_2\ (\text{adsorbed}) + C^{13}O\ (\text{adsorbed})$$

$$R = C \cdot f(pCO_2) \cdot \varphi(pCO)$$

According to the present observations, the adsorptions of carbon monoxide and carbon dioxide were both rather weak and the adsorbed amount of each reactant in each separated adsorption isotherm at 900°C. was simply proportional to its pressure. However, since these results were obtained for the total surface of the quartz vessel, when each reactant is adsorbed on each different surface (without mutual displacement) and the adsorption of carbon monoxide on the active surfaces for this reaction is moderate the rate of this exchange reaction follows[16]

$$R = k \cdot \frac{pCO}{1 + b \cdot pCO} \cdot pCO_2$$

This rate law coincides well with expression (4).

Moreover, since the catalytic activities of various kinds of quartz vary considerably when the adsorptions of carbon monoxide and carbon dioxide on the different active surfaces are both moderate, the rate of this exchange reaction seems to follow[17]

$$R = k \cdot \frac{pCO}{1 + b \cdot pCO} \cdot \frac{pCO_2}{1 + b' \cdot pCO_2} \approx k \cdot pCO^m \cdot pCO_2^n$$

The rate law thus obtained is in good agreement with the results of Norris and Ruben ($m \approx 0.7$, $n \approx 0.85$).

On the other hand, one may derive the similar rate law when two reactant species are both moderately adsorbed on the same surface and $1 \gg (b \cdot pCO)^2$, $(b' \cdot pCO_2)^2$,

$$R = k \cdot \frac{pCO \cdot pCO_2}{(1 + b \cdot pCO + b' \cdot pCO_2)^2} \approx k \cdot pCO^m \cdot pCO_2^n$$

However, unfortunately, the present results of this exchange reaction are unexplained by the adsorptions of two reactant species on the same surface. And from the fact that the value of the apparent activation energy of this exchange reaction obtained by the present author is in good agreement with that of Norris and Ruben, it seems probable that the reaction, both in the present author's and in that of Norris and Ruben, obeys a similar mechanism.

From these reasons mentioned above, though the present results are well explained by both mechanisms (1) and (2), the latter seems more probable to the present author.

In both mechanism (1) and (2), it is also necessary to ascertain the influence of the side reaction on the quartz surface.

$$2CO \rightleftarrows CO_2 + C$$

This reaction on a nickel catalyst was investigated in detail by Rhi.[18]

The present results in testing for this reaction, using the same quartz vessel, are shown in Table 3. Table 3 shows that this reaction

Table 3

The Decomposition of Carbon Monoxide (at 900°C.).

Initial Pressure pCO (mm.Hg. at 0°C.)	Time t (min.)	CO_2, formed (vol. %)
10.9	60	0.7
10.7	180	1.0
21.2	60	1.2
21.2	120	1.5
30.6	30	1.1
30.6	63	1.9
30.9	120	2.4

slightly occurs at the temperatures of these experiments. However, as it was also suggested by Brandner and Urey, since the pressure of the gas mixture and the percentage of carbon monoxide was not sufficiently high in any present exchange experiment to cause deposition of massive carbon on the walls of the quartz vessel, the influence of this side reaction on the present exchange reaction appears to be very small.

The mechanism suggested by Brandner and Urey is an excited water gas reaction on the walls of the quartz vessel.

(16) See, for example: G. M. Schwab, *Zeit. Elektrochem.*, **35**, 573 (1929).
($2CO + O_2 = 2CO_2$, on SiO_2).

(17) See, for example: C. R. Prichard and C. N. Hinshelwood, *J. Chem. Soc.*, **127**, 1546 (1925).

(18) T. Rhi, *Rev. Phys. Chem. Japan*, **8**, 89 (1934); **10**, 200 (1936).

$$H_2 = H_2^*$$
$$C^{13}O_2 + H_2^* \rightleftarrows C^{13}O + H_2O^*$$
$$H_2O^* \rightarrow H_2O$$
$$(H_2^*) + (H_2O^*) = \text{constant}$$

They considered that their mechanism might be supported, though it was not entirely free of difficulties, by the fact that the exchange rate was markedly accelerated by adding hydrogen or water vapor.

As has been mentioned, the study of the catalytic water gas reaction on the surface of a heated platinum wire is a famous one.

And it seems also probable that hydrogen and water vapor are strongly adsorbed on quartz at the temperatures of these experiments and, then, they cause a marked acceleration of this exchange reaction.

Indeed, as seen in Table 2, since the values of x (percentage ratio, $C^{13}O_2$ to total CO_2) are markedly decreased in these experiments, the addition of water apparently causes a pronounced acceleration of this exchange reaction. However, it must be noticed that in each run of adding water the final concentration of carbon dioxide is also considerably increased and, then, this acceleration is only apparent and not true. The true acceleration caused by adding water must be much smaller than this, and may be measured by $(C^{13}O_2)/(C^{13}O_2)_0$ in Table 2, where $(C^{13}O_2)_0$ and $(C^{13}O_2)$ each denotes the concentration of $C^{13}O_2$ at the initial and given time respectively. Accordingly, the present results shown in Table 2 indicate that the true acceleration is somewhat increased with the water contents. This would seem inconsistent with Brandner and Urey's important assumption in their mechanism, because their mechanism is based on the assumption that the surface is completely covered by these molecules of H_2^* and H_2O^* and that the total amount of these molecules is constant. And it seems also very difficult for the present author to suppose that in each exchange experiment of no additives the considerable amount of water vapor remained in the reaction vessel. Moreover, unfortunately, Brandner and Urey's mechanism fails to explain the fact of the exchange rate in the present experiments obeying expression (4).

The present author calculated the rate constant, k', on the basis of Brandner and Urey's rate law and mechanism. Although each value of k' (at 900°C.) given in Table 1 apparently indicates rather good agreement, this may be attributed to the fact that the value of $1 + b \cdot pCO/pCO + pCO_2$ in the present experiments at 900°C. is not very different from the others.

From these reasons it seems inevitable for the present author to consider that the mechanism suggested by Brandner and Urey (a excited water-gas reaction) is, in itself, a different reaction from the present exchange reaction, though it contains many interesting suggestions.

Conclusions

It has been concluded that this exchange reaction is heterogeneous and catalytic.

The rate of this reaction has the form of a product of adsorption isotherms. The probable mechanism—and then the probable rate determining process—of this exchange reaction seems to be a bimolecular exchange (oxidation) reaction between the two reactant species adsorbed on quartz. Although a similar mechanism was already suggested by Norris and Ruben, they had failed to confirm the heterogeneity of this reaction.

The present results are somewhat different from those of Norris and Ruben. In the present experiments, it seems probable to consider that each reactant is adsorbed on each different surface and the adsorption of carbon monoxide on the active surfaces for this exchange reaction is moderate, but carbon dioxide is rather weakly adsorbed.

The results obtained by Norris and Ruben suggest to us that the adsorption of the two reactant species in their experiments are both moderate and not very different.

It is supposed that the observed difference between the results of Norris and Ruben and that of the present author may be attributed to the difference in the catalytic activity of quartz.

The present exchange reaction is somewhat accelerated by adding water. Probably it may depend on the occurrence of the water gas reaction,

$$CO_2 + H_2 \rightleftarrows CO + H_2O$$

Although Brandner and Urey proposed this mechanism (an excited water gas reaction) for the present exchange reaction, their mechanism does not satisfy the present results of this exchange reaction.

Therefore, so far as the present experiments are concerned, the present author considers that the reaction mechanism is fundamentally different in the presence and in the absence of water vapor or hydrogen.

The author wishes to express his grateful

thanks to Professor T. Titani of Osaka University who kindly offered his precious sample of C^{13} isotope and also many helpful suggestions on this problem, and to Professor O. Toyama of Naniwa University for his kind discussions.

The author is also greatly indebted to Dr. T. Kambara of the Central Laboratory of Hitachi Factory for using his mass spectrometer.

Department of Chemistry, Faculty of Education, Naniwa University, Sakai, Osaka

Dichroisms of Benzene Rings. IV. The Dichroisms of Diphenyldiacetylene and Naphthazarine

By Kazuo NAKAMOTO

(Received September 27, 1952)

Introduction

In the former papers of this series,[1] remarkable dichroism of the benzene ring has been found in common aromatic crystals and molecular compounds. From the viewpoint of quantum mechanics, however, the triple bond is expected to show more remarkable dichroism than the double bond because the former has two π-electrons in each carbon atom. So it is of interest to measure the dichroism of the triple bond and to compare it with that of the benzene ring.

In the present study, the dichroism of diphenyldiacetylene whose crystal structure had been perfectly determined by X-ray analysis has been measured quantitatively in the ultraviolet region. The result seems noteworthy, indicating remarkable dichroism of the triple bond independent of the dichroism of the benzene ring.

Of particular interest in the field of molecular structure is the problem of determining whether naphthazarine, 5,8-dihydroxy-1,4-naphthoquinone, exists as a molecular compound similar to quinhydrone or as the monomer in crystalline state. The result of the dichroism measurement has led us to the conclusion that a formation of molecular compound is not probable so far as the assumed orientation of molecules is correct.

Experimental

Materials.—(1) Diphenyldiacetylene—Colourless acicular crystals were obtained by recrystallization from an alcoholic solution. M. p. 87°. Monoclinic system. Straight extinction. Dichroism can not be observed with the naked eye. (2) Naphthazarine—The Friedel-Crafts synthesis between hydroquinone and maleic anhydride[2] was employed for the preparation of this substance. Recrystallization from a ligroin solution produced violet needle crystals similar to quinhydrone. Since naphthazarine slowly decomposes on heating in the air, its melting point was identified as the diacetate (m. p. 192°). Monoclinic system. Straight extinction. Thin crystals show slight dichroism; rose, when viewed with linearly polarized light whose electric vector vibrates parallel to the c-axis (needle axis), and rose red, with the light vibrating parallel to the b-axis.

Measurements.—Dichroisms of the crystals were measured quantitatively by the microscopic method with microcrystals as described before[1]. Spectra of the alcoholic solutions were measured by photographic method using the rotatory sector. In each graph, the ordinates, α and ε denote absorption coefficient per mm. of the crystal, and molar extinction coefficient of the solution, respectively.

Results and Discussion

(1) **Diphenyldiacetylene.**—In 1940, Wiebenga[3] studied the crystal structure of diphenyldiacetylene and succeeded in its Fourier analysis. According to his result, planar molecules of diphenyldiacetylene are piled up along the c-axis, making their molecular planes almost parallel to the a-axis and inclined by an angle of 25° referred to the b-axis.

(1) K. Nakamoto, *J. Am. Chem. Soc.*, **74**, 390, 392 and 1739 (1952).

(2) K. Zahn and P. Ochwat, *Ann.*, **462**, 81 (1928).

(3) E. H. Wiebenga, *Z. Krist.*, **102**, 193 (1940).

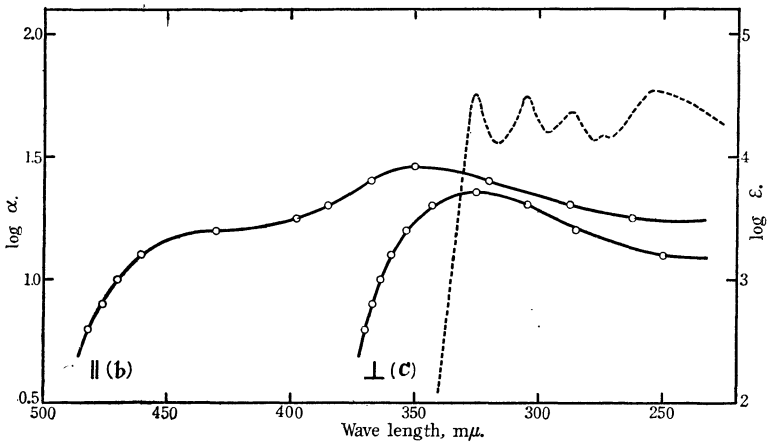

Fig. 1.—Absorption spectra of diphenyldiacetylene.

Absorption spectra by linearly polarized light with the electric vectors vibrating parallel to the *b*- and *c*-axes, respectively, are recorded in Fig. 1. Numerical data characterizing these spectra are given in Table 1.

Table 1

	1st band (acetylene band)		2nd band (benzene band)	
	λmax.	log αmax.	λmax.	log αmax.
b-abs.	430	1.20	350	1.45
c-abs.			325	1.30

The absorption spectrum of diphenyldiacetylene in an alcoholic solution is also given in Fig. 1 (dotted line). As is clearly shown in the spectra of diphenylpolyin series,[4] the four distinct bands at 326, 305.3, 287.4 and 275.5 mμ are the absorptions due to the acetylene group in the molecule. The next broad band appeared at 255 mμ is attributed to the absorption resulting from the π-electrons of the benzene rings.

As is seen above, the acetylene band is bathochromic in respect to the benzene band. This relation may hold also for the spectra in crystalline state. In the *b*-absorption of crystalline state, therefore, the first band at 430 mμ and the second band at 350 mμ are concluded to be due to the acetylene group and the benzene ring, respectively. In the *c*-absorption, however, only one maximum which may be ascribed to the benzene band appears at 325 mμ, because the acetylene band is too weak in this polarized light. Nevertheless, we can expect that the *b*-absorption of the acetylene band is bathochromic and hyperchromic to the *c*-absorption from experimental analogy between the dichroism of the benzene ring and that of the acetylene group.

Comparing the result of X-ray analysis with the above spectroscopic discussion, we may conclude that the absorption parallel to the acetylene bond and the benzene rings is bathochromic and hyperchromic to the absorption perpendicular to them. Thus the acetylene group shows the same dichroic property as the benzene ring, except the former indicates more remarkable dichroism than the latter.

(2) **Naphthazarine.**—It has been a subject of much discussion both experimental and theoretical to decide whether naphthazarine exists as a molecular compound similar to quinhydrone or as the monomer in crystalline state. In an attempt to solve this problem, measurements of the dichroism of naphthazarine crystals have been made in the visible and ultraviolet region. As to the X-ray study on this crystal, Palacios and Salvia[5] have measured only the dimension of its unit cell and no further detailed study has been undertaken.

According to their result, the unit cell of naphthazarine crystal[6] is as follows:

$$a=3.85,\ b=8.02,\ c=14.5\ \text{Å}.\ \beta=97°6'$$

Considering that a is nearly equal to ordinary

(4) M. Nakagawa et al., *J. Chem. Soc. Japan*, **72**, 561 (1950); 73, 141 (1951).
For another example, see W. D. Celmer and I. A. Solomons, *J. Am. Chem. Soc.*, **74**, 3843 (1952).

(5) J. Palacios and R. Salvia, *Anales. soc. espan. fis. quim.*, **32**, 49 (1934).

(6) Naphthazarine has at least two modifications. The one was recently used by Rogers for the measurement of magnetic anisotropy (*J. Am. Chem. Soc.*, **69**, 1506 (1947)). The other was studied by Palacios and Salvia as stated above, and used here for the dichroism measurement.

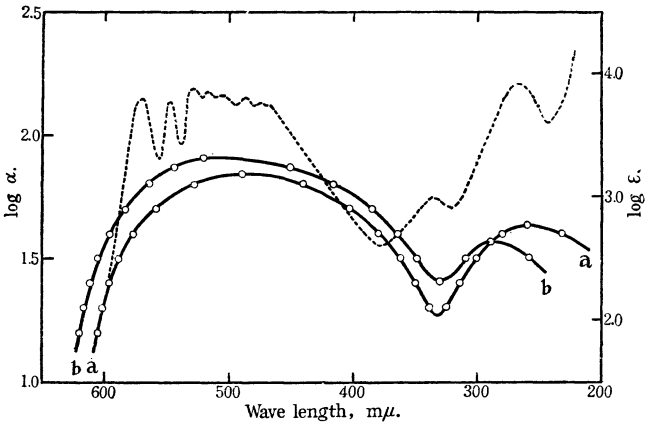

Fig. 2.—Absorption spectra of naphthazarine.

distance which separates aromatic layers, it seems probable that the molecules are piled up along the a-axis. Thus, the absorption spectra by linearly polarized lights with the electric vector vibrating parallel to the a- and the b-axes have been measured. Their curves and numerical data are given in Fig. 2 and Table 2, respectively.

Table 2

	$\lambda_{max.}$	$\log \alpha_{max.}$	$\lambda_{max.}$	$\log \alpha_{max.}$
a-abs.	490	1.84	250	1.64
b-abs.	510	1.92	290	1.57

The absorption spectrum of naphthazarine in an alcoholic solution is also shown in Fig. 2 (dotted line). It has a broad intense band with vibrational structure between 570~470 mμ, which may be ascribed to the absorption principally due to the π-electron system in the molecule. The first bands at 510 and 490 mμ in crystalline state coincide with the above π-band in liquid state. Therefore we conclude that the π-band is bathochromic and hyperchromic in the b-absorption rather than in the a-absorption.

Conforming the probable orientation of molecules with the above result, we can reach the conclusion that the absorption parallel to the molecular plane is bathochromic and hyperchromic to the absorption perpendicular to it. In other words, the general rule about the dichroism of molecular compounds does not hold here and naphthazarine indicates similar dichroic property to common aromatic crystals. This conclusion suggests to us that a possibility of forming a molecular compound like quinhydrone is not probable in the present case.

If there exists any overlap of the π-orbitals that are thrust out perpendicularly from each molecular plane, the feature of the spectra would be expected to produce a marked change.[1]

Summary

Absorption spectra of diphenyldiacetylene and naphthazarine in crystalline state as well as in solution have been measured quantitatively in the visible and ultraviolet region. In the former compound, it has been found that the acetylene group indicates similar dichroic property to the benzene ring except for the fact that the dichroism of the former is more remarkable than that of the latter. From the dichroic property of naphthazarine, it has been concluded that the substance exists as the monomer and does not form the molecular compound like quinhydrone even in crystalline state.

The author wishes to express his sincere thanks to Prof. R. Tsuchida for his kind guidance and encouragement throughout this work. Appreciation is also expressed to Dr. Nakagawa for the gift of diphenyldiacetylene used in this work.

Department of Chemistry, Faculty of Science, Osaka University, Osaka

Estimation of the Amount of Hydration of Alcohols

By Tunetaka SASAKI and Tatuya YASUNAGA

(Received December 11, 1952)

Introduction

The present authors have already calculated the volume of water of hydration (abbreviated to call hydration volume) of inorganic ions, assuming that both solute and hydration water are incompressible, and they have confirmed that such an assumption was permissible, for the values thus obtained ran parallel with the heat of hydration and electrostriction.(1) A similar calculation cannot however be applied in the case of hydration of alcohols in aqueous solution because the incompressibility of solute and hydration water, especially the latter, cannot be assumed. This comes chiefly from the difference between a strong interaction of ion~water dipole in the case of the aqueous electrolyte solution and a weak interaction of dipole~dipole or of hydrogen bond frequently pointed out to form in the case of aqueous solution of nonelectrolyte.(2) This problem can however be attacked from a somewhat different direction if we take up the sound velocity in aqueous solution instead of the compressibility.

Principle of Calculation

Recently, Rao(3) has pointed out that the function,

$$v^{1/3}M/D=V \qquad (1)$$

where v is the velocity of sound, M the molecular weight, and D the density, is a constant, characteristic of a pure liquid, and is additive and constitutive in that it may be computed by summing increments assigned to atoms and bonds. Lagemann and Corry(4) however proposed an alternative procedure for computing this constant, that is, there is an additivity only of what they choose to call "*bond velocities*" shown in the following table.

Table 1

Bond	Bond Increment	Bond	Bond Increment
C—H	95.2	C—Cl	230
C—C	4.25	C=C	129
C—O	34.5	C=O	186
O—H	99.0		

Now, we assume that this additivity rule also applies in the case of an ideal solution, just as the similar rule applies in the case of molecular polarization. Thus for an ideal solution

$$V_1N_1+V_2N_2=v^{1/3}\frac{M_1N_1+M_2N_2}{D} \qquad (2)$$

is assumed to hold, where N represents the molal fraction. In the case of an aqueous alcohol solution however, the above relation does not hold, because the solution is not a mere mixture of alcohol and water molecules. We may rather assume a ternary mixture composed of alcohol, bound or hydration water and free or solvent water for such a solution. Then we get the following equation instead of the equation (2),

$$V_1(N_1-x)+V_2N_2+V_1'x=v^{1/3}\frac{M_1N_1+M_2N_2}{D} \qquad (3)$$

where x and V_1' are the molal fraction and molecular sound velocity of hydration water respectively. From the equation (3), we obtain the amount of hydration per mole solute,

$$\frac{x}{N_2}M_1=\left[v^{1/3}\frac{M_1N_1+M_2N_2}{D}-(V_1N_1+V_2N_2)\right]\times M_1/V_1'V_1)N_2 \qquad (4)$$

Experimental Results and Discussions

First of all we checked the validity of the above mentioned additivity rule of bond velocity for water which differs widely in nature from other organic liquids checked by Lagemann and Corry.(4) We could confirm that

(1) T. Yasunaga and T. Sasaki, *J. Chem. Soc. Japan*, **72**, 316 (1951).
(2) H. S. Frank and M. W. Evans, *J. Chem. Phys.*, **13**, 507 (1945), A. L. Robinson, *J. Chem. Phys.*, **14**, 588 (1946).
(3) M. R. Rao, *J. Chem. Phys.*, **9**, 682 (1941).
(4) R. T. Lagemann, and J. E. Corry, *J. Chem. Phys.*, **10**, 739 (1942).

Table 2

Fraction by volume of heptane in mixture at 20°C.	Sound Velocity m./sec.	Density d_4^{20}	$V_1N_1+V_2N_2$	$v^{1/3}(M_1N_1+M_2N_2)/D$	% error
0.000	1039.4	0.6278	1163.2	(1163.2)	0.00
0.223	1058.4	0.6416	1245.6	1244.3	0.10
0.409	1082.3	0.6519	1314.3	1311.9	0.18
0.607	1107.1	0.6622	1387.5	1392.1	0.33
0.806	1130.1	0.6737	1461.0	1463.1	0.14
1.000	1152.4	0.6849	1532.7	(1532.7)	0.00

the equation (1) gave a numerical value of 201 for V of water while we obtained the value of 198 as twice the value of OH bond velocity. Thus we can safely apply the additivity rule for at least the pure liquids concerned.

Further we made an experimental confirmation of the equation (2). Fortunately we found data available for this purpose which has been offered by Jacobson[5] for the case of the mixture of heptane and pentane. In this case also, as is shown in Table 2, an excellent agreement can be seen between $V_1N_1+V_2N_2$ and $v^{1/3}(M_1N_1+M_2N_2)/D$.

We then proceeded to study the validity of the equation (3) or (4), for the case of aqueous alcohol solutions.

Here we employed the fixed frequency type acoustic interferometer reported in a previous paper[6] to measure the sound velocity in a liquid mixture. The sound velocity measured was shown as a linear function of concentration in Fig. 1. From this figure, we can obtain the value for v of the equation (4), for a given concentration. To estimate the value V_1' in the equation (4), we assumed that hydration of alcohol is chiefly due to the hydrogen bridge between alcohol and water molecules, and approximated the hydration water to be ice. The value V_1' can then be calculated from the equation (1) using the values for ice. Thus we obtained $V_1'=259.7$.

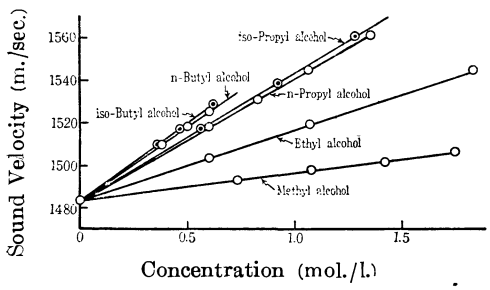

Fig. 1.—Sound velocity of aqueous alcohol solution at 20°C.

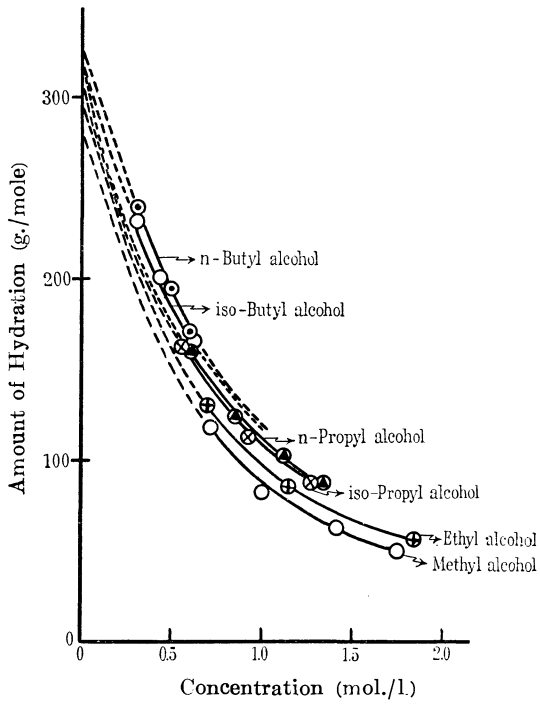

Fig. 2.—Amount of hydration per mole of alcohol at 20°C.

Using these values we calculated the amount of hydration as a function of concentration, from the equation (4). The results were shown in Fig. 2. In this figure we note a set of parallel curves for alcohol homologues. We fan also see that the amount of hydration increases with the number of carbon atoms in a molecule at constant concentration, and decreases with the concentration for one and the same alcohol which is in accord with the general behavior of the hydration. Further we compared the above value of amount of hydration (at 1 mol/liter concentration) with the known value of heat of hydration which was calculated for alcohols by Butler.[7] A

(5) B. Jacobson, *Arkiv Kemi.*, **2**, 177 (1950).
(6) T. Yasunaga, *J. Chem. Soc. Japan*, **72**, 87 (1951).
(7) J. A. V. Butler, "Structure and Molecular Forces in (a) Pure Liquids and (b) Solution", *Faraday Society*, 229 (1936).

fairly good proportionality between these quantities is noticed in Fig. 3. The fact again leads us to the conclusion that the amount of hydration hereby obtained is the quantity closely related to the actual amount of water of hydration.

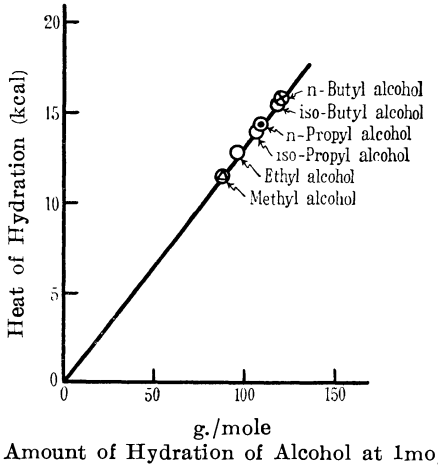

Fig. 3.—Relation between heat of hydration and amount of hydration at 1 mol/l.

Summary

The amount of hydration for alcohols in aqueous solution was estimated, assuming that the molecular sound velocity of a solution can be calculated from that for each constituent of the solution and their molal fraction, thereby regarding the water of hydration as the third component different from the free solvent and rather resembling ice as far as the sound velocity is concerned. The quantities thus calculated showed the general behavior of hydration water and also proved to be proportional to the heat of hydration.

A part of the cost of this study has been defrayed from the Scientific Research Expenditure of the Ministry of Education given to one of the authors.

Department of Chemistry, Faculty of Science, Kyushu University, Fukuoka.

On the Relation between Viscosity and Critical Micelle Concentration of Detergent Solutions*

By Naoyasu SATA and Kiyoshi TYÛZYÔ

(Received August 2, 1952)

Introduction

The viscosity of detergent solutions has been investigated for a long time, but almost all investigations before 1935 were carried out in the region of concentrated solutions owing to the insufficient knowledge about the structure of micelles in this period.(1) Thereafter, there was also no research which dealt with the relation between viscosity and micelle-structure. In 1939, Hess, Philippoff and Kiessig found a method of determining critical micelle concentration (CMC) of soap solutions from their viscosity and measured viscosities of several soap solutions for a wide range of concentration.(2) Although this is a remarkable investigation, it did not yet try to discuss the size and shape of micelle from viscosity data, because the systematic investigation of micelle-structure began gradually at that period. However, after 1940, new interesting phenomena (e. g., solubilization,(3) spectral dye(4)) were found and several new physical methods (e. g., long spacing X-ray diffraction,(5) light scattering(6)) were applied to the micelle-investigation, so that knowledges concerning micelle increased suddenly. We can remember the

* Part of this paper was presented at the 5th Annual Meeting of the Chemical Society of Japan, April, 1952 in Tokyo.

(1) E. L. Lederer, "Kolloidchemie der Seifen" 1932, S. 141.

(2) K. Hess, W. Philippoff and H. Kiessig, *Kolloid-Z.*, **88**, 40 (1939).

(3) J. W. McBain and R. C. Merrill, *Ind. Eng. Chem.*, **34**, 915 (1942).

(4) M. L. Corrin and W. D. Harkins, *J. Am. Chem. Soc.*, **69**, 679 (1947).

(5) W. D. Harkins, R. W. Mattoon and M. L. Corrin, ibid., **68**, 220 (1946).

(6) P. Debye, *J. Colloid Sci.*, **3**, 407 (1948).

discovery of 1st and 2nd CMC, theories of spherical, cylindrical and lamellar micelle, etc.

Therefore it seems necessary to review the existing many viscosity data again, under the light of the new structural theory of micelles.

We want to remark first the superiority of the viscosity-method in comparison with other methods of CMC-determination; secondly describe our new simple method of determining 1st and 2nd CMC from viscosity and finally discuss the relation between molecular weight of micelle and characteristic constants concerning viscosity which we have newly discovered.

Comparison of Variable Methods of Determining CMC

Variable methods have been proposed hitherto for CMC-determination, and it is convenient to classify them as follows. (Table 1) In the 2nd and 3rd column are expressed the possibilities of various methods to determine 1st and 2nd CMC respectively in which positive and negative use is expressed with ⊕ and ⊖. In the 4th column are tabulated the possibilities of giving the information concerning the shape of micelle. The 5th column shows the accuracy of the methods in which many ⊕ signs express higher accuracy. The 6th column shows the degree of the experimental difficulty of the method and also number of ⊕ signs corresponds to its degree. Moreover, methods are classified in (I) and (II) groups before the 1st column. To (I) belong the methods which cause the change of the state of micelle at the measurement and also the change of CMC. (Generally, CMC falls by adding other substances.) (II) contains methods which cause no changes relatively.

Investigating Table 1, it is clear that light scattering is the best, and spectral dye method is the simplest. 2nd CMC can be determined only by diffusion and X-ray method. Moreover, there are a few methods which give some information about the shape of micelle. From all view points, we could conclude that light scattering method is the best among many methods. But this method requires an especially precise experiment under troublesome conditions and is not easy to perform. After all, there is no method which gives 1st and 2nd CMC, shape of micelle and moreover is easy to perform. The new viscosity method which we propose, gives 1st and 2nd CMC and has the possibility of giving the information concerning size of micelle, if very high accuracy is not demanded. That is why we insist upon this new viscosity method as a practical and useful one. (Viscosity method in Table 1 is not ours but that of Hess and others.)

The Method of Determining 1st CMC from Viscosity

Hess, Philippoff and Kiessig were the first who found the method of determining CMC from

Table 1

Methods of Determining CMC

	Method	1st CMC	2nd CMC	Size & Shape of Micelle	Accuracy of Method	Difficulty of Method	Literature
(I)	Solubilization	+	−	−	++	++	(7)
	Spectral Dye	+	−	−	++	+	(4)
	Diffusion	+	+	+	+	+++	(8), (9), (10)
(II)	Osmotic Coefficient	+	−	−	+	++	(11)
	Conductivity	+	−	−	+	++	(12)
	Density	+	−	−	+	+	(9), (13)
	Viscosity	+	−	−	+	+	(2)
	Surface Tension	+	−	−	+	+	(14)
	Light Scattering	+	−	+	+++	+++	(15), (16)
	X-rays	−	+	+	+	+++	(2), (17)
	Membrane Potential	+	−	−	+	++	(18)
	Flow Birefringence	−	−	+	+	+++	(19)

(7) R. S. Stearns, H. Oppenheimer, E. Simon and W. D. Harkins, *J. Chem. Phys.*, **15**, 496 (1947).

(8) G. S. Hartley and D. F. Runnicles, *Proc. Roy. Soc.*, **A168**, 420 (1938).

(9) R. J. Vetter, *J. Phys. Colloid Chem.*, **51**, 262 (1947).

(10) H. Okuyama, S. Saito and K. Tyuzyo, presented at the 4th Year Meeting of the Chemical Society of Japan in Tokyo, 1952.

(11) J. W. McBain and A. P. Brady, *J. Am. Chem. Soc.*, **65**, 2072 (1943).

(12) J. W. McBain, Frontiers in Colloid Chemistry, p. 113 (1950).

(13) K. A. Wright and H. V. Tartar, *J. Am. Chem. Soc.*, **61**, 544 (1939).

(14) A. E. Alexander, *Trans. Faraday Soc.*, **38**, 248 (1942).

(15) P. Debye, *J. Phys. Colloid Chem.*, **53**, 1 (1949).

(16) P. Debye, Ann. N. Y. Acad. Sci., **51**, 575 (1949).

(17) R. W. Mattoon, R. S. Stearns and W. D. Harkins, *J. Chem. Phys.*, **16**, 644 (1948).

(18) C. W. Carr, W. F. Johnston and I. M. Kolthoff, *J. Phys. Colloid Chem.*, **51**, 636 (1947).

(19) H. A. Scheraga and J. K. Backus, *J. Am. Chem. Soc.*, **73**, 5103 (1951).

η_r (relative viscosity) or $1/[\eta]$ ($[\eta]$ is the solpe of η_r vs. C-curve.) We have already discovered that η_{sp}/C_m vs. concentration curve of Potassium-caprate becomes minimum at 1st CMC[10]. (η_{sp}: specific viscosity $=\eta_r-1$, C_m: soap conc. in mol./l.) Further examining the existing data, we found, almost without exceptions, the curve with one maximum and minimum as Fig. 1. Namely, η_{sp}/C_m becomes minimum at some value of C_m, i. e. C_{m1}, and C_{m1} value is somewhat lower than C'_{m1} which is obtained from the knick of η_r, in many cases. Moreover, η_{sp}/C_m becomes maximum in lower part of C_{m1} in many cases. As the examples, we show the data of Dodecylamine-hydrochloride at 20° and 30°C. in Fig. 2[20] and

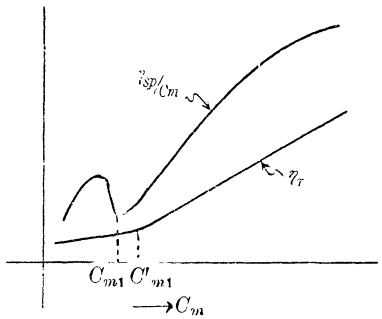

Fig. 1

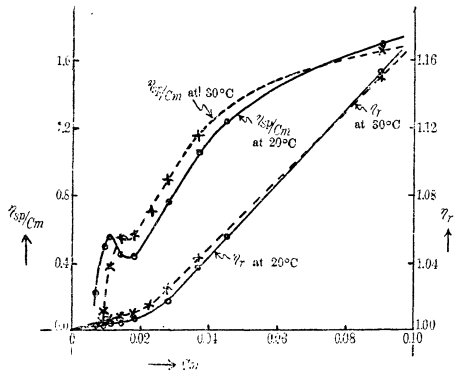

Fig. 2.—Dodecylamine-hydrochloride at 20 and 30°C. (K. Tyûzyô)

Table 2

1st CMC determined by the new Viscosity-Method

Substance	Temp. (°C)	1st CMC(A)	CMC from η_r	C_{m1}	Author	Literature
Na-caprylate	20	—	(0.36)	0.07(E)	Lamm, Högberg (1940)	(21)
Na-nonylate	20	0.22	0.22	0.24	Hess, Philippoff Kiessig (1939)	(2)
Na-caprate	20	0.10	0.12(B)	0.10(B)	Lamm, Högberg (1940)	(21)
K-caprate	20	0.10	0.08(C)	0.07(C)	Okuyama, Tyuzyo Saito (1951)	(10)
Na-laurate	20	0.025	0.096	0.031	Hess, Philippoff Kiessig (1939)	(2)
Dodecylamine-HCl	20	0.0132	0.023	0.015	Tyuzyo (1951)	(20)
	30	0.0132	0.020	0.016	Tyuzyo (1951)	(20)
Na-dodecyl-sulfate	40	0.010	0.012	0.012	Wright, Tartar (1939)	(13)
	70	0.012	0.017	0.014	Wright, Tartar (1939)	(13)
Na-oleate	20	0.001	0.23(D)	—(D)	Hess, Philippoff Kiessig (1939)	(2)
Hexanolamine-caprylate	20	—	0.35	0.26	Gonick (1946)	(22)
Aerosol-MA	25	—	0.029	0.027	Vetter (1947)	(9)

(A) 1st CMC in the 3rd column is the average value derived from the several different methods.

(B) Sodium-caprate has two minimum and the larger one coinsides with 1st CMC.

(C) In Potassium-caprate, CMC from η_r is closer to 0.10 than C_m, but in this case, 0.044 n KOH is added as the swamping electrolyte for diffusion and so CMC must somewhat fall. Therefore, the method of η_{sp}/C_m is not inferior than the one of η_r even in this case.

(D) 1st CMC of Sodium-oleate cannot be determined from viscosity method becaues its value (0.001) is too small. The value (0.23) of Hess and others is very large. Perhaps they mistook 2nd CMC for 1st CMC. (Also see Section 4.)

(E) C_{m1} of Sodium-carylate is too small contrary to expectation.

(F) Sodium-dodecylsulfate has no minimum at 50 and 60°C. It has only a knick at 70°C.

(G) Both Sodium-capronate and Sodium-valeriate have no minimum. It seems probable that there exist no micelles in the studied range of concentration.

(20) K. Tyuzyo, Unpublished.
(21) O. Lamm and H. Högberg, *Kolloid-Z.*, **91**, 10 (1940).
(22) E. Gonick, *J. Am. Chem. Soc.*, **68**, 177 (1946).

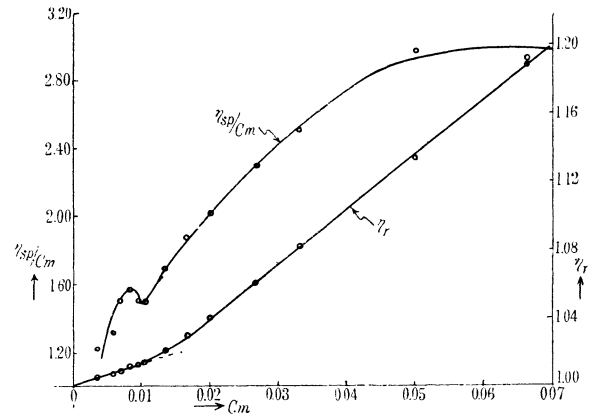

Fig. 3.—Na-dodecylsulfate at 20°C.
(Hess, Philippoff, Kiessig)

Sodium-dodecylsulfate at 20°C. in Fig. 3.[2] All the numerical data are summarized in Table 2. From Tab. 2, we see that the coincidence of C_{m1} and 1st CMC from other methods is satisfactory. Moreover, because C_{m1} corresponds to the distinct "minimum" of η_{sp}/C_m vs. C_m curve, it could be determined more accurately than the rather vague "knick" of η_r.

The Method of Determining 2nd CMC from Viscosity

2nd CMC is defined with the concentration where I-band in X-ray diffraction begins to appear,[17] but almost no other physico-chemical properties are investigated in such a region of high concentration. Only a few abnormalities were found in diffusion measurement.[9][10]

Now, we can presume that above 1st CMC, concentration of detergent monomer in solution which is in equilibrium with micelle is almost constant and unchanged.[16] Accordingly, we make the following operations.

$$C^\circ_m = C_m - C_{m1} \tag{1}$$

$$\eta^\circ_{sp}/C^\circ_m = (\eta^\circ_r - 1)/(C_m - C_{m1}) = (\eta_r/\eta_{r\min})^{-1}/(C_m - C_{m1}) \tag{2}$$

where,

C°_m: detergent concentration defined with equation (1)
C_m: detergent concentration in mol./l.
C_{m1}: 1st CMC derived from above viscosity method
$\eta_{r\min}$: relative viscosity of solution against water at 1st CMC

If we plot $\eta^\circ_{sp}/C^\circ_m$ against C°_m, we obtain the curve as Fig. 4 almost without exceptions.[23] As the examples, we have shown in Fig. 5 and Fig. 6

(23) There are only few data on the viscosity measurement over the wide range of concentration, and so in some cases we connect two independent data.

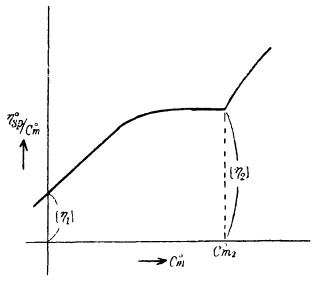

Fig. 4.

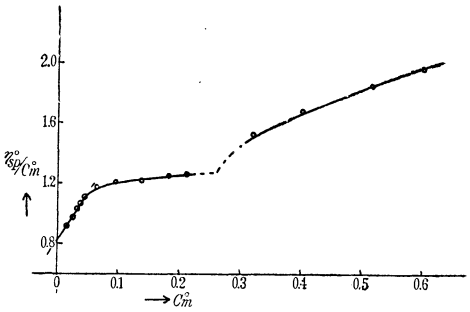

Fig.5.—Na-nonylate at 20°C.
(Hess, Philippoff, Kiessig)

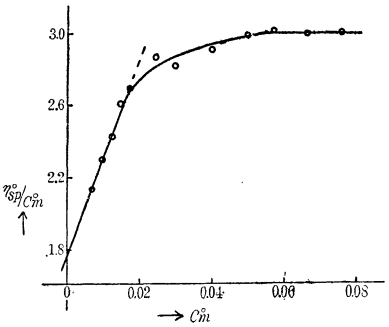

Fig. 6.—Na-dodecylsulfate at 20°C.
(Hess, Philippoff, Kiessig)

the results of sodium-nonylate and sodium-dodecylsulfate.[2] From the figures, we see that $\eta^\circ_{sp}/C^\circ_m$ increases linearly with C°_m as long as C°_m is small and thereafter passing a knick, converges to the constant value, i. e. $[\eta_2]$ in Fig. 4. Then the second and more sharp knick appears when C°_m reaches to some value, i. e. C°_{m2} from where $\eta^\circ_{sp}/C^\circ_m$ increases suddenly again. After all, $[\eta_1]$ and $[\eta_2]$ are defined with the following equations.

$$[\eta_1] = \lim_{C^\circ_m \to 0} (\eta^\circ_{sp}/C^\circ_m) \tag{3}$$

$$[\eta_2] = \lim_{C^\circ_m \to C^\circ_{m2}} (\eta^\circ_{sp}/C^\circ_m) \tag{4}$$

The meaning of $[\eta_1]$ and $[\eta_2]$ will be explained in the next section. Moreover, we have C_{m2} from the next equation.

Table 3

2nd CMC determined by the new Viscosity-Method

Substance	Temp. (°C.)	C_{m2}(*) in wt. %	2nd CMC in wt. %	Method of determining 2nd CMC	Author	Literature
Na-nonylate	20	9~10	—	—	—	—
K-caprate	—	—	22.9	X-rays	Mattoon, Stearns, Harkins (1948)	(17)
K-laurate	20	10.7~13.1	12.20	X-rays	〃 〃 〃	〃
K-myristate	20	8.0~10.7	7.16	X-rays	〃 〃 〃	〃
Na-palmitate	60	5.6~ 6.7	—	—	—	—
Na-stearate	60	3.1~ 3.7	—	—	—	—
Na-dodecyl-sulfate	40	6~9	4~5	X-rays	Hess, Philippoff Kiessig (1939)	(2)
	70	6~9				
Na-oleate	20	4.39	7.2	Viscosity	Hess, Philippoff Kiessig (1939)	(2)
			4~5	X-rays	〃 〃 〃	〃
			5~6	Diffusion	Okuyama, Tyuzyo, Saito (1951)	(10)
Aerosol-MA	25	2.99	4.5	Partial specific Volume	Vetter (1947)	(9)
			2.5	Diffusion	〃	〃

(*) In many cases, $\eta_{sp}^{\circ}/C_m^{\circ}$ vs. C_m° curve gives no sharp knick so that C_{m2} is expressed in an extended range and not a fixed value. For this fact, the method itself is not responsible but the insufficiency of the experimental data is the real reason.

$$C_{m2}=C_{m1}+C_{v\,2}^{\circ} \qquad (5)$$

In the Table. 3 are shown C_{m2}-values from above method and the existing values of 2nd CMC. It will be understood from the table that our C_{m2} values fairly coincide with 2nd CMC obtained from other methods. This method of determining 2nd CMC seems to be quite satisfactory at the present stage. (The data of X-rays are not quite accurate themselves.)

Table 4

Values of $[\eta_1]$ and $[\eta_2]$

Substance	M	Temp. (°C.)	$[\eta_1]$	$[\eta_2]$
Na-caprylate	166.21	20	0.65	0.87
Na-nonylate	180.23	20	0.81	1.28
Na-caprate	194.25	20	0.67	—
	〃	20	1.19	—
K-caprate	210.35	20	0.87	—
Na-laurate	222.30	20	1.18	(2.2)
K-laurate	238.40	20	—	2.6
K-myristate	266.48	20	—	3.3
Na-Palmitate	278.42	60	—	2.0
Na-stearate	306.48	60	—	2.5
Na-dodecylsulfate	302.37	20	1.78	3.0
		40	2.23	2.65
		70	1.94	2.57
Dodecylamine-HCl	221.80	20	0.88	2.0
		30	0.94	1.9
Na-oleate	304.34	20	1.35	—
		20	—	3.81
Aerosol-MA	388.46	25	1.73	1.84
Hexanolamine-caprylate	221.80	25	1.13	—

The Meaning of $[\eta_1]$ and $[\eta_2]$

We tabulate in Table. 4 $[\eta_1]$ and $[\eta_2]$ values obtained from above method. M in the second column of the table is the molecular weight of the detergent monomer. $[\eta_1]$ would be the related quantity to the micelle molecular weight (M_m) from the analogy of high polymer solutions. But unfortunately, M_m has hardly ever been measured accurately up to this time. And so it is impossible to compare $[\eta_1]$ with M_m directly. Therefore, for convenience, we plotted $[\eta_1]$ and $[\eta_2]$ against M (monomer molecular weight) in Fig. 7 and Fig. 8.

The following facts are recognizable from these figures.

(a) Fatty acid anionic soap series lie almost on the straight line.

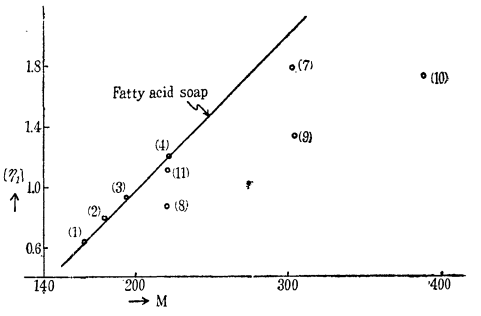

(1) Na-caprylate; (2) Na-nonylate; (3) Na-caprate; (4) Na-laurate; (5) K-laurate; (6) K-myristate; (7) Na-dodecyl-sulfate; (8) Dodecylamine-HCl; (9) Na-oleate; (10) Aerosol MA; (11) Hexanolamine-caprylate

Fig. 7.—Relation between $[\eta_1]$ and M.

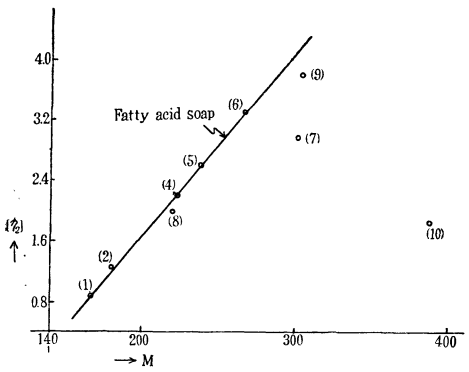

Fig. 8.—Relation between $[\eta_2]$ and M

(b) $[\eta_1]$ of sodium-oleate is exceptionally small, whereas its $[\eta_2]$ is not very small.

(c) $[\eta_1]$ and $[\eta_2]$ of sodium-dodecylsulfate are both abnormally small.

(d) $[\eta_1]$ of dodecylamine-hydrochloride is smaller than that of anionic soap, but $[\eta_2]$ is almost equal.

(e) $[\eta_1]$ and $[\eta_2]$ of aerosol-MA (sodium-methylamyl-sulfosuccinate) are both much smaller than those of ordinary fatty acid soap.

Discussion

(I) The phenomenon that η_{sp}/C_m becomes minimum at C_{m1} (Section 3) may probably be due to the result of the electrostatic interaction, owing to the strong electrolytic character of soap molecules. (η_{sp}/C_m of polyelectrolyte solutions passes generally a minimum value at some concentration.) However, most recently, R. Goto, N. Koizumi and T. Sugano found that η_{sp}/C_m of polyethleneoxide-monoalkylether solutions (nonionic detergent) also reaches a minimum in the neighbourhood of CMC.[24] Therefore, this phenomenon seems to be common to ionic and nonionic detergent which cannot be explained simply with the electrostatic force. We have no adequate explanation for this phenomenon.

(II) It is very particular that $\eta^{\circ}_{sp}/C^{\circ}_m$ converges to $[\eta_2]$. This is a completely different behavior compared with high polymer solutions of which η_{sp}/C_m is proportional to the square of concentration and so increases very rapidly in the region of high concentration. There seem to be three cases.

(i) Micellar size increases with concentration, but its shape does not change.

(ii) Shape changes with increasing concentration, whereas its size stays unchanged.

(iii) Size increases and shape also changes with increasing concentration.

Which of those three possibilities is most reasonable cannot still be decided. The recent investigation of flowbirefringence of detergent solutions[19] seems to be important in order to aquire some information of the micelle size and shape at moderately high concentration. At present, there is no direct means to determine both micellar size and shape simultaniously over wide range of concentration. Our discussion therefore is obliged to be limited to the indirect one. The most effective method, i. e. light scattering, can decide M_m only at low concentration and is not applicable at high concentration. Moreover, in the condition without adding electrolyte, it is impossible to dicide the micelle shape from the assymmetry of the scattered light, because micelle is too small in this condition. On the other hand, X-ray method gives some information of micelle size and shape at high concentration, but cannot be applied to low concentration. With diffusion method, it is necessary to add some swamping electrolyte in the soap solution, nevertheless micelle size is given only under some assumptions concerning hydration. At any rate, for detailed analysis of th above phenomena, many experimental data are still lacking.

(III) It must be remarked that $[\eta_1]$ and $[\eta_2]$ and M (monomer molecular weight) has a linear relation for fatty acid homologue. The fact that sodium-oleate dislocates the linearity could be explained from abnormal physical properties of oleic acid based on its cis-configuration. For example, it has abnormal low meltingpoint (14°C.) and high density (0.895). Aerosol-MA dislocates also, but it is natural if we remember that its micelle is quite different from ordinary soap because its monomer has the hydrophilic group nearly at the center. The difference between cationic and anionic soap micelles may be based upon the difference of the hydrophilic character of their hydrophilic group. The difference between sodiumdodecylsulfate and fatty acid soap is due also to the same cause. If M_m of several detergents are measured accurately by the light scattering, we can expect that the relation such as $[\eta_1]=KM_m^n$ may be concluded from those data.

Summary

(1) Several methods of determining CMC are compared and criticised.

(2) A new method of determining 1st CMC from viscosity is experimentally established.

(24) R. Goto, N. Koizumi and T. Sugano, presented at the 5th Annual Meeting of the Chemical Society of Japan in Tokyo, 1952.

(3) A new method of determining 2nd CMC from viscosity is established by transforming concentration and viscosity in the new variables.

(4) Of each soap, characteristic constants $[\eta_1]$ and $[\eta_2]$ are discovered, and it is shown that a definite relation is concluded between these values and monomer molecular weight.

(5) The theoretical explanation of these newly found phenomena has not yet been made.

Department of Chemistry, Faculty of Science, Osaka University, Osaka

New Spraying Reagents for the Detection of Reducing Sugars on the Paper Chromatograms

By Susumu HIRASE, Choji ARAKI and Susumu NAKANISHI*

(Received September 19, 1952)

Since paper chromatography was first applied to carbohydrates by Partridge,[1] various spraying reagents have been reported for the detection and identification of sugars separated on a paper chromatogram. Acidic solutions of aromatic amines such as aniline[2] and benzidine,[3] or of phenols such as resorcinol and naphthoresorcinol,[4] have been most frequently employed as spraying reagents. Their use depends upon the formation of furfural or its derivative by the action of an acid upon the sugar, and its subsequent condensation with an amine or phenol to give a colored compound. Among them, amine reagent is generally sensitive to aldoses, but is not so sensitive to ketoses and sometimes gives only faint spots. Whereas the sensitivity of phenol reagent to ketoses is excellent, its sensitivity to aldoses is moderately poor. Therefore, for complete detection of components in a mixture of unknown sugars by means of paper chromatography, such disadvantage has been experienced that both amine and phenol reagents must be applied.[5] If, however, aminophenols, carrying amino and phenolic hydroxyl groups, are used instead of an amine or phenol alone, they may be expected to be universal reagents in order to detect both aldoses and ketoses in one spraying operation. In this expectation, several aminophenols have been examined as the color reagents for reducing sugars, and an alcoholic solution of *o*-aminophenol acidified with phosphoric acid has been found to be the most useful one in respect of its universal sensitivity for various types of sugars and its specific coloration.

Experimental

Spraying Reagents: Of aminophenols were examined *o*-, *m*- and *p*-aminophenol, 1-amino-2-naphthol, 2,4-diaminophenol and 2-amino-resorcinol, the last two being used in the form of their hydrochlorides because of the unstability of their free bases. The reagent was prepared before use by dissolving 0.15 g. of each aminophenol in 20 cc. of ethanol and acidifying it with 10 cc. of 50% (w/w) phosphoric acid.

General Procedure: By means of micropipettes, the solutions of various concentrations of a sugar were spotted side by side at intervals of 2 cm. on a starting line of a filter paper sheet (Tōyō filter paper No. 2) so that each spot carried 1, 2, 3, 5, 10, 15 and 20 μg. of the sugar, respectively. The chromatogram was irrigated in the ascending technique with the upper layer of a mixture of butanol, ethanol and water (4:1:5 V/V), the solvent being allowed to advance about 30 cm. from the sugar starting line. The paper was then dried, sprayed with the reagent, and heated in an oven at 105° for a few minuites until a series of sugar spots with successively decreasing intensities was revealed in decreasing order of sugar quantity. The background of the paper remained almost unaffected. Thus, the minimum quantity of the sugar which was detected by each reagent was measured, and the color of the spots was also observed. Experiments were repeated several times for each of L-arabinose, D-xylose, D-ribose, L-rhamnose, D-glucose, D-mannose, D-galactose, D-fructose, L-sorbose, D-tagatose, lactose, sucrose,

* Faculty of Engineering, Dōshisha University, Kyoto.

(1) S. M. Partridge, *Nature*, **158**, 270 (1946).
(2) S. M. Partridge, ibid., **164**, 444 (1949).
(3) R. H. Horrocks, ibid., **164**, 443 (1949).
(4) W. G. C. Forsyth, ibid, **161**, 239 (1948).
(5) S. Hirase and C. Araki, *Memoirs of Faculty of Industrial Arts, Kyoto Technical University*, **1**, 19 (1952)

Table 1

The Observed Color and the Sensitivity (in μg. unit) of Each Sugar Class to Various Aminophenol Reagents

Sugar Classes	Aminophenols											
	o-Aminophenol		*m*-Aminophenol		*p*-Aminophenol		1-Amino-2-naphthol		2,4-Diaminophenol*		2-Aminoresorcinol*	
Pentose	Blue	1	Brown	2	Reddish brown	5	Blue	5	Dark blue	1	Blue	5
Methylpentose	Cherry red	5	Brown	5	Yellowish brown	5	Purple	15	Orange	5	Orange red	15
Aldohexose	Brown	5	Brown	5	Yellowish brown	5	Brown	15	Brown	5	Brown	15
Ketohexose	Lemon yellow	1	Lemon yellow	1	Lemon yellow	1	Lemon yellow	1	Lemon yellow	1	Lemon yellow	1
Lactose	Brown	5	Brown	5	Brown	5	Brown	15	Brown	5	Brown	15
Sucrose	Yellow	1	Yellow	1	Yellow	1	Yellow	1	Yellow	1	Yellow	1
Uronic acid	Blue	1	Reddish brown	1	Reddish brown	1	Blue	1	Blue	1	Blue	1

* u ed as its hydrochloride since its free base was unobtainable.

D-glucuronolactone, D-mannuronolactone and D-galacturonic acid. The results are summarized in the accompanying table.

Results

It will be seen from the table that all of the reagents are more or less effective to detect sugars, though the preliminary expectation is not completely satisfied. Generally speaking, they are particularly sensitive to ketoses and ketose-containing sucrose, giving a yellow color. Uronic acid or its lactone is also detectable with superior sensitivity. With regard to aldoses, pentose can be detected more sensitively than methylpentose and aldohexose, and gives the same coloration as that of uronic acid or its lactone.

Among these reagents, *o*-aminophenol reagent is found to be the most valuable one, for it detects as little as 1~5 μg. of each sugar and yields a specific color with each particular class of sugars. Although 2,4-diaminophenol reagent also seems to be possessed of these advantages, it is inferior to the former due to its unstability. With *o*-aminophenol reagent, it is easily achieved to decide the sugar class to which an unknown sample belongs, and, moreover, methyl glycosides give the same colorations as those of their parent sugars. For example, methyl xyloside and methyl glucoside give blue and brown color, respectively. Sugar alcohols are lacking in any coloration.

The authors wish to express their hearty thanks to Mr. K. Yamanouchi for his kind assistance in the course of this study.

Institute of Chemistry, Faculty of Industrial Arts, Kyoto Technical University, Kyoto

Studies on the Mechanism of the Electrolytic Formation of Perchlorate.* I.

By Kiichiro SUGINO and Shigeru AOYAGI

(Received November 17, 1952)

Introduction and Outline of the Research

Preparation of peracids is the typical electro-process which can not practically succeed by any other method. Especially, the production of perchlorate or persulphate is one of the most important electrolytic processes now operated in the world.

Anodic potential of the formation of perchlorate has been considered to be very high and this electrolytic preparation has been successfully accomplished only by the use of smooth platinum anode which has the highest oxygen overvoltage. One of the authors has already developed a new electrolytic process of this production using lead peroxide anode instead of platinum. In this case, in order to increase the oxygen overvoltage of lead peroxide anode, a small amount of sodium fluoride must be added in the electrolyte. The reason for these devices is that even if the anodic potential of the formation of perchlorate is very high, it can not proceed unless at the lower potential than that of oxygen evolution. But the anodic potential of the formation of perchlorate has not yet been accurately determined and the variation of it with the concentration of chlorate has also remained unknown. Therefore, the present study seeks to measure the anodic potential of perchlorate formation accurately and at the same time to present the most probable mechanism of this anodic process.

Twenty five years ago, the polarographic method was proposed by Heylovský and Shikata and the electrolytic reduction potential of organic compounds which is lower than that of hydrogen evolution at the dropping mercury cathode and the variation of it with the concentration of the depolariser can now be measured very easily by that method. So the authors tried to apply the same method to the anodic process of peracid formation to determine the potential at which the reaction occurs. If the anodic potential of perchlorate formation is lower than that of oxygen evolution at platinum anode, a typical anodic polarogram will be obtained by a platinum micro-anode, just the same as the cathodic polarogram of the reduction process described above. The resulting polarogram assumed is shown in Fig. 1.

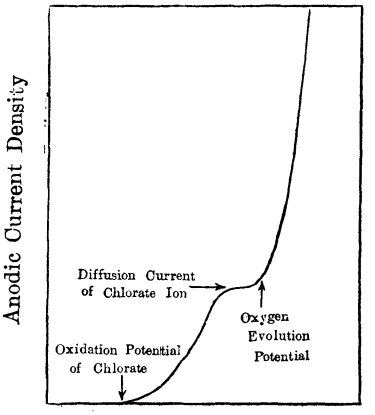

Fig. 1.

And the variation of the anodic potential with the concentration of chlorate will be approximately represented by the following formula.

$$E=\frac{RT}{2F}\ln\frac{K}{C_{ClO_3^-}\cdot a^2_{OH^-}}$$

where $C_{ClO_3^-}$ is the concentration of chlorate having a definite value and K is a constant. If these assumptions are verified by the experiments, the formation of perchlorate must be expressed by the following mechanism;[1]

$$2OH^- - 2e \rightarrow 2OH \rightarrow O + H_2O$$
$$ClO_3^- + O \rightarrow ClO_4^-$$

Upon these assumptions, the current-

* This papar was already given in the lecture at the general meetings of the Electrochem. Soc. of Japan held on May 1949, April 1950 and April, 1952.

(1) Bennett and Mack, *Trans. Electrochem. Soc.*, **29**, 323 (1916).

potential curves of the electrolytic oxidation of chlorate were measured polarographically under various conditions. The nature of the polarogram thus obtained was quite different from that of the usual oxidation-reduction process as shown in Fig. 1 and from the polarogram, it was pointed out that the anodic potential of the oxidation of chlorate might be higher than that of oxygen evolution. And even the phenomenon which was probably the limiting current of the discharge of OH^- ion could also be seen in the polarogram. These results were not able to be completely explained by the usual mechanism described above. In order to explain the results more suitably, the authors proposed an alternative mechanism, in which the discharge of chlorate ion and the subsequent combination and hydrolysis of ClO_3 were assumed.(2)(3) This mechanism has already been proposed by other investigators, but no experimental verifications were found in the literature of the subject.

The research has been further continued to confirm the above results. For this purpose, the electrolysis of chlorate solution at definite anodic potential was carried out and the anodic current density and the current efficiency of perchlorate formation at that current density were plotted against the anodic potential applied. A current-potential curve like the polarogram was obtained from these experiments and it was observed that the current efficiency of perchlorate formation increased with increasing current density due to the increase of anodic potential applied. And in spite of no perchlorate formation in the electrolysis of a very dilute aqueous solution of chlorate, it was also observed that when the same amount of chlorate dissolved in a concentrated perchlorate solution was electrolysed (this is the case of practical perchlorate cell), perchlorate was formed in a fair current efficiency. In addition to this, perchlorate solution itself gave an analogous polarogram as chlorate in which the discharge potential of perchlorate ion was observed at higher value than that of oxygen evolution. From these experiments, it was made clear that the first step of perchlorate formation was probably the discharge of chlorate ion. And it may be supposed that the reason for the possibility of discharge of chlorate ion is not only the high oxygen overvoltage of special anodic materials, but also the lack of water in the neighbourhood of the electrode surface due to the extraordinarily high salt concentration of the electrolyte and also to the strong hydration power of existing ions. (The latter was verified by further experiment.) These results will be reported successively. In this paper, only results obtained from the measurement of anodic polarogram of the electrolysis of chlorate and a possible mechanism based upon the polarogram were given.

(2) Oechsli, *Z. Electrochem.* **9**, 807 (1903).
(3) Knibbs and Palfreeman, *Trans. Faraday Soc.*, **16**, 402 (1920).

(Part I) Anodic polarogram of the Electrolysis of Chlorate by a Platinum Microanode

Measurement of Current-potential Curves

A micro-rotating platinum electrode and a smooth platinum plate of sufficiently large area were used as the anode and the cathode respectively. The details of the cell design and the measurement circuit are shown in Fig. 2-b and Fig. 2-a.

(1) **Electrolytic Cell.** — The section of the platinum wire of 0.3 mm. diameter sealed in a glass tube was used as the anode, the area of which was about $10^{-3}\sim10^{-4}$ cm^2. The cathode was a platinum plate of 10 cm^2. Throughout the following electrolysis, the current being less than 7×10^{-4} amp., the potential drop across the electrolyte did not amount to 10 mv. which was the limit of accuracy of our potential measurement. The stem of the anode—a glass tube—was rotated at 1000 r. p. m.. Although the significance of this rotation is not very important, it prevents the accumlation of oxygen gas on the surface of the anode and maintains the thickness of the anodic diffusion layer unchanged during the measurement and so a better reproducibility in the measured current-potential curves may be expected.

(2) **Polarograph.** — The sensitivity of the galvanometer used was 3.5×10^{-6} amp./mm./m..

(3) **Apparatus for the cathodic potential measurement.**—Since the cathode has a large area and the current is very small, the polarisation at cathode is generally considered to be very small. But in our case, it was found that it amounted to about 500 mv. for the cathodic current density of 3.5×10^{-3} amp./cm^2.. Thus, the cathodic potential must be measured continually throughout the current-potential curve measurement. For this purpose, the simple apparatus illustrated in Fig. 2-a was sufficient and also very convenient, the sensitivity of which was 3 mv., and the range of measurement, -450 mv.$\sim$ $+450$ mv..

(4) **Temperature.** — The electrolytic cell and the calomel electrode were immersed in a thermostat regulated at 17°C$\pm$0.02°.

(5) **Electrolyte.**—1$\sim$6 mol./l. aqueous solutions of sodium chlorate were used. It is seen that the use of such a high concentration of the

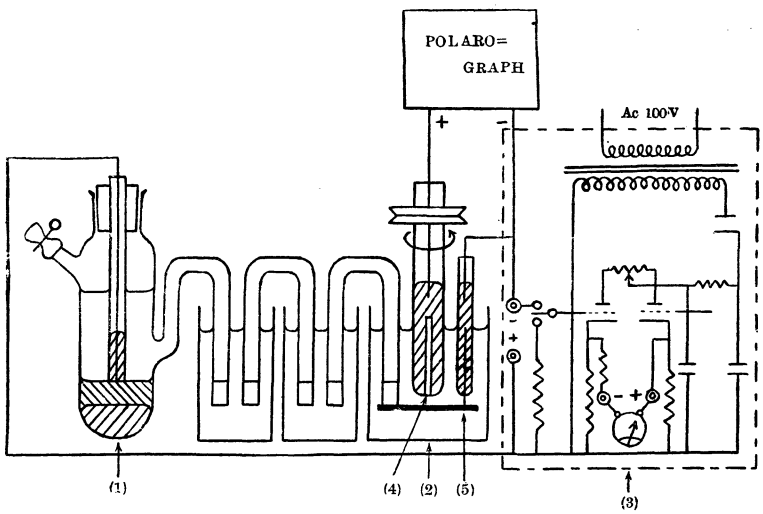

Eig. 2 a.—(1) Calomel Electrode (Saturated KCl Type)
(2) Electrolytic Cell, (3) Valve Voltmeter,
(4) Anode. (5) Cathode.

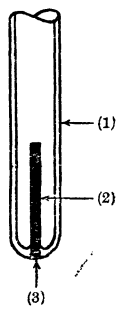

Fig. 2 b.—(1) Glass Tube
(2) Platinum Wire
(3) Anode Surface

electrolyte, together with the relatively large anodic current density mentioned above, makes the condition of our current-potential curve measurement deviate from that of the ideal polarographic method. But it was confirmed that for wellknown anodic processes (which occur at lower potential than that of oxygen evolution), usual polarograms were always given by the use of the same apparatus and under the same measuring conditions as described later.

Results and Discussion

The polarograms for various concentrations of sodium chlorate solutions are shown in Fig. 3. The abscissa corresponds to the anodic potential (the numerical values of which were obtained by subtracting the cathodic potential from the cell voltage and by referring to the hydrogen scale). The ordinate corresponds to the apparent anodic current density in amperes per dm^2. Its value, however, was not so reliable in consequence of the obscurity of the true apparent area of the anode.

The potentials of the second stage were seen to be:

about	2.1 V	for	5.6 M	solution
	2.1 〃	〃	4.0	〃
	2.2 〃	〃	2.8	〃
	2.4 〃	〃	2.0	〃
	2.4 〃	〃	1.4	〃

Some characteristics of the polarograms obtained may be summarized as follows:

(1) In a moderately concentrated solution of chlorate, two stages of potential were definitely observed, as shown in Fig. 3.

(2) In the first or lower stage, the potential has a value of about 1.7—1.9 v. On the other hand, in the second or higher stage, the potential has a higher value than 2.3 v.

(3) Contrary to the usual polarogram, the height of the wave of the first potential stage was seen to be reversely proportional to the concentration of chlorate. It lowered as the

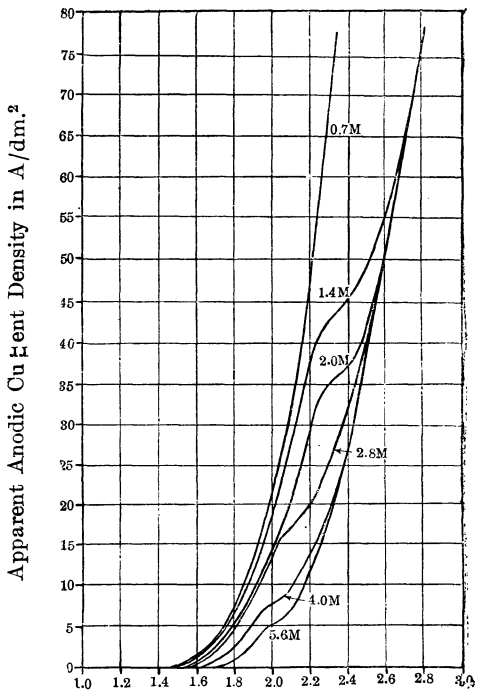

Fig. 3.

concentration of chlorate increased.

(4) For a sufficiently dilute solution, this wave height grew so high that it reached beyond the range of the measurement, a simple exponential curve being observed.

If an analogous interpretation would be made for our polarogram to ordinary ones of the cathodic process, the first or lower stage should be the potential of the oxidation of chlorate and the second or higher one of oxygen evolution. This, however, must be decidedly denied by the fact that the height of the wave corresponding to the first stage is reversely proportional to the concentration of chlorate. In addition to this, the value of the potential of first stage was found to correspond to the one of oxygen evolution. (The reversible oxygen potential, E_{O_2/OH^-}, is about 0.8 v. for any solution of *p*H 7 and estimating about 1v. of oxygen overvoltage of a smooth polainum plate at the current density of 1 amp./dm^2., the actual oxygen evolution potential for any solution concerned amounts to about 1.8 v.) So, among two potential stages mentioned above, the lower one may be supposed, on account of its value of potential, to be a potential corresponding to the electrolysis of water or the evolution of oxygen gas. If the lower stage is regarded as the potential of oxygen evolution, the higher one may be of the oxidation of chlorate. Thus, our polarograms should be classified in another type of current-potential curve from the ordinary one. And it is obviously certain that the oxidation of chlorate occurs at some higher potential than that of oxygen evolution. This fact is not able to be explained by an usual following mechanism.

$$2OH^- - 2e \rightarrow 2OH \rightarrow O + H_2O$$
$$ClO_3^- + O \rightarrow ClO_4^-$$

So an alternative mechanism already proposed by other investigators was adopted by the authors in which the discharge of chlorate ion was assumed. A supposed mechanism may be formulated as follows

$$2ClO_3^- - 2e \rightarrow 2ClO_3$$
$$2ClO_3 + H_2O \rightarrow HClO_3 + HClO_4$$

$$\left.\begin{array}{l} 2ClO_3^- - 2e \rightarrow 2ClO_3 \\ 2ClO_3 \rightarrow ClO_3 - O_3Cl \\ ClO_3 - O_3Cl + H_2O \rightarrow HClO_3 + HClO_4 \end{array}\right\} (2)$$

Later, in order to confirm the accuracy of our polarographic method, one of the authors has carried out the measurement of current-potential curves of several typical anodic reactions (electrolysis of KCl, KBr, KI, $NaNO_2$, $Na_2S_2O_3$, Na_2SO_3 etc.) which seemed to occur at lower potential than that of oxygen evolution. In the polarograms thus obtained, the potential stages corresponding to each anodic reaction were observed definitely at lower potential than that of oxygen evolution. These results showed that the polarogram of the electrolytic oxidation of chlorate described above and the proposed mechanism based on the polarogram were both probably correct.

Further, in view of the prospective discussion of the dependence of the discharge of chlorate ion on the mechanism of perchlorate formation, it is necessary to know the true formation of perchlorate at the potential of second stage in Fig. 3. For this purpose, in the following research, the electrolysis of chlorate solution was carried out at a definite anodic potential, corresponding to the second stage in Fig. 3. under various conditions. Many interesting phenomena were observed and from the results obtained, our conclusion based upon the polarogram was seen to increase its appropriateness. These results will be reported hereafter.

The cost of this research has been mainly defrayed from the Grant in Aid for Fundamental Scientific Research of the Ministry of Education to which the authors' thanks are due.

Laboratory of Organic Electrochemistry and Biochemistry, Tokyo Institute of Technology, Tokyo

The Oxygen Equilibrium of Hemerythrin and Bohr Effect

By Masaji KUBO

(Received October 15, 1952)

The transfer of oxygen from the external environment into the tissues of various animals is accomplished by respiratory pigments capable of combining with oxygen when its partial pressure is high and of giving it up when the pressure is low. There are four different types of the pigments, hemoglobin, chlorocruorin, hemerythrin and hemocyanin. The first three contain iron while hemocyanin is a copper compound. Surely hemoglobin has been studied in the most extensive way.(1) Among the iron-containing respiratory pigments, hemerythrin is interesting in view of the fact that although the common property as an oxygen transporter confers upon all these types of molecules their biological analogy, the chemical properties of hemerythrin are very markedly different from those of hemoglobin and chlorocruorin. Oxygen combines with hemoglobin(2) or chlorocruorin(3) in definite proportion of one molecule per one atom of iron, whereas the gas combines with hemerythrin(4) in the proportion of one molecule per three atoms of iron in the pigment molecule. Besides hemerythrin is not a heme derivative as are hemoglobin and chlorocruorin.(2)(5) The oxygen dissociation curve of hemerythrin from sipunculus under physiological conditions has already been studied by Florkin.(2) The present investigation was undertaken in order to examine more closely the oxygen equilibrium and Bohr effect, which together with magnetic studies to be reported later will reveal some features of interest concerning the function of iron atoms in the molecule.

Preparation of Hemerythrin Solution.—The coelomic fluid of a species of sipunculid worm called phascolosoma from the Marine Biological Laboratory in Woods Hole was centrifuged to throw down the dark red violet corpuscles. The sediment was washed several times with 2.5% sodium chloride solution to remove the plasma completely. It was made up to 60% of the original volume with distilled water and left to stand in an icebox for about two hours to lake the corpuscles. The stroma was removed by centrifuging and the dark red violet solution after filtration through a hard filter paper was ready for use. The solution contained a minute amount of sodium chloride originating from the washing solution. This does not affect the results at all. The exact control of the concentration was unnecessary in the present experiment. Still the difference between the optical densities of reduced and oxygenated solutions gives an accurate relative concentration for each solution. The simultaneous determination of optical density difference and iron content for one solution to be reported in the following paper can convert the relative value to the absolute concentration in gram atoms of iron per cc.

Apparatus.—The apparatus used was essentially the same as that used in the earlier experiments(1) on hemoglobin. The spectrophotometric method was employed for the determination of the degree of oxygenation of hemerythrin. As a constant light source a 6 V., 30 W. microscope lamp was used. It was run from two heavy duty accumulators connected in parallel. The light was filtered through an interferance filter backed by a blue masking filter to get monochromatic light of wavelength 4760 A. This wavelength was chosen as satisfying the basic requirement that it should be readily transmitted by both reduced and oxygenated hemerythrin solution, although much more readily by the former than the latter. The monochromatic light was then passed through an optical cell having a path length of 2.5 mm. for the light through the solution. Only 1 cc. of solution was enough to fill the cell. The cell was really a part of a tonometer made of glass, which could be evacuated and sealed by a rubber vaccine cap. The total volume enclosed in the vessel amounted to 292.5 cc. The light transmitted by the cell fell on a photomultiplier tube RCA 931. The current thus produced was passed through a suitably chosen high grade resistor and the resulting voltage drop was measured by means of a potentiometer with a Millivac vacuum tube millivoltmeter as a detector of the balancing point.

Experimental Procedure

The tonometer containing the oxygenated

(1) D. W. Allen, K. F. Guthe and J. Wyman, *J. Biol. Chem.*, **187**, 393 (1950).
(2) R. A. Peters, *J. Physiol.*, **44**, 131 (1912).
(3) H. M. Fox, *Proc. Roy. Soc. London*, B **115**, 368 (1934).
(4) M. Florkin, *Arch. intern. physiol.*, **36**, 247 (1933).
(5) R. Kobert, *Arch. ges. Physiol.*, **98**, 411 (1903) : G. F. Marrian, *Brit. J. Exptl. Biol.*, **4**, 357 (1927).

hemerythrin solution was evacuated and equilibrated three times with the atmosphere of 99.9% pure commercial nitrogen saturated with water, until the dark red violet solution changed into a pale milky white, almost colorless solution of reduced hemerythrin. The measurement of optical density of the medium was made putting the tonometer in the optical system. Then a desired amount of air was introduced into the tonometer through the vaccine cap by means of a syringe and hypodermic needle, calibrated as to the volume of delivery. The resulting oxygen pressure in the tonometer could be calculated from the volume of air introduced, that of the gas phase in the tonometer and the known composition of air, with due correction for the humidity of air. The correction was also made for the amount of oxygen taken up by the solution. It could be calculated from the volume of the solution, the concentration in gram atoms of iron per cc., and the percentage saturation of the hemerythrin with oxygen as given by the photometric measurements to be described in the following paragraph. This correction was usually small, amounting to less than a few per cent of the calculated pressure of oxygen. After the measurement of optical density of the solution at 20°C. for twelve different oxygen pressure was over, the last measurement was made on essentially 100 per cent oxygenated hemerythrin obtained by exposing the solution to atomospheric air. Because hemerythrin has high oxygen affinity, it was unneccessary to use pure oxygen at this point. The degree of saturation Y with oxygen of the hemerythrin solution was calculated as

$$Y=\frac{D-D_{\mathrm{red}}}{D_{\mathrm{ox}}-D_{\mathrm{red}}} \qquad (1)$$

where D's denote optical densities of the solution in equilibrium with oxygen of partial pressure p, completely deoxygenated and oxygenated solutions respectively. Since we were interested only in the difference of optical densities, it was convenient to use a neutral filter made of a piece of photographic film of appropriate darkness to reduce the value of I_0, the intensity of incident light, so as to make it match that of I, the intensity of light emerging from the cell. It should be noted that no knowledge of the extinction coefficients and the exact concentration was required for the calculation of Y values.

The prime requirement in this kind of experiment was accuracy as well as speed, since proteins are known to be subject to denaturation especially in solutions of pH values far apart from that of physiological condition. The agreement of individual data of I/I_0 was within 1%. The difference between the optical densities of reduced and oxygenated solutions amounted to about 1.3. Hence the probable error in the degree of saturation is estimated to be less than 1%. The crucial point seemed to lie not in physico-chemical measurement but rather in the biochemical problem of how to prepare definite specimens and how to minimize the effect of denaturation. The whole physico-chemical measurement comprizing twelve different values of oxygen pressure could be carried out in six hours. Thus a fresh sample could always be prepared on the day of measurement and used.

Results and Discussion

The first two experiments were made on unbuffered hemerythrin solutions of concentration 5.16 and 6.31×10^{-6} gram atoms of iron per cc. respectively. The pH value of the solution in oxygenated state as measured by a glass electrode was 6.25 pretty close to the isoelectric point 5.85.[6] The unbuffered solution was fairly stable and a solution left overnight in an icebox gave results practically identical with those of a fresher sample.

The degree of partial saturation Y with oxygen is plotted as a function of $\log p$, the logarithm of oxygen pressure in mm. Hg., in

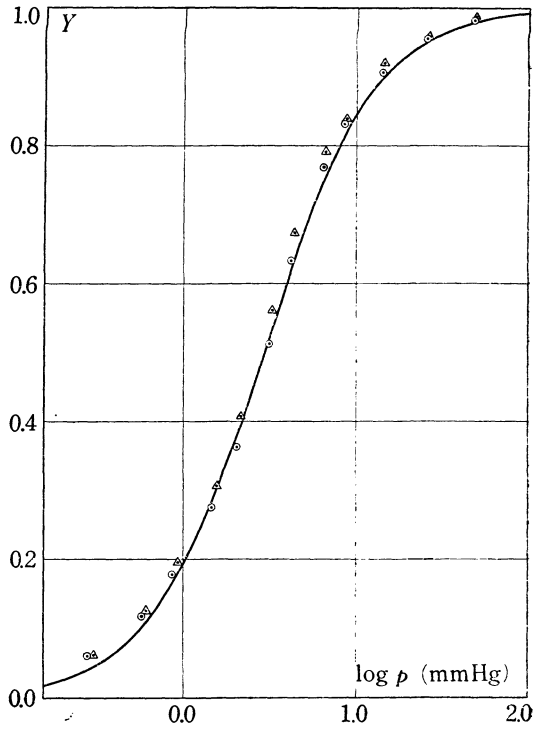

Fig. 1.—The degree of saturation with oxygen of hemerythrin as a function of the logarithm of the partial pressure of oxygen. 20°C., unbuffered, pH = 6.25. The circular points represent data on the solution of iron concentration 5.16×10^{-6} g. atom/cc., and the triangular points those of 6.31×10^{-6}. The full line depicts the empirical formula (2).

(5) J. Roche, *Ann. Rev. Biochem.*, **5**, 463 (1936).

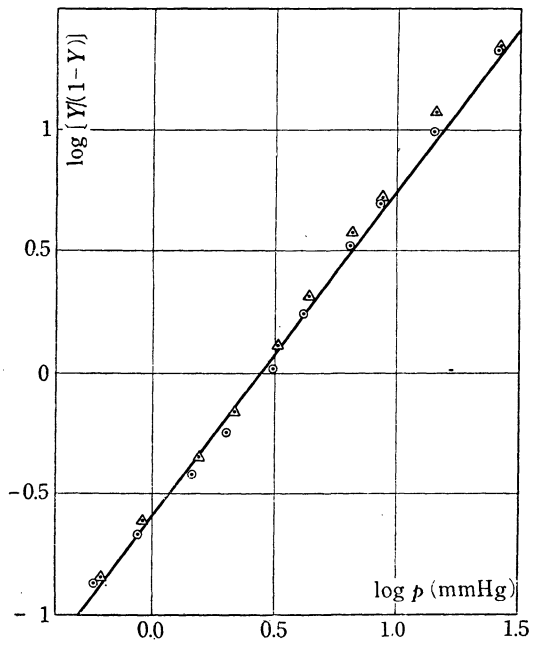

Fig. 2.—The dependence of $\log[y/(1-y)]$ upon $\log p$.

Fig. 1. The functional relation between Y and $\log p$ can be represented by the following empirical formula.

$$Y=\frac{1}{2}+\frac{1}{2}\tanh\left(2.303\frac{n}{2}\log\frac{p}{p_{1/2}}\right) \quad (2)$$

with $n=1.37\pm.05$ and $\log p_{1/2}=0.46\pm.02$. This is mathematically equivalent to the statement that $\log[Y/(1-Y)]$ is a linear function of $\log p$,

$$\log\frac{Y}{1-Y}=n(\log p-\log p_{1/2}) \quad (3)$$

as shown in Fig. 2. In fact the values of n and $\log p_{1/2}$ mentioned above were obtained in this way. From the equation (2) it is clear that $p_{1/2}$ is nothing but the partial pressure of oxygen in equilibrium with the solution in which the amount of oxygenated hemerythrin is just the same as that of the reduced form. The interpretation of the physical meaning of n in terms of the theory of linked groups is given in a paper by Wyman.[7] It will be found that the equation (3) can be written in an alternative way as follows.

$$\frac{Y}{1-Y}=\left(\frac{p}{p_{1/2}}\right)^n=Kp^n \quad (4)$$

or Hill's empirical equation:

$$Y=\frac{Kp^n}{1+Kp^n} \quad (5)$$

The constant K in the equation (4) may be interpreted, formally at least, as the equilibrium constant for the hypothetical reaction:

$$M+nX=MX_n \quad (6)$$

$n=1$ would mean that all the oxygen attaching centers in the molecule are mutually independent, whereas $n=2$ that two centers are linked together so that an oxygen molecule attached to one center induces another oxygen molecule to combine with the molecule at once. The value $n=1.37$ in this case suggests that the oxygen combining centers in hemerythrin molecule are not completely independent, but the stabilizing interaction is weak, weaker at least than in the case of hemoglobin, in which case n was found to be 2.8.[7] This conclusion will be important in the interpretation of magnetic susceptibility of hemerythrin.

$\log p_{1/2}=0.46$ gives $p_{1/2}=2.9$ mm. Hg. Florkin[8] studied the oxygen dissociation curve of hemerythrin from sipunculus, and found for $p_{1/2}$ the value of 8 mm. Hg. at 19°C. It is doubtful that the disagreement is really significant in view of the fact that these samples were extracted from different animals and that the conditions were slightly different.

Finally the curve of Fig. 1 has a very slight but unmistakable asymmetry which cannot be ascribed to experimental errors. Wyman and others[1] found that the similar asymmetry in the case of hemoglobin disappeared for a freshly prepared material. In the present case even freshly prepared solution gave slight asymmetry of the curve and a material left to stand overnight revealed no sign of increased asymmetry.

Bohr Effect.—Further studies were made on the effect of pH on the oxygen equilibrium of hemerythrin. The measurements were made on solutions at 20°C. prepared in the same way as before, buffered with mixtures given in Table 1 chosen to get desired pH values, which were actually measured by a glass electrode. The oxygen equilibrium curves obtained were very similar to that of the unbuffered solution, except the case for pH=4.4, in which case though the curve was symmetrical it was less steep. The values of n and $\log p_{1/2}$ are summarized in Table 2. In the case of pH=4.4, slight denaturation was

(7) J. Wyman, *Adv. Protein Chem.*, **4**, 407 (1948).

(8) M. Florkin, *C. R. Acad. Sci.*, **195**, 832 (1932).

Table 1

Concentration of Hemerythrin (g. atom Fe/cc.)	Buffer Solution	Buffer Concentration	*p*H Value
4.95×10^{-6}	Na_2HPO_4-citric acid	0.035 M	4.4
5.16, 6.31	Unbuffered	—	6.25
4.10	K_2HPO_4-KH_2PO_4	0.095	6.8
5.55	Borax-boric acid	0.022	8.8

Table 2

*p*H	n	$\log p_{1/2}$
4.4	1.11±.05	0.57±.02
6.26	1.37±.05	0.45±.02
6.8	1.35±.05	0.44±.02
8.8	1.27±.05	0.46±.02

clearly perceptible by the appearance of fine pale yellow suspensions, and at *p*H=2.7 or 10.0 denaturation was so rapid that measurement could not be made at all. If progressive denaturation takes place, the decrease of concentration decreases D_{ox} in the equation (1) and results in the overestimation of Y in the lower left branch of the curve in Fig. 1, while in the upper right branch the simultaneous decrease of D and D_{ox} gives rise to the underestimation of Y, with the consequent flattening of the sigmoid curve. Taking this into account, we can conclude that within the *p*H range of stable hemerythrin solution there is no dependence of oxygen equilibrium upon *p*H, i.e., Bohr effect is absent. So that no oxygen-linked acid groups are present in hemerythrin molecule, unlike the case of hemoglobin.

Summary

The oxygen equilibrium of hemerythrin and its Bohr effect were studied by spectrophotometric method. It was found that the oxygen combining centers in this molecule are not completely independent but the stabilizing effect is weak. The value of n in Hill's equation is equal to 1.37. The partial pressure of oxygen in equilibrium with the solution of 50% saturated hemerythrin is 2.9 mm. Hg. Within the *p*H range of stable hemerythrin solution, there is no dependence of oxygen equilibrium upon *p*H, hence no oxygen-linked acid groups are present in hemerythrin molecule.

The present experiments were made at the Biological Laboratories, Harvard University. I wish to express my sincere thanks to Professor Jeffries Wyman, Jr. for his kind suggestions and advices.

Chemical Department, Faculty of Science, Nagoya University, Nagoya

Dipole Moments of Methyltropolones and their Bromoderivatives*

By Yukio KURITA, Toshikuni MIZUNO, Toshio MUKAI and Masaji KUBO

(Received November 19, 1952)

Proceeding with our work on the dipole moments of tropolone and its derivatives,[1] we made experiments on three methyltropolones and seven of their bromoderivatives. They were synthesized by one of us[2] and his collaborators. The position of substituents, which had already been inferred from evidences in organic syntheses,[2] could be confirmed by this physico-chemical method.

Experimental Results.—The apparatus and the method of measurement are already given in our previous paper.[1] The results are shown in Tables 1 and 2. The only datum found in literature to be compared with the present results is that of the compound II measured by Tyrell and Mills.[3]

* Read before the scientific meeting of the Chemical Society of Japan held on April 4, 1952.

(1) Y. Kurita, T. Nozoe and M. Kubo, *Bull. Chem. Soc. Japan*, **24**, 10, 99 (1951).

(2) T. Nozoe, T. Mukai, M. Kunori, T. Muroi and K. Matsui, *Sci. Reports Tohoku Univ.*, 1, **35**, 242 (1952).

(3) R. D. Haworth and J. D. Hobson, *J. Chem. Soc.*, **1951**, 561.

Table 1

Dielectric constant and density increments

	Compounds	w $\times 10^5$	$\Delta\varepsilon$ $\times 10^4$	Δd $\times 10^5$
I	Methyltropolone	192	192	47
	m. p. 50.5—51°	360	346	88
	25°	542	497	139
II	Methyltropolone	336	418	83
	m. p. 74—76°	598	728	141
	30°	940	1143	217
III	Methyltropolone	150	211	36
	m. p. 108—110°	331	422	75
	25°	512	663	123
IV	Bromomethyltropolone	321	267	128
	m. p. 123°	595	445	158
	25.6°	1086	899	458
V	Bromomethyltropolone	227	230	114
	m. p. 83—85°	514	507	215
	25°	674	677	282
VI	Bromomethyltropolone	230	80	138
	m. p. 171—172.5°	334	129	161
	25°	549	191	209
VII	Dibromomethyltropolone	271	158	123
	m. p. 140°	532	324	257
	30°	834	524	410
VIII	Tribromomethyltropolone	265	82	140
	m. p. 99.5—100.5°	588	176	309
	25°	766	225	421
IX	Bromomethyltropolone	213	194	94
	m. p. 115°	412	355	183
	30°	545	515	216
X	Dibromomethyltropolone	205	139	104
	m. p. 140°	404	283	202
	30°	630	404	321

Table 2

Dipole moments of methyltropolones and their derivatives

	t(°C.)	ε_1	d_1(g./cc.)	α	β(g./cc.)	$P_{2\infty}$(cc.)	R_D(cc.)	μ(D)
I	25	2.2753	0.87129	8.69	0.263	255.5± 1.0	37.1	3.27±.01
II	30	2.2637	0.86637	12.02	0.222	340.9± 1.6	37.1	3.88±.01
III	25	2.2744	0.87132	12.48	0.240	354.0± 8.2	37.1	3.94±.05
IV	25.6	2.2693	0.87036	8.38	0.455	375.9±20.6	44.8	4.05±.13
V	25	2.2727	0.87163	9.94	0.373	445.2± 8.2	44.8	4.42±.05
VI	25	2.2732	0.87221	3.39	0.224	192.0±13.6	44.8	2.68+.12
VII	30	2.2605	0.86614	6.51	0.510	406.6± 3.2	52.6	4.19±.02
VIII	25	2.2732	0.87124	2.86	0.554	247.6± 5.2	60.4	3.02±.04
IX	30	2.2608	0.86648	9.54	0.372	453.8±34.4	44.8	4.51±.19
X	30	2.2644	0.86627	6.22	0.509	389.5±21.2	52.6	4.27±.13

Their value of 3.9 D is in good agreement with ours.

Discussion.—The theoretical values for the moments of these compounds with substituents at various presumed positions were calculated as in our previous reports. The bond moment of methyl group substituted in tropolone was assumed to be equal to that in toluene; μ(C–CH$_3$) $=-0.4$ D. The calculated values are compared with the experiment in Table 3. We could thus determine definitely the position of substituents for all the compounds studied, except the compound V, for which we wish to defer our final decision.

Table 3

The position of substituents in methyl tropolones and their derivatives

Compounds	μ_{obs}(D)	μ_{calc}(D)	The position of substituents
I	3.27	3.41	3-Methyltropolone
II	3.88	3.76	4-Methyltropolone
III	3.94	3.90	5-Methyltropolone
IV	4.05	4.17	7-Bromo-3-methyltropolone
		1.95	5-Bromo-3-methyltropolone
V	4.42	4.24	3-Bromo-4-methyltropolone
		4.45	7-Bromo-4-methyltropolone
VI	2.68	2.27	5-Bromo-4-methyltropolone
		2.82	3,5-Dibromo-4-methyltropolone
		3.13	5,7-Dibromo-4-methyltropolone
VII	4.19	4.42	3,7-Dibromo-4-methyltropolone
VIII	3.02	2.93	3,5,7-Tribromo-4-methyltropolone
IX	4.51	4.48	3-Bromo-5-methyltropolone
X	4.27	4.56	3,7-Dibromo-5-methyltropolone

Summary

The dipole moments of three methyltropolones and their bromoderivatives were measured in benzene solution at 25° or 30°. The values obtained were compared with the theoretical data for the moments of these compounds with substituents at various presumed positions.

The final decision of the position of substituents were made as shown in Table 3.

We wish to express our thanks to Prof. T. Nozoe of Tohoku University for his kind suggestions and encouragement. Our thanks are also due to the Ministry of Education for aid in this research.

Chemical Institute, Faculty of Science, Nagoya University, Nagoya
Chemical Institute, Faculty of Science, Tohoku University, Sendai

Studies on Pyrethrins
The Synthesis of Some β-Keto Esters

By Masanao MATSUI, Tokuji YAMAGUCHI, Takeaki KATO and Giichi FUNAZO

(Received June 16, 1951)

Several methods are reported to prepare β-keto-esters through the condensation of methyl ketones and ethyl carbonate. The typical methods are those which use, as condensation agent, sodium alcoholate,[1] sodamide[2] and more recently sodium hydride.[3] Though the reaction yields depend upon the character of methyl ketones which are used, the best results can generally be obtained by employing sodium hydride, and the next best by sodium alcoholate. The sodamide method yields usually poor results, but is exempted from inconveniences which accompany the former two methods such as the work in the stream of nitrogen gas or the stirring under reduced pressure and the use of large excess of diethyl carbonate.

We, therefore, investigated the method to increase the condensation yield in the reaction by sodamide. We performed the reaction and found that the low yield of the reaction is due to the formation of urethan by a side reaction of this condensation.

A mechanism of this condensation proposed by Levine[2] is as follows;

(I) $CH_3COR+NaNH_2 \longrightarrow (CH_2COR)^-Na^+ + NH_3$

(II) $C_2H_5OCO_2C_2H_5+(CH_2COR)^-Na^+ \longrightarrow RCOCH_2COOC_2H_5+NaOC_2H_5$

(III) $RCOCH_2CO_2C_2H_5+(CH_2COR)^-Na^+ \longrightarrow (RCOCHCOOC_2H_5)^-Na^+ + CH_3COR$

or $RCOCH_2CO_2C_2H_5+NaNH_2 \longrightarrow (RCOCHCOOC_2H_5)^-Na^+ + NH_3$

The equations are correct as far as the mechanism is concerned, but the following side reactions also occur in reality. A part of ammonia produced in (I) and (III) reacts with diethyl carbonate and yields urethan and alcohol when two molecules of sodamide are used for one molecule of methyl ketones

(IV) $C_2H_5OCO_2C_2H_5+NH_3 \longrightarrow NH_2CO_2C_2H_5+C_2H_5OH$

and the alcohol which is produced reacts with sodium enolate of the methyl ketone or with sodamide to produce ammonia.

(V) $C_2H_5OH+(CH_2COR)^-Na^+ \longrightarrow CH_3COR+C_2H_5ONa$

or $C_2H_5OH+NaNH_2 \longrightarrow C_2H_5ONa+NH_3$

The methyl ketone liberated by this reaction reacts sodamide and liberates ammonia, and ammonia repeats the reactions already described though ammonia decreases gradually by escaping from the reaction system. Thus we found that in order to minimize the reaction between ammonia and diethyl carbonate, it is necessary to produce sodium enolate of the methyl ketone at first, and in order to complete enolization of the methyl ketone or to complete the production of keto ester as far as possible, it is also necessary to employ more than two molecules of sodamide and more than one molecule, or probably more than two molecules, of diethyl carbonate to one molecule of the methyl ketone.

By using a methyl ketone, sodamide and diethyl carbonate in the molar ratio of 1:3:3 in the procedure described in the experimental part, we succeeded in obtaining almost the same yields of β-keto ester (See Table 1) as in the case of sodium hydride when the methyl

(1) Wallingford et al., *J. Am. Chem. Soc.*, **63**, 2252 (1941).
(2) R. Levine and C. R. Hauser, *J. Am. Chem. Soc.*, **66**, 1768 (1944).
(3) S. B. Soloway and F. B. LaForge, *J. Am. Chem. Soc.*, **69**, 2677 (1947).

Table 1

ketones	products	b. p.	n_D (temp., °C.)	yield %				Analytical Data %	
				$NaOCH_3$ method	old $NaNH_2$ method	NaH method	the present method	Found	Calcd.
Methyl ethyl ketone	Ethyl 3-oxo-valerate	91—93°/ 17 mm	1.4183 (23°)		13[2]		11	C 57.62 H 7.83	C 58.33 H 8.33
Methyl n-propyl ketone	Ethyl-3-oxo-caproate	93-95.5°/ 15 mm	1.4240 (30°)		19[2]		48	OC_2H_5 28.6	OC_2H_5 28.2
Allyl-acetone	Ethyl 3-oxo-6-heptenoate	95-100°/ 11 mm	1.4414 (22°)	70[4]		77[4]	70	OC_2H_5 25.8	OC_2H_5 26.5
Methallyl-acetone	Ethyl 3-oxo-6-methyl-6-heptenoate	105-115°/ 12.5 mm	1.4493 (15°)			70[4]	70	C 64.87 H 8.65	C 65.21 H 8.70
5-Hepten-2-one	Ethyl 3-oxo-6-octenoate	90-104°/ 7 mm	1.4397 (30°)			85[8]	69.5	OC_2H_5 25.0	OC_2H_5 24.4
6-Hepten-2-one	Ethyl 3-oxo-7-octenoate	102-120°/ 9.5 mm	1.4384 (30°)				75.5	OC_2H_5 24.9	OC_2H_5 24.4
Piperonyl-acetone	Ethyl 3-oxo-5-(3, 4-methylene-dioxyphenyl)-valerate	160-163°/ 3 mm	1.5111 (30°)				32	C 63.32 H 6.10	C 63.63 H 6.07
Furfuryl-acetone	Ethyl 3-oxo-5-furylvalerate	110-120°/ 3 mm	1.4758 (16°)				22	C 64.78 H 7.05	C 62.86 H 6.67
Benzyl-acetone	Ethyl 3-oxo-5-phenyl-valerate	129-138°/ 7 mm	1.4972 (17°)				40.9	C 71.43 H 7.34	C 70.91 H 7.21
Tetrahydro-furfuryl-acetone	Ethyl 3-oxo-5-(2-tetrahydro-furfuryl) valerate	110-117°/ 3 mm	1.4448 (31°)				38	OC_2H_5 23.62	OC_2H_5 21.08

ketone is stable to alkali.

This research is a part of the synthetic study of pyrethrin and cinerin homologues and several 3-methyl-2-cyclopenten-4-ol-1-ones (See Table 2)—some of them are not yet known—have been synthesized by the condensation of methyl glyoxal with these keto esters through the methodes of LaForge et al.[4] or Matsui et al.[5]

Experimental

A. Methyl Ketones

(1) **6-Hepten-2-one.**—Buten-(1)-ol-(4) (b. p. 112-114°) was prepared in 30% yield from allyl bromide and paraformaldehyde, and 4-bromobutene-(1) (b. p. 94-100°) in 64% yield from this butenol by the method of Linstead and Rydon.[6] A solution of sodium methylate prepared by dissolving 12 g. (ca. 0.5 mol.) of sodium in 200 cc. of absolute methanol was cooled to 15° and 70 g. (0.54 mol.) of ethyl acetoacetate was added to the stirred solution. After 1.5 hrs. 68 g. (0.5 mol.) of the above 4-bromobutene was added at once and the reaction was completed by refluxing for five hours. Most of the methanol was removed by distillation and water was added to the residue. Crude ethyl α-3-butenylacetoacetate separated as an upper layer and weighed 57.7 g..

One hundred and thirty eight grams of this crude keto ester and 70 g. of potassium hydroxide in 1.3 l. of water were stirred at 20° for 7 hrs.. The oil was extracted with petroleum ether and discarded. A mixture of 50 cc. of concentrated sulfuric acid and 80 cc. of water was added to the aqueous solution and the mixture was warmed under stirring on a water bath until the evolution of carbone dioxide ceased. The upper oily layer was separated, and the aqueous layer was saturated with sodium chloride and was extracted with petroleum ether. The oil and the petroleum extracts were combined and washed with dilute alkali and saturated sodium chloride solution and dried with potassium carbonate. After evaporation of the solvent, the residue was distilled. 6-Hepten-2-one distilled at 145-150°, yield 42 g. (50 % of the theory based on the crude ester)

(2) **Piperonylacetone.**— One hundred fifty grams of piperonylideneacetone was dissolved in

(4) M. S. Schechter, N. Green and F. B. LaForge, *J. Am. Chem. Soc.*, **71**, 3165 (1949).

(5) M. Matsui, T. Kato et al, *J. Chem. Soc. Japan, Pure Chem. Sect.*, **71**, 235 (1950).

(6) *J. Chem. Soc.*, **1934**, 1996

(7) Kaufmann and Radosevic, *Ber.*, **49**, 679 (1916).

(8) F. B. LaForge et al., *J. Am. Chem. Soc.*, **70**, 3708 (1948).

Table 2

2-Substituted 3-methyl-2-cyclopenten-4-ol-1-ones

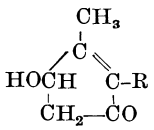

	b. p.	n_D	yield %*	Analytical Data
Methyl	108–110°/ 0.29 mm.	1.5079/ 26°	31	Found: C, 68.01; H, 7.85. Calcd. for $C_7H_{10}O_2$: C, 66.67; H, 7.92%.
Ethyl	132–135°/ 1.3 mm.	1.5082/ 28.5°	30.8	Found: C, 68.40; H, 8.37. Calcd. for $C_8H_{12}O_2$: C, 68.57; H, 8.57%.
Allyl	132–135°/ 1 mm.	1.5141/ 25°	34	Semicarbazone, m. p. 210° Found: C, 56.73; H, 7.20. Calcd. for $C_{10}H_{15}O_2N_3$: C, 57.40; H, 7.23%.
Methallyl	121–126°/ 0.2 mm.	1.5120/ 12°	24	Semicarbazone, m. p. 208–209° Found: C, 59.10; H, 7.25; N, 19.01. Calcd. for $C_{11}H_{17}O_2N_3$: C, 59.19; H, 7.68; N, 18.83%.
2-Butenyl (trans-cinerolone)	127–132°/ 0.5 mm.	1.5096/ 18.5°	45	Semicarbazone, m. p. 208–209° Found: C, 59.79; H, 7.53: N, 19.28. Calcd. for $C_{11}H_{17}O_2N_3$: C, 59.19; H, 7.68; N, 18.83%.
3-Butenyl	126–132°/ 0.5 mm.	1.5151/ 18°	41	Semicarbazone, m. p. 187° Found: C, 59.73; H, 7.40; N, 19.09. Calcd. for $C_{11}H_{17}O_2N_3$: C, 59.19; H, 7.68; N, 18.83%.
Benzyl	161–165°/ 0.15 mm.	1.5680/ 21°	20	Semicarbazone, m. p. 215–216°. Found; C, 64.79; H, 6.48; N, 16.41. Calcd. for $C_{14}H_{17}O_2N_3$: C, 64.87; H,6.56; N, 16.23%.
Piperonyl	146–150°/ 0.23 mm.	1.5670/ 23°	21	Found: C, 68.84; H, 5.21. Calcd. for $C_{14}H_{14}O_4$: C, 68.29;H, 5.59%.
Furfuryl	140–143°/ 0.6 mm.	1.5352/ 16°	38	Semicarbazone, m. p. 201–202° (from ethanol). Found: C, 56.98; H, 6.79; N, 16.97. Calcd. for $C_{12}H_{15}O_3N_3$: C, 57.83; H, 6.02; N,1 6.86%. 3,5-Dinitrobenzoate, m. p. 168–169° Found: C, 55.71; H, 4.28; N, 7.18 Calcd. for $C_{18}H_{14}O_8N_2$: C, 55.95; H, 3.65; N, 7.25%. p-Nitrobenzoate, m. p. 108–109° Found: C, 63.38; H, 4.94; N, 4.10. Calcd. for $C_{18}H_{15}O_6N$: C, 63.34; H, 4.43; N, 4.16%.
Tetrahydrofurfuryl	113–120°/ 0.1 mm.	1.5095/ 19°	4	Found: C, 68.15; H, 7.06. Calcd. for $C_{11}H_{16}O_3$: C, 67.35; H, 8.16%.

* The yields are based on the ester used.

300 cc. of ethyl acetate and reduced with an equivalent amount of hydrogen at 10 atm. in the presence of 10 g. of Raney nickel at room temperature to piperonylacetone, b. p. 152-158°/5 mm. (the reported b. p. 164-5°/12 mm.[7]), yield 105 g. (71% of theory).

(3) Tetrahydrofurfurylacetone.

(i) Tetrahydrofurfurylpropanol-(2). Two hundred and eighty grams of furfurylidene acetone was hydrogenated with 4 equivalent molecules of hydrogen at 40 atm. in the presence of 25 g. of Raney nickel together with some water at 90-120°. The product, boiling 122-131°/24 mm., n_D^{22} 1.4519, was collected, yield 175 g. (62% of theory) (Found: C, 66.14; H, 10.88. Calcd. for $C_8H_{16}O_2$: C, 66.66; H, 11.11%.)

(ii) Tetrahydrofurfurylacetone. Seventy-two grams of tetrahydrofurfuryl-propanol was oxidized with a mixture of 49 g. of potassium bichromate, 70 g. of concentrated sulfuric acid and 250 cc. of water at 60°. The product was extracted with ether. After distillation 31 g. of tetrahydrofurfurylacetone, boiling at 112-115°/28 mm., n_D^{27} 1.4414, was obtained; 2.4-Dinitrophenylhydrazone, yellow crystal, m. p. 76.5°-78.5°C. (Found: N, 17.51. Calcd. for $C_{14}H_{18}O_5N_4$: N, 17.34%).

B. β-Keto-Esters

The general procedure is as follows: one mol. of a methyl ketone is added at a time under stirring to about 3 mols. of sodamide in 1 l. of dry ether at 0° in an ice bath; after 15 minutes the bath is removed and stirring is continued another one hour and then refluxed 15 minutes in a water bath. The bath is replaced by the ice bath and about three mols. of diethyl carbonate is dropped as rapidly as possible. Stirring and refluxing is continued for 4 hours. After cooling three mols. of glacial acetic acid is added and then 600 cc. of water. The upper ether layer is separated and the ether is recovered by distillation. The residual oil is dissolved in an equal volume of petroleum ether and washed several

times with an equal volume of water in order to remove a small quantity of urethan. The urethan can be recovered by extracting the water solution with ether. The petroleum ether solution is dried on anhydrous sodium sulphate or magnesium sulphate. After evaporation of the petroleum ether, the β-keto ester is distilled under reduced pressure.

Summary

A new procedure for preparing β-keto esters from methyl ketones, sodamide and diethyl carbonate using these reagents in the molar ratio of 1:3:3 is reported. The yields of β-keto esters approach to those of the preparation using sodium hydride as condensing agent. Furthermore, some cyclopentenolones were prepared from the β-keto esters synthesized by this procedure.

We are greatly indebted to Dr. Ryo Yamamoto for the valuable advices and to the Ministry of Education for research grants of 1950.

Laboratory of Sumitomo Chemical Co. Ltd. Osaka

The Co-ordinate Compounds of Iron with Some Hydroxycarboxylic Acids

By Kazuo SHIBATA and Tazuhiko NOGUCHI

(Received August 18, 1952)

Sulphosalicylic acid has widely been used for the colorimetric determination of ferric iron in solutions, but of the details of physico-chemical properties of the complex formed by co-ordination of hydroxycarboxylic acid of this sort we have only rudimentary information at present. The present work was carried out with the purpose of clarifying some properties of co-ordinate compounds of tri-valent iron with sulphosalicylic acid and related substances, dealing in particular with the determination of the number of ligands chelating with iron and the equilibrium constants between them. The compounds studied were salicylic, sulphosalicylic and 2-hydroxy-3-naphthoic acids, which all, with their hydroxyl group situated in the ortho position to the carboxyl group, form stable complexes with iron.

Methods

The concentration of the complexes formed in solutions was determined spectrophotometrically, using an Adam Hilger monochrometer for visible region combined with the photo-multiplier-tube 931-A. The thickness of the cell compartments used was 1 cm. The mixture of ethanol and water (1:1 in volume) was generally used as the solvent, the purpose of which was to prevent the precipitation of the complexes formed. The standard solution of iron was prepared by dissolving pure iron wire into dil. hydrochloric acid by heating. The ferrous ion in the solution was oxidized by $KClO_3$.

The reaction between acids and iron was observed by the following procedure. 5 cc. of the alcoholic solution of hydroxycarboxylic acid was added to 5 cc. of ferric iron aq. solution. After a while, the absorbance, $E=\log_{10}I_0/I$ (I_0, incident light; I, transmitted light) of the solution was observed at the wave-length of the absorption maximum of the complex formed. As the equal amounts of solutions were mixed together, the solution at the beginning of reaction contained half the concentrations of each component in the original solution, which were denoted by C_f (concentration of iron in g. atoms/l.) and C_h (concentration of hydroxycarboxylic acids in mol./l.), respectively.

Results

(1) **Determination of the Number of Chelating Ligands.**—By a preliminary experiment it was confirmed that the positions of absorption maxima shown by the complexes of sulphosalicylic acid, salicylic acid and 2-hydroxy-3-naphthoic acid were 5100 Å., 5300 Å. and 5900 Å., respectively, in 50% ethanol aq. solution. For sulphosalicylic acid, the absorption maximum was measured in water, which was found to be 4900 Å. The absorbance E of the reaction mixtures was measured using monochromatic light corresponding to the absorption maximum of each complex.

Using a definite concentration of iron solution

($C_f = 0.91 \times 10^{-3}$) the change of E in function of C_h was followed. The experimental curves shown in Fig. 1 indicate that at lower concentrations of C_h, E is proportional to C_h, but with the increase of C_h, E increases more slowly and finally reaches a constant value. It was confirmed that the maximum value of E did not increase any more, even when solid hydroxycarboxylic acid was added to the mixture.

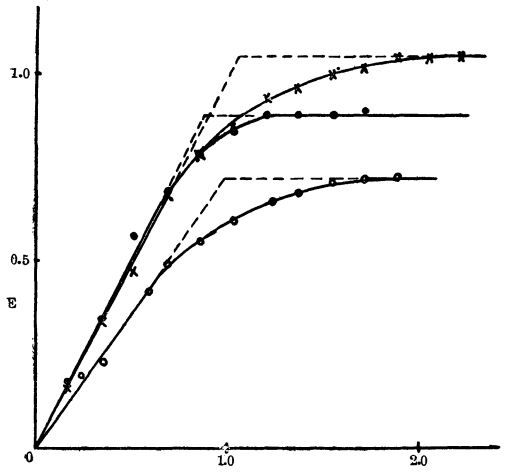

C_h in 10^{-3} mol./l. unit.
● Sulphosalicylic acid
× 2-Hydroxy-3-naphthoic acid
○ Salicylic acid

Fig. 1.

It is obvious that, in the region of linear proportionality, almost all of the hydroxycarboxylic acid added had co-ordinated with iron, while after reaching a constant value of E, almost all of the iron ion was bound. Hence, the value of C_h at the crossing point of the two dotted extrapolated lines shown in Fig. 1 must indicate the upper-most quantity of hydroxycarboxylic acid which can chelate with all iron ions present. These values of C_h were found to be 0.98 for salicylic acid, 0.90 for sulphosalicylic acid and 1.05 for 2-hydroxy-3-naphthoic acid, which all coincide with the value of C_f within the experimental error. A similar experiment was carried out with sulphosalicylic acid, using pure water as solvent. Also in this case, the molecular ratio of chelating agent to iron was found to be one to one.

In Fig. 2 are shown the results of experiments in which the change of E in function of C_f at a definite value of C_h (4.0×10^{-3}) was determined. The distinct linear ascent of the curves shows that under the conditions studied all iron ions have been bound by hydroxycarboxylic acids. The values of tangents of these lines also indicate that the combinations occur at the ratio of one to one.

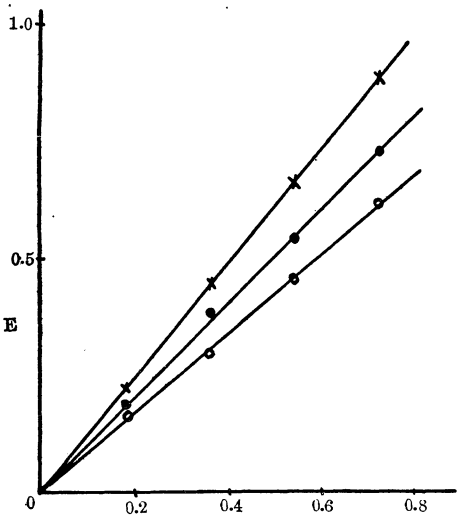

C_f in 10^{-3} g.-atoms/l. unit.
● Sulphosalicyilc acid
× 2-Hydroxy-3-naphthoic acid
○ Salicylic acid

Fig. 2.

(2) The equilibrium constant between iron and hydroxycarboxylic acids.—In so far as Beer's law holds, the concentration of a complex in solution must be proportional to the absorbance E of the solution; namely,

$$E = A[\mathrm{HFe}] \qquad (1)$$

where (HFe) stands for the concentration of chelated compounds and A for the proportionality constant. The value of A may be estimated either from the value of C_f and the maximum value of E in the experiment shown in Fig. 1, or from the tangent of straight lines in Fig. 2. The values of A thus obtained were 850 for salicylic acid, 1020 for sulphosalicylic acid and 1230 for 2-hydroxy-3-naphthoic acid.

Since the number of ligands chelating with one iron ion was found to be one, the equilibrium between the reaction components may be represented by

$$\mathrm{H} + \mathrm{Fe} \rightleftarrows \mathrm{HFe}$$

$$K = \frac{[\mathrm{HFe}]}{[\mathrm{H}][\mathrm{Fe}]} \qquad (2)$$

where H represents the molecule of hydroxycarboxylic acid and K the equilibrium constant. Since C_f and C_h are the concentrations at the beginning of reaction, they are

$$C_f = [\mathrm{Fe}] + [\mathrm{HFe}] \qquad (3)$$

$$C_h = [\mathrm{H}] + [\mathrm{HFe}] \qquad (4)$$

Substituting equations (3) and (4) in equation (2), we get

$$[\mathrm{HFe}]^2 - (C_f + C_h + 1/K)[\mathrm{HFe}] + C_f C_h = 0$$

Dividing this equation by [HFe], we obtain

$$Z \equiv [HFe] + C_f\left(\frac{C_h}{[HFe]} - 1\right) = C_h + \frac{1}{K} \qquad (5)$$

By applying the data shown in Fig. 1 to this equation, the value of K can be calculated; namely, if we plot the values of Z of the left-hand side of equation (5) against the values of C_h, the points must be on a straight line having a slope of unity and the intersection across the ordinate should be $1/K$. As will be seen from Fig. 3, the linear relationship holds satisfactorily except for the cases of very low concentrations. From the reciprocals of the intersections determined by the method of least square, the values of K of salicylic acid and 2-hydroxy-3-naphthoic acid were found to be 13,900 and 10,900, respectively.

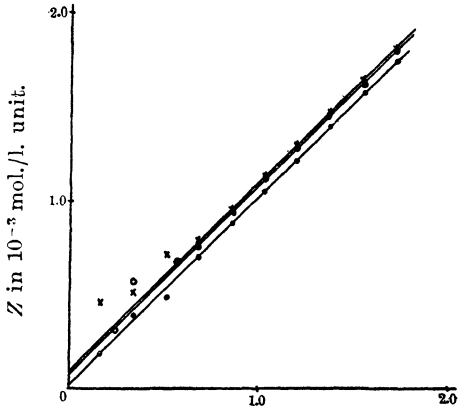

C_h in 10^{-3} mol./l. unit.
● Sulphosalicylic acid
× 2-Hydroxy-3-naphthoic acid
○ Salicylic acid

Fig. 3.

As for the value for sulphosalicylic acid, the intersection was so close to the origin of co-ordinates that the value of K could not be estimated accurately by the above method. Therefore, a resort was had to the following procedure to determine the value in this case. If the mixture contains two kinds of hydroxy-carboxylic acids, H_1 and H_2, the equilibrium to be established between them and the iron ion will be;

$$H_1 + Fe \rightleftarrows H_1Fe$$
$$H_2 + Fe \rightleftarrows H_2Fe$$

Therefore,

$$\frac{K_1}{K_2} = \frac{[H_1Fe](C_2 - [H_2Fe])}{[H_2F\,](C_1 - [H_1Fe])} \equiv K' \qquad (6)$$

where

$$C_1 = [H_1Fe] + [H_1]$$
$$C_2 = [H_2Fe] + [H_2]$$

and K' stands for K_1/K_2.

If the concentrations of the H_1Fe and H_2Fe are estimated experimentally, K' can be calculated, and if K_2 is known K_1 may be obtained from K' and K_2.

As the hydroxycarboxylic acid (H_2) with known equilibrium constant (K_2) we used 2-hydroxy-3-naphthoic acid, which was mixed with sulphosalicylic acid (H_1) in 5 cc. of alcoholic solution and this was added to 5 cc. of iron aq. solution. The absorbances of the solution were measured at the two wave-lengths corresponding to the absorption maxima of H_1Fe and H_2Fe. The values of absorbance thus obtained, which may be denoted by E_1 and E_2, respectively, cannot be regarded as being proportional to the concentrations of the corresponding complexes formed, because the two absorption bands are appreciably broad and overlap with each other at both wavelengths. The situation is schematically illustrated in Fig. 4, where the curve I+II is the absorption curve of the solution obtained, which is thought to be the sum of the curves of I and II for H_1Fe and H_2Fe existing in the solution. The actual absorbance, which is proportional to the concentration of each complex is denoted by E_1' and E_2', respectively, in Fig. 4. Therefore, E_1 and E_2 may be reduced to E_1' and E_2' by solving the following equations;

$$E_1 = E_1' + \frac{E_1''}{E_2'} E_2'$$
$$E_2 = E_2' + \frac{E_2''}{E_1'} E_1'$$

where E_1'' and E_2'' are the absorbances of H_2Fe and H_1Fe at the wave-lengths corresponding to the absorption maxima of H_1Fe and H_2Fe, respectively. The ratios E_1''/E_2' and E_2''/E_1', which can be determined experimentally, may be regarded to be constant independent of the concentrations. From the values of E_1' and E_2' thus obtained, the concentrations of H_1Fe and H_2Fe were calculated using the constant A already determined for each complex.

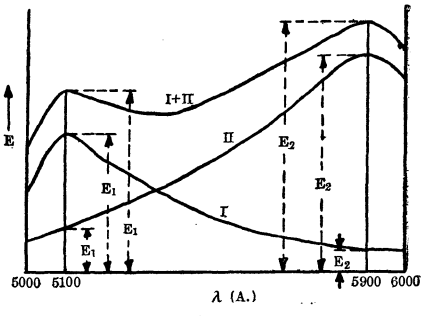

Fig. 4.

Experiments conducted with varying concentrations of H_1, H_2 and Fe, yielded the results shown in Table 1. As may be seen, the value K' calculated from different sets of experiment

showed an excellent agreement, giving a mean value of $K'=2.84$. Since K_2 is 10,900, the value of K_1 (equilibrium constant of Fe-sulphosalicylic acid-complex) is 31,000.

Table 1.

C_1	C_2	C_f	K'
0.720×10^{-3}	0.720×10^{-3}	0.720×10^{-3}	2.76
0.480 〃	0.720 〃	0.480 〃	2.82
0.720 〃	0.480 〃	0.480 〃	2.87
0.688 〃	0.688 〃	0.480 〃	2.90

A similar experiment carried out using salicylic acid and 2-hydroxy-3-naphthoic acid gave the results: (K_1 for salicylic acid):(K_2 for 2-hydroxy-3-naphthoic acid)=1.30. This value coincides fairly well with the value 1.28 calculated from the K-values which have already been determined separately for both substances.

Discussions and Summary

Chelating action of salicylic, sulphosalicylic and 2-hydroxy-3-naphthoic acids towards iron was investigated quantitatively, and it was found that they combine with one-to-one molecular ratio with iron. In order for these substances to be used as colorimetric reagents for the determination of iron, it is desirable that the reagents as well as their complexes be well soluble in water, and that the equilibrium contants of the complexes be sufficiently large so that the proportionality between the absorbance caused by complex and the concentration of iron or chelating agent may hold in a wide range. In this respect sulphosalicylic acid may be regarded as most suitable, among the three hydroxycarboxylic acids studied, as a reagent for iron determination. In view of the fact that the introduction of sulphonyl group into salicylic acid caused the increase of K, it may be expected that a more suitable iron reagents would be obtained by further introduction of sulphonyl group in salicylic acid.

The authors wish to express their thanks to Prof. Hiroshi Tamiya for his guidance and his constant encouragement during the course of this study.

The Tokugawa Institute for Biological Research, Tokyo and Faculty of Science and Engineering, Waseda University, Tokyo

Rheology of Coal. IV. Strength and Fracture of Coal

By Katsuya INOUYE and Hideo TANI

(Received July 30, 1952)

Introduction

As well demonstrated by such example as that tar, which is usually accepted as a "ductile" material, is "brittle" under impact, or that rubber, which is typically "elastic" at ordinary conditions, becomes "brittle" at liquid air temperatures, the mechanical properties of solids are functions of, at least, time and temperature.

Coal is not, of course, a simple solid, but is of extreme complexity and variety. One of the present authors (K. I.) has tried experiments on the Young's modulus[1] and internal viscosity[2][3] of coal, which might be able to propose an aspect on the structure and properties of coal from the rheological standpoints, in order to give more straightforward interpretations of the complex properties of coal. As one of the important rheological characteristics of coal, brittleness or strength for rupture is considered in this paper in the light of the facts disclosed in these preceding studies.

The strength of coal is a very important property in various fields of industry concerning coal. First, the mechanical strength is a leading factor for the efficient coal mining, whether the coal is mined by machines or by hands. The fracture of coal during the transportation or coal cleaning is a factor to determine the saleable output rate for definite purposes. The furnace or oven in which the coal is burned or carbonized desires stable

(1) K. Inouye, *J. Colloid Sci.*, **6**, 190, (1951).
(2) K. Inouye, *This Bulletin*, **26** 84 (1953).
(3) K. Inouye, *This Bulletin*, **26**, 157 (1953).

mechanical property of the coal used. There is no doubt of the importance of the strength when the coal is treated in a powdered form, as in floatation, briquetting etc.

In these cases, the coal is subjected to various kinds of stresses, especially varying duration of load. As described above, the coal strength is a function of time, so that the phenomena concerning the strength or fracture should be considered from the standpoint that one cannot speak of a definite characteristic strength of the solid, although some influences of inner flaws and chemical environments in the coal should not be neglected.

F. W. Preston and others[4] have shown, in their experiments on the fatigue of glass that the strength of glass is a simple function of time under a constant load,

$$\log t = -a/m + 1/fm \qquad (1)$$

where, f is the stress required to break a solid, t its duration of application, and a and m are constants. Each sample is thus defined by the inclination factor m (termed fatigue modulus) and by the point t_0, where the line intersects the time axis.

N. W. Taylor[5] has proposed a theory which connects f with t. The slow process preceding fracture is shown to be the orientation of the atomic network contained in an elementary prism of length $r = \lambda_0 E/f$, where E is Young's modulus and λ_0 is the critical elongation required for fracture. The rate-controlling factor is the activation energy, $E\alpha/f$, for the orientation or rearrangement of the atomic network under the stress. The theory has lead to the equations,

$$t = (1/k_0)e^{E\alpha/fKT} \qquad (2)$$

and

$$\log t = -\log k_0 + (E\alpha/2.3\,KT)/f \qquad (3)$$

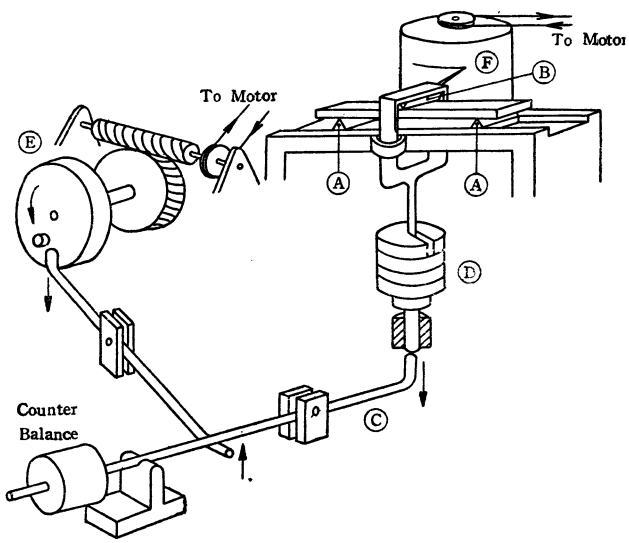

Fig. 1.—Experimental Apparatus

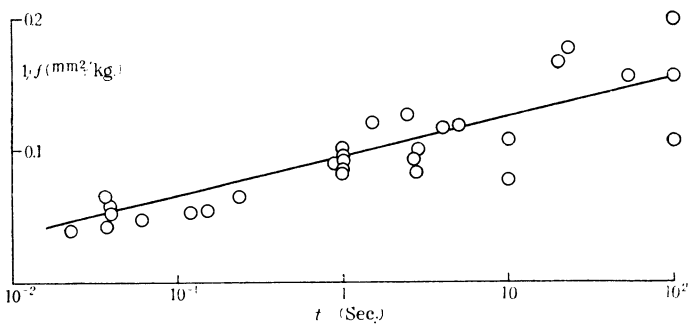

Fig. 2.—$1/f$ versus t for window glass

where K is the Boltzmann constant, T the absolute temperature and α and k_0 are constants. It is noteworthy that the logarithmic expression has the same form as the empirical relation by Preston et al.

The present authors have constructed an apparatus to measure the breaking stress at varying durations of load and, after some preliminary tests with glass in order to check the above-mentioned logarithmic relation between stress and time by their own apparatus, the breaking experiments were carried out on coal to interpret the fracture.

Apparatus and Experimental Procedures

Fig. 1 shows the apparatus schematically. The specimen, cut in a rectangular bar with the accuracy of 1% in each dimension and parallel to the bedding plane, is set on two wedge-shaped metals (A). The stress is applied by another wedge-shaped metal (B) just touched to the centre line in the upper surface of the specimen, when

(4) J. L. Glathart and F. W. Preston, *J. Appl. Phys.*, **17**, 189, (1946).
T. C. Baker and F. W. Preston, *J. Appl. Phys.*, **17**, 170, (1946).
(5) N. W. Taylor, *J. Appl. Phys.*, **18**, 943, (1947).

the shaft (C) is removed from the position of supporting the weight (D). The short duration of application can be changed by a gear and cam mechanism (E) driven by motor, covering the range of 1 sec. to 0.01 sec. The actual time of applied stress was measured by the recording dram method (F), a longer period than 1 second by the stopwatch.

The experimental procedure begins with a measurement to try to break the specimen at a certain time of load, t_1, with continuously changing weight, w, and if the specimen does not fracture at w_m but does at w_n, the breaking strength at t_1, f, is calculated from the equation,

$$f = \frac{3\,w_n l}{2bt^2} \tag{4}$$

where, l is the span length, b the breadth and t the thickness of the specimen, assuming that the coal fractures is a dynamic solid.

The possible maximum error of the experiment is considered as follows: errors in dimensions of the specimen are ±3%, errors in measuring the weight ±6%, and errors in measuring the time, which however vary with the time range, are ±5% at maximum cases. The total error is, therefore, ±14% at its maximum.

All specimens were examined after being set

Table 1
Fracture Experiments of Coal Samples

Sample	Block No.	Average ash %, dry basis, in vol. (ϕ)	Ash % of specimen (dry basis) in weight	Ash % of specimen (dry basis) in volume (ϕ)	$1/f$ (mm²/kg)	t (sec)
American (Bituminous, strongly-caking)	I	13.0	13.08	8.19	1.28	3×10^{-2}
			19.00	12.34	1.48	1.5
			19.56	12.73	1.54	3.2×10^{-2}
	II	65.0	67.93	55.97	1.18	2×10^{-2}
			69.50	58.57	1.62	1.5
			80.05	70.65	1.52	0.5
			80.07	70.38	1.78	3.5
	III	86.0	90.64	85.32	0.68	300
			91.15	86.07	0.58	4×10^{-2}
			91.37	86.40	0.66	50
			91.56	86.84	0.64	2.5×10^{-1}
Takashima (Bituminous, caking)	I	1.4	2.32	1.41	2.86	2×10^{-2}
			2.33	1.41	3.24	30
			2.37	1.44	2.32	4×10^{-2}
			2.91	1.77	3.90	300
	II	3.0	4.48	2.74	2.24	300
			4.75	2.89	2.00	0.1
			5.03	3.07	1.84	100
			5.49	3.37	2.18	2×10^{-2}
	III	10.0	12.13	7.65	0.84	1.3×10^{-1}
			17.80	11.50	0.64	4.6×10^{-1}
			22.07	14.52	0.98	5
Yubetsu (Producer gas coal)	—	—	22.99	16.61	0.38	1
			27.33	18.41	0.51	4
			28.69	19.42	0.38	4×10^{-2}
			29.43	20.00	0.46	0.5
			29.92	20.39	0.44	10
			31.38	21.53	0.44	3×10^{-2}
			40.63	29.11	0.62	24
			53.15	40.50	0.37	0.2
			55.10	42.41	0.50	3
			57.16	44.46	0.37	5×10^{-2}
			57.83	45.14	0.73	70
Shosaku (Anthracite)	—	3.6	5.64	3.46	1.18	2
			5.72	3.51	1.06	3×10^{-2}
			5.78	3.55	1.12	0.1
			5.83	3.59	1.36	2
			7.21	4.45	1.12	0.1
			7.24	4.47	1.18	2×10^{-2}

into the dessicator of 76% relative humidity for about one month to avoid the influence of the moisture.

Tests on Glass

Approximately 30 specimens were prepared from a piece of window glass and tested by the apparatus. The time for fracture covered the ranges from 5×10^{-2} to 10^3 second. The values of $1/f$, or brittleness index, are plotted against $\log t$ in Fig. 2.

It would appear that the $1/f$ values are more dispersed in the range of longer duration than the shorter. It was, however, assumed that the linear relationship between $1/f$ and $\log t$ is valid in this case. The fatigue modulus, m, obtained using the statistical method is 2.90×10^{-2} mm^2./kg. This value is quite reasonable in comparison with those given by Preston et al.

Brittleness Data of Coals

The coals examined were selected from the same species whose structures were previously discussed in the preceding articles of this study. (For the descriptions of samples, see the reference 2 or 3.)

The brittleness data are given in Table 1 with ash concentrations. The ash contents are recalculated in volume percentages, ϕ, because its significant meaning to the properties has been proposed in the author's preceding reports. Several blocks were chosen for each sample and the specimens were made from each block. After the fracture measurements, the actual ash concentrations were obtained for each specimens, which showed, of course, some deviations; the table also gives the mean values, which were obtained by analyses of mixed powdered samples.

Fatigue Modulus and Activation Energy

The $1/f$ values were plotted against $\log t$ for each block and, assuming the linear relationship between $1/f$ and $\log t$, the fatigue modulus, m, they were obtained from the lines on the graph. The validity of the linear reltionship was better for the anthracite and also the producer gas coal; both showed higher strength and slight deviation in strength with the change of ash concentration than the bituminous coals did. The statistical considerations of the dependence of strength on various factors will be described further in the next paper of this study. Fig. 3 shows the $1/f$ versus $\log t$ relationship for Yubetsu coal. Two values with larger deviation at the durations longer than 10 sec. were omitted from the linear relation.

From Equations (1) and (3),

$$m=2.3\,KT/E\alpha \qquad (5)$$

and,

on the other hand, the molal activation energy for fracture is,

$$U=NE\alpha/f \qquad (6)$$

where, N=Avogadro's number and hence $NK=R=2$ cal./mol. Therefore, from (5) and (6), U can be calculated from the experimentally known data of m. U values in Table 2 were calculated at first in functions of $1/f$, and then for breaking time of 10^{-2} sec. and 10^2 sec., where T was taken as 288°K (15°C.), the mean room temperature during the experiments.

Table 2

Activation Energy for Fracture

Sample	$m\times10^2$ (mm^2/kg)	$t=10^{-2}$ sec		$t=10^2$ sec	
		f (kg/mm^2)	U (Kcal/mol)	f (kg/mm^2)	U (Kcal/mol)
American					
I	18.9	0.82	8.52	0.53	13.2
II	22.0	0.88	6.88	0.49	12.3
III	2.30	1.71	33.8	1.49	38.7
Takashima					
I	31.8	0.42	10.0	0.28	15.2
II	5.52	0.50	48.0	0.45	53.4
III	11.0	1.52	7.94	0.99	12.2
Yubetsu	2.72	2.69	18.2	2.13	22.5
Shosaku	12.2	1.02	10.7	0.64	16.9

The values of f and U express the strength of coal in absolute units at different ranges of duration of load. It is noteworthy that in each cases the rupture can occur less easily with short time of application of stress than with longer deformation. In other words, the coal can be broken with less force when it is applied a for longer time than at short application. The total molal energy required to

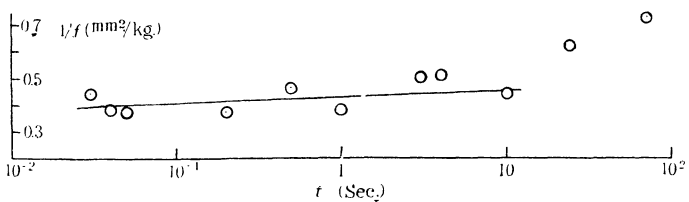

Fig. 3.—$1/f$ versus $\log t$ for Yubetsu producer gas coal.

"activate" the fracture is, however, larger when the deformation is applied for longer duration.

The stress for fracture, f, is larger for the specimen with higher ash concentration (Refer the variations between each result of American coal and of Takashima coal). A remarkable maximum in U values for Takashima coal seems to be difficult to be interpreted; it may be connected with the fact that the Young's modulus of this sample shows a minimum at $\phi=2$ and a maximum at $\phi=8$. (This fact will be reported in detail in Rheology of Coal VI by the present authors.)

The comparison of the strength and the activation energy between species of coals is rather of indefinite conclusion, because of the unequality of analytical composition, although some absolute expressions of industrially empirical strength can be shown.

The comparison of results for Takashima II ($\phi=3.0$) and Shosaku anthracite ($\phi=3.6$) may be interesting; these differences indicate that the bituminous coal is more "brittle" than the anthracite, when applied with stress of short duration, because the ratio of f between the samples is 2.04 at $t=10^{-2}$ sec.; while the difference in strength is slight under long duration of stress, because the ratio is 1.47 at $t=10^{2}$ sec. The comparison of American I ($\phi=13.0$) and Takashima III ($\phi=10.0$) may suggest the fact that the American bituminous coal is of lower strength than the Japanese bituminous coal. These considerations are readily understood if one refers to the results on the Young's modulus and internal viscosity for these coals.[1][2] The detailed discussions with further experimental results will be reported in the next paper.

The authors express their thanks to Dr. M. Kurokawa and Mr. A. Baba for interest in the investigation.

Shigen-Gijyutsu-Shikenjo
(Resources Research Institute)
Saitama-Kawaguchi, Japan

Research on the Crystal Structure of R_3O_5 Type Oxides and Classification of sixfold co-ordinated Oxide Crystals

By Goro YAMAGUCHI

(Received November 7, 1952)

Introduction

The data of crystal structure of pseudo-brookite ($Fe_2O_3 \cdot TiO_2$), a natural mineral, is as follows.[1]

Pseudo-brookite $Fe_2O_3 \cdot TiO_2$ Orthorhombic

V_h^{17}=Bbmm a=9.79 kX

Z=4 b=9.93 kX

c=3.725 kX

In the previous paper,[2] the author found that $Al_2O_3 \cdot TiO_2$ and $MgO \cdot 2TiO_2$ have the same crystal structure as $Fe_2O_3 \cdot TiO_2$ (R_3O_5 type) and

Table 1

Expected Formula	Mixing Molar Ratio of Powdered Oxides	Sintering Temp. (°C.)	Time (h)	Result*
$Fe_2O_3 \cdot TiO_2$	1 : 1	1250	1	○
$Fe_2O_3SnO_2$	1 : 1	1000, 1250	1	×
$Al_2O_3 \cdot TiO_2$	1 : 1	1250, 1400	1	○
$Al_2O_3 \cdot SnO_2$	1 : 1	1000, 1250	1	×
$MgO \cdot 2TiO_2$	1 : 2	1400	1	○
$MgO \cdot 2SnO_2$	1 : 2	1250	1	×
$CoO \cdot 2TiO_2$	1 : 2	1250, 1400	1	○
$NiO \cdot 2TiO_2$	1 : 2	1250, 1400	1	×
$ZnO \cdot 2TiO_2$	1 : 2	1250	1	○
$ZnO \cdot 2SnO_2$	1 : 2	1250	1	×

* ○…the R_3O_5 type is found by X-rays.
×…the R_3O_5 type is not found.

(1) W. L. Bragg, "Atomic structure of minerals", (1937).

(2) G. Yamaguchi, *J. Ceram. Assoc. Japan*, **55**, 94, (1947).

described a clasification of sixfold coordinated oxide crystals, but, in this paper, other R_3O_5 type oxides and many examples of crystals fitted and not fitted in this classification, shall be described.

Synthetic experiment of R_3O_5 type oxides

Powdered simple oxides were mixed in a definite ratio and sintered at a constant temperature. After cooling, the sintered products were analyzed by X-ray method and their crystal structure was determined. Conditions of synthesis and the results are shown in Table 1, but these conditions are only typical examples of synthesis.

Values of latice constants

Obtained latice constants are shown in Table 2.

Table 2

	Experimental Data (spacing in kX)				Calculated Latice Const		
	d_{002}	d_{130}	d_{322}	d_{320}	a	b	c
$Fe_2O_3 \cdot TiO_2$	1.866	1.969	1.541	2.727	9.80	9.93	3.733
$Al_2O_3 \cdot TiO_2$	1.798	1.905	1.485	2.641	9.46	9.58	3.596
$MgO \cdot 2TiO_2$	1.867	1.978	1.543	2.739	9.84	9.98	3.734
$CoO \cdot 2TiO_2$	1.862	1.960	1.536	2.713	9.75	9.88	3.724
$ZnO \cdot 2TiO_2$	1.867	1.965	1.540	2.723	9.78	9.90	3.734

Table 3

Type	Positive Results	Negative Results.
RO (NaCl or MgO type)	$Li_2O \cdot Fe_2O_3$ (800)*, $Li_2O \cdot Al_2O_3$ (800), $Li_2O \cdot TiO_2$ (1000)	$Li_2O \cdot Cr_2O_3$, $Li_2O \cdot SnO_2$
R_3O_4 (spinel type)	Al_3O_4 (fused),(3) $MgO \cdot Al_2O_3$ (1250), $CoO \cdot Al_2O_3$ (1200), $NiO \cdot Al_2O_3$ (1100), $CuO \cdot Al_2O_3$ (1100), $ZnO \cdot Al_2O_3$ (1100), $MnO \cdot Al_2O_3$ (1100), $MgO \cdot Fe_2O_3$ (1250), $CoO \cdot Fe_2O_3$ (1250), $NiO \cdot Fe_2O_3$ (1250), $Li_2O \cdot 5Al_2O_3$ (800), $Li_2O \cdot 5Fe_2O_3$ (800), $MgO \cdot Cr_2O_3$ (1250), $2MgO \cdot TiO_2$ (1250), $2ZnO \cdot TiO_2$ (1250), $2MgO \cdot SnO_2$ (1250), $2ZnO \cdot SnO_2$ (1250), $2CoO \cdot SnO_2$ (1250), $CoO \cdot MgO \cdot TiO_2$ (1250) [8.43]†, $CoO \cdot ZnO \cdot TiO_2$ (1250) [8.44], $CoO \cdot MgO \cdot SnO_2$ (1250) [8.57], $CoO \cdot ZnO \cdot SnO_2$ (1250) [8.58], $NiO \cdot CoO \cdot TiO_2$ (1250) [8.40], $NiO \cdot ZnO \cdot TiO_2$ (1250) [8.40], $NiO \cdot MgO \cdot SnO_2$ (1250) [8.54], $NiO \cdot ZnO \cdot SnO_2$ (1250) [8.53], $CuO \cdot MgO \cdot TiO_2$ (1100) [8.43], $CuO \cdot CoO \cdot TiO_2$ (1100) [8.43], $CuO \cdot ZnO \cdot TiO_2$ (1000) [8.44], $MnO \cdot MgO \cdot TiO_2$ (1100) [8.46], $MnO \cdot CoO \cdot TiO_2$ (1100) [8.47], $MnO \cdot MgO \cdot SnO_2$ (1250) [8.64], $MnO \cdot CoO \cdot SnO_2$ (1250) [8.66]	$Li_2O \cdot 5Cr_2O_3$, $2NiO \cdot TiO_2$, $2NiO \cdot SnO_2$, $NiO \cdot MgO \cdot TiO_2$, $NiO \cdot CoO \cdot SnO_2$, $CuO \cdot MgO \cdot SnO_2$(?)**, $CuO \cdot CoO \cdot SnO_2$(?), $CuO \cdot ZnO \cdot SnO_2$, $2CuO \cdot TiO_2$, $2CuO \cdot SnO_2$, $MnO \cdot ZnO \cdot TiO_2$, $MnO \cdot ZnO \cdot SnO_2$, $2MnO \cdot TiO_2$,†† $2MnO \cdot SnO_2$
$RO_{4/3 \sim 3/2}$ (imperfect spinel type)	$MgO \cdot xAl_2O_3$ (sintered or fused), $CoO \cdot xAl_2O_3$ (sintered), $NiO \cdot xAl_2O_3$ (sintered), $x > 1$; $Li_2O \cdot yAl_2O_3$ (Sintered) $y > 5$	
R_2O_3 (Cr_2O_3 type)	$MgO \cdot TiO_2$ (1250), $CoO \cdot TiO_2$ (1250), $NiO \cdot TiO_2$ (1250), $(0.8NiO \cdot 0.2CoO) \cdot TiO_2$ (1250), $(0.9NiO \cdot 0.1CoO) \cdot TiO_2$ (1250)	$CuO \cdot TiO_2$, $MgO \cdot SnO_2$, $NiO \cdot SnO_2$
R_3O_5 ($Fe_2O_3 \cdot TiO_2$ type)	$Fe_2O_3 \cdot TiO_2$ (1400), $Al_2O_3 \cdot TiO_2$ (1400), $MgO \cdot 2TiO_2$ (1400), $CoO \cdot 2TiO_2$ (1400), $ZnO \cdot 2TiO_2$ (1400)	$Al_2O_3 \cdot SnO_2$, $MgO \cdot 2TiO_2$, $Fe_2O_3 \cdot SnO_2$, $MgO \cdot 2SnO_2$, $CoO \cdot 2SnO_2$, $ZnO \cdot 2SnO_2$
RO_2 (SnO_2 type)	TiO_2, SnO_2	

* ( )……one example of sintering temp. (°C) in author's experiment.

† [ ]……latice constant (kX) of spinel which is not listed in "Crystal Structure, Vol. 2" by Wyckoff.

** (?)……doubtful.

†† $2MnO \cdot TiO_2$ is listed as spinel in the Wyckoff's book.

(3) "Aluminium suboxide" G. Yamaguchi, *J. Electrochem. Assoc. Japan*, **14**, 106(1946); *J. Ceram. Assoc. Japan*, **55**, 42 (1947). *Bull. Chem. Soc. Japan*, **23**, 90 (1952)

Classification of sixfold coordinated oxide crystals and results of synthesis.—Four types of the oxide crystals (RO, R_3O_4, R_2O_3, RO_2)are known, but the author proposes to add the new type, R_3O_5, according to the results of this paper, and the imperfect spinel type ($RO_{4/3\sim3/2}$). The author's extended classification with examples of positive and negative results is as Table 3.

Result

1. Latice constants of R_3O_5 type crystals ($Fe_2O_3 \cdot TiO_2$, $Al_2O_3 \cdot TiO_2$, $MgO \cdot 2TiO_2$, $CoO \cdot 2TiO_2$, $ZnO \cdot 2TiO_2$) are determined.

2. Crystal structures of interoxide compounds of metals, whose coordination number of oxygen is six, are classified into six types; RO(NaCl or MgO type), R_3O_4 (spinel type), $RO_{4/3\sim3/2}$ (imperfect spinel type), R_2O_3 (Cr_2O_3 type), R_3O_5($Fe_2O_3 \cdot TiO_2$ type), RO_2(SnO_2 type). Between interoxide compounds of the same type, formation of solid solution is expected.

3. SnO_2 fits into this theory only in the case of spinel formation.

4. NiO and CuO have almost no acidic property, so that in the cases of formation of R_3O_4 and R_3O_5, they act peculiarly.

5. The author proposes to give the name of "definite ratio solid solution" to crystals of those interoxide compounds when metal atoms are distributed at random at latice points.

Department of Applied Chemistry,
Faculty of Engineering,
the University of Tokyo, Tokyo

LETTER

Phase Transition in the Crystals of Trimethylacetic Acid

By Yoshiyuki NAMBA, Tsutomu ODA and Hisao HAYASHI

(Received December 24, 1952)

In a previous paper,[1] it has been reported that trimethylacetic acid (pivalic acid) crystallizes in a face-centered cubic lattice, the molecules taking orientational or rotational disorder. It has been also optically observed that, on cooling the crystal, it transforms into a birefringent mass. This optical measurement is in harmony with the external observation made by Butlerow[2] who pointed out that this subs ance solidified at the ordinary temperature in a transparent mass, and that when cooled down to about 0°C. it was converted into a snow-like mass. As a continuation of our previous work dilatometric measurements on these transition phenomena and an X-ray study on the structure of the low temperature modification have been carried out.

Dilatometric measurements were made at a temperature range from −20° to 40°C., choosing mercury as the dilatometer liquid. As the result it has been found that the transition is accompanied by abrupt contraction of the volume as the temperature is lowered and occurs really at −2°C., and at 7°C, when the temperature is raised. The relative value of the volume change $\Delta V/V_{15°}$ is approximately 8% and larger than that of fusion. This fact suggests that the transition is accompanied by remarkable enhancement of molecular motion.

In order to confirm this expectation, we prepared complete rotation photographs of single crystals of the low temperature modification, using almost the same method as in the previous paper,[1] except with a cooling apparatus of the Ubbelohde-Woodward type.[3] In this case, as we expected, the intensity of reflection dose not decrease so rapidly with increasing scattering angle as in the high temperature modification. The reflections could not be indexed with the cubic lattice as reported by Butlerow.[2]

Therefore, considering the above mentioned birefringence, this modification should possess

(1) Y. Namba and T. Oda, This Bulletin, **25**, 225(1952).
(2) A. Butlerow, *Ann.*, **173**, 355 (1874).
(3) A. R. Ubbelohde and I. Woodward, *Proc. Roy. Soc.* A, **188**, 358 (1947).

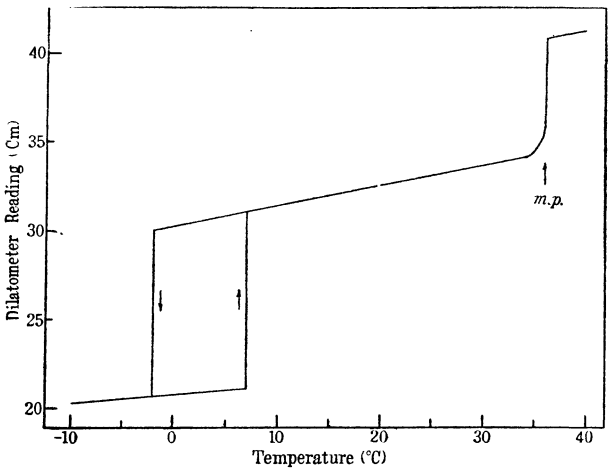

Fig. 1.—Dilatometric curve of $(CH_3)_3CCO_2H$.

a lower symmetry than cubic.

As a conclusion it may be said as ascertained that the intense molecular rotation in the high temperature modification is stopped below the transition and the molecules take an ordered arrangement, in the lattice of low symmetry.

Furthermore, the small changes in volume and entropy[4] at the fusion point indicate that the crystal above the transition temperature may be taken as a good example of organic plastic crystals.[5]

In conclusion, we wish to express our thanks to Professors I. Nitta and S. Seki of the Osaka University for their kind interest throughout this experiment and to Dr. E. Matsumura for his aid in the preparation of the materials.

Chemical Laboratory Osaka Liberal Arts University, Osaka

(4) J. Pirsch, *Ber.*, **70**, 12 (1937).

(5) J. Timmermans, *J. Chim. Phys.*, **35**, 331 (1938).

Physico-Chemical Studies on Molecular Compounds. III. Vapor Pressures of Diphenyl, 4, 4'-Dinitrodiphenyl, and Molecular Compound between Them

By Syûzô SEKI and Keisuke SUZUKI

(Received August 26, 1952)

Introduction

In a previous paper,[1] we have reported the vapor pressures of quinhydrone and of the molecular compound between hexamethylbenzene and picryl chloride. These molecular compounds (M. C.'s for brevity) are constructed with (1:1) molar ratio of the component molecules, and the benzene nuclei of them are arranged in nearly parallel positions alternately. Now, there are recently known some M. C.'s which are considerably different from those in the molecular arrangement as well as in their composition. According to James, Saunder, and others,[2] 4,4'-dinitrodiphenyl (D. N. D. for brevity) forms a number of M. C.'s with diphenyl and its derivatives. Their general type of crystal structure stands in contrast in such points as that the component molecules are packed in nearly perpendicular positions to each other and that the molar ratios differ from M. C. to M. C., giving no (1:1) molar ratios. In these respects, it will be of some interest to study the present materials in comparison with the substances already reported and also in relation to the urea-adducts[3] having some resemblance in their molecular arrangements, as well as to the molecular sieve actions of some zeolite crystals.[4]

Experimental

Apparatus.—The vapor pressures as well as the variations of composition of the solid phase as the evaporation proceeds were measured by the effusion method. The details of the apparatus were already reported in a previous paper,[5] so that its description may be omitted here.

Samples.—*Diphenyl*: The product "Zur Analyse" of Dr. Theodor Schuchart was recrystallized from glacial acetic acid solution. m. p. 69.5°~69.8°C.

D. N. D.: The material was prepared through nitration of diphenyl with fuming nitric acid, and then the product was recrystallized once from ethyl alcohol and further twice from acetone, finally being subjected to fractional sublimation under high vacuum (10^{-5} mm. Hg.) at about 120°C. m. p. 237.0°~237.5°C.

M. C. (1:3): Two acetone solutions containing diphenyl (somewhat in excess of the calculated 1:3 ratio) and D. N. D. were mixed at a little below the boiling point and then M. C. was precipitated by slow cooling of the mixture at a rate of about 10°C./hour. m. p. 194°~225°C.* The reason for such a wide range of melting process will be explained in a later section.

Results

The vapor pressures of diphenyl and D. N. D. are given in Tables 1 and 2 and illustrated in Fig. 1. The vapor pressure equations derived from them are also given in the bottoms of each table. The relation of the vapor pressures of (1:3) M. C. (vapor pressures

Table 1
Vapor Pressure Values of Diphenyl

t°C.	$P_{mm.Hg.} \times 10^3$
14.3	2.33
14.8	2.38
16.8	3.16
19.7	4.19
22.0	5.44
23.8	6.44
25.6	7.78
27.6	9.23
28.0	9.44
29.9	11.9
31.3	13.8
34.1	17.4

$$\log P = 11.003 - 3918.2/T$$
$$T = 273.14 + t$$

(1) I. Nitta, S. Seki, H. Chihara and K. Suzuki, *Sci. Papers Osaka Univ.*, No. 29 (1951).
(2) (a) W. S. Rapson, D. H. Saunder and E. T. Stewart, *J. Chem. Soc.*, **1946**, 1110; (b) D. H. Saunder, *Proc. Roy. Soc.*, **A190**, 508 (1947); (c) J. N. van Niekerk and D. H. Saunder *Acta Cryst.*, **1**, 44 (1948); (d) R. W. James and D. H. Saunder, *Proc. Roy. Soc.*, **A190**, 518 (1947).
(3) A. E. Smith, *Acta Cryst.*, **5**, 224 (1952).
(4) R. M. Barrer, *Quart. Rev.*, **3** 293 (1949).
(5) I. Nitta, S. Seki, M. Momotani and K. Sato, *J. Chem. Soc. Japan*, **71**, 378 (1950).

* Rapson et. al. 191°~221°C. see ref. (2a).

Table 2
Vapor Pressure Values of D. N. D.

t°C.	$P_{mm.Hg.} \times 10^3$
138.1	2.92
139.7	3.85
140.5	3.49
143.2	4.38
146.0	5.04
148.1	6.15
150.3	7.10
152.3	8.60
155.3	9.72

$\log P = 10.744 - 5458.2/T$

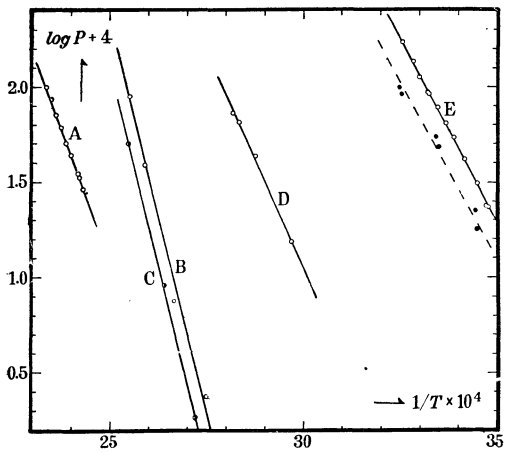

Fig. 1.—Vapor pressures of D. N. D. (A), (1:6) M. C. (B and C), (1:3) M. C. (D), and Diphenyl (E)
dotted line: Bright's values

calculated from the effusion velocity through an orifice of unit area) with the variation of effused amount are shown in Fig. 2. At relatively lower temperatures (e. g. curve (a) at 63.7°C. in the figure), the curves are composed of two regions: In the initial part, the vapor pressures are almost constant up to about 4.5% of the effused amounts, and then decrease remarkably. The position of the point B, at which the velocity begins to slow down, is more distinct at lower temperatures. But, as the temperature rises, the horizontal part (A-B) begins to incline downwards and the position of B becomes less distinct, moving to a region of somewhat smaller amounts of effusion. It is confirmed by the experiments that the material evaporated in the region (A-C) consists entirely of diphenyl. It is by the introduction of its molecular weight into the effusion equation that the vapor pressures at various stages of effusion as shown in the Fig. 2 are obtained. Extrapolating the curve to the zero point of effusion, we obtained the

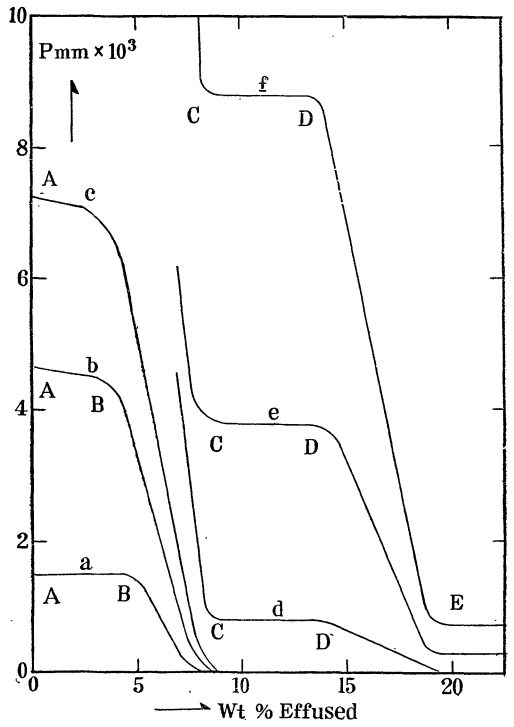

Fig. 2.—Vapor pressure change of M. C. with variation of effused amount
Experimental temperatures are as follows:
a: 63.7°C.; b: 74.5°C.; c: 79.9°C.;
d: 105.5°C.; e: 112.8°C.; f: 118.7°C.

Table 3
Vapor Pressure Values of (1:3) M. C.

t°C.	$P_{mm.Hg.} \times 10^3$
63.7	1.54
74.5	4.33
79.9	7.14
81.6	7.36

$\log P = 10.722 - 4555.9/T$

vapor pressure data of (1:3) M. C. at the initial stage of sublimation as given in Table 3 and Fig. 1. As the vapor pressure is increased by raising the temperature of the experiment, there appears another horizontal portion in the region exceeding about 8% of the effused amount. This composition is corresponding to nearly (1:6) molar ratio and the constancy of vapor pressure implies the occurence of another new sort of M. C. By the microscopic observation of the sample at this stage of effusion (8%), it is found that the original (1:3) M. C. is completely converted into another sort of woolly small crystalline aggregate, which shows a distinct melting point (m. p. 210°C.).

As is evident from Fig. 2, this horizontal

portion (C-D) is not inclined as the temperature rises and the position of point D remains always at the constant value of abscissa (13±0.5%) within the experimental error. The large portion of the material effused in the region of (C~D) is found to be diphenyl. Since the determinations of the composition of effused substances by chemical analysis is difficult on account of their small amount, we have estimated the composition of the solid phase and molecular weight of effused substances approximately in the following manner. Assuming that the partial vapor pressures of D. N. D. are equal to those of pure D. N. D. at the same temperatures, then the value of abscissa at which the diphenyl molecules contained in the solid phase is exhausted may be calculated to be 18.6% from the observed rate of effusion and original composition of (1:3) M. C, In fact, the point where the vapor pressures reach those of pure D. N. D. is found to be 18.7±0.3%, proving the adequacy of the above assumption.

On this basis, the vapor pressures of (1:6) M. C. are calculated as given in Table 4 and Figs. 1 and 2. It was found also that the vapor pressures of this M. C. are influenced by the history of their preparation. That is, the product prepared from the decomposition of fresh (1:3) M. C. shows higher vapor pressures (line B in Fig. 1 and (a) in Table 4) than those from the (1:3) M. C. stored for about a month in a desiccator (line C in Fig. 1 and (b) in Table 4). The values of thermodynamic functions derived from the vapor pressure data of all the specimens are given in Table 5.

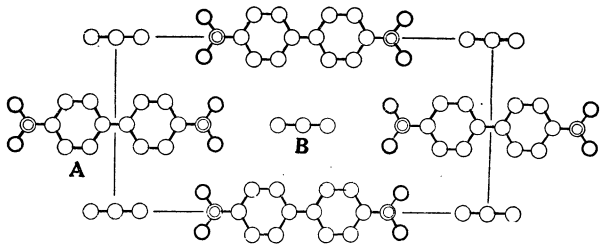

Fig. 3.—Idealized structure of a series of (1:3) M. C.
A: D. N. D. Molecules.
B: Diphenyl molecules or its derivatives.

Table 4
Vapor Pressure Values of (1:6) M. C.

(a)		(b)	
t°C.	$P_{mm.Hg.} \times 10^3$	t°C.	$P_{mm.Hg.} \times 10^3$
90.5	0.238	94.5	0.184
101.8	0.760	105.5	0.910
112.8	3.89	119.5	1.84
118.7	8.90		
$\log P = 18.361 - 8016.2/T$		$\log P = 18.987 - 8349.6/T$	

Although the final product beyond the point D shows the same Debye photograph as well as the same melting point with those of pure D. N. D., the vapor pressures are of a little higher values (not more than 5%) than the D. N. D. prepared by the ordinary method.*

Discussion

The results of vapor pressures obtained in the present investigation may be discussed first in comparison with the data already reported by other investigators. Among the substances measured by us, only the vapor pressure of diphenyl was measured by Wolf[6] and Bright.[7] The former reported merely a value of the heat of sublimation (16.4±0.2 kcal./mol.), which is considerably smaller than ours (17.9±0.4 kcal./mol.), while the heat of sublimation obtained by Bright(17.4±0.7 kcal./mol.) is in good agreement with ours, their vapor pressure values being, however, somewhat lower than ours as shown in Fig. 1.

Table 5
Enthalpy, Entropy and Standard Free Energy Changes of Sublimations*

Substances	ΔH kcal./mole	ΔS e. u./mole	$\Delta F^{298.1}$ kcal./mole
Diphenyl	17.94±0.41	37.14±1.36	6.89±0.81
(1:6) M. C. (a)	36.70±1.79	70.88±4.79	15.58±3.32
(1:6) M. C. (b)	38.23±0.70	73.75±1.86	16.24±1.25
(1:3) M. C.	20.86±0.41	35.90±1.44	10.15±0.84
D. N. D.	24.99±0.44	36.01±0.80	14.25±0.68

† The thermodynamic fuctions of M. C's are corresponding to those of their decomposition processes, in exact sense (see in the text).

* Similar facts were also found in the cases of α-quinol and picryl chloride produced by decomposition of the M. C.

(6) K. L. Wolf and H. Weghofer, *Z. Physik. Chem.* **B39**, 194 (1938).
(7) N. F. H. Bright, *J. Chem. Soc.*, **1951**, 624.

Now, we may proceed to the problems of M. C. Although the characteristic features of the crystal structure of the (1:3) M. C. were mentioned briefly in the last section, it may be desirable to explain them somewhat more in detail for the consideration of the evaporation processes. In this M. C., the D. N. D. molecules form layers in face-centered array, as shown in Fig. 3. The D. N. D. molecules A in the figure lying in this layer are so arranged that a gap is left between the nitro groups of adjacent D. N. D. molecules. By superposing such layers with a spacing of 3.5 A., these gaps will produce a set of tubular cavities, also in face-centered array, running through the whole structure. The molecules of diphenyl or its derivatives (B in Fig. 3) occupy these tubular cavities, as shown end-on in the figure. Thus the directions of the long axes of B molecules is exactly or nearly perpendicular to the layers containing D. N. D. molecules. The ratio of the number of B molecules to that of D. N. D. molecules varies from compound to compound, and depends on the length of B molecules rather than on their chemical nature, and, indeed, it has been found possible to predict the molar ratio in M. C. from a knowledge of such molecular length, indicating no localized bonding between A and B molecules. The non-integral ratio (1:3.33) of the M. C. with 4-chlorodiphenyl is the most remarkable example.[2a][2d]

Turning to the evaporation process of (1:3) M. C., we can find a situation similar to that of the two M. C.'s reported in the previous paper,[1] i. e. the preferred evaporation of the more volatile component occurs, and the vapor pressures, the compositions of gaseous as well as of crystalline phase change with the progression of evaporation. When examined in more detail, however, the behavior of the M. C.'s of the present series is different in several points. As shown in Fig. 2 the vapor pressure-composition curve has, instead of one in the cases of previously reported substances, two horizontal regions followed by more gently sloped region than the M. C.'s previously reported.

From the standpoint of phase rule considerations, the horizontal parts, the constant pressure regions, which are independent on the compositions (A-B and C-D), mean the coexistence of one gas and two solid phases, whereas the other sloping regions (B-C and D. E) mean the presence of one gas and one solid phase.

In the cases of M. C.'s reported in a previous paper[1] the evaporation of the more volatile component necessitates the collapse of the original mother crystals on account of the features of the molecular arrangements in which each of the component molecules are piled up alternately. Accordingly, when the molecules of a more volatile component evaporate, the less volatile component molecules must be separated from the original crystals and recrystallized at a considerably rapid rate. Indeed, we obtained a wider range of horizontal parts of vapor pressures in these M. C.'s, implying that adequate conditions for the coexistence of the two solid phases are realized easily.

On the other hand, in the present M. C. the selective evaporation of the more volatile component would not necessitate the collapse of the mother crystals on account of the above mentioned structural characteristics. Indeed, the first horizontal parts (A-B) do not cover so wide a region as that of the M. C. previously reported and tend to slope at higher temperatures (e. g. the curve at 79.9°C.). This sloping tendency means the formation of a solid-solution-like structure resulting from the violent thermal motions of B component molecules along the tubular cavities.

Similar curves have been found recently in the hydrogen-titanium system by A. D. Mc. Quillan.[8] In this system, the lattice structure of titanium changes, appearing in the three types of interstitial compounds of α, β and γ, as the amount of hydrogen in the solid phase increases. In the midway regions between the definite composition of these interstitial compounds, they also show a solid-solution-like behavior. As is well known, such a phenomenon is frequently observed also in the hydration process of some sorts of gels and other hydrates[9] in which so-called "vagabond waters" are contained.

The wide range of melting phenomena observed in the present (1:3) M. C. described in the second section may be attributed to the formation of a solid solution owing to the partial evaporation of diphenyl. The comparison of the ΔH value of the (1:3) M. C. in Table 4 with that of the component crystals indicates also that the interaction of each component is not greatly strengthened by the formation of M. C.

When the amounts of effusion exceed about 8% of the original weight which corresponds to the molar ratio of about (1:6), the vapor pressure again retains a constant value, implying the coexistence of the two new solid phases. The existence of this (1:6) M. C. has

(8) A. D. Mc. Quillan, *Proc. Roy. Soc.*, **A204**, 309 (1951).
(9) W. Eitel, "Physikalische Chemie der Silikate", 1941, S. 517.

not been known yet for D. N. D.-diphenyl system. Such a large deviation of molar ratio from (1:1) may be very scarce for crystalline M. C. of aromatic nitrocompound-aromatic hydrocarbon (or aromatic amine, phenol) systems.* The distinct melting point (see section 2), the invariance of the flatness of vapor pressure in the region (C-D) as well as the constancy of the position of point D at various temperatures, and the values of thermodynamic functions given in Table 3 may be looked upon as the evidences of the considerably-stable structure of this (1:6) M. C. Although its crystal structure is not yet known, the mobility of the diphenyl molecule in this (C-D) region may be supposed to be restrained more strongly than the (1:3) M. C.

It is worth while to note, however, that the free energy of (1:6) M. C. prepared from two samples of the (1:3) M. C.'s which had been preserved for different periods of time, differs somewhat in each case. For the elucidation of this ageing effect, however, a further detailed investigation will be necessary.

In conclusion the authors wish to express their sincere thanks to Professor Nitta for his gracious encouragement and suggestions during this work. The expense of this investigation was defrayed from the funds of Taniguchi Kôgyô Shôreikai as well as from the Scientific Research Expenditure Grant from the Ministry of Education to which the authors' thanks are due.

Department of Chemistry, Faculty of Science, Osaka University, Osaka

* It is known that the urea-adducts (see ref (3)), M. C. between desoxycholic acid and aliphatic long chain compounds (Y. Go and O. Kratky, *Z. Physik. Chem.*, **B26**, 439 (1934)), gas hydrate (W. F. Clanssen, *J. Chem. Phys.*, **19**, 259 (1951); H. V. Stackelberg and H. R. Muller, *Naturwiss.*, **38**, 456 (1951) **39**, 20 (1952): L. Pauling and R. E. Marsh, *Proc. Nat. Acad. Art and Sci.*, Feb (1952)) and other so-called "clathrate compounds" (D. E. Powell, H. M. Powell, *J. Chem. Soc.*, **1947**, 208; **1948** 571, 815) show such anomalous molar ratio.

On the Harkins—Jura's Adsorption Isotherm and Its Constants.

By Tomohiko SAKAKI

(Received August 27, 1952)

I. Introduction

W. D. Harkins and G. Jura[1] obtained experimentally the following equation of state for the condensed films spread on the surface of liquid:

$$\pi = b - a\sigma \tag{1}$$

where π is the surface pressure, σ is the area per molecule of the film, and b and a are constants. They also found that the above linear relationship is applicable to adsorbed films on solids.

Equation (1) can be transformed into an adsorption isotherm expressed in terms of equilibrium pressure p and adsorbed volume v_a,

$$\log_{10}\frac{p}{p_0} = B - \frac{A}{v_a^2} \tag{2}$$

with

$$A = a\Sigma^2 V^2 / 2\times 2.303 NRT \tag{3}$$

and

$$B = A/v_s^2$$

where Σ is the surface area of adsorbent, V the volume of one mole of ideal gas at N. T. P., N Avogadro number, p_0 the saturation pressure, and v_s the adsorbed volume at p_0.

Eq. (2) gives Type II isotherms which are in good agreement with the experimental curves up to $p/p_0 = 1/3$ or higher. Moreover, the surface area Σ is proportional to the square root of A;

$$\Sigma = kA^{1/2} \tag{4}$$

Harkins and Jura regarded k in (4) as being characteristic to each adsorbate and independent of the adsorbents. Thus they have given the values of k to the four kinds of vapors, calculating from their isotherms on the anatase powder the area of which had been determined

(1) W. D. Harkins and G. Jura, *J. Am. Chem. Soc.*, **66**, 1366 (1944); *J. Chem. Phys.*, **11**, 430 (1943); ibid, **11**, 431 (1943).

Table 1

The H. J. Constants

Adsorbate	Temp. (°K)	k (m.²/cc.)	A (cc./gr.)²[a]	CAT (cal./mole·1/cm.⁴)[b]	σ_0 (Å.²)[c]	CAT σ_0^2 (cal./mole)
N_2	77.4	4.01	11.8	159. $\times 10^{70}$	16.2	417
H_2O	298.	3.83	12.9	668. × 〃	10.5	734
n-C_4H_{10}	273.	13.6	1.02	48.4× 〃	32.1	499
n-C_7H_{16}	273.	16.9	0.664	31.5× 〃	45.	640

(a) The value of 13.8 m.²/gr. was used for Σ.

(b) $C=\dfrac{N^2R\ln_{10}}{V^2\Sigma^2}$

(c) The values of σ_0 for water and n-butane were calculated from the liquid densities according to B. E. T.. The value for n-heptane was determined from crystallographic data. (See Reference (1)).

by the "absolute method"[2] (Table 1). It is possible, therefore, to estimate the surface areas of solids using Eqs. (2) and (4) and Table 1 from the adsorption isotherms of these vapors on the solids, without the assumption of a molecular area of the adsorbate. This is called the "relative method" by the original authors.

There are, however, a few ambiguous points in the above-mentioned theory of adsorption. First, though Eq. (2) is considered to be applicable to multimolecular adsorption, the theoretical basis for this is not obvious. Secondly the assumption that the values of k are independent of adsorbents should be examined in more detail.

II. Thermodynamic Considerations

We shall begin by considering an adsorbed film composed of N_A molecules of the vapor adsorbed on a crystalline solid surface, having equilibrium pressure p at T°K below the critical temperature. If the same vapor has the saturation pressure p_0 in equilibrium with its liquid (or solid) at T°K, the difference in molar free energy between the film and the liquid, $\bar{F}$ is given by

$$\bar{F}=RT\ln\frac{p}{p_0} \qquad (5)$$

On the other hand $\bar{F}$ is formally written as

$$\bar{F}=(H_A-E_L)-T\bar{S} \qquad (6)$$

where H_A is the molar differential enthalpy of adsorption, E_L the enthalpy of condensation per mole, and S the difference in the molar entropy between the two states.

From (5) and (6) we get

$$\ln\frac{p}{p_0}=-\frac{\bar{S}}{R}+\frac{1}{RT}(H_A-E_L) \qquad (7)$$

Now H_A is the function of the adsorbed amount N_A, the form of which is determined experimentally. When $p\to p_0$, $H_A\to E_L$; hence $\bar{S}$ is a function of N_A as well, and approaches zero as p tends to reach p_0. If H_A and $\bar{S}$ are expressed as functions of N_A, $H_A(N_A)$ and $\bar{S}(N_A)$, the observed isotherm is

$$\ln\frac{p}{p_0}=-\frac{\bar{S}(N_A)}{R}+\frac{1}{RT}\{H_A(N_A)-E_L\} \qquad (8)$$

For convenience, introducing v_a in place of N_A,

$$v_a=V\cdot N_A/N.$$

Eq. (8) can be written as

$$\ln\frac{p}{p_0}=-\frac{\bar{S}(v_a)}{R}+\frac{1}{RT}\{H_A(v_a)-E_L\} \qquad (9)$$

The dimensional consideration leads to the fact that H_A and $\bar{S}$ are the functions of degree of coverage, θ, given by

$$\theta=N_A/N_0$$

where N_0 is the number of molecules adsorbed on the surface when it is covered with a complete monomolecular layer. Thus Eq. (8) is rewritten as

$$\ln\frac{p}{p_0}=-\frac{\bar{S}(\theta)}{R}+\frac{1}{RT}\{H_A(\theta)-E_L\} \qquad (10)$$

When the degree of coverage reaches θ, the work required to evaporate all the molecules of the film is

(2) W. D. Harkins and G. Jura, *J. Am. Chem. Soc.*, **66**, 1362 (1944).

Table 2

The Enthalpy Functions in the System of H_2O-Anatase

Range	Integral Enthalpy, h_a	Molar Differential Enthalpy, H_A
v_a, 0.68—3.25 cc./gr. p/p_0, 0 —0.10 〃	$h_{a1}=-0.461(v_a)^{5/8}+\frac{v_a}{V}E_L$ Eq. (13)	$H_{A1}=-6460(v_a)^{-3/8}+E_L$ Eq. (16)
v_a, 2.09—6.16 〃 p/p_0, 0.02—0.55 〃	$h_{a2}=-1.446+\frac{1.50}{v_a}+\frac{v_a}{V}E_L$ Eq. (14)	$H_{A2}=-\frac{33600}{v_a^2}+E_L$ Eq. (17)
v_a, 6.16—∞ 〃 p/p_0, 0.55—1.00 〃	$h_{a3}=-1.315+\frac{0.634}{v_a}+\frac{v_a}{V}E_L$ Eq. (15)	$H_{A3}=-\frac{14200}{v_a^2}+E_L$ Eq. (18)

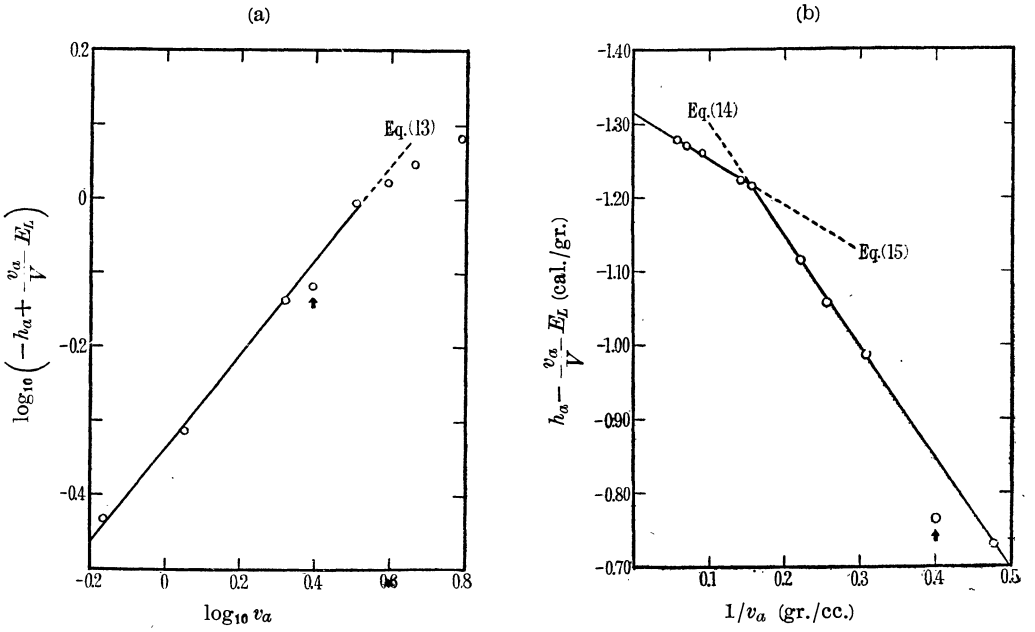

The arrowed point $\left(v_a=2.49\text{ cc./gr.},\ h_a-\frac{v_a}{V}E_L=0.762\text{ cal./gr.}\right)$ lies neither on the line of (a) nor on that of (b).

Fig. 1.—The Variation of the Integral Enthalpy of Adsorption with v_a in the System of H_2O—Anatase

$$F_a=\frac{1}{N}\left\{-T\int_0^{N_A}\bar{S}(N_a/N_0)dN_A+\int_0^{N_A}H_A(N_A/N_0)dN_A+KN_A\right\} \quad (11)$$

where K is a constant.

By definition the surface pressure of the film is given by

$$\pi=-\left(\frac{\partial F_a}{\partial \Sigma}\right)_{T,\,N_A}=-\frac{1}{\sigma_0}\left(\frac{\partial F_a}{\partial N_0}\right)_{T,\,N_A} \quad (12)$$

π is calculated from the isotherm, using Eqs. (11) and (12).

III. The Isotherm and Heats of Adsorption in the System of H_2O—Anatase

Harkins and Jura[3] measured the heats of immersion into water of the anatase samples, on which various quantities of water vapor had been adsorbed. The integral enthalpies, h_a's, of this case are known from the results of this experiment.

The formulae listed in column 2 of Table 2 correctly represent the original data[4] written in terms of cals. per one gram of the adsorbent as illustrated in Fig. 1 (a) and (b). The variation of the molar differential enthalpy H_A with v_a, derived from these formulae, are

(3) W. D. Harkins and Jura, *J. Am. Chem. Soc.*, **66**, 919 (1944).

(4) Table I in the reference (3).

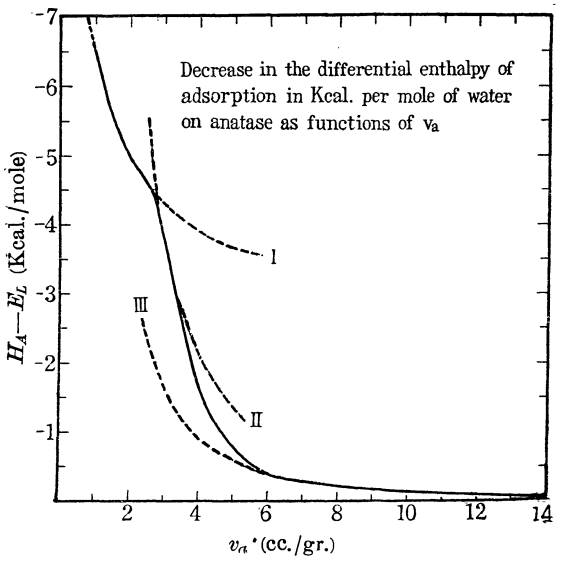

Fig. 2.

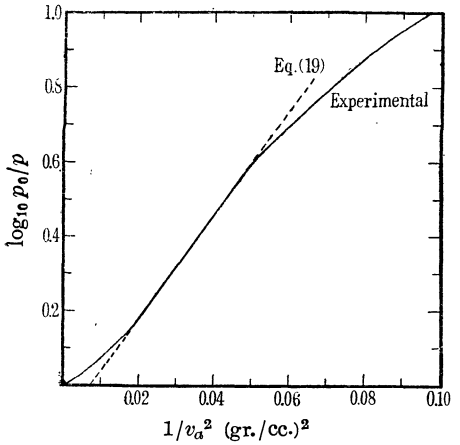

Fig. 3.—The Adsorption Isotherm of H_2O on Anatase Plotted According to H. J.

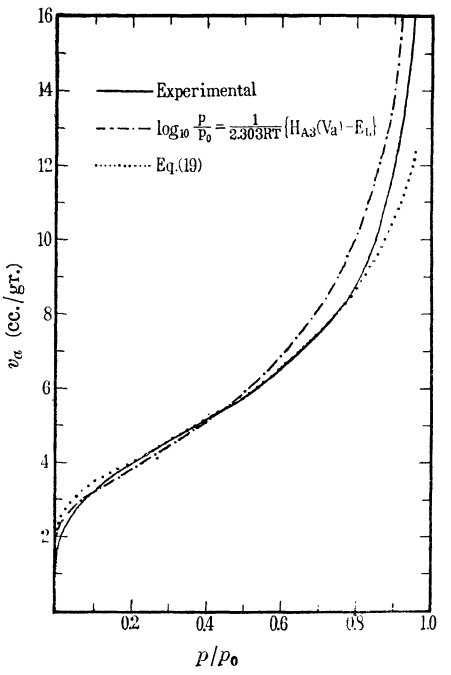

Fig. 4.—Adsorption Isotherm of Water on Anatatse at 25°C.

shown in Fig. 2 and column 3 of Table 2. In Fig. 2, curve I represents $H_{A1}(v_a)$, curve II $H_{A2}(v_a)$ and curve III $H_{A3}(v_a)$, respectively. It is to be noted that Eq. (13) is very similar to the empirical formula suggested by Lamb and Coolidge[5] on the integral heats of adsorption of various organic vapors on charcoal. As v_a is increased, $-H_{A1}(v_a)$ decreases slowly towards E_L, whereas $-H_{A2}(v_a)$ and $-H_{A3}(v_a)$ rapidly decrease and asymptotically approach E_L.

It seems that $H_{A1}(v_a)$ represents the change of H_A in the process of packing the first layer, $H_{A3}(v_a)$ in the formation of the higher layers and $H_{A2}(v_a)$ in the intermediate state. In Fig. 2 the full line gives the variation of H_A through the whole region in a smooth curve.

In Fig. 3 are presented the adsorption data[6] of water vapor on one gram of the anatase sample at 25°C. plotted according to the original authors. The straight line is obtained in the relative pressure range 0.3—0.7 (v_a varies in this region from 4.7 to 7.4 cc./gr.). We obtain as the H. J. isotherm in this case,

$$\log_{10}\frac{p}{p_0}=0.070-\frac{12.9}{v_a^2} \qquad (19)$$

while, inserting $H_{A3}(v_a)$ of (18) to (9), we get

$$\ln\frac{p}{p_0}=-\frac{\bar{S}(v_a)}{R}-\frac{1}{RT}\cdot\frac{14200}{v_a^2}$$

or

$$\log_{10}\frac{p}{p_0}=-\frac{\bar{S}(v_a)}{4.58}-\frac{10.4}{v_a^2} \qquad (20)$$

By comparing (19) and (20), it may be concluded that the general tendency of the adsorption is mainly determined by the enthalpy part of the isotherm in the medium region of relative pressure. That the function $H_{A3}(v_a)$ is adopted instead of $H_{A1}(v_a)$ and $H_{A2}(v_a)$, is because it not only represents the actual enthalpy change in the medium the higher

(5) A. B. Lamb and A. S. Coolidge, *J. Am. Chem. Soc.*, **42**, 1146 (1920).

(6) W. D. Harkins and G. Jura, *J. Am. Chem. Soc.*, **66**, 1356 (1944).

pressure regions but also reflects the outline of the whole isothermal variation as shown in Fig. 4.

IV. The Harkins—Jura's Theory and the Constants in Their Isotherm

In the case of the water vapor—anatase system, it has been found that $H_A - E_L$ is inversely proportional to v_a^2 in the later stage of adsorption, and that it determines the outline of the isotherm. If it is admitted that these conclusions generally apply to the H. J. type isotherms, a reasonable solution to the questions raised at the beginning of this paper is obtained.

(i) Multimolecular Adsorption and H_A (v_a).—We have in general

$$\log_{10}\frac{p}{p_0} = -\frac{\bar{S}(v_a)}{2.303R} + \frac{1}{2.303RT}\{H_A(v_a) - E_L\} \quad (21)$$

According to the above viewpoint, we put

$$H_A(v_a) - E_L = -K_n/v_a^2 \quad (22)$$

where K_n is a constant.

Provided that the first term of the right-hand side of (21) is neglected, the fact that the H. J. isotherm contains the inverse square term of v_a is necessarily ascribed to the form of H_A (v_a) given by (22).

Eq. (22) suggests the picture on the potential field in the neighbourhood of the adsorbent surface, namely in the early stage of adsorption the molecules are settled in the deep potential near the surface, while as the adsorption proceeds the packing of the molecules is gradually extended to the place of flattened potential further from the surface and finally those occupying the furthest sites evolve only the heat of condensation. These situations are characteristic of the multimolecular adsorption, and are roughly reflected on the form of H_A (v_a) in Eq. (22). We may hence deduce the conclusion that this form of $H_A(v_a)$ and consequently the H. J. isotherm are peculiar to the multimolecular adsorption.

Generalizing Eq. (2), we have the following isotherm,

$$\log_{10}\frac{p}{p_0} = B - \frac{A}{v_a^n} \quad (23)$$

where n is a constant.

The second term of the right-hand side of (23) seems to be of an adequate form to represent the variation of the enthalpy part in the later stage of adsorption. On account of this the similar interpretations can be applied to this case.

(ii) The H. J. Constants and the "Relative Method".—As mentioned in Sec. II, the differential enthalpy is essentially the function of θ. Introducing v_m in place of N_0,

$$v_m = V\frac{N_0}{N}$$

Thus (22) is rewritten as

$$H_A(\theta) - E_L = -K_m(v_m/v_a)^2 \quad (24)$$

where K_m is the constant equal to K_n/v_m^2.

If we recall the preponderance of the enthalpy part in the medium pressure region, we put

$$\frac{A}{v_a^2} \approx \frac{1}{2.303RT}\{-H_A(\theta) + E_L\} \quad (25)$$

where A is the constant in Eq. (2).

As v_m is given by $V N_0/N$ or $V\Sigma/N\sigma_0$*, (24) and (25) give

$$A \approx \frac{K_m}{2.303RT}\frac{V^2\Sigma^2}{N^2\sigma_0^2} \quad (26)$$

Since Σ is naturally common for the same adsorbent, AT is expected to be proportional to K_m/σ_0^2, and $AT\sigma_0^2$ to K_m, provided that (25) is valid. It is seen from column 5 of Table 1 that the order of magnitude in AT is reverse to the size of molecule, i. e., water > nitrogen > n-butane > n-heptane. This is quite natural, so far as AT is inversely proportional to σ_0^2. In column 6 are shown the probable values of σ_0 at the temperatures listed in column 2. Eq. (24) indicates that K_m is the excess molar differential enthalpy at $v_a = v_m$, so that the polyatomic molecules or the molecules having large dipole moment should have great values of K_m. This is the same with $AT\sigma_0^2$, regarded as to be proportional to K_m. The result given in the last column is just as expected; the order in $AT\sigma_0^2$ is water > n-heptane > n-butane > nitrogen.

v_a in Eq. (2) remains definite at $p = p_0$ unless B is zero. In Fig. 4, however, the experimental curve increases towards infinity as p approaches p_0, though B is determined as 0,070 in this case. Hence it is to be noted that B is not always equal to the actual value of A/v_s^2.

* σ_0 is the area per molecule at $N_a = N_0$, given by Σ/N_0.

From the above point of view, it is possible to give a support to the "relative method". Provided that "heats of adsorption (of a vapor) seem to be roughly the same whether the adsorbent is charcoal, a metal or an oxide[7]", K_m is a peculiar constant to the vapor and independent of adsorbents, so that, roughly speaking, the constant k of (4) depends solely on the kind of vapors at a definite temperature. This is consistent with the original authors' viewpoint.

(iii) The Two-Dimensional Equation of State.—If the contributions of the entropy term to the free energy of the film is ignored according to the results in (i) and (ii), the work required to evaporate N_a adsorbed molecules into the vapor phase can be approximated by the energy of desorption of the film, q_a, in the medium pressure region.

From (24), we have

$$H_A(\theta)-E_L=-K_m(v_m/v_a)^2$$
$$=-K_m(N_0/N_A)^2$$

The corresponding h_2, which has the integrated form of H_A, is written as

$$-h_a=\frac{N_A}{N}E_L+k_2-k_1\frac{N_0^2}{N_A} \qquad (27)$$

where k_2 and k_1 are constants.

Thus q_a is given by

$$-q_a=\frac{N_A}{N}Q_L+k_2-k_1\frac{N_0^2}{N_A} \qquad (28)$$

(7) S. Brunauer, "The adsorption of Gases and Vapors", Vol. I, p 240, Princeton University Press, Princeton, N. J. (1945).

where Q_L is the molar heat of condensation. Provided that the right-hand side of (27) or (28) is composed of a power series of N_0^n/N_A^{n-1}, we can put

$$k_2=k_3N_0$$

where k_3 is a constant.

Hence we obtain

$$-F_a\approx\frac{Q_L}{N}N_A+k_3N_0-k_1\frac{N_0^2}{N_A} \qquad (29)$$

Substituting (29) into (12), we reach the equation of state from which Harkins and Jura started,

$$\pi\approx b-a\sigma$$

with

$$b=k_3/\sigma_0$$
$$a=2k_1/\sigma_0^2.$$

V. Acknowledgement

The author is grateful to Prof. Isamu Sano of this Institute for his interest and encouragement. He is also indebted to Dr. Yutaka Miyahara of this Instisute, to Dr. Keizo Suzuki of Gifu University, and to Dr. Yuzuru Ôshika of Kobayashi Institute of Physical Research, for their helpful advice. The cost of this research has been defrayed from the Scientific Research Grant of the Ministry of Education.

Chemical Institute, Faculty of Science,
Nagoya University, Chikusa,
Nagoya, Japan

Equilibrium of the CO_2-NH_3-Urea-H_2O System under High Temperature and Pressure. III. Effect of Water Added on Liquid-Vapor Equilibrium

By Schôhachi KAWASUMI

(Received August 28, 1952)

It was found by Fichter and Becker[1] experimentally in 1911 that the initial presence of water has a strongly depressing influence on the conversion of ammonium carbamate to urea. This fact was later substantiated by several investigators. To date no one, however, has satisfactorily shown the effect of water added to ammonium carbamate on the liquid-vapor equilibrium of the system. The present paper covers a study of the variation

(1) Fichter and Becker, *Ber.*, **44**, 3473 (1911).

of the equilibrium pressure, the liquid and vapor compositions and densities with an increase in the amount of water in the original charge.

Measurements were begun after heating the system at 160°C. for 20 to 24 hours. Since the equilibrium of the system is dependent on the weight of the carbamate in a given reaction volume as reported in the previous paper,[2],[3], experiments were conducted in which the initial loading density of ammonium carbamate (D) was 0.60 g./cc. Mole ratio of water added to ammonium carbamate (W) was varied from 0.20 to 1.00. Consequently the total loading density including water added is over 0.60 g./cc.

Experimental Results and Discussion

Equilibrium Pressure: Results of investigation of the effect of water added on the equilibrium pressure which was measured from the carbamate side of the reaction and also from the urea and water side by means of an apparatus reported in the previous paper[2] are shown graphically in Fig. 1. The figure shows the equilibrium pressure

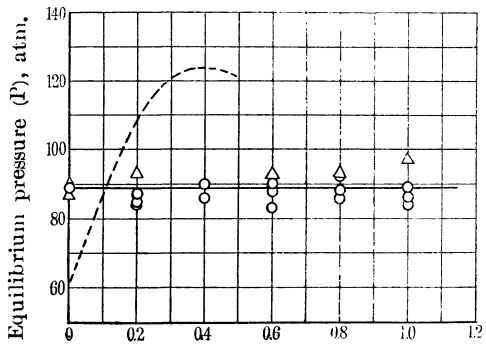

Fig. 1.—Effect of water added to ammonium carbamate on the equilibrium pressure

Curve	Investigator	Temp. °C.	Initial Content
----	Krase and Gaddy[4]	150	Carbamate and Water
——	Present Measurement at D=0.60 g./cc.	160	○ Urea and Water △ Carbamate and Water

to be approximately constant independent of mole ratio of water added to ammonium carbamate and of the kinds of starting materials within the experimental error. Only a study of the effect of water on the equilibrium pressure has been performed by N. W. Krase and V. L. Gaddy.[4] They showed that an increase in the percentage of water is accompanied by an increase in the total pressure of the charge as shown in Fig. 1, and gave a possible explanation that it is because of an increase in partial pressure of carbon dioxide as an increased percentage of ammonia was removed from the vapor phase on account of its greater solubility in water with increasing amount of water added. It is impossible to criticize their experiments since they made no reference to the apparatus and method of pressure measurement. Accordingly, the discrepancy between the two experimental results is obscure.

Vapor- and Liquid-Compositions: The effects of water added to the system on mole ratios (R' and S') of ammonia and water, respectively, to carbon dioxide in the vapor phase and on mole ratio (R) of unconverted ammonia to carbon dioxide in the liquid phase, measured by the methods reported in the previous paper,[3] are shown in Fig. 2 and 3 respectively. Both the

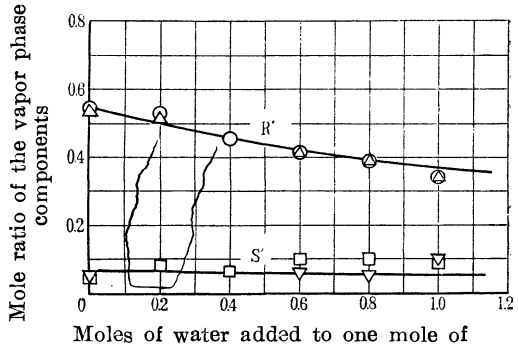

Fig. 2.—Effect of water added to ammonium carbamate on the vapor composition at 160°C. and D=0.60 g./cc.

Symbol	Initial Content	Mole Ratio
○	Urea and Water	Ammonia to Carbon Dioxide (R')
△	Carbamate and Water	
□	Urea and Water	Water to Carbon Dioxide (S')
▽	Carbamate and Water	

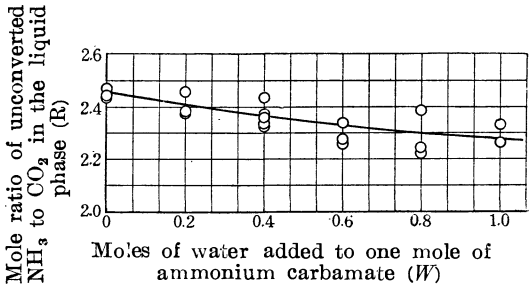

Fig. 3.—Effect of water added to ammonium carbamate on the liquid composition at 160°C. and D=0.60 g./cc.

(2) S. Kawasumi, This Bulletin, **24**, 148 (1951).
(3) S. Kawasumi, ibid., **25**, 227 (1952).
(4) N. W. Krase and V. L. Gaddy, *J. Ind. Eng. Chem.*, **14**, 611 (1922).

vapor- and the liquid-compositions become richer in carbon dioxide with the increase of mole ratio (W) of water added to ammonium carbamate, and mole ratio (S') of water to carbon dioxide in the vapor phase is approximately constant independent of the amount of water added.

Equilibrium Yield of Urea: It is evident that added water causes the equilibrium yield of urea to fall off, so that the best yield is obtained with pure ammonium carbamate. The results of the present study of the relation between the equilibrium yield of urea (Y) and mole ratio (W) of water added to ammonium carbamate are shown in Fig. 4 together with the results of other investigators.[4],[5],[6].

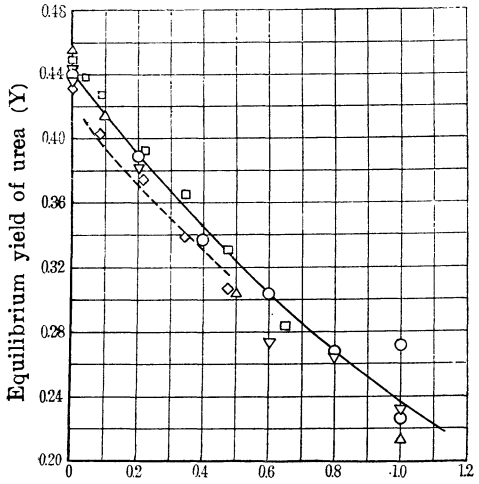

Fig. 4.—Effect of water added to ammonium carbamate on the equilibrium yield of urea

Symbol	Investigator	Initial content	Temp., °C.	D, g./cc.
—○—, —▽—	Present measurement	Urea and water; Carbamate and water	160	0.60
△	Kitawaki, Hori and Shimoda[6]		160	0.65
◇	M. Tokuoka[5]		150	0.50
□	M. Tokuoka[5]		150	0.90
------	Krase and Gaddy[4]		150	—

Volume of Liquid Phase: The relation between percentage of volume of the liquid phase, which was measured by the method reported in the previous paper,[3] and mole ratio (W) of water added to ammonium carbamate is shown in Fig. 5. The liquid volume increases linearly from 48.0% to 61.0% by the addition of one mole of water to one mole of ammonium carbamate.

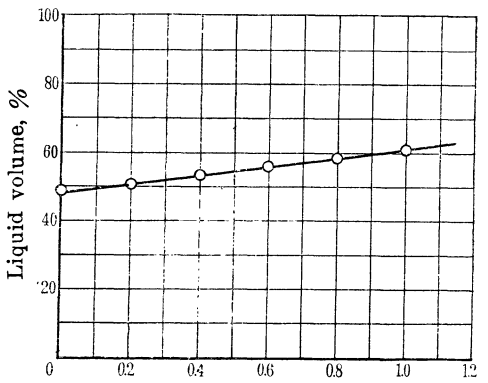

Fig. 5.—Relation between liquid volume and water added at 160°C. and $D=0.60$ g./cc.

Effect of Water on Liquid-Vapor Equilibrium Compositions

The liquid-vapor equilibrium compositions at 160°C. and $D=0.60$ g./cc., which were calculated from the above-mentioned data on the same assumption and by the same method

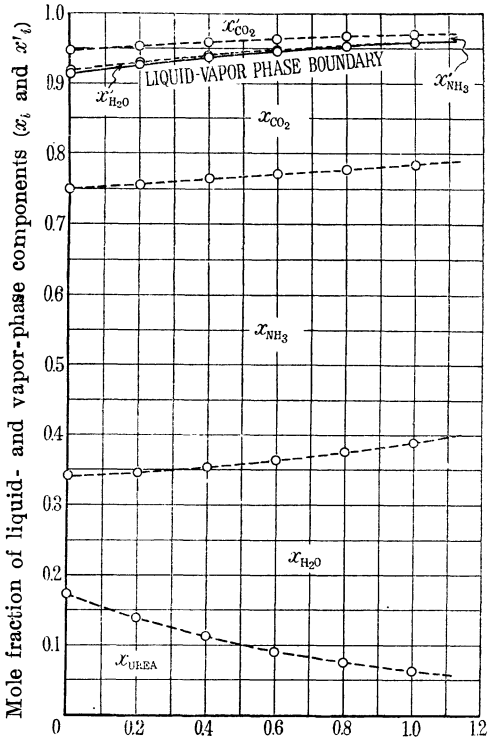

Fig. 6.—Liquid-vapor equilibria diagram of the CO_2-NH_3-Urea-H_2O system in the presence of water added.
(Temp. = 160°C. and $D=0.60$ g./cc.)

(5) M. Tokuoka, *J. Agr. Chem. Soc. Japan*, **10**, 1333 (1934), ibid. **11**, 107 (1935), ibid. **11**, 174 (1935).
(6) Kitawaki, Hori and Shimoda, *Bull. Gov. Chem. Ind. Res. Inst. Tokyo*, **32**, No. 6 and 10 (1937).

Table 1

Effect of Water Added to Ammonium Carbamate on Liquid and Vapor Phase Compositions in Equilibrium State at 160°C. and D=0.60 g./cc. (c=7.685 mole/l.)

W, mole water/mole carbamate			0	0.20	0.40	0.60	0.80	1.00
P, atm.			89	89	89	89	89	89
R'			0.547	0.500	0.460	0.425	0.395	0.370
S'			0.066	0.062	0.060	0.057	0.056	0.054
R			2.460	2.410	2.365	2.330	2.300	2.275
Y			0.442	0.390	0.345	0.304	0.268	0.237
Equilibrium Concentration,	mole/l.	n'_{CO_2}	1.031	1.006	0.964	0.927	0.886	0.847
		n'_{NH_3}	0.564	0.503	0.444	0.394	0.350	0.313
		n'_{H_2O}	0.068	0.062	0.058	0.053	0.050	0.046
		n_{CO_2}	3.257	3.682	4.070	4.422	4.740	5.016
		n_{NH_3}	8.012	8.873	9.624	10.304	10.902	11.413
		n_{Urea}	3.397	2.997	2.651	2.336	2.059	1.822
		n_{H_2O}	3.329	4.472	5.667	6.894	8.157	9.461
	mole fraction	N'_{CO_2}	0.620	0.640	0.658	0.674	0.690	0.702
		N'_{NH_3}	0.339	0.320	0.303	0.287	0.272	0.260
		N'_{H_2O}	0.041	0.040	0.039	0.039	0.038	0.038
		N_{CO_2}	0.181	0.184	0.185	0.185	0.183	0.181
		N_{NH_3}	0.445	0.443	0.437	0.430	0.422	0.412
		N_{Urea}	0.189	0.150	0.120	0.097	0.080	0.066
		N_{H_2O}	0.185	0.223	0.258	0.288	0.315	0.341
d', g./cc.			0.109	0.109	0.108	0.110	0.110	0.111
d, g./cc.			1.131	1.133	1.139	1.132	1.135	1.139
K_{N_1}			0.974	0.926	0.876	0.817	0.773	0.733

as reported in the previous paper,[3] are shown in Table 1. A plot of mole fraction (x_i and x'_i) of components in the two phases against mole ratio (W) of water added to ammonium carbamate is drawn in Fig. 6. From these results, it has become evident that a large percentage of water added to the system exists in the liquid phase, and consequently the volume of the liquid phase increases with an increase of the amount of water added. It may be concluded that the constancy of the equilibrium pressure independent of the amount of water added to the system is because of a decrease in total mole of components in the vapor phase on account of their greater solubility in water as well as of a decrease in the volume of the vapor phase with an increase of the amount of water added.

The equilibrium constants K_{N_1} of the following reaction represented by mole fraction N_i

$$CO_2+2NH_3 \rightleftarrows CO(NH_2)_2+H_2O \qquad (1)$$

$$K_{N_1}=\frac{N_{Urea}N_{H_2O}}{N_{CO_2}N^2_{NH_3}}$$

are shown in the last line of Table 1. As the values of K_{N_1} show a tendency to decrease gradually with an increase of water added to the system at a given temperature, K_{N_1} is not an equilibrium constant in the true sense of the term. The equilibrium constant should be calculated on the other assumption and discussed from the other stand-point.

Liquid- and Vapor-Density

Results of calculation of the liquid- and vapor-density (d and d') at 160°C. and over the range of mole ratio (W) from 0.20 to 1.00 of water added to ammonium carbamate are shown in Table 1. Both densities are approximately constant independent of the amount of water added. In general, the vapor-density increases linearly with the rise of pressure as shown in the previous paper.[3] Therefore, the constancy of the equilibrium pressure independent of the amount of water added will also be reasonable from the results of calculation of the vapor-density, since it undergoes little change by the addition of water.

Summary

(1) The effect of water added to ammonium

carbamate on liquid-vapor equilibrium of the CO_2-NH_3-Urea-H_2O system was investigated at 160°C. and a loading density of ammonium carbamate 0.60 g./cc. and over the range of mole ratio from 0.20 to 1.00 of water added to ammonium carbamate.

(2) The equilibrium pressure is approximately constant independent of the amount of water added within the range of the experimental conditions. Both the vapor- and the liquid-compositions become richer in carbon dioxide, and the equilibrium yield of urea decreases with an increase of the amount of water added.

(3) The results of calculation of the compositions and densities of the liquid- and the vapor-phases in the equilibrium state when water ranging from 0.20 to 1.00 mole was added to one mole of ammonium carbamate have been shown.

Research Department, Niihama Works,
Nissin Chemical Co., Ltd., Niihama.

Equilibrium of the CO_2-NH_3-Urea-H_2O System under High Temperature and Pressure. IV. Effect of Loading NH_3-CO_2 Mole Ratio on Equilibrium Pressure and Vapor Composition

By Schôhachi KAWASUMI

(Received August 28, 1952)

In 1918 Fichter, Steiger and Stanisch[1] found ammonia to exert a beneficial influence for the formation of urea from ammonium carbamate only when moderate amounts were used in their experiment in which they heated ammonium carbamate with ammonia. H. J. Krase and V. L. Gaddy[2] later obtained the yield of urea of 80 to 85% calculated on ammonium carbamate initially charged in the presence of as much as 300% excess ammonia at a temperature of 155°C. They explained that an excess amount of ammonia over that combined as carbamate acts as a dehydrating agent, removing the water from the active mass, thus preventing its reaction with urea and thereby shifting the equilibrium toward the urea side. They found also that an excess amount of carbon dioxide added to carbamate exerts no such effect. In the same way, Hori and Ogami[3] investigated the yield of urea in the presence of excess ammonia over the temperature range from 130° to 180°C. and found excellent agreement with the mass law according to the equation:

$$CO_2+2NH_3 \rightleftharpoons CO(NH_2)_2+H_2O \quad (1)$$

However, the equilibrium constant of the equation (1) employed by them was represented by mole fraction derived from the initial loading composition and the yield of urea without distinction between the liquid- and vapor-compositions. It is evident that the liquid-vapor phase equilibrium of the system is dependent upon the loading density of the initial content in the reaction vessel in the presence of excess ammonia or carbon dioxide as well as in the stoichiometrical loading mole ratio of $2NH_3$ to $1CO_2$.[4]

No one, to my knowledge, has shown the effect of excess ammonia or carbon dioxide added to ammonium carbamate on the liquid and vapor phase equilibrium. The effects of the variation of the loading mole ratio of ammonia to carbon dioxide over the range from 1.60 to 3.40 on the equilibrium pressure and the composition of the vapor phase are described in this paper.

Experimental Procedure

The equilibrium pressure and the composition of the vapor phase were respectively determined

(1) Fichter, Steiger and Stanisch, *Verhandl. Naturforsch. Ges. Basel*, **28**, II, 66 (1918); *Chem. Abst.*, **14**, 540 (1920).

(2) H. J. Krase and V. L. Gaddy, *J. Am. Chem. Soc.*, **52**, 3088 (1930).

(3) Hori and Ogami, *J. Soc. High Pressure Gas Ind. Japan*, **6**, 256 (1942).

(4) S. Kawasumi, This Bulletin, **24**, 148 (1951).

with the methods reported in the previous papers[4][5] after heating the reaction vessel at 160°C. for 20 to 24 hours. The starting materials were prepared by loading ammonium carbamate or equi-molar urea and water into the reaction vessel with a constant loading density of 0.60 g./cc., followed by the addition of the required amounts of liquid ammonia or solid carbon dioxide to it by the procedure described below. Consequently, the total loading density including excess liquid ammonia or solid carbon dioxide was more than 0.60 g./cc. The amount of liquid ammonia and solid carbon dioxide added to one mole of carbamate ranged from 0.10 to 1.40 moles and from 0.10 to 0.25 moles, respectively. In other words, the range of the loading mole ratio of ammonia to carbon dioxide covered in the present study was 1.60 to 3.40.

Procedure for Loading Liquid Ammonia:—Loading of excess liquid ammonia was accomplished by a special method measuring its weight directly without such a steel weighing pipette as employed by Krase and Gaddy,[2] or steel bomb equipped with a liquid level indicator in order to measure its volume as usually employed. Ammonium carbamate or equi-molar urea and water was weighed out accurately in a glass beaker, as large as the reaction vessel can hold as shown in Fig. 1, which was put on the left pan

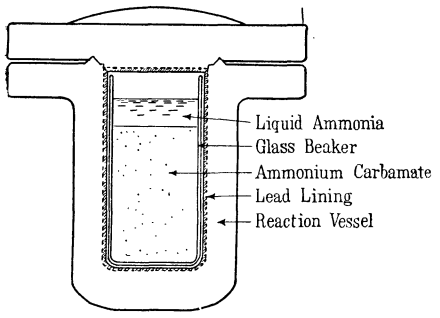

Fig. 1.—Experimental apparatus.

of the balance. After the balance weight equivalent to the required amount of liquid ammonia to be added to carbamate was put on the right pan, liquid ammonia withdrawn previously from its bomb in an open vessel was poured on the above content in the glass beaker on the left pan. Since the vaporisation of ammonia initially charged induces the cooling of the glass beaker and its content due to the latent heat of the vaporisation, it is possible to charge a required amount of liquid ammonia, accurately, into the beaker. This mixture was introduced into the reaction vessel together with the beaker, and then the vessel was closed as quickly and securely as possible, to prevent the loss of material by leakage. If the procedure was finished within a few minutes, only a negligibly small quantity of gaseous ammonia was lost during the above manipulation.

Procedure for Loading Solid Carbon Dioxide:—A required quantity of solid carbon dioxide was weighed out and then as soon as it was introduced into the reaction vessel in which ammonium carbamate was previously charged, the reaction vessel was closed as quickly as possible.

Experimental Results and Discussion

Relation between Equilibrium Pressure and Loading Composition:—The effect of the loading mole ratio of ammonia to carbon dioxide (L) on the equilibrium pressure (P) has been investigated at a temperature of 160°C. from several starting materials, which were prepared by adding liquid ammonia or solid carbon dioxide respectively to ammonium carbamate only, an equi-molar mixture of urea and water, or an equi-molar mixture of carbamate, urea and water which were loaded at a constant density of 0.60 g./cc. in each case.

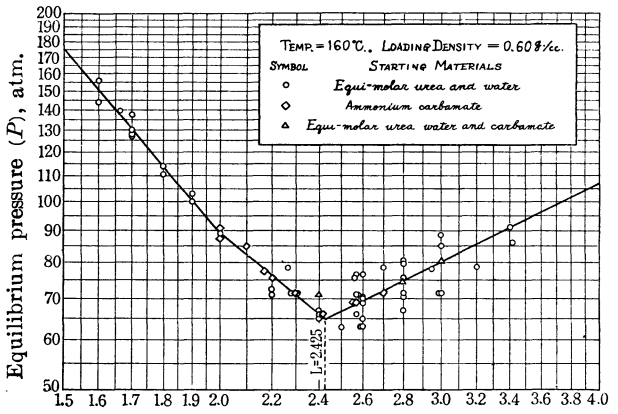

Fig. 2.—Equilibrium pressure of the CO_2-NH_3-Urea-H_2O system in the presence of excess ammonia or carbon dioxide at 160°C.

The results of these experiments are shown by three straight lines as a plot of the logarithm of P against the logarithm of L in Fig. 2. The equilibrium pressure rises up with increasing the excess amount of carbon dioxide and it reaches 150 atmospheres at a loading mole ratio $L=1.60$. No one, to my knowledge, has shown the relation between P and L, and yet it has usually been conjectured that the same pressure rise may be observed with increasing the excess amount of ammonia.

(5) S. Kawasumi, This Bulletin, **25**, 227 (1952).

Dr. S. Kodama,[6] Professor of Kyoto University, however, suggested three years ago that the equilibrium pressure had a tendency to decrease with excess ammonia, when it was added to ammonium carbamate, to the minimum. The present measurements at 160°C. have also shown the system definitely to exert the minimum pressure at a loading mole ratio $L=2.43$. The reason why the minimum pressure is caused by the addition of excess ammonia is explained in the following section. The results of these experiments are represented by three empirical equations as shown in Table 1. A discontinuous point at a loading mole ratio of $2NH_3$ to $1CO_2$, where only carbamate or equi-molar urea and water were initially loaded in the reaction vessel, may possibly be attributed to the fact that the total loading density is minimum at this point.

Table 1

Empirical Equations for the Equilibrium Pressure of the CO_2-NH_3-Urea-H_2O System in the Presence of Excess Ammonia or Carbon Dioxide at 160°C. and $D=0.60$ g./cc.

Range of L	Empirical Equation
1.60—2.00	$P=459.5\,L^{-2.372}$
2.00—2.43	$P=273.4\,L^{-1.618}$
2.43—3.40	$P=26.75\,L$

where P= pressure, atm. and L= loading mole ratio of NH_3 to CO_2

Relations between the equilibrium pressure and the loading composition over the temperature range from 130° to 190°C. are shown in Fig. 3. These experiments were performed with the initial mixtures of equi-molar urea and water and excess ammonia. The loading mole ratio of ammonia to carbon dioxide at which the system exerts the minimum equilibrium pressure varies from 2.4 to 2.5 with the rise of temperature from 130° to 190°C. as indicated by a broken line in Fig. 3.

Relation between Vapor Composition and Loading Composition :—Mole ratios of ammonia to carbon dioxide (R') and of water to carbon dioxide (S') in the vapor phase in the equilibrium with the liquid phase have been determined at a temperature of 160°C. and over the range of the loading mole ratio $L=1.60$ to 3.40. A plot of the logarithm of the measured mole ratios of R' and S' against the logarithm of L is respectively shown in Fig. 4, in which $R'-L$ relation at 160°C. is represented by the following equation.

$$R'=L^{6.764}/2\times10^2.$$

At $L=2.43$ where the system exerts the minimum equilibrium pressure at 160°C. as

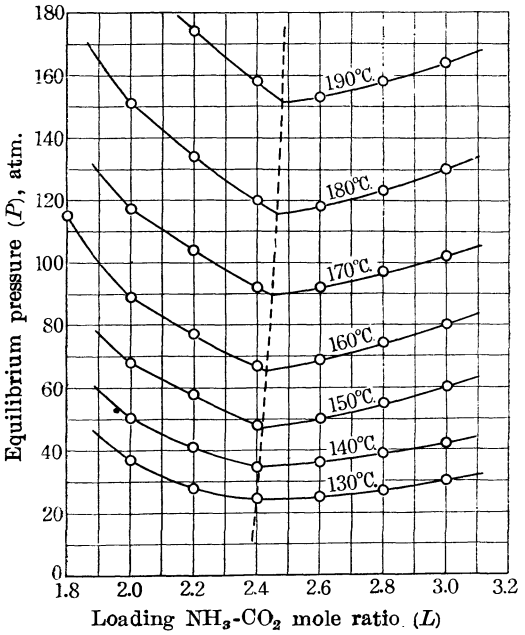

Fig. 3.—P-L-T relations of the CO_2-NH_3-Urea-H_2O system

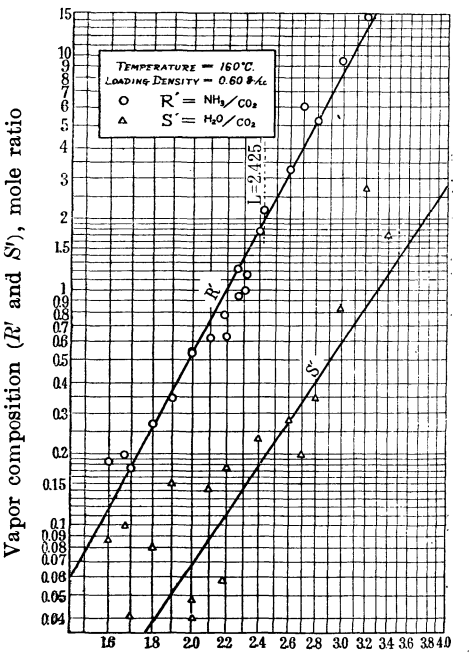

Fig. 4.—Vapor composition of the CO_2-NH_3-Urea-H_2O system in the presence of excess ammonia or carbon dioxide at 160°C.

(6) S. Kodama, *Unpublished report at Research Department, Nissin Chem. Co.* (1950).

pointed out in the preceding section, definitely $R'=2.00$, that is to say, the mole ratio of ammonia to carbon dioxide in the vapor phase is equivalent to the composition of ammonium carbamate.

Relation between Vapor Cmposition and Equilibrium Pressure : —For the purpose of studying the relation between the vapor composition and the equilibrium pressure, the partial pressures of each of the components (p_{CO_2}, p_{NH_3} and p_{H_2O}) in the vapor phase under several conditions have been calculated from the previous investigations of the author[4],[5] assuming the vapor to be a perfect gas. Table 2~4 show respectively the variations of the partial pressure with the temperature at a constant loading density (D) of 0.60 g./cc., the variation with the loading density of ammonium carbamate in the absence of excess ammonia or carbon dioxide, and the variation with the amount of water added to one mole of carbamate (W) at a constant temperature of 160°C. Table 5 shows the results of calculation from the present measurement of the vapor compositions under the conditions of $L=1.6$—3.0, $D=0.60$ g./cc. and 160°C.

Table 2

Relation between Partial Pressure of the CO_2-NH_3-Urea-H_2O System and Temperature at Constant Loading Mole Ratio $L=2.00$ and Loading Density of 0.60 g./cc.

Temp., °C.	Partial Pressure, atm. p_{CO_2}	p_{NH_3}	p_{H_2O}	$K_p\times10^{-5}$
140	33.4	15.7	1.4	0.115
150	43.7	22.0	2.3	0.486
160	55.2	30.2	3.6	1.81
170	69.9	41.4	5.7	6.83
180	86.1	55.9	9.0	24.2

Table 3

Relation between Partial Pressure of the CO_2-NH_3-Urea-H_2O System and Loading Density at Constant Temp.=160°C. and Loading Mole Ratio $L=2.00$

D, g./cc.	Partial Pressure, atm. p_{CO_2}	p_{NH_3}	p_{H_2O}	$K_p\times10^{-5}$
0.20	27.2	37.0	4.5	1.70
0.40	39.9	32.5	4.1	1.73
0.60	55.2	30.2	3.6	1.81
0.80	74.2	30.0	3.3	2.20
1.00	100.6	32.6	3.3	3.53

Table 4

Relation between Partial Pressure of the CO_2-NH_3-Urea-H_2O System and Added Water at Constant Temp.=160°C., Loading Mole Ratio $L=2.00$, and Loading Density $D=0.60$ g./cc.

Added water, mole/mole, carbamate	Partial Pressure, atm. p_{CO_2}	p_{NH_3}	p_{H_2O}	$K_p\times10^{-5}$
0	55.2	30.2	3.6	1.81
0.20	57.0	28.5	3.5	1.62
0.40	58.5	27.0	3.5	1.49
0.60	60.0	25.6	3.4	1.34
0.80	61.3	24.2	3.5	1.26
1.00	62.5	23.1	3.4	1.13

Table 5

Relation between Partial Pressure of the CO_2-NH_3-Urea-H_2O System and Loading Mole Ratio at Constant Temp.=160°C. and Loading Density $D=0.60$ g./cc.

L, Loading mole ratio	Partial Pressure, atm. p_{CO_2}	p_{NH_3}	p_{H_2O}	$K_p\times10^{-5}$
1.60	127.9	19.9	3.2	1.62
1.80	86.0	24.6	3.4	1.77
2.00	55.2	30.2	3.6	1.81
2.20	35.4	36.7	3.9	1.86
2.40	21.8	40.4	3.8	1.35
2.62	15.0	50.6	3.9	1.50
2.80	11.2	59.6	4.2	1.67
3.00	7.4	68.4	4.2	1.46

According to trial calculations of $K_p=p_{CO_2}p^2_{NH_3}p_{H_2O}$ which are shown in these Tables, the logarithm of K_p is a linear function of the temperature over the range between 140° and 180°C. as shown in Fig. 5, while at a constant temperature of 160°C. $K_p\times10^{-5}$ is

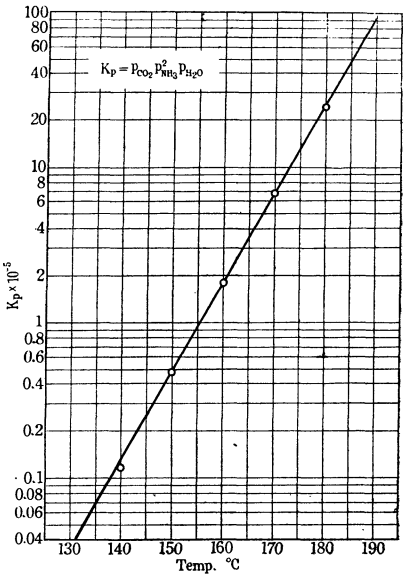

Fig. 5.—K_p-Temp. relation at $L=2$ and $D=0.60$ g./cc.

approximately constant (1.1～3.5) independent of D, W and L within the range of the present experimental conditions.

The approximate constancy of K_p seems to show that at least for practical purposes the assumption, that the activity of ammonium carbonate in the liquid phase is 1, is allowable. If we take such assumption as ammonium carbonate dissociates according to the equation:

$$(NH_4)_2CO_3(l) \rightleftharpoons CO_2(g)+2NH_3(g)+H_2O(g),$$

the equilibrium constant must be constant as follows.

$$K_p = P^4 N'_{CO_2} N'^2_{NH_3} N'_{H_2O} \equiv \text{a constant at } 160°C.$$

where P is the total pressure of the system and N_i' is the mole fraction of i-component in the vapor phase.

$$N'_{CO_2}+N'_{NH_3}+N'_{H_2O}=1$$

Accordingly,

$$K_p = P^4 N'^2_{NH_3}(1-N'_{NH_3}-N'_{H_2O})N'_{H_2O}$$

Supposing that N'_{H_2O} is constant,

$$\frac{\partial P}{\partial N'_{NH_3}} = \frac{K_p^{1/4}(3N'_{NH_3}+2N'_{H_2O}-2)}{4N'^{3/2}_{NH_3}N'^{-1/4}_{H_2O}(1-N'_{NH_3}-N'_{H_2O})^{5/4}}$$

At a vapor composition where the system exerts the minimum pressure,

$$\frac{\partial P}{\partial N'_{NH_3}}=0$$

Therefore,

$$3N'_{NH_3}+2N'_{H_2O}-2=0$$

or

$$R' \equiv \frac{N'_{NH_3}}{N'_{CO_2}} = 2$$

Thus, it has been verified that the mole ratio of ammonia to carbon dioxide in the vapor phase under the minimum pressure of the system at a given temperature is equal to that of ammonium carbamate independent of the amount of water in the vapor.

Effect of Temperature on Relation between Vapor- and Loading Composition: —Mole ratio of ammonia to carbon dioxide in the vapor phase (R') has also been determined at 140° and 180°C. as well as 160°C. over the range of the loading mole ratio L= 2.0—3.0.

The experimental results and empirical equations for R'—L relations are given in Fig. 6. These three straight lines intersect at a

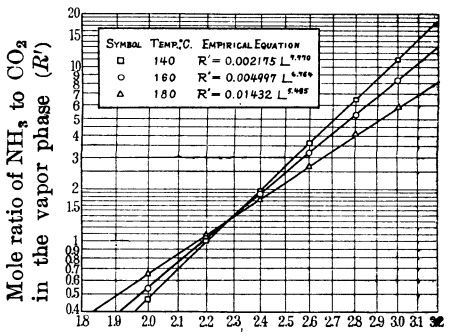

Fig. 6.—R'-L relations at 140°, 160° and 180°C.

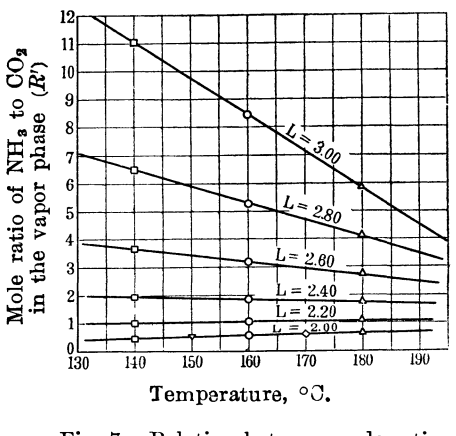

Fig. 7.—Relation between mole ratio of NH_3-CO_2 in the vapor phase and temperature over the range of L=2～3

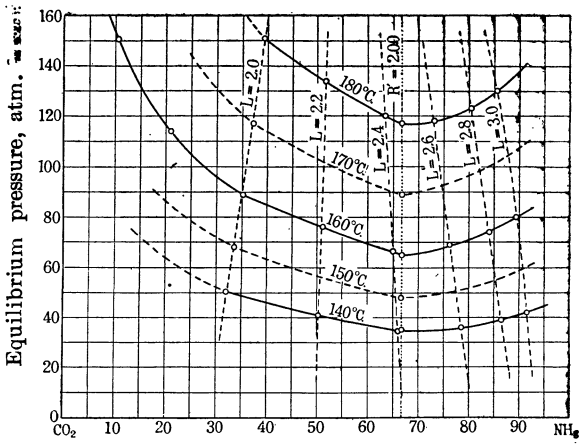

Fig. 8.—Equilibrium pressure-vapor composition diagrams for the CO_2-NH_3-Urea-H_2O system

point near $L=2.28$, where R' is constant independent of temperature. R' is also a linear function of temperature at a given loading composition as shown in Fig. 7.

From the above data, such a relation as shown in Fig. 8 is derived between the equilibrium pressure and ratio of ammonia to carbon dioxide in the vapor phase over the temperature range from 140° to 180°C. With a rise of temperature and a consequent increase of total pressure, the vapor composition becomes richer in ammonia at any loading composition less than $L=2.28$, while it becomes richer in carbon dioxide at more than $L=2.28$.

Summary

(1) For the purpose of studying the liquid-vapor equilibria of the CO_2-NH_3-Urea-H_2O system in the presence of excess ammonia and carbon dioxide respectively over that combined as ammonium carbamate, the equilibrium pressure and vapor composition of the system under high temperature and pressure have been determined over the range of the loading NH_3-CO_2 mole ratio from 1.60 to 3.00.

(2) The experiments which were performed with an initial loading density of ammonium carbamate into a reaction vessel of 0.60 g./cc. and at a temperature of 160°C. have definitely shown the system to exert the minimum pressure and simultaneously to have the vapor composition of $2NH_3$ to $1CO_2$ at a loading mole ratio of 2.43 NH_3 to $1CO_2$.

(3) The relation between the equilibrium pressure and the mole ratio of NH_3 to CO_2 in the vapor phase has been given diagrammatically over the temperature range from 140° to 180°C.

The writer wishes to express appreciation for the kind guidance and the advice received throughout this work from Dr. Shinjiro Kodama, Prof. of Kyoto University, and for the encouragement received from Dr. Kenji Fujimura, the chief of the Research Department.

Research Department, Niihama Works,
Nissin Chemical Co., Ltd., Niihama

Heats of Wetting of Polysaccharides. III. Heats of Wetting of Acetylated and Methylated Polysaccharides

By Toshio NAKAGAWA

(Received September 13, 1952)

Introduction

The origin of the heat developed when a polysaccharide is thrown into water, is generally ascribed to the interaction between the hydroxyl group of the substance and water molecule. But surprisingly, few experimental facts supporting this opinion have been reported. If this supposition is correct, the heat of wetting of a polysaccharide whose hydroxyl groups are substituted with less hydrophilic groups will become smaller than that of the mother substance.

The author measured the heats of wetting of acetylated starch, glycogen, inulin and konjacmannan, also that of methylated inulin, and obtained smaller values than those of their respective mother substances.

Experimental

Heats of wetting were measured with the apparatus described in the first report of this series[1] under evacuated condition.

The samples of acetylated and methylated polysaccharides were prepared with the following methods.

(1) **Acetylated starch.**—Acetylation was carried out following the method of Kerr and Cleveland[2] who had acetylated limit dextrin. Potato starch, which had been washed thoroughly by methanol with Soxhlet's extractor, was ground to a powder and subjected to acetylation.

(2) **Acetyl glycogen.**— Glycogen purified as

(1) T. Nakagawa, This Bulletin, **25**, 169 (1952).
(2) R. W. Kerr and F. C. Cleveland, *J. Am. Chem. Soc.*, **71**, 3455 (1949).

described in the first report,[1] was acetylated with a similar method.

(3) **Acetyl inulin.**—Powdered inulin (β form) was treated as reported by W. N. Haworth, E. L. Hirst and E. G. V. Percival.[3] The acetylated substance was purified by recrystallization from methanol.

(4) **Acetyl konjacmannan.**—From the preliminary examination, it became clear that β-konjacmannan is not suitable as a starting substance, so the acetylation was performed with α-konjacmannan.

Acetyl determinations were carried out by the method described by W. N. Haworth et al[4] and the result was as follows:

acetyl starch	43.5 %
acetyl glycogen	—
acetyl inulin	45.0 %
acetyl konjacmannan	44.8 %

(5) **Methyl inulin.**—Methyl inulin was obtained by the simultaneous deacetylation and methylation of acetyl inulin.[3]

The above-mentioned five samples were subjected to heat measurements after drying in Abderhalden's desiccator under 2/100 mm. Hg at 65°C.

(3) W. N. Haworth, E. L. Hirst and E. G. V. Percival, *J. Chem. Soc.*, 2384 (1932).

(4) W. N. Haworth and H. R. L. Streight, *Helv. chim. Acta.*, **15**, 609 (1932).

Results and Discussion

The heats of wetting of the above-mentioned substances are arranged in Table 1. in comparison with those of their mother substances.

Table 1

cal./g.

Acetyl starch	5.4	Starch	native	28.2
			pasted	24.6
			retrograded	25.6
Acetyl glycogen	3.1	Glycogen		23.5
Acetylkonjacmannan	6.5	Konjacmannan	α	23.7
			β	16.2
Acetyl inulin	0.3	Inulin	β	23.1
Methyl inulin	1.3		α	17.9
			retrograded	21.2

We see that the acetylated and methylated polysaccharides have much lower values than their mother substances. This fact may give a strong support to the opinion that the heats of wetting of polysaccharides are mainly attributed to the interaction between the hydroxyl groups and water.

The author wishes to express his sincere thanks to Prof. Sameshima for his kind guidance and encouragement.

Chemical Department, Faculty of Science Tokyo University, Tokyo.

Sedimentation Volume of Alginic Acid Powder in Electrolyte Solution

By Shigeru MIYAMOTO and Tunetaka SASAKI

(Received October 4, 1952)

Although there have been many studies on alginic acid and its salts, few studies have been carried out on the properties of alginic acid powder as a dispersed phase. In the present paper, it was attempted to study the colloid chemical properties such as sedimentation volume, degree of swelling, electrokinetic potential and cation exchange capacity of alginic acid powder in electrolyte solution.

Experimental

Alginic acid powder was prepared as follows. Alginic acid was precipitated from sodium alginate solution (polymerization degree being about 198) by adding hydrochloric acid, washed, and it was then dissolved in sodium carbonate solution. This procedure was repeated three times, after which alginic acid was precipitated, washed with water, methanol and ether, and then dried at 50°C for five hours. Dry alginic acid was ground in an agate mortar and the portion of 200~280 mesh was taken and kept in a glass bottle. The size and shape of particles were such that their longer axis was between about 0.02 and 0.1 mm. and the ratio of longer to shorter axis was less than about 1.4. The ash content of the sample was about 0.2 %. Electrolytes used were also purified by the usual method.

Sedimentation Volume.—10 cc. of an electrolyte solution was pipetted in a flat bottom glass tube of 1cm. inner diameter and 19 cm. height. 0.3 g of alginic acid powder was then added and the tube was shaken vigorously. The sedimentation volume reached a constant value after 3~7 days which was recorded as an equilibrium value.

Swelling Degree.—Sedimentation volume is considered to increase with increasing degree of coagulation[1],[2],[3],[4] as well as the swelling of the powder. Assuming that the sedimentation volume is proportional to the swollen volume when the coagulation degree does not change, the following relation is obtained.

$$S=(V_w \cdot X/X_w-v_w)/v_w \qquad (1)$$

Here, S is the swelling degree of alginic acid, V_w the sedimentation volume in water, X_w and X the swollen volume in water and in an electrolyte solution respectively, all referred to one gram of dry alginic acid. The quantity v_w is an apparent volume per gram of dry powder under the same degree of coagulation as in water. X and v_w are calculated by the following relations.

$$X=\{U-(W-p \cdot w_0)/d\}/p \qquad (2)$$

$$v_w=V_w/X_w \cdot \rho \qquad (3)$$

Here, U and W are the volume and weight of electrolyte solution with swollen alginic acid containing p gram of dry acid, respectively, w_0 the weight of swollen alginic acid per gram of dry substance, and d and ρ, densities of electrolyte solution and dry alginic acid, respectively. Of these quantities, w_0 was obtained by the measurement, in dry and swollen state, of the weights of alginic acid film prepared on a microscopic slide.

Coagulation Degree.—In general, the sedimentation volume increases with the increasing degree of coagulation. Assuming that swelling and coagulation contribute to the sedimentation volume additively, coagulation degree C is expressed as follows.

$$C=(V_E-V_w \cdot X/X_w)/v_w \qquad (4)$$

Here, V_E is the sedimentation volume in an electrolyte solution. The value of C in water was taken as the standard. From (1) and (4),

$$\Delta v \equiv S+C=(V_E-v_w)/v_w \qquad (5)$$

results, which means that the specific sedimentation volume Δv is the sum of the degrees of swelling and coagulation.

Electrokinetic Potential.—Cataphoretic velocity and ζ-potential of alginic acid were measured for particles suspended in various electrolyte solutions. Namely, a dilute suspension of alginic acid is introduced in U-tube and the sedimentation velocity u_1 is measured under a definite gradient of electrostatic field E. The field is reversed and the velocity u_2 is measured again. Then the following relation holds.

$$G+k\zeta E=au_1 \qquad (6a)$$

$$G-k\zeta E=au_2 \qquad (6b)$$

Here, G represents the force due to gravity and k and a, two constants. Then,

$$\zeta=a(u_1-u_2)/2k \cdot E \qquad (7)$$

gives ζ-potential when we use proper value for a/k[5].

Cation Exchange Amount.—Alginates formed by mixing alginic acid powder and the electrolyte solutions of varying concentration were washed and burnt in a crucible. Cation exchange amounts for the electrolytes of various concentrations were estimated from the amount of metal oxide formed. Values of pH of electrolyte solutions were 1.5~1.8 for cupric, aluminum and ferric chlorides.

Experimental Results

Preliminary experiments were carried out to study the effects of temperature, particle size and the redispersion upon the sedimentation volume as shown in Tables 1 and 2.

Table 1

Effects of temperature, particle size on sedimentation volume*

Temp. (°C.)	Particle Size (Mesh)	Sed. Vol. in 3N KCl Solution(cc./g.)
0	280<	7.9
10	〃	7.0
37	〃	5.9
10	〃	7.0
10	200~280	5.4
10	110~150	4.3
10	70~100	4.4

Table 2

Effect of redispersing the sediment on sedimentation volume*

Temp. (°C.)	Particle Size (Mesh)	Sed. Vol. (cc./g.) in 3N KCl after Repeated Disp.			
		0	1st	2nd	3rd
10	280<	7.9	6.2	5.9	5.8

The maximum error introduced in the sedimentation volume measurement was ±13% for

(1) P. Ehrenberg, "Bodenkolloide", p. 83, 84, Dresden (1918).
(2) A. v. Buzágh, *Kolloidchem. Beih.*, **32**, 114 (1931).
(3) G. F. Kandilarou, *Kolloid-Z.*, **90**, 320 (1940).
(4) W. Gallay and J. E. Puddington, *Can. J. Research*, **21** B, 171 (1943); **22** B, 16 (1944).
(5) H. A. Abramson, "Electrokinetic Phenomena", p. 111, Chem. Catalog, New York (1934).
* Alginic acid powder stored for about five months after purification was used.

thorium nitrate solution and about ± 7 % for most other cases. Values of sedimentation volume in various electrolyte solutions are shown in Fig. 1.* Values of pH of these solutions were 2.0~2.2

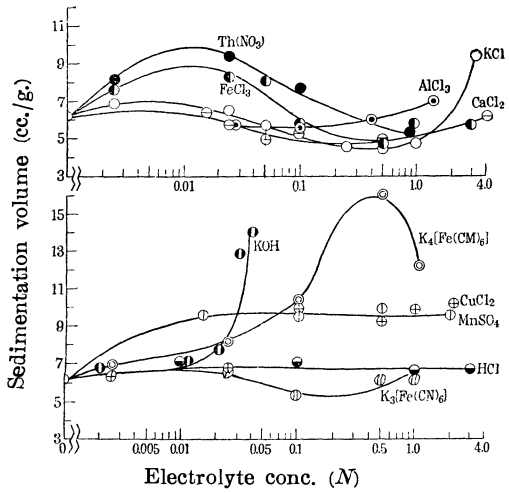

Fig. 1.—Sedimentation volume of alginic acid powder in various electrolyte solutions.

for potassium and calcium chlorides, 1.5~1.8 for cupric, aluminum and ferric chlorides and 1.7~1.9 for thorium nitrate. The effects of its change on the sedimentation volume proved to be negligible. We can see as a whole in this figure that the sedimentation volume exhibits a maximum at relatively low concentration of electrolyte and minimum in the region of larger concentration. The maximum is especially marked in the case of thorium and ferric salts. We should, however, note the anomalous case for potassium hydroxide and potassium ferrocyanide where the anomalies are due perhaps to a strong basicity and negative polyvalency. We then calculated the swelling degree S according to the equation (1) which was

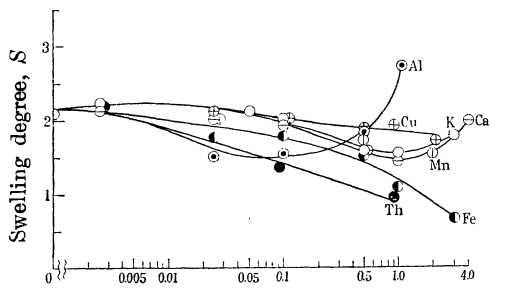

Fig. 2.—Values of swelling degree in various electrolyte solutions.

shown in Fig. 2. The swelling generally decreases with increasing concentration of electrolyte. It increases, however, at fairly large concentrations for some electrolytes. Further, the coagulation degree C was shown in Fig. 3 a. In the cases of

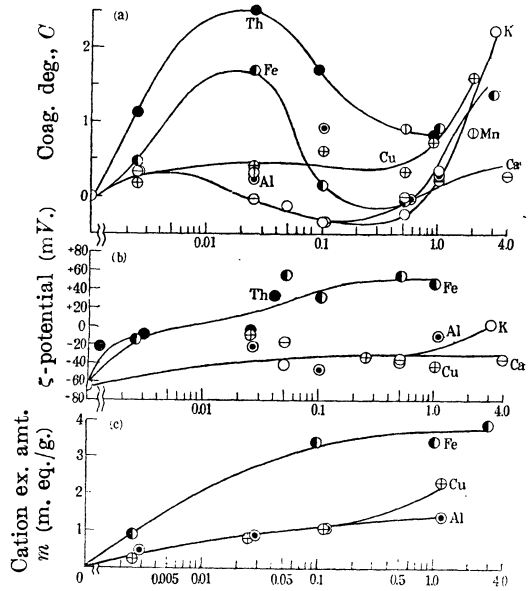

Fig. 3.—Coagulation degree, electrokinetic potential and cation exchange amount of alginic acid powder in various electrolyte solutions.

ferric chloride and thorium nitrate, the values of C showed a marked maximum at about 0.01 N of electrolyte concentration, while the rest of the salt gave rather a flat maxima at the same region of concentration. At higher concentration region, the values of C after passing a minimum tended to increase for all cases examined.

The electrokinetic potential was calculated using the equation (7), and shown in Fig. 3 b. For the calculation, a/k was equated to $4\pi\eta/D$, (η, being the viscosity coefficient and D the dielectric constant of water) according to the classical Helmholtz theory, since we were not interested here in the exact evaluation of a/k. It can be confirmed that the inversion of sign of ζ-potential takes place with increasing concentrations of electrolyte in the cases of ferric chloride and thorium nitrate and the isoelectric points of alginic acid particle correspond to the maxima of coagulation degree. Besides, the values of swelling degree S and coagulation degree C in various solutions of electrolytes with common cation or anion were measured and shown in Table 3. It seems that the differences of the effects of various electrolytes on coagulation degree are explained by the difference in amount of cation exchange adsorption which was shown in Fig. 3 c.

From this table, the following series of decreas-

* Here a fresh sample of alginic acid was used.

ing order were obtained for anions (or cations) composing salt of common cation (or anion), with regard to the degrees of swelling and coagulation.

Table 3
Swelling and coagulation degrees in solutions of electrolytes with common cation or anion

Electrolyte	Conc. (N)	Sed.Vol. (cc./g.)	Swollen Wt., w	Swell. Deg., S	Coag. Deg., C
NH_4Cl	3.00	6.7	2.46	+1.08	+1.45
NaCl	3.00	6.8	2.56	+1.11	+1.47
KCl	3.00	9.4	2.93	+1.73	+2.22
$MgCl_2$	3.00	5.7	2.38	—	—
$CaCl_2$	3.00	5.6	2.51	—	—
$BaCl_2$	3.00	5.9	2.66	—	—
KCl	1.00	4.6	2.23	+1.52	−0.11
KBr	1.00	5.0	2.27	+1.52	+0.11
KNO_3	1.00	5.3	2.43	+1.78	0.0
KI	1.00	6.2	2.51	+1.69	+0.58
KCNS	1.00	7.2	2.33	+1.61	+1.16

Swelling $K>Na>NH_4$, $Ba>Ca>Mg$, $NO_3>I>CNS>Br=Cl$

Coagulation $K>Na>NH_4$, $CNS>I>Br>NO_3>Cl$

Discussion

Effects of temperature, particle size and redispersing the sediment once settled on the sedimentation volume of alginic acid in 3 N potassium chloride solution shown in Table 1 and 2 seem to indicate the effects of coagulation which has a profound influence upon this phenomenon. According to Buzágh[6], the adhesion force which brings about the coagulation of particles decreases at first and then increases with the rise of temperature in aqueous solution. The coagulation degree may also increase in the case of small particles. The decrease of sedimentation volume caused by redispersing the sediment may be explained by the destruction of the structure once formed by coagulation. Decrease of sedimentation volume in water which is observed on a sample kept dry for several months, may be due to the decrease of swelling. It can be seen in Figs. 2 and 3 a that the contribution of swelling to the sedimentation volume is as a whole larger than that of coagulation in most electrolyte solutions. But in solutions of ferric chloride and thorium nitrate, coagulation is pronounced and swelling effect is weak. In fact, coagulation of particles was observed by the naked eye and the microscope in these solutions. Maxima of coagulation degree were observed at relatively small concentration of ferric chloride and thorium nitrate as shown in Fig. 3 a. These maxima corresponded to the isoelectric points which were detected by the electrokinetic potential measurement. Thus a coagulation degree can be estimated from electrokinetic data. This is similar to the cases of quartz[7] and calcium carbonate[8] powder reported by Buzágh. Increase of the electrokinetic potential is due to the adsorption of polyvalent cations on alginic acid which is evident from the comparison of potential with cation exchange amount m.

(6) A. v. Buzágh, loc. cit. (2).

Summary

The sedimentation volume and swelling degree of alginic acid in electrolyte solutions were measured and the coagulation degree was calculated from these values. It was observed that the coagulation degree showed large values, giving maxima at relatively low concalculated from these values. It was observed nitrate. These maxima corresponded to the isoelectric points shown on the electrokinetic potential curve. A close correlation was seen among coagulation degree, electrokinetic potential and cation exchange amount.

The cost of this research has been defrayed from the Scientific Research Expenditure of the Ministry of Education given to one of the authors.

Department of Chemistry, Faculty of Science, Kyûshû University, Fukuoka.

(7) A. v. Buzágh, *Kolloid-Z.*, **51**, 230 (1930); **52**, 46 (1930); **76**, 2 (1936).
(8) A. v. Buzágh, *Kolloid-Z.*, **83**, 279 (1938).

Electrolytic Reduction of Aromatic Carboxylic Acids III. Reduction of Phenylacetic Acid[1]

By Shin-ichi Ono and Tadao Hayashi

(Received October 24, 1952)

In the previous papers we reported that the electrolytic reduction of benzoic acid[2] at a Pb cathode gave a benzyl alcohol. On the other hand, the reduction of cinnamic acid[3] at a Pb or a Hg cathode gave no γ-phenylpropyl alcohol but gave rise to bimolecular compounds as well as β-phenylpropionic acid.

Already Inoue[4] reported that the reduction of phenylacetic acid with a Pb cathode in the alcoholic acid solution gave a β-phenylethyl alcohol (53.4%) and a small amount of phenylpinacone. Marie[5] also reported that the carboxyl group in phenylacetic acid could be reduced to alcohol (33%), but gave no pinacone. The result of the former is different from the latter.

In this paper, it is intended to discuss the reduction of phenylacetic acid in relation to the results obtained from both benzoic- and cinnamic-acids, especially in regard to the formation of the alcohol from carboxylic acid. Another object of this study is to investigate the effect of platinized platinum cathode (Pt-Pt) in the course of the electrolytic reduction.

Experimental

(1) Materials.—Phenylacetic acid was a commercial product, and further purified by recrystallization. It had a m. p. of 76°C. Cathodes used were the same materials as in the case of previous paper.[3]

(2) Reduction Method.—The reduction, including the case of high pressure of hydrogen, was carried out in the same manner as described in the previous paper.[3] In the case of Pb, Hg and Hg-Zn cathodes, usually three times the theoretical amount of current was used.

(3) Isolation and Estimation of Products.—(i) Reduction at Pb-, Hg- and Hg-Zn cathodes When the reduction was completed, the catholyte was diluted with water, and then extracted with ether. After the evaporation of the ether, the remaining liquid was steam-distilled.

The distillate from steam-distillation was extracted again with ether. The ether solution was dried with anhydrous sodium sulfate. After the vaporization of the ether, an oily liquid was obtained. The liquid contained ethyl phenylacetate, phenylethyl alcohol and small amounts of phenylethyl phenylacetate, and the latter was distilled under diminished pressure, b. p. 110~116°/7 mm.Hg., m. p. 29°C. The oily liquid was saponified with 20% alcoholic potassium hydroxide solution, and extracted with ether. The ether solution was dried with anhydrous sodium sulfate. After the vaporization of the ether, the colorless fragrant oil was fractionated at 98~102°/11 mm.Hg. The fraction has d_4^{20} 1.0325 and n_D^{20} 1.5217 (Found: C, 78.15; H, 8.10. Calculated for $C_6H_5CH_2CH_2OH$: C, 78.68; H, 8.19%). Thus it can be regarded as phenylethyl alcohol.

The residual solution from steam-distillation was neutrallized with potassium hydroxide, and then extracted with ether. The evaporation of the ether gave a small amount oily liquid from which no pinacone compound was obtained.

(ii) Reduction at a Pt-Pt Cathode. After completing the reduction, the catholyte was diluted with water, and extracted with ether, and then dried over anhydrous sodium sulfate. After the vaporization of the ether, the remaining liquid was distilled under diminished pressure. The two fractions, (f_1) 65~80°/6 mm.Hg and (f_2) 114~119°/6 mm.Hg were obtained.

Redistillation of (f_1) gave a liquid, b. p. 68~70°/6 mmHg. d_4^{25} 0.9475, n_D^{25} 1.4472. The fraction (f_1) was saponified with 20% alcoholic potassium hydroxide solution, and extracted with ether. The ether solution was dried with anhydrous sodium sulfate. After the vaporization of the ether, the residual liquid was distilled under diminished pressure. The fraction has 117~119°/6 mm.Hg, d_4^{25} 0.9953, n_D^{25} 1.4590 (Found: C, 67.52; H, 9.79. Calculated for $C_6H_{11}CH_2COOH$: C, 67.60; H, 9.86%). Thus the fraction (f_1) can be regarded as ethyl cyclohexylacetate.

The fraction (f_2) was distilled again under diminished pressure, and gave a liquid, b. p. 117~119°/6 mmHg, d_4^{22} 0.9955, n_D^{22} 1.4588 (Found: C, 67.73; H, 9.78. Calculated for $C_6H_{11}CH_2COOH$: C, 67.60; H, 9.86%). Thus it can be regarded as cyclohexylacetic acid.

(1) This paper was presented at the regular meeting of the Chemical Society of Japan, held at kyoto, on May, 1951.
(2) S. Ono and T. Yamauchi; *This Bulletin*, **25**, 404 (1952).
(3) S. Ono and T. Hayashi; ibid. **26**, 11 (1953).
(4) H. Inoue; *J. Soc. Chem. Ind. Japan*, **24**, 914 (1921).
(5) M. Marie; *Bull. Soc. Chim.*, **25**, 512 (1919)

Results and Discussions

(1) Formation of Phenylethyl alcohol.—The optimum conditions for the preparation of phenylethyl alcohol from phenylacetic acid at a Pb cathode are shown in the Table 1.

Table 1

Optimum conditions for the formation of phenylethyl alcohol

Investigator	$PhCH_2COOH$ (g.)	EtOH (cc.)	H_2SO_4 (%) (g.)	Current quantity (A. hrs.)	Yield (%)
Marie[5]	20	20	50 50	40	33
Inoue[4]	20	20	75 70	40	53.4
Authors	13.6	40	50 50	30	28
〃	13.6	40*	50 50	30	35.3

Current density: 10 amp/dm.^{2} Temp: 60°C.

*, Cellosolve was used as a solvent instead of EtOH.

It is a well-known fact that the ester compound is not suitable for the preparation of the corresponding alcohol by the electrolytic reduction, as is seen in the case of benzoic acid.[6] Comparing the results of Table 1, it is surprizing that Inoue's condition gave the yield higher of alcohol, even though his condition seems to be more likely to give the ethyl phenylacetate than those of other's.

In the present experiment, it was found that the cellosolve is available as a solvent to avoid the formation of ester compound.

We have found that the electrolytic reduction of the carboxyl group is most easily possible when it is directly attached to an aromatic ring in a series of carboxylic acid, such as benzoic acid. In the case of phenylacetic acid, the carboxyl group is isolated by the CH_2-linkage from the phenyl group; therefore, it is expected that the electronic interaction between phenyl and carboxyl groups would be less effective than in the case of benzoic acid. That is, the yield of alcohol from phenylacetic acid is smaller than that from benzoic acid. Cinnamic acid or phenylpropionic acid gave no γ-phenylpropyl alcohol as stated in the previous paper.[3] It may be expected that the relative ease of the reduction of carboxyl group is closely related to the nature of R-groups. (R=Ph-, $PhCH_2$- or $PhCH_2CH_2$-)

(2) Effect of Cathode.—In the present experiment, lead (Pb), zinc amalgam (Hg-Zn), mercury (Hg) and platinized-platinum (Pt-Pt) cathodes were used in order to determine the effect of cathode materials on the reduction products. Pb, Hg-Zn and Hg cathodes were observed to act analogously, giving the phenylethyl alcohol.

We have found that Pb cathode is preferable to Hg-Zn or Hg cathode, for the formation of phenylethyl alcohol.

On the other hand, the reduction at a Pt-Pt cathode gave rise to cyclohexyl compounds and it seemed that the behavior of the Pt-Pt cathode was quite the same as in the case of benzoic-and cinnamic-acids.[7]

(3) Effect of Solvents.—(i) **Reduction at a Pb Cathode** When sulfuric acid and ethanol are used as a catholyte, we have found that the 50% of sulfuric acid solution is available for the formation of phenylethyl alcohol. In the case of high concentration of sulfuric acid solution, the yield of phenylethyl alcohol is decreased by the formation of ethyl phenylacetate which will be less reactive for the formation of phenylethyl alcohol. We have studied that when 75% of sulfuric acid and ethanol are used as a catholyte, more than 60% of phenylacetic acid is esterified without using the current at 60°C.

To avoid the esterification, ethyl acetate and cellosolve were used as a solvent, and the later gave the better yield. Results are shown in the Table 2.

Table 2

Effect of Solvents

Catholyte: Phenylacetic acid 13.6 g, Sulfuric acid 40 cc., Solvent 40 cc. Current density: 10 amp/dm.^{2} Current quantity: 30 A·hrs. Cathode: Lead (1.0 dm.^{2})

Run No.	Solvent	Temp. (°C.)	Phenylethyl alcohol (%)
1	MeOH	50	25.0
2	EtOH	60	28.0
3	$CH_3COOC_2H_5$	60	29.0
4	$C_2H_5OCH_2CH_2OH$	60	35.3

Table 3

Effect of Acid concentration

Catholyte: Phenylacetic acid 13.6 g, EtOH 40 cc., Sulfuric acid 40 cc. Cathode: Pt-Pt sheet (1 dm.^{2}). Current quantity: 28 A. hrs. (Theor. 16.1 A. hrs.). Temperature: 30~35°C.

Conc. of H_2SO_4%	C. D. amp/dm.^{2}	product f_1 (g.)	f_1 (%)	f_2 (g.)	f_2 (%)	Yield f_2(Total)* (%)	C. E. (%)
28	2	6.0	35.3	6.0	42.3	79.4	45.7
50	2	9.5	55.9	3.0	21.1	77.9	44.8
75	2	10.5	61.8	1.5	10.6	72.8	41.9

Products: f_1; Ethyl cyclohexylacetate.
f_2; Cyclohexylacetic acid.

* Sum of f_2 and cyclohexylacetic acid produced from the hydrolysis of f_1.

(6) (a) For example, Swann, *Trans. Electrochem. Soc.* **75**, 411 (1939), and reference (2).
(b) S. Ono and J. Nakaya reported at the regular meeting of the Chemical Society of Japan held at Tokyo, April, 1951. that the electrolytic reduction of ethyl phenylacetate at Pb cathode gave no phenylethyl alcohol.

(7) c. f. Part I and II of this series, ref. (2) and (3).

(ii) **Reduction at a Pt-Pt Cathode** It was seen from the data in the table 3 that the yield of ethyl cyclohexylacetate was increased and the yield of cyclohexylacetic acid was decreased with the increase of the acid concentration. In the same acid concentration, it was found that better yields could be obtained at a lower current density (Table 4).

Table 4
Effect of Current Density

Catholyte: Phenylacetic acid 13.6 g, EtOH 40 cc., 50 % sulfuric acid 40 cc. Cathode: Pt-Pt sheet (1 dm.^{2}). Current quantity: 28 A. hrs. (Theor. 16.1 A. hrs.). Temperature: 30~35°C.

C. D. (amp/dm.^{2})	Yield (%)	C. E. (%)
0.5	81.5	46.9
1.0	80.2	4[illegible].1
2.0	76.5	44.0
3.0	74.6	42.9
4.0	75.5	43.4
5.0	75.5	43.4

Product; Cyclohexylacetic acid.

(4) **Effect of High Pressure.**—In a series of this investigation, the special study was made in order to know the effect of external pressure in the course of electrolytic reduction of phenylacetic acid.

Table 5
Effect of high pressure

(a) Reduction of Phenylacetic acid at a Pb Cathode

Catholyte: Phenylacetic acid 13.6 g., Sulfuric acid 40 cc., Cellosolve 40 cc. Cathode: Lead sheet (1 dm.^{2}). Current quantity: 30 A. hrs. (Theor. 10.7 A. hrs.). Temperature: 50~55°C.

H_2SO_4 (%)	C. D. (amp/dm.^{2})	Press. of H_2 (atm.)	Yield (%)	C. E. (%)
50	5.0	—	33.0	11.7
〃	〃	25	32.5	11.6
〃	〃	35	33.8	12.0
75	5.0	—	25.5	9.1
〃	〃	40	26.4	9.4
〃	10.0	40	32.4	11.5
28	5.0	—	30.3	10.8
〃	〃	20	31.5	11.2
〃	10.0	40	32.8	11.7

Product: Phenylethyl alcohol.

The reduction was undertaken at the high pressure of hydrogen (15~40 atm.). In the case of the reduction at a lead cathode, the product was quite the same as the ordinary pressure. Results are given in the Table 5. Among these data, a slight increase in the product was observed at the high pressure, but an increase of the hydrogen pressure made no clear effect on the product. If, in the case of Pt-Pt cathode, we may assume that the reduction consists mainly in the catalytic mechanism, it can be expected that there is some correlation between the reduction products and the external pressure. But we have fairly comparable data in this experiment; (Table 6), therefore, further studies must be made to clarify this problem.

Table 6
Effect of high pressure

(b) Reduction of phenylacetic acid at Pt-Pt Cathode.

The electrolytic conditions are the same as tab'e 4, except the external pressure of hydrogen.

C. D. (amp/dm^2)	Press. of H_2 (atm.)	Yield (%)	C. E. (%)
3·0	—	74.6	42.9
〃	15	75.5	43.4
〃	30	76.0	43.7
4.0	25	76.8	44.2
〃	35	76.0	43.7
5.0	25	78.2	45.0
〃	40	79.0	45.4

Product: Cyclohexylacetic acid.

Summary

(1) The electrolytic reduction of phenylacetic acid at a Pb, a Hg-Zn, a Hg or a Pt-Pt cathode was studied. It was confirmed that phenylethyl alcohol could be produced from phenylacetic acid using Pb, Hg-Zn and Hg cathodes. The Pt-Pt cathode was observed to behave catalitically in the course of reduction and gave rise to cyclohexylacetic acid.

(2) The relative ease of the reduction of the carboxylic acid to alcohol was closely related to the nature of the group which lies between phenyl and carboxyl radical.

(3) The effect of high pressure of hydrogen was discussed on the electrolytic reduction of phenylacetic acid.

The authors express their sincere thanks to Dr. N. Sugiyama, Prof. of the Tokyo University of Education for his kind advice and discussions.

Department of Chemistry, Faculty of Education, Naniwa University, Osaka.

Dichroic Study on Polyvinylalcohol Fiber
III. Double Refraction of Polyvinylalcohol Fiber

By Saburo OKAJIMA, Yasuji KOBAYASHI and Ryuzo YAMADA

(Received November 6, 1952)

In the preceding paper the change of the dichroism of the model filament of polyvinylalcohol (PVA) by stretching is reported. Now the intrinsic double refraction of the same filament after stretching and heat-treatment under various conditions is given. As the dichroism and intrinsic double refraction can indicate the orientation of the molecules and it is known that the double refraction of the fiber is affected by the crystallinity, so there may be a possibility to know separately these two factors, the orientation and the crystallinity, by comparing these two measures.

In this report the double refraction of PVA filament which has previously been treated variously was observed as the preliminary experiment on the determination of the above two factors.

Experiment

(I) Preparation of the isotropic model filament and the method of stretching.—The isotropic filament of PVA was melt-spun as described in the first report of this study.[1] The stretching of the isotropic model filament was also carried out similarly as previously,[2] but now it is known that a filament is not stretched uniformly along the axis and this is not due to the irregular structure of the sample but to the stretching conditions. This is clearly shown by the following experiment: A pair of filaments, *a* and *b*, in Fig. 1, on which many small points had been marked with a special ink, were attached parallel to a stretching frame and stretched under various conditions and the degrees of stretching were observed along their axes by comparing the corresponding distances between the marks before and after stretching. Fig. 1 shows the distribution of the stretching degree (v) along the axes of a pair of filaments which had been attached to the same frame and, therefore, stretched at the same time. We can see from the figure some interesting facts, as follows:

(a) The end parts near the clamps are elongated more and the middle part is comparatively uniform. The tendency becomes remarkable as the total stretching degree grows larger.

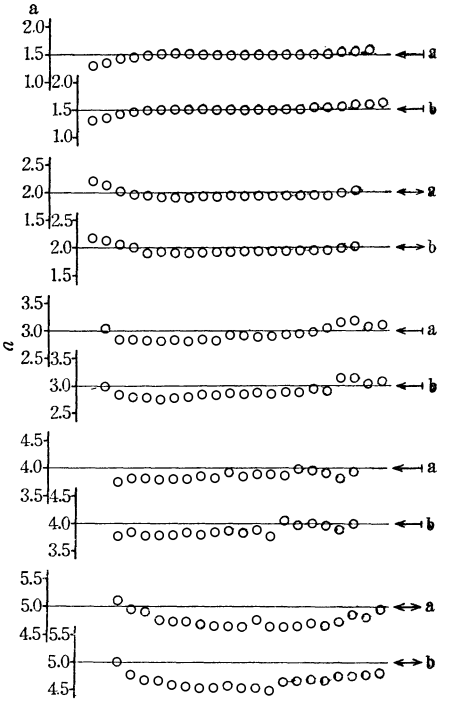

Fig. 1.

(b) The correspondence of the stretching of the two parallel filaments, *a* and *b*, is very good irrespective of the irregularity of deformation above. So the phenomenon is not caused by the irregular structure of the sample along the axis.

(c) The distribution of v along the filaments is nearly symmetrical. This is irrespective of the fact that either both ends of the filament are pulled away or only one end is pulled away, fixing the other end. These types of stretching are shown by ←→ and → in the figure.

Taking this irregularity into consideration, the test pieces used for the measurements of the intrinsic double refraction (Γ) and v were taken from the middle part of the stretched filament in the following experiments.

(II) Determination of Γ.—Some test pieces taken from the middle part of the stretched filament was comented to a frame prepared from a brass plate of 0.4 mm thickness (Fig. 2 a). A

(1) S. Okajima and Y. Kobayashi, *J. Soc. Chem. Ind. Japan*, **54**, 791 (1951).
(2) S. Okajima and Y. Kobayashi, This Bulletin, **25**, 268, (1952).

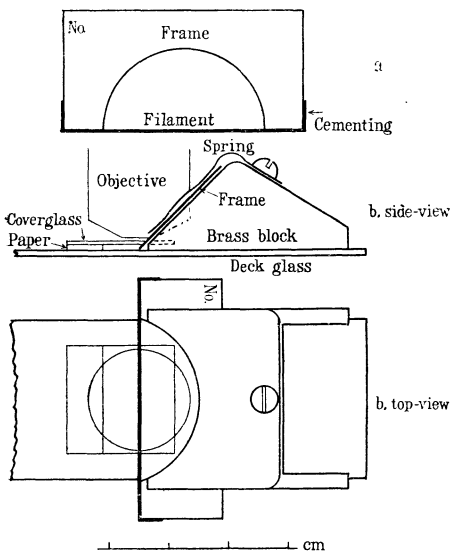

Fig. 2.

benzene-alcohol solution of benzylcellulose was used as the cementing material.

This frame with a test piece is attached with a pair of springs to one side of a brass block which was placed on the stage of a polarization microscope (Fig. 2 b). This brass block was prepared in such a way that the above brass plate inclines by 45° to the horizontal plane. Then dropping the brass plate and reattaching it to the block, nearly the same portion of the filament can be again observed microscopically from the direction perpendicular to the first one. Then if the retardation R and width D of the same portion of the test piece are measured from the two directions perpendicular to each other, and if these two measures are R_1, D_1 and R_2, D_2, then Γ of that part is given by R_1/D_2 and R_2/D_1. The suffixed 1 and 2 mean the first and second measurements.

If the filament is not exactly circular, then D_1 differs slightly from D_2 and the above device gives a good result. Furthermore, when the section of the filament is too elliptic and the cover glass is pressed slightly, the filament against the deck glass owing to the surface tension of the mountant, the larger diameter is liable to be observed under a microscope, so now it is devised to insert a piece of paper of an appropriate thickness between the cover and deck glasses to give a sufficient space for the filament to take a free state.

The mountant was prepared by adding some cedar oil to tricresylphosphate to adjust the refractive index to that of PVA, 1.535. This mountant is vaporisable with difficulty and very suitable for our purpose.

The sample was stocked in a vacuum P_2O_5-desiccator over 15 hours and mounted in the above liquid. The magnification of the microscope was 400×.

The measurment of the retardation was carried out as usual partly by observing the diffraction colour and partly by using compensater, using D-line, as the light source.

Experimental Results

The samples were conditioned at the various humidities at 20° and 30°C. and stretched under the same conditions. They were treated as described above and the change of the double refraction by stretching were observed. The result is shown by the curve (a) in each figure below. Some of the samples were washed out with carbon tetrachloride or ether to remove the mountant and then heated in an air-oven controlled at 140 ±3°C. for various periods of time, after being conditioned in a desiccator containing the saturated solution of ammonium sulfate (81% RH at 20°C.). Some of them were washed, conditioned and heated again and again and the change of their Γ by the heat treatment were traced. The results are summarised below.

Fig. 3 shows the carried out result of experiment at 30°C. and 100% RH. The curve a is the relation of Γ versus v, which is a saturation type. The points ○ and ● are obtained by two different observers with using two samples spun separately, but they coincide well; therefore, the reproducibility of the experiment can be said to be very good.

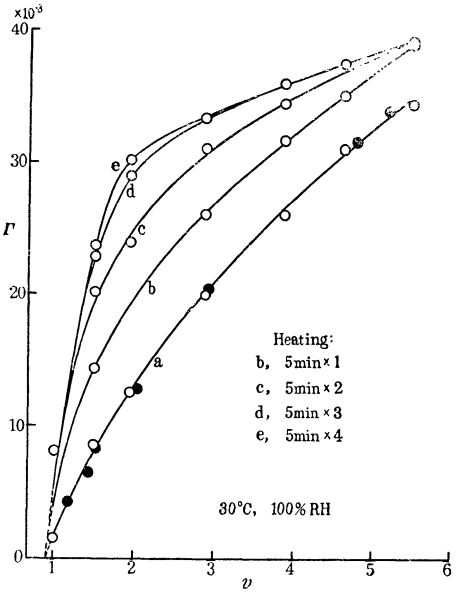

Fig. 3.

The curve b (5 min. heating ×1) is almost parallel to a and the others c~e are not parallel but their end points converge to one point and only the middle parts rise stepwise in the order c to e. Therefore the increment of Γ by heating at 140°C. is not uniform relative to v, but the change is largest at $v \fallingdotseq 2$ and the filament of the highest orientation attains the equilibrium state

after short heating, while some four heatings are required at $v \fallingdotseq 2$.

Fig. 4~7 show the similar experiments stretched at 30°C. and 93% RH, at 20°C. and 100% RH, at 20°C. and 93% RH, at 20°C. and 81% RH respectively. The character of each case is similar to that of Fig. 3. The saturated state is obtained by heating for 15~30 min. in all experiments.

In the case of Fig. 6 the sample b' was heated for 15 min. immediately after vacuum drying and had not been conditioned, and the curve b' is somewhat lower than the corresponding curve b, which was heated after the ordinary conditioning. The curves b and b' shift to c and c' respectively by the secondary heating of 15 min. after ordinary conditioning, where c' is also below the corresponding c. Therefore some amount of moisture in the filament seems to have a good effect upon the raising of Γ, although the moisture in the filament vaporises rapidly in such an open heating. The phenomenon is not the problem of the rate of change and it remains after reaching the equilibrium state.

The stretching at 20°C. and 81% RH is very poor as shown in Fig. 7; this fact has been pointed out already in the previous paper with using dichroism.

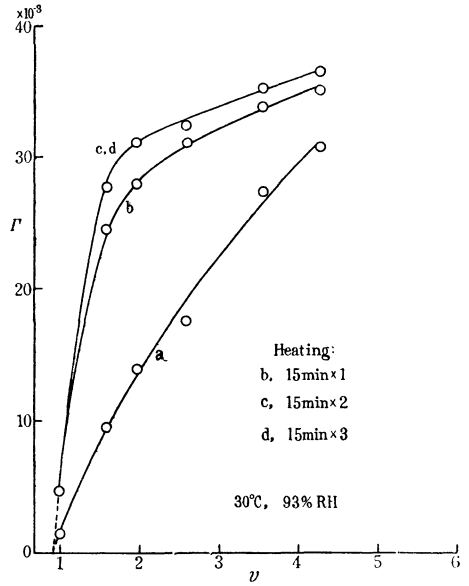

Fig. 4.

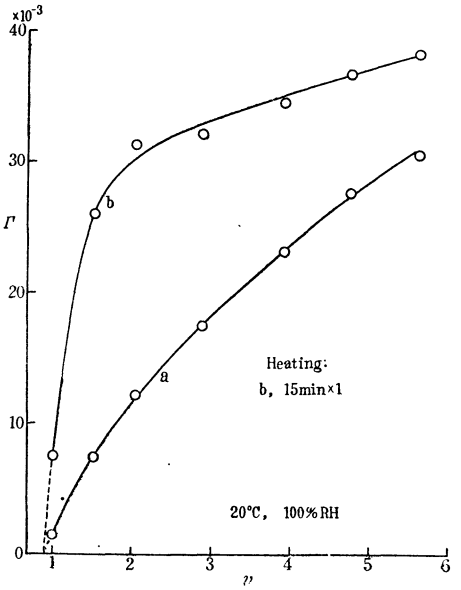

Fig. 5.

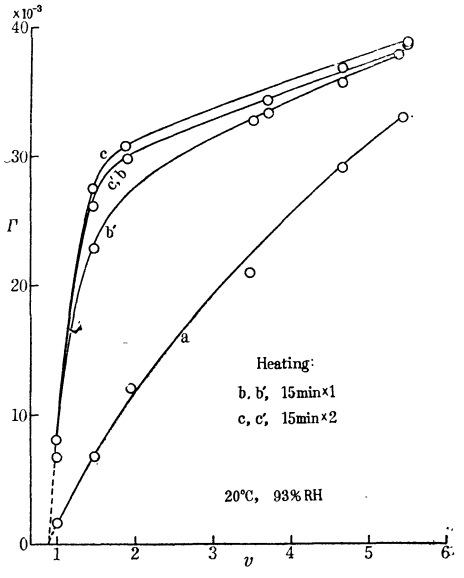

Fig. 6.

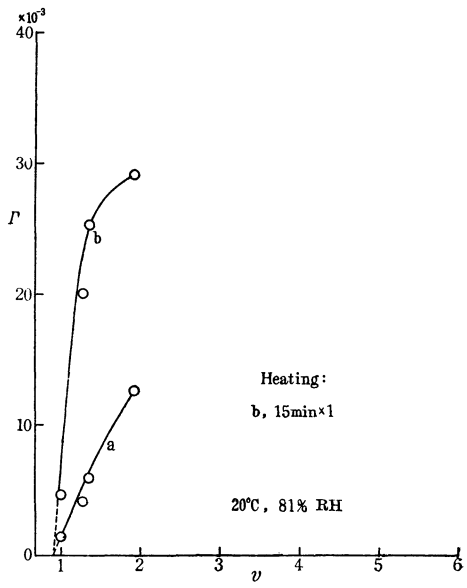

Fig. 7.

Now summing up the curve *a* and the one heated to equilibrium in each experiment, it is indicated as shown in Fig. 8, that the rise of Γ by stretching becomes sharper as the stretching is carried out at lower humidity and higher temperature, while the difference disappears when these samples are heated to equilibrium and the original curves converge nearly to one relation, where the maximum value of Γ amounts to $38\sim 39\times10^{-3}$.

Now an experiment was made, in which the filament stretched at 20°C. and 100% RH were heated at 140°C. for 25 min., when one half of it (*b*) was treated as before but immediately after vacuum drying, while the other half (*c*) was heated at the same temperature after conditioning at 20°C. and 81% RH and at the higher humidity by supplying the water vapor. As shown in Fig. 9 the moisture effect is clearly recognized here also, but the effect is not similar to the case of Fig. 6 and it is in the reverse direction and, therefore, the optimum moisture content seems to exist for the raising of Γ. The difference here is also considered, not to be caused by the different rate of change as the effect remains in the equilibrium state, which is attained by repeating the heat-treatment for 60 min.

In this experiment also a filament (●) was stretched very slowly (8 hours were required for the total stretching) as compared to the experiment hitherto described, in which the stretching was carried out within 10 seconds. According to the figure the slower stretching is more effective to raise Γ but the maximum value does not change so much.

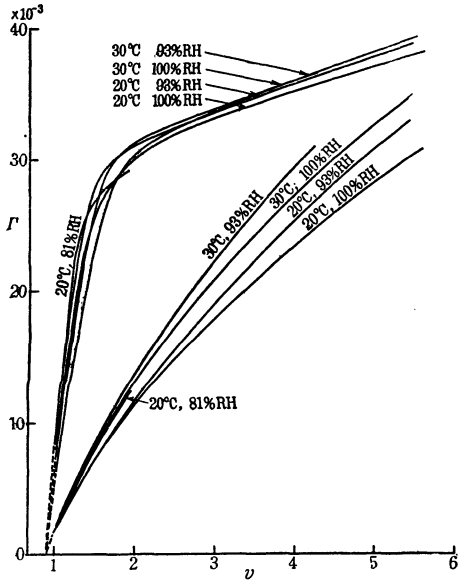

Fig. 8.

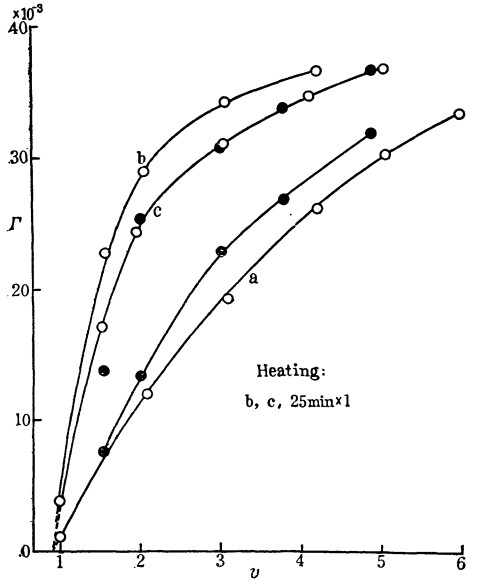

Fig. 9.

Discussion

A similar stretching experiment has been carried out and the change of the dichroism by stretching has been reported in the preceding paper. Now comparing the experimental results obtained under the similar conditions in the preceding paper to these in the present study, the similar trends are seen. In both cases the change of the measures becomes less sharp as the moisture content increases. But there are small discrepancies in detail; for example, the dichroic curve of a filament of higher moisture is sigmoid but the birefringence curves are all saturation type as shown above.

This is certainly because the dichroic data indicate principally only the orientation of PVA molecules independently on the crystallinity, while Γ relates also to the crystallinity. According to K. H. Meyer[3] PVA partly crystallize by stretching only and then the orientation curves indicated by the dichroism and the double refraction may be different. But quantitative study on the crystallization of PVA is not yet reported and this is an important problem for the vinylon industry of Japan. The detailed comparison of the two orientation curves will be given in the following paper.

The authors are indebted to Dr. Yazawa for the sample of PVA used, for which their thanks are due.

Faculty of Engineering, Yamagata University, Yonezawa, and Faculty of Engineering, Tokyo Metropolitan University

(3) K.H. Meyer, "Natural and synthetic high polymers."

The Resonance Energy and the Hindering Potential Barrier of the C-C axis of Glyoxal

By Mikio KATAYAMA

(Received November 6, 1952)

Introduction

There have been few investigations on the hindering potential about single bonds of aliphatic compounds which have conjugated double bonds. In these compounds the molecular structures are so remarkably influenced by quantum-mechanical resonance, that the potential barrier about the bond has to be calculated by taking into account the resonance energy. The hindering potential of butadiene[1] was discussed by calculating the energies of several structures of butadiene, by the method of Goeppert-Mayer and Sklar, but owing to the uncertainty of the correction of the energy zero of these structures, it was not possible to obtain a precise value of the hindering potential. On the other hand, Penny and Sutherland[2] calculated the hindering potential of O-O axis in H_2O_2 and of N-N in H_2N-NH_2 molecule by the use of Heitler-London's method. In this article the same method will be applied for the case of glyoxal having conjugated double bonds.

By electron diffraction investigation the stable structure of glyoxal molecule was determined to be planar and of the trans[3] form. Accordingly, in order to calculate the hindering potential barrier of glyoxal, it is sufficient to compute the difference between the energies of the perpendicular form and of the planar one. For the stable planar configuration the structure A and the structure B in Fig. 1 are considered as the possible non-polar resonance structures, while for the perpendicular configuration, the structure B is to be put aside from our consideration, since in this position the two double bonds do not resonate absolutely.

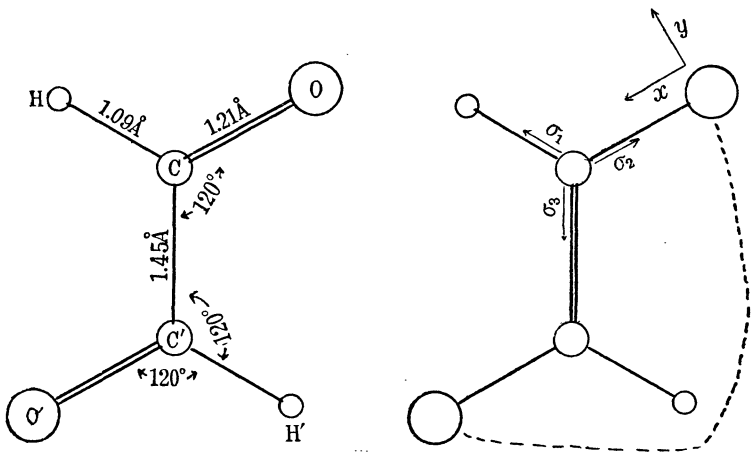

Structure A Structure B

Fig. 1.—The Configuration of Glyoxal molecule

§ 1. The case in which the structure a alone is considered

When we assume the molecule has only the form A, the wave function of this molecule in Heitler-London's approximation is expressed as follows:

$$\Psi_A = \{\psi^O{}_y(1)\psi^O{}_y(2)\}(\psi^H(3;\psi_{\sigma_1}(4))(\psi^O{}_x(5)\psi_{\sigma_2}(6))$$
$$(\psi^O{}_\pi(7)\psi^C{}_\pi(8))(\psi_{\sigma_3}(9)\psi'_{\sigma_3}(10))$$

(1) M. Katayama and Y. Morino; *Reports of the Institute of Science Technology, University of Tokyo*, **5**, 19, (1951).

(2) W. G. Penny and G. B. B. M. Sutherland: *J. Chem. Phys.*, **2**, 492 (1934).

(3) J. E. Lu Valle and V. Schomaker: *J. Am. Chem. Soc.*, **61**, 3520 (1939).

$$\{\psi^{O}_{y'}(11)\psi^{O}_{y'}(12)\}(\psi^{H'}(13)\psi_{\sigma_1'}(14))$$
$$(\psi^{O}_{x'}(15)\psi_{\sigma_2'}(16))(\psi^{C}_{\pi'}(17)\psi^{C}_{\pi'}(18)) \quad (1)$$

where bracket { } means a lone pair, and bracket ( ) a pair bond: for example,

$$(\psi^{H}(3)\psi_{\sigma_1}(4)) = \frac{1}{2}(\psi^{H}(3)\psi_{\sigma_1}(4)$$
$$+\psi^{H}(4)\psi_{\sigma_1}(3))(\alpha(3)\beta(4)-\alpha(4)\beta(3)) \quad (2)$$

and ψ^{H} denotes the wave function of hydrogen, and ψ_{σ_1}, ψ_{σ_2} and ψ_{σ_3} the hybridized wave functions of carbon atoms. The wave functions of π-electrons of oxygen and carbon atoms are designated by ψ^{O}_{π} and ψ^{C}_{π}, the directions of the coordinate axis being shown in Fig. 1. In this expression, 1s electrons of carbon atoms and 1s and 2s electrons of oxygen atoms are ignored. Thus in this approximation the energy of certain states of the molecule may be expressed by the following formula:

$$W = H(E) - 2\sum J_{pp'} - \sum J_{pt} + \sum J_{qr} - \frac{1}{2}\sum J_{rs} - \sum u J_{tt'} \quad (3)$$

where $H(E)$ denotes the coulomb energy, $J_{pp'}$ the exchange energy between the wave functions of the electrons of different lone pairs, J_{pt} those between an electron of a lone pair and the other electron which does not belong to the lone pair, J_{qr} those between the electrons which make the same bond, J_{rs} those between the electrons which make different bonds, $J_{tt'}$ those between electrons which do not make a bond or a lone pair. u is the element of representation of symmetry group. The last term will be used in the calculation on §2.

In order to calculate the energy difference due to the rotation about the C-C axis, it is sufficient to ignore from Eq. (2) the terms which do not vary with the rotating angle about the central C-C axis. Thus the remaining energy may be expressed as follows:

$$\begin{aligned} W(\varphi) = 4\{&U(yO:yO')+U(yO:H')+U(yO:xO') \\ &+U(yO:\sigma_2')+U(yO:O\pi') \\ &+U(yO:C\pi')+U(yO:\sigma_1')\} \\ +2\{&U(H:\sigma_1')+U(H:xO')+U(H:\sigma_2') \\ &+U(H:O\pi')+U(H:C\pi')+U(\sigma_1:xO') \\ &+U(\sigma_1:\sigma_2')+U(\sigma_1:O\pi')+U(\sigma_1:C\pi') \\ &+U(xO:\sigma_2')+U(xO:O\pi')+U(xO:C\pi') \\ &+U(\sigma_2:O\pi')+U(O\pi:C\pi')+U(\sigma_2:C\pi')\} \\ &+U(H:H')+U(\sigma_1:\sigma_1')+U(xO:xO') \\ &+U(\sigma_2:\sigma_2')+U(C\pi:C\pi')+U(O\pi:O\pi') \end{aligned} \quad (4)$$

where $U(a:b) = Q(a:b) - \frac{1}{2}J(a:b)$. The coulomb and the exchange energies, $Q(a:b)$ and $J(a:b)$, have respectively the following expression:

$$\left.\begin{aligned} Q(a:b) &= \int \psi_a(1)\psi_b(2)H\psi_a(1)\varphi_b(2)d\tau \\ J(a:b) &= \int \psi_a(1)\psi_b(2)H\psi_a(2)\psi_b(1)d\tau \end{aligned}\right\} \quad (5)$$

where H means Hamiltonian of $(a:b)$ system. It would be desirable to calculate the integrals, but unfortunately, the tables of these integrals given by Kotani[4] et al, are not available for this case, because the integrals to be used in the present calculation are those between the atoms farther apart than those given in their tables. Hence, for simplicity, the coulomb energy is assumed to be 20% of the Morse function and the exchange energy the remaining part of the Morse function. The dissociation energies,[5] the equiliblium distances and the vibrational frequencies are listed in Table 1, which are used to calculate the Morse functions. For the exchange integral between the π-electrons the value calculated by Penny[6] in ethylene molecule, 0.75 e. v., is used.

Table 1
Constants for Morse function

Bond	Dissociation Energy kcal.	Equilibrium Distance A.	Frequencies $cm.^{-1}$
H—H	102.4	0.74	4375
O—H	113.1	0.97	3660
O—O	34.3	1.32	1304
C—O	81.8	1.43	1030
C—C	83.0	1.54	990
C—H	92.3	1.10	2930

If the directions of the bondings of the two different atoms make the angles θ_1 and θ_2 with the line drawn through the nuclei of the two atoms, the exchange integral between these two electrons may be written in the following expression:

$$J(xO:xO') = J'(xO:xO')\cos^2\theta_1\cos^2\theta_2 + J_{\perp}(xO:xO')\cos\varphi\sin^2\theta_1\sin^2\theta_2 \quad (6)$$

where $J'(xO:xO')$ represents the exchange integral derived from Morse function, and $J_{\perp}(xO:xO')$ means the one between the perpendicular components of the wave functions to the O—O line. In order to estimate the value of $J_{\perp}(a:b)$, if both electrons, a and b, are referred to p-electrons, $J_{\perp}(a:b)$ has the same value as the exchange energy between π-electrons, and if a and b are referred to p-electron and hybridized sp^2-electron respectively, or both of them are referred to hybridized sp^2-electrons, the values of $J(a:b)$ are taken as 2/3 or 4/9 as those of π-electrons. φ represents the angle of rotation.

(4) M. Kotani et al: *Proc. Phys-Math. Soc.*, **20**, Extra No. (1938); **22**, Extra No. (1940).
(5) R. H. Gillette and A. Sherman: *J. Am. Chem. Soc.*, **58**, 1135 (1936).
(6) W.G. Penny: Proc. *Phys. Soc. London*, **46**, 333 (1934).

about the C—C axis, the zero of the angle being at the position where the molecule has the planar trans form. The calculated energies of the planar and perpendicular models of glyoxal by the method stated above are listed in Table 2. It is well established by this calculation that, if this molecule has the wave function Ψ_A only, i. e. if only the type A of molecule exists, the perpendicular form is more stable than the planar one.

§ 2. The case of the resonance between the structure A and B

It is evident that the molecule of the glyoxal has not only the contribution of the structure A, but also of other forms such as the structure B. In this paragraph the calculation is performed, considering the structure A and B as the resonance form. The structure B is represented by the following wave function:

$$\Psi_B = \{\psi'_y(1)\psi^O{}_y(2)\}(\psi_{\sigma_1}(3)\psi^H(4))(\psi_{\sigma_2}(5)\psi^O{}_x(6))$$
$$(\psi_{\sigma_3}(7)\psi_{\sigma_3'}(8))(\psi^C{}_x(9)\psi^C{}_{\pi'}(10))$$
$$\{\psi^O{}_{y'}(11)\psi^O{}_{y'}(12)\}(\psi_{\sigma_1'}(13)\psi^{H'}(14))$$
$$(\psi_{\sigma_2'}(15)\psi^O{}_{x'}(16))(\psi^O(17)\psi^{O'}{}_{\pi}(18)) \quad (7)$$

As the result of the resonance between the structure A and B, the energy of the molecule is calculated from the following secular equation,

$$\begin{vmatrix} M_{11}-W & M_{12}-\frac{1}{2}W \\ M_{12}-\frac{1}{2}W & M_{22}-W \end{vmatrix} = 0 \quad (8)$$

$$M_{11} = Q + 2J(O\pi : C\pi) - \frac{1}{2}\{J(O\pi : O\pi') + J(C\pi : C\pi')\}$$

$$M_{12} = \frac{1}{2}M_{11} + \frac{3}{4}\{J(C\pi : C\pi') + J(O\pi : O\pi')\} - \frac{3}{2}J(C\pi' : O\pi)$$

$$M_{22} = Q + J(C\pi : C\pi') + J(O\pi : O\pi') - J(C\pi : O\pi)$$

In this equation, M_{11} is the energy of the molecule when only the structure A is considered. The result of this calculation indicates that the energy of the ground state in the trans form is about 5.12 kcal. lower than the case of the structure A alone considered, if the resonance between two non-polar structures is considered. It will be evident that the cis-form is also stabilized by the resonance which has almost the same energy, so that the same amount of resonance energy is tentatively assumed for the cis-form. The calculated value of the energy of each form is shown in the lower part of Table 2. It can easily be seen that the planar form is more stable than the perpendicular one.

Table 2
Relative Energies of Several Configurations

	trans form	cis form	perpendicular form
Structure A only considered	33.72 kcal.	32.83 kcal.	30.13 kcal.
Resonance between the structures A and B being considered	28.60	27.71	30.13

Discussion and Acknowledgement

The calculation stated above indicates that the structure A gives the more stable perpendicular form than the planar ones, while the resonance between A and B makes the planar one more stable than the perpendicular one. Thus it may be concluded that the cons deration of the conjugation of double bonds contributes several kilocalories to the hindering potential about the central single bond, while the energy of the perpendicular form is the same as that in the case where only the form A is considered. The hindering potential of glyoxal has not been determined experimentally, but in the molecules of oxalyl-chloride it was confirmed by electron diffraction and dipole moment measurements[7] that the hindering potential is about 5 kcal., the trans-form being the most stable position. The value 1.5 kcal.~2.4 kcal. obtained in this article is practically of the same order.

This calculation indicates that the cis-form is more stable than the trans-form, contrary to the observed result. This disagreement might be due to the approximate nature of the calculation; for instance, to the exclusion of the 1s and 2s electrons of O atoms. Moreover, it would be reasonable to take into account the polar structure as one of the canonical set. But, the higher order approximation as this ought not to be performed since the values J and Q used in this calculation are comparatively rough.

The author takes this best opportunity to express his real appreciation for the valuable advice and understanding of Prof. Yonezo Morino and Assistant Professor Saburo Nagakura.

Department of Chemistry, Faculty of Science, Tokyo University

(7) Y. Morino et al: unpublished.

Dipole Moments of Bromotropolones, Thujaplicins and Related Compounds*

By Yukio KURITA, Tetsuo NOZOE and Masaji KUBO

(Received November 11, 1952)

We have already measured the dipole moments of tropolone and some of its derivatives,[1][2][3] and discussed the results in relation to the molecular structure of these compounds and to the electronic structure of tropolone as derived from molecular orbital treatment. The present investigation was undertaken in order to determine the position of substituents in seven new kinds of tropolone derivatives synthesized by one of us (Nozoe) and his collaborators. From the studies on magnetic susceptibility, Hazato and his collaborators suggested that tribromotropolone lacks aromatic properties characteristic of tropolone derivatives.[4] We hoped that the dipole moment measurement would reveal some feature of interest concerning the peculiarity of this compound. Nozoe has reported that unlike other tropolone derivatives α-thujaplicin forms two kinds of crystals of different melting points.[5] It seemed to be interesting to decide whether the difference of the two forms is due merely to the arrangement of molecules in crystals or whether the two crystals are made up of molecules of different molecular structure such that they give different dipole moments in solution.

Experimental Method and Results.—All the measurements were made in benzene solution at 25°C. The dielectric constant was measured with the apparatus reported in the previous paper.[1] The materials used were synthesized and purified in the laboratory of organic chemistry in Tohoku University. The amount of each sample at our disposal was less than 0.3 g. and we were obliged to be satisfied with measurements on solutions of a few different concentrations. As some of these compounds were hygroscopic, we employed a modified Hedestrand method similar to that introduced by Halverstad and Kumler[6] for obtaining specific polarization $p_{2\infty}$ at infinite dilution, differing in the fact that densities were used rather than specific volumes.

$$p_{2\infty}=p_1+C\alpha-\frac{p_1}{d_1}\beta \tag{1}$$

Here p_1 and d_1 denote the specific polarization and density of the solvent, α and β are the rates of change of the dielectric constant ε and density d with weight fraction w,

$$\varepsilon_{12}=\varepsilon_1+\alpha w_2,\quad d_{12}=d_1+\beta w_2 \tag{2}$$

and

$$C=3/d_1(\varepsilon_1+2)^2 \tag{3}$$

where the suffixes 12, 1 and 2 signify the solution, solvent and solute respectively. The crucial data affecting the value of $p_{2\infty}$ were α and β. In evaluating the values for these two constants with equation (2), we used the data on solution alone to minimize the possible effect of moisture content. The probable errors $\delta\alpha$ and $\delta\beta$ estimated by least square method gave for the probable error $\delta p_{2\infty}$ the value

$$\delta p_{2\infty}=C\,|\,\delta\alpha\,|+\frac{p_1}{d_1}\,|\,\delta\beta\,| \tag{4}$$

The probable error $\delta\mu$ in dipole moments was due partly to the assumption that the sum of the electronic and atomic polarization P_E+P_A is equal to the molecular refraction calculated for D-line. Shiratori and Kinumaki[7] reported that the exaltation of molecular refraction is fairly great in these compounds. The atomic polarization of these compounds is supposed to be high owing to the possible vibration of a proton participating in hydrogen bond formation. Fortunately orientation polarization is in general much higher than P_E+P_A in the present case, hence the errors in P_E and in P_A do not affect the value for the moments in an appreciable manner. The results of measurements together with the estimated* errors are given in Tables 1 and 2.

* Read before the scientific meeting of the Chemical Society of Japan held on July 5, 1952.

(1) Y. Kurita, T. Nozoe and M. Kubo, This Bulletin, **24**, 10 (1951).

(2) Y. Kurita and M. Kubo, ibid., **24**, 13 (1951).

(3) Y. Kurita, T. Nozoe and M. Kubo, ibid., **24**, 99 (1951).

(4) G. Hazato, J. Maruha, T. Ikegami and H. Kon, reported at the annual meeting of the Chemical Society of Japan on April 8, 1951.

(5) T. Nozoe, Y. Kitahara, K. Yamane and T. Ikemi, *Proc. Japan Acad.*, **27**, 193 (1951).

(6) I. F. Halverstadt and W. D. Kumler, *J. Am. Chem. Soc.*, **64**, 2988 (1942).

(7) K. Shiratori and S. Kinumaki, reported at the annual meeting of the Chemical Society of Japan on April 4, 1952.

* Excluding errors due to P_E and P_A.

Table 1

Dielectric constant and density increments of benzene solutions at 25°C.

	Compounds	Melting points	w $\times 10^5$	$\Delta\varepsilon$ $\times 10^3$	Δd $\times 10^4$
I	Bromotropolone	190°[ab]	429	12	15
			781	21	32
II	Bromotropolone	108°[ab]	329	26.3	10.8
			568	46.3	—
			1090	89.0	45.5
			1682	141.3	73.5
III	Dibromotropolone	161°[b]	227	15	8
			856	45	43
			1250	69	66
IV	Tribromohinokitiol	90.5°[c]	371	10	16
			836	21	41
			1057	29	52
V	α-Thujaplicin A	34°[d]	344	26.6	6.2
			657	49.8	11.1
			1023	77.9	18.3
VI	α-Thujaplicin B	25.5°[d]	347	26.7	7.9
			788	61.2	15.8
			1284	97.1	24.5
VII	Dibromo-α-thujaplicin				
		80—1°	309	8	13
			633	17	26
			1113	30	46

(a) T. Nozoe, S. Seto, Y. Kitahara, M. Kunori and Y. Nakayama, *Proc. Japan Acad.*, **26**, No. 7, 38 (1950).
(b) T. Nozoe, Y. Kitahara, K. Yamane and A. Yoshikoshi, ibid., **27**, 18 (1951).
(c) T. Nozoe, T. Mukai, K. Takase and A. Matsukuma, ibid., **27**, 152 (1951).
(d) T. Nozoe, Y. Kitahara, K. Yamane and T. Ikemi, ibid., **27**, 193 (1951).

Hedberg[8] and that carried out in our laboratory.[9] (2) The bond moment was assumed to have the same value as in the corresponding benzene derivative, i. e., $\mu(C\text{-}Br)=1.5\,D$, $\mu(C\text{-}i\text{-}C_3H_7)=-0.65\,D$, $\mu(C\text{-}NO_2)=4.0\,D$. (3) The substitution by electrophilic atoms and groups such as bromine and nitro-group are most liable to take place at carbon atoms 3(ortho), 5(para) and 7 (ortho'). This was derived from our molecular orbital treatment[2] and is in conformity with the results in organic synthesis.* (4) The moment of tropolone, 3.5 *D*** in magnitude, lies along a line pointing from the center of the ring to the middle point of two oxygen atoms with its positive end at the ring. That this assumption holds approximately is supported by our previous conclusion from dipole moment measurement.[1] The calculated moments were compared with the experimental data and the position of substituents was determined as shown in Table 3.

Table 3

The position of substituents in tropolone derivatives

Compounds	μobs	μcalc	Position of substituents
Bromotropolone	2.07	2.00	5 or *p*
Bromotropolone	3.91	4.10	3 or *o*
Dibromotropolone	3.57	4.16	3, 7 or *oo'*
Tribromohinokitiol	3.05	3.10	3, 5, 7 or *oo'p*
α-Thujaplicin A	3.37	3.42	3 or *o*
α-Thujaplicin B	3.37	3.42	3 or *o*
Dibromo-α-thujaplicin	2.82	3.03	5, 7 or *po'*

In general the agreement between the observed and the calculated moments is good, considering the approximations made in the calculation. The slight dscrepancy in the case of *oo'*-dibromotropolone may be due to the strong steric and induction effects between oxygen and bromine atoms, as was also the case in *oo'*-dibromohinokitiol.[3] In tribromohinokitiol, the agreement is as good

Table 2

Molecular polarizations and dipole moments at 25°C.

	ε_1	d_1, g./cc.	α	β, g./cc.	P, cc.	R_D, cc.	μ, D
I	2.274	0.8709	2.56	0.483	128	40.3	2.07
II	2.2705	0.87069	8.48	0.463	354.2± 2.8	40.3	3.91±.02
III	2.2753	0.87100	5.23	0.566	309 ±14	48.1	3.57±.10
IV	2.2725	0.87117	2.72	0.525	260 ±16	69.6	3.05±.13
V	2.2730	0.87133	7.55	0.179	278.5± 2.0	46.3	3.37±.02
VI	2.2736	0.87153	7.51	0.177	279.6± 3.9	46.3	3.37±.03
VII	2.2726	0.87153	2.74	0.411	224.6± 1.7	61.9	2.82±.02

Discussion.—In order to determine the position of substituents in these molecules, we calculated the values of the moments for various possible isomers with the following assumptions. (1) The tropolone ring has a regular heptagon form. Hence the bond monents lie along the lines from the center of the ring to their respective carbon atoms. This assumption is supported by an electron difraction experiment by Heilbronner and

(8) E. Heilbronner and K. Hedberg, *J. Am. Chem. Soc.*, **73**, 1386 (1951).
(9) M. Kimura and M. Kubo, This Bulletin, **26**, 250 (1953).
* Cf. reference (a) and (b) of Table 1.
** Recalculated using Halverstadt-Kumler's method.

as can be expected, while such was not the case in tribromotropolone.[1] We recalculated the moment for the latter using the Halverstadt-Kumler's method instead of graphical extrapolation and obtained the moment value 2.46 *D*, which is close to the theoretical value of 2.66 *D*. Hence we can conclude that the successive substitution by bromine in tropolone or hinokitiol do not affect the structure or the electronic state of tropolone ring, though Hazato[4] reported the peculiarity of tribromotropolone. Our conclusion is in conformity with Kimura's result on electron diffraction that in tribromotropolone the structure of tropolone ring is nearly identical with that of tropolone.[9]

In view of the fact that the Halverstadt-Kumler's method gives better results than the ambiguous graphical extrapolation, we have recalculated the data on α-dinitrohinokitiol (m. p. 155°),[1] for which we could not get a definite conclusion. The observed value recalculated is 4.79 *D* and this is in good agreement with the theoretical value of 4.5 *D* for 5,7(or *po'*)-dinitrohinokitiol. This assignment can explain the results in organic synthesis[10] adequately.

The two crystal forms of α-thujaplicin gave an identical moment. The conceivable two molecular forms of α-thujaplicin, i. e., 3-isopropylcycloheptatriene-2,4,6-ol-2-one-1 and 3-isopropylcycloheptatriene-2,4,6-ol-1-one-2 are expected to have values for their moments different from each other by an amount of about 0.4 *D* due to the induction effect. This should surely be detectable by experiment. The absence of such a difference indicates that the two crystal forms give identical molecules in solution. Probably the molecules in the two crystal forms are the same with each other, the difference being attributable to the arrangement of molecules in crystals.

(10) T. Nozoe, Y. Kitahara, K. Yamane and K. Yamaki, *Proc. Japan Acad.*, **26**, 14 (1950).

Summary

The dipole moments of seven tropolone derivatives were measured in benzene solution at 25°C. The values obtained are: bromotropolone (m. p. 190°C., 5-bromo-), 2.07 *D*; bromotropolone (108°C., 3-bromo-), 3.91 *D*; tribromohinokitiol (90.5°C., 3,5,7-tribromo-), 3.05 *D*; α-thujaplicins, both A (34°C.) and B (25.5°C.) form, 3.37 *D*; dibromo-α-thujaplicin (80°C., 5,7-dibromo-), 2.82 *D*. By analysing the results obtained, the position of substituents in these molecules were determined and are given immediately after each name of these compounds in parentheses. The two crystal forms of α-thujaplicin with different melting points give an identical moment in solution. α-Dinitrohinokitiol of m. p. 155°C. is 5,7 (or *po'*)-dinitrohinokitiol.

We wish to express our thanks to Mr. T. Mizuno for his help in our experiment. Our thanks are also due to the Ministry of Education in aid of this research.

Chemical Institute, Faculty of Science, Nagoya University, Nagoya
Chemical Institute, Faculty of Science, Tohoku University, Sendai

Magnetic Susceptibilities of Reduced and Oxygenated Hemerythrins

By Masaji KUBO

(Received November 13, 1952)

The molecular weight of hemerythrin, an iron-containing respiratory pigment, determined by Adair's osmotic pressure method is 66,000.[1] Since hemerythrin contains 1.01% of iron, one molecule of hemerythrin contains twelve iron atoms. The molecule combines with oxygen in the proportion of one oxygen molecule to three atoms of iron,[2] hence the number of oxygen molecules fully combined with a hemerythrin molecule is four. This seems to be very peculiar in view of the fact that in two other iron-containing respiratory pigments, hemoglobin and chlorocruorin, the number of iron atoms in a molecule is equal to the number of oxygen molecules which can combine with it. To elucidate the problem more closely, I have undertaken magnetic susceptibility measurements on hemerythrin. Similar measurements, adopted by Pauling and

(1) A. Roche and J. Roche, *Bull. soc. chim. biol.*, **17**, 1494 (1935).
(2) M. Florkin, *Arch. intern. physiol.*, **36**, 247 (1933).

Coryell,[3] have led to a great extension of the structural knowledge of hemoglobin and related compounds.

Apparatus.—For the determination of magnetic susceptibility, a simple Gouy magnetic balance was employed. A test tube, filled with solution to a definite level, was suspended from a balance between the poles of a magnet. The test tube was 25 cm. long and 8.9 mm. in outer diameter, and the magnetic pole pieces were 7.2 cm. in vertical length and separated by 1.2 cm. The liquid meniscus was at the center of a strong homogeneous field of intensity H. The top and bottom ends of the tube were in a region of weak field H'. The current through the coil of the electromagnet was adjusted exactly to 9.7 amp; with this current magnetic saturation was almost attained. H and H' amounted to 1.03×10^4 and 2.2×10^2 oersteds respectively, hence H'^2 is entirely negligible compared with H^2. The effect of the residual magnetic field after the current was switched off was also small and need not be considered.

The magnitude of downward force f experienced by the tube along its length is given by the expression,

$$f=\frac{1}{2}(\kappa_{\text{gas}}-\kappa_{\text{liq}})H^2A=g\Delta w.$$

where κ_{gas}, κ_{liq} are the volume susceptibilities of the gas and liquid in the tube, A is the cross-sectional area of the liquid column having the value of $\pi(6.9/2)^2$ mm.^{2}, g the gravitational constant, and Δw the apparent increase in weight of the tube on application of the magnetic field.

The magnetic balance was operated at room temperature (25°), and was calibrated with distilled water saturated with air and its magnetic susceptibility per unit volume was set equal to -0.719×10^{-6}. The susceptibility per unit volume of the solution under investigation was calculated from

$$\frac{\kappa_{\text{gas}}-\kappa_{\text{sol}}}{\kappa_{\text{air}}-\kappa_{\text{water}}}=\frac{\Delta w_{\text{sol}}}{\Delta w_{\text{water}}}$$

To fill the upper part of the tube, 99.9% pure commercial nitrogen was used for reduced hemerythrin and air for oxygenated hemerythrin and water. It would be more desirable to use nitrogen in place of air to saturate the water and to remove dissolved oxygen completely from it. However, we had to use air for oxygenated hemerythrin and hence the effect of dissolved air is worth our attention. On the assumption of the additivity of magnetic susceptibility, the increase of susceptibility due to the paramagnetic contribution of dissolved oxygen can be calculated from the known solubility of the gas in water and the molecular susceptibility of oxygen, with the aid of Curie's law. The correction amounted to $+0.0009\times10^{-6}$, which is entirely negligible in comparison to -0.719×10^{-6} of pure water. It was of course ascertained that no bubbles of air came out of water or solution on the wall of the container during measurement. The value of π_{gas} is -0.00040×10^{-6} for nitrogen, which is entirely negligible compared with κ_{sol}, and $+0.0294\times10^{-6}$ for air. Two calibrated test tubes were used; one for reduced hemerythrin and the other for the oxygenated preparation in order to carry out the magnetic measurements at the same time.

Material.—The oxygenated hemerythrin solution was prepared as described in the preceding paper.[4] All the measurements on magnetic susceptibility, optical density, density, and the chemical analysis of iron were made on one and the same solution. These measurements were made in one day, except the iron analysis which took a longer time. The blood cells were washed during the previous evening and allowed to hemolyse overnight. One test tube for magnetic measurement was filled with approximately 5 cc. of the solution. Another part of the solution was deoxygenated in a tonometer, to which a test tube was attached by means of a rubber tube, according to the procedure already given.[4] After deoxygenation was complete, a portion of the solution was transferred to the test tube which was filled to the desired level for the magnetic measurements. The rubber tube was clamped on and a rubber stopper was inserted through the rubber tube to seal the test tube. In this case a very small quantity of air remaining in the rubber tube between the clamped part and the stopper was driven out by a stream of nitrogen injected through the rubber wall by means of a syringe and hypodermic needle.

It was of prime importance in this experiment that the concentration of deoxygenated and oxygenated solutions remained equal in spite of the repeated partial evacuation with an aspirator and equilibration with water-saturated nitrogen. To determine whether appreciable loss of water occurred, measurements were made on the optical density of the original oxygenated solution D_{ox}, that of deoxygenated solution D_{red}, and that of the latter solution exposed to and equilibrated with atmospheric air D'_{ox}. $D_{\text{ox}}-D_{\text{red}}$ and $D'_{\text{ox}}-D_{\text{red}}$ agreed with each other within 0.8%. Incidentally, this can be used to convert the relative concentrations in terms of optical density given in the previous paper into concentrations in terms of the iron content. The specific gravity of the solution at room temperature (25°) was found to be 1.018.

Determination of Iron Content.—The solution (16.408 g.) was dried in air at 100° (dry protein: 0.0221 g. per cc. of solution), and the iron content was determined by the thiocyanate method. A Coleman spectrophotometer was used for color comparison with green light of wave-length

(3) L. Pauling and C. D. Coryell, *Proc. Natl. Acad. Sci. U. S.*, **22**, 210 (1936); C. D. Coryell and F. Stitt, *J. Am. Chem. Soc.*, **62**, 2942 (1940).

(4) M. Kubo, This Bulletin, **26**, 189 (1953).

525 mμ. The concentration of the solution was found to be 7.88×10^{-6} g. atoms of iron per cc.

Results and Discussion

The results of magnetic measurements are summarized in Table 1. The susceptibility of reduced hemerythrin solution is higher while

Table 1

Magnetic Susceptibilities of Reduced and Oxygenated Hemerythrin Solutions at 25°.

	Δw(mg.)	Δw_{water}(mg.)*	$\kappa\times10^6$
Reduced	11.9	16.4	−0.543
Oxygenated	16.35	16.1	−0.731

* Two values do not agree with each other exactly, because different test tubes were used for them.

that of the oxygenated solution a little lower than that of water. It is obvious that although masked by the diamagnetic effect of the solvent and the protein part of hemerythrin, paramagnetic contribution attributable to iron is surely present in the reduced state, whereas such contribution is doubtful in oxygenated solution. The difference of molecular susceptibilities of reduced and oxygenated hemerythrin molecules is given by

$$\chi_{red}-\chi_{ox}=12\times\frac{-0.543+0.731}{7.88}=0.286\,\text{cm.}^3,$$

in which the factor 12 is introduced to take account of the fact that one molecule of hemerythrin contains twelve iron stoms. The difference method is particularly elegant because of the automatic cancellation of the effect of minute quantities of impurities such as indifferent proteins and sodium chloride, which might have come from blood cells and the solution used to wash them respectively, and of the diamagnetic term χ_0 in

$$\chi=\chi_0+N\frac{\mu^2}{3kT}$$

where μ denotes magnetic moment and other notations have their usual significances.

The change in magnetic susceptibility is, to be sure, closely connected with an iron atom or atoms directly combined with oxygen and those affected by it. In a complex molecule such as hemerythrin containing many iron atoms, there is a certain ambiguity as to the interpretation of μ. Let us assume that the different magnetic groups acting at the same time as oxygen-combining centers are oriented entirely independently of one another in the external magnetic field, as if located in separate molecules. This assumption will be justified, since as revealed by the studies on oxygen equilibrium[4] the mutual interaction between these centers is weaker, indicating greater distance between them, than in the case of hemoglobin, for which Pauling and Coryell[5] have given ample reasons for believing that the different magnetic groups in the molecule are magnetostatically independent. The further assumption will be made that the four groups in question are equivalent. Otherwise we would have obtained a more complicated shape of the oxygen equilibrium curve. Then we have

$$\chi_{red}-\chi_{ox}=\frac{4N}{3kT}\left(\mu^{*2}_{red}-\mu^{*2}_{ox}\right)$$

in which μ^* denotes the magnetic moment of each group acting as an oxygen combining center. Quantum mechanical considerations give for a magnetic moment

$$\mu^2=g^2\beta^2J(J+1)$$

where g is the gyromagnetic ratio, β is the Bohr magneton, $eh/4\pi mc$ in Gaussian units, the numerical value of which is 9.2726×10^{-21} erg gauss^{-1} or erg$^{1/2}$ cm.$^{3/2}$, and J the resultant angular momentum in units $h/2\pi$. Neglecting contributions due to orbital moments, and putting $g=2$ and $J=n/2$ for electrons, where n denotes the number of unpaired electrons, we have

$$\mu=\sqrt{n(n+2)}\beta$$

for the effective moment. In connection with the assumption that the spins only are involved, it will be worthwhile to point out that the orbital moments are appreciable for rare earth elements but are probably not very large for other transition group elements.[6] μ in this general treatment corresponds μ^* in this particular problem of a complex molecule. Hence

$$\chi_{red}-\chi_{ox}=\frac{4N\beta^2}{3kT}\left[n(n+2)_{red}-n(n+2)_{ox}\right]$$

Putting numerical values in the equation, we have

$$n(n+2)_{red}-n(n+2)_{ox}=171$$

There is no ad hoc reason to assign any particular value to n_{red} or n_{ox}. The assumption

(5) L. Pauling and C. D. Coryell, *Proc. Natl Acad. Sci. U. S.*, **22**, 159, 210 (1936).

(6) Cf. for example P. W. Selwood, Magnetochemistry, Interscience Publ. Inc., New York, 1943, p. 144.

that the oxygenated group has no unpaired electrons, $n_{ox}=0$, will give for the number of unpaired electrons in the deoxygenated group the value of 12.1 per three atoms of iron, which fixes the lower limit of n_{red}. This fact can hardly be explained if we suppose that only four of the twelve iron atoms of a hemerythrin molecule play a role in combining with four oxygen molecules and that other eight iron atoms remain indifferent. It is known that the iron in hemerythrin is in the ferrous state and that if it is oxidized to the ferric state, the resulting methemerythrin has a brownish color which no longer disappears when its solution is subjected to a vacuum or to the action of a reducing agent.[7] In an isolated ferrous ion or in a hydrated ferrous complex ion $[Fe(OH_2)_6]^{++}$, in which the bonds between the iron atoms and water molecules are essentially ionic or the ion-dipole type, the six outer electrons in excess of those required to form a completed argon shell occupy five $3d$ orbitals, and give rise to a normal state in which four of the electron spins are unpaired. In a covalent ferrous complex ion such as $[Fe(CN)_6]^{-IV}$, on the other hand, the six outer electrons of iron occupy three $3d$ orbitals with their spins paired, the other two $3d$ orbitals forming octahedral bond orbitals with one $4s$ and three $4p$ orbitals, resulting in no unpaired electrons. Therefore irrespective of whether the bonds of iron atoms are ionic or covalent it is very improbable that three ferrous iron atoms contained in a reduced hemerythrin group can have more than twelve unpaired electrons. Hence we can conclude that the number of unpaired electrons in a group acting as an oxygen combining center in reduced state, n_{red}, is twelve.

The calculated value of n_{red} is rather insensitive to the assumed value of n_{ox} so long as the latter is less than three, the calculated value of n_{red} being 12.1~12.4 for the assumed value of n_{ox} ranging from 0 to 2. Hence we have no means to decide from experimental data alone which of the three values $n_{ox}=0$, 1, 2 is correct. In fact the neglect of orbital contributions to the moment overestimates the number of unpaired electrons, while the assumption of complete coupling between different iron atoms in a group underestimates the number. Theoretically $n_{ox}=1$ or 2 is improbable and the most probable one among these three values will be $n_{ox}=0$.

Reduced hemerythrin, like ferrohemoglobin, must therefore be regarded as containing an ionic type of bonding of all iron atoms, whereas in oxygenated hemerythrin all the bonds are essentially covalent in nature. It is a very remarkable fact that oxygen molecules combining with the pigment molecule exert such a profound influence on the electronic structure of all iron atoms present. Pauling and Coryell[8] suggest as the most probable linkage of an oxygen molecule or carbon monoxide molecule coordinated with an iron atom in hemoglobin the following formulas:

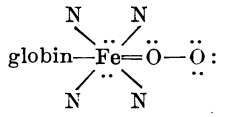

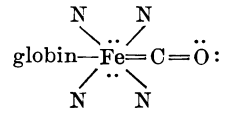

resonating between other possible electronic structures. In this connection it is important to point out that the similarity of hemerythrin and hemoglobin lies in their physiological function as oxygen-transporters rather than in their chemical properties. Unlike hemoglobin, hemerythrin does not combine with carbon monoxide. In fact Florkin[9] found that hemerythrin combined with the same amount of oxygen whether the partial pressure of carbon monoxide was 4 or 150 mm. Hg., and Roche[10] found that bubbling carbon monoxide through a hemerythrin solution brought about no change in its spectrum. This fact makes it very likely that the combination of oxygen with hemerythrin takes place in a quite different manner from that of oxygen with hemoglobin. At present our knowledge on the structure of hemerythrin molecule is so limited that it is almost impossible to propose any definite idea to explain how an oxygen molecule can affect the electronic states of all the three iron atoms in the group. Possibly these iron atoms are coupled with each other in a polynuclear complex so as to be able to transmit the effect of the change of electronic state directly to others. We may have in the diamagnetic state of oxygenated hemerythrin a situation similar to that in certain polynuclear complexes such as iron enneacarbonyl, in which two iron atoms, with an odd number of electrons, coexist in the same molecule, and yet the molecule is diagmagnetic. A possible explanation is that there is some kind of electron pairing taking place, because of the proximity of the iron atoms to one another.

(7) G. F. Marrian, *Brit. J. Exptl. Biol.*, **4**, 357 (1927); M. Florkin, loc. cit.; J. Roche, *Bull. soc. chim. biol.*, **15**, 1415 (1933).

(8) L. Pauling and C. D. Coryell, loc. cit.

(9) M. Florkin, loc. cit.

(10) J. Roche, loc. cit.

Summary

The magnetic susceptibilities of reduced and oxygenated hemerythrin solutions of the same concentration were measured by a Gouy magnetic balance at 25°. The susceptibility of the reduced solution was found to be higher than that of the oxygenated one, indicating a paramagnetic contribution of iron atoms in the reduced molecule. With the assumptions that the four groups acting as oxygen combining centers in the molecule are equivalent to one another and that they are magnetostatically independent, the number of unpaired electrons in the group was calculated to be twelve in the reduced state and zero in the oxygenated preparation. In the reduced state the bonds of the iron atoms are ionic or ion-dipole type in nature. A profound change in the electronic structure takes place when oxygen molecules are combined with the hemerythrin molecule. An oxygen molecule not only loses its own paramagnetism, but also affects all three iron atoms in the group in such a way that the bond type is essentially covalent. These iron atoms are supposed to be coupled with each other in a polynuclear complex so as to be able to transmit the effect of the change of electronic state directly to the others.

The present experiments were made at the Biological Laboratories, Harvard University and the magnetic measurement at the Department of Metallurgy, Massachusetts Institute of Technology. I wish to express my sincere thanks to Prof. Jeffries Wyman, Jr. for his interest and suggestions and to Prof. Albert R. Kaufmann of MIT for giving me facilities to use his magnetic balance.

Chemical Department, Faculty of Science, Nagoya University, Nagoya

The Dipole Moments of Fluorenone Peroxide and Bishydroperoxide

By Keniti HIGASI

(Received November 19, 1952)

In 1940, Wittig and Pieper[1] prepared a new monomeric peroxide, viz., the so-called "fluorenone peroxide"[1] and discussed its structure. They regarded the formula (I) as unsatisfactory, because the yellow color of the crystal seemed to reveal a ketonic double bond. And they favored the oxo-öxide structure (II) instead, which appeared to agree with many of its properties, including its solubilities.

In 1942, Prof. Murakami, of Osaka University, offered me this substance prepared by the Wittig and Pieper's method and we measured its dipole moment in benzene at room temperature. It was then evident from the observed value of its moment, viz., 3.1D that the ring structure (I) which has a smaller moment than 2D should be ruled out. Further, the oxo-öxide structure which corresponds to a large moment of about 6D could not represent the actual state of the molecule. In the preceding article[2] it was suggested, therefore, that resonance occurs among various structures including (II), resulting in a lesser moment.

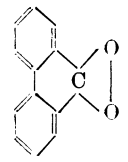

(I)

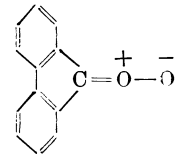

(II)

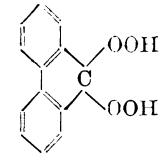

(III)

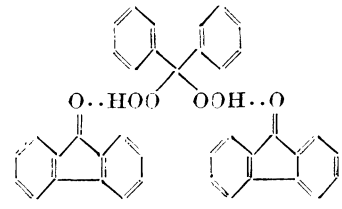

(IV)

(1) G. Wittig und G. Pieper, *Ber.*, **73**, 295 (1940).

(2) K. Higasi, *Bull. I. P. C. R. Tokyo*, **21**, 1147 (1942).

In 1949, Criegee, Schnorrenberg and Beck[3] reported that Wittig's "fluorenone peroxide" is not a simple substance but a mixture of two molecules of fluorenone and one molecule of its bishydroperoxide (III). In benzene solution this molecular compound (IV) dissociates into the three components, giving a monomeric value in the molecular weight determination.

In the present note I wish to report the result of a reexamination of our data from the view-point of Criegee and his pupils. From the apparent polarization of "fluorenone peroxide", the total polarization of the molecular compound (in a dissociated state) was calculated, and then by subtracting the polarizations of two fluorenone molecules,[4] the polarization of the bishydroperoxide (III) was obtained. The dipole moment thus evaluated for the latter substance was 2.4D* in benzene (with fluorenone).

The polarity of the bishydroperoxide (III) arises chiefly from the two C—O dipoles and two O—H dipoles. Besides these, there are small moments induced in the hydrocarbon residue, but a correction for them may be included in the resultant moment for C—O dipoles, which are in a fixed position to the plane of rings. In contrast to these, the two O—H dipoles can rotate around two axes of rotation, viz., the C—O, and O—O linkages (Fig. 1). As a first approximation we may regard the polarity of the molecule as consisting of three independently rotating dipoles, viz., one for O-C-O dipole of 1.0D, and the other two of 1.53D each for the O—H groups.[5] This rough picture was in fact in good accord with the observed moment, giving 2.38D as the calculated moment.**

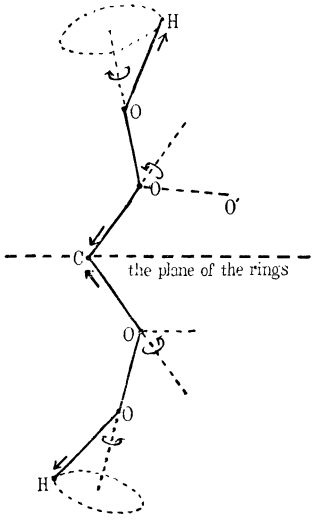

Fig. 1.—The axes of rotation in bishydroperoxide

Further, it is of interest to find that the apparent polarization of fluorenone peroxide increases with the increase in concentration, and that the bishydroperoxide reveals the same tendency but that it is even more pronounced. In Fig. 2 the molecular polarization of the bishydroperoxide was plotted against the mole fraction of the solute and compared with the curve for fluorenone itself.

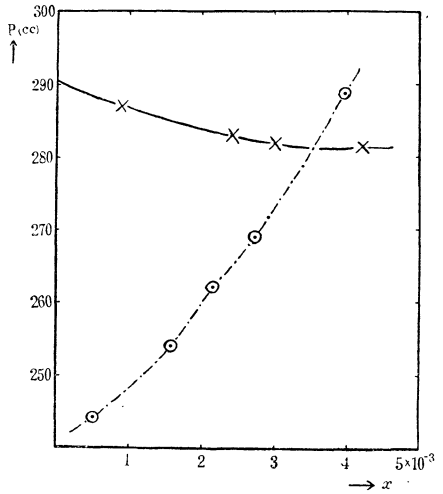

Fig. 2.—Molecular polarization in benzene solution at 25°C (P) and mole fraction (x).
× Fluorenone (Le Fèvre et al[4])
⊙ Bishydroperoxide (Higasi, the sample B*)

The increase in polarization with increasing concentration may be accounted for by making any of the following two assumptions. First, we regard it as characteristic of the solute with O—H group, e.g., the polarizations of alcohols in hexane. Secondly, the bishydroperoxide has a strong tendency to interact with one or two molecules of fluorenone, thus forming very polar complexes. The latter interpretation may be the more plausible,

(3) R. Criegee, W. Schnorrenberg and J. Beck, *Ann.*, **565**, 7 (1949).

(4) E. D. Hughes, C. G. Le Fèvre, R. J. W. Le Fèvre, *J. Chem. Soc.*, 207 (1937).

* The sample A (m. p. 107°~8°) gave 3.1D for fluorenone peroxide and 2.4 D for the bishydroperoxide, while the sample B (m. p. 104°) gave 3.2 D and 2.9 D, respectively. The sample A was recrystallized from B (Cf. Wittig and Pieper: m. p. 108°).

(5) C. P. Smyth, *J. Phys. Chem.* **41**, 209 (1937); and other papers.

** The moment of the bishydroperoxide m is calculated as $m^2=1\times1.0^2+2\times1.53^2$.

because the chance for the association in this type is twice that in the former.

In conclusion, it may be safely stated that a better explanation of our dielectric measurement can be obtained from the work of Criegee and his school than from that of Wittig and Pieper.

I wish to thank Professor M. Murakami of Osaka for the gift of materials and also Doctor R. K. Start of Obuse for his generous assistance in the preparation of the English manuscript.

Institute of Applied Electricity,
Hokkaido University, Sapporo

Electron Diffraction Investigation on Tropolone*

By Masao KIMURA and Masaji KUBO

(Received November 19, 1952)

We have already measured the dipole moments of tropolone and some of its derivatives in benzene solution.[1] The high moments of tropolone were explained adequately by taking into account the contribution of various resonance structures with a formal positive charge at the ring carbon atoms. The resonance was supposed to give a certain amount of double bond character to each bond in the ring, resulting in a coplanar heptagon configuration. The supposition was still too indirect to allow a definite conclusion and hence we undertook an electron diffraction experiment on tropolone to get more direct evidence in support of a regular heptagon ring. After the experiment was complete, an experiment similar to ours was published by Heilbronner and Hedberg[2] and X-ray study by Robertson[3] on the copper complex of tropolone. Though our results were essentially the same as those of Heilbronner and Hedberg, we think it worthwhile to report them in detail, because we could explain the appearance of a peak in the radial distribution function which they failed to assign to any possible distance, and in addition we could deal with the two C-O distances in more extensive manner, the results of which will be of much interest concerning the possible symmetry of this molecule.

Material and Experimental Method.—The tropolone sample (m. p. 50~51°) was synthesized and purified at the laboratory of organic chemistry, Tohoku University.[4] It was evaporated at a temperature several degrees higher than its melting point, and was led through a high temperature nozzle into a vacuum chamber to interfere with an electron beam of 0.05~6 A. wavelength calibrated with a gold foil. The diffraction photographs were prepared in the usual way.[5] The camera distance was 11 cm.

Experimental Results.—The visual intensity curve obtained is shown in Fig. 1 (V_1).* The q ($=10s/\pi$) values for the maxima and minima of diffraction halos are given in Table 1.

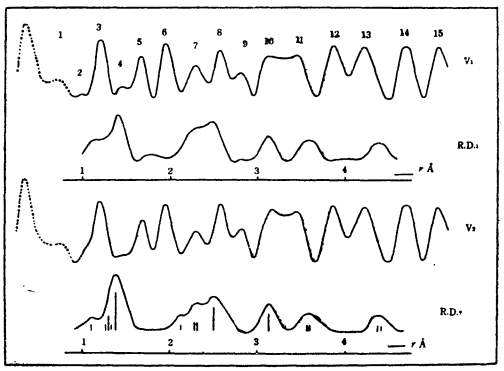

Fig. 1.—Visual curve and the radial distribution function of tropolone

* Read before the scientific meeting of the Chemical Society of Japan held on April 4, 1952.

(1) Y. Kurita, T. Nozoe and M. Kubo, This Bulletin **24**, 10, 99 (1951).

(2) E. Heilbronner and K. Hedberg, *J. Am. Chem. Soc.* **73**, 1386 (1951).

(3) J. M. Robertson, *J. Chem. Soc.*, **1951**. 1222.

(4) T. Nozoe, S. Seto, Y. Kitahara, M. Kunori and Y. Nakayama, *Proc. Japan Acad.*, **26**, (7) 38 (1950).

(5) M. Kimura, *Chemical Researches*, **9**, 53 (1951).

* The dotted portion was obtained from the theoretical intensity curve calculated for the molecular structure inferred from the preliminary radial distribution function, which was derived from the full line part of the visual intensity curve.

Table 1

The q values for the maxima and minima of diffraction halos

Max.	Min.	q	Max.	Min.	q
1		10.06		9	49.04
	2	12.10	9		51.59
2		14.68		10	54.23
	3	16.62	10		58.74
3		19.10		11	62.61
	4	21.78	11		65.18
4		24.10		12	68.20
	5	26.13	12		72.32
5		28.43		13	75.89
	6	31.04	13		79.60
6		33.91		14	85.00
	7	37.39	14		89.03
7		40.89		15	92.99
	8	43.70	15		96.51
8		46.47			

The radial distribution function,

$$rD(r) = \sum_{q=1}^{\max} I_q \exp(-aq^2) \sin\left(\frac{\pi}{10} qr\right)$$

calculated from the visual intensity curve V_1 is shown in Fig. 1 (RD_1). Here notations have their usual significances and the constant a was chosen so that $\exp(-aq^2) = 0.1$ at $q_{\max}$. The peaks at 1.39 and 3.13 A. are sharp and hence the values are accurate. Those at 3.59 and 4.38 A. are distinct but broad, presumably due to the close proximity of two different distances.* The humps at 1.10, 2.30 and 2.48 A. are less distinct and are not suitable for obtaining accurate values for the distance. Of the three weak maxima at 1.75, 2.80 and 4.02 A., the latter two seem to be insignificant, while the first one corresponds evidently to the fairly conspicuous peak at 1.73 A. of Heilbronner and Hedberg. These peaks and humps can be explained properly except the three weak maxima as shown in Table 2 (3rd and 4th columns) with the following two assumptions. (1) The tropolone ring has a plane regular heptagon form shown in Fig. 2 with edges 1.39 A. long. (2) Each of the C-O bonds of 1.30 A. in length lie along a line bisecting the respective $\angle$CCC angle.

The C-O distance of 1.30 A., O-O distance of 2.52 A. and C-H distance of 2.13 A. will be masked respectively by peaks at 1.39, 2.51 and 2.28 A. The flat peak at 1.75 A. less obvious than that of Heilbronner and Hedberg does not correspond to any possible distance. We suspected that the appearance of this peak might be due to the inaccuracy of intensity estimation by visual method on the 1st, 2nd, 4th, 7th and 9th maxima. We therefore tried to modify the visual curve V_1 in such a way that the ghost disappears. The resulting curve and the radial distribution function obtained from it are shown in Fig. 1 (V_2 and RD_2). The three ghosts in question disappear in the radial distribution function. The curve V_2 is in conformity with the visual estimation except that here the 2nd and 4th weak maxima in V_1 appear as inflection points. It is very hard to determine accurately the intensity of such maxima by visual method. In fact it is known that a weak maximum observed by naked eyes, if examined by microphotometry on a diffraction photograph taken with a sector, turns out to be an inflection point of the curve. Hence we believe that V_2 rather than V_1 is nearer the truth and wish to point out that in view of the fact that the whole visual curve affects the radial distribution function, it is possible that small errors in visual curve may give rise to fortuitous maxima in radial distribution function. The interatomic distances from the modified radial distribution function RD_2 are given in the last column of Table 2. The agreement with the calculated values is excellent.*

In order to determine C-O distance which was masked by a very strong peak at 1.39 A. in the radial distribution function, we calculated the theoretical intensity curve

Table 2

Interatomic distances in tropolone

Bond	Ratio of Z_iZ_j/r_{ij}	Interatomic distance, A. calc.	obs. RD_1	obs. RD_2
C_1-C_2	18	1.39	1.39	1.39
C_1-C_3	11	2.51	2.48	2.51
C_1-C_4	8	3.12	3.13	3.13
O_1-C_2	8	2.28	2.30	2.32
C_1-O_1	7	1.30	—	—
O_1-C_3	5	3.61	3.59	3.60
O_1-C_4	4	4.40	4.38	4.39
O_1-O_2	3	2.52	—	—
C-H	3	1.10	1.10	1.10
C···H	3	2.13	—	2.13

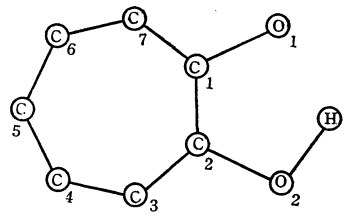

Fig. 2.

* Another explanation that this is due to the vibrational motion of atoms is less likely, because we should then expect similar broadening for the peak at 3.13 A as will be clear in later paragraphs.

* Vertical bars in Fig 1 (RD_2) indicate distances calculated for the best model. The heights of the bar are drawn proportional to Z_iZ_j/r_{ij}.

$$I(q)=\sum_{i<j}\sum \frac{Z_iZ_j}{r_{ij}} \sin\left(\frac{\pi}{10} qr_{ij}\right)^{*}$$

for various values of C_1-O_1 and C_2-O_2 distances ranging from 1.18 to 1.38 A. Here Z_i and Z_j denote the atomic numbers of i- and j-atoms respectively and r_{ij} the distance between them. The ring was assumed to have a regular heptagon form with C-C distance equal to 1.39 A. The line along the C-O bond was assumed to bisect ∠CCC angle. The effect of hydrogen atom could be neglected. A part of the results are summarized in Table 3 and Fig. 3.

Table 3

Various models for the theoretical intensity curves

Model	C_1-O_1 distance, A.	C_2-O_2 distance. A.
1	1.26	1.26
2	1.30	1.30
3	1.34	1.34
4	1.22	1.30
5	1.22	1.38
6	1.26	1.34
7	1.30	1.38

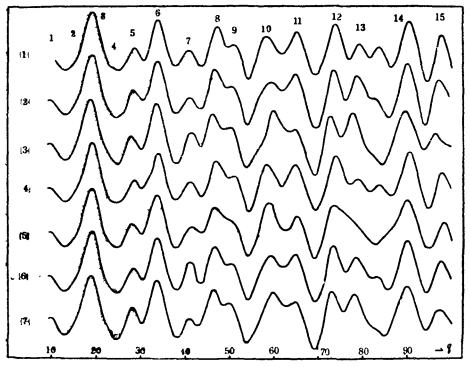

Fig. 3—Theoretical intensity curve

The following experimental facts will serve as a criterion to discard some of the presumed values of C-O distance. (1) The 10th and 11th maxima in the visual intensity curve with nearly equal intensity are broad. (2) The 12th and 13th maxima have nearly equal strength and are sharp. It was found that if the two C-O distances were assumed to have equal length (Cf. models 1~3), a distance of 1.26 as well as 1.34 A. does not fit the experiment. If the two C-O distances are different, we have naturally a variety of choice, though a distance less than 1.22 A. or greater than 1.40 A. (Cf. models 4 and 5) for one of the two C-O bonds does not give any theoretical intensity curve in agreement with the experiment. If we take vibrational motion into account, the theoretical intensity curve changes in such a way that both the 10th and the 11th maxima become a little flatter, the degree of change being greater for the former than for the latter and that the shelf at the lower right foot of the 13th maximum becomes less obvious. These changes, however, do not alter the conclusions derived for the fixed model. After closer examination,** we found that the best fit with experiment could be obtained for the model 6. The agreement of this model with experiment and the broad peak at 3.60 and 4.39 A. in the radial distribution function seem to imply that tropolone is a mobile tautomeric system of unsymmetrical molecules with the hydrogen atom not occupying a position midway between the two oxygen atoms. The unsymmetrical structure was also favored by Dewar,[6] Cook[7] and others[8] and by Nozoe.[9]

Summary

The molecular structure of tropolone was studied by the electron diffraction method. The most plausible model was found to be a plane regular heptagon form with C-C distance 1.39 A. long and C-H distance 1.10 A., having two slightly different C-O distances, i.e., C-O =1.34 A. and C=O=1.26 A.

We wish to express our thanks to Prof. Nozoe of Tohoku University for providing us with the material prepared for use in the present investigation and to Prof. Morino of Tokyo University for valuable discussions. Our thanks are also due to the Ministry of Education for grants in aid of this research.

Chemical Department, Faculty of Science, Nagoya University, Nagoya

* The effect of vibration of atoms in the molecule, which is not taken into account in this equation, did not affect appreciably the position of maxima and minima and also the relative intensity of maxima lying close together. This will be explained in detail later.

** It was found that a deviation less than 5° of C-O directions in or out of the ring plane does not affect appreciably the theoretical intensity curve. The deviation of this direction greater than about 5° is unlikely, though it may afford another possibility of explanation for the broadness of peaks at 3.60 and 4.39 A.

(6) M. J. S. Dewar, *Nature*, **155**, 50, 141, 479 (1945).
(7) J. W. Cook, A. R. Gibbs, R. A. Raphael and A. R. Somerville, *J. Chem. Soc.*, **1951**, 503.
(8) H. P. Koch, ibid., **1951**, 512; G. P. Scott and D. S. Tarbell, *J. Am. Chem. Soc.*, **72**, 240 (1950).
(9) T. Nozoe, T. Mukai and J. Minegishi, *Proc. Japan Acad.*, **27**, 419 (1951); N. Yui and T. Nozoe, *Sci. Reports Tohoku Univ.*, **35**, 83 (1951).

Antituberculous Compounds. II. Thiosemicarbazones from Benzalacetones[1]

By Tamio NISHIMURA

(Received November 25, 1952)

In a previous communication the author has reported the synthesis of *p*-acetamidocinnamaldehyde thiosemicarbazone as a vinylog of Tibion.[2] In our laboratory this thiosemicarbazone has been shown not to have antituberculous activity over that of Tibion in an *in vivo* test.[3] But in connection with this study, it would be interesting to compare the antituberculous activity of the thiosemicarbazones previously reported with that of other vinylogous thiosemicarbazones having similar structure. For this purpose the author synthesized *p*-acetylaminobenzalacetone thiosemicarbazone (V) and 1-(*p*-nitrophenyl)-2-bromo-1-butene-3-one thiosemicarbazone (VIII), according to the following scheme.

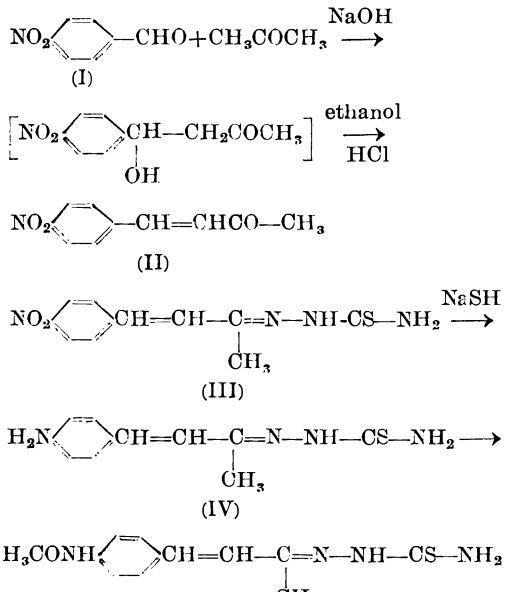

(1) A part of this study was presented at the annual meeting of the Chemical Society of Japan in Tokyo on April 5, 1952.

(2) T. Nishimura, This Bulletin, **25**, 54 (1952).

(3) K. Mizunoe, Unpublished data.

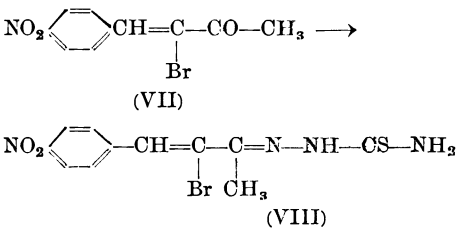

(VII)

(VIII)

p-Nitrobenzaldehyde (I) was prepared from *p*-nitrotoluene as described before.[2] According to the method of Baeyer and Becker,[4] (I) was condensed with acetone and dehydrated to produce *p*-nitrobenzalacetone (II), without giving good results. However, it was found that the condensation reaction proceeded smoothly at room temperature when a mixture of acetone and water (1:1) was used. On condensation and dehydration, Baeyer and Becker's so called "*p*-nitrodicinnamyl methyl ketone"[4] was obtained in a considerable amount. The condensation product, 4-hydroxy-4-(*p*-nitrophenyl)-2-butanone was extracted with ether and dehydrated with hydrochloric acid without isolating it in a crystalline state. (II) was condensed with thiosemicarbazide in ethanol to give *p*-nitrobenzalacetone thiosemicarbazone (III) which was reduced to *p*-aminobenzalacetone thiosemicarbazone (IV) with sodium hydrogen sulfide. *p*-Acetamidobenzalacetone thiosemicarbazone (V) was obtained by acetylation of (IV) with acetic anhydride in ethanol.

1-(*p*-Nitrophenyl)-1, 2-dibromobutan-3-one (VI) was obtained by the action of bromine on (II) in glacial acetic acid, which was converted to 1-(*p*-nitrophenyl)-2-bromo-1-buten-3-one (VII) by dehydrobromination with potassium carbonate or pyridine.

Experimental[5]

***p*-Nitrobenzalacetone** (II).—A mixture of 30.2g. (0.2 mole) of *p*-nitrobenzaldehyde, 60 ml. of acetone and 60 ml. of water in a 300 ml. Erlenmeyer flask was made slightly alkaline by adding

(4) A. Baeyer and P. Becker, Ber. **16**, 1968 (1883).

(5) All temperatures are uncorrected.

4 drops of 10% sodium hydroxide solution. The mixture was shaken for 25 minutes at room temperature while *p*-nitrobenzaldehyde disappeared, yielding a small amount of undissolved "*p*-nitrodicinnamyl methy ketone." The reaction mixture was neutralized with 10% hydrochloric acid and extracted with 120 cc. and then 60 cc. of ether. The ether extracts were combined, filtered and concentrated on a water bath. The concentrated solution was mixed with 60 cc. of ethanol and 40 cc. of 10% hydrochloric acid, heated for 4 hours on a steam bath and allowed to stand overnight at room temperature. Precipitated yellow crystals were collected on a filter, recrystallized from 120 cc. of ethanol and dried in a desiccator, yielding 20.1 g. (53%) of the desired product, m. p. 107—108°. "*p*-Nitrodicinnamyl methyl ketone" (m.p. 244°) which did not dissolve in ethanol on recrystallization amounted to 6.7 g.

***p*-Nitrobenzalacetone thiosemicarbazone** (III).—Into a hot solution of 4.7 g. of thiosemicarbazide in 200 cc. of ethanol was added 9.6 g. of *p*-nitrobenzalacetone and the mixture was heated on a steam bath, giving 12.2 g. (92%) of the thiosemicarbazone, m. p. 240° (decomp.) (Found: N, 21.10% Calcd. for $C_{11}H_{12}O_2N_4S$: N, 21.21%).

***p*-Aminobenzalacetone thiosemicarbazone** (IV).—A mixture of 4 cc. of 2*N*-sodium hydroxide and 20 cc. of ethanol was saturated with hydrogen sulfide. To this solution was added 1.2 g. of *p*-nitrobenzalacetone thiosemicarbazone in one portion, and the mixture was refluxed for one hour. After cooling, the precipitated crystals were collected, washed with ethanol and water, yielding 0.9 g. (75%) of the desired product melting at 191° (decomp.). This material was dissolved in 7 cc. of pyridine and the solution was filtered. 7 cc. of water was added to the solution and it was allowed to stand overnight in an ice-box. Separated crystals were filtered and washed with ethanol and water, giving 0.8 g. of the same m. p. (Found: N, 23.93%, Calcd. for $C_{11}H_{14}N_4S$: N, 23.92%).

***p*-Acetylaminobenzalacetone thiosemicarbazone** (V).—A mixture of 0.6 g. of *p*-aminobenzalacetone thiosemicarbazone, 10 cc. of ethanol and 0.4 cc. of acetic anhydride was heated on a steam bath until complete dissolution took place. The solution was allowed to stand overnight at room temperature. Crystals were filtered and washed with ethanol and water, giving 0.5 g. (70%) of the desired product melting at 220—221°(decomp.). After recrystallization from 40 cc. of ethanol, there was obtained yellow plate melting at 223° (decomp.). Further recrystallization did not change the m. p. (Found: N, 20.12%. Calcd. for $C_{13}H_{16}ON_4S$: N, 20.28%).

1-(*p*-Nitrophenyl)-1,2-dibromobutane-3-one (VI).—3.2 g. of bromine was added with stirring to a solution of 3.8 g. of *p*-nitrobenzalacetone in 20 cc. of glacial acetic acid. The mixture was allowed to stand for two hours at room temperature and then overnight in an ice-box. Separated crystals were filtered and washed with ethanol and water to give 4.4 g. (63%) of the desired product melting at 118° (decomp.). The m. p. of a small sample recrystallized from glacial acetic acid (or ethanol) was 128° (decomp.) (Found: C, 34.69; H, 2.96; Br, 45.33%. Calcd. for $C_{10}H_9O_3NBr_2$: C, 34.21; H, 2.58; Br, 45.54%).

1-(*p*Nitrophenyl)-2-bromo-1-buten-3-one (VII).—(a) A solution of 1.8 g. of 1-(4-nitrophenyl)-1,2-dibromobutane-3-one in 5 cc. of pyridine was heated for five minutes on a steam bath, followed by addition of 5 cc. of water. After cooling, 1.2 g. (89%) of the desired product melting at 119—120° was obtained. Recrystallization from ethanol gave the pure material melting at 120—121° (Found: C, 44.68; H, 3.28; N, 5.28% Calcd. for $C_{10}H_8O_3NBr$: C, 44.46; H, 2.99; N, 5.19%).

(b) 0.8 g. of bromine was added to a solution of 0.9 g. of 4-nitrobenzalacetone in 5 cc. of glacial acetic acid and the mixture was allowed to stand for 15 minutes. This was followed by the addition of 0.4 g. of anhydrous potassium carbonate. When the evolution of gas had ceased, the mixture was heated on a steam bath for 30 minutes and then 2 ml. of water added. On cooling, resulting crystals were collected and washed with water. The yield of the product melting at 118—119° was 1.0 g. (77%).

1-(*p*-Nitrophenyl)-2-bromo-1-buten-3-one thiosemicarbazone (VIII).—To a hot solution of 0.5 g. of thiosemicarbazide in 25 cc. of ethanol was added 1.4 g. of 1-(*p*-nitrophenyl)-2-bromo-1-buten-3-one and the mixture was refluxed for 20 minutes on a steam bath to give 1.3 g. (75%) of the desired product melting at 182° (decomp.). The crude material was dissolved in 7 cc. of pyridine and reprecipitated by adding 5 cc. of water to the solution to yield the pure substance melting at 191° (decomp.) (Found: Br, 23.05; N, 16.59% Calcd. for $C_{11}H_{11}O_2N_4BrS$: Br, 23.29; N, 16.32%).

The author wishes to express his sincere thanks to Mr. T. Nagano and Miss. M. Ito of our laboratory for some of the micro-analyses in this work.

The expense of this work was partly defrayed by Grant in Aid for the Miscellaneous Scientific Research, given by the Educational Ministry to which the author's thanks are due.

Chemical Laboratory,
The Kitasato Institute, Tokyo, Japan

Determination of Small Quantity of Pentosan in Cellulosic Materials

By Tōru ABE, Kei MATSUZAKI, Akira HATANO and Hiroshi SOBUE

(Received November 25, 1952)

I. Introduction

It is well known, that the phloroglucin method gives high values of pentosan content, on account of oxymethyl furfural produced from hexosan by acid distillation. In the case of chemical pulps especially high α pulps for cellulose ester or rayon tire cords, the apparent pentosan from hexosan becomes several times the true value and results in inaccuracy. Therefore, many methods have been advised to reduce or remove the influence of hexosan.

1) Barbituric acid method[1][2]

2) Decomposition of oxymethyl furfural by redistillation[3][4]

3) Dissolving oxymethyl furfural-phloroglucide by treatment with alcohol[3][5]

4) Colorimetry[6]~[9]

5) Determination utilizing the difference of the rates of thermal decomposition between furfural and oxymethyl furfural[10][11]

The method 1) gives lower values because of the solubility of the condensate in hydrochloric acid solution. As to the method 2), oxymethyl furfural is not only incompletely removed but also furfural is decomposed considerably. As for the method 3), the difference between the decomposition rates of oxymethyl furfural and furfural was smaller than expected and a good result was not obtained.

The method 3) is not a perfect one, but in Japan, phloroglucin method is predominantly adopted. So it is not useless to investigate the method more thoroughly. Colorimetric method 4) is promising as it is claimed that the influence of hexosan is under 0.1%. Then in this research, both the treatment of the phloroglucide with ethanol and the colorimetric method were investigated and the results were compared with barbituric acid, bromate and the usual phloroglucin methods, with special attention to the influence of hexosan on pentosan determination.

II. Improvement of Phloroglucin Method

1) **Experimental Procedures.**—The amounts of furfural and oxymethyl furfural produced by acid distillation, depend on the weight of the sample, distillation apparatus, variety and concentration of the acid, and rate and time of distillation. So, at first, these conditions were determined as follows:

The sample was weighed into a distillation flask (300 cc.) and 100 cc. of 12% hydrochloric acid solution was added and the mixture was heated in an oil bath. The temperature of the bath was regulated to obtain 30 cc. of the distillate in ten minutes and this was about 170°C. During the course of distillation, when every 30 cc. of the distillate was obtained, 30 cc. of 12% hydrochloric acid solution was tapped into the flask. To the total distillate (360 cc.), 40 cc. of phloroglucin-12% hydrochloric acid solution (7.33 g./l.) was added and the solution was kept standing for sixteen hours at 20°C. The phloroglucide was filtered on a glass filter 1G4, then 60 cc. of 95% ethanol was added to the precipitate in the glass filter and the mixture was kept standing for ten minutes at 60°C. The alcohol-insoluble residue was filtered on the glass filter and this procedure was repeated three times. In some cases, the initial phloroglucide was once dried at 105°C. and then treated with alcohol. Solubility in alcohol was calculated from the amount of phloroglucide before and after the alcohol-treatment and the portion dissolved in the mother liquor (hydrochloric acid solution) was

(1) E. Unger and R. Jäger, *Ber.*, **36**, 1222 (1903).
(2) S. Takehara, *J. Soc. Chem. Ind., Japan*, **47**, 74 (1944).
(3) K. Oshima and K. Kondo, *J. Coll. Agr. Hokkaido Imp. Univ.*, **16**, 52 (1926).
(4) C. Kullgren and H. Tydén *Cellulosechemie*, **11**, 15 (1930).
(5) T. Fukai and W. Nakajima, *J. Soc. Brewing, Japan*, **23**, No. 9, 18, No. 10, 18 (1928).
(6) G. E. Youngburg and G. W. Pucher, *J. Biol. Chem.*, **61**, 741 (1924).
(7) R. E. Peeves and J. Munro, *Ind. Eng. Chem., Anal. Ed.*, **12**, 551 (1940).
(8) R. A. Stillings and B. L. Browning, *Ind. Eng. Chem., Anal. Ed.*, **12**, 499 (1940).
(9) K. Kawamura and T. Higuchi, *J. Soc. Textile Cellulose Ind. (Japan)*, **7**, 95 (1951).
(10) T. Fujimura, *J. Soc. Textile Cellulose Ind. (Japan)*, **7**, 29 (1951).
(11) T. Fujimura, *J. Chem. Soc. Japan, Ind. Chem. Soc.*, **54**, 271 (1951).
(12) H. F. Launer and W. K. Wilson, *J. Res. Natl. Bur. Stand.*, **22**, 471 (1939).
(13) S. Takehara, *J. Soc. Chem. Ind., Japan*, **46**, 449 (1943).
(14) M. Hamada and I. Takano, *J. Agr. Dep. Kyushu Imp. Univ.*, **9**, No. 1 (1940).
(15) W. Gierisch, *Cellulosechemie*, **6**, 61, 81 (1925).

not considered. For calculation of xylose or pentosan content, the dissolved portion of the phloroglucide was assumed 5.2 mg. in 400 cc. of the mother liquor, even when the alcohol treatments were made.

2) Experimental Results.—(a) Influence of times of the alcohol treatment.—By means of one treatment, alcohol-soluble part was largely removed and completely eliminated by the operations of three times as shown in Table 1.

Table 1

Effect of Times of Alcohol-Treatment on Solubility in Alcohol

Glucose (g.)	3.0108	3.0091
Total phloroglucide (g.)	0.0320	0.0329
Alcohol-insoluble phloroglucide (g.)		
Time of treatment		
1	0.0142	0.0154
2	0.0137	0.0148
3	0.0137	0.0149
4	0.0138	0.0147
5	0.0139	0.0147

(b) Apparent pentosan content from glucose, xylose and arabinose.—According to Kröber, conversion ratios of xylose and arabinose to furfural were 88% and 73% respectively. He constructed his table in supposition that the pentosan in wood is a mixture of an equal amount of xylose and arabinose. Our experiment showed that these values were 86% and 72% respectively, and glucose also yielded phloroglucide which corresponded to 1.9% pentosan when calculated from Kröber's table. When the fresh, wet phloroglucides were treated with ethanol, 82% of the one from glucose was dissolved in ethanol but also 10~11% of those from xylose and arabinose were dissolved. After the precipitate was once dried, the alcohol-soluble portion was considerably lowered as shown in Tables 2 and 3. In the tables each experiment was duplicated and averaged.

(c) Influence of the amount of phloroglucin added, on the alcohol-soluble portion.—The

Table 2

Apparent Pentosan from Glucose (3.000 g.)

Condition of phloroglucide treated with alc.		Phloroglucide, mg.	Apparent pentosan, %*	Solubility, %
dry	before alc.	59.2	1.90	60.3
	after alc.	23.5	0.86	
wet	before alc.	—	—	82.1
	after alc.	10.6	0.47	

* Based on the weight of glucose and calculated from Kröber's table.

Table 3

Conversion ratios of Xylose and Arabinose to Furfural (sample, each 0.100 g., and the ratios were calculated from the amount of phloroglucide)

	Condition of phloroglucide treated with alc.		Phloroglucide, mg.	Conversion ratio, %	Solubility, %
Xylose	dry	before alc.	101.6	86.1	4.0
		after alc.	97.5	82.8	
	wet	before alc.	—	—	10.8
		after alc.	90.6	77.3	
Arabinose	dry	before alc.	84.0	71.9	1.5
		after alc.	82.7	70.9	
	wet	before alc.	—	—	10.0
		after alc.	75.6	65.2	

previous experiment showed that both the furfural- and oxymethyl furfural phloroglucide were divided into two parts, alcohol-soluble and -insoluble. It is clear that the cause is not the solubility of the precipitate in alcohol, such as in low-molecular weight compounds. Because the weight of the dissolved portion reached a constant value as the treatments were repeated.

Goodwin and Tollens[16] observed that, at room temperature, one mole of furfural condensed with one mole of phloroglucin under separation of one mole of water, but at 80°C. the precipitate was formed under dehydration of three moles of water. This indicates the oomposition of the phloroglucide is not constant and it is probable that this variation in composition would have effects on the solubility in alcohol. Then various amounts of phloroglucin were added to furfural and oxymethyl furfural solution, and the solubilities in alcohol of the phloroglucides produced were determined. 1 g. of furfural, purified twice by vacuum distillation, was dissolved in 1 l. of 12% hydrochloric acid solution, of which 10 cc., 30 cc., 50 cc. and 100 cc. were taken out and each was diluted to 360 cc. with 12% hydrochloric acid solution. To these solutions, the phloroglucin solution was added so as to make molar ratio of furfural to phloroglucin 1 : 2, 1 : 3, 1 : 5 and 1 : 10 and each was diluted with 12% hydrochloric acid solution to make the total volume 400 cc., The weights of the phloroglucides and their solubilities in alcohol were tabulated in Table 4. The solubilities were determined on the undried, wet samples, that were the same in the following experiments.

The table shows that the greater the ratio of phloroglucin to furfural, the larger is the solubility in alcohol of the precipitate. The amount of the phloroglucide (including alcohol-soluble part) always agreed well with the calculated value from the assumption that one mole of furfural condensed with one mole of phloroglucin under dehydration of two moles of water.

(16) W. C. Goodwin and B. Tollens, *Ber.*, **37**, 915 (1904).

Table 4

Effect of Phloroglucin added on the Solubility of Furfural-Phloroglucide in Alcohol

Furfural : Phloroglucin	Furfural	10 mg.	30 mg.	50 mg.	100 mg.
	Phloroglucide, theoretical	19.4 mg.	58.1 mg.	96.9 mg.	193.8 mg.
	Phloroglucide, observed, %*				
1 : 2	without alc.	93.8	100.3	99.1	—
	with alc.	69.5	88.6	91.1	95.5
1 : 3	without alc.	95.4	99.9	99.5	—
	with alc.	66.9	83.0	88.2	94.1
1 : 5	without alc.	93.8	100.6	99.9	—
	with alc.	54.1	78.3	84.9	91.7
1 : 10	without alc.	97.9	100.0	99.5	—
	with alc.	68.5	76.2	82.6	—

* Based on the theoretical amount.

Table 5

Effect of Phloroglucin added on the Solubility of Oxymethyl Furfural-Phloroglucied in Alcohol

Phloroglucin added*	Phloroglucide, observed, mg.		Apparent pentosan, %
1 : 2	without alc.	63.0	2.0
	with alc.	11.5	0.5
1 : 3	without alc.	63.3	2.0
	with alc.	10.8	0.5
1 : 5	without alc.	60.3	1.9
	with alc.	10.3	0.5
1 : 10	without alc.	60.9	2.0
	with alc.	11.0	0.5

* Based on apparent pentosan, 2% of the sample (glucose, 3.000 g.)

Next, similar procedures were applied to the oxymethyl furfural obtained from glucose by distillation with hydrochloric acid solution. From Table 5, it seems that neither the amount of phloroglucide nor its solubility in alcohol are influenced by the amount of phloroglucin added. But the color of the precipitate varied from brown to yellowish brown as the added amount was increased. This would indicate the composition of the phloroglucide varied according to the ratio of phloroglucin to oxymethyl furfural but its influence is not remarkable as the amount of the precipitate is small.

From the fact that the solubility of furfural-phloroglucide in alcohol increased with the amount of phloroglucin added, it is desirable to adjust the amount of phloroglucin added twice the theoretical. Therefore, expe iments were made on the mixtures of glucose and xylose (3 g. of glucose 10, 30, 50 and 100 mg. of xylose) adding twice plus the theoretical amount of phloroglucin to the distillate.

Results in Table 6 indicate the alcohol-extraction is useful especially for pentosan-poor samples,

Table 6

Solubility of Phloroglucide from Glucose-Xylose Mixtures

Sample, glucose 3 g. plus xylose, mg.	Xyolse, observed, mg.	
	without alc.	with alc.
10	72.6	17.0
30	90.5	36.1
50	105.5	58.7
100	151.8	112.0

but even in those cases, the amount of xylose observed is always greater than the true value. This is due to the presence of a greater amount of alcohol-insoluble phloroglucide from oxymethyl furfural than an alchool-soluble part of furfural-phloroglucide.

(d) **Discussion.**—The amount of alcohol-soluble phloroglucide of furfural increased with the amount of phloroglucin added. This indicates that the structure of furfural-phloroglucide is not constant. But, as above mentioned, the total amount of phloroglucide is independent of the phloroglucin added and consistent with the assumption that one mole of furfural condenses with one mole of phloroglucin under dehydration of two moles of water. From these results, the condensate is thought to be a relatively high-molecular compound as in furfural resin, with structures of chain type or more probably net-work type, and not to be a low-molecular compound. The size and shape of the condensate would vary with phloroglucin added and influence the solubility in alcohol. A distinct conclusion, however, can not be made without elementary analysis and molecular weight determination of the condensate.

In the case of oxymethyl furfural, the added amount of phloroglucin dose not influence the solubility in alcohol but the color change above mentioned may show structural variation of the condensate similar to the case of furfural-phloroglucide. In both cases, if the precipitate was

once dried, the solubility in alcohol was lowered perhaps by increased condensation. Even when wet, undried precipitate was treated with alcohol, and the solubility was considerably influenced by the method of filtration and the duration of time from filtration to the alcohol-treatment.

In conclusion, the alcohol-treatment of phloroglucide is useful to reduce remarkably the influence of hexosan on pentosan determination, but has the defects that the influence is not completely removed and the experimental reproducibility is not good because of complicated factors.

III. Colorimetry with Aniline and Comparison with Other Methods

1) Experimental Procedures.—Pentosan determination by colorimetry was in most cases applied to furfural produced by acid-distillation, but sometimes also applied to pentose itself obtained by acid hydrolysis.[17] Many color reagents such as benzidine,[18] xylidine,[19] orcin,[20] aniline[6]~[9] and p-bromoaniline[21] were used. It soon became evident from the preliminary work that the method of Stillings & Browning[8] gave good results. Then, this method was adopted with the following modifications.

Acetic acid-aniline reagent was prepared by dissolving 50 cc. of aniline in 500 cc. of glacial acetic acid. To 10 cc. of the neutralized distillate 50 cc. of the aniline solution was added and kept standing for half an hour at 25°C. Transmittancy of the solution was determined by the Hitachi EPO type photometer with a filter of 520 mμ, and compared with standard solution of furfural. In this and following experiments distillation was continued to 270 cc. to save the time of distillation. Furthermore, too long distillation gave rise to much quantity of oxymethyl furfural produced by side reaction (cf. Fig. 1).

2) Experimental Results.— Stability of the color reaction with aniline depends on temperature. As temperature lowers, rate of decolorization decreases and the stability increases as shown in Fig. 2. Colorimetry with aniline was applied to glucose-xylose mixtures and the results were compared with other methods as shown in Table 7. In Table 8, pentosan content in some cellulosi

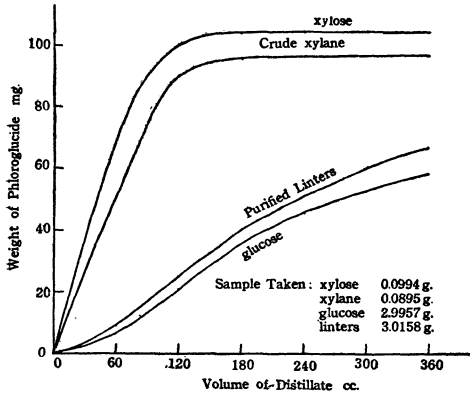

Fig. 1.—Effect of volume of distillate on the amount of phloroglucide produced.

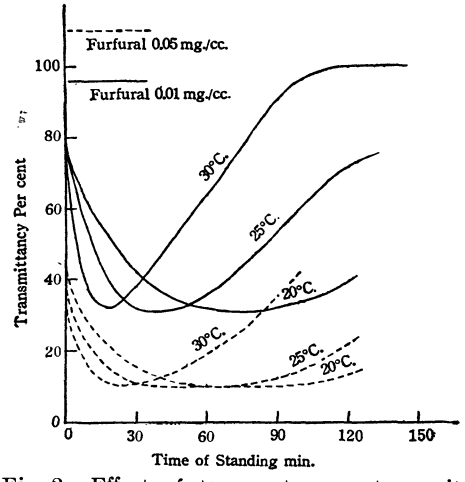

Fig. 2.—Effect of temperature on transmittancy.

Table 7

Comparison of Various Methods for Pentosan Determination

Sample, g.		Xylose, % theoretical	Xylose, % observed				
			Barbituric acid	Bromate	Phloroglucin		Colorimetry
Glucose	Xylose				without alc.	with alc.	
3.00	0	0	0	2.1	2.0	0.5	0.1
3.00	0.01	0.33	0	2.2	2.4	0.6	0.3
3.00	0.03	0.99	0	3.1	3.0	1.2	1.0
3.00	0.05	1.63	0	3.6	3.5	1.9	1.5
3.00	0.10	3.23	2.5	4.9	4.9	3.6	3.3

(17) G. L. Miller, R. H. Golder and E. E. Miller, *Anal. Chem.*, **23**, 903 (1951).
(18) R. A. McCance, *Biochem. J.*, **20**, 1111 (1926).
(19) K. Sumikura and Z. Nakamura, *Labr. Biol. Tottori Coll.*, 158 (1928).
(20) Analysis Comittee of the Central Laboratory of the Cellulose Industry, *Svensk Papperstid.*, **54**, 179 (1951).
(21) E. W. Rice, *Anal. Chem.*, **23**, 1501 (1951).

materials was determined by colorimetry. It was assumed that, in Table 8, pentosan in the samples was only xylan[22] and in Tables 6~8, conversion ratio of xylose to furfural was 86%.

Table 8

Pentosan Content in Some Cellulosic Materials (Colorimetrically Determined)

Sample	Pentosan, %
Unbleached pulp for viscose rayon	2.46
Purified pulp for cellulose ester	0.61
Rayaceta	0.74
Secondary cellulose acetate from Rayaceta	0.25
Secondary cellulose acetate (Hercules)	0.37
Secondary cellulose acetate (Eastman)	0.36
Viscose staple	0.92
Viscose rayon	0.53
Bleached linters	0.25
Raw Egypt cotton (alcohol-benzene extracted)	0.50

3) **Discussion.**—Table 7 shows that, for the estimation of a small quantity of pentosan, the colorimetry is superior to other methods. The next one is phloroglucin method with the alcohol-treatment. But, as already mentioned before, experimental reproducibility of the latter is inferior to that of the colorimetry and the method gives high values to pentosan-poor materials and presumably low values for pentosan-rich ones, because of partial solubility of furfural and oxymethyl furfural-phloroglucide in alcohol. Barbituric acid method[1] gives always low values and especially for the samples, in which pentosan content is under 1.5%, no precipitate being formed. Bromate method[23] (not corrected for oxymethyl furfural) agrees very well with phloroglucin method[24] without the alcohol-treatment but they give a higher result (about 2%) than the true value. This higher value (2%) might seem too large as compared with the values reported by other investigators but it may be accounted for by the differences in distillation apparatus and conditions which affect the amount of oxymethyl furfural as mentioned before, or for the characteristics of cellulose materials as pointed out by Meller.[25]

In conclusion, colorimetry is superior to other methods for the determination of a small quantity of pentosan. Phloroglucin method with alcohol-treatment considerably removes the influence of hexosan and has a limited usefulness.

Summary

1. For the estimation of a small quantity of pentosan in cellulosic materials, an improvement of phloroglucin method and colorimetry with aniline were investigated on mixtures of glucose and xylose, and the results were compared with bromate, the usual phloroglucin and barbituric acid methods.

2. Treatment of the undried phloroglucide with alcohol remarkably removes the influence of hexosan on pentosan determination but it is not complete. As the solubility of the furfural-phloroglucide increases with phloroglucin added, it is desirable to increase the amount of the latter to twice the theoretical.

3. Colorimetry with aniline is superior to other methods. The color reaction is stable at low temperatures.

4. Pentosan contents of some cellulosic materials, such as rayons, pulps and cellulose acetates, are tabulated.

We express thanks to Masao Moriya for his earnest aid throughout the experiment. The expense of this work was defrayed from the Scientific Research Encouragement Grant of the Department of Education.

Department of Applied Chemistry, Faculty of Engineering, Tokyo University, Tokyo

(22) H. Sobue and A. Hateno, *J. Chem. Soc. Japan, Ind. Chem. Sec.*, **55**, 131 (1952).

(23) *Tappi Standard* T 19 m-50 (1950).

(24) *Tappi Standard* T 223 m-48 (1943).

(25) A. Meller, *Paper Trade J.*, **124**, No. 9, 104 (1947); **125**, No. 11, 57 (1947).

The Normal Vibrations of Some Silicon Tetrahalides as Calculated by Urey-Bradley Field

By Yuzo KAKIUTI

(Received November 27, 1952)

Assuming the Urey-Bradley field, Simanouti calculated the normal frequencies of many polyatomic molecules which are in good agreement with the observed values.[1][2][3] In the present paper, the normal frequencies of some silicon tetrahalides were calculated using the similar type of potential field, according to which the potential energy of a molecule can be expressed as follows,

$$V=\sum_i\left[K'_i r_i \Delta r_i+\frac{1}{2}K_i(\Delta r_i)^2\right]+\sum_{i<j}\left[H'_{ij}r^2_{ij}\Delta\alpha_i+\frac{1}{2}H_{ij}(r_i\cdot\Delta\alpha_{ij})^2\right]+\sum_{i<j}\left[F'_{ij}q_i\cdot\Delta q_{ij}+\frac{1}{2}F_{ij}(\Delta q_{ij})^2\right],$$

where the notations same as those given in reference (1) are used. K, H and F denote stretching, bending and repulsive force constants, respectively. The values of these force constants were determined so as to give the best fit with the observed frequencies of $SiCl_4$, $SiBr_4$ and SiI_4, taking the equilibrium bond distances Si-Cl, Si-Br and Si-I as 2.01, 2.15 and 2.43 A, respectively (see Table 1). Here

Table 1

Values of the force constants (K, H, F, $F'\times10^{-5}$ dyne/cm and $\kappa\times10^{11}$ dyne.cm)

$SiCl_4$		$SiBr_4$		SiI_4	
K (Cl) =	2.59	K (Br) =	2.02	K (I) =	1.48
H (Cl) =	0.059	H (Br) =	0.051	H (I) =	0.044
F (Cl) =	0.29	F (Br) =	0.23	F (I) =	0.16
F' (Cl) =	−0.029	F' (Br) =	−0.023	F' (I) =	−0.016
κ (Cl) =	0.21	κ (Br) =	0.18	κ (I) =	0.14

The κ's denote the intramolecular te: sions.

we assumed that F' value is about—10 % of F value.[4] Some of these values agree very well with those given in reference (3). Using

Table 2

Calculated *vs.* observed frequencies (cm^{-1})

Class		Obs.[5]	Calc.	Diff. %
$SiCl_4$	A_1	424	424	0
	E	150	150	0
	F_2	221	220	−0.5
		610	608	−0.3
$SiBr_4$	A_1	249	250	+0.4
	E	90	91	+1.1
	F_2	137	138	+0.7
		487	488	+0.2
SiI_4	A_1	168	168	0
	E	63	63	0
	F_2	94	94	0
		405	405	0
$SiClBr_3$	A_1	159	159	0
		288	291	+1.0
		579	584	+0.9
	E	101	102	+1.0
		173	162	−6.4
		498	491	−1.4
$SiCl_2Br_2$	A_1	111	111	0
		182	181	−0.5
		326	329	+0.9
		563	565	+0.4
	B_1	191 (?)	187	−2.1
		605	604	−0.2
	B_2	174	174	0
		508	494	−2.8
	A_2	122	123	+0.8
$SiCl_3Br$	A_1	191	187	−2.1
		368	370	+0.5
		545	540	−0.9
	E	135	134	−0.7
		205	206	+0.5
		610	606	−0.7
$SiClI_3$	A_1	114	117	+2.6
		220	228	+3.6
		557	570	+2.3
	E	73	74	+1.4
		134	138	+3.0
		411	436	+6.1

(1) T. Simanouti, *J. Chem. Phys.*, **17**, 245 (1949).
(2) T. Simanouti, *ibid.*, **17**, 734 (1949).
(3) T. Simanouti, *ibid.*, **17**, 848 (1949).
(4) T. Simanouti, to be published shortly.
(5) M. L. Delwaulle, *J. Phys. Chem.*, **56**, 355 (1952).

Class		Obs.[5]	Calc.	Diff. %
$SiCl_2I_2$	A_1	83	83	0
		160	161	+0.6
		276	281	+1.8
		538	544	+1.1
	B_1	?	165	
		589	599	+1.7
	B_2	149	150	+0.7
		418, 436	421	
	A_2	111	114	+2.7
$SiCl_3I$	A_1	169	165	−2.4
		333	333	0
		519	511	−1.5
	E	123	125	+1.6
		197	199	+1.0
		600	603	+0.5

the common values of these force constants, the normal frequencies of $SiCl_4$, $SiBr_4$, SiI_4, $SiCl_3Br$, $SiCl_2Br_2$, $SiClBr_3$, $SiCl_3I$, $SiCl_2I_2$ and $SiClI_3$ were calculated in the same way as in reference (1), where we assumed that the force constants relating to both unlike halogen atoms X and Y have the average values of two force constants which are concerned with each of them. The results are shown in Table 2. The calculated frequencies are in general in good agreement with the observed values.

The writer wishes to express his sincere thanks to Prof. S. Mizushima at Tokyo Univ. and Dr. T. Simanouti for their kind guidance.

Faculty of Science,
St. Paul's University (Rikkyo Daigaku), Tokyo

Antituberculous Compounds. III. N-Acyl Derivatives of *p*-Aminocinnamaldehyde and *p*-Aminobenzaldehyde thiosemicarbazones[1]

By Tamio NISHIMURA

(Received November 29, 1952)

Several N-acyl derivatives of *p*-aminocinnamaldehyde thiosemicarbazone were prepared in order to study the effects of a variety of acyl groups on its antituberculous activity. In the course of this study, it was found that *p*-dimethylacrylylaminocinnamaldehyde thiosemicarbazone, when tested by subcutaneous injection of its oily suspension,[2] had markedly reduced toxicity compared with other thiosemicarbazones prepared in this laboratory. As it was considered that this effect would be due to the presence of α,β-double bond in dimethylacrylyl radical, the experiment was extended to combine α,β-unsaturated acids having fewer carbon atoms with *p*-aminocinnamaldehyde and *p*-aminobenzaldehyde thiosemicarbazones. The preparation of the higher analogs was not undertaken since the higher acyl groupings seemed to decrease the activity.[3]

Dimethylacrylic acid was prepared by the usual method.[4][5][6] Dimethylacrylyl chloride was first prepared by the action of thionyl chloride on dimethylacrylic acid[7] in unsatisfactory yields, but later phosphorus trichloride was found to give a better yield and pure material. Phenylacetyl chloride and cinnamyl chloride were employed in the experiments, in the form of etheral solutions without isolation of the substances.[8] Methacrylic acid was prepared by hydrolysis of methyl methacrylate[9] and the corresponding chloride was obtained according to the method described by Rehberg et al.[10] *p*-Aminocinna-

(1) Most part of this study has been presented before the annual meeting of the Chemical Society of Japan in Tokyo on April 5, 1952.

(2) Toraichi Takebe, Unpublished data.

(3) Katsuhiko Tago, Unpublished data; Robert Behnish, Fritz Mietsch and Hans Schmidt, *Am. Rev. of Tuberc.*, **61**, 1 (1950).

(4) J. B. Conant and Neal Tuttle, *Org. Syn.* Col, Vol. 1, p. 193.

(5) J. B. Conant and Neal Tuttle, ibid., p. 338.

(6) Barbier and Léser, *Bl.* (3) 33, 815.

(7) H. Staudinger and E. Ott. *Ber.*, **44**, 1636 (1911).

(8) G. A. Schmidt and David A. Shirley, *J. Am. Chem. Soc.* **71**, 3804 (1948).

(9) Ryozo Inoue, *J. Soc. Chem. Ind., Japan*, **45**, 385 (1942).

(10) C. E. Rehberg, Marion B. Dixon and C. H. Fisher, *J. Am. Chem. Soc.* **67**, 208 (1945).

Table 1

Thiosemicarbazones

Aldehydes	Yield %	Solvent for recrystallization	M. P. °C	Empirical formula	Nitrogen % Calcd.	Nitrogen % Found
p-Benzoylamino-cinnamaldehyde[a]	43	pyridine and water	233—4 (decomp.)	$C_{17}H_{16}ON_4S$	17.23	17.37
p-Phenylacetylamino-cinnamaldehyde[b]	39	pyridine and water	223 (decomp.)	$C_{18}H_{18}ON_4S$	16.56	16.65
p-Dimethylacrylyl-aminocinnamaldehyde[a]	53	pyridine and water	234—5 (decomp.)	$C_{15}H_{18}ON_4S$	18.55	18.27
p-Dimethylacrylyl-aminobenzaldehyde[a]	39	glacial acetic acid	224 (decomp.)	$C_{13}H_{16}ON_4S$	20.27	20.17
p-(*p*-Tolylsulfonyl)-aminocinnamaldehyde[a]	73	pyridine and water	241—2 (decomp.)	$C_{17}H_{16}O_2N_4S_2$	14.94	15.06
p-*n*-Caproylamino-cinnamaldehyde[a]	46	ethanol	197	$C_{16}H_{22}ON_4S$	17.60	17.44
p-*n*-Caproylamino-benzaldehyde[a]	53	ethanol	201 (decomp.)	$C_{14}H_{20}ON_4S$	19.16	18.84

(a) Pure chloride was used. The reaction was carried out in pyridine.

(b) This substance was prepared as with *p*-cinnamylaminocinnamaldehyde thiosemicarbazone.

maldehyde and *p*-aminobenzaldehyde thiosemicarbazones could be prepared smoothly by the reduction of the corresponding nitrothiosemicarbazones with sodium hydrogen sulfide.[11]

All the N-acyl derivatives of *p*-aminocinnamaldehyde and *p*-aminobenzaldehyde thiosemicarbazones except for succinoyl and crotonyl derivatives were obtained by the action of acid chloride or its etheral solution on the amino thiosemicarbazones in pyridine. An attempted preparation of the crotonyl derivatives in pyridine did not succeed, but Schotten-Baumann's reaction in methyl acetate gave the desired products in reasonable yields. The compounds not described in the experimental part are listed in Table 1.

Biological evaluations of these thiosemicarbazones will be published elswhere. This paper is concerned only with their synthesis and characterization.

Experimental[12]

β, β-Dimethylacrylyl Chloride.—A mixture of 10 g. of dimethylacrylic acid and 7.5 g. of phosphorus trichloride was warmed at 60—75° for 3.5 hours. The crude chloride obtained by distillation under reduced pressure was further subjected to distillation under ordinary pressure and a portion boiling at 145—150° and amounting to 7.7 g. (65%) was collected.

***p*-Aminobenzaldehyde Thiosemicarbazone.**—200 cc. of ethanol and 80 cc. of 2 N-sodium hydroxide solution were mixed, saturated with hydrogen sulfide and 22.4 g. of *p*-nitrobenzaldehyde thiosemicarbazone was added in one portion. The whole mixture was then refluxed on a steam bath for 30 minutes, while the crystals of the nitro thiosemicarbazone completely disappeared. A resulting dark red colored solution was allowed to stand at room temperature overnight and the separated crystals were collected on a filter, and were washed thoroughly with ethanol and water. Dried material, m. p. 197—198° (decomp.) weighed 14.5 g. (75%).

***p*-Succinoylaminocinnamaldehyde Thiosemicarbazone.**—A mixture of 2.2 g. of *p*-aminocinnamaldehyde thiosemicarbazone, 1.0 g. of succinic anhydride and 20 cc. of ethylacetate was refluxed for 30 minutes. The precipitate was collected, dissolved in sodium hydroxide solution, and the filtered solution was acidified with 10% hydrochloric acid to give 2.2 g. (70%) of the desired product melting at 189° (decomp.). A small sample was recrystallized from ethanol to yield a pure product, m. p. 207—208° (decomp.) (Found: N, 17.47%. Calcd. for $C_{14}H_{16}O_3N_4S$; N, 17.50%).

***p*-Crotonylaminobenzaldehyde Thiosemicarbazone.**[13]—To a mixture of 3.9 g. of *p*-aminobenzaldehyde thiosemicarbazone, 10 cc. of 2N-sopium hydroxide solution and 60 cc. of methylacetate were added dropwise. And then a solution of 2.1 g. of crotonyl chloride in 10 cc. of methylacetate at 5—10° was added with stirring. Yellow crystals were collected, washed with methylacetate and dried, yielding 2.4 g. (46%) of the desired product melting at about 240° (decomp.). On dissolving it in 36 cc. of pyridine and adding 110 cc. of water to the solution, long needles (2.0 g.) of the same m. p. separated. For microanalysis a portion was further recrystallized from ethanol (Found: N, 21.04. Calcd. for $C_{12}H_{14}ON_4S$: N, 21.36%).

(11) Tamio Nishimura, This Bulletin, **25**, 54 (1952).

(12) All temperatures are uncorrected.

(13) Crotonyl chloride was prepared by the action of phosphorus trichloride on α-crotonic acid.

***p*-Crotonylaminocinnamaldehyde Thiosemicarbazone.**[15] — From 2.2 g. of *p*-aminocinnamaldehyde thiosemicarbazone, 2.4 g. (83%) of the acylated product melting at 222° (decomp.) was obtained in a manner similar to that described above. It was dissolved in 16 cc. of pyridine and 30 cc. of water was added to the solution. Yellow crystals (1.1 g.) of m. p. 227° (decomp.) were collected, redissolved in 20 cc. of pyridine and 40 cc. of water was added to the solution, giving 1 g. (35%) of the pure material melting at 234° (decomp.). An additional recrystallization was without effect on the m. p. (Found: N, 19.40%. Calcd. for $C_{14}H_{16}ON_4S$: N, 19.43%).

***p*-Cinnamoylaminocinnamaldehyde Thiosemicarbazone.**—A mixture of 0.74 g. of cinnamic acid and 0.60 g. of thionyl chloride was heated at 70—90° for an hour and the unreacted thionyl chloride removed by distillation. The residual acid chloride dissolved in ether was added dropwise and with stirring to a cold solution of 1.1 g. of *p*-aminocinnamaldehyde-thiosemicarbazone in pyridine and the reaction mixture was poured into 150 cc. of ice water. The solid was recrystallized by means of pyridine and water; yield 0.6 g. (33%) m. p. 243° (decomp.) (Found: N. 15.60%. Calcd. for $C_{19}H_{18}ON_4S$: N, 15.96%).

***p*-Methacrylylaminobenzaldehyde Thiosemicarbazone.**—A mixture of 1.3 g. of methacrylic acid and 0.7 g. of phosphorous trichloride was kept at 60—70° for fifteen minutes and then at room temperature for two hours. The upper layer was added dropwise to a cold solution of 2 g. of *p*-aminobenzaldehyde thiosemicarbazone in 10cc. of pyridine. After standing at room temperature for an hour, 15 cc. of water was added to the reaction mixture and allowed to stand in an ice box over-night. The separated solid, after recrystallizations from pyridine and water, gave 0.4g. of colorless plate melting at about 216° (decomp.) (Found: N, 20.93%, Calcd. for $C_{12}H_{14}ON_4S$: N, 21.36%).

The author is much indebted to Mr. T. Nagano for the micro-analyses in this work. The expense of this work was partly defrayed by a Grant in Aid for the Miscellaneous Scientific Research, given by the Educational Ministry to which the author's thanks are due.

Chemical Laboratory,
The Kitasato Institute, Tokyo, Japan

Dephosphorylation of Nucleic Acids, Mononucleotides and Casein by Lanthanum and Cerium Hydroxide Gels

By Michio SHIMOMURA and Fujio EGAMI

(Received December 3, 1952)

E. Bamann[1] has found that certain metal hydroxide gels, especially those of lanthanum and cerium, have catalytic effect on the hydrolysis of phosphate esters. Since nucleic acids are also phosphate esters, we studied the behavior of yeast ribonucleic acid towards lanthanum hydroxide gel and have found that it is easily dephosphorylated.[2] Independently of us, and probably of Bamann, K. Dimroth and his coworkers quite recently reported the similar effects of metal hydroxide gels.[3] J. E. Backer and F. W. Allen,[4] on the other hand, showed that pyrimidine nucleotides could be hydrolysed into nucleosides and inorganic phosphate under similar conditions.

The present paper deals with our recent studies on the catalytic effects of lanthanum and cerium hydroxide gels.

Materials

Two preparations, free acid and sodium salt, of brewer's yeast RNA, designated as RNA Preparation 1 and 2, were used. These were extracted by the method of Clarke and Schryver.[5] In obtaining Preparation 2, the chloroform method of Sevag et al.[6] was used. The phosphorus content of the two preparations was 6.5 and 8.7 per cent, respectively. The highly polymerized preparation of the sodium salt of calf spleen DNA, containing 7.4 per cent phosphorus, was

(1) E. Bamann, *Angew. Chem.*, **52**, 186 (1939).
(2) F. Egami and M. Shimomura, *Science (Japan)*, **18**, 472 (1948).
(3) K. Dimroth, L. Jaenicke and D. Heinzel, *Ann. Chem.*, **566**, 206 (1950). K. Dimroth, L. Jaenicke and I. Vollbrechtshausen, *Z. physiol. Chem.*, **289**, 71 (1952).
(4) J. E. Backer and F. W. Allen, *J. Biol. Chem.*, **188**, 59 (1951).
(5) G. Clarke and S. B. Schryver, *Biochem. J.*, **11**, 319 (1937).
(6) M. G. Sevag, D. B. Lackman and J. Smolens, *J. Biol. Chem.*, **124**, 425 (1938).

kindly supplied by Dr. A. Sibatani. Desoxyribo-, a-ribo-, b-ribo and 5'-ribocytidylic acid were kindly supplied by Dr. W. E. Cohn. The phosphorus content of commercial casein prepared by the method of Hammersten was 0.80 per cent.

Lanthanum carbonate was prepared from industrial lanthanum oxide. Since the latter contained silicates and metaphosphates, which hinder the action of lanthanum hydroxide and disturb the estimation of phosphoric acid detached from substrates, these impurities were removed during the course of preparation of the carbonate by heating with hydrochloric acid and then with sodium hydroxide and finally by treating the mixture with ammonium molybdate. Cerium carbonate was likewise prepared from industrial cerium oxide.

Experimental Conditions

The reaction mixture in a typical experiment for the measurement of dephosphorylation of RNA: 100 mg. of lanthanum carbonate were suspended in distilled water and dissolved by the addition of hydrochloric acid in a 50 cc. Erlenmeyer flask. Then it was adjusted to *p*H 8.0 by aqueous ammonia, thus lanthanum hydroxide was precipitated. To this suspension, 1 cc. of 1 per cent RNA solution, 10 cc. of 0.1 N sodium veronal-hydrochloric acid buffer, *p*H 8.0, and water were added till the final volume was 20 cc. RNA formed additional precipitate with lanthanum ion, known as a powerful precipitating reagent for nucleic acids.[7] The flask was rubber-stoppered, shaken vigorously to make the suspension homogeneous and immersed in a water-bath, which was held at desired temperature (time zero.). The mixture was shaken occasionally during the hydrolysis to avoid precipitation. Aliquots of 1 to 2 cc. were withdrawn at various time intervals, cooled to room temperature if necessary, and analysed for inorganic phosphate. Similar conditions were also used when the dephosphorylation of phosphoric esters other than RNA were tested.

Analytical Methods

Total Phosphorus.—The phosporus content of the various preparations was measured by the method of Lieb and Wintersteiner.[8]

Inorganic Phosphate.—In the reaction mixtures, phosphate was found only in the precipitate and was completely absent in the supernatant. Samples for analysis, therefore, were withdrawn carefully avoiding uneven sampling.

In reaction mixtures containing nucleic acid or protein, the bulk of these substances was precipitated by the addition of an equal volume of 10 per cent trichloroacetic acid. This technique permitted the direct colorimetric determination of the phosphate in the supernatant according to the method of Fiske and Subbarow.[9] The decrease of the colour intensity due to the presence of lanthanum was negligible within concentrations used. A slight turbidity which appeared on addition of the molybdate was removed by centrifugation.

Reducing Power.—If the glycosidic linkage in nucleosides is broken during the hydrolysis of RNA, the appearance of a reducing group is to be expected. This was measured by the ferricyanate reduction method of Fujita and Iwatake,[10] in which the lanthanum contained in the test samples was removed together with cadmium hydroxide.

Orcinol Reaction for the Estimation of RNA and Diphenylamine Reaction for the Estimation of DNA—Methods described by Kerr and Seraidarian[11] and by Dische[12] were used respectively; the presence of lanthanum did not disturb the estimations.

Experimental

Effect of Temperature.—Fig. 1 shows the dephosphorylation reaction of RNA by lanthanum hydroxide gel at various temperatures. It was observed that 95 per cent of the total phosphate groups of RNA were transformed into inorganic phosphate in 24 hours both at 90° and at 100°. In a control experiment at 80°, in which lan-

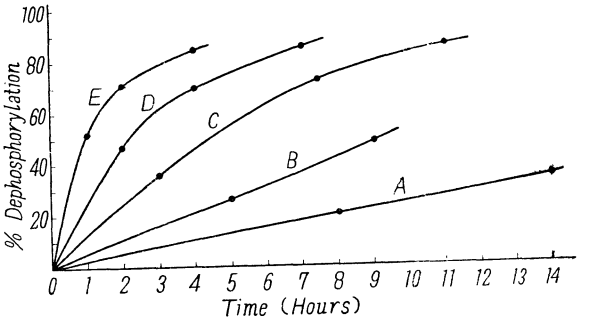

Fig. 1.—Effect of temperature on the hydrolysis of ribonucleic acid under the influence of lanthanum hydroxide. Each reaction mixture contained 10 mg. of RNA Preparation 2, lanthanum hydroxide (from 100 mg. of lanthanum carbonate), and 10 cc. of 0.1 N veronal buffer, *p*H 8.0, the total volume 20 cc. Curves A, B, C, D and E are at 60°, 70°, 80°, 90° and 100°, respectively. Curves D and E reached at 95 per cent dephosphorylation in 24 hours.

(7) E. Hammersten and T. Theorell, *Acta Med. Scand.*, **68**, 226 (1928).

(8) H. Lieb and O. Wintersteiner, *Mikrochemie*, **2**, 78 (1924).

(9) C. H. Fiske and Subbarow, *J. Biol. Chem.*, **66**, 375 (1925).

(10) A. Fujita and D. Iwatake, *Biochem. Z.*, **242**, 43 (1932).

(11) S. E. Kerr and K. Seraidarian, *J. Biol. Chem.*, **159**, 211 (1945).

(12) Z. Dische, *Mikrochemie*, **2**, 26 (1930).

thanum was omitted, no formation of inorganic phosphate was observed. On the other hand, the dephosphorylation of RNA was very slow at low temperatures. The amount of inorganic phosphate was only 2 per cent at 28° and 0 per cent at 5° after 5 days.[13]

The activation energy of the dephosphorylation reaction of RNA under the influence of lanthanum hydroxide was calculated from Fig. 1. The reaction was approximately of the first order, at least before 80 per cent dephosphorylation. Log k and $1/T$ were in linear relation between 60° and 100°. The activation energy was 20,200~20,400 cal.

Effect of *p*H. — The influence of *p*H on the lanthanum hydroxide is illustrated in Fig. 2. Optimal *p*H lies between 8.0 and 9.0.

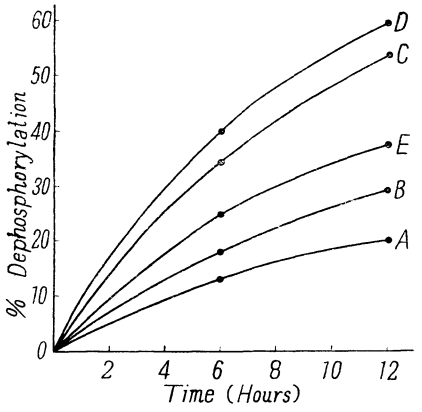

Fig. 2.—Effect of *p*H on the hydrolysis of ribonucleic acid under the influence of lanthanum hydroxide. Curves *A*, *B*, *C*, *D* and *E* are at *p*H 6.0 (citrate buffer), 7.0 and 8.0 (veronal buffer), 9.0 and 10.0 (ammonium buffer), respectively. Temperature 70°. Other conditions similar to Fig. 1.

Effect of the Quantity of Lanthanum hydroxide.—The catalytic effect of lanthanum hydroxide increased with increasing quantity (Fig. 3). The atomic ratio of lanthanum/phosphorus in the reaction mixture in which 10 mg. of lanthanum carbonate was used was approximately 1 (Curve *B*). After 40 hours Curves *B*, *C* and *D* reached 100 per cent, whereas Curve A barely reached 70 per cent. This was understandable since the phosphate formed during the hydrolysis of RNA hindered the catalytic effect by firmly attaching itself to lanthanum.

Natures of the Hydrolysis Product—RNA was almost completely dephosphorylated under the relatively mild conditions, and the nucleosides, the dephosphorylation product, were expected to remain unaltered under these conditions. The

(13) The data at low temperatures reported in the previous paper (2) had been slightly higher, since the inorganic phosphate had been estimated by the method of Bell and Doisy, and hence the colour due to silicates had been contaminated.

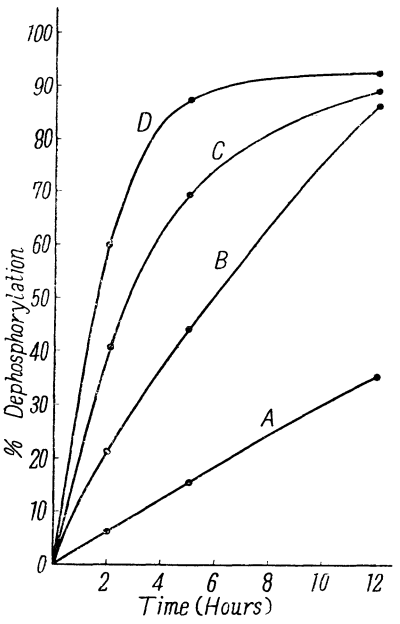

Fig. 3.—Effect of the amount of lanthanum hydroxide on the hydrolysis of ribonucleic acid. Curves *A*, *B*, *C* and *D* were obtained with lanthanum hydroxide produced respectively from 5, 10, 30 and 100 mg. of lanthanum carbonate. Temperature 90°. Other conditions similar to Fig. 1.

Table 1

Reducing Power and Colour Intensity of Orcinol Test during Dephosphorylation of RNA

Time, hrs	Dephosphorylation, %	Reducing Power† mg. glncose	Orcinol Test†† %
0		0.00	103
1		0.00	100
12		0.00	100
25		0.00	100
39		0.00	97
43	98	0.01	97
Calculation		1.25*	

The reaction mixture contained 50 mg. of RNA Preparation 2, lanthanum hydroxide obtained from 500 mg. of the carbonate, and 25 cc. of 0.1 M veronal buffer, *p*H 8.0, in a total volume of 50 cc. Temperature, 80°. 3 cc. of reaction mixture was used for each estimation of reducing power.

† Reducing power measured with 3 cc. aliquots and expressed as mg. glucose.

†† The colour intensities measured were compared with the standard RNA solution containing RNA in the same concentration as the original reaction mixture.

* On the complete hydrolysis of the glycosidic linkages.

reducing power of ribose should appear, if the glycosidic linkages in the nucleosides were broken; Table 1 shows that no reducing group was liberated. The colour intensity of the orcinol test for ribose also remained constant within experimental error.

Dephosphorylation Process and Confirmation of Ribonucleosides as the Final Products by Means of Periodate Oxidation.—The splitting of linkages between the bases and ribose groups may be detected by the periodate test.[14] One mole of periodate should be consumed per one mole of nucleosides, if these linkages remain intact, whereas, 4 moles should be consumed, if the breakdown is complete. Moreover, the course of the hydrolysis of RNA might be investigated by this periodate oxidation method, since 5'-ribonucleotides consume one mole of periodate per mole, but 2'- and 3'-ribonucleotides would not. For example, the formation of periodate consuming products would precede the dephosphorylation when RNA is hydrolysed through the intermediate 5'-ribonucleotides.

Since measurement was greatly disturbed by the existence of lanthanum salt, samples were mixed with an equal volume of 0.2 M phosphate buffer, *p*H 7.0, thus inducing the complete precipitation of lanthanum in the form of insoluble phosphate. After standing for about 10 minutes and centrifugation, aliquot of these supernatants was used for the periodate test. Another aliquot of these supernatants was examined by the orcinol test for ribose. The result of this test showed that the amount of RNA removed together with lanthanum was relatively small (Column 3, Table 2). Table 2 shows that the consumption of periodate precedes the dephosphorylation. It may be explained by the fact shown below (see Table 3) that the phosphate at 2'- or 3'-carbon atom is split off preferentially in comparison to that at 5'-carbon atoms. The fact that the final product consumes approximately one mole of periodate per mole of total phosphorus confirms the already mentioned finding that nucleosides are the final hydrolysis product.

Preparation of Ribonucleosides.—60g. of lanthanum carbonate were suspended in distilled water and dissolved by the addition of distilled hydrochloric acid. After precipitating lanthanum hydroxide from the solution by the addition of concentrated aqueous ammonia, the precipitate was washed thoroughly with dilute aqueous ammonia by centrifugation in order to remove the chlorine ion. The precipitate was finally suspended in distilled water. To this lanthanum hydroxide suspension was added RNA solution containing 20 g. of RNA Preparation 1. This mixture was adjusted at *p*H 8 to 9 with aqueous ammonia or with sulphuric acid. Total volume was about 1.5 liter. The mixture was heated to 80° and maintained at this temperature for about 40 hours. Aqueous ammonia was added occasionally to prevent lowering of *p*H. Then, the precipitate was filtered off and washed with 1.5 liter of hot water. (Protein, contained in the RNA Preparation, was adsorbed to, and inorganic phosphate, produced by the hydrolysis of RNA, was also bound with lanthanum hydroxide. Nucleosides went into the filtrate.) Lanthanum in the filtrate was precipitated quantitatively by the addition of oxalic acid and filtered by suction. The filtrate was concentrated to a volume of 300 cc. under reduced pressure at about 50° and then filtered while warm. Guanosine settled out from the filtrate in long needles upon freezing overnight. This was recrystallized from hot water. The yield was 2.1 g. Picric acid solution was then added to the filtrate of guanosine until there was no further precipitation of adenosine picrate. The picrate was filtered off and a second crop was obtained when the filtrate was concentrated to 400 cc. and allowed to stand in a refrigerator. The picrate was crystallized from hot water in the form of platelets. The yield was 4.0 g. Finnlly cytidine picrate was obtained in the form of long crystalline needles from the filtrate of adenosine picrate by the method of Levene.[15] The yield was 3.2 g.

Behaviour of Desoxyribonucleic Acid.—No dephosphorylaton of DNA was observed under

Table 2

Periodate Consumption by Hydrolysis Product in the Course of Dephosphorylation of RNA

Time, hrs	Dephosphorylation, %	Colour intensity of orcinol test, %	Periodate, consumption mole	Periodate consumption Colour intensity of orcinol test, mole
0	0	73	0.025	0.034
2	25	78	0.59	0.76
5	54	96	0.84	0.87
8	72	96	1.06	1.10
23	99	104	1.22	1.17

The reaction mixture contained 100 g. of RNA Preparation 2 and lanthanum hydroxide obtained from 300 g. of the carbonate. Total volume, 20 cc.; *p*H, 8.0; temperature, 80°. No buffer was used and occasional addition of N sodium hydroxide prevented the lowering of *p*H.

(14) R. Adams, "Organic Reaction," New York, **2**, 341 (1944).

(15) P. A. Levene, *J. Biol. Chem.*, **25**, 103 (1916).

the same conditions as shown in Curve 3 in Fig. 1 even after 48 hours. The supernatant of the reaction mixture at 48 hours gave negative diphenylamine test, although, in the case of RNA, the colour intensity of the orcinol test of the supernatant increased with increasing dephosphorylation of RNA. DNA, even after the depolymerization by heating in 0.25 N sodium hydroxide at 80° for 20 minutes, was not dephosphorylated under the influence of lanthanum hydroxide.

Dephosphorylation of Nucleotides.—Contrary to DNA, desoxyribocytidylic acid was dephosphorylated. Table 3 shows the dephosphorylation of desoxyribo- and ribonucleotides. b-Cytidylic acid is dephosphorylated more easily than a-cytidylic acid and 5'-cytidylic acid most slowly.

Table 3

Dephosphorylation of Various Cytidylic Acids

Time, hrs.	Desoxyribo-, %	a-Ribo-, %	b-Ribo-, %	5'-Ribo-, %
3	60	57	89	30
6	88	85	97	43
Control				
12	0	3.0		

The reaction mixture contained lanthanum hydroxide obtained from 30 mg. of the carbonate, nucleotide (1.92 mg. desoxyribo-; 2.08 mg. a-ribo-; 2.31mg. b-ribo-; 2.05mg. 5'-ribocytidylic acid, in each case), and 1 cc. of M ammonium buffer, *p*H 9, and the volume was made to 12 cc. with distilled water.

Table 4

Catalytic Effect of Lanthanum Hydroxide on Dephosphorylation of Casein

Time, hrs	Dephosphorylation at 25°, %	Dephosphorylation at 70°, %	Control, at 70°, %
18.5		71	20
21.5	0		
42.5		98	34

Each reaction mixture contained 50 mg. of casein, lanthanum hydroxide obtained from 150 mg. of the carbonate, 1 cc. of M ammonium buffer, *p*H 9, and the total volume was made to 10 cc. with water. In the control experiment, water replaced lanthanum hydroxide.

Dephosphorylation of Casein.—Casein was not dephosphorylated at room temperature, 25°, as Bamann has shown (1). But at 70°, the catalytic effect of lanthanum hydroxide was observed (Table 4).

Summary

1. The dephosphorylation reaction of RNA by lanthanum hydroxide gel was further studied. The activation energy of the reaction is 20,200~20,400 cal. Optimal *p*H is between 8 and 9.

2. RNA is hydrolysed almost completely into nucleosides and inorganic phosphate at 90° in 40 hours at *p*H 8. The formation of nucleosides as the final product of hydrolysis was shown from the reducing power measurements and periodate consumption of products.

3. DNA is not dephosphorylated at all under conditions where RNA is almost completely dephosphorylated. This may be related to the structural difference of DNA and RNA.

4. Preparative method for ribonucleosides from RNA under catalytic effect of lanthanum hydroxide was described. Ribonucleosides are obtained in good yields.

5. Desoxyribo-, a-ribo-, b-ribo-, and 5'-ribocytidylic acid are all subject to catalytic dephosphorylation. 5'-Ribocytidylic acid is dephosphorylated most slowly.

6. Cerium hydroxide can be used as catalyst of the reaction in the same way with lanthanum hydroxide.

7. The dephosphorylation of casein is considerably accelerated by lanthanum hydroxide at 70° but not at 25°.

Part of the cost of this investigation was defrayed from the Scientific Research Encouragement Grant from the Ministry of Education.

Chemical Institute, Faculty of Science, Nagoya University

Polarographic Behavior of Cinnamic-, Styrylacetic- and Crotonic- Acids[1]

By Shin-ichi ONO and Tadao HAYASHI

(Received December 20, 1952)

Introduction

Several authors have already measured the reduction potentials of cinnamic acid[2] and crotonic acid[3] in various solutions.

In connection with the electrolytic reduction of cinnamic acid,[4] the authors have undertaken the polarographic observation of cinnamic-, styrylacetic- and crotonic acids, in order to know the relation between the reducibility and the structure of molecules and also the reduction of carbon-carbon double bond in these acids at a dropping mercury electrode.

Experimental

Dioxane-water mixture containing 50% dioxane was used as a solvent, with several types of supporting electrolytes. Since the decomposition potential of buffer-solutions was found to be less negative than the reduction potential of the double bond in these acids, special care was taken for the selection of supporting electrolytes. In the experiments which will be discussed, unbuffered electrolytes were usually used. The supporting electrolytes used were as follows:

(a) Acid media
  (1) HCl—0.1N LiCl System
  (2) HCl—0.1N $SrCl_2$ 〃
  (3) HCl—0.1N $CaCl_2$ 〃

(b) Neutral media
  (1) $(CH_3)_4NBr$ (0.1N), $(CH_3)_4NI$ (0.05N)
  (2) LiCl. KCl, NaCl, NH_4Cl (0.1N)
  (3) $CaCl_2$, $SrCl_2$, $BaCl_2$ (0.1N)

(c) Alkaline media
  (1) LiOH (0.1N)

The dropping mercury electrode had the following characteristics. At a pressure of 50 cm of mercury, the droptime in 50% Dioxane-0.1N $(CH_3)_4NBr$ was 3.98 sec. (Open circuit). The value of m was 1.01 mg. sec.$^{-1}$, with a calculated value of $m^{2/3}t^{1/6}$ of 1.267 mg.$^{2/3}$t$^{-1/2}$ (Open circuit).

Table 1

Half-wave Potentials and Diffusion Currents of Polarographic Waves of Styrylacetic and Crotonic Acids. (50% Dioxane)

Sample (mol.)	Electrolyte	Half-wave Potential (volt vs. S. C. E.)	I_l (μA.)	I_l/C.
Styrylacetic acid				
4×10^{-3}	0.1N $(CH_3)_4NBr$	−1.70	4.56	1.14
1 〃	〃	−1.64	1.06	1.06
2 〃	0.05N $(CH_3)_4NI$	−1.69	2.40	1.20
1 〃	〃	−1.64	1.16	1.16
2 〃	0.1N LiCl	−1.65	2.40	1.20
2 〃	0.1N $SrCl_2$	−1.64	2.80	1.40
2 〃	0.1N $CaCl_2$	−1.60	2.20	1.10
2 〃	0.1N LiOH	—		
Crotonic acid				
5×10^{-3}	0.1N $(CH_3)_4NBr$	−1.73	9.12	1.82
2 〃	〃	−1.70	3.38	1.69
2 〃	0.1N LiCl	−1.66	3.04	1.52
2 〃	0.1N $SrCl_2$	−1.65	2.72	1.31
2 〃	0.1N LiOH	—		

(1) This paper was presented at the Annual meeting of the Chemical Society of Japan, held in Tokyo, on April 1952. This paper shall be "Part IV of Electrolytic Reduction of Aromatic Carboxylic Acids".

(2) (a) L. Schwaer, *Collection Czechoslov. Chem. Commun.*, **7**, 326, (1935).
(b) G. Semerano and A. Chisini, *Gazz., Chim. Ital.*, **66**, 510, (1936).
(c) S. Wauzonek, S. C. Wang and P. Lyons, *J. Org. Chem.*, **15**, 593, (1950).

(3) (a) K. Shoji, *Sc. P. (Japanese)*, **9**, 69, (1930).
(b) M. v. Stackelberg and W. Stracke, *Z. Elektrochem.*, **53**, 118, (1949).

(4) S. Ono and T. Hayashi, This Bulletin, **26**, 11, (1953).

The electrolytic cell was a simple cylindrical shape with a mercury pool anode, and was provided with side arms for anode connection and for admission of hydrogen for the removal of dissolved oxygen.

The anode potential was measured against a saturated calomel electrode (S.C.E.). The current-voltage curve was photographically recorded with A Model SH Shimazu Polarograph, which has a current scale calibrated in microamperes (Sensibility ; 8.0×10^{-3}microamp./mm./m.). All the experiments were carried out at room temperature. (15°±1°C).

All samples were prepared by the usual method, and purified by recrystallization. Cinnamic acid, m.p. 133—133.5°C, styrylacetic acid, m.p. 87—87.5°C, crotonic acid, m.p. 71—72°C.

Dioxane was purified by refluxing with sodium for 12 hours and by distillation.

The purified samples were dissolve in dioxane to the concentration of 1×10^{-2}mol/1, as a stock solution.

Polarographic results

(1) **Electroreduction in neutral and alkaline solutions.**—Both styrylacetic acid and crotonic acid gave a single wave, corresponding to the deposition of hydrogen ion in neutral solution, whereas they gave no polarographic (reduction) wave in alkaline solution. Table 1 shows the observed half-wave potentials and diffusion currents of styrylacetic and crotonic acids.

On the other hand, cinnamic acid gave a well-defined two-step polarographic wave in neutral solutions, and the first wave diminished by the addition of alkali.

Typical polarograms are given in Fig. 1, using a 0.05N $(CH_3)_4NI$ solution as a supporting electrolyte.

Table 2 shows a summary of the observed half-wave potentials and diffusion currents of cinnamic acid. In the presence of NH_4Cl, KCl, or NaCl as a supporting electrolyte, the second wave of cinnamic acid overlapped the decomposition potentials of these cations; therefore, it was difficult to distinguish "the real reduction wave" of the carbon-carbon double bond. However, if we used solutions of LiCl, $SrCl_2$, $CaCl_2$, $(CH_3)_4NI$, or $(CH_3)_4NBr$, as a supporting electrolyte, cinnamic acid gave a well-defined two-step reduction wave.

It was an interesting fact that the half-wave potentials of the second wave became more positive by 0.12 volt for $SrCl_2$ and by 0.15 volt for $CaCl_2$ than those for $(CH_3)_4NBr$.

We found, when $(CH_3)_4NBr$ was used, that the half-wave potentials of cinnamic acid were independent of the concentration of cinnamic acid,

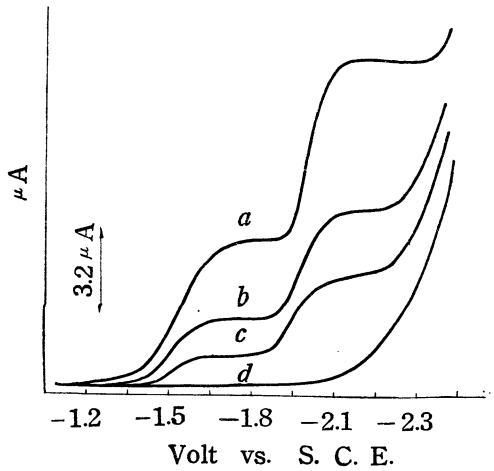

Fig. 1.—A typical polarograme of Cinnamic acid in 0.05 N $(CH_3)_4NI$ (containing 50% Dioxane, 0.001% gelatine)
(a) 4×10^{-2}M. of sample. (b) 2×10^{-3}M. (c) 1×10^{-3}M. (d) Residual Current.

Table 2

Half-wave Potentials and Diffusion Currents of Cinnamic Acid in Neutral or Alkaline Solution. (50% Dioxane, with 0.001% gelatin)

Cinnamic acid (mol.×10^{-3})	Electrolyte	First wave			Second wave		
		$\pi_{1/2}$ (Volt vs. S. C. E.)	I_l (μA.)	I_l/C.	$\pi_{1/2}$ (Volt vs. S. C. E.)	I_{il} (μA.)	I_d/C.
5.0	$(CH_3)_4NBr$	−1.53	5.76	1.15	−2.03	9.28	1.86
4.0	〃	−1.52	4.08	1.02	−2.02	7.20	1.80
2.0	〃	−1.50	2.16	1.08	−2.01	3.68	1.84
1.0	〃	−1.49	1.05	1.05	−1.98	1.85	1.85
4.0	$(CH_3)_4NI$	−1.56	4.16	1.04	−2.05	6.88	1.72
2.0	〃	−1.52	2.16	1.08	−2.01	3.52	1.76
1.0	〃	−1.55	1.10	1.10	−1.99	1.78	1.78
2.0	LiCl	−1.54	2.24	1.12	−1.99	5.84	2.92
2.0	$SrCl_2$	−1.55	2.40	1.20	−1.89	3.52	1.76
2.0	$CaCl_2$	−1.53	2.24	1.12	−1.86	3.52	1.76
4.0	LiOH	—			−1.97	11.00	2.75
2.0	〃	—			−1.96	5.40	2.70
1.0	〃	—			−1.95	2.80	2.80

and the height of waves increased linearly with the concentration.

It was made clear that lithium cinnamate gave a single wave corresponding to the reduction of cinnamate anion, by using 0.1N LiOH solution.

(2) **Electroreduction in acid solution.**—In the case of 0.1N HCl solution as a supporting electrolyte, cinnamic-, styrylacetic- and crotonic-acids gave no reduction waves of carbon-carbon double bond, owing to the decomposition potential of hydrogen ion in the bulk of HCl solution. (Decomposition potential of hydrogen ion was measured at ca. −1.16 volt. vs. S. C. E.)

Another attempt was made to investigate the polarographic behavior of cinnamic acid in some unbuffered acid solutions.

Table 3 shows a summary of the observed half-wave potentials and diffusion current of cinnamic acid in acid solution. The second wave (I_d) which corresponds to the reduction of carbon-carbon double bond, was diminished linearly with the increase of the concentration of HCl, while the first wave (I_l) grew remarkably large, owing to the decomposition of hydrogen ion.

(3) **Electroreduction of ethyl cinnamate.**—We have undertaken the polarographic observation of ethyl cinnamate in neutral and also alkaline solutions.

Ethyl cinnamate gave a single wave which might correspond to the reduction of carbon-carbon double bond in a neutral solution (0.1N $(CH_3)_4NBr$), whereas it gave a double wave in

Table 3

Half-wave Potentials and Diffusion Currents of Cinnamic Acid in Acid Solution. (50% Dioxane, 0.004—0.005% gelatin)

Cinnamic acid (mol.)	HCl (N.×10⁻³)	Electrolyte	First wave $\pi_{1/2}$ (Volt vs. S. C. E.)	First wave I_l (μA.)	First wave I_l/C.	Second wave $\pi_{1/2}$ (Volt vs. S. C. E.)	Second wave I_d (μA.)	Second wave I_d/C.
2×10⁻³	0.5	0.1N $CaCl_2$	−1.55	3.2	1.60	−1.89	2.9	1.45
〃	1.0	〃	−1.50	4.5	2.25	−1.89	1.5	0.75
(c. f.	1.0	〃	−1.47	2.5)				
5×10⁻³	—	0.1N $CaCl_2$	−1.55	5.2	1.04	−1.87	7.8	1.54
〃	0.5	〃	−1.55	6.0	1.20	−1.87	6.8	1.36
〃	1.0	〃	−1.50	7.2	1.44	−1.88	5.8	1.16
〃	5.0	〃	−1.49	22.2	4.44	−1.77	3.4	0.68
(c. f.	5.0	〃	−1.53	24.4)				
5×10⁻³	—	0.1N $SrCl_2$	−1.55	5.4	1.08	−1.90	9.4	1.88
〃	0.5	〃	−1.54	6.4	1.28	−1.90	8.6	1.72
〃	1.0	〃	−1.50	8.2	1.64	−1.92	7.4	1.25
〃	5.0	〃	−1.47	25.4	5.08	−1.79	5.6	1.12
(c. f.	5.0	〃	−1.51	25.5)				
1×10⁻²	—	0.1N $SrCl_2$	−1.57	12.8	1.28	−1.97	18.0	1.80
〃	1.0	〃	−1.54	14.8	1.48	−1.96	16.4	1.64
〃	2.0	〃	−1.53	20.4	2.04	−1.97	13.2	1.32
〃	5.0	〃	−1.48	33.2	3.32	−1.86	10.4	1.04
〃	10.0	〃	−1.47	99.6	9.96	−1.86	6.8	0.68
(c. f.	1.0	〃	−1.55	3.2)				

Table 4

Half-wave Potentials and Diffusion Currents of Ethyl Cinnamate. (50% Dioxane)

Sample (mol.)	Electrolyte	First wave* $\pi_{1/2}$ (Volt vs. S. C. E.)	First wave* i_d (μA.)	Second wave $\pi_{1/2}$ (Volt vs. S. C. E.)	Second wave i_d (μA.)
5×10⁻³	0.1N $(CH_3)_4NBr$	−1.69	13.1	—	—
1×10⁻³	〃	−1.68	2.6	—	—
4×10⁻³	0.1N LiOH	−1.65	.....**	−1.97	.....**
2×10⁻³	〃	−1.66	.....	−1.96	.....
1×10⁻³	〃	−1.67	.....	−1.96	.....

* This first waves have different meaning for those of Table 2.

** i_d value are omitted, because they are changeable with the lapse of hydrolysis.

alkaline solution (0.1N LiOH).

Table 4 gives the observed half-wave potentials and diffusion currents of ethyl cinnamate. Comparing the results obtained from both cinnamic acid and its ester in the same supporting electrolyte, it was clear that the half-wave potential of ethyl cinnamate was more positive than that of cinnamic acid. The appearance of the double wave in the reduction of the ethyl cinnamate in alkaline solution can be attributed mainly to the reduction of two different forms, that is, ethyl cinnamate and cinnamic acid resuling from

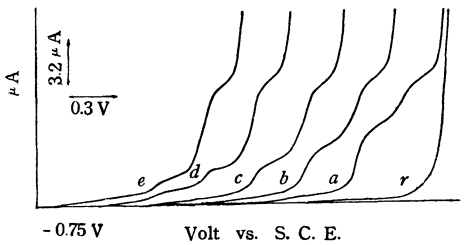

Fig.—2.—A polarogram for the hydrolysis of Ethyl Cinnamate. (Supporting media: 50% Dioxane 0.1N LiOH, Sample: 1.5×10^{-3}M.) (R) Residual Current. (a) Initial state, (b), (c), (d), (e) states after the lapse of respectively 40 min., 80 min., 120 min., 160 min., from (a).

hydrolysis. Fig. 2 shows a polarograme for the hydrolysis of ethyl cinnamate. The first wave was observed to have diminished by the hydrolysis. The total wave heights were constant and they were twice as large as the height of cinnamic acid in the same concentration. Detailed discussion on this phenomenon will be presented in another paper.

Discussion

It has been pointed out that the electroreducibility of a carbon-carbon double bond was closely related to the nature of the conjugated system of the double bond in the study of polarographic reduction of several unsaturated acids.[2a]

It was found in the present experiment that cinnamic acid gave only the polarographic wave corresponding to the reduction of carbon-carbon double bond. The electroreduction of cinnamic acid gave two-step polarographic waves in neutral solution. Under these conditions, there would be neutral molecules, dissociated cinnamate anions and hydrogen ions in the vicinity of the electrode surface and these species would contribute to the potential determining step. The following characteristic kinds of behavior were observed;

(1) Well-defined two-step reduction wave was obtained in a neutral solution.

(2) The first wave was observed to diminish by addition of alkali.

(3) Lithium cinnamate gave a single wave either in neutral or in alkaline solution.

(4) The heights of the first wave and the heights of the second wave were both proportional to the concentration of samples.

(5) Total wave heights of both the first and the second waves remained constant when alkali was introduced into a neutral solution.

In the initial stage of waves (first wave), therefore, this phenomenon may be considered as being due to the discharge of hydrogen in the bulk of solution. This is true because at such *p*H values (*p*H>6) the concentration of the undissociated acid becomes negligibly small and the cinnamate anion may be reduced directly on the electrode surface.

Another interesting result which was obtained was that the half-wave potentials of the carbon-carbon double bond, in the case of divalent cations as a supporting electrolyte, were shifted and became less negative than in the case of the monovalent cation. (Table 5) The effect of divalent cations can be explained by the ionic activity of these cations that form the metal complex with carbonyl anion and tend to diffuse to the electrode surface by the electrostatic interaction.

It has been mentioned that[4] the electrolytic reduction of cinnamic acid in acid solution with mercury cathode, gave rise to bimolecular compounds, which were produced by the dimerization of free radicals, Ph-$\dot{C}$HCH$_2$COOH obtained from cinnamic acid. But in alkaline solution, no bimolecular compounds were produced; that is, only hydrocinnamic acid was given.

If we assume that the polarographic reduction process will take place in the same manner as in the case of so-called electrolytic reduction, it may be expected that there will be considerable change in the polarograms obtained from acid

Table 5

Effect of Cations on the Half-wave Potentials of Cinnamic acid. (50% Dioxane)

Sample (2.0×10^{-3} mol.)	Cation	Electrolyte	Half-wave Potential (Volt vs. S. C. E.)	I_d (μA.)	I_d/C.
Li cinnamate	$(CH_3)_4N^+$	0.1N $(CH_3)_4NBr$	−1.98	6.0	3.00
〃	Li^+	0.1N LiCl	−1.93	8.5	4.25
〃	Sr^{++}	0.1N $SrCl_2$	−1.88	5.8	2.90
〃	Ca^{++}	0.1N $CaCl_2$	−1.84	5.5	2.75
Ba cinnamate	Ba^{++}	0.1N $(CH_3)_4NBr$	−1.92	5.8	2.90
Ca cinnamate	Ca^{++}	〃	−1.90	5.7	2.85

solution, compared with that in neutral or alkaline solution. But, in the present experiments, no clear effect of hydrogen ion concentration could be established, since the half-wave potential of carbon-carbon double bond was observed to be more negative than the decomposition potential of hydrogen ion.

Summary

1) In neutral solution, both styrylacetic acid and crotonic acid gave a single wave (ca. −1.6——1.7 *v.*), on the other hand cinnamic acid gave a well-defined two-step polarographic wave (ca. −1.5 *v.* and ca. −2.0 *v.*) corresponding to the reduction of carbon-carbon double bond. The half-wave potentials of cinnamic acid were shifted by the presence of divalent cations.

2) Ethyl cinnamate gave a single wave (ca. −1.7 *v.*) in neutral solution, but in alkaline solution it gave two waves (ca. −1.7 *v.* and ca. −2.0 *v.*). The first wave was observed to diminish by the hydrolysis in alkaline solution.

The authors wish to express their thanks to Dr. I. Tachi of the Univ. of Kyoto, and his collaborator for the discussion of the results.

Department of Chemistry,
Faculty of Education, Naniwa University, Osaka

Dipole Moments of Tropone, 2-Phenyltropone, Tropolone Methyl Ether and their Derivatives*

By Yukio KURITA, Shuichi SETO, Tetsuo NOZOE and Masaji KUBO

(Received December 23, 1952)

Hitherto we studied the dipole moments of tropolone (or cycloheptatriene-ol-2-one-1) and its derivatives.[1~5] The characteristic feature of the molecules of these compounds is that the electronic structures with a negative charge at the carbonyl oxygen and a positive charge at one of the carbon atoms in the ring contribute appreciably to the normal state. The same situation is expected[6~8] for tropone (or cycloheptatrienone), one of the simplest and the most fundamental compounds with a cycloheptatriene ring. The determination of the dipole moment of tropone made in the present investigation will throw light on the theory of the π-electron problem as applied to the charge distribution in this molecule.

We have also carried out measurements on the dipole moments of eleven of its derivatives. All the compounds studied were synthesized* and purified by one of us (T.N.) and his collaborators at the laboratory of organic chemistry, Tôhoku University.

Experimental Method and Results

All the measurements were made in benzene solution at 25° except in one case (compound VII) for which the temperature was varied from 20° to 40°. The apparatus and the method of measurement were the same as used in our earlier works. The Halverstadt-Kumler's method was employed throughout. The moment of tropolone was remeasured, in view of its importance, to get more accurate value from data at various concentrations. The results are shown in Tables 1 and 2, where the same notations are used as those in the previous reports.

Discussion of Results

Tropone.—The value 4.17 D for the moment of tropone is in fair agreement with that of Giacomo and Smyth, 4.30 D.[10] The large

* Read before the scientific meeting of the Chemical Society of Japan (A Symposium on Tropolone Chemistry) held on July 5, 1952.

(1) Y. Kurita, T. Nozoe and M. Kubo, This Bulletin, **24**, 10 (1951).

(2) Y. Kurita and M. Kubo, ibid., **24**, 13 (1951).

(3) Y. Kurita, T. Nozoe and M. Kubo, ibid., **24**, 99 (1951).

(4) Y. Kurita, T. Nozoe and M. Kubo, ibid., **26**, 242 (1953).

(5) Y. Kurita, T. Mizuno, T. Mukai and M. Kubo, ibid., **26**, 192 (1953).

(6) T. Nozoe, T. Mukai, K. Takase and T. Nagase, *Proc. Japan Acad.*, **28**, No. 9, 477 (1952).

(7) H. J. Dauben and H. J. Ringold, *J. Am. Chem. Soc.*, **73**, 876 (1951).

(8) W. von E. Doering and F. L. Detert, ibid., **73**, 876 (1951).

* See literatures at the end of Table 1.

(10) A. D. Giacomo and C. P. Smyth, *J. Am. Chem. Soc.*, **74**, 4411 (1952).

Table 1

Dielectric Constant and Density Increments, 25°

	Compounds	$w\times10^5$	$\Delta\varepsilon\times10^4$	$\Delta d\times10^5$
I	Tropone[a]	208	439	46
	b. p. 84—85°(6 mm.)	439	862	100
		737	1364	154
		1070	1998	224
II	2-Phenyltropone[b]	225	225	—
	m. p. 85—86°	380	—	79
		804	760	192
		1184	1087	267
III	4-Bromo-2-phenyl-	151	60	21
	tropone[c]	366	99	101
	m. p. 88°	627	195	196
		841	289	290
IV	3,7-Dibromo-	331	156	113
	2-phenyltropone[d]	470	223	182
	m. p. 118°	842	387	351
		1328	611	575
V	2-(*p*-Methoxy-	317	269	73
	phenyl)-tropone[e]	506	416	105
	m. p. 54.5—55.0°	875	670	244
VI	Tropolone methyl	341	538	80
	ether[f]	612	1065	149
	(oil)	1119	1941	278
VII	(Tropolone methyl ether)$_2$·H_2O,[f]		m. p. 41°	
	20°	253	438	—
		358	650	45
		558	993	105
	30°	253	411	65
		358	608	98
		558	930	142
	40°	253	366	10
		358	555	86
		558	874	168
VIII	*o*-Bromotropolone	160	242	67
	methyl ether A	252	393	107
	(7-Bromo-2-	335	514	141
	methoxy-tropone)[g]	563	876	239
	m. p. 91—91.5°	1077	1670	488
IX	*o*-Bromotropolone	319	187	113
	methyl ether B	613	356	263
	(3-Bromo-2-	1081	589	430
	methoxy-tropone)[g]	1490	867	637
	m. p. 76—77°			
X	α-Thujaplicin	433	430	80
	methyl ether B[h]	694	710	120
	m. p. 72°	1224	1250	210
XI	*m*-Methyltropolone	200	320	48
	methyl ether A	297	543	84
	(6-Methyl-2-	527	891	135
	methoxy-tropone)[i]	627	1160	168
	m. p. 95.5-96°			
XII	Tropolone[j]	471	578	114
	m. p. 51°	864	993	227
		1187	1361	309
		1911	2206	488
		2378	2705	613

(a) T. Nozoe, T. Mukai, K. Takase and T. Nagase, *loc. cit.* reference (6).
(b) T. Nozoe, T. Mukai and J. Minegishi, *Proc. Japan Acad.*, **27**, 419 (1951).
(c) T. Nozoe, S. Seto and S. Ito, ibid., to be published shortly.
(d) T. Nozoe, T. Mukai and I. Murata, ibid., **28**, 142 (1952).
(e) T. Nozoe, S. Seto, T. Ikemi and T. Sato, ibid., **28**, No. 8, 413 (1952).
(f) T. Nozoe, S. Seto, T. Ikemi and T. Arai, ibid **27**, 102 (1951).
(g) T. Nozoe, Y. Kitahara and S. Masamune, ibid., **27**, 649 (1951).
(h) T. Nozoe, Y. Kitahara, K. Yamane and T. Ikemi, ibid., **27**, 193 (1951).
(i) P. Akroyd, R. D. Haworth and J. D. Hobson, *J. Chem. Soc.*, **1951**, 3427.
(j) T. Nozoe, S. Seto, Y. Kitahara, M. Kunori and Y. Nakayama, *Proc. Japan. Acad.*, **26**, No. 7, 38 (1950).

increase, about 1.1 D), in the moment of this molecule over that of cycloheptanone, 3.04D,[11] indicates the importance of the contribution of polar structure B.

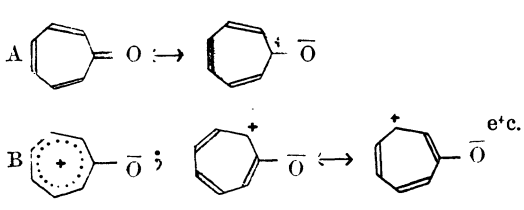

Sutton[12] pointed out that the moments of various unsaturated ketones and aldehydes with conjugated C=C double bonds fit in well with calculated values, if we give mesomeric moments of 0.1 D and 0.2 D respectively to C—C bonds adjacent to the carbonyl group and to the next C=C bonds, each lying along its respective bond. The correction of mesomeric effect can only partly explain the increase of moment of tropone over that of cycloheptanone. The calculated value is 3.5D, still smaller than the observed value by an amount of 0.7 D. This may be attributed to an additional effect due to the formation of cycloheptatrienone ring. In fact, the difference

(11) Hs. H. Günthard and T. Gäumann, *Helv. Chim. Acta.*, **34**, 39 (1951).
(12) J. B. Bentley, K. B. Everard, R. J. B. Marsden and L. E. Sutton, *J. Chem. Soc.*, **1949**, 2957.

Table 2

Dipole Moments of Tropone and Related Compounds in Benzene Solution at 25°

Compounds		ε_1	d_1(g./cc.)	α	β(g./cc.)	$P_{2\infty}$(cc.)	R_D(cc.)	μ(D)
I		2.2788	0.87121	17.98	0.204	387± 4	30.9[a]	4.17±.03
II		2.2751	0.87144	9.01	0.234	355± 8	55.1	3.82±.05
III		2.2719	0.87075	3.36	0.387	215±12	62.9	2.73±.11
IV		2.2732	0.87078	4.54	0.461	346±12	70.7	3.67±.01
V		2.2772	0.87084	7.15	0.316	332± 9	61.4	3.63±.05
VI		2.2668	0.87127	17.92	0.254	494± 1	37.2	4.72±.01
VII	20°	2.2816	0.87605	18.06	0.300	1045±29	78	6.81±.10*
	30°	2.2617	0.86616	16.88	0.246	1005±26	78	6.78±.10*
	40°	2.2384	0.85443	16.55	0.502	980±26	78	6.80±.10*
VIII		2.2721	0.87124	15.56	0.458	666± 2	45.0	5.51±.01
IX		2.2724	0.87112	5.71	0.436	269±11	45.0	3.31±.08
X		2.2716	0.87156	10.34	0.165	397± 4	51.1	4.11±.02
XI		2.2683	0.87131	18.67	0.272	565±21	41.7	5.06±.10
XII		2.2759	0.87113	11.26	0.258	289± 3	32.5[b]	3.53±.02

(a) R_D observed is 33.9 cc.[8]

(b) R_D observed is 37.46 cc. and the value extrapolated to infinite wavelength is 34.30 cc.[9]

* Apparent moments.

of 0.7 D is very close to the moment of 0.85D calculated theoretically for heptafulvene.[13] The magnetic susceptibility measurements by Maruha and Hazato[14] also indicate the importance of the electronic structures of the type B.* If we assume that the structure A has a moment 3.0 D and the structure B has 16.8 D, the contribution x of the polar form B can be calculated from

$$3.0(1-x)+16.8\,x=4.17$$

as $x=0.082$. There are six individual structures for B. Hence the contribution of each polar structure is 0.014, giving an effective positive charge 0.014 e to each of the six ring carbon atoms. Brown[15] in his molecular orbital treatment gave an effective charge of 0.06—0.11 e. This is not surprising, since the neglect of mutual repulsion between electrons, made in simple molecular orbital method, will always give too high value for the theoretical moment.

2-Phenyltropone and its derivatives.— The moment of 2-phenyl-tropone is smaller than that of tropone, due to the induction effect. Presumably the benzene ring is nearly perpendicular to the plane of cycloheptatriene ring to minimize steric hindrance. The absorption spectra studied by Tsuboi[16] also indicate that the degree of conjugation between the two rings is not great. With the assumption that the cycloheptatriene ring has a regular heptagon form, that the moment of 2-phenyltropone, 3.82 D in magnitude, lies along the C=O bond direction and that the value of C—Br bond moment is 1.5 D, the moment of 4-bromo-2-phenyltropone was calculated to be 2.6 D, a little lower than the observed value of 2.73 D. Actually owing to induction effect, the moment of 2-phenyltropone makes an angle of a few degrees with the C=O direction towards phenyl-group. This with C—Br moment gives a greater resultant moment in agreement with experiment. The moment calculated for 3,7-dibromophenyltropone in a similar manner is 4.4 D to be compared with the observed value of 3.67 D. The difference of this order of magnitude may be attributed to the induction and steric effects.

The position of methoxy-group in 2-(*p*-methoxyphenyl)-tropone has already been determined by us[17] from evidences in organic synthesis. Hoping to confirm the conclusion, we calculated the moment for *p*-position with reasonable assumptions. The calculated value of 3.9 D agrees fairly well with the observed value of 3.63 D.**

(9) T. Shiratori and S. Kinumaki, private communication.

(13) E. D. Bergmann, E. Fischer, D. Ginsberg, Y. Hirshberg, D. Lavie, M. Mayot, A. Pullman and B. Pullman, *Bull. Soc. Chim. France*, **1951**, 684.

(14) J. Maruha and G. Hazato private communication.

* See also the literature (a) of Table 1.

(15) R. D. Brown, *J. Chem. Soc.*, **1951**, 2670.

(16) M. Tsuboi, private communication.

(17) T. Nozoe, S. Seto, T. Ikemi and T. Sato, *loc. cit.* reference (e) of Table 1.

** The theoretical value is rather insensitive to the presumed position of methoxy-group (3.9 D for *para*, 3.9 D for *meta* and 3.4 D for *ortho*-substitution). It is therefore impossible from the dipole moment data alone to determine the position.

Table 3

Dipole Moments of Methyl Ethers of Tropolone Derivatives

2-Methoxy-tropones	*cis*-Position	Perpendicular form	*trans*-Position	Observed (D)
3-Bromo-	3.4—4.4	4.1—4.9	4.7—5.4	3.31
7-Bromo-	4.0—4.6	5.3—5.7	6.3—6.7	5.51
6-Methyl-	3.3—4.2	4.3—5.0	5.1—5.7	5.06
7-Isopropyl-*	2.9—3.8	3.8—4.6	4.6—5.2	4.11

Tropolone methyl ether and its derivatives.—The moment of tropolone methyl ether was estimated from those of tropone and methoxy-group with due regard to the mesomeric moments of O—C (ring) bond. The calculated moment is 3.1—3.9 D for *cis*-configuration, i.e., for methyl group near the oxygen atom of C=O in the ring plane, 5.1—5.6 D for *trans*-configuration and 4.2—4.8 D for the structure in which the methoxy-group lies in a plane perpendicular to the ring. The possible explanation of the observed moment, 4.72 D, is either that the methoxy-group is out of the ring plane to minimize steric hindrance or that both *cis*- and *trans*-configurations are present to give an intermediate moment. A similar conclusion can also be derived for substituted methoxytropones as shown in Table 3.

In particular, the moment of 3-bromo-2-methoxytropone is very close to the theoretical value for *cis*-configuration. Probably the methoxy-group is repelled by the great steric repulsion of bromine atom at 3-position. This will render the molecule less stable than that of 7-bromo-2-methoxytropone in good agreement with the fact that the former is more liable to aromatization than the latter.[18] Mills and Tyrell[19] in their preliminary measurements gave for the moment of *m* (β in their notation)-methyltropolone methyl ether A the value of 4.9 D in agreement with ours. Sutton and Saxby[20] also measured the moment** of this compound and supported the constitutions proposed by Akroyd and others.

The moment of tropolone methyl ether hydrate is independent of temperature and the dependence of the dielectric constant and density of the solution upon concentration is normal. This fact suggests no association taking place. The observed apparent moment of 6.80 D agrees within experimental errors with

$$\bar{\mu} = [2\mu^2(\text{trop. meth. eth.}) + \mu^2(H_2O)]^{1/2}$$
$$= (2 \times 4.72^2 + 1.75^2)^{1/2} = 6.9 \text{ D}.$$

Hence we conclude that in benzene solution the hydrate dissociates into three separate *molecules*.

Summary

The dipole moments of tropone, 2-phenyltropone, tropolone methyl ether and their derivatives were measured in benzene solution at 25°. The increase of moment of tropone over that of cycloheptanone was adequately explained by mesomeric effect and an additional effect due to the formation of cycloheptatriene ring. The latter effect was supported by the theoretical moment for heptafulvene. The moments of various derivatives were compared with the theoretical data. The agreement between them confirmed the correctness of the position of substituents in these compounds already determined or inferred from the standpoint of organic syntheses. The apparent moment of tropolone methyl ether hydrate indicates that in benzene the hydrate dissociates into three separate molecules.

We wish to express our thanks to Mr. Y. Kitahara and Mr. T. Mukai of Tôhoku University for their collaboration in the syntheses of these compounds. Our thanks are also due to the Ministry of Education in aid of this research.

Chemical Institute, Faculty of Science, Nagoya University, Nagoya
Chemical Institute, Faculty of Science, Tôhoku University, Sendai

* The position of isopropyl-group was determined by T. Nozoe, S. Seto, T. Ikemi and T. Sato from evidences in organic chemistry, the details of which will be published shortly.

(18) T. Nozoe, Y. Kitahara and S. Masamune, *loc. cit.* reference (g) of Table 1.

(19) R. D. Haworth and J. D. Hobson, *J. Chem. Soc*, **1951**, 561.

(20) P. Akroyd, R. D. Haworth and J. D. Hobson, *loc. cit.* reference (i) of Table 1.

** Unfortunately their value is not given in the paper.

Derivatives of dl-Aminopropanediols*

By Chieko URAKAMI and Kasumi KAKEDA

(Received January 9, 1953)

Since the structure of chloramphenicol was proven[1] by a group of workers at the laboratories of Parke Davis & Co. to be *D*-(levo)-threo-2-dichloroacetamido-1-*p*-nitrophenyl-1, 3-propanediol, a number of papers dealing with the preparation of its analogs have appeared, but esterification of the hydroxyl groups of the chloramphenicol type compounds have not been attempted. It might be possible to maintain bacteriostatic activity by dropping off the *p*-nitrophenyl group from the chloramphenicol molecule and by esterifying the hydroxyl groups with *p*-nitrobenzoic or fatty acids of varied chain lengths since certain esters of glycerol[2] have been reported to be active against *Mycobacterium tuberculosis*. As far as we are aware, there have been reported no cases where the haloacylaminopropanediols have been esterified with the acids we used in this experiment.

A number of functional derivatives of the following three types of compounds were prepared (Table 1, 2 and 3).

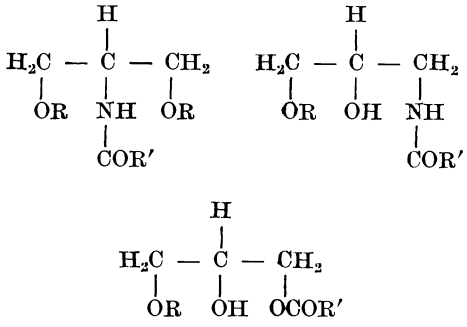

R=H or acyl group,
R′=haloalkyl group

1- and 2-Aminopropanediols were prepared

Teble 1

1-Aminopropanediol Series, $CH_2(OR)CH(OH)C\overset{*}{H}_2NHCOCHCl_2$

No.	R	M. P. °C	$n_D^{12.5}$	Calcd. C	Calcd. H	Calcd. N	Found. C	Found. H	Found. N
I	H	59.0—59.5		29.70	4.49	6.93	29.17	4.29	6.78
II	$C_6H_{17}CO$	55.5—56.5 (from absol. MeOH)		49.13	7.36	4.09	48.90	7.70	4.13
III	$C_{11}H_{23}CO$	70.5—71.0 (〃)		53.12	8.13	3.64	53.32	8.36	3.41
IV	p-$O_2NC_6H_4CO$	138.0—138.5 (〃)		41.04	3.44	7.98	41.44	4.01	7.67
V	i-C_3H_7CO	155—170/1.5×10^{-4}mm.Hg.*	1.492	39.70	5.51	5.15	38.28	5.08	5.39
VI	i-C_4H_9CO	150—170/8×10^{-4}mm.Hg.*	1.486	41.98	5.99	4.89	43.76	5.91	5.08

* Bath temperature.

Reaction Condition

No.	Reaction time	Yield%	Solubility: MeOH	EtOH	AcMe	Et_2O	AcOH	AcOEt	$CHCl_3$	C_6H_6	Petr. ether	H_2O
II	20 hrs.	27	+	+	+	+	+	+	−	−	−	−
III	24 hrs.	43	+	+	+	+	+	+	+	+ (hot)	+ (hot)	−
IV	2 weeks	34	+	+	+	−	+	+	+ (hot)	−	−	−
V	24 hrs.	58	+	+	+	+		+	+	−	+ (hot)	−
VI	24 hrs.	65	+	+	+	+		+	+	−	+ (hot)	−

* Part of this work was presented at the Fifth Annual Meeting of the Chemical Society of Japan, April 1952.

(1) M. C. Rebstock, H. M. Crooks, Jr., and J. Controulis, *J. Am. Chem. Soc.*, **71**, 2458, 2163 (1949).

(2) Th. Wagner-Jauregg and H. Arnold, *Ber.*, **70**, 1459 (1937); H. Arnold, ibid., **71**, 1505 (1938); ibid., **73**, 90 (1940).

Table 2

2-Aminopropanediol Series, $CH_2(OR_1)CH(NHCOCHCl_2)CH_2(OR_2)$

No.	R_1	R_2	M. P. °C.*	Calcd. C	Calcd. H	Calcd. N	Found. C	Found. H	Found. N
VII	H	H	143.5—144.0	29.70	4.49	6.93	30.25	5.97	6.84
VIII	$C_8H_{17}CO$	$C_8H_{17}CO$	50.0—51.0	57.24	8.56	2.90	58.34	8.27	2.82
IX	$C_{11}H_{23}CO$	$C_{11}H_{23}CO$	68.5—69.0	61.04	9.42	2.23	60.90	9.22	2.47
X	p-$O_2NC_6H_4CO$	H	141.0—142.0	41.04	3.44	7.98	41.49	3.34	7.67
XI	$C_{15}H_{31}CO$	$C_{15}H_{31}CO$	80.0—81.0	65.46	10.24	2.06	66.21	10.04	2.21
XII	$C_{17}H_{35}CO$	$C_{17}H_{35}CO$	80.0—80.5	66.99	10.56	1.90	67.97	10.39	1.99

* Recrystallized from abs. EtOH.

Reaction Condition

No.	Reaction time	Yield%	Solubility: MeOH	EtOH	AcMe	Et_2O	AcOH	AcOEt	$CHCl_3$	C_6H_6	Petr. ether	H_2O
VIII	3 days	83 (crude)	+	+	+	+			+	−	−	−
IX	3 days	83 (crude)	+	+	+	+			+	−	−	−
X	5 days	73 (crude)	+	+	+	−		+	+	−	−	−
XI	24 hrs.	78 (crude)	+	+	+	+	+		+	−	−	−
XII	24 hrs.	77 (crude)	+	+	+	+	+		+	−	−	−

Table 3

Halogenated Acyl Ester Series, $CH_2(OCOC_{11}H_{23})CH(OH)CH_2(OR)$

No.	R	M. P. °C.	Calcd. C	Calcd. H	Found. C	Found. H
XIII	$CHCl_2CO$	175—178/10^{-2}mm.Hg.*	52.90	7.84	52.61	7.50
XIV	CH_2ClCO	50.0—50.5 145—155/10^{-2}mm.Hg.*	58.19	8.19	58.57	8.78

* Bath temperature.

Reaction Condition

No.	Reaction time	Yield%	Solubility: MeOH	EtOH	AcMe	Et_2O	AcOEt	$CHCl_3$	C_6H_6	Petr. ether	H_2O
XIII	24 hrs.	82	+	+	+	+	+	+	−	−	−
XIV	24 hrs.	68	+	+	+	+	+	+	−	−	−

according to the method described in the literature.[3~5] The amino group was acylated first with methyl dichloroacetate and then one or both hydroxyl groups were esterified with long chain aliphatic acids or p-nitrobenzoic acid.

Since it has been observed that the acyl migration[6][7] takes place from the oxygen of the hydroxyl group to the nitrogen of the amino group in acyl derivatives of the aminopropanediol in an alkaline solution and vice-versa in an acid solution, the confirmation of the chemical costitution of the final compounds prepared was desirable. If the 2-hydroxyl group in the 1-acyl-amino-2, 3-propanediol and the 1, 3-hydroxyl groups in the 2-acylamino isomer were left free, the migration of the acyl group from the nitrogen of the amino group to the oxygen of the hydroxyl groups to the 2- and 1 or 3-posititions, respectively, would occur on treatment with phosphorus pentachloride. Therefore, the hydroxyl groups were acylated previous to the treatment with

(3) E. Abderhalden and E. Eichwald, *Ber.*, **47**, 2888 (1913).
(4) E. Schmidt and R. Wilkendorf, *ibid.*, **52**, 398 (1919).
(5) H. Schlenk and B. W. De Haas, *J. Am. Chem. Soc.*, **73**, 3921 (1951).
(6) Max Bergmann and S. Sabetay, *Z. physical. Chem.*, **137**, 47 (1924).
(7) Carlo G. Alberti, XII Int. Congr. Meeting in New York, Sept., 1951.

phosphorus pentachloride. 1-Dichloroacetamido-3-lauroyloxy-2-propanol was esterified with stearoyl chloride and the resulting product was treated with phosphorus pentachloride,[8] followed by deamination with nitrous acid to give 1-lauroyl-2-stearoylglycerol, which was then esterified with stearoyl chloride. The final product melted at 56.0~57.0°C. and showed no depression of its m. p. when mixed with an authentic sample (m. p. 54.0°C.[9]) prepared according to Fischer's method.[10] Similarly, deamination was carried out with 2-dichloroacetamido-1, 3-dilauroyloxypropane.

This procedure proves that no migration of the dichloacetyl group or no interchange of the haloacyl with other acylgroup has taken place. The preparation of 1-lauroyloxy-2, 3-distearoyloxy from 1-dichloroacetamido-3-lauroyloxy-2-propanol shows that the monoacylation of the primary alcohol has taken place during the acylation of the haloacylaminopropanediol. Therefore, it is reasonable to state that the rest of the compounds prepared possess the structures as indicated.

Experimental

dl-Dichloroacetamidopropanediol (I).—A mixture of 18 g. (0.197 mol) of 1-aminopropanediol (140~140.5°C./6~6.5 mm) and 30 g. (0.209 mol) of methyl dichloroacetate was refluxed on the water bath for 1½ hrs. The methanol formed was removed and the residue was washed by decantation five times with 30 cc. portions of petroleum ether and dried over conc. sulfuric acid paraffin in a vacuum desiccator to induce crystallization. The crude product was dissolved in ethyl acetate, the solution filtered, the solvent removed and the residue washed with petroleum ether. The yield was quantitative.

1-Dichloroacetamido-3-lauroyloxy-2-propanol (III).—To a mixture of 8 g. (0.039 mol) of dl-dichloroacetamidopropanediol, 30 cc. of chloroform and 4 g. of pyridine, cooled to zero degree, was added dropwise 8 g. (0.037 mol) of lauroyl chloride* under constant stirring. The reaction mixture was allowed to stand at room temperature for 24 hrs., acidified with 1/2 N sulfuric acid and extracted with ether. The ether extract washed with a 5% solution of sodium carbonate followed by water and dried over anhydrous sodium sulfate. It was then filtered and the residue obtained after removal of the solvent was allowed to stand at −18°C. to allow crystallization to take place. The crude product was dried in a vacuum desiccator over conc. sulfuric acid, and purified by recrystallization from absolute methanol. The crude product weighed 10 g. (71% of theoretical yield), and pure product melting at 70.5~71.0°C. weighed 6 g. (43% of theoretical yield). The compounds 1-dichloroacetamido-3-nonoyloxy-2-propanol (II) and 1-dichloroacetamido-3-*p*-nitrobenzoloxy-2-propanol (IV) were prepared by the similar method described above.

dl-1-Dichloroacetamido-3-isobutyroyloxy-2-propanol (V).—To a solution of 6 g. (0.029 mol) of dl-dichloroacetamidopropanediol and 3 g. of pyridine in 5 cc. of chloroform was added, under cooling, 3.5 g. (0.026 mol) of isobutyroyl chloride and allowed to stand at room temperature for 24 hrs. The reaction mixture was treated in the manner similar to the method described for the preparation of 1-dichloroacetamido-3-lauroyloxy-2-propanol. Since it was found to be a liquid compound, the crude product was extracted with ether, the solvent removed, the residue extracted with alcohol, and the residue obtained after removing the alcohol was subjected to high vacuum distillation.

The 1-dichloroacetamido-3-isovaleroyloxy-2-propanol (VI) was prepared similarly.

1-Lauroyloxy-2, 3-distearoyloxypropane.—For the confirmation of the structure of 1-dichloroacetamido-3-lauroyloxy-2-propanol, one gram (0.0026 mol) of 1-dichloroacetamido-3-lauroyloxy-2-propanol was dissolved in a mixture of 10 cc. of chloroform and 2.5 g. of pyridine, the resulting mixture treated, under cooling, with 0.85 g. (0.0028 mol) of stearoyl chloride and the reaction mixture allowed to stand for 2 days. The subsequent treatment of the reaction mixture was carried out in the manner similar to the method described previously. The pure compound melted at 66~67°C.

The compound thus obtained was treated with phosphorus pentachloride according to the method described in the literature[8] to obtain the hydrochloride salt of 1-amino-2-stearoyloxy-3-lauroyloxypropane. The product was then deaminated with nitrous acid to give 1-lauroyl-2-stearoyl glycerol, which was then esterified with stearoyl chloride in the presence of pyridine. The purified triglyceride melting at 56.0~57.0°C. showed no depression of its melting point when mixed with the sample prepared according to Fischer's method.[10] (Reported m. p. 54.0°C.[9])

The total amount of lauric acid obtained by hydrolysis of 1-dichloroacetamido-3-lauroyloxy-2-propanol with 0.1 N sodium hydroxide was found quantitative.

2-Dichloroacetamidopropanediol (VII).—2-Aminopropanediol[5] was treated with methyl dichloroacetate in the manner described for the preparation of the dl-dichloroacetamido isomer. The crude product was purified once from a mixture of methanol and petroleum ether and then from absolute alcohol, m. p. 143.5−144.0°C. The yield was quantitative.

(8) Max Bergmann, E. Brand and F. Dreyer, *Ber.*, **54**, 935 (1921).

(9) B. F. Daubert, *J. Am. Chem. Soc.*, **66**, 291 (1944). Daubert prepared this compound by the reduction of 1-lauroyloxy-2, 3-dielaidoyloxypropane.

(10) E. Fischer, *Ber.*, **53**, 1589 (1920).

* Lauric acid used in this experiment was a c. p. grade of Matheson product.

2-Dichloroacetamido-1, 3-dilauroyloxypropane (IX).—A solution of 1.2 g. (0.0060 mol) of 2-dichloroacetamidopropanediol in a mixture of 30 cc. chloroform and 10 g. of pyridine was treated, under cooling, with 1.8 g. (0.0082 mol) of lauloyl chloride, the reaction mixture allowed to stand for three days, and treated in the manner described for the preparation of 1-dichloroacetamido-3-lauroyloxy-2-propanol. Compounds 2-dichloroacetamido-1, 3-dinonoyloxypropane (VIII), 2-dichloroacetamido-1-*p*-nitrobenzoyloxy-3-propanol (X), 2-dichloroacetamido-1, 3-dipalmitoyloxypropane (XI),* 2-dichloroacetamido-1, 3-distearoyloxypropane (XII),* were prepared according to the method mentioned above.

1-Chloroacetyl-3-lauroyl glycerol (XIV).—A solution of 4.5 g. (0.016 mol) of monolaurin (m.p. 62~63°C)[10] and 1.5 g. of pyridine in 15 cc. of chloroform was treated, under cooling, with 2.5 g. (0.022 mol) of monochloroacetyl chloride and the resulting reaction mixture was worked up as described previously. The product was taken up in ether, the solvent removed, and the residue subjected to high vacuum distillation.

Compound 1-dichloroacetyl-3-lauroyl glycerol (XIII) was prepared in the similar manner.

1, 3-Dilaurin.—Upon treatment of compound 2-dichloroacetamido-1, 3-dilauroyloxypropane with phosphorus pentachloride followed by nitrous acid, as described for the 1-compound, 1, 3-dilauryl glycerol, m. p. 56~57°C. was obtained. This product showed no depression of its melting point when mixed with the sample (m. p. 56~57°C.) prepared according to the method of Daubert[11] (reported m. p. 58°C.). The hydrolysis of 2-dichloroacetamido-1, 3-dilauroyloxypropane with 0.1 N NaOH gave quantitative recovery of lauric acid.

* Palmitic and stearic acids used were c. p. grades obtained from the "Delta Chemical Works", m. p. 61-62°C and 68-69°C, respectively.

Summary

Derivatives of 1-aminopropanediol, 2-aminopropanediol and the halogenated acyl esters of glycerol have been prepared. The amino group has been acylated with haloalkylacyl group and one or both hydroxyl groups with aliphatic acids of various chain lengths. Preliminary experimental results have shown that these compounds exhibit bacteriostatic activity in vitro against mycobacterium tuberculosis, avian. The chemical constitution of the isomeric products, the 1-amino and 2-amino derivatives, has been confirmed. The preparation of the optical active forms of the aminopropanediols are now in progress.

Osaka City University, Department of Home Economics, Osaka

(11) B. F. Daubert, *J. Am. Chem. Soc.*, **66**, 289 (1944).

LETTER

Diallylsilanediol, $(CH_2=CH-CH_2)_2Si(OH)_2$

Rokuro ŌKAWARA, Kōhei HASHITANI and Takeo WATASE

(Received April 25, 1953)

Organosilanediol is an interesting compound in the study of silicones. While saturated silanediols have been described in various papers, unsaturated silanediols have not been previously reported. Recently Frish, Goodwin and Scott[1] prepared a series of organosilanediols which have one unsaturated and one saturated hydrocarbon radical on the same silicon atom. But the one which has two unsaturated hydrocarbon radicals on the same silicon atom has not been prepared. We wish now to report on diallylsilanediol which has been prepared directly from diallyldichlorosilane with a similar principle as that of Lucas and Martin.[2]

In a three-necked 2 l.-flask, an efficient stirrer and two dropping funnels were inserted in each neck. As a hydrolyzing mixture, saturated sodium chloride solution (270 g.) with an excess of solid sodium chloride and ethyl ether (400 cc.) were used. Redistilled (30 g.) diallyldichlorosilane (*Anal.* Cl: Calcd. 39.2,

(1) K. C. Frisch, P. A. Goodwin and R. E. Scott, *J. Am. Chem. Soc.*, **74**, 4584 (1952).

(2) G. R. Lucas and R. W. Martin, *J. Am. Chem. Soc.*, **74**, 5225 (1952).

Found 39.3) prepared by the direct method was diluted with ethyl ether (200 cc.) and 1 N-sodium hydroxide solution were placed in each dropping funnel. By using methyl orange as indicator the two solutions were added differentially to the hydrolyzing mixture with vigorous stirring. During the course of addition the temperature of the mixture was kept below 4°C. and the color change of methyl orange was carefully controlled between slight red and orange, because *p*H of the mixture has a great influence on the yield. Sodium chloride was added at a time when the solid disappeared from the hydrolyzing mixture.

After the addition, the ether layer was separated and completely dehydrated on sodium sulfate. Then ether was distilled off on a water-bath below 40°C., or better aspirated off. The product, oily matter and crystalline solid were washed with a little quantity of petroleum ether (yield 21 g., 87% of the theory). A sample for analysis was recrystallized from ethyl ether, m. p. 81°C., d^{10} 1.105. *Anal.* Calcd. for $C_6H_{12}O_2Si$ (144.2): C, 50.09; H, 8.57; Si, 19.38; hydroxyl, 23.9%. Found: C, 49.96; H, 8.39; Si, 19.44; mol. wt. 147 (in dioxane), 144.9 (from X-ray analysis); hydroxyl (Karl Fischer) 22.5%. Iodine value I_0: Calcd. 352, Found 355.*

Details on the preparation and properties of this compound will be reported later.

We thank Mr. M. Kakudo for the X-ray analysis and Takeda Yakuhin Kōgyō Laboratory for the determination of carbon and hydrogen.

Department of Applied Chemistry, Faculty of Engineering, Osaka University, Osaka

* The high iodine values (I_e) proportional to the excessa mount (e) of Wijs reagent were observed. The value I_0 was obtained from the several I_e values by extrapolating graphically when $e \to 0$.

The Formation of Cycloöctatetraene in the Thermal Polymerization of Acetylene

By Zenichiro KURI

(Received April 28, 1953)

The success of the detection of cycloöctatetraene (C. O. T.) in the photopolymerization products of acetylene and a theory on the mechanism of its formation have already been reported.[1] Extending this to the thermal polymerization, the author found C. O. T. here also in the products. Reppe,[2] too, supposed that it might exist in the thermal polymerization products, but he failed to demonstrate it.

The apparatus, the analysis of C. O. T., and others were the same as in the former experiment, except that an electric furnace (12 cm. in length) was used in place of a mercury lamp. The linear flow rate of acetylene through the reaction tube was maintained at 2.6 cm. /

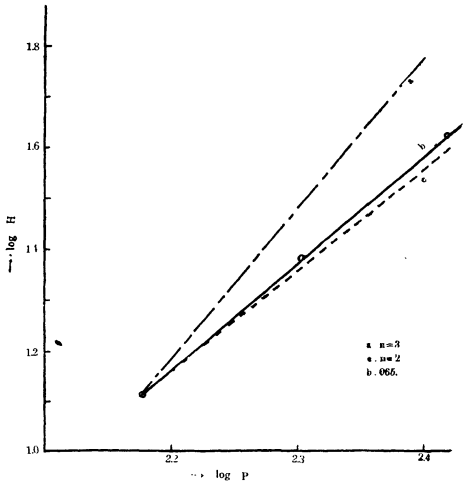

Fig. 1.—H: Rate of formation of C·O·T.
P: Pressure of acetylene.

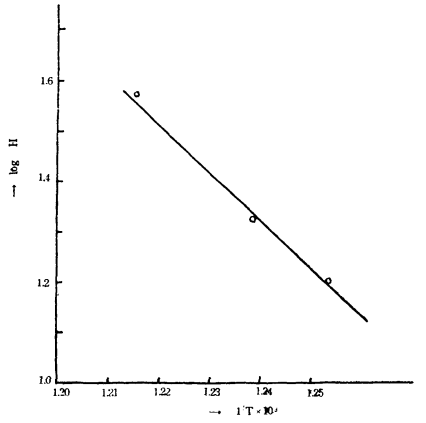

Fig. 2.—H: Rate of formation of C·O·T.
1/T: Reciprocal of the temperature °K.

(1) Z. Kuri and S. Shida, This Bulletin, **25**, 116(1952).
(2) J. W. Reppe, Acetylene Chemistry (P. B. Report 18852-s) p. 151 (1945).

sec. (A) The pressure was changed from 150 to 250 mm. Hg. The temperature was kept constant at 550°C. Fig. 1 shows the logarithm of the rate of C. O. T. formation (expressed in the height, mm, of the polarographic diffusion current) vs. the logarithm of pressure of acetylene, where $n=2$ and $n=3$ means the second and the third order reaction, respectively, in respect to acetylene. The slope indicates the reaction to be practically of the second order. (B) The temperature was changed from 525° to 550°C. The pressure of acetylene was kept constant at 250 mm.Hg. Fig. 2 shows the logarithm of the rate of C. O. T. formation vs. the reciprocal of the temperature. From the slope one gets the activation energy of C. O. T. formation, 44.3 Kcal. Details of the experiment and the reaction mechanism will be published later. The author is grateful to Dr. S. Shida for his helpful discussion.

Laboratory of Physical Chemistry,
Tokyo Institute of Technology.
Ookayama, Meguro-ku, Tokyo

Electrostatic Lattice Energy of $PbSO_4$, $BaSO_4$, $SrSO_4$ and $CaSO_4$[1]

By Yosio SAKAMOTO

(Received March 1, 1952)

§ 1. Lattice-Energy Problem on the Complex Ionic Crystal

The lattice energy of ionic crystals of simple composition and structure has been studied fairly completely, though this subject still leaves room for more thorough consideration at least in some particular aspects, for instance, in the strict application of thermodynamics. On the contrary, few researches have been made into ionic crystals of so complex a structure that the degree of their symmetry is small or their atoms form into partial groupings. One of the chief purposes of the author is to study these complex ionic crystals, especially to elucidate[2] physicochemical properties of radical ions, the properties not a few of which (e. g., the energies fo hydration) have remained quite obscure.

Among the ionic crystals whose lattice energies have so far been evaluated by means of computing lattice sums,[3] those which belong to the rhombic system have the smallest degree of symmetry. No more than two studies[4][5] have been made on these rhombic crystals, which, moreover, contain radical ions. In the one case,[4] however, the treatment seems to be unsatisfactory, and in the latter[5] the spatial arrangement of the ions is orderly enough.

On the other hand, the ionic arrangement in the rhombic crystals of lead sulfate, in which Dr. Kobayashi[2] was interested, and of the alkaline earth sulfates is relatively irregular and complex. So, first, for the rectangular crystal lattice of any complexity a set of expressions of Madelung's coefficient[6] is derived, and then verified in two simple cases by means of numerical application. The mode of calculation based on this set of expressions will produce effectually an exact and precise result with minimum effort, even for the cases considerably complicated.

§ 2. A Set of Expressions for the Calculation of Madelung's Coefficient M_d

2.1) The crystal lattice in general.[7]—The electrostatic potential energy per mol., Φ_1, of a crystal lattice is expressed by

$$\Phi_1 = -Ne^2 M_d / d \tag{1}$$

where d is a quantity proportional to length, and M_d Madelung's coefficient[6] referred to d. M_d may be represented, through Ewald's method,[8] by a set of expressions suitable for the calculation of its value, thus:

$$M_d = -\{(d/\delta)^3 L/\pi + \bar{Y} + Y/s - \varepsilon d/\sqrt{\pi}\}\sum_h z_h^2;$$

$$L = \mathrm{S}'_{\bar{l}} w_l L_l,\ L_l = e^{-\kappa\lambda_l}/\lambda_l,\ \kappa = (\pi/\varepsilon d)^2,$$

$$\lambda_1 = |\vec{q}^1 d/2\pi|^2,\ w_l = 1 + (2/s)X_l,$$

$$X_l = (\nu/\sum_h z_h^2)\sum'_{(kk')} z_k z_{k'} \cos(\vec{q}^l \vec{r}_{kk'});$$

$$\bar{Y} = \mathrm{S}'_{\bar{l}} \bar{Y}_l,\ \bar{Y}_l = G(\varepsilon d\bar{\eta}_l)/\bar{\eta}_l,\ \bar{\eta} = |\vec{r}^{\,l}|/d;$$

$$Y = (\nu/\sum_h z_h^2)\mathrm{S}_l \sum'_{(kk')} z_k z_{k'} Y^l_{kk'},$$

$$Y^l_{kk'} = G(\varepsilon d\eta^l_{kk'})/\eta^l_{kk'},\ \eta^l_{kk'} = |\vec{r}^{\,l}_{kk'}|/d;$$

$$s = \sum_k 1 = \sigma\sum_h 1 = \sigma\nu,\ h = 1, 2, \cdots\cdots \nu;$$

$$\bar{l} = (\bar{l}_1, \bar{l}_2, \bar{l}_3),\ \bar{l}_i = -l_i;$$

$$i = 1, 2, 3; \tag{2}$$

(1) (a) "Lattice Energy of $PbSO_4$, $BaSO_4$, $SrSO_4$ and $CaSO_4$." Unpublished thesis, Hirosima Univ., 1942; revised and enlarged, 1946—51, ("Physical Chemistry of a Radical Ion SO_4--,") Jan. 1951—; (b) "Lattice Energy..... I. Electrostatic Potential Energy." Oral report, *Nippon-Buturi-Gakkai.St* **4**, 64 (1949).

(2) This intention was suggested to me in 1942 by the late Prof. Yōzo Kobayashi (1895—1945).

(3) In regard to ionic crystals with radical ions several reports have been issued since 1926 on the (electrostatic) lattice energy whose values were obtained by means of computing lattice sums; these radical ions are: CO_3--, NO_3-, BO_3---, HF_2-, N_3-, BF_4-, NH_4+, $CN-$, $OH-$, $SH-$, $SeH-$, C_2--, O_2-, and O_3-. On the other hand, Kapustinskiĭ (1933, 1943) offered a general expression that gives, without performance of lattice summations, a rough value of the lattice energy, and for radical ions it has been utilized since 1935 by several Soviet investigators; above all, extensively by Yatsimirskiĭ since 1947.

(4) B. Y. Oke: (a) *Proc. Indian Acad. Sci.*, **4A**, 1 (1936); (b) ibid., **5A**, 326 (1937).

(5) T. Matsuhara [-bara] and T. Nagamiya, *Sci. Papers Osaka Univ.*, No. 14, pp. 17 (1949).

(6) As for a crystal with the structure of small degree of symmetry the constancy of the so-called Madelung's constant is not perfect; accordingly, it might be proper to adopt the term "coefficient" (or "factor") in general as a substitute for the term "constant."

(7) Cf.: M. Born, "Atomtheorie des festen Zustandes," 1923, from which are taken several symbols used here: δ, a_i, s, $\vec{r}^{\,l}_{kk'}$ etc., l_i etc., S, Σ, S' etc., $\vec{q}^{\,l}$, — on Y, ε, and $G(x)$. Notice: C. N. Wall, *Phys. Rev.*, **36**, 1243 (1930); R. H. Canfield, ibid., **40**, 1034(1932); W. J. Taylor, *idid.*, **77**, 763 (1950); G. Molière, *Z. Krist.*, **101**, 383 (1939).

(8) P. P. Ewald, *Ann. Physik*, [4] **64**, 253 (1921).

where h ("intramolecular index") and ν correspond to k and s, resp., σ is the number of the "molecules" in a cell, z_h the valency of an ion as particle h, and S with $\bar{l}$ and $\sum$ with (kk') denote such a summation that a pair of indices l & $\bar{l}$ and a pair of permutations of indices kk' & $k'k$, resp., be counted once only.

In the case of a z-z-valent compound it is suitable for comparison to introduce a derived quantity M_a/z^2. The linear size, χ, of a molecule may be defined by

$$\chi=(V/N)^{1/3}=\delta/\sigma^{1/3} \tag{3}$$

where V is the molal volume; and the adoption of M_χ as M_a is also valuable in some cases.

2.2) The rectangular crystal lattice.—The preceding set of expressions of M_a may be specified so as to fit to the rectangular crystal lattice in the following form:

$$\delta^3=\prod_i a_i;\quad L=\frac{1}{2}\mathrm{S}'_{\mathring{l}}c_l L_l+(2/s)\,\mathrm{S}'_{\bar{l}}X_l L_l,$$

$$\lambda_l=(d/a_1)^2\sum_i (a_1/a_i)^2 l_i^2,$$

$$X_l=(\nu/\sum_h z_h^2)\sum'_{(kk')} z_k z_{k'}\cos 2\pi\sum_i (k_i-k_i')l_i;$$

$$\bar{Y}=\frac{1}{2}\mathrm{S}'_{\mathring{l}}c_l\bar{Y},\quad \bar{\eta}=(a_1/d)\{\sum_i (a_i/a_1)^2 l_i^2\}^{\frac{1}{2}};$$

$$\overset{\mathring{l}}{\eta}_{kk'}=(a_1/d)\{\sum_i (a_i/a_1)^2(k_i-k_i'+l_i)^2\}^{\frac{1}{2}};$$

$$\mathring{l}=(\mathring{l}_1,\ \mathring{l}_2,\ \mathring{l}_3),\ \mathring{l}_i=|\,l_i\,|\,;$$

$$c_l=2^\mu,\ \mu=0,\ 1,\ 2,\ 3; \tag{4}$$

where S with $\mathring{l}$ denotes such a summation that a set of like cells with one and the same value of $\mathring{l}$ be counted once only, c_l is the number of these like cells in a set, and μ the number of the non-zero components of $\mathring{l}$.

In case that X_l depends solely on the absolute values (regardless of the signs) of the components of l, i. e.,

$$X_l=X_l(\mathring{l}) \tag{5}$$

further simplification may be brought about, thus

$$L=\frac{1}{2}\mathrm{S}'_{\mathring{l}}c_l w_l L_l \tag{6}$$

In § 3.2 and 4 the numerical calculation of $M_\delta(=Ma_1\delta/a_1)$ is made in the two selected cases:

$$\text{(1)}\quad \varepsilon=\varepsilon^0=\pi/d \qquad \text{(2)}\quad \varepsilon=\varepsilon'=\pi/d\sqrt{2}$$
$$\text{with } d=a_1 \text{ (but finally } d=\delta) \tag{7}$$

§ 3. Verification of the Expressions of M_δ

3.1) The cubic case NaCl.[9a]—After the expressions of M_δ for the cubic crystal lattice had been derived from those given in § 2, they were applied to the case of NaCl, the numerical calculations with the three selected values of ε producing for M_δ the values $3.495129189266_{48\pm17}$, $\cdots\underline{6}3_{24\pm48}$, and $\cdots\underline{6}3643_{25\pm17}$ molec^{-1}. cell$^{-1/3}$. These values coincide not only with each other perfectly but also with Emersleben's corresponding one practically. This fact seems to support the reliability of all the above-mentioned expressions for M_a or M_δ and of the mode of handling them.

3.2) The rhombic case $CaCO_3$.[9b]—The expressions of M_δ given in § 2 were applied to the rhombic case of $CaCO_3$, and the numerical calculations (cf. Eq. 7), being carried out by use of the same data for the crystal structure as used by Oke[4] but in a fashion somewhat different from his, produced for M_δ the values 12.84723_9 and $\cdots 3_3$ molec^{-1}. cell$^{-1/3}$. The fact that they perfectly coincide will be satisfactory. While, on the other hand, the agreement between each of them and Oke's corresponding one is not satisfactory, since there is a discrepancy of 11% between them. This poor agreement, however, was found[9c] to be caused by the inaccurateness in the value of Oke.

§ 4. Calculation[10] of Madelung's Coefficient M_δ

With the two applications in § 3 as preliminary, the set of expressions of M_δ is now applied to the crystals of the four sulfates in which the author has become interested. These four cases shown in the title are designated by a', a'', a''', and b, resp.

4.1) Data for the crystal structure[11][12]—

State: 0—30° C, 1 atm. Rhombic; a: $BaSO_4$ type, b: $CaSO_4$ type; $\sigma=4$ molec. cell^{-1};
$\nu=2$ part. molec^{-1}—$Me^{++}+SO_4^{--}$[13] (8)

In Case a, an approximate fraction is selected for the value of each parameter, and the adopted values are:[14]

$$v\approx\frac{24}{72},\quad u\approx\frac{23}{72},\quad v'\approx\frac{50}{72},\quad u'\approx\frac{68}{72} \tag{9a}$$

(9) For details, see the three papers (a, b, and c) in *J. Sci. Hiroshima Univ.*, Ser. A, **16**, No. 3 (1953), where (a) Emersleben's and (c) Oke's works are touched upon with comment.

(10) For details, see *J. Sci. Hiroshima Univ*, Ser. A, **16**, No. 3 (1953).

(11) Mainly, R. W. G. Wyckoff: (a) "The Structure of Crystals," 2. ed., 1931—see also (b) "Crystal Structures," Vol. II, 1951.

(12) The values of $a:b:c$ are taken from: "J. D. Dana: The System of Mineralogy," 6th ed., 1915. For its 7th ed., Vol. II, 1951, see Note 4b of Ref. 10.

(13) Here, the electricity is assumed to be located at the center of SO_4^{--} (i. e., of its S) as well as of Me^{++} as a point charge.

(14) The magnitudes of the error thereby caused are: -42, 36, -3, 14; -55, 14, -3 124; and -55, -14, -3, 14 (resp.)$\times 10^{-4}$. If we adopt $u'\gtrsim 67/72$ instead, each last number becomes -124, -14, or -124, resp.

Table 1

i							1, +2								2, −2
ii	1				2			3			4				5—8
iiia	$\frac{1}{4}$,	v,	u		$\frac{3}{4}$,	$-v$,	$-u$	$\frac{1}{4}$,	$\frac{1}{2}-v$,	$\frac{1}{2}+u$	$\frac{3}{4}$,	$\frac{1}{2}+v$,	$\frac{1}{2}-u$		(v', u')
iiib	u,	$\frac{1}{4}$,	0		$-u$,	$\frac{3}{4}$,	0	$\frac{1}{2}+u$,	$\frac{1}{4}$,	$\frac{1}{2}$	$\frac{1}{2}-u$,	$\frac{3}{4}$,	$\frac{1}{2}$		(u')
Case	a′				a″			a‴						b	
iv	1:1.28939:1.57032				1:1.31359:1.63040			1:1.28005:1.55790						0.89325:1:1.0008	
v	0.33_{75}	0.69_{47}			0.33_{88}	0.69_{47}		0.33_{88}	0.69_{47}					0.65	0.15
	0.31_{58}	0.94_{50}			0.31_{80}	0.93_{20}		0.32_{08}	0.94_{30}						

i: h, z_h. ii: k. iii: Atomic positions. iv: $a_1:a_2:a_3$ (a:) $=b^*:c^*:a^*=b:c:2a$ or (b:) $=a^*:b^*:c^*=a:b:c$, where a^*, b^*, c^* are the (röntgenoscopical) lattice constants and $a:b:c$ is the (morphometrical) axial ratio. v: Parameters (a:) $\begin{matrix}vv'\\uu'\end{matrix}$ or (b:) uu'.

In Case b, without artificial approximation,

$$u=\frac{13}{20},\quad u'=\frac{3}{20} \tag{9b}$$

4.2) Calculated values of M_δ (to be amended in § 6).—Each couple (cf. Eq. 7) of numerical values for M_δ obtained by calculation is given in Table 2. The coincidence between them seems

Table 2

M_δ	$PbSO_4$	$BaSO_4$	$SrSO_4$	$CaSO_4$
Case 1	13.16377_3	13.18779_4	13.15651_2	13.50363_5
〃 2	$\ldots75_8$	$\ldots78_5$	$\ldots51_0$	$\ldots62_7$

so perfect that they conform to the verification of accounts in Ewald's method. Every one of these four values might be acceptable, from the standpoint assumed in the author's other paper,[15] as of reasonable magnitude.

§ 5. Estimation of the Uncertainty in the Calculated Value of M_δ

5.1) General remark.—The error with which the value of M_δ calculated in this mode is expected to be accompanied may be analyzed—as mentioned in Ref. 9b, § 2.3—into three sorts of errors, which are to be discussed in some detail.

5.2) The error from computation.—The main error (i) of computation comes from that reduction of the decimal to its approximate fraction which is done in Eq. 9a concerning the parameters of atomic positions. A rough value for it has been merely indirectly estimated to be 0.2%.[16] On the other hand, the ordinary computational error (ii) must be only subordinate, because the two calculated values for M_δ coincide to the extent of 10^{-4}%.

5.3) The error from theory.—Several assumptions underlying the method of this calculation are to be mentioned here. The matters concerning the grain size, the imperfection of a crystal (such as the mosaic structure and the lattice defect), and the thermal motion of the constituent particles may be insignificant in ordinary cases; the question of chemical purity of the material will rather be regarded as a matter of experiment.

On the other hand, several difficulties are encountered when we consider the following aspects peculiar to our subject. The character of the bonds between ions in these crystals is—though mainly ionic—in a fair measure, covalent owing to the small degree of symmetry in the crystal structure and of uniformity in the ionic distribution, not a little polarizability of the radical (sulfate) ion in particular, the bivalency of the ions, and the great polarizing influence by lead ion and that by calcium ion. Yet, this crystal system retains rectangular symmetry, the distribution of the neighboring anions around a cation (or the reverse) is passably uniform and the coordination number[17] of an ion is no less than some value between 5 and 7, the deformability of sulfate ion is by no means great,[18] and the shape of sulfate ion is of regular tetrahedron, though slightly distorted. Consequently, the assumption[13] made about the distribution of electric charges, i. e., the purely ionic bonding between point charges (with certain integral multiples of the electric elementary quantum) at the assigned sites, will be practically not far from reality. Furthermore, it is to be noticed that the electrostatic potential energy of a crystal lattice may be regarded as a quantity *defined*, in a

(15) Ref. 9c, Art. V.

(16) In Case b, which is free from this error and in which the crystal structure bears a close resemblance to that in Case a, another calculation has been executed with the values $u-\frac{1}{2}=u'=0.1$ (besides, 0, 0.05, 0.2, and 0.25), producing for M_δ the numerical value 12.9941_1. Certain considerations have then been made with such materials as Eq. 9b, Note 14, and Table 7 of Ref. 10 (including the sub-table for $CaSO_4$ with $u'=0.1$) and with a certain possible supplementary assumption.

(17) In these crystals we cannot definitely assign to this quantity any discrete number. Cf. Table 6 of Ref. 10, where γ_p is proportional to the interionic distance and (a) the five or (b) the three $-\frac{1}{2}d_{kk'p}$'s are, so to speak, the "components" of the coordination number.

(18) "[Geiger-Scheel.] Handbuch der Physik," Bd. XXIV/2 (2. Aufl.), 1933, Kap. 6 (by H. G. Grimm and H. Wolff), Ziffn. 61, 64—66, esp. Tab. 62.

certain sense (so far as the present state of our knowledge is concerned), on the basis of an assumption such as mentioned above, the possibility[19] of the subsequent step to approximation being left to a later estimation of the whole potential energy (or, further, the total energy in the thermodynamic signification).

The magnitude of the error originating from theory is, accordingly, somewhat indefinite, and so it is difficult to be estimated; still the author will give it a value 0.5%, if necessary.

5.4) The error from experiment.—M_δ depends upon the axial ratio ($a:b:c$) and the parameters of atomic positions (briefly, parameters). These quantities vary with temperature and pressure and, from a practical viewpoint, with chemical purity (and certain physical matters mentioned in Art. 3). The error due to these variations and that due to measurement constitute together the total experimental error.

In regard to variation in the magnitudes of the parameters we have as yet no information, while the magnitudes of the variabilities of $a:b:c$ are known for some of these crystals and are shown in Table 3.[20]~[25] It will be seen from this table that any datum with such specification as "at some ordinary temperature and pressure" suffices for our present purpose and, at the same time, that the experimental error in $a:b:c$ of No. 1 is less than 0.3%. The effect of uncertainty in $a:b:c$ upon M_δ is not simple in nature and might scarcely be estimated exactly unless we execute several sets of calculations. Nevertheless, the author will try to form a very rough estimate of it.

Table 3

No.	a′	b
1	0.78516:1:1.28939	0.89325:1:1.0008
2	0.7852 (−62°) 1.2891	0.8911 (−64°) 0.9996
3	0.7894 (514°) 1.2870	0.8996 (500°) 1.0025
4	7.3 −3.6	15.1 5.5
	a″	a‴
1	0.81520:1:1.31359	0.77895:1:1.28005
2	0.8161 (−60°) 1.3121	0.7785 (−62°) 1.2821
3	0.8124 (570°) 7.3047	0.7794 (550°) 1.2780
4	−5.9 −11.7	1.5 −6.7
5	1.431 2.252 1.490†	1.920 1.851 1.490
6	−6.7 −10.0	0.54 −6.4
7	5.221 6.757 5.194	6.222 4.406 4.462
8	1.25 2.05	−1.41 −0.072
9	$0.81\frac{6}{2}:1:1.31\frac{5}{0}$	$0.7\frac{9717}{6964}:1:1.\frac{30010}{25506}$
10	0.8146 :1:1.3119	0.78093:1:1.28324††
11	0.81439:1:1.31223	——

1: Axial ratio (a. r.) adopted in Table 1. 2, 3: A. r. at the temp. indicated. 4, 6: Mean increments per deg. in a. r., in 10^{-6} deg.$^{-1}$. 5: Coeffs. of linear thermal expansion at 0—100° C, in 10^{-5} deg^{-1}. 7: Linear compressibilities at 23—26° C, 0 atm., in 10^{-7} bar^{-1}. 8: Increments per bar in a. r., in 10^{-7} bar^{-1}. 9: A.-r. of various minerals. 10: A. r. of a pure mineral. 11: A. r. from a^*, b^*, c^* adopted by Wyckoff. † For the new data, see S. S. Sharma, *Proc. Indian Acad. Sci.*, **33A**, 283 (1951). †† See also Note 4b of Ref. 10.

Now the three crystals of the barite type have been considered, in Eq. 9a, to have the same value for each parameter, and so the distinction between these crystals will remain solely in $a:b:c$. These calculations may, therefore, be regarded as having been made on such a crystal of one and the same compound as with three different experimental values for $a:b:c$. There is then constructed a table (Table 4a) that shows the relation between M_δ and $a:b:c$. It is seen from this table that, for this special case (in which a/b and c/b alter alike in both magnitude and sign), the quotient $2M_\delta/\{(b/a)\Delta(a/b)+(b/c)\Delta(c/b)\}$ is at most *ca.* 0.07.[24]

Table 4a

No.	(1)	(2)	(3)	(4)	(5)	(6)	(7)	(8)
$BaSO_4$ ···					···			
B—P	300, 242	376, 186	281			240	18.2	0.065
$PbSO_4$ ···					···			
P—S	62, 93	80, 73	76			73	5.5	0.072
$SrSO_4$ ···					···			

1: A. r. in Table 3, No. 1. 2: Differences in a. r. between the crystals, as indicated by B—P or P—S. 3: Quotients (2)÷(1). 4: Arithmetical mean of the quotients in (3). 5: M_δ in Table 2. 6: Difference in M_δ similar to (2). 7: Quotient (6)÷(5). 8: Quotient (7)÷(4). In Nos. 2-4, 6, and 7 the unit is 10^{-4}.

(19) E. g., the mode of treatment in Ref. 5.

(20) Nos. 2, 3. R. Kolb's, through *Chem. Zentr.*, **1911**, I, 1317.

(21) Nos. 5, 9, 10. "Gmelins Handbuch," 8. Aufl. The values for a^*, b^*, c^* recommended in this book give 0.81342 : 1 : 1.31066.

(22) No. 7. Values calculated by the present author from: P. W. Bridgman, *Proc. Am. Acad. Arts Sci.*, **77**, 187 (1949).

(23) No. 11. Ref. 11b. In this book Walton and Walden's work is cited; their values for a^*, b^*, c^* of a pure artificial crystal at 24—30°C give 0.81326 : 1 : 1.31124.

(24) In a preliminary calculation (Case α) I adopted for $a:b:c$ the values derived from those of the lattice constants quoted in Ref. 11a. The values (Case α) that correspond to those (Case β) in Table 4a are: No. 1—0.816630 : 1 : 1.316079, 0.785316 : 1 : 1.288104, 0.779851 : 1 : 1.276119; No. 5—13.188_2, 13.163_7, 13.157_2; No. 8—0.063, 0.061; and for $CaSO_4$ No. 1—0.893525 : 1 : 1.001439; No. 5—13.50251. If we construct a table which is similar to Table 4a and in which a combination $\beta\alpha$ is taken for each crystal, the values corresponding to those in Table 4a, No. 8, in the order of B, P, S, and C, are: 0.049, -0.00_6, −0.059, and −0.175. If such a weighted mean as $\{10(b/a)\Delta(a/b)+(b/c)\Delta(c/b)\}/11$ is taken instead of the arithmetical mean in No. 4, the above-mentioned eight values for No. 8 become: 51, 70; 51, 69; 50, 02±20, 74, and −246 (resp.) $\times 10^{-3}$. After such complementary considerations it will be found admissible to adopt the magnitude *ca.* 0.07 for Case a or α. −0.2 for Case b.

After all, the error (i) in M_δ due to uncertainty in $a:b:c$ will not exceed $(0.3\% \times 0.07 \approx)$ 0.02% in Case a, while in Case b,[24] possibly, 0.05%. On the other hand, the error (ii) due to uncertainty in the parameters does not, presumably, differ much from the amount 0.2% mentioned in Art. 2 in Case a, and in Case b this error is estimated[25] to be *ca.* 0.4%.

§ 6. Values of M_δ with Their Probable Errors

The purity of the materials whose values of the axial ratio are adopted in these calculations (§ 4) is unknown to the present author. With respect to $BaSO_4$ and $SrSO_4$, however, certain reported values are for chemically pure crystals or are designated as recommended ones.[26] They are now adopted and the values of M_δ in Table 2 are amended by utilizing the consideration made in § 5.4. In Table 5 each final value of M_δ is given, to which both its probable error, estimated[27] in § 5, and its corresponding axial ratio

Table 5

Madelung's Coefficients (M_δ) of the Sulfates at 0—30°C

(δ: Mean lattice constant. Unit: $molec^{-1}.cell^{-1/3}$)

	$PbSO_4$	$BaSO_4$
M_δ	13.164±0.7%	13.187±0.7%
$a:b:c$	$0.78_{52}:1:1.28_{94}$	0.814:1:1.312
	$SrSO_4$	$CaSO_4$
M_δ	13.159±0.7%	13.504±0.9%
$a:b:c$	$0.78_{69}:1:1.28_{32}$	$0.89_{32}:1:1.00_{08}$

are appended. The corresponding values of M_χ/z^2 are: 2.0_{73}, 2.0_{77}, 2.0_{72}, and 2.1_{27} (resp.) $molec^{-4/3}$.-$valency^{-2}$.

§ 7. Rates of Variation in M_δ with Temperature and Pressure

By utilizing the consideration made in § 5.4 a rough estimation of the variability of (viz. the rate of variation in) M_δ with temperature or pressure has been made,[28] producing the results: $-(\partial M_\delta/\partial T)_P{}^*/M_\delta$, in $10^{-7}\,deg^{-1}$: 5, −4 or −4,[29] 0.9 or 0.1, and −20; $(\partial M_\delta/\partial P)_T{}^*/M_\delta$, in 10^{-9}-bar^{-1}: —, 8, −7, and —; for Cases a′, ...b, resp.; where * means that the parameters of atomic positions are assumed to be kept constant. Thence it is seen that the (absolute) magnitudes of these two quantities are 10^{-2} of those of the mean linear thermal expansibility and of the mean linear compressibility, respectively.

§ 8. Values of the Electrostatic Lattice Energy Φ_1

The molal electrostatic potential energy, Φ_1, of a crystal lattice may be computed by use of Eq. 1 with $d=\delta$; while (cf. Eqs. 3, 4)

$$\delta^3 = a_1 a_2 a_3 = \sigma V/N = \sigma M/\rho N \qquad (10)$$

where M is the gram-formula mass and ρ the density. The values of Φ_1 thus computed[30] are shown in Table 6.[31] Every one of them is accurate to *ca.* 1%, but the relative error, viz. the

Table 6

Electrostatic Lattice Energies (Φ_1) of the Sulfates, with their corresponding quantities of ρ and δ, at 25° C

		$PbSO_4$	$BaSO_4$
i	ρ	6.37±0.02	4.49±0.01
ii	δ	6.812±0.007	7.015±0.005
iii	$-\Phi_1$	641.6±5.1	624.1±4.8
		$SrSO_4$	$CaSO_4$
i	ρ	3.97±0.01	2.98±0.02
ii	δ	6.748±0.006	6.719±0.015
iii	$-\Phi_1$	647.5±5.1	667.3±7.5

Unit. i: $g.\,cm^{-3}$ ii: $Å.\,cell^{-1/3}$
iii: $kcal.\,mol^{-1}$

error in each difference between them, may probably be much less than (possibly, *ca.* 1/6 of) the corresponding sum of their independent errors. (This statement is valid also for M_δ in § 6.)

The rate of variation in Φ_1 with temperature or pressure will be approximately equal to the minus mean linear thermal expansibility or the mean linear compressibility, resp., if we refer to § 7 and assume that the corresponding rate of variation in M_δ due to the parameters of atomic positions may be small enough.

Summary

A plan for investigation of the physical chemistry of radical ions is stated with especial reference to the strict treatment of the lattice-energy problem and the treatment of complex ionic crystals. First, the expressions suitable for the practical numerical calculation of

(25) The experimental error in u or u_I being supposed to be 0.005, an interpolation is made between the values 13.50 and 12.99—refer to Note 16 and Tables 1 (v) and 2.

(26) Cf. Table 3 (Nos. 10, 11) and Notes 21, 23.

(27) In Case a the errors 2-i and 4-ii are counted once collectively.

(28) The materials in Tables 3 (Nos. 2—8) and 4a (No. 8) and in Note 24 have been used.

(29) A set of the data in Ref. † of Table 3 leads to −5 for both 25° and 0—100° C.

(30) The values adopted are: M's, and N, e, and cal in *J. Am. Chem. Soc.*, **74**, 2447, 2699 (1952); σ in Eq. 8; and ρ's selected from various sources, esp. from Liter. 4b of Ref. 10.

(31) The corresponding values of the lattice constants a^*, b^*, c^*, in kx. $cell^{-1/3}$, computed by use of the values of $a:b:c$ in Table 5 and of λ_g/λ_s (1.00202 kx. $Å^{-1}$), are: 8.439, 5.374, 6.929; 8.850, 5.436, 7.132; 8.342, 5.341, 6.854; and 6.218, 6.961, 6.967; resp.

Madelung's coefficient of the general and the rectangular crystal lattice are derived from Ewald's original general expressions. Next, they are verified in the two simple cases, NaCl and the rhombic $CaCO_3$, by means of numerical application. Then, they are applied to the more complex cases, i. e., the rhombic crystals of $PbSO_4$, $BaSO_4$, $SrSO_4$, and $CaSO_4$, with SO_4^{--} which is assumed to be a point charge. The degree of accuracy of the calculated values is further discussed; and, in connection with it, an attempt is made to estimate the extent of variability of Madelung's "coefficient" (or "constant," as it is called). Finally, the electrostatic lattice energy is evaluated.

I express my sincere thanks to the late Dr. Y. Kobayashi, who introduced me to this problem. I am grateful to Professor Tamamushi for his encouragement and kindness in reading my original manuscript. I am also indebted to Assist. Prof. M. Miura, who has afforded facilities for continuing my work, and to Assist. Prof. E. Hirahara for his valuable advice.

Department of Chemistry, Hirosima University of Literature and Science, Hirosima

The Separation of Isotopes by Countercurrent Gaseous Exchange Column. I. Transport Equation and Over-All Separation

By Kunihiko KIGOSHI

(Received August 1, 1952)

Introduction

Taylor and others[1][2] have observed a very efficient isotope separation with experiments on the countercurrent gaseous exchange column. Bernstein and Taylor[2] have used a hot wire type thermal diffusion column with a top reservoir filled with carbon dioxide and a bottom reservoir in which a chemical converter reduces carbon dioxide to carbon monoxide. The column consisted of a water-jacketed glass tube 1.0 cm. in diameter and 110 cm. long. When it ran two or three days with hot wire temperature 1150°C., the heavy isotope C^{13} was concentrated 1.5 times to the initial concentration at the bottom reservoir. This over-all separation is much greater than that of ordinary thermal diffusion.

To account for its high efficiency, Bernstein and Taylor[2] have treated the problem with the simplified flow pattern and idealized two cases; diffusion rate limited case and exchange rate limited case. However, the treatment of this problem is so simplified that it cannot explain the mechanism of isotope separation by this column. The exchange reaction between carbon dioxide and monoxide had been studied by Brandner and Urey,[3] and recently Norris and Ruben[4] reexamined this problem. Though their results are not entirely conclusive it may be said that the reaction velocity is very slow at the temperature below 700°K., and at the higher temperature the reaction velocity increases as the ordinary chemical reactions. Since the diffusion rate is proportional to the square of temperature, it may be reasonable to assume that above the certain temperature T_b the reaction is very rapid compared with the diffusion process. At the region where temperature is below T_b the exchange reaction may be considered very slow compared with the diffusion process, therefore we may treat the behavior of heavy isotope C^{13} in carbon dioxide and carbon monoxide separately. In the region where the temperature is higher than T_b, the equilibrium of the isotopic exchange reaction,

$$C^{12}O_2+C^{13}O \rightleftarrows C^{13}O_2+C^{12}O$$

holds with the equilibrium constant $\alpha(T)$ of this temperature. Under these situations the mechanism of the isotope enrichment by countercurrent gaseous exchange column can

(1) T. I. Taylor and R. B. Bernstein, *J. Am. Chem. Soc.*, **69**, 2076 (1947); T. I. Taylor and W. Spindel, *J. Chem. Phys.*, **16**, 635 (1948).

(2) R. B. Bernstein and T. I. Taylor, *J. Chem. Phys.*, **16**, 903 (1948).

(3) J. Brandner and H. C. Urey, ibid., **13**, 351 (1945).

(4) T. H. Norris and S. Ruben, ibid., **18**, 1595 (1950).

be solved using no more serious assumptions and simplified cases.

Descriptions of Experimental Conditions and Notations

Suppose two different gases of species 1 and 2 each has the same element A, and there are two isotopes A^i and A^j. When we write AB for the gas molecule of species 1 and AC for species 2, the chemical exchange reaction,

$$A^iB+A^jC\rightleftarrows A^jB+A^iC \qquad (1)$$

takes place very rapidly compared with the diffusion process at the temperature higher than T_b and slowly enough at the temperature below T_b.

The apparatus is supposed to be an ordinary hot wire type thermal duffusion column, and its dimensions are as follows; r_1, r_2=radius of cooled cylinder and hot wire, Z=length of column, T_1 and T_2 are absolute temperatures of cooled cylinder and hot wire respectively. r and z are radial and vertical (along the column) coordinates; $r_2\leq r\leq r_1$, $0\leq z\leq Z$.

The gas in the apparatus is a mixture of AB and AC. c_1, c_2=fractional molar concentration of species 1(AB) and 2(AC); $c_1+c_2=1$. ν_1, ν_2= fractional molar concentration of isotope A^i of the species 1 and of species 2. ν=fractional molar concentration of isotope A^i as a whole; $\nu=c_1\nu_1+c_2\nu_2$. D_1, D_2=self diffusion coefficient of species 1 and 2. λ=thermal conductivity, η=viscosity, ρ=density of gas mixture. M_1, M_2=molecular weight of AB and AC, $\bar{M}$=mean molecular weight; $\bar{M}=c_1M_1+c_2M_2$.

Isotopic Transport

The consideration about the distribution of different gases in the thermal diffusion column treated here is based on the theory which had been developed by Furry, Jones and Onsager.[5] Suppose species 1 concentrates to the hot part of the column by thermal diffusion, the transport τ_1 (mol./sec.) of species 1 along the column is given by Furry and Jones[6][7] as follows,

$$\bar{M}\tau_1=Hc_1c_2-(K_c+K_d)(dc_1/dz) \qquad (2)$$

where H, K_c and K_d are given by expressions (52), (40) and (47). Regarding the flow of gas, the equation of flux (mol./sec. cm.) of species 1 was given by Furry, Jones and Onsager[5] as follows,

$$\boldsymbol{J}_1=(\rho/\bar{M})[\boldsymbol{v}c_1+D'_1(-\operatorname{grad} c_1+\alpha_t c_1c_2 \operatorname{grad}\ln T)] \qquad (3)$$

and a corresponding equation holds for $\boldsymbol{J}_2$. Where $\boldsymbol{v}$ is velocity vector of convective flow, D'_1 is diffusion coefficient of species 1 in the gas mixture and α_t is thermal diffusion constant for the mixture of two different gases. The isotopic exchange reaction and the separation of isotope in the column are treated here at the situation in which the steady state was attained about the distribution of two gases of species 1 and 2. Then we have

$$\operatorname{div}\boldsymbol{J}_1=\operatorname{div}\boldsymbol{J}_2=0 \qquad (4)$$

Regarding the flow of isotope in the gas of species 1, the equation of flux of A^i is

$$\boldsymbol{I}_1=\nu_1\boldsymbol{J}_1-(\rho D_1c_1/\bar{M})(\operatorname{grad}\nu_1-\alpha_1(1-\nu_1)\nu_1 \operatorname{grad}\ln T) \qquad (5)$$

and the flux of A^i in the gas of species 2 is

$$\boldsymbol{I}_2=\nu_2\boldsymbol{J}_2-(\rho D_2c_2/\bar{M})(\operatorname{grad}\nu_2-\alpha_2(1-\nu_2)\nu_2 \operatorname{grad}\ln T) \qquad (6)$$

where α_1 and α_2 are isotopic thermal diffusion constants for gases of species 1 and 2 respectively. We assume that the time variation of ν_1 and ν_2 at each point in the tube is negligible, i. e. stationary or quasistationary state with respect to the isotopic distribution in the column. This assumption holds not only at the final equilibrium but also during the approach to equilibrium when both reservoirs are sufficiently large. From these conditions we have

$$\operatorname{div}\boldsymbol{I}_1=\operatorname{div}\boldsymbol{I}_2=0 \quad (T<T_b) \qquad (7)$$

at the point where the temperature is below T_b. In the region where the temperature is higher than T_b, the exchange reaction (1) takes place. Then in this region we have only one equation,

$$\operatorname{div}(\boldsymbol{I}_1+\boldsymbol{I}_2)=0 \quad (T\geq T_b) \qquad (8)$$

and in this region ν_1 and ν_2 are related by equilibrium canstant

$$\nu_2/\nu_1=\alpha(T) \quad (T\geq T_b) \qquad (9)$$

The application of equations (5), (6) and (2) on equation (7) gives

(5) W. H. Furry, R. C. Jones and L. Onsager, *Phys. Rev.*, **55**, 1083 (1939).
(6) R. C. Jones and W. H. Furry, *Rev. Mod. Phys.*, **18**, 151 (1946).
(7) W. H. Furry and R. C. Jones, *Phys. Rev.*, **69**, 459 (1946).

$$\boldsymbol{J}_1 \operatorname{grad} \nu_1 - \operatorname{div}(\rho D_1 c_1 \operatorname{grad} \nu_1)/\bar{M}=0 \quad (T<T_b) \tag{10}$$

$$\boldsymbol{J}_2 \operatorname{grad} \nu_2 - \operatorname{div}(\rho D_2 c_2 \operatorname{grad} \nu_2)/\bar{M}=0 \quad (T<T_b) \tag{11}$$

in the same way we have from equations (8) and (9)

$$\boldsymbol{J}_1 \operatorname{grad} \nu_1 + J_2 \operatorname{grad}(\alpha\nu_1) - \operatorname{div}(\rho D_1 c_1 \operatorname{grad} \nu_1 + \rho D_2 c_2 \operatorname{grad}(\alpha\nu_1))/\bar{M}=0 \quad (T\geq T_b) \tag{12}$$

where we neglected the third terms of equations (5) and (6) which are derived from thermal diffusion of isotope in each of two gases. Because we are now interested in the case having a large separation factor which would never be explained by thermal diffusion. We can see from equation (3) that the z-component j_{iz} of the vector $\boldsymbol{J}_i$ $(i=1, 2)$ is sufficiently large compared with other components except the small region where v_z becomes zero. Then from equations (10), (11) and (12), neglecting the radial components of $\boldsymbol{J}_i$ we have

$$j_{iz}(\partial\nu_1/\partial z) - r^{-1}(\partial/\partial r)\rho D_i c_i r(\partial\nu_i/\partial r)/\bar{M}=0 \quad (i=1, 2)\ (T<T_b) \tag{13}$$

$$j_{1z}(\partial\nu_1/\partial z) + j_{2z}(\partial\nu_2/\partial z) - r^{-1}(\partial/\partial r)\rho r[D_1 c_1(\partial\nu_1/\partial r) + D_2 c_2(\partial\nu_2/\partial r)]/\bar{M}=0 \quad (T\geq T_b) \tag{14}$$

In the above equations the terms containing $(\partial^2\nu_1/\partial z^2)$ and $(\partial^2\nu_2/\partial z^2)$ are omitted. These terms represent the effects of diffusion of isotope along the column which are separately treated in the equation of isotopic transport. The term $D_1\rho(\partial c_1/\partial z)(\partial\nu_1/\partial z)\bar{M}$ and corresponding term of species 2 are also omitted in (13) and (14), since the diffusion along the column is small enough compared with the convective flow. The neglect of these terms in equations (13) and (14) gives only a slight effect as much as the neglect of radial components of $\boldsymbol{J}_i$ in equations (10) and (11).

Now we introduce the functions L_i and L which are defined as follows,

$$\int_{r_1}^{r} 2\pi r j_{iz} dr = L_i(r) \quad (i=1, 2) \tag{15}$$

$$L_1(r) + L_2(r) = L(r) \tag{16}$$

Using the above equations we can integrate (13) and (14),

$$(\partial\nu_1/\partial z)L_i(r) = 2\pi\rho D_i c_i r(\partial\nu_i/\partial r)/\bar{M} \quad (i=1, 2)\ (T<T_b) \tag{17}$$

$$(\partial\nu_1/\partial z)L_1(r) + (\partial\nu_1/\partial z)L_2(r) = 2\pi\rho r[D_1 c_1(\partial\nu_1/\partial r) + D_2 c_2(\partial\nu_1\alpha/\partial r)]/\bar{M} \quad (T\geq T_b) \tag{18}$$

since $\partial\nu_1/\partial r$ and $\partial\nu_2/\partial r$ must vanish at the walls and we neglect small differences between $\partial\nu_1/\partial z$ and $\partial\nu_2/\partial z$, and their dependence on radial coordinate. By means of equation (15) the total flow of gases of species 1 and 2 are given by

$$-\tau_i = L_i(r_2) \quad (i=1, 2) \tag{19}$$

As the total flow of gas as a whole is zero, we get

$$\tau_1 + \tau_2 = 0 \tag{20}$$

At any point $\operatorname{div}(\boldsymbol{I}_1+\boldsymbol{I}_2)$ is zero then, total transport (τ = mol./sec.) of isotope A^i along the tube is independent of z, i. e.,

$$\tau = \int_{r_2}^{r_1} 2\pi r(j_{1z}\nu_1 + j_{2z}\nu_2)dr - (\partial\nu_1/\partial z)\int_{r_2}^{r_1} 2\pi\rho r(D_1 c_1 + D_2 c_2)dr/M = \text{const.} \tag{21}$$

The first term of equation (21) represents the transport of isotope by the convective flow of gases and the second term is derived from the vertical diffusion of isotope. When the small radial variations of c_1 and c_2 are neglected, the second term becomes the same as the case of thermal diffusion column, and we can use the results of Furry and Jones[6][7] as follows,

$$(\partial\nu_1/\partial z)\int_{r_2}^{r_1} 2\pi\rho r(D_1 c_1 + D_2 c_2)dr/\bar{M} = [c_1(K_d)_1/\bar{M} + c_2(K_d)_2/\bar{M}](\partial\nu_1/\partial z) \tag{22}$$

where $$(K_d)_i = 2\pi(\rho D_i)_1 r_1^2 k_d \quad (i=1, 2) \tag{23}$$

They tabulated the numerical values of k_d for the different values of (T_2/T_1) and (r_1/r_2) in the case of a Maxwellian gas. The subscript 1 of (ρD_i) emphasizes that the quantity in parethesis is to be evaluated at T_1. Using equation (15), partial integration of the first term of equation (21), gives

$$\int_{r_2}^{r_1} 2\pi r(j_{1z}\nu_1 + j_{2z}\nu_2)dr = \int_{r_2}^{r_b} 2\pi r\nu_1(j_{1z} + \alpha j_{2z})dr - \int_{r_1}^{r_b} 2\pi r(\nu_1 j_{1z} + \nu_2 j_{2z})dr = \tau_1\nu_1(r_b) + \tau_2\nu_2(r_b) - \int_{r_2}^{r_b}[(\partial\nu_1/\partial r)(\tau_1 + L_1)$$

$$+(\partial\nu_2/\partial r)(\tau_2+L_2)]dr$$
$$+\int_{r_1}^{r_b}((\partial\nu_1/\partial r)L_1+(\partial\nu_2/\partial r)L_2)dr$$

where r_b is radial coordinate, the temperature of which is T_b. According to (15), (9), (20), (17) and (18) the above expression becomes

$$\nu_1\tau_1(1-\alpha(T_b))+\int_{r_2}^{r_b}\frac{D_2c_2(\tau_1+L_1)-D_1c_1(\tau_2+L_2)}{D_1c_1+D_2c_2}\nu_1\frac{d\alpha}{dr}dr+\int_{r_1}^{r_b}\frac{\bar{M}}{2\pi\rho r}\left(\frac{L^2_1}{D_1c_1}+\frac{L^2_2}{D_2c_2}\right)\frac{\partial\nu_1}{\partial z}dr+\int_{r_b}^{r_2}\frac{\bar{M}}{2\pi\rho r}\left(\frac{L^2}{D_1c_1+D_2c_2}\right)\frac{\partial\nu_1}{\partial z}dr \quad (24)$$

We may regard in expression (24) the functions ν_1 and $\partial\nu_1/\partial z$ depend only on z. By expressions (22) and (24), the isotopic transport given by (21) becomes as follows,

$$\tau=A\nu_1-(B_c+B_d)\partial\nu_1/\partial z \quad (25)$$

where

$$A=\tau_1(1-\alpha(T_b))+\int_{r_2}^{r_b}\frac{D_2c_2(\tau_1+L_1)-D_1c_1(\tau_2+L_2)}{D_1c_1+D_2c_2}\frac{d\alpha}{dr}dr \quad (26)$$

$$-B_c=\frac{\bar{M}}{2\pi}\left[\int_{r_1}^{r_b}\left(\frac{L_1^2}{D_1c_1}+\frac{L_2^2}{D_2c_2}\right)\frac{dr}{\rho r}+\int_{r_b}^{r_2}\frac{L^2}{D_1c_1+D_2c_2}\cdot\frac{dr}{\rho r}\right] \quad (27)$$

$$B_d=(c_1(K_d)_1+c_2(K_d)_2)/\bar{M} \quad (28)$$

Evaluation of integrals in B_c is simply performed when some approximations are introduced for L_1, L_2 and diffusion coefficients. In expression (27) diffusion coefficients D_1 and D_2 are contained in positive terms, therefore we can substitute these coefficients by mean value $\bar{D}$ without great error.

The main part of j_{1z} is convective flow along the tube. Then we may put

$$j_{1z}=\rho c_i v/\bar{M} \quad (i=1,2) \quad (29)$$

in equation (15), where v is z-component of convective flow $\boldsymbol{v}$. This is very close approximation since the effects of diffusion are small enough compared with convective flow. We can remove c_i from under the integral sign of (15), because c_i varies only slightly with T. Then we may substitute L_i by c_iL. Using above approximation we obtain

$$-B_c=\frac{\bar{M}}{2\pi}\int_{r_1}^{r_2}\frac{L^2}{\rho\bar{D}r}dr \quad (30)$$

In order to evaluate the second term of expression (26) we use the following approximation which is similar to one applied to L_i in the above case;

$$\tau_i+L_i=\int_{r_2}^{r}2\pi rj_{iz}dr\cong c_iL$$

By this approximation we can rewrite equation (26) as follows,

$$A=\tau_1(1-\alpha(T_b))+\frac{c_1c_2(D_2-D_1)}{c_1D_1+c_2D_2}\int_{r_2}^{r_b}L\frac{d\alpha}{dr}dr \quad (31)$$

Convective Flow

Except the both ends of the tube, temperature gradient is determined by conduction alone, and in this region we have

$$2\pi Q=2\pi r\lambda(-dT/dr) \quad (32)$$

where $2\pi Q$ is heat flow by conduction per unit length of the tube, in cal./cm. sec.

The hydrodynamical equation of steady viscous flow in cylindrical coordinates is

$$r^{-1}(\partial/\partial r)r\eta(\partial v/\partial r)=dp/dz+\rho g \quad (33)$$

where p is pressure and g is acceleration of gravity. We assume that the velocity is entirely in z direction, and it is independent of z. Using equation (33) we have

$$Q^2(d/dT)\lambda^{-1}r^{-2}(d/dT)\eta\lambda^{-1}(dv/dT)=g(d\rho/dT) \quad (34)$$

Convective flow v must vanish at the walls;

$$v(T_1)=v(T_1)=0 \quad (35)$$

We have from equations (15), (16) and (29),

$$L=\int_{r_1}^{r}2\pi r\rho vdr/\bar{M} \quad (36)$$

From this equation we can see that L is the total flow of convection at the outside of the cylindrical part of radius r. Then we have

$$L(r_1)=L(r_2)=0 \quad (37)$$

Differentiate equation (36) with respect to r, and using equation (32) we have

$$v=-(\bar{M}Q/2\pi\lambda r^2)(dL/dT) \quad (38)$$

Substitution of equation (38) in (34) gives a differetial equation for L,

$$\frac{\bar{M}c^3}{2\pi}\frac{d}{dT}\frac{1}{r^2\lambda}\frac{d}{dT}\frac{\eta}{\lambda}\frac{d}{dT}\frac{1}{r\lambda\rho}\frac{dL}{dT}=g\frac{d\rho}{dT} \tag{39}$$

From (35), (37) and (38) the boundary conditions are

$$L(r_1)=L(r_2)=L'(r_1)=L'(r_2)=0 \tag{39}'$$

The function L obtained from (39) and (39)′ is identical to

$$(2\pi\rho\bar{D}/\lambda Q^3\bar{M})G$$

where G is the function used by Furry and Jones[6][7]. Therefore we can use their results of calculation about the integral contained in equation (30), and we have

$$B_c=K_c/\bar{M}=(2\pi/9!)(\rho^3g^2/\eta^2\bar{D})_1\cdot r^8{}_1k_c/\bar{M} \tag{40}$$

where values of k_c are tabulated for Maxwellian gases by Furry and Jones[6] for various combinations of (T_2/T_1) and (r_1/r_2). In order to evaluate the integral in equation (31), we have to solve the differential equation (39). Using the assumption that the quantities λ, η and ρD are proportional to T, an assymptotic solution of equation (39) for extreme cylindrical case $(r_2/r_1\to 0)$ has been given by Furry and Jones[7];

$$L(T)=2\pi\bar{M}(\rho g/\eta)_1\cdot r^4{}_1t^3{}_1\exp(2t^2{}_1)\gamma(t) \tag{41}$$

$$\gamma(t)\cong\frac{\gamma_\infty-(\gamma''/t_2)}{1-(\delta''/t_2)},$$

$$\delta''=\left[\exp(-t^2{}_1)\Big/\int_{t_1}^{\infty}\exp(-x^3)dx\right]-t_1$$

Where variable t is defined by

$$t=(\lambda/QT)^{1/2}T \tag{42}$$

and t_1 and t_2 are values of t at $T=T_1$ and T_2 respectively. The numerical values of γ_∞ and γ'' as the functions of t were tabulated by Furry and Jones.[7] Using these results we obtain the expression for the integral in (31) in terms of known functions as follows,

$$H_b=\int_{r_2}^{r_b}L(d\alpha/dr)dr$$
$$=(2\pi/\bar{M})(\rho g/\eta)_1r^4{}_1t^3{}_1\exp(2t^2{}_1)$$
$$\times[h_b-(h''_b/t_2)]/[1-(\delta''/t_2)] \tag{43}$$

$$h_b=-\int_{t_b}^{\infty}\gamma_\infty(d\alpha/dt)dt \tag{44}$$

$$h''_b=-\int_{t_b}^{\infty}\gamma''(d\alpha/dt)dt$$

Equilibrium Separation Factor

We proceed from the equation for transport of isotope A up to the tube:

$$\tau=A\nu_1-(B_c+B_d)(d\nu_1/dz) \tag{45}$$

where A is given by (31) and (43);

$$A=\tau_1[1-\alpha(T_b)]+[c_1c_2(D_2-D_1)/\bar{D}]H_b \tag{46}$$

B_c is given by equation (40), and B_d is given by equation (28);

$$B_d=K_d/\bar{M}=2\pi(\rho\bar{D})_1r^2{}_1k_d/\bar{M} \tag{47}$$

The approximation was used to derive above equations that we put D_1 and D_2 are equal to $\bar{D}$ except the case which contains their difference.

In the final equilibrium state τ is zero all along the tube. Putting $\tau=0$ in (45) we obtain

$$A\nu=(B_c+B_d)(d\nu/dz) \tag{48}$$

The integral of (48) gives a ratio of the concentration of isotope A in the top and the bottom reservoirs. In general case the distinction between ν_1 and ν_2 is not necessary when we consider the large separation of isotope in both reservoirs. The functions of z in equation (48) are ν and A which depends z through c_1c_2 in (46). Then integral of (48) is

$$(1-\alpha(T_b))Z+\frac{D_2-D_1}{\bar{D}}H_b\int_0^Z c_1c_2dz$$
$$=(B_c+B_d)\ln\left(\frac{\nu(Z)}{\nu(0)}\right) \tag{49}$$

where $\nu(0)$ and $\nu(Z)$ are values of ν at the bottom and the top reservoirs respectively.

By the similar way we obtain from equation(2)

$$(H/\bar{M})\int_0^Z c_1c_2dz=\tau_1Z$$
$$+(K_c+K_d)(c_1(Z)-c_1(0))/\bar{M} \tag{50}$$

where $c_1(Z)$ and $c_1(0)$ are c_1 at the bottom and the top reservoirs. Substitution of (50), (40) and (47) into (49) leads to the expression for over-all separation S as follows,

$$\ln S=\ln\left(\frac{\nu(Z)}{\nu(0)}\right)=\left[(1-\alpha(T_b))\right.$$
$$\left.+\frac{D_2-D_1}{\bar{D}}\frac{H_b}{H/\bar{M}}\right]\frac{\tau_1Z}{B_c+B_d}$$
$$+\frac{D_2-D_1}{\bar{D}}\frac{H_b}{H/\bar{M}}(c_1(Z)-c_1(0)) \tag{51}$$

When we use the approximate formula (41), H becomes

$$H=2\pi(\rho^2 g/\eta)_1 r^4_1 t^3_1 \exp(2t^2_1)\frac{h_\infty-(h''/t_2)}{1-(\delta''/t_2)} \tag{52}$$

where $$h_\infty=\int_{t_1}^{\infty}\alpha_t(\gamma_\infty/t)dt$$

$$h''=\int_{t_1}^{\infty}\alpha_t(\gamma''/t)dt \tag{53}$$

The expressions (53) and (43) give

$$\frac{H_b}{H/\bar{M}}=\frac{h_b-(h_b''/t_2)}{h_\infty-(h''/t_2)} \tag{54}$$

Discussion

From rather surprisingly simple results given by equation (51) we can easily calculate overall separation S, since B_c, B_d and $(c_1(Z)-c_1(0))$ may be determined from experimental conditions, and H_b/H may be numerically calculated by expression (54) when we know the temperature T_b.

The details of experimental verification of equation (51) will be reported in part 2 on this Bulletin.

We shall now discuss the functioning of gaseous exchange column. The remixing effects of the diffusion of isotope along the tube and of the countercurrent in the tube are represented by $B_d d\nu_1/dz$ and $B_c d\nu_1/dz$ respectively in the transport equation (45). It is reasonable that an appropriate approximation leads these terms to the expressions which are identical for the ordinary thermal diffusion as shown by equation (40) and (47). The initial isotopic transport obtained by putting $d\nu_1/dz=0$ in equation (45) is rather complicated, but its meaning is clear. When the ratio ν_2/ν_1 is $\alpha(T_b)$ at any point in the tube,

$$\nu_1\tau_1(1-\alpha(T_b))=\tau_1\nu_1+\tau_2\nu_1\alpha(T_b)$$

is transport of isotope A along the tube. Whereas in the equilibrium region ($T\geq T_b$) α varies with temperature. If we assume the self diffusion coefficient D_1 is larger than D_2, the radial variation of ν_1 may not be large, but the radial variation of α results in a strong variation of ν_2. The deviation of transport estimated in the first term of the expression (46) is corrected by the second term which is derived from such an asymmetric variation of ν_1 and ν_2 between r_2 and r_b. An application of (46) to the experiments of Bernstein and Taylor[2] shows that the first term is negligibly small compared with the second term. Therefore we may conclude that the transport of isotope in the equilibrium region results in the high efficiency of the gaseous exchange column. Perphaps there is another possibility to obtain the high efficiency by the mode of operation in which τ_1 takes large value by the thermal dissociation with suitable gas. In this case the transport of gases must be recalculated with the equilibrium constant of thermal dissociation.

Summary

The theoretical treatment of the countercurrent gaseous cxchange method for the separation of isotopes is developed here. The equation of transport is derived with the assumption that the equilibrium of the isotopic exchange reaction holds only in the sharply defined region in which temperature is higher than T_b. An appropriate approximation leads the transport equation to one which is formally similar to the transport equation of thermal diffusion column. The mechanism of isotope enrichment by countercurrent gaseous exchange method is discussed using the transport equation. The equilibrium separation factor is also derived from the transport equation.

Department of Physics and Chemistry, Gakushuin University, Mejiro Tokyo

Purification and Characterization of Tobacco Mosaic Virus

By Itaru WATANABE and Yoshimi KAWADE

(Received October 13, 1952)

Since the isolation and crystallization of tobacco mosaic virus (TMV), by Stanley[1] studies on physicochemical properties of viruses have greatly advanced, especially by taking advantage of the ultracentrifuge for purification. Ultracentrifugal purification of TMV now seems to be a well-established method; a preparation with high degree of homogeneity is, nevertheless, not easy to obtain. Only a few comprehensive studies on the properties of TMV particles are found in the literature which are based on simultaneous measurements of various physicochemical characteristics of a purified solution. In this paper the results obtained by the authors during the last few years[2] are shown, concerning the ultracentrifugal purification of TMV and characterization of purified preparations, by various means among which a sample of high degree of homogeneity is included.

Experimental

A. Purification of TMV.

1. Ultracentrifuge.—The ultracentrifuge used is an air-driven, vacuum-type one[3] first constructed in Japan at the end of 1948, some details of which were reported previously.[4][5]

2. Materials.—Tobacco leaves infected with tobacco mosaic disease were kindly supplied by Dr. J. Hitaka of the Tobacco Experimental Station at Hatano, Kanagawa Prefecture. Xanthi was used for the starting plant in our earlier experiments, but it was found that brownish pigments were not completely removed even after several cycles of alternate high and low speed centrifugations. In later experiments, therefore, we used mainly the infected leaves of White Burley, for it was found much easier to remove colored materials by centrifugation only.

The virus studied here is believed to be the ordinary strain of tobacco mosaic virus.

3. Purification Procedures.—Of the several preparations obtained, the purification methods of TMV-8 and -9 are described, which follow essentially those of Stanley.[6]

Young White Burley tobacco plants were harvested about two or three weeks after inoculation with TMV. The leaves were frozen in a refrigerator and ground through a meat chopper after three weeks (TMV-8); or they were frozen with solid carbon dioxide and ground the following day (TMV-9). On grinding, solid K_2HPO_4 was added amounting to 2.5% of the fresh weight of the leaves to maintain the *p*H of the expressed juice near neutrality. The juice was clarified by centrifugation and then subjected to three (TMV-8) or five (TMV-9) cycles of alternate high and low speed centrifugations. The high speed runs to obtain the virus pellets were made for one hour at 30,000 R. P. M. (65,000×g) or for half an hour at 36,000 R. P. M. (95,000×g), and those of low speed to remove heavier impurities, at 9,000 to 12,000 R. P. M. (6,000 to 10,000×g) for about 15 minutes. The solvents used to dissolve the pellets of TMV were 0.1M phosphate buffer at *p*H 7.0 for the first two cycles and 0.01M for the others. The final pellets so obtained were practically pigment-free. They were dissolved in 0.01M phosphate buffer at *p*H 7.0 and stored in a cold room near 0°C.

4. Yields.—Biological assays by the half leaf method on *Nicotiana glutinosa* were performed only qualitatively, and it was found that no serious loss or inactivation of TMV had occurred during the isolation processes by comparing the infectivity of purified preparation with that of original juice.

The yields of purified virus were found to be about the same order as that reported by other workers[7][6][9] and are shown in Table 1.

Table 1
Yields of Purified TMV

Sample	Total amount of TMV obtained, g.	Mg. TMV per g. of original plant	Mg. TMV per cc. of plant juice
TMV-8	0.030	1.0	1.2
TMV-9	1.07	1.4	1.8
	(1.5)	(2.0)	(2.5)

( )···Including less pure TMV

(1) W. M. Stanley, *Science* **81**, 644 (1935).
(2) A brief preliminary report, I. Watanabe, Y. Otsuka, and S. Mizushima, *Repts. Radiation Chem. Research Inst., Tokyo Univ.*, No. 5, 10 (1950).
(3) E. G. Pickels, *Rev. Sci. Instruments*, **9**, 358 (1938).
(4) S. Sasaki and O. Taniguchi, *J. Japan Soc. Mech. Eng.*, **54**, 255 (1951).
(5) I. Watanabe and Y. Kawade, *Chemistry and Chem. Industry*, **5**, 585 (1952).
(6) W. M. Stanley, *J. Am. Chem. Soc.*, **64**, 1804 (1942).
(7) W. M. Stanley, in R. Doerr und C. Hallauer, "*Handbuch der Virusforschung*", I, Vienna (1938), pp. 447—546.
(8) H. K. Schachman and W. J. Kauzmann, *J. Phys. Colloid Chem.*, **53**, 150 (1949).
(9) F. C. Bawden, "*Plant Viruses and Virus Diseases*", Waltham (1950).

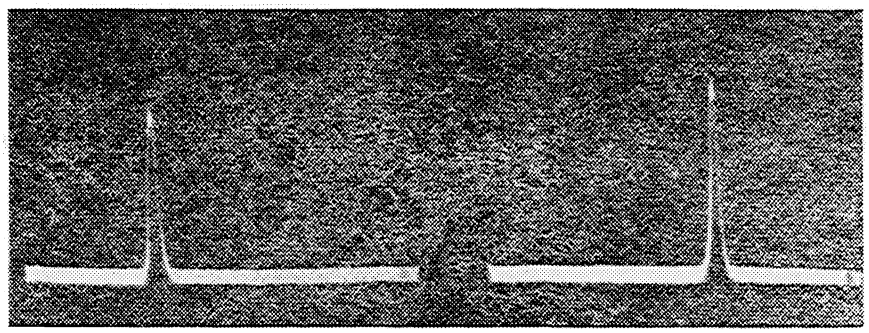

← Ascending → Descending

Fig. 1.—Electrophoretic pattern of 0.44% solution of TMV-9 in 0.2 ionic strength phosphate buffer at *p*H 7.7[16]

B. Homogeneities and Properties of Purified TMV.

Some chemical and physical properties of purified TMV have been examined to test its homogeneity and to determine size and shape of the virus particles.

1. Chemical Analyses.—An aliquot of the purified stock solution (TMV-9) was dialyzed against distilled water, and precipitated by acidified ethanol. The precipitate, washed and dried, was dissolved in weak alkali and submitted to analyses for nitrogen by the micro Kjeldahl method, phosphorus by King's method,[10] and pentose nucleic acid by the orcinol method.[11] Dische's diphenylamine test[12] for DNA was found entirely negative. The results are shown in Table 2 and are in good agreement with the values reported by previous investigators.[9][13]

Table 2

Chemical Analyses of Purified TMV

(Sample: TMV-9)

	N %	P %	N/P	PNA %	DNA %
	16.6	0.51		6.2$_7$	0.0
	16.7	0.50		5.8	0.0
Average	16.7	0.51	33	6.0	0.0

2. Physical Measurements.—Electrophoretic measurements of purified preparations were carried out in a Tiselius-type[14] apparatus, equipped with a Svensson optical system,[15] in phosphate buffers of various ionic strengths at *p*H 7.7 and the details will be published elsewhere.[16] In all preparations examined, except in the case only a single boundary was found in the electrophoretic pattern of TMV-8, and the boundary remained very sharp during the course of electrophoresis (forexample, see Fig. 1). A small amount of an unidentified slower component was seen in the pattern of TMV-8. The electrophoretic mobilities were calculated from the descending patterns and in Table 3 are shown the representative data of TMV-9 at 0°C.

Diffusion constants were measured refractometrically by the Svensson schlieren method[15] using a Neurath-type[17] diffusion cell under

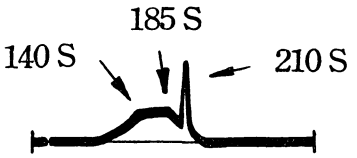

→ $S_{20,w}$

Fig. 2.—Tracing of sedimentation pattern of 0.51% solution of TMV-8 in 0.01M phosphate buffer at *p*H 7.0[18]

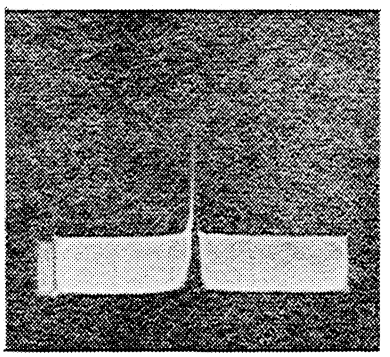

→

Fig. 3.—Sedimentation pattern of 0.61% solution of TMV-9 in 0.01M phosphate buffer at *p*H 7.0[18]

(10) E. J. King, *Biochem. J.*, **26**, 292 (1932).
(11) S. E. Kerr and K. Seraidarian, *J. Biol. Chem.*, **159**, 211 (1945).
(12) F. Seibert, *J. Biol. Chem.*, **133**, 593 (1940).
(13) W. M. Stanley and M. A. Lauffer, in T. M. Rivers, "*Viral and Rickettsial Infections of Man*", Philadelphia (1948), pp. 18—66.
(14) A. Tiselius, *Trans. Faraday Soc.*, **33**, 524 (1937).
(15) H. Svensson, *Kolloid-Z.*, **87**, 181 (1939).
(16) I. Watanabe and N. Ui, in preparation.
(17) H. Neurath, *Science*, **93**, 431 (1941).
(18) I. Watanabe, Y. Kawade, and S. Mizushima, *J. Chem. Soc. Japan, Pure Chem. Sect.*, **73**, 828 (1952).

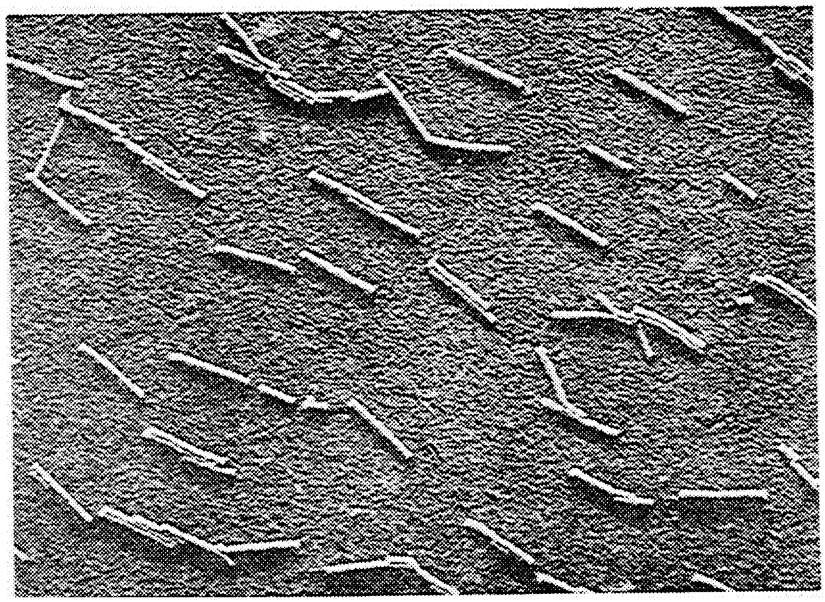

Fig. 4.—Typical electron micrograph of centrifugally purified TMV (TMV-9) photographed by Japan Electron Optics Co., Tokyo. Magnification 35,000 and chromium shadow cast.

various conditions in phosphate buffers. The most reliable value of diffusion constant of the preparation of TMV-9 is shown in Table 3.

Sedimentation studies were carried out in 0.01M phosphate buffer at *p*H 7.0 by using an air-driven analytical ultracentrifuge.[18] TMV-8 proved very inhomogeneous and showed three components in sedimentation pattern (see Fig. 2). The sedimentation constants ($s_{20,w}$) of these three peaks were 210, 185, and 140 S (S: Svedberg unit), when corrected for viscosity of the solution, and would correspond roughly to dimer, monomer, and half-length particle of TMV, respectively. On the other hand, TMV-9 gave a single sharp boundary shown in Fig. 3, suggesting a high degree of homogeneity. It may be stated that such an exceedingly sharp boundary of TMV has not been reported except by Schachman.[19] The sedimentation constant was calculated to be 157S, corrected for viscosity of the solvent, and 185S, corrected for viscosity of the solution according to Lauffer[20] (see Table 3). The latter value is in close agreement with those reported by other workers[8][20][21] for monomeric TMV.

Viscosity was measured in 0.01M phosphate buffer at *p*H 7.0 by an Ostwald-type viscosimeter with low velocity gradient (about 100 sec.$^{-1}$). TMV-8 gave a volume fraction intrinsic viscosity of about 40. This slightly low value of intrinsic viscosity as compared with that of TMV-9 is probably due to the presence of a large amount of shorter (half-length) particles in TMV-8 (see Fig. 2). The viscosity of TMV-9 showed a considerable decrease with time; the intrinsic viscosity at equilibrium state was estimated to be 50 (Table 3).

Electron microscopic observations were made on various samples and in Fig. 4 is shown one of the representative micrographs of purified TMV-9. No extraneous materials have been observed in any. It is apparent that the particles of length about 300 mμ predominate in number in each case. Shorter and longer

Table 3
Physical Data of Purified TMV
(Sample: TMV-9)

Electrophoretic Mobility (at 0°C. in phosphate buffer of ionic strength 0.2 and *p*H 7.7)	$u_D = -7.0_5 \times 10^{-5}$ cm.^{2}/sec. volt
Diffusion Constant	$D_{20,w} = 0.4 \times 10^{-7}$ cm.^{2}/sec.
Sedimentation Constant	$s_{20,w} = 185$ S* (corrected by solution viscosity) = 157 S (0.5%) (corrected by solvent viscosity)
Intrinsic Viscosity (Volume Fraction)	$[\eta]_V = 50$
(Partial Specific Volume)	($V = 0.73$)**

* S is a Svedberg unit and a sedimentation rate equal to 10^{-13} cm./sec. in a unit centrifugal field.

** The value obtained by Lauffer.[22]

(19) H. K. Schachman, *J. Am. Chem. Soc.*, **73**, 4808 (1951).
(20) M. A. Lauffer, *J. Am. Chem. Soc.*, **66**, 1195 (1944).
(21) G. Schramm und G. Bergold, *Z. Naturforsch.*, **2b**, 10 (81947).
(22) M. A. Lauffer, *J. Am. Chem. Soc.*, **66**, 1188 (1944).

Table 4
Size and Shape of TMV Particles
(Sample: TMV-9)

Methods	Mol. Wt. (10^6)	Frictional Ratio, f/f_0	Axial Ratfo, a/b	Length, a (mμ)	Diameter, b (mμ)
Sedimentation and Viscosity	37	2.2	24	310	13
Sedimentation and Diffuion	42	2.3	28	360	13
Diffusion and Viscositys	53	2.2	24	360	15
Electron Microscope and X-Ray Diffraction	45		20	300	15.2*

* The value obtained by Bernal and Fankuchen from the X-ray diffraction experiments[25]

particles are, however, always present; and even in our most homogeneous preparation, TMV-9, the distribution is broader than reported by American investigators.[22][23][24] Electron micrographs of the original extract for TMV-7 were also taken and it was found that a considerable amount of shorter rods had been already present in plant juice. It might, therefore, be difficult, if not impossible, to ascribe the presence of the short rods entirely to the break-up of the monomer virus rods due to mechanical stresses during centrifugation.

3. Size and Shape of TMV Particles.—The physical data mentioned above are summarized in Table 3. Size and shape of TMV can be determined by various combinations of viscosity, diffusion, and sedimentation data in conjunction with the partial specific volume.[22] The results of the various methods of determining the dimensions of the particles of TMV-9 are shown in Table 4. In these calculations Lauffer's value[22] of partial specific volume was temporarily adopted. It can be seen that the agreement between the various methods is excellent considering the experimental errors and uncertainties in the calculation methods of determining the size and shape of such highly asymmetric particles. It must be, however, borne in mind that these values are not conclusive, since the concentration dependence of sedimentation constant has not yet been measured exactly in our case and the determinations of various physical constants have not been made at the same time. The latter consideration seems important because of the observed change in the viscosity of solutions of TMV-9 with the lapse of time.

Discussion

In the ultracentrifugal purification of viruses, it seems primarily important to take care of the choice of suitable starting materials. In fact, it was found in our experiments that the leaves of Xanthi contained pigment which was difficult to remove from the virus fraction and that in this respect White Burley was superior to Xanthi. It is also essential to remove heavier materials as completely as possible in the first clarification of the expressed juice. Otherwise, green impurities remaining in the turbid supernatant, once sedimented by high speed centrifugation and redissolved in buffer solution, become somewhat difficult to be removed by subsequent centrifuga tion and complicate the further purification procedure.

It is clear from the results of chemical and physical measurements on purified TMV that the purity of centrifugally isolated TMV, especially of TMV-9, was very high, so to say, in a chemical sense. The homogeneities of preparations, however, were not always so good. TMV-9 showed a single sharp boundary both in sedimentation and electrophoretic patterns. On the contrary, three peaks appeared in the sedimentation pattern of TMV-8. But this marked heterogeneity was not detected in the electrophoretic measurements, which showed only one main peak except a presence of a small amount of slower component. This apparent discrepancy in sedimentation and electrophoretic patterns of TMV-8 may be ascribed to some difference of sensitivities of sedimentation and electrophoretic analyses in detecting the heterogeneity of length of rod-like particles such as TMV. Another possible explanation, however, cannot be excluded; that is, a certain change in molecular state might have occurred during the preservation, since the electrophoretic measurements were made immediately after the purification of TMV-8 while the ultracentrifugal analysis was performed nearly three months after it. This marked heterogeneity found in sedimentation pattern could not be detected also in diffusion pattern of TMV-8, the measurements of which were made at the same time as the electrophoretic experiments.

TMV-9, on the other hand, showed no evidence of heterogeneity and a single sharp boundary was obtained both in sedimentation and electrophoretic patterns, as mentioned above*; nevertheless, a rather broad distribution was observed in the electron micrographs. In view of the high sensitivity of ultracentrifuge in detecting hetero-

(23) G. Oster, C. A. Knight, and W. M. Stanley, *Arch. Biochem.*, **15** 279 (1947).

(24) R. C. Williams and R. L. Steere, *J. Am. Chem. Soc.*, **73**, 2057 (1951).

(25) J. D. Bernal and I. Fankuchen, *J. Gen. Physiol.*, **25**, 111 (1941).

* Even after storage in a cold room near 0°C. for more than six months, TMV-9 still retained a fairly good homogeneity in sedimentation pattern.[18]

geneity (presence of short rods) of TMV[13] and a possible change of distribution in length during the preparation of specimen for electron microscopic examination, it might be not unreasonable to conclude that TMV-9 has a high degree of homogeneity and that shorter rods observed in electron micrographs are, at least in part, artefacts. It must be remembered, however, that there still remain other possibilities concerning the origin of these short rods which are seen also in other samples; first, they may be present in the original expressed juice and secondly, they may arise from the break-up of the longer particles as a result of mechanical stresses during the preparation.[26]

It is rather curious that TMV-8, although purified under very similar conditions as TMV-9, showed the marked heterogeneity. In this respect, it would be necessary to point out that in the case of TMV-8, the leaves were frozen in a refrigerator and treated three weeks after the harvest, while in TMV-9, the harvested leaves were frozen with solid carbon dioxide and treated in the following day. These differences in the time of storage of leaves might have caused the unexpected difference in homogeneities of TMV-8 and -9. It seems very desirable, anyway, to start the purification of virus as soon as possible after the harvest of leaves.

Schachman and Kauzmann[6] studied the aggregation effect of phosphate buffer during the purification and storage of TMV and found that isolation of TMV by centrifugation in 0.1M phosphate followed by water leads to the best preparation. Considering their experimental results, however, we used 0.01M phosphate buffer instead of water and the final solution was also stored in the same buffer. Very good results were obtained in this case too. But the solution stored in 0.01M phosphate buffer showed considerable decrease in viscosity with the lapse of time, as mentioned above. This change in viscosity seems very interesting, but other measurements must be performed during storage before a clear explanation can be made about it.

Electrophoretic mobility, diffusion constant, sedimentation constant, and intrinsic viscosity were determined on the most homogeneous preparation, TMV-9. The size and shape of TMV particles were also calculated by various combinations of diffusion constant, sedimentation constant, and intrinsic viscosity and an excellent agreement was found between the results of these indirect physico-chemical procedures and direct observation with the electron microscope.

Since the degree of homogeneity of a purified TMV preparation with respect to the length of the rod-like particle is known to vary various factors, including the purification procedures employed, the nature of the solvent used for preservation, etc.,[27] it is necessary to assess the degree of homogeneity of the specimen when its physicochemical properties are to be studied. Among the numerous investigations on the determination of size and shape of TMV, those of Lauffer[22] and of Schramm and Bergold[21] have been probably the most comprehensive in this respect, but even their samples were apparently inhomogeneous judging from the sedimentation patterns obtained by them. Studies on homogeneous solution of such highly asymmetric particles will be greatly valuable in establishing the hydrodynamic theory underlying the measurements of sedimentation, diffusion, viscosity, etc.

Summary

Tobacco mosaic virus (TMV) was purified by differential centrifugation in a vacuum-type, air-driven ultracentrifuge, first constructed in Japan.

The yield of purified TMV was high and about 2 mg. per cc. of the original plant juice.

Chemical analyses and physico-chemical examinations (including electrophoresis, sedimentation, diffusion, viscosity and electron microscope measurements) were carried out on the purified preparations to test their purities and homogeneities. It was found that the purity of ultracentrifugally isolated TMV was very high in a chemical sense. Although the homogeneity with respect to the length of particles was not always so good, one preparation, TMV-9, was found to have a high degree of homogeneity by the sedimentation and electrophoresis patterns. The size and shape of TMV particles were determined on this preparation by several methods.

The authors wish to express their appreciation of the interest and suggestions of Prof. S. Mizushima of the Department of Chemistry, University of Tokyo, throughout the course of this work. They are also indebted to Prof. S. Sasaki and Prof. O. Taniguchi, Tokyo Institute of Technology, for their kind advices about ultracentrifuge and to Dr. J. Hitaka, Tobacco Experimental Station at Hatano for tobacco leaves. They also wish to acknowledge the technical assistance of Mr. M. Nakamura. Part of the expense of this investigation was defrayed by a Grant in Aid for Scientific Research by the Ministry of Education.

Institute of Science and Technology,
Tokyo University, Tokyo

(26) T. Sigurgeirsson and W. M. Stanley, *Phytopathology*, **37**, 26 (1947).

(27) See, e. g., refs. (26), (24), and (8).

Dosage volumétrique du manganèse et du chrome par le péroxyde d'argent

(Reçu le 18 Novembre, 1952)

Par Motoharu TANAKA

Introduction

Le péroxyde d'argent est un oxydant énergique qui a déjà donné des résultats satisfaisants dans le dosage colorimétrique du manganèse[1] et du chrome[2] et dans le dosage volumétrique du cérium.[3] Ce réactif pourra trouver d'autres applications dans la chimie analytique. Nous présentons l'utilisation possible de ce réactif dans le dosage volumétrique du manganèse et du chrome.

Manganèse[4]

Jusqu'à présent on a employé généralement les trois méthodes suivantes pour le dosage volumétrique du manganèse:

1°)[5] Titrage du permanganate qu'on obtient par l'oxydation d'ion manganeux à l'aide d'un oxydant quelconque.

2°)[6] Titrage direct de l'ion manganeux par une solution titrée de permanganate.

3°)[7] Titrage de l'excès de fer ferreux en traitant le bioxyde de manganèse par une solution titrée de permanganate.

Parmi les trois, la première méthode est la plus ordinaire, et on y emploie divers oxydants comme le persulfate d'ammonium, le bismuthate de sodium et le péroxyde de plomb.

Pour ces deux derniers, il faut filtrer l'excès de l'oxydant après oxydation. Quant au persulfate, l'inhabileté peut provoquer la destruction du permanganate formé dans l'ébullition qui est faite pour éliminer l'excès de l'oxydant. De plus, quand on se sert d'acide arséneux pour le titrage direct du permanganate, on observe parfois au terme de la réaction la recoloration due à la destruction incomplète de l'excès de persulfate.

Les résultats suivants ont prouvé que le péroxyde d'argent est applicable au dosage volumétrique du manganèse avec succès.

Réactifs nécessaires

1°) Péroxyde d'argent (en suspension dans l'eau distillée).

2°) Acide sulfurique (1:1).

3°) Solution titrée de permanganate de potassium.

4°) Solution titrée d'oxalate de sodium.

Mode opératoire

A la solution normale d'acide sulfurique qui contient moins de 2 mg. de manganèse,[8] ajouter en agitant du péroxyde d'argent. Après oxydation complète, ajouter de l'acide sulfurique jusqu'à 3N, chauffer sur le bain-marie pendant 2 minutes pour détruire l'excès d'oxydant. Traiter la solution obtenue avec une quantité connue d'une solution centinormale d'oxalate de sodium, dont l'excès sera titré à l'aide d'une solution centinormale de permanganate.

Exactitude de la méthode

Nous avons répété les titrages sur diverses quantités de manganèse. Les expériences nous révèlent que l'on peut estimer la teneur en manganèse avec un écart absolu inférieur à 0,003 mg. Le tableau 1 reproduit les résultats.

Exemples d'analyse

L'analyse de divers aciers nous permet d'établir le tableau 2. L'emploi des deux méthodes ne garantit pas toujours des résultats identiques. Mais l'inspection précise a prouvé qu'il y a, dans le procédé par le persulfate, un certain point difficile, qui nous amène souvent

(1) Y. Murakami, Ce Bulletin, **22**, 159 (1949); M. Tanaka, *J. Chem. Soc. Japan, Pure Chem. sect.*, **72**, 29 (1950).

(2) M. Tanaka, Ce Bulletin, **23**, 165 (1950).

(3) K. Kimura et Y. Murakami, *Mikrochemie*, **36**, 727 (1950).

(4) Ce rapport a été présenté au "Symposium" de la chimie analytique de la Société chimique du Japon ayant lieu à Sendai, le mois de Nov. 1951.

(5) H. D. Hillson, *Ind. Eng. Chem. Anal. Ed.*, **16**, 560 (1944). H. Marshal, *Chem. News*, **83**, 76 (1901). Fred. C. T. Daniels, *Ind. Eng. Chem.*, **6**, 658 (1914). Z. S. Moukhina et N. V. Zolotareva, *Zab. Lab.*, **3**, 881 (1934); *Ann. chim. analyt. chim. appl.* (3) **17**, 216 (1935).

(6) Luciano Barzaghi, *Anais. assoc. quim. Brasil*, **2**, 187 (1943); *C. A.*, **38**, 4214 (1944); M. Marqueyrol et L. Toquet, *Ann. chim. analyt. chim. appl.*, (2), **9**, 289, 324 (1927); J. Pattinson, *J. Chem. Soc.*, **35**, 365 (1879); J. Majdel, *Z. Anal. Chem.*, **81**, 14 (1930).

(7) P. Nicolardot et al., *Compt. rend.*, **170**, 808 (1920).

(8) Il est nécessaire que la concentration de manganèse soit inférieure à 0,05 mg. par centimètre cube. La présence du phosphate favorise l'oxydation du manganèse et en même temps élimine la teinte jaune du fer.

Tableau 1
Exactitude de la méthode (Manganèse)

Mn présent (mg.)	Mn trouvé (mg.)	Ecart absolu (mg.)	Erreur relative (%)
0.081	0.081	0	0
〃	0.080	−0.001	−1.3
〃	0.082	+0.001	+1.3
0.402	0.404	+0.002	+0.5
〃	0.405	+0.003	+0.7
〃	0.403	+0.001	+0.3
0.558	0.557	−0.001	−0.2
0.810	0.810	0	0
〃	0.812	+0.002	+0.3
〃	0.810	0	0
1.620	1.620	0	0
〃	1.618	−0.002	−0.1
〃	1.618	−0.002	−0.1

Tableau 2
Exemples d'analyse (I)

Echantillon	Mn trouvé (%) Méthode du persulfate	Méthode du péroxide d'argent	Remarque
Acier à la silice	0.79[a]	0.787	Cr 0.07%
Acier au tungstène	0.50[b]	0.498	Cr 0.09%
Acier	0.17[a]	0.171	
Acier	0.47[a]	0.503	
		0.502	
Acier au chrome et manganèse	9.66[a]	9.48	Cr18.06%
		9.48	
		9.45	
Acier rapide[c]	0.078	0.0780	Cr 3.87%
Acier au nickel et chrome[c]	0.45	0.454	Cr 0.78%
Gueuse[c]	0.77	0.776	

a) Résultats obtenus à la Faculté des sciences mécaniques, Université de Nagoya.
b) Résultat obtenu à Daido-Seikô Co.
c) Echantillon d'étalon du Japon. Les résultats de l'analyse donnés dans la première colonne sont donc les moyennes de plusieurs valeurs.

à un mauvais résultat, tandis que notre méthode par le péroxyde d'argent facilement donne les meilleurs resultats.

Influences des divers éléments

Parmi les éléments qui peuvent exister dans les échantillons ordinaires, seule une grande quantité de chrome fait obstacle à la méthode du péroxyde d'argent en rendant difficile la perception du terme du titrage. Mais on peut facilement séparer la plupart du chrome d'avec le fer et le manganèse en employant le péroxyde de sodium ou l'eau oxygénée et la soude caustique. L'emploi de l'oxalate tolère la présence d'une petite quantité de chrome.

On peut facilement neutraliser la gêne du chloride par addition simple de l'ion mercurique.[9]

Chrome[10]

Il y a beaucoup de chimistes qui ont essayé le dosage volumétrique et colorimétrique du chrome en se basant sur le fait qu'on peut oxyder le chrome trivalent en hexavalent. L'oxydation du chrome peut être faite dans le milieu alcalin et dans le milieu acide. Pour cette dernière voie d'analyse on emploie divers oxydants énergiques (bromate de potassium,[11] chlorate de potassium,[12] permanganate de potassium,[13] persulfate de potassium en présence de nitrate d'argent,[14] et acide perchlorique[15] etc.). Mais on y rencontre souvent les difficultés, par exemple nécessité de filtration ou de destruction ennuyeuse de l'excès de l'oxydant.

P. F. Urone et H. K. Anders[16] se sont servis avec succès le bismuthate de sodium dans le dosage colorimétrique de cet élément.

Le péroxyde d'argent a pu trouver une nouvelle application, comme on le verra, dans le dosage volumétrique du chrome. Les résultats obtenus ont été satisfaisants comme dans le cas du dosage volumétrique du manganèse.

Réactifs nécessaires

Acide sulfurique (1:1).
Acide phosphorique à 85%.
Péroxyde d'argent en suspension dans l'eau distillée.
Solution titrée de sulfate ferreux.
Solution titrée de permanganate de potassium.
Solution titrée d'oxalate de sodium.

Mode opératoire

On ajoute du péroxyde d'argent à la solution d'acide sulfurique (environ 1N) contenant le chrome (moins de 2 mg.). On la chauffe sur le bain-marie bouillant pendant deux minutes pour éliminer l'excès du péroxyde, Quand une grande quantité de fer existe, il faut décolorer

(9) M. Tanaka, *J. Chem. Soc. Japan. Pure chem. sect.*, **72**, 136 (1950).
(10) Ce rapport a été déjà présenté à l'assemblée annuelle de la Société analytico-chimique du Japon, a Kyoto, au mois d'Octobre, 1952.
(11) I. M. Kolthoff et E. B. Sandell, *Ind. Eng. Chem., Anal. Ed.*, **2**, 140 (1930).
(12) F. H. Storer, *Amer. J. Science*, (2), **45**, 190 (1868).
(13) W. W. Scott, Standard Methods of Chemical Analysis, 5 th Ed., 495 (1939).
(14) H. Pinsl, Archiv f. Eisenhüttenwesen, **10**, 139 (1936). Fred. C. T. Daniel, op. cit. Willard et Young, *Ind. Eng. Chem.*, **20**, 769 (1928).
(15) L. Bertiaux, R. Chataigner et al., *Chim. anal.*, **33**, 129 (1951); S. Schuldiner et F. B. Clardy, *Ind. Eng. Chem., Anal. Ed.*, **18**, 728 (1946).
(16) P. F. Urone et H. K. Anders. *Anal. Chem.*, **22**, 1317 (1950).

la teinte jaune provenant de cet élément par addition de l'acide phosphorique. Sinon, cette coloration gêne plus ou moins la perception du terme du titrage.

Après refroidissement on verse dans la solution oxydée l'excès de la solution titrée de sulfate ferreux. Puis on le titre avec le permanganate de potassium.

Exactitude de la méthode

Nous avons répété les titrages des solutions dont les teneurs en chrome sont 0.2～1.5 mg. Quand il existe plus de chrome que 2 mg., l'oxydation en est incomplète. Nous donnons ci-dessous les résultats:

Tableau 3

Exactitude de la méthode (Chrome)

Cr présent (mg.)	Cr trouvé (mg.)	Ecart absolu (mg.)
1.580	1.578	−0.002
〃	1.583	+0.003
〃	1.580	±0.000
1.056	1.054	−0.002
〃	1.052	−0.004
〃	1.062	+0.006
0.524	0.526	+0.002
〃	0.509	−0.015
〃	0.516	−0.008
0.208	0.208	±0.000
〃	0.213	+0.005
〃	0.210	+0.002
1.056[a])	1.048	−0.005

a) Nous avons ajouté du manganèse. Cet élément, qui est oxydé par le péroxyde d'argent, est ensuite réduit par les gouttes d'une solution centinormale d'oxalate de sodium.

Influences des éléments étrangers

Si le manganèse existe, cet élément est transformé à l'étape permanganique par le péroxyde d'argent. Mais on peut facilement réduire ce permanganate par introduction de l'acide chlorhydrique ou de l'oxalate sans réduction du chromate formé. Donc dans ce dernier cas il suffit de commencer le titrage du chrome après le dosage volumétrique du manganèse, si l'on emploie la méthode présentée plus haut.

La plus grande partie du fer et du manganèse qui co-existent est facilement séparée d'avec le chrome selon les deux manières suivantes:

1° Après la réduction du fer et du manganèse à l'étape bivalente, on ajoute une solution de bicarbonate de sodium à 8% jusqu'au moment ou l'on observe la précipitation, et on y en verse 4 cc. de plus. On fait bouillir pendant une minute. On filtre le précipité rapidement autant qu'il est possible. On peut reprendre tout le chrome dans le précipité.

2° Quand on verse la solution contenant fer, manganése, chrome et l'excès du phosphate[9] dans la solution bouillante de péroxyde de sodium, fer et manganèse se précipitent et on reprend le chrome dans le liquide filtré.

La présence du vanadium ne gêne pas le dosage.

Exemples d'analyse

Voici les résultats d'analyse des aciers:

Tableau 4

Exemples d'analyse (II)

Echantillons	Cr trouvé (%) Méthode par péroxyde d'argent	Cr trouvé (%) Méthode par permanganate	Remarque
Acier à la silice et manganèse	0.073	0.07[a])	Mn 0.79%
Acier au tungstène	0.094	0.09[b])	Mn 0.50%
Acier au chrome et manganèse	18.05 18.05 18.04	18.06[a])	Mn 9.66%
Acier au nickel, chrome et molybdène	1.23	1.20[a])	Mn 0.81%
Acier au nickel et chrome	1.73	1.68[a])	Mn 1.10%
Acier au nickel et chrome[c])	0.780	0.78	Mn 0.45%
Acier rapide[c])	3.86 3.88 3.88	3.87	Mn 0.078%

a) Résultats obtenus à la faculté des sciences mécaniques, Université de Nagoya.
b) Résultat obtenu à Daidô-Seikô Co.
c) Echantillons d'étalon du Japon. Les resultats de l'analyse donnés dans la deuxième colonne sont donc les moyennes de plusieurs valeurs.

On peut comparer les résultats par le péroxyde d'argent avec ceux par le permanganate de potasse.

Résumé

Nous avons présenté l'utilisation possible du péroxyde d'argent pour le dosage volumétrique du manganèse et du chrome. Nous résumons notre étude:

1°) Même les débutants peuvent employer cette méthode qui assure les résultats exacts.

2°) Le péroxyde d'argent est suffisamment puissant, et l'oxydation par ce réactif et la

(17) Evans, *Analyst*, **46**, 285 (1921). La présence de l'excès du phosphate protège de chrome de co-précipiter avec le fer.

destruction de son excès sont complètes.

3°) Comme il a été déjà indiqué,[1] la durée de conservation du péroxyde d'argent est presque infinie (on peut l'employer sans aucun souci de son changement même un an après la préparation).

4°) Le titrage de l'excès d'oxalate de sodium permet la présence d'une quantité de chrome telle qu'elle ne fait pas obstacle par l'intensité de sa coloration jaune. Aussi, peut-on estimer le manganèse et le chrome simultanéement.

Nous ne voulons pas manquer, en terminant, de remercier cordialement Monsieur le Professeur Sugawara qui nous a encouragé pendant cette recherche et Monsieur le Professeur Hirano qui a mis à notre diaposition des échantillons d'acier nécessaires.

Institut de chimie, Faculté des Sciences,
Université de Nagoya

On the Ring-Opening Reactions of the Furan Compounds. I. The Synthesis of 1, 4-Pentadien-3-one-1, 5-dicarboxylic Acid from 2-Furanacrylic Acid

By Hiroshi MIDORIKAWA

(Received January 13, 1953)

In the ring opening of furan compounds by hydrogen peroxide, 2-furanacrylic acid behaved peculiarly, by giving 1,4-pentadien-3-one-1,5-dicarboxylic acid in fairly good yield. This reaction is analogous to the bromine and subsequent silver oxide oxidation[1] by which 2-furanpropionic acid gives furonic acid as illustrated below:

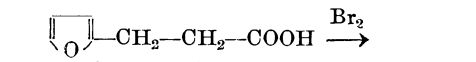

2-furanpropionic acid

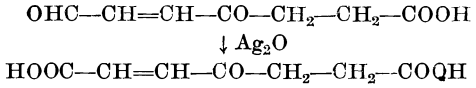

furonic acid

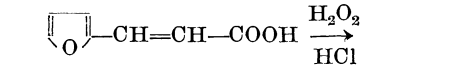

2-furanacrylic acid

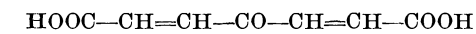

1, 4-pentadien-3-one-1, 5-dicarboxylic acid

Straus[2] had already synthesized it from 2,4 - dibromopentan - 3- one - 1,5 - dicarboxylic acid methyl ester. He reported that the acid decomposes "stürmisch" at 230° and its methyl ester is acted upon by sunlight. In this experiment, the acid decomposed gently at 236°, and pale yellow crystals of the methyl ester were changed to white granular crystals by exposure to direct sunlight. But the photochemical change took place also with the free acid. That is to say, the acid of pale yellow crystals was changed to an acid of hygroscopic white powder by direct sunlight, the methyl ester of which was identified with the 1,4-pentadien-3-one-1,5-dicarboxylic acid methyl ester exposed to direct sunlight. Since it had already been reported that the methyl ester is polymerised to a dimer by direct sunlight,[3] the free acid may be polymerised to a dimer.

On reducing the acid by aluminium amalgam, γ-ketopimelic acid was obtained. By potassium permanganate oxidation, the acid gave oxalic acid and fumaric acid, but no maleic acid. It is assumed, therefore, that two double bonds of the acid have the trans structure as follow:

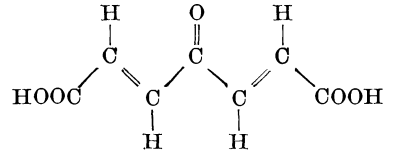

Its carbonyl group reacted upon phenylhydrazine with formation of phenylhydrazone.

α - Methyl - β - (2 - furyl) - acrylic - acid, α-phenyl-β-(2-furyl)-acrylic acid and α-cyano-β-(2-furyl)-acrylic acid did not undergo such a furan ring opening by hydrogen peroxide.

(1) A. Baeyer, *Ber.*, **10**, 395 (1877).
(2) F. Straus, *Ber.*, **37**, 3297 (1904).
(3) H. Stobbe and E. Färber, *Ber.*, **58**, 1551 (1925).

Experimental

1,4-Pentadien-3-one-1,5-dicarboxylic acid.—Furanacrylic acid 4.8 g. was suspended in a mixture of 40 cc. 35% aqueous hydrogen peroxide and 5 cc. conc. hydrochloric acid, and the vessel was kept for five days in water at room temperature (about 28°), when orange crystals were formed at the bottom. The cyrstals were filtered and washed with methanol to remove unchanged furanacrylic acid. Yield, 2.2 g. From the filtrate was obtained 0.3 g. of the acid by concentration on the water-bath. The resulting acid was dissolved in boiling water, decolourized by active charcoal and crystallised in pale yellow hexagonal plates on cooling. It melted at 236° with decomposition.

	H	C
Anal. Calcd. for $C_7H_6O_5$:	3.55	49.39
Found:	3.53	49.38

When the acid dissolved in a mixture of phenylhydrazine and acetic acid was left overnight, the phenylhydrazone crystallised out. It formed red needles by recrystallisation from a mixture of methanol and water; m. p. 182-3°.

	H	C	N
Anal. Calcd. for $C_{13}H_{12}O_4N_2$:	4.61	59.97	10.76
Found:	4.52	59.48	10.56

1,4-Pentadien-3-one-1,5-dicarboxylic acid methyl ester.—0.5 g. of the acid was esterified by refluxing for thirty minutes with 3 cc. methanol and 0.2 g. conc. sulfuric acid. On cooling the whole the methyl ester was separated out and recrystallised in pale greenish yellow needles from ethyl acetate; m. p. 171-2°.

	H	C
Anal. Calcd. for $C_9H_{10}O_5$:	5.08	54.52
Found:	5.01	54.57

Its phenylhydrazone was obtained by the same method as the acid, and recrystallised from methanol; lustrous yellow leaflets; m. p. 153-4°.

	H	C	N
Anal. Calcd. for $C_{15}H_{16}O_4N_2$:	5.59	62.45	9.71
Found:	5.25	62.11	9.48

3-Pentanone-1,5-dicarboxylic acid (γ-ketopimelic acid).—To the 20 cc. aqueous solution of the 1 g. acid neutralised by sodium carbonate, was added 0.2 g. aluminium amalgam and left at room temperature for a day. After filtering off aluminium hydroxide, the filtrate was acidified with hydrochloric acid and evaporated to dryness on the water-bath. From the residue, γ-ketopimelic acid was extracted with methanol and recrystallised from a mixture of methanol and chloroform. Yield, about 0.1 g., m. p. 142-3°.

	H	C
Anal. Calcd. for $C_7H_{10}O_5$:	5.79	48.25
Found:	5.57	48.25

Oxidation of 1,4-pentadien-3-one-1,5-dicarboxylic acid.—To 1.7 g. of the acid suspended in 50 cc. water was added drop by drop with stirring at about 15° a potassium permanganate solution which consisted of 5 g. potassium permanganate and 70 cc. water. After about thirty minutes, the reaction was over. The reaction mixture was filtered, neutralised with acid, concentrated on the water-bath and shaken up with ether upon acidification. From the ether solution were obtained two compounds. The one was soluble in water and melted at 100-1°. Yield, 0.1 g.. The mixed melting point of oxalic acid with it showed no depression. The other was insoluble in water and melted at 275° in a sealed tube. Yield, 0.1 g. It was identified with fumaric acid.

	H	C
Anal. Calcd. for $C_4H_4O_4$:	3.47	41.36
Found:	3.73	41.39

Photochemical changes of 1,4-pentadien-3-one-1,5-dicarboxylic acid and its methyl ester.—The methyl ester placed in a covered glass vessel was exposed to direct sunlight for a few hours with frequent stirring. The pale greenish yellow crystals of methyl ester changed into a white powder. It was recrystallised in colourless rhombs from ethyl acetate and melted at 239° with decomposition as reported by Straus. Similarly, the acid changed into a hygroscopic white powder by exposure to direct sunlight. The recrystallisation was unsuccessful. It melted at about 221° with decomposition.

	H	C
Anal. Calcd. for $C_7H_6O_5$:	3.55	49.39
Found:	3.87	48.59

0.5 g. of the acid sufficiently exposed to sunlight was esterified by refluxing for thirty minutes with 3 cc. of methanol and 0.3 g. of conc. sulfuric acid. The methyl ester crystallised out and was recrystallised from ethyl acetate. It formed colourless rhombs and melted at 237° with decomposition.

	H	C
Anal. Calcd. for $C_9H_{10}O_5$:	5.08	54.52
Found:	4.86	54.00

The mixed melting point of this methyl ester and the photochemically changed methyl ester showed no depression.

Summary

2-Furanacrylic acid gave 1,4-pentadien-3-one-1,5-dicarboxylic acid in a fairly good yield by treatment with aqueous hydrogen peroxide containing hydrochloric acid. This acid underwent the same photochemical change by direct sunlight as its methyl ester.

This acid was reduced to γ-ketopimelic acid by aluminium amalgam, and oxidised to fumaric and oxalic acids by potassium permanganate. It is assumed that the two double bond have the trans structure. The phenylhydrazones of the acid and the methyl ester were obtained.

The Scientific Research Institute, Tokyo

The Visible Absorption Spectra and Binding Energy of Quinhydrone-Type Molecular Compounds

By Hiroshi TSUBOMURA

(Received February 17, 1953)

Introduction

Although quinhydrone and homologous molecular compounds have been well known for many years, the nature of the intermolecular binding force has not yet been thoroughly clarified. Recently, some interesting results concerning this problem have been obtained. Osaki and Matsuda[1] have, through the analysis of the x-ray pattern of quinhydrone crystal, determined the structure of this compound. K. Nakamoto[2] observed the dichroism of the visible absorption spectra of quinhydrone crystal, and found that "the spectrum by the light with the electric vector abundant with the parallel component to the benzene ring is more bathochromic and hyperchromic than the one with the electric vector abundant with the perpendicular component to the benzene ring". Seki and others[3] determined the heat of formation of quinhydrone from its component-molecules as 5.39 kcal./mol. by the measurements of the heat of solution and the vapor pressure. This would be the first reliable experimental data of the binding energy of this compound.

The present author has determined the heat of association of quinhydrone and some homologues in dilute solutions by measuring quantitatively the absorption spectra of the solutions of quinone and the compounds which combine with it (in this research, hydroquinone, dimethylhydroquinone and phenol, hereafter called B compounds) in various concentrations and temperatures. The visible absorption spectra of these systems in various concentrations were measured by L. Michaelis and S. Granick. They treated the results with the theory of chemical equilibrium and reported that the molecular compounds in solutions are in a dimeric form, $Q_1 \cdot B_1$, without regard to their compositions in the solid state. However, they had no intention of deriving the heat of association from these measurements, though the determination of these values is, in principle, possible.

In the second part of this paper, a structure of these molecular compounds will be proposed on the basis of some experimental knowledge concerning these compounds. On this assumed structure, the origin of the binding force and the visible absorption spectra of these molecular compounds are discussed.

Part I. The Determination of the Heat of Association in Solution by the Measurements of the Visible Absorption Spectra

Principle of the Experiment

The principle of deriving the experimental equilibrium constant of association and the molecular extinction coefficient of the molecular compound is the same as that which was employed by Benesi and Hildebrand.[5] Namely, if we designate the total molar concentration of quinone and a B compound by c^0_Q and c^0_B, the extinction coefficient of the molecular compound by d_X, and its molecular extinction coefficient by ε_X, then the linearity relation

$$c^0_Q/d_X = 1/(K \cdot \varepsilon_X \cdot c^0_B) + 1/\varepsilon_X \qquad (1)$$

(1) Osaki and Matsuda, *Acta Cryst.* (to be published). Their results were quoted in Nakamoto's paper (ref. (2)).

(2) K. Nakamoto, *J. Am. Chem. Soc.* **74**, 1738 (1952).

(3) S. Seki, *Kagaku*, **22**, 416 (1952). Detailed information will be published in the near future in this bulletin.

(4) H. A. Benesi and J. H. Hildebrand, *J. Am. Chem. Soc.*, **71**, 2703 (1949).

holds between (c^0_Q/d_λ) and $(1/c^0_B)$, if the equilibrium is expressed by the formula $Q+B \rightleftarrows QB$ and if $c^0_Q \ll c^0_B$. We found that equation (1) really holds for all molecular compounds we investigated, agreeing with Michaelis' results. Then, we can calculate the equilibrium constant K and the molecular extinction coefficient ε_λ using the least square method.

Since quinone, unfortunately, has absorption in the visible region, it is necessary to select some wave lengths which are most suitable for the experiment, i. e., wave lengths, in which the absorption of the molecular compound is sufficiently strong and the absorption of quinone is negligibly small. In the case in which the absorption of quinone is not small enough to be ignored even in the most suitable region of wave length, d_λ was calculated by the formula

$$d_\lambda = d_{obs} - d'_Q - d^0_B \qquad (2)$$

where d^0_Q and d'_B are the absorption of the total quinone and the B compound present in the solution including those which are associated. These d^0_Q and d^0_B were calculated from the molecular extinction coefficients of these compounds in a free state and their concentrations in each ternary system.* Of course, we should use d_Q and d_B that are the absorption of free quinone and the B compound present in the system instead of the d^0_Q and d^0_B. However, the small magnitude of d^0_Q and d^0_B as compared to d_λ and the small degree of association of the molecular compounds reasonably permit the approximation.

The heat of association ΔH can be determined from the equilibrium constants at two different temperatures by use of the following formula

$$\Delta H = -RT_1 \cdot T_2/(T_1-T_2) \cdot \ln K_1/K_2 \qquad (3)$$

Experimental

Spectrophotometric measurements were made with the Beckman spectrophotometer, Model DU.

The solvent used should have the following properties:

1. Its absorption in the visible region is negligible.
2. It dissolves considerable amounts of the compounds under the investigation.
3. It has no particular influence on the association of the molecular compounds.

Cyclohexane was used as a solvent which generally fulfills these conditions. However, only for the case of quinone-hydroquinone system, 0.05M. aqueous solution of hydrogen chloride was used, since hydroquinone is quite insoluble in cyclohexane. It is known that hydroquinone dissolved in water is a little unstable under the contact of air. However, we can believe that this compound remained unchanged in such a dilute acid as above mentioned during the spectrophotometric measurements, because it was verified that the ultraviolet absorption spectrum of this compound in such a solution did not change at all for at least 30 hours.

The method of purification of cyclohexane and phenol was described elsewhere.[6] Quinone was synthetized by the oxydation of hydroquinone by sodiumbichromate,[7] and recrystalized several times out of benzene (m. p. 114—115°C). Hydroquinone was recrystalized from mixtures of benzene and methanol (m. p. 172—173°C). Dimethylhydroquinone was recrystalized from methanol (m. p. 56.0—56.2°C). The ultraviolet absorption spectra of all these compounds were checked before experiment and identity of them with the results described in literatures was confirmed.

During the measurement of absorption, the constancy of the temperature of the samples was maintained by use of a thermospacer equipped in the spectrophotometer (±1°C). Stoppered cells, which were 1 cm in width, were used.

Results

The approximate ranges of the concentrations of quinone and the B compounds in each spectrophotometric measurements were given in Table 1. These ranges of concentration were chosen so that the extinction coefficients of the ternary systems at the optimum wave lengths lie between 1 and 2. In order to apply Eq. (1), the concentration of the quinone were always made below 10% of that of the B compounds. This also decreases the error due to the visible absorption of quinone.

Table 1

	concn. of quinone	concn. of B
1	0.0033 M	0.05—0.46 M
2	0.0045 M	0.06—0.4 M
3	0.003 M—0.007 M	0.15—1.2 M

1: quinone-hydroquinone system
2: quinone-phenol system
3: quinone-dimethylhydroquinone system

For the purpose of testing the accuracy of the values derived, the same experiments were made for more than two wave lengths. The results were shown in Table 2. Since in the cases of the quinone-phenol and quinone-dimethylhydroquinone systems the attempt to derive ε_λ's for the higher temperatures was unsuccessful, ε_λ's for the lower temperatures were used in the calculation of K's for the higher temperatures, by the assumption that there is no great difference between ε_λ's foe these two temperatures respectively. Although the values given in this table

* In this calculation, it was assumed that the absorption spectra of quinone and the B compounds are not shifted from those in a free state. This assumption is necessary, bnt, strictly speaking, is not in general true. For example, hydrogen-bonding between quinone and a B compound may cause a slight shift of their spectra.

(5) H. Tsubomura, *J. Chem. Soc. Japan*, **73**, 920 (1952).
(6) Organic Syntheses, **1**, 469.

Table 2

The ε_1, K_1 and the ε_2, K_2 correspond to the data for lower and higher temperatures respectively

B compound	wave length (in mμ)	ε_1	ε_2	K_1	K_2	K_1/K_2	ΔH (kcal./mol.)
hydroquinone	500	630	730	1.01	0.49	2.1	4.8
	520	510	600	1.10	0.46	2.4	5.7
phenol	330	1180	1180	1.23	0.71	1.7	4.4
	350	1110	1110	1.11	0.57	1.9	5.0
	400	850	850	1.06	0.56	1.9	5.0
dimethyl-hydroquinone	380	340	340	0.51	0.30	1.7	4.2
	390	310	310	0.69	0.43	1.6	3.8
	400	355	355	0.61	0.43	1.4	2.7

Table 3

B compound	solvent	K_1 (t°C)	K_2 (t°C)	K_1/K_2	ΔH (kcal./mol.)	λmax (mμ)	εmax
hydroquinone	0.05 M HCl aq. solution	1.06 (20°)	0.48 (49°)	2,2	5.2	440	890
phenol	cyclohexane	1.13 (16°)	0.61 (39°)	1.9	4.8	315	1200
dimethyl-hydroquinone	cyclohexane	0.60 (25°)	0.39 (49°)	1.6	3.5	413	370

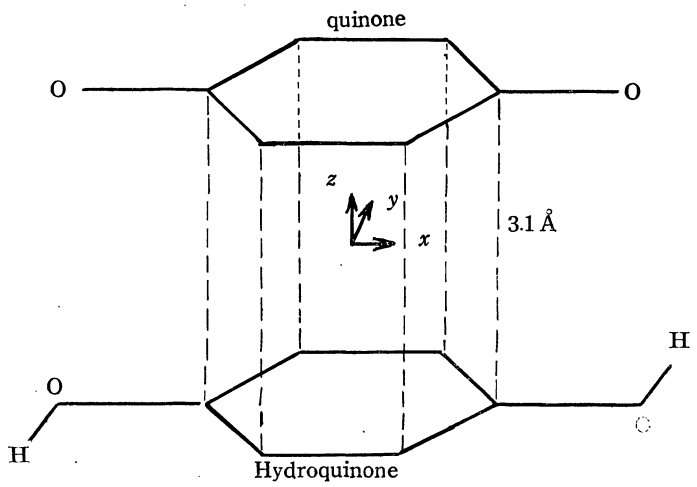

Fig. 1.

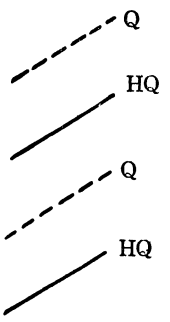

Fig. 2

are not perfectly accurate, it may be regarded that they show us the general trends of the binding energies and the absolute intensities of the visible absorption of these molecular compounds. The average values of K_1, K_2, K_1/K_2 and ΔH, with λmax and εmax which were obtained from the measurements of the whole spectra were given in Table 3.**

Detailed discussion on these results will be given in the second part of this paper with the theoretical treatment of these molecular compounds.

** It is to be noted here that we should be careful in comparing the heat of association of quinone-hydroquinone system with that of quinone-phenol system because these two were measured in different solvents.

Part II. Theory of the Intermolecular Binding Energies and the Electronic States of Quinhydrone and Homologous Molecular Compounds

The molecular structure of quinhydrone and homologues

As previously mentioned, quinhydrone and homologous molecular compounds in dilute solutions are of the form $Q_1 \cdot B_1$. We assume the structures of these associated molecules as those in which two benzene rings are piled up so that one ring is situated just above the other and the planes of these two rings are parallel. For example, the structure of quinhydrone is assumed as given in Fig. 1.

The basis of this assumption is as follows: The

occurance of a new visible absorption in these molecular compounds shows that there is considerable electronic interaction between molecules. Therefore, the structure of the molecular compound must be assumed in such a way as to make an electronic interaction between molecules possible. The structure shown in Fig. 1 will correspond to the strongest electronic interaction and smallest steric repulsion between two component-molecules. On the other hand, the X-ray analysis of Osaki and Matsuda shows that, in the quinhydrone crystal, the quinone and hydroquinone molecules are piled up one upon another in a way shown in Fig. 2; this structure differs from the one shown in Fig. 1 in that the benzene ring of, e. g., quinone is not situated just above the benzene ring of, e. g., hydroquinone. It may be conceived that this deformation is caused by the complicated interacting forces between every atom in the crystal. However, in a dilute solution, where the quinhydrone molecules are separated from each other, there is no reason for the centers of the two benzene rings not to lie on a common normal.

Here, a note on the binding state of the hydrogen atom in quinhydrone should be given. M. Davies[6] measured the infrared absorption spectra of quinhydrone crystal in the 3 μ region and found a peak at 3.10 μ corresponding to the hydroxyl stretching mode. Applying Badger's rule, he was lead to the conclusion that the hydroxyl bond distance is about 1.0Å, which is nearly the same as that of alcohol. According to his results, it is reaonably accepted that the two hydrogen atoms in quinhydrone are definitely bonded to the oxygen atoms, and it is improbable that a peculiar valency state exists in which the hydrogen atoms are equally bonded to the two molecules. In other words, quinhydrone is made up of quinone and hydroquinone molecules which are mutually perturbed.

The nature of the binding energies of quinone and the B compounds

It can be definitely concluded that hydrogen bonding is not a substantial cause of the binding of quinone and the B compounds, from the fact that some compounds which have no group acting as a proton donor, e. g., dimethylhydroquinone, can also combine with quinone.

If we assume the structures of the molecular compounds to be as shown in Fig. 1, it will be clear that a hydrogen bond is unable to form between two component-molecules. For the hydroxyl group in a normal hydroquinone or phenol lies in the plane of benzene ring and, therefore, is nearly perpendicular to the line connecting the two oxygen atoms of quinone and hydroquinone or phenol. It is evident that in such a structure a hydrogen bond cannot be formed, since this bond is believed to be mainly electrostatic. If the hydrogen atom of hydroquinone elevates itself from the plane of the ring, hydrogen bond would be formed. However, in this case the conjugation of the lone pair electron of oxygen with the benzene π-electrons which give rise to a considerable stabilization of the hydroquinone molecule would be destroyed. Of course, it is supposed that there are hydrogen-bonded quinone and hydroquinone or phenol molecules in a dissolved state. However, the hydrogen bond will probably be formed between molecule-pairs which, different from those of which molecular compound is composed, are situated in such a manner as shown in Fig. 3. We can suppose that the electronic interaction

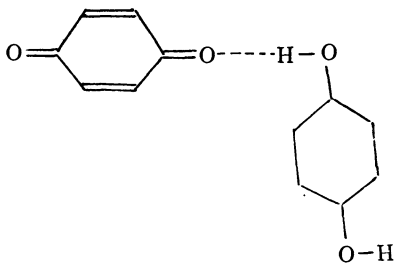

Fig. 3.

between these hydrogen-bonded molecules is negligibly small, and therefore the visible absorption spectra cannot arise from them. As the heat of association given in Table 3 is derived from visible absorption spectra, and the formation of a hydrogen bond is supposed not to disturb that of quinhydrone, we may conclude that the energy of the hydrogen bond is not included in the heat of association given in Table 3.

Briegleb and others[9] have laid stress on the so-called "Dipolinduktions-effekt" in interpreting the association of aromatic nitro-compounds and aromatic hydrocarbons. They insisted that this dipole-induction effect, together with the dispersion force which is an intermolecular binding force working more or less between every pair of molecules, are the main causes of binding in these molecular compounds. It seems, however, that this theory cannot fully explain the intermolecular binding force of quinhydrone.

The author calculated roughly the energy contribution of the dipole-induction effect for quinhydrone based on the molecular structure shown in Fig. 1. It consists mainly of the force between the dipole of the carbonyl group of quinone (about 3.8 *D*) and that of hydroquinone induced by it, and is estimated as about -1 kcal./mol. On the other hand, the interaction between permanent dipoles of quinone and hydroquinone is estimated to be about $+0.8$ kcal./mol., and almost cancels the energy of attraction of the dipole-induction effect. Also, there seems to be no reason why

(7) M. Davies, *J. Chem. Phys.*, **8**, 577 (1940).

(8) G. Briegleb, "Zwischenmolekulare Kräfte und Molekülstruktur", Ferdinand Enke, Stuttgart, 1937, p. 104.

the dispersion force between quinone and the *B* compounds should be particularly greater than those between others which are known to make no molecular compounds.* Moreover, the dipole-induction effect, or other electrostatic interaction cannot explain the change of the absorption spectra with the formation of the molecular compounds.

Theory of electronic interaction

The measurements of the static dielectric polarization of benzene-iodine mixtures,[10] or other similar systems[11] strongly suggest that the intermolecular binding of these molecular compounds is of some kind of a coordination linkage, that is, the molecular compounds are made up of two molecules, one of which has a low ionization potential and the other has a strong electron affinity, and an electron of the former is partially transferred to the latter, forming an intermolecular covalent bond. R. S. Mulliken[12] formulated this idea using the quantum-mechanical resonance theory and explained the absorption spectra of the molecular compounds. In order to test whether this theory is applicable to the quinhydrones or not, the author made a semi-quantitative treatment of the electronic states of these molecular compounds using molecular orbital method, and compared the results with absorption data.

To proceed the theoretical analysis, it is first necessary to know the electronic states of free quinone and the free B compounds. Among the electronic orbitals of quinone and B compounds, only π-orbitals are important here because the intermolecular interaction between the σ- and inner shell orbitals of quinone and the *B* compounds are far smaller than those between π-orbitals. First, the quinone-hydroquinone system is discussed.

Quinone-hydroquinone system

The π-molecular orbitals of quinone and hydroquinone constructed by the linear combination of $2p\pi$-AO's of carbon and oxygen atoms have been calculated by Nagakura and Kuboyama[13] with a simple LCAO method, using resonance integrals and coulomb integrals which are suitably made self-consistent.** The energy levels of the MO's derived by them are given in Fig. 4. Quinhydrone belongs to the symmetry group C_{2v} in our assumed structure, and therefore there are four

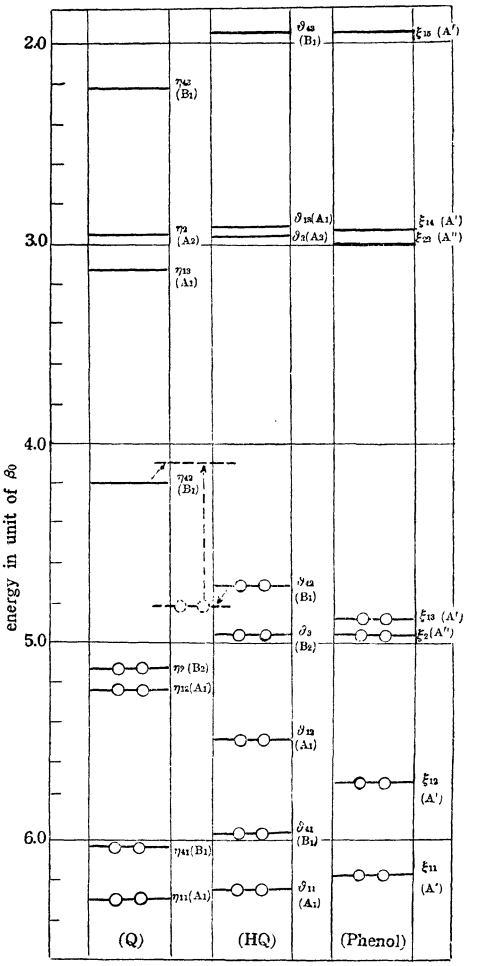

Fig. 4.—The energy levels of MO's of quinone, hydroquinone and phenol

irreducible representations A_1, A_2, B_1 and B_2.[14] The names of the irreducible representations to which each MO belongs are also given in Fig. 4. It is to be noted that the MO's of quinone and hydroquinone are very much alike since these are constructed by AO's which are similar in position as well as in number, the only difference between these two molecules being that an oxygen atom of hydroquinone has two π-electrons while that of quinone has but one. As a result, the MO of hydroquinone denoted as ϑ_{42} in Fig. 4 is a filled orbital, while the corresponding MO of quinone denoted as η_{42} is an empty one, and this difference gives slight modifications of all MO's of the one molecule as compared to the latter. Now, it can be supposed easily from experimental evidences that, relatively speaking, hydroquinone has a low ionization potential and quinone has a

* Here, we regard the dispersion force as expressible in the formula of $U=-I_1 \cdot I_2/(I_1+I_2)\times(\sigma_{1\,2})\times 3/2R^6$,

(9) F. Fairbrother, *J. Chem. Soc. (London)*. **1948**, 1051.

(10) J. Weiss and H. Kronberger, *J. Chem. Soc. (London)*, **1942**, 245.

(11) R. S. Mulliken, *J. Am. Chem. Soc.*, **74**, 811 (1952).

(12) S. Nagakura and A. Kuboyama (*unpublished results*).

** The same method was used in the calculation of the energy levels of furan, pyrrole and thiophen. See, "S. Nagakura and T. Hosoya, This Bulletin, **25**, 179 (1952)".

(13) Here the notations are the same as those used by Eyring et al. See, "Eyring, Walter and Kimball, Quantum Chemistry, Appendix VII". The operation σ_v is taken as the reflection in the plane including four oxygen atoms.

strong electron affinity. This corresponds to the fact that the difference between the energies of ϑ_{42} and η_{42} is small. (See, Fig. 4). In addition, these two orbitals belong to the same irreducible representation in the over-all symmetry of the molecular compound. From these facts, it can be seen that an intermolecular conjugation between ϑ_{42} and η_{42} (which results an partial migration of an electron that is originally occupying ϑ_{42} to η_{42}) is easily produced. And, in the first approximation, only the consideration of this conjugation is sufficient in the treatment of the intermolecular conjugation as a whole.

The reason for this is given briefly as follows: Since migration is possible only between two MO's belonging to the same irreducible representation, we can see that the following intermolecular migrations of electrons from hydroquinone to quinone may be possible,

$$\vartheta_{42}\rightarrow\eta_{43},\ \vartheta_{41}\rightarrow\eta_{42},\ \vartheta_{12}\rightarrow\eta_{13},\ \text{etc.}$$

But these migrations are thought to be far less possible than that of $\vartheta_{42}\rightarrow\eta_{42}$, because in such cases the energy difference between MO's are much greater than that between ϑ_{42} and η_{42}. Next, we should note that intermolecular conjugations may occur between two filled orbitals of hydroquinone and quinone, e. g., ϑ_3 and η_3, ϑ_{12} and η_{12} etc. However, such conjugations between filled orbitals produce no effect but an increase of total electronic energy, which, as Parr and Mulliken have pointed out,[14] is attributable to the exchange repulsion between molecules.

Now we can set up the total electronic wave function of quinhydrone in the ground state as an anti-symmetrized product of one-electron MO's.

$$\begin{aligned}\Psi_g = n_g(18!)^{-1/2}\sum_{\nu}(-1)^{l}\,\mathrm{P}\,&\eta_{11}(1)\eta_{11}(2)\eta_{12}(3)\eta_{12}(4)\\ &\cdots\cdots\vartheta_{11}(9)\vartheta_{11}(10)\vartheta_{12}(11)\vartheta_{12}(12)\ \cdots\cdots\\ &\phi_g(17)\phi_g(18)\times\alpha_1\beta_2\alpha_3\beta_4\cdots\cdots\alpha_{17}\beta_{18}\end{aligned}\qquad(4)$$

$$\phi_g(\nu)=a_0\vartheta_{42}(\nu)+b_0\eta_{42}(\nu)\qquad(5)$$

Since a complete treatment of the MO's including eighteen electrons is extremely difficult, we are ought to be satisfied by a simple approximation in which the energy of the migrating electrons is expressed as

$$E(\nu)=\int\phi(\nu)H_\nu\phi(\nu)d\tau_\nu\qquad(6)$$

Here, H_ν is the total hamiltonian for the migrating electron including the kinetic energy operator of an electron, the potentials of atomic cores and other electrons. Then, the minimization of $E(\nu)$ leads to the secular equation,

$$\begin{vmatrix} W_{42}-E & \beta \\ \beta & W'_{42}-E \end{vmatrix}=0\qquad(7)$$

where W_{42} and W'_{42} are the coulomb integrals of the MO ϑ_{42} and η_{42}, respectively, and β is the resonance integral over them. Solving (7), we get the lower and upper roots, E_g and E_e;

$$E_{g,\,e}=(W_{42}+W'_{42})/2\pm\{(\Delta W/2)^2+\beta^2\}^{1/2}\qquad(8)$$

in which, $\Delta W=W'_{42}-W_{42}$. a_0 and b_0 can be immediately calculated from E_g. We get another wave-function ϕ_e corresponding to the upper level, E_e. This is approximately given by the following formula.

$$\phi_e=b_0\vartheta_{42}-a_0\eta_{42}\qquad(9)$$

As is shown lately, a_0 is nearly one and b_0 is far smaller than a_0. Hence, it can be said that ϕ_g is much alike to ϑ_{42} and ϕ_e is much alike to η_{42}. Therefore, if we assign the visible absorption of quinhydrone to the transition from ϕ_g to ϕ_e, it has the character of an intermolecular charge-transfer spectra and agrees with Nakamoto's experimental results (ref. (2)). Other transitions of this molecular compound which have the electric moment normal to the benzene rings cannot be found in this region of wave length.

Next, we will calculate the transition moment of this transition. The total electronic wave function of quinhydrone in the singlet excited state is given in a way similar to (4).

$$\begin{aligned}\Psi_e = n_e(18!)^{-1/2}\sum_{\nu}(-1)^{p}\,\mathrm{P}\,&\eta_{11}(1)\eta_{11}(2)\eta_{12}(3)\eta_{12}(4)\\ &\cdots\cdots\vartheta_{11}(9)\vartheta_{11}(10)\vartheta_{12}(11)\vartheta_{12}(12)\ \cdots\cdots\\ &\phi_g(17)\phi_e(18)\times\alpha_1\beta_2\alpha_3\beta_4\ \cdots\cdots\\ &(2)^{-1/2}(\alpha_{17}\beta_{18}-\alpha_{18}\beta_{17})\end{aligned}\qquad(10)$$

The transition moment μ is, for definition, given by

$$\mu=e\int\Psi_e^*\Big(\sum_{\nu yz}x\Big)\Psi_g d\tau\qquad(11)$$

As a result of calculation, μ is approximately given by

$$\mu\fallingdotseq ea^3{}_0b_0R/\sqrt{2}\qquad(12)$$

in which R being the distance between two molecules. From (8), we can see that a_0 and b_0 depend on β and ΔW. Since resonance integrals are in many cases proportional to the corresponding overlap integrals, we calculated the overlap integral between ϑ_{42} and η_{42} in order to know the magnitude of β. This can be expanded in terms of overlap integrals between AO's and can be easily calculated. If we use Slater type AO's with screening constants $z_c=3.25$, $z_o=4.55$, the result was 0.043. Then, we calculate β from the resonance integral β_0 and the overlap integral s_0 between two adjacent carbon atoms of benzene in the following way,***

(14) Parr and Mulliken, *J. Chem. Phys.*, **19**, 1273 (1951).

*** Such a procedure is often used in the calculation of the resonance integrals between two π-orbitals. Though we are here dealing with resonance integrals between two σ-orbitals, the situation is conceivable to be nearly the same.

Table 3

(The unit of W's is in β_0)

ΔW	$\Delta E(=E_e-W'_{42})$	a_0	b_0	μ_{calc}	E_e-E_f	f_{obs}	μ_{obs}
$\beta=0.2\,\beta_0$							
0.5	0.070	0.945	0.331	2.94 D	0.64 (6800 Å)	0.014	1.14
0.7	0.055	0.963	0.265	2.49 D	0.81 (5370 Å)		
0.9	0.044	0.978	0.216	2.13 D	0.99 (4390 Å)		
1.1	0.035	0.985	0.172	1.73 D	1.17 (3720 Å)		
$\beta=0.1\,\beta_0$							
0.9	0.012	0.992	0.119	1.22 D	0.92 (4740 Å)		

$$\beta=\beta_0\times s/s_0$$

we get $\beta=0.17\,\beta_0$. It was suggested by Mulliken and others that the overlap integral between bonded atoms or molecules is supposed to be greater than that which is calculated from the Slater AO's. Therefore, in this case, we tentatively assume that β is the order of $0.20\,\beta_0$. The estimation of ΔW is also difficult. But, fortunately, the variation of this does not influence the transition moment significantly. We estimated that it lies in a region from 0.5 to $1.0\,\beta_0$*, and calculated various a_0, b_0 values using various ΔW in this region. From these values, the transition moment μ can be calculated. On the other hand, experimental oscillator strength was calculated from the absorption data in solution using the following formula,

$$f_{obs}=(nc^2m/N\pi e^2)\times 10^3\int\varepsilon d\nu^{(15)}\fallingdotseq 0.1875\times 10^{-8}n\varepsilon_{max}\cdot\Delta\nu \quad (13)$$

in which n is the index of refraction of the solution and $\Delta\nu$ is the distance between two points in the absorption curve at which the intensity is half the maximum value. Applying the Lorentz-Lorenz correction to this,[16] we can get f_{obs} in gaseous state, and from it the μ_{obs} can be calculated. The calculated and experimental μ's are given in Table 3. The transition energy depends mainly on ΔW, and the value of ΔW which gives a transition energy most close to the experimental one is seen to be $0.9\,\beta_0$. For reference, the oscillator strengths using $\beta=0.10\,\beta_0$ are also given using $\Delta W=0.9\,\beta_0$. These results show that the charge transfer spectra proposed here may have sufficiently strong oscillator strength to be correlated with the values experimentally obtained.

Although it is dangerous to refer to the total π-electronic energy of the molecular compound from the simple MO theory, it can be supposed that this intermolecular conjugation between filled and unfilled MO's will produce a decrease of electronic energy. If this is true, such a decrease of electronic energy by intermolecular conjugation will be the most characteristic part of the intermolecular binding energy of these molecular compounds.

Other quinhydrone-type molecular compounds

The π-electronic state of dimethylhydroquinone is quite similar to that of hydroquinone. Hence, we can expect that the π-electronic interaction between quinone and dimethylhydroquinone is also quite similar to that of quinone-hydroquinone system. From the experimental results shown in Part I., it can be seen that the molecular compound of dimethyl hydroquinone has a considerably lower absorption intensity and binding energy than that of hxdroquinone. This can be understood in the following way. The intermolecular distance of this molecular compound is supposed to be made larger than in the case of hydroquinone because the methyl group will considerably increase the steric repulsion between molecules. The resonance integral between ϑ_{42} and η_{42} will become smaller owing to the large intermolecular distance, and this will decrease the intensity of the charge transfer spectra and the charge transfer force.

In order to discuss the case of quinone-phenol molecular compound, we should know the electronic state of phenol. The author calculated the LCAO MO energy levels of phenol by use of the same method as was adopted in the calculation of quinone and hydroquinone. The energy levels obtained are given also in Fig. 4. We assume that the symmetry group of quinone-phenol molecular compound is C_{1h} (see, ref. (14)), that is, it has only one plane of symmetry (xz plane in Fig. 1). The names of the irreducible representations to which the MO's of phenol belong in the overall symmetry of the molecular compound are given in Fig. 4. On the other hand, the irreducible representations of the MO's of quinone written in Fig. 4 are transformed in this case in the following way,

$$A_1,\ B_1 \rightarrow A',\quad A_2,\ B_2 \rightarrow A''.$$

As a result, the highest filled MO of phenol, ξ_{13}, and the lowest unfilled MO of quinone, η_{42}, belong to the same irreducible representation in the C_{1h}

* The ΔW calculated as the energy difference between η_{42} and δ_{42} in Fig. 4 is $0.5\beta_0$. On the other hand, the electron affinity for η_{42} orbital was calculated to be about 8.0 ev., with a method similar to that employed by Sklar[16] in the calculation of the electron affinity of benzene ring of substituted benzens. This corresponds roughly to $\Delta W=1.0\beta_0$.

(15) A. L. Sklar, *J. Chem. Phys.*, **7**, 992 (1939).

symmetry of the molecular compound. From the stand-point analogous to that in the former discussions, we may conclude that, in this molecular compound, the conjugation between ξ_{13} and η_{42} is predominant. By the calculation of the AO coefficients of the MO's of phenol, we can see that the AO coefficients of ξ_{13} are very much like those of ϑ_{42} in hydroquinone and therefore it is conceivable that the overlap integral between ξ_{13} and η_{42} is of nearly the same magnitude as that between ϑ_{42} and η_{42}. The calculated value of the former integral is really 0.040, in close agreement with the latter. Hence, we may expect that the resonance integral between ξ_{13} and η_{42} is also as large as that between ϑ_{42} and η_{42}. The ionization potential of phenol is supposed to be larger than that of hydroquinone, because the energy level of the highest filled orbital of phenol is lower than that of hydroquinone. Hence, ΔW in quinone-phenol system is expected to be larger than that of quinone-hydroquinone system. The change of ΔW, however, does not influence the absorption intensity seriously as was previously stated. Therefore, we deduce that the absorption intensity of quinone-phenol system is of the same order of magnitnde with that of quinone-hydroquinone system. Also, the charge transfer force as a contribution of the binding energy in this molecular compound is expected to be the same as quinone-hydroquinone system. However, as the change of ΔW directly changes the transition energy, we should expect that the peak wave-length of quinone-phenol system will be shorter than that of quinone-hydroquinone system. These considerations agree with experimental results.

Summary

The absolute intensities of the visible absorption spectra and the binding energies of quinhydrone-type molecular compounds have been determined by the measurements of their absorption intensities in solutions. The visible absorption spectra of these molecular compounds can be explained as the charge-transfer spectra of the π-electrons of quinone and the B compounds. The intensity of these charge-transfer spectra can be calculated roughly by setting up linear combination of the lowest unfilled MO of quinone and the highest filled MO of the B compound, and the results agree qualitatively with the experimentally derived absorption oscillator strengths. This charge-transfer resonance is thought to be the most characteristic part of the intermolecular binding energy in these molecular compounds.

The author's sincere thanks are due to Prof. K. Kozima for his encouragement, and to Prof. S. Nagakura and Mr. A. Kuboyama who permitted the author to use the results of their calculation and the spectrophotometer of their laboratory.

Tokyo Institute of Technology,
Meguroku, Tokyo

The Separation of Isotopes by Countercurrent Gaseous Exchange Column. II. Experimental Tests of the Theory

By Kunihiko KIGOSHI

(Received February 18, 1953)

In order to test the theory developed in part 1, the isotope separation of carbon by the countercurrent gaseous exchange column was carried out by hot wire type thermal diffusion column. The isotopes used for this experiments are C^{12} and C^{14}, and the gaseous species for the exchange reaction are carbon dioxide and carbon monoxide. Taylor and Bernstein[1] had performed similar experiments on the separation of C^{13} and C^{12} but we need thorough investigation of this experiment and reliable data on the over-all separation factors for various filament temperatures.

Equilibrium constants for many isotopic exchanges have been studied by Urey and his co-workers[2]. The results of their calculation and the theory on the gaseous exchange column enable us to predict the possibilities of the high efficient isotope separations by the gaseous-chemical exchange method.

(1) R. B. Bernstein and T. I. Taylor, *J. Chem. Phys.*, **16**, 903 (1948).

(2) H. C. Urey, *J. Chem. Soc.*, 562 (1947); H. C. Urey and L. J. Greiff, *J. Am. Chem. Soc.*, **57**, 321 (1935).

Experimental Apparatus

Figure 1 is an illustration of the apparatus arrangement. The exchange column was constructed by a water jacketed glass tube of 12.7 mm. in diameter and 150 cm. long. The filament used in the experiments was a platinum wire of 0.7 mm. diameter and it was hung from the top of the column. The centering of the filament was made by five spacers of a small piece of nichrome wire. At the bottom of the column a 70 g. weight was attached to the end of the filament to keep the filament taut. Electrical contact was made by a steel rod (13 cm. long) which was attached to the weight keeping the contact to the mercury pool at the bottom of the column. Constant electric power supply for filament heating was obtained using a ballast tube which has a plateau of characteristic curve between 28~40 volt with 8.5 amp. Power regulation was made by two autotransformers F. T and S. T in Figure 1. When the voltage applied to the ballast tube was adjusted to proper value we could obtain an almost constant power supply for filament heating within the input voltage variations between 90~100 volt.

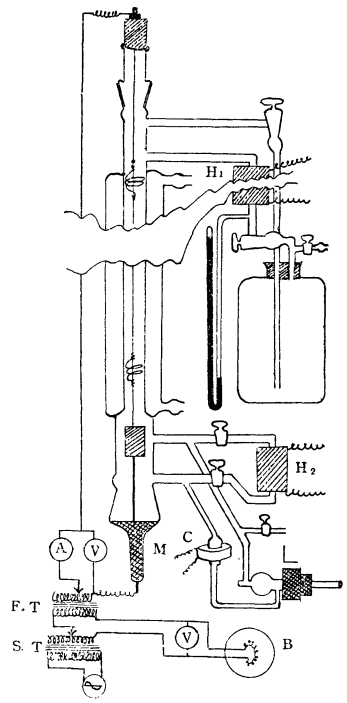

Fig. 1.—Experimental apparatus, H_1; electric furnace for circulation, H_2; Zn-reducer, C; gas circulation pump, M; mercury pool, L; Lauritsen electroscope, B; ballast tube, F. T. and S. T; autotransformers, A; ammeter, V; voltmeter

A top gas reservoir was a glass bottle of 22 l which was connected to the top of the column by two glass tubings. One of these was heated by an electric furnace in order let the gas in the reservoir flow to the top of the column. Flow velocity was measured in the preliminary experiments and we found that it was about 200 cc. per minute. To the bottom reservoir a zinc reducer was attached for reducing carbon dioxide to carbon monoxide. Temperature of the reducer was maintained to 400°C. by an electric furnace which was regulated by an automatic temperature regulator. The volume of the bottom gas reservoir was 250 cc. including the reducer and the ionization chamber of the Lauritsen type electrometer.

Carbon dioxide generated from sodium carbonate and sulfuric acid was introduced into the previously evacuated apparatus through two gas washing bottles with water. The active isotope C^{14} of two or three microcuries was previously mixed into the sodium carbonate used for the gas generation. It has been found by Brandner and Urey[3] that the water vapour or hydrogen is good catalysis for the isotopic exchange reaction between carbon dioxide and carbon monoxide. Increase of reaction velocity reduces the temperature T_b. Therefore we can expect the increase of separation factor by the presence of these gases. To saturate the water vapour in the bottom reservoir a little amount of water was introduced on the mercury pool. In all essential respects the details of operation of the separation column were the same as have been described by Bernstein and Taylor[1].

Measurements of Isotopic Ratio C^{14}/C^{12}

A concentration of C^{14} was measured by Lauritsen type electrometer having an ionization chamber of 160 cc. content. The gas of the bottom reservoir was circulated through the ionization chamber by a magnetically operated gas circulation pump with the flow velocity 30 cc. per minute. Ionization current produced by β-rays from C^{14} depends not only on the concentration of C^{14} but also the composition of gases in the ionization chamber. Therefore we have to know the relation between concentration of C^{14} and ionization current produced in the various mixtures of gases. Results on the measurements of ionization current of the Lauritsen electrometer at various compositions and pressure are represented in Figure 2. In these experiments the concentration of C^{14} was maintained constant (about 6 μc./mol.) and ionization current was expressed in div./sec. Pressure-ionization current curves for carbon dioxide and carbon monoxide showed similar variation. We obtained the similar curves for the mixtures of both gases although these were not represented in Figure 2. The linear dependences of ionization current on the composition of the mixture of two different gases are represented by curves 3 and 4 in Figure 2.

(3) J. D. Brandner and H. C. Urey, *J. Chem. Phys.*, **13**, 351 (1945).

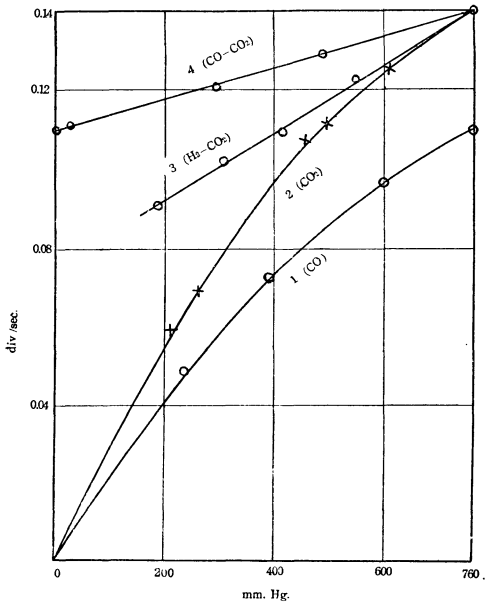

Fig. 2.—Pressure and composition dependence of ionization current with constant amount of C^{14}, Curve 1; pure CO, abscissa is total pressure. 2; pure CO_2, abscissa is total pressure. 3; H_2-CO_2 mixture, abscissa is partial pressure of CO_2 (total pressure is 760 mm. Hg.). 4; CO-CO_2 mixture, abscissa is partial pressure of CO_2 (total pressure is 760 mm. Hg.).

If we measure ionization current and pressure and composition of the samples using Figure 2 we can easily obtain the ionization current which would be observed if pure carbon dioxide is introduced under the standard pressure in the ionization chamber with the same amount of active isotope. The corrected ionization current thus obtained may be regarded to be proportional to C^{14} concentration, because a linear dependence of the ionization current on C^{14} concentration holds in a wide range of the concentration[4].

High content of hydrogen was observed in the bottom reservoir at the initial stage of the separation process. However after a few hours' operation, the hydrogen content in the bottom reservoir became less than 0.5 %, therefore the corrections to the measured activities were made only for carbon monoxide contents in the ionization chamber.

Results

Some of the typical changes of C^{14} concentration at the bottom reservoir are shown in Figure 3. We may see that the continuous operation of about fifty hours is ample time to obtain the equilibrium state. The estimation of the initial isotopic transport τ_0 was made by the initial increase of the heavy isotope in the bottom reservoir. The values of initial isotopic transport and over-all separation in the equilibrium states for various filament temperatures are tabulated in Table 1.

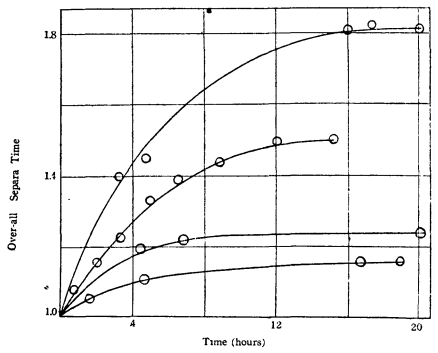

Fig. 3.—Dependence of over-all separation on time

Table 1

Run	$c_1(0)$	$c_1(Z)$	P mm.Hg.	T_2 °C.	S	τ_0/ν ×10⁷mol./sec. Obs.	Calc.
11	85.7	14.2	715	680	1.16	0.9~1.1	0.97
12	80.4	20.4	780	800	1.24	1.5~1.8	1.14
13	68.6	11.8	780	900	1.29		1.35
14	54.0	13.4	750	1100	1.64	2.2~2.5	1.90
15	93.0	30	755	650	1.19		0.95
16	75.0	24.2	746	1170	1.82	3.4~4.5	2.23
17	52	15	750	1130	1.68		2.05
18	85	21	772	1030	1.52	1.8~2.4	1.68
19	65.7	17.5	756	715	1.18	1.0~1.6	0.99
20	52.9	10.6	755	510	1.15		0.92

Values of isotopic transport, over-all separation and experimental conditions at final equilibrium states

$c_1(0)$ = CO% in the bottom reservoir,
$c_1(Z)$ = CO% in the top reservoir,
P = total pressure in the column,
T_2 = filament temperature,
S = over-all separation,
τ_0 = initial transport of C^{14} along the column,
ν = C^{14} concentration at the initial state

The filament temperature was measured by the thermal expansion of the filament. A linear expansion coefficient of 1.00×10^{-5} cm./cm., deg. for platinum wire was used for this measurement. This expansion coefficient was obtained from the measurements on the expansion of our platinum filament without any spacers. A platinum wire with 50~100g. weight at the end was hung outside the column and the temperature of electrically heated platinum wire was measured with optical pyrometer. The observed linear expansion coefficient was independent of the amount of weight

(4) F. C. Henriques, Jr., and C. Margnetti, *Ind. Eng. Chem.*, Anal. Ed., **18**, 417 (1946).

and was in accordance to other observations[5]. The uniformity of the temperature along the column was examined by optical pyrometer and we found almost uniform heating except the small regions (about 10 cm.) near the spacers at which the temperature was lower than other parts, but it did not exceed 100°C. Therefore the difference between measured temperature and maximum temperature of filament was ignored in our experiments.

Occasionally compositions of gases in the bottom and the top reservoirs were examined by ordinary gas analysis using few cc. of the samples. The bottom gas always contained 50~90 percent carbon monoxide and the required corrections on the activity measurements were made according to the measured gas compositions as described in the preceding section. Since the samples were small compared with the amount of gases in reservoirs, we ignored their effects on the time variation of isotopic concentration.

From the change of composition of the top reservoir we could obtain the net transport τ_1 of carbon monoxide along the tube. Observed value was $\tau_1=2.9\pm0.5$ cc./min. The results were insufficient in accuracy for the determination of τ_1. Perhaps the errors of the measurements were derived from the non-uniformity of gases in the top reservoir. Then in order to obtain an accurate value of transport we undertook the preliminary experiments. A well stirred bottom gas reservoir of two liters was filled by carbon monoxide at the initial states. The variations of the composition in this reservoir were measured during two or three hours' operations with the filament temperatures between 700 and 1000°C. We obtained $\tau_1=3.3\pm0.2$ cc./min. for these filament temperatures. The results were also not accurate enongh to obtain a dependence of τ_1 on the filament temperature, but rather good compared with the results from the top gas analysis; therefore we used $\tau_1=3.3$ cc./min. in our latter treatment.

Discussion of Results

In the theoretical consideration, the over-all separation of our experiments was given by the formula (51) in part 1. In this formula H_b/H was estimated by equation (54) which was valid only in the extreme case $r_2/r_1\to0$, but this approximation did not yield good results in the cases of our experiments. Therefore we had to use the original form of γ instead of the expression of γ described in equations (41). An exact expression of γ had been given by Furry and Jones[6] and the results of numerical calculation of γ for $r_1/r_2=18.2$, $T_2/T_1=10/3$, 11/3, 4, 13/3, 14/3 and 5 are illustrated in Figure 4. We can estimate H_a and H_b by the numerical integrations of the following expressions.

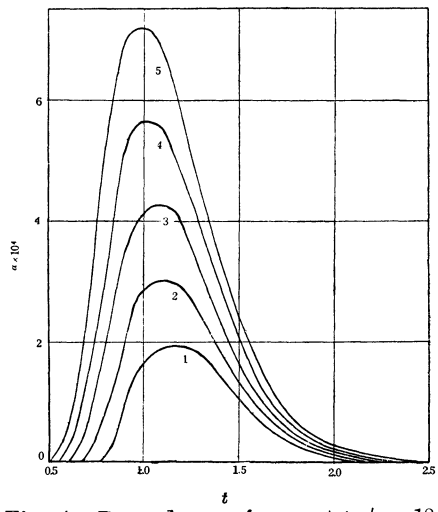

Fig. 4.—Dependence of γ on t ($r_1/r_2=18.2$). Curve 1; $T_2/T_1=10/3$, 2; $T_2/T_1=11/3$, 3; $T_2/T_1=4$, 4; $T_2/T_1=13/3$, 5; $T_2/T_1=5$

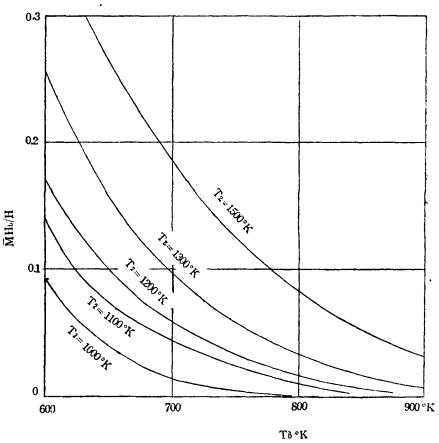

Fig. 5.—Dependence of $\bar{M}H_b/H$ on T_b

$$H/\bar{M}=a\int_{t_1}^{t_2}\alpha_t\frac{\gamma}{t}dt \qquad (1)$$

$$H_b=a\int_{t_b}^{t_2}\gamma\frac{d\alpha}{dt}dt \qquad (2)$$

where $a=2\pi(\rho^2g/\eta)_1\cdot r_1^4t_1^3\exp(2t_1^3)$, and α_t is thermal diffusion constant for the mixture of carbon dioxide and carbon monoxide. We used $\alpha_t=0.10$ which was obtained from the experimental data of Kitagawa and Wakao[7]. Expression (1) had been derived by Furry and Jones and expression (2) was obtained from equations (41) and (43) in part 1.

The results of numerical calculation of $\bar{M}H_b/H$ are graphically represented in Figure 5. Where

(5) Randolt and Börnstein, "Physik.-Chem. Tab. Eg III c" p. 2212.

(6) W. H. Furry and R. C. Jones, *Phys. Rev.*, **69**, 459 (1946).

(7) H. Kitagawa and M. Wakao, *J. Chem. Soc. Japan*, **62**, 100 (1941).

we assumed $T_1 = 300°K$, we neglected the temperature dependence of α_f. The equilibrium constant α for the isotopic exchange reaction

$$C^{14}O + C^{12}O_2 \rightleftarrows C^{12}O + C^{14}O_2 \qquad (3)$$

was calculated following the method adoped by Urey[2]. The results of numerical calculation of equilibrium constant

$$\alpha^{14} = \alpha = \frac{[C^{12}O][C^{14}O_2]}{[C^{14}O][C^{12}O_2]}$$

are shown in Figure 6 with the same constant α^{13} for the equilibrium between C^{12} and C^{13}.

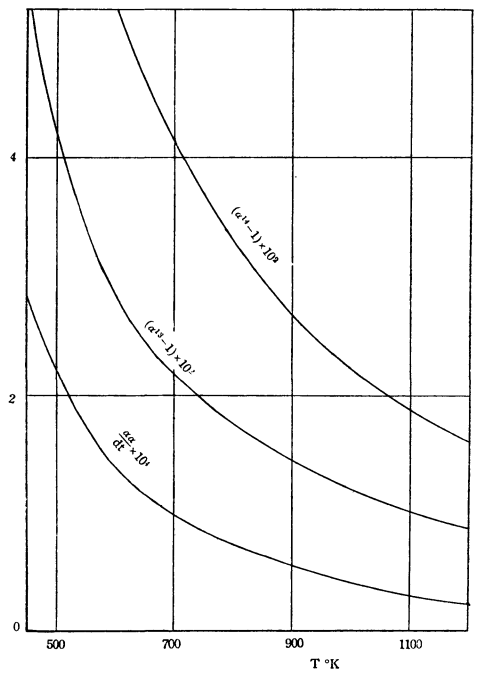

Fig. 6.—Temperature dependences of equilibrium constants $\alpha(=\alpha^{14})$, α^{13}, and $d\alpha/dT$

Our experiments were performed with the isotopic mixture which contains minute quantity of the heavy isotope C^{14} in the natural isotopes of carbon. Therefore the equilibrium constant α may be regarded as an isotopic ratio $\alpha = [C^{14}O_2]/[C^{14}O]$ at the equilibrium (3).

The over-all separation S was estimated by the following expression derived in part 1.

$$-\ln S = \ln \frac{\nu(Z)}{\nu(0)} = \left[1 - \alpha(T_b) + \frac{D_2 - D_1}{\bar{D}} \frac{\bar{M}H_b}{H}\right] \times \frac{\tau_1 Z}{B_c + B_d} + \frac{D_2 - D_1}{\bar{D}} \frac{\bar{M}H_b}{H} (c_1(Z) - c_1(0)) \qquad (4)$$

where $\nu(Z), \nu(0)$ = fractional molar concentration of C^{14} at the top and the bottom of the column, D_1, D_2 = self diffusion coefficient of carbon monoxide and carbon dioxide, $\bar{D}$ = mean value of D_1 and D_2, Z = column length, and $c_1(Z)$, $c_1(O)$ = fractional molar concentration of carbon monoxide at the top and the bottom of the column. A value of $(D_1 - D_2)/\bar{D} = 0.461$ was obtained from the self diffusion coefficients of carbon dioxide and carbon monoxide[8]. If an appropriate value of T_b is assumed, we may obtain over-all separation S using the experimental data on the value of transport (τ_1) of carbon monoxide along the tube and the concentrations of carbon monoxide in the top and the bottom reservoirs at a final equilibrium state. Assuming $T_b = 600$, 700, 750, 800, 850, and 900°K., the numerical evaluation of expression (4) was performed, and obtained the values of $\ln S$ as functions of filament temperature T_2 are illustrated in Figure 7. In these calculations B_c and B were obtained by substituting into equations (40) and (47) the following numerical data,

$\rho = 1.46 \times 10^{-3}$	$T_1 = 300°K.$
$\eta = 165 \times 10^{-6}$	$r_1 = 0.635$
$\bar{D} = 0.141$	$r_2 = 0.035$
$\bar{M} = 36$	$c_1(0) - c_1(Z) = 0.7$

In practice, $c_1(0) - c_1(Z)$ changed in each experimental case, but the second term of equation (4) did not exceed 5 % of the total value; therefore the variation of $c_1(0) - c_1(Z)$ was ignored in our treatment.

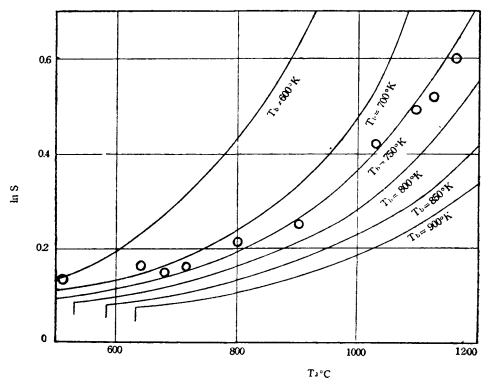

Fig. 7.—Dependence of calculated and observed over-all separation on the filament temperature

In Figure 7 we plotted ln S obtained from the experimental values of Table 1. Perhaps an appreciable error would be introduced concerning the temperature measurements of the filament. However within limits of error, observed over-all separations coincide with the calculated values for $T_b = 750°K$ as illustrated in Figure 7. The observed over-all separations in the cases of low filament temperatures were rather large compared with the expected values. These discrepancies between experimental values and theoretical values may be attributed to the neglect of isotopic

(8) J. H. Jeans, "The Dynamical Theory of Gases" (1925) p. 321.

enrichment by the ordinary thermal diffusion in the theoretical treatment of this report.

The theoretical estimation on the isotopic transport is made by equation (45) in part 1. Since there is no isotopic concentration gradient along the column at the initial state, an initial transport can be obtained putting $d\nu_1/dz=0$, then we have,

$$-\tau_0=(\tau_1)_{t=0}=\left[(1-\alpha(T_b))\tau_1+c_1c_2H_b\frac{D_2-D_1}{\bar{D}}\right]\nu_1$$

Using equation (2) in part 1, it becomes

$$-\tau_0=\left[1-\alpha(T_b)+\frac{D_2-D_1}{\bar{D}}\frac{\bar{M}H_b}{H}\left(1+\frac{B_c+B_d}{\tau_1}\frac{dc_1}{dz}\right)\right]\nu_1\tau_1. \qquad (5)$$

The substitutions of the values of $\bar{M}H_b/H$ for $T_b=750$°K. and of other constants corresponding to the experimental conditions in equation (5) yielded calculated initial isotopic transports tabulated in Table 1. On account of the difficulties in the determination of the initial slopes of curves such as in Figure 3, we can not draw any detailed conclusion from the small discrepancies between calculated and observed values in Table 1, but these experimental evidences support our theoretical interpretation.

At the cylindrical region of the column at T_b°K., we assumed that both variations of the isotopic composition by exchange reaction and by diffusion process maintain balance. Therefore it will be possible to estimate a parameter T_b from the data on the diffusion coefficients and reaction velocity of the exchange reaction. Unfortunately we have no satisfactory knowledge on the kinetics of isotope exchange reaction between carbon monoxide and carbon dioxide, although there have been detailed studies[3][9]. However we may construct a most efficient apparatus using the obtained theoretical results, because T_b takes a constant value for an isotopic exchange reaction employed for the experiments.

The high efficiency of the isotope separation in our experiments at the elevated filament temperatures was caused by the high value of $\bar{M}H_b/H$ in expression (4). On the similar base it is supposed that the rise of cold wall temperature brings high over-all separation factor. The elevation of the temperature in the whole tube results in decreasing of t_b—the lower limit of integral (2)—with respect to the curves of γ. A steep increase of γ with the decrease of t also yields a steep increase of $\bar{M}H_b/H$ by the elevation of the tube temperature, because a range of integration of H_b depends on t_b as was shown by expression (2).

Summary

The separation of carbon isotope C^{14} by the countercurrent gaseous exchange method has been studied using a hot wire type thermal diffusion column. The isotopic exchange reaction employed for the experiments was a reaction between carbon dioxide and carbon monoxide. The separation column was constructed with a water-jacketed glass tube of 150 cm. long and 12.7 mm. in diameter. An electrically heated platinum wire was placed at the center of the tube, and its temperature was measured by thermal expansion of the wire. The column was filled with carbon dioxide. A converter was put at the bottom of the column in order to reduce carbon dioxide to carbon monoxide. The concentration of C^{14} at the bottom of the column was measured by a Lauritsen type electrometer. The over-all separations at the equilibrium states were observed for the various filament temperatures between 570 and 1170°C. The dependence of over-all separation on the filament temperature and initial isotopic transports were in reasonable agneement witd theoretical estimates.

Department of Physics and Chemistry, Gakushuin University, Mejiro, Tokyo

(9) T. H. Norris and S. Ruben, *J. Chem. Phys.*, **18**, 1595 (1950).

On the Ring-Opening Reactions of the Furan Compounds. II. The Synthesis of γ, ζ, ι-Triketobrassylic Acid from Difurfurylideneacetone

By Hiroshi MIDORIKAWA

(Received February 21, 1953)

It had already been found that furfurylideneacetone yields γ, ζ-diketocaplyric acid[1] by refluxing with alcoholic hydrochloric acid. By a similar furan ring opening, γ, ζ-diketosebacic acid was synthesized from δ-furfurylidenelevulinic acid.[2] In the present report, γ, ζ, ι-triketobrassylic acid was obtained from difurfurylideneacetone by the same procedure. This reaction is illustrated below.

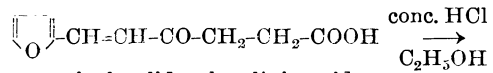

δ-furfurylidenelevulinic acid

γ, ζ-diketosebacic acid

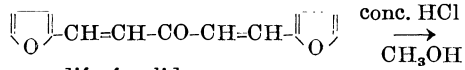

difurfurylideneacetone

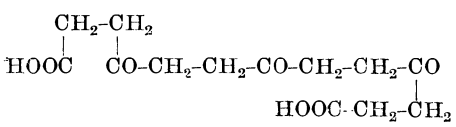

γ, ζ, ι-triketobrassylic acid

This acid gave an oily matter when combined with phenylhydrazine.* The semicarbazone and the hydrazone of this acid did not crystallize out. It was readily esterified by refluxing with alcohol and sulfuric acid. In the case of difurfurylidene-methyl-ethyl ketone (I), difurfurylidenecyclohexanone (II) and furfurylidenediethyl ketone (III), the similar ring opening reaction did not take place with the same procedure as δ-furfurylidene levulinic acid and difurfurylidene acetone.

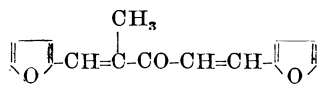

I

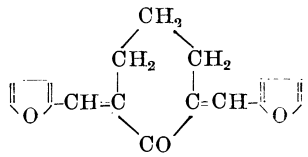

II

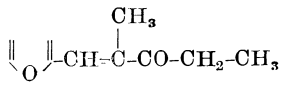

III

These furfurylidene ketones have a branched chain at the carbon atom between the furfurylidene and the carbonyl goups. It seems that the ring opening is hindered by the presence of the branched chain.

Experimental

Difurfurylideneacetone.—20 g. furfural and 6 g. acetone were dissolved in 270 cc. water, and 30 g. 10% aqueous caustic soda solution was introduced at once. After stirring for four and a half hours, the reaction was over. Then, neutralised with sulfuric acid, it was left overnight and solidified. Yield, 20g.. It was recrystallized from ligroin; yellow prisms; m. p. 60—1°; lit.[3] m. p. 60—1°.

γ, ζ, ι-Triketobrassylic Acid.—A mixture of 13 g. difurfurylidene acetone, 130 cc. conc. hydrochloric acid and 200 cc. methanol was refluxed on the water-bath for three hours. The reaction mixture was evaporated on the water-bath to remove hydrogen chloride, water being repeatedly added to it. The residue was extracted with a sufficient quantity of boiling water, and the extract was concentrated on the water-bath, after being decolorized with active charcoal. On cooling, colorless foliated crystals separated out from it, and were recrystallized from water. Yield, 1.5 g.; m. p. 168—9°; readily soluble in water, methanol and acetic acid on heating; insoluble in benzene, chloroform, acetone and ether.

(1) E. A. Kehrer and P.Igler, *Ber.*, **32**, 1177 (1899).
(2) E. A. Kehrer and E. Hofacker, *Ann.*, **294**, 167 (1897).
* Kehrer and Hofacker had reported that the diphenylhydrazone of γ, ζ-diketosebacic acid is difficult to crystallize.

(3) L. Claisen and A. C. Ponder, *Ann.*, **223**, 146 (1884).

	C	H
Anal. Calcd. for $C_{13}H_{16}O_7$:	54.52	6.33
Found:	54.59	6.23

Esterification of γ, ζ, ι-Triketobrassylic Acid. —0.5g. of the acid was boiled in a mixture of 2 cc. methanol and 0.1 cc. conc. sulfuric acid for thirty minutes. On cooling the reaction mixture, the methyl ester was separated out. It was recrystallized from water. Yield, 0.4 g.; colorless needles; m. p. 92—3°.

	C	H
Anal. Calcd. for $C_{15}H_{22}O_7$:	57.29	7.06
Found:	57.20	7.20

0.3 g. of the acid was esterified by refluxing with 2 cc. ethanol and 0.1 cc. conc. sulfuric acid for thirty minutes. The ethyl ester was recrystallized from water; colorless leaflets: m. p. 63—4°.

	C	H
Anal. Calcd. for $C_{17}H_{26}O_7$:	59.61	7.63
Found:	59.66	7.36

Difurfurylidenecyclohexanone, difurfurylidene-methyl-ethyl ketone and furfurylidene diethyl ketone were synthesized by the same method as difurfurylidene acetone.

Summary

The γ, ζ, ι-triketobrassylic acid which is a new triketo-dicarboxylic acid was obtained from difurfurylidene acetone by the ring opening.

The similar ring opening did not take place in difurfurylidene cyclohexanone, difurfurylidene-methyl-ethyl ketone and furfurylidene-diethyl ketone which have a branched chain at the carbon atom between the furfurylidene and the carbonyl groups. It seems that the ring opening reaction is hindered by the presence of the branched chain.

The Scientific Research Institute Tokyo

The Dielectric Constant of Dispersion of Spherical Particles

By Masaji KUBO and Sankichi NAKAMURA

(Received February 23, 1953)

The dielectric constant of emulsions and suspensions and the magnetic permeability of compressed powders have been studied theoretically and experimentally in view of their scientific as well as of their technical importance. Many empirical and theoretical equations have been proposed for disperse systems composed of two different phases. Almost all the empirical formulas assume that some function of dielectric constant ε changes linearly with the volume fraction ϕ.

$$f(\varepsilon)=\phi_1 f(\varepsilon_1)+\phi_2 f(\varepsilon_2) \qquad (1)$$

where suffixes denote the two components constituting the heterogeneous system. The following functions have been proposed.

$f(\varepsilon)=\varepsilon$ (2)
$f(\varepsilon)=1/\varepsilon$ (3) } Wiener's limiting formulas

$f(\varepsilon)=\log\varepsilon$ (4) Lichtenecker

$f(\varepsilon)=(\varepsilon-1)/(\varepsilon+2)$ (5) Clausius-Mosotti

$f(\varepsilon)=(\varepsilon-1)/(\varepsilon+u)$ (6) Wiener

Here u is a constant dependent on the form of the particles. Since earlier works on the problem have already been reviewed by Heymann[1] and Voet,[2] our references to such works need not be comprehensive. The Wiener's limiting formula (2) applies strictly to such heterogeneous systems, in which each single part of the components is cylindrical in shape with the generating line of the cylindrical surface parallel to the electric vector, while the formula (3) to systems in which all the boundary surfaces between the phases are planar and perpendicular to the field. To be sure, the actual heterogeneous systems of interest are very different from these limiting cases. In fact we may expect for instance that an oil-in-water emulsion has a different dielectric constant from that of a water-in-oil emulsion with the same volume fraction of the oil. In fact Goto and Koizumi[3] found that such was actually the case. Therefore we should reject the additive rule of the form (1).

(1) E. Heymann, *Kolloid-Z.*, **66**, 229 (1934).
(2) A. Voet, *J. Phys. Coll. Chem.*, **51**, 1037 (1947).
(3) R. Goto and N. Koizumi, *Rep. Inst. Chem. Research, Kyoto Univ.*, **18**, 121 (1949); R. Goto, *Rev. High Molecules*, **5**, 47 (1951).

and derive a theoretical formula taking into account the non-equivalence of the dispersion medium and the disperse phase. Such an attempt has already been made by Wiener[4] and by Bruggeman.[5] The original paper by Wiener was not available to the writers. His formula for the dielectric constant of a dispersion of concentration ϕ in volume fraction is

$$\frac{\varepsilon-\varepsilon_0}{\varepsilon+2\varepsilon_0}=\frac{\varepsilon_1-\varepsilon_0}{\varepsilon_1+2\varepsilon_0}\phi \qquad (7)$$

for spherical particles of dielectric constant ε_1 dispersed in a medium of dielectric constant ε_0. Piekara[6] derived the same formula with the aid of Wiener's proportionality postulate. That is, he calculated the dielectric constant of dispersion of spherical particles in vacuum and assumed that the same equation holds for a dispersion in a homogeneous medium if in the original equation ε and ε_1 are substituted by $\varepsilon/\varepsilon_0$ and $\varepsilon_1/\varepsilon_0$ respectively. This procedure lacks an adequate theoretical justification. In addition he employed Mosotti's inner field, which has nothing to do with dispersions of particles of greater size than molecular dimensions. Bruggeman proposed the following formula.

$$\frac{\varepsilon_1-\varepsilon}{\varepsilon_1-\varepsilon_0}\left(\frac{\varepsilon_0}{\varepsilon}\right)^{1/3}=1-\phi \qquad (8)$$

He employed Rayleigh's formula,[7] which gave the dielectric constant increment due to the introduction of spherical particles arranged regularly at the lattice points of a simple cubic lattice into a homogeneous phase. Then he ignored higher terms of ϕ. The result is equivalent to that derived from the assumption of Wiener's proportionality postulate, the difference between his theory and Wiener's being that instead of using Mosotti's inner field he integrated a differential equation containing $d\varepsilon/d\phi$. Hence it is not surprising that these two formulas give an identical value for $d\varepsilon/d\phi$ at $\phi=0$.

The present writers have taken a different method of approach avoiding the use of the Wiener's proportionality postulate and obtained an entirely different theoretical formula. The basic assumptions underlying the writers' derivation are as follows. Each particle of the disperse phase is spherical in shape. The radius of the sphere is very small compared with the dimension of the whole heterogeneous system, enabling us to ignore the effect of boundary of the whole system. But it is very great in comparison to the molecular dimensions so that the disperse phase and the dispersion medium can be considered to be homogeneous media characterized by their respective dielectric constants alone. The particles are assumed to have no net charge. If the particles are not so finely dispersed, the effect of polarization will be more important than that of charges at the boundary surfaces. The system may be polydisperse, i. e., the radius of the particles may not be uniform. For the time being, let us assume that all the particles have a radius a.

Suppose a dispersion containing n particles of disperse phase per unit volume. The volume fraction ϕ is given by

$$\phi=\frac{4\pi}{3}a^3n. \qquad (9)$$

Let us imagine $\Delta\nu$ spheres of radius a in unit volume. The number of spheres is so small that the distance between them is very great compared with the radius a. Take out the matter in the spheres and substitute it with a medium of dielectric constant ε_1. If such substitution were made on a homogeneous medium of dielectric constant ε, we could give an expression for the dielectric constant increase. We assume that the same formula for the dielectric constant change is approximately valid for the result of substitution applied on an already existing dispersion containing n particles per unit volume. This means that the heterogeneous system can well be represented by a homogeneous system of the same dielectric constant. Actually the system under consideration is not perfectly static, i. e., the particles already present are moving with respect to the newly inserted spheres. Hence the averaging may be justified to a certain extent. The assumption would be exact if the particles already present were much smaller in size than those introduced. In our case, however, the representation of a heterogeneous system by an average homogeneous phase is an approximation. It will be worthwhile to mention that Brinkman[8] applied the same idea to the theory of viscosity of concentrated suspensions and solutions and obtained a good viscosity formula.

When a sphere of dielectric constant ε_1 is introduced into a homogeneous medium of dielectric constant ε subjected to a uniform

(4) O. Wiener, *Abh. Königl. sächs. Ges. Wiss. Math. Phys. Kl.*, **32**, 509 (1912).
(5) D. A. G. Bruggeman, *Ann. Physik*, (5) **24**, 636 (1935).
(6) A. Piekara, *Kolloid-Z.*, **59**, 12 (1932).
(7) Rayleigh, *Phil. Mag.*, (5) 34, 481 (1892).
(8) H. C. Brinkman, *J. Chem. Phys.*, **20**, 571 (1952).

electric field E_0, the field is distorted in such a way[9] that outside the sphere, its effect is equivalent to a dipole at the center pointing to the field direction, which we shall call x-direction, with its moment equal to

$$m=\frac{\varepsilon_1-\varepsilon}{\varepsilon_1+2\varepsilon}a^3E_0. \tag{10}$$

The potential outside the sphere is given by

$$V=-E_0x+\frac{m}{r^2}\cos\theta \tag{11}$$

where r is the distance between the dipole and the point P in question and θ is the angle between r and the x-direction. On the other hand the sphere is uniformly polarized with a modified field given by

$$F=\frac{3\varepsilon}{\varepsilon_1+2\varepsilon}E_0. \tag{12}$$

Outside the sphere the x-component of the field due to a dipole m is given by

$$\begin{aligned}F_x&=\left(-\frac{\partial V_m}{\partial r}\right)\cos\theta-\left(-\frac{1}{r}\frac{\partial V_m}{\partial\theta}\right)\sin\theta\\&=\frac{m}{r^3}(3\cos^2\theta-1)\end{aligned} \tag{13}$$

where V_m denotes the dipole potential given by the second term in the right-hand side of equation (11). The x-component of the induced moment in a volume element at P is

$$\begin{aligned}&\chi F_x r^2\sin\theta dr d\theta d\phi\\&=\frac{(\varepsilon-1)m}{4\pi r^3}(3\cos^2\theta-1)r^2\sin\theta dr d\theta d\phi\end{aligned} \tag{14}$$

where χ denotes the electric susceptibility or polarizability per unit volume. If we integrate (13) over θ from 0 to π, and over r from a to infinity, the integral over θ vanishes,

$$\int_0^\pi(3\cos^2\theta-1)\sin\theta d\theta=0 \tag{15}$$

while that over r becomes infinity.*

$$\int_a^\infty\frac{dr}{r}=\Big|\ln r\Big|_a^\infty. \tag{16}$$

From the physical point of view, it is unlikely that the effects of volume elements far from the center of the sphere are appreciable. Let us assume that the dipole field smaller than a certain value F_c can contribute to the induced moment only in a negligible magnitude. Since the dipole field is given by

$$\begin{aligned}F_m&=\left[\left(-\frac{\partial V_m}{\partial r}\right)^2+\left(-\frac{1}{r}\frac{\partial V_m}{\partial\theta}\right)^2\right]^{1/2}\\&=\frac{m}{r^3}(3\cos^2\theta+1)^{1/2}\end{aligned} \tag{17}$$

the integration over r should be extended to

$$b=\left(\frac{m}{F_c}\right)^{1/3}(3\cos^2\theta+1)^{1/6}. \tag{18}$$

Therefore the increase of moment due to the introduction of the sphere is

$$\begin{aligned}\Delta M_{\text{out}}&=\iiint\chi F_x r^2\sin\theta dr d\theta d\phi\\&=\iiint\frac{(\varepsilon-1)m}{4\pi r^3}(3\cos^2\theta-1)r^2\sin\theta dr d\theta d\phi\\&=\frac{\varepsilon-1}{2}m\int_0^\pi(3\cos^2\theta-1)\left[\int_a^b\frac{dr}{r}\right]\sin\theta d\theta.\end{aligned} \tag{19}$$

Owing to the logarithmic form of (16) and the relation (15), the constant b does not affect the integral. In other words the absolute value of the ambiguouly chosen F_c is not important. Then we have

$$\begin{aligned}\Delta M_{\text{out}}&=\frac{\varepsilon-1}{2}m\int_0^\pi(3\cos^2\theta-1)\frac{1}{6}\\&\quad\times\ln(3\cos^2\theta+1)\sin\theta d\theta\\&=\frac{\varepsilon-1}{2}m\frac{1}{6}\int_{-1}^1(3x^2-1)\ln(3x^2+1)dx.\end{aligned} \tag{20}$$

The integration by parts gives

$$\begin{aligned}\Delta M_{\text{out}}&=-(\varepsilon-1)m\int_0^1\frac{x^4-x^2}{3x^2+1}dx\\&=-(\varepsilon-1)m\left|\frac{x^3}{9}-\frac{4x}{9}+\frac{4\sqrt{3}}{9\times3}\arctan\sqrt{3}x\right|_0^1\\&=\frac{\varepsilon-1}{3}m\left(1-\frac{4\pi}{9\sqrt{3}}\right)\\&=\frac{(\varepsilon_1-\varepsilon)(\varepsilon-1)}{3(\varepsilon_1+2\varepsilon)}ca^3E_0\end{aligned} \tag{21}$$

where

$$c=1-\frac{4\pi}{9\sqrt{3}}=0.1939. \tag{22}$$

(9) Cf. R. Becker, "Theorie der Elektrizität". I. Teubner, Leipzig and Berlin, 1933, p. 77.

* Higasi[10] in his theory of the solvent effect on dipole moments considered that the product of the two integrals vanishes.

(10) K. Higasi, *Sci. Pap. Inst. Phys. Chem. Research*, **28**, 284 (1936).

The increase of moment inside the sphere is obviously

$$\Delta M_{\text{in}}=\left(\frac{\varepsilon_1-1}{4\pi}F-\frac{\varepsilon-1}{4\pi}E_0\right)\frac{4\pi a^3}{3}$$
$$=\frac{(\varepsilon_1-\varepsilon)(2\varepsilon+1)}{3(\varepsilon_1+2\varepsilon)}a^3E_0. \quad (23)$$

Hence for $\Delta\nu$ such spheres far apart from each other, the increase of polarization is

$$\Delta P=(\Delta M_{\text{out}}+\Delta M_{\text{in}})\Delta\nu$$
$$=\frac{(\varepsilon_1-\varepsilon)[(2+c)\varepsilon+(1-c)]}{3(\varepsilon_1+2\varepsilon)}a^3E_0\Delta\nu. \quad (24)$$

The increase of the dielectric constant of the whole system is therefore

$$\Delta\varepsilon=\frac{4\pi\Delta P}{E_0}$$
$$=\frac{(\varepsilon_1-\varepsilon)[(2+c)\varepsilon+(1-c)]}{(\varepsilon_1+2\varepsilon)}\left(\frac{4\pi a^3}{3}\right)\Delta\nu. \quad (25)$$

By the removal of $\Delta\nu$ spheres of the initial dispersion of concentration ϕ, followed by substitution with the medium of disperse phase, we take out $\phi\Delta\nu$ particles on the average and add $\Delta\nu$ particles anew. Hence the increase in the number of particles of the disperse phase is

$$\Delta n=(1-\phi)\Delta\nu. \quad (26)$$

Combining these two equations, we have

$$\frac{\Delta\varepsilon}{\Delta n}=\frac{(\varepsilon_1-\varepsilon)[(2+c)\varepsilon+(1-c)]}{(\varepsilon_1+2\varepsilon)(1-\phi)}\left(\frac{4\pi a^3}{3}\right) \quad (27)$$

or

$$\frac{\varepsilon_1+2\varepsilon}{(\varepsilon_1-\varepsilon)[(2+c)\varepsilon+(1-c)]}d\varepsilon=\frac{d\phi}{1-\phi}, \quad (28)$$

Therefore

$$\int_{\varepsilon_0}^{\varepsilon}\frac{\varepsilon_1+2\varepsilon}{(\varepsilon_1-\varepsilon)[(2+c)\varepsilon+(1-c)]}d\varepsilon=\int_0^{\phi}\frac{d\phi}{1-\phi} \quad (29)$$

where ε_0 denotes the dielectric constant of the pure dispersion medium. The integration can be evaluated immediately and we have

$$\frac{3\varepsilon_1}{(2+c)\varepsilon_1+(1-c)}\log\frac{\varepsilon_1-\varepsilon}{\varepsilon_1-\varepsilon_0}$$
$$-\frac{(2+c)\varepsilon_1-2(1-c)}{[(2+c)\varepsilon_1+(1-c)](2+c)}\log\frac{(2+c)\varepsilon+(1-c)}{(2+c)\varepsilon_0+(1-c)}$$
$$=\log(1-\phi) \quad (30)$$

where the base of the logarithm may be either e or 10. This equation gives the relation between ε and ϕ, if ε_0 and ε_1 are known. It will be remarked that in this derivation the radius a of particles has been eliminated completely. Therefore the absolute value of the radius is trivial and the uniformity of the particle size is not a necessary condition for the derivation of this equation. For conducting particles we may put $\varepsilon_1=\infty$. Then we have

$$-\frac{1}{2+c}\log\frac{(2+c)\varepsilon+(1-c)}{(2+c)\varepsilon_0+(1-c)}$$
$$=\log(1-\phi). \quad (31)$$

This relation is applicable to metal sols of spherical particles.

Equations in magnetostatics are similar in form to those in electrostatics. If magnetic permeabilities are approximately equal to unity, the second term of the left-hand side of the equation (30) vanishes. This condition is satisfied for dia- or paramagnetic solid powder in air. Then the following simple relation holds for the magnetic permeability μ

$$\frac{\mu_1-\mu}{\mu_1-\mu_0}=1-\phi. \quad (32)$$

That is, the magnetic permeability of a heterogeneous system changes linearly with the volume fraction. Linearity holds also between the magnetic susceptibility and the volume fraction. This relation is used for the measurement of the magnetic susceptibilities of solids by the powder method.

A comparison of the relation (30) with the Bruggeman's formula will be of interest. If we substitute E_0 in the first line of (23) by F, a procedure which is not justified of course, and let $\Delta M_{\text{out}}=0$ or $c=0$, we have

$$\frac{\varepsilon_1+2\varepsilon}{3\varepsilon(\varepsilon_1-\varepsilon)}d\varepsilon=\frac{d\phi}{1-\phi} \quad (33)$$

instead of (28). Integration gives

$$\log\frac{\varepsilon_1-\varepsilon}{\varepsilon_1-\varepsilon_0}-\frac{1}{3}\log\frac{\varepsilon}{\varepsilon_0}=\log(1-\phi) \quad (34)$$

which is identical with the Bruggeman's formula (8).

Though at first sight our theoretical formula and those by Wiener and Bruggeman seem to cover the whole volume fraction range from 0 to 1, the volume fraction of a disperse phase can never be higher than $\pi/3\sqrt{2}=74.0$ %. It is expected that these theories will become inadequate when the volume fraction approaches this limiting value.

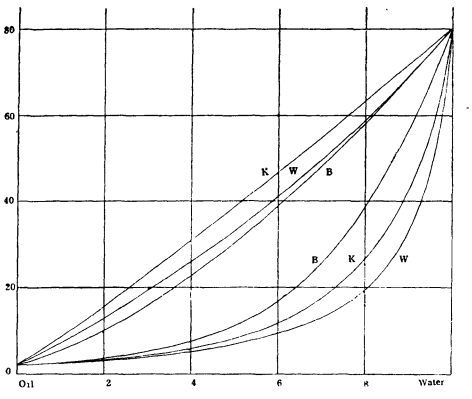

Fig. 1.—The dielectric constants of an oil-in-water type emulsion (upper three curves) and a water-in-oil type emulsion (lower three curves) after the theories of Wiener (W), Bruggeman (B) and the present writers (K)

As an example we have drawn in Figure 1 the dependence of dielectric constant upon the volume fraction for dispersions of water-in-oil and oil-in-water types, taking the dielectric constants of water and oil to be equal to 80 and 2 respectively. For comparison, curves from the formulas of Wiener and Bruggeman are also given. It will be seen that though the functional forms of the three theoretical formulas are entirely different, the curves are similar to each other in their general trend. Namely, the dielectric constant of an oil-in-water type emulsion is higher than that of the water-in-oil type emulsion of the same volume fraction. The curve for the oil-in-water type emulsion is slightly convex to the abscissa, while the deviation from linearity is considerable for the water-in-oil type emulsion. These theoretical conclusions are in conformity with experiments.[11] Most of the experiments which have hitherto been made[12] deal with dilute dipsersions, in which the disperse phase has higher dielectric constant than that of the dispersion medium. In this case the three theories give nearly coincident results. Up to the present, the Bruggeman's formula has been tested and is supposed to be fairly satisfactory. A quantitative comparison of the three theoretical formulas will be made in the succeeding paper.

Summary

The dielectric constant of the dispersion, in which spherical particles of dielectric constant ε_1 are dispersed in a medium of dielectric constant ε_0, has been worked out theoretically without employing Wiener's proportionality postulate. The following equation has been derived for the relation between the dielectric constant ε of the dispersion and the volume fraction ϕ of the disperse phase.

$$\frac{3\varepsilon_1}{(2+c)\varepsilon_1+(1-c)}\log\frac{\varepsilon_1-\varepsilon}{\varepsilon_1-\varepsilon_0} - \frac{(2+c)\varepsilon_1-2(1-c)}{[(2+c)\varepsilon_1+(1-c)](2+c)}\log\frac{(2+c)\varepsilon+(1-c)}{(2+c)\varepsilon_0+(1-c)} = \log(1-\phi)$$

where $c=1-4\pi/9\sqrt{3}$

Chemical Department, Faculty of Science, Nagoya University, Nagoya

(11) R. Goto and N. Koizumi, loc. cit.

(12) A. Voet, loc. cit. F. Wachholtz and A. Franceson, *Kolloid-Z.*, **92**, 158 (1940); A. Piekara, ibid., **49**, 97 (1929); **58**, 283 (1932).

Heterogeneous Structure of Rayon. III. Peeling-off by Heterogeous Nitration

By Saburo OKAJIMA, Shigeru HAYAMA and Kiyoshi WATANABE

(Received March 5, 1953)

In the preceding papers[1] the authors studied the conditions of peeling-off the rayons by heterogeneous acetylation and reported some results obtained by applying this method for several types of rayons. The results are very interesting but it requires too long acetylation up to some hundred to one thousand hours at 60°C. and the reaction is followed by remarkable degradation of cellulose, which will

(1) S. Okajima, S. Hayama and K. Kobayashi, This Bulletin, **25**, 271, 275 (1952).

be a disadvantage in some cases.

As is well known, the ordinary nitration of cellulose proceeds very smoothy with little degradation, but the reaction velocity is too large to be used for our present purposes. Furthermore the ordinary nitration is said not to be fiber-heterogeneous. But according to S. Watanabe,[2] the nitration in organic diluents proceeds with moderate speed and in the case of the natural fibers the reaction seems to be fibrillar-heterogeneous under appropriate conditions. Therefore this type of nitration is very interesting also for our study and some peeling-off examination was made by nitration.

In this report the conditions under which the nitration proceeds fiber-heterogeneously with moderate speed are described and the radial distributions of the orientation degrees in some rayons obtained by this method are compared to those obtained previously by heterogeneous acetylation.

Conditions of Fiber-heterogeneous Nitration

Using a HNO_3—$(CH_3CO)_2O$—CCl_4 system as the nitration bath, the conditions in which a fiber-heterogeneous nitration proceeded with moderate speed was determined. Pieces of an ordinary viscose rayon on the market were extracted with ether and hot water (60°C.) as described previously, and were used as the samples by drying in vacuum immediately before nitration. After nitration for various hours at room temperature the samples were washed with CCl_4 and then thoroughly with water (60°C.) and air dried.

The reaction type varies with the composition of the acid mixture, which was examined by observing the nitrated products under a polarization microscope. If the reaction is fiber-heterogeneous the nitrated sheath of each filament can be clearly recognized, as the birefringence of the cellulose differs remarkably from that of the nitrocellulose.[3] And moreover when such a fiber is swollen in the acetone-water mixture (2:1) only the nitrated sheath swells and a clear demarcation appears between the nitrated and unreacted parts of celluloses and after dissolving away with pure acetone, a slender core remains, which shows some lateral striations as does the original fiber. A permutoid reaction does not indicate such a behavior and the fiber swells homogeneously. Therefore the reaction type can easily be distinguished by such tests.

As to the conditions, dilution ratio DR, nitric acid ratio NAR and bath raio BR are defined as follows:

DR: Weight of $HNO_3+(CH_3CO)_2O$/Weight of CCl_4,

NAR: Weight of HNO_3/(Weight of $HNO_3+(CH_3CO)_2O$),

BR: Weight of the total acid mixture/Weight of the cellulose.

The reaction velocity is dependent on these factors, and the conditions are selected in such a way that the nitration is completed in about 7 hours at room temperature.

The results are summarized in Tables 1 and 2, according to which the following facts are seen: (1) DR has little effect on the type of reaction and the velocity within such experiments. (2) NAR are very effective and at 55% NAR the reaction is too speedy to be followed and at 45% it is too slow. (3) NAR affects also the type of reaction; at 55% NAR the fiber extracted with acetone becomes slender but the lateral striations disappear, and the nitration is of slight permutoid.

Table 1

Effect of the Bath Composition, $T=20$°C.

Exp. No.	DR	NAR(%)	t (hr.)	Reaction type
1	1/5	50	2	F. H.*
2	1/10	50	2	F. H.
3	1/10	50	15	Completely reacted
4	1/5	55	0.5	F. H.
5	1/5	55	1	Completely reacted
6	1/5	45	22	F. H. but the reaction is too slow

* Fiber-heterogenous

Table 2 indicates the effect of AR, according to which the yarn reacts too rapidly at AR=1/2.5 and the optimum value is 1/5~1/10.

Table 2

Effect of DR and BR, T=13°C. and NAR=50%.

Exp. No.	DR	BR	t (hr.)	Type of reaction
1	1/2.5	230	3	Completely reacted
2	1/5	200	3	F. H.
3	1/10	182	3	F. H.
4	1/15	178	3	F. H.
5	1/20	175	3	F. H.
6	1/10	182	8	Nearly completely reacted

To summarize, the best conditions for our purpose are as follows:

DR=1/5~1/20,

NR=50%,

providing $t=0$~7 hrs and T=15~20°C.

Peeling-off by Nitration

The conditions of nitration used for peeling-off is now determined; it is applied to some rayon samples. Those results are summarized in the following tables and figures, where the notations used are the same as described previously unless being noted specially.

(2) S. Watanabe, *J. Soc. Chem. Ind. Japan*, **45**, 832 (1942), **47**, 561 (1944).

(3) Ambronn und Frey, "Polarisationsmikroskop", 1926, S. 169; K. Kanamaru, *Helv. Chim. Acta*, **18**, 1429 (1934).

Table 3

Viscose Rayon V−1

(1) NAR=50%, DR=1/10, BR=180, T=18°C.

Not denitrated. * indicates the value after denitration.

t, hr	5/61	10/60	25/60	1	2	3-20/60	4-40/60	7
$W'/W-1$, %	4.1	6.0	9.2	14.2	21.8	26.0	41.1	55.0
L_T/W, %	3.1	5.1	8.7	14.2	21.4	30.7	44.5	55.7
N, %	1.01	1.74	2.54	3.68	5.28	6.11	8.40	10.05
$x/3(N)$, %	4.0	7.0	10.6	16.0	24.2	29.3	44.3	57.2
$x/3$, %	4.9	7.2	11.0	17.0	26.2	31.2	49.3	66.0
P_r, %	1.6	2.6	4.4	7.4	11.4	16.8	25.5	33.4
$\Gamma \cdot 10^3$	21.5	—	18.2	17.5	16.0	16.2	—	—
$\Gamma \cdot 10^3$*	20.4	21.2	19.6	17.0	17.1	16.2	16.5	16.3

(2) NAR=50%, DR=1/10, BR=150, T=18°C.

Not denitrated.

t, hr	5/60	10/60	25/60	1	2	3-30/60	5-15/60	7-20/60
$W'/W-1$, %	4.4	5.7	8.2	13.2	19.3	28.4	36.2	53.5
L_T/W, %	6.5	5.4	7.5	8.2	—	26.8	34.3	—
N, %	1.27	1.49	2.38	3.42	4.50	6.60	7.70	9.25
$x/3(N)$, %	5.0	5.9	9.9	14.8	20.0	32.7	40.1	51.3
$x/3$, %	5.3	6.8	9.8	15.8	23.2	34.1	42.2	64.2
P_r, %	2.6	2.7	3.8	4.3	—	14.4	19.0	—
$\Gamma \cdot 10^3$	—	—	—	—	—	—	—	—

Table 4

Cuprammonium Rayon C

(1) NAR=50%, DR=1/10, BR=220, T=18.5°C.

Not denitrated. * indicates the values after denitration.

t, hr	5/60	10/60	25/60
$W'/W-1$, %	24.9	39.2	69.0
L_T/W, %	20.2	36.6	72.5; 77.2*
N, %	5.78	8.94	12.34
$x/3(N)$, %	27.3	49.0	79.5
$x/3$, %	29.9	47.0	82.8
P_r, %	10.8	20.4	47.5; 52.2*
$\Gamma \cdot 10^3$	—	—	— 28.1*

(2) NAR=50%, DR=1/15, BR=212, T=16°C.

Not denitrated.

t, hr	5/60	9/60	15/60	26/60	42/60
$W'/W-1$, %	6.3	13.8	19.3	29.0	38.3
L_T/W, %	3.4	4.8	12.8	25.8	36.0
N, %	2.17	3.39	4.64	7.15	8.70
$x/3(N)$, %	8.9	14.6	20.8	36.2	47.2
$x/3$, %	7.6	16.6	23.2	34.8	46.0
P_r, %	1.7	2.4	6.5	13.6	20.0
$\Gamma \cdot 10^3$	—	—	—	—	—

(3) NAR=46%, DR=1/10, BR=154, T=14°C.

Denitrated. "L_T/W* indicates the values before denitration.

t, hr	3/60	6/60	12/60	24/60	50/60	30/60**	35/60***
$W'/W-1$, %	3.1	6.1	9.2	15.4	21.8	39.0	42.8
L_T/W*, %	0.0	0.0	1.9	10.3	19.3	35.6	37.3
L_T/W, %	2.6	4.8	—	15.4	23.8	40.6	42.0
N, %	1.06	1.95	2.52	3.75	5.55	7.97	9.25
$x/3(N)$, %	3.3	8.0	10.3	16.7	26.1	42.1	51.1
$x/3$, %	3.7	7.3	11.0	18.5	26.2	46.8	51.4
P_r, %	1.3	2.4	—	8.0	12.7	22.9	23.8
$\Gamma \cdot 10^3$	31.4	31.8	—	31.3	30.8	30.4	29.9

** NAR=56%, DR=1/10, BR=220, T=2°C.

*** NAR=60%, DR=1/10, BR=220, T=2°C.

Table 5

Tire cord T

(1) NAR=50%, DR=1/10, BR=220, T=12°C. Denitrated. L_T/W^* indicates the values before denitration.

t, hr	40/60	1	1-20/60	1-40/60	2
$W'/W-1$, %	16.2	22.8	29.0	38.3	46.0
L_T/W^*, %	14.2	21.7	28.1	35.8	42.5
L_T/W, %	17.2	—	—	38.8	45.5
N, %	4.11	5.73	6.64	8.56	9.30
$x/3(N)$, %	18.1	27.1	33.0	46.2	51.3
$x/3$, %	19.4	27.4	34.8	46.0	55.2
P_r, %	9.0	11.1	15.5	21.6	26.2
$\Gamma \cdot 10^3$	33.6	—	—	32.7	32.0

(2) NAR=50%, DR=1/10, BR=220, T=10°C. Denitrated. L_T/W^* indicates the values before denitration.

t, hr	10/60	30/60	1-40/60	3-30/60
$W'/W-1$, %	5.6	10.2	20.1	53.1
L_T/W^*, %	3.1	7.9	19.4	53.0
L_T/W, %	5.5	10.1	—	56.1
N, %	1.54	2.66	4.81	9.26
$x/3(N)$, %	6.1	11.2	21.9	51.3
$x/3$, %	6.7	12.2	24.1	63.7
P_r, %	2.8	5.1	—	33.7
$\Gamma \cdot 10^3$	33.7	33.7	—	30.6

(3) NAR=50%, DR=1/10, BR=220, T=14°C. Denitrated. L_T/W^* indicates the values before denitration.

t, hr	55/60	1-50/60	2-20/60	3
$W'/W-1$, %	26.6	56.9	71.1	85.2
L_T/W^*, %	24.8	55.8	73.4	—
L_T/W, %	27.7	—	76.0	—
N, %	5.91	9.92	11.28	—
$x/3(N)$, %	28.1	56.1	67.9	—
$x/3$, %	31.9	68.3	85.3	—
P_r, %	15.0	33.5	51.0	—
$\Gamma \cdot 10^3$	33.2	—	30.4	—

Some of the previous samples are used also here in order to compare the acetylation and nitration results.

The notation in the above tables are defined below:

t: Duration of nitration, hr.

W: Weight of the sample used for nitration, g.

W': Weight of the nitrated yarn, g.

L_T/W: Extracted portion (by acetone) of the nitrated yarn. The percentage is expressed on the cellulose base.

N: Nitrogen content (%) of the nitrated yarn, determined with Lunge nitrometer.

P_r: Peeled-off portion of the single filament, expressed on the percentage of the original diameter.

Experimental Results

(1) Nitration.—In Fig. 1 the weight increase W'/W is plotted against the nitrogen content of the nitrated yarn, where the curve is the theoretical relation. The observed points of cuprammonium yarn (×) are on the theoretical curve, but the highly nitrated products of the other two samples (○ and ▲) deviate upward from the relation. The cause is not yet clear but this is certainly because the nitrogen content which is obtained is too low; of course in the case of the cuprammonium yarn it is said to be correctly obtained. Then it can be said, at least, that no part of the nitrated yarn disperses away in the nitration bath as the yarn does during acetylation, and then $\log(W'/W-1)$ versus $\log t$ is expected to be linear. Fig. 2 shows that this is the case.

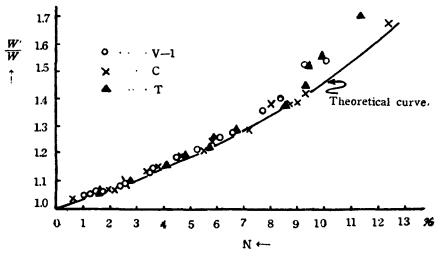

Fig. 1.

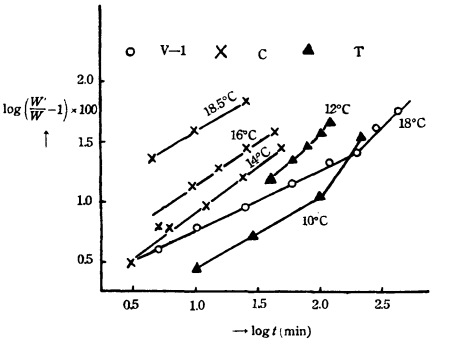

Fig. 2.

The knick points are seen on the relations of $V-1$ and T, but none on that of C. This relates probably to the existence of the skin, which will be studied precisely in the future.

The temperature coefficient of the nitration reaction is considerable.

(2) The weight of the peeled-off portion.—If the nitrated OH is x mols per 162 g of cellulose, W'/W is expressed by the following function of x.

$$W'W-1=45/162 \cdot x$$

Assuming now that all the NO_2-groups are concentrated to the nitrated shell to constitute

trinitrocellulose[1] and this triester is extracted by acetone to give L_T, then L_T/W must be $x/3$. These relations are shown in Fig. 3, where $W'/W-1$ is plotted on the abscissa instead of $x/3$. x can be also calculated from the observed values of N %, which is given in Table 3~5 by $x/3(N)$, but this value which is obtained seems to be too low and the discussion is now ommitted here.

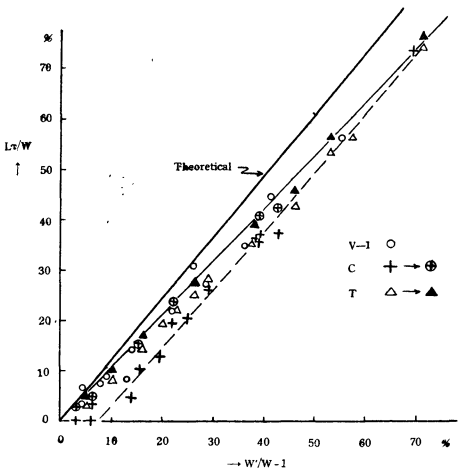

Fig. 3.

The observed points of each sample are on the separate lines, but they are all smaller than the corresponding theoretical values. It is worth while especially to note that the cuprammonium rayon whose N % is lower than 1.5% can not be extracted to any extent. This fact indicates that the assumption taken for the above calculation does not hold exactly and the next consideration can be given for one of the reasons.

A diffuse layer may exist between the trinitrocellulose (in the practical meaning) shell and the cellulose core, part of which then remains unextracted on the cellulose core and gives a greater value of the unextracted residue W', if the residue is considered as described above, and therefore the extracted portion L_T will be smaller as compared to the value from $W'/W-1$. And indeed when the unextracted residue is treated with NH_4SH alcoholic solution, L_T/W approaches to the theoretical; In the figure the point △ of T and + of C shift to the corresponding values is indicated by ▲ and ⊕ respectively.

These corrected points belong to a line which starts from the origin, but the inclination of the line differs from that of the theoretical line. This means that the part of the diffuse layer remains undissolved and the amounts increase as the nitration proceeds because the layer as it diffuses, becomes broader and broader toward the center of the filament.

Of course acetone dissolves not only trinitrocellulose but also lower nitrates, so the above consideration is a first approximation. But in this case L_T/W calculated from W'/W must be still larger.

Radial Distribution of Γ

The thickness of the peeled-off shell, P_r, was calculated from the values of L_T/W, where the extracted yarn with acetone was followed by the complete denitration with NH_4SH alcoholic solution, which was prepared by the well known method.[5]

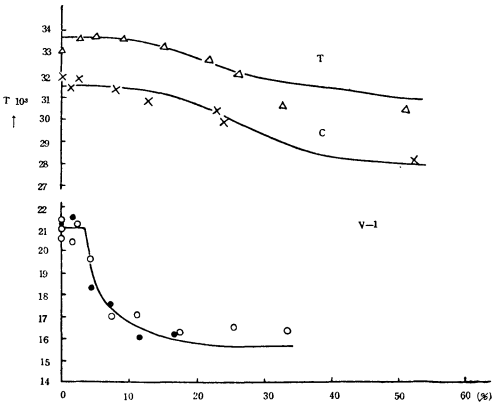

Fig. 4.

The intrinsic double refraction, Γ, of the peeled-off core was measured as described in the preceding paper. The double refraction of the extracted filament changes but slightly by denitration (rf. Fig. 4, ○ and ● of V—1 are the values before and after the denitration respectively) but the treatment is necessary to obtain the reasonable value of P_r, as the surface layer of the core contains some low substituted nitrocellulose before denitration.

The relation of Γ and P_r are shown in Fig. 4, where P_r of V—1 is exceptionaly calculated from L_T/W before denitration. Even in this case Γ is the double refraction after denitration. The observed points are plotted in the figure, where the curves are the relation taken from the second report of this series, obtained by the acetylation method. In the cases of the tire cord and cuprammonium rayons Γ of the original filaments differs tolerably from the corresponding values of the previous measurements, so the previous curves are shifted upwards in the figure so that the origins coincide in both measurements. This discrepancy of Γ is probably caused by the fact that the composition of the immersion liquids used for the present measurement of the refractive indices differs from those of the previous one. In the case of V—1 the same liquid compositions

(4) J. Chédin, *Kolloid. Z.* **125**, 65 (1952).

(5) Dorée, "The Method of Cellulose Chemistry", 1933, P. 227.

were used and such a phenomenon is not observed and therefore the correction is unnecessary.

Then the observed points nearly agree with the previous curves in all cases. So now it is proved that the nitration method is also suitable for the peeling-off and it is superior in some cases, where the speedy reaction with no degradation is required. Such examples will be reported in the near future.

The cost of this research has been defrayed by the Grant in Aid for Fundamental Scientific Research from the Ministry of Education, to which the authors' thanks are due.

Faculty of Engineering,
Yamagata University, Yonezawa
and
Faculty of Engineering,
Tokyo Metropalitan University, Tokyo

Vat Dyes of Pyrazoloanthrone Series. IV. Constitution and Properties of N-alkyl Derivatives of Pyrazoloanthrone Yellow[1]

By Toshio MAKI and Takashi AKAMATSU

(Received March 5, 1953)

The actual existence of the two isomers of N-alkyl derivatives of pyrazoloanthrone, 9-N-alkyl form (I) and 1-N-alkyl isomer (II), was shown in our previous report.[2] We have then pointed out the tautomerism of Pyrazoloanthrone Yellow (2, 2'-dipyrazoloanthronyl) (III $\rightleftarrows$ IV, R=H)

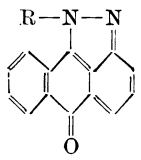

(I)

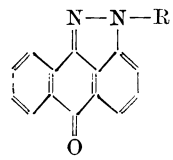

(II)

and established the constitution of the two isomers of its N, N'-dialkyl derivatives. Thus, 9-N, 9'-N'-dialkyl formula (III) has been given to the rubine red dyes and 1-N, 1'-N'-dialkyl structure (IV) to the orange isomers.[3]

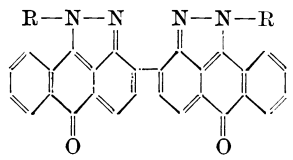

(III)

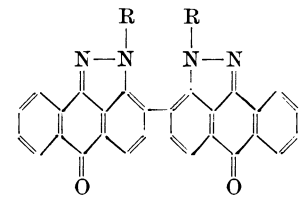

(IV)

The methyl (R=CH_3) and ethyl (R=$CH_2 \cdot CH_3$) compounds were already described in our preceding report.[3] We have now prepared hitherto unknown N, N'-di-n-propyl (III, IV, R=$CH_2 \cdot CH_2 \cdot CH_3$) and N, N'-di-n-butyl (III, IV, R=$CH_2 \cdot CH_2 \cdot CH_2 \cdot CH_3$) derivatives by the alkylation of Pyrazoloanthrone Yellow with the corresponding alkyl *p*-toluenesulfonate. In all cases rubine red vat dyes (III) of higher light fastness and orange isomers (IV) of lower light fastness were simultaneously produced, and the former dyes were the principal products (72~75% of the theory). The rubine red dyes are nearly insoluble in organic solvents, while the orange isomers so very easily soluble, that the quantitative separation of the two isomers can simply be carried out using *o*-dichlorobenzene.

	Yield (% of the theory)	
	Rubine red dyes (III)	Orange isomers (IV)
R=CH_3	75.1%	21.4%
R=$CH_2 \cdot CH_3$	74.9	23.8
R=$CH_2 \cdot CH_2 \cdot CH_3$	72.6	26.8
R=$CH_2 \cdot CH_2 \cdot CH_2 \cdot CH_3$	72.3	27.3

(1) Read before the 5th Annual Meeting of the Chemical Society of Japan on April 5, 1952.

(2) T. Maki and T. Akamatsu, *J. Chem. Soc. Japan, Ind. Chem. Section*, **54**, 281 (1951).

(3) T. Maki and T. Akamatsu, *J. Chem. Soc. Japan, Ind. Chem. Section*, **54**, 326 (1951); See also *J. C. S.*, **1952**, 1631, 1637~8.

Various coloring properties of the four principal rubine red vat dyes are compared.

Constitution (III)	Streak	Conc. H_2SO_4	Vat	On cotton	
				Shade	Light fastness
$R=CH_3$	Purple red	Red orange	Blue (A)	Rubine red	5~6(B)
$R=C_2H_5$[4]	Purple red	Red orange	Blue (A)	Rubine red	6 (A)
$R=n\text{-}C_3H_7$	Purple red	Red orange	Blue (C)	Rubine red	5~6(C)
$R=n\text{-}C_4H_9$	Purple red	Red orange	Blue (B)	Rubine red	5~6(D)

In the column of vat, (A) means easily soluble, (B) and (C) soluble with some difficulty. Under the light fastness, (A), (B), (C) and (D) denote the order of fastness. (A) is the highest among the four compounds.

More accurate comparison of the four rubine red dyeings were carried out using self recording G. E. spectrophotometer with 1% cotton dyeings (IN method) and the obtained reflectance curves (Fig. 1) were analysed according to the I. C. I. system.[5]

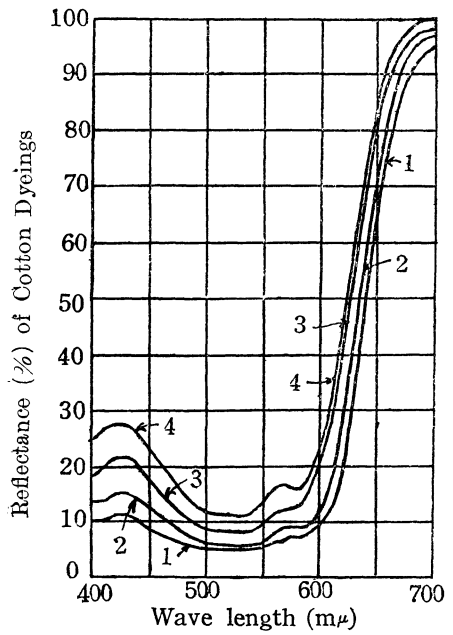

1·····(III), R=CH_3
2·····(III), R=C_2H_5
3·····(III), R=n-C_4H_9
4·····(III), R=n-C_3H_7

Fig. 1

Constitution (III)	R=CH_3	R=C_2H_5	R=n-C_3H_7	R=n-C_4H_9
Trichromatic coefficient x	0.4352	0.4252	0.3894	0.4137
Trichromatic coefficient y	0.2725	0.2609	0.2625	0.2650
Brightness Y(%)	9.16	11.47	19.46	16.07
Dominant wave-length (mμ)	495.1c	496.9c	499.2c	497.0c
Color purity (%)	41	44	36.2	40

Comparing the dominant wave-lengths it is known that the shade of the N, N'-dimethyl derivative is most reddish and that of the N, N'-di-n-propyl derivative most bluish although their differences are not very remarkable. It was unexpected that the n-butyl is less bluish than the n-propyl homologue. The shade of the N, N'-diethyl compound shows the highest color purity (i. e. most monochromatic) among the four, while lower brightness (Y) of the N, N'-dimethyl and diethyl compounds is shown due principally to their stronger dyeing powers. The order of the cotton dyeing powers is: methyl>ethyl>n-butyl>n-propyl.

Vinylon[6] fibres and cloths, to which most vat dyes are not satisfactorily applicable, can be dyed in rubine red shades by a modified IN method with these N, N'-dialkylated Pyrazoloanthrone Yellow, in which the N, N'-di-n-propyl compound gives the most clear and strong red dyeings of sufficient intensity. The washing fastness of vinylon dyeings of the *n*-propyl derivative was excellent, light fastness about 5 grade, their fastness to rubbing, however, was not very high (nearly 3 grade). The order of the vinylon dyeing powers is: n-propyl>ethyl>n-butyl>methyl.

Experimental Part

N, N'-Di-*n*-propyl Derivatives of Pyrazoloanthrone Yellow.—1.32 g. (1 mol. ratio) of Pyrazoloanthrone Yellow[3] was converted into nearly 20% paste by the usual method, heated on a water bath with 4 g. of 90% sodium hydroxide and 4 cc. of water, diluted with 62 cc. of cold water, the N, N'-disodium salt thus formed was filtered and without washing perfectly dried in vacuum at room temperature. This was then finely powdered and boiled under reflux with stirring in 26 g. of *o*-dichlorobenzene with 1.93g. (3 mol. ratio) of n-propyl p-toluenesulfonate (b. p. 4 mm. 145±3°) for 6 hours. When the hot solution was filtered and washed with alcohol and hot water the rubine red compound (III, R=$CH_2\cdot CH_2\cdot CH_3$) was obtained as an insoluble

(4) According to our studies this must be the true constitution of Indanthren Rubine R. See reference (3).
(5) A. C. Hardy, Handbook of Colorimetry.
(6) Polymerized vinyl alcohol partially acetallized (ca. 35%) with formaldehyde.

crystalline powder. Yield was 1.14 g. (72.61% of the theory). From the *o*-dichlorobenzene filtrate crude orange isomer (IV, $R=CH_2\cdot CH_2\cdot CH_3$) was collected after steam distillation. Yield was 0.42 g. (26.75% of the theory), the total yield corresponds to 99.36% of the theory.

The insoluble rubine red compound is a brown red powder, having a purple red streak, dissolves in conc. sulfuric acid with red orange color, from which by gradual addition of water successively resulted yellow-orange solution, yellow solution, yellow precipitate and at last purple red precipitate. Hydrosulfite vat, which is a little less easily soluble than other three N,N'-dialkyl derivatives, is blue, and cotton is dyed in clear purple-red shade by IN method (2% dye). When the substance was dissolved in 20 parts of 98.5% sulfuric acid and 8.2 cc. of water added dropwise with external cooling to produce 70% sulfuric acid the insoluble part (92%) was the rubine red dye of highest purity. Found: N, 10.68; Calculated for $C_{34}H_{26}O_2N_4$ (III, R=n-C_3H_7): N, 10.72 %.

The crude orange isomer, which had been obtained by steam distillation from the *o*-dichlorobenzene filtrate, was further purified by dissolving in monochlorobenzene, shaking with active coal, filtering and adding alcohol to the concentrated filtrate. It is an orange brown crystalline powder with an orange streak. Conc. sulfuric acid solution is red orange, from which orange precipitate resulted by the addition of water. From a blue hydrosulfite vat (IN) it dyes cotton red-orange of lower light fastness than the rubine red isomer. Found: N, 10.62; Calculated for $C_{34}H_{26}O_2N_4$ (IV, R=n-C_3H_7): N, 10.72%.

Vinylon fibres can be dyed by a modified IN method using dye paste. The dye bath consisted of 120 cc. of water, 3 cc. of 25% sodium hydroxide, 0.8 g. of hydrosulfite and 0.4 cc. of turkey red oil and vatted at 60° for 15 min. The fibres were dyed at 50° for 90 min. and after air oxidation, washing and acidification treated with soap solution (0.2:100) at 60° for 30 min. Sufficient intensity is obtained with 2% dye.

N,N'-Di-*n*-butyl Derivatives of Pyrazoloanthrone Yellow.—2.19 g. (1 mol. ratio) of Pyrazoloanthrone Yellow was converted into N,N'-disodium salt using 8 g. of 90% sodium hydroxide as in the case of the above n-propyl compounds. This was then as a dry, fine powder boiled with 44 g. of o-dichlorobenzene and 3.42 g. (3 mol. ratio) of n-butyl *p*-toluenesulfonate (b. p. 3.5 mm. 140~145°) for 6 hours and filtered hot. The yield of insoluble crystalline powder of the rubine red compound (III, $R=CH_2\cdot CH_2\cdot CH_2\cdot CH_3$) was 1.96 g. (72.33% of the theory), while the amount of the soluble orange isomer (IV, $R=CH_2\cdot CH_2\cdot CH_2\cdot CH_3$) was 0.74 g. (27.31% of the theory). The total yield was 99.64% of the theory. Their color reactions and dyeing properties are on the whole similar to those of the corresponding n-propyl derivatives. The comparison of the homologous rubine red dyes are given in the general part of this paper. The rubine red n-butyl compound of the highest purity remained insoluble (93%) by the treatment with 70% sulfuric acid. Found: N, 10.17; Calculated for $C_{36}H_{30}O_2N_4$ (III, R=*n*-C_4H_9): N, 10.18%.

The orange isomer was purified a in the case of the n-propyl compound with monochlorobenzene, active coal and alcohol and the orange brown crystalline powder thus obtained was analysed. Found: N, 10.11; Calculated for $C_{36}H_{30}O_2N_4$ (IV, R=n-C_4H_9):N, 10.18%.

Measurement of Reflectance Curves of the Cotton Dyeings.—1% IN cotton dyeings were carefully prepared using the rubine red vat dyes purified with 70% sulfuric acid. The dyes were converted into paste form before dyeing. The reflectance (%) of the cotton dyeings was measured by self recording G. E. spectrophotometer taking a similarly treated, undyed cotton cloth as the standard in order to cancel the absorption effect of the latter. The light source C of the I. C. I. system was used.

The authors express their gratitude to The Government Industrial Research Institute, Tokyo for the measurement of reflectance curves using self recording G. E. spectrophotometer.

Dyestuffs Research Laboratory,
Department of Applied Chemistry,
Tokyo University, Tokyo

A Reinvestigation of the Structure of Ethylene Oxide by Electron Diffraction

By Masato IGARASHI

(Received March 5, 1953)

Recently, Cunningham, Boyd, Gwinn, Myer, and Le Van investigated the structure of ethylene oxide by microwave spectrum,[1] and gave the results different from those of Ackermann and Mayer's earlier electron diffraction study[2] (Table 1). The difference is very large in the C—C distance. Therefore we have reinvestigated the structure by electron diffraction.

Ethylene oxide was prepared from ethylene chlorohydrin and lime. Electron diffraction photographs were obtained by the apparatus with a camera distance of about 9 cm and an electron wave length of about 0.055 Å. The maxima and minima of diffraction halos were measured by the visual method on the photographs; the q values are given in Table 2 and represented by the arrows in Fig. 1 ($q = (40/\lambda)\sin\phi/2$, where λ is the electron wave length and ϕ is the scattering angle).

A the atomic distances are equal to those of Ackermann and others, and in model B they are equal to those of Cunningham and others while in models C and D only the C—C distances are varied from those of B. The theoretical intensity curves (Fig. 1) were calculated by the well-known formula,[3]

$$I = \sum_{ij}(Z_i Z_j / r_{ij}) \exp(-a_i q_r^2) \sin(\pi q r_{ij}/10)$$

where r_{ij} is the distance between the atoms i and j, and Z_i is the atomic number of the atom i. The value of the coefficient a_{ij} was assumed to be 0.00016 for bonded hydrogen terms, 0.0004 for unbonded hydrogen terms, and zero for all the others. The theoretical values of q and their ratio to the observed values at the maxima and minima are shown in Table 2. It is clear that the models B and C fit better with the observed than the other

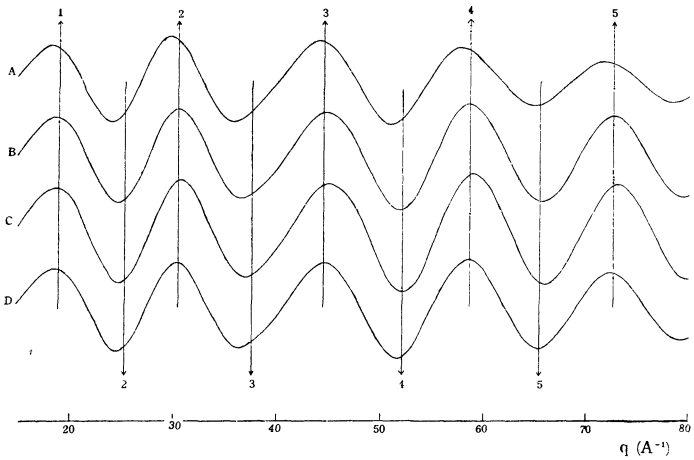

Fig. 1.—Theoretical intensity curves

The molecular models used for the correlation methods are compared in Table 1. In model models. Thus we can conclude that the C—C distance is 1.46±0.03 Å, supporting the results of the microwave spectroscopy.

(1) G. L. Cunningham, A. W. Boyd, W. D. Gwinn, and W. I. Le Van; *J. Chem. Phys.* **17**, 211 (1949); G. L. Cunningham, A. W. Boyd, R. J. Myer, W. D. Gwinn, and W. I. Le Van, ibid. **19**, 676 (1951).

(2) P. C. Ackermann and J. E. Mayer, *J. Chem. Phys.* **4**, 377 (1936).

(3) S. Spurr and V. Schomaker, *J. Am. Chem. Soc.* **64**, 2693 (1942).

Table 1

	(a) Cunningham	(b) Ackermann	(c) Models used for our study			
			A	B	C	D
C—C	1.472A	1.56±0.05A	1.56A	1.47A	1.44A	1.50A
C—O	1.436A	1.45±0.05A	1.45A	1.44A	1.44A	1.44A
C—H	1.082A	1.05±0.07A	1.05A	1.08A	1.08A	1.08A
∠H—C—H	116°41′		109.5°	116°41′	116°41′	116°41′
∠H_2—C—C	159°25′		151°	159°25′	159°25′	159°25′

Table 2

Max.	Min.	q_{obs}	q_{calc} A	q_{calc} B	q_{calc} C	q_{calc} D	q_{calc}/q_{obs} A	q_{calc}/q_{obs} B	q_{calc}/q_{obs} C	q_{calc}/q_{obs} D
1		18.9	18.2	18.6	18.7	18.5	0.962	0.983	0.988	0.978
	2	25.3	24.2	24.8	24.9	24.6	0.965	0.980	9.984	0.972
2		30.45	29.7	30.5	30.7	30.6	**0.975**	**1.002**	**1.008**	**0.998**
	3	37.6	35.8	36.7	37.1	36.5	0.952	0.976	0.987	0.971
3		44.5	44.2	44.6	44.9	44.5	**0.994**	**1.003**	**1.010**	**1.001**
	4	52.1	51.2	51.9	52.2	51.7	0.982	0.996	1.002	0.992
4		58.65	57.8	58.6	59.0	58.4	**0.986**	**0.999**	**1.006**	**0.996**
	5	65.4	65.0	65.8	66.1	65.4	0.994	1.006	1.011	1.000
5		72.6	71.6	72.6	73.2	72.3	0.986	1.000	1.008	0.996
				Average			0.979	0.996	1.002	0.992
				Average deviation			0.012	0.008	0.008	0.009

Values in Gothics were doubly weighted in computing averages.

The author wishes to express his gratitude to the late Professor H. Oosaka and to Professor A. Kotera for their kind guidance during the course of this research.

Department of Chemistry, Faculty of Science, Tokyo University of Education, Tokyo

4,4′-Dimethoxy-2,2′-dihalogeno-α,α′-dialkylstilbenes, Their Ultraviolet Absorption Spectra and Estrogenic Action

By Michinori ŌKI[1]

(Received March 9, 1953)

The essential features of the molecular structure favorable for the development of a strong estrogenic activity are two groups carrying active hydrogen atoms or producing such in vivo, located at an optimum distance from each other, and an optimum thickness.[2] Diethylstilbestrol, 4-$HOC_6H_4CEt=CEtC_6H_4OH$-4′, acquires its favorable molecular structure by virtue of the steric effect of the two ethyl groups at the α,α′-positions which force the benzene rings to rotate to a suitable extent. The smaller activity of 4,4′-dihydroxy-α,α′-dimethylstilbene (dimethylstilbestrol), 4-$HOC_6H_4CMe=CMeC_6H_4OH$-4′, is attributed to its thinner structure formed by the smaller steric effect of the methyl groups. It has been reported by Hudson and Walton[3] that 4,4′-dihydroxy-2,2′,α,α′-tetramethylstilbene, 4,2-

(1) Present address: Department of Chemistry, Faculty of Science, Tokyo Metropolitan University, Meguro, Tokyo.

(2) M. Ōki and Y. Urushibara, This Bulletin, **25**, 109 (1952).

(3) B. J. F. Hudson and E. Walton, *J. Chem. Soc.*, **1946**, 85.

Table 1

Estrogenic Activity of 4,4′-Dimethoxy-2,2′-dihalogeno-α,α'-dialkylstilbenes, 4,2-$CH_3OXC_6H_3CR=CRC_6H_3XOCH_3$-2′,4′.

	Substance	Melting point or Boiling point	Minimum active dose in mice
(I)	R=CH_3, X=Cl	[112—113°]	200 γ (5.9×10^{-7}mol.)
(II)	R=CH_3, X=Br	[117.5—119.5°]	200 γ (4.7× 〃)
(III)	R=CH_3, X=I	[159—160°]	500 γ (9.6× 〃)*
(IV)	R=C_2H_5, X=Cl, trans	[105.5—106.5°]	100 γ (2.7× 〃)
(V)	R=C_2H_5, X=Br, trans	[114.5—115°]	100 γ (2.2× 〃)
(VI)	R=C_2H_5, X=I, trans		200 γ (3.6× 〃)
(VII)	R=C_2H_5, X=Cl, cis	(88—89°/0.07 mm.)	1 mg.
(VIII)	R=C_2H_5, X=Br, cis	(87—89°/0.04 mm.)	1 mg.
(IX)	R=C_2H_5, X=I, cis	(108—110°/0.02 mm.)	1 mg.

* Active in 75 % animals.

Table 2

Absorption and Estrogenic Activity of 4,4′-Dimethoxy-α,α'-dialkylstilbenes, 4-$CH_3OC_6H_4CR=CRC_6H_4OCH_3$-4′.

Substance		Melting point	$\lambda_{max.}$(mμ)	$\varepsilon_{max.}\times10^{-4}$	Minimum active dose in mice
(X)	R=CH_3	141.5—143°	247	2.85	100 γ (3.7×10^{-7}mol.)
(XI)	R=C_2H_5	121.5—123°	236	2.20	2.5 γ (0.084× 〃)

$HOMeC_6H_3CMe=CMeC_6H_3MeOH$-2′,4′, is a strong estrogen. Then it comes out that the methyl groups at 2,2′-positions may coöperate with the methyl groups at α,α'-positions to produce a molecular structure favorable for estrogenic action. As the bromine atom possesses a van der Waals radius nearly equal to that of the methyl group, it might be expected that introduction of bromine atoms into the 2,2′-positions of the 4,4′-dihydroxy-α,α'-dimethylstilbene would give also a potent estrogen, although it has been indicated that the bromine atoms in 4,4′-dimethoxy-α,α'-dibromostilbene, 4-$MeOC_6H_4CBr=CBrC_6H_4OMe$-4′, appear to have a smaller steric effect on the rotation of the benzene rings than that of the methyl groups in the corresponding α,α'-dimethyl compound.(4)

The present paper records the results of the investigations on the effect of introduction of two equal halogen atoms into the 2,2′-positions of 4,4′-dimethoxy-α,α'-dimethylstilbene and 4,4′-dimethoxy-α,α'-diethylstilbene (diethylstilbestrol dimethyl ether). The general principle of preparations, which are described in details in the Experimental Part, was as follows:

2-Halogeno-4-methoxy-acetophenone or -propiophenone, prepared from *m*-halogenoanisole and acetyl chloride or propionic anhydride, was transformed into the hydrazone. The hydrazone was oxidized to the diazomethane with yellow mercuric oxide. Treatment of the diazomethane with sulfur dioxide followed by decomposition of the resulting ring-sulfone gave the final product. Estrogenic potency was taken as an evidence for the structure of the product and as the basis for distinguishing the trans-form from the cis-form. Only the trans-form of each dimethyl compound was obtained, while in the cases of the diethyl compounds fractional distillation of the products gave geometrical isomerides.

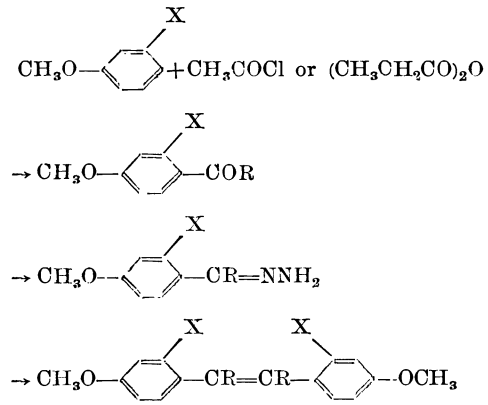

(R=CH_3 or C_2H_5; X=Cl, Br, or I)

The ultraviolet absorption curves of the trans-compounds are shown in Figs. 1 and 2. The absorption data of the parent compounds are given in Table 2. The trans-diiodo-diethyl compound (VI) was not obtained in a pure state and was not included in the

(4) M. Ōki, This Bulletin, **26**, 37 (1953).

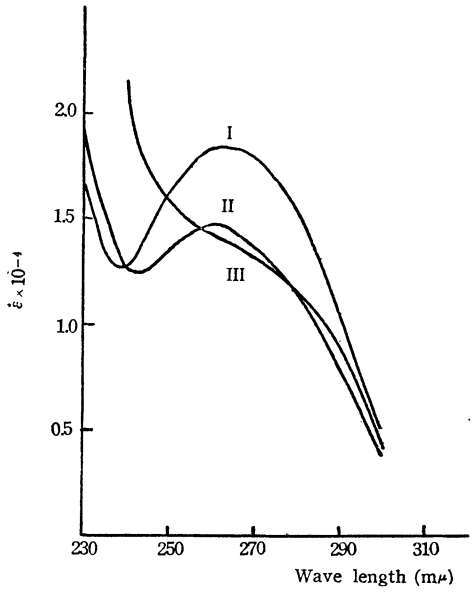

Fig. 1.—Ultraviolet absorption spectra of 4,4'-Dimethoxy-2,2'-dichloro-α,α'-dimethylstilbene ( ), 4,4'-Dimethoxy-2,2'-dibromo-α,α'-dimethylstilbene (II), and 4,4'-Dimethoxy-2,2'-diiodo-α,α'-dimethylstilbene (III)

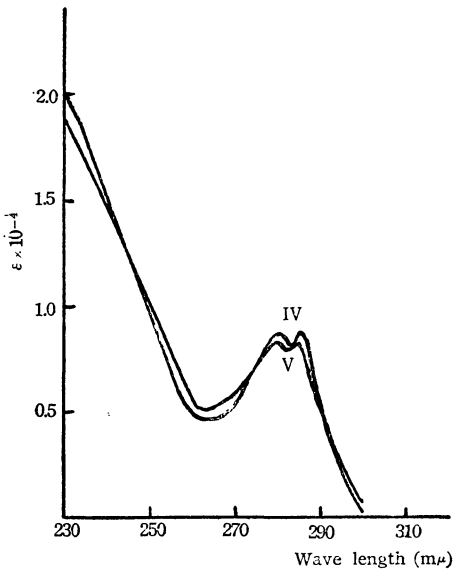

Fig. 2.—Ultraviolet absorption spetra of 4,4'-Dimethoxy-2,2'-dichloro-α,α'-diethylstilbene (IV) and 4,4'-Dimethoxy-2,2'-dibromo-α,α'-diethylstilbene (V).

absorption measurement. The dimethyl compounds and the diethyl compounds, respectively, showed absorption maxima at the same wave lengths irrespective of the kinds of halogen atoms at 2,2'-positions, although the diiodo-dimethyl compound (III) gave no maximum but a shoulder. Provided that the observed absorptions are those depending on the conjugation of the system comprising the benzene rings and the central ethylenic linkage, this may suggest that the halogen atoms at 2,2'-positions in any of the substances examined have little steric influence on the rotation degree of the benzene rings, because it would be less plausible to consider alternatively that they had definite and equal influence in spite of their different bulks. Then it may be said that the alkyl groups at α,α'-positions alone determine the rotation degree of the benzene rings, and the 2,2'-dihalogeno-compounds retain the structures of the parent compounds except the halogen atoms present in place of the hydrogen atoms at 2,2'-positions.

However, it remains unexplained why the bathochromic effect of the halogen substitution is greater in the diethyl compounds than in the dimethyl compounds. The observed absorptions of the dimethyl compounds and those of the diethyl compounds might not correspond to each other, because they appear characteristically different both in the shapes and in the extinction coefficients.

The minimum active doses were determined by the vaginal smear test with ovariectomized mice, substances in camellia oil being injected subcutaneously in two portions. The results given in Table 1 indicate that the diethyl compounds are stronger than the corresponding dimethyl compounds, and, either in the diethyl or in the dimethyl series, the dichloro-compound and the dibromo-compound have nearly the same potency, while the diiodo-compound a weaker potency. The liquid isomerides of the diethyl compounds showed very weak activities, indicating that they were cis-forms. The activities of the parent compounds are given in Table 2 with the absorption data. Comparison of the activities of the dihalogeno-derivatives with those of the parent compounds shows that the halogen substitution at 2,2'-positions reduced the activity, slightly in the dimethyl series, while profoundly in the diethyl series. The reduction of the activity was probably caused, at least partly, by the fattening of the molecules by the halogen atoms, and it is quite natural to suppose that the sharp peak of activity peculiar to the optimum structure of diethylstilbestrol may be very sensitive even to a slight deformation of the structure.

Experimental Part

4-Methoxy-2-chloroacetophenone.—To a

mixture of 14.3 g. of 3-chloroanisole, prepared from 3-methoxybenzenediazonium chloride and cuprous chloride,[5] and 16.0 g. of anhydrous aluminum chloride in 30 c.c. of carbon disulfide, 7.9 g. of acetyl chloride were gradually added with good stirring and cooling. The reaction mixture was left to stand for 30 minutes at room temperature and then gently boiled for 30 minutes. The upper carbon disulfide layer was decanted off. After treated with ice and hydrochloric acid (20 c.c.), the mixture was extracted with benzene. The benzene solution was washed with 10% aqueous sodium hydroxide and then with water, dried over calcium chloride, and distilled under a reduced pressure. 4-Methoxy-2-chloroacetophenone distilled over at 139–141° (10 mm.) and solidified on cooling. Recrystallization from petroleum ether gave colorless needles melting at 26–27°. Yield 11.5 g. (62% of the theory). Found: Cl, 19.15. Calculated for $C_9H_9O_2Cl$: Cl, 19.20%.

The 2, 4-dinitrophenylhydrazone was obtained in yellowish orange needles melting at 181–183°, when recrystallized from ethyl acetate. Found: N, 15.58; Cl, 9.56. Calculated for $C_{15}H_{13}O_5N_4Cl$: N, 15.36; Cl, 9.72%.

4-Methoxy-2-bromoacetophenone. — Obtained in the same way as 4-methoxy-2-chloroacetophenone by using 18.7 g. of 3-bromoanisole, prepared from 3-methoxybenzenediazonium bromide and cuprous bromide.[6] 4-Methoxy-2-bromoacetophenone distilled at 149–151°(8 mm.) or 163–166°(15 mm.). It solidified on cooling in a refrigerator to large prisms melting below the room temperature (23°). Yield 13.5 g. (59% of the theory). Found: Br, 34.72. Calculated for $C_9H_9O_2Br$: Br, 34.89%.

The 2, 4-dinitrophenylhydrazone was obtained in reddish yellow needles melting at 193–194°, when recrystallized from ethyl acetate. Found: N, 13.67; Br, 19.76. Calculated for $C_{15}H_{13}O_5N_4Br$: N, 13.69; Br, 19.53%.

4-Methoxy-2-iodoacetophenone.— Synthesized in the same way as described for 4-methoxy-2-chloroacetophenone from 23.4 g. of 3-iodoanisole, prepared by the decomposition of 3-methoxybenzenediazonium chloride in an acidic potassium iodide solution.[7] 4-Methoxy-2-iodoacetophenone distilled at 168—170° (9.5 mm.) or 158—159° (6 mm.) and was recrystallized from petroleum ether. Colorless needles melting at 68—70°. Yield 15.8 g. (55% of the theory). Found: I, 45.52. Calculated for $C_9H_9O_2I$: I, 45.97%.

The 2,4-dinitrophenylhydrazone was prepared as usual and recrystallized from ethyl acetate. Red needles melting at 108.5—109°. Found: N, 12.40; I, 27.87. Calculated for $C_{15}H_{13}O_5N_4I$: N, 12.28; I, 27.82%.

4-Methoxy-2-chloropropiophenone.— A mixture of 14.3 g. of 3-chloroanisole and 30.0 g. of anhydrous aluminum chloride in 50 c.c. of carbon disulfide was treated with 10.5 g. of propionic anhydride analogously as in the preparation of its lower homolog. 4-Methoxy-2-chloropropiophenone distilled at 152–153° (12 mm.). Yield 12.2 g. (61% of the theory). Found: Cl, 18.02. Calculated for $C_{10}H_{11}O_2Cl$: Cl, 17.85%.

The 2, 4-dinitrophenylhydrazone was prepared as usual and recrystallized from ethyl acetate-alcohol. Orange leaflets melting at 168–169°. Found: N, 15.55; Cl, 9.50. Calculated for $C_{16}H_{15}O_5N_4Cl$: N, 15.45; Cl, 9.77%.

4-Methoxy-2-bromopropiophenone.—Prepared in the same way as 4-methoxy-2-chloropropiophenone, 18.7 g. of 3-bromoanisole being used instead of 3-chloroanisole. 4-Methoxy-2-bromopropiophenone distilled at 146–147° (6 mm.). Yield 15.7 g. (65% of the theory). Found: Br, 32.94. Calculated for $C_{10}H_{11}O_2Br$: Br, 32.88%.

The 2, 4-dinitrophenylhydrazone was prepared as usual and recrystallized from ethyl acetate-alcohol. Orange leaflets melting at 154–155°. Found: N, 13.51; Br, 19.68. Calculated for $C_{16}H_{15}O_5N_4Br$: N, 13.76; Br, 19.62%.

4-Methoxy-2-iodoprcpiophenone. — Prepared in the same way from 23.4 g. of 3-iodoanisole. 4-Methoxy-2-iodopropiophenone distilled at 158–162°(6 mm.) and solidified on cooling. Recrystallization from petroleum ether gave colorless plates melting at 61–63°. Yield 17.3 g. (58% of the theory). Found: I, 43.86. Calculated for $C_{10}H_{11}O_2I$: I, 43.75%.

The 2,4-dinitrophenylhydrazone was prepared as usual. Recrystallization from ethyl acetate gave orange-yellow needles melting at 161-162°. Found: N, 12.78; I, 28.23. Calculated for $C_{16}H_{15}O_5N_4I$: N, 12.56; I, 27.94%.

4-Methoxy-2-chloroacetophenone-hydrazone.—A solution of 4-methoxy-2-chloroacetophenone (5.0 g.) and hydrazine hydrate (1.6 g.) in hot propyl alcohol (5 c.c.) was refluxed for 5 hours on an oil bath. Crystals separating on cooling were collected and recrystallized from alcohol. Colorless needles melting at 138–139°. Yield 0.2 g. (4% of the theory). Found: N, 14.22; Cl, 18.09. Calculated for $C_9H_{11}ON_2Cl$: N, 14.10; Cl, 17.85%. On standing it decomposed probably to an azine.

(5) F. Leverdin and F. Eckhard, *Ber.*, **32**, 2626 (1899).
(6) Cf. H. R. Snyder and Z. Wicks, Jr., "Organic Syntheses", Vol. 24, p. 22.
(7) A. Baeyer and V. Villiger, *Ber.*, **35**, 3026 (1902).

All the ketones described above gave poor yields of hydrazones even when heated with hydrazine hydrate in ethanol for 5 hours.

4,4′-Dimethoxy-2,2′-dichloro-α,α′-dimethylstilbene (I).—A suspension of 3.0 g. of the above hydrazone and 5.5 g. of yellow mercuric oxide in 30 c.c. of petroleum ether was shaken for 8 hours at 12–16°. The resulting red solution containing the diazomethane was filtered from solids. To the filtrate cooled in ice-water, a rapid stream of sulfur dioxide was passed until the color disappeared. The solvent was distilled off from the reaction mixture and the remainder was heated at 160–200° to complete the decomposition. The oil solidified on cooling and was purified by chromatographical separation followed by recrystallization from benzene-petroleum ether. Pale yellow needles melting at 112–113°. Yield 0.4 g. (16% of the theory). Found: Cl, 21.32. Calculated for $C_{18}H_{18}O_2Cl_2$: Cl, 21.03%.

4-Methoxy-2-bromoacetophenone-hydrazone.—Treatment of the ketone (13.5 g.) with hydrazine hydrate (3.5 g.) in propyl alcohol gave difficultly crystallizable hydrazone, which was directly used in the next reaction. On long standing at a cool place it solidified and was recrystallized from alcohol. Colorless needles melting at 88–90°. Found: N, 11.60; Br, 32.98. Calculated for $C_9H_{11}ON_2Br$: N, 11.48; Br, 32.74%.

4,4′-Dimethoxy-2,2′-dibromo-α,α′-dimethylstilbene (II).—A suspension of the above crude hydrazone and yellow mercuric oxide in petroleum ether was treated in an analogous way as described for the dichloro-compound (I). Recrystallization from benzene-petroleum ether gave 4,4′-dimethoxy-2,2′-dibromo-α,α′-dimethylstilbene in pale yellow needles melting at 117.5–119.5°. Yield 0.3 g. (3% of the theory). Found: Br, 37.73. Calculated for $C_{18}H_{18}O_2Br_2$: Br, 37.51%.

4-Methoxy-2-iodoacetophenone-hydrazone.—Prepared in the same way. The crystalline product obtained in colorless needles melting at 158–160° after recrystallization from benzene-petroleum ether was not the expected hydrazone. The major part of the product was an oil and used in the next step without purification.

4,4′-Dimethoxy-2,2′-diiodo-α,α′-dimethylstilbene (III).—Prepared from the above crude hydrazone in the same way as the dichloro-compound (I). Chromatographical separation followed by recrystallization from benzene-alcohol or ethyl acetate gave pale yellow plates melting at 159–160°. Yield 0.03 g. from 3.0 g. of the crude hydrazone (1% of the theory). Found: I, 49.12. Calculated for $C_{18}H_{18}O_2I_2$: I, 48.80%.

4-Methoxy-2-chloropropiophenone-hydrazone.—Prepared in the same way as the acetophenone-hydrazones. The oily hydrazone was used without purification.

4,4′-Dimethoxy-2,2′-dichloro-α,α′-diethylstilbene (IV) (VII).—Prepared in the same way as the corresponding dimethyl compound (I). Five hours' shaking was sufficient for oxidation. Distillation of the product gave a pale yellow oil boiling at 125–145° (0.5 mm.) and another yellow viscous oil boiling at 210–220° (0.5 mm.). Redistillation of the former gave a colorless oil boiling at 88–89° (0.07 mm.). Found: Cl, 19.52. Calculated for $C_{20}H_{22}O_2Cl_2$: Cl, 19.41%. The latter fraction solidified on standing at a cool place for a long time and was recrystallized from alcohol. Colorless prisms melting at 105.5–106.5°. Found: Cl, 19.53. Calculated for $C_{20}H_{22}O_2Cl_2$: Cl, 19.41%. Yield 0.8 g. of the liquid compound and 1.5 g. of the solid isomeride from 10.0 g. of the starting ketone (25% of the theory).

The estrogenic activities showed that the liquid compound was the cis-form and the solid the trans-form. The same holds good for other diethyl compounds described below.

4-Methoxy-2-bromopropiophenone-hydrazone.—Obtained as an oily substance and used without purification.

4,4′-Dimethoxy-2,2′-dibromo-α,α′-diethylstilbene (V) (VIII).—Prepared from the above crude hydrazone. Distillation of the product gave a pale yellow oil boiling at 135–140°(0.3 mm.) and a yellow viscous oil boiling at 190–205°(0.25 mm.). The former was refined to a colorless oil boiling at 87–89°(0.04 mm.). Found: Br, 35.02. Calculated for $C_{20}H_{22}O_2Br_2$: Br, 35.19%. The higher boiling fraction solidified on standing at a cool place for a long time and was recrystallized from alcohol. Colorless prisms melting at 114.5–115°. Found: Br, 35.23. Calculated for $C_{20}H_{22}O_2Br_2$: Br, 35.19%. Yield 1.2 g. of the liquid cis-isomeride and 1.7 g. of the solid trans-isomeride from 10.0 g. of the starting ketone (31% of the theory).

4-Methoxy-2-iodopropiophenone-hydrazone.—Obtained as an oily substance and used without purification.

4,4′-Dimethoxy-2,2′-diiodo-α,α′-diethylstilbene (VI) (IX).—Synthesized from the above hydrazone. Distillation of the product gave a yellow oil boiling at 65–120°(0.03 mm.)

and a residue. The distillate was refined to a colorless oil boiling at 108–110°(0.02 mm.). Found: I, 46.58. Calculated for $C_{20}H_{22}O_2I_2$: I, 46.74%. The residue did neither distil even at 200°(0.0005 mm.) nor solidify. It was fractionated through an alumina column in benzene solution and the solvent was evaporated in vacuo. A heavy viscous oil. Found: I, 45.82. Calculated for $C_{20}H_{22}O_2I_2$: I, 46.74%. Yield 1.3 g. of the cis-isomeride and 2.0 g. of the trans-isomeride from 10.0 g. of the starting ketone (33% of the theory).

Ultraviolet absorption spectra. — They were recorded with a Beckman Model DU photoelectric quarz spectrophotometer in 95% ethanol. The length of solutions was 5 mm. and the concentrations were 0.02 to 0.05 millimol per litre.

The author wishes to thank Professor Y. Urushibara for his kind guidance. Thanks are also due to Mr. F. Ueno of the Teikoku Hormone Manufacturing Co., Ltd., Kawasaki, for the bio-assays and to the Ministry of Education for the Grant in Aid for Fundamental Scientific Research.

Department of Chemistry,
Faculty of Science, Tokyo University.

Radiometric Determination of Small Amounts of Thallium

By Tomitaro ISHIMORI

(Received March 17, 1953)

In 1940, a method of gravimetric determination of thallium which is based on the quantitative precipitation of thallium as $[Co(NH_3)_6](TlCl_6)$ was first reported by G. Spacu and A. Pope.[1] They determined about 100 mg. thallium by their method.

In 1949, examining this method carefully, Y. Murakami[2] improved it slightly and ascertained its excellent selectivity. According to this author an amount of thallium as small as 5 mg. could be determined precisely. In this paper, a new method of radiometric determination of smaller amounts of thallium, i. e. 3 mg. —0.5 microg. thallium is proposed.

This method consists in the precipitation of thallium by radioactive hexammine cobaltic trichloride which is labelled with cobalt-60 and the measurement of radioactivity of the precipitate which is due to the radioactive cobalt combined with hexachlorothallic ion as hexammine cobaltic ion. As the precipitation of thallium with hexammine cobaltic trichloride is highly selective, the method will be applied in various cases. However, the presence of radioactive thallium will disturb the determination. Therefore, for example, the determination of thallium contents in radioactive minerals will not be successful.

Further, it must be added that another method of radiometric determination of micro-amounts of thallium had been reported by H. Moureu et al.[3] in 1944. Their method is based on the formation of radioactive thallium iodide.

Experimental Part

(1) **Apparatus.**—Chemical procedures are operated in a microbeaker. For the filtration of the precipitate a filter-tube with a layer of sintered glass is used. The filtering surface is covered with fibres of filter paper, suspended in the water, by sucking up through the tube.

For the measurement of radioactivity, a Lauritsen electroscope made by the Scientific Research Institute, Tokyo, and a Geiger-Müller counter with a scaler of 32 which is prepared by Prof. T. Sasaki, Kyushu University, are used.

(2) **Reagents.**—Stock solution of thallium nitrate is prepared by dissolving thallous nitrate (Merck reagent), and standardised by the Spacu's method. Diluting this stock solution, a series of standard solutions (acidified slightly with nitric acid) is prepared.

Solution of potassium chlorate: 1 g. potassium chlorate is dissolved in 15 cc. distilled water.

Solution of hexammine cobaltic trichloride: According to the amounts of thallium to be determined, either the solution of the precipitant (A) or that of (B) is used.

Solution of the precipitant (A): 0.05 *M* aqueous solution of the hexammine cobaltic trichloride which is prepared by the Biltz's method[4] from 10 g. cobalt chloride containing about 2.5 mg. cobalt-60 chloride. This solution is used for the

(1) G. Spacu und A. Pope, *Z. Anal. Chem.* **120**, 322 (1940).

(2) Y. Murakami, This Bulletin **22**, 206 (1949).

(3) H. Moureu, P. Chovin and R. Daubel, *Chem. Abst.* **40**, 1752 (1946): *Compt. rend.* **219**, 127 (1944).

(4) H. Biltz, "Übungsbeispiel aus der anorg. Experimentalchemie", Leipzig, **1913**, s. 165.

determination of 3.1—0.034 mg. thallium.

Solution of the precipitant (B): About 0.05 *M* aqueous solution of the hexammine cobaltic trichloride which is prepared as above from 0.5g. cobalt chloride containing about 5 mg. cobalt-60 chloride. This solution is used for the determination of less than 30 microg. thallium.

(3) **Procedure.**—A known quantity of a thallium solution is taken from a burette into a microbeaker. 0.5 cc. of 1% ammonium chloride, 1—2 drops of hydrochloric acid (1:1) and 3—5 drops of potassium chlorate solution are added to the beaker. Thallium is oxidised to the thallic state by gentle boiling on a hot plate. When the volume of the liquid is reduced to less than one half, the beaker is removed from the hot plate and cooled on standing. The total volume of the solution must be 0.5—2 cc. Then 2—5 drops of the radioactive hexammine cobaltic trichloride reagent are added, until the solution is coloured orange red. If the amount of thallium present is less than about 30 microg., the precipitate is scarcely seen or is not seen at all. In such cases, it is preferable to leave it overnight. In other cases, the precipitate is formed immediately and it is necessary to leave it only for a short time. The precipitate formed as above is filtered with the above-mentioned filter-tube, and washed four times with small portions of 2% hydrochloric acid. Filtrate and washings are discarded. About 1 cc. of 3% hydrogen peroxide and a few drops of acetic acid are added to the beaker which contains the precipitate and filter-tube. After dissolving the precipitate by heating on a water bath, the solution is poured into a glass dish through the filtertube by suction. Several times the filter-tube and the inside of the beaker are rinsed with small portions of distilled water. All these washings are transferred into the glass dish. The combined solution in the glass dish is evaporated up on a water bath. After cooling, the radioactivity of the glass dish which contains the residue is measured.

(4) **Measurement of Radioactivity.**—Measured radioactivity of each specimen which is corrected for the natural leaks or natural counts is represented by divisions per minute (d/m), or counts per minute (c/m). The specimen obtained from 1.55 mg. Tl by using the solution of precipitant (A) is reserved as the standard of radioactive $[Co^*(NH_3)_6](TlCl_6)$. Shortly after the measurement of the radioactivity of each specimen, the radioactivity of the standard, $(d/m)_s$ or $(c/m)_s$, is measured in the condition of the same geometry. The ratio $(d/m)/(d/m)_s$ or $(c/m)/(c/m)_s$ is not affected by the variation of the sensitivity of the Lauritsen electroscope or the Geiger-Müller counter and the decay of the radioactivity of cobalt-60. So far as the reagent of the same bottle is used, the specific activity of the reagent is constant and the ratio $(d/m)/(d/m)_s$ or $(c/m)/(c/m)_s$ will depend only on the amount of thallium.

(5) **Results Obtained.**—The results for 3.1—0.034 mg. Tl are shown in Table 1. All these results are obtained by using the solution of the precipitant (A). From the Table 1 we can see that there are no serious differences between the results obtained by Geiger-Müller counter and those obtained by Lauritsen electroscope and that the relation between the amount of thallium and the ratio $(c/m)/(c/m)_s$ is almost linear. The deviations of $(c/m)/(c/m)_s$/mg. Tl of the each experiment from the mean value of $(c/m)/(c/m)_s$/ mg. Tl, 0.701, are calculated in the fourth column, and from the mean value of the deviations we can estimate the accuracy of the determination.

Table 1
Results for 3.1—0.034 mg. Tl

mg. Tl (taken)	Measured by G. M. Counter		% Deviation	Measured by Lauritsen Electroscope
	$\frac{(c/m)}{(c/m)_s}$	$\frac{(c/m)/(c/m)_s}{\text{mg. Tl}}$		$\frac{(d/m)}{(d/m)_s}$
3.100	2.196	0.708	1.0	2.184
2.790	1.853	0.664	−5.3	1.857
2.325	1.534	0.659	−5.9	1.630
2.108	—	—	—	1.468
2.015	1.411	0.700	0.0	1.329
1.721	—	—	—	1.115
1.550	1.000	0.645	−8.0	1.000
1.225	0.871	0.711	1.4	0.867
0.744	0.493	0.662	−5.6	0.505
0.482	0.347	0.719	2.6	0.360
0.449	0.300	0.668	−4.7	0.303
0.360	0.273	0.755	7.7	0.259
0.228	0.171	0.750	7.0	0.163
0.130	0.098	0.753	7.4	0.096
0.077	0.064	0.831	18.5	0.059
0.034	0.020	0.588	−16.0	0.019
0.000	0.000	—	—	0.000
mean	—	0.701	±6.5	—

Table 2
Results for 24.6—0.46 microg Tl

microg Tl (taken)	$(d/m)/(d/m)_s$	$\frac{(d/m)/(d/m)_s}{\text{microg Tl}}$	% Deviation
24.6	0.619	0.0251	−14.4
23.4	0.657	0.0281	− 4.1
21.6	0.594	0.0275	− 6.1
18.4	0.517	0.0281	− 2.7
15.4	0.465	0.0302	3.1
12.9	0.370	0.0287	− 2.1
9.08	0.226	0.0248	−15.4
5.95	0.152	0.0255	−13.0
3.85	0.117	0.0303	3.4
1.86	0.063	0.0338	15.4
1.24	0.045	0.0363	23.8
0.46	0.015	0.0326	11.3
0.00	0.000	—	—
mean	—	0.0293	±9.5

If the amount of thallium is calculated from the following equation (1), the accuracy of the method will be in the order of $\pm(6-7)\%$.

$$\text{mg. Tl} = (c/m)/(c/m)_s/0.701 \qquad (1)$$

The results for 24.6—0.46 microg. Tl obtained by using the solution of the precipitant (B) are shown in Table 2. In these cases the radioactivity is measured only by the Lauritsen electroscope. From Table 2 we can see that the linear relation between the amount of thallium and ratio $(d/m)/(d/m)_s$ is not so good and that although more than about five micrograms thallium may be calculated from the following equation (2), it is preferable to use a working curve in the determination of thallium less than about five micrograms.

$$\text{microg. Tl} = (d/m)/(d/m)_s/0.029 \qquad (2)$$

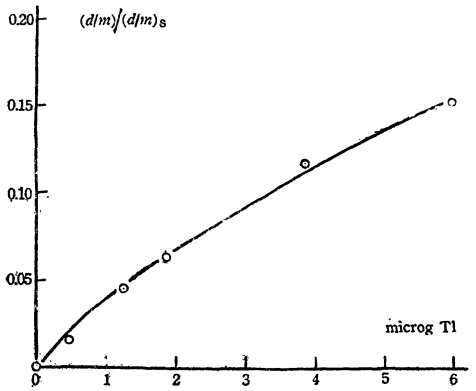

Fig. 1.—Working Curve for Determination of minute Amounts of Thallium

Fig. 1 shows the working curve for the determination of minute amounts of thallium. Roughly speaking, the error in the determination of the minute quantities of thallium is estimated about ten per cent or more.

(6) Application. — The method is applied to the determination of the thallium contents in volcanic rocks in the following procedure[5]:

To about 2 g. of finely divided rock powder in a platinum dish add about 8 cc. of 6N sulfuric acid and about 12 cc. of hydrofluoric acid. Evaporate to dryness and fume off the excess sulfuric acid avoiding decomposition of ferric sulfate. Take up the residue in a little water and again fume off the sulfuric acid. Treat the residue with water; warm to bring all soluble material into solution. Cool the solution and make up to about 100 ml. Reduce thallium to thallous state with hydroxylamine hydrochloride and add 5 cc. of 10% potassium cyanide and 5 cc. of 10% ammonium citrate. Adjust the *p*H to about 10 adding dilute ammonium hydroxide dropwise. Extract the mixture with four 10—15 cc. portions of 0.1% dithizone in chloroform. Combine the extracts and wash with 20—50 cc. of (1:1000) ammonium hydroxide. Separate the chloroform layer and shake the aqueous phase with a few cc. of dithizone solution to recover any thallium that may have passed into the ammonia solution. Shake the combined chloroform extracts with 10 cc. of (1:100) nitric acid and separate the chloroform layer. The aqueous layer is transferred to a microbeaker and evaporated to about 1 cc. or less. The resultant solution is treated as (3) using solution of precipitant (B).

To examine the recovery of thallium, known quantities of thallium standard solution are diluted to about 100 cc. and treated with dithizone following the above-mentioned procedure. Results are considerably low as shown in the Table 3.

Table 3
Recovery of Thallium

microg Tl (taken)	$(d/m)/(d/m)_s$	microg Tl (found) (a)	microg Tl (found) (b)	% Recovery
14.8	0.398	—	13.5	91
3.8	0.092	2.8	3.1	73—81

(a): calcd. from Fig. 1 (b): calcd. from Eq. (2)

Table 4
Thallium contents of Rocks

Sample	microg Tl (added)	$(d/m)/(d/m)_s$	microg Tl (found) (a)	microg Tl (found) (b)	%Tl
2.11 g. Liparite (Kozusima, Izu)	none	0.029	0.8	1.0	0.00005
2.04 g. 〃 (〃)	6.1	0.139	5.1	4.7	—
1.77 g. Basalt (Fuji)	none	0.003	0.1	—	0.00000

(a): calcd. from Fig. 1 (b): calcd. from Eq. (2)

The results obtained on two Japanese volcanic rocks are shown in Table 4. These values will be low from the above-mentioned results of examination of the extraction of thallium, but it will be sure that the thallium content of the liparite is in the order of $10^{-5}\%$.

Further study on the determination of thallium content of silicate rocks is to be continued.

The auther wishes to express his sincere thanks to Prof. Sinnosuke Matuura for the opportunity to carry out this investigation and to Mr. Tohru Nozaki for his assistance in the experiment.

(5) c. f. F. J. Welcher, "Organic Analytical Reagents". Vol. 3, D. Van Nostrand Co, New York, (1949), p. 544.

Chemical Laboratory, Faculty of Science, Kyushu University

The Raman Spectrum of Cyanuric Acid

By Mitsuo ITO

(Received April 6, 1953)

Introduction

From the experimental results of the ultra-violet absorption spectra, E. Agallidis and his coworkers as well as I. M. Klotz and Themis Askounis have concluded that enol-and keto-formal cyanuric acids coexist in aqueous solution in the tautomeric relation.[1],[2] In the present work, the author tried to ascertain this from the view-point of Raman spectrum, and computed further approximate force constants for both forms by simple calculations.

Experimental

For photographing Raman spectra a powerfully light-gathering spectrograph constructed by us was used. It had two dense flint prisms (height 4.5 cm, side length 6 cm), a collimator lens (diameter 9 cm., focus 45 cm.) and a camera lens (diameter 8 cm., focus 21 cm.). Two glass mercury lamps were used as the light source, placed on both sides of the wood-type Raman tube. The exposure time, on "Oriental" Hyper Panchromatic plates, ranged from 10 to 100 hours.

A sample of pure cyanuric acid, recrystallized from water three times, was dissolved in a hydrogen chloride acidic and a caustic soda alkaline solution. As the concentration of the aqueous solution at room temparature could not be made greater than about 10 %, although water seems to be the best solvent for the acid, a rather long exposure time was needed to record measurable Raman lines. During the exposure hot water was circulated continually through the outer jacket of the wood tube in order to prevent the precipitation of crystal.

Table 1 lists wave number shifts measured in the Raman spectra of both the acidic and alkaline solutions, with indications of their relative intensities and exciting mercury lines.

Discussion

As shown in Table 1, there are some Raman lines which have nearly coinciding wave number shifts, but with changing relative intensities observed in the two solutions. For example, 708 cm.$^{-1}$ measured for the alkaline solution and 715 cm.$^{-1}$ measured for the acidic solution, giving the same Raman shift within experimental error, shows a much greater intensity in the alkaline solution. Other such examples are found in the pairs of 331 and 329, 432 and 425, and 1410 and 1421 cm.$^{-1}$.

Table 1

Observed Raman lines of cyanuric acid in the acidic and alkaline solutions

Alkaline solution			Acidic solution		
Wave number shift (cm.$^{-1}$)	Exciting mercury line	Relative intensity	Wave number shift (cm.$^{-1}$)	Fxciting mercury line	Relative intensity
331	e	3	329	e	1
432	e	3	425	e, k	1
456	e, k, i	1			
572	e, k, i	2			
708	e, —e, k	8	715	e, k	3
			816	e, k	3
853	e	3	853	e, k, i	6
923	e, k	3	921	e	4
1090	k, i	2			
			1371	e, k, i	2
1410	k, i	4	1421	e, k, i	2
			1636	k, i	5
			3446	e, k, i	6
			3488	e, k	4

(1) E. Agallidis, H. Fromherz and A. Hartmann, *Ber.*, **71**, 1391 (1938).

(2) I. M. Klotz and Themis. Askounis, *J. Am. Chem. Soc.*, **69**, 801 (1947).

On the other hand, there are some pairs of lines whose intensities are in the reverse ratio, that is, strong in the acidic and weak in the alkaline solution. The pairs 853 and 853, and 923 and 921 cm.$^{-1}$ belong to this type.

Such a change of relative intensities of the corresponding Raman lines can be readily understood by assuming that tha enol-and keto-formal cyanuric acids coexist in aqueous solution and that the equilibrium between them changes with the *p*H of the solution. This assumption is in agreement with and supports the result of ultra-violet absorption.[1],[2]

In caustic soda alkaline solution, cyanuric acid exists more stably in the form of cyanuric acid ion represented by formula (1) in Fig. 1, while in acidic solution the keto form represented by (11) is more stabilized. Then the Raman lines which are stronger in the alkaline solution must be due to (1), and those stronger in the acidic solution to (11). Accordingly the shifts 331, 432, 708 and 1410 cm.$^{-1}$ are attributed to (1), and those of 853, 921, 1636, 3446 and 3488 cm.$^{-1}$ to (11).

Let us consider first the frequencies of totally symmetric vibrations of the cyanuric acid ion of form (1). X-ray diffraction studies show that the symmetry in cyanuric acid crystal is D_{3h}.[3]

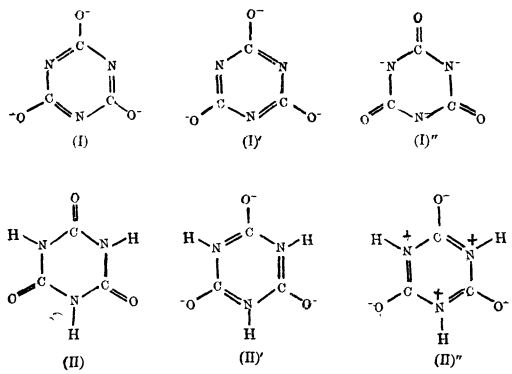

Fig. 1.—Resonance structures for cyanuric acid of enol-and keto-forms.

Assuming the same symmetry also for the ion (1), there are in all three totally-symmetric vibrations. As totally-symmetric vibrations generally appear strongly in the Raman effect,[4] it is reasonable to consider that among the four strong lines attributed by us to (1) (either one of 331 or 432, 708 and 1410 cm.$^{-1}$) the first one is probably the totally-symmetric deformation vibration of the six-membered ring, the second the totally-symmetric breathing vibration of the whole ion, and the last the totally-symmetric stretching vibration of the carbon and oxygen atoms.

On a crude assumption that cyanuric acid ion resonates only between the two Kekulè-like structures (1) and (1)′ in Fig. 1, the totally-symmetric vibration frequencies were calculated using the valence-force-field model.[4]

For the force constants the following values were used:

k (C—O) $=5.00\times10^5$ dyne/cm.,[5]
k (C—N) $=7.6\times10^5$ dyne/cm.,[5]
δ ($\angle$NCN) $=0.23\times10^5$ dyne/cm.,[6]
δ ($\angle$CNC) $=0.32\times10^5$ dyne/cm.,[6]

where k and δ refer to stretching and bending vibrations respectively. The three totally-symmetric vibration frequencies and the corresponding vibrational types are

481 cm.$^{-1}$: deformation vibration,
904 cm.$^{-1}$: breathing vibration,
and 1288 cm.$^{-1}$: stretching vibration of the c-o bonds.

These calculated frequencies, however, do not agree well with the Raman frequencies observed above, meaning that the force constants used are not suitable. An attempt was made then to derive more reasonable force constants by substituting the obsered Raman frequencies into the final equations of the frequency calculation and to interpret their meaning. For this purpose 708 and 1410 cm^{-1} were taken as the two totally-symmetric non-deformation vibrations because of their prominent intensities. For the remaining totally-symmetric frequency we may choose either 331 or 431 cm.$^{-1}$.

If we chose 431 cm.$^{-1}$, some force constants would come out negative. Therefore we took

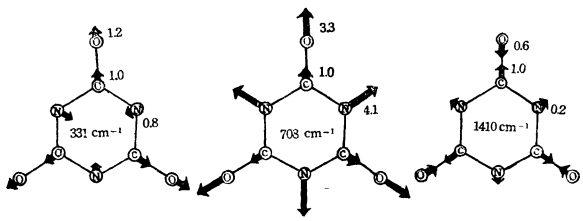

Fig. 2.—Calculated totally-symmetric vibrational frequencies and modes of the cyanuric acid ion.

(3) E. H. Wiebenga and N. F. Moermann, *Z. Krist.*, **99**, 217 (1938).
(4) G. Herzberg, "Raman and infrared spectra of polyatomic molecules," Van Nostrant, N. Y., (1945).
(5) Hibben, "Raman effect and its chemical application", Reinhold, N. Y., (1939).
(6) L. Kellner, *Proc. Roy. Soc. London*, **177**, 456 (1941).

331 cm.$^{-1}$ as the frequency of the third totally-symmetric vibration. The force constants calculated on the above assumptions are

k (C—O) $=6.71\times10^5$ dyne/cm.,
k (C—N) $=5.71\times10^5$ dyne/cm..

In Fig. 2, the calculated vibrational modes are shown for each frequency.

Comparing the above force constants with those already known for other molecules, the k value for the c-o bond may be explained as the result of addition of a slight double-bond character to that of the formal single bond, and the k value for the C—N bond caused by the actual bond having a more single-bond character than the formal one-and-half-bond. Thus the cyanuric acid ion gets some resonance contribution also from the keto-ionic structure as well as from the kekulé-like structures, as shown in Fig. 1.

Next, we applied the same consideration to the keto-formal structure (II) which is stable in acidic solution. Assuming also the symmetry D_{3h} for this structure, the totally-symmetric vibrations are four in number theoretically, i. e. in addition to the three vibrational types mentioned above for the cyanuric acid ion there is one more totally-symmetric stretching vibration of the N—H bond.

With the same procedures the four totally-symmetric vibration frequencies belonging to the formula (II) in Fig. 1 were calculated, using the following force constants

k (C=O) $=11.6\times10^5$ dyne/cm.,[5]
k (C—N) $=4.85\times10^5$ dyne/cm.,[5]
k (N—H) $=6.20\times10^5$ dyne/cm.,[5]
δ ($\angle$NCN) $=0.23\times10^5$ dyne/cm.,[6]
δ ($\angle$CNC) $=0.32\times10^5$ dyne/cm.,[6]

The resulting frequencies are

353 cm.$^{-1}$: deformation vibration,
769 cm.$^{-1}$: breathing vibration,
1811 cm.$^{-1}$: stretching vibration of the C=O bond,
3346 cm.$^{-1}$: stretching vibration of the N—H bond.

These frequencies are again very different from the observed Raman values 853, 1636, etc. In order to obtain a better agreement, we mnst adopt a larger and a smaller force constant for the C-N and the C=O bond respectively. The binding strength of the C-N bond in thit molecule should be larger than that of the formal C-N bond, and the C=O bond of it should be weaker than in the formal C=O bond. Accordingly some amount of the resonance contribution from the ionic structures (II)′ and (II)″ in Fig. 2 may be expected.

Although it is certain that cyanuric acid takes predominantly the keto-form in the acidic solution and enol-form in the alkaline solution, respectively, only the extreme structures (I) and (II) cannot explain the facts.

For example, the reported atomic distances in crystalline cyanuric acid are 1.28 A for the C-O bond and 1.37 A for the C-N bond,[3] both of which are intermediate between the normal single and the normal double bond lengths.

This fact is also confirmed by magnetic susceptibility measurements.[7] In the case of cyanuric acid in acidic or alkaline solution the structural contribution of the enol-or the keto-form appears much more dominant than in the case of crystal, depending on the pH value of the solution.

Finally, the author wishes to express his hearty thanks to Professor S. Imanishi, and to Assistant Professor Y. Kanda for their kind guidance. He also thanks Mr. Furukawa for his assistance in the experimental part of the work.

Department of Chemistry,
Faculty of Science, University of Kyushu,
Fukuoka

(7) J. Maruyoshi, *J. Chem. Soc. Japan*, **71**, 627 (1950).

Theoretical Study on the Polarographic Limiting Currents. I. Revised Equation for the Diffusion Currents*

By Hiroaki MATSUDA

(Received April 9, 1953)

Criticism of the Revised Equations Already Reported

Recently H. Strehlow and M. von Stackelberg,(1) J. J. Lingane and B. A. Loveridge(2) and T. Kambara, M. Suzuki and I. Tachi,(3) taking the curvature of dropping mercury electrode into consideration, derived the following revised expression of Ilkovič equation representing the mean diffusion current $\bar{i}_d(\mu A)$.

$$\bar{i}_d = 607n{*C}D^{1/2}m^{2/3}\tau^{1/6}(1+AD^{1/2}m^{-1/3}\tau^{1/6}) \quad (1)$$

In this equation, n, ${*C}$, D, m and τ are the number of electrons associated with the electrode reaction, the concentration of depolarizer in the bulk of solution in millimol/l, the diffusion constant of depolarizer in cm.^{2}/sec., the rate of flow of mercury in mg./sec. and the drop time in sec., respectively; A is a coefficient of interest to be discussed.

Strehlow and von Stackelberg have obtained the value $A=17$, upon solving the so-called Stackelberg's integral equation(4) representing the "differential thickness of diffusion layer" denoted by δ.(5) It seems, however, that the conclusion $A=17$ has not a good theoretical ground owing to the error contained in the integral equation employed by them, as given below. They define the "integral thickness of diffusion layer", denoted by Δ, by the relationship:

$$\Delta = \frac{2}{{*C}}\int_{r_0}^{\infty}({*C}-C)dr \quad (2)$$

and upon assuming that $4\pi r_0^2 \cdot \Delta$ is proportional to the total amount of reduction product, they derive

$$\Delta = \frac{2D}{r_0^2}\int_0^t r_0^2\delta^{-1}dt \quad (3)$$

where t is the time. These assumptions stated by them are not right in tri-dimensional problem, although they are legitimate in uni-dimensional one. This can be readily seen, when we treat a stationary spherical electrode, in which the quantity $4\pi r_0^2\Delta$ is clearly not proportional to the amount of reduction product, and thus Eq. (3) does not hold. In order to define the integral thickness of diffusion layer in such a rational way, as Eq. (3) can hold in the case of stationary spherical electrode, we should use the following equation instead of Eq. (2).

$$\Delta' = \frac{2}{{*C}r_0^2}\int_{r_0}^{\infty}({*C}-C)r^2dr \quad (4)$$

It can be shown that in the case of diffusion at a stationary spherical electrode Δ' and δ are given by

$$\Delta' = 4\sqrt{\frac{Dt}{\pi}}\left(1+\frac{\sqrt{\pi Dt}}{2r_0}\right) \quad (5)$$

$$\frac{1}{\delta} = \frac{1}{r_0}+\frac{1}{\sqrt{\pi Dt}} \quad (6)$$

Elimination of t from Eqs. (5) and (6) leads to the relationship between Δ' and δ, which holds for the stationary electrode of spherical form; thus it is found that

$$\Delta' = \frac{4}{\pi}\frac{r_0\delta}{r_0-\delta}\left(1+\frac{\delta}{2(r_0-\delta)}\right) \quad (7)$$

If we assume that Eq. (7) holds for the diffusion at the dropping electrode, upon eliminating Δ' from Eqs. (3) and (7), we obtain the following integral equation:

$$\pi D\int_0^t r_0^2\delta^{-1}dt = r_0^3\left\{2\frac{\delta}{r_0-\delta}+\left(\frac{\delta}{r_0-\delta}\right)^2\right\} \quad (8)$$

---

* A part of this paper was read at the 5th Annual Meeting of the Chemical Society of Japan, April 4, 1952, Tokyo.

(1) H. Strehlow and M. von Stackelberg, *Z. Elektrochem.*, **54**, 51 (1950).

(2) J. J. Lingane and B. A. Loveridge, *J. Am. Chem. Soc.* **72**, 438 (1950).

(3) T. Kambara, M. Suzuki and I. Tachi, This Bulletin **23**, 219 (1950).

(4) M. von Stackelberg, *Z. Elektrochem.*, **45**, 466 (1939).

(5) The differential thickness of diffusion layer is defined as follows:

$$\delta = {*C}/(\partial C/\partial r)_{r=r_0}$$

In this equation, C, r_0 and r are the concentration of depolarizer at an arbitrary point in the diffusion layer, the radius of mercury drop and tbe distance of any point from the center of drop, respectively.

This equation is the Stackelberg's integral equation determining the thickness δ in the case of spherical diffusion at a mercury drop expanding symmetrically. This equation has been already derived by Kambara, Suzuki and Tachi,[3] and upon solving this equation by means of an approximate calculation, they have shown the value of A to be 29.3.[6] The present author expands the quantity δ into the power series of $(m^{-1/3}D^{1/2}t^{1/6})$; i. e.

$$\delta=(D^{1/2}t^{1/2})\sum_{j=0}^{\infty}\beta_j(m^{-1/3}D^{1/2}t^{1/6}),$$

and then by comparing the means of comparison of coefficients, the β's are determined; thus Eq. (8) can be solved more precisely and the value of $A=31.2$ is obtained.

The above stated procedures are all based on the assumption that Stackelberg's integral equation, i. e. Eq. (7) showing the relationship between the differential and integral thicknesses of diffusion layer at a stationary spherical electrode, is valid even in the case of a dropping electrode. However, this assumption seems to have no theoretically concrete basis.

On the other hand, the intuitive consideration of Lingane and Loveridge[2] gave the value $A=39$. Kambara and Tachi[7] approximately solved the differential equation proposed by D. MacGillavry and E. K. Rideal[8] and the result was $A=39$; but the accuracy of this approximate calculation seems considerably inferior.

On account of these circumstances, it may be significant to consider here again the theoretical revision of Ilkovič equation. In this paper the solution of MacGillavry-Rideal differential equation by means of the method, that has been employed in the field of hydrodynamics by Th. von Kármán[9] and K. Pohlhausen[10] in order to evaluate the velocity distribution in the boundary layer, will be demonstrated and the expression for the limiting diffusion current will be shown. Further, the shielding effect of capillary will be considered theoretically. Finally, the revised Ilkovič equation representing the diffusion current in amalgam polarography will be also shown.

(6) T. Kambara and I. Tachi, This Bulletin, **25**, 284 (1952).
(7) T. Kambara and I. Tachi, This Bulletin, **23**, 225 (1950).
(8) D. MacGillavry and E. K. Rideal, *Rec. trav. chim.*, **56**, 1013 (1937).
(9) Th. von Karman, *Z. angew. Math. u. Mech.*, **1**, 233 (1921).
(10) K. Pohlhausen, ibid., **1**, 252 (1921).

Theoretical Derivation of the Revised Equation for the Diffusion Current

The movement of solution in the vicinity of mercury drop appears to be very complicated; now let us assume that the solution around the mercury drop is pushed away by the concentric expansion of drop, the volume of which increases at a constant rate. Then we can find $C(r, t)$ the concentration of depolarizer in the diffusion layer, by solving the following MacGillavry-Rideal differential equation:

$$\frac{\partial C}{\partial t}=D\frac{1}{r^2}\frac{\partial}{\partial r}\left(r^2\frac{\partial C}{\partial r}\right)-\frac{a^3}{3r^2}\frac{\partial C}{\partial r} \qquad (9)$$

where

$$a=(3m/4\pi d)^{1/3}$$

In this equation d represents the density of mercury at 25°C.

The initial and boundary conditions are clearly given by

$$C={}^*C \quad \text{for} \quad t=0,\ r>r_0;$$
$$C=0 \quad \text{for} \quad r=r_0,\ t>0;$$
$$C={}^*C,\ r^2\frac{\partial C}{\partial r}=0 \quad \text{for} \quad r\to\infty,\ t>0.$$

$^*C$ represents here the concentration of depolarizer in the bulk of solution, and the radius of mercury drop r_0 is given by

$$r_0=at^{1/3}=\left(\frac{3}{4\pi d}\right)^{1/3}m^{1/3}t^{1/3}=0.260m^{1/3}t^{1/2}(\text{mm})$$

Upon multiplying the both sides of Eq. (9) by r^2, and integrating the equation thus obtained with respect to r from r_0 to infinity, it can be readily seen that

$$\frac{\partial}{\partial t}\int_{r_0}^{\infty}({}^*C-C)r^2dr=Dr_0^2\left(\frac{\partial C}{\partial r}\right)_{r=r_0}.$$

Since the diffusion constant of depolarizer is very small, the inhomogeneity of concentration distribution occurs only in the vicinity of electrode surface; therefore, the integration interval from r_0 to infinity shown in the above equation may be replaced by that from r_0 to $\delta'(t)$, resulting in no appreciable deviation. Here, $\delta'(t)$ is a function of time, and represents the thickness of layer, in which the inhomogeneity of concentration arises, i. e. the thickness of diffusion layer. Writing

$$r=r_0+x,$$

then it is found that

$$\frac{\partial}{\partial t}\int_0^{\delta'}(^*C-C)(r_0+x)^2dx=Dr_0^2\left(\frac{\partial C}{\partial x}\right)_{x=0} \tag{10}$$

This equation corresponds to the integro-differential equation of von Kárman in hydrodynamics; in order to solve this equation, we will at first expand the quantity $^*C-C$ in the power series of x; i. e.

$$^*C-C=^*C\frac{x}{r_0+x}\left(1+\sum_{j=1}^{l}A_jx^j\right) \tag{11}$$

When the l unknown coefficients A_j ($j=1,2,\ldots,l$) are determined as functions of δ' and r_0 with the aid of l suitable boundary conditions, then insertion of Eq. (11) into Eq. (10) gives an ordinary differential equation of first order demonstrating δ'. Upon integrating the differential equation thus obtained, we can find δ' as a function of time, from which the proper expression for the diffusion current is derived.

(i) At first we will put $l=6$; then the following boundary conditions are found, by which A_j ($j=1,2,\ldots,6$) are to be determined.

$$\left.\begin{aligned}&(C)_{x=\delta'}=^*C;\ \left(\frac{\partial C}{\partial x}\right)_{x=\delta'}=0;\\&\left(\frac{\partial^2C}{\partial x^2}\right)_{x=\delta'}=0;\ \left(\frac{\partial^3C}{\partial x^3}\right)_{x=\delta'}=0;\\&\left(\frac{\partial^4C}{\partial x^4}\right)_{x=\delta'}=0;\\&\left[\frac{\partial^2\{(r_0+x)C\}}{\partial x^2}\right]_{x=0}=0\end{aligned}\right\} \tag{12}$$

The first five equations result from the fact that the concentration C in the diffusion layer should vary as continually as possible and be connected with the bulk concentration $^*C$ at $x=\delta'$. The last condition is obtained when the relation $r=r_0+x$ is inserted into Eq. (9) and then $x=0$ is put therein. Upon determining the coefficients A_j by the aid of conditions shown by Eq. (12), it is found that $^*C-C$ is given by

$$^*C-C=^*C\frac{r_0}{r_0+x}\left\{1-3\left(\frac{x}{\delta'}\right)+10\left(\frac{x}{\delta'}\right)^3-15\left(\frac{x}{\delta'}\right)^4+9\left(\frac{x}{\delta'}\right)^5-2\left(\frac{x}{\delta'}\right)^6\right\} \tag{13}$$

Insertion of Eq. (13) into Eq. (10) gives the following ordinary differential equation of first order, by which δ' is to be determined.

$$\frac{d}{dt}\left(\frac{3}{14}r_0^2\delta'+\frac{1}{28}r_0\delta'^2\right)=Dr_0^2\left(\frac{1}{r_0}+\frac{3}{\delta'}\right) \tag{14}$$

Now writing

$$\delta'=(D^{1/2}t^{1/2})\sum_{j=0}^{\infty}\alpha_j(a^{-1}D^{1/2}t^{1/6})^j$$

and inserting this equation into Ep. (14), we can determine α_j's by the method of comparison of coefficients; thus the solution of Eq. (14) is given by the equation in form of following power series.

$$\delta'=(D^{1/2}t^{1/2})\left\{2\sqrt{3}+\frac{4}{5}(a^{-1}D^{1/2}t^{1/6})-\frac{19}{75}\sqrt{3}(a^{-1}D^{1/2}t^{1/6})^2+\frac{856}{6375}(a^{-1}D^{1/2}t^{1/6})^3-\ldots.\right\} \tag{15}$$

Since the diffusion current i_d is equal to the number of mols of depolarizer reaching the surface of dropping electrode in unit time multiplied by nF, it is found that

$$\begin{aligned}i_d&=4\pi r_0^2\cdot nF\cdot D\left(\frac{\partial C}{\partial r}\right)_{r=r_0}\\&=4\pi r_0^2\cdot nF\cdot D\cdot{}^*C\left(\frac{1}{r_0}+\frac{3}{\delta'}\right)\end{aligned}$$

When the expression for δ' given by Eq. (15) is inserted into the above equation, then we obtain the following equation showing the instantaneous diffusion current, in which the usual conventional units are employed.

$$i_d=709\,n^*CD^{1/2}m^{2/3}t^{1/6}\{1+35.5(D^{1/2}m^{-1/3}t^{1/6})+266(D^{1/2}m^{-1/3}t^{1/6})^2-\ldots.\} \tag{16}$$

Accordingly the mean diffusion current is shown by

$$\bar{i}_d=608n^*CD^{1/2}m^{2/3}\tau^{1/6}\{1+31.1\,(D^{1/2}m^{-1/3}\tau^{1/6})+207(D^{1/2}m^{-1/3}\tau^{1/6})^2-\ldots.\} \tag{17}$$

(ii) In order to execute the calculation of higher order approximation, the value $l=10$ will be chosen; for the determination of A_j ($j=1,2,\ldots,10$) to the six boundary conditions shown by Eq. (12) the following four conditions will be added.

$$\left.\begin{aligned}&\left(\frac{\partial^5C}{\partial x^5}\right)_{x=\delta'}=0;\ \left(\frac{\partial^6C}{\partial x^6}\right)_{x=\delta'}=0;\\&\left(\frac{\partial^7C}{\partial x^7}\right)_{x=\delta'}=0;\\&\left[\frac{\partial^4}{\partial x^4}\{(r_0+x)C\}\right]_{x=0}+4\frac{a^3}{D}\frac{1}{r_0^3}\left(\frac{\partial C}{\partial x}\right)_{x=0}=0\end{aligned}\right\} \tag{18}$$

The last condition can be obtained, when r in Eq. (9) is replaced by (r_0+x) and then equation thus obtained is twice differentiated with respect to x and further $x=0$ is put therein.

When the quite analogous mathematical procedures shown in the case of $l=6$ are carried out, then we find the following equation representing the instantaneous and mean diffusion current; i. e.

$$i_d=709n^*CD^{1/2}m^{2/3}t^{1/6}\{1+36.3(D^{1/2}m^{-1/3}t^{1/6}) +343(D^{1/2}m^{-1/3}t^{1/6})^2-\ldots.\} \quad (19)$$

$$\bar{i}_d=608n^*CD^{1/2}m^{2/3}\tau^{1/6}\{1+31.7\,(D^{1/2}m^{-1/3}\tau^{1/6}) +267(D^{1/2}m^{-1/3}\tau^{1/6})^2-\ldots.\}. \quad (20)$$

Although the accuracy of mathematical treatment can be increased with the increasing greater value of l, the numerical calculation thereof becomes more and more complicated. Furthermore, the comparison of Eq. (16) with (19) and (17) with (2) clearly indicates that the coefficients of the first, second and third terms, appearing in the above stated two calculations, show no considerable differences. Hence the approximate calculation with $l=10$ may be satisfactorily precise.

NOTE:—In the case of uni-dimensional diffusion, coresponding to the Ilkovič equation, the solution can, as well known, be obtained rationally; when the above developed approximate treatment is applied to this case with the value $l=10$, the following equations for the instantaneous and mean diffusion current are derived.

$$i_d=709n^*CD^{1/2}m^{2/3}t^{1/6}$$
$$\bar{i}_d=608n^*CD^{1/2}m^{2/3}\tau^{1/6}$$

Comparison of these equations with the Ilkovič equation indicates that the coefficients 707 and 607 obtained by Ilkovič are converted into 709 and 608, respectively, by the present approximate method. Therefore the above derived coefficients 709 and 608, which appear in Eqs. (16), (17), (19) and (20) showing the instantaneous and mean diffusion current, may be replaced by the values 707 and 607, respectively.

Shielding Effect of the Capillary Tube

In the above quoted mathematical treatment, it is assumed that the mercury drop hangs freely in solution and expands concentrically. In fact, however, at the upper end of drop the capillary tube exists, and accordingly the diffusion of depolarizer from the region neighbouring the upper part of drop is prevented.

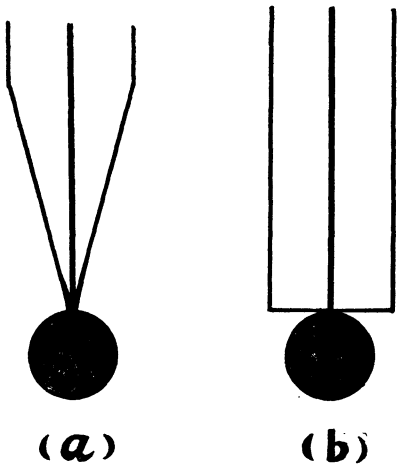

Fig. 1.

In the case of the tapering capillary tube as illustrated in Fig. 1 (a), the shielding effect of capillary may be considerably lessened; but with the capillary of thick wall as shown in Fig. 1 (b) this effect should be taken into account.

Next we will consider how the diffusion current will be affected by the shielding effect due to such a capillary as shown in Fig. 1(b). In order to treat this problem precisely, we must integrate the differential equation representing the cylindrically symmetric diffusion with the boundary conditions which are so complicated that it appears almost impossible. Hence we may be satisfied with the treatment based on the simplified model as follows.

Since the total current I, which has flowed in the time interval from $t=0$ to $t=t$, is obviously equal to the number of mols of depolarizer, which have disappeared from the solution in the same time interval, multiplied by nF, the diffusion current i_d is given by

$$i_d=\frac{dI}{dt}=nF\frac{d}{dt}\iiint_V(^*C-C)r^2\sin\theta dr d\theta d\varphi \quad (21)$$

where the region of integration V covers all the space in diffusion layer. In the preceding treatment, the region of integration is regarded to be the spherical shell surrounded by two spheres of radii r_0 and $r_0+\delta'$, owing to the assumption of free existence of mercury drop in solution. The upper part of this spherical shell, however, is in fact partly covered by the lower tip of capillary tube, as illustrated by the shaded portion in Fig. 2, and so the decrease in the concentration of depolarizer in this shielded part has no effect on the current

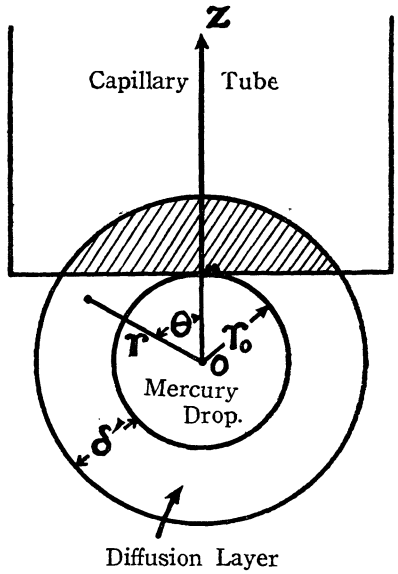

Fig. 2.—Schematic representation of shielding effect due to capillary tube.

intensity. Hence, in order to consider the shielding effect of capillary, the proper region of integration must be limited to the part of spherical shell which is really occupied by solution. Therefore, as to the three variables, r, θ and φ, the limits of integration should be $r_0 \to r_0+\delta'$, $\cos^{-1}(r_0/r) \to \pi$ and $0 \to 2\pi$, respectively. With these considerations, Eq. (21) is written in the form:

$$i_d = nF\frac{d}{dt}\int_0^{2\pi} d\varphi \int_{r_0}^{r_0+\delta'} (*C-C)r^2 dr \times \int_{\cos^{-1}\frac{r_0}{r}}^{\pi} \sin\theta d\theta$$

Upon executing the calculation with the value $l=10$ after inserting the expression for $*C-C$ given by Eq. (11) into the above equation, we can obtain the following equation for diffusion current.

$$i_d = 709n^*CD^{1/2}m^{2/3}t^{1/6}\{1+23.5(D^{1/2}m^{-1/3}t^{1/6}) +62.9(D^{1/2}m^{-1/3}t^{1/6})^2-\ldots.\} \quad (22)$$

Whence the mean diffusion current is found to be

$$\bar{i_d} = 608n^*CD^{1/2}m^{2/3}\tau^{1/6}\{1+20.6(D^{1/2}m^{-1/3}\tau^{1/6}) +49.0(D^{1/2}m^{-1/3}\tau^{1/6})^2-\ldots.\} \quad (23)$$

Revised Equation for the Diffusion Current in Amalgam Polarography

Next, employing the similar mathematical procedure as is already shown above, we will derive the revised Ilkovič equation showing the diffusion current observed in amalgam polarography.

Although the movement of mercury in the drop electrode seems very complicated, the diffusion process of amalgamated metal may be regarded to proceed in a spherical mercury drop expanding concentrically, provided that the rate of flow of mercury is not seriously great. Then the distribution of concentration $C_M(r,t)$ of amalgamated metal in the mercury drop is represented by the following equation.

$$\frac{\partial C_M}{\partial t} = D_M\frac{1}{r^2}\frac{\partial}{\partial r}\left(r^2\frac{\partial C_M}{\partial r}\right)-\frac{a^3}{3r^2}\frac{\partial C_M}{\partial r} \quad (r\leqq r_0) \quad (24)$$

Here, D_M is the diffusion constant (cm.^{2}/sec.) of amalgamated metal in mercury.

Further the initial and boundary conditions are given by

$$\left.\begin{aligned} &C_M = *C_M \quad \text{for} \quad t=0 \ (r<r_0);\\ &C_M = 0 \quad \text{for} \quad r=r_0 \ (t>0);\\ &C_M = *C_M,\ \frac{\partial C_M}{\partial r}=0 \quad \text{for} \quad r=0 \ (t>0)\end{aligned}\right\} \quad (25)$$

where $*C_M$ represents the concentration of amalgamated metal in the bulk of mercury.

Multiplying the Eq. (24) by r^2 and then integrating with respect to r from zero to r_0, it can be readily seen that

$$\frac{\partial}{\partial t}\int_0^{r_0}(*C_M-C_M)r^2dr = -D_M r_0^2\left(\frac{\partial C_M}{\partial r}\right)_{r=r_0}$$

Since it may be assumed that the thickness of diffusion layer $\delta'_M(t)$ is much smaller than r_0, the integration from zero to r_0 may be replaced by that from $r_0-\delta'_M$ to r_0; then putting $r=r_0-x$, we have

$$\frac{\partial}{\partial t}\int_0^{\delta'_M}(*C_M-C_M)(r_0-x)^2dx = D_M r_0^2\left(\frac{\partial C_M}{\partial x}\right)_{x=0} \quad (26)$$

As shown by Eq. (11), the quantity $*C_M-C_M$ will be expanded into the power series of x; i. e.

$$*C_M-C_M = *C_M\frac{r_0}{r_0-x}\left(1+\sum_{j=1}^{l}B_j x^j\right) \quad (27)$$

Then, taking $l=10$, and employing the similar boundary conditions as shown by Eqs. (12) and (18), we can determine the coefficients B_j $(j=1,2,\ldots,10)$ as the functions of δ'_M and r_0. Next, insertion of Eq. (27) into Eq.

(26) gives then an ordinary differential equation of first order, by which δ'_M is demonstrated; upon integrating this equation, we can obtain δ'_M as a function of t. The diffusion current can be easily found therefrom, and the result is

$$i_d = -709n^*C_M D_M^{1/2} m^{2/3} t^{1/6} \times \{1 - 34.9(D_M^{1/2} m^{-1/3} t^{1/6}) + 199(D_M^{1/2} m^{-1/3} t^{1/9})^2 - \ldots\} \quad (28)$$

Further the mean diffusion current is manifested by

$$\bar{i}_d = -608n^*C_M D_M^{1/2} m^{2/3} \tau^{1/6} \times \{1 - 30.5(D_M^{1/2} m^{-1/3} \tau^{1/6}) + 155(D_M^{1/2} m^{-1/3} \tau^{1/6})^2 - \ldots\} \quad (29)$$

In the case of amalgam polarography, since the diffusion layer is built up inside the mercury drop, the shielding effect due to capillary tube is expected to be of little importance, so that it may be ignored.

Comparison with Experimental Data

(A) Mean Diffusion Current.— Recently, in order to verify the validity of the revised Ilkovič equation, many investigators have carried out precise experiments, in which the drop time and the rate of outflow of mercury are variously changed with many capillaries of different characteristics; these experiments shows that Eq. (1) holds for the drop time longer than the critical drop time. And as for the numerical value of the coefficient A appearing in the second term of Eq. (1), the experimental results can be classified into the following two cases. I. e., Lingane with Loveride[11] and L. Meites with T. Meites[12] have found the result $A=31.5\pm4.6$, in the case with reductions of several ionic species. On the other hand, von Stackelberg and his collaborators[13] have found that $A=17\pm3$ agrees well with the results; it must be noted here especially that W. Hans and W. Jensch[14] have found that $A=16.1\pm1.5$ is adequate according to their elaborated studies on the polarographic reduction of hydrogen ion. The result observed by the former group of investigators, i. e. $A=31.5\pm4.6$, is in good agreement with Eq. (20), in which the shielding effect of capillary tube is ignored, while $A=17\pm3$ observed by the latter group is in fairly good harmony with Eq. (23), in which the shielding effect is taken into consideration. Which is then more adequate of these two numerical values proposed for the coefficient A? This will be judged by many accurate experimental studies in future.

As to the case of amalgam polarography, Strehlow and von Stackelberg[1] have experimented with cadmium amalgam, and shown that Eq. (29) holds when no phenomenon of "Spüleffekt" appears. Further, R. C. Turner and C. A. Winkler[15] have also confirmed the fact that in the case of lead and cadmium amalgam Eq. (29) agrees well with the experimental findings when m is lesser than 1.2 mg./sec.

(B) Current-Time Curve.—With variable ionic species, the diffusion current-time curve during one drop-life has been investigated oscillographically by Mc Kenzie,[16] Taylor, Smith and Cooter,[17] Mac Donald and Wetmore,[18] and Kambara, Suzuki and Tachi.[3] According to these experiments, although at the last two thirds of drop-life Eq. (22) holds semi-quantitatively, the current intensity at the first one third of drop-life is found to be very small; i. e. a perfect deviation from Eq. (22) is reported. The extraordinary small current flowing in the youth of drop-life will be explained by considering some or all of the following facts, that have been ignored in the above mathematical treatment. (1) In the present calculation, it is assumed that m is constant; but it is well known that m may become considerably small in the youth of drop-life, because the back pressure due to the interfacial tension must increase with the decreasing radius of drop.[19] (2) Owing to the electrolytic reaction at the preceding drop, the succeeding drop is dipped into the solution of lower concentration of depolarizer than that of bulk; i. e. there exists at the beginning of renewed drop-life already a diffusion layer around the drop.[20] (3) At the very infancy of drop-life the diffusion layer is so thin, that the rate-determining process depends not

(11) J. J. Lingane and B. A. Loveridge, *J. Am. Chem. Soc.*, **66**, 1425 (1944); *Anal. Chem.*, **21**, 52 (1949). Cf. *Reference* (2).

(12) L. Meites and T. Meites, *J. Am. Chem. Soc.*, **72**, 3686 (1950), **73**, 395 (1951).

(13) H. Strehlow and M. von Stackelberg, *Z. Elektrochem.*, **54**, 51 (1950) H. Strehlow, O. Madrich and M. von Stackelberg, ibid., **55**, 244 (1951).

(14) W. Hans and W. Jensch, ibid. **56**, 648, (1952).

(15) R. C. Turner and C. A. Winkler, *Cad. J. Chem.*, **29**, 469 (1951), *Chem. Abst.* **46**, 2421 (1952).

(16) H. A. McKenzie, *J. Am. Chem. Soc.*, **70**, 3147 (1948).

(17) J. K. Taylor, R. C. Smith and I. L. Cooter, *J. Reserch Natl. Bur. Standards*, **42**, 387 (1949).

(18) J. J. MacDonald and F. E. Wetmore, *Trans. Faraday Soc.*, **47**, 533 (1951).

(19) I. M. Kolthoff and J. J. Lingane, "Polarography" vol. 1, p. 76 (1952) Intersci. Publ.

(20) L. Airey and A. A. Smales, *Analyst*, **75**, 287 (1950).

solely on diffusion velocity and the rate of electrode process must be taken into account at the same time.[21]

(C) Ratio of the Mean Diffusion Current $\bar{i}_d$ to the Maximum Value of Instantaneous Current $i_{max.}$ — According to the Ilkovič equation, the ratio $i_d/i_{max.}$ becomes $6/7=0.857$. On the other hand, according to the present revised equations (22) and (23) this is given by

$$\frac{\bar{i}_d}{i_{max}} = \frac{6}{7} - 2.5(D^{1/2}m^{-1/3}\tau^{1/6}) + 45(D^{1/2}m^{-1/3}\tau^{1/6})^2 - \cdots$$

E.g., employing the numerical values given by $D=0.72\cdot10^{-5}$cm.^{2}/sec.; $m=2.305$ mg./sec.; $\tau=3.488$ sec., it is found that $\bar{i}_d/i_{max}=0.851$, while the experimental value observed by Taylor, Smith and Cooter[17] is 0.813. Thus the revised equation approaches somewhat nearer to the experimental result than the original Ilkovič equation; neverthless neither of the two theories is seen to be in complete harmony with the experiments.

(21) T. Kambara and I. Tachi, This Bulletin **25**, 135, 281 (1952); H. Matsuda, Presented at the 5th Annual Meeting of Chem. Soc. of Japan, April 1952.

Summary

In order to integrate the MacGillavry-Rideal differential equation, representing the diffusion process at the dropping mercury electrode, the present author employed the von Kárman-Pohlhausen method. Thus the following revised expression of the Ilkovič equation showing the mean diffusion current is derived, in which the shielding effect due to the capillary tube is also treated theoretically.

$$\bar{i}_d = 608n^*CD^{1/2}m^{2/3}\tau^{1/6}\{1+20.6(D^{1/2}m^{-1/3}\tau^{1/6}) + 49.0(D^{1/2}m^{-1/3}\tau^{1/6})^2 - \cdots\}$$

The analogous treatment is also applied to the case of amalgam polarography, and the following equation for the mean diffusion current is obtained.

$$\bar{i}_d = -608n^*C_M D_M^{1/2}m^{2/3}\tau^{1/6} \times\{1-30.5(D_M^{1/2}m^{-1/3}\tau^{1/6}) + 155(D_M^{1/2}m^{-1/3}\tau^{1/6})^2 - \cdots\}$$

The author wishes to express his hearty thanks to Dr. T. Kambara for his steady encouragement and help.

Goverment Chemical Industrial Research Institute, Tokyo

Vat Dyes of Acenaphthene Series. V. Constitution of Dibromoanthanthrone (Indanthrene Brilliant Orange RK).[1]

By Toshio MAKI and Harukichi HASHIMOTO

(Received May 19, 1953)

A brilliant reddish orange vat dye of excellent fastness (light 7~8), commercially known as Indanthrene Brilliant Orange RK, has been obtained by direct bromination of anthanthrone. Among various methods of bromination it has been acknowledged in our laboratory that only the bromination in oleum (about 8% SO_3) in the presence of a little iodine gives the best result by the application of the least amount of bromine.[2] The crude product, however, contains a small quantity of orange brown impurity and, according to our experiment, the purification can be most effectively carried out by using 92~94% sulfuric acid, in which the pure reddish orange dibromoanthanthrone is insoluble.

The constitution of the dibromoanthanthrone was hitherto not at all experimentally determined and only by assumption 4, 10-dibromo formula (II-A) has usually been suggested,[3] but sometimes the other 2, 8-dibromo structure

(1) Read before the 5th Annual Meeting of the Chemical Society of Japan on April 5, 1952.

(2) G. P. 478738, *Frdl.* **16**, 1417; See also PB 84316-3471, *FIAT* **1313**, Vol. II, 90.

(3) Rowe, "The Development of the Chemistry of Commercial Synthetic Dyes (1856~1938), 87; PB 84316-3471.

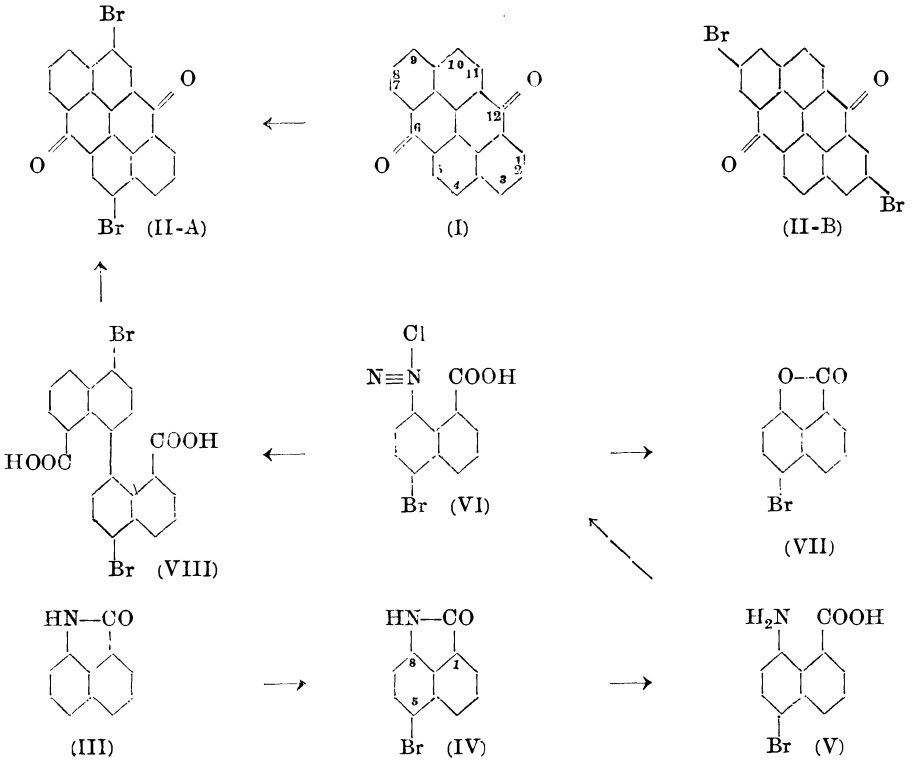

(II-B) is also adopted.[4]

We have now brominated naphthostyril (III) in acetic acid solution and found that the product is 5-bromonaphthostyril (IV) (m.p. 257°), which had been obtained by Eckstrand[5] from 5-bromo-8-nitro-1-naphthoic acid by reduction. The constitution of the bromonaphthostyril was further confirmed by converting it, after hydrolyzing the styril ring, into 5-bromo-8-hydroxy-1-naphthoic acid lactone (VII) (m. p. 193°) by diazotization and heating with dilute sulfuric acid. From this 5-bromonaphthostyril (IV) we have synthesized 4, 10-dibromoanthanthrone (II-A) via dibromodinaphthyl-dicarboxylic acid (VIII) by application of the diazo reaction and ring formation in conc. sulfuric acid analogous to the synthesis of anthanthrone from naphthostyril.[6] Our method of applying an ammoniacal solution of reduced copper sulfate and precipitated metallic copper was also useful for this diazo reaction.

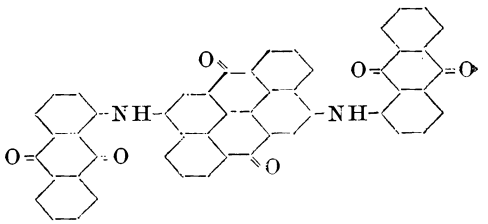

(IX)

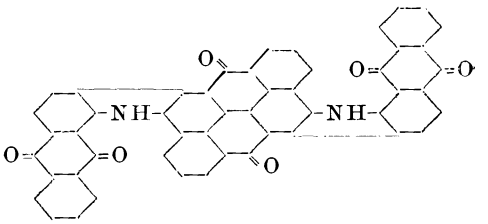

(X)

4, 10-Dibromoanthanthrone (II-A) thus synthesized is completely identical with the brilliant reddish orange dibromoanthanthrone (Indanthrene Brilliant Orange RK), which had been obtained by the direct bromination of anthanthrone. They are identical not only in their dyeings and color reactions, but in all other chemical reactivity and condensation products, for example in the formation of grayish violet di-α-anthraquinonyl-diimide

(4) *FIAT* **1313**, Vol. II, 89.
(5) Eckstrand, *J. prakt. Chem.* [2] **38**, 173, 281 (1888); *Ber.* **19**, 1136, 1139 (1886).
(6) T. Maki, H. Hashimoto and K. Kamada, *J. Chem. Soc. Japan, Ind. Chem. Section*, **55**, 483 (1952); See also PB 84316-3480; *FIAT* **1313**. Vol. II, 90.

(IX) and olive gray biscarbazole derivative (X).

Thus, as in the case of benzanthrone[7] the diphenyl residue in the molecule of anthanthrone is also found to be reactive to halogenation and in the present case p-and p'-position to the centre union are brominated. Indanthrene Brilliant Orange GK must similarly has 4, 10-dichloro structure. The formula (II-B) given in FIAT[4] is improbable as the constitution of Indanthrene Brilliant Orange RK, but may be rather that of the orange brown isomeric dibromoanthanthrone, which has been found by us as an impurity of the bromination and soluble in 90% sulfuric acid.

Experimental Part

Direct Bromination of Anthanthrone.—Anthanthrone (1.50 g., 1 mol. ratio)[6] was dissolved in 45 g. of oleum (8% SO_3) with 0.075 g. of iodine and 1.10 g. (2.8 atomic ratio, 70% of the apparent theory) of bromine was dropped down with stirring in about 30 min. at room temperature. It was then heated to 60° and kept at this temperature for 5 hours. The product was poured into ice water, the precipitate was collected, treated with 500 cc. of 1% aqueous sodium bisulfite, 500 cc. of 1% aqueous sodium carbonate and after acidification with dilute hydrochloric acid washed thoroughly with cold water. The yield of the crude product, a dark red orange powder, was 2.20 g. (96.8% of the theory). Found. Br, 38.40; calcd. for $C_{22}H_8O_2Br_2$ (II-A): Br, 34.44%. The crude dibromoanthanthrone (1 part), as a fine powder, was heated with 30 parts of 92% sulfuric acid on a water bath for 30 min. and allowed to stand over-night at room temperature. The black brown insoluble part was collected on a glass filter and when this was carried into water a brilliant red orange precipitate resulted, which was filtered and washed neutral. The yield was 72% of the crude product, corresponding to 69.7% of the theory from anthanthrone. Found: Br, 33.95; calcd. for $C_{22}H_8O_2Br_2$ (II-A): Br, 34.44%. Clear red orange powder, soluble in conc. sulfuric acid with clear green color. Hydrosulfite vat (IK) is violet red, from which brilliant reddish orange cotton dyeing is obtained. The shade of the dyeing is quite identical with that of the commercial Indanthrene Brilliant Orange RK[8].

In the above purification the concentration of sulfuric acid has unusually sensitive effect both on the yield of dye and on the shade of dyeing. Thus, the similar treatment with 94% sulfuric acid gives dibromoanthanthrone of the highest purity as the insoluble part, whose cotton dyeing is more clear and brilliant than that of the commercial dye, but the yield of the purification was 62% of the crude product. A dye almost identical with the commercial product, but of rather slightly yellowish shade, is obtained using 90% sulfuric acid in 84% yield of the crude product.

The part soluble in 90% sulfuric acid was obtained as a dark brown powder when the acid filtrate was poured into water. Its amount was ca. 14% of the crude dibromoanthanthrone. It dyes cotton in orange brown from a violet red hydrosulfite vat (IK); The solution in conc. sulfuric acid is dark green. This substance is a hitherto unknown impurity and our analysis indicates that it is an isomer of dibromoanthanthrone. We suggest the formula (II-B) as its probable constitution taking into consideration the reactivity of the remaining diphenyl residues in the molecule. Found: Br, 31.74; calcd. for $C_{22}H_8O_2Br_2$ (II-B): Br, 34.44%.

5-Bromonaphthostyril (IV).—To the solution of 5.08 g. (1 mol. ratio) of naphthostyril[6] in 51 g. of glacial acetic acid 4.55 g. (1.9 atomic ratio, 95% of the theory) of bromine, dissolved in 23 g. of glacial acetic acid, was added dropwise at 25° in 3 hours and agitated further 4 hours at the same temperature. After standing over-night the crystalline precipitate was collected and washed with water. Its yield was 6.19 g. (83.2% of the theory), m. p. 250.5~257.5° (corr.). By recrystallization from 10 parts of glacial acetic acid greenish yellow needles melting at 256.5~260.5° (corr.) were obtained. The yield was 76% of the crude product. Found: Br, 31.99; calcd. for $C_{11}H_6ONBr$ (IV): Br, 32.22%. This is identical with the 5-bromonaphthostyril (m. p. 257°) obtained by Eckstrand[5] from 5-bromo-8-nitro-1-naphthoic acid by reduction.

Conversion of Bromonaphthostyril into 5-Bromo-8-hydroxy-1-naphthoic Acid Lactone (VII).—The bromonaphthostyril (2,48 g. 1 mol. ratio), which had been obtained by the bromination of naphthostyril, was dissolved in 15 g. of 10% aqueous sodium hydroxide by heating on a water bath and diluted with 20 cc. of water. After ice cooling 0.69 g. of sodium nitrite (1 mol. ratio), dissolved in 4 cc. of water, was added to the solution and diazotized at 0° by giving 17 cc. of ice cooled 4 N hydrochloric acid and stirring further 20 min. The diazo solution was slowly poured into 100 g. of hot 20% sulfuric acid on a boiling water bath. The evolution of nitrogen gas ceased in ca. 20 min. and the color of the precipitate changed into yellow from brown. The heating was continued for further 30 min., then it was allowed to cool and the precipitate collected. Light brown powder of m.p. 182~187° (corr.), the yield was 2.24 g. or 89.9% of the theory. After crystallizing from 10 parts of glacial acetic acid 1.72 g. (76.8% of the crude product) of light brown needles melting at 191° (corr.) were obtained. By further recrystallization a sample of constant m. p. 193° (corr.) was obtained. Found: Br, 31.82; calcd. for $C_{11}H_5O_2Br$ (VII): Br 32.09%.

(7) T. Maki and Y. Nagai, *J. Soc. Chem. Ind. Japan, Suppl.* **38**, 491 B (1935); T. Maki, and T. Aoyama, *J. Soc. Chem. Ind. Japan, Suppl.* **38**, 636 B (1935); T. Maki and Y. Nagai, *Ber.* **70**, 1837 (1937); T. Maki and A. Kikuchi, *Ber.* **71**, 2031, 2036 (1938); T. Maki and A. Kikuchi, *J. Soc. Chem. Ind. Japan*, **50**, 141 (1947).

(8) The dyestuff content of the commercial Indanthrene Brilliant Orange RK (I. G.) was 75.6% and actual bromine content of this dyestuff was found to be 32.25%.

This substance was identical with 5-bromo-8-hydroxy-1-naphthoic acid lactone of Eckstrand[5] (m. p. 192°).

Synthesis of 4, 10-Dibromoanthanthrone (II-A) from 5-Bromonaphthostyril. — Two mol. ratio (5.0 g.) of copper sulfate ($CuSO_4 \cdot 5H_2O$) was dissolved in 20 cc. of water, 24 g. of 25% aqueous ammonia added and the solution was completely (rather to a faintly red color) decolorized by introduction of sulfur dioxide under ice cooling. To this solution of cuprous oxide complex, 10 g. of 25% aqueous ammonia and freshly precipitated metallic copper paste (1 mol. ratio)[9] were added.

5-Bromonaphthostyril (2.48 g., 1 mol. ratio), dissolved in 15 g. of 10% aqueous sodium hydroxide, was diazotized using 0.69 g. of sodium nitrite and 17 cc. of 4 N hydrochloric acid at 0° for 20 min., as in the case of the lactone (VII), and cooled to −5°. The diazo solution was poured into the copper solution at −5°, stirred at this temperature for 1 hour, allowed to rise in 2 hours to 20° and then stirred further 2 hours at 20°. After standing over-night the solution was filtered and dibromodinaphthyldicarboxylic acid (VIII) was precipitated from the filtrate with hydrochloric acid. Yield of a light brown powder was 1.69 g. This was dissolved without purification in 17 g. of conc. sulfuric acid, kept in a boiling water bath for 1 hour and after cooling poured into ice water. The precipitate was collected, washed neutral and heated with 300 cc. of 5% aqueous sodium carbonate in order to remove carbonate soluble impurities. The yield of dibromoanthanthrone, a dark red orange powder, was 1.41 g. or 60.8% of the theory. Further purification was carried out by heating 1 part of the finely powdered crude product with 30 parts of 92% sulfuric acid 30 min. in a boiling water bath and allowing to cool, when pure 4, 10-dibromoanthanthrone (II-A) was obtained as an insoluble precipitate. The Yield was 1.24 g. or 87.9% of the crude product. Found: Br, 33.94; calcd. for $C_{22}H_8O_2Br_2$ (II-A): Br, 34.44%.

It is a clear reddish orange powder, soluble in conc. sulfuric acid with clear green color and brilliant reddish orange cotton dyeing is obtained from a violet red hydrosulfite vat (IK). This synthetic 4, 10-dibromo compound is completely identical with the direct brominated dibromoanthanthrone in dyeings and all color reactions.

Condensation of Dibromoanthanthrone with 1-Aminoanthraquinone.[10]—One mol. ratio (1.00 g.) of the synthetic dibromoanthanthrone (Br, 33.94%), 2 mol. ratio (0.962 g.) of 1-aminoanthraquinone, 0.4 mol. ratio (0.069 g.) of precipitated cupric oxide and 2 mol. ratio (0.457 g.) of anhydrous sodium carbonate were boiled with 29.4 g. of nitrobenzene under reflux and stirring for 3 hours. Alcohol (15 g.) was added at 70° and after agitated for 30 min. the product was allowed to stand over-night. The precipitate was collected, washed with alcohol, heated with 200 cc. of dilute hydrochloric acid (1: 50) for 30 min. in a water bath, filtered and thoroughly washed with hot water. Yield was 1.534 g (94.1% of the theory). Violet gray powder, hardly soluble in organic solvents, soluble in conc. sulfuric acid with blue green color, from which violet precipitate separated by adding water. It dyes cotton grayish violet from a violet red vat (IK). The substance is completely free from bromine. Found: N, 3.49; calcd. for $C_{50}H_{24}O_6N_2$ (IX): N, 3.74%.

Dibromoanthanthrone (Br, 33.65%) obtained by the direct bromination of anthanthrone gave also quite the same di-α-anthraquinonyl-diimide (IX) both in yield and properties. Found: N, 3.57; calcd. for $C_{50}H_{24}O_6N_2$ (IX): N, 3.74%.

The carbazolation to the substance (X) was carried out by heating 1.00 g. of the diimide (IX) with 8.0 g. of anhydrous aluminium chloride and 2.0 g. of dry sodium chloride at 180° (oil bath temperature) for 6 hours and treating as usual with water and hydrochloric acid. The yield of the crude product was 1.00 g. It was then, as a dry fine powder, agitated with 10 cc. of 3.7% sodium hypochlorite solution and 5 cc. of water 1 hour at room temperature and 3 hours under reflux on a boiling water bath. The precipitate was collected, acidified with hydrochloric acid and then washed neutral. Yield was 0.94 g. Black powder, hardly soluble in organic solvents, soluble in conc. sulfuric acid with yellowish green black color, from which yellowish green black precipitate separated by the addition of water. Hydrosulfite vat (IK) is dark violet red and cotton is dyed in olive gray shade. Found: N, 3.71; calcd. for $C_{50}H_{20}O_6N_2$ (X): N, 3.76%.

The direct brominated dibromoanthanthrone gave also via the above diimide quite the same biscarbazole derivative (X) both in yield and properties. Found: N, 3.82; calcd. for $C_{50}H_{20}O_6N_2$ (X): N, 3.76%.

Dyestuffs Research Laboratory, Department of Applied Chemistry, Tokyo University, Tokyo

(9) Prepared from 2.5 g. of copper sulfate in 16 cc. of water by the addition of 0.03 cc. of turkey red oil and then 0.78 g. of zinc dust followed by decantation and washing.

(10) Compare with G. P. 485961, 487023, *Frdl.* **16**, 1422, 1424.

LETTER

A New Method of Measuring he Surface Tension of Liquids by Using the Vertical Liquid Jet

By Toshio IKEDA

(Received May 7, 1953)

Lately the present writer has derived the following theoretical approximation formula[1] for the "starting critical flow rate, V_c", the lowest flow rate necessary to change the tripping flow of the vertical jet into the laminar one:

$$V_c \fallingdotseq \pi r^{3/2}\sqrt{2\gamma/\rho} \qquad (1)$$

where r is the inner radius of the nozzle, γ, the surface tension of liquid, and ρ, the density of the liquid, and this formula proved to be accurate for the nozzle of the radius less than 0.05 cm. experimentally. Using this relation, one can calculate the tension of the surface that is newly developing.

Experimental Results

The liquids used were of the "chemical pure" grade. The capillary nozzle that was drawn out of a glass tube was about 10 cm. long, having the circular tube section of which inner and outer radii were 0.0375 and 0.1102 cm. respectively, and it was fixed in the direction of the gravity, joined by a short rubber tube directly to a glass siphon that was dipped into the liquid in a large glass reservoir (about 12 cm dia.).

The rate of the jet flow was regulated by changing the level of the liquid, or by sliding the reservoir upwards or downwards. The value of V_c was estimated from the volume of the liquid that ran down for ten seconds after the first development of the normal laminar jet flow, and was always accurate within 0.001 cc. per second at the room temperature.

The results are listed in Table 1. The values of γ calculated by the formula[1] and those of the static surface tensioa,[2] γ_0, for most liquids agree very well; but the reason why some anomalies, such as for water, chloroform, and carbon-tetrachloride, occur is yet to be known.

Therefore, this method could be used, if one were very careful for measuring the surface tension of liquids, the degree of accuracy here being at least 97 or 98 percent.

Department of Chemistry, the Liberal Arts Faculty, Shizuoka University.

Table 1

Liquids	Temp. °C.	ρ g./cc.	V_c cc./sec.	$\gamma_{calc.}$ dynes/cm.	γ_0 dynes/cm.
Water	15.5	0.998	0.282	88.7	73.23
Methyl alcohol	16.0	0.796	0.156	21.6	23.45
Ethyl alcohol	17.3	0.792	0.160	22.6	22.0
Aceton	19.5	0.792	0.160	22.6	23.14
Chloroform	15.6	1.50	0.110	20.2	26.9
Carbon tetrachloride	15.2	1.60	0.109	21.2	26.24
n-Hexane	16.8	0.660	0.150	16.6	17.76
Toluene	15.5	0.866	0.171	28.2	28.72
Chlorobenzene	17.2	1.108	0.159	31.2	33.84
Nitrobenzene	20.5	1.203	0.181	43.9	43.00

(1) T. Ikeda, *Reports of the Liberal Arts Faculty, Shizuoka Univ., Ser. B, No.* **3**, 20 (1952).

(2) Landolt-Börnstein, "Phys. Chem. Tabellen", I, (1923) p. 208.

Eine Neue Methode zur Darstellung von Eisenrhodanidenlösung mit dem Kationenaustauschenden Harze

Von Masatoshi FUJIMOTO

(Eingegangen am 18. April, 1953)

Um eine chlor- und ammonium- (oder einwertigen metall-) ionenfreie Lösung von Eisenrhodaniden darzustellen, hat der Verfasser mit einem kationenaustauschenden Harze folgendes Experiment ausgeführt.

Die hier angewandte Darstellungsmethode beruht auf den zwei folgenden Reaktionen.

$NH_4SCN+HR \rightleftharpoons HSCN+NH_4R$ (Ionenaustausch),

$xHSCN + Fe(OH)_3 \rightleftharpoons H_{x-3}Fe(SCN)_x^{3-x} + 3H_2O$ (Neutralisierung bzw. Komplexbildung): HR (NH_4R) bedeutet ein kationenaustauschendes Harz von H- (NH_4-) Form und x, die Integrale, 3, 4, 5, und 6.

Der Versuch wird folgenderweise durchgeführt

1. Darstellung von Eisenhydroxyd—Auf gewöhnlicher Weise, d. h., aus einer Lösung des Eisensesquichlorides und verdünntem Ammoniakwasser, stellt man einen Niederschlag des Eisenhydroxydes dar und wäscht auf einem aschenfreien Filtrierpapier mit heissem destilliertem Wasser völlig aus, bis mit Silbernitrat keine Chlorionen in 5–10 ccm. des Filtrates nachgewiesen werden.

2. Darstellung der Rhodansäure durch Kationenaustausch—Man stellt eine Säule[1] des kationenaustauschenden Harzes (HR) auf, wodurch eine ungefähr 0.1- bzw. 0.3 M. wässerige Lösung des Ammoniumrhodanides stöchiometrisch in die freie Rhodansäure (HSCN) übergeführt wird.

3. Darstellung von Endprodukt—Die so hergestellte wässerige Lösung von freier Rhodansäure wird sofort auf den in einem Trichter (Abb. I) befindlichen Eisenhydroxydniederschlag hinzugefügt.—Sobald die Rhodansäure auf den Niederschlag zu tropfen beginnt, färbt sich die in C angesammelte Lösung schwarzblutrot.

Als Beispiel wird folgendes gezeigt

Mit einer Säule von Amberlite IR-120 (HR, 30 Maschen, 10 ccm. und 16 cm. lang), aus 50 ccm. von 0.15 M. Lösung des Ammoniumrhodanides und 5 ccm. von 0.42 M. Lösung des Eisensesquichlorides, hat der Verfasser eine klare schwarzrote wässerige Lösung von Eisenrhodanid gewonnen, in welcher nur kleinste Menge der Chlorionen (nach der Oxydation mit heisser konzentrierter Salpetersäure mit Silbernitrat geprüft) und der Ammoniumionen (mit Nesslerschem Reagens nachgewiesen) enthalten war.

Laboratorium der analytischen Chemie, Chemisches Institut der wissenschaftlichen Fakultät, Tokyo Universität, Tokyo.

(1) Vgl. H. Kakihana, Dieses Bulletin **22**. 242 (1949).

Über die Einwirkung des Bromwasserstoffs und des Sauerstoffs auf α,β-ungesättigte Ketone. I. Eine neue Spaltungsreaktion durch Sauerstoffeffekt[1]

Von Hazime KASIWAGI

(Eingegangen am 12, Juli, 1952)

Hinsichtlich des Verhaltens der α,β-ungesättigten Carbonsäuren gegen Bromwasserstoff sind mehrere Ergebnisse unter Berücksichtigung des Sauerstoffeffekts angekündigt worden[2,3], während man dagegen in Bezug auf den bei den entsprechenden Ketonen aufzutretenden Sauerstoffeffekt nur sehr arme Kenntnisse besitzt. Der Grund liegt wohl darin, dass die Ketone dieser Art unter Vereinigung mit Halogenwasserstoff Molekülverbindungen bilden, und zwar mit solcher Schnelligkeit, dass man nicht im Stande ist, die Bildung der Molekülverbindung zu verlangsamen, um dadurch die anomale Additionsreaktion zu verwirklichen. Kann der von dem Sauerstoffeffekt hervorgerufene, anomale Reaktionsprozess eigentlich bei den α,β-ungesättigten Ketonen nicht stattfinden? Von solcher Überlegung aus hat der Verfasser die Reaktionen einiger ungesättigten Ketone näher studiert und eine dem Sauerstoffeffekt zuzuschreibende, bemerkenswerte Erscheinung beobachtet. Im folgenden wird die Einzelheiten der Untersuchung dargelegt.

Lässt man den Bromwasserstoffstrom in die Benzol-, Petroleumäther-, Tetrachlorkohlenstoff-, bzw. Schwefelkohlenstoff-lösung von Chalkon (I) einleiten, so färbt sich die Lösung bald orangengelb, was der Entstehung der Molekülverbindung des Hydrobromids A nach Vorländer u. s. w.[4] zu verdanken ist. Die Lösung sich jedoch bald darauf entfärbt unter Bildung vom weissen Niederschlag des Hydrobromids B, d. h. des normalen Additionsprodukts.

Das weisse Additionsprodukt ist gewöhnlich sehr unbeständig, nämlich zersetzt sich die aus Benzalaceton durch die Addition des Chlorwasserstoffs erhaltene Verbindung unter Abspaltung von dem letzteren, sobald sie aus dem Reaktionsraum herausgenommen wird[5]. Bei Chalkon oder seinen Homologen, spaltet das Additionsprodukt wie bei Benzalaceton, von der Wärme oder überflüssiger Menge Base, z. B. Pyridin beeinflusst, leicht den Bromwasserstoff ab und geht in das ursprüngliche ungesättigte Keton zurück.

Der Additionsprozess wird ferner davon nicht beeinflusst, ob der heftige Sauerstoffstrom in Vereinigung mit dem Bromwasserstoffstrom in die Ketonlösung durchgeleitet wird oder nicht, und eine identische Additionsverbindung wird gewonnen, nämlich die Orientation des Bromwasserstoffs bleibt bei der Addition zur Ketonen unter wechselnden Bedingungen unveränderlich. So erhält man als Additionsprodukt nur dieselbe Verbindung, nämlich Phenyl-β-bromhydrostyrylketon (III) aus I und *p*-Tolyl-β-bromhydrostyrylketon (IV) aus 4'-Methylchalkon (II), jedoch keineswegs die Verbindungen, nämlich α-Bromhydroketon, Dibromid oder ihre Oxydationsprodukte, deren Bildung auf den Sauerstoffeffekt zurückzuführen ist. Dabei ist es angenommen worden, dass, wenn eine von dem Sauerstoffeffekt herrührende Reaktion wirklich stattfinden kann, das freie Radikal, das den Reaktionsprodukten als die Durchgangsstufe notwendig ist, vielleicht die Form, $C_6H_5CHCHBrCOC_6H_5$ hätte, weil diese infolge der grösseren Beständigkeit durch die Konjugierung seines freien Elektrons zur Phenylgruppe wohl als die geeignetere Form anzusehen ist. Da solche anomale Reaktionsprodukte, wie oben erwähnt, nicht erhalten worden sind und auch die Abscheidung des Wassers und des Broms, die im meisten Fall mit Sauerstoffeffekt eng zusammenhängt, im Laufe der Reakution niemals bemerkt worden ist, liegt es nahe zu behaupten, dass der Sauerstoffeffekt bei den α,β-ungesättigten Ketonen, wie I und II, nicht auftreten könnte. Lässt man aber Bromwasserstoff auf eine stark verdünnte Petroleumäther- oder Ligroin-

1) Eingebracht in der zweiten Jahresversammlung der Japanischen Chemischen Gesellschaft, Tokyo, 1949.

2) F. R. Mayo und C. Walling, *Chem. Rev.*, **27**, 351(1940), dort befinden sich mehrere Literaturen, ausserdem O. Simamura, Dieses Bulletin, **17**, 327 (1942); O. Simamura und M. Takahashi, ibid., **22**, 60 (1949) u.s.w..

3) M. Takahashi, Vortrage auf der dritten (Kyoto, 1950) und der vierten (Tokyo, 1951) Jahresversammlung der Japanischen Gesellschatt.

4) D. Vorlander und C. Tubandt, *Ber.*, **37**, 1652 (1904).

5) L. Francesconi und G. Cusmano, C. **1908**. II., 1102.

lösung ungesättigter Ketone unter Durchleiten des heftigen Sauerstoffstroms einwirken, so strömt die Reaktionsflüssigkeit, die normalerweise das Additionsprodukt ausfällt, ein augenreizenden Geruch aus. Dieser Geruch kann vielleicht nicht der Bildung des β-Bromhydroketons oder seines sekundären Umwandlungsprodukts, sondern dem Verlauf einer anderen Reaktion als normaler Addition zugeschrieben werden. Obwohl es nicht gelungen ist, die riechende Substanz zu isolieren, führt diese Tatsache zur Erwartung, dass der Sauerstoffeffekt auch bei den α,β-ungesättigten Ketonen stattfinden könnte.

Aus diesem Grunde hat der Verfasser als ein anderartiges ungesättigtes Keton, das α-Bromchalkon (ω-Brom-ω-benzyliden-acetophenon V) dargestellt und den bei ihm auftretenden Sauerstoffeffekt untersucht. Durch Addition des Bromwasserstoffs unter den gewöhnlichen Bedingungen, worin die Konzentration des Ketons verhältnismässig grösser ist, kann man ein Dibromid des Ketons I erhalten. Bezüglich Chalkondibromids sind stereomerisch zweierlei Stoffe bekannt, nämlich das eine mit Schmelzpunkt von 157.2～8.2°C. und das andere von 120～1°C. Beim genannten Fall entsteht fast ausschliesslich das Dibromid von tieferem Schmelzpunkt, wie Abell es bereits bestätigt hat[6]. Dabei ist der Einfluss des heftigen Sauerstoffstroms nicht beobachtet worden, der mit Bromwasserstoff in die Lösung von gleicher Konzentration durchgeleitet wird, da dasselbe Dibromid aus der Reaktionsflüssigkeit sich niederschlägt.

Bei starker Verdünnung mit Petroleumäther läuft die Reaktion etwas abweichend, nämlich nach der Beendigung der Reaktion nimmt die Petroleumätherlösung eine eigentümliche gelbe Farbe an und scheidet eine dünne Schicht von blutroter Farbe. Die Lösung wird durch ihren heftigen augenreizenden Geruch gekennzeichnet, der auch bei der Reaktion des Ketons I oder II, freilich hier aber viel schwächer, wahrgenommen wird. Ferner bemerkt man weisse prismatische Kristalle die sich an dem Boden und der Wand bilden. Aus der Petroleumätherlösung ist ferner durch Behandlung mit Sodalösung ein saurer Stoff zn erhalten, der sich als mit dem obigen Kristall identisch erweist, und zwar als Benzoesäure. Da die Benzoesäure schon aus der Wand des Reaktionsgefässes sich ausgeschieden ist, verdankt sie ihre Bildung der eigentlichen Reaktion. Daher kann man mit Recht annehmen, dass das ungesättigte Bromketon V unter der Bedingung, die für den Auftritt des Sauerstoffeffekts verantwortlich ist, sich oxydativ abbauen und dadurch die Benzoesäure und die heftig augenreizende Substanz sich bilden mögen. Die am Boden abgesunkene blutrote Schicht besteht aus Wasser, aber zeigt negative Jodkali-Stärke-Reaktion. Daraus folgt, dass kein Brom während der Reaktion gebildet wird.

Der Streitpunkt, um den Reaktionsmechanismus in Bezug auf das Bromketon V klar zu machen, besteht zuerst in der Entscheidung, woran die Kohlenstoffkette des Ketons V abspaltet und darauf die Bildung der Benzoesäure beruht.

Um diesen Punkt aufzuklären, ist die gleiche Reaktion des α-Brom-4'-methyl-chalkon (ω-Brom-4-methyl-ω-benzyliden-acetophenon VI) untersucht worden. Falls die Reaktion in einer ziemlich konzentrierten Lösung durchgeführt wird, findet keine dem genannten Effekt eigentümliche Erscheinung statt (genau wie beim ungesättigten Bromketon V), sondern kann man nur ein bei 156.5～7.5°C. schmelzendes gesättigten Dibromid des Ketons II erhalten[7]. In grösserer Verdünnung unter Durchströmung des Bromwasserstoffs und des Sauerstoffs verläuft hingegen die Reaktion anders, aber ganz ähnlich der Reaktion des Ketons V unter derselben Bedingungen. Nach Beendigung der Reaktion, erhält man aus der gelben Petroleumätherlösung einen sauren Stoff, der einen Schmelzpunkt von 174～7°C. aufweist und mit der *p*-Toluylsäure übereinstimmt. Da keine andere saure Substanz daraus zu gewinnen ist, mag die während der Reaktion des Ketons VI gebildete saure Substanz nur aus *p*-Toluylsäre bestehen. Diese Tatsache genügt, um herauszustellen, dass das Loslösen der Kohlenstoffkette zwischen dem Carbonylkohlenstoff und seinem α-Kohlenstoffatom stattfindet.

Die Mengen der beinahe unter gleichen Bedingungen aus den ungesättigten Ketone V und VI gebildeten Säuren werden auf der Tabelle verglichen. Man ersieht daraus, dass es eine Zersetzung bei dem nicht sub-

6) Robert D. Abell, *J. Chem. Soc.*, **101**, 998 (1913).

7) Dieses gesättigte Dibromid stimmt vielleicht mit dem Dibromid von tieferem Schmelzpunkt überein, das C. Weygand und A. Matthes (*Ber.*, 59, 2247 (1926)) durch fraktionierende Umkristallisation des aus 4-Methyl-chalkon durch Addition des Broms unmittelbar gebildeten Dibromidsgemisches, als das Isomere des bei 175～6°C. schmelzendes Dibromids, erhalten, und dem sie den Schmelzpunkt von 140～1°C. verliehen haben. Wegen der ausserst geringen Gehalt des rohen Produkts an demjenigen Dibromid (höchstens 2% d. Theor.), ist es aber sehr schwierig, ihn rein zu erhalten. Nicht nur das, ist es mit Recht anzunehmen, dass das Dibromid von tieferem Schmelzpunkt, wie beim Fall von Keton V, vorzüglich aus dem ungesättigten Bromketon VI durch Addition des Bromwasserstoffs zu gewinnen sei, deshalb soll als der Schmelzpunkt desjenigen Dibromids der oben angedeutete, auf dieser Reaktion von mich ermittelte Wert, nämlich 156.5～7.5°C., ausgewählt werden eher als der von C. Weygand und A. Matthes.

stituierten Keton weit heftiger als bei dem substituierten ist.

Mengen der durch den Sauerstoffeffekt gebildeten aromatischen Säuren

R	$C_6H_5CH=CBr-COC_6H_4R$	Lösungsmittel	RCOOH	
	gr.	ccm.	gr.	mol.%
H	3.45	100	0.52	35.8
H	3.68	145	0.53	34.0
p-CH_3	3.29	75	0.18	12.3
p-CH_3	2.00	65	0.12	13.3
p-CH_3	2.00	70	0.06	6.7

Dass die Bildung der aromatischen Carbonsäuren aus den Ketonen V und VI dank des Sauerstoffeffekts hervorgebracht wird, ist auch durch die Tatsache unterstützt worden, dass in Gegenwart von der kleinsten Menge des Brenzkatechins, eines bekannten Antioxidants, weder das Wasser noch die Substanz von augenreizendem Geruch auch unter Durchleiten des Sauerstoffstroms gebildet und nur das Dibromid von tieferem Schmelzpunkt als Reaktionsprodukt erhalten wird.

Dass die Einwirkung des Sauerstoffs allein nicht genug ist, um die genannte Zersetzung der Ketone V und VI hervorzubringen, sei noch hinzugefügt. Wie später in der nächsten Mitteilung hingewiesen werden soll, wird die saure Substanz stets vom gewissen bromierten Reaktionsprodukt begleitet und für gebildet durch die Zersetzung des bromhaltigen Radikals angesehen.

Hier seien einige Angaben über das verwandte α-Bromketon VI gegeben. Dieses Keton wird aus dem Dibromid von höherem Schmelzpunkt, 177.0~177.5°C.,[8] nach dem von Abell in Bezug auf das Keton V beschriebenen Verfahren[9] durch Abspaltung von Bromwasserstoff und Behandlung seiner alkohlischen Lösung mit wasserfreiem Kaliumacetat dargestellt.[10] Das Keton gibt durch Einwirkung des Hydroxylamins in alkalischer Methanollösung die bei 131~2°C. schmelzenden, weissen Nadeln des 3-Phenyl-5-*p*-tolylisoxazols, der auch aus dem Dibromid durch das gleiche Verfahren erhältlich ist. Seine Struktur wird gemäss dem Beispiel des 4'-Bromchalkons und anderen Analogen entschieden.[11]

Beschreibung der Versuche

Chalkon und 4-'Methyl-chalkon sind aus Benzaldehyd durch Kondensation mit Acetophenon bzw. Methyl-*p*-tolylketon dargestellt worden. Beim letzteren, das bei 76.5~77.5°C. zu schmelzen ist[12], steigt aber der Schmp. durch Umkristallisation aus Methanol sehr schwierig auf. Reineres Präparat ist dadurch erhältlich, dass man das rohe Keton II durch Addition des Bromwasserstoffs in β-Bromhydroketon überführt, auf dem Wasserbad zum Abspalten des Bromwasserstoffs erhitzt, und den so erhaltenen Rückstand aus Methanol umkristallisiert. So gewinnt man aus dem rohen Produkt von Schmp. 72.5~75°C. ein Präparat, das durch einmaliges Umkristallisieren aus Methanol einen Schmp. von 75.8~77.2°C. aufweist, während das nur durch Umkristallisation gereinigte Keton bei 73~6°C. schmiltzt. **3-Phenyl-5-p-tolylisoxazolin.** Nach dem von Blatt betreffs 4'-Bromchalkons beschriebenen Verfahren[13] erhielt man aus 2.2 gr. Keton II über dessen Oxim 1.3 gr. bei 80~6°C. schmelzender Substanz, die, dreimal aus Äthanol umkristallisiert, bei 93.0~94.5°C. schmiltzt N%: beob. 5.72, ber. für $C_{16}H_{15}ON$ 5.91.

Einwirkung von Bromwasserstoff auf Ketone I und II. a. Reaktion in Benzol. Löst man das Ketone in 5~6 Teile Benzol auf und leitet bromfreien, getrockneten Bromwasserstoff ein, so bildet sich Hydrobromid B fast quantitativ. Beim Keton I scheidet sich der grösste Teil des Produkts als weisser Niederschlag aus der Lösung ab, dagegen bleibt das Hydrobromid B des Ketons II in der Lösung, da die Löslichkeit des letzteren in Benzol recht grösser ist. Schmp. des Hydrobromids des Ketons II (IV): 103~109°C., Br%: beob. 26.53, ber. für $C_{16}H_{15}OBr$ 26.40. Wenn man einen heftigen Sauerstoffstrom mit dem Bromwasserstoff durchleitete, wurde keine merkliche Abänderung beobachtet. Die Anwesenheit der Feuchtigkeit übt ebenfalls keinen Einfluss aus. **b. Reaktion in Ligroin.** Man löst 0.58 gr. Keton II in 60 ccm. bei 90~105°C. siedendem Ligroin und leitet Bromwasserstoff mit einem heftigen Sauerstoffstrom eiskalt ein. Die Lösung scheidet nach Farbeänderung, wie bei der Reaktion in Benzol der Fall ist, weissen Niederschlag des Hydrobromids ab, wobei allmähliche Entfärbung stattfindet. Nach Beendigung der Reaktion wird der Niederschlag (Schmp.: 103~7°C.) filtriert und das Lösungsmittel unter vermindertem Druck bis zu einem Volum von 3 ccm. abgedampft, wodurch weitere Menge Kristalle (Schmp.: 95~104°C.) gewonnen wird. Die erhaltenen Kristalle (sämtlich 86% d. Theor.) stimmt mit *p*-Tolyl-β-bromhydrostyrylketon überein. Durch fortgesetztes Abdampfen des Ligroinfitrats auf dem wasserbade bleibt ein schwarzbraunes, etwas reizend riechendes Öl zurück. Weitere Behandlung wurde nicht ausgeführt. Bromhydroketone III und IV sind sehr unbeständig und, durch Wärme so wie auch eine Base beeinflusst, bilden sich in die ungesättigten Ketone zurück unter Abspaltung von Bromwasserstoff. Nämlich folgendermassen: wenn man 0.43 gr. Keton III in 10 ccm. Benzol löst und in

8) C. Weygand, *Ber.*, **57**, 416 (1924).
9) R. D. Abell, loc. cit., 1002.
10) C. Weygand, *Ann.*, **459**, 112 (1927); ibid., **472**, 178 (1929).
11) A. H. Blatt, *J. Am. Chem. Soc.*, **53**, 1139 (1931); P. Barnes und L. B. Dudson, ibid., **67**, 132 (1945).
12) 4'-Methyl-chalkon ist polymorph und die durch dieses Verfahren zuerhaltende Substanz, die den oben angedeuteten Schmp. hat, ist von Weygand als α-Form genannt worden. C. Weygand und A. Matthes, *Ann.*, **449**, 30 (1926).
13) A. H. Blatt, loc. cit.

Gegenwart von 0.42 gr. Pyridin (3.5 mol. Äquiv.) drei Tage stehen lässt, so ändert sich die Farbe allmählich zu gelb und der aus ihr durch Abdampfen des Benzols bei Zimmertemperatur erhaltene Kristall schmiltzt bei 50~90°C., was die Abspaltung von Bromwasserstoff recht erheblich aufweist. **Pyrazolinderivate.** Die obenewähnten Ketone III und IV geben durch Reagieren mit Phenylhydrazin quantitative Menge der Pyrazolinderivate. Die aus dem Keton III erhaltene Verbindung ist 1,3,5-Triphenyl-pyrazolin und stimmt mit dem Stoff, den Knorr aus Phenylhydrazon des Chalkons I[14] und H. Rupe & F. Schneider durch Einwirkung des Phenylhydrazins auf Phenyl-β-chlor-hydrostyrylketon[15] erhielten, überein. Schmp.: 135~6.5°C. N%: beob. 9.14; ber. für $C_{21}H_{18}N_2$ 9.40. Wird das Keton IV mit überflüssigem phenylhydrazin (etwas mehr als 2 Mole) versetzt und das Ganze gut geknetet, so wird es zur gelben Masse unter nicht gelinder Wärmeentwicklung. Nach dem Erkalten wird es durch Zugabe verdünnter Salzsäure vom überflüssigen Hydrazin befreit und aus Äthanol-Benzol kristallisiert. 1,5-Diphenyl-3-*p*-tolyl-pyrazolin stellt bei 153.5~4.5°C. schmelzende Nadeln und eine bläulich fluoreszierende Lösung dar, wie die des Triphenylpyrazolins. N%: beob. 9.18; ber. für $C_{22}H_{20}N_2$ 8.97.

Ungesättigte Bromketone V und VI. a. Keton V wurde aus Chalkondibromid von höherem Schmp. nach dem von Abell beschriebenen Verfahren dargestellt. Das Keton destilliert sich bei 194~7°C. unter 5 mm. Druck (nach Abell, 230~1°C., 18 mm.) und stelt schwach gelblich gefärbte Kristalle von Schmp. 43~4°C. dar. Br%: beob. 27.89; ber. für $C_{15}H_{11}OBr$ 27.78. **b. 4'-Methyl-chalkondibromid.** Löst man 30 gr. 4'-Methyl-chalkon (II) in 250 ccm. Schwefelkohlenstoff auf und lässt 22 gr. Brom eiskalt eintropfen, so wird die theoretische Menge von Dibromid (51.5 gr.) erhalten. Das Dibromid ist schwer löslich in Äthanol und zwar werden nicht mehr als 1.6 gr. desselben in 100 ccm. siedendes Äthanols gelöst. Man erhält aus dem oben erwähnten Rohprodukt, dreimal mit Benzol umkristallisiert, 44 gr. Dibromid von Schmp. 177.0~177.5°C. Br%: 42.02; ber. für $C_{16}H_{14}OBr_2$ 41.85. Anderseits wurde das Dibromid von tieferem Schmp., das dem Chalkondibromid von Schmp. 120~1°C. entspricht, aus Bromketon VI (s. unten auf c) durch Addition des Bromwasserstoffs dargestellt. Man Löst 1.05 gr. Keton in 8 ccm. Schwefelkohlenstoff auf und leitet der getrockneten Bromwasserstoff ein. Es scheidet sich 0.87 gr. des weissen Niederschlags ab, ferner wird aus der Lösung ein Ertrag von 0.38 gr. hinzugesetzt. Durch mehrmalige Umkristallisation der beiden Präparate aus Äthanol steige der Schmp. je bis auf 155.5~6.8° und 140~4°C. Hierauf führt man die Mischprobe mit der gleichen Menge Dibromid von höherem Schmp. aus, so schmelzen die beiden Präparate je bei 140~150° und 142~166°C., nämlich ist die Schmelzpunktserniederung beim ersteren auffallender als beim letzteren. Daher kristallisiert man das erstere noch dreimal mit Äthanol, um die bei 156.5~7.5°C. schmelzende weisse Nadeln zu gewinnen. Br%: 41.98; ber. für $C_{16}H_{14}OBr_2$ 41.85. **c. Bromketone VI** wurde nach dem genau ähnlichen Verfahren wie beim Keton V dargestellt. Sdp.: 212~4°C. unter 7 mm. Druck. Das destillierte Öl erstarrt durch Abkühlung mit Eis. Es wird gereinigt, indem man es auf der Tonplatte ausbreitet und zum Befreien von öligen Unreinigkeiten mit Petroleumäther behandelt. Schmp.: 62~4°C. Br%: 26.70; ber. für $C_{16}H_{13}OBr$ 26.54. **d. 3-Phenyl-5-p-tolyl-isoxazol.** 1.50 gr. des Ketons VI werden in 35 ccm. Methanol gelöst, mit 0.69 gr. Hydroxylaminhydrochlorid, gelöst in 1.25 ccm. Wasser, versetzt und zum Sieden erhitzt. Wird eine konzentrierte Lösung von 1.67gr. kaustischen Kalis darin hinzugesetzt, so findet sogleich eine heftige Reaktion statt und ändert sich die Farbe der Flüssigkeit von Gelb zu Orange. Nach Beendigung der Reaktion fallen weisse Nadeln aus der sich kühlenden Lösung, die hierdurch wieder entfärbt. Man erhält 0.95 gr. Isoxazol, der aus Methanol umkristallisiert, bei 131~2°C. schmilzt. N%: beob. 5.8; 5.68 ber. für $C_{15}H_{13}ON$ 5.96. Derselbe Isoxazol kann auch bei der Einwirkung des Hydroxylamins auf 4'-Methyl-chalkondibromid in alkalischem Medium nach dem gleichen Verfahren gewonnen werden.

Die Einwirkung des Bromwasserstoffs auf die Bromketone V und VI. a. Reaktion in Schwefelkohlenstoff. Löst man 1.58 gr. Keton in 8 ccm. Schwefelkohlenstoff auf und leitet den Bromwasserstoff ein, so trübt sich die Lösung weiss und die Reaktion vollendet während einer Viertelstunde, wodurch sämtlich 2.04 gr. des Dibromids gebildet werden. Der Ertrag ist fast quantitativ, darunter 1.06 gr. erhält man als Niederschlag, der bei 119.0~120.5°C., und den übrigen Teil, 0.98 gr. von Schmp. 108~114°C. aus dem Filtrat. In Bezug auf das Keton VI sind Einiges über die Reaktion schon im vorausgehenden Abschnitt erwähnt. Der Einfluss des Sauerstoffstrom auf den Verlauf der Reaktion hinsichtlich dieser Ketone kann nicht bemerkt werden, nämlich verändern sich die Ausbeute und der Schmp. des Produkts nicht. **b. Reaktion in Petroleumäther. Keton V.** 3.45 gr. Keton werden in 100 ccm. bei 75~90°C. siedendes Petroleumäthers und eiskalt gehalten, und ein heftiger Sauerstoffstrom mit Bromwasserstoffstrom wird durchgeleitet. Nach Verlauf von halb bis anderthalb Studen trübt sich die Lösung (vor dem Trüben wird nur das unveränderliche, ungesättigte Keton aus der Lösung zurückgewonnen), dann scheidet sich eine dünne Schicht von blutroter Farbe auf dem Boden ab. Hierauf nimmt die Lösung eine auffallende, gelbe Farbe an, die sich von der dem ungesättigten Keton zuzuschreibenden, schwach gelben Farbe deutlich unterscheidet, ferner wird sie durch den stark augenreizenden Geruch gekennzeichnet. Auf dem Bodem und der Wand des Reaktionsgefässes bilden sich prismatische Kristalle von Schmp. 117~120°C. Sie stimmen mit dem Dibromid von tieferem Schmp. nicht überein, sondern ergibt sich durch Mischprobe als identisch mit Benzoesäure. Die Lösung wird zusammen mit den Kristallen mit konzentrierter Bicarbonatlösung durchgeschüttelt und aus

14) *Ber.*, **21**, 1209 (1888).
15) ibid., **28**, 957 (1895).

geäthert. Nach Abdampfen der Ätherlösung bleiben 0.52 gr. Kristalle übrig, die nach Umkristallisation aus Wasser bei 121～2°C. schmelzen und ebenfalls sich als Benzoesäure erweisen. Die von Petroleumäther abgeschiedene, an dem Boden niedergelassene Schicht, deren Menge nach einer Reine von den bezüglich 2～4 gr. Ketons V durchgeführten Versuchen 0.8～1.5 gr. beträgt, ist als Wasser anzunehmen, da sie leichte Löslichkeit im Wasser und mit wasserfreiem Kupfersulfat eine positive Reaktion aufweist. Darin befindet aber das Brom sich nicht, da die Jodkali-Stärke-Reaktion negativ ist. **Keton VI.** Werden 2.00 gr. Keton in 65 ccm. von demselben Lösungsmittel aufgelöst und nach dem gleichen Verfahren wie beim Keton V der Einwirkung des Bromwasserstoffs und des Sauerstoffs erlitten, so wird keine Veränderung als bei der Reaktion betreffs des vorangehenden bemerkt und verläuft die Reaktion ganz ähnlich, nämlich ändert sich die Farbe der Lösung nach einigem Zeitverlauf zu gelb, bildet sich eine dünne Schicht von Wasser und die Lösung kommt stark augenreizend zu riechen. Der mit konzentrierter Bicarbonatlösung ausgeschüttelte saure Stoff beträgt 0.12 gr., der aus Wasser auskristallisiert, bei 174～7°C. schmiltzt und mit *p*-Toluylsäure übereinstimmt, da er mit derselbe Säure zusammengeschmolzen, keine Schmelzpunktserniederung zeigt. Ferner schmiltzt der aus dem Filtrat durch Abdampfen des Wassers in kleiner Menge gewonnene, saure Stoff bei 165～175°C. und ergibt sich auch als *p*-Toluylsäure. Die Benzoesäure ist darin nicht gefunden worden. **c. Einfluss des Brenzkatechins.** 2.50 gr. Ketone VI werden mit 0.04 gr. des Brenzkatechins in 70 ccm. desselben Lösungsmittels aufgelöst und nach dem auf vorangehendem Abschnitt beschriebene Verfahren behandelt. Es bilden sich allmählich weisse Kristalle an der Wand. Die Reaktionsflüssigkeit riecht nach Verlauf von zwei und halb Stunden keineswegs augenreizend, und keine Bodenschicht wird bemerkt. Es bildet sich auch kein saurer Stoff. Die Menge des Niederschlags beträgt 1.33 gr., der nach Umkristallisation aus Benzol-Alkohol einen Schmp. von 152～5°C aufweist und mit dem Dibromid von tieferem Schmp., d.h. dem normalen Additionsprodukt übereinstimmt.

Zusammenfassung

Die Untersuchung über die Einwirkung des Bromwasserstoffs und des Sauerstoffs auf einige α,β-ungesättigte Ketone zeigt, dass der Sauerstoffeffekt bezüglich Chalkons und 4'-Methylchalkons nicht bemerkt werden, aber bei ihren α-Bromderivaten findet eine merkwürdige Erscheinung, d.h. die Abspaltung der Kohlenstoffkette zwischen den Atomen des Carbonylkohlenstoffs und seines α-ständigen statt, die Bildung der aromatischen Carbonsäure zur Folge hat. Dies ist eine von dem Sauerstoffeffekt begleitete, neu gefundene Abspaltungsreaktion und zwar wird in Gegenwart von einem Antioxidant, Brenzkatechin ganz und gar untergedrückt. Von der Menge des hierbei entstandenen sauren Stoffs aus ist es auch klargemacht, dass die Zersetzung bei α-Bromderivat des Chalkons im Vergleich mit dem entsprechenden des 4'-Methylchalkons erheblicher ist.

Chemisches Institut,
Fakultät der Naturwissenschaften,
Tokyo Universität, Tokyo

Rheology of Coal. V. Some Factors Affecting the Strength of Coal

By Katsuya INOUYE and Hideo TANI

(Received August 19, 1952)

Introduction

The authors already attempted in Part IV[1] an absolute expression of the strength of coal from measuring the stress required to fracture, f, and the duration of the stress, t, and hence the strength was discussed by the values of "fatigue modulus" and molal activation energy for fracture. Further results are described in this paper with statistical treatment on the factors affecting the strength of coal. The stress at rupture and activation energy, which should have been compared for samples with constant analytical composition and also at same duration of stress, are again given for several typical cases using the statistical correlation equations of f upon t and ash concentration.

Further Experiments on the Fracture of Coal

Table 1 shows the values of f, t covering mainly the range of 2 to 0.1 second, Young's

modulus from the vibrational method, E_d, Young's modulus from the static (bending) method, E_s, as well as ash content in weight % and in volume %, ϕ. The measurements were carried cut for f and t by the previously described apparatus to measure the breaking strength at varying durations 5 of load[1]. The dynamic Young's modulus was obtained by the acoustic method measuring the resonant frequency of the rectangular specimen at audiofrequencies[2]. The static Young's modulus was calculated by measuring the deformation of the specimen end by reflection of light from the mirror cemented on one of the ends, at bending of the rectangular specimen when the stress is applied to the center of the length and the specimen is supported with two wedge-shaped metals at near positions to the ends. The experimental apparatus used includes that for the fracture measurement and is schematically shown in Fig. 1. The equation by which the static modulus of elasticity, E_s, was calculated is as follows:

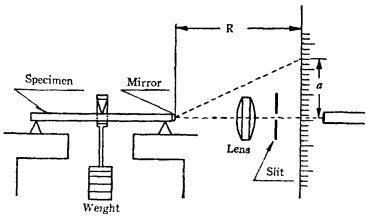

Fig. 1.—Apparatus measuring the Static Young's Modulus

$$E_s=\frac{3Wl^2R}{2b\tau^3a},$$

where W is the weight, l the span length of specimen, b the breadth, τ the thickness, R the distance between scale and the mirror cemented on one end of the specimen, and a the deviation of the reflected light spot.

The W/a value was taken from the "elastic" strain-stress relation, i.e., the linear relationship which is obtained from the total strain minus plastic deformation remaining after unloading.

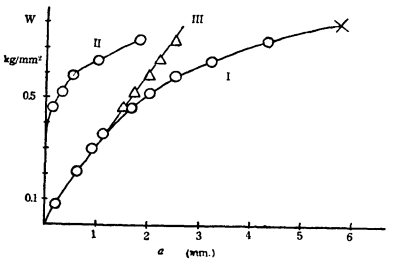

Fig. 2.—An Example of Static Measurement
I, Total Strain
II, Plastic Deformation
III, "Elastic" Strain (I−II)
The crossing denotes the breaking point.

Fig. 2 shows an example of the static experiments for a sample from American coal.

The samples of coal examined were selected from the species which had been discussed in the preceding articles of this study, i.e., American bituminous (strongly-caking) coal, Takashima bituminous (caking) coal, Toro bituminous (weakly-caking) coal and Shosaku anthracite. The descriptions of the samples in general properties are given in Part II or III[3,4]. All specimens were cut from blocks in rectangular bar with the accuracy of 1% in each dimension and parallel to the bedding plane. The measurements were carried out after putting the samples in the dessicator of 76% relative humidity for 6 months to avoid the influences owing to the moisture in the sample.

Table 1

Strength, Young's Moduli and Properties of Coal

Sample	t (sec.)	f (kg./mm.²)	$E_d\times10^{-10}$ (dyne/cm.²)	$E_s\times10^{-10}$ (dyne/cm.²)	Ash Content (dry basis) In weight (%)	Ash Content (dry basis) In volume (ϕ)
American (Bituminous, strongly-caking)	0.1	1.16	7.35	1.19	55.16	42.05
	0.1	0.09	1.89	0.12	4.45	2.72
	0.1	0.19	2.84	0.19	5.07	3.07
	0.1	0.16	3.34	0·23	2.87	1.74
	0.1	0.81	13.4	1.20	52.02	39.41
	0.5	0.53	3.94	0.55	9.90	6.28
	0.5	0.20	4.14	0.23	5.03	3.08
	0.5	0.66	14.6	1.15	80.05	70.65
	1	0.09	2.65	0.15	1.77	0.87
	2	0.69	7.86	0.92	87.40	80.61

1) K. Inouye, This Bulletin, **26**, 200 (1953).
2) K. Inouye, *J. Colloid Sci.*, **6**, 190 (1951).
3) K. Inouye, This Bulletin, **26**, 84 (1953).
4) K. Inouye, This Bulletin, **26**, 157 (1953).

Takashima	0.1	0.15	4.59	0.17	3.40	2.27
(Bituminous,	0.1	0.37	3.40	0.59	20.59	13.46
caking)	0.1	0.22	2.91	0.20	1.61	0.97
	0.1	0.40	3.98	0.42	4.02	2.44
	0.1	0.50	3.08	0.42	4.75	2.89
	0.1	0.40	4.19	0.43	8.59	5.34
	0.5	0.11	2.27	0.10	2.80	1.69
	1	0.29	2.96	0.28	3.70	2.25
	60	1.03	4.74	0.62	2.12	1.28
Toro	0.1	0.12	2.27	0.13	6.94	4.28
(Bituminous,	0.1	1.09	4.52	0.65	6.05	3.72
weakly-caking)	0.1	0.46	2.97	0.37	7.91	4.90
	0.1	1.05	6.83	0.65	10.43	6.53
	0.5	0.68	3.71	0.44	10.35	6.48
	0.5	0.16	2.37	0.18	1.14	0.69
	1	0.93	4.49	0.51	6.45	3.97
	2	1.40	3.94	0.73	9.04	5.63
	2	0.28	3.44	0.19	7.48	4.63
	10	0.31	3.55	0.14	5.80	3.56
Shosaku	0.1	1.14	7.90	0.91	8.80	5.47
(Anthracite)	0.1	0.92	9.35	0.90	8.51	5.30
	0.1	0.28	7.70	0.36	7.83	4.85
	0.1	1.00	11.5	0.74	6.68	4.11
	0.1	0.41	6.87	0.44	6.31	3.88
	0.5	1.21	9.83	0.80	4.94	3.02
	0.5	0.57	5.98	0.57	8.98	5.59
	2	0.85	7.49	0.67	5.64	3.46

Strength and Young's Modulus

Some correlations have been expected between the Young's modulus which expresses the bond strength in the solid and the breaking strength. Tables 2 and 3 show the statistical expressions of the correlation. On the whole, samples with high elastic constant show high strength, assuming the duration of load, t, is always constant; in these calculations the Young's modulus is assumed to be independent of the resonant frequency at which the measurement was carried out, and also the dependence of f on t is ignored. In other words, the errors shown in the table contain the errors owing to these possible dependencies.

It would, however, appear that a strong correlation of strength exists upon the static Young's modulus rather than the dynamic Young's modulus. This fact will be naturally accepted as the fracture experiments have been carried out at the range of t mainly of 2 to 0.1 second, longer duration comparing with the rate of deformation by the acoustic method when the resonant frequency was approximately 5,000 c/s.

Reading the figures in Tables 2 and 3, E values are given in 1×10^{10} dyne/cm.^{2} unit, f in 1×10^8 dyne/cm.^{2} unit.

Table 2
Strength and Static Young's Modulus

Sample	Correlation Coefficient	Regression Line of E_s upon f	Standard Error	Test of Correlation
American	0.94	$E_s=0.05+1.27\ f$	0.16	<0.01
Takashima	0.70	$E_s=0.16+0.48\ f$	0.12	<0.05
Toro	0.84	$E_s=0.13+0.44\ f$	0.12	<0.01
Shosaku	0.94	$E_s=0.24+0.60\ f$	0.07	<0.01

Table 3
Strength and Dynamic Young's Modulus

Sample	Correlation Coefficient	Regression Line of E_d upon f	Standard Error	Test of Correlation
American	0.69	$E_d=2.35+8.92\ f$	3.11	<0.05
Takashima	0.36	$E_d=2.99+1.28\ f$	0.79	<0.3
Toro	0.71	$E_d=2.53+2.12\ f$	0.86	<0.05
Shosaku	0.63	$E_d=5.80+3.42\ f$	1.27	<0.1

Dynamic Young's Modulus and Static Young's Modulus

The dynamically obtained elastic constant is remarkably larger than the static modulus of elasticity; the experimental result is understood from the general concept in rheology that the static deformations force the material deform accompanied with some flows. This characteristic is recognized especially in American bituminous coal, with 35% volatile matter in mean value, having remarkable difference between two series of elastic moduli.

The statistical calculations in Table 4 suggest high correlation between E_d and E_s. Comparing also E_d and E_s in Table 1 for each specimen, it may be significant to note the facts, (1) for each coal, E_s variations owing to every affecting factor are less than E_d variations, (2) in the range of low ash content, E_d/E_s ratio is markedly large, probably because of the influence of viscous flow, as low ash content means high content of bituminous matter which acts as the plasticizer (refer Part I and II of this study), and (3) E_d/E_s ratio is large especially for the bituminous coals. These points appear to support the proposed concept of coal structure from the rheological standpoint; one of the authors' (K. I.) previous experiments has shown that, in strongly-caking coals, ash is the centre of solvation of organic coal molecules, just like a "filler" in the plastics, and the molecules with weaker intermolecular forces, surrounding such a rigid micelle structure of solvated molecules, act as a "plasticizer", especially when the whole system is carbonized, during which a softening of the system at say 400~500°C. is characteristically to be accomplished. The weakness of intermolecular forces of "plasticizer" molecules makes them distinguished in being easily extracted by solvents. Therefore, for example, the so-called bitumen (extract by benzene up to 300°C. at 50 atmosphere) content, B, is a function of ash concentration in volume, ϕ, as $\phi=a/B^2$ [2]. It would be natural to interpret the wide difference between E_d and E_s for low ash content samples as a phenomenon based on remarkable viscous flow by weakly combined molecules. However, the authors consider that more detailed measurements by a refined apparatus would be necessary for further discussions.

Table 4

Young's Moduli from Dynamic and Static Methods

Sample	Correlation Coefficient	Regression Line of E_d upon E_s	Standard Error	Test of Correlation
American	0.90	$E_d=1.12+8.60\ E_s$	1.89	<0.01
Takashima	0.53	$E_d=2.66+2.68\ E_s$	0.72	<0.1
Toro	0.75	$E_d=2.12+4.26\ E_s$	1.01	<0.05
Shosaku	0.52	$E_d=5.32+4.48\ E_s$	1.40	<0.2

Correlation of Strength on Ash Content

As one of the authors (K. I.) has proposed in the preceding paper[2], Young's modulus is a linear function of ash concentration (dry basis) in volume %, ϕ, for each species, and hence the properties of the coal are characterized by the solvation factor, K, of molecules around ash and also the modulus at $\phi=0$, E_0. If the theory is valid, and if the fact is accepted that the strength is also a linear function of E (especially the static Young's modulus, as described above), the strength is expected to be in simple relationship with ϕ.

Table 5

Strength and Ash Content

Sample	Range of ϕ (%)	Correlation Coefficient	Regression Line of f upon ϕ	Standard Error	Test of Correlation
American	0.9— 3.1	0.73	$f=0.045+0.037\ \phi$	0.03	<0.2
	6.3—13.5	0.53	$f=0.35\ +0.028\ \phi$	0.13	<0.3
	42.0—87.0	0.53	$f=0.045+0.014\ \phi$	0.35	<0.1
	0.9—87.0	0.80	$f=0.085+0.016\ \phi$	0.29	<0.01
Takashima	1.0— 2.0	−0.62	$f=1.32\ -0.665\ \phi$	0.21	<0.2
	2.0— 4.0	0.57	$f=0.001+0.14\ \phi$	0.11	~0.2
	4.0—22.3	0.75	$f=0.065+0.063\ \phi$	0.30	<0.1
	1.0—22.3	0.46	$f=0.36\ +0.03\ \phi$	0.33	<0.05
Yubetsu	8.8—16.9	0.63	$f=0.68\ +0.048\ \phi$	0.13	<0.3
	19.2—30.3	−0.66	$f=3.93\ -0.090\ \phi$	0.39	<0.2
	8.8—30.3	0.26	$f=1.26\ +0.024\ \phi$	0.49	<0.5
Shosaku	3.0— 5.6	−0.45	$f=1.93\ -0.24\ \phi$	0.39	<0.1

Table 5 shows the f—ϕ relationship for three present samples (Toro coal was omitted for low correlation) as well as Yubetsu coal, a producer gas coal. (Data for Yubetsu coal are shown in Table 1 of Part IV.) The dependence of t upon f is ignored in these calculations. The calculations were carried out for several ranges of ϕ of each coal; the correlation differs with the ϕ ranges. The better correlations in accordance with the division have led the authors to consider the properties of samples for each divided range of ϕ. One example will be discussed in the next paper for Takashima coal.

Correlation of Strength upon Ash and Time

The strength is the function of not only ϕ, but is correlated with both ϕ and t. A formulation between $1/f$, ϕ (or $1/\phi$) was tried using also data reported in Part IV of the study. The multiple correlation coefficients suggest, however, that a better formula could be found; low correlation may be due to the assumption that $1/f$ is in a linear relationship with ϕ (or $1/\phi$) and also with logt.

For an example of the calculation, a formula for American coal, which showed best correlation within the samples examined, is given in Table 6.

Table 6

Strength, Time and Ash Content

Sample	Multiple Correlation Coefficient	Regression Line of $1/f$	Standard Error
American	0.87	$1/f=1.09+11.2\frac{1}{\phi}+0.445 \log t$	1.45

The molal activation energy for fracture, U, is obtained according to Equations (5) and (6) of Part IV of the study, i.e.,

$$U=\frac{2.3KTN}{fm},$$

where, K is the Boltzman constant, T the absolute temperature, N the Avogadro's number and m is a "fatigue modulus", i.e., the inclination of the linear relationship between $1/f$ and $\log t$. In Table 2 of the preceding paper, U values were given however for samples with varying ash concentration. It was therefore apparently difficult to compare the values for the optional conditions.

Using the formula in Table 6 between $1/f$, $1/\phi$ and $\log t$ for American coal, U values can be obtained and compared at assumed constant ash concentration and at the same values of t. Table 7 shows the U values for several typical cases.

Table 7

Strength and Molal Activation Energy for Fracture at $t=0.1$, 1 and 10 sec and $\phi=1$, 5 and 10%

Sample	t (sec)	$\phi=1$		$\phi=5$		$\phi=10$	
		f (kg/mm²)	U (Kcal/mol)	f (kg/mm²)	U (Kcal/mol)	f (kg/mm²)	U (Kcal/mol)
American	0.1	0.084	35.2	0.35	8.6	0.57	5.3
	1	0.081	36.4	0.30	9.9	0.45	6.6
	10	0.079	38.0	0.27	11.2	0.38	7.9

The temperature was assumed as 15°C, the average room temperature during the experiments. The American bitumious coal is remarkably weak at low ash contents and at the same time needs high activation energy for fracture. The dependence of strength on duration of load, t, is also obtained. Such a treatment would enable to describe the strength of the coal in more definite expression than routine methods used in coal industry.

The authors hereby express their thanks to Dr. M. Kurokawa and Mr. A. Baba for interest in this investigation.

Shigen-Gijutsu-Shikenjo
(Resources Research Institute)
Saitama-Kawaguchi, Japan

The Diamagnetic Sucseptibilities and Anisotropies of the Polynuclear Aromatic Compounds

Hideo AKAMATU and Yoshio MATSUNAGA

(Received January 20, 1953)

Introduction

Aromatic compounds show the large diamagnetic anisotropies, the values of the principal susceptibility normal to the planes of molecules are abnormally large compared to that in the planes. The phenomenon has been explained by the presence of the non-localized electrons in these molecules, one π-electron per aromatic carbon atom, which are free to circulate, under the influence of the magnetic field, from one atom to the other along the aromatic rings. The behaviour is closely analogous to the electric current induced in a conducting network.[1~8]

In general, the diamagnetic anisotropy for a molecule can be estimated from the magnetic data which are observed along the principal axes of a crystal, combined with the informations about the orientation of the molecules in it. Several investigations[9] for aromatic compounds have been made in this way. Such a method is the orthodox one, neverthless, it can not be applied to the substances whose crystal structures have not been fully analysed. Moreover, frequently, we can not obtain the single crystals large enough in size to be able to be used for the magnetic measurement, especially when the molecular weight becomes larger. In such a case, the specimens are made of fine crystals in the powder form, and it is merely the values of the mean susceptibility that we can know. Fortunately, however, in the case of the planar molecules as the condensed polynuclear aromatic compounds, it is able to evaluate approximately the diamagnetic anisotropies from the values of the mean susceptibility. The method has been devised by Hazato[10] and by Pacault[11].

Let K_1, K_2 and K_3 be the principal mole susceptibilities for a molecule, where K_1 and K_2 are those in the plane of molecule, and K_3 is that perpendicular to the plane. Then the mean mole susceptibility χ_M will be expressed by

$$\chi_M = 1/3\,(K_1+K_2+K_3) \qquad (1)$$

It can be assumed that $K_1 \fallingdotseq K_2$ for the planar structure of molecule. Then the diamagnetic anisotropy of the molecule is expressed as

$$\Delta K = K_3 - K_1 = 3\,(\chi_M - K_1) \qquad (2)$$

The anisotropic part of the susceptibility, ΔK, is due to the circulation of the π-electrons in the plane of molecule, whereas K_1 (and K_2) is the isotropic part and will be the sum of the atomic susceptibilities based on the distribution of electrons being spherical symmetry. The approximate expressions for K_1 have been made by several authors. Pauling[7] has assumed the atomic susceptibility of aromatic carbon, aside from the p_z-electron, being $3/4\,(-6.0\times10^{-6})$. On the other hand, Hazato and Pacault have used the Pascal's empirical formula in a modified way, i.e.,

$$\chi(\mathrm{C}=) = \chi(\mathrm{C}) + 1/4\cdot\lambda\,(\mathrm{C}=\mathrm{C}-\mathrm{C}=\mathrm{C}) = (-6.0+10.56/4)\times10^{-6} = -3.36\times10^{-6} \qquad (3)$$

was assumed by Hazato, and

$$\chi(\mathrm{C}=) = \chi(\mathrm{C}) + 1/2\cdot\lambda\,(\mathrm{C}=\mathrm{C}) = (-6.0+5.45/2)\times10^{-6} = -3.28\times10^{-6} \qquad (3)'$$

was assumed by Pacault. In this way, K_1 for hydrocarbons is expressed as

$$K_1 = \Sigma\chi(\mathrm{C}=) + \Sigma\chi(\mathrm{H}) \qquad (4)$$

Better results in the way of the latter authors are given than the former. In the present report, $\chi(\mathrm{C}=) = -3.36\times10^{-6}$ was used following Hazato, combined with $\chi(\mathrm{H}) = -2.93\times10^{-6}$.

1) E. Hückel, *Z. Physik.*, **83**, 632 (1933).
2) A. R. Ubbelohde, *Nature*, **132**, 1002 (1933).
3) F. London, *J. phys. radium.*, **8**, 397 (1937); *J. Chem. Phys.*, **5**, 837 (1937).
4) H. Brooks, *J. Chem. Phys.*, **9**, 463 (1941).
5) B. Pullman et al., *J. phys. radium.*, **12**, 652, 717 (1951); **13**, 15 (1952).
6) R. McWeeny, *Proc. Phys. Soc.*, **A64**, 261, 921 (1951).
7) L. Pauling, *J. Chem. Phys.*, **4**, 673 (1936).
8) K. Lonsdale, *Proc. Roy. Soc.*, London, **A159**, 149 (1937).
9) K. S. Krishnan, *Nature*, **130**, 313, 698 (1932); K. Lonsdale and K. S. Krishnan, *Proc. Roy. Soc. London*, **A156**, 597 (1936); S. Banerjee, *Z. Krist.*, **100**, 316 (1939).
10) G. Hazato, *J. Chem. Soc. Japan*, **64**, 483 (1943); H. Shiba and G. Hazato, This Bulletin, **22**, 92 (1949).
11) A. Pacault, *Bull. Soc. Chim. France*, **1949**, D. 1).

Experimental

Materials.—A part of the materials was obtained from the commercial products, neverthless, most materials were synthesized by Mr. T. Handa in our laboratory. All of the materials were carefully purified by the usual method. In each case, the repeated sublimation *in vacuo* was applied to the last process of the purification. As the molecular weight increases, no good solvent can be found for the polynuclear aromatic compounds, in consequence, the ordinary method of purification including the dissolution process can not be applied. Even in such a case, the method of sublimation *in vacuo* gives the favourable results. Some details for the materials have been given in a previous report[12].

Magnetic Measurements.—The Gouy method was employed for the measurements of the magnetic susceptibility. The specimen tube was made of a cylindrical glass tube, which was separated into two sections by a glass partition. The upper half was packed with the sample, while the lower half was permanently evacuated. This was suspended between the poles of a magnet, hanging from an arm of an analytical balance, so that the lower end of the sample column was nearly at the centre of the poles, while the lower portion of the tube extended below the magnetic field. The dimension of the sample container was about 33 mm. in height (about half the length of the total tube) and about 0.094 sq. cm. in cross section, in one example. The diameter of the pole face is 20 mm., and the gap between the poles is 8 mm.

Taking water as the standard substance, the mass susceptibility, χ, is given by

$$\chi=(\kappa^*-\kappa_0)\frac{V}{F^*-F_0}\cdot\frac{F-F_0}{m}+\frac{\kappa_0}{d} \quad (5)$$

where m, d are the mass and the density, respectively, of the sample, κ^*, κ_0 are the volume susceptibilities of water and air respectively, F^*, F are the apparent changes in weight on application of the magnetic field when the tube is filled with water, and with the sample occupying the same volume V as water respectively, and F_0 is that for the empty tube. Hence, $V/(F^*-F_0)$ is the cell-constant. The values of κ^* and κ_0 were assumed to be -0.720×10^{-6} and $+0.0294\times10^{-6}$ respectively at 20°C. A constant magnetic field, about 23,000 oersteds was applied in every case. It is known by investigators that the accuracy of measurements on powdered samples is limited by the uniformity and reproducibility of packing. It seems preferable to pack the sample as close as possible.

Among a series of measurements, the calibration was checked with naphthalene from time to time. The mass susceptibility of naphthalene estimated in our experiment was $-(0.720\pm0.001)\times10^{-6}$.

Results

The results are shown in Table 1 for hydrocarbons as well as in Table 2 for quinones. In these tables, the values of the diamagnetic anisotropy calculated by equation (2) and (3) are given in column 6. The values for the low molecular weight members, taken from the International Critical Tables, are also shown for comparison.

For quinones, the calculations of ΔK were made by using the value of $+1.73\times10^{-6}$ for $\chi(O)$, with the assumption that the carbon atoms in the carbonyl radical would be aromatic; in consequence, $\chi(C)$ for these carbon atoms was also assumed to be -3.36×10^{-6}, instead of -6.00×10^{-6} for aliphatic carbon. This latter assumption is preferable, since the calculated value of ΔK for *p*-benzoquinone is not far from 40.6[13] which was evaluated by Lonsdale and Krishnan[9] from the anisotropy of the crystal, and ΔK calculated for anthraquinone is not far from 165 which was supposed by Banerjee[9]. Which assumption would be made, the difference will be small for compounds with the higher number of carbon atoms.

Table 1

Diamagnetic Susceptibilities and Anisotropies of Condensed Polynuclear Aromatic Hydrocarbons

Substance			Mass Suscept. $(-\chi\cdot10^{-6})$	Mole Suscept. $(-\chi_M\cdot10^{-6})$	Aniso-tropy $(-\Delta K\cdot10^{-6})$	$\sqrt{\overline{r^2}}$ (Å)	(p)
Benzene	C_6H_6		0.712*	55.6	54	1.44	(6)
Naph-thalene	$C_{10}H_8$	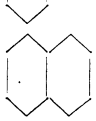	0.717*	91.9	105	1.57	(10)

12) H. Inokuchi, S. Shiba, T. Handa, and H. Akamatu, This Bulletin, **25**, 229 (1952).

13) The factor -1×10^{-6} is to be understood with all values of susceptibility and anisotropy in the following discussion.

Anthracene	$C_{14}H_{10}$	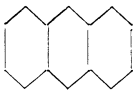	0.726*	129.4	159	1.64 (14)
Phenanthrene	$C_{14}H_{10}$	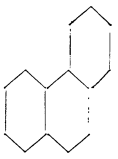	0.718*	127.9	155	1.61 (14)
Pyrene	$C_{16}H_{10}$	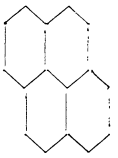	0.731±0.001	147.9	197	1.70 (16)
Perylene	$C_{20}H_{12}$	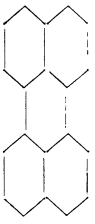	0.662±0.002	166.8	193	1.51 (20)
Anthanthrene	$C_{22}H_{12}$	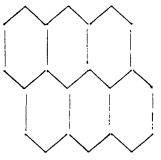	0.739±0.002	204.2	285	1.75 (22)
Dibenzpyrene	$C_{24}H_{14}$	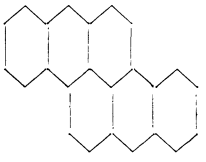	0.706±0.002	213.6	276	1.65 (24)
Mesonaphthodianthrene	$C_{28}H_{14}$	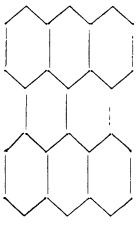	0.612±0.001	214.6	238	1.42 (28)
Dibenzcoronene	$C_{30}H_{14}$	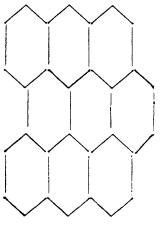	0.778±0.003	289.4	443	1.87 (30)
Pyranthrene	$C_{30}H_{16}$	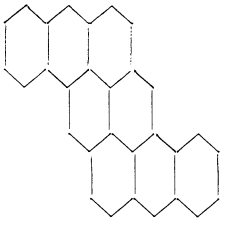	0.709±0.002	266.9	358	1.68 (30)

Indanthrazine	$C_{28}N_2H_{16}$	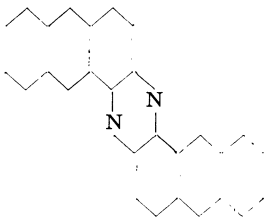	0.646±0.002	245.7	330	1.61 (30)
Ovalene	$C_{32}H_{14}$	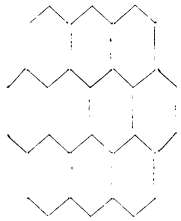	0.888±0.007	353.8	616	2.12 (32)
Violanthrene	$C_{34}H_{18}$	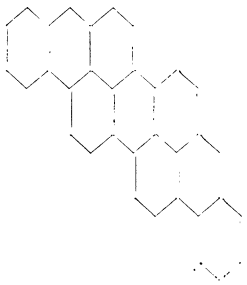	0.641±0.002	273.5	320	1.49 (34)

* International Critical Tables

Table 2

Diamagnetic Susceptibilities and Anisotropies of Condensed Polynuclear Quinones

Substance			Mass Suscept. $(-\chi\cdot10^{-6})$	Mole Suscept. $(-\chi_M\cdot10^{-6})$	Anisotropy $(-\Delta K\cdot10^{-6})$	$\sqrt{\bar{r}^2}$ (Å)	(p)
p-Benzoquinone	$C_6H_4O_2$	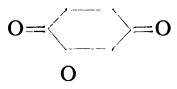	0.382*	41.3	39	1.24	(6)
Anthraquinone	$C_{14}H_8O_2$	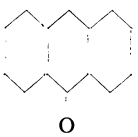	0.575*	119.6	158	1.62	(14)
Phenanthrenequinone	$C_{14}H_8O_2$	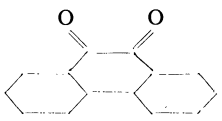	0.502±0.001	104.5	113	1.38	(14)
Benzanthrone	$C_{17}H_{10}O$	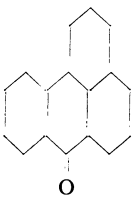	0.620±0.003	142.9	175	1.56	(17)

Dibenz-phenan-throne	$C_{21}H_{12}O$	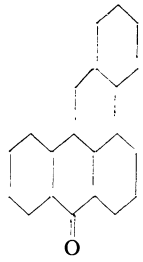	0.716±0.002	200.5	295	1.82 (21)
Anthan-throne	$C_{22}H_{10}O_2$	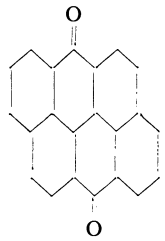	0.581±0.002	178.1	235	1.59 (22)
Dibenz-pyrene-quinone	$C_{24}H_{12}O_2$	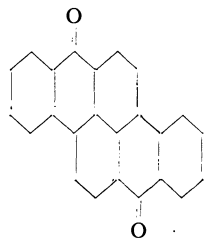	0.551±0.001	183.1	212	1.44 (24)
iso-Dibenz-pyrene-quinone	$C_{24}H_{12}O_2$	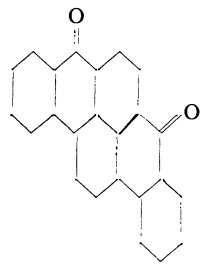	0.586±0.001	194.6	247	1.56 (24)
Meso-naphtho-dianthrone	$C_{28}H_{12}O_2$	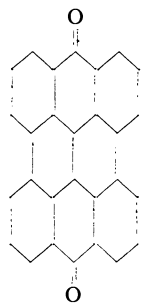	0.583±0.003	221.8	288	1.56 (28)
Helian-throne	$C_{28}H_{14}O_2$	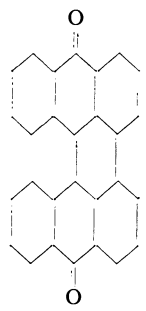	0.497±0.003	189.9	175	1.21 (28)

Pyranthrone	$C_{30}H_{14}O_2$	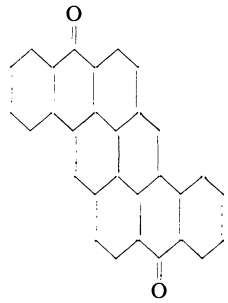	0.616±0.003	250.3	335	1.62 (30)
Flavanthrone	$C_{28}N_2H_{12}O_2$	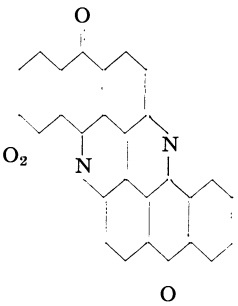	0.590±0.001	241.0	361	1.68 (30)
Violanthrone	$C_{34}H_{16}O_2$	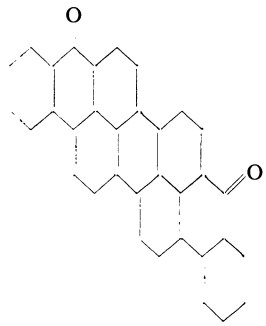	0.449±0.003	204.8	159	1.05 (34)
iso-Violanthrone	$C_{34}H_{16}O_2$	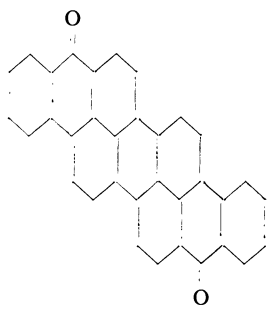	0.473±0.002	215.9	193	1.16 (34)

* International Critical Tables

It will be seen from the results that, in general, the diamagnetic anisotropy becomes progressively large with the increase in the number of rings. However, the increment in the anisotropy by the increase in the number of rings is not made by a simple way, but strikingly depends upon the shape of the molecule or the way of the aromatic condensation. Therefore, to see the rate of increment in the anisotropy, it is desirable to know some quantity assigned to each one carbon atom or π-electron. Since the anisotropy is caused by the circulation of the π-electrons in the molecular plane, their contribution to the anisotropy can be expressed, conveniently, by the Langevin theory as,

$$\Delta K = -(Ne^2/4mc^2)\sum_p \overline{r^2} = -4.248\cdot10^{-10}\cdot p\cdot\overline{r^2} \quad (6)$$

where $\sqrt{\overline{r^2}}$ is the average effective radius of the π-electron orbitals, p is the number of the π-electrons, and the other symbols have the usual meanings. The calculated values of $\sqrt{\overline{r^2}}$ are given in the last column

in the tables with the values of p assumed.

For benzene, the average radius of the π-orbitals is calculated as 1.44 A., and this average may be compared with 1.39 A., the radius of the benzene nucleus itself. As the condensation of rings increases, from benzene, through naphthalene, anthracene, pyrene, anthanthrene, dibenzcoronene, to ovalene, the average π-orbital radii become progressively large. The final product of the aromatic condensation is to be found in graphite, whose average π-orbital radius is about 8 A., calculated from Krishnan's data[14] in the same way.

The large value of the average π-orbital radius means that some fractions of π-electrons occupy the orbits whose radii are larger than that of a single benzene ring, in other words, their mobile or non-localized character is increased in the statistical sense. This occurrs among the above molecules.

On the other hand, there are molecules whose average π-orbital radii are relatively small, notwithstanding the fact that they are made of a large number of rings. For violanthrene, as an example, $\sqrt{\bar{r}^2}$ is 1.49 A. which is merely comparable to benzene.

In Fig. 1, the average π-orbital radii are plotted against the number of π-electrons, refering to the molecular structures. It will be seen in this figure, that the molecules occupying the upper positions are made of the closely compact arrangement of rings, while the molecules occupying the lower positions are made of the extended or concave arrangement of rings. The molecules discussed above belong to the former group, while in the latter group the π-electrons must be more or less localized in the statistical sense.

Perylene and Meso-naphthodianthrene— It is worth while to comment on perylene and meso-naphthodianthrene. For perylene, the diamagnetic anisotropy has beeen evaluated by Shiba and Hazato[10], as ΔK (perylene) $/\Delta K$(naphthalene)$=1.96\sim2.02$, and from this result, they assumed that the perylene molecule has two predominant naphthalene nuclei and the central hexagon in this molecule has a special structure which does not contribute to the diamagnetic anisotropy. From the results of the calculation of the diamagnetic anisotropy by London's method, Hazato[15] showed that this argument is supported when it is assumed that the central hexagon bonds have nearly the single bond character. Moreover, when the central hexagon is assumed to be equivalent to the other rings, a little paramagnetism is anticipated[16]. In the usual chemical language, the perylene molecule is not made of an aromatically conjugated system of the molecule as a whole but separated into two naphthalene nuclei. (Fig. 2 a). When this is not the case, the molecule would have the quinoid structure with excess electrons. (Fig. 2 b). This leads to the localization of the π-electrons. Therefore it would not be unreasonable to anticipate that the diamagnetic anisotropy of perylene may be smaller than twice that of naphthalene.

The mole susceptibility of perylene has

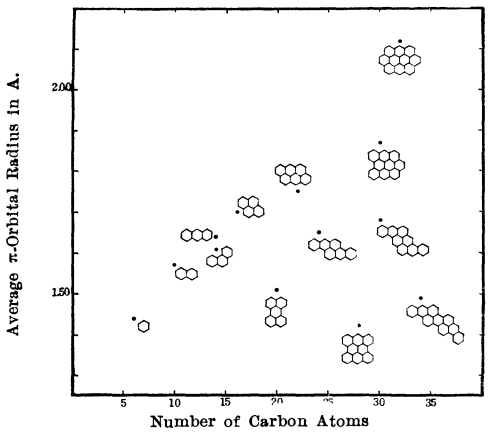

Fig. 1. The average π-orbital radii are plotted against the number of carbon atoms (or π-electrons), refering to the molecular structures.

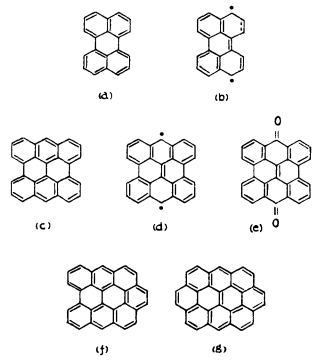

Fig. 2. (a) (b): Perylene, (c) (d): Meso-naphthodianthrene, (e): Meso-naphthodianthrone, (f): Dibenzcoronene, (g): Ovalene.

14) K. S. Krishnan, *Nature*, **133**, 174 (1934).

15) G. Hazato, This Bulletin, **22**, 151 (1949).

16) In the calculation by Hazato for this case, no definite value was obtained, neverthless, our recalculation shows that ΔK(perylene)/ΔK(naphthalene)$=-0.08$, neglecting the overlap integral.

been found to be 171 by Shiba and Hazato, while it is 165.0 by Pacault[17], and 166.8 in the present report. The smaller value of ΔK is evaluated from both of the latter rather than from the former; neverthless, the difference will not be large. Therefore, the contribution from the quinoid structure to the wave function of perylene will not be very large, at least from the magnetic standpoint.

Meso-naphthodianthrene is in the same situation as perylene. (Fig. 2 c, d). In this case, however, the diamagnetic anisotropy is much smaller than twice that of anthracene, i.e., $\Delta K(M.\ N.)/\Delta K(\text{anthracene})=1.5$. The average π-orbital radius is merely comparable to that of benzene. This means that the localization of π-electrons occurrs much more strongly in meso-naphthodianthrene than in perylene. This is in agreement with the empirical fact that the former is more chemically reactive than the latter, i.e., it is easy to synthesize ovalene from meso-naphthodianthrene by the reaction with maleic anhydride, while it is difficult to synthesize coronene from perylene.

In dibenzcoronene, the aromatically conjugated system can be completed at least of the molecule as a whole, (Fig. 2 f); then the diamagnetic anisotropy as well as the average π-orbital radius jumps to the higher value. This is further increased in ovalene. (Fig. 2 g).

The colour of meso-naphthodianthrene is deep green, while meso-naphthodianthrone is brownish green, dibenzcoronene is brown, and ovalene is reddish orange. It is interest that the former has the deepest colour among these. This may be associated to the structure in which the contribution from the large electric moment takes place; this leads to the quinoid type structure with the excess electrons in pairs making the formal charge. The triplet state may be conceivable too, whose paramagnetic contribution cancels the diamagnetic property in part. However, this fact has not yet been ascertained.

The similar discussion must also be extended to the molecules with long shaped structure, such as violanthrene, since their diamagnetic anisotropies are small.

Quinones

In the calculation of the average π-orbital radii of quinones, it was assumed that the π-electrons of all carbon atoms, including the carbonyl radical, contribute to ΔK. For *p*-benzoquinone, the average π-orbital radius is 1.24 A. when calculated with six π-electrons in this way, whereas 1.52 A. with four π-electrons omitting two combined to oxygen atoms. In the present report, the calculation followed the former way, and assumed that the difference in the values between *p*-benzoquinone and benzene is due to the localization of the π-electrons caused by the carbonyl radicals. In consequence, the evaluated values of the average π-orbital radii for quinones, in general, become a little smaller than that for the corresponding hydrocarbons. This difference ($\Delta\sqrt{\overline{r^2}}$) is about 0.2 A. This is the case of *p*-benzoquinone, phenanthrenequinone, anthanthrone, and dibenzpyrenequinone.

Neverthless, for meso-naphthodianthrone, the values of ΔK and $\sqrt{\overline{r^2}}$ are much larger than that of corresponding meso-naphthodianthrene. It will be understood from the discussion in the preceding section, when we remember that passing from meso-naphthodianthrene to meso-naphthodianthrone the aromatically conjugated system of the molecule as a whole can be completed, and this leads to the delocalization of excess electrons in the former. (Fig. 2 e).

The opposite case to this is seen, when passing from violanthrene to violanthrone. The diamagnetic anisotropy of violanthrone is abnormally small; the average π-orbital radius is only 1.05 A. In this case, again, the molecule can not be made of an aromatically conjugated system as a whole but separated into two benzanthrone nuclei. The overlapping effect of this and the elongated structure of this molecule strikingly decreases the diamagnetic anisotropy. The value of ΔK of violanthrone is not only far smaller than twice that of benzanthrone, but it is even smaller than that of benzanthrone itself.

From the results discussed above, it may be concluded that, when a molecule can not be made of an aromatically conjugated system as a whole but separated into two predominant nuclei, the larger the nuclei are, the more strongly the diamagnetic anisotropy falls off.

The Tables contain the results on a few aza-aromatic compounds[18]. The magnetic property of the aza-aromatic ring is quite like that of the benzene ring. This is clearly shown when comparing the result on flavanthrone with that on pyranthrone.

17) A. Pacault, *Ann. chim.* [12] **1**, 257 (1946).

18) In the calculation of K_1, $\chi(\text{N=})=\chi(\text{>C=N-})-\chi(\text{C=})=[(-6.00-5.57+8.16)-(-3.36)]\times10^{-6}=-0.05\times10^{-6}$ was assumed, from the Pascal's constants and equation (3).

Summary

The magnetic susceptibilities of condensed polynuclear aromatic compounds with higher molecular weights (ten hydrocarbons and twelve quinones) have been measured by the Gouy method, and the diamagnetic anisotropies have been approximately evaluated.

The diamagnetic anisotropy becomes progressively large as the number of rings increases, when the aromatic condensation takes place in the manner of the closely compact arrangement of rings; while, when it is not the case, it depends strikingly upon the molecular structure.

When the diamagnetic anisotropy has a smaller value, notwithstanding the molecule is made of a large number of rings, the localization of the π-electrons or some other excited states must be assumed. Such a case is found, when a molecule is not made of the aromatically conjugated system as a whole but separated into two predominant nuclei, as meso-naphthodianthrene and violanthrone, or when a molecule is made of a long shaped structure as pyranthrene or violanthrene.

Acknowledgement

The authors express their hearty thanks to Mr. T. Handa who prepared most materials used in this study, and to Mr. H. Inokuchi for the collaboration throughout this investigation. The cost of this study was defrayed from the grant of the Ministry of Education, to which the authors' thanks are due.

Department of Chemistry,
Faculty of Science,
Tokyo University, Tokyo

Physico-chemical Studies on Molecular Compounds. IV. Heats of Solution of Crystalline Quinone, Hydroquinone and Quinhydrone into Acetone and Heat of Formation of Crystalline Quinhydrone

By Keisuke SUZUKI and Syûzô SEKI

(Received February 23, 1953)

Introduction

Although there have appeared already numerous investigations on the crystalline molecular compounds from the standpoint of organic chemistry in crystalline states, physico-chemical studies concerning the interaction energies between component molecules are very scanty in comparison with those in solution. The heat of formation of the molecular compound in solution, however, involves ambiguous energy quantities referring to the solvation energy, the accurate estimation of which is difficult on account of the unknown relative molecular arrangement.

On the other hand, during the past several years, a considerable number of complete crystal structure determinations of molecular compounds have been performed, so that it is much more suitable to determine the interaction energies of these materials. For this purpose, we have determined in a previous report,[1] indirectly the interaction energy of quinhydrone, its crystal structure being completely determined in this laboratory[2]. In the present investigation, we have undertaken to determine this energy more accurately by direct measurements of heats of solution of quinhydrone as well as those of component crystals.

Experimental

a) Apparatus and procedures.—The calorimeter used for the present work is in principle identical with that reported in a previous paper[3]. A few points improved now are as follows:

1) I. Nitta, S. Seki, H. Chihara and K. Suzuki, *Sci. Paper Osaka Univ.* No. 29 (1951).
2) I. Nitta, K. Osaki and H. Matsuda (to be published).
3) S. Seki and K. Suzuki, This Bulletin, **26**, 63 (1953).

i) In order to hold the constancy of temperature of the thermostat more accurately, the whole apparatus was surrounded by an air thermostat, the temperature of which was controlled within the accuracy of 0.1~0.2°C and held ca. 0.2°C below the temperature of the water thermostat. For the regulation of temperature of the inner water jacket, five helical glass tubes of ordinary toluene regulators were connected in parallel (ca. 400 cc.) and the portion of mercury-platinum contact was dipped into the water in order to avoid the temperature fluctuation of the outer atmosphere.

As the results of these improvements the temperature of the inner water jacket was held to be constant within the accuracy of 0.0001°C.

ii) Instead of the precision type voltmeter and ammeter used previously for the determination of water equivalent of the calorimeter, Yokogawa P-7 type low voltage potentiometer and potential divider (resistance, 29330 ohm; magnification, 99.708 : 1) were used for the measurement of voltage drop of the calorimeter heater, and the current through the heater was calculated by the measurement of the potential drop of manganin standard resistance (9.9967 ohm at 25°C, immersed in special transformer oil) connected in series with the heater. As the change of resistance of the standard resistance and potential divider due to Joule's heat was very small, its effects can be ignored. The correction for the amount of current through the circuit of the potential divider was taken into consideration. The circuit for the determination of water equivalent is shown in Fig. 1.

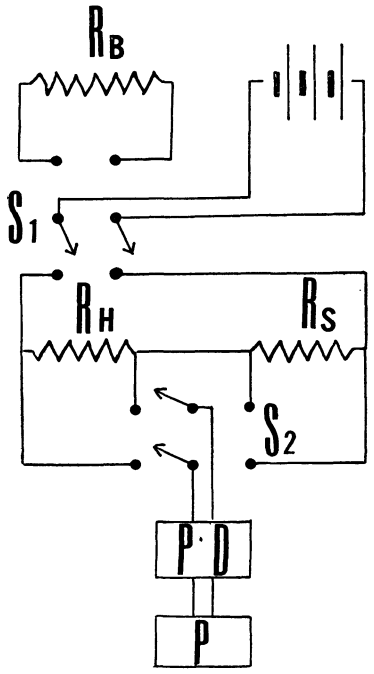

Fig. 1.—Calorimeter heating circuit

S_1, S_2: switches
R_H : calorimeter heater
R_S : standard resistance
R_B : ballast resistor
P : potentiometer
PD : Potential divider

iii) For the accurate determination of the heat of solution of crystalline materials, it is very desirable to dissolve a specimen as quickly as possible into the solvent. For this purpose, we have chosen acetone as the solvent. As a dissolving device, we have adopted the method of breaking a thin glass bulb (capacity: ca. 2 c.c.) containing a powdered specimen. In this way, about 80% of the samples dissolve within fifteen seconds and the whole process of dissolution was accomplished within about three minutes. The endothermic effect due to the evaporation of acetone into the air bubbles liberated from the glass bulb was calibrated before the experiment and found to be expressed approximately by the following relation;

$$\Delta H_b = 0.10 \times v \text{ cal}$$

ΔH_b: heat absorbed,
v: empty space of the bulb in cc.

b) Samples

i) *Hydroquinone* (*Hq*): The product of Wakô Pure Chemicals Ltd. was recrystallized twice from ethyl alcohol and then subjected to fractional sublimation under high vacuum (10^{-5} mm. Hg) at 100°C. (Melting point: 172.5~173.0°C.) This material has three modifications[4] (α, β and γ). The material obtained by this operation was ascertained to be of the α-form by taking the Debyephotograph. To exclude the possibility of coexsistence of the minute amount of the γ-form, the sample was powdered in agate mortar and stored for about four months in a vacuum desiccator.

ii) *Quinone* (*Q*): *Hq* prepared as mentioned above was oxidized by sulfuric acid and aqueous solution of $K_2Cr_2O_7$, then recrystallized from benzene and ligroin, and finally subjected to fractional sublimation under high vacuum at room temperature using solid carbon dioxide as the cooling material. (Melting point: 115.0~115.5°C.)

iii) *Quinhydrone* (*QH*): Equimolar *Q* and *Hq* prepared by the above mentioned methods are dissolved into acetone. Then this solution was evaporated gradually at room temperature for about one day. The precipitated *QH* at the bottom of the beaker was stored in a darkened desiccator together with pure *Q* in order to prevent frac-

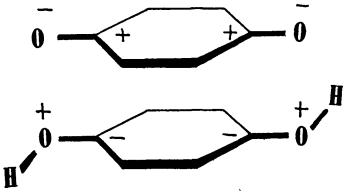

Fig. 2.—A model for quinhydrone by Murakami

4) W.A. Caspari, *J. Chem Soc.* **129**, 2944 (1926); **131**, 1093 (1927) H.M. Powell and P. Riesz, *Nature* **161**, 52 (1948).

tional evaporation[1] of Q from the QH crystals. (Melting point: 169.5~170.0°C C.*)

Results and Discussion

a) Experimental results.—All measurements were carried out at about 24°C and their results are given in Table 1. As the solvent for the determination of the heat of solution of Q, pure acetone as well as acetone solution already containing equimolar Hq were used to see if the molecular compound formation be possible in the solution. As is shown in the table, two values of heats of solution for these solvents were equal within the experimental error.

Table 1

Heats of solution of QH, Hq and Q

Sample	Exptl. No.	m	N	t°C	ΔH kcal/mol.
Quinhydrone	1	0.01 384	494	24.02	9.142
	2	0.01 373	499	24.03	9.179
	3	0.01 393	491	24.14	9.119
	Average				9.147±0.012
Hydroquinone	4	0.01 394	491	24.06	−0.380
	5	0.01 439	476	24.10	−0.358
	Average				−0.369±0.008
Quinone*	6	0.01 435	477	24.00	4.157
	7	0.01 399	490	23.98	4.100
	Average				4.129±0.022
Quinone	8	0.01 394	491	23.98	4.114±(0.02)

m: mole number of the sample used.
N: mole number of acetone to dissolve one mole of solute.
t°C: average temperature of the measurement.
ΔH: +sign is taken for the endothermic process.
*: for the solvent containing equimolar Hq.

b) Heat of solvation of quinone and hydroquinone. Energy of hydrogen bond between acetone and hydroquinone.—Prior to the discussions on the problems of molecular compound formation, the solution state of each component will be discussed here. As is well-known, the heat of solvation at infinite dilution ΔH^{∞}_{soln} is given by the following equation

$$\Delta H^{\infty}_{solv}=\Delta H^{\infty}_{soln}-\Delta H_{sub}$$

where ΔH^{∞}_{soln} is the heat of solution at infinite dilution, ΔH_{sub} the heat of sublimation of the crystals. The heat of solution obtained by the present investigation correspounds to that at a finite concentration, so that the heat of dilution brought to the infinite dilution should be added over this experimental value to evaluate ΔH^{∞}_{soln}. As for the heat of dilution of Hq, it is guessed to be less than 100 cal/mol. from the considerations of the data of heats of dilution[5] of aqueous solution at the concentrated state in connection with the data on the degrees of association of phenol in non-polar solvent determined by infra-red absorption spectra[6]. Presumably this correction factor is much less for Q. Since the orders of magnitudes of these corrections are smaller than or equal to the experimental errors of the heats of sublimation, it may be approximately correct to substitute ΔH_{soln} (under experimental condition) for ΔH^{∞}_{soln} for the present discussion. ΔH^{∞}_{solv} in Table 2 were calculated on this assumption by use of the heats of sublimation measured by us.[1] In the table also the values for aqueous solutions and that of resorcinol are given for reference.

There exists evidently considerable difference between the heats of solvation for acetone of Hq and Q, respectively, as seen in the table. This fact may be explained in the following way:

Considering the process of dissolution of a molecule into a solvent, heat of solvation of a molecule consists of the following two parts;

* The samples preciptated from aqueous or alcoholic solutions, the products prepared from the melts of the equimolar components, the product of Kahlbaum Co., etc. exhibit lower melting points as well as wider melting ranges than the sample mentioned above.

5) "International Critical Table."
6) W. Lütcke and R. Mecke, *Z. Electrochem*, **53**, 241 (1949).

namely, (I) the heat necessary to create a cavity which holds a solute molecule in solvent (endothermic) and (II) the heat evolved due to the interaction between a solute molecule and surrounding solvent molecules. Of these two, the former may be looked upon to be approximately equal for *Q* and *Hq*, because of their nearly equal size and shape. Hence, the difference should be attributed to the second effect, of which van der Waals interaction between solvent and solute molecules may be also nearly equal. Accordingly, the difference 9.64 kcal/mol. should be attributed to the hydrogen bond formation of O–H·····O=C type as shown in Fig. 3, whereas the *Q* molecule does not form such a hydrogen bond.

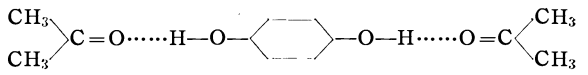

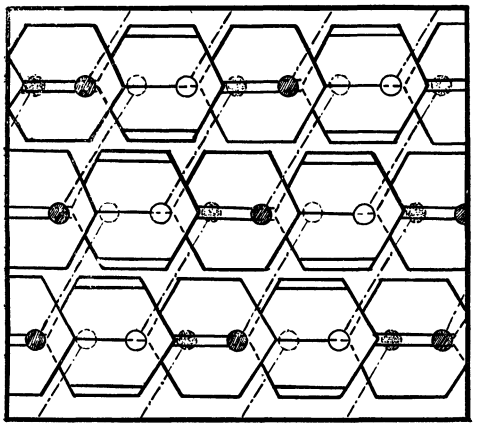

Fig. 3.—A schematic representation of molecular packing in quinhydrone crystal
Hatched circles: oxygen atoms of quinone
White circles: oxygen atoms of hydroquinone
——•——•——: hydrogen bonds

In general, the energy of hydrogen bond determined in a solution state has always some ambiguities, as the estimation of the differece of the solvation energies of associated and non-associated molecules is difficult. In the present case, however, they are cancelled empirically by the solvent effect of *Q* molecule having nearly equal size, shape and numbers of electrons. The energy of hydrogen bond $\frac{1}{2}(9.64)=4.82$ kcal/mol determined is somewhat smaller than that of formic acid dimer[7] (6.3 kcal/mol.) having similar type of hydrogen bond (O—H·····O=C). This small difference may be attributed to the weaker proten donating power of hydroquinone and to the weaker proton accepting power of acetone molecule.

The smaller difference between the heats of hydration of *Q* and *Hq* (5.35 kcal/mol: see Table 2) in comparision with that of heats of solvation for acetone indicates a possibility of hydrogen bond formation of *Q* molecule in aqueous solution where the water molecules play a dual role of proton donor as well as of proton acceptor. For the quantitative ex-

Table 2

Heats of solution, hydration, solvation and related data of *Hq*, *Q* and resorcinol. unit: kcal/mol.

Substances		Water		Acetone	
	ΔH_{sub}	ΔH_{soln}	ΔH_{hyd}	ΔH_{soln}	ΔH_{solv}
Quinone	16.38±0.14 (a)	4.69 (c)	11.69	4.11	12.27
Hydroquinone	21.54±0.22 (a)	4.50 (d)	17.04	−0.37	21.91
Resorcinol	22.8 ±0.4 (b)	4.0 (e)	18.8	—	—

a: See reference (1)
b: K.L. Wolf and H.G. Trieschmann, *Z. physik. Chem.*, B 27, 37 (1934).
c: Schreiner, 4.69 kcal at room temp. N=1830;
d: Schreiner, 4.50 kcal at room temp. N=360. (sample crystallized from glacial acetic acid), 4.56 kcal at room temp. N=360 (sample sublimed at ordinary pressure); Kolossowsky, 4.46 kcal at 16°C, N=282; We have adopted average value of Schreiner and that of Kolossowsky.
e: Robertson and Ubbelohde, 4.12 kcal at 18°C N=410 (α-modification), 3.90 kcal at 18°C N=410 (β-modification); We have adopted the average of their values.

7) As to the estimation of hydrogen bond energy of formic acid dimer, see I. Nitta, S. Seki and K. Suzuki, This Bulletin **24**, 64 (1951).

planation of this difference, however, further informations on the nature of proton accepting power of the phenol derivatives may be neccessary[8].

c) Molecular compound formation.—Now, we should like to proceed to the problem of molecular compound formation. According to many physico-chemical investigations carried out hitherto,[9] the following chemical equilibrium;

$$QH \rightleftarrows Q + Hq$$

in water, alcohol and liquid ammonia is always largely shifted to the right hand side at room temperatures, and the amount of *QH* molecules is only 6% even at the saturated solution. Therefore, in the case of dilute solution where the present work was done*, the amount of *QH* would be considered to be negligible. Indeed, in the present experiment, the fact that the heat of solution of *Q* for pure acetone is equal to that for acetone solution containing equimolar *Hq* within the experimental error (ca. 20 cal.) is concordant with this expectation.

On the basis of these discussions given above and from the data of heat of solution, we are now in a position to calculate the heat of formation of *QH* crystals from the component crystals at 24°C. The heat of formation at O°K. can also be estimated employing the specific heats data measured by Lange[10]. These two values together with the corresponding changes of entropy and Gibbs free energy which are calculated by assuming the validity of the third law of thermodynamics, are all given in Table 3. In the Table, the heats of formation of *QH* (the first row) calculated from other thermodynamic investigations are also given for reference. Of these the second one (4.7 kcal.), which was estimated from our previous investigation on the vapor pressure of *Q*, *Hq* and *QH*[1], is nearly equal to the value determined directly in this work. Also the same quantities determined from the electrode potential etc., and from the heats of combustions are given. As they are derived from the difference of several thermodynamic quantities, they cannot be free from considerable error. The heat of sublimation of *QH* (43.31 kcal in the last row), which cannot be estimated accurately from the vapor pressure measurement*, was determined directly by the summation of heats of sublimation of each component crystals (21.54 kcal. for *Hq* and 16.38 kcal. for *Q*) and heat of formation of *QH* (5.386 kcal.).

Table 3

Some thermochemical data of crystalline quinhydrone

ΔH_{form} at 24°C	-5.387 ± 0.042 (-4.7 ± 1.0, (a) -8.1 ± 2.1, (b) $-4.3\pm$? (c))
ΔH_{form} at 0°K	-5.26
ΔG_{form} at 24°C	-3.67
ΔS_{form} at 24°C	-6.28
ΔH_{sub}	43.31 ± 0.42

unit: energy, in kcal/mol.
entropy in e.u/mol.

a: value estimated from vapor pressure. see ref. (1)

b: value estimated from heat of combustion. These data are taken from the following; Quinone: 654.8 (Berthelot, Louginin); 659.2 (Berthelot, Recoura); 656.6 (Schreiner, Berner); 656.3 (Swietoslawsky from Valeur's data); average value 656.7 ± 0.6 Hydroquinone: 685.9 (Berthelot, Louginin); 685.8 (Stohnann, Langbeim); 684.7 (Baker); 684.0 (Swietoslawsky); 682.6 (Berner, Schreiner); average value 684.6 ± 0.4 Quinhydrone 1331.5 and 1334.8 (two different samples, Berner, Schreiner); average value 1333.2 ± 1.1.

c: value estimated from electrode potential, specific heats and third law by Schreiner.

Finally, a few words may be added here on the heat of formation of *QH*. Our result (5.386 kcal./mol.) is considerably different from the heat of formation of *QH* in aqueous solution (2.35 kcal.) determined by Berthoid.[9b] The discrepancy, however, is a matter of course, since our value is for the crystalline state and the latter for the aqueous solution state in which the hydration process plays a complex role**.

d) Nature of intermolecular forces in

8) In the case of aliphatic alcohols, we have analysed this problem somewhat more in detail. see ref. (3).

9) a) Vapor pressure depression of ammonia solution: I. Shaltenstein and A.M. Monoszon, *Z. Phys Chem.*, **A165**, 147 (1933).
b) Solubility in acqeous solution: A. Berthoid and S. Kunz, *Helv. Chim. Acta.* **21**, 17 (1938).
c) Absorption spectra in aqueous and alcoholic solutions: L. Michaelis and S. Grannick, *J. Am. Chem. Soc.*, 66, 1023 (1944).
d) Diamagnetic susceptibility: L. Michaelis, M.P. Schubert, R.K. Reber, J. A. Kuck and S. Grannick, *J. Am. Chem. Soc.* **60**, 1678 (1938).

* Judging from the heat of dissociation of *QH* (2.35 kcal/mol) measured by Berthoid et. al. (9b), the amount of *QH* may be less than 1% at the present experimental condition.

10) The values of Lange are put in order by Schreiner, *Z. phys. Chem.*, **117**, 57, (1925).

* The value given in a previous paper corresponds to the decompositional sublimation to form 95% *Q* vapor and 5% *Hq* vapor and leave α-Hydroquinone as a residue.

** The solvent effects for the heat of formation of (1:1) molecular compounds between trinitrobenzene and naphthalene (or anthracene) are known from the spectroscopic measurements of Briegleb et. al.; *Z. physik. Chem.*, **B19**, 255 (1932).

crystalline *QH*.—We may now discuss the nature of intermolecular forces on the basis of our experimental results. As regards the origin of these intermolecular forces of *QH*, there have been already put forward several explanations. These are:

i) ordinary covalent bond.
ii) ionic binding: i. e. the electrostatic coulombic attraction between ions. (Q^+Hq^- or Q^-Hq^+)
iii) coupling of two semiquinones.
iv) hydrogen bond.
v) a) dispersion forces.
b) dipole or multipole interactions.
c) induction forces.
d) charge transfer forces, etc.

The first theory of ordinary covalent bond is excluded by the two facts that the magnitude of interaction energy (5 kcal.) is too small to be an ordinary covalent bond energy and that the intermolecular distances which have been determined by the X-ray method are very much longer than the sum of covalent radii.

The second ionic binding theory can not explain the small amount of heat of sublimation which is in same order to those of ordinary molecular crystals. The magnetic property of this crystal also disagrees with the complete ionized structure, for the odd electron configuration of molecules should exhibit the paramagnetic effect, whereas this crystal actually is diamagnetic[11]. The explanation of ionic binding by Weiss et al. based on the non-additivity of molar polarization of *QH* from those of the components is not always conclusive for the evidence of the ionic structure of component molecules[12].

The third one, the semiquinone theory disagrees also wrth the fact of diamagnetic property of *QH*.

As regards the fourth, *Hq* and *Q* molecules are really combined with each other by hydrogen bond as shown in Fig. 3. Although the crystal structure of α-*Hq* is not yet known, it is quite likely that these molecules in crystals would be also linked together by hydrogen bonds, in some analogy to the crystal structure of β-*Hq*, α or β-resorcinol and phlorogrucinol, in each of which hydrogen bonds combine these molecules.

The energy of hydrogen bond (C=O····H—O) in *QH* crystal will be estimated from the values of formic acid dimer (6.3 kcal.) or of acetone·*Hq* associate (4.8 kcal). On the other hand, the energy of hydrogen bond of *Hq* can be taken to be about 4.0 kcal./mol. by the comparison of the heat of sublimation of *Hq* with that of *p*-Xylene[13]. Hence, the contribution of hydrogen bond energy for the molecular compound formation is estimated to be from 4.6 to 1.6 kcal. (12.6—8.0) or (9.6—8.0). Although the color effect of *QH* would not be explained essentially by this effect, the hydrogen bond formation would contribute to a certain extent for molecular compound formation. As shown in Table 4, the facts that

Table 4

Crystalline molecular compounds between quinone and other substances (*B* component)

Group	Substances	Molar ratio *Q* : *B*
I	phenol, *o*-, *m*-, *p*-cresol, hydroquinone methy ether	1 : 2
II	hydroquinone, *p*-toluidine, *p*-nitroaniline	1 : 1
III	resorcinol, pyrocatechol, α-, β-naphthol	1 : 1 and other ratio
IV	(a) pyrogallol, (b) phenylenediamine	(a) 3 : 1 (b) 2 : 1
V	*o*-, *m*-nitroaniline	None
VI	hydroquinone dimethyl ether	None
VII	benzene, toluene, xylene, naphthalene, tolane, azobenzene, nitrobenzene	None
VIII	anthracene	1 : 1
IX	phenanthrene	1 : 6
X	aliphatic hydrocarbons, ethers, aldehydes ketones	None
XI	aliphatic alcohols, acids, amides	None

the molar ratios of molecular compounds I, II, III and IV groups are parallel with the numbers of hydrogen atoms in hydroxyl or amino groups and that there can not be formed stable crystals of molecular compounds in the combinations of V, VI, VII and X groups having no hydroxyl groups, suggest a role of hydrogen bond for the molecular compound formation. However, it may be safely said that this effect is not a very decisive one, as is evidently seen in the cases of VIII, IX and X.

11) S. Banerjee, *Z. Krist.*, **100**, 316 (1939); H. Mikhail and F.G. Baddar, *J. Chem Soc.*, **1944** 540

12) The disagreement between the molar polarization of *QH* and the sum of those for component crystals may be also explained by the anisotropy of electron distribution and by the change of atomic polarizability caused by hydrogen bond formation. Indeed, the other crystals measured by them which deviate remarkably from the additivity involves the N—H···O or O—H···O hydrogen bonds. See: J. Weiss, H. Kronberger, *J. Chem. Soc.*, **1944** 464.

13) Heat of sublimation of *p*-Xylene: 13.5 kcal/mol., Linder's value from Landolt-Börnstein's Table.

Next, we proceed to the fifth. The ordinary dispersion effect has not been hitherto taken nto consideration at all, since it can not explain the reasons, why the compound formation takes place between a pair of specified molecules and also why such a remarkable change of color[14] accompanies this process. Indeed, this effect may be ignored, in the case of a compound formation in solution, but it is worth while to reexamine it for the case of crystalline state where the packing of molecules plays a much more important role than in the case of solution state, as the dispersion forces are sensitive to the mode of molecular packing. For example, the difficulty of compound formation between aliphatic and aromatic molecules (see examples X and XI in table 4), the non-existence of crystalline molecular compounds of the systems such as I_2-benzene, and tetranitromethane-diphenylmethane (typical examples of molecular compounds in solutions) may be attributed to the unfavourable packing of component molecules because of the considerable difference of their sizes and shapes.

As a measure of the dispersion energy contribution for the heat of sublimation of the *QH*, twice the heat of sublimation of *p*-Xylene (isoelectronic molecule to *Q* and *Hq*) may be tentatively adopted. Then, it is found that the contribution of the dispersion energy to the heat of sublimation is estimated to be about 60% of the total and that the sum of this contribution and the hydrogen bond energy estimated above is not yet sufficient to explain the total observed (see Table 5). The facts that the density of *QH* (1.41) is larger than those of *Q* (1.32) and *Hq* (1.33) and that the nearest intermolecular[2] distance between *Hq* and *Q* molecules lying parallel in *QH* crystal (3.2A) is abnormally shorter than those of any aromatic compounds, suggest also there are partaking other sorts of attraction forces between component molecules.

Table 5

Contribution of the various kinds of energy to the heats of sublimation of *Q*, *Hq*, and QH, and to the heat of formation of *QH*.
(unit: kcal/mol.)

	Heat of sublimation			Heat of Formation
	Hq	*Q*	*QH*	
Total	21.54	16.38	43.31	5.386
Hydrogen bond	8.0	0	12.6 ~ 9.6	4.6 ~ 1.6
Dispersion	13.5	13.5	27	0
Others	0	2.9	3.7 ~ 6.7	0.8 ~ 3.8

Recently, Murakami[15] put forward a theory for the intermolecular forces of *QH* type molecular compounds. From the point of view of resonance theory, he supposed the π-electron charge distributions of *Q* and *Hq* as shown in Fig. 4. If we assume to put *Hq* molecule just upon *Q* molecule in a parallel position as shown in the figure, the charges of opposite signs in respective molecules come to the nearest, so that we can expect there will arise strong electrostatic attraction between them. He postulated this is the cause of the molecular compound formation, and also explained qualitatively the shift of absorption band to the longer wave length as well as the simultaneous intensity increase of the band. His theory is, however, of qualitative nature, so we have attempted here to evaluate the π-electron charge distribution semi-quantitatively. Assuming the molecular symmetry of *Hq* molecule approximately to be D_{2h} the electron charge density[16] of *Hq* molecule was computed by the simple LCAO-MO theory. In this case, the coulombic integrals of oxygen and adjacent atoms as well as the resonance integrals between oxygen and adjascent atoms were calculated by the use of Jaffe's parameter for phenol[17], all the overlap integrals being ignored. The results obtained as well as the corresponding values for *Q* obtained by Coulson et al.[18] are

14) The absorption spectra of *QH* in crystalline state: K. Nakamoto, *J. Am. Chem. Soc.*, **74**, 1739 (1952).
15) H. Murakami, *Sci. Paper Osaka Univ.* No. 18 (1949).
16) C.A. Coulson, H.C. Longuet-Higgins, *Proc. Roy. Soc.*, A **192**, 16 (1947).
17) H.H. Jaffe, *J. Chem. Phys.* **20**, 279 (1952).
18) C.A. Coulson, Valence p. 256 (Oxford Univ. Press. 1952). [After completion of this work, we became aware of the similar calculations on *Q* by Dr. Nagakura (Tokyo University), who kindly gave us the opportunity of reading his manuscript in advance of publication.

* Here, a simple relation $e=\frac{\mu_{C-O}}{r}$ (e: formal charge, μ_{C-O}: the bond moment of C—O: r: the atomic distance between C and O atoms) is applied, assuming that the μ_{C-O} of *Hq* and *Q* is equal to that of aliphatic compound ($\mu_{C-O}=0.8$ D). But, as

Table 6

Calculated molecular orbitals of hydroquinone (D_{2h})

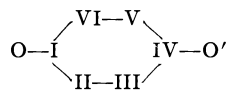

Symmetry character	Energy	Normalized M. O.
b_{3g}	$\alpha-1.987\ \beta$	$0.4013(I-IV)-0.0916(O-O')-0.4066(II-III-V+VI)$
b_{1u}	$\alpha-1.028\ \beta$	$0.5550(I+IV)-0.2057(O+O')-0.2737(II+III+V+VI)$
a_{1u}	$\alpha-\beta$	$0.5000(II-III+V-VI)$
b_{3g}	$\alpha+0.285\ \beta$	$0.2408(I-IV)-0.6100(O-O')+0.1873(II-III-V+VI)$
b_{1u}	$\alpha+0.573\ \beta$	$0.0729(I+IV)+0.6605(O+O')-0.1709(II+III+V+VI)$
b_{2g}	$\alpha+\beta$	$0.5000(II+III-V-VI)$
b_{3g}	$\alpha+1.382\ \beta$	$0.5300(I-IV)+0.3465(O-O')+0.2225(II-III-V+VI)$
b_{1u}	$\alpha+2.134\ \beta$	$0.4322(I+IV)+0.1517(O+O')+0.3811(II+III+V+VI)$

Table 7

Calculated π-electron densities and charge distributions of hydroquinone and quinone molecule

			O	I	II
Hq	electron density		1.902	1.062	1.018
	charge distribution	π	0.098	−0.062	−0.018
		σ	−0.118	+0.118	—
		total	−0.020	+0.056	−0.018
Q	charge distribution	π	−0.48	+0.34	+0.07
		σ	−0.14	+0.14	—
		total	−0.62	+0.48	+0.07

given in Table 6 and 7. As is shown in Table 7, the charge distributions of the π-electrons are in agreement qualitatively with Murakami's theory. However, if we take into consideration further the resultant contributions of σ-electrons of C—O* bond, the signs of the charge densities remains unchanged in the case of *Q*, while those of *Hq* change their signs and become nearly uniform. Moreover, it should be noticed that, as already shown in Fig. 3, the oxygen atoms of *Hq* actually do not lie just upon the oxygen atoms of *Q*, but rather upon the centers of benzene nuclei in the crystalline *QH*. Such a relative arrangement of component molecules is also known in the case of molecular compound between *s*-trinitrobenzene and *p*-iodoaniline[19] in the crystalline state. These two facts, i.e. the closer approach of the polarizing dipole of one component molecule to the polarizable benzene nucleus of the other, and the nearly uniform distribution of electronic charges of *Hq* molecule, will imply that the interaction energy due to the Murakami theory seems to be not so predominant. And such a relative arrangement of component molecules suggests the important role of induction effect as pointed out by Briegleb[20]. However, more precisely, each component molecule is situated in a quadrupole field resulting from the antiparallel dipole pairs of the upper and lower molecules of the other component, so that the situation is more complicated than the simple case of Briegleb.

Finally, the theory proposed recently by Mulliken[21] seems to be very significant for the explanation of the interaction energy as well as the color effect of molecular compounds in general. For the confirmation of this theory, however, thermal investigation is not sufficient and there will be necessary presumably electrical, photoelectrical, spectroscopic studies, etc.

the degrees of hybridization of the AOs of carbon atoms in aliphatic single bonds and of aromatic σ-bonds is different, this assumption is not so exact.

19) H.M. Powell, G.H. Huse and P.W. Cooks, *J. Chem. Soc.*, **1943**, 153.

20) G. Briegleb and J. Kambeitz: *Z. physik. Chem.*, B **25**, 251 (1934).

21) R.S. Mulliken, *J. Am. Chem. Soc.*, **64**, 811 (1952).

In conclusion the authors wish to express their sincere thanks to Professor Nitta for his valuable suggestions and to Mr. Osaki for his helpful discussions. The cost of this research was defrayed from the funds of Taniguchi Kôgyô Shôreikai as well as from the Scientific Research Expenditure Grant from the Ministry of Education to which the thanks of the present authors are due.

Department of Chemistry,
Faculty of Science
Osaka University, Osaka

Surface Chemistry of High Polymers. I. Non-electrolytic Flexible Linear Polymers at Air/Water Interface

Toshizo ISEMURA, Hiroshi HOTTA and Teruo MIWA.

(Received March 2, 1953)

Introduction

It is a well-known fact that some natural polymers such as protein[1,2,3] and some synthetic polymers such as polymethacrylates[4,5] and polypeptides[6] spread as a monolayer at both air/water and oil/water interfaces. It is expected that the molecular structure, the kinds as well as the amounts of polar groups and also the size of non-polar or polar side chains will affect the behaviour of surface films of the polymers. Studies on the surface films of polymers of known structure will give some information for the elucidation of the behaviour of important natural polymers as proteins. The shape of the polymer molecules at the interface is probably different under the influence of the surface force from that in the bulk phase. The shape of the polymer molecule at the interface in relation to its molecular structure and the kinetic unit of the molecule at the interface are problems to be investigated. It is also very interesting to investigate the mechanical properties of the surface film of the polymer in relation to the molecular structure and to compare with the properties in the bulk system.

At the outset, the linear non-electrolytic polymers, namely, polyvinyl acetate, polyvinyl stearate and some copolymers of different compositions between vinyl acetate and vinyl stearate were studied at the air/water interface by measuring surface pressure-area and surface potential-area relations. In the present paper, the results obtained and some considerations on the results will be presented.

Experimental

Materials—Polyvinyl acetate was prepared from vinyl acetate by emulsion polymerization using ammonium persulphate as the catalyst. In most of the experiments, polyvinyl acetate was used in that condition if no special indication was given. However, reacetylated polyvinyl acetate was sometimes used for the elimination of the effects of branched polymers. Polyvinyl acetate was hydrolysed to polyvinyl alcohol, which was again tranformed into polyvinyl acetate by acetylation using acetic anhydride. Polyvinyl stearate and the copolymers of vinyl acetate and vinyl stearate were prepared by Prof. S. Murahashi and Mr. S. Otsuka in our institute. The composition of these copolymers are shown in Table I. These polymers were spread on distilled water from benzene solution.

Methods and Apparatus—Surface pressure was measured by three methods. In low pressure region less than ca. 3 dynes/cm, it was measured by film balance of Adam type of double torque system using torsion wires of phosphor-brone of 0.12 mm. and 0.07 mm. in diameters. The molecular weight determination was carried out by this method. In high pressure region, surface pressure was measured by either hanging plate or ring method.

In the experiments with the film balance of Adam type or hanging plate type, the polymer was spread on the substrate in a rectangular tray $16 \times 60 \times 1.2$ cm. by an automatic microvolume pipette so as to occupy more than 100 A^2. per monomer. The surface concentration was changed by compression with a paraffined glass barrier in the usual manner. On the other hand, the surface concentration was changed with successive addition by injection through a micrometer syringe

1) I. Langmuir and V. J. Schaefer, *Chem. Rev.*, **24**, 181 (1939).
2) H.B. Bull, "Advances in Protein Chemistry," **3**, 95(1947).
3) C.W.N. Cumper and A.E. Alexander, *Trans. Faraday Soc.*, **46**, 235 (1950).
4) D.J. Crisp, *J. Colloid Sci.*, **1**, 49 (1946).
5) D.J. Crisp, ibid., **1**, 161 (1946).
6) T. Isemura and K. Hamaguchi, This Bulletin, **25**, 40 (1952).

Table 1

Composition of Copolymers Used in the Present Experiment

Sample	Initial mole percentage of vinyl stearate at synthesis	Mole percentage of vinyl stearate in copolymer	Mean molecular weight per vinyl unit
A (Acetate)	0	0	86
E	10	—	—
B	20	20.0	130
C	50	58.6	217
D	80	82.6	272
S (Stearate)	100	100	310

when the surface pressure was measured by the ring method using a glass cylinder. The details of the technique of successive injection method will be given in the next paper in relation to the investigation of the oil/water interface.

Surface potential was measured by vibrating electrode method. The apparatus used was essentially the same as used in our previous investigation, however, with some necessary modification to adapt it for the present purpose.[7]

Results

The experimental results obtained are shown in Figs. 1~7, in which the notations of curves are common in Table I, respectively. Polyvinyl acetate gave a film of expanded type as shown in Figs. 1 and 2. The degree of polymerization gave no appreciable effect on the F—A curve. Polyvinyl acetate prepared by reacetylation showed no essential difference on F—A curve from that of the original polyvinyl acetate. The FA—F curve of the polyvinyl acetate was not strictly linear but slightly convex upward, and was almost independent of the degree of polymerization. If the linear relation between FA and F is assumed, the molecular weight of the spread polymers may be determined from Fig. 3 as in the case of proteins. The molecular weights thus determined were 7,000~10,000 as shown in Table II, and were extraordinarily less than that determined from its intrinsic viscosity $[\eta]$, using the relation[8]

$$\bar{P}=(\text{Antilog}\frac{[\eta]}{0.28}-1)\times 2000 \ , \quad \ldots\ldots(1)$$

and not to be compared with it.

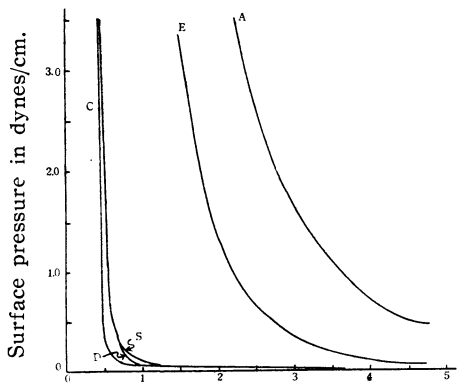

Area in m²/mg

Fig. 1 The F-A curves of vinyl polymers by Adam's balance.

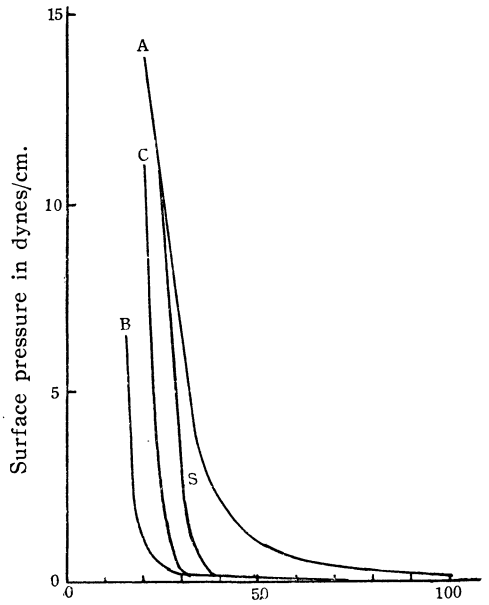

Area per vinyl unit in A²

Fig. 2 The F-A curves of vinyl polymer by hanging plate method.

7) H. Hotta and T. Isemura, This Bulletin, **25**, 101 (1952).

8) I. Sakurada and T. Chiba, *J. Soc. Chem. Ind. Japan*, **47**, 135 (1944).

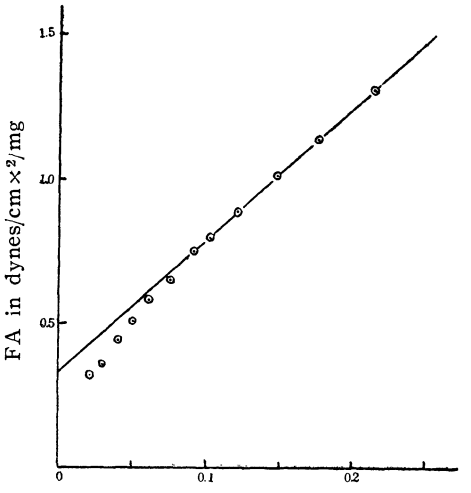

Surface pressure in dynes/cm.
Fig. 3 The FA-F curve of polyvinyl acetate (sample "c")

On the other hand, FA—F curve for polyvinyl stearate was linear as shown in Fig. 4. Its molecular weight from this curve was 41,000.

In the experiments shown in Fig. 1, the reading of surface pressure was taken 30 seconds after every compression. In the ex-

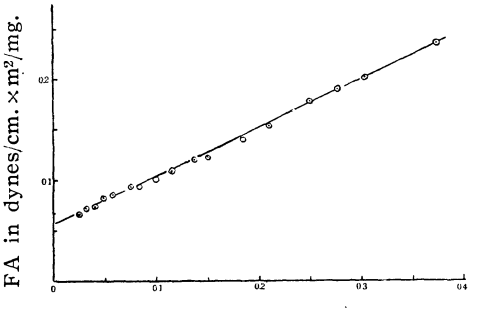

Surface pressure in dynes/cm.
Fig. 4 The FA-F curve of polyvinyl stearate

Table 2

Molecular Weight of Vinyl Polymers Used in the Present Experiment

Polymer	Sample	Molecular weight from pressure Surface	Viscosity	Osmotic pressure
Polyvinyl acetate	a	10,000	58,820	—
	b	7,020	69,350	—
	c	7,920	110,500	—
	d	9,240	—	110,000±5,000
Polyvinyl stearate	e	41,000	—	70,000

Sample "a" was prepared by reacetylation of sample "b".

periments shown in Fig. 2, the rate of compression was 1 A².⁄monomer/2 minutes. The surface pressure of the polyvinyl acetate was not changed with time after every compression up to 7 dynes/cm. However, with the copolymers and polyvinyl stearate, the pressure was changed considerably with time after every compression, when the surface pressure exceeds 0.2 dynes/cm. The limiting area per monomer determined by extrapolation of linear portion of F—A curve to zero pressure was about 55 A². for polyvinyl acetate. Polyvinyl stearate gave a coherent film and its limiting area per monomer was 30 A². The condensation of film by the introduction of vinyl stearate in the copolymer was considerable. The limiting area per monomer was less than that of polyvinyl stearate, if the copolymer contains more than 20% of vinyl stearate. In Fig. 5 are shown the F—A curves obtained by successive injection method.

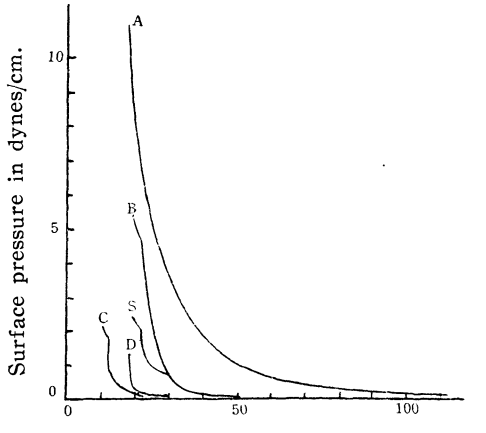

Area per vinyl unit in A
Fig. 5 The F-A curves of vinyl polymers by successive injection method

The surface potential and surface moment are shown in Figs. 6 and 7. The surface

moment per monomer, μ, was calculated from Helmholtz's formula,

$$\mu = \frac{\Delta V}{4\pi n} \quad \text{.....(2)}$$

using the average ground molecular weight in Table I, where ΔV is the surface potential, and n the number of monomer unit per unit area. Fig. 6 is the results obtained by compression method, and Fig. 7 that by successive injection method. When the experiments were carried out by the compression method, the surface potential was fluctuated markedly until the surface area per monomer decreased to far less than 100 A^2. The reliable values were obtained only in the region shown in Fig. 6. In spite of the fairly good reproducibility of F—A curves, the reproducibility of the surface potential curves was not satisfactory and was dependent on the composition of the polymers. Its reproducibility of polyvinyl acetate was the highest, and next highest was that of polyvinyl stearate. The order of reproducibility was as follows,

$$A > S > D > C > B.$$

The results shown in Figs. 5 and 7 were those obtained by the successive injection method as already mentioned. The area is the apparent area calculated from the injected amount, simply by dividing the total area by the injected mass. In this case, the fluctuation of surface potential, as observed in the compression method, was hardly observed at all.

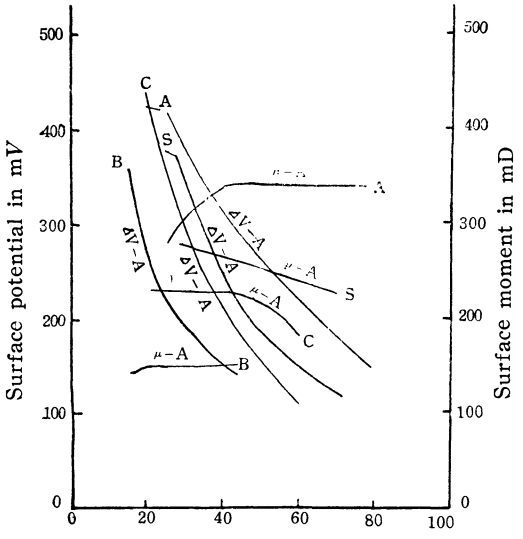

Area per vinyl unit in A^2.

Fig. 6 The ΔV-A and μ-A curves of vinyl polymers by successive injection method.

The fluctuation of surface potential, observed in the region of low surface concentration in the case of the compression technique, is probably caused of inhomogeneity of the surface layer. The compression of the film by the barrier from one side often causes

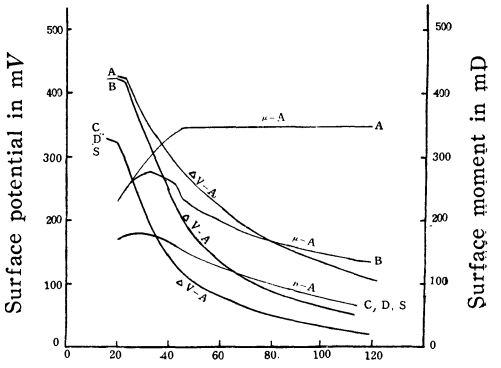

Area per vinyl unit in A^2.

Fig. 7 The ΔV-A and μ-A curves of vinyl polymers by compression method.

accidental condensation and accompanies the heterogeneity of the film. Consequently, the change does not always follow the course of equilibrium. The instability of the film of copolymers with small content of vinyl stearate may be attributed to this accidental change appearing at the various parts of the film.

Discussion

Polyvinyl acetate gave the film of expanded type with free space between the chains. If stearate groups are substituted for the acetate groups in polyvinyl acetate, the mutual cohesion between side chains is considerably increased and the film tends to condense. With polyvinyl stearate film, the specific area is usually less than with polyvinyl acetate, and the expanded region at low surface pressure is lacking. The limiting area per monomer of the film of copolymer with moderate content of vinyl stearate was found often to be even less than that of polymer containing only vinyl stearate as shown in Fig. 2. It may happen that the attraction of hydrocarbon chains of stearate compresses the vinyl acetate groups from the interface into aqueous phase.

From simple thermodynamic calculations, it may be found that the inclination of the FA—F curve, i.e. α, in

$$FA = \beta + \alpha F \quad \text{.....(3)}$$

corresponds to the co-area of the molecule.[9] From these considerations, it was concluded that the co-area of polyvinyl acetate is 60 A^2./monomer and that for polyvinyl stearate is 25 A^2./monomer. The limiting areas per monomer for polyvinyl acetate and stearate were 55 A^2. and 30 A^2. respectively as mentioned above. These areas are nearly equal to the co-areas estimated from equation (3). The co-area of the polyvinyl stearate thus estimated is plausible if we recognize that the stearate side chains project out of the water surface and that they are closely packed. However, the co-area of the polyvinyl acetate is much larger than that estimated from molecular model, even if the side chains are lying flat. In the film of polymer with short side chains such as polyvinyl acetate, the motion of the segment of chain is so violent that the co-area is nearly twice the area per monomer estimated from the molecular model owing to the elimination of the restriction of molecular motion by the attraction between side chains. According to the analogous calculation with b in the van der Waals' equation, the co-area must be twice of actual area in two dimensional gas.

From the surface moment data, it can be concluded that the orientation of the side chains of polymer are not affected very much by the compression up to the area of 40 A^2./monomer with polyvinyl acetate and to 28 A^2./monomer with polyvinyl stearate film. Below 40 A^2./monomer the surface moment of polyvinyl acetate decreased gradually. These results are readily explained using the model of polymer film assumed by us just mentioned above. With the film of polyvinyl acetate the area, where the surface moment begins to decrease, corresponds to the area where the film begins to change to coherent type from an expanded film. For the polyvinyl acetate film is of expanded type having free space between chains, and the film changes to a coherent film if it is compressed to less than 40 A^2./monomer, where the change of μ begins to appear. On the other hand, with the film of polyvinyl stearate, stearate groups in a polymer molecule project out of water phase and mutually interact so that the side chains have definite orientation even if the surface concentration is low. The μ begins to change when the film is compressed after the coherent film is completely formed. The areas where μ deviates from a constant value, are also parallel to the co-areas of the polymers mentioned above.

Surface potential of polyvinyl acetate reached the saturated value of 420 mV below 25 A^2./monomer, and that of polyvinyl stearate 370 mV below 28 A^2./monomer, respectively. Surface potential-area curves change the inclination at these areas. At these points a part of ester groups was probably removed from the interface, and the film was partially collapsed. From F—A curves, however no indication of discontinuity was detected at these points.

The surface potential curves of the copolymers were continuous far below these areas. It seems probable that the attraction between the hydrocarbon chains of stearate groups suppresses the vinyl acetate groups from the interface into aqueous phase if surface pressure is sufficiently high. Consequently the film was gradually changed into so-called "overfilm". The relatively remarkable change of surface pressure with time after every compression and the small values of μ, found with these copolymer films, agree with our views mentioned above.

The F—A curve of polyvinyl stearate showed almost the same feature as that of polyoctadecyl methacrylate studied by Crisp,[5] suggesting that structures and shapes of molecules in both films are almost identical. The limiting area found by Crisp for polyoctadecyl methacrylate was 30.5 A^2./monomer, while that for polyvinyl stearate found by us was 30.0 A^2. However, the surface moment of polyvinyl stearate per monomer was 278 mD, whereas that of polyoctadecyl methacrylate per monomer found by Crisp was 460 mD. This far smaller surface moment of polyvinyl stearate than that of polyoctadecyl methacrylate is readily understood in the light of molecular orientation at the interface. The principal difference between them may be governed by the orientation of C=0 bond as shown in Fig. 8.

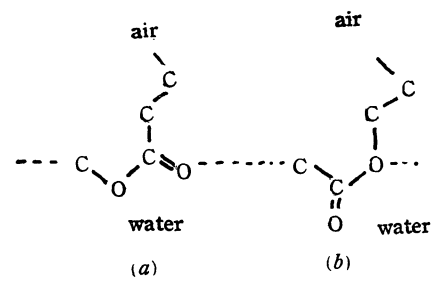

Fig. 8 Orientation of side chain at the air/water interface;
(a) polyvinyl stearate;
(b) polyoctadecyl methacrylate.

As mentioned above, the results obtained

9) H.B. Bull, *J. Biochem.*, **185**, 27 (1950).

by two different methods of changing surface concentration of the polymer did not agree with each other, especially, in high surface concentration. Unlike the compression method, the spread molecules would not be in the unusually forced orientation, if the surface concentration of the film was changed by successive injection method. However, the injected polymer would not be spread at the interface as a monolayer when the surface concentration exceeded a certain value and the film was closely packed by its own spreading pressure. For these reasons, the area per monomer shown in Figs. 5 and 7 are only apparent. On the other hand, the orientation of the molecule spread by this method may be more natural than that studied by the compression method. Recently, B.D. Powell and A.E. Alexander[10] studied the monolayers of copolymers between vinyl pyridine and styrene with the two different methods. They found smaller surface potential by the successive injection method than by the compression method. They attributed this to the "edge effect." In our opinion, however, this phenomenon may be closely connected with the difference of the facility of spreading of the film by these two methods. Surface potential-area curves with polyvinyl acetate film obtained by these two methods coincided with each other. The F—A curves, however, did not coincide with each other, especially, in high surface concentration. The F—A curve obtained by the compression method was almost consistent with that obtained at the oil/water interface, on which we will report in the following paper. These results are all comprehended in the light of the molecular flexibility which will be discussed also in the following paper in some details. The discrepancy between the F—A curves observed by two different methods may be caused by the fact that the surface concentration near the ring can not only reach an equilibrium value within relatively short time interval after every injection, but also can reach it after formation of a fresh surface by raising the ring. That may be the essential difficulty inherent in the study of surface film of polymer by means of the ring method.

10) B.D. Powell and A.E. Alexander, *J. Colloid Sci.* **7**, 432 (1952).

Summary

The surface films of some linear non-electrolytic polymers such as polyvinyl acetate, polyvinyl stearate and copolymers between them were studied at the air/water interface by measuring surface pressure, and surface potential in relation to the area occupied per monomer.

The surface concentration was changed by two different methods, namely by the compression with barrier and by the successive addition by injection with micrometer syringe.

Polyvinyl acetate gave the film of expanded type and was hardly affected by its degree of polymerization. Polyvinyl stearate gave the film of coherent type and its F—A curve resembled that of polyoctadecyl methacrylate. The copolymer with moderate content of vinyl stearate showed the smaller limiting area per monomer than polymers of its constituents.

The results were discussed in relation to the molecular model and to the methods adopted to change the surface concentration.

In conclusion, the authors express their hearty thanks to Prof. S. Murahashi and Mr. S. Otsuka in our institute who kindly supplied copolymers to them. The cost of this research has been partly defrayed from the Scientific Research Encouragement Grant from the Ministry of Education, to which the authors' thanks are due.

The Institute of Scientific and Industrial Research, Osaka University, Sakai, Osaka

Surface Chemistry of High Polymers. II. Non-electrolytic Flexible Linear Polymers at Oil/Water Interface

By Hiroshi HOTTA

(Received march 2, 1953)

While the properties and structures of insoluble films at the air/water interface are now known in some detail,[1] there are few investigations at the oil/water interface in spite of emphasis on its necessity.[2,3,4,5,6] In the present investigation the films of amilan and copolymers of vinyl acetate and stearate were studied to obtain informations on the general behaviour of non-electrolytic flexible linear polymer at oil/water interface. The experimental method was similar in principle to that developed by Alexander *et al.*[2,3,4,5]

From the present investigation, it has been concluded that these linear polymer molecules behave freely at the oil/water interface, for the lateral cohesion between them becomes much weaker than at the air/water interface and their non-polar side chains are removed from the interface into the oil phase. The length of the segment of kinetic unit for these polymers at the interface was estimated by adopting the statistical treatment of flexible linear polymer in the bulk solution with some modifications to adapt to the surface film. The results will be given in the following lines in detail.

Since there is the case that the behaviour of monolayer is very different between air water and oil/water interface so far as the side chains are concerned, which was confirmed by our investigation, we cannot always infer the phenomena in the living body from the result of the film at the air/water interface alone. Therefore we need by all means the experiment at the oil/water interface also for this purpose.

Experimental Method

Materials—Amilan (ε-aminocaproic acid polymer) was purified by dissolving in formic acid and reprecipitated by water, and spread from the solution dissolved in a mixture of concentrated sulphuric acid (10%), isopropyl alcohol (40%) and water (50%). Copolymers of vinyl acetate and stearate were spread from benzene solution. Although these copolymers were the same as those which had been used previously at the air/water interface,[7] their compositions, calculated from the analysis, were shown again in Table I for convenience.

Petroleum ether (b.p.=100~140°C. and $d.=0.75$) used as the oil phase was purified repeatedly with various agents from commercial Gum Gasoline. The distilled water was used as the water phase.

Spreading Technique—The oil/water interface was formed and cleaned by the technique developed by Alexander and Teorell.[2] The dimensions of the trough were also almost the same as theirs. The samples were spread from the micrometer-syringe at the interface by adding *ca.* 3×10^{13}

Table 1

Composition of Copolymers Used in the Present Experiment

Sample	Initial mole percentage of vinyl stearate at synthesis	Mole percentage of vinyl stearate in copolymer	Mean molecular weight per vinyl unit
A (Acetate)	0	0	86
B	20	20.0	130
C	50	58.6	217
D	80	82.6	272
S (Stearate)	100	100	310

1) N. K. Adam, "The Physics and Chemistry of Surfaces" (1938).
2) A. E. Alexander and T. Teorell, *Trans. Faraday Soc.*, **35**, 727 (1939).
3) A. E. Alexander, "Surface Chemistry" (1949), p. 123.
4) C. W. N. Cumper and A. E. Alexander, *Trans. Faraday Soc.*, **46**, 235 (1950).
5) A.J.G. Allen and A.E. Alexander, ibid., **46**, 316 (1950).
6) D. F. Cheesman, *Biochem. J.*, **50**, 667 (1952).
7) T. Isemura, H. Hotta and T. Miwa, This Bulletin, **26**, 380 (1953).

monomer units per square centimetre at a time.

Interfacial Tension—The interfacial tension was determined by Alexander's ring method,[3] in which the displacement of a ring at maximum pull is read by an optical lever. The ring used was made of platinum-10% iridium wire of a diameter of 0.30 mm, and the diameter of the ring was 2.70 cm. It was cleaned and leveled by Harkins and Jordan's method.[8] The correction factor of the ring (1.022) was determined experimentally at zero pressure.

On the investigation of insoluble monolayer, one of the sources of error inherent in the ring method is owing to the appreciable extension of interface at both the inside and outside of the ring at breaking point. This effect has been studied experimentally by Alexander and Teorell.[2] Nevertheless, it seemed that the effect was slight except at the higher pressure in our present case, as a result of comparison with the other method.

All measurements were made ten minutes after the successive injection of spreading solution, and at room temperature (20~23°C.) without any special temperature regulation, but the variation of temperature during the course of measurement to obtained a single curve never exceeded one degree. The effect of the interval of successive measurements with amilan film was examined, and its result is shown in Fig. 1.

Results and Discussion

Amilan—At first, it was examined how long we must wait before measurement for perfect spreading of the sample after every injection of the polymer solution at the interface. After some preliminary experiments, it was found that ten minutes after every injection was sufficient for perfect spreading. The results are shown in Fig. 1, together with the result at the air/water interface, measured by this method of successive injection used at the oil/water interface.

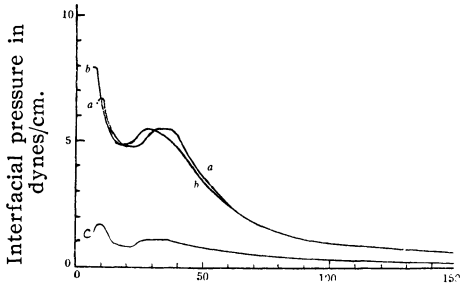

Area in A². per monomer

Fig. 1 The π-A curves of amilan:
curve a— at petroleum ether/water interface, measured at 10 mins. after injection;
curve b— at petroleum ether/water interface, measured at 3 mins. after injection;
curve c— at air/water interface, measured at 10 mins. after injection.

In the π-A curve of amilan, it was found the characteristic transition region of van der Waals' type as shown in Fig. 1. Since the appearance of the transition point may be dependent on the strength and distribution of hydrophilic groups, namely, the activation energy transition as discussed later in detail, these conditions may be just optimum for the appearance of such a "superpressed" phenomenon in this case. The first kink point, 38A²., and the again rapidly rising point 18A²., are comprehended in terms of the transition between the flat-in-interface and bent-into-oil phase forms of the hydrocarbon part of the main chain. These dimensions are consistent with that computed by Stuart's model.

Copolymers—The π-A curves of vinyl copolymers at the oil/water interface are shown in Fig. 2., in which the notations of curves are common in Table 1, respectively. The ordinate of the figure is interfacial pressure in dynes/cm., and the abscissa is surface area in A². per vinyl unit, calculated from the mean molecular weight in Table 1.

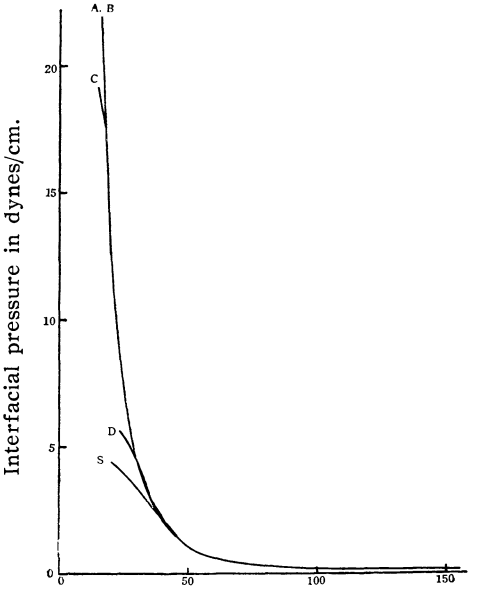

Area per vinyl unit in A²

Fig. 2 The π-A curves of vinyl polymers at the petroleum ether/water interface.

All these π-A curves of vinyl copolymers fall on the same curve of polyvinyl acetate independent of the content of stearate in con

8) E. D. Harkins and H. F. Jordan, *J. Am. Chem. Soc.*, **52**, 1751 (1930).

trast with much dependence on its content at the air/water interface.[7] However, these curves deviate from this common curve at any wider area with increasing content of vinyl stearate. The areas of deviation are shown in Table 2. These areas can be calculated as the product of the area of vinyl stearate (37 A^2.) and its mole fraction in copolymer as shown in the Table. From these facts it may be concluded that all copolymers at the oil/water interface behave freely, liberating from lateral cohesion, so that the side chains are removed into oil phase. This deviation area of polyvinyl stearate is fairly greater than the limiting area at the air/water interface, obtained in the preceding paper.[7] It is because the free micro-Brownian motion of stearyl group in the oil phase does not permit the neighbouring stearyl group to approach. Upon consideration of the fact that the deviation from the common curve is due to the mutual hindrance of such a micro-Brownian motion, we can understand the proportionality of this area in the films of high stearate content, and the disappearance of this point in those of low stearate content, as shown in the Table 2.

Table 2

Kink Point from Common Curve

Sample	Kink point in A^2.	
	obs.	calc.
A	not found	—
B	not found	—
C	22.6	21.7
D	30.7	30.6
S	37	37

General Behaviour of Film of Non-electrolytic Flexible Linear Polymer

Now, the general behaviour of these non-electrolytic flexible linear polymers at the oil/water interface will be discussed in the light of the above-mentioned facts. On the consideration of such a general problem, we must distinguish between the effect of backbone and that of side chain. Since the latter has remarkably steric factors, the problem becomes very complicated. At the oil/water interface, however, the former effect is essential before the surface concentration is fairly high, for the side chains may be dissolved in the oil phase as mentioned above.

In general the interfacial pressure, π, is expressed thermodynamically as

$$\begin{aligned}\pi &= \gamma_i - \gamma_f \\ &= -\left(\frac{\partial F_i}{\partial A_f}\right)_{T,\Sigma} \\ &= -\left(\frac{\partial H_i}{\partial A_f}\right)_{T,\Sigma} + T\left(\frac{\partial S_i}{\partial A_f}\right)_{T,\Sigma} \qquad \text{.....(1)} \\ &\qquad (\Sigma = A_i + A_f),\end{aligned}$$

where A, F, H, S and γ are surface area, free energy, heat content, entropy and interfacial tension, respectively, and the subscripts f and i refer to film and interface, respectively. In equation (1), the first term corresponds to adhesion of polymer to substrate and cohesion between chains, and the second term to kinetics of chain. Therefore, the stronger the hydrophility of the polar group in the chain is, the more distinct the transition point may be. Conversely, when the hydrophility is weak, this polar group cannot already restrain the behaviour of the chain, and the transition point becomes indistinct. It is evidently shown in both our polymers. Sorption of water on these polymers was studied as a measure of extent of hydrophility by some investigators.[9,10] Their results are shown in Table 3 for comparison with the present inference.

Table 3

Moles of Polar Groups per 100 gr. of Polymer Compared with Moles of Water Vapour Sorption at 0.9 Relative Vapour Pressure

Polmer	Moles of polar group	Moles of water vapour
Polyvinyl acetate	1.16	0.17
Polyglycin-DL-alanine	1.56	1.72

Now, the oil/water interface will be compared with the air/water. The polymer molecule behaves generally freely in the former not only by the dissolution of side chain into oil phase as mentioned above, but also by the liberation from lateral cohesion, because the heat of mutual separation of molecules at the interface is scarcely required in such a present case as "like dissolves like." On the other hand, the molecules at the air/water

9) M. Dole and A. D. McLaren, *J. Am. Chem. Soc.*, **69**, 651 (1947).
10) B. Katchnan and A. D. McLaren, ibid., **73**, 2125 (1951).

interface seem to be frozen in themselves by cohesion even at relatively low surface concentration. Therefore, the change of free energy in respect to surface area should be far greater in the latter. But, in the case when the molecule is free even in the latter, there would be no difference between both interfaces. Such a fact is also shown in the case of polyvinyl acetate as confirmed by our investigation. On the other hand, amilan shows the difference in spite of having no side chain. It may be due to the strong polarity of its polar group, which is also confirmed by Table III. The discussions in the preceding paper[7] can be also understood only on the ground of these inferences.

As mentioned above, the linear polymer is flexible at the oil/water interface as in organic solvent, and even if the polymer has side chains, its non-polar side chain is removed into oil phase. Therefore, by neglecting the effect of side chain, we may apply the statistical treatment of flexible linear polymer with some modifications to the surface chemistry of the present polymers at the oil/water interface. That is, the relation between the interfacial pressure, π, and the surface area per monomer unit, A, may be expressed in the form as

$$\pi A = \frac{kT}{n}\left(1+\frac{b}{A}\right) \qquad \cdots\cdots(2)$$

The physical meaning of the coefficients, n and b, in this equation will be mentioned below.

Therefore, when we plot the product of πA against the reciprocal of A as shown in Fig. 3, and extrapolate this curve to infinity of area, the length of segment of long chain molecule can be obtained, that is, n-mer is the kinetic unit of these polymers in the interface. The obtained results are listed in Table IV, in which the number of atoms in each unit chain of both polymers is nearly 50 atoms in consideration of the side chain in vinyl copolymer. We must now again remember the extent of error inherent in the ring method as mentioned above. On the other hand, Flory had estimated from the activation energy of flow in viscosity that there are approximately 32 atoms in each segment of flow of polyesters in organic solvent.[11]

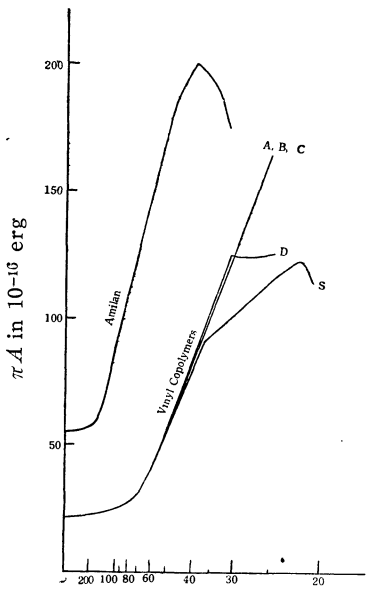

Fig. 3 The πA-$1/A$ curve of polymer at the petroleum ether/water interface.

Table 4

Length of Segment of Linear Polymer at the Oil/Water Interface

Polymer	$(\pi A)_{A=\infty}$	n	Number of atoms in each segment of backbone chain
Amilan	55×10^{-16} erg	7.2	50
Vinyl Copolymer	21×10^{-15}	19	38

The physical meaning of coefficient, b, in the second term of equation (2) in the dilute region may be considered to be analogous to that of bulk solution.[12]

From the curves in Fig. 3, we can readily determine the point, from which the interaction between the chains becomes more predominant, for the kink points appear clearer in these curves. The negative slope appears when some atoms in the backbone chain are removed from interface by either bending or collapsing. The kink points listed in Table II were thus determined. The linear range of the curve corresponds to the range of interaction of the same order. The rapidly rising point in this curve, which may correspond to that of beginning of mutual interaction and of rising of surface viscosity, is

11) P. J. Flory, *J. Am. Chem. Soc.*, **62**, 1057 (1940).
12) For example, H. Mark and A. V. Tobolsky, "Physical Chemistry of High Polymeric Systems" (1950), p. 263.

nearly 70 A^2. per vinyl unit for this copolymer, and 150 A^2. per monomer for amilan. On considering an atom unit instead of a monomer unit, these areas are identical on account of the above-mentioned correction of the side chain effect. The π-A curves of both polymers should be also considered on the same universal ground of an atom unit in the interface.

This flexibility phenomenon is observed not only at the oil/water interface. The determination of the molecular weight of high polymers has recently been tried by monolayer method[13,14] among other bulk methods, and it was confirmed by many investigators that the agreement with the molecular weight obtained by other methods is sufficient.[15] On the other hand, it is reported that this method is unsuitable for some polymers such as polyvinyl acetate.[7,16] Especially, it was found in the preceding paper that the molecular weight of polyvinyl acetate obtained by this method is independent of the degree of polymerization, and, as mentioned above, its π-A curves at the air/water and oil/water interface are almost identical. Moreover, its surface potential-area curves at air/water interface, measured by both methods of compression and successive injection, are also entirely identical, as mentioned in the preceding paper.[7] From these phenomena it is clear that we should consider the flexibility of linear polymer also to some extent at the air/water interface. On the other hand, πA-π curve is linear in the case of the rigid molecule such as protein[14] even at the oil/water interface.[5] However, even in the case of protein, it is recently reported that the existence of surface submolecule should be considered in the non-Newtonian region in the experiment of surface viscosity.[17]

In conclusion, the author expresses his hearty thanks to Prof. T. Isemura for his kind guidance throughout the present work, and to Prof. S. Murahashi and Mr S. Otsuka in our institute who kindly supplied copolymers to him. The cost of this research has been partly defrayed from the Scientific Research Encouragement Grant from the Ministry of Education, to which the author's thanks are due.

The Institute of Scientific and Industrial Research, Osaka University, Sakai, Osaka

13) J. Guastalla, *Compt. rend.*, **208**, 1078 (1939).
14) For example, H. B. Bull, *J. Biochem.*, **185**, 27 (1952).
15) For example, M. Abribat and J. Pouradier, *Compt. rend.*, **227**, 1101 (1948).
16) G. C. Benson and R. L. McIntosh, *J. Colloid Sci.*, **3**, 323 (1948).
17) M. Joly, "Surface Chemistry" (1949), p. 157.

Adiabatic Compressibility of Aqueous Solution. II. Amino Acids, Amides and related Compounds*

(Received March 10, 1953)

by

Yutaka MIYAHARA

The ultrasonic investigation of aqueous solution of amino acids, amides and related compounds will be presented in this paper, in continuation of the previous study of organic acids.[1] As has been reported previously, the adiabatic compressibility of aqueous solution, obtained by measuring ultrasonic velocity, gives much informations about the interactions between solute molecules and those of water.

In addition to a number of investigations in this field carried out in Japan, which were referred to in the previous paper, several studies have been reported in foreign literatures. The first application of ultrasonics to

* Presented at the Symposium of Colloid Chemistry held at Fukuoka on November 16, 1952.

1) Y. Miyahara, This Bulletin, **25**, 326 (1952).

the study of solvation was reported by Passynsky.[2] He estimated the amount of hydrated water of strong electrolytes,[2] non-electrolytes[3] and colloids[4] in his series of investigations. He assumed that the volume of the incompressible part of the solution, obtained from the ratio of compressibilities of solution and solvent, corresponds to the solvation volume. However, since this volume included that of the solute molecule, as is shown by the comparison of his equation with ours, which has been reported in the previous paper, the stated assumption could not fully be accepted.

More recently, Jacobson[5] has studied the liquid mixtures, aqueous solution of non-electrolytes, amino acids and proteins. His treatment was based on the same picture as that adopted by us, and he introduced a correction term in his equation of compressibility of solution, representing the effects of electrostriction and of breaking of hydrogen bond of surrounding water by inserted solute molecules.

On the other hand, Gucker and co-workers[6] treated this problem from an entirely different viewpoint in their study on amino acids solutions. Their investigation was based on Kirkwood's theories of mutual interaction and solvation of zwitter ion. This may also be another important way to attack this problem.

Experimental

The velocity of ultrasonic waves in solution was measured with an ultrasonic interferometer and has been briefly described in the previous paper. The details shall be presented herein. The sectional diagram of the interferometer is shown in Fig. 1. The reading scale on which the reflector is carried was part of a commercial sliding type traveling micrometer (Shimazu Scientific Co.). This scale was furnished with a vernier, graduated to 1/100 mm. The essential part of the cell was made of brass, coated with silicone resin, NS NO. 150. The crystal was cemented with the same resin. As has been shown in the wiring diagram in the previous paper, the single-tube oscillator was used to drive the crystal of the interferometer. Hence, the frequency of ultrasonic waves varied markedly in the vicinity of the points at which standing waves occured. In order to obtain the wave length at a definite frequency, the reading was made at a moment when the current flowing in the microammeter was at a minimum and the beat frequency

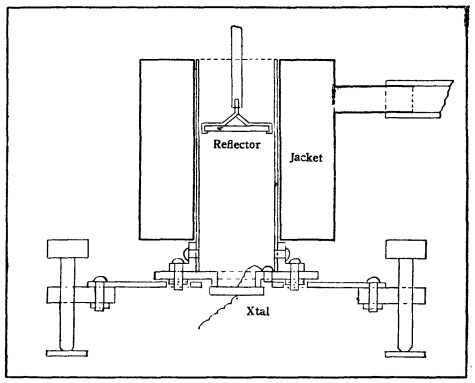

Fig. 1.

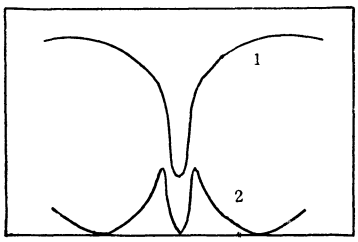

Position of Reflector

Fig. 2.

1.....Current
2.....Beat frequency

became zero. This condition was secured by a manual adjustment for each measurement run. The relations between beat frequency, current dips and position of reflector thus adjusted are shown in Fig. 2. By these methods the frequency of ultrasonics when standing waves were set up, could be adjusted to the standard. The frequency of a commercial radio station, JOAR, 1090KC. was used as a standard, and beats were detected with a superheterodyne radio receiver. The resonance frequency of the X-cut crystal used was 1270 KC. The temperature of the cell was held constant by circulating water from a thermostat through a jacket around the interferometer. The velocity measurements were made at 30.0°C.

The materials investigated were as follows;

2) A. Passynsky, *Acta Physicochim.* U.R.S.S., **11**, 606(1938).
3) A. Passynsky, *Acta Physicochim.* U.R.S.S., **22**,137(1947).
4) A. Passynsky, Acta Physicochim. U. R. S. S., **22**, 263 (1947).
5) B. Jacobson, *Arkiv För Kemi*, **2**, 177 (1950).
6) F. T. Gucker, F. W. Lamb, G. A. Marsh and R. M. Haag, *J. Am. Chem. Soc.*, **72**, 310 (1950).

Material	Source	Original Purity	Times of Recrystallization
Urea		c.p.	3
Thiourea		c.p.	3
Urethan		c.p.	3
Urotropine	Takeda	c.p.	1
Creatinine	Fisher	c.p.	0
Glycine	E. Merk	g.p.	0
α-Alanine	Ishizu	g.p.	1
L-Leucine	Takeda	c.p.	1
DL-Valine	Matheson	c.p.	1
DL-Methionine	Takeda	c.p.	1
L-Proline	Takeda	c.p.	1

Results and Discussion

The experimental results of ultrasonic velocity and other related values are given in Tables 1-11. The notations used are as follows;

c .....ultrasonic velocity in solution,
c_0.....ultrasonic velocity in water,
V_0 ...apparent volume of water in solution defined as

$$V_0=(D_s-x)/D_w$$

x .....concentration of solute in gram per cc. solution,
D_s.....density of solution at 30°C.,
D_w ...density of water at 30°C.,
K.....defined as

$$K=V_0-\kappa/\kappa_0$$

κ .....adiabatic compressibility of solution,
κ_0 ...adiabatic compressibility of water.

The physical meanings were explained in the previous paper.

Table 1
Urea

No.	x	c/c_0	κ/κ_0	V_0	K
1	0.0303	1.0082	0.9759	0.9778	0.0019
2	0.0312	1.0083	0.9758	0.9769	0.0011
3	0.0333	1.0090	0.9738	0.9754	0.0016
4	0.0386	1.0102	0.9701	0.9715	0.0014
5	0.0426	1.0111	0.9674	0.9684	0.0010

Table 2
Thiourea

No.	x	c/c_0	κ/κ_0	V_0	K
1	0.0330	1.0070	0.9776	0.9758	−0.0016
2	0.0294	1.0065	0.9793	0.9785	−0.0008
3	0.0354	1.0082	0.9747	0.9740	−0.0007
4	0.0355	1.0077	0.9755	0.9740	−0.0015
5	0.0342	1.0072	0.9769	0.9750	−0.0019
6	0.0300	1.0064	0.9795	0.9780	−0.0015

Table 3
Urethan

No.	x	c/c_0	κ/κ_0	V_0	K
1	0.0294	1.0076	0.9818	0.9739	−0.0079
2	0.0350	1.0091	0.9781	0.9691	−0.0090
3	0.0324	1.0086	0.9794	0.9713	−0.0081
4	0.0339	1.0090	0.9785	0.9699	−0.0086
5	0.0332	1.0089	0.9790	0.9704	−0.0086

Table 4
Urotropine

No.	x	c/c_0	κ/κ_0	V_0	K
1	0.0195	1.0046	0.9871	0.9844	−0.0027
2	0.0180	1.0042	0.9881	0.9857	−0.0024
3	0.0180	1.0044	0.9877	0.9857	−0.0020
4	0.0202	1.0044	0.9871	0.9840	−0.0031

Table 5
Creatinine

No.	x	c/c_0	κ/κ_0	V_0	K
1	0.0192	1.0059	0.9836	0.9857	0.0021
2	0.0213	1.0066	0.9816	0.9841	0.0025

Table 6
Glycine

No.	x	c/c_0	κ/κ_0	V_0	K
1	0.0301	1.0131	0.9622	0.9824	0.0202
2	0.0116	1.0052	0.9850	0.9932	0.0082
3	0.0155	1.0069	0.9801	0.9910	0.0109
4	0.0192	1.0088	0.9746	0.9891	0.0145

Table 7
α-Alanine

No.	x	c/c_0	κ/κ_0	V_0	K
1	0.0289	1.0135	0.9646	0.9803	0.0157
2	0.0324	1.0152	0.9605	0.9777	0.0172

Table 8
L-Leucine

No.	x	c/c_0	κ/κ_0	V_0	K
1	0.0144	1.0075	0.9826	0.9882	0.0056
2	0.0153	1.0083	0.9809	0.9875	0.0069
3	0.0110	1.0059	0.9863	0.9911	0.0048

Table 9
DL-Valine

No.	x	c/c_0	κ/κ_0	V_0	K
1	0.0201	1.0103	0.9754	0.9844	0.0090
2	0.0132	1.0070	0.9832	0.9898	0.0066
3	0.0202	1.0109	0.9741	0.9844	0.0103

Table 10
DL-Methionine

No.	x	c/c_0	κ/κ_0	V_0	K
1	0.0101	1.0040	0.9892	0.9929	0.0037
2	0.0101	1.0040	0.9891	0.9930	0.0039
3	0.0191	1.0076	0.9794	0.9865	0.0071
4	0.0163	1.0062	0.9832	0.9883	0.0051

Table 11
L-Proline

No.	x	c/c_0	κ/κ_0	V_0	K
1	0.0160	1.0068	0.9820	0.9886	0.0066
2	0.0190	1.0073	0.9802	0.9865	0.0063

The molar value, K_m of the respective substances, which is calculated by the method of least squares assuming that it is independent of concentration, is also listed in Table 12 and Table 13, as well as those calculated from the data of Passynsky, Jacobson and Gucker. K_m is defined as

$$K_m = MK/x$$

where M is the molecular weight; it is related to the commonly used apparent compressibility by the following equation:

$$K_m = -\Phi/\kappa_0$$

where Φ is defined as

$$\Phi = (1000/c)\kappa - (1000D_s/c - M)\kappa_0/D_w$$ *

(1) **Amides and Related Compounds**—The influences of the radicals which directly interact with the surrounding water molecules upon the values of K_m were studied quantitatively in the previous paper, and it was shown that the values of K_m could be expressed as the sum of $K_{m,r}$ assigned to the individual radicals for a series of homologous molecules.

This additive law does not hold strictly in the present case which includes various types of molecules. However, the qualitative tendency may still remain; negative values for those of hydrophobic radicals, such as methylene and thioketone could also be assigned. The effects of radicals such as acid amides and non-ionic amines are relatively small, in marked contrast to those of amino radicals in amino acids.

(2) **Amino Acids**—In spite of the fact that the various amino acids investigated had alkyl chains of different lengths, which would reduce K_m to negative values, it was found that K_m was almost constant for the various compounds.

This may be interpreted as follows: the magnitude of the effect of metheylene radicals on K_m is very small as compared with that of ionized groups. Therefore it may not

Table 12
K_m

	30°C*	25°[6]	20°[5]	20°[3]
Urea	2.3			2.0
Thiourea	−3.1			
Urethan	−23			
Urotropine	−19			
Creatinine	13			
Glycolamide		−6.0	2.0	
Lactamide		−9.5	−5.4	

Table 13
K_m

	30°*	25°[6]	20°[5]	20°[3]
Glycine	52	60	60	58
α-Alanine	48	59	58	60
β-Alanine		61	60	
L-Leucine	56			
DL-Valine	56			
DL-Methionine	53			
L-Proline	42			

be illogical to suspect that when a molecule has hydrophobic radicals such as methylene radicals together with ionic groups, the effect of the former on K_m is entirely masked by the strong electrical force of the latter, since the weak interaction between such hydrophobic radicals and the surrounding water molecules are non-electrical in nature.

Assuming that the water in the nearest vicinity of the zwitter ion becomes incompressible by the strong electrostatic force, as in the case of strong electrolytes, the amount of hydrated water is found to be about 54 g./mol., or three molecules per on pair of zwitter ion. This values may be some measure of hydration of zwitter ion in comparison with that of strong electrolytes.

A part of the cost of this research was defrayed from the Scientific Research Encouragement Grant from the Ministry of Education.

Chemical Institute,
Faculty of Science,
Nagoya University,
Chikusa, Nagoya

* c . . . mole per 1000 cc. solution

* Present data

Constant Current Coulometric Method in Argentometric Titration of Thiourea

By Masaki NAKANISHI and Hanako KOBAYASHI

(Received May 15, 1953)

Introduction

Several methods are available for the determination of thiourea in which are included, besides well-known Volhard's silver nitrate method in an ammoniacal solution, iodine titration by Reynolds[1], oxidimetric method by Cuthill[2], selenious acid method by Werner[3] and sulfur determination method proposed by Wiesenberger[4] and Akita[5]. When thiourea is mixed with ammonium thiocyanate, the analysis of the former only, or of both is carried out according to the methods published by Salkowski[6], Reynolds[1] and Kodama[7].

These methods are, however, limited to a comparatively larger amount of thiourea. It is desirable to find out a reliable and accurate micromethod by which a milligram amount or less of thiourea is precisely determined. The object of this paper is to present a coulometric titration method for the microanalysis of thiourea.

The constant current coulometric method was applied to this purpose and the results obtained were satisfactory. As is observed in Table 1 and 2, milligram and submilligram quantities of thiourea were determined with a tolerable precision.

In the method described below, thiourea was treated with silver bromide solution in ammonia and the liberated bromide ion, which is equivalent to thiourea, was titrated with the anodically generated silver ion rather than with a standard solution. The electrolysis current was automatically controlled to be constant during the electrolysis; thus the amount of the generated silver ion was exactly determined as the product of current and time according to Faraday's law.

Because the titrant could be added in very small increments, the coulometric titration is a suitable means to the microanalytical treatment. In contrast to the ordinary titration, the standardization and storage problems of solutions are avoided, therefore high precision is attained by the constant current coulometric titration especially when it is applied to microanalyses.

In the preliminary experiments a small amount of thiourea was titrated in an ammoniacal medium with the anodically generated silver ion, which procedure is analogous to the Volhard's titration of thiourea. Results obtained were fairly accurate when the concentration of ammonia exceeds $2N$ in the electrolyte. But the objection is that the reaction is somewhat time-consuming. This difficulty was overcome by the present method, replacing thiourea by the equivalent bromide ion.

Apparatus

A weighing bottle of brown glass (about 70 ml.) with the ground glass stopper was used as the

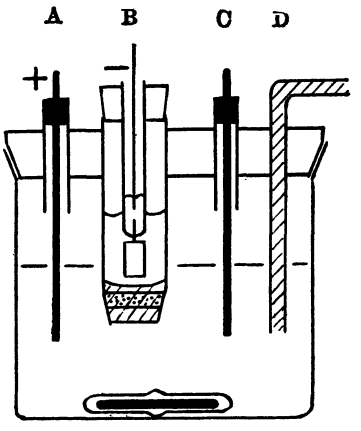

Fig. 1. Schematic diagram of the electrolysis cell
A: Generator anode, Ag rod.
B: Generator cathode, Pt sheet.
C: Indicator electrode, Ag rod.
D: Agar KNO_3 bridge.

1) J. E. Reynolds and E. A. Werner, *J. Chem. Soc.*, **83**, 6 (1903).
2) R. Cuthill and C. Atkins, *J. Soc. Chem. Ind.*, **56**, 5 (1937).
3) A. E. A. Werner, *Analyst*, **65**, 286 (1940).
4) E. Wiesenberger, *Mikrochimie ver. Mikrochim. Acta*, **29**, 73 (1941).
5) T. Akita and K. Takagishi, *Plastics* (in Japanese), **1**, 22 (1950).
6) Salkowski, *Ber.*, **26**, 2498 (1893).
7) S. Kodama and others, *J. Chem. Ind. Japan*, **54**, 184 (1951).

electrolysis cell. The sample to be analysed was weighed directly in it. Another rubber stopper was prepared to which electrodes were firmly settled and arranged for electrolysis as shown in Fig. 1. Generator cathode (B in the figure) is a smooth platinum plate (6×15mm) dipped in the saturated potassium nitrate solution, which is isolated from the solution to be analysed with a sintered glass disk and agar.

The solution was vigorously stirred with a magnetic stirrer. The whole cell is preferably enclosed in a dark case to eliminate the photochemical change of silver bromide.

As the source of the constant current for electrolysis the line-operated device of Carson[8] was utilized. The value of current was measured at intervals during electrolysis from the IR-drop across a standard resistor to ascertain the constancy. Actually the current was stable enough and no appreciable drift was observed. The quantity of silver ion generated is calculated as the product of current and time, the latter having been measured with a stop-watch.

The electrolysis was interrupted at appropriate intervals and followed by the measurement of potential of the indicator electrode. The end-point of the titration was determined in the same way as in the conventional potentiometric titration.

Procedure and Results

Procedure. The aqueous solution or the solid sample of thiourea is weighed directly in the electrolysis cell. When a larger volume of solution than several milliliters is dealt with, evaporate to a few milliliters. Then the silver bromide solution in ammonia is added drop by drop to a slight excess. Without filtering the precipitate of silver sulfide formed, the solution is gently warmed at 60 to 70°C till the odour of ammonia disappears. Precautions must be taken against drying up the solution. This process is accomplished in a dark place to avoid the photochemical decomposition of silver bromide which has been separated out. Next about 5g. of potassium nitrate is added and the solution is made up to about 50ml. with water, acidified with dilute sulfuric acid. After arranging the electrodes to the cell, the electrolysis is started with a constant current of an appropriate value. The end-point is informed with the aid of the potentiometric method.

NOTES. The ammoniacal silver bromide solution is prepared as follows. The purified silver bromide which is prepared from silver nitrate and potassium bromide and recrystallised from ammonia is dissolved to saturation in concentrated ammonia. This work is performed under a photographic lamp in a dark room. The ammoniacal solution thus prepared is stable against light if no residue of the solute is present.

Sulfuric acid is the most preferable to acidify the solution after the reaction between thiourea and silver bromide has been completed. With acetic acid, the measuring process is time-consuming although no serious interference results. Nitric acid is disapproved because it attacks silver electrodes even when diltute and gives considerable negative results.

To bring the reaction between thiourea and silver bromide to completion, subsequent removal of ammonia is inevitable. Expelling ammonia with a strong base is not recommended. In the procedure described above the solution was gently warmed at 60 to 70°C over an electric heater of small wattage. Precautions must be taken against bubbling and complete evaporation. To make the removal of ammonia easy, the preliminary concentration of the original solution to a small volume is advisable and the large excess of the silver bromide solution is rather objectionable.

Repeatability. To have a knowledge of the repeatability of this method a series of experiments were made taking about 3.9 mg. of thiourea in each. About 4ml. of the silver bromide solution was added and the constant current of about 10 mA. was used for electrolysis. The results obtained are shown in Table 1. Observed values are fairly accurate. The mean of the errors is −0.0076 mg. for these seven samples and the standard deviation 0.011 mg. for each value.

Table 1

Determination of Thiourea, (A)

Amount of Thiourea	Current	Equiv. Point (sec.)		Error	
(mg.)	(mA.)	Calc.	Found	mg.	%
3.936	10.010	997.5	999.7	0.009	0.22
3.942	9.999	999.1	996.9	−0.009	−0.22
3.940	9.996	998.9	996.0	−0.011	−0.29
3.995	10.005	999.5	992.4	−0.027	−0.71
3.937	10.000	998.1	998.9	0.003	0.08
3.939	10.010	998.8	997.3	−0.006	−0.15
3.939	10.021	997.4	999.6	0.009	0.22

Table 2

Determination of Thiourea, (B)

Amount of Thiourea	Current	Equiv. Point (sec.)		Error	
(mg.)	(mA.)	Calc.	Found	mg.	%
0.3982	10.001	100.9	101.7	0.0031	0.79
0.3926	10.003	99.5	103.6	0.0161	4.1
0.1969	5.986	83.4	86.2	0.0067	3.4
0.1963	5.959	83.5	85.3	0.0043	2.2
0.1965	5.783	86.2	87.2	0.0024	1.2
0.0312	0.876	87.6	89.2	0.0006	1.8
0.0312	0.882	88.2	95.5	0.0026	8.3
0.0312	0.899	88.1	93.5	0.0019	6.1
0.0312	0.889	89.0	83.3	−0.0020	−6.4

8) W. N. Carson, *Anal. Chem.*, **22**, 1565 (1950).

Analysis of Decreased Amounts of Thiourea. As this method is intended rather for the microanalysis, decreased amounts of thiourea were treated, the results of which are shown in Table 2. Absolute errors in mg. are passably small, but the relative errors are no longer ignored, therefore the limitation lies at several hundredths milligram of thiourea. It is obvious from the table that the use of smaller electrolysis current is profitable for smaller amounts of thiourea, because the smaller the current is, the longer time is taken to the end-point. Thus the error due to time-measurement is reduced.

Simultaneous Analysis of Thiourea and Thiocyanate

Microanalytical determination of thiourea and ammonium thiocyanate in the mixture is often sought for.

The present method, when applied to the mixture, gives the sum of both substances, because thiocyanate is titrated argentometrically together with bromide and only one inflection occurs on the potentiometric curve owing to the similar solubilities of their silver salts.

Titration of thiourea only with the electrolytically generated iodine, modified method of Reynolds[1], was also not available because iodine titration is valid only for macroanalysis.

Léon's device[9] gives a useful information to the present purpose, as be succeeded in the simultaneous analysis of bromide and thiocyanate with the potentiometric titration in an 80 to 90% acetone solution. This device was introduced and the simultaneous analysis of thiourea and thiocyanate was attempted in an acetone solution using the present method. The acetone solution made a clear-cut distinction of thiourea from thiocyanate and two inflections appeared on the potential-time curve due to bromide and thiocyanate respectively. Mixtures of various proportions were treated, the results of which are tabulated in Table 3.

Table 3

Simultaneous Analysis of Thiourea and Thiocyanate in 90% Acetone Solution
1 coulomb = 0.3945mg. thiourea, 0.7889mg. thiocyanate

Thiourea	Thiocyanate	Current	Equiv. Point Found (sec.)		Error (%)	
(coulomb)	(coulomb)	(mA.)	Thiourea	Thiocyanate	Thiourea	Thiocyanate
7.484	2.526	10.013	760.4	252.6	1.7	0.12
7.482	2.526	10.011	757.2	255.4	1.3	1.2
7.978	3.959	10.032	816.6	391.3	2.5	−0.68
7.971	3.956	10.009	804.9	402.2	1.1	1.7
4.806	5.435	10.019	488.3	539.8	1.6	−0.22
4.806	5.435	10.067	483.5	544.0	1.3	0.95
4.806	5.435	10.018	485.2	553.7	1.1	2.0
4.983	9.782	10.008	514.0	985.5	3.2	1.1
4.981	9.777	10.006	514.1	983.3	3.3	0.58
2.502	7.547	10.001	254.0	758.4	1.6	0.48
2.504	7.553	9.993	252.9	756.4	1.0	0.01

A little less accurate values are found compared with those in a pure solution. This procedure is, however, simple and easy for the simultaneous analysis, if such an error is within allowance.

Summary

The coulometric method with a constant current was used for the microanalysis of thiourea.

An ammoniacal solution of silver bromide was added to thiourea solution and the liberated bromide equivalent to thiourea was titrated with electrolytically generated silver ion in an acid solution. A milligram amount of thiourea was satisfactorily determined with the standard deviation of about 0.01 mg. and the method is also applicable to submilligram amounts of thiourea.

Simultaneous analysis of thiourea and ammonium thiocyanate in a mixture was made using 90% acetone solution.

Laboratory of Chemistry, Faculty of Science, Ochanomizu University, Tokyo

9) C. Léon, *Compt. Rend.*, **232**, 170 (1951).

On the Infrared Frequency Shift in the Liquid State and its Relation to the Atomic Polarization

By Eizi HIROTA

(Received May 27, 1953)

Introduction

It is a well-known fact that the infrared frequencies of molecules in the liquid states are, in general, lower than those in the gaseous states. This fact implies that the molecules are slightly deformed in condensed phase by the intramolecular field due to the surrounding molecules. The deformation of molecules in a static external field is, on the other hand, indicated as the so-called "atomic polarization." Therefore the frequency shift in the liquid state may have some relation to the atomic polarization. Kirkwood, West, and Edwards[1] studied the frequency shift of HCl, but their work was limited to a simple molecule such as HCl and not extended to the relation of the frequency shift with the atomic polarization. Here the frequency shift will be treated as a more general problem and connected with the atomic polarization.

Atomic Polarization

The atomic polarization induced by ith infrared active normal vibration is given by[2]

$$P_{Ai}=\frac{1}{3}\frac{4\pi N}{3}\alpha_{Ai}=\frac{4\pi N}{9}\frac{e_i^2}{4\pi^2 m_i\nu_i^2} \quad (1)$$

where N denotes Avogadro's number, e_i the effective charge, m_i the effective mass, and ν_i the frequency of the ith normal vibration. The factor 1/3 in Eq. (1) takes account of the fact that the vibration under consideration has only one degree of freedom rather than three as does the isotropic oscillator.[3] As a whole it gives rise to

$$P_A=\sum_i P_{Ai}=\frac{4\pi N}{9}\sum_i\frac{e_i^2}{4\pi^2 m_i\nu_i^2} \quad (1')$$

where the summation is extended over all the infrared active vibrations.

Frequency Shift

A) A Simple Treatment (Heteronuclear diatomic molecules, with only one normal mode).—Let us consider first a simple case in which the molecule has one vibrational degree of freedom (e.g. HCl). In view of the complexity of the intramolecular force field in the liquid phase one can not obtain a satisfactory expression for it. But Onsager[4] gave an ingeneous method of evaluating the intramolecular force by solving an electrostatic equivalence. Let us make a spherical cavity in the liquid phase with dielectric constant ε, whose radius is denoted by a, and put at its center the electric moment $\boldsymbol{m}$. Then this dipole polarizes the surrounding medium and produces a "reaction field" $\boldsymbol{R}$ at its own place, which is given by

$$\boldsymbol{R}=\frac{2(\varepsilon-1)}{2\varepsilon+1}\frac{\boldsymbol{m}}{a^3} \quad (2a)$$

where

$$\boldsymbol{m}=\boldsymbol{\mu}+e\boldsymbol{x} \quad (3a)^{*)}$$

and $\boldsymbol{\mu}$ denotes rigid dipole of the molecule, e the effective charge, and $\boldsymbol{x}$ the displacement of the nucleus (treated as a vector quantity; the directions of $\boldsymbol{\mu}$ and $\boldsymbol{x}$ coincide with the axis of the molecule in this case). This field stabilizes the molecule by the amount,

$$-\Delta E=\frac{1}{2}\boldsymbol{R}\boldsymbol{m}=\frac{\varepsilon-1}{2\varepsilon+1}\frac{1}{a^3}(\boldsymbol{\mu}+e\boldsymbol{x})^2 \quad (4a)$$

so that the force constant for the molecular vibration is decreased in the liquid phase by the amount,

1) W. West and R.T. Edwards, *J. Chem. Phys.*, **5**, 14 (1937); J. G. Kirkwood, ibid., **2**, 351 (1934) Cf. E. Bauer and M. Magat, *Physica*, **8**, 718 (1938).

2) J. H. Van Vleck, "The Theory of Electric and Magnetic Susceptibilities", Oxford University Press, London, 1932. pp.42f. & 361t.

3) Reference 2, p.46.

4) Lars Onsager, *J. Am. Chem. Soc.*, **58**, 1486 (1936 .

*) It may be artued that the Onsager's model is an electrostatical one and, therefore, cannot be adequately applied to the time-dependent phenomena such as vibrations of nuclei. But when the wave-length of the radiation is far greater than the size of the radiating system (the molecule in this case), one can treat this process as a "quasi-stationary" one.

$$-\Delta f=-\frac{\partial^2 \Delta E}{\partial x^2}=\frac{2(\varepsilon-1)}{2\varepsilon+1}\frac{e^2}{a^3}=2ce^2 \quad (5a)$$

where

$$c=\frac{\varepsilon-1}{2\varepsilon+1}\frac{1}{a^3}$$

It follows that the fundamental frequency in the liquid phase, ν', is related to that in the free state, ν, by the relation:

$$\nu'=\left(\nu^2-2c\frac{e^2}{4\pi^2 m}\right)^{\frac{1}{2}}\cong\nu\left[1-\frac{ce^2}{4\pi^2 m\nu^2}\right] \quad (6a)$$

or

$$\frac{\Delta\nu}{\nu}=\frac{\nu-\nu'}{\nu}=c\frac{e^2}{4\pi^2 m\nu^2}=c\alpha_A \quad (7a)$$

where m is the effective mass of the harmonic oscillator composed of the diatomic molecule. Inserting this relation into Eq. (1'), we obtain

$$P_A=\frac{4\pi N}{9}\frac{1}{c}\frac{\Delta\nu}{\nu}=\frac{2\varepsilon+1}{3(\varepsilon-1)}\frac{M}{d}\frac{\Delta\nu}{\nu} \quad (8a)$$

where M and d denote molecular weight and density of the liquid respectively, which are related to a by

$$\frac{4\pi}{3}a^3=\frac{M}{N\cdot d}$$ (4)

It is necessary to compare this simple and rather straightforward derivation of $\Delta\nu$ with the result obtained by Kirkwood, whose idea was only quoted by West and Edwards and not given in details.[1] Their expression is

$$\frac{\Delta\nu}{\nu}=\frac{\varepsilon-1}{2\varepsilon+1}\frac{1}{a^3}\frac{(\mu_1^2+2\mu_0\mu_2)}{4\pi^2 m\nu^2} \quad (7a')$$

where

$$\mu_1=[(\partial\mu)/(\partial x)]_{x=0},\ \mu_2=[(\partial^2\mu)/(\partial x^2)]_{x=0}$$

and

$$\mu_0=[\mu]_{x=0}$$

This differs from Eq. (7a) only in the point that Kirkwood took into account the anharmonicity of vibration by introducing the second derivative of the dipole moment with x.

B) More General Treatment (Polyatomic molecules, with more than one infrared active normal mode).—The principle of the calculation is, in general, the same as that used in A) except the introduction of the polarizability α, which is, according to Onsager, given by

$$\alpha=\frac{n^2-1}{n^2+2}a^3 \quad (8)$$

where n stands "internal refractive index". The total electric moment induced in the center of the cavity is given by

$$\boldsymbol{m}=\boldsymbol{\mu}+\alpha\boldsymbol{R}+\sum_i e_i'\boldsymbol{Q}_i \quad (5b)$$

in which $\boldsymbol{R}$ is given by the same expression as Eq. (2a) and e_i' denotes $e_i/\sqrt{m_i}$ *) and $\boldsymbol{Q}_i$ the ith normal coordinate (treated as a vector quantity).**)

Combination of Eqs. (2a) and (3b) affords, by means of Eq. (8),

$$\boldsymbol{R}=\frac{2(n^2+2)(\varepsilon-1)}{3(2\varepsilon+n^2)}\frac{1}{a^3}[\boldsymbol{\mu}+\sum_i e_i'\boldsymbol{Q}_i] \quad (9)$$

and

$$\boldsymbol{m}=\frac{(n^2+2)(2\varepsilon+1)}{3(2\varepsilon+n^2)}[\boldsymbol{\mu}+\sum_i e_i'\boldsymbol{Q}_i]$$

$$=C[\boldsymbol{\mu}+\sum_i e_i'\boldsymbol{Q}_i] \quad (10)$$

In this case the energy of stabilization becomes

$$-\Delta E=\frac{1}{2}\boldsymbol{R}\boldsymbol{m}=\frac{\varepsilon-1}{2\varepsilon+1}\frac{C^2}{a^3}[\boldsymbol{\mu}+\sum_i e_i'\boldsymbol{Q}_i]^2 \quad (4b)$$

which is considered as a perturbing potential. Changing the variables from $\boldsymbol{Q}_{is}'$ to ξ_{is}', i.e.,

$$\boldsymbol{Q}_i=\boldsymbol{\xi}_i+\boldsymbol{Q}_{io}$$

($\boldsymbol{Q}_{io}$: a constant to be determined)

and choosing $\boldsymbol{Q}_{io}$ to satisfy the relations

$$\lambda_i\boldsymbol{Q}_{io}^2-R'e_i'(\boldsymbol{\mu}\boldsymbol{Q}_{io})-R'\frac{e_i^2}{m_i}\boldsymbol{Q}_{io}^2$$

$$-R'\sum_j e_i'e_j'(\boldsymbol{Q}_{io}\boldsymbol{Q}_{jo})=0$$

where and

$$\lambda_i=4\pi^2\nu_i^2 \qquad R'=\frac{2(\varepsilon-1)}{2\varepsilon+1}\frac{C^2}{a^3}$$

the perturbing potential Eq. (4b) reduces to, except constant terms,

$$-\Delta E=\frac{1}{2}R'[\sum_i\frac{e_i^2}{m_i}\xi_i^2+2\sum_i\sum_j e_i'e_j'(\xi_i\xi_j)] \quad (4b')$$

in which the second terms depend only upon the cross products of ξ_{is}' and, therefore, may

*) It is to be noted that the dimension of $\boldsymbol{Q}_i$ is $[M]^{\frac{1}{2}}[L]$.
**) See Discussion.

be neglected in the first order approximation. The change in ν_i, in this order of approximation, turns out to be

$$\nu_i' = \left[\nu_i^2 - \frac{2(\varepsilon-1)}{2\varepsilon+1}\frac{C^2}{a^3}\frac{e_i^2}{4\pi^2 m_i}\right]^{\frac{1}{2}}$$

$$\cong \nu_i\left[1-\frac{\varepsilon-1}{2\varepsilon+1}\frac{C^2}{a^3}\frac{e_i^2}{4\pi^2 m_i \nu_i^2}\right] \quad (6b)$$

or

$$\frac{\Delta\nu_i}{\nu_i} = \frac{\nu_i-\nu_i'}{\nu_i} = \frac{\varepsilon-1}{2\varepsilon+1}\frac{C^2}{a^3}\frac{e_i^2}{4\pi^2 m_i \nu_i^2} \quad (7b)$$

Thus, similarly to Eq. (8a), the total atomic polarization is given by

$$P_A = \frac{4\pi N}{9}\frac{2\varepsilon+1}{\varepsilon-1}\frac{a^3}{C^2}\sum_i \frac{\Delta\nu_i}{\nu_i} \quad (8b)$$

$$= \frac{2\varepsilon+1}{3(\varepsilon-1)}\frac{1}{C^2}\frac{M}{d}\sum_i \frac{\Delta\nu_i}{\nu_i} \quad (8b')$$

where the summation is extended over the terms due to the infrared active vibrations and

$$C = \frac{(n^2+2)(2\varepsilon+1)}{3(2\varepsilon+n^2)} \quad (11)$$

stands for a small correction due to the polarizability, reducing to 1 in the limit $n^2=1$.

Comparison with Experiments

In order to check the relation obtained above, two quantities should have been measured : i.e., the frequency shift $\Delta\nu$ and the atomic polarization P_A. But unfortunately precise data have not been available for either of them. The following are several examples useful at present to confirm the results.

Ex. 1. Hydrogen Chloride.—West and Edwards[1] observed the fundamental frequencies of HCl in the gaseous state and in CCl_4 solution, which are 2886 cm.$^{-1}$ and 2833 cm.$^{-1}$ respectively. Inserting this date and $\varepsilon=2.23$, the dielectric constant of carbon tetrachloride, in Eq. (8a) one obtains $P_A=1.0$ cc. Using the frequency 2780 cm.$^{-1}$ in pure HCl liquid obtained by Hettner[5], $P_A=0.8$ cc. These should be compared with the value $P_A=1.25$ cc. obtained from the measurement of the dielectric constant of the gaseous HCl by Zahn[6].

Ex. 2.—Water in carbon tetrachloride solution.—The molecule H_2O has three infrared active modes, the two of which were measured by Borst, Buswell, and Rodebush[7] in its CCl_4 solution. The results are as follows: for the fundamental frequency of 3652 cm.$^{-1}$, $\Delta\nu=43$ cm.$^{-1}$ and for $\nu=3756$ cm.$^{-1}$ $\Delta\nu=44$ cm.$^{-1}$. Assuming $\Delta\nu=20$ cm.$^{-1}$ for the remaining bending vibration (1595 cm.$^{-1}$), one can calculate $P_A=0.8$ cc. (See Table 1.). Various values of P_A have been obtained experimentally, only three of which are quoted here: $P_A=3.2$ cc. was obtained by the measurement of infrared dispersion[8], $P_A=2.0$ cc. by the dielectric constant of the solid[9] and $P_A=0.1$ cc.

Table 1

Frequency Shift of H_2O[7]

ν in Gas (cm.$^{-1}$)	ν in CCl_4 solution (cm.$^{-1}$)	$\Delta\nu$ (cm.$^{-}$)	$\Delta\nu/\nu$
1595	—	(20)	(0.0125)
3652	3609	43	0.0118
3756	3712	44	0.0117
			$\sum\Delta\nu/\nu$ 0.036

Table 2

Frequency Shift of CH_3I[11]

Symmetry	ν in Gas (cm.$^{-1}$)	ν in Liquid (cm.$^{-1}$)	$\Delta\nu$ (cm.)	$\Delta\nu/\nu$
A_1	532	552	10	0.0188
E	883	887	−4	−0.0091*)
A_1	1250	1242	8	0.0064
E	1441	1429	12	0.0166
A_1	2967	2950	17	0.0057
E	3058	3050	8	0.0052
				$\sum\ \nu/\nu$ 0.0527

*) This term is neglected for the calculation of $\Delta\nu/\nu$.

5) G. Hettner, *Zeits. f. Physik*, **89**, 234 (1934).
6) C. T. Zahn, *Phys. Rev.*, **24**, 400 (1927).
7) L. B. Borst, A. M. Buswell, and W. H. Rodebush, *J. Chem. Phys.*, **6**, 61 (1938).
8) C. H. Cartwright and J. Errera, *Proc. Roy. Soc.*, **A154**, 138 (1937).
9) J. Errera, "Polarisation dielectrique," quoted in Reference 8.

by the dielectric constant of the gas[10].

Ex. 3. Methyl Iodide.—From the results of Fenlon, Cleveland, and Meister[11] (Table 2) with Eq. (8b) one obtains $P_A=1.6$ cc., which should be compared with 1.4 cc., the value obtained by C.P. Smyth[12].

Ex. 4. Benzene.—Using the available data for $\Delta\nu$[13,14] (Table 3), one can estimate very roughly the value of P_A for C_6H_6, resulting to 1.9 cc., which agrees fortuitously with the value of Smyth[12] 1.9 cc.

Discussion

It should be noted here that the effective charges, $e_i's$, in Eq. (3) and others are those for the vibrations of molecules in the condensed phase and may differ from $e_i's$ defined by Eq. (1) or by Eq. (1'), the coincidence of both expressions being a formal one. This discrepancy might, if it were a real one, afford apparently greater "atomic polarization". An assumption is also made about the nuclear motion; that is, the vibration of nucleus is trated here simply by assuming no electrical and no mechanical anharmonicity. Since the errors originating from this treatment are not large, this solution may be allowed for the present as an approximate one.[15]

Table 3
Frequency Shift of C^6H^6

Symmetry	ν in Gas (cm.$^{-1}$)[13]	ν in Liquid (cm.$^{-1}$)[14]	ν (cm.$^{-1}$)	$\Delta\nu/\nu$
A_{2u}	671	675	−4	−0.0024*)
E_{1u}	1037	1036	1	0.0020
E_{1u}	1485	1478	7	0.0094
E_{1u}	3099	3089	10	0.0064
				$\sum\Delta\nu/\nu$ 0.0178

*) This term is neglected for the calculation of $\Delta\nu/\nu$.

Onsager's theory assumes that the geometry of the cavity is a spherical one and the dipole of the molecule is considered to be concentrated at the center of this sphere. It has already been pointed out by Wada[16] that these two assumptions are serious, and for a special case of 1,2-dichloroethane a more precise model was proposed to give a satisfactory result. In fact, the dipole induced by the infrared active normal vibration is not obviously a point one, contradicting the assumptions of Onsager's theory. However, if we are allowed to assume Onsager's theory at least as the first approximation, the theory stated above provides the effective charge for a normal vibration of the molecule from the frequency shift of the vibration. Detailed discussions are postponed, because of deficiencies in the accuracy on the theoretical as well as the experimental sides. Nevertheless, it is very interesting to note that the atomic polarization, which is a quantity difficult to measure, can be obtained by the frequency shifts in infrared absorption bands.

The author wishes to express his gratitude to Prof. Y. Morino for his kind advice and discussions. He is also indebted to Prof. M. Yasumi for his valuable criticisms.

Department of Chemistry,
Faculty of Science,
Tokyo University, Tokyo

10) P. Debye and H. Sack, "Handb. d. Radiologie", IV. Akad. Verlag., Leipzig. 1934.
11) P. F. Fenlon, F. F. Cleveland, and A. G. Meister, *J. Chem. Phys.*, **19**, 1561 (1951).
12) C. P. Smyth, *J. Chem. Phys.*, **1**, 247 (1933).
13) G. Herzberg, "Molecular Spectra and Molecular Structure", Band II., D. Van Nostrand Co. New York, 1949.
14) American Petroleum Institute Research Project 44, Serial No. 307, 498 and 499.
15) B. L. Crawford, Jr., and H. L. Dinsmore, *J. Chem. Phys.*, **18**, 983 (1950), B. L Crawford, Jr., *J. Chem, Phys.*, **20**, 977 (1952).
16) A. Wada, Private communication. See also D. G. Frood and A. J. Dekker, *J. Chem. Phys.*, **20**, 1030, (1952).

On the Separation of Phosphorus and Iron by Means of Cation Exchange Resin

By Yukichi YOSHINO

(Received December 16, 1952)

The rapid and accurate method of determination of phosphorus by means of ion-exchange column was for the first time proposed by Helrich and Rieman[1] for the analysis of phosphate rocks. The author once attempted to apply this method to the determination of phosphorus in the iron-bearing samples for the purpose of geochemical studies on the distribution of phosphorus in the limonite ores of Japan.[2] But, owing to the incompleteness of the separation of phosphoric acid from tervalent iron by cation exchange resin, the attempt did not succeed. Later, the problem of interference of ferric iron was pointed out by several workers.[3,4,5] In connection with it, the author had observed the same phenomena in the studies of ion-exchange separation of arsenic acid from ferric ion and the problem could be solved by previous reduction of the test solution by sulfur dioxide.[6]

It is now proved that the same techniques are also applicable to the quantitative separation of phosphate ion from tervalent iron by cation exchange resin. This paper also describes some investigations on the behavior of phosphorus on the column using P^{32} tracer as well as high frequency oscillators.

Experimental

The Cation Exchange Resins and Reagents.—Amberlite IR-120 and Amberlite IR-112 (A. G.) (both 50 to 100 mesh) were used.

Both acetate and borate comparison buffers were prepared according to Helrich and Rieman's original paper,[1] except that, in place of methyl red, bromocresol green indicator was added to acetate buffer. Carbonate free 0.1 *N* sodium hydroxide solution was standardized against 0.1 *M* potassium dihydrogen phosphate solution from *pH* 4.63 to *pH* 8.98 using comparison buffers.[4]

Ion Exchange Separation of phosphate Ion from Tervalent Iron by Reduction with Sulfur Dioxide.—To a mixture of 10cc. of 0.1*M* ferric chloride solution and a definite volume of 0.1 *M* potassium dihydrogen phosphate solution, add 1*N* hydrochloric acid of one tenth of the total volume in order to prevent formation of precipitate. Heat the solution on a water bath and pass a rapid current of sulfur dioxide for about half an hour in order to convert ferric ion into ferrous state. Then, pass the solution through a column of sodium form cation exchanger at a rate of 1—2cc. per minute. Wash with 30cc. of distilled water in several portions at the same rate. The effluent and washings are collected in a 100cc. Erlenmeyer flask, into which a small piece of porcelain is added as a boiling chip. Then, attach a glass joint spray trap and outlet tube bending downward. Heat flask gently and expel a greater part of excess sulfur dioxide. Add bromine water until coloration takes place and again distil off the excess of bromine. Rinse the attachments with a small volume of water and cool the solution. Then, add 0.25cc. of bromocresol green indicator and neutralize with 1*N* sodium hydroxide until indicator turns slightly blue. Adjust the *pH* at 4.63 with 0.1*N* hydrochloric acid and 0.1*N* sodium hydroxide using acetate buffer. Then, add 0.3 cc. of phenolphthalein and titrate with standard sodium hydroxide solution to the *pH* 8.98 using borate buffer. Table 1 shows the results obtained in such determinations.

Determination of Phosphate in Ferric Oxide Deposit and Vivianite.—Weigh out about 1 gram of fine powdered sample and treat with 20 cc. of aqua regia. Evaporate the so-

---

* Presented at the First Annual Meeting of the Japan Society for Analytical Chemistry, Kyoto, Oct. 30 to Nov. 1 1952.

1) Helrich, K. and Rieman, W., *Anal. Chem.*, **19**, 651 (1947).

2) Yoshino, Y., *J. Chem. Soc. Japan, Pure Chem. Sect.*, **72**, 503 (1951).

3) Kubo. S. and Tsutsumi, C., *Bull. Chem. Soc. Japan*, **23**, 187 (1950).

4) Goudie, A. J. and Rieman, W., *Anal. Chem.*, **24**. 1067 (1952).

5) Salmon, J.E., *J. Chem. Soc.* 2316 (1952).

6) Yoshino, Y., This Bulletin, **24**, 39 (1951).

Table 1

Separation of Phosphate from Ferric Iron

Phosphate ion taken (m. mol.)	Phosphate ion found (m. mol.)	Error (%)	Resin (g.)
1.000	0.998	−0.2	5 (Amberlite IR-120)
1.000	1.006	+0.6	5 („)
1.000	0.999	−0.1	5 („)
0.500	0.498	−0.4	7 („)
2.000	2.005	+0.25	10 (Amberlite IR-112)

lution to syrupy state and add 5 cc. of concentrated hydrochloric acid and dry up. Repeat this operation once more. Then, add 10 ml. of 1*N* hydrochloric acid. The solution is heated and filtered. Collect the filtrate and washings in a 100 cc. measuring flask and fill up to the mark with water. Taking aliquot portion of the sample solution, phosphate content was determined according to the same procedure as was described in a previous paragraph. The comparison of results obtained by both ion-exchange* and gravimetric method weighing as $Mg_2P_2O_7$ is given in Table 2.

Tracing of Phosphate Ion on Elution by Means of Radioactive P^{32}—The acidified solution containing 1 millimol of ferric chloride and potassium phosphate labeled with 0.3 microcurie of P^{32}* was passed in a bed of 10 grams of sodium form Amberlite IR-120. The column was washed with 0.01 *N* hydrochloric acid up to 450 cc. The percentage of phosphate in each step of filtrate was estimated by the radioactivity measurement. The results obtained are shown in Table 3.

It is observed that under these conditions, the percentage of separation of phosphate from tervalent iron becomes remarkably less,

Table 2

Determination of Phosphorus in Iron-bearing Samples

Sample	P_2O_5(%) Gravimetric	Ion Exchange	No. of detn.	Difference
Ferric oxide deposit of Meiji-yu Hot Spring, Nagano Pref.	8.94	8.96	3	+0.02%
Vivianite from Himeshima mine, Ôita Pref.	24.44	24.14	1	−0.30%

Table 3

Phosphate added (m.mol.)	% of Phosphate found in the Effluent and Washings: Effluent+50 cc.,	50~150,	−250,	−350,	−450cc.,	Total
2.000	85.0	6.6	3.5	(2.4)		97.5
1.000	71.9	7.8	3.2	2.3	1.2	86.4
0.100	45	13	7.7	7.0	6.0	78.7
0	6.1	3.6	2.5	2.4	1.9	16.5

the less the ratio of P/Fe in test solution. The gradual flowing out of phosphate ion in the washings may be due to the relatively weak linkage between phosphorus and ferric iron. This situation is quite similar to that observed in the system of arsenic acid and tervalent iron.[5]

Examination of the Distribution of Phosphate held on the Column using P^{32} and High Frequency Oscillators.—The solution containing 1 millimol of ferric chloride and 1 millimol of phosphoric acid labeled with about 10 microcurie of P^{32} was passed through a column of hydrogen form Amberlite IR-120 (0.9 cm.^{2} × 11 cm.) and the column was washed with 30 cc. of water in three portions. Then, 3 cc. of hydrogen form resin was packed to

* 10 grams of Amberlite IR-112 (A.G.) were employed.

* Obtained through the Isotopes Division or the Atomic Energy Commission. Decay and radiation properties were scanned and identified.

the head. The glass tubing was enveloped with a lead sheet having a window (10×10 mm.) and sliding the tube, vertical distribution of the radioactivity was measured by a Lauritsen electroscope. At the same time, a radioautograph was taken using X-ray film.

Fig. 1 represents the results obtained. The radioactivity is observed to be concentrated at the head of the original bed.

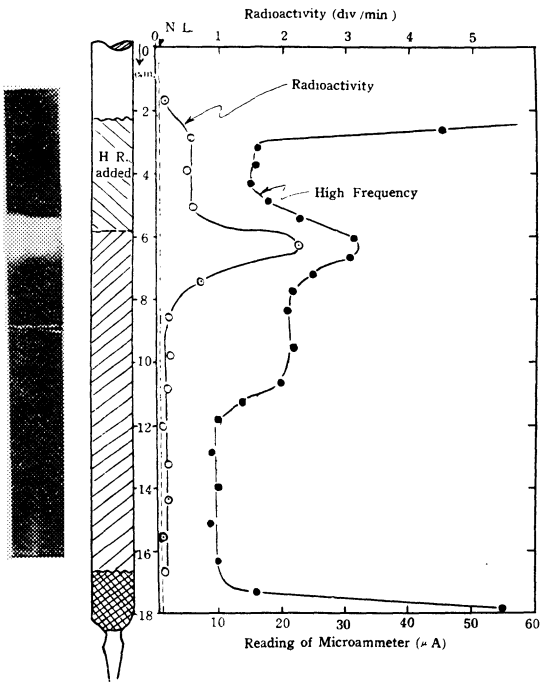

Fig 1

Then, the column was subjected to high frequency measurements[7] and the results are shown also in Fig. 1. The peak of the reading of a microammeter, which may be due to the band of ferric ion adsorbed, coincides with that of radioactivity. The position of the iron band could be also detected by the color change when Amberlite IR-112 was used.

From these experiments, it may be concluded that the holding of phosphate ion on the column is caused by direct interaction between phosphate and ferric iron. Whether this is due to the formation of complex or physical absorption is not known as yet.

Acknowledgements

The author wishes to express his appreciation to Prof. Wm. Rieman III of the Rutgers University for his advice and encouragement. He is also indebted to Dr. N. Matsuura for his kind guidance on radioactive tracer techniques, to Dr. M. Honda for the high frequency measurements and to the Ministry of Education for a Grant in Aid for Fundamental Scientific Research.

Institute of Chemistry, College of General Education, University of Tokyo, Meguroku, Tokyo

7) M. Honda,, *J. Chem. Soc. Japan, Pure Chem. Sect.*, **73**, 529 (1952).

Researches by the Chromatography. IV. On the Impurities of Cotton Cellulose and Wood Cellulose

By Akira HATANO and Hiroshi SOBUE

Introduction

In previous papers[1,2,3] we have reported some preliminary investigations carried out in order to determine qualitatively or quantitatively the hydrolyzate of some species of wood pulps by means of paper chromatography. From these investigations it was evident that glucose, xylose, mannose, arabinose, galactose and uronic acids of these sugars are the building units of the polysaccharides of the wood pulps investigated. Recently remarkable progress has been made

1) H. Sobue and A. Hatano, *J. Chem. Soc. Japan, Ind. Chem. Sect.*, **54**, 460 (1951).
2) H. Sobue and A. Hatano, ibid. **55**, 131 (1952).
3) H. Sobue, K. Matsuzaki, A. Hatano and Y. Arisawa, *J. Soc. Tex. Cell. Ind. Japan*, **8**, 79 (1952).

in the purification of wood pulps in both scientific and industrial fields, and high grade wood pulps are now being appreciated as the materials for tire cord rayon, acetate rayon, nitrocellulose, Bemberg etc. instead of cotton linters.

A number of research workers have studied the difference of the chemical components, morphological structures, fine structures, chain length distribution and reactivity or accessibility between these two different cellulosic materials[4]. The authors have studied their impurities and obtained some interesting results, which are expected to offer a number of unsolved problems. These will be described below.

Materials and Methods

Egyptian cotton linters (Gossypium cananilles), Japanese red pine (Pinus densiflora) and Japanese beech (Fagus crenata) were used as the materials. Their chemical composition is analysed by Tappi standard method and is tabulated in Table 1. The

Table 1

Chemical Components of Cotton Linters, Red Pine and Beech

	Cotton Linters	Red Pine	Beech
	%	%	%
Total Cellulose	99.0	54.7	56.8
Alpha Cellulose	96.8	38.3	41.5
Beta Cellulose	1.1	4.2	7.2
Ash	0.18	0.27	0.33
Resin	0.45	3.08	2.67
Lignin	—	28.0	23.6

raw cotton is extracted with alcohol-benzene (1 : 1) for six hours and boiled carefully with 1% sodium hydroxide for fifteen hours. The sample is washed with water and then with diluted acetic acid and washed again with water and dried in air. Thus, purified cotton is obtained. The material is infused in 69% sulfuric acid and kept for three days at 0~5°C, and this sulfuric acid solution is diluted into 2% sulfuric acid with water and hydrolysis is carried out under boiling. The hydrolyzate is neutralized with barium carbonate and concentrated by evaporation in a vacuum. The aliquot of the concentrated solutions is placed on one end of a filter-paper strip and developed with *n*-butanol-acetic acid-water (4 : 1 : 1) and partitioned into its component. Toyo filter paper No. 50 is used exclusively in these experiments. Standard sugars and amino acids are obtained from commercial sources. Strips are dried in air and some of them are sprayed with an acetone solution of ninhydrin and the amino acids are identified. Some of them are sprayed with a *n*-butanol solution of anilin-hydrogen-phthalate, and the monosaccharides and uronic acids are identified.

Experimental Results and Discussion

In the hydrolyzates of raw cotton linters, there are found arabinose and small amounts of galactose, galacturonic acid and glucuronic acid. It is not clear whether these uronic acids are the original components of linters or produced in the process of hydrolysis. According to the result of determination with a photoelectric photometer[1], arabinose is about 1.5% of glucose in the hydrolyzates. Pectin has been noticed in raw cotton linters and is said to be present in the fiber inner surface, primary wall or secondary wall with the components of wax. A long time ago, Ehrlich[5] et al. stated that pectin is composed of 4 moles of *dl*-galacturonic acid, 1 mole of *l*-arabinose and 1 mole of *d*-galactose. But the details on the relationship between cellulose and arabinose, galactose etc. will be discussed in the following paper.

The hydrolyzate of purified cotton linters contains almost no impurities besides the traces of arabinose and glucuronic acid. This fact shows that the prification of cotton linters is easy and is thought to be an important difference from the case of wood pulps[2,3].

The amino acids in the hydrolyzates of the samples which show positive ninhydrin reactions are cystine, aspartic acid, asparagine, arginine, glutamic acid, alanine and tryptophane. The *Rf* value of various amino acids are illustrated in Table 2.

Table 2

Rf Values of Amino Acids in Butanol-Acetic Acid-Water (4 : 1 : 1) mixed Solution at 25°C.

Amino Acids	*Rf* Value
Crystine	0.08
Arginine	0.14
Aspartic Acid	0.24
Glutamic Acid	0.31
Asparagine	0.37
Alanine	0.43
Tryptophane	0.60

All of these amino acids are contained in any of the cotton linters, red pine and beech,

4) J.W. Bailey, *Ind. Eng. Chem.*, **30**, 40 (1938); A. Meller. *Paper Trade J.*, **124**, No. 9, 104 (1947); W. Klauditz, *Holz Roh-u Werkstoff*, **4**, 314 (1941); E.J. Lorand and E.A. Georgi, *J. Am. Chem. Soc.*, **59**, 1166 (1937); H. Haas, *Das Papier*, **2**, 397 (1948); R. Bartunek, *Cellulosechemie*, **22**, 56 (1944).

5) F. Ehrlich, *Z. Angew. Chem.*, **43**, 1072 (1930).

Raw cotton linters have been found to contain, besides glucose, about 1.5% arabinose, and a small amount of glactose, glucuronic acid and galacturonic acid.

The amounts of the various amino acids contained in the hydrolyzates of raw cotton linters, red pine and beech are somewhat different from each other, but the kinds of the amino acids are the same and they are assumed to be cystine, aspartic acid, aspargine, arginine, glutamic acid, alanine and tryptophane.

Glutamic acid changes to pyrrolidoncarboxylic acid in the process of hydrolysis of the materials and shows special colorizations reactions with ninhydrin and bromo-phenol-blue indicator.

Purified cotton linters and sulfate rayon pulps treated by alkali cooking do not contain any amino acid, but sulfite rayon pulps contain cystine, alanine and pyrrolidoncarboxylic acid.

Faculty of Engineering,
University of Tokyo, Tokyo

LETTER

Further Notes on Protamines[1]

By Toshio ANDO, Koichi IWAI, Makoto YAMASAKI, Chieko HASHIMOTO, Masami KIMURA, Shin-ichi ISHII and Takaaki TAMURA

(Received June 23, 1953)

It has recently been shown by the present authors[2] that our clupein has alanine as the *N*-terminal residue of the molecule, while salmine has proline. Further investigations showed that all the specimens of our clupein (from *Clupea pallasii* obtained in Hokkaido, Japan in 1947), either prepared by the classical methods of Rasmussen[3] and Felix[4] or by the recent one of Mirsky,[5] or prepared from the material caught in another year (1951), also have only alanine as their *N*-terminal residue.

Furthermore, manometric determination by Van Slyke method of amino nitrogen gave 0.22% N for the free base of clupein (amino N found: 0.1704 mg. from 78.44 mg. clupein. M.W. of clupein calculated therefrom: 6,400), while almost none for salmine (amino N found: 0.0225 mg. from 49.52 mg. salmine, i.e. 0.046% N) in accordance with the fact that the terminal proline gives no detectable amino nitrogen by the present method. This substantiated enough our results above obtained.

The disagreement shown in the *N*-terminal residue of clupein molecule between the result above obtained in our laboratory and that described by German researchers[6,7] who asserted that proline occupied the position, seems to be attributable to the species difference of materials used. One of the latter (Felix) described that *Clupea harengus* was used. It is of interest that a slight difference in species of herrings may cause such a distinction in a part of their sperm protamine molecules. Salmine in its turn, notwithstanding its origins either from the genus *Oncorhynchus* as in Japan[2] (*Onc. keta*) and Canada[8] (*Onc. tschawytscha*?) or from the genus *Salmo* as in Europe[9] (*Salmo salar*?), has always been shown to have proline as the *N*-terminal amino acid.

As for melecular weight, repeated estimations on both protamines by various methods such as methoxyl determinations of the esters (M.W. of clupein: ca. 6,100[10] and 10,800[11], M.W. of salmine: ca. 6,100[10] and 7,300[11]), intensity measurements of absorption near

1) The present paper was read by one of the authors (C.H.) before the symposium on protein structure held on April 26, 1953 in Tokyo University.
2) T. Ando, et al., This Bulletin, **25**, 132 (1952).
3) K. E. Rasmussen, *Z. physiol. Chem.*, **224**, 97 (1934).
4) K. Felix, et al., ibid., **249**, 111 (1937).
5) A. E. Mirsky, et al., *J. Gen. Physiol.*, **30**, 101 (1946).
6) K. Felix, et al., *Z. physiol. Chem.*, **286**, 67 (1950).
7) E. Waldschmidt-Leitz, et al., *Experientia*, **7**, 183 (1951).
8) S. F. Velick, et al., *J. Biol. Chem.*, **191**, 233 (1951).
9) R. R. Porter and F. Sanger, *Biochem. J.*, **42**, 287 (1948).
10) The result of repeated esterifications.
11) The result of once esterification.
12) The similar result has been obtained by means of diffusion-viscosity measurements by K. Iso, T. Kitamura and I. Watanabe in this institute (unpublished).

ultra-violet region of the DNP-derivatives (the former: ca. 5,600~7,200, the latter: ca. 6,100~6,800), electrometric titrations of protamines (the former: ca. 4,600, the latter: ca. 4,400) and also manometric determination of amino nitrogen in clupein as shown above, may lead to the conclusion that both protamines should probably have the molecular weight of nearly the same order[12] (6,000~7,000).

The arginine content in clupein also was successfully determined (87.8±2%) by chromatographic method using Amberlite XE-64 and citrate buffer solution (0.2 *M*, *p*H, 6.50). Further experiments on probable fractionations of protamines and accurate determinations of constituent amino acids are yet in progress. Details will be fully reported later.

Institute of Science and Technology,
Tokyo University, Komaba-machi,
Meguro-ku, Tokyo

A Remark on Solvent Power of Various Solvents for High Polymers

By Toru KAWAI

(Received January 23, 1953)

The process of the interaction of long chain molecules with low molecular weight solvent molecules, which includes solubility, swelling, and plasticization, is of great importance both to research and to industry. The definition of solvent power still lacks precision; namely, the term of "good" or "bad" solvent has been employed vaguely in the discussions of viscosity, osmotic pressure, swelling, and other measurements.

The empirical parameter μ, which was introduced by Huggins[1] in his statistical treatment of high polymer solutions is well used as a measure of thermodynamic interaction between polymer and solvents. Although this parameter μ can be considered as a measure of solvent power, it cannot always explain the experimental results of viscosity, osmotic pressure, and swelling measurements. Indeed, systematic study, choosing various liquids for one polymer substance, reveals that the second virial coefficient in osmotic pressure expression represented by power series expansion in polymer concentrations, intrinsic viscosity and swelling ratio do not always show a good correspondence to the μ values. In this paper we shall analyse the meaning of μ in a more improved and empirically satisfying approximation, considering principally the volume effect of the solvent, and shall examine some experimental results in the light of this procedure.

Analysis of Parameter μ

From the well-known Flory-Huggins' theory of high polymer solutions the partial molal free energy of solvent is expressed by

$$\Delta\bar{F}_1=RT\{\ln(1-v_2)+(1-1/x)v_2+\mu v_2^2\} \quad (1)$$

where v_2 is volume fraction of polymer, and x the volume ratio of polymer molecule to solvent molecule (number average). With the use of Eq. (1) justified to a large measure by experiment, a more careful consideration of the parameter μ is desirable. In the initial statistical treatment of Huggins,[1] μ consisted of a term $1/z'$, introduced from the calculation of the entropy of mixing (z': effective co-ordination number in hypothetical lattice sites[1]), to which was added a contribution from the heat of mixing. As mentioned in the later sections, the necessity of choosing unreasonably low values of z (co-ordination number) to fit the data has lead to abandonment of this original interpretation, but the separation of μ into entropy and heat terms is of quite general validity, and we may write[2]

$$\mu=\mu_S+\mu_H \quad (2)$$

Let us first consider μ_S for athermal solutions. In Table 1 the expressions of μ_S are summarized, being calculated from the results of the statistical evaluation of the entropy of dilution by several authors[1][3][4][5].

Table 1

Theoretical Expression of μ_S by Several Authors

Authors	$\Delta\bar{S}_1$	μ_S
Flory[3]	$-R[\ln(1-v_2)+v_2]$	0
Huggins[1]	$-R[\ln(1-v_2)-(1-1/x)(Z'/2)\ln\{1-)2v_2/Z')\}]$	$(1-1/x)/Z'$
Miller[4]	$-R[\ln(1-v_2)-(Z/2)\ln\{1-(2/Z)v_2(1-1/x)\}]$	$(1-1/x)^2/Z$
Guggenheim[5]	$-R[\ln(1-v_2)-(Zq_1/2)\ln\{1-(2/Zq_2)(x_2-x_1)v_2/x_2)\}]$ $(q=\{x(Z-2)+2\}/Z)$	$(1-1/x)^2/Z$ $(x_2\gg x_1)$

Except Flory's original formulation[3], the theoretical expressions of μ_S are nearly equal to $1/z$. Experimentally μ_S falls between 0.3 and 0.5, far too high to be explained as merely $1/z$. This discrepancy is well interpreted in the following sections by consider-

1) M. L. Huggins, *Ann. N. Y. Acid Sci.*, 43, 1 (1942).
2) Within the accuracy of experiments μ is nearly independent on polymer concentration for many systems, but the μ_S or μ_H is not constant except in very dilute range. Therefore, our discussion is limited to that of high dilution.
3) P. J. Flory, *J. Chem. Phys.*, 9, 660 (1941).
4) A. R. Miller, *Proc. Camb. Phil. Soc.*, 35, 109 (1942); ibid., **39**, 54, 131 (1943).
5) E. A. Guggenheim, *Proc. Roy. Soc.*, A**183**, 203 (1944).

ing chiefly the effect of segment size.

In the case when the heat of dilution is not zero, we must consider the problem of the preferential ordering induced in the solution by difference in the interaction energy. However, it was shown by Orr[6] and Guggenheim[7] that this effect does not introduce a serious error for high polymer solutions, and therefore, we shall neglect this effect for the time being. Thus we must consider the nature of μ_S and μ_H separately, in considerable detail, examining error due to over-simplified approximations or inadequate assumptions in the existing theories, which are not always applicable to the actual systems.

The Effect of Segment Size

In the majority of the existing theories of high polymer solutions, it has been assumed that the unit segment of polymer chain and solvent molecule are the same in shape and size. It requires that a section of the polymer chain which occupies a volume equal to that of one solvent molecule is also not very different in shape from the solvent molecule, and that it is equally free to occupy any one of $(z-1)$ cells in purely stereometric mean without considering the flexibility of the polymer chain. Considering the effect of flexibility of the chain also in addition to the above hindrance, perhaps steric in nature, Flory[8] modified his initial formulation of the entropy of dilution. If the solvent molecule is very small, or if there are limitations on the tortuosity which the chain may comfortably assume, then the size of the section of the chain which is free to orient itself at random, irrespective of the orientation of the preceding sections, may be equivalent to the volume occupied by several solvent molecules. Thus, he constructs a new lattice in which one cell will accomodate either β solvent molecules or one segment of the polymer chain, and obtains the same results as that of the writer[9] when the volume of "segment" is larger than that of solvent molecule as mentioned later. In the earlier papers[9][10], the writer calculated this effect of size and shape of solvent molecule and polymer "segment", and the result obtained may be written (Eqs. (9) and (11) in reference 9),

when $V_1 > V_2$,

$$\Delta\bar{S}_1 = -R\{(V_1/V_2[\ln v_1 + (1+1/x)v_2 + \mu_S v_2^2] + [1-(V_1/V_2)](\ln v_1 + v_2)\} = R[(V_1/V_2 x)v_2 + (1/2 - \mu_S V_1/V_2) v_2^2 + \cdots\cdots] \quad (3)$$

when $V_1 < V_2$,

$$\Delta\bar{S}_1 = -(RV_1/V_2)[\ln v_1 + (1-1/x)v_2 + \mu_S v_2^2] = R(V_1/V_2)[v_2/x + (1/2 - \mu_S)v_2^2 + \cdots], \quad (4)$$

where V_1 and V_2 are molal volumes of solvent molecule and polymer "segment" respectively. Here, we assume the "segment" as a unit submolecule which must be determined by steric factor only[11], and is characteristic to the polymer chain without regard to the types of the solvent, whereas Flory[8] assumed it as a section of the polymer chain which occupies a volume equal to the solvent molecule. Considering that the above approximation of Flory may not be allowed when the section of the polymer chain extremely differs in shape from the solvent molecule the validity of the usual expression of the entropy of mixing, $\Delta S = -R[N_1 \ln v_1 + N_2 \ln v_2]$, fails when the section of polymer chain and the solvent molecule are extremely different in shape from each other even if the molal volumes are the same (See Eq. (8) in reference (9).) It is therefore evident that our assumption on the "segment" is more reasonable than that of Flory. Furthermore, it may be proper that this effect of segment size is separated from the effect of flexibility of the chain as in our treatment. Thus, we can improve the degreeof approximation because the term $(1-2\mu_S)$ may be considered as a probability factor modifying the purely random probability of finding adjacent polymer segments, whereas the Flory's modification was applied to his first approximation treatment[3] of high polymer solutions, which is an obvious oversimplification, as Flory himself recognized. It must be noted here that all the factors except the effect of the "segment" size are involved in μ_S in our treatment, because this treatment is proved to be very useful although it must be regarded as semi-empirical, and the theoretical limitations for further analysis of μ_S are increasingly apparent. In these factors, however, the effect of flexibility of the polymer chain is supposed to play the most important role, and hereafter, we are to employ f instead of μ_S which

6) W. J. C. Orr, *Trans. Faraday Soc.*, **11**, 320 (1944).
7) E. A. Guggenheim, *Proc. Roy. Soc.*, A**183**, 213 (1944).
8) P. J. Flory, *J. Chem. Phys.*, **10**, 51 (1942).
9) T. Kawai, This Bulletin, **25**, 336 (1952).
10) T. Kawai, This Bulletin, **24**, 269 (1951).

11) The types of the hypothetical lattice sites are determined by the stereometric relation between the solvent and the polymer (the shape and size of the solvent molecule and the polymer "segment"). However, the "segment" should be determined uniquely by the stereometric factors of the polymer molecule itself.

was usually employed and which involved the effect of segment size. This parameter f corresponds to the μ_S value theoretically estimated when the polymer segment and the solvent molecule are the same in shape and size (its value is nearly equal to $1/z$)[12], and depends upon properties (mainly flexibility) of the polymer chain alone. Thus, Eqs. (3) and (4) may be rewritten
when $V_2<V_1$,

$$\Delta\bar{S}_1=R[(V_1/V_2x)v_2+\{1/2-(fV_1/V_2)\}v_2^2+\cdots\cdots] \quad (5)$$

when $V_2<V_1$,

$$\Delta\bar{S}_1=R[(V_1/V_2)\{v_2/x+(1/2-f)v_2^2+\cdots\cdots\}] \quad (6)$$

Application of The Above Treatment to The Osmotic, Viscosimetric and Swelling Measurements

We are going to examine the effect of segment size mentioned above on the results of the measurements of osmotic pressure, viscosity, and swelling ratio. Combining the expression of the partial heat of dilution of the solvent,

$$\Delta\bar{H}_1=KV_1v_2^2 \quad (7)[13]$$

with Eqs. (5) and (6), the usually employed μ may be expressed by

$$\mu=fV_1/V_2+KV_1/RT, \quad (8)$$

when, $V_2<V_1$ and

$$\mu=1/2-(V_1/V_2)(1/2-f)+KV_1/RT, \quad (9)$$

when $V_2>V_1$.

Osmotic Pressure: The second virial coefficient, A_2, in osmotic pressure expression represented by power series expansion in polymer concentrations, may be given as follows;

when $V_2<V_1$,

$$A_2=(RT/\rho^2V_1)(1/2-\mu)=(RT/\rho^2\{1/2V_2-f/V_4+K/RT\} \quad (10)$$

when $V_2>V_1$,

$$A_2=(RT/\rho^2\{1/2-f)/V_2+K/RT\} \quad (10)$$

(ρ is density of the polymer). Therefore, the order of magnitude of the A_2, values (accordingly the slope of the line drawn through points of π/C plotted against C) obtained in a series of measurements with a polymer substance and different solvents, may not always agree with that of the $(1/2-\mu)$ values. One of such examples was reported in an earlier paper.[14]

Viscosity: The intrinsic viscosity of dilute solutions of a given high polymer varies with the nature of the solvent. For flexible linear polymers, this variation of intrinsic viscosity may, according to Flory[15], be treated as a swelling phenomenon, and be interpreted in terms of the interaction between solute and solvent molecules, although only the long range interferences between segments belonging to remotely connected portions of the chain were considered in his treatment. In an earlier paper[16] the writer formulated exactly the relation between intrinsic viscosity and the thermodynamic parameter μ. This formulation was exactly equivalent to that for swelling phenomenon. Thus, we shall confine ourselves to show that the above treatment, in which the effect of "segment" size has been considered, can be applied to the formula of swelling equilibrium.[17]

Swelling:—According to Flory-Rehner,[18] when solvent in gel is in equilibrium with excess solvent, the condition attained is that the partial molal free energy of the solvent in the gel equals zero;

$$\Delta\bar{F}_{1g}=\Delta\bar{F}_{1m}+\Delta\bar{F}_{1el}=RT\{\ln(1-v_{2g})+v_{2g}+\mu_g v_{2g}^2\}+RT(\rho V_1/M_c)v_{2g}^{1/3}=0 \quad (12)$$

, where ΔF_{1m} is the osmotic and ΔF_{1el} the elastic contribution to the partial molal free energy. The notation of this equation is similar to what is usually employed.

Here, applying the above effect of "segment" size to Eq. (12), there is obtained

$$\ln(1-v_{2g})+v_{2g}+f(V_1/V_2)v_{2g}^2+(KV_1/RT)v_{2g}^2+AV_1v_{2g}^{1/3}=0 \quad (13)$$

when $V_2<V_1$, and

12) B. H. Zimm, *Am. Chem. Soc.*, Meeting Sept. 1947.

13) For application to the case in which strong mutual energy exists between unlike pairs, the constant K is employed here in a rather empirical meaning, instead of the form $\Delta\bar{H}_1=V_1[(\Delta E_1/V_1)^{1/2}-(\Delta E_2/V_2)^{1/2}]^2$ ($\Delta E_i/V_i$: cohesive energy density).

14) K. Ishikawa and T. Kawai, *J. Chem. Soc. Japan* (Ind. Chem. Section), **55**, 73 (1952).

15) P. J. Flory, *J. Chem. Phys.*, **17**, 103 (1949).

16) T. Kawai, This Bulletin, **25**, 341 (1952).

17) Yamaguchi deduced analogous results concerning the relation between intrinsic viscosity and the nature of solvents from an entirely different procedure (B. Yamaguchi and T. Oki. Paper read at the rheological meeting held by the Chemical society, the High Polymer Society, and the Physical society, on 4th, Dec. 1952, in Tokyo.)

18) P. J. Flory and J. Rehner Jr., *J. Chem. Phys.*, **11**, 512 (1943).

$$(V_1/V_2)[\ln(1-v_{2g})+v_{2g}+fv_{2g}^2]+(KV_1/kT)v_{2g}^2+AV_1v_{2g}^{1/3}=0 \quad (14)^{19)}$$

, when $V_2>V_1$.

Hence,

$$\mu_g=(V_1/V_2)f+KV_1/RT$$

, when $V_2<V_1$, and (15)

$$\mu_g={}^1/_2-(V_1/V_2)({}^1/_2-f)+KV_1/RT$$

, when $V_2>V_1$. (16)

Therefore, when $V_2>V_1$, volume swelling ratio ($={}^1/v_{2g}$) is a function of $({}^1/_2-\mu_g)/V_1$, and is independent upon V_1. When $V_2<V_1$, volume swelling ratio may be determined in somewhat different manner from the case when $V_2>V_1$. These problems will be discussed in the next section in more detail, being compared with experimental results.

Comparison with Experimental Results

Eqs. (13) and (14) will be tested from the measurement of the swelling of Boyer and Spencer[20] on styrene-divinylbenzene gels, which is one of the systematic studies in a large number of liquids differing widely in chemical type and in solvent power for a gel sample. In Table 2, one of their experimental results is analysed, attempting to show the better correspondence of the observed volume swelling ratio ${}^1/v_{2g}$ with $({}^1/_2-\mu_g)/V_1$ calculated from the above procedure, rather than with the parameter μ_g which have been usually interpreted in terms of the Flory-Rehner theory.

Table 2

Swelling of 0.0333% Divinyl Benzene Gels in Various Solvents at 23°C.

Solvents	Volume Swolling Ratic	μ_g	$(1/2-\mu_g)/V_1 \times 10^4$	$(1/2-\mu_g+\Delta\mu)/V_1\times 10_4$	V_1
Phenyl Cyclohexane	18.57	0.417	4.85	6.02(14)	171
sym-Tetrachloroethane	23.92	0.417	7.83	9.72 (1)	106
Styrene	21.96	0.424	6.61	8.35 (5)	115
Phenyl Acetylene	22.43	0.426	6.73	8.54 (4)	110
o-Xylene	20.98	0.427	6.03	7.69 (7)	121
m-Xylene	20.02	0.433	5.45	7.07 (9)	123
p-Xylene	19.63	0.436	5.18	6.80(11)	124
Toluene	20.72	0.440	5.63	7.51 (8)	107
Trichloroethylene	21.84	0.444	6.23	8.45 (6)	89.9
Thiophene	22.99	0.450	6.31	8.83 (2)	79.3
cis-Dichloroethylene	22.49	0.453	6.19	8.82 (3)	75.9
Cyclohexanone	19.08	0.453	4.53	6.45(13)	104
Tetrahydrofuran	21.0	0.455	2.18	3.00	217
Dimethylfuran	18.00	0.458	2.87	5.71(16)	104
sym-Triethylbenzene	13.72	0.458	2.27	3.35(18)	103
Perchlorethylene	18.31	0.459	3.99	5.93(15)	120.9
Pyridine	19.82	0.464	4.46	6.94(10)	80.7
Ethylidene Chloride	18.41	0.469	0.83	1.37	372
trans-Dichloro-1-nitroethane	19.24	0.469	3.70	6.08(12)	83.8
Nitrobenzene	15.72	0.475	2.44	4.39(17)	103
Aniline	11.99	0.503	−0.33	1.86(19)	91.4
Diethyl Carbonate	10.79	0.503	−0.25	1.40(20)	122
Ethyl Chloroacetate	10.29	0.510	−0.94	0.94(22)	106
r-Valerolactone	10.96	0.510	−1.10	1.10(21)	91.0
Propylene Oxide	12.7	0.590	−14.4	−1.01	69.4
Ethyl Laurate	65.3	0.570	−2.63	−11.5	266

The order of magnitude of the volume swelling ratios for the liquids given in Table 2 does not always correspond to that of the μ_g valves[21]. On the other hand, the order of their magnitude shows a better correspondence with that of the $({}^1/_2-\mu_g)/V_1$ values. (The larger the $({}^1/_2-\mu_g)/V_1$ values, the greater

19) Speculation of the "network" theory of Flory-Rehner leads to the conclusion that ΔF_{el}, the elastic contribution to the partial molal free energy, should be expressed by the form $AV_1v_{2g}^{1/3}$, where A is a constant characteristic to the network structure, rather than by the form $(\rho V_1/M_c)v_{2g}^{1/3}$, which involves M_c explicitly.

20) R. F. Boyer and R. S. Spencer, *J. Polymer Sci.*, **3**, 97 (1948).

21) In many cases, the molal volumes of solvents do not differ very much from each other, and in such cases, the order of magnitude of the volume swelling ratios agrees with that of the μ_g values.

the solvent power, whereas the smaller the μ_g, the greater the solvent power.)

However, the regularity of this correspondence fails for a few liquids which are given under the line of ethylchloroacetate in Table 2. These discrepancies are completely removed by applying the following correction. In an earlier paper[22] it was pointed out that the values of μ_g calculated from swelling measurements are usually larger than those of μ obtained by osmotic measurements, and that, generally, the magnitude of these discrepancies is about 0.02[22] (which was determined approximately from many experimental results). These corrected values, $(1/2-\mu_g+\Delta\mu)/V_1$, are given in the fourth column in Table 2, where the number in the parentheses shows the order of magnitude of these values. A satisfactory correspondence is obtained between the volume swelling ratio and these values, whereas such a complete correspondence fails for the μ_g values. Now, there are three exceptional cases of tetrahydrofran, ethyl laurate and ethyliden chloride, in which the V_1 values are much larger than in the other cases. This exception may be well interpreted by Eq. (15), although the solvent power of these three liquids cannot be compared with that of the other liquids due to the uncertainty of the V_2 value[23].

This paper was read at the Meeting of Soc. of High Polymer, Japan, in Kanazawa, on 8th Nov., 1952.

The author expresses his apprecation to Professor H. Maeda and K. Makishima for their encouragement and support of this work.

Laboratory of Textile Chemistry,
Tokyo Institute of Technology, Tokyo

22) T. Kawai, This Bulletin, **24**, 691 (1951). Probably, these discrepancies are due to over-simplification in the network theory of Flory (See P. J. Flory, *J. Chem. Phys.*, **18**. 108 (1950).

23) In the writer's opinion, the V_2 values should be determined through systematic study of experimental results, employing Eqs. (15) and (16). In this experiment of Boyer and Spencer, available data is too scanty to discuss quantitatively the case of $V_2>V_1$. From Table 2, the value of V_2 of this polymer is supposed to be about 100. It must be noted, however, that Eq. (16) may hold approximately even in the range $V_1>V_2$ so long as the difference between V_1 and V_2 is not considerably large, because the μ value should, according to Eqs. (15) and (16), decrease as V_1 increases ($V_1<V_2$), and become equal to that calculated from Eq. (1) when $V_1=V_2$, and then increases ($V_1>V_2$).

Studies of Molecular Structures by Electron Diffraction. I. The Molecular Structure of Monofluoro- and Monobromobenzenes

By Tooru YUZAWA (†) and Mashio YAMAHA

(Received February 26, 1953)

The molecular structures of monofluoro- and *o*-difluorobenzenes with regards to the C-F distance from the resonance theory were investigated by Dr. H. Oosaka[1] using electron diffraction method. Recently a new apparatus which is capable of giving photographs of large scattering angle diffraction pattern has been constructed in our laboratory. We have reinvestigated the molecular structure of monofluorobenzene and also investigated the structure of monobromobenzene and determined the lengths of C-F, C-Br and C-C bonds using this new apparatus.

Experimental

The new apparatus is of the vertical hot cathode type, and the accelerated electron beam from the cathode is focused by an electromagnetic coil. The camera length is about 91 mm. The wave length of the electron beam is 0.062~0.054 Å, which is calibrated by the gold photographs.

Monofluorobenzene (boiling point: 85.0°C.) was synthesized[2] by the following reaction:

$$C_6H_5NH_2+HBF_4+NaNO_2 \xrightarrow[\text{ice cold}]{HCl} C_6H_5N_2BF_4 \xrightarrow{heat} C_6H_5F+N_2\uparrow+BF_3\uparrow.$$

Commercial monobromobenzene was purified by distillation. (Boiling point: 154.0°C.).

Results and Discussion

The theoretical intensity curves for several assumed molecular models have been calculated by the formula[3],

$$I=k\sum_i\sum_j Z_iZ_j/r_{ij}\cdot\exp(-b_{ij}q^2)\cdot\sin qr_{ij},$$

where $q=10s/\pi, s=(4\pi\sin\theta/2)/\lambda$, θ the scattering angle, and λ the wave length of the beam. The thermal vibration factore exp $(-b_{ij}q^2)$ is ignored here[4].

In Table 1 are shown the assumed interatomic distances of the molecular models with marks from A to H for fluorobenzene and from J to O for bromobenzene. The coplanarity of the benzene ring and the attached halogen atom is assumed for all models. The visual intensity curves of ten or more photographs of each substance are compared with the theoretical curves in Figs. 1 and 2. The q-values at the measured maxima and ratios $q/q_{obs.}$ with the deviations of the theoretical q-values from the observed are listed in Tables 2 and 3 for each substance.

Table 1

Assumed Molecular Models Corresponding Interatomic Distances (cf. Figs. 1 and 2)

	C—C	1.38	1.40	1.42 (Å)
C—F:	1.27 (Å)	A	D	
	1.31	B	E	(H)
	1.35	(C)	F	
C—Br	1.86	J	L	(N)
	1.88	K	M	O

In order to determine the consistent molecular models, we have compared the shapes and q-values of maxima of theoretical curves. and found the following characteristic features

For monofluorobenzene, 1) the 7th maximum is influenced by C—C distance variation, 2) the 4 th and the 6 th maxima, and the separation between the 3rd and the 4th change by C—C and C—F distances, and 3) the shape of the 9th and the 10th maxima has the characteristic feature for C—F variation, and it also depends slightly on the thermal vibration of the molecule (See Fig. 1).

For monobromobenzene, 1) generally, the q-values of intense maxima shift sligtly by the variation of C—C distance, and 2) the 6th, 8th and 11th maxima as well as the shape of the 4th maximum change with C—Br (See Fig. 2).

These considerations lead us to the conclusion that:

1) H. Oosaka, This Bulletin. **15**, 31 (1940). cf. C. Finbak & O. Hassel, *Arch. Math. Naturvidenskab*, **45**, No. 3,8 (1941).

2) "Organic Synthesis" XIII. p. 46.

3) R. Spurr and V. Schomaker, *J. Am. Chem. Soc.*, **64**, 2693 (1942). cf. L. Pauling and L. O. Brockway, *J. Am. Chem. Soc.*, **57**, 2684 (1935).

4) The influence of various thermal vibrations is small as will be seen in our next report on difluorobenzenes (5).

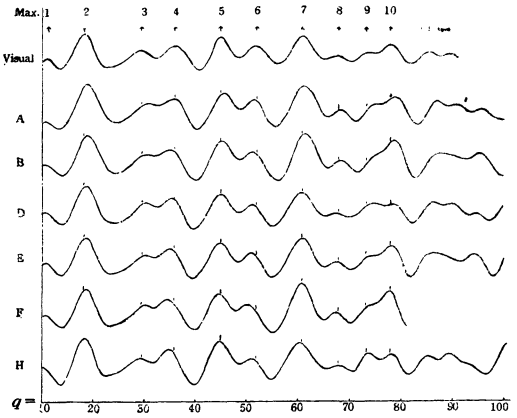

Fig. 1. Theoretical and Visual Intensity Curves for Monofluorobenzene.
The measured q-values of maxima are shown by arrows and dots on each curve. (These are the same in Fig. 2.)

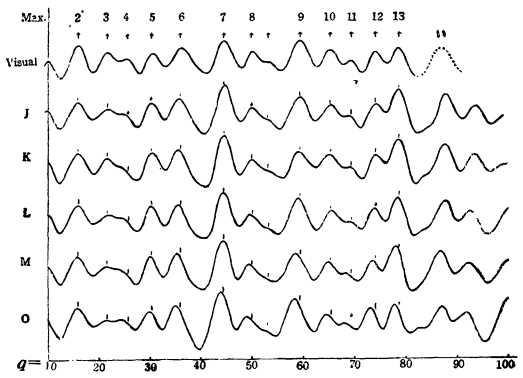

Fig. 2. Theoretical and Visual Intensity Curves for Monobromobenzene

Table 2

Observed q-values and the Comparison of Measured and Theoretical Values for Monofluorobenzene.

Models		A	B	D	E	F	
Max.	$q_{obs.}$	q/q_o dev. (q's)	q/q_o dev. (q's)	q/q_o dev. (q's)	q/q_o dev. (q's)	q/q_o dev. (q's)	wt.
1	11.05	— —	— —	— —	— —	— —	
2	18.05	1.042+0.75	1.042+0.75	1.036+0.65	1.025+0.45	1.019+0.35	1
3	29.35	1.048+0.41	1.024+0.7	1.031+0.9	1.028+0.8	1.024+0.7	1
4	35.80	0.997−0.1	0.986−0.5	0.989−0.4	0.972−1.0	0.964−1.3	2
5	44.80	1.018+0.8	1.011+0.5	1.009+0.4	0.998−0.1	0.996−0.2	2
6	51.90	0.990−0.5	0.983−0.9	0.981−1.0	0.976−1.2	0.970−1.5	1
7	60.66	1.012+0.9	1.011+0.6	0.996−0.2	0.996−0.2	0.996−0.2	2
8	67.62	1.012+0.8	1.012+0.7	1.004+0.3	0.999−0.1	0.998−0.1	1
9	diffuse						
10	77.31	1.023+1.4	1.017+0.9	1.015+0.7	1.009+0.3	1.001−0.3	1
*							
mean av.		1.017_8	1.010_6	1.007_5	1.000_2	0.995_2	
av. dev.		0.014_9	0.013_1	0.015_2	0.016_0	0.014_8	
wt. mean av.**		1.015_5	1.008_6	1.004_9	0.997_0	0.993_1	
mean sq.av.dev.		0.78	0.63	0.58	0.68	0.76	

* See Fig. 1. for outer halos.

** Used weights for each maximum are shown in the last column. In these average values the contribution of the C-C variation is predominant.

Table 3

Observed q-values and the Comparison of Measured and Theoretical Values for Monobromobenzene.

Models		J	K	L	M	O
Max.	$q_{obs.}$	q/q_o dev. (q's)	q/q_o dev. (q's)	q/q_o dev. (q's)	q/q_o dev. (q's)	q/q_o dev. (q's)
2	15.97	1.005+0.08	0.996−0.07	0.996−0.07	0.989−0.17	0.989−0.17
3	21.56	1.020+0.4	1.007+0.14	1.011+0.24	1.009+0.19	1.011+0.24
4	25.65	— (−0.6)	— —	— —	— (−0.8)	— —
5	30.40	1.007+0.2	1.005+0.15	0.997−0.1	0.993−0.2	0.987−0.4
6	35.97	0.997−0.12	0.988−0.42	0.990−0.37	0.988−0.42	0.979−0.8
7	44.47	1.005+0.2	1.002+0.1	0.997−0.12	0.996−0.2	0.991 —
8	49.95	1.001+0.15	0.999−0.05	0.994−0.3	0.989−0.5	0.979−0.8
	shelf					

9	59.44	$1.003+0.06$	$0.994-0.3$	$0.991-0.5$	$0.986-0.8$	$0.982-1.1$
10	65.30	$1.006+0.4$	$0.997-0.2$	$0.999-0.05$	$0.992-0.5$	$0.989-0.8$
11	69.40	$0.996-0.3$	$0.994-0.4$	$0.994-0.4$	$0.987-0.9$	$0.984-1.1$
*						
mean av.		1.004_4	0.997_9	0.996_6	0.992_3	0.989_0
av. dev.		0.004_7	0.004_2	0.004_0	0.004_9	0.005_6
mean sq. av. dev.		0.24	0.24	0.28	0.48	0.74

* See Fig. 2 for outer halos.

C—F = 1.30±0.03 Å for monofluorobenzene, C—Br = 1.86±0.02 Å for monobromobenzene, and C—C = 1.39±0.02 Å for the both.

This C—F length of monofluorobenzene is shorter than the previously reported value 1.34 Å[1], but is more accurate since the outer halos are taken into account in this case. We are investigating the carbon-halogen distances of various halogenated benzenes containing fluorine atom. For instance, the value 1.30 Å for C—F bond are obtained for *m*- and *p*-difluorobenzenes[5].

The Pauling formula, which shows the shortening of the bond length in the molecule with resonance structures, is

$$R = R_s - (R_s - R_d)\,(3x/2x+1),$$

where x is the double bond character, R_s and R_d are the interatomic distances[6] for a single and double bond respectively, and R is the resultant intermediate distance. The values of x estimated from our observed bond lengths are 29% for C—F of monofluorobenzene and 25% for C—Br of monobromobenzene. If we use the corrected values of R_s, 1.355 Å for C—F and 1.883 Å for C—Br, which are the length of the normal single bond proposed by Pauling and Schomaker[7], we obtained 16.9% for C—F and 13.3% for C—Br.

5) Published shortly (we have investigated for p- and o-fluorochlorobenzenes, p-fluorobromobenzene and m- and p-difluorobenzenes).

6) L. Pauling, "The Nature of the Chemical Bond" p. 175 (1940).
R_S=1.41Å, 1.91Å for C-F, C-Br respectively, and R_d=1.21Å, 1.81Å for C=F, C=Br respectiveiy.

7) L. Pauling and V. Schomaker, *J. Am. Chem Soc.*, **63**, 37 (1941).
$R_{AB}=R_A+R_B-\beta|x_A-x_B|$, values for C-F, C-Br bonds are as follows:
R_C=0.77Å*, R_F=0.72Å, R_{Br}=1.14Å*, x_C=2.5, x_F=4.0, x_{Br}=2.8, β=0.09. C-F: 0.77+0.72—0.09(4.0—2.5)=1.355Å, C-Br: 0.77+1.14—0.09(2.8—2.5)=1.883Å.
* proposed by Pauling and Huggins.

Summary

The molecular structures of monofluorobenzene and monobromobenzene have been investigated by the electron diffraction method. The C—F and C—Br distances in each molecule have been determined as 1.30±0.03 Å and 1.86±0.02 Å respectively. These distances are shorter than the case in which the bonds have the normal single bond characters. The double bond characters for these bonds have been calculated and obtained 16.9% for C—F and 13.3% for C—Br, in which we have considered the corrected single bond lengths in both cases.

Acknowledgment

We would express our deep gratitude to the late Professor H. Oosaka for his guidance, especially for having suggested to us the study of this problem; to Mr. M. Tanaka, Director of Kichô Shindôsho Factory, for having offered to us very useful material for the construction of the apparatus; and also to Mr. S. Uchida for his kind help in its actual construction.

Department of Chemistry, Faculty of Science, Tokyo University of Education, Tokyo

New Colorimetric Microdetermination of Vanadium in Natural Waters*

Ken SUGAWARA, Motoharu TANAKA and Hideo NAITÔ

(Received March 2, 1953)

I. General description

A new colorimetric method of the determination of vanadium was established which allows to separate and determine a few μg. of this element with a two figure accuracy from a bulk of water as large as 20 liters.

The procedure consists of three main steps: (1) Coprecipitation of the element with ferric hydroxide. (2) Separation of vanadium from the coprecipitant and other accompanied elements. (3) Final colorimetry of vanadium oxinate in amyl alcohol.

The concentration by coprecipitation saves much time, which is required in the ordinary evaporation method, and avoids at the same time loss of vanadium into a large bulk of residue, produced when the latter method is applied.

The intense coloration of vanadium oxinate in amyl alcohol makes the determination of a few μg. of the element possible[1], a quantity lying close to the limit in the current phosphotungstovanadate method[2].

II. Procedure

Step 1. Take a sample of 5 to 20 liters depending upon the probable content of vanadium. Acidify with hydrochloric acid, add ferric nitrate solution to give a solution containing 10 mg. of iron per liter and then 1 cc. of 1 M sodium hypochlorite solution per one liter. While warming on a water bath the solution is neutralized with 2 N ammonium hydroxide to bromthymol blue or bromcresol purple and then filtered.

Step 2. Ignite the paper and its contents in a platinum crucible. The ash is ground with 3 g. of anhydrous sodium carbonate in an agatemortar, transferred in a platinum crucible and fused for 40 to 60 minutes by a full burner. The cake obtained is transferred into a small beaker and the crucible is rinsed with hot water. Add 2 to 5 drops of hydrogen peroxide, then 30 to 40 cc. of water in order to digest the entire mass. When digestion is complete, the contents of the beaker are filtered through a small filter paper of fine texture which is previously washed with 20% hot solution of sodium carbonate. Wash the residue with hot 2% sodium carbonate solution.

Step 3. The joint filtrate is neutralized to p-nitrophenol by sulfuric acid in expelling the liberated carbon dioxide. Add 2.5 cc. of 4 N sulfuric acid in excess and set the solution aside to cool to room temperature. Add 1 cc. of 5% malonic acid solution and 0.5 cc. of 2% oxine solution. The whole is transferred into a separatory funnel and mixed with 4 cc. of 4 N sodium acetate for buffer with constant stirring. Add 3 cc. of chloroform, shake for one minute and the layers are left to separate. The chloroform layer is drawn off into a platinum crucible. Add 1 cc. of chloroform to the funnel to wash its stem. Then 2 cc. of chloroform and 0.2 cc. of oxine solution are added. Shake vigorously. After leaving it to stand still, the chloroform layer is drawn out into the platinum crucible. Two to three extractions are sufficient to remove all the oxinate when the last chloroform extract remains faintly yellowish due to oxine itself.

Step 4. Add 1 g. of sodium carbonate to the united chloroform extract, evaporate to dryness at a lower temperature on a water bath. The residue is heated by a burner in order to destroy the organic matter and finally fused by a full burner.

Step 5. The melt is digested with water, filtered and neutralized to p-nitrophenol. Adding 1 cc. of 4 N sulfuric acid, the solution is once heated to boil and left with immersing in cold water. The volume of the solution is made up to 70 to 100 cc. Add 0.5 cc. of the oxine solution and 6.0 cc. of 2 N ammonium hydroxide with constant stirring. In case any white precipitate is formed, the solution should be diluted till it dissolves. Transfer the solution into a separatory funnel, add 10 cc. of benzene and shake vigorously for one minute. Two benzene extractions remove ferric oxinate completely.

Step 6. The remaining aqueous layer is mixed with 4 cc. of sodium acetate solution and 4.5 cc. of 4 N sulfuric acid, whereby the pH is adjusted to about 4.

Add 0.2 cc. of the oxine solution and extract with amyl alcohol. The extraction is repeated till the final fraction bears no perceptible coloration. The united extract is transferred into a

---

* The following two methods have been proposed for similar purposes: (1) M. Ishibashi, T. Shigematsu and Y. Nakagawa, *Bull. Inst. Chem. Research*, Kyoto Univ., Kyoto Japan. **24**, 68 (1951), (2) J. M. Bach and R. A. Treiles, *Bol. obras sanit. nacion Buenos Aires*, **5** 127 (1941); *Chem. Abstracts*, **36**. 859 (1942); ibid., **35**, 545 (1941). In the former vanadium is coprecipitated with ferric cupferronate and determined by the current phosphotungstovanadate method, while in the latter the oxinate is extracted by isoamyl alcohol.

1) E. Sudo, *J. Chem. Soc. Japan*, **72**, 817 (1951).

2) E. B. Sandell, "Colorimetric Determination of Traces of Metals" Interscience Publishers Inc. New York, p. 607 (1950).

10 cc. measuring flask and diluted to the mark with amyl alcohol. Then the optical density of the solution is determined by the spectrophotometer at wavelength of 475 mμ.

III. Discussion

1) Ferric hydroxide as coprecipitant.—The recovery of vanadium in the coprecipitation with ferric hydroxide is practically 100% at the *pH* ranges of bromthymol blue and bromcresol purple. The following experiment showed this.

Various amounts of iron and vanadium were added to dilute hydrochloric acid solution, neutralized with ammonium hydroxide to different kinds of indicator whose *Hp* ranges differ. The vanadium content of the formed precipitate was determined (See Table 1).

Table 1

Optimum *pH* Range for the Coprecipitation of Vanadium with Ferric Hydroxide

Indicator	*pH* range	V added μg.	V found μg.	Error %
Methyl orange	3.1—4.5	27.9	26.0	−6.8
Bromcresol purple	5.2—6.8	27.9	28.0	+0.4
Bromthymol blue	6.0—7.6	27.9	28.1	+0.7
Phenolphthalein	8.0—9.8	27.9	26.7	−4.3
Ammonia in excess		27.9	26.4	−4.7

It is also notable that five dissolution-precipitations of the precipitate did not give any loss.

2) Amount of iron required for the complete precipitation of vanadium.—Seven mg. of iron per liter is sufficient to precipitate 0—27.9 μg. of vanadium and an amount up to 150 mg. gives no interference. Table 2 shows it.

Table 2

Coprecipitation of Vanadium with Ferric Hydroxide

Fe added mg.	V added μg.	V found μg.	Error %
150	0	< 1.0	
150	27.9	26.8	− 3.9
100	27.9	27.6	− 1.1
50	27.9	27.6	− 1.1
10	27.9	28.1	+ 0.7
10	27.9	28.3	+ 1.4
10	27.9	28.0	+ 0.4
7	27.9	27.9	0.0
7	27.9	28.1	+ 0.7
5	27.9	26.2	− 6.1
5	279	239	−14.3
2	27.9	17.8	−36.2
0	27.9	1.3	−95.4

3) Separation of iron from vanadium.—Oxine gives colored compounds with various kinds of elements other than vanadium, which can be extracted by organic solvents. Thus careful separations of these elements are required to precede a successful determination of vanadium.

Iron is the first to be considered, its separation being caused at two different stages in the writers' procedure; (1) leaching process of the melt of carbonate fusion and (2) oxinate extraction by benzene.

According to E. B. Sandell the recovery of vanadium at (1) is complete for silicate materials. The writers confirmed it on melts particularly rich in iron as shown in Table 3

Table 3

Separation of Vanadium from Iron in Step (1)

Fe added mg.	V added μg.	V found μg.	Error %
50	27.9	27.7	−0.7
50	27.9	27.6	−1.1
150	0	<1.0	

In order to check the point (2), the following experiment was done.

Different amounts of iron and vanadium were added to a series of 50 cc. waters, containing 3 g. of sodium carbonate, which were divided into four groups to be treated in different ways. Group 1. After being neutralized with sulfuric acid to phenolphthalein, oxine was added and the formed ferric oxinate was separated by shaking with benzene. Groups 2 and 3. After being neutralized with sulfuric acid, 1 cc. and 0.5 cc. of 2 *N* sodium carbonate solution were added respectively and then oxine. The formed oxinate was

extracted by benzene. Group 4. 1 cc. of 4 *N* sulfuric acid was added in excess after it was neutralized. Oxine was then added and the solution was made alkaline with 6 cc. of 2 *N* ammonium hydroxide. The formed oxinate was extracted. The residual solutions from the four different treatments were regulated to *pH* 4 with a mixture of sulfuric acid and sodium acetate, then extracted by amyl alcohol. Vanadium was determined in the extract. Table 4 shows the result in which Group 4 gives the best result.

Table 4

Separation of Vanadium from Iron in Step (2)

	Fe added μg.	V added μg.	V found μg.	Error %
Group 1	0	55.8	55.0	− 1.4
	0	0	<1.0	
	100	55.8	47.3	−13.7
Group 2	0	55.8	55.1	− 1.3
	100	0	<1.0	
	100	55.8	55.1	− 1.3
	100	55.8	61.3	+ 9.9
Group 3	100	55.8	54.0	− 2.9
	100	55.8	55.0	− 1.4
Group 4	100	55.8	56.0	+ 0.4
	100	55.8	55.9	+ 0.2
	100	55.8	55.8	0
	100	55.8	56.3	+ 0.9

4) **Interference by other elements.**—Aluminum, manganese and silicon are other elements which are usually encountered in tural waters and coprecipitated with iron, thus probably causing some interference.

Aluminum.—A greater part of aluminum moves into the filtrate, when the melt from carbonate fusion is leached and expected to be extracted by organic solvents, in forming oxinate at a *pH* range 4.5—9.8[3]. The oxinate formation, however, can be avoided by masking the element with malonic acid in a slightly acidic solution. The following experiment shows it.

A series of acid solutions containing various amounts of vanadium, 10 mg. of aluminum and 50 mg. of iron was treated with ammonium hydroxide. The precipitates obtained were processed following the steps 2—6 in the procedure to determine vanadium. The result is given in Table 5.

Manganese.—Manganese is reduced by hydrogen peroxide to form precipitate in step 2 of the procedure. In case the manganese content is large, there may form a large bulk of precipitate with a considerable retention of vanadium. However it was shown that an amount of manganese up to 50 mg. does not matter as shown in Table 5.

Table 5

Interferences by Aluminium and Manganese

		Fe added mg.	V added μg.	V found μg.	Error %
Al	10 mg.	50	0.0	<1.0	
	„	„	27.9	27.7	−0.7
	„	„	11.2	10.9	−2.7
	„	„	5.6	5.5	−1.8
Mn	5 mg.	10	27.9	27.9	0
	50	„	27.9	26.4	−5.4

3) E. Sudo, *J. Chem. Soc. Japan*, **72**, 718 (1951).

Table 6

Examples of Application

Description	Sample taken	V added	V found
Ground water rich in silicate from a well in the campus of Nagoya University (126 mg. SiO_2/L)	10 L		13.7 μg.
	10 „	11.2 μg.	24.6 „
Surface water of Lake Yogo-ko, Shiga Pref. (Aug., 1951)	20 „		8.9 „
Surface water of Lake Kizaki-ko, Nagano Pref. (Dec., 1952)	20 „		3.9 „
A spring water from Higashiyama area, Nagoya City	20 „		0.8 „
Bottom deposits of Lake Yogo-ko	24.7 mg.		0.018%*
	24.7 „		0.017 „
	24.7 „		0.018 „

* by the current phosphotungstovanadate method.

Silicon.—Silicon in the water is coprecipitated with iron and separates as jelly, when the melt from carbonate fusion is leached and neutralized, thus any vanadium is probably retained. However the retention does not occur so long as the silica content of the water does not exceed 126 mg. per liter: an analysis of a 10 liter sample of well water originally containing 1.26g. of SiO_2 and 13.7 μg. of vanadium, with an additional 11.2 μg. of the latter element, gave a satisfactory vanadium value, 24.6 μg. (See Table 6).

5) **Colorimetry.**—The following is notable concerning the colorimetry of vanadium oxinate in amyl alcohol.

a) The Lambert-Beer's law is strictly obeyed from 0.00 up to 10.0 μg. of vanadium per ml. In case the optical density at 475 mμ is measured, using "Coleman model 14 Universal spectrophotometer", the following relation holds good;

$$X = \frac{E - 0.023}{0.0117}$$

where X—the amount of vanadium in μg. per 10 ml. of amyl alcohol
E—the optical density when an accessory "round cuvette", with effective cell thickness 13.06 mm., is used

b) The color developed undergoes no measurable change within 24 hours.

c) The recovery of vanadium by extraction depends largely on the quality of amyl alcohol. Hence a careful purification of amyl alcohol is needed and a preliminary test of its quality by extracting a known amount of vanadium is recommended.

6) **Appilcation to silicate materials.**—The present method, originally developed for water analysis, may be applied to common silicate materials. An example of its application to the bottom deposits of Lake Yogo-ko, Shiga Prefecture, is given in comparing with the value for the same sample by the current phosphotungstovanadate method at the bottom of Table 6, in which some data for terrestrial waters are collected.

The writers wish to express their deepest thanks to the Trustees of the Elizabeth Thompson Science Fund who decided to donate a grant for supplying the Faculty of Science, Nagoya University, with a universal type Coleman spectrophotometer by the aid of which the present research was accomplished.

Chemical Institute, Faculty of Science, Nagoya University

The Crystal Structure of Chlorodinitro-triammine-cobalt. III.

By Yoshimichi TANITO, Yoshihiko SAITO and Hisao KUROYA

(Received March 18, 1953)

Introduction

In the absorption spectra of aqueous solution of chlorodinitrotriammine-cobalt III, $[Co(NH_3)_3(NO_2)_2Cl]$, the third absorption band was found at $\lambda = 2500$Å with log $\varepsilon = 4.4$[1], and therefore, it has been postulated that two of the negative radicals are co-ordinated in trans-positions with respect to each other. Since there are three negative ligands in the molecule, there remain the following two possibilities about the configuration of this molecule as shown in Fig. 1.

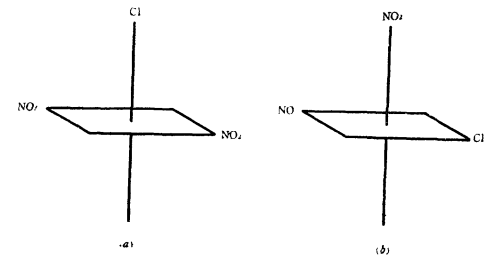

Fig. 1 Two possible forms of $[Co(NH_3)_3(NO_2)_2Cl]$, having two negative radicals in *trans* positions.

1) M. Kobayashi, A. Hagitani, and I. Mita: *J. Chem. Soc. Japan*, 58 (1937) 391.

In order to decide between (a) and (b) we have attempted to investigate the crystal structure of this compound by means of X-rays.

Unit Cell and Space Group

Chlorodinitro-triammine-cobalt (III) was prepared from trinitro-triammine-cobalt (III) and hydrochloric acid according to the method described by Jörgensen.[2] The crystals for this work were grown by slow evaporation of saturated aqueous solution containing a small amount of acetic acid at about 20° C. in a dessicator containing calcium chloride.

They are dark red tetragonal bipyramids, the effective dimensions of which are 0.4 mm. in each dimensions.

Making use of these crystals, oscillation photographs were taken around the [110] and [001] axes.

The unit cell dimensions were found from high order reflections. They are:

$$a=9.87\pm0.02\ \text{Å},\quad c=16.51\pm0.05\ \text{Å}.$$

The unit cell contains eight formula units. The calculated density is 1.961 g./cc., whereas the observed value was 1.952 g./cc. determined at 10°C. by the pyknometer method.

The Laue symmetry was found to be C_{4h}-$4/m$.

The systematic absences are: (hkl) present only with $h+k+l=$even, $(hk0)$ present only with $h=2n$, $k=2n$, and $h+k=4n$, and $(00l)$ present only with $l=4n$, so that the space group is C_{4h}^{6}-$I4_1/a$.

The intensities of the diffraction maxima were estimated visually by comparison with a time-exposure calibrated standard and converted into structure amplitudes in the usual way, which were later placed on an absolute scale by comparison with the calculated values.

Analysis

The space group $I4_1/a$ possesses sixteen general positions, and since the unit cell contains eight units of $[Co(NH_3)_3\ (NO_2)_2\ Cl]$, it may be concluded that 16 N (nitro), 16 N (ammonia), and 32 O probably lie in general positions, while the other 8 Co, 8 Cl and 8 N ammonia) must occupy special positions.

The possible eight fold special positions for these Co, Cl and N atoms are: $(00z)$, etc., which lie on two fold axes, sets of symmetry centres at (0, 1/4, 1/8), etc., or (0, 1/4, 5/8) etc., or otherwise, two sets of four fold positions at (000), $(00\frac{1}{2})$, etc., in the four fold inversion axes.

It is quite natural to assume an octahedral co-ordination around a cobalt atom as shown in Fig. 1.

Since the symmetry $\bar{1}$ and also $\bar{4}$ cannot be achieved by any octahedral arrangement of the ligands around a central atom, it may be concluded that the cobalt atom lies on a two-fold axis, having two NO_2 and two NH_3 groups in trans-positions with respect to each other, and a Cl atom and one NH_3 group being on the two-fold axis (Fig. 1 (a)).

A trial model of a molecule was derived from the knowledge of interatomic distances and bond angles found in our previous works on cobaltic complexes.[3][4][5] The approximate coordinates for those atoms which lie on the symmetry axis were easily deduced from packing considerations.

A Patterson projection P (xy) was synthesized, from which the azimuthal orientation of the complex molecule could be readily deduced.

Approximate coordinates for all the atoms were then written down, and the structure amplitudes for about 60 planes $(hk0)$ and $(h0l)$ were calculated. The agreement was reasonably good, and enabled a start to be made with the process of refinement by means of Fourier syntheses. These parameter values were used for a calculation of the signs of the $F(hkl)$ values, the origin of coordinates being shifted on a center of symmetry at (0, 1/4, 1/8).

Successive refinement of these parameter values was made by two dimensional Fourier syntheses $\rho(xy)$ and $\rho(xz)$. Then Fourie syntheses along lines parallel to the c-crystal axis were made at the values of x and y obtained from the two-dimensional projection. It was found that the maxima on these lines were sharp, and by taking these new maxima as new z-coordinates and then repeating the process of structure amplitude calculation and Fourier syntheses, refinement was achieved fairly rapidly. After five stages of these refinement processes all the $F(hkl)$ values were involved in a final set of line syntheses. One of the results is shown in Fig. 2. Finally, all the structure amplitudes were inserted as terms of a three-dimensional Fourier syntheses which was computed in sections perpendicular to c axis at the values obtained in the line syntheses for Co, $O_{(1)}$ and $O_{(2)}$. The result is shown in Fig. 3. The final parameter values obtained from these Fourier syntheses are listed in Table 1.

2) S. M. Jörgensen: *Z. anorg. Ch.* **7**. 310 (1894); **13**, 180 (1897).

3) Y. Tanito, Y. Saito and H. Kuroya: This Bulletin, **25**, 188 (1952).

4) Y. Tanito, Y. Saito and H. Kuroya: This Bulletin, **25**, 328 (1952).

5) A. Nakahara, Y. Saito and H. Kuroya: This Bulletin, **25**, 331 (1952).

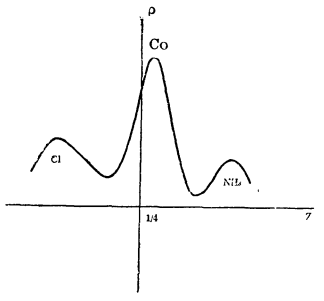

Fig. 2 Electron density along *a* two-fold axis, showing positions of Cl, Co and NH_3

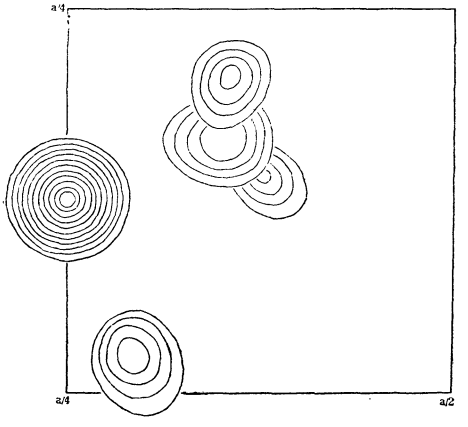

Fig. 3 Superposition of three-dimensional Fourier sections for [Co $(NH_3)_3$ $(NO_2)_2$ Cl]. Those for Cl and NH_3 (1) are not shown, which lie above and below Co respectively. The electron-density contours are drawn to an arbitrary scale.

Table 1.
Parameter Values Found for [Co $(NH_3)_3$ $(NO_2)_2$ Cl] (Values in fractions of the cell dimensions)

	x	*y*	*z*
Co	0	0	0.267
Cl	0	0	0.128
N (1) (ammonia)	0	0	0.382
N (2) (ammonia)	0.077	−0.186	0.267
N	0.187	0.075	0.267
O (1)	0.215	0.180	0.304
O (2)	0.275	0.015	0.230

The atomic scattering factors used in computing the structure amplitudes were those given in the International Tables. The value of B in the temperature factor was given the value 2.5 Å^2.

The figure of merits $\Sigma||F_o|-|F_c||/\Sigma|F_o|$ is 0.26 for all the (*hkl*) data, for which only observed 330 reflections up to $\sin\theta/\lambda=0.49$ have been included. Fig. 4 gives a general indication of the agreement between the calculated and experimental F values.

Description of the structure

The crystal consists of [Co $(NH_3)_3$ $(NO_2)_2$ Cl] molecules and Fig. 5 gives a perspective drawing of the structure. Interatomic distances and interbond angles are listed in Table 2.

A molecule of [Co $(NH_3)_3$ $(No_2)_2$ Cl] is illustrated in Fig. 6. It has a two fold axis of symmetry. Two nitro-groups and two ammonia molecules, NH_3 (2), are co-ordinated to a cobalt atom in trans-positions respectively.

These four nitrogen atoms form a square around a cobalt atom within experimental

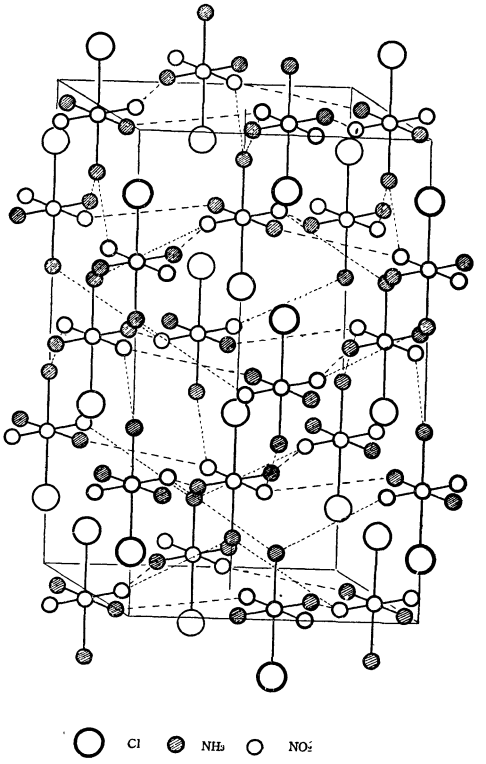

Fig. 5 A perspective drawing, showing the packing of the molecules in [Co $(NH_3)_3$ $(NO_2)_2$ Cl]. Circles are not drawn strictly to scale. Oxygen atoms are omitted.

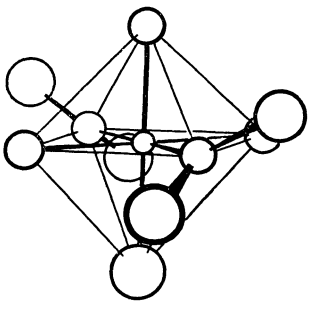

Fig. 6 The molecule of chlorodinitro-triammine-cobalt (III).

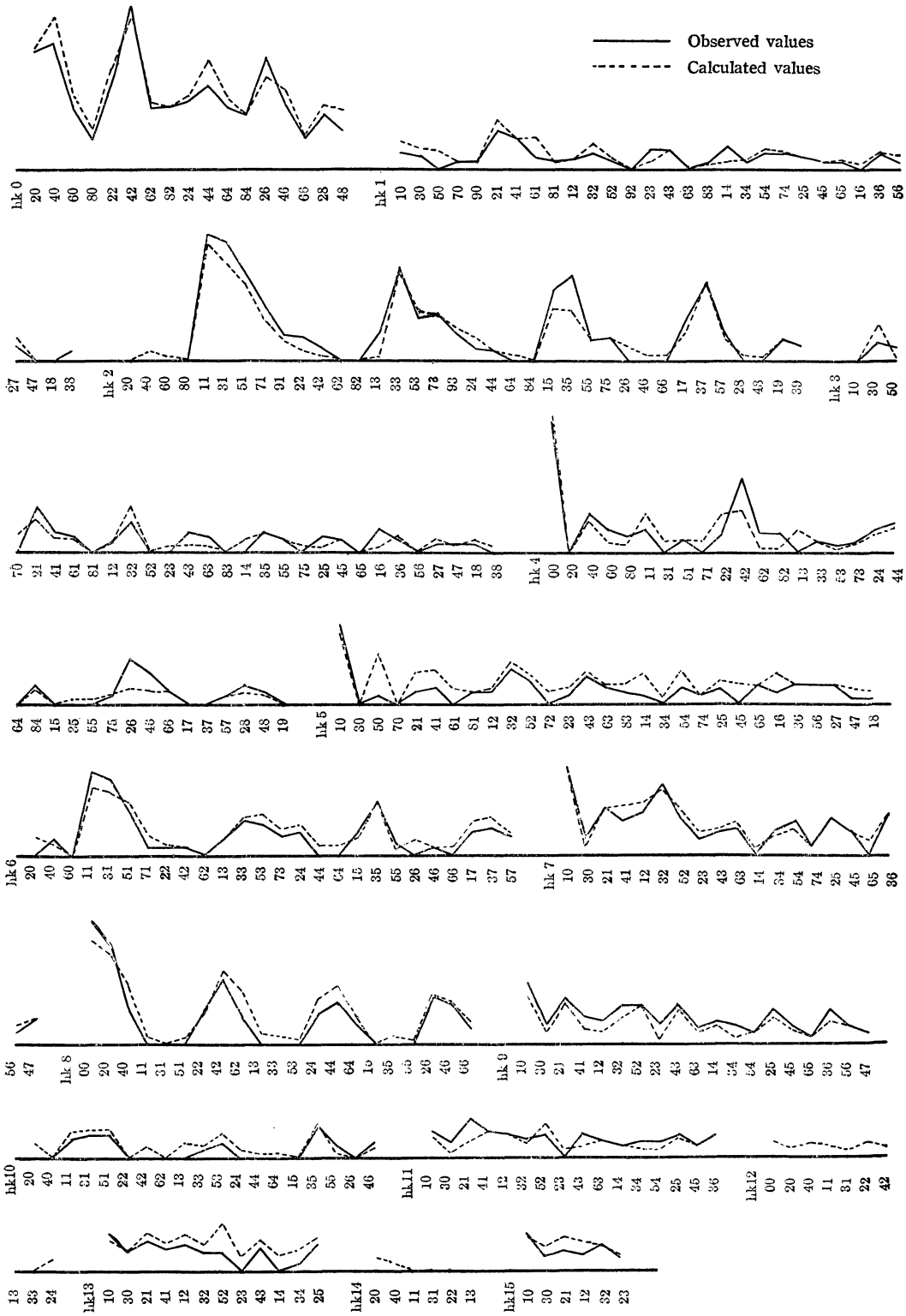

Fig. 4 Observed and calculated F's

Table 2
Calculated Interatomic Distances and Bond Angles (Values in A Maximum errors about ±0.05 A and ±4°.)

	within a molecule			between molecules	
Co	N (1) (ammonia)	1.90	O (1)	N (2) (ammonia)	2.84
	Cl	2.30	O (2)	N (1) (ammonia)	2.75
	N (2) (ammonia)	1.99	N (1) (ammonia)	Cl	3.68
	N	1.99		Cl	3.99
N	O (1)	1.24	Cl	Cl	4.24
	O (2)	1.22			
O (1)	O (2)	2.12			
∠ ONO		119°			

errors, being 1.99 Å apart from it. On a line through a cobalt atom and perpendicular to the plane of four nitrogen atoms are a Cl atom and a NH_3 (1) group at 2.30 Å and 1.90 Å respectively, thus forming a distorted octahedron around a metal atom. These interatomic distances are in good agreement with those found in the structures of [Co $(NH_3)_3$ $(NO_2)_3$], [Coen$_2$ Cl_2] Cl · HCl · $2H_2O$ and [Co $(NH_3)_3$ H_2OCl_2] Cl.[3)4)5)]

The shape and size of the nitro-groups (N . . . O=1.24, 1.22 Å and ∠ONO=119°) are also in agreement with our previous results as well as with those in the case of KNO_2 recently determined very accurately.[6)] The plane containing a nitro-group is inclined at an angle of about 34.8° with the plane of four nitrogen atoms. Thus there exist two kinds of molecules in the crystal, each being the mirror image of the other.

The closest approach of molecules is between NH_3 of one molecule and O of a nitro-group of the other. The unusual short NH_3 . . . O distances of 2.75 and 2.85 Å suggest probable hydrogen bonding between molecules.

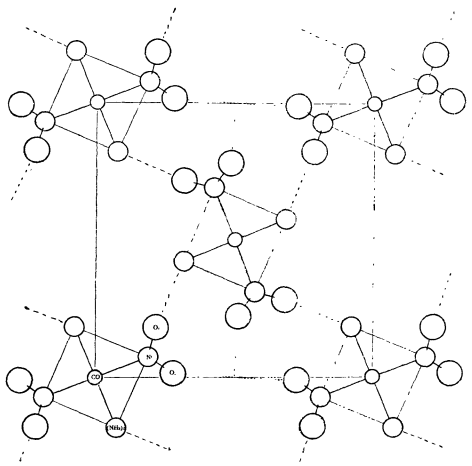

Fig. 7 Portion of the structure projected upon a plane perpendicular to [001], showing NH_3 . . . O linkages. Broken lines represent linkages in the layer, and dotted lines indicate those between layers.

Such hydrogen bonds were also found in the structure of trinitrotriammine-cobalt (III).[3)] Molecules are arranged approximately in a layer parallel to (001) which is shown in Figs. 5 and 7. Each layer comprises equal numbers of two kinds of molecules above-mentioned.

The main forces acting between molecules in the layer seem to be NH_3(2) . . . O(1) interactions which are indicated in the figure by broken lines. These (001) layers are held together by hrdrogen bonds between NH_3 (1) of one layer and O (2) of a nitro-group of the molecule belonging to the adjacent layer. These bonds are also shown by dotted lines in Figs. 5 and 7.

Thus each molecules are bound together by these two kinds of hydrogen bonds, forming a three-dimensional net work.

Summary

The crystal structure of [Co $(NH_3)_3$ $(NO_2)_2$ Cl] is tetragonal, with eight formula units in a cell of dimensions $a=9.87$ Å and $c=16.51$ Å.

The space group is C_{4h}^5-I $4_1/a$. The determination of atomic parameters was made by three dimensional Fourier syntheses. The configuration of the complex molecule is described.

Two nitro-groups are found to be in trans-positions with respect to each other. The main forces acting between these molecules in the crystal seem to be O . . . H-N bonds between the oxygen atoms of the nitro-group and the ammonia of the other. Molecules are linked together by these hydrogen bonds, forming a compact three-dimensional network in the crystal.

The authors desire to express their hearty thanks to Professor I. Nitta and Professor R. Tsuchida for their kind advice and encouragement throughout this work. Part of the cost of this study has been defrayed from the research grant from the Ministry of Education.

Institute of Polytechnics, Osaka City University, Osaka

6) G. B. Carpenter: *Acta Cryst.* **5**, 132 (1952).

Surface Chemistry of Synthetic Protein Analogues. II. Temperature Dependence of the Force-Area Relations of Some Polypeptides Monolayers and Thickness of the Monolayer*

By Toshizo ISEMURA and Kozo HAMAGUCHI

(Received March 20, 1953)

Introduction

Previously, the authors studied the various kinds of the behavior of the monolayers of some synthetic polypeptides as the model of natural proteins.[1] The polypeptides were of non-ionic side chains from four to ten carbon atoms in length. The force-area relations of the films were first investigated. From the results obtained, it was concluded that poly-DL-α-aminocaproic acid resembles exceedingly natural proteins among others. It has the side chains of four carbon atoms and its limiting area occupied by the film at zero compression was ca. 15 Å^2 per amino-acid residue. On the other hand, it was found that a plateau which is a part of high compressibility appears in the force-area (F-A) curves of the monolayers of polypeptides of longer side chains such as poly-DL-α-aminocaprylic acid, poly-DL-α-aminocapric acid, poly-DL-α-aminolauric acid and poly-γ-benzyl-DL glutamate. The F-A curves of these polypeptides monolayers were quite different in shape from those of natural proteins. The end of the plateau was always about 15 Å^2 per residue with all these films mentioned above. This area corresponds to the area per residue calculated from X-ray data of close packed chains of polypeptide of β-keratine type. (when the side chains were compressed away from the surface and the backbones were closely packed.). The resemblance between F-A curves of the protein monolayer and that of synthetic polypeptide of short side chains such as poly-DL-α-aminocaproic acid is due principally to the fact that natural proteins have on the average the side chains of effective length of three carbon atoms or less.

In the previous paper, the appearance of the plateau in the F-A curve was attributed to the reorientation of the polymer molecule caused by the compression of monolayer. To prove our supposition, the energy required for reorientation was evaluated and the thickness of the monolayer before and after transition was determined. In the course of experiments, it was found that the plateau of the F-A curves moves to the lower pressure region with the rise of temperature. From the relation of temperature and the pressure of transition from one state of the film to the other reoriented state, the heat of transition was estimated by the aid of two-dimensional equation of Clapeyron-Clausius.

On the other hand, these polypeptides films were transferred on the optical guage made of the built-up film of barium stearate under the spreading pressures under and above the transition pressure using the various piston oils. Then, the thickness of the built-up film of these polypeptides films was measured optically.

From the experimental results, our views of the reorientation at the plateau in F-A curve were justified for the most part.

Experimental Methods

Surface pressure was measured by the hanging plate method as reported in the previous paper. Distilled water was used as substrate, for the monolayer of these polypeptides is scarcely affected by the acidity or basicity of the substrate, as reported in the previous paper. To regulate the temperature of the substrate in the trough, the glass hose was dipped in the trough, through which water at constant temperature was circulated from a thermostat.

The films of these polypeptides were built up on the optical guage made of barium stearate multilayers by Langmuir-Blodgett's technique[2,3]

---

* This paper was presented before the "Symposium on the Studies on Protein Structure" which was held under the auspices of the Chemical Society of Japan, in Oct. 31-Nov. 1, 1952.

1) T. Isemura and K. Hamaguchi, This Bulletin, **25**, 40 (1952). T. Isemura, K. Hamaguchi, H. Tani. J. Noguchi and H. Yuki, *Nature*, **168**, 165 (1951).

under various spreading pressures of piston oils such as castor oil, tricresyl phosphate and some piston oils of low spreading pressure. Piston oils of low spreading pressure were prepared by mixing ethyl myristate with liquid paraffin[4] and their spreading pressure was measured by film balance beforehand for use. The thickness of the films of these polymers was determined optically by Blodgett's method.[3]

Poly-DL-α-aminocaproic acid film could not be transferred on the optical guage by dipping the plate vertically into the water covered with monolayer. However, it was transferred if the plate was inserted into the aqueous phase at an angle of 15° with the water surface and then withdrawn holding the plate at the same inclination. Polypeptide films other than that of poly-DL-α-aminocaproic acid were built up in the usual manner.

Results

The observed force-area relations at various temperatures are shown in Figs. 1–4.

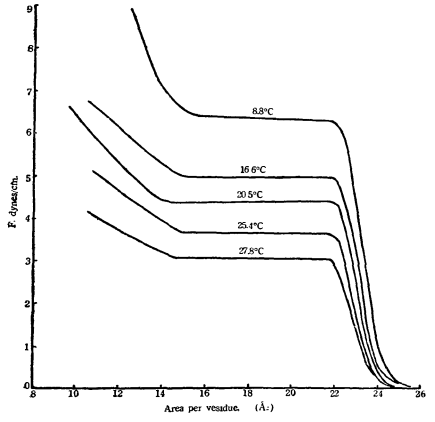

Fig. 1.—Poly-DL-α-aminolauric acid

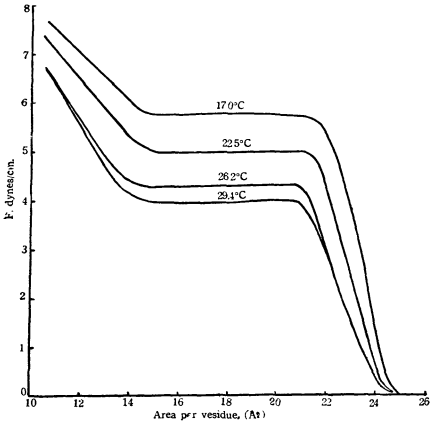

Fig. 2.—Poly-DL-α-aminocapric acid

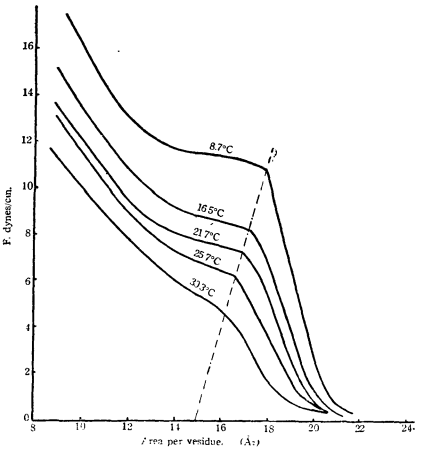

Fig. 3.—Poly-DL-α.aminocaprylic acid

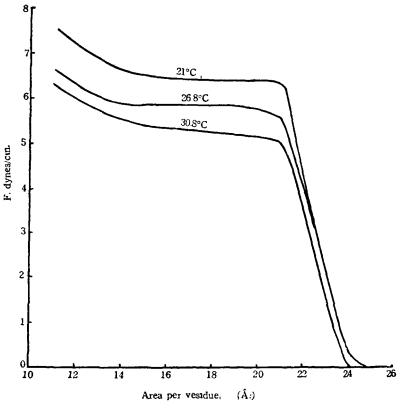

Fig. 4.—Poly-γ-benzyl-DL-glutamate

The force-area relation of the polymer film of short side chains such as poly-DL-norleucin was hardly influenced by the change of temperature. However, the force-area curves of the surface films of the polymers with longer side chains, such as poly-DL-α-aminolauric acid, poly-DL-α-aminocapric acid, poly-DL-α-aminocaprylic acid and poly-γ-benzyl-DL-glutamate were profoundly affected by the change of temperature. The plateau which appears in the F-A curves of monolayers of these polymers, passes to the lower pressure region with the rise of temperature of the substrate water. Nevertheless, the area at which the plateau begins to appear and the area at the end of the plateau, where the surface pressure begins to increase again were always nearly the same and independent of temperature. Moreover, the area of the end of the plateau was constant, namely, 15 Å^2 irrespective of the kind of polypeptides. The behavior of the monolayer of poly-DL-α-aminocaprylic acid was somewhat different from that of three other polypeptides. Although the plateau passes to the lower pressure region with the rise of temperature, the plateaus are not parallel to the area axis. In this case, their inclinations increase gradually and the area at which the plateau begins to appear, shifts to a

2) K. B. Blodgett, *J. Am. Chem. Soc.*, **57**, 1107 (1935).
3) K. B. Blodgett and I. Langmuir, *Phys. Rev.*, **53**, 909 (1938).
4) Norris and Taylor, *J. Chem. Soc.*, **1938**, 1719.

smaller area with the rise of temperature. The F-A curves of the monolayer of poly-DL-α-aminocaprylic acid may be an intermediate case between monolayers of polypeptide of shorter side chains and those of longer side chains.

The thickness of the built-up films of these polypeptides are shown in Table 1. The observed thickness h_3 indicated in the Table is not the value actually observed but the thickness which the built-up film should have, if the deposition ratio were unity. For comparison, the calculated thickness is also shown in the Table. h_1 is the thickness obtained by dividing the density of the polypeptide with the area per amino-acid residue at the spreading pressure of the piston oil used, which can be estimated from F-A curve. h_2 is the thickness of the film estimated by using the molecular model by Stuart, when the polypeptide chain is of β-keratine type and is compressed closely so as to project the side chains of the one side of the backbone and to push the side chains of the other side into the water.

Table 1.

Polypeptides	Spreading Pressure F (dynes/cm.)	Thickness (Å) calculated h_1	calculated h_2	observed h_3
Poly-DL-α-aminocaproic acid	3.1	10.7	11.7	11.1
Poly-DL-α-aminocaprylic acid	5.8	10.1	—	9.0
	9.5	15.0	16.4	15.6
Poly-DL-α-aminocapric acid	3.1	9.6	—	9.4
	9.5	24.0	21.3	22.7
Poly-DL-α-aminolauric acid	3.1	9.6	—	9.5
	5.8	23.9	26	20.7

Discussion

In the previous paper, the appearance of the plateau in the F-A curve was attributed to the reorientation of the polymer molecule caused by compression of monolayer. If we assume that both films before and after reorientation are two different surface phases, the surface pressure at which the plateau appears in the F-A curve, is the pressure of a phase transition. If this transition pressure was plotted against the temperature, straight lines were obtained for every polypeptide as shown in Fig. 5. dF/dT was readily evaluated from this figure. Inserting this value into two-dimensional Clapeyron-Clausius' equation, the change of enthalpy by the phase transformation of the film at any temperature can be evaluated as follows:

$$\Delta H^S = T \cdot \Delta A \frac{dF}{dT}$$

where F is the surface pressure of transition, ΔH^S the change of heat content per ground mole of the surface film, T transition temperature and ΔA the change of area per mole of ground molecule. If we assume a relation between the internal energy of surface film and its heat content, namely

$$H^S = U^S + FA,$$

we can estimate the change of internal energy of surface film as follows

$$\Delta U^S = \Delta H^S - F \cdot \Delta A.$$

The calculated changes of enthalpy and changes of internal energy of the phase change of the polypeptide monolayers are shown in Table 2.

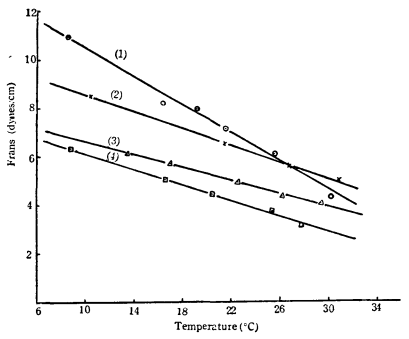

Fig. 5.—Transition pressure-temperature relation (1) Poly-DL-α-aminocaprylic acid; (2) poly-γ-benzyl-DL-glutamate; (3) Poly-DL-α-aminocapric acid; (4) Poly-DL-α-aminolauric acid.

Table 2.

	ΔH^S (cal./ground mole)	ΔU^S (cal./ground mole)
Poly-DL-α-aminolauric acid	567 (25.4°C)	608
Poly-DL-α-aminocapric acid	395 (26.2°C)	440
Poly-DL-α-aminocaprylic acid	285 (25.4°C)	302
Poly-γ-benzyl-DL-glutamate	498 (21.6°C)	565

The difference of internal energy between both states before and after the phase transformation decreases with the length of the side chains of the polypeptide. From the figures in the Table, it may be expected that the energy required for the phase transformation must be very small if the side chains were of four carbon atoms or less. This is caused perhaps by the following reasons. The ratio of two axes of the cross section of the polypeptide molecule perpendicular to the direction of the main chain is not widely different from unity. The thermal energy will readily exceed the energy needed for the transformation. In fact, no plateau was found in the F-A curve of polypeptides of side chains of four carbon atoms such as poly-DL-α-aminocaproic acid, copolymer of glycine-alanine and natural proteins. A report on the monolayer of the copolymer of glycine-alanine, will be given in the following paper in some details. In the cases of polypeptides of short side chains and proteins, the difference of energy between two states may be negligible and reorientation of the molecule occurs without any difficulty. After the reorientation is completed, the film just becomes incompressible and the surface pressure rises suddenly even with a small decrease of area.

It is very interesting that the heat content of the condensed phase of the film is more than that of the expanded phase, contrary to many usual cases met in three dimensions. In the case of polypeptide film, the more condensed phase is of high entropy. The order of the reoriented, condensed film may be worse than that of the film lying flat on the substrate. The order of magnitude of ΔU^S is far less than that of any kind of bonding such as hydrogen linkage. So, the energy change found in the present case is insufficient to break such linkages and may be spent principally for the reorientation.

Recently, Dervichian reported[5] that the plateau would appear in the force-area curve when the film of natural proteins, such as, serum albumin and egg albumin, was compressed relatively rapidly and continuously. Howover, the plateau would disappear from F-A curve if the film was compressed intermittently. He explained his experimental result as follows. There are some modifications in protein film and the transformation between them takes some time, and so, the surface pressure rises if the film is rapidly compressed, before a modification of larger area is transformed to a modification of smaller area.

5) D. G. Dervichian, *Kolloid-Z.*, **126**, 15 (1952).

If our views of reorientation of polypeptide films are accepted and it is assumed that it needs some time for reorientation of the side chains even in the polypeptides of short side chains such as natural proteins, the facts found by Dervichian can be readily explained.

The film of poly-DL-α-aminocaprylic acid gives an intermediate film between that of poly-DL-α-aminocaproic acid or natural proteins and that of the polypeptides which show a distinct plateau in the F-A curve. In this case, the plateau found in F-A curves are not completely parallel to the area axis but somewhat inclined. The less inclined the plateau is, the lower the temperature is. In other words, the more compressible the film at the plateau is, the lower the temperature is. Moreover, the area at which the transformation begins, moves to the smaller area with the rise of temperature, while the area at which the film begins to transform is almost entirely independent of temperature with the polypeptide film of side chains longer than eight carbon atoms or more in length. The points at which the transformation begins to occur lie nearly on a straight line which intercepts the area axis at about 15 Å^2, as shown in Fig. 3. It may be inferred that the plateau will completely disappear from the F-A curve at about 46°C. and it may be presumed that F-A curve of the film becomes that of poly-DL-α-aminocaproic acid.

As previously mentioned, the plateau appears even in the F-A curve of natural proteins, if the film is compressed rapidly and continuously, for it takes some time to reorient such short side chains found in proteins. In our present experiment, when the area occupied by the film is decreased intermittently. Accordingly, it seems reasonable that the polypeptide such as poly-DL-α-aminocaproic acid which resembles protein shows no plateau in F-A curve.

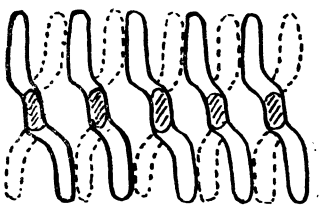

Fig. 6.—Close packed state of DL-polypeptide

To prove our supposition on the reorientation of the polymer, the determination of the thickness of the monolayer is the most direct method. It is expected that a distinct difference will be found between the thickness of monolayers built up at the pressure of more than the pressure at which the plateau ap-

pears and that built up at the pressure less than the transition pressure. And this is the case. After the reorientation was completed, the film assumed the shape shown in Fig. 6. With proteins and synthetic polypeptides of short side chains, only the built-up film of this orientation may be obtained. Whereas, with polypeptide films of longer side chains the other type of built-up film in which the side chains lie flat was also obtained.

With poly-DL-α-aminocaproic acid, the thickness of the film was 11.1 Å at pressure as low as 3.1 dynes/cm. In this case, the observed thickness, h_3, is in good agreement with h_1 and h_2. It suggests that the reorientation of the film is already completed. With poly-DL-α-aminocaprylic acid film, the thickness of the monolayer built up at 5.8 dynes/cm. (this pressure is less than the transition pressure) was 9.0 Å, whereas the thickness of the monolayer built up at 9.5 dynes/cm. (this pressure is more than the transition pressure) was 15~16 Å. This value is in good agreement with h_2. Although similar results were obtained with the monolayers of poly-DL-α-aminocapric acid and poly-DL-α-aminolauric acid, the thickness of the monolayer built up at the pressure higher than the transition pressure was nearly equal to but slightly less than the thickness evaluated by using Stuart models.

(for the most part.) These results support our views on the reorientation of the side chains of polypeptide.

Summary

In the force-area curves of the monolayer of synthetic polypeptides of longer side chains, a plateau which is a region of very high compressibility appears. The appearance of the plateau can be attributed to the reorientation of the polymer molecule at the interface. The pressure at which the plateau appears, decreases with the rise of temperature. From the temperature dependence of this pressure, the heat of transformation was evaluated.

The polypeptides of shorter side chains of four carbon atoms or less in length scarcely need any energy for reorientation. Accordingly, no plateau was found with these polypeptides. The thickness of the monolayer of these polypeptides at the pressure above and under the transition pressure was determined optically by Langmuir-Blodgett technique. The thickness of the monolayer observed was compared with that calculated by using Stuart model (for the most part.) Our views on the reorientatoin of the film were ascertained.

The authors wish to express their sincere thanks to Dr. H. Tani and Mr. H. Yuki in the Faculty of Science, Osaka University and to Dr. J. Noguchi at Kanazawa University who gave them the valuable samples of synthetic polypeptides. The authors' thanks are also due to Mr. R. Onishi for his assistance. A part of the expense for the experiment has been defrayed from a grant given by the Ministry of Education to which the authors' thanks are due.

The Institute of Scientific and Industrial Research, Osaka University, Sakai, Osaka

Studies on the Molecular Structures of Gaseous Acetamide and N-methylacetamide by Electron Diffraction

by Masao KIMURA and Michiro AOKI

(Received April 1, 1953)

Introduction

In many problems of the structure of protein, it is essential to determine the probable dimension of the polypeptide chain. Recently Corey and Donohue carried out X-ray diffraction experiments on DL-alanine, L-threonine, β-glycylglycine and N-acetylglycine, and suggested the probable dimension of the polypeptide chain to be as follows[1]: C=O 1.23 Å, C-N 1.32 Å, αC—C 1.53 Å, αC—N 1.47 Å, $\angle$NCO 122°, $\angle\alpha$CCO 121°, $\angle$CNαC 120° and $\angle$CαCN 110°. In the present investigation the molecular structure of gaseous acetamide, units of the polypeptide chain, and of gaseous N-methylacetamide, the simplest

1) R. B. Corey, J. Donohue, *J. Am. Chem. Soc.*, **72**, 2899 (1950).

molecule with a peptide linkage, were determined by electron diffraction and were compared with the result obtained from the X-ray diffraction experiments of some proteins.

Senti and Harker[2] determined the structure of acetamide using X-ray diffraction by crystal to be as follows: C=O 1.28 Å, C—N 1.38 Å, C-C 1.53 Å, ∠NCO 122° and ∠CCO 129°. No reports have ever been published regarding the structure of N-methylacetamide.

Experiment

The boiling points of acetamide and N-methylacetamide are 222°C and 206°C respectively. These compounds were vaporized by the use of a high temperature nozzle shown in Fig. I. The temperature of vapors could easily be raised up to 200°C by heating a nichrome wire coiled around a sample holder. The amount of the vapor could be regulated by a needle.

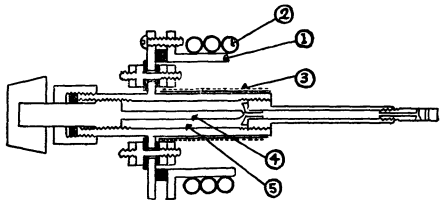

Fig. 1.—Diagram of the high temperature nozzle: (1) camera; (2) pipe coiled for coiled pipe for water cooling through which water is flowed; (3) nichrome wire; (4) needle; (5) sample holder.

The positions of maxima and minima of halos were estimated visually and were listed in Table 1. The visual curves are shown in Fig. 2V and Fig. 3v.

2) F. Senti, D. Harker, *J. Am. Chem., Soc.*, **62**, 2008 (1940).

Table 1

Observed Values for Acetamide and N-methylacetamide*.

Max.	Min.	q		Max.	q	
		Acetamide	N-methylacetamide		Acetamide	N-methylacetamide
	2	15.36	14.14	6	53.23	53.30
2		19.40	18.65	7	61.54	60.15
	3	24.01	24.33	8	68.18	69.14
3		27.81	27.97	9	77.03	76.76
	4	31.96	31.45	10	84.67	86.15
4		36.35	35.31	11	93.00	94.13
	5	40.56	40.75	12	100.55	
5		44.37	44.26			
	6	49.16	49.27			

* The observed values for the 1st maximum and the 7th, 8th, 9th, 10th, 11th and 12th minima were inaccurate and were not listed in this table. These values were not used for quantitative comparison.

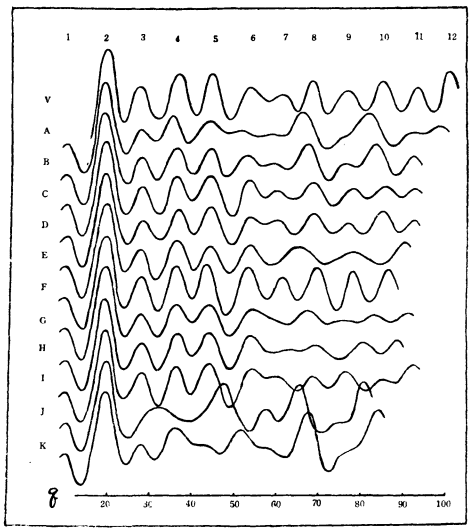

Fig. 2.—Visual and theoretical curves for acetamide.

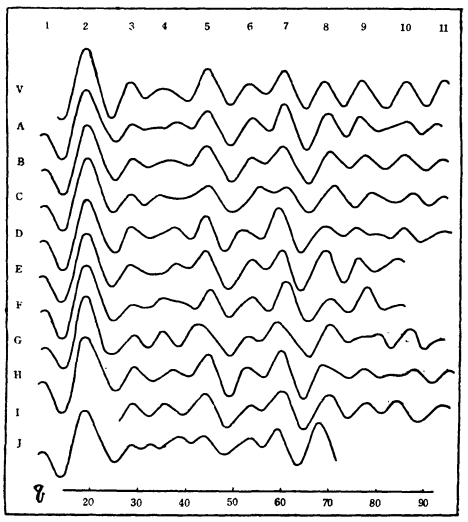

Fig. 3.—Visual and theoretical curves for N-methylacetamide.

The theoretical intensity curves,

$$I(q)=\sum_{i}\sum_{\neq j}(Z_iZ_j/r_{ij})\exp(-a_{ij}q^2)\sin(\pi qr_{ij}/10)$$

were computed for various models and were compared with the visual curve. Here notations have their usual significances and $\exp(-a_{ij}q^2)$ is a factor relating to the intramolecular vibration.

Because the theoretical intensity curves for acetamide were not affected appreciably by vibrations, a_{ij}'s could be taken as zero. For N-methylacetamide, the rotational vibration about carbon nitrogen bond cannot be neglected, therefore a a_{ij}'s were taken as either zero or 0.0004 for both C—C pair and C—O pair (Fig. 4).

Table 2
Models Assumed for Acetamide

model	C—N (Å)	C=O (Å)	C—C (Å)	∠NCO (degree)	∠CCO (degree)
A	1.37	1.25	1.54	122	120
B	„	1.23	1.54	124	122
C	„	1.21	1.54	126	120
D	„	„	1.52	124	124
E	„	„	1.57	126	118
F	„	1.21	1.54	128	120
G	„	„	„	124	120
H	„	„	„	126	118
I	„	1.19	1.54	126	124
J	1.38	1.28	1.53	122	129
K	1.32	1.23	1.53	122	121

Table 3
Models Assumed for N-methylacetamide

model	C—N (Å)	∠CNC (degree)	
A	1.45	115	trans
B	„	„	trans, vibrating
C	„	110	trans, rigid
D	„	120	trans, rigid
E	1.49	115	trans, rigid
F	1.39	„	trans, rigid
G	1.45	115	cis, rigid
H	„	„	twisted by 30 degrees from trans
I	„	„	free rotating
J	1.47	120	trans

Acetamide.—It was assumed that C-H 1.09 A, N-H 1.02 Å, ∠CCH 109°28′, ∠CNH 107° and that C, C, N and O atoms are coplaner. Because of many parameters involved, first the C—N distance was kept at 1.37 Å and the theoretical intensity curves were computed for various values of C-C, ∠NCO and ∠CCO, where the C=O distance was presumed to be 1.25 Å, 1.23 Å, 1.21 Å or 1.19 Å. Some of them are reproduced in Fig. 2.

(a) *Case of* C=O 1.25 Å: The theoretical curve for the model having the values of C-C 1.54 Å, ∠NCO 122° and ∠CCO 120° (Fig. 2A) did not agree with the visual curve, because the 6th and 7th maxima were too low; the 9th maximum appeared as a shelf and the q values of maxima were smaller than those in the visual curve. Even if different values were used for C—C, ∠NCO and ∠CCO with the values of model A, the 7th maximum disappeared and the theoretical curve in agreement with the visual curve could not be obtained.

(b) *Case of* C=O 1.23 Å: For the model having C—C 1.54 A, ∠NCO 124° and ∠CCO 122° (Fig. 2B), the theoretical curve obtained was similar in shape to the visual curve, except that the positions of maxima and minima disagreed with the observed values. If we assumed 1.57 Å for C—C distance, which was longer than the value of model B, the 8th, 9th and 11th maxima became higher, while the 6th and 7th maxima became lower. If we assumed 1.52 Å for C—C distance, which was shorter than the value of model B, the 6th, 7th, 8th, 10th, 11th and especially the 9th maxima became too low. These two theoretical curves appeared to be worse than the curve for model B. If C—C distance, ∠NCO and ∠CCO were varied properly, in the only case of about 1.52 Å, the theoretical curve could be obtained with the features similar to the visual curve. But the positions of maxima and minima shifted to q values smaller than the observed one.

(c) *Case of* C=O 1.21 Å: For the model having C—C 1.54 Å, ∠NCO 126° and ∠CCO 120° (Fig. 2C)~124°, the theoretical curves showed good agreement with the visual curve in features and the positions of maxima and minima. In order to determine the acceptable range of parameters, C—C, ∠NCO, and ∠CCO, their values were varied from the values of model C. When ∠NCO and ∠CCO were kept at the value of model C and C—C distance was assumed to be 1.52 Å, no good theoretical curve could be obtained. But in this case, if ∠NCO and ∠CCO were varied properly, an acceptable theoretical curve could be obtained, for example, as shown in the curve of ∠NCO 124° and ∠CCO 124° (Fig. 2D). When ∠NCO and ∠CCO were kept at the value of model C and C—C distance was assumed to be 1.57 A, no curve could be obtained in agreement with the visual curve, even though we took any value of ∠NCO and ∠CCO (for example Fig. 2E). When C—C and ∠CCO were kept at the value of model C and ∠NCO was larger or smaller by two degrees than the angle of model C, acceptable theoretical curves could not be obtained as shown in Fig. 2F or G respectively. Finally if C—C and ∠NCO were kept at the value of model C and ∠CCO was smaller by two degrees than the angle of model C, no acceptable theoretical curve (Fig. 2H) could be obtained. In this case if ∠CCO was 126°, the theoretical curve was entirely similar to that of model H and therefore could not be accepted.

(d) *Case of* C=O 1.19 Å: For the model having C—C 1.54 Å, ∠NCO 126° and ∠CCO 124°, the theoretical curve (Fig. 2I) could be obtained in agreement to some extent with the visual curve, but it cannot be accepted as a better model from the point of view of the relations of the 8th and 9th, or of the 10th and 11th maxima.

Even though C—C, ∠NCO and ∠CCO were varied properly, satisfactory theoretical curves could not be obtained.

According to the results of interpretation outlined above, if we assume 1.37 Å for C—N distance, the value of 1.21 Å is the best and the values of 1.23 Å—1.19 Å are acceptable for C=O distance. For other parameters, ∠NCO, ∠CCO and C—C distance, fairly wide ranges of values are permissible to obtain theoretical curves similar to the visual one. Thus ∠NCO 128°~132°, C—C 1.50 Å~1.56 Å and ∠CCO 118°~126° may be adopted as the widest range of the values. Furthermore quantitative comparison with the visual curve was made for the positions of maxima and minima in several better theoretical curves.

Thus the structure of acetamide was determined as follows:

C=O	1.21 Å±0.02 Å,	∠NCO	125°±3°
C—N	1.36 Å±0.02 Å,	∠CCO	122°±4°
C—C	1.53 Å±0.03 Å,		
C—H	1.09 Å (assumed),	∠CCH	109°28′ (assumed)
N—H	1.02 Å (assumed),	∠CNH	107° assumed)

and C, C, N and O atoms assumed lying in one plane.

The structure obtained by Senti and Harker and the probable dimension of a polypeptide chain given by Corey and Donohue give theoretical curves shown in Fig. 2J and K respectively. They disagree definitely with the visual curve.

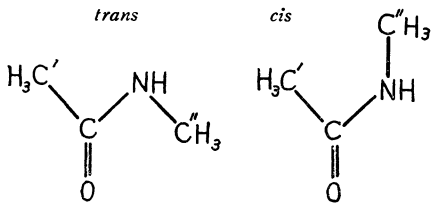

Fig. 4.—N-methylacetamide

N-methylacetamide. The photograph was analysed assuming a molecular structure similar to acetamide obtained above and using second C″—N distance, ∠C″NC and a rotational angle of the methylgroup about C″—N bond axis as parameters.

In the case of the trans configuration (Fig. 4), the theoretical curve having the values of C″—N 1.45 Å and ∠CNC 115° agreed to some extent with the visual curve, but the 4th and 11th maxima did not agree with those of the visual curve (Fig. 3A). If we took into account the rotational vibration of methyl group about C″—N bond axis, the theoretical curve was in satisfactory agreement with the visual curve (Fig. 3B). When C″—N was kept at 1.45 Å and ∠CNC was varied to 110° (Fig. 3C), even if we took the vibrational effect into account, no acceptable theoretical curve could be obtained. when C″—N was kept at 1.45 Å and ∠CNC was varied to 120° (Fig. 3D), the 7th maximum seemed to be too high compared with the 6th. But this model should not be discarded, entirely because, if the vibration is taken into account, the theoretical curve becomes more similar to the visual one than the theoretical curve for model 3D.

When ∠CNC was kept at the value of model A and C″—N distance was varied to 1.49 Å or 1.39 Å, the theoretical curves were obtained as shown in Fig. 3E and F respectively. Both curves are unacceptable.

In the case of the cis configuration (Fig. 4), the theoretical curve Fig. 3G was obtained using the same value of C″—N distance and ∠C″NC as model A. The curve was not in agreement with the visual one in regard to the positions of the 5th, 6th, 7th and 10th maxima and the feature of the 4th maximum. It could not be revised even if we took into account the rotational vibration of a methyl group. In the theoretical curve (Fig. 3H) computed for the model with the methyl group twisted by 30 degrees from the *trans* configuration, the 6th and 8th maxima shifted to smaller values and the similarity to the visual curve became worse in the feature of the curve. But the theoretical curves for the models with the methyl group twisted within about 30 degrees, could not be discriminated from the visual one. Further the theoretical curve for the model whose methyl group rotates freely about C—N bond axis (Fig. 3 I), does not better account for the visual one than the curves for the *trans* configuration, but this also cannot be discarded.

According to the result mentioned above, it is most probable that N-methylacetamide has the trans configuration and its methyl group oscillates about C—N bond axis. But the structures whose methyl group rotates freely may also be probable. The conclusion from the measurement of dipole moment in solution[3] is that N-methylacetamide has the *trans* configuration. Further from the viewpoint of steric repulsion, the *trans* configuration is more favorable than the *cis* configuration.

with the known structure of acetamide the structure of N-methylacetamide was determined as follows:

C″—N	1.44 Å±0.04 Å
∠C″NC	117°±5°

trans configuration.

The theoretical curve for N-methylacetamide was computed using the structure of a polypeptide chain obtained by Corey and Donohue and is shown in Fig. 3J. It could be distinguished definitely from the visual curve.

Discussion of Results

Our results differ definitely from the values

3) S. Mizushima, T. Shimanouchi, S. Nagakura, K. Kuratani, M. Tsuboi, H. Baba, O. Fujioka, *J. Chem. Soc. Japan* **71**, 32 (1950): *J. Am. Chem. Soc.*, **72**, 3490 (1950).

obtained by Senti and Harker, but do not differ very much from the probable dimension of a polypeptide chain proposed by Corey and Donohue. The result obtained by Senti and Harker seems to be not very accurate. It has already been mentioned that the probable dimension of a polypeptide chain obtained by Corey and Donohue does not give a satisfactory theoretical curve.

The discrepancy between the results obtained by us and by Corey and Donohue may be supposed to be due to the difference in materials used and in the states of aggregation. Namely, Corey and Donohue used as samples β-glycylglycine, N-acetylglycine and so on while we used acetamide and N-methylacetamide morover they determined the crystal structures, while we determined the structures in the gaseous state.

As it is unlikely that the former difference will give rise to an appreciable change in the molecular structure, it will be more adequate to consider that the latter is the main cause of the difference between the results obtained by us and by Corey and Donohue, i. e. to suppose that the hydgrogen bond, which is absent in the gaseous state but exists in the crystalline state, plays a major role

Acetamide will have the resonance structures shown by

$$CH_3\text{-}\overset{\overset{O}{\|}}{C}\text{-}NH_3 \text{ (A)} \quad \text{and} \quad CH_3\text{-}\overset{\overset{+}{|}}{C}\overset{O^-}{=}NH_2 \text{ (B)}$$

as the extreme cases, hence by the hydrogen bonds the contribution of the structure (B) becomes greater in the crystal line state than in the gaseous state. As a result, C=O distance will tend to be longer and C—N distance to be shorter in the crystal.

The change in the structure of acetamide due to the formation of a hydrogen bond is supported by another fact. N-methylacetamide in dilute benzene solution shows an infrared absorption maximum of C=O vibration at 1700 cm^{-1} in extreme dilution, but its wave number shifts to 1640 cm^{-1} as the concentration increases[5] owing to the hydrogen bond between solute molecules.

Summary

1) The molecular structures of acetamide and N-methylacetamide were determined using electron diffraction by gases. The results were compared with the values obtained from X-ray diffraction by crystals.

2) C=O distance is longer in the crystalline state than in the gaseous state, while C—N distance is shorter in the crystalline state than in the gaseous state. This is due to the hydrogen bond which is absent in the gaseous state but exists in the crystalline state.

We wish to express our sincere thanks to Professor S. Mizushima and Professor Y. Morino of Tokyo University who supplied us with the sample of N-methylacetamide used in this experiment. We also wish to thank Professor M. Kubo of Nagoya University for his helpful advice.

Department of Chemistry,
Faculty of Science,
Nagoya University

Studies of Molecular Structures by Electron Diffraction. II. The Structures of *o*-,*p*-Fluorochrolobenzene and *p*-Fluorobromobenzene

By Hajime Oosaka† and Yûmi Akimoto

(Received May 1, 1953)

Introduction

Recently the molecules of fluorine substituted benzene derivatives have been the subjects of several investigations. Early electron diffraction results on fluorobenzene and *o*-difluorobenzene by the visual method was reported by one of the authors.[1] The quoted bond lengths, C—F, have been 1.34± 0.04 Å and 1.35±0.03 Å respectively. A little later a discrepant result was reported by Finbak and Hassel[2] who found 1.31±0.03Å for the C—F distance in fluorobenzene by the sector method.

It was, therefore, decided to carry out the

1) H. Oosaka, This Bulletin, **15**, 31 (1940).

2) C. Finbak and O. Hassel, *Arch. Math. Naturvidenskab*, XLIV (1941); O. Hassel and H. Viervoll, *Acta Chim. Scand.*, **1**, 149 (1947).

extensive measurement on the various fluorobenzene derivatives. Not long afterward, some of our collaborators have reported the result of reinvestigation of fluorobenzene.[3] And, in this paper, the molecular structures of *o*-, *p*-fluorochlorobenzene and *p*-fluorobromobenzene are to be reported as a second part of this series.

Materials

Each fluorobenzene derivative was prepared from corresponding nitroaniline by the successive diazotations. All steps are too familiar to describe in detail but the step, Schiemann reaction, where a fluorine atom is introduced into the aromatic nucleus.

Schiemann Reaction.[4]—(The following procedures are common to the three compounds mentioned above.)

(A) Preparations of Diazonium Fluoborates.—To a mixture of 100 cc. of 40% fluoboric acid and 50 cc. of water is added 0.25 mole of well ground corresponding halogenated aniline. The solution (or suspention) is cooled to 5°C., and a saturated solution of 17.3 g. (0.25 mole) of sodium nitrite is added slowly, the temperature being kept under 20°C. The precipitate is washed with cold water, cold methanol and ether successively. The yields are 92% (o-$BF_4N_2ClC_6H_4$), 89% (p-$BF_4N_2ClC_6H_4$) and 93% (p-$BF_4N_2BrC_6H_4$).

Meigs[5] reported that the temperature of the reacting mixture may rise to 30°C. without ill effect during the diazotation of aniline in fluoboric acid solution. Carrying out the diazotations for several numbers of compounds,[6] we extended Meigs' conclusion over nearly all monohalogenoaniline. Table 1 serves to confirm this conclusion by showing the yields obtained under several different temperatures, in case of the diazotation of *p*-fluorochloroaniline, as an example.

Table 1
Temperature Effect for the Diazotation of *p*-chloroaniline

Sample	Temp. of bath (°C)	Max. temp. of reacting mixture (°C)	Yield (%)
1	15	30	78.5
2	7	18	88.7
3	0 (ice)	10	86.1
4	−10 (ice-NaCl)	0	84.7

All the other halogenated anilines can be treated likewise: there are no troubles up to 20°C. However, in case of nitroanilines, the reacting mixture must be kept under 7°C, because considerable decomposition occurs even at about 10°C. A more severe condition is necessary in case of tetrazotation: decomposition begins at about −8°C.

(B) Decompositions of Diazonium Fluoborates.—Decompositions were carried out according to the direction of Organic Reactions.[4] The yields were 68% (o-$FClC_6H_4$), 72% (p-$FClC_6H_4$), and 74% (p-$FBrC_6H_4$).

Each sample was distilled before use.

Experimental

Electron diffraction photographs of *p*-fluorochlorobenzene were taken in the apparatus of Brockway type with the camera distance of 13.4 cm. For the other two compounds a new camera, previously described,[3] was used.[7] About eight photographs were taken for each compound under different conditions, and were measured visually in the usual way. The electron wave length was determined to be 0.052~0.064 Å by caribration against gold leaves.

Theoretical intensity curves were calculated by the following equation.

$$I(s)=\sum_i\sum_j Z_iZ_j \exp(-a_{ij}s^2)\frac{\sin sl_{ij}}{sl_{ij}}$$

where $s=(4\pi/\lambda)\sin\theta/2$, l_{ij}: the distance between the i-th and j-th atoms, Z: the atomic number, a: the coefficient of thermal vibration, λ: the wave length, and θ: the scattering angle. (For *p*-fluorobromobenzene and *o*-fluorochlorobenzene, modified parameter $q(=(40/\lambda)\sin\theta/2)$ was used in place of s.[8]

For hydrogen, an effective value, 1.25, was used in order to approximate better to its low-angle scattering relative to carbon and halogen atoms.

***p*-Fluorochlorobenzene.**—In computing theoretical intensity curves, assumptions were made as below: (1) C—C=1.40 Å, (2) C—H=1.04 Å, (3) ∠H—C—C=∠Hal.—C—C=120°, (4) the molecule has a planar skeleton. The parameter values were made for fourteen models over the following ranges: C—Cl=1.66~1.72 Å, C—F=1.27~1.41 Å. All interactions involving hydrogen atoms were included, except H—H terms. The thermal term was neglected since the high-angle scattering region hardly contributed to the determination of parameters. Typical curves are shown in Fig. 2, and the values of the parametersin Fig. 1.

Curve C is inconsistent with the experimental data for lack of max. IV. Curves G and H can be rejected because max. III is too large. In

3) T. Yuzawa and M. Yamaha, in press.
4) A. Roe, "Organic Reactions" Vol. V, Chap. IV. p. 193.
5) Meigs, U. S. pat. 1,916, 327 (C.A., **27**, 4539 (1933)).
6) *p*-Fluoroaniline, *o*-, *m*-, *p*-chloroaniline, *o*-, *p*-bromoaniline, *p*-iodoaniline and *o*-, *m*-, *p*-nitroaniline were diazotized for this purpose. Tetrazotations were carried out also.
7) Because of the accomplishments of a new apparatus and calculation tables in q scale in the midst of our research, such disorepances were introduced unavoidably.
8) R. Spurr and V. Schomaker, *J. Am. Chem. Soc.* **64**, 2693 (1942).
9) On account of possible majority of thermal vibration on Br···F, some additional curves were calculated with suitable values of a_{ij} for all terms, but the resulting changes were insignificant but for max. IX.

curve F, max. III is larger still compared with max. II. Curves A and B are borderline cases since max. VI is too weak as compared with max. V. Furthermore, curve B can probably be eliminated because of the disappearance of shelf II.

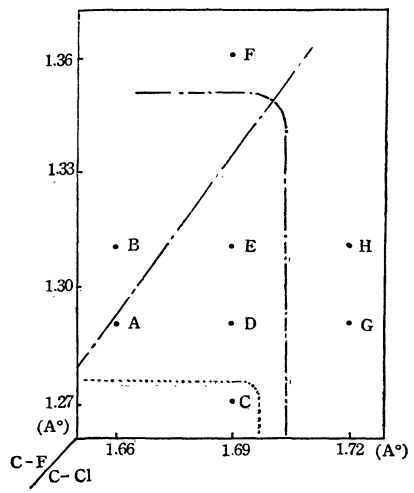

Fig. 1.—Parameter chart for *p*-fluorochlorobenzene

The position of the letters indicate the parameters of the models for which intensity curves were computed. The dashed and dotted lines indicate where particular features of the intensity curves were sufficiently different from the visual curve to make them unacceptable.

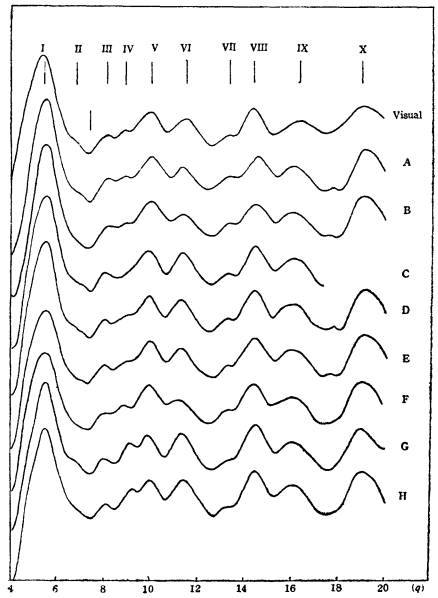

Fig. 2. Theoretical intensity curves for *p*-fluorochlorobenzene.

The best agreement with the observed pattern would be given by a model located about the midway between D and E. Finally we have C—F=1.30±0.03 Å, and C—Cl=1.68±0.02 Å. (The quantitative comparisons are in Table 2.)

Table 2

p-Fluorochlorobenzene

Max.	Min.	Obs. (*s*)	$s_c./s_o.$ A	$s_c./s_o.$ D	$s_c./s_o.$ E
I		5.381	1.022	1.025	1.022
II		(6.778)			
	III	7.336	0.988	0.993	0.988
III		8.082	1.007	0.994	0.992
IV		8.890	1.006	1.000	0.996
V		9.935	1.006	0.997	1.000
VI		11.509	0.984	0.980	0.973
VII		(13.398)	(0.996)	(0.988)	(0.985)
VIII		14.381	1.008	1.001	1.000
IX		16.349	0.984	0.979	0.981
X		19.016	1.003	1.003	1.001
Average, 9 features			1.001	0.997	0.995
Mean deviation, Δ			0.011	0.009	0.010
Mean square root, $(\Delta^2)^{1/2}$			0.012	0.013	0.014

***p*-Fluorobromobenzene.**—Theoretical curves were calculated over the following parameter ranges: C—Br=1.84~1.90 Å, C—F=1.27~1.33 Å. The assumptions were made just as those of fluorochlorobenzene. Typical ones of these curves are shown in Fig. 4, and the values chosen for the parameters in Fig. 3.

In order to avoid laborious computation in a literal treatment of the thermal factors, a_{ij} was neglected over all models and a procedure was

adopted wherein two curves were plotted for several models. The light curves represent only the scattering due to non hydrogen distances and the bonded C—H distances; in addition to these terms, the heavy curves include the non-bobded C···H and Hal.···H terms. The heavy curves are significant for small q and the light curves for large q.

Curve A may be excluded because of the intense max. III. Dislocation of max. V eliminated curve J and put curve I on a borderline. For the remaining curves, there are not any sufficient reasons to eliminate them qualitatively. Indeed curves F, G and H lack max. VI, and curves B, C and F show max. XI distinctly. However, they are too weak to be decisive criteria hence the thermal effects may weaken these tendencies.

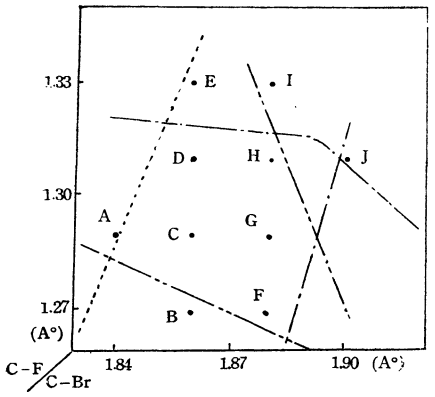

Fig. 3.—Parameter chart for p-fluorobromobenzene.

The quantitative comparisons are tabluated in Table 3. As the final result we obtain C—F = 1.30±0.03 Å and C—Br = 1.87±0.02 Å.

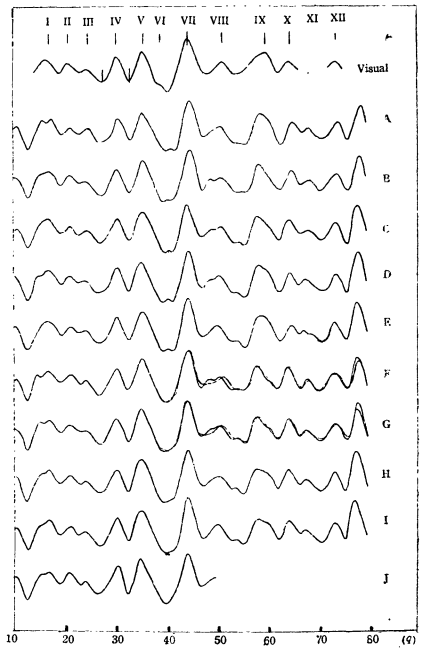

Fig. 4.—Theoretical intensity curves for p-fluorobromobenzene.

Table 3

p-Fluorobromobenzene

Max.	Min.	Obs. (q)	$q_c./q_o.$ C	D	G
I		16.68	0.999	1.006	1.006
II		20.86	1.006	1.016	1.006
III		24.61	(0.980)	(0.980)	(0.976)
	IV	27.46	(0.977)	(0.970)	(0.984)
IV		30.08	1.007	1.004	1.004
	V	33.03	0.993	0.990	0.984
V		35.59	0.986	0.986	0.992
VI		(38.8)			
VII		44.42	0.999	1.008	1.000
VIII		51.35	0.993	0.985	0.993
IX		59.99	(0.958)	(0.963)	(0.953)
X		64.60	1.003	1.001	1.000
XI		73.76	1.003	1.002	1.002
Average, 9 features			0.999	1.000	0.999
			1.001	**1.002**	**1.000**
Mean deviation, Δ			0.005	0.008	0.005
Mean square root, $(\Delta^2)^{1/2}$			0.007	0.010	0.007

	B	E	F	H
Average, 9 features	1.003	1.001	0.998	0.998
	1.006	**1.002**	**1.001**	**0.999**
Δ	0.010	0.009	0.008	0.007
$(\Delta^2)^{1/2}$	0.011	0.012	0.010	0.008

Black style numerals indicate the values obtained from temperature-factored curves.

o-Fluorochlorobenzene.—In this case, we cannot always assume the coplanarity of all atoms. Using the sector method, Bastiansen and Hassel[10] concluded that the forces acting between C-halogen atoms tend to bring the halogen atoms out of the plane of the benzene ring. However, as opposed by Morino,[11] this result is inconceivable theoretically.

No matter which they may be, in computing theoretical intensity curves this problem has no significiant base of arguments; no important difference on the shapes of the curves were found between the coplanar model and non coplanar one, and hence the molecule was assumed to have a planar skelton in this case.

Parameter ranges were taken as: C—Cl=1.67~1.75 Å, C—F=1.29~1.37 Å, F—Cl=2.90~3.04 Å. The assumption and the thermal factors were treated in a way similar to the case of *p*-fluorobromobenzene. Fig. 5 and Table 4 show typical curves and their parameters of twenty-one models which have been tested.

Curves A, B, F, G, and H are rejected because they show considerably different shapes in the region q=20~30. Curves C, D and E are mostly acceptable, though curve E is rather a borderline case since max. V and XII are somewhat out of step with the observed ones.

However when we examine them more strictly, they show several difficulties: max. VI is too much weaker than the observed, max. XI is too strong relative to max. X. Spreading the ∠Hal.—C—C over 120°, we can remove these difficulties, and curves K and L show the best agreement with the observations. Even curve J shows the fit better than curve C. Curves I and M are borderline cases.

Quantitative comparisons are given in Table 5. The final structure is C—F=1.30±0.03 Å, C—Cl=1.69±0.02 Å, and ∠F—C—C (adjacent of Cl)=∠Cl—C—C (adjacent of F)=121±1°.

Table 4
Parameters for *o*-fluorochlorobenzene

Model number	C—Cl (Å)	C—F (Å)	Cl—F (Å)	F—C—C (adj. of Cl), Cl—C—C (adj. of F)
A	1.67	1.29	2.90	120°
B	1.67	1.33	2.91	120°
C	1.70	1.29	2.92	120°
D	1.70	1.31	2.92	120°
E	1.70	1.33	2.93	120°
F	1.71	1.29	2.92	120°
G	1.73	1.31	2.94	120°
H	1.73	1.35	2.96	120°
I	1.67	1.29	2.95	121°
J	1.70	1.29	2.95	120°45′
K	1.70	1.29	2.99	121°40′
L	1.70	1.31	2.99	121°30′
M	1.71	1.31	2.99	121°20′

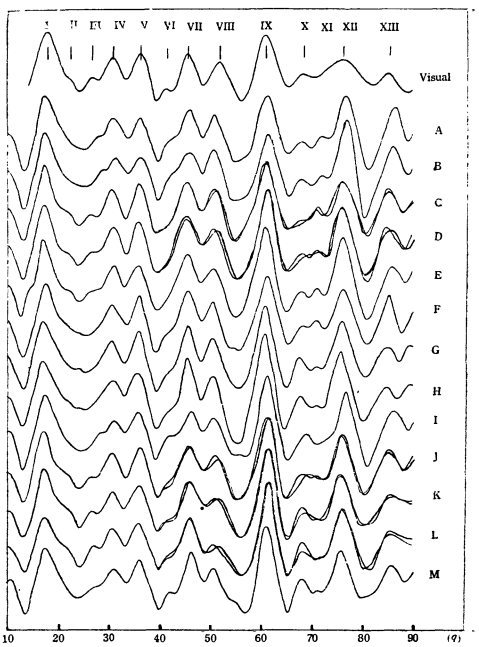

Fig. 5.—Theoretical intensity curves for *o*-fluorochlorobenzene.

10) O. Bastiansen and O. Hassel, *Acta Chim. Scand.*, **1**, 489 (1947).
11) Y. Morino, Discussion on the Inter- and Intramolecular forces, Tokyo, June, 1952.

Table 5

o-Fluorochlorobenzene

Max.	Obs. (q)	$q_c./q_o.$		
		C	J	K
I	17.76	(0.976)	(0.979)	(0.979)
II	(22.28)			
III	26.42	1.001	1.006	1.000
IV	30.56	1.001	1.002	1.004
V	36.29	0.992	0.989	0.989
VI	41.38	/	(1.000)	(1.000)
VII	45.62	1.000	1.001	1.003
VIII	51.98	0.978	0.981	0.981
IX	60.82	1.009	1.007	1.007
X	68.41	(0.994)	(0.996)	(0.994)
XII	76.39	1.002	0.998	0.992
XIII	85.30	0.999	0.999	1.001
Average, 8 features		0.997	0.998	0.996
		0.999	**0.999**	**0.998**
Mean deviation, Δ		0.005	0.006	0.007
Mean square root, $(\Delta^2)^{1/2}$		0.008	0.008	0.008
		D	E	L
Average, 8 features		0.998	0.995	0.997
		1.000	/	**0.998**
Δ		0,009	0.009	0.010
$(\Delta^2)^{1/2}$		0.012	0.010	0.012

Black style numerals indicate the values obtained from temperature-factured curves.

Discussion

We must confess that the value of C—F distance reported earlier by one of us is inadequate.[1] In the earlier work, patterns were detectable only up to $s=15$. It is certain that the impropriety was originated from this experimental limitation.

C—Cl and C—Br distances do not contradict that of the previous works published by several authors.

In case of *o*-fluorochlorobenzene, the reason for a deviation of ∠Hal.—C—C from the value of 120° is chiefly a result of repulsion between halogen atoms. The distance to be expected in absence of such deviation must be smaller than the sum of van der Waals radii, which should be at least 3.0 Å. The slight increment of Hal.—C distance which has been found in several *o*-halogenobenzenes, were not observed. This fact may be explained as the repulsive force is not so sufficiently large as to demand the visible stretching of Hal.—C bonds in this case.

Summary

The molecular structures of *o*-, *p*-fluorochlorobenzene and *p*-fluorobromobenzene have been investigated by the electron diffraction method. The following values have been obtained by the analysis based on coplanar structures; C—F = 1.30±0.03 Å, C—Cl = 1.68±0.02 Å for *p*-fluorochlorobenzene; C—F = 1.30±0.03 Å, C—Br = 1.87±0.02 Å for *p*-fluorobromobenzene; and C—F = 1.30±0.03 Å, C—Cl = 1.69±0.02 Å, and ∠C_1—C_2—F = ∠C_2—C_1—Cl = 121±1° for fluorochlorobenzene. C—C = 1.40 Å, C—H = 1.04 Å are assumed throughout the analysis.

The authors wish to express their sincere thanks to Prof. A. Kotera for his continued encouragement to this research. They are also indebted to Mr. M. Yamaha and Mr. M. Igarashi for their helpful discussions and suggestions. A part of the cost of this research has been defrayed from the Scientific Research Encouragement Grant from the Ministry of Education, to which the authors' thanks are due.

Chemical Laboratory, Tokyo Bunrika University, Tokyo

The Structure of Surface Denatured Protein. V. The Surface Film of Diketo-piperazine

Kazutomo IMAHORI

(Received August 8, 1952)

Introduction

Many investigations have been made about the properties of monolayers of proteins. Rideal[1] and Alexander[2] insist that the unfolded polypeptide chain has β-keratine configuration, while Isemura[3] has explained his results by using Mizushima and Shimanouchi's model. But none has regard for the existence of diketopiperazine configuration on the surface. It may not be probable that polypeptide chain has diketopiperazine configuration on the water surface. Yet, the existence of diketopiperazine configuration cannot be denied until the limiting area of diketopiperazine film is determined.

The author has investigated the diketopiperazine monolayer and obtained the value of limiting area from the results of F—A, V—A and η—A curves.

Experimental

Material—Diketopiperazine is prepared from glycine by Dr. Tadao Sugita, in the Institute of Chemistry, Faculty of Science, University of Tokyo, and is recrystallized several times. This is spread on the surface of KCl solution of about 0.2 N concentration from the solution in the mixed solvent of dichloracetic acid and benzene. The spread film is uniform as checked by the constancy of surface potential within the error of 1 mV.

Measuring Apparatuses—Surface pressure was measured by a modified Wilhelmy balance, which has been described in the Part I of this series[4]. Surface potential is measured by the apparatus described in Part III of this series[5]. Viscosity of monomolecular film can be measured by the method of flowing out through a capillary canal[6], by the method of the oscillation of a ring in the monolayer[7] or by the method of rotation of a ring (analogous to a cell of Couette) in the monolayer[8].

The apparatus and the procedure of the present measurements are essentially the same as those described by Joly[6]. A diagram of the apparatus used is shown in Fig. 1. This consisted essentially of a brass tray T, containing a canal C and two Wilhelmy balances W and W'. The canal is 1.1 cm long and 0.062 cm broad, and have door D at its end, which controls the flow of monomolecular film. Harkins[9] gave for this case the following equation,

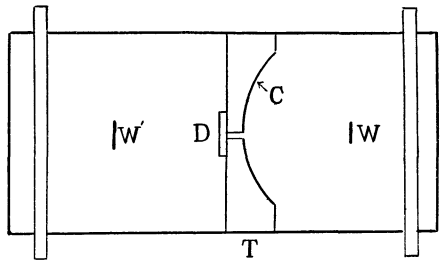

Fig. 1

$$\eta = \frac{\alpha}{Q} \cdot \frac{d^3}{12} - \frac{d \cdot \eta_0}{\pi}$$

where α is the film pressure gradient, Q the quantity of the film which passes through the canal in unit time, d the breadth of the canal and η_0 the viscosity of the substrate.

Thus, the surface viscosity η can be determined by the measurement of the quantity Q.

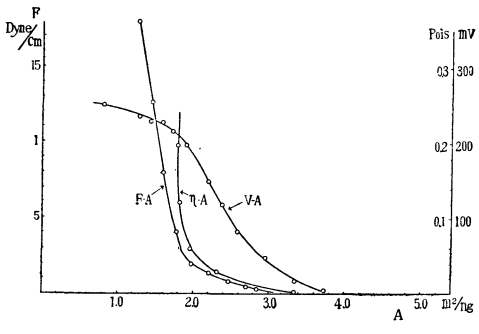

Fig. 2

1) E. K. Rideal, *Proc. Roy. Soc.* (*London*) **A137**, 70 (1932).
2) C. W. N. Cumper and A. E. Alexander, *Trans. Farad. Soc.*, **46**, 240 (1950).
3) T. Isemura and K. Hamaguchi, This Bulletin, **25**, 40 (1952).
4) K. Imahori, This Bulletin, **25**, 7 (1952).
5) K. Imahori, This Bulletin, **25**, 13 (1952).
6) M. Joly, *Kolloid Zeits.*, **89**, 26 (1939).
7) L. Fourt, *J. Phys. Chem.*, **43**, 887 (1939).
8) R. Chaminade, D. G. Dervichian et M. Joly, *Journ. Chim. Phys.*, **47**, 883 (1950).
9) W. Harkins, *J. Chem. Phys.*, **5**, 601 (1937), **6**, 53 (1938).

Results

The F—A curve in Fig. 2 shows the plot of the film pressures in dyne per centimeter against the film areas in square meters per milligram. The measurements were done as carefully as possible. The film was compressed slowly with small decrements. Ample time was allowed after each decrease in area for the attainment of equilbrium surface pressure. The result shows that the limiting area of this curve is 1.85 m^2/mg.

The V—A curve in the figure shows the plot of the surface potentials of the film in millivolt against the film areas in square meters per milligram. The curve shows that the limiting area is 1.82 m^2/mg.

The η—A curve in the figure shows the plot of the surface viscosity in pois against the film area in square meters per milligram. All the experiments, represented by the circlets in the figure, were carried out under surface pressure differences below 2.5 dyne per centimeter. In the figure, sudden increase in slope of the curve occured at 1.82 m^2/mg and this shows that the limiting area is 1.82 m^2/mg.

Discussions

The above three curves show that the limiting area of diketopiperazine monomolecular film is 1.82—1.85 square meters per milligram. The mean of the three values is 1.83 m^2/mg (or 34.6 $Å^2$ per one diketopiperazine molecule).

The crystal structure of diketopiperazine has been determined by Corey[10] by X-ray diffraction. From this result, the limiting area per one diketopiperazine molecule is to be 35.5 $Å^2$ when diketopiperazine molecule are orientated flat on the surface (the broad side on) perhaps in such a way as shown in Fig. 3.

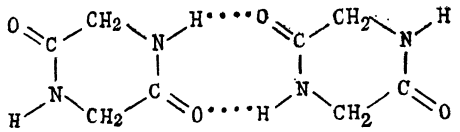

Fig. 3

Comparing this result with that obtained by author's experiment, we can say the following: The diketopiperazine molecules lie flat when they are expanded on the water surface. But when the film is compressed below the limiting area, diketopiperazine molecules probably begin to rise on the surface.

On the other hand, the author has obtained the limiting area of the horse serum albumin molecule to be about 9820 $Å^2$ [4]. The chemical constitution of the serum albumin molecule has been determined by several authors[11] and it is calculated that one serum albumin molecule contains about 780 amino acid residues. Thus, the mean limiting area per one amino acid residue becomes to be 12.5 $Å^2$. This value is far less than the limiting area of the diketopiperazine film (17.3 $Å^2$/amino acid residue) and, it can be denied that the polypeptide chain of the serum albumin shows diketopiperazine configuration as it is spread on the surface.

The value of 14.7 $Å^2$ is obtained by Isemura[3] for synthetic protein analogues and also by Alexander for the alanine-polymer[2]. And it is obvious that synthetic protein analogues also does not show the diketopiperazine confiuration, when they are spread on the water surface.

As Isemura has insisted, the above value of 14.7 $Å^2$ can be explained most perfectly by using Mizushima and Shimanouchi's E-type model,[12] while one amino acid residue of B-type molecule would cover about 10 $Å^2$. Dr. T. Shimanouchi and the present author has ascertained these two values from the experiments of glycine-polymer monolayer, which will be published in other report.

Anyhow, from these values, the configuration of polypeptide chain of surface denatured serum albumin does not comprise the diketopiperazine ring. Probably, it is the mixture of B-and E-type of Mizushima and Shimanouchi's model[12].

Summary

1. The curves of the surface pressure against area, the surface potential against area, and surface viscosity against area were obtained with diketopiperazine. All the three curves show the limiting area to be about 1.83 m^2/mg or 34.6 $Å^2$ per molecule.

2. Comparing this result with that obtained by Corey, diketopiperazine molecules are thought to lie flat on the surface.

3. The above value is far larger than the limiting areas of native serum albumin or synthetic protein analogues. And the polypeptide chain will not show the diketopiperazine configuration on the surface.

The author wishes to express his hearty thanks to professors S. Mizushima and B.

10) R. B. Corey, *J. Amer. Chem. Soc.*, **60**, 1598 (1938).

11) W. Steine & S. Moore, *J. Biol. Chem.*, **178**, 79 (1949), E. Brand et al., *J. Amer. Chem. Soc.*, **67**, 1524 (1945).

12) S. Mizushima & T. Shimanouchi. This Bulletin, **21**, 1 (1948).

Tamamushi for their kind advice and encouragement. The author also owes much to Dr. T. Shimanouchi to whom the author's thanks are due. The expense of this work has been defrayed from the Grant in Aid for Fundamental Scientific Research from the Ministry of Education.

Chemical Institute, College of General Education, University of Tokyo

Intermolecular Charge-Transfer Spectra. I. Halogen-Aromatic Complexes

Hideo MURAKAMI

(Received February 17, 1953)

Introduction

Recently, Mulliken developed the theory of intermolecular charge-transfer spectra[1,2]. According to him, the concept of intermolecular charge-transfer spectra gives a reasonable explanation for many cases, such as halogen-aromatic complexes, organic molecular compounds, hydrated anions, etc. In the present paper, we shall study the characteristic absorption bands (λ_{max}: 2,800 Å~3,300 Å, ϵ_c: 7,000~14,000) of halogen-aromatic complexes, especially the dependence of the absorption intensity on the structure of aromatic components. In the case of methyl derivatives of benzene, experimental results indicate that the true molar extinction coefficient ϵ_c decreases with introducing methyl groups into an aromatic component. On the contrary, the above-mentioned theory indicates the increase of ϵ_c for the same condition as above, and Mulliken himself admits the difficulty of this contradiction. The chief object of the present paper is to solve this puzzle.

When halogen derivatives of benzene are used as aromatic components, the observed values of ϵ_c are mysterious. The reasonable interpretation for these results will also be given.

Absolute Intensity

In the case of hydrated anions, Rabinowitch introduced the idea of electron transfer spectra to explain the characteristic strong absorption band[3]. He attributed it to such an electron transfer from anion to water molecule as follows.

$$X^-\cdot(H_2O) \xrightarrow{h\nu} X\cdot(H_2O)^-$$

As was emphasized by Rabinowitch, the absorption intensity which corresponded to the above process was very large (ϵ~10,000).

It is obvious that anion X^- and molecule H_2O are chemically saturated. Therefore, we cannot expect the usual valence bond between them. Then the distance R between them may be approximately given by addition of their respective van der Waals radius. Consequently, R becomes relatively large compared with the usual covalent bond distances. This situation indicates the small overlapping between orbital functions of two components. Taking this fact into account, the above-described large absorption intensity is somewhat surprising.

Recently, Mulliken gave the quantum mechanical formalism to the idea of electron transfer spectra (in Mulliken's nomenclature, intermolecular charge-transfer spectra), and showed that large absorption intensity was understandable even when the intermolecular distance R was relatively large.

Now, we summarize the essence of Mulliken's theory in the suitable form for the present study. In complex A·B, A and B represents the acceptor and donor respectively. Then, two sorts of wave functions, ψ_0 and ψ_1, are defined. Firstly, ψ_0 is a "no-bond" wave function with respect to covalent bonding, that is

$$\psi_0=\psi(A\cdot B) \qquad (1)$$

Secondly, ψ_1 is a "dative" wave function corresponding to the transfer of an electron from B to A accompanied by the establishment of a weak covalent bond, that is

$$\psi_1=\psi(A^-—B^+) \qquad (2)$$

Using these wave functions, the wave function of the ground state N of any complex A·B is approximated by

1) R. S. Mulliken, *J. Am. Chem. Soc.* **72**, 600 (1950).
2) R. S. Mulliken, *J. Am. Chem. Soc.* **74**, 811 (1952).
3) E. Rabinowitch, *Rev. Mod. Phys.*, **14**, 112 (1942).

$$\psi_N = a\psi_0 + b\psi_1 \qquad (3)$$

In loose complexes, the relation $a^2 \gg b^2$ is expected. Further, we can expect that the overlap integral

$$S = \int \psi_0 \psi_1 dv \qquad (4)$$

is very small*, and neglect it in the following rough approximation.

From Eq. (3), the energy of the ground state is given by the lower root of the seqular equation

$$\begin{vmatrix} W_0 - W & H_{01} \\ H_{01} & W_1 - W \end{vmatrix} = 0 \qquad (5)$$

where

$$W_0 = \int \psi_0 \boldsymbol{H} \psi_0 dv \ , \quad W_1 = \int \psi_1 \boldsymbol{H} \psi_1 dv$$

$$H_{01} = \int \psi_0 \boldsymbol{H} \psi_1 dv \qquad (6)$$

$\boldsymbol{H}$ is the exact Hamiltonian operator for the entire system. The solution of Eq. (5) is given as

$$W = (W_1 + W_0)/2 \pm [(W_1 - W_0)^2 + 4H_{01}^2]^{\frac{1}{2}}/2 \qquad (7)$$

In case of loose complex, we can expect the relation

$$1 \gg 4H_{01}^2/(W_1 - W_0)^2 \qquad (8)$$

Taking this relation into account, we expand the second term of the right hand side of Eq. (7), then

$$\left.\begin{aligned} W_N &\simeq W_0 - H_{01}^2/(W_1 - W_0) \\ W_E &\simeq W_1 + H_{01}^2/(W_1 - W_0) \end{aligned}\right\} \qquad (9)$$

where W_N and W_E represents the energy of normal and excited state respectively. These are familiar second-order perturbation equations, and correspond to Mulliken's equations in which the overlap integrals S are taken as zero. The wave function ψ_E which belongs to the eigenvalue W_E takes the following formula

$$\psi_E = a\psi_1 - b\psi_0 \qquad (10)$$

The ratio of the coefficients a and b is easily given as follows,

$$\pm\rho = b/a \simeq -H_{01}/(W_1 - W_0) \qquad (11)$$

Using Eqs. (3) and (10), the dipole moment μ_{EN} of transition $(\psi_E \to \psi_N)$ is given as

$$\mu_{EN} = -e\int \psi_E \vec{r}\, \psi_N dv \simeq eab(\vec{r}_B - \vec{r}_A) \qquad (12)$$

where $\vec{r}_B$ and $\vec{r}_A$ represents the radius vector from origin of arbitrary coordinate to the center of two components B and A, respectively. So long as the wave functions ψ_N and ψ_E are normalized, the condition $a^2 \gg b^2$ requires that a is very near to unity and b is relatively small compared with unity. Under such a condition, the dipole moment μ_{EN} is very sensitive to the value of b and, according to Mulliken, a relatively small value of b is sufficient to explain the observed large absorption intensity. At the present stage, however, the reliable and exact determination of the value of b has not been established yet.

Relative Intensity (Analysis of Experimental Results)

In 1938, Aickin, Bayliss and Rees studied the absorption spectra of bromine in solution and observed the new intense absorption bands in the neighbourhood of 2950 Å in case of aromatic solvents[4]. They interpreted these bands, however, as bromine bands which were enormously enhanced by the solvent effect. Later, Benesi and Hildebrand investigated the absorption spectra of iodine in aromatic solvents[5]. The intense absorption bands which were analogous to those of bromine solutions were observed. Moreover, they found that the extinction coefficient of these bands was directly proportional to the iodine concentration using aromatic solvents. This fact indicates the existence of the equilibrium as follows,

$$I_2 + Ar \rightleftarrows I_2 \cdot Ar$$

where Ar denotes the aromatic hydrocarbon, and $I_2 \cdot Ar$ denotes the iodine-aromatic complex.

They considered that the above-mentioned intense absorption bands in the near ultraviolet region were due to only the presence of the complex $I_2 \cdot Ar$, and determined the

* The exact determination of the value of S is somewhat difficult. In case of iodine-benzene complex, Mulliken considered that the upper limit of S is the order of 0.1–0.2. According to our estimate, however, the overlap integral between π-orbital of benzene and σ-orbital of iodine do not exceed 0.02 so long as we assume the usual Slater type functions and the same model of complex as that of Mulliken.

4) R. G. Aickin, N. S. Bayliss and A. L. G. Rees, *Proc. Roy. Soc.* (London), **A169**, 234 (1938).

5) H. A. Benesi and J. H. Hildebrand, *J. Am. Chem. Soc.*, **71**, 2703 (1949).

true molar extinction coefficient ϵ_c of complex by taking into account the equilibrium constant for the above reaction. The results are given in Table 1. Keefer and Andrews performed the same experiment using chlorine, bromine and iodine monochloride instead of iodine and obtained the interesting results as shown in Table 1 and 2[7,8]. From these results, we can extract some noticeable relations as follows:

Table 1
Experimental Values of λ_{max} and ϵ_c

Aromatic Component	I_2-Aromatic Complexes		Cl_2-Aromatic Complexes	
	λ_{max} (A)	ϵ_c	λ_{max} (A)	ϵ_c
Benzene	2970	15400		9090
m-Xylene				6340
Mesitylene	3330	9300		

Table 2
Experimental Values of λ_{max} and ϵ_c

Aromatic Component	Br_2-Aromatic Complexes		ICl-Aromatic Complexes	
	λ_{max} (A)	ϵ_c	λ_{max} (A)	ϵ_c
Benzene	2920	13400	2870	9900
Toluene	3010	10500	2940	9050
t-Butylbenzene			2900	8470
o-Xylene	3130	8200	3030	7720
m-Xylene	3120	10100	3010	9000
p-Xylene	3060	7300	2950	7200
Chlorobenzene	2860	7300	2870	5650
Bromobenzene	2880	7600	2890	5750
Iodobenzene	3100	17000		

a) When toluene or *t*-butylbenzene is used as aromatic component instead of benzene, the true molar extinction coefficient ϵ_c derceases to some extent.

b) When xylene or mesitylene are used instead of benzene, ϵ_c decreases further except in the case of *m*-xylene. In the case of *m*-xylene complex, ϵ_c is almost the same as in toluene complex.

c) When chlorobenzene or brombenzene is used, ϵ_c is small and the same order of *o*-or *p*-xylene. In case of iodobenzene complex, howeuer, ϵ, is larger than that of benzene complex.

d) Now, we compare ϵ_c of Br_2-complex with those of corresponding ICl-complexes. (See Table 2). To extract the interesting regularity, we define the ratio k of ϵ_c as follows.

$$k_1 = \frac{\epsilon_c \text{ of } Br_2\text{-substituted benzene complex}}{\epsilon_c \text{ of } Br_2\text{-benzen complex}}$$

$$k_2 = \frac{\epsilon_c \text{ of ICl-substituted benzene complex}}{\epsilon_c \text{ of ICl-benzene complex}}$$

The values of k_1 and k_2 for various aromatic components are easily calculated using ϵ_c in Table 2, and shown in Table 3. Then, it is obvious that in any case the relation

Table 3
Comparison of k_1 and k_2

Aromatic Component	k_1	k_2
Benzene	1.00	1.00
Toluene	0.78	0.91
o-Xylene	0.61	0.78
m-Xylene	0.75	0.91
p-Xylene	0.54	0.73
Chlorobenzene	0.54	0.57
Bromobenzene	0.57	0.59

$$k_2 > k_1$$

exists without exception.

The main object of this paper is to explain the above-mentioned relations a), b), c) and d) considering the relative configuration of two components from the statistical point of view.

As is described in a) and b), true molar extinction coefficient ϵ_c decreases with introducing metyl groups into the aromatic components. According to Mulliken's theory, the reverse is predicted. As shown in Table 4, the ionization potential of an aromatic molecule decreases with introducing methyl groups[8]. This makes the value of $(W_1 - W_0)$ smaller, and according to Eq. (11), the value of $\rho = b/a$ larger. Consequently, Eq. (12) predicts the increase of dipole moment μ_{EN}, that is, the increase of absorption intensity. At first sight, the contradiction of experimental and theoretical results seems very difficult to solve. We can show, however, that the harmony between them is obtainable by the examination of a model.

Table 4
Lowest Ionization Potential (in ev)[8]

Aliphatic Compound	I. P.	Aromatic Compound	I. P.
Methane	13.1	Benzene	9.24
Ethane	11.6	Toluene	8.92
Propane	11.3	*t*-Butylbenzene	8.5*
Methyl Chloride	11.25	*o*-Xylene	8.3*
Ethyl Chloride	10.89	*m*-Xylene	8.3*
Methyl Bromide	11.17	*p*-Xylene	8.3*

6) R. M. Keefer and L. J. Andrews, *J. Am. Chem. Soc.*, **72**, 4677, 5170 (1950).
7) L. J. Andrews and R. M. Keefer, *J. Am. Chem. Soc.*, **73**, 462 (1951).
8) W. C. Price, *Chem. Rev.*, **41**, 257 (1947).

Ethyl Bromide	10.92 10.24[a]	Chlorobenzene	9.42[b]
Methyl Iodide	9.49	Bromobenzene	9.41[b]
Ethyl Iodide	9.34 9.295[a]	Iodobenzene	9.10[b]

* These value have been estimated by consideration of spectroscopic features other than Rydlberg series, and probably less accurate.

a) W. C. Price, *J. Chem. Phys.*, **3**, 365 (1935).

b) J. D. Morrison and H. J. C. Nicholson, *J. Chem.* Pys., **20**, 1021 (1952).

Relative Intensity (Statistical Consideration)

For the relative configuration of two components in the complex, Mulliken assumed the model, in which iodine or bromine molecule rests on the benzene molecule with its axis parallel to the plane of the benzene and its center on the sixfold axis of the benzene. It is obvious that this model is the most compact one, and stable on account of van der Waals interaction. Moreover, according to Mulliken's opinion, the resonance energy $-H_{01}^2/(W_1-W_0)$ between ψ_0 and ψ_1 in the ground state is larger in this model than in the other. (See Eq. (9)). Then, it is an interesting and important problem to compare the magnitude of van der Waals interaction energy with that of resonance stabilizing energy.

Experimentally, Cromwell and Scott measured the heat of formation of iodine-benzene complex.[9] Their results indicate that ΔH is approximately -1.4 Kcal./mol. This value is smaller than the energy in weak hydrogen bond and is the order of magnitude which is understandable as mere van der Waals interaction energy. Further, Ham, Rees and Walsh found out that the infrared spectra of saturated solution of iodine in the purified mesitylene was indistinguishable from that of mesitylene[10]. These results probably indicate that the main interaction is the van der Waals type, and the resonance type (in Mulliken's nomenclature, charge-transfer force) is smaller compared with the former.

If the van der Waals type is predominant and the resonance type is negligible compared with the former, Mulliken's idealized model needs some revision for halogen-substituted benzene complexes. For example, when the aromatic component is monosubstituted benzene, we can consider the two configurations (α) and (β) in Fig. 1, and can expect almost the same stability for them considering van der Waals type interaction. Then it occurs that (α) and (β) type complexes exist in solution with almost equal statistical weight.

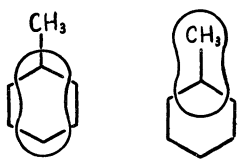

(α) Fig. 1 (β)

In case of model (β), the overlapping between π-orbital of aromatic component and σ-orbital of halogen component is decreased considerably, and the distance between centers of two components is slightly lengthened. These situations make the value of H_{01} smaller and of (W_1-W_0) slightly larger. Remembering Eqs. (11) and (12), we can expect the decrease of coefficient b, and then of dipole moment μ_{EN}.

In the experimental determination of ϵ_c, it was assumed that all the complexes had the same absorption intensity. As is shown before, however, this assumption is not a reasonable one, and the experimental values are nothing but the statistical mean for complexes (such as models (α) and (β)) which have their own various absorption intensities.

a) Bromine-Toluene Complex.—As idealized model, we consider the two relative configurations (α) and (β) which are shown in Fig. 2.

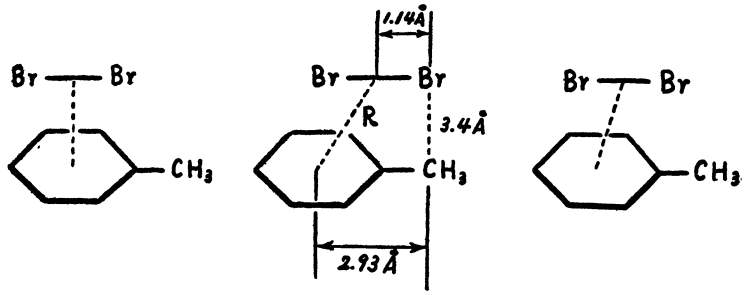

(α) (β) (γ)
Fig. 2

9) T. M. Cromwell and R. L. Scott, *J. Am. Chem. Soc.*, **72**, 3825 (1950).

10) N. S. Ham, A. L. G. Rees and A. Walsh, *J. Chem. Phys.*, **20**, 1336 (1952).

In model (α), all conditions are equal to that of an idealized model for bromine benzene complex which has been postulated by Mulliken, except the decrease of ionization potentical of aromatic component by amount of 0.32 ev. (See Table 4). Since the decrease of ionization potential causes the decrease of (W_1-W_0) by almost the same amount, it is expected that the wavelength λ_{max} at maximum absorption of toluene complex shifts towards the longer side. Taking $\lambda_{max}=2920$ Å. of benzene complex as origin, the decrease of (W_1-W_0) by amount of 0.32 ev. predicts $\lambda_{max}=3160$ Å. for model (α) of bromine-toluene complex. This is longer than the experimental value 3010 Å. As is easily shown, the absorption intensity of bromine-toluene complex in model (α) is almost the same as that of bromine-benzene complex, that is, $\epsilon_c^{(\alpha)}\sim13400$. (See Table 2).

In model (β), the intermolecular distance R which combines the center of bromine molecule and center of benzene ring is lengthened by the amount of 0.44 Å. This causes the decrease of absolute value of Coulombic energy by the amount of 0.48 ev in excited state. If the effect of polarization is taken into account, this value may become smaller to some extent. The decrease of absolute value of Coulombic energy tends to conpensate the variation of ionization potential and exchange interaction energy. Therefore, we assume that (W_1-W_0) is equal to that of bromine-benzene complex. Then λ_{max} in model (β) is expected to be 2920 Å. (See Table 2). In model (β), as discussed before, the overlapping between π-orbital of benzene ring and σ-orbital of bromine may decrease and this causes the decrease of ϵ_c considerably. The exact calculation of ϵ_c in model (β) is somewhat defficult; then we postulate that the value of ϵ_c in model (β) is the half of that in model (α) as tentative one, that is, $\epsilon_c^{(\beta)}\sim6700$.

Now, we bring up the third assumption that models (α) and (β) have almost equal stability and exist in solution with almost equal statistical weight. Then the molar extinction coefficient of bromine-toluene complex is give by

$$\epsilon_c=(\epsilon_c^{(\alpha)}+\epsilon_c^{(\beta)})/2=10500$$

The observed ϵ_c is just 10500 (See Table 2). On account of the superposition of two bands, the wavelength at absorption maximum becomes to lie in the middle of λ_{max} which are predicted for models (α) and (β), then approximately at about 3040 Å. The observed value is 3010 Å. The same result is obtainable by postulating model (γ) instead of the third assumption. In model (γ), the relative position of bromine to benzene ring is in the middle of models (α) and (β).

b) Bromine-Xylene complexes.—When *o*- or *p*-xylene is used as aromatic component, we can expect the three relative configurations as shown in Fig. 3. Then, as is postulated in bromine-toluene complex, we assume that these configurations have almost the same stability. Using the same values of $\epsilon_c^{(\alpha)}$ and $\epsilon_c^{(\beta)}$ as those used before, we obtain ϵ_c of bromine-xylene complex as follows.

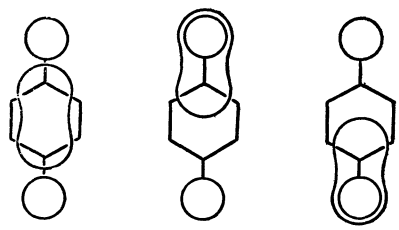

Fig. 3.

$$\epsilon_c=(\epsilon_c^{(\alpha)}+2\epsilon_c^{(\beta)})/3=8933$$

The observed value is 8200 for *o*-xylene complex, and 7300 for *p*-xylene complex.

In case of *m*-xylene complex, the observed value of ϵ_c is very large, that is 10100. This fact indicates that model (α) is more stable than model (β) and predominant statistically in solution. Consequently, we must consider that the benzene ring in *m*-xylene has a larger van der Waals attraction than that in *o*- or *p*-xylene.

According to experimental results of Platt and Klevens, the intensity of $N\rightarrow V$ type transition of π-electron in *m*-xylene is larger than that in *o*- or *p*-xylene.[11] The experimental total oscillator strength f of this transition is 1.46 for *m*-xylene and 1.22~1.23 for *o*- or *p*-xylene. According to our tentative estimate, this strong $N\rightarrow V$ type transition contributes considerably to the van der Waals interaction, and the larger f value of *m*-xylene may probably sufficient to explain the required larger van der Wasls attraction of benzene ring in *m*-xylene.

c) Bromine-Halogenobenzene Complexes.—When chlorobenzene or bromobenzene is used as aromatic component the observed ϵ_c is very small, and it has the same order with $\epsilon_c^{(\beta)}$ (See Table 2). This requires that model (β) is more stable than model (α), and almost all the complexes exist in the con-

11) J. R. Platt and H. B. Klevens, *Chem. Rev.*, **41**, 301 (1947).

figuration of model (β). If we take into account the interaction between large dipole of C—Cl or C—Br bond and the induced dipole in bromine molecule, the above requirement may probably be understandable.

On the contrary, when iodobenzene is used as aromatic component, the observed ϵ_c is very large. In case of iodobenzene, the ionization potential of substituted iodine (9.295 ev.) is almost equal to that of benzene (9.24 ev.) (See Table 4). Then, being different from other cases, π-electrons in substituted iodine can contribute to intermolecular charge-transfer spectra as well as π-electron in benzene ring. Consequently, the magnitude of H_{01} in model (β) may be equal to or larger than that in model (α). This situation may probably explain the observed large ϵ_c.

d) Iodine Monochloride-Aromatic Complexes.—As is shown in Table 3, there exists the relation,

$$k_2 > k_1$$

This relation requires that the stability of model (α) relative to model (β) is larger in ICl-aromatic complexes than in corresponding Br_2-aromatic complexes. This requirement may be understandable considering the interaction between large dipole of ICl and the induced dipole in the benzene ring.

The above discussions all concern the halogen-aromatic complexes. We can expect the validity of the analogous discussions for the other molecular compounds, such as quinhydron type molecular compounds. The detailed study for these cases will be reported later.

Summary

The intermolecular charge-transfer spectra of halogen-aromatic complexes have been studied theoretically. Especially, the dependence of absorption intensity on the structure of aromatic component has been investigated. To solve the discrepancies between experimental results and Mulliken's theoretical predictions, we have introduced the statistical consideration for the relative configurations between two components. Using some reasonable assumptions, we have obtained the satisfactory agreement between theoretical predictions and experimental results, at least qualitatively.

The author wishes to express his sincere thanks to Prof. S. Akabori for his encouragement and interest in the course of this work, and also to Mr. I. Tanaka and Y. Mori for their valuable discussions.

Faculty of Science, Osaka University, Osaka

Intermolecular Charge-Transfer Spectra. II. Pressure Effect on the Characteristic Absorption Spectra of Molecular Complexes

Hideo MURAKAMI

(Received March 20, 1953)

Previously, Gibson and Loeffler studied the absorption of visible light by solutions of amins in nitrobenzene under large hydrostatic pressures, and observed the significant change of absorption as a function of pressure.[1] Recently, Shuler presented a free electron model to explain the characteristic absorption spectra of molecular complexes, especially the above-mentioned pressure effect on these spectra.[2] According to our opinion, however, Shuler's theory is not a suitable one for the explanation of the present problem, at least in its original form. In the following discussion, we show that the kinetic consideration of Gibson and Loeffler combined with Mulliken's theory[3] may probably be sufficient to explain the observed pressure effect.

Discussion on Shuler's Theory

The essence of Shuler's theory can be summarized as follows. When two one dimensional conjugated molecules, A and B, ap-

1) R. E. Gibson and H. Loeffler, *J. Am. Chem. Soc.* **62**, 1324 (1940); See also, **61**, 2877 (1939).
2) K. E. Shuler, *J. Chem. Phys.*, **20**, 1865 (1952).
3) R. S. Mulliken, *J. Am. Chem. Soc.*, **74**, 811 (1952).

proach sufficiently close, the potential for π-electrons can be expressed by the idealized model as shown in Fig 1. Then, the pene-

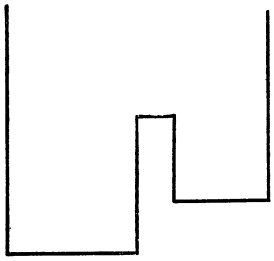

Fig. 1—One-dimensional unsymmetrical potential model for molecular complex.

tration of the central potential barrier by π-electrons produces a splitting of energy levels in the resulting two minimum potential. It was difficult, however, to obtain these splittings quantitatively for the unsymmetrical potential as described above, and Shuler assumed the simplified symmetrical potential as shown in Fig. 2. For this model, each

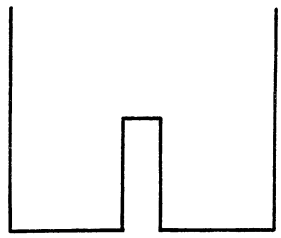

Fig. 2.—Simplified symmetrical potential model which is assumed by Shuler for molecular complex.

original energy level of the free molecule splits into two, and this situation is shown in Fig. 3. On account of the assumption of

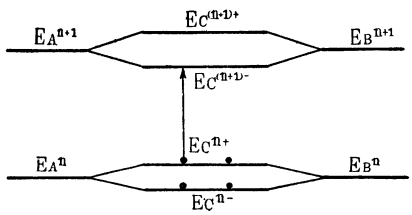

Fig. 3.—Splitting of energy levels by complex formation in case of symmetrical potential

symmetrical potential, one has the simple relationship

$$E_A{}^n = E_B{}^n \tag{1}$$

for all the energy levels of the conjugated molecular partners. Taking the splitting of each level into account, the energy levels E_C of the complex which correspond to the energy levels $E_A{}^n$ and $E_B{}^n$ of A and B can be expressed as follows:

$$E_C{}^{n+} = E_A{}^n + \varepsilon^n \tag{2}$$

$$E_C{}^{n-} = E_A{}^n - \epsilon^n \tag{3}$$

where $2\epsilon^n$ is the delocalization energy for the n the level. If $E_C{}^{n+}$ is the highest filled level of the complex, the main absorption band is then due to the transition

$$E_C{}^{n+} \longrightarrow E_C{}^{(n+1)-}$$

where

$$E_C{}^{(n+1)-} = E_A{}^{(n+1)} - \epsilon^{(n+1)} \tag{4}$$

and the wavelength λ_C of this absorption peak is given by

$$\lambda_C = \frac{hc}{\Delta E} = \frac{hc}{[E_A{}^{(n+1)} - E_A{}^n] - [\epsilon^{(n+1)} + \epsilon^n]} \tag{5}$$

Now, Shuler postulated that the effect of pressure reduced the width and height of central potential barrier corresponding to the closer approach of both components. This situation produces an increase of delocalization energy ϵ on account of easier penetration by π-electrons through the barrier. Consequently, as is seen in Eq. (5), the increase of ϵ produces an increase of λ_C, so long as one assumes the constancy of $[E_A{}^{(n+1)} - E_A{}^n]$. Thus, Shuler's theory predicts the shift of main absorption band towards the longer wavelength side at higher pressure.

We must emphasize, however, that the assumption of symmetrical potential is not adequate to amine-nitrobenzene complexes. In these cases, the potentials are rather unsymmetrical as shown in Fig. 4. And so, the condition of Eq. (1) becomes no longer valid. Then, Eqs. (2), (3), (4) and (5) lose their validity. According to Mulliken's theory, the characteristic absorption band of molecular complex (A B) corresponds essentially to the transition, as follows.

$$(A\,B) \longrightarrow (A^- - B^+)$$

That is, one electron is transferred from B to A in the process of optical transition. In a free electron model, this situation should be expressed by the transfer of a π-electron from level N_B to level $(M+1)_A$ as shown in Fig. 4. Further, in the case of an unsymmetrical model, the delocalization energy may be mainly due to the small amount of penetration of π-electron from level N_B to

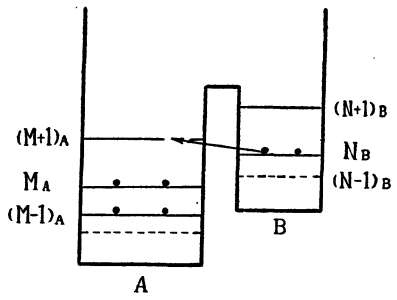

Fig. 4.—Expected relative height of energy level in case of unsymmetrical potential. (In the present case, component A and B corresponds to nitrobenzene and dimethylaniline respectively).

level $(M+1)_A$ through the potential barrier. Thus, the application of Shuler's model may probably be limited to the self-complex such as benzene-benzene complex.

Discussion on Absorption Intensity

The typical experimental results of Gibson and Loeffler are shown in Fig. 5 for 50% solution of dimethylaniline in nitrobenzene at 45°. The results are given as transmission curves. Curve 1 and 3 is the case of solution in 0.5 cm. cell at 1 bar and 1000 bars respectively. Curve 2 and 4 is the case of solution in 0.9 cm. cell at 1 bar and 1000 bars respectively. It must be emphasized that these curves are nothing but a very small portion of the complete absorption band, and the behaviours at the region of absorption maximum under the influence of pressure are not observed. Then, we cannot conclude directly

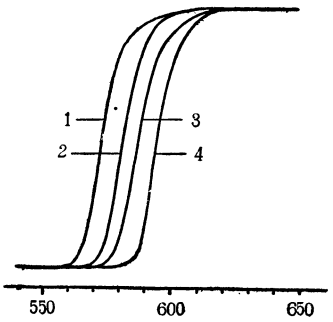

Wave length, mμ (approx.)

Fig. 5.—Transmission curves for 50% solution of dimethylaniline in nitrobenzene at 45°
1, solution in 0.5 cm cell at 1 bar;
2, solution in 0.9 cm cell at 1 bar;
3, solution in 0.5 cm cell at 1000 bars;
4, solution in 0.9 cm cell at 1000 bars.

the shift of absorption bands towards the longer side so long as the data are limited to the above mentioned ones.

Moreover, the comparison between curves 1 and 2 suggests that the pressure effect is mainly due to the intensification of light absorption. In case of curve 2, the absorbing layer is increased 1.8-fold in thickness compared with curve 1. Consequently, we can expect that the degree of light absorption is also increased by the same amount. This situation appears in Fig. 5 as if the absorption band is pushed towards the longer wavelength side, although the location of the absorption band should be the same in either case. If we assume that the pressure effect is only due to the intensification of light absorption, the distance between curves 1 and 3 or curves 2 and 4 requires that the absorption intensity is 2.5~3.5-fold increased under the pressure of 1000 bars, at least in the region of the observed wavelength.

At the present stage, we cannot give any conclusion whether the wavelength at absorption maximum shifts towards the longer or shorter side, or remains at the same position under the effect of pressure. On the other hand, however, we can give a rather definite explanation of the intensification of light absorption, as follows.

Gibson and Loeffler assumed that the absorption of visible light by the solution was proportional to the average time the active groups of unlike molecules spent very close to each other, i.e., to the probability of finding two unlike molecules at very short distances apart and suitably oriented in the solution. Using kinetic consideration and some empirical relations which were obtained by them, they showed that the above hypothesis was sufficient to explain the intensification of light absorption due to the increase of pressure at constant temperature or the elevation of temperature at constant volume. Then, the remaining task is to base the hypothesis of Gibson and Loeffler by Mulliken's theory on intermolecular charge-transfer spectra.

According to Eq. (12) in Part I, the dipole moment of charge-transfer spectra is approximated by the formula

$$\mu_{EN} \simeq e_{ab}(\vec{r}_B - \vec{r}_A) \qquad (6)$$

were

$$b/a \simeq -H_{01}/(W_1 - W_0) \qquad (7)$$

As has been discussed in Part I, dipole moment μ_{EN} is sensitive to the value of H_{01}. Since absorption intensity f_{EN} is proportional

to the square of μ_{EN}, f_{EN} is much more sensitive to the value of H_{01}. Further, as can easily be seen from Eq. (6) in Part 1, the value of H_{01} is very sensitive to the overlap between the wavefunctions (in the present case, between that of π-electron systems) of both components. The degree of overlap depends very much on the distance and relative orientation between both components. Consequently, the increase of the probability of finding two unlike molecules, A and B, at very short distances apart and suitably oriented in a solution makes the absorption intensity much larger. Thus, the hypothesis of Gibson and Loeffler is based by the theory of intermolecular charge-transfer spectra.

The author wishes here to express his sincere gratitude to Prof. S. Akabori for his interest and encouragement throughout the study of this series.

Faculty of Science, Osaka University, Osaka

Physicochemical Properties of the Surface of Aqueous Solutions VI. Breaking of the Solid Surface

By Hideo KIMIZUKA

(Received May 14, 1953)

In one of our preceding papers, the study on the mechanical properties of the surface of a solution[1] was carried out in relation to the foam stability and a further investigation was continued on the mechanical behavior of the surface[2]. As to the foam stability, however, it may be pointed out that the formation of the coherent adsorbed layer though closely related is not an exact explanation for the stabilizing action of the foam, because the mechanical behaviors thereby investigated was that of the surface film suffering no destruction. On the other hand, some complicated phenomena such as an irreproducibility in the surface tension value[3], and the membrane effect were observed when the surface tension was measured with a solution forming a solid film. So a further study on the mechanical property of the film near the yield point, where so-called time dependent phenomena[4,5] were frequently observed, was attempted to obtain a more plausible explanation for these phenomena.

1) H. Kimizuka and T. Sasaki, This Bulletin, **24**, 230 (1951).
2) H. Kimizuka and T. Sasaki, This Bulletin, **25**, 318 (1952); H. Kimizuka, ibid, **26**, 30, (1953).
3) du Noüy, "Surface Equilibria of Biological and Organic Colloids" *J. Am. Chem. Soc.*, Monograph Series No. 27, Chemical Catalog Comp. Inc., New York (1926).
4) W. F. Busse, E. T. Lessig, D. L. Loughborough and L. Larric, *J. App. Phys.*, **13**, 715 (1942).
5) H. Kubota, *Oyo Butsuri* (*J. App. Phys.*), **17**, 286 (1948).

Experimental and Result

In the present study, the solutions used were chosen so that the liquid might form a solid film[2]. In the first place, a distribution of the life-time of the aqueous film was observed under a constant tension using du Noüy's tensiometer. A platinum ring of the tensiometer, 1.5 cm. in diameter, was just touched to a fresh surface of 1% saponin solution contained in a shallow glass vessel, 6 cm. in diameter and 1.3 cm. in depth. A constant tension was applied to the ring and the breaking time, t, elapsed before the detouchment of the ring from the surface was measured. The experiments were carried out at 28±1°C. The results showed that N, the number of breakings which occurred after a time t, was empirically approximated by the equation,

$$N = N_0 e^{-mt} \qquad (1)$$

where N_0 and m are constants excepting the case in the region of the smaller time. The results of similar experiments under diffrent tensions were shown in Fig. 1. For water, ethyl alcohol and its aqueous solution, m was either zero or infinity.

A measurement of the breaking time as a function of stress was carried out by means of the torsion ring method. The apparatus[2]

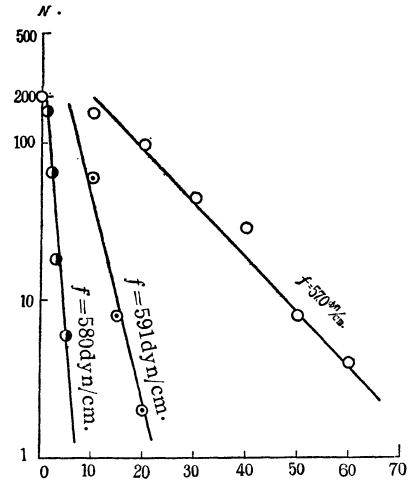

Fig. 1. Distribution of breaking time with constant tension. Saponin solution (10g./l.).

used was essentially the same as described already, but in this case a suspension wire with a torsion constant, κ, of 5.35 dyn. cm. and a platinum ring with diameter of 2.0 cm. was used and the inner cylinder was removed. The breaking time, τ, elapsed before the sudden increase in a strain of the surface, $d\theta$ was measured under a constant torsional force, f ($=\kappa\theta_0$, θ_0 being a torsion angle) for 1 g./l. saponin solution aged for one hour. The temperature of this and all of the following experiments was 10±1°C. One of the results is shown in Fig. 2. The following relation can then be found to hold as shown in Fig. 3 a,

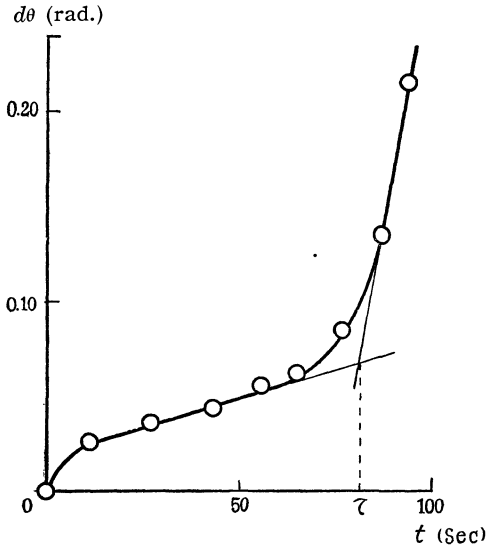

Fig. 2. Strain~time curve near rupture of absorbed layer of saponin solution (1g./l.) aged for 1 hr. $f=\kappa\theta_0=22.8$ dyn. cm.

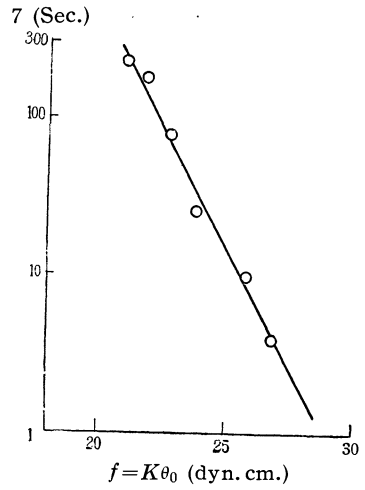

Fig. 3 a. Breaking time as a function of stress. Saponin solution (1g./l.).

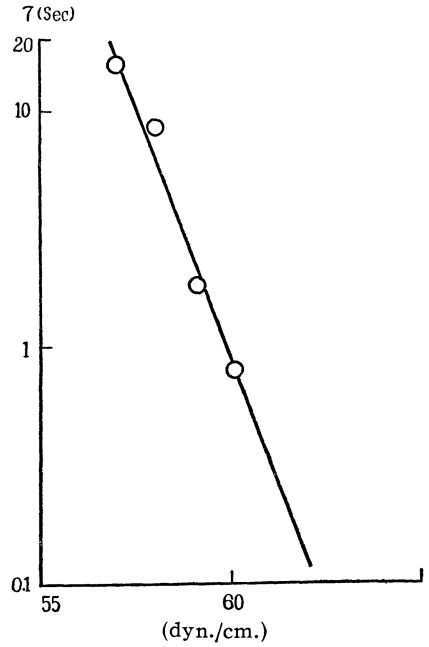

Fig. 3 b. Breaking time as function of stress. Saponin solution (10g./l.).

$$\log\tau = a - bf \qquad (2)$$

where a and b are constants.

The torsion ring method was also applied for the measurement of yield value. Immediately after a breaking of the surface by rotating the top of torsion wire with the

angle of θ_r under the condition of $\tau \fallingdotseq 0$, the top was returned to the initial position and θ_a, an angle at which the motion of the ring was stopped, was measured. Thus we obtained the values $\kappa\theta_r$ and $\kappa\theta_a$ which were considered to correspond to the yield value of breaking and solidifying respectively. The membrane effect[1], M, was measured by the capillarimeter with a radius of 0.0284 cm. Now it can easily be seen that $\kappa\theta_r$ and $\kappa\theta_a$ should correspond to M_r and M_a respectively, where M_r and M_a represent the membrane effect acting on the receding and advancing meniscii in the capillary tube. Here the true surface tension is assumed to be situated between the two apparent surface tensions and $M=M_r+M_a$. Both the measurements of the yield value and the membrane effect were carried out for the surfaces of solutions containing various substances aged for one hour. The result is shown in Fig. 4, in which the ordinate represents M; the abscissa, $F_0=\kappa(\theta_r+\theta_a)$.

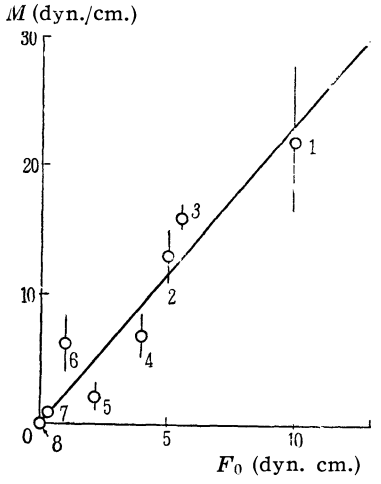

Fig. 4. Membrane effect versus yield value of adsorbed layer diagram for solutions. 1, 0.25 g./l. saponin solution; 2, 0.10g./l. saponin solution; 3, 1g./l. egg albumin solution; 4, 10g./l. peptone solution; 5, 5g./l. polyvinyl alcohol solution; 6, 5×10^{-3} M./l. night blue solution; 7, 5g./l. gum arabic solution; 8, water.

A method for the measurement of the surface tension was devised as follows. A platinum ring of the du Noüy's tensiometer was just touched to the surface of a solution, which was pulled upward by the applied force, and a rise of liquid meniscus was measured. Under such a condition, the principal section of the free liquid surface is represented as shown by a curve AB in Fig. 5. In this figure, A shows a cross section of the

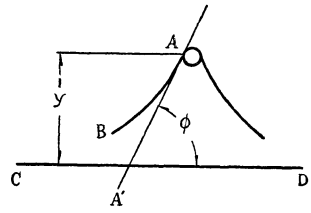

Fig. 5.

platinum ring and AA' is a tangent to the curve AB at the point of contact A, and makes an angle ϕ with the horizontal surface of liquid. Then a rise of meniscus y is given by the equation[6],

$$\rho g y^2 = 2\sigma(1-\cos\phi), \qquad (3)$$

where ρ is the density of liquid; g, the gravity constant and σ, the surface tension. Now if f is a force exerted by the ring per unit length,

$$f=\sigma \sin\phi. \qquad (4)$$

A simple calculation* using Eqs. (3) and (4) leads to the expression,

$$\lim_{y\to 0}\frac{df}{dy}=(\rho g\sigma)^{\frac{1}{2}}$$

or

$$\sigma=\frac{1}{\rho g}\left(\lim_{y\to 0}\frac{df}{dy}\right)^2 \qquad (5)$$

This relation holds fairly well for ethyl alcohol solutions with varying concentrations as shown in Fig. 6, where σ is measured by the usual method. In the case of the surface exhibiting the nature of a solid film, σ in Eq. (5) should be replaced by σ' of the following equation,

$$\sigma'=\sigma+Ed\zeta, \qquad (6)$$

where E is the elastic constant and $d\zeta$, an increase in surface area with relation to y. Since the condition of $y\to 0$ corresponds to that of $d\zeta\to 0$, σ' is equal to σ in such a case and again the Eq. (5) is valid, namely the equation gives a true surface tension even when the surface film becomes somewhat

6) F. C. Chapman and N. Davy, "Properties of matter". Blackie & Son Ltd., London and Glasgow, (1936) p 104.

* If we assume further the condition of $f=\sigma$ and therefore $\phi=\pi$ 2 in this calculation, $\sigma=\frac{1}{2}\rho g y_0^2$ results, where y_0 is y when $\phi=\frac{\pi}{2}$, a maximum rise of the meniscus. This equation was confirmed by the experiment using ethyl alcohol solution with varying concentration. The result is shown in Fig. 8.

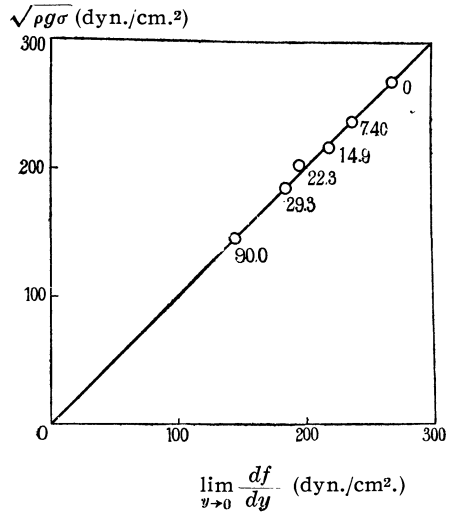

Fig. 6. Relation between $\lim_{y\to o}\frac{df}{dy}$ observed and $\sqrt{\rho g\sigma}$ calculated. Number listed at each point represents the concentration (%) of aqueous ethyl alcohol solution.

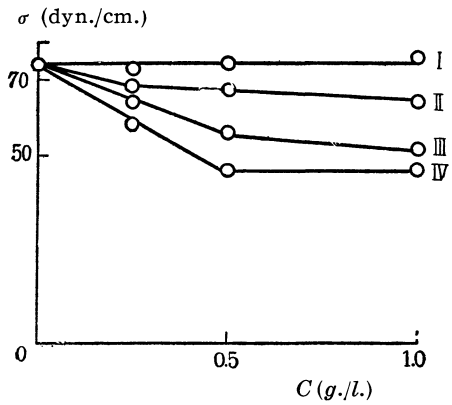

Fig. 7. Surface tensions of saponin solution. Each curve shows the values of surface tension measured by the ring method (II), present method (III) and capillary method (I and IV which correspond to receding and advancing meniscii respectively.).

solid in nature. Thus the present method was adopted for the measurement of surface tension of the saponin solution aged for one hour. The values obtained for various concentrations were plotted in Fig. 7, together with those of apparent surface tension obtained by the capillary rise method with receding and advancing conditions, and the ring method.

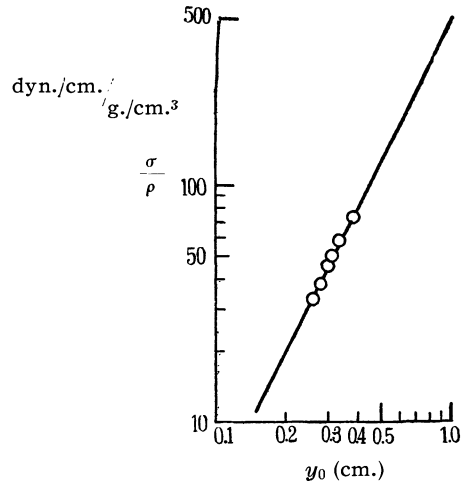

Fig. 8. Ethyl alcohol solution.

Discussion

It has frequently been pointed out for the measurement of surface tension of such a solution as saponin solution that the reproducible results could hardly be obtained even when the experimental conditions such as temperature, concentration and time of ageing were carefully controlled[3]. Among the other factors which are responsible for such a fluctuation, the breaking of the solid film hereby formed can be considered most important. In fact, if the measurement is carried out by means of du Noüy's tensiometer, the measured "surface tension" may actually be the force required for the breaking of the surface film. Results obtained as shown in Fig. 1 evidently show this fact. Kubota[5] obtained a similar result for the breaking of glass which he accounted for by introducing the probability of breaking, m, which was independent of time. Now it was confirmed that in the case of common liquids, m sharply changed from zero to infinity as the external force increased, whereas in the case of saponin solution m changed gradually from zero to infinity.

We should like further to refer to the equations (1) and (2). The phenomena expressed by these equations are liable to conflict with each other. As shown in Fig. 1, however, the deviation from the constancy of the value of m was observed in the region of shorter time, and in fact a frequency of occurrence of breaking showed a maximum in this range of time. A time, τ, at which the maximum frequency was observed was again related with the corresponding stress, f, by the equation (2). This was shown in Fig. 3b.

This relation was further confirmed by the measurement of the thin film withdrawn from the surfaces of 1% solutions of saponin and egg albumin, which was not given here. A possibility may further be considered that the surface tension effect would also be the cause of this phenomenon, but the result of the torsion ring method may exclude such a possibility, since here the surface area is kept constant and the motion of the ring is free from the action of surface tension. Thus the coincidence of the results of both techniques gives us the confirmation that they can be explained by the same mechanism, the breaking of a solid film. A similar relation was also observed for the breaking of high polymer[4] and was also treated theoretically[7]. These fact together with our former result[2] lead us to the opinion that the rupture of an aqueous saponin film rather resembles the breaking of a solid body such as glass or high polymer, and should not be treated as the rupture of the ordinary liquid film. Thus the breaking of the surface film, proved to occur in some range of stress, may result in the irreproducibility of apparent surface tension, if we do not specify the time required for the rupture of film, for instance, to be sufficiently small. A number of explanations[8] for the foam stability have already been presented, but they all neglected to take into account of this fact.

As shown in Fig. 4, the membrane effect was proportional to the yield value of the solid film, which was valid for the several solutions. This will be a confirmation of the view presented in a preceding paper[9] that the membrane effect is a measure of the strength of the surface.

As pointed out before, the irregularity of surface tension is due to the rupture of solid film, so a method free from such an influence is required for a measurement of true surface tension. The technique devised proved to be applicable for common liquids as shown in Fig. 6, which showed a good agreement with the result obtained by the usual method for ordinary solutions. On the other hand, the apparent surface tension of saponin solution measured by the usual method was somewhat higher than that by the present method as shown in Fig. 7. This probably means that the usual method involves an inevitable rupture of surface film. Fig. 7 also showed that the true surface tension is situated between two apparent surface tensions measured previously by a capillarimeter[9].

7) A. Tobolsky and H. Eyring, *J. Chem. Phys.*, **11**, 125 (1943).
8) T. Sasaki, *Kagaku no Ryoiki*, **5**, 16 (1951).
9) H. Kimizuka and T. Sasaki, *Memoirs of the Faculty of Science, Kyushu University, Ser. C*, **1**, 197 (1950).

Summary

(1) The rupture of aqueous saponin film was studied by measuring the variation of the frequency of the breaking with tension as well as by measuring the breaking time as a function of stress. The results showed that the irreproducibility of the observed data upon surface tension was due to the breaking of the solid film and this mechanism was also responsible for the nature of the stability of such a foam as that produced by saponin, which was also considered to consist of solid film.

(2) A new method for the measurement of surface tension, applicable to the solution forming a solid adsorbed layer, was presented.

(3) It was shown that the membrane effect is a breaking stress of the adsorbed layer.

In conclusion, the author expresses his hearty thanks to Prof. T. Sasaki for his kind guidance and encouragement throughout this study and he is also indebted to Dr. T. Tanaka of this University for his kind suggestion and criticism. A part of the cost of this research has been defrayed from the Scientific Research Expenditure of the Ministry of Education given to Professor Sasaki.

Department of Chemistry, Faculty of Science, Kyushu University, Fukuoka

Synthesis and Dielectric Polarization of 9-Anthranol

By Kenkichi NUKADA and Yoshié BANSHO

(Received June 23, 1953)

Introduction

K. H. Meyer reported in 1911 on the synthesis of 9-anthranol, which is the simplest substance in leuco-compounds of anthraquinone series, and also on its behaviour in several organic solvents.[1] He observed that 9-anthranol exhibited strong fluorescence in some solvents and explained that there might exist in solution a chemical equilibrium between anthrone and 9-anthranol, the reaction velocity

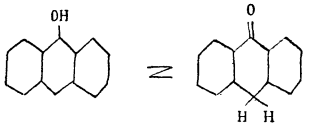

9-Anthranol Anthrone

Fig. 1

and equilibrium constant of which depended on solvent. Bäckström et al. pointed out an iodine titration method for the quantitative analysis of 9-anthranol.[2] Le Fèvre et al. investigated the dielectric behaviour of the same substance and its methyl ether. However, the above-mentioned authors could not prepare pure 9-anthranol. The present authors have established the best condition of synthesis of 9-anthranol and measured the dipole moment of it by the solution method. The reproducibility was satisfactory.

Experimental

Synthesis

The original procedure of Meyer[1] and the modified one of Bäckström and Beatty[2] have been traced, but the purity of 9-anthranol prepared in this way was unsatisfactory. The authors have synthesized 9-anthranol of high purity by improving these two methods. They have found that it was important to operate the synthesis continually in a stream of nitrogen (to prevent oxidation) and to maintain the temperature as low as possible (to prevent isomerisation) during the preparation. The result of synthesis had good reproducibility.

Anthrone was prepared from anthraquinone (Org. Syn. Coll. vol. 1, p. 60) and recrystallised twice from mixed solvent of benzene and petroleum ether (3:1). m.p. 154.7°C.

The apparatus is shown schematically in Fig. 2, and the procedure is as follows:

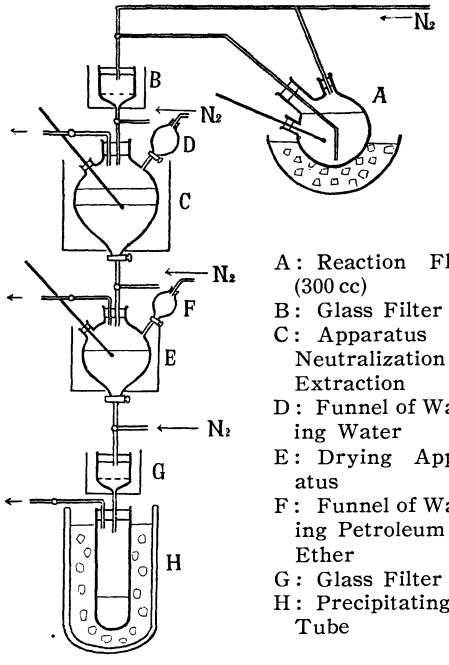

A: Reaction Flask (300 cc)
B: Glass Filter
C: Apparatus for Neutralization and Extraction
D: Funnel of Washing Water
E: Drying Apparatus
F: Funnel of Washing Petroleum Ether
G: Glass Filter
H: Precipitating Tube

Fig. 2. Apparatus for Synthesis of 9-Anthranol

3.0 g. of fine powdered anthrone was boiled in 180 g. of 10% aqueous solution of sodium hydroxide for about ten minutes in a stream of nitrogen, and as soon as the boiling was over, 300 g. of ice pieces were added and the flask was cooled rapidly by an ice sodium chloride bath set outside. When the temperature of the solution lowered to −5°C, the flask was arranged as indicated in Fig. 2, A, and cooled to maintain this temperature.

Apparatus for neutralization and extraction, C, which contained 120 cc. of toluene, 300 cc. of distilled water, 300 g. of ice pieces and 15 cc. of 98% sulphuric acid, was cooled from outside by solid carbon dioxide to maintain −5°C. The solution of sodium salt of 9-anthranol was poured directly into C in a stream of nitrogen and shaken; the

1) K. H. Meyer, *Ann.*, **379**, 37 (1911).
2) H. Bäckström and H. Beatty, *J. Phys. Chem.*, **35**, 2549 (1949).
3) C. L. Angyal and R. J. W. Le Fèvre, *J. Chem. Soc.*, **1950**, 562.

precipitated 9-anthranol was extracted in upper toluene layer. Then by the pressure of nitrogen the water layer was removed, the toluene layer was washed with 200 cc. of distilled water and the water layer was removed similarly. The yellow emulsion was sent into a drying apparatus F which contained 80 g. of fresh calcined and oxygen-free anhydrous sodium sulphate, and was shaken at −5°C. 20 cc. of petroleum ether (b.p. 60~70°C.) was cooled beforehand at ca. −70°C. in a precipitating tube H which was immersed in a solid carbon dioxide-methanol bath; the clear dried 9-anthranol toluene solution was then poured into petroleum ether through the glass filter G by the suction and the pressure of nitrogen. Sodium sulphate was washed with 60 cc. of petroleum ether (b.p. 60~70°C) and solution in H was diluted simultaneously. The pale yellow precipitate of 9-anthranol was deposited immediately and the precipitation was accomplished in an hour. The precipitate was filtered in a stream of nitrogen as rapidly as possible, washed with 50 cc. of petroleum ether (b.p. 45~50°C), then taken in a vacuum desiccator and sucked by a vacuum pump for half an hour at 0°C to remove petroleum ether contained in crystal. Then the product was dried for about ten hours over phosphorous pentoxide in a vaccum at the same temperature. The yellow fine crystal of 9-anthranol was enclosed in ampouls in a stream of nitrogen. yield: 1.5—1.7 g.

Infrared spectrum of 9-anthranol suspended in Nujol was measured and a strong absorption band of OH group was observed.

Notice

1) Water and toluene used in the synthesis were distilled in a stream of nitrogen, so that they were free from oxygen.

2) It was necessary to cool all the apparatus, A to G, at −3 ~ −5°C by small pieces of solid carbon dioxide.

3) All the transfusions of liquid were made in a closed apparatus by the suction or under the pressure of nitrogen, and the whole time of preparation was within half an hour.

4) Oange-yellow to red crystal was deposited, if the temperature rose or the air leaked into the apparatus. The product prepared in this way could not be used as a sample for the measurement of dielectric constant because the reproducibility of results was unsatisfactory.

Behaviour in Solvent

9-Anthranol was dissolved in several solvents and the times t's required for the complete disappearance of fluorescence of solutions were measured. (Table 1). According to Meyer,[1] t was a function of the reaction velocity of tautomerism.

In ethanol, dioxane and ether t's were large and the reactions were supposed to be slow. However in carbon disulphide, carbon tetrachloride, acetone and pyridine no fluorescence appeared and the reactions were supposed to be very fast. In benzene t was large and as the number of methyl groups of benzene ring increased, t decreased. In petroleum ether, n-heptane and cyclohexane t's were large but practically these solvents could not be used in the dielectric measurement because the solubilities in these were very small.

As the suitable solvents the authors then chose benzene, dioxane and toluene for the following experiments.

Table 1

The Times Required for the Complete Disappearance of Fluorescence at 7°C.

Solvent	Solubility	t (hours)
Benzene	+	22
Toluene	+	10
m-Xylene	+	5
Chlorobenzene	+	0.5
Methanol	+	6.5
Ethanol	+	ca. 50
n-Buthanol	+	7
i-Amyl Alcohol	+	17
Ether	+	24
Dioxane	++	ca. 60
Petroleum Ether (b.p. 40~60°C.)	−	24
n-Heptane	−	24
Cyclohexane	−	23
Acetic Acid	+	1
Chloroform	+	0.2
Carbontetrachloride	+	No fluorescence
Carbon Disulphide	+	„
Acetone	+	„
Pyridine	++	„

The symbols are: ++ very great, + ordinary, − very small.

Dielectric Measurements

Solvent: All the solvents were purified according to the methods in "Organic Solvents".[4]

Density: Ostwald-type pycnometer was used.

Instrument: Usual Heterodyne-beat type oscillator designed and constructed by one of the authors (Nukada) was used to measure dielectric constants of solutions.[5] Capacities of sample cells were from 50 pF to 80 pF.

The synthesized sample had to be stored in nitrogen atomosphere at low temperature and to be dissolved in solvents as quickly as possible. When the purity of a sample was low or the temperature of solution too high, 9-anthranol changed into anthrone and the fluorescence of the solution vanished rapidly.

4) A. Weissberger and E. Proskauer, "Organic Solvents", Oxford University Press, 1935, p. 106, 107, 140.

5) e.g. see J. W. Baker and L. Groves, *J. Chem. Soc.*, **1939**, 1144.

Table 2

The Dielectric Constants and the Densities of 9-Anthranol in Several Organic Solvents.*) **) ***)

i) Solvent: Benzene, 6.3°C.

ω	ε_{12}	v_{12}
0.01297	2.345	—
0.00885	—	1.1164
0.00485	2.325	1.1178
0.00165	2.318	1.1190

$\varepsilon_1=2.313$ $v_1=1.1193$
$\alpha=23.0$ $\beta=-0.397$
$p_{20}=0.634$ $P_{20}=123$ cc
$\mu=1.72$ D

ii) Solvent: Benzene, 15°C.

ω	ε_{12}	v_{12}
0.02197	—	1.1240
0.01654	2.338	—
0.01299	2.330	—
0.00877	2.317	1.1281
0.00860	2.315	—
0.00520	2.309	1.1295
0.00386	2.304	—
0.00234	—	1.1303
0.00165	2.299	—

$\varepsilon=2.294$ $v_1=1.1309$
$\alpha=26.7$ $\beta=-0.332$
$p_{20}=0.73$ $P_{20}=142$ cc
$\mu=1.99$ D

iii) Solvent: Dioxane, 15°C.

ω	ε_{12}	v_{12}
0.01424	2.336	0.9578
0.01044	—	0.9588
0.00380	2.306	0.9605
0.00229	2.303	0.9610

$\varepsilon_1=2.298$ $v_{12}=0.9614$
$\alpha=26.7$ $\beta=-0.264$
$p_{20}=0.63$ $P_{20}=122$ cc
$\mu=1.82$ D

iv) Solvent: Benzene-Dioxane Mixture, 15°C (Mol fraction B : D = 10 : 1)

ω	ε_{12}	d_{12} (g/cc)	P_2 (cc)
0.01555	2.352	0.9089_2	162
0.01296	2.341	0.9076_8	159
0	2.295	0.9028_5	—

$P_{20}=161$ cc $\mu=2.20$ D

v) Solvent: Benzene-Dioxane Mixture, 15°C (Mol fraction B : D = 100 : 1)

ω	ε_{12}	d_{12} (g/cc)	P_2 (cc)
0.02150	2.350	0.8979_9	138
0.00914	2.313	0.8935_7	132
0	2.291	0.8911_3	—

$P_{20}=135$ cc $\mu=1.91$ D

vi) Solvent: Toluene, 15°C.

ω	ε_{12}	d_{12} (g/cc)	P_2 (cc)
0.02117	2.444	0.8788	115
0.01605	2.440	0.8776	128
0.00826	2.426	0.8767	134
0.00409	2.409	0.8728	132
0	2.398	0.8713	—

$P_{20}=133$ cc $\mu=1.88$ D

*) The symbols used in this Table are the same as those of Halverstadt and Kumeler.[7] ε_{12}: dielectric constant of solution, v_{12} ($=1/d_{12}$): specific volume of solution (cc/gr), ω: concentration (weight percent), P_2: solute molar polarization, P_{20}: solute molar polarization at infinite dilution, p_{20}: solute specific polarization at infinite dilution: $\alpha=\frac{d\varepsilon_{12}}{d\omega}$, $\beta=\frac{dv_{12}}{d\omega}$, ε_1: dielectric constant of solution at infinite dilution, v_1: specific volume at infinite dilution, μ: dipole moment (Debye unit).

The values of α, ε_1, β and v_1 were calculated utilizing the statistical method of least squares.

**) In calculation of the orientation polarization the authors have assumed that the sum of electric polarization and atomic one was equal to the molar refraction MR_D for sodium D line. For 9-anthranol $MR_D=58$ cc.

***) μ were calculated as

$$\mu=0.0128\times\sqrt{(P_{20}-MR_D)T}$$

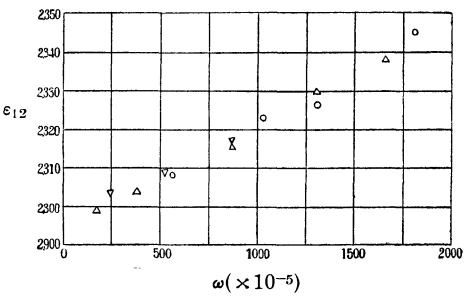

Fig. 3. Relation between ω and ε_{12}
Solvent: Benzene. 15°C.
Symbols △, ▽ and ○ represent the results of several experiments under the same condition.

Results

Dielectric constants and densities of several solutions were measured at various concentrations. (Table 2).

All the $\omega\sim\varepsilon_{12}$ curves became straight lines except for toluene solution.[6]

The dipole moments of 9-anthranol in benzene and dioxane solutions were calculated by Halverstadt-Kumler's equation[7] and the moments in other solutions by the usual method.[8] The results are in Table 3. Since in solutions there exists a chemical equilibrium

6) Fig. 3 shows the result of several measurements under the same experimental condition. Unlike the case of other samples, (e.g. anthrone in benzene, Denys, I. Coomber and J. R. Partington, *J. Chem. S.oc*, **1938**, 1444,) the curves were not fine straight lines. This deviation means probably the unstability of 9-anthranol in solvents.

7) I. F. Halverstadt and W. D. Kumler, *J. Am. Chem. Soc.*, **64**, 2988 (1942).

8) P. Debye, "Polare Molekeln". Leibzig, 1929.

between 9-anthranol and anthrone, values in Table 3 do not mean the "exactly true value of dipole moment of 9-anthranol" but should be regarded as a "nearly true one", because in such solvents the velocity constants are small. Le Fèver et al. measured the dipole moment of 9-anthranol methyl ether. (1.5 D). Noting a difference of 0.4~0.5 D between phenol and its methyl ether, they supposed that 9-anthranol had a moment of 1.9~2.0 D.[3] The authors' result agrees with this supposition.

Table 3

The Dipole Moments of 9-Anthranol in Several Organic Solvents

Solvent	Temp	Moment (Debye Unit)
Benzene	6.3°C	1.72 D
Benzene	15 °C	1.99 D
Benzene : Dioxane (100 : 1)	15 °C	1.91 D
Benzene : Dioxane (10 : 1)	15 °C	2.20 D
Dioxane	15 °C	1.82 D
Toluene	15 °C	1.88 D

In benzene-dioxane mixture, the moment values are comparable with Nagakura and Baba's result on phenol.[9]

In toluene $\omega \sim \varepsilon_{12}$ curve was not a straight line.

It may be reasonable to explain the stabilisation of 9-anthranol by the assumption that in benzene[10] and dioxane[11] OH-group of 9-anthranol makes weak combination with solvent and the potential barrier between anthrone and 9-anthranol becomes higher, hydrogen atom of 9-anthranol's OH is thus hindered from shifting to the position "10" of anthracene ring. The results in Table 1 also support this asumption except for acetone and pyridine, in which the stabilisation of 9-anthranol by the combination O···H—O and N···H—O can be expected, but the causes of these exceptions are not plain now.

9) S. Nagakura and H. Baba, *J. Am. Chem. Soc.*, **74**, 5693 (1952).

10) There is a coupling of π-electrons of benzene with proton of OH-group in solute molecule. (W. Lütte and R. Mecke, *Z. Elektrochem.* **53**, 241 (1949).)

11) In dioxane a hydrogen bond between solvent and solute may exist.

Summary

1) The condition of synthesis to obtain pure 9-anthranol was established.

2) Times required for the complete disappearance of fluorescence of solution were measured and assumed to be measures of reaction velocities of tautomerism from 9-anthranol to anthrone. In ethanol, ether, dioxane and benzene the reaction velocities were small.

3) Dielectric constants of 9-anthranol in benzene, dioxane, benzene-dioxane mixtures and toluene solutions were measured. Reproducibility was satisfactory. In the said solvents 9-anthranol was relatively stable and $\omega \sim \varepsilon_{12}$ curves were straight lines except in toluene.

4) The stability of 9-anthranol in solvent was supposed to be increased, by an interaction between π-electrons of solvent and proton of solute O—H group in the case of benzene, or by O···H—O combination in the case of dioxane.

The authors' thanks are due to the kind guidance of Mr. Y. Mashiko and Mr. E. Koike, the Technical Officials of this Institute, and Assistant Prof. S. Nagakura, Tokyo University and to the advices in experiment of Mr. S. Saeki and Mr. K. Fujii, this Institute.

The Government Chemical Industrial Research Institute, Tokyo

Rheology of Coal. VI. The Micelle Structure in Relation to Anomalies of Rheological Properties of A Bituminous Coal

By Katsuya INOUYE and Hideo TANI

(Received August 25, 1952)

Introduction

The linear relationships between ash concentration in volume percentage and some rheological properties of coals[1,2,3] have made one of the authors (K. I.) propose a theory on the structure of coals, especially for caking coals, in which the coal molecules "solvate" around ash particles as a filler in formation of a micelle-like structure.

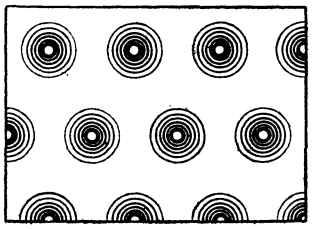

Fig. 1-a. Model of the Structure of Caking Coals.

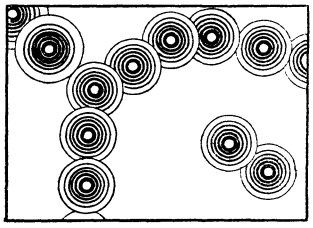

Fig. 1-b. Scaffolding Structure of Micellar Spheres.

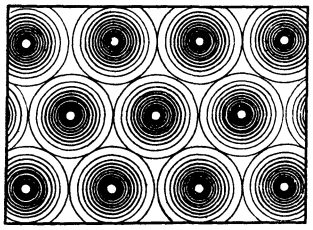

Fig. 1-c. Close-packed state.

The "free" molecules freed from solvation forces act as a plasticizer when the whole system is carbonized. The model would thus appear able to illustrate the cause of caking properties which means and necessitates the mobile condition of the system in caking temperature range, according to the theory, by the "plasticizer effect" of the matrix of micellar system, notwithstanding whether or not the *intra*-micellar changes have to occur. Fig 1-a illustrates the structural model of strongly-caking coal. The concentration of blackening means the strength of intermolecular forces, and the circles represent ash particles as skeletons. High concentration around the circles means strong solvation. For weakly or non-caking coals, the concentration around ash is low and at the same time blackening of the background must be strong; in such conditions thermal mobility of the whole system at higher temperatures cannot be accomplished.

The validity of this model with micelle and matrix may be well demonstrated by using carbon black as rigid micelle spheres and bakelite "A" as more freely combined matrix[4]. This black mixture, preferably with addition of a small amount of alcohol, when "carbonized" up to say 120°C, fuses (cakes) and remarkably swells, resulting in a very porous hard substance which very much resembles coke.

In this paper, the authors make mention of discussing the anomalous behavior of a Japanese bituminous coal, Takashima, in its rheological properties to discuss the model structure by an actual example.

Elasticity, Viscosity and Strength

Takashima bituminous coal, mined in Kyushu, Japan, having the average volatile matter of approximately 38% (d. a. f.), has been distinguished in the authors' experiments by wide distribution of ash concentration between various specimens from 1 to 20 in weight %.

1) Elasticity: Prat I of this study, K. Inouye, *J. Colloid Sci.* **6**, 190, (1951).
2) Internal Viscosity: Part II, K. Inouye, This Bulletin, **23**, 84, (1953).
3) Breaking Strength: Part V, K. Inouye and H. Tani, This Bulletin, **26**, 359, (1953).
4) K. Inouye, Unpublished experiments.

The modulus of elasticity values by resonant frequency method previously reported[1] and further data showed that the variation curve of elastic constant with ash concentration has some ranges of entirely different inclination, as shown in Fig 2. It is noteworthy that a minimum of the elastic moduli exists at $\phi=2$, and also that the elasticity decreases again in the range of 8~10% of ϕ. (ϕ is the ash content in volume percentage, dry basis.)

The experiments of internal viscosity from measuring the vibrational decrement at audiofrequencies[2], which suggested that the same relationships as in the Young's modulus experiments exist also in the viscosity data, led to an interesting fact of Fig. 2 that for Takashima coal a minimum at $\phi=2\%$ and second maximum at $\phi=10$ were recognized for the internal viscosity also.

Furthermore, the strength for rupture of the rectangular specimen[3] showed a variation of the strength factors with ϕ in nearly the same form, as illustrated in Fig. 2. The statistical correlation of the breaking strength upon ash concentration[3] has already suggested that the correlation must be considered for every individual range of ash concentration.

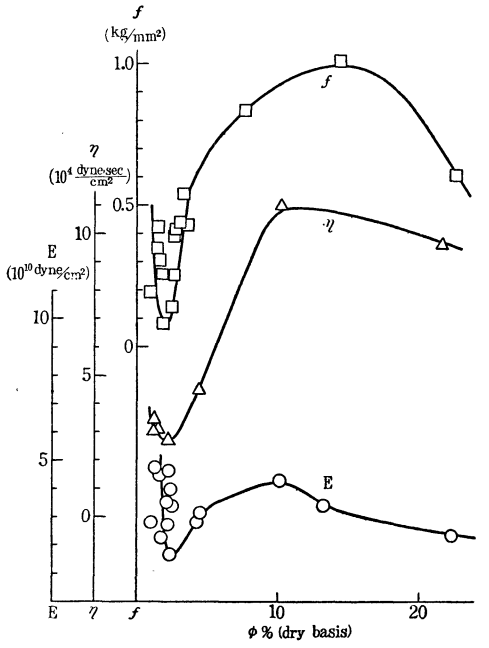

Fig. 2. Varication of Rheological Properties with Ash Concentration.
E: Young'g Modulus
: Internal Viscosity
f: Breaking Strength

An Interpretation of Variations in Rheological Properties

It is recognized in the rubber science that the loading with carbon black to improve mechanical properties of rubber causes perturbation of the stresses and strains set up in the body, and hence this leads to an increase in the elastic and viscosity constants, i, e., a stiffening of the solid, in linear relationships with carbon content.[5,6] Tensile strength, for instance, increases by the loading. However, the changes of strength are considered to be not in linear relationship with loading but in varying manner according to the ranges of loading. E. Guth[6] suggested that the decrease of the tensile strength of rubber-carbon black system for small loadings is caused by the stress concentrations occurring around the carbon particles when the stress is applied, and the increase of the strength for greater loadings by the tendency of the carbon black particles (perhaps of the "solvated" micellar spheres) to form chains and finally some type of network. This increase with loading continues up to the point where the suspension becomes a dilution of carbon by rubber. He made mention of carbon content for the first range as up to 10% by volume, for the second 10 to 30%.

Such descriptions are apparently very suggestive for the present case of coal, by the close similarity of the fundamental characteristics, in spite of the numerical differences. The minimum of Young's modulus, internal viscosity coefficient and breaking strength at 2% of ash content by volume appears to correspond to the state where the micelle spheres, in which the ash particles as nuclei solvate coal molecules, first contact each other to form a scaffolding structure, as schematically illustrated in Fig 1-b. In other words, the modellic picture as Fig. 1-a, homogenious in distribution of the micelles, may not represent the actual structure, because if all micellar spheres could touch each other even at the ash concentration of 2% by volume, the dimension of a micellar sphere must be very large.

If the maximum of the rheological properties at approximately 8 to 10% by volume of ash means the point where the micellar spheres exist in a closed-packing state, as Fig. 1-c, the total internal surface of the micellar system is calculated as,

$$S=\frac{m(\text{area of a sphere})}{m(\text{volume of a sphere})d}$$
$$=m4\pi R^2/m(4/3)\pi R^3 d$$
$$=3/Rd,$$

where S is the total specific surface area per one gramme of the coal, m the number of micellar spheres per gramme, R the radius of the sphere and d is the true density. Hence the radius of the micelle can be obtained if the specific internal surface area of the sample with 10% of ash content by volume is known. A specimen with 10.13% of ϕ was examined at first for Young's modulus (4.19×10^{10} dyne/cm²) and internal viscosity coefficient (1.1×10^{5} dyne. sec/cm²) to ascertain

5) H. M. Smallwood, *J. Appl. Phys.*, **15**, 758, (1944).
6) E. Guth, *J. Appl. Phys.*, **16**, 20, (1945).

to assume as the appropriate sample for this purpose, and then powdered. The range of particle size of 30 to 60 Tyler mesh was chosen to measure the specific surface area by the iodine adsorption method at 25.0°C[7]. Using the obtained value of specific area, 9.51×10^4 cm²/g (dry basis), and the density measured in methanol at 25.0°C, 1.24, R was calculated as 2,540Å. As the value of ϕ of this sample is 10.13%, the radius of the ash particle is estimated as 1,160 Å; the value of the radius of "filler" particle in coal is in the same order, but slightly larger, as those of some kinds of carbon blacks[8]. The value of the micellar radius may mean, on the other hand, that solvation forces or internal pertubation caused by ash particles reach in the space of radius of approximately 2,500 Å. However, it may not be true that the dimension of ash particles is always constant overall the ranges of ash concentration, but varying dimensions according to the ash content and therefore to the variation of micellar structure itself are more probable.

Shigen-Gijyutsu-Shikenjo
(Resources Research Institute)
Saitama-Kawaguchi, Japan

(7) K. Inouye, *J. Fuel Soc. Japan*, **29**, 112, (1950).

(8) J. Sameshima, H. Akamatsu, K. Inouye, S. Kawamura, R. Matsuura, H. Hamada and K. Tamaru, *Rev. Modern Colloid Sci. Japan*, Vol. **1**, 250, (1948). R. B. Anderson and P. H. Emmett, *J. Appl. Phys.*, **19**, 367, (1948)

On the Ring-opening Reactions of the Furan Compounds. III. On the Condensation of Furfural with Methyl Ethyl Ketone by Alkali

By Hiroshi MIDORIKAWA

(Received March 20, 1953)

In the case of condensation of furfural with methyl ethyl ketone by alkali, there are two possibilities, as illustrated in the accompanying equation:

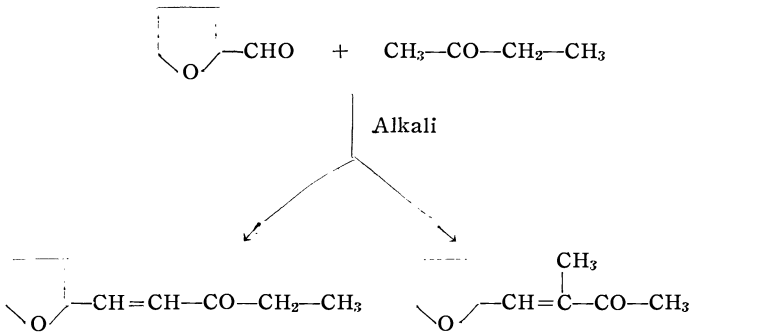

1-(2-furyl)-1-penten-3-one (I)

4-(2-furyl)-3-methyl-3-buten-2-one (II)

Kashiwagi[1] and the other[2] indicated that the condensation product was II. But they gave no satisfactory confirmation of its structure.

On the other hand, Hunsdiecker[3] and the others[5] reported that the condensation product which they assumed to be I afforded γ,ζ-dioxopelargonic acid by ring-opening in alcoholic hydrochloric acid. The work done to date seems to be not yet clear.

In the present experiment, the condensation was carried out at reaction temperatures 0° and 60°.

At reaction temperature 0°, furfural underwent principally the aldol condensation with methyl ethyl ketone. The resulting aldol was easily dehydrated with acetic anhydride or dilute hydrochloric acid to yield the unsatu-

1) I. Kashiwagi: This Bulletin, **2**, 310 (1927).
2) D. M. Al'vin Gutzatz: *C. A.*, **30**, 3591 (1936).
3) H. Hunsdiecker: *Ber.*, **75B**, 447 (1942).

ated ketone, which gave a semicarbazone of foliated crystals melting at 212~4°. This unsaturated ketone was smoothly oxidised to α-methyl-2-furanacrylic acid III by sodium hypochlorite. It is undoubted, therefore, that this unsaturated ketone is II and the reaction sequence is shown as follows:

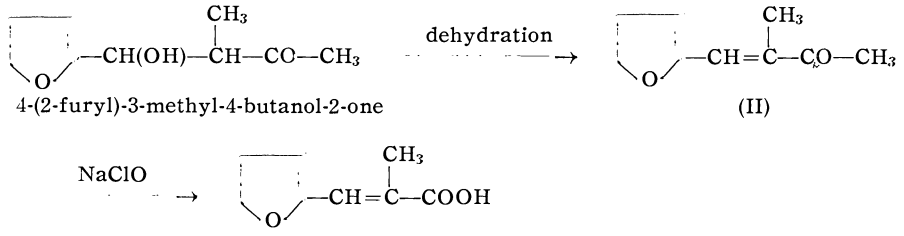

4-(2-furyl)-3-methyl-4-butanol-2-one (II)

α-methyl-2-furanacrylic acid (III)

From the condensation product at reaction temperature 60° was obtained a mixture of two semicarbazones, which consisted of a larger part of needles melting at 182~4° and a smaller part of foliated crystals melting at 212~4°. The latter was identical with the semicarbazone of II. This condensation product, on sodium hypochlorite oxidation, afforded III in a very poor yield. It seems certain that the semicarbazone of needles melting at 182~4° is that of I. Furthermore, this condensation product, on ring-opening in alcoholic hydrochloric acid, gave a dioxocarboxylic acid in a fairly good yield.

On the other hand, the condensation product at reaction temperature 0°, after dehydration with acetic anhydride, gave the same dioxocarboxylic acid by ring-opening in alcoholic hydrochloric acid as the condensation product at reaction temperature 60°, but its yield was very poor.

From these results, it may be inferred that the dioxocarboxylic acid was γ,ζ-dioxopelargonic acid arising from the ring-opening of I as illustrated below, and the condensation product at reaction temperature 0° contained a small amount of I accompanying 1-(2-furyl)-1-pentanol-3-one, and II failed to give a dioxocarboxylic acid by ring-opening in alcoholic hydrochloric acid.

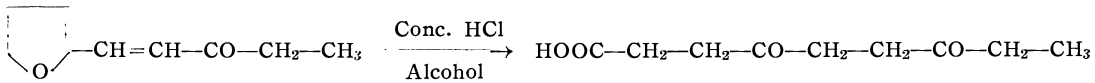

(I) γ,ζ-dioxopelargonic acid

The semicarbazones obtained here were converted to the 2,4-dinitrophenylhydrazones respectively. It is interesting that the 2,4-dinitrophenylhydrazone of red needles (m.p. 184~5°) and the one of carmine rhombic plates (m.p. 212~3°) were detected to be those of II. The former was obtained directly from the condensation product at reaction temperature 0°, and the latter from the unsaturated ketone obtained by dehydration of this condensation product. These two 2,4-dinitrophenylhydrazones on recrystallisation did not shift to each other, which may be those of cis- and trans-isomers of II.

The semicarbazones of I and II, together with their 2,4-dinitrophenylhydrazones, are shown in the accompanying table.

	Semicarbazone	2,4-dinitrophenylhydrazone
1-(2-furyl)-1-penten-3-one	colourless needles, m.p. 182~4°	red needles m.p. 205~6°
4-(2-furyl)-3-methyl-3-buten-2-one	colourless leaflets, m.p. 212~4°	carmine rhombic plates, m.p. 212~3°
		red needles, m.p. 184~5°

Detection of the 2,4-dinitrophenylhydrazones obtained from the condensation product at reaction temperature 25° indicated the presence of I, II and 4-(2-furyl)-3-methyl-4-butanol-2-one.

Experimental

Condensation at 60～5°.—A solution of furfural (12 g.) and methyl ethyl ketone (24 g.) in water (200 cc.) was mechanically stirred at 60～5° and 5% aqueous caustic soda (20 cc.) was at once run in. After stirring for 1.5 hrs., the reaction mixture was neutralised with dil. sulfuric acid, the oily layer separated, and the aqueous solution extracted twice with benzene. The separated oil and the benzene extract were combined. The benzene solution was dried over calcium chloride and the benzene removed. From the remaining oil was collected a fraction (10 g.) distilling at 128～9°/22 mm.

	H	C
Anal. Calcd. for $C_9H_{10}O_2$:	6.71%	71.96%
Found:	6.72%	71.31%

This fraction gave a mixture of two semicarbazones which consisted of a larger part of needle crystals (m.p. 182～4°) and a smaller part of foliated crystals (m.p. 212～4°). The former was more soluble in methanol than the latter.

The needles (this was considered to be 1-(2-furyl)-1-penten-3-one semicarbazone)

	H	C	N
Anal. Calcd. for $C_{10}H_{13}O_2N_3$:	6.32%	57.94%	20.28%
Found:	6.27%	57.90%	20.08%

The foliated crystals (4-(2-furyl)-3-methyl-3-buten-2-one semicarbazone)

	H	C	N
Anal. Calcd. for $C_{10}H_{13}O_2N_3$:	6.32%	57.94%	20.28%
Found:	6.42%	58.12%	19.85%

The semicarbazone of needle crystals was converted to a 2,4-dinitrophenylhydrazone of carmine needle crystals (m.p. 205～6°).

	H	C	N
Anal. Calcd. for $C_{15}H_{14}O_5N_4$:	4.27%	54.53%	16.96%
Found:	4.05%	54.43%	17.09%

The semicarbazone of foliated crystals was converted to a 2,4-dinitrophenylhydrazone of carmine rhombic crystals (m.p. 212～3°).

	H	C	N
Anal. Calcd. for $C_{15}H_{14}O_5N_4$:	4.27%	54.53%	16.96%
Found:	4.10%	54.84%	17.14%

Aldol Condensation at 0～3°.—Into a stirred solution of furfural (15 g.) and methyl ethyl ketone (20 g.) in water (350 cc.) was at once introduced 10% aqueous caustic soda (10 cc.) at 0～3°, after stirring for 4.5 hrs. at 0～3°, the reaction mixture was neutralised with dil. sulfuric acid, the oily layer was separated and the aqueous solution extracted twice with ether. The separated oil and the ether extract were combined. Fractionation of the ether solution, after drying over calcium chloride for a brief time, gave a pale yellow oil (10 g.), b.p. 117～8°/10mm., which was considered to chiefly contain 4-(2-furyl)-3-methyl-4-butanol-2-one.

	H	C
Anal. Calcd. for $C_9H_{12}O_3$:	7.19%	64.24%
Found:	6.79%	65.13%

This fraction afforded a 2,4-dinitrophenylhydrazone of unsaturated ketone $C_9H_{10}O_2$, which was recrystallised from pyridine-methanol; microscopic carmine needles; m.p. 184～5°. This was considered to be the 2,4-dinitrophenylhydrazone of 4-(2-furyl)-3-methyl-3-buten-2-one.

	H	C	N
Anal. Calcd. for $C_{15}H_{14}O_5N_4$:	4.27%	54.53%	16.96%
Found:	4.14%	55.03%	16.93%

Dehydration of Aldol.—The foregoing aldol (6 g.) was gently refluxed with acetic anhydride (6 g.) for 3 hrs. Fractionation of the reaction mixture gave a yellow oil (4 g.), b.p. 124～5°/20 mm.

	H	C
Anal. Calcd. for $C_9H_{10}O_2$:	6.71%	71.96%
Found:	6.43%	71.00%

This fraction gave the semicarbazone of foliated crystals (m.p. 212～4°) and the 2,4-dinitrophenylhydrazone of rhombic crystals (212～3°).

The aldol was also dehydrated by heating with 5% hydrochloric acid on the water-bath for a short time, giving the same semicarbazone and 2,4-dinitrophenylhydrazone.

Oxidation by Sodium Hypochlorite.—Anhydrous sodium carbonate (7 g.) and bleaching powder (10 g.) were mixed in water (30 cc.) After a brief time, the resulting calcium carbonate was filtered off, the filtrate was diluted to 40 cc. with water and 1 g. caustic soda was added.

The oil (1 g.) obtained by the dehydration of the aldol was suspended in the sodium hypochlorite solution (8 cc.) prepared above and the vessel was kept for two days in water at room temperature, with occasional shaking. Then, the reaction mixture was acidified with dil. hydrochloric acid to yield α-methyl-2-furanacrylic acid (0.35 g.) It was recrystallised from hot water; colourless needles; m.p. 116～7°; lit.[4] m.p. 116°.

	H	C
Anal. Calcd. for $C_8H_8O_3$:	5.29%	63.13%
Found:	5.34%	63.15%

4) I. Kashiwagi: This Bulletin, **2**, 318 (1927).

The condensation product at reaction temperature 60～5° gave a trace of α-methyl-2-furanacrylic acid under the same conditions.

Ring-opening in Alcoholic Hydrochloric Acid.—The condensation product (2 g.) at reaction temperature 60～5° was refluxed with alcohol (4 cc.) and conc. hydrochloric acid (1.5 cc.) on the water-bath for 3 hrs. The reaction mixture, after addition of water, was evaporated to dryness on the water-bath. The residue was extracted with a sufficient quantity of boiling water; the extract, after decoloursing with active charcoal, was evaporated up. The dioxocarboxylic acid which was considered to be γ,ζ-dioxopelargonic acid was obtained as a crystalline mass (0.35 g.) on cooling and recrystallised twice from ligroin; colourless hexagonal plates; m.p. 83～4; lit.[5] m.p. 84～5°.

		H	C
Anal.	Calcd. for $C_9H_{14}O_4$:	7.58%	58.03%
	Found:	7.55%	57.54%

The dehydration product from the aldol gave a very small amount of colourless tabular crystals by the same procedure; m.p. 83～4°. The mixed melting point of the specimen with the foregoing dioxocarboxylic acid showed no depression.

Condensation at Ordinary Temperature(25°).—A mixture of furfural (10 g.), methyl ethyl ketone (20 g.), 10% aqueous caustic soda (10 cc.) and water (250 cc.) was stirred for 5 hrs. at about 25°. By the same procedure as described above, a pale yellow oil (8 g.) distilling at 131～5°/22 mm. was obtained, which gave a mixture of the three species of 2,4-dinitrophenylhydrazone mentioned above. These 2,4-dinitrophenylhydrazones were separable from the mixture by virtue of their pyridine solubility. The 2,4-dinitrophenylhydrazone of m.p. 212～3° was the least soluble and that of m.p. 185～6° was the most soluble.

5) F. L. Breusch and E. Ulusoy: *C. A.*, **42**, 5850 (1948).

Summary

It seems that furfural can react with methyl ethyl ketone in two ways by alkali.

In the condensation at 0～3°, the main product was 4-(2-furyl)-3-methyl-4-butanol-2-one. This aldol was easily dehydrated to 4-(2-furyl)-3-methyl-3-buten-2-one, which was oxidised to α-methyl-2-furanacrylic acid by sodium hypochlorite.

In the condensation at 60～3°, the main product was the furfurylidene ketone, which gave the semicabazone melting at 182～4° and the dioxocarboxylic acid by ring opening in alcoholic hydrochloric acid. It is presumed that this ketone is 1-(2-furyl)-1-penten-3-one, and the dioxocarboxylic acid resulting from it is γ,ζ-dioxopelargonic acid.

It is also interesting that two species of 2,4-dinitrophenylhydrazone were obtained with respect to 4-(2-furyl)-3-methyl-3-buten-2-one.

The author wishes to thank Messrs. K. Furuhashi and K. Muto for micro-analyses.

Scientific Research Institute
Komagome, Tokyo

Studies on the Chemical Constitution of Agar-agar. XV.[1] Exhaustive Mercaptolyses of Agar-agar[2]

By Choji ARAKI and Susumu HIRASE

(Received April 22, 1953)

Agar-agar, a gel-forming polysaccharide extracted from certain species of red sea weeds, has long been known to produce D-galactose on acid-hydrolysis. C. Araki, one of the present authors, revealed that 3,6-anhydro-L-galactose besides D-galactose is a-constitutional monosaccharide, on the bases that he isolated agarobiose[3] (4-D-galactopyranosyl-3,6-anhydro-L-galactose) from partial hydrolysis products of agar, and that he could obtain 2-methyl 3,6-anhydro-L-galactose dimethylacetal[4] from methylated agar as well as 3,6-anhydro-L-galactose dimethylacetal[5] from agar itself by the methanolysis method. Jones and Peat were of the opinion that 3,6-anhydro-L-galactose might arise secondarily from L-galactose-6-sulfate during some chemical operations[6]. Further evidence, however, which excludes the possibility of the latter opinion, is now made available by the mer-

1) Part XIV: C. Araki, *J. Chem. Soc. Japan*, **65**, 725 (1944). Works on this subject are reviewed by C. Araki in "A Summary of Organic Chemical Investigations on Agar-agar", Memoirs of the Faculty of Industrial Arts, Kyoto Technical Univ., **2**(B), 17 (1953), written in English.

2) Read at the Ordinary Meeting of the Kinki Branch of the Chemical Society of Japan in September, 1950.

3) C. Araki, *J. Chem. Soc. Japan*, **65**, 533, 627 (1944).

4) C. Araki, *J. Chem. Soc. Japan*, **61**, 775 (1940).

5) C. Araki, *J. Chem. Soc. Japan*, **65**, 725 (1944).

6) W. G. M. Jones and S. Peat, *J. Chem. Soc.*, **1942**, 225.

captolysis of agar.

Mercaptolysis[7], substantially hydrolysis followed by simultaneous mercaptalation, has proved in a few cases[8] to be successful in isolating aldose components as their crystalline mercaptals. This has led the authors to apply the procedure to establish the constitutional sugars of agar.

Mercaptolysis of agar was accomplished by dissolving it in concentrated hydrochloric acid with ice-cooling and by stirring the solution with addition of ethylmercaptan for forty eight hours. Neutralization of the reaction mixture followed by evaporation produced well-known crystalline D-galactose diethylmercaptal, which was also identified by oxidation to mucic acid and acetylation to characteristic pentaacetate.

A filtered solution from crystals mentioned above was then extracted with ether in Soxhlet's percolator. Ether extracts yielded crystalline 3,6-anhydro-L-galactose diethylmercaptal, and small amounts of crystalline DL-galactose diethylmercaptal and of xylose diethylmercaptal-containing sirup. 3,6-Anhydro-L-galactose diethylmercaptal, which gave crystalline tri-*p*-nitrobenzoate, was identified by conversion to free sugar and then to crystalline diphenylhydrazone[5] and phenylosazone[5]. Further confirmative evidence was provided by comparison with the authentic specimen prepared for the first time. DL-Galactose diethylmercaptal, also a new compound, giving crystalline pentaacetate, was confirmed by its optical inactivity, its oxidation to mucic acid and by the preparation of an authentic sample.

As the residue obtained by evaporation of the solution, from which the monosaccharide derivatives mentioned above had been removed, seemed to comprise oligosaccharide diethylmercaptals, it was submitted to a second mercaptolysis for forty eight hours to yield monosaccharide units. Crystalline diethylmercaptals of D-, 3,6-anhydro-L- and of DL-galactose were isolated again. The non-crystalline residue of the second mercaptolysis products was further effected by the third mercaptolysis, the same products being isolated in a crystalline state. In the last two cases, no xylose derivative could be found. Thus repeated exhaustive mercaptolyses of agar furnished crystalline specimens of diethylmercaptals of D-galactose, 3,6-anhydro-L-galactose and of DL-galactose in yields of 30.2%, 24.4% and 1.0% to agar employed, respectively.

It may not be a matter of surprise that such an acid sensitive sugar as 3,6-anhydro-L-galactose was out of perfect degradation in the presence of a strong mineral acid, inasmuch as 2-desoxy-aldohexose, which has been accepted as an acid-sensitive sugar equal to 3,6-anhydro-aldohexose, affords its stable mercaptal[9] under the similar condition. With regard to DL-galactose, one of the authors reported that he could not find it in the hydrolysate of agar extrated from *Gelidium amansii*[10], but afterwards it was isolated from an agarous substance of *Camphaephora Hypraeides*, J. Ag[11]. As commercial agar, employed in this investigation, is generally prepared by extracting a mixture of *Gelidium amansii* and several other species of sea weeds, it may be possible to assume that DL-galactose derivative isolated above arises from other species than *Gelidium amansii*. Xylose was also detected[12] in the hydrolysis products of commercial agar, but further evidence will be necessary for its conclusive identification.

From these results it is concluded that 3,6-anhydro-L-galactose as well as D-galactose is a chief constitutional sugar in the agar molecule, just as one of the authors has stated. Moreover, it may be of interest that derivatives of D-galactose and 3,6-anhydro-L-galactose can be isolated approximately in equal yield. This suggests that these two sugars are involved in almost equal amounts in the molecule of agar. But it would be still difficult to conclude that these two sugars comprise the main bulk of the molecule, as the exhaustive experimental conditions employed above have made it impossible to deal with the whole material quantitatively.

Experimental

Unless otherwise stated, concentration and evaporation of the solution were carried out under reduced pressure below 40°. Analyses for the thioethoxyl group are according to the method of the present authors[13]. All m.ps. are uncorrected.

7) M. L. Wolfrom, L. W. Geoges and J. C. Sowden, *J. Am. Chem. Soc.*, **60**, 1026 (1938); M. L. Wolfrom, D. R. Myers and E. N. Lassettre, ibid., **61**, 2172 (1939).

8) I. R. Hooper, L. H. Klemm, W. J. Polglase and M. L. Wolfrom, *J. Am. Chem. Soc.*, **68**, 2120 (1946); **69**, 1052 (1947); P. W. Kent, *Nature*, **166**, 442 (1950).

9) W. G. Overend, M. Stacey and J. Stanek, *J. Chem. Soc.*, **1949**, 2481; W. G. Overend, F. Shafizadeh and M. Stacey, *J. Chem. Soc.*, **1950**, 671.

10) C. Araki, *J. Chem. Soc. Japan*, **58**, 1214 (1937).

11) C. Araki, Collection of Treatises in Commemoration of the 45th Anniversary of Kyoto Technical College, pp 69 (1948).

12) S. Hirase and C. Araki, Memoirs of the Faculty of Industrial Arts, Kyoto Technical Univ., **1**, 19 (1952).

13) The method will be published elsewhere.

I. Mercaptolysis of agar-agar.—Commercial powdered agar (60.0 g., dry weight 49.1 g.), placed in a three-necked flask fitted with a mechanical stirrer, dropping funnel and calcium chloride tube, was dissolved in concentrated hydrochloric acid (*d* 1.20, 200 g.) by stirring and ice-cooling; the agar dissolved gradually in 40 mins. into a deep brown solution. Ethylmercaptan (80 g.) was then added from the dropping funnel with vigorous stirring in three portions so that the temperature did not exceed 10°. After addition, the stirring was continued for 48 hrs., maintaining the temperature at 10~12°. The reaction mixture was neutralized by pouring it on excess lead carbonate suspended in water (1 l.). Precipitates of the excess lead carbonate and lead chloride formed were removed by filtration and washing with cold water (1 l.). The combined filtrate and washings were saturated with hydrogen sulfide,

Operations for Mercaptolysis Products of Agar-agar.

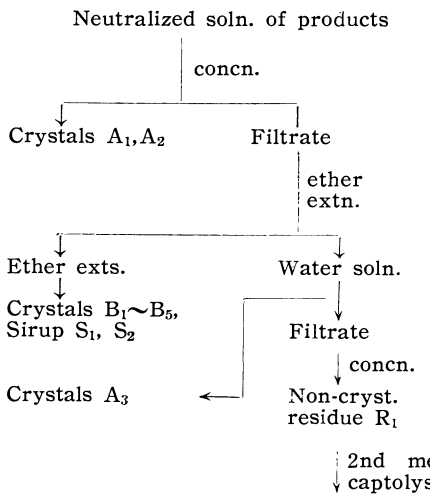

the precipitate of lead sulfide being removed by filtration. The filtrate was then neutralized with silver carbonate after removal of hydrogen sulfide in vacuo, and filtered before and after a second treatment with hydrogen sulfide. The solution thus obtained was operated as shown in the accompanying diagram and as described below.

II. Isolation and confirmation of D-galactose diethylmercaptal.—The neutralized solution obtained above was concentrated until it gave rise to crystalline magma. The crystals (A_1) were filtered, washed with cold water and dried; yield 7.25 g., m.p. 139~140°, $[\alpha]_D^{15}$ −4.3° in water. The second crop of the crystals (A_2) was obtained by concentrating the combined filtrate and washings mentioned above to about 200 cc., and allowing it to stand overnight in an ice-box; yield 1.95 g., m.p. 140~141°, $[\alpha]_D^{15}$ −4.6° in water. Crystals A_1 and A_2 were combined and recrystallized from alcohol. Pure D-galactose diethylmercaptal was btained as prismatic needles, m.p. 141~142°, $[\alpha]_D^{15}$ −4.65° in water (*c* 0.680), −3.99° in pyridine (*c* 1,003). Its m.p. was not depressed on admixture with an authentic sample (m.p. 142°)[14].

Anal. Found: C, 41.65; H, 7.99; SC_2H_5, 42.75. Calcd. for $C_{10}H_{22}O_5S_2$: C, 41.93; H, 7.74; SC_2H_5, 42.68 %.

Oxidation of the crystals mentioned above with nitric acid (*d* 1.15) yielded mucic acid, m.p. 212°, not depressed on admixture with an authentic specimen (m.p. 214°).

Pentaacetyl D-*galactose diethylmercaptal*[15]: m.p. 76~77°, $[\alpha]_D^{18}$ +11.31° in chloroform (*c* 2.210).

III. Isolation and confirmation of 3,6-anhydro-L-galactose diethylmercaptal.

a) Isolation:—Combined filtrate and washings from A_2, described in **II**, were concentrated to about 150 cc., and extracted with ether in a Soxhlet's percolator.

The first extract (20 hrs.) on cooling gave crystals (B_1, 6.95 g.), m. p. 102~5°, $[\alpha]_D^{12}$ +11.0° in water. The ethereal filtrate from B_1 on evaporation furnished further crops of crystals (B_2, 1.17 g.), m.p. 102~5°, $[\alpha]_D^{12}$ +10.8° in water. The mother liquor from B_2 was concentrated to a sirup (S_1, 1.20 g.), $[\alpha]_D^{12}$ −1.6° in water.

The second extract (30 hrs.) afforded crystals (B_3, 0.58 g.), m.p. 109~116°, $[\alpha]_D^{12}$ +1.7° in water, filtrate from which on evaporation gave further crystals (B_4, 0.22 g.), m.p. 102~5°, $[\alpha]_D^{12}$ +13.3° in water. Mother liquor from B_4 was concentrated to a sirup (S_2, 0.45 g.), $[\alpha]_D^{12}$ −6.1° in water.

The third extract (70 hrs.) gave crystals (B_5, 0.75 g.), m.p. 115~121°, $[\alpha]_D^{12}$ −2.5° in water. Ethereal filtrate from B_5 left nothing on evaporation.

The crystals B_1, B_2 and B_4, showing the same properties, were combined and recrystallized from ethyl acetate (40 cc.), yielding almost pure 3,6-anhydro-L-galactose diethylmercaptal (5.20 g.), m.p. 104~7°, $[\alpha]_D^{25}$ +12.1° in water. An additional product (2.61 g., m.p. 103~6°, $[\alpha]_D^{25}$ +11.8° in water), was recovered by evaporating the mother liquor. A pure substance was obtained after several recrystallizations from ethyl acetate containing a small amount of petroleum ether (b. p. 40~70°), forming silky needles with m.p. 110~111° and $[\alpha]_D^{14}$ +14.09° in water (c 1.636), −21.11° in ethanol (c 1.041) and −26.25° in pyridine (c 1.638). Its m.p. was not depressed on admixture with the authentic specimen, the preparation of which is described in **III—d.** It was readily soluble in water, methanol, ethanol and pyridine, moderately soluble in ether, acetone, ethyl acetate and chloroform, and practically insoluble in benzene and petroleum ether. It gave a Seliwanoff's ketose reaction.

14) E. Fischer, *Ber.*, **27**, 678 (1894); R. M. Hann, W. D. Maclay and C. S. Hudson, *J. Am. Chem. Soc.*, **61**, 1270 (1939).
15) M. L. Wolfrom, *J. Am. Chem. Soc.*, **52**, 2467 (1930).

Anal. Found: C, 44.48; H, 7.68; SC_2H_5, 45.65. Calcd. for $C_{10}H_{20}O_4S_2$: C 44.75; H, 7.51; SC_2H_5, 45.55 %.

b) Tri-*p*-nitrobenzoyl 3,6-anhydro-L-galactose diethylmercaptal:—To a solution of 3,6-anhydro-L-galactose diethylmercaptal (0.50 g.), isolated above, in pyridine (10 cc.) was added *p*-nitrobenzoyl chloride (1.20 g.). The reaction mixture, after being allowed to stand 2 days, was treated in the usual manner. Recrystallization of the product from ethanol containing a small amount of ethyl acetate furnished colorless fine needles of tri-*p*-nitrobenzoate (0.50 g.), m.p. 140~142°, $[\alpha]_D^6$+18.48° in chloroform (c 0.974).

Anal. Found: N, 5.64; S, 8.91. Calcd. for $C_{31}H_{23}O_{13}N_3S_2$: N, 5.86; S, 8.96 %.

c) 3,6-Anhydro-L-galactose:—To a solution of 3,6-anhydro-L-galactose diethylmercaptal (5.32g.) in water (50 cc.), held in a three-necked flask equipped with a mechanical stirrer, finely powdered lead carbonate (15 g.) and a solution of mercuric chloride (11 g.) in water (200 cc.) were added. Rapid stirring was maintained for 3 hrs. at room temperature. The reaction mixture was then filtered, a small amount of lead carbonate being placed in a filter flask. The filtrate was concentrated to about 20 cc. in the presence of lead carbonate. Unaffected mercaptal and excess mercuric chloride were removed by exhaustive extraction with ether until nothing came into the extract. The remaining water solution was concentrated to dryness by repeatedly adding absolute ethanol and distilling it off. The residue was dissolved in absolute ethanol, insoluble lead compounds were removed by filtration, and the filtrate was concentrated to a glassy solid of 3,6-anhydro-L-galactose (2.90 g.), $[\alpha]_D^{25}$−39.4° (initial) in water (c 1.75), −25.2° (24 hrs., constant). It reduced cool Fehling's solution, showed strong Seliwanoff's reaction, and restored the color to Schiff's reagent.

Diphenylhydrazone[5]: m.p. 154°, $[\alpha]_D^{15}$ − 34.31° (initial) in methanol (c 1.370), −24.09° (24 hrs.).

Phenylosazone[5]: m.p. 217°, $[\alpha]_D^{15}$−75.38° (initial) in pyridin-methanol (2 : 3) (c 0.738), −53.48° (24 hrs.).

d) 3,6-Anhydro-L-galactose diethylmercaptal from corresponding dimethylacetal:—A solution of 3,6-anhydro-L-galactose dimethylacetal (2.50 g.) in concentrated hydrochloric acid (2.5 g.) was shaken for 1 hr. with ethylmercaptan (1.6 g.) with ice-cooling. Small pieces of ice were added to induce crystallization, and separated crystals of the mercaptal were filtered, washed with small portions of ice-water, and dried over potassium hydroxide in vacuo; yield 2.37 g., m.p. 105~8°. Several recrystallizations from ethyl acetate containing a small amount of petroleum ether (b. p. 40~70°) gave silky needles, m.p. 110~111°, $[\alpha]_D^{15}$ +14.36° in water (c 1.253), −21.03° in ethanol (C 1.617) and −26.32° in pyridin (C 1.140).

Anal. Found: C, 44.49; H,7.73; SC_2H_5, 45.43. Calcd. for $C_{10}H_{20}O_4S_2$: C, 44.75; H, 7.51; SC_2H_5, 45.55 %.

IV. Isolation and confirmation of DL-galactose diethylmercaptal.

a) Isolation:—Crystals B_3 and B_5, described in **III-a,** were considered to be mixtures from their ill-defined m.ps. These were combined and divided into two components by fractional crystallizations from acetone. From the less soluble fraction, D-galactose diethylmercaptal (0.48 g.) was obtained, m.p. alone and mixed m.p. 139~140°, $[\alpha]_D^{12}$−4.40° in water. DL-Galactose diethylmercaptal was accumulated in the more soluble fraction. The crude crystals (0.55 g.). m.p. 123~5°, were purified by further recrystallizations from ethanol, forming prismatic needles, m.p. 127°, $[\alpha]_D^{15}$±0° in water (c 0.676) and pyridine (c 0.711). Its m.p. was not depressed on admixture with an authentic specimen, of which preparation is described in **IV-c.**

Anal. Found; C, 41.71; H, 7.84; SC_2H_5, 42.75. Calcd. for $C_{10}H_{22}O_5S_2$: C, 41.93; H, 7.74; SC_2H_5, 42.68 %.

The substance gave mucic acid on oxidation with nitric acid (d 1.15), m.p. 212°, undepressed when mixed with an authentic sample (m.p. 214°).

b) Pentaacetyl DL-galactose diethylmercaptal:—The crystals (0.20 g.) obtained above were acetylated with pyridine and acetic anhydride in the usual way. The product was recrystallized by dropping water to its methanolic solution, forming prisms (0.28 g.), m.p. 112~113°, $[\alpha]_D^{17}$± 0° in chloroform (c 0.954).

Anal. Found: C, 48.17; H, 6.71; SC_2H_5, 24.51; CH_3CO, 43.85. Calcd. for $C_{20}H_{32}O_{10}S_2$: C, 48.37; H, 6.50; SC_2H_5, 24.61; CH_3CO, 43.33 %.

c) DL-Galactose diethylmercaptal from dulcitol:—Dulcitol (5.0 g.) was oxidized with 3 % hydrogen peroxide according to literature[16] on the subject. The reaction product, however, was converted to diethylmercaptal, without direct isolation of DL-galactose, by the action of concentrated hydrochloric acid (2 g.) and ethylmercaptan (2 g.). The mercaptal obtained was purified by recrystallizations from ethanol, yielding prismatic needles (0.80 g.), m.p. 125~127°.

Anal. Found: C, 41.72; H, 7.95; SC_2H_5, 42.43. Calcd. for $C_{10}H_{22}O_5S_2$; C, 41.93; H, 7.74; SC_2H_5, 42.68 %.

V. Detection of xylose diethylmercaptal.

A small portion of each of sirups S_1 and S_2, the separation of which is described in **III-a,** was treated with mercuric chloride and mercuric oxide to yield free sugar. Both of resulting products were shown to be mixtures of xylose and 3,6-anhydro-L-galactose by paper chromatography. Hence, S_1 and S_2 were combined and extracted with cold benzene. Extract on solvent removal gave a colorless sirup (1.40 g.), $[\alpha]_D^{17}$−7.7° in water, SC_2H_5 46.89 (calcd. for $C_9H_{20}O_4S_2$: 47.64 %). An attempt to crystallize xylose diethylmercaptal or its acetate was unsuccessful.

16) C. Neuberg and J. Wohlgemuth, *Z. physiol. Chem.*, **36**, 219 (1902).

VI. Second mercaptolysis.

The residual water solution from ether extraction, described in **III-a,** was diluted with water to 200 cc. after the removal of ether in vacuo, and allowed to stand in an ice-box for a week. A small amount of crystals of D-galactose diethylmercaptal was deposited; yield 0.90 g., m.p. and mixed m.p. 137~139°, $[\alpha]_D^{15}$ −4.9° in water. The filtrate was concentrated to a sirup, which was dried by repeated additions of absolute methanol followed by evaporation, yielding an amorphous solid (R_1); yield 29.0 g., $[\alpha]_D^{13}$ −7.5° in water, SC_2H_5 22.62 % (hexobiose and hexotriose diethylmercaptals require SC_2H_5 27.2 and 22.6 %). It did not reduce a hot Fehling's solution, the observation excluding the possibility of the existence of ketose components.

R_1 was dissolved in concentrated hydrochloric acid (120 g.) and stirred with ethylmercaptan (40 g.) at 10~12° for 48 hrs. The reaction products were treated quite in the same manner as before; the yields of crystalline diethylmercaptals of D-galactose, 3,6-anhydro-L-galactose and of DL-galactose were 8.09 g., 7.29 g. and 0.23 g., respectively. No sirup containing xylose derivative could be found. The residue (R_2), corresponding to R_1 in the first series, was obtained as amorphous solid (12.7 g.), $[\alpha]_D^{21}$ −6.8° in water, SC_2H_5 22.10 %. This did not reduce a hot Fehling's solution.

VII. Third mercaptolysis.

R_2 obtained above was again submitted to mercaptolysis with concentrated hydrochloric acid (60 g.) and ethyl mercaptan (30 g.) at 10~12° for 48 hrs. The procedure was essentially the same as in the preceding two cases, except for being carried out on a smaller scale. The yields of crystalline dietylmercaptals of D-galactose, 3,6-anhydro-L-galactose and of DL-galactose isolated herein were 4.88 g., 4.22 g. and a trace, making the total yield 23.55 g., 19.85 g. and 0.78 g., respectively. No xylose derivative was found in this case. The residue (R_3), corresponding to R_1 in the first series, was brown a sirup (3.1 g.), $[\alpha]_D^{24}$ −1.7° in water, SC_2H_5, 21.05 %.

The authors wish to express their thanks to Mr. K. Arai for the microanalyses for carbon, hydrogen and nitrogen, and to Mr. K. Yamanouchi for his assistance in this work. This research has been aided by the Grant for Scientific Research from the Ministry of Education.

Institute of Chemistry,
Faculty of Industrial Arts,
Kyoto Technical University, Kyoto

Electronic Remarks on the Origin of the Anomalous Color of Some Organic Iron. III. Complex Salts

By Kôzô Sone

(Received May 18, 1953)

Introduction

The absorption spectra of chelate compounds of Fe (II) were studied by the present author[1] and he came to the conclusion that unsaturated intramolecular chelate rings formed between Fe and chelating organic compound would probably act as the new chromophore to produce the new absorption bands in the visible region. The several compounds of Fe (III) containing ligands such as acetylacetone[2] or 8-quinolinol were found also to show a similar intense absorption band as Fe (II) compounds. Other examples of such an intense absorption bands, those of Fe (III) chelate compounds of 1-nitroso-2-naphthol and nitrosophenylhydroxylamine will be reported in this paper.

The Fe (III) complexes of NCS^- and N_3^- ions[3] and the enolic and phenolic substances[4] all show intense, distinct bands in the visible region and from the fact that these bands are also completely different from the band of Fe^{+++} ion or from those of the ligands, it is likely that these bands also belong to the

1) K. Sone, This Bulletin, **25**, 1 (1952); *J. Am. Chem. Soc.* in press.

2) K. Sone, I. Miyake, H. Kuroya, K. Yamasaki, *J. Chem. Soc. Japan*, **69**, 70 (1948).

3) A.v. Kiss et al., *Z. anorg. allg. Chem.*, **244**, 98 (1940); J. Badoz-Lambling, *Bull. soc. chim. France*, **1950**, 1195.

4) F. Wesp and W.R. Brode, *J. Am. Chem. Soc.*, **56**, 1037 (1934); H. Henecka, *Ber.*, **81**, 179 (1948); see also H. Henecka, "Chemie der Beta-Dicarbonyl-Verbindungen", p. 110, Springer-Verlag, Berlin, 1950.

same kind as those absorption bands of the above mentioned chelate complexes.

From all these facts it seems clear that the Fe^{++} ion posesses a peculiarly high ability to produce anomalously deep-colored organic complexes. Indeed it was pointed out by Yoe[5] that among about 5000 organic substances studied, about 1200 were found to produce intensely colored complexes with iron, while no other metal showed such a high ability for color production.

In the present article, discussions will be made on this problem from the standpoint of the electronic theory of organic chemistry and it will be shown that by the application of this theory a number of features of these colorations can be explained satisfactorily.

Experimental

A Beckman model DU spectrophotometer and a Coleman universal spectrophotometer were used in the spectral measurements. The results of absorption spectra were shown in Fig. 1 in which the ordinate expresses the value of molecular extinction coefficient ε calculated by the familiar formula $\varepsilon = \frac{log\ I_c/I}{c.d.}$

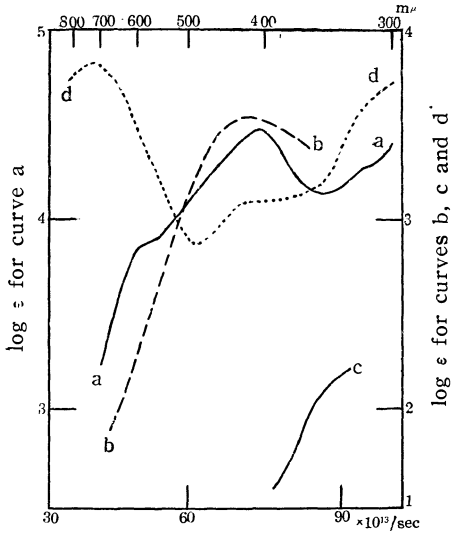

Fig. 1.—Curve a: Tris (1-nitroso-2-naphthol) iron in chloroform, b: Tris (nitrosophenylhydroxylamine) iron in chloroform, c: Ammonium salt of nitrosophenylhydroxylamine (cupferron) in water, d: Colloidal solution of Prussian blue.

The tris (1-nitroso-2-naphthol) iron (III) was prepared after Ilinsky and Knorre[6]. Chloroform solutions of the above complex and of tris (nitrosophenylhydroxylamine) iron (III) were used for spectral measurements. Concentrations used were 1/1500 mole for tris (1-nitroso-2-naphthol) iron and 1/5000 mole for tris (nitrosophenylhydroxylamine) iron respectively.

Colloidal solution of Prussian blue prepared by mixing aqueous solutions of $K_4[Fe(CN)_6]$ and iron alum was also studied. The final concentration of Fe^{++} and Fe^{+++} were 1/2000 and 1/4000 mole respectively. The ε value was calculated for one atom of Fe^{+++}.

Discussion

The tris (nitroso-naphthol) iron has a band at 407 mμ. The longer wave length side of this band shows a hump at ca. 600 mμ. This means the probable existence of a new band in this region which is responsible for the dark color, almost black of this iron complex. This color is in contrast with the nitrosonaphtholates of other metals such as Co, Cu and Pd which are mostly red or brown.

The iron (III) complex of nitrosophenylhydroxylamine which contains 3 molecules of the ligand shows a strong band at 420 mμ which is quite different from the absorption of the ligand itself (Fig. 1, curve c.). The color of this iron complex is red which is in contrast with complexes of other metals. For example, complexes of Cr, Ni and Co are green and pink[7] and similar to their hydrated ions in the color.

The number and shapes of the anomalous absorption bands in the above-mentioned Fe (III) complexes are considerably different in each case, and therefore it will be rather difficult to give a general treatment to explain their origins. In addition, it is also known from magnetochemical observations[8] that the Fe-ligand coordinate bonds in the dipyridyl and phenanthroline complexes are of covalent character, while most of the other complexes with anomalous absorption only contain ionic linkage. Therefore there certainly exists a considerable difference between the electronic structures of these two types of complexes. Nevertheless, it is fairly clear that by the combination of the Fe (III) ion and all these organic ligands some completely new electron transitions which were absent beforehand become possible.

In regard to the origin of the appearance of such transition, it can be pointed out that the redox transition between the Fe^{++} and

5) J. H. Yoe, *Anal. Chem.*, **20**, 393 (1948).
6) M. Ilinsky and J. Knorre, *Ber.*, **18**, 2728 (1885).
7) V. Anger, L. Lafontaine, C. Caspar, *Compt. rend.*, **180**, 376 (1925).
8) B. Werbel, V.H. Diebler and W.C. Vosburgh, *J. Am. Chem. Soc.*, **65**, 2329 (1943): A.E. Martell and M. Calvin "Chemistry of the Metal Chelate Compounds", **1952**, p. 214

Fe^{++} ions occurs with relative ease in contrast with the other heavy metals, such as Co, Ni and Cu which have strong tendencies to keep their most stable valence states. This indicates that the energy difference between these two valence states is relatively small.

Now if an organic ligand which can cause the anomalous absorption with Fe (III) and which generally contains conjugated double bonds and is therefore rich in the mobile π-electrons, approaches the Fe^{+++} ion, the electronic structure (B) shown below becomes possible,

$$\underset{(A)}{Fe^{+++} + :R} \longleftrightarrow \underset{(B)}{Fe^{++} + .R} \qquad (1)$$

i.e., one electron is partially transferred from :R to Fe^{+++}, producing a Fe^{++} ion and a free radical ·R derived from the ligand.

These two structures (A) and (B) will make possible the condition of mutual resonance and therefore the structure (B) will, to a certain extent, contribute to the resonance of the whole system containing Fe^{+++} and R^- together.

The present author assumes that the establishment of this resonance system (1) and the occurrence of electron transitions between the new energy states produced by such resonance could be the true origin of the anomalous absorption bands of the above-mentioned Fe (III) complexes.

The assumption of the existence of such a resonance system may be supported by the following facts of organic chemistry. Dewar[9] described that when some aromatic amines are oxidized by $FeCl_3$, the first step is the reaction of the type

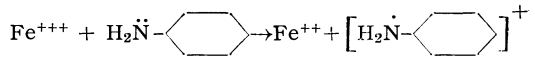

which looks quite analogous to the above mentioned resonance formula, and from this fact it is also very probable that this reaction proceeds through the formation of an intermediate complex,

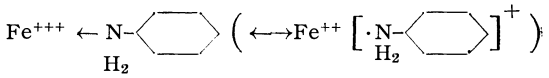

in which the two electronic states corresponding to the (A) and (B) given above are in resonance. Similar assumption of the one-electron transfer is generally accepted also to explain the oxidation and oxidative decomposition of phenols, facts which are important for the later discussions.

From these considerations, it will be quite reasonable to assume that, in the well-known

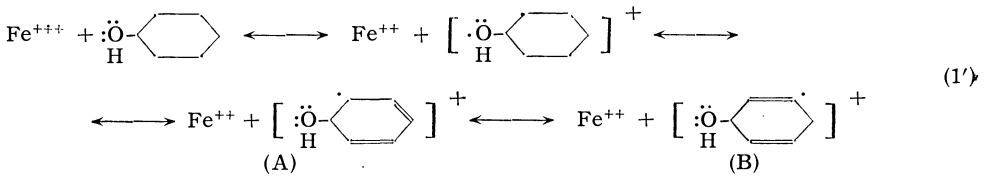

(1′)

reaction of the Fe^{+++} ion and phenol, the Fe^{+++} ion will show some properties of the Fe^{++} ion, and the phenol molecule will acquire some properties of the free radicals as shown schematically in (1′). Under this assumption, a number of experimental data on the Fe^{+++} ~phenol reaction can be explained satisfactorily.

(1) When an anionoid, or electron-donating group (alkyl, halogens, NH_2, OH etc.) is substituted in the benzene nucleus of phenol, the electron transfer from the phenolic OH to the Fe^{+++} ion will be more or less facilitated, thus promoting the contribution of the structure (B) in the resonance system (1′), and therefore increasing the mobility of the whole π-electron system, shifting the absorption band to the longer wave length, and making the phenol molecule highly reactive owing to its free-radical character enhanced by the substituted group.

(2) When a cationoid, or electron-attracting group (CHO, COOH, NO_2 etc.) is substituted, the electron transfer from OH to Fe^{+++} will become rather difficult, shifting the band towards the shorter wave length and thereby stabilizing the ligand molecule from reacting away.

These conclusions coincide completely with the experimental data of Wesp and Brode[4]. According to them,

(1) In the alkyl-, halogen-, NH_2- and OH-substituted phenols, the position of the band is generally shifted to longer wave length from the position found for the unsubstituted phenol and, in the case of its *o*- and *p*-derivatives, the produced colored complexes are very unstable, changing rapidly into the Fe^{++}

9) M.J.S. Dewar, "The Electronic Theory of Organic Chemistry", 1949, p. 248; L. Fieser and M. Fieser, "Organic Chemistry", 1950, p. 677.

ion and resinous substances which are formed from the oxidative polymerization of the respective phenols. With *m*-derivatives the band shifts are much less, or even in the opposite direction and the complexes are somewhat more stable.

These facts can be explained if the following two assumptions are made. Namely, (i) the coordinated phenol molecule with some enhanced free radical character polymerizes into the resinous matter, leaving the iron which is now in the Fe (II) state; (ii) since the m-substituent is difficult to resonate with the OH group, it cannot greatly influence the resonance of the whole system in such a way as the o- and p-substituents do.

It might be added that the same kind of band shift and instabilization of complexes occurs in the case of thiophenol, whose SH group is much more deformable than the OH group of phenol.

(2) In the case of the CHO-, COOH- and NO_2-substituted phenols the band is shifted to the shorter wave length than in the case of phenol, and the resulting complexes become very stable.

Wesp and Brode also observed that the Fe (III) complexes of naphthols are generally colored in blue or green, and thus absorb light at longer wave length than phenols, and this fact is explained easily if the greater mobility of the π-electrons in the naphthalene ring compound with benzene ring is taken into account.

Recently Henecka[4] measured the absorption spectra of the color reactions of two series of enolic substances with Fe^{+++}. The structures of their complexes are, respectively,

(A) acetylacetone type,

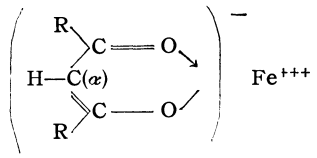

and (B) acetoacetate type.

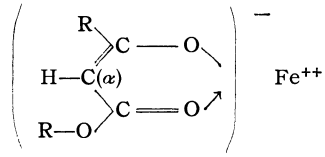

From his experimental data it can be observed that: (1) the absorption maximum for a compound of type (A) is generally located at a shorter wave length than that of the corresponding compound of type (B) with silmilar substituent groups, (2) when the H atom on the α-position in both types is replaced by alkyl, Cl-, or OR-group (i.e. anionoid group), the band is shifted to the longer wave length, while RCO-, RO_2C- or CN-group (i.e. cationoid groups) shifts the band in the opposite direction. It is very remarkable that these relationships are quite analogous to those observed by Wesp and Brode for the phenols. The relationship (1) can be readily understood because the compound of type (B) is that of type (A) substituted with an anionoid OR group.

In this way, the general characteristics of the Fe^{+++}~phenol and enol colorations can be explained adequately, and other anomalous colorations of the Fe (III) complexes can be considered in analogous manners. There exist some experimental evidences which support this point of view; for example, Linhard and Weigel[10] indicated that the strong absorption band at 300~330 mμ shown by the rhodanato- and azido-complexes of Co (III) originates from the following electron transition:

$$\left[Co^{(+++)}\ X^{(-)}A_5\right]^{++} \xrightarrow{h\nu} \left[Co^{(++)}\ X\ A_5\right]^{++}$$

($A=NH_3$, $X^-=NCS^-$ or N_3^-)

which is virtually an electron transfer from the ligand to the central metal. If their arguments are correct it will be fairly probable that the strong bands at 450~500 mμ of the Fe^{+++}~NCS^- and Fe^{+++}~N_3^- complexes are also of the same origin, i.e., they are derived from the electron transfers which are closely related to the resonance of type (1). The change between the Fe (III) and Fe (II) in this case, however, would occur much more easily than that between the Co (III) and Co (II) in the ammine complexes, and this will cause the absorption band of Fe^{+++} complex appear in the longer wave length, as is observed experimentally.

It is also conceivable that the anomalous colors of the Fe (II) chelates, which the author formerly considered to be due to the special ring formation[1], might be in fact, due to the resonance of the type

$$Fe^{++} + :R \longrightarrow Fe^{+++} + :R^{-}$$

i.e. the reverse of that assumed for the Fe (III) complexes[11]. The possibility of the

10) M. Linhard and M. Weigel, *Z. anorg. allg. Chem.*, **267**, 113, 121 (1951).

11) Interesting remarks concerning such colorations were made by P. Krumholz (*Nature*, **167**, 570 (1951).

production of deep colors as the result of the resonance between the metallic complex ion and the organic molecules was also indicated by the study of Kröhnke[12] on some deeply colored organic ferrocyanides, and further examples of similar anomalous colorations of iron complexes are found in the books of Feigl[13].

It may be added that some of the absorption spectra of anomalously colored complexes such as $Fe^{+++}\sim NCS^-$ or $Fe^{++}\sim$phenanthroline complexes show apparent similarities to that of the Prussian blue solution, which certainly contains a resonance system between the Fe^{++} and Fe^{+++} ions through the coordinated CN^- ions. (cf. Fig. 1, curved). These apparent similarities seem to give further support to the point of view discussed throughout this article.

The author wishes to express his thanks to Prof. K. Yamasaki for his guidance, and also to Mr. M. Kobayashi of Tokyo University and to Mr. K. Nakanishi of Nagoya University for their valuable advice and suggestions.

Aichi College of Liberal Arts
(Aichi-Gakugei-Daigaku)
Higashiku, Nagoya

12) F. Kröhnke, *Ber.*, **83**, 35 (1950).
13) F. Feigl, "Chemistry of Specific, Selective and Sensitive Reactions", New York, 1949.

An Improved Accurate Film Balance*

By Kiyoshi INOKUCHI

(Received May 29, 1953)

Introduction

Measurement of low film pressure is a matter of increasing importance for the study of monomolecular layers. The apparatus for measuring film pressures generally falls into three types, i. e., dipping slide type, two-dimensional aneroid type, and float balance type. The dipping slide method, introduced by Dervichian[1], and Harkins and Anderson[2] is uniquely simple and yields reliable value when properly used. Bull[3], and Abribat et al.[4] recently used this type of apparatus for the monolayers of various macromolecules, such as proteins or long chain polymers, and obtained the molecular weight of the film molecules. The main drawback of this method, however, lies in the fact that the measurements become unreliable whenever the decreasing film pressures are involved. It requires, moreover, careful choice of materials for dipping slide, since a small change of contact angle of the slide owing to the deposition of monolayer may introduce large errors.

The aneroid type of balance, originated by Marcelin,[5] was recently modified by Puddington[6] and Kalousek.[7] The feature of this type is the fact that the movable float, indispensable for the float balance, is eliminated, and the construction is comparatively simple. The principal objection to this type, however, may be the difficulty of obtaining the absolute calibration for it, and the difficulty of removing the contamination which may, more or less, occur inside the enclosed area.

On the other hand, the float balance has an advantage over the above two methods, since it eliminates their objections and permits wide application. Although the disadvantage of this type lies in the comparatively laborious technique for preventing leakage at both ends of the float, it is a matter of technique which could be overcome in some way. Adam

* Presented at the Symposium on Colloid Chemistry of the Chemical Society of Japan, Nov. 1951, Tokyo.

1) D. G. Dervichian, *J. Phys. Radium*, **6**, 221, 429 (1935).
2) W. D. Harkins and T. F. Anderson, *J. Am. Chem. Soc.*, **59**, 2189 (1937).
3) H. B. Bull, ibid., **67**, 4, 5 (1945).
4) M. Abribat and J. Pouradier, *Compt rend*, **227**, 1101 (1948).
5) A. Marcelin, *Ann. physique*, **4**, 505 (1925).
6) I. E. Puddington, *J. Colloid Sci.*, **1**, 505 (1946).
7) M. Kalousek, *J. Chem. Soc.*, **1949**, 894.

and Jessop's[8] apparatus, an adaptation of Langmuir's[9] balance for low pressure measurement, is too complicated in construction and laborious in operation. Sensitive float balances were presented by Marcelin,[10] Moss and Rideal,[11] and Guastalla,[12] and have proved their merits for measuring extremely low pressure. These apparatus, however, are not extensively used because of their unfavorable design for routine work. Thus, a generally accessible apparatus is now wanted, which enables film pressures of the order of millidynes per cm. to be accurately measured with ease of operation. The present paper deals with an improved apparatus and technique for use which meet all the requirements stated above.

Construction

The apparatus to be described is of float balance type. The elevation views of the construction are illustrated in Fig. 1. The apparatus provides a vertical torsion wire (1), which suspends a torsion weight (2). Below the torsion weight, a cramp (3) for the wire is provided, which can be raised or lowered by turning the knob (4). This cramp fixes the weight at raised position and protects the torsion wire from accidental shock when the

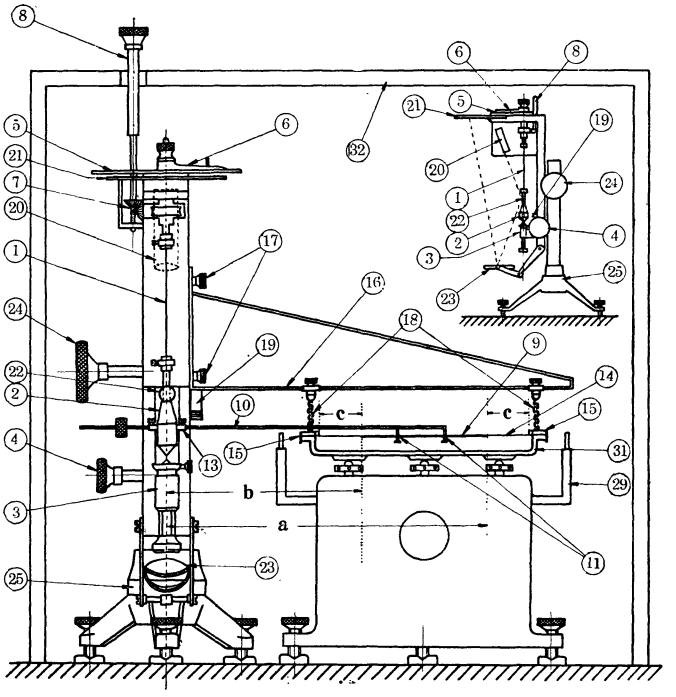

Fig. 1.—Elevation views of construction

apparatus is out of measurement. Lowering the cramp makes the torsion weight free and sets the apparatus ready for use. At the top of the apparatus, a reading scale (5) is provided with a pointer (6), which is coaxial to the torsion head. The torsion head is connected to the knob (8) through the gear-wheel (7). Thus, the rotation of the torsion head is transmitted finely by the manual movement of this knob from the outside of the cabinet (32). The torsional angle of the torsion head can be read down to 0.1 degree by means of the vernier of the pointer.

On the surface of water, a paraffin-waxed mica strip (called a float (9) hereafter) is placed. The float is supported by the arm (10) which extends above the surface of water in parallel with the length of the float. The connection of the float with the supporting arm is as follows. The arm has two needles (11), which penetrate the float through two holes respectively. The holes are so loosely bored that the float can be moved freely according to the change of water level, but they are tight enough to follow the horizontal movement of

8) N.K. Adam and G. Jessop, *Proc. Roy. Soc.*, **110A**, 423 (1926).
9) I. Langmuir, *J. Am. Chem. Soc.*, **39**, 1848 (1917).
10) A. Marcelin, *Ann. physique*, **4**, 481 (1925).
11) S. A. Moss and E. K. Rideal, *J. Chem. Soc.*, **1933**, 1525.
12) M. J. Guastalla, *Cahier de physique* **10**, 36 (1942).

the float. The end of the supporting arm is fixed to the torsion weight (2) by the small stopper (13).

The leakage of the film past the ends of the float is prevented by thin silk threads (14) treated with paraffin or vaseline. The metal blocks (15) which ride on the rims of the trough (31) serve the purpose to fix the threads on the rims rapidly and surely with simple technique. At the side of the apparatus, a frame (16) of L-form is equipped being fixed by the screws (17). From the horizontal arm of this frame hang two short chains (18), which suspend the above metal blocks in such a way that the metal blocks just mount on the rims of the trough when the apparatus is just in condition for measurement. When it is necessary to wash the float, it is removed from the position (13) and attached to the clip (19) of the frame (16), which is removable from the system as a whole.

The apparatus also provides the optical system in order to visualize the fine dislocation of the float and to carry out the measurement rapidly in continuous work. A bulb and the convex lens with a slit, both assembled in a container (20), are attached behind the scale (5). Outside the scale, a frosted glass (21) with adjustable scale is attached on which the light image is projected. The torsion weight also provides a small mirror (22) which is movable with the rotation of the float. The other mirror (23), equipped at the lower part of the apparatus is about 4 cm. in diameter and the reflecting plane is adjustable to all direction by manuplation. The path of the light is arranged in such a way that the light image of the slit is reflected via both the moving mirror (22) and the fixed mirror (23) on the frosted glass (21).

By turning the knob (24), the apparatus can be raised until the float leaves the surface of the water. In such position, the apparatus can be turned around the vertical axis of the stand (25). By turning it to the right, the apparatus is made parallel to the length of the trough.

Performance

Operation of apparatus.—The supporting arm of the float is fixed to the clip (19) of the frame, and thin silk threads, treated with paraffin or vaseline, are set across the gaps between both ends of the float and the metal blocks so as to make nearly semicircles. The frame (16) is then dismantled from the apparatus and the floating barrier is allowed to be washed under the tap water. After the washing is over, the frame is reassembled to the apparatus. The apparatus is so set that the length of the float becomes parallel to that of the trough. The supporting arm of the float is removed from the clip of the frame and fixed to the stopper of the torsion weight. After cleaning of water surface, the apparatus is so turned that the length of the float is at right angles to the trough. By turning the knob (4), the cramp (3) is lowered in order to let the weight be free; then, by turning the knob (24), the apparatus is lowered slowly down until the float, as well as threads, is allowed to swim on the surface of the water and the metal blocks come to ride on the rims of the trough (Fig. 2.).

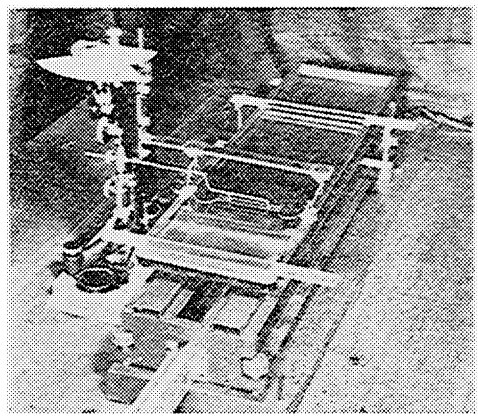

Fig. 2.—Apparatus ready for measurement.

The position of the pointer (6) is set to zero; the light image on the adjustable scale is brought to zero position by manuplating the mirror (23). The film-forming substance is now spread on the surface of water. Since the dislocation of the float due to the film pressures deflects the light image on the frosted glass, zero adjustment is conducted by turning the knob (8) so that the image returns to zero position of the scale. The film pressures exerted here, can be calculated from the readings of the angles thus distorted.

Determination of Film Pressures.—When the torsional angle of α radians is required to bring the dislocated float to zero position, the following equation will hold between the film pressures and the torsional angles

$$\int_{b-c/2}^{a+c/2} F x dx = \frac{F}{2}(a^2-b^2+ac+bc)=\alpha k \quad \text{.....[1]}$$

where F represent the film pressures in dyne per cm., k, the torsion constant of the wire, x, the distance from the torsion wire, a, the distance from the torsion wire to the distant end of the float, b, that to its nearer end, and c, the distance of the gaps at both ends of the float, respectively (see Fig. 1). From the equation [1], follows

$$F=\frac{2\alpha k}{(a+b)(a-b+c)} \quad \text{.....[2]}$$

When the measuring of a, b, and c, are 20.0 cm., 12.0 cm. and 3.0 cm. respectively, using torsion

wire of phosphor bronze of 0.273 mm. in diameter and 8.0 cm. in length gives the sensitivity of 0.273 dynes per cm. per scale degree and the measurable upper limit of about 40 dynes per cm. For lower pressures, the thinner wires are employed. The wire of 0.101 mm. in diameter and 8.0 cm. in length was found suitable for lower pressure measurement, giving the sensitivity of 0.004 dynes per cm. per scale degree and the measurable upper limit of about 0.7 dynes per cm. The torsion constant of the wire was obtained from the period of swing of a torsion weignt whose moment of inertia is possible to compute.

Cleaning of Water Surface.—Sweeping with a moving barrier, made of a paraffined glass rod, does not give perfectly clean surface of water, since the rubbing of the glass rod against the rims of the trough may more or less cause scratching of the paraffin surface. So, a rubbingless barrier is desired in which no scratching might occur. The suggestion is given by the method described by Guastalla.[12] The principle is that a band of talc powder which is sprinkled on the surface, is used as a barrier to arrest the contamination, and the driving of the talc powder thus formed is conducted by air-jet. The scheme of the sweeping is illustrated in Fig. 3. A long glass

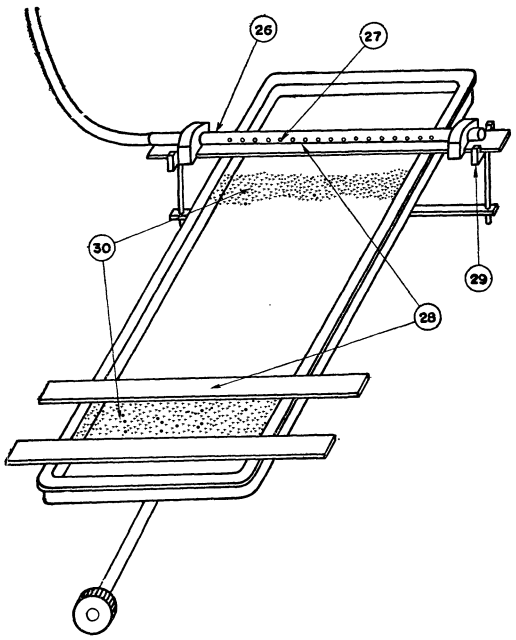

Fig. 3.—Schematic illustration of sweeping of water surface by talc blowing method.

tube (26), with fine orifices (27) along its length, is mounted on the movable glass rod which is held by a rod carrier (29) a short distance above the surface. Talc powder, purified by washing with water, alcohol, and benzene, and then heated properly, is spread on the surface at one side of the trough in the form of a band. Compressed air, filtered by cotton plug and purified by bubbling through the column of water, is sent out from the orifices of the glass tube. The movement of the glass rod with the above glass tube is conducted so that the air stream from the orifices blows off the talc barrier (30) to the opposite side of the trough. When the impurities are collected into the corner of the trough, the glass rod is lowered so as not to be in contact with water, in the order to prevent the talc powder from floating back. Such operation is repeated until the surface pressure attains a constant value.

Prevention of Leakage past the Threads by Sprinkling Talc Powder.—When the measurements are performed in a high pressure region, the operation which is recommended is that a small amount of purified talc powder is sprinkled around the solid-thread connections before the spreading of materials. This operation, though not always necessary, is useful for eliminating the possibility of leakage around the threads, and guarantees the measurement of high pressures up to 30 dynes per cm. or more.

Example

Fig. 4 shows an example of the force-area curve of myristic acid at the air-water interface, measured with this apparatus. The

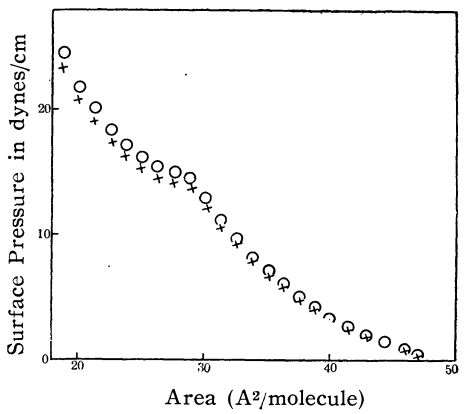

Fig. 4.—Force-area curve of myristic acid on 0.01 N hydrochloric acid at 18.0C°. Circles indicate the pressures determined by this apparatus, while crosses, the pressures by dipping slide method.

results obtained were in good accordance with that of Harkins.[13] The results, moreover, were referred to the one with simultaneous measurement using the dipping slide method. A fairly good agreement was obtained between the two methods. In details, however, it was found that the pressures obtained with the dipping slide method were

13) W. D. Harkins, "Physical Chemistry of Surface Films" p. 112, Reinhold Publ. Co. (1952).

** Purest sample (m.p. 54.5°C) given through the courtesy of Dr. H. Fukuba of the Nutritional Chemical Laboratory of this University, to whom the author's thanks are due.

consistently a little lower than those with this apparatus, and such a trend was emphasized in the higher pressure region, especially above the kink point of the curve. Harkins and Anderson[2] obtained just the same trend with pentadecylic acid and lecithin when they compared the values from both methods of dipping slide and of float balance, and they attributed this discrepancy partly to the errors made in the calibration of film balance. It is, however, noteworthy that the same tendency was obtained under the present experimental condition, where a different type of balance was used. This fact may suggest that this discrepancy may not be of accidental nature as they say, but of something essential associated with the instrumentation. It is rather reasonable to think that the discrepancy is due wholly to the increasing contact angle of the dipping slide owing to the deposition of the monolayer substance.

Summary

An improved apparatus and technique for measuring low film pressures, have been described. Although the apparatus bears resembalance to the Marcelin's balance, the following improvements were achieved in order to enable the low pressure measurement to be generally accessible.

(1) The main construction is laid beside the trough, unlike the usual apparatus whose construction is placed above the surface of water. This design is well suited for minimizing the chance of contamination which more or less occurs on the surface during assembling or operation of the instrument.

(2) Since one of the disadvantages of this type balance lies in the possibility of leakage at the solid-thread connections, especially at the connection between rims of the trough and thread, properly designed metal blocks are used to ensure the perfect connection with simple technique.

(3) An important point in the design of the apparatus is that it should be capable of easy dismantling and reassembling, so that the operation of cleaning can be easily conducted. This requirement is satisfied by the use of a carrier for the float and threads which is easily removable from the main construction of the apparatus.

(4) The float is so designed that the connection between the float and the supporter is an independent bearing, when the float is allowed to be in contact with the water surface. Owing to such construction, the change of water level during run does not matter.

(5) The optical system, which makes the deflection of the floating barrier visible, is equipped with the apparatus. Since the frosted glass, on which the light image is projected, lies just beside the reading scale, observations can be made with no unnecessary delay.

These designs meet well the requirements for measuring low film pressures. Continuous use for eighteen months has shown the apparatus to be very convenient and reliable.

The author wishes to express his hearty thanks to Prof. Taro Tachibana for his helpful advice and encouragement.

Department of Chemistry,
Faculty of Science,
Ochanomizu University, Tokyo

The Catalytic Action of Organic Peroxides on the Polymerization of Ethenoid Compounds. II. The Activity of Substituted Benzoyl Peroxides on the Polymerization of Vinyl Acetate

By Matsuji TAKEBAYASHI, Tadao SHINGAKI and Yasumasa ITO

(Received May 29, 1953)

In the previous work[1] of this series it was established that the activity of symmetrical *m*- and *p*-substituted benzoyl peroxides on the mean velocity of polymerization of styrene is inversely proportional to the square root of the dissociation constants of the corresponding substituted benzoic acids,* and that the rate of polymerization is in a parallel relation

1) M. Takebayashi and T. Shingaki, This Bulletin, **26**, 137 (1953).

*) The mean velocity of polymerization was measured after eighteen hours at 60° C.

to the rate of decomposition of the peroxides. The present paper is concerned with a comparative investigation of the activity of the peroxides on the polymerization of vinyl acetate and of styrene.

The polymerization of vinyl acetate has been carried out with 1/30 mol. of vinyl acetate and 1/3000 mol. of symmetrical *m*- and *p*-substituted benzoyl peroxides at 40°C. and 60°C. in the absence of air, and the effect of peroxides on the rate of polymerization has been measured. The results obtained are summarized in Table 1. In Fig. 1, the overall velocity (v_{Br}) of polymerization is plotted against the square root of the dissociation constants (K) of the corresponding substituted benzoic acids.

Table 1

Rate of Polymerization of Vinyl Acetate

Substituted benzoyl peroxide	Rate of polymerization (%)		$v_{Br} \times 10^3$, mol./l., min.	
	at 40°C., for 18 hrs.	at 60°C., for 2 hrs.	at 40°C.	at 60°C.
p,p'-Dimethoxy	99.9	98.3	9.91	87.8
m,m'-Dimethoxy	45.2	87.1	4.49	77.8
p,p'-Dimethyl	49.8	96.8	4.94	86.5
m,m'-Dimethyl	37.0	91.4	3.67	81.6
Unsubstituted	46.2	92.0	4.58	82.2
p,p'-Dichloro	31.4	83.8	3.12	74.8
m,m'-Dichloro	6.6	16.8	0.66	15.0
p.p'-Dicyano	4.1	9.0	0.41	8.0
m,m'-Dicyano	3.4	5.9	0.34	5.3
p,p'-Dinitro	0.7	2.4	0.07	2.1
m,m'-Dinitro	1.0	3.6	0.10	3.2
None	0.0	0.3		

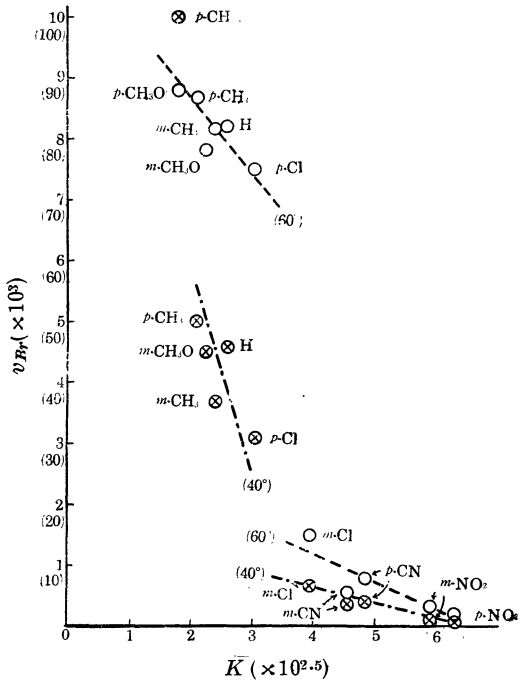

Fig. 1.—Polymerization of vinyl acetate in the presence of substituted benzoyl peroxides at 40°C. and 60°C.

* The numbers in parentheses are those for the data at 60°C.

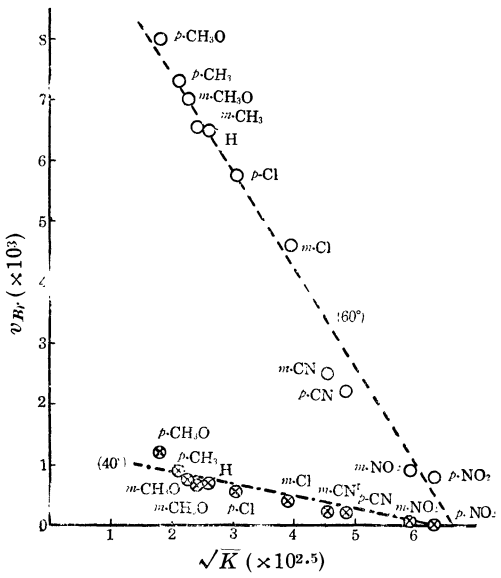

Fig. 2.—Polymerization of styrene in the presence of substituted benzoyl peroxides at 40°C. and 60°C.

Table 2

Rate of Polymerization of Styrene

Substituted benzoyl peroxide	Rate of polymerization (%) at 40°C., for 70 hrs.	Rate of polymerization (%) at 60°C.,* for 18 hrs.	$v_{Br}\times10^3$, mol./l., min. at 40°C.	$v_{Br}\times10^3$, mol./l., min. at 60°C.
p,p'-Dimethoxy	59.1	99.8	1.18	7.98
m,m'-Dimethoxy	36.9	85.7	0.74	6.85
p,p'-Dimethyl	44.3	91.6	0.89	7.32
m,m'-Dimethyl	33.1	82.0	0.66	6.56
Unsubstituted	35.1	81.5	0.70	6.52
*p,p'*Dichloro	28.6	71.9	0.57	5.75
m,m'-Dichloro	22.3	57.3	0.45	4.58
p,p'-Dicyano	10.3	28.3	0.21	2.26
m,m'-Dicyano	9.7	31.5	0.19	2.52
p,p'-Dinitro	1.4	10.1	0.03	0.81
m,m'-Dinitro	3.1	11.2	0.06	0.89
None	1.1	1.5		

* The data at 60°C. are quoted from the previous paper.

Comparing the results with those obtained in the polymerization of styrene, which are shown in Table 2 and Fig. 2, remarkable differences are recognized in the activity of peroxides and the velocity of polymerization.

In the polymerization of vinyl acetate the peroxides are divided into two groups according to their activities, the one containing effective peroxides, such as dimethoxy-, dimethyl-and *p,p'*-dichloro-benzoyl peroxides,and the other less effective ones, such as *m,m'*-dichloro-, dicyano-, and dinitro-benzoyl peroxides. And the activity of peroxides in each group is nearly inversely proportional to $\sqrt{K}$ at the experimental conditions (Fig. 1), while in the polymerization of styrene the same relation has been satisfied for all peroxides used (Fig. 2).

The polymerization of vinyl acetate proceeded more rapidly than that of styrene, as had been reported.[2] This tendency was observed to be remarkable in the presence of effective peroxides, where the velocity of polymerization of vinyl acetate was found to be about six[3] and over ten times as large as that of styrene at 40°C. and 60°C., respectively. While in the presence of less effective peroxides, the velocity of polymerization of vinyl acetate was observed to be only about two and three times as large as that of styrene at 40°C. and 60°C., respectively.

In the next place, the authors investigated the kinetic order of the thermal decomposition of the peroxides in vinyl acetate at 40°C. and 60°C. by the iodometric method according to the direction of Swain and his co-workers.[4] The decomposition was observed to be of first order at 40°C., but not always exactly so at 60°C. perhaps because of the fact that the polymerization proceeded so rapidly that the condition of decomposition of the peroxides was changed to some extent during the reaction. The rate constant (k_1) is given in Table 3, and that (k_1') in styrene is added in it for the sake of comparison.

Table 3

Rate Constant of Decomposition of Substituted Benzoyl Peroxides

Substituted benzoyl peroxide	$k_1\times10^4$, min.$^{-1}$ at 40°C,	$k_1\times10^4$, min.$^{-1}$ at 60°C.	log (k/k_0) at 40°C.	log (k/k_0) at 60°C.	$k_1'\times10^4$, min.$^{-1}$ at 60°C.
p,p'-Dimethoxy	7.36		0.25		17.7
m,m'-Dimethoxy	3.91	34	−0.02	0.0	12.0
p,p'-Dimethyl	4.60		0.05		12.7
m,m'-Dimethyl	2.99	34	−0.14	0.0	11.3

2) For examples: G. V. Schulz and E. Husemann, *Z. physik. Chem.* (B) **39**, 246 (1938); A. C. Cuthbertson, G. Gee and E. K. Rideal, *Proc. Royal Soc.* A, **170**, 300 (1939); G. M. Burnett, *Quarterly Revs.* **4**, 292 (1950).

3) Only in the presence of *p,p'*-dimethoxy-benzoyl peroxide, the polymerization velocity of vinyl acetate was found to be about nine times as large as that of styrene at 40°C.

4) C. G. Swain, W. H. Stockmayer and J. T. Clarke, *J. Am. Chem. Soc.*, **72**, 5426 (1950).

Unsubstituted	4.14	34	0.00	0.0	11.05
p,p'-Dichloro	2.14	18	−0.30	−0.27	9.9
m,m'-Dichloro	1.61	3.2	−0.41	−1.03	8.1
p,p'-Dicyano	0.70	1.8	−0.77	−1.28	4.6
m,m'-Dicyano	0.69	1.8	−0.78	−1.28	4.8

The data given in Table 3 indicate that the greater the electron-repelling effect of substituents, the more rapidly the peroxides decompose in vinyl acetate as well as in styrene, and that the effective peroxides decompose about two to three times more rapidly in vinyl acetate than in styrene at 60°C., while less effective ones decompose about two or three times more slowly, suggesting the solvent effect. Fig. 3 shows the relation between the velocity of polymerization of vinyl acetate and log (k/k_0), where k_0 and k are the rate constants of benzoyl peroxide and substituted benzoyl peroxides, respectively.

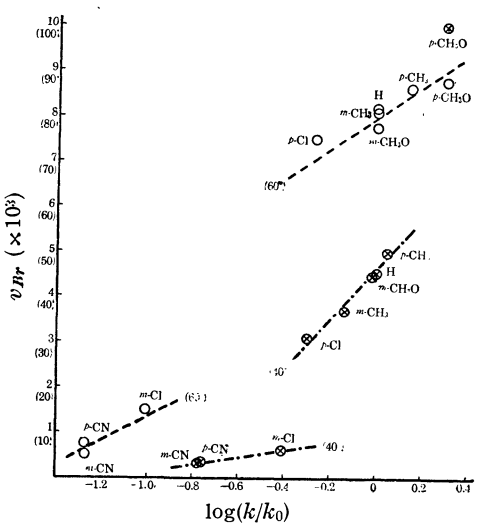

Fig. 3.—Correlation of extrapolated first order rate constants with v_{Br} in vinyl acetate at 40°C. and 60°C.

* The numbers in parentheses are those for the data at 60°C.

The results indicate also that the peroxides are divided into two groups according to their activities, contrary to the results obtained in the polymerization of styrene, and that the activity of peroxides in each group is nearly proportional to log (k/k_0). The above facts lead us to the reasoning that the velocity of polymerization is affected not only by the rate of decomposition of peroxides but also by the activity of radicals derived from peroxides.

Considering that the thermal decomposition of peroxides in vinyl acetate is an uni-moiecular reaction, the radicals acting as the initiator of the polymerization are suggested to be various kinds of benzoate radical RCOO and of aryl radical R, produced by loosing carbon dioxide from the radical RCOO. Then the authors measured the amount of carbon dioxide generated from the peroxides (2/3000 mol.) in vinyl acetate (2/30 mol.).

In the experiments at 40°C. for eighteen hours, carbon dioxide was not generated from all the peroxides except *p,p'*-dimethoxy-benzoyl peroxide. Therefore, it is supposed that the radical acting as the initiator is chiefly RCOO, except in the case of *p,p'*-dimethoxy-benzoyl peroxide. The effects of various kinds of radical RCOO, which should be produced from the peroxides, on the velocity of polymerization were estimated per mol. of RCOO as shown in Table 4.

Table 4

Effect of the Radical RCOO on the Polymerization

Substituted benzoyl peroxide	Extent of decomposition (%)	Amount (M) of RCOO ($\times 10^{-4}$ mol.)	v_{Br}/M (mol./l., min.)
*m,m'*Dimethoxy	34	2.3	0.19
p,p'-Dimethyl	39	2.6	0.19
m,m'-Dimethyl	28	1.9	0.19
Unsubstituted	36	2.4	0.19
p,p'-Dichloro	21	1.4	0.21
m,m'-Dichloro	16	1.0	0.06
p,p'-Dicyano	7	0.5	0.08
m,m'-Dicyano	7	0.5	0.07

The data in Table 4 lead us to the conclusion that there are two groups in the activity of the radical RCOO. From *p,p'*-dimethoxy-benzoyl peroxide 5×10^{-4} mol. of carbon dioxide was produced. The conspicuous effect of the peroxide on the velocity of polymerization is supposed to depend on the activities of *p*-methoxy-benzoyl and *p*-methoxy-phenyl radicals besides the large rate of decomposition of the peroxide.

In the experiments at 60°C. for two hours, on the contrary, carbon dioxide was generated from effective peroxides, not from less effective ones. The result also suggests that two types of radical, RCOO and R, react as the initiator in the presence of effective peroxides, while the radical RCOO reacts chiefly

in the presence of less effective ones. The amounts of carbon dioxide generated are listed in Table 5.

Table 5

Amount of Carbon Dioxide Generated from Peroxides at 60°C.

Substituted benzoyl peroxide	Amount of carbon dioxide ($\times 10^{-4}$ mol.)
p,p'-Dimethoxy	6.8
m,m'-Dimethoxy	3.0
p,p'-Dimethyl	4.5
m,'m-Dimethyl	3.2
Unsubstituted	3.3
p,p'-Dichloro	2.7

The data are in a similar order to those found for the velocity of polymerization at 60°C. in the presence of effective peroxides.

Experimental

Materials.—The vinyl acetate employed was washed several times with water[5], dried over anhydrous sodium sulfate, and fractionated in the atmosphere of nitrogen just before use. b.p. 72°C. All substituted benzoyl peroxides were prepared and purified as described in the previous paper.[1]

Polymerization of Vinyl Acetate.—A peroxide (1/3000 mol.) and vinyl acetate (1/30 mol.) were taken in the reaction tube, the tube cooled in a mixture of solid carbon dioxide and alcohol, and sealed off in a vacuum. The sealed tube was immersed in a thermostat of 40°C. or 60°C. for the reaction time, then removed and cooled in an ice-salt-bath. Unchanged vinyl acetate was driven off in a vacuum and the weight of poly-vinyl acetate was measured. In another experiment, the reaction products were dissolved in acetone and the polymer was precipitated by adding water to the solution. The weight of polyvinyl acetate was almost equal to that of the case mentioned above.

Decomposition of Peroxides.—Owing to the high-volatility of vinyl acetate, the apparatus and experimental procedure were somewhat modified compared with those in the case of the decomposition in styrene. The main part of the apparatus is shown in Fig. 4.

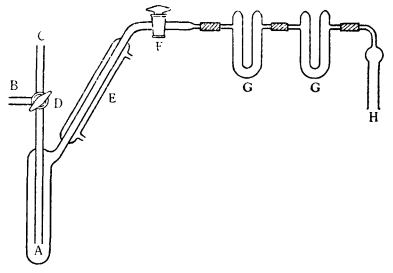

Fig. 4

A is the reaction tube of 22 mm. diameter and 35 cc. capacity, B the inlet tube for nitrogen, C the tube for evacuation, E the cooler with cold water, and G the soda-lime tube for the absorption of carbon dioxide produced. During the reaction a soda-lime tube H was attached to G.

A mixture of peroxide (2/3000 mol.) and vinyl acetate (2/30 mol.) was taken in A and tube A was cooled in solid carbon dioxide and alcohol. After the cock F was closed and the reaction tube evacuated through C, the cock D was closed. Then the tube A was immersed in a thermostst of 40°C. or 60°C. for the reaction time. When the requied time was over, A was cooled again at -30~35°C. in a mixture of solid carbon dioxide and alcohol, the cock F opened, passing pure nitrogen through B into the whole apparatus, and the weight of carbon dioxide absorbed in G was measured. The amount of carbon dioxide was verified by the blank test.

Summary

(1) The activity of symmetrical *m*- and *p*-substituted benzoyl peroxides on the rate of polymerization of vinyl acetate has been investigated at 40°C. and 60°C. in the absence of air.

(2) The peroxides have been divided into two groups according to their activities. The activity of peroxides in each group is nearly inversely proportional to the square root of the dissociation constants of the corresponding substituted benzoic acids in the experimental conditions.

(3) The thermal decomposition of the peroxides in vinyl acetate has been observed to be of first order at 40°C., but not always exactly so at 60°C.

(4) In the decomposition of the peroxides at 40°C., carbon dioxide was not generated from all the peroxides excluding *p,p*-dimethoxybenzoyl peroxide; while in the decomposition at 60°C., carbon dioxide was produced from effective peroxides, such as dimethoxy-, dimethyl-, and *p,p'*-dichloro-benzoyl peroxides.

(5) It has been confirmed that the velocity of the polymerization is affected not only by the rate of decomposition of the peroxides but also by the activity of radicals derived from the peroxides.

(6) The results have been compared with those obtained in the polymerization of styrene.

The authors express their hearty thanks to the Ministry of Education for a grant.

Chemical Laboratory, South College, Osaka University, Osaka

5) S. Okamura, "*Kobunshi-tembo*," **2**, 125 (1950).

LETTER

Separation of Selenium and Tellurium by Means of Cation Exchange Resin

Fumio AOKI

(Received September 4, 1953)

In the cource of studying the analysis of high purity selenium the writer faced the need of separating selenium from tellurium. Reduction of selenite by sulphur dioxide is not only tedious but also unreliable when the amount of tellurium is less than the order of milligram.

A new method by Johnson and Kwan[1] is found to be difficult to perform. Yoshino[2] pointed out that selenium (as selenite) passes through cation exchange resin except when a large amount of iron is present, but he did not mention the behavior of tellurium.

The writer has observed that selenium can be separated from tellurium by applying the solution on a cation exchange resin column.

Experimental

(1) Test solutions:—(a) 99.95% selenium was dissolved in nitric acid, evaporated to dryness, sublimed twice, and the resultant selenium dioxide was dissolved in water. (b) 99.5% tellurium was dissolved in nitric acid, evaporated to dryness, dissolved in the least possible amount of nitric acid; then filtered, and the filtrate was evaporated to drive off most of nitric acid.

The precipitated tellurous acid was washed with hot water, and finally dissolved in the least possible amount of nitric acid. Concentration of each solution was determined gravimetrically.

(2) Resin column:—10 ml. of Amberlite IR 120 (60 mesh) was used as HR type.

(3) Procedure:—25 ml. of slightly acid (<0.05 N) solution, containg 50 to 1000 γ of either selenium or tellurium or both, was dropped on the resin column at the rate of 2 ml./min., followed by 100 ml. of water, 100 ml. of 0.3 N hydrochloric acid and 100 ml. of 3 N hydrochloric acid. Every 25 ml. portion of the passed solution was examined for selenium and tellurium. The examination was made by the stannous chloride reduction method.

(4) Results:—Selenium was found in the first and second portions of the passed solution and in the third portion it was only faintly detected. In the fourth and fifth portions neither selenium nor tellurium seemed to be present. Tellurium appeared from the sixth to the ninth portion.

When the original solution contains iron, lead or copper in comparable amount to selenium or tellurium, heavy metals are separated as well as selenium and tellurium. Heavy metals are, of cource, found in the portions later than the tenth.

Government Chemical Industrial Research Institute, Tokyo-Hatagaya

1) R. A. Johnson, F. A. Kwan: *Anal. Chem.*, **23**, 651 (1951).
2) Y. Yoshino: *J. Chem. Soc. Japan*, **71**, 577 (1950).

Radiometric Det rmination of Small Amounts of Potassium

By Tomitaro ISHIMORI and Yoshimasa TAKASHIMA

(Received May 29, 1953)

Sodium cobaltinitrite, the well-known reagent for both the gravimetric and the indirect colorimetric determinations of potassium[1], was used in the radiometric determination of potassium by R. Ehrenberg[2] and M. Ishibashi et al[3]. As it was difficult to obtain artificial radioactive substances, they were obliged to use natural radioactive indicators. Therefore, tedious chemical procedures were necessary before beginning the measurement of radioactivity. Their methods are schematically shown in Table I.

TABLE I SCHEMES OF RADIOMETRIC METHODS FOR POTASSIUM

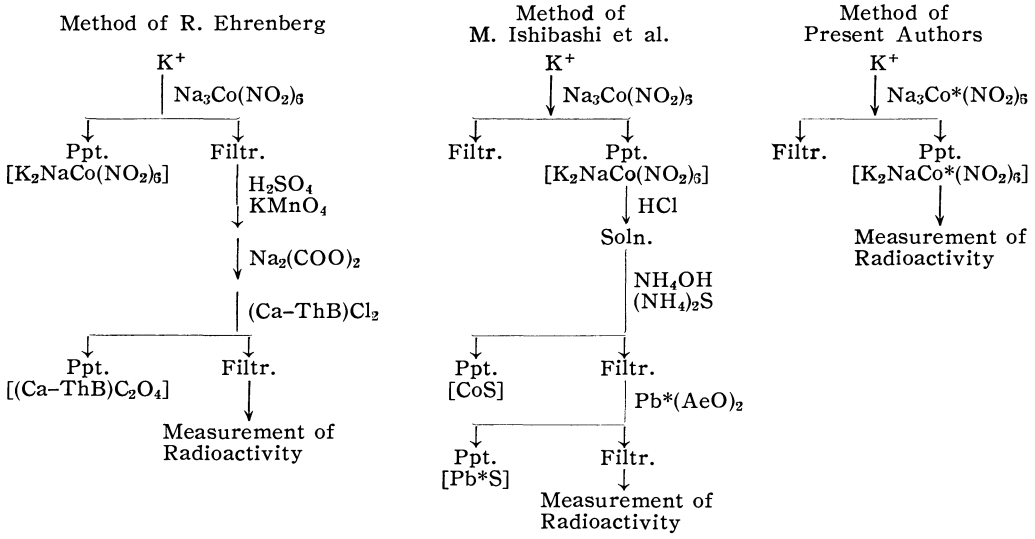

In recent years, the artificial radio-isotope of cobalt (cobalt-60) is easily obtainable from the Atomic Energy Commission of U.S.A., so the present authors investigated a simplified radiometric determination of small amounts of potassium using radioactive sodium cobaltinitrite labelled with cobalt-60 as precipitant.

(1) Determination of (8~0.3) mg. Potassium—Various amounts of the standard solution of recrystallised potassium chloride are taken and radioactive $K_2NaCo^*(NO_2)_6$ is precipitated according to the following procedure.

The relation between the relative intensity of the radioactivity of the precipitate and the amount of potassium taken is investigated.

(a) Preparation of the Radioactive Precipitant I—According to the usual method[1,3] a solution of sodium cobaltinitrite labelled with cobalt-60, $Na_3Co^*(NO_2)_6$, is prepared as the precipitant.

First, the following two solutions are prepared.

Solution (A)	cobalt nitrate	21 g.
	cobalt-60 chloride	about 0.7 mc.
	water	42 cc.
	acetic acid	10.4 cc.
Solution (B)	sodium nitrite	100 g.
	water	150 cc.

Next, the solution (B) is added to the solution (A) and the nitrogen oxide formed by the double decomposition of the salts is expelled by passing the air through the combined solution. Any precipitate formed is filtered off and the filtrate which contains sodium cobaltinitrite labelled with cobalt-60 is used as the precipitant.

In this paper, the precipitant thus prepared will be called the precipitant I.

(b) Procedure—According to the usual method[1], radioactive potassium-sodium cobaltinitrite,

1) R. Fresenius u. G. Jander, "Handbuch d. Analytischen Chemie", 3 Teil, Bd. Ia, Julius Springer, Berlin, 1940, p. 172.
2) R. Ehrenberg, *Microchem. Pregl Festschr.*, 61, (1929), *C.A.*, **24**, 2395; *Biochem. Z.*, **197**, 467 (1928), *C.A.*, **23**, 51.
3) M. Ishibashi and H. Kishi, *J. Chem. Soc. Japan*, **57**, 1039 (1936).

$K_2NaCo^*(NO_2)_6$ is precipitated by the precipitant described in (1, a). A definite amount of the standard solution of potassium chloride is poured slowly into a platinum or quartz crucible which contains 5 cc. radioactive precipitant I and 1 cc. of 1N nitric acid. Then some water is added until the total volume of the resultant solution amounts to 16 cc.

After standing over-night, the yellow precipitate of radioactive potassium-sodium cobaltinitrite is filtered on a glass filter and washed with about 20 cc. of 0.01N nitric acid and then with about 10 cc. of 95% alcohol. The washing solution is drained off by suction and the washed precipitate is dried at 110°C. in an air bath for about one hour. After cooling, the radioactivity of the precipitate on the glass filter is measured by a Geiger-Müller counter made by the Nuclear Instrument and Chemical Corporation, U.S.A.

The precipitate obtained from 3.145 mg. potassium is reserved as the standard of the radioactivity and the intensities of the activity of the precipitates obtained from the solutions containing various amounts of potassium are compared respectively with the standard. The relative intensity thus obtained is not affected by the decay of cobalt-60 or the daily variation of the sensitivity of the instrument for the measurement of radioactivity.

(c) **Results**—Results of the experiments are shown in Table II and Figure 1 and 2.

TABLE II RESULTS OF (1)

mg. K (Taken)	Relative Intensity of Radioactivity
7.863	2.27
6.291	1.82, 1.98
4.718	1.58, 1.47
3.145	1.00*, 0.98
1.573	0.45, 0.47, 0.48, 0.48
1.258	0.37, 0.40
0.943	0.28, 0.28
0.629	0.16, 0.16
0.315	0.04, 0.05

(*) Taken as the standard. The activity of the standard is about 1960 c/min. It shows slight variations according to the daily variation of the sensitivity of the counter.

In Figures 1 and 2, the almost linear relationships between the relative radioactivities and the amounts of potassium taken are shown in a fairly wide range of amounts of potassium, so we conclude that we can determine the amounts of potassium radiometrically according to the above-mentioned procedure, using Figures 1 and 2 as working curves.

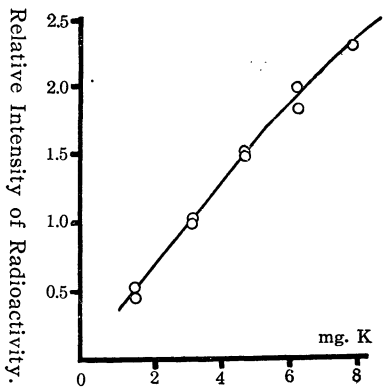

Fig. 1 Working curve of (1)

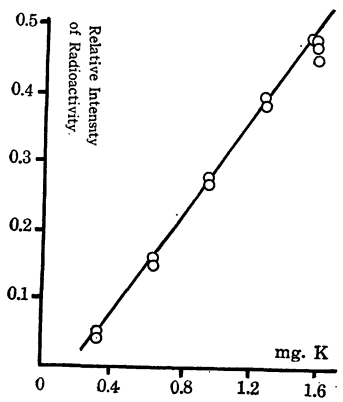

Fig. 2 Working curve of (1)

(2) **Determination of (0.8~0.16) mg. Potassium**—The relation between the relative intensity of the radioactivity of the precipitate formed and the amount of potassium taken is investigated following the same procedure as described in (1, b), and using the precipitant having a stronger specific activity, which is prepared as follows.

For the measurement of radioactivity, the same standard as (1, b) is used.

(a) **Preparation of Precipitant II**—The precipitant II is prepared from the following two solutions, (C) and (D), in the same way as described in (1, a).

Solution (C)	cobalt nitrate	15 g.
	cobalt-60 chloride	about 4.5 mc.
	acetic acid	7.5 cc.
	water	30 cc.
Solution (D)	sodium nitrite	72 g.
	water	108 cc.

(b) **Results**—Results are summarized in Table III and the relation between the rela-

Table III Results of (2)

mg. K (Taken)	Relative Intensity of Radioactivity	Mean
0.786	2.00, 1.82, 1.88, 1.86	1.89
0.629	1.48, 1.39, 1.50, 1.54, 1.56	1.49
0.472	0.98, 0.85, 1.11, 0.92	0.97
0.315	0.29, 0.29, 0.34	0.31
0.157	0.05, 0.07, 0.13, 0.16	0.10

tive intensity of the radioactivity of the precipitate and the amount of potassium taken is shown in Figure 3. As seen in Figure 3, the deviation of each experiment is larger than in Figure 1 or 2. The working curve of Figure 3 is shaped S, while those of Figure 1 and 2 are almost linear.

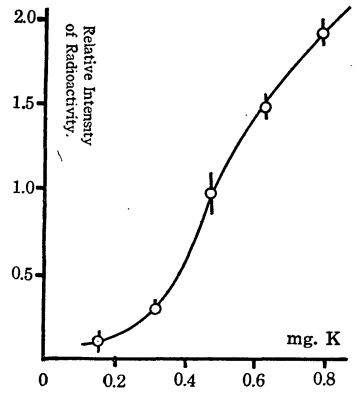

Fig. 3 Working curve of (2)

(c) **Application of the Above Method to the Determination of Potassium in Silicate rocks**—The determination of potassium contents in two kinds of andesite is tried by the above described radiometric method, combined with the method of J. Lawrence Smith for the isolation of alkali chlorides, using about 200 mg. of each sample. Comparison of the values thus obtained with those obtained by the usual gravimetric method as potassium chloroplatinate is shown in Table IV.

Table IV Determination of Potassium Content of Andesite

Sample	% K_2O obtained gravimetrically	% K_2O obtained radiometrically
(A)	0.46, 0.40	0.39, 0.39
(B)	0.40, 0.33, 0.37	0.32, 0.32

(3) **Determination of (0.126~0.0016) mg. Potassium**—In the experiments for the minute quantities of potassium, the precipitation and the filteration must be done microchemically, and the precipitant with a much higher specific activity must be used. Further, cautions against the contamination by potassium from glass-wares must be taken.

(a) **Standard Solution of Potassium Chloride**—The stock solution which contains 1.5010 g. potassium chloride per litre is diluted just before use and a series of dilute standard solutions of potassium chloride is prepared.

(b) **Preparation of Radioactive Precipitant III**—The precipitant III. is prepared from the following two solutions, (E) and (F), in the same way as described in (1, a) in a smaller scale.

Solution (E)	cobalt nitrate	1 g.
	cobalt-60 chloride	about 6.7 mc.
	acetic acid	0.5 cc.
	water	2 cc.
Solution (F)	sodium nitrite	4.8 g.
	water	72 cc.

(c) **Procedure**—Five drops of the precipitant III and one drop of 1N nitric acid are put into the platinum crucible which contains 0.5 cc. of standard solution of potassium chloride prepared as described in (3, a). After leaving it over-night, the precipitate formed is filtered off with a micro filter-tube[4] and washed with 0.5 cc. of 0.01N nitric acid and then three times with 0.7 cc. alcohol. The washed precipitate in the platinum crucible is dissolved in hot water. The solution is transferred to a glass dish through the filter-tube and evaporated up on a water bath.

The radioactivity of the residue in the glass dish is measured with Lauritsen electroscope, made by the Scientific Research Institute, Tokyo. For the measurement of radioactivity, an arbitrarily selected specimen is used as the standard and the ratio of the intensities of the radioactivity of each specimen and the standard is calculated.

(d) **Results**—Results are shown in Table V and Figure 6. The relation between the relative intensity of the measured radioactivity and the amount of potassium is linear, so that the quantitative determination of the minute amounts of potassium can be carried out in the procedure described in (3, c).

4) E. Beryl Daw, "Quantitative Organic Microanalysis", J. & A. Churchill Ltd., 1937, p. 96,

TABLE V RESULTS OF (3)

mg. K (Taken)	Relative Intensity of Radioactivity
0.0000	0.003, 0.003
0.0016	0.004, 0.005
0.0047	0.023, 0.025
0.0094	0.052, 0.061
0.0236	0.14, 0.12
0.0394	0.23, 0.24
0.0630	0.36, 0.36
0.1260	0.69, 0.70

The activity of the standard is about 347 div./min. It shows slight variations according to the daily variation of the sensitivity of the electroscope.

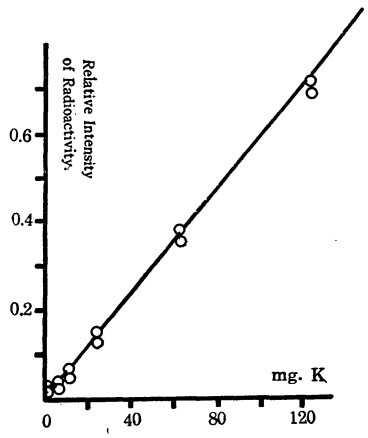

Fig. IV Working curve of (3)

(e) **Applications of the Above Method**— (i) The potassium contents of two samples of silicate rocks; andesite found in Kurofuyama, ASAMA[5] and the standard sample of diabase sent from the U. S. Geological Survey, W-I[6], are determined according to the following procedure:

About 20 mg. of the powdered sample is treated according to the J. Lawrence Smith method to obtain the total alkali chlorides. The chlorides are dissolved in a little water and treated as (3, c). A platinum or quartz crucible is used as a microbeaker and all filtrations are done with a micro filtertube.

In Table VI, the values thus obtained are

TABLE VI DETERMINATION OF POTASSIUM CONTENT OF SILICATE ROCKS

Sample	% K_2O obtained gravimetrically	% K_2O obtained radiometrically
Andesite (Kurofuyama)	0.85*	0.54, 1.07***
Standard Sample of Diabase	0.78**	0.77***, 0.88***

(*) Value given by I. Iwasaki.
(**) Value reported from our laboratory.
(***) Value obtained by the extrapolation of the working curve.

compared with those obtained by the usual method. The coincidences are fairly good and we conclude that this method will be effective for the microdetermination of potassium in silicate rocks.

(ii) The potassium content of the tap water which is supplied to our laboratory is determined in our micro-radiometric method.

The procedure is as follows: About ten grams of the tap water is taken in a platinum crucible and evaporated to about 0.5 cc. on a water bath. After cooling, the evaporate is treated as described in (3, c).

The determinations are done with 10 g. and 15 g. of the water, and potassium with the concentrations of 0.083 and 0.087 millimole per litre are obtained respectively. Although the presence of ammonium ion disturbs the determination, the ammonium content of the sample is estimated to be 0.006 millimole per litre by the colorimetric method, so that our value for potassium should be reliable.

The authors wish to express their sincere thanks to Prof. Sinnosuke Matuura for the facilities accorded to them during this investigation, to Prof. Iwaji Iwasaki for providing samples of andesite and to Mr. N. Kokubu for determining the ammonium content of the tap water.

Department of Chemistry,
Faculty of Science,
Kyushu University

5) I. Iwasaki, *J. Chem. Soc. Japan*, **57**, 1324 (1936).
6) W. G. Schlecht, *Anal. Chem.*, **23**, 1568 (1951).

On the Distribution of Nutrient Salts in the Equatorial North Pacific*

By Rinnosuke FUKAI

(Received May 30, 1953)

Introduction

Among the factors which govern the distribution of chemical constituents such as nutrient salts and dissolved oxygen in sea water, in addition to the hydrographical movements of sea water, it is clear that the biological factor, namely consumption or regeneration of the constituents by living organisms or from their corpses, play an important rôle in natural processes. Since 1937, various investigators[1] have discussed this problem in connection with the existence of the oxygen minimum layer in the oceans, and it has generally been accepted that the biological factor cannot be ignored in natural processes. As the author had an opportunity of analysing the water samples collected from the equatorial region of the North Pacific Ocean, where the movements of sea water represent a characteristic feature of the tropical region, the distribution of nutrient salts has been investigated taking the biological factor into consideration.

Samples and Analytical Methods

Water samples were collected by members of the Nankai Regional Fisheries Research Laboratory (Kôchi, Kôchi Prefecture, Japan) when the marine observations on the fishing ground of tunny were carried out aboard "F.R.S. Tenyô Maru" in the summer of 1951. The analysis of the samples except those of dissolved oxygen was carried out by the author at the Tôkai Regional Fisheries Research Laboratory (Tokyo, Japan) after about four weeks standing. The chemical constituents analysed were chlorine, phosphate-phosphorus and nitrate-nitrogen. Dissolved oxygen was determined by a member of the Nankai Regional Laboratory aboard the ship. As the area in which the observations were carried out was within a district of high temperature, the water samples to be analysed for phosphate and nitrate were carefully preserved by adding chloroform-toluol mixture and mercuric chloride solution respectively immediately after the sampling, in order to prevent bacterial growth. Although some changes in phosphate contents in the samples collected from the upper layers containing living organisms must be expected even if the above mentioned procedure has been adopted, serious errors will not be introduced since the phosphate contents of the upper layers are much lower than those of the deeper layers.

The analytical methods adopted were as follows: chlorine: titration method proposed by Fajans using uranine as the indicator[2]; phosphate: colorimetric determination by Denigès-Atkins using Beckman's Model DU Quartz spectrophotometer[3]; nitrate: colorimetric method with Harvey's reduced strychnine reagent[4].

Data for nutrient salts obtained from the equatorial region of the Pacific were accumulated through the observations made on board the "Carnegie" and the "Dana". But the data obtained from this region are much fewer than those from the equatorial Atlantic and there is a lack of systematic data in the Eastern Hemisphere. The data dealt with in this paper were obtained along the longitude 150°E and 160°E between the equator and latitude 20°N. Twelve samples were collected at each station from different layers above a depth of 1000 meters. Collection was carried out at about 50 stations, then about 600 samples were collected and analysed.

The distribution of the constituents was considered on the basis of the data obtained from longitudinal section along 150°E, since the conditions along 160°E did not differ significantly from those along 150°E.

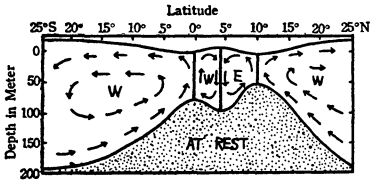

Fig. 1. Schematic representation of the vertical circulation within the equatorial region of the Atlantic. W: westward current. E: eastward current. (After Defant, 1936).

* Contribution B-No. 113 from the Tokai Regional Fisheries Research Laboratory, Tokyo, Japan.

1) H. R. Seiwell, *Papers in Phys. Oceanogr. and Meteor.*, **5**, No. 3 (1937); H. U. Sverdrup, *J. Conseil permanent intern. pour l'exploration de la mer*, **13**, 163 (1938).

2) Y. Miyake, This Bulletin, **14**, 29 (1939).

3) R. Fukai, *J. Oceanogr. Soc. Japan*, in press.

4) H. Wattenberg, *Rapp. et Proc.-Verb. des Reunions, Conseil permanent intern. pour l'exploration de la mer*, **103**, 1 (1937).

Results and Discussion

1. General Feature of Water Movements in the Region in Question—A. Defant[5] derived theoretically a schematic representation of vertical circulation of water within the equatorial region of the Atlantic as shown in Fig. 1. According to the schema, convergence (sinking of water) or divergence (upwelling of water) is developed at the boundary between the currents, and it is expected that the distribution of chemical constituents may fit with the schema. Based upon the data obtained on board the "Carnegie" (1929), Sverdrup et al[6]. recognised the close agreement between the water movements and the distribution of the constituents in the upper layers.

2. Chlorinity Distribution in the Longitudinal Section—The data for chlorine determination were given in term of chlorinity. In Fig. 2, distribution of chlorinity in the

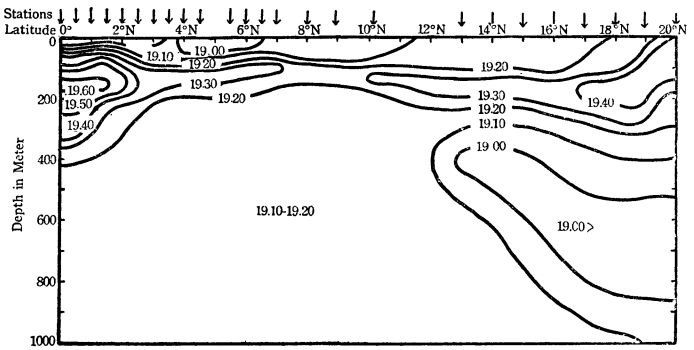

Fig. 2. Chlorinity distribution in the longitudinal section along 150°E. Units: %.

longitudinal section along 150°E is given. In this figure, it is obvious that the intermediate water of the North Pacific appears within the depths between 400 m. and 800 m. at lat. 12°N and northwards. As going to the south, the water below the intermediate layer becomes homogeneous and the characteristic water of the equatorial region having high chlorinity (Cl>19.30%) appears in the upper layer. But whether the water movement has influence on the distribution of chlorinity is not clear.

3. Distribution of Dissolved Oxygen and Phosphate-phosphorus in the Section—The distributions of dissolved oxygen and phosphate are illustrated in Figs. 3 and 4, respec-

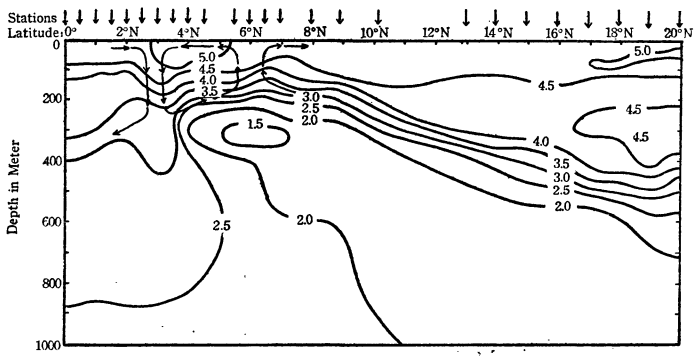

Fig. 3. Distribution of dissolved oxygen in the longitudinal section along 150°E. Units: O_2 ml. per liter.

tively. In these figures, the corresponding distribution of these constituents with the schema presented by Defant is clearly shown. The convergence occuring near lat. 3°N and divergence near 6°N are recognised. The water movements suggested by the distribution of the constituents are shown by the arrows. From these figures, it is concluded that the vertical movements of water affect

5) A. Defant, Deutshe Atlantische Expd. *Meteor*, Bd. VI, Teil I (1936).
6) H. U. Sverdrup et al., "The Oceans", Prentice-Hall, New York, 1946, p. 711.

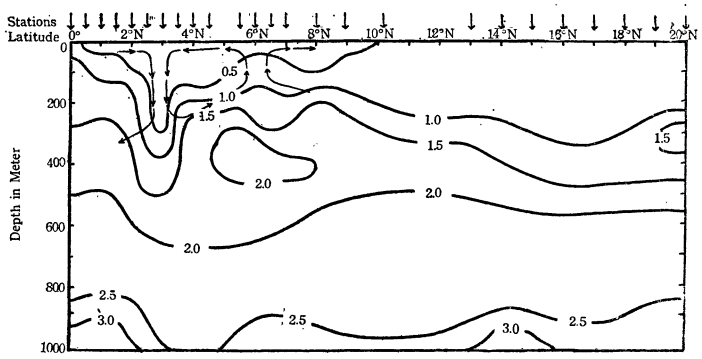

Fig. 4. Phosphate distribution in the longitudinal section along 150°E. Units: μg. -atoms PO_4-P per liter.

the distribution of the constituents at a depth as low as 500 m.

Although the water movements affect decidedly the distribution of the constituents in the region in question, it cannot be explained simply by the structure of water movements that a pool of minimum content of dissolved oxygen or maximum content of phosphate appears at a depth of about 300 m. The extreme value of the constituents in an enclosed domain should appear only when the decomposition of dead organisms, namely the consumption of dissolved oxygen or the regeneration of phosphate takes place within the domain[7]. It is a remarkable fact that the domain lies just below the divergence, for areas in which upwelling of water is taking place have high fertility due to the nutrient salts transported from the layers below, and are able to support larger populations of organisms than other areas. If a greater quantity of dead organisms in this area decomposes while sinking, decomposition processes occuring in this water column will be more vigorous than those in other areas. In consequence, it is probable that the maximum decomposition may occur in the above mentioned domain.

4. Relationship between Oxygen Minima and Maxima of Nutrient Salts—Before considering the decomposition processes quantitatively, the vertical distribution of the constituents is given in Fig. 5. From the figure, it can be seen that the extreme values of these constituents appear in close correlation with each other and are centered at a depth of 300 m. Although vertical distributions of phosphate and nitrate seem to be in parallel correlation, it is noteworthy that the gradient of phosphate increment is larger than that

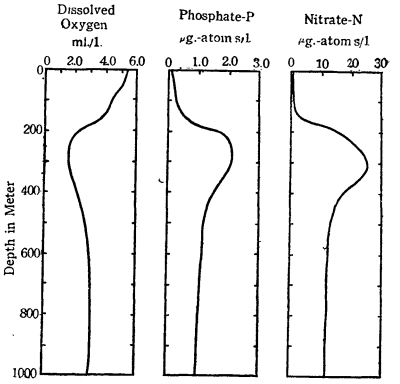

Fig. 5. Typical vertical distributions of dissolved oxygen, phosphate-phosphorus and nitrate-nitrogen in the Equatorial North Pacific based on the data obtained at Station 29 (lat. 4°30′N, long. 150°02′E).

of nitrate increment at depths within 200～300 m. This may be attributed to the difference in the rates of liberation between phosphate and nitrate *in situ*, as the author has recently pointed out[8]. Due to the lack of available data for nitrate, further detailed discussion concerning the vertical distribution of nutrient salts is impossible.

5. Quantitative Consideration on the Rate of Decomposition—In order to obtain quantitative knowledge upon the rate of decomposition in connection with the appearence of oxygen minima and nutrient salts maxima, computations were carried out introducing some simplifying assumptions.

If we consider a cube of sea water of a unit volume *in situ*, the change of concentration of the constituents affected by the biological factor in this cube can essentially be expressed[9].

7) G. A. Riley, *Bull. Bingham Oceanogr. Collection*, **8**, Article 1 (1951).

8) R. Fukai, This Bulletin, **25**, 323 (1952).

9) H. U. Sverdrup, *J. Conseil permanent intern. pour l'exploration de la mer*, **13**, 163 (1938).

$$\frac{\partial c_o}{\partial t} = R + \frac{\partial}{\partial x}\left(\frac{Ax}{\delta}\cdot\frac{\partial c}{\partial x}\right) + \frac{\partial}{\partial y}\left(\frac{Ay}{\delta}\cdot\frac{\partial c}{\partial y}\right) + \frac{\partial}{\partial z}\left(\frac{Az}{\delta}\cdot\frac{\partial c}{\partial z}\right) - \left(V_x\frac{\partial c}{\partial x} + V_y\frac{\partial c}{\partial y} + V_z\frac{\partial c}{\partial z}\right) \quad \text{.....(1),}$$

where, C_o: Concentration of the constituent in the cube,
δ: Specific gravity of sea water,
R: Biological rate of change,
A_x, A_y, A_z: Coefficents of eddy diffusivity along x-, y- and z-axis, respectively,
V_x, V_y, V_z: Current velocity components along x-, y- and z-axis, respectively.

We take x-axis from the east to the west, y-axis from the south to the north and z-axis from the surface to the bottom and make the following assumptions.

1. Steady state has been established. In other words, the distribution of the concentration is not altered in the course of time.
2. The distribution of the concentration is homogeneous along the east-west axis.
3. Current velocities except along the east-west axis, are negligibly small in the computation.

Under these assumptions, equation (1) is reduced as follows:

$$R = -\left[\frac{\partial}{\partial y}\left(\frac{Ay}{\delta}\cdot\frac{\partial c}{\partial y}\right) + \frac{\partial}{\partial z}\left(\frac{Az}{\delta}\cdot\frac{\partial c}{\partial z}\right)\right] \quad \text{.....(2).}$$

Assumptions 1 and 2 are supposed to be reasonable, because the difference between the distribution pattern along 150°E and that along 160°E is small. Assumption 3 is also likely correct since the vertical current velocity is nearly equal to zero at depths such as an oxygen minimum layer and horizontal current velocity along y-axis, V_y, may also be ignored because it does not exceed the order of 0.5 cm./sec.

Now let us assume that δ equals unity and A_y and A_z are constant and rewrite the equation (2) into a finite form. Then we may obtain.

$$R = -\left[A_y\frac{\delta^2 c}{\delta y^2} + A_z\frac{\delta^2 c}{\delta z_2}\right] \quad \text{.....(3).}$$

We cannot calculate the values of R unless the values of A_y and A_z are known. However, the derivation of physical coefficents, A_y and A_z, from the present data is difficult. Accordingly, the values which have been obtained so far for these coefficents in various regions[10] are introduced. Thus, the values of R are calculated by introducing the gradients of the concentration near 300 m. depth. The results are shown in the tables. Tables I and II indicate the rate of phosphate liberation and oxygen consumption, respectively. As it is considered that $A_y = 10^7$ C.G.S.[11] and $A_z \leqq 10$ C.G.S.[12] in the layer in question, the rate of $3\sim8\times10^{-8}$ μg.-atoms PO_4-P/1. sec. for phosphate liberation and of $3\sim12.5\times10^{-8}$ ml. O_2/1. sec. for oxygen consumption may be estimated. Knowledge concerning the biological rate of change *in situ* has scarcely been accumulated. The values here proposed are about ten times higher than those proposed by Riley in 1951.[7] But, these values are prolobly reliable, for they are estimated for a particular layer within the tropical region of high temperature, while Riley's values are those for the whole Atlantic Ocean.

TABLE I

VALUES CALCULATED FOR PHOSPHATE LIBERATION

Units: 10^{-8} μg.-atoms PO_4-P/1. sec.

A_z/ A_y	10^6	10^7	10^8
0	0.3	3.4	34
10	5.1	8.2	39
50	24	27	58

TABLE II

VALUES CALCLATED FOR OXYGEN CONSUMPTION

Units: 19^{-8} ml. O_2/1. sec.

A_z/ A_y	10^6	10^7	10^8
0	−0.4	−3.6	−36
10	−9.3	−12.5	−45
50	−45	−49	−81

Summary

The present author carried out the determination of nutrient salts of the water samples collected from the equatorial region of the North Pacific in 1951, and their distributions have been investigated taking the biological factor into consideration.

The author found that the distributions of nutrient salts were closely connected with the structure of the movements of sea water in this region and that the effect of water movements was extended to a depth of 500 m. On the other hand, it is suggested that the oxygen minima and nutrient salts maxima developed just below the divergence are caused by the biological factor.

10) H. U. Sverdrup et al., "The Oceans", Prentice-Hall, New York, 1946, p. 484.
11) R. B. Montogomery and E. Palmen, *J. Marine Res.*, **3**, 112 (1940).
12) H. R. Seiwell, *Papers in Phys. Oceanogr. and Meteorol.*, **3**, No. 1 (1935).

The estimations of biological rate of change of the constituents in the layer in which the decomposition processes might occur were made, introducing some simplifying assumptions. As the results, the values of $3\sim8\times10^{-8}$ μg.-atoms PO_4-P/1 ; sec. for phosphate liberation and $3\sim12.5\times10^{-8}$ ml. O_2/1. sec. for oxygen consumption were obtained. These values are probably reliable as the measure indicating the rate of decomposition processes which take place in the subsurface layer within the region in question.

The author desires to express his hearty thanks to Prof. Kenjirô Kimura of Tokyo University and Dr. Masao Migita of the Tokai Regional Fisheries Research Laboratory for their valuable advice. Many thanks are also due to Mr. Hiroshi Yabe and other members of the Nankai Regional Laboratory who have placed water samples at the author's disposal.

Tokai Regional Fisheries Research Laboratory, Tokyo, Japan

Spectrochemical Study of Microscopic Crystals. IV. The Dichroism of the Tetrahalogeno-Complex Type[1]

By Shoichiro YAMADA and Ryutaro TSUCHIDA

(Received June 25, 1953)

Previously the present authors[2,3] reported on the dichroism of tetra-co-ordinated planar complexes of platinum(II) and palladium(II), and reached the conclusion that the dichroisms of these planar complexes can be classified into two types; that is, the "tetrahalogeno-complex type" and the "tetracyano-complex type." Both the types have been found to show the following common rule as to the second band: the ∥-absorption[4] is hyperchromic to the ⊥-absorption[4] in palladium complexes, and the ∥-and ⊥-absorptions in platinum complexes show the band with maximum absorption coefficient of almost equal magnitude. The main difference between the two is that in the former type the second band of the ∥-absorption lies in the longer wave-length than the ⊥-absorption whereas in the latter it holds the relation reverse to the above. It seemed of interest to investigate the cases with other planar tetra-co-ordinated complexes. In the present work, the dichroisms of crystals of K_2PdI_4, $K_2Pd(SCN)_4$ and $K_2Pt(SCN)_4$ have been measured and the results of the measurements have been discussed in association with the previous data[2,3] on dichroisms of planar complexes.

1) Presented in part at the Symposium on Co-ordination Compounds, Tokyo, November 13, 1951.
2) S. Yamada, *J. Am. Chem. Soc.*, **73**, 1182 (1951).
3) S. Yamada, H. Yoneda and R. Tsuchida, *J. Chem. Soc. Japan*, **69**, 145 (1948).
4) ∥- or ⊥-absorption represents, respectively, absorption by polarized light with its electric vector parallel or perpendicular to the plane of the complex.

Experimental

Materials.—$K_2Pd(SCN)_4$ was prepared in red hexagonal prisms from potassium tetrachloro-palladate (II) and potssium thiocyanate. The crystal shows dichroism on the prism face, i. e,, orange-red and yellow, and exhibits an oblique extinction. Dichroism measurements were made on the prism face by polarized lights with their electric vectors along the directions of extinction.

K_2PdI_4 was prepared in black, rhombic tablets with metallic lustre by adding a concentrated solution of potassium tetrachloro-palladate (II) to a hot solution of potassium iodide. The crystal exhibits a straight extinction. Dichroism can be recognized under the microscope with a thin crystal; that is, it appears brownish black and greenish black by polarized lights with their electric vectors along the c-and a-axes, respectively. Dichroism measurements were made in these directions; c-and a-absorptions represent absorptions by polarized lights with their electric vectors along the c-and a-axes, respectively.

$K_2Pt(SCN)_4$ was prepared in orange, hexagonal prisms by the method of Buckton[5]. The crystal exhibits an oblique extinction on the prism face, and appears yellow and yellowish orange by polarized light with electric vector along the directions of extinction. Dichroism measurements were performed along the directions of extinction, that is, the a-and b-directions in the figure (Fig. 3).

$K_2PdBr_4.2H_2O$ was prepared by the method of Gutbier and Krell.[6] The brown prismatic crystals obtained belong to the rhombic system, and

5) G. B. Buckton, *Ann.*, **92**, 286 (1854).
6) A. Gutbier and A. Krell, *Ber.*, **38**, 2385 (1905).

show a marked dichroism on the prism face. Dichroism measurements were made on this face by polarized lights with electric vectors parallel and perpendicular to the principal axis. Although the dichroism of the crystal had been reported in the previous paper,[2,3] measurements in the present work have been extended to the region of longer wave-length and smaller extinction coefficients. The crystal structure of the compound has not yet been analyzed. However, we concluded in the previous report[3] that the complex ions in the crystal are arranged parallel to each other with their planes perpendicular to the c-axis. ∥-and ⊥-absorptions are designated on the basis of the above presumption.

Measurements.—Quantitative dichroism measurements were performed by the microscopic method.[7] The crystals used in the measurements were several hundredths of mm. thick. α denotes extinction coefficient per mm. of the crystal. Molecular absorption coefficients, k, were estimated from the relation, $k=10M\alpha/\rho$, where M and ρ represent, respectively, the molecular weight of the compound and the density of the crystal. Results of the measurements are shown in the Figures 1~4 and tabulated in the Tables I~III.

Absorption spectra of aqueous solutions of $K_2PdBr_4.2H_2O$ and $K_2Pd(SCN)_4$ were determined by the photographic method using a sector-photometer, and that of $K_2Pt(SCN)_4$ was determined with a Beckman quartz-spectrophotometer model DU.[8]

Results and Discussion

Potassium Tetrathiocyanato-palladate (II).—A striking difference is observed between the two component absorptions in Fig. 1.

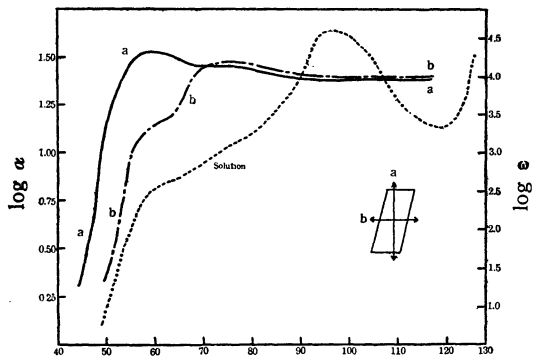

Fig. 1. Absorption spectra of $K_2Pd(SCN)_4$

Comparing the result of the present measurements with existing data on absorption spectra of other palladium complexes,[2,3] it is reasonable to suppose that in the absorption spectra of the crystal the band at $\nu=60\times10^{13}$/sec. corresponds to the second band,[9] and that the flat absorption in the shorter wave-length region consists of the third[9] and SCN-specific bands.[10] The first band[9] may be so small that it is probably covered under the large second absorption band. The rule as to the dichroism of planar complexes of palladium, which was reported previously,[2] states that the second band of the ∥-absorption is hyperchromic to that of the ∥-absorption. Therefore, the absorption curve "a" of the thiocyanato-complex may reasonably be assigned to the ∥-absorption. From the absorption curves, the following conclusion may be reached for the above complex-salt; the ∥-absorption is bathochromic to the ⊥-absorption. This is the case with the "tetrahalogeno-complex type.[2]" Consequently, tetrathioacyanato-palladium (II) complex is supposed to fall into the group of the tetrahalogeno-complex type."

Potassium Tetraiodo-palladate (II).—A rather remarkable dichroism can be recognized, as shown in Fig. 2. The band at $\nu=40$

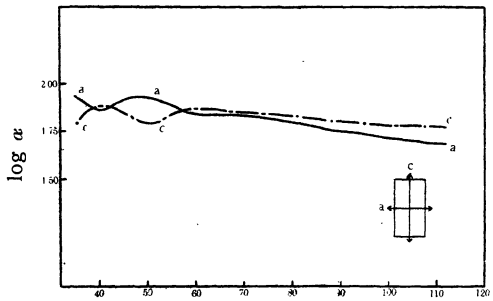

Fig 2. Absorption spectra of K_2PdI_4.

in the c-absorption is considered to be the second band, and the broad absorption extending from $\nu=60$ to shorter wave-length region is supposed to be the superposition of the third and I-specific bands. With the a-absorption, the second band lies in the near infrared region. The broad absorption curve in the visible and shorter wave-length region consists of the third and I-specific bands. It is readily seen that for the second band the following relation exists; the a-absorption is bathochromic and hyperchromic to the c-absorption. With tetrachloro-and tetrabromo-palladate (II) ions, the following rule has been established[2]: the ∥-absorption of the second

7) R. Tsuchida and M. Kobayashi, "The Colours and the Structures of Metallic Compounds," Zoshindo, Osaka, Japan, 1944, p. 180; This Bulletin, **13**, 619 (1938); *J. Chem. Soc. Japan*, **60**, 769 (1939).

8) The authors are indebted to the Analytical Laboratory of our department for the measurement of absorption spectra of $K_2Pt(SCN)_4$ with a Beckman spectrophotometer.

9) About the first, second and third absorption bands, see R. Tsuchida, This Bulletin, **13**, 388 and 436 (1938).

10) R. Tsuchida and M. Kobayashi, This Bulletin, **13**, 476 (1938).

band is bathochromic and hyperchromic to the ⊥-absorption. Since it seems reasonable to assume that the tetraiodo-palladate (II) ion shows a dichroism of the same type as those of the tetrachloro-and tetrabromo-palladate (II) ions, the following presumption may be reached that the a-absorption corresponds to the ∥-absorption and the c-absorption to the ⊥-absorption. Moreover, comparing the dichroism of potassium tetraiodo-palladate (II) with those of tetrachloro- and tetrabromo-complexes and judging from the relation between the dichroisms and the external forms with the latter two crystals, in both of which the planes of the complex ions are perpendicular to the c-axis,[3] it may be concluded that in the crystal of potassium tetraiodo-palladate (II) the complex-ions are arranged at least almost parallel to each other with their planes perpendicular to the c-axis.

Potassium Tetrathiocyanato-platinate (II). (Fig. 3.)—In the b-absorption the small inflexion at $\nu=68$ corresponds to the second band and the broad absorption stretching over the

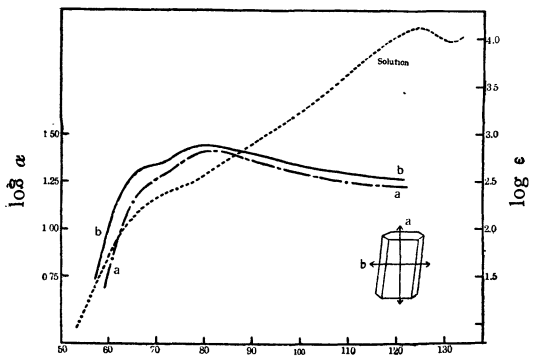

Fig. 3. Absorption spectra of $K_2Pt(SCN)_4$

shorter wave-length region consists of the third and SCN-specific bands. Similarly, in the a-absorption, the inflexion at $\nu=70$ corresponds to the second band and the broad absorption curve in the shorter wave-length region consists of the third and specific bands. The first band may be concealed under the large second band, as in the case of potassium tetrathiocyanato-palladate (II). No very great difference can be recognized between the a- and b-absorptions, but these absorptions seem to represent the characteristic feature of the dichroism of the planar tetrathiocyanato-complex. Thus for the second absorption band is found the following relation: the b-absorption is bathochromic and hyperchromic to the a-absorption.

TABLE II
ABSORPTION MAXIMA OF TETRATHIOCYANATO-COMPLEX COMPOUNDS

		ν 10^{13}/sec.	log α	ν 10^{13}/sec.	log α
$K_2Pt(SCN)_5$	∥	67	1.31	80	1.44
	⊥	71	1.25	83	1.42
$K_2Pd(SCN)_4$	∥	58	1.54	73	1.44
	⊥	62	1.14	75.8	1.48

Since the tetrathiocyanato-platinate (II) ion is reasonably supposed to belong to the group of complexes which show a dichroism of the "tetrahalogeno-complex type," as in the case of the tetrathiocyanato-palladate (II) ion, it is considered that the b- and a-absorptions are abundant, respectively, with the parallel and perpendicular components of the planar complex ion, though the a- and b-absorptions may not completely coincide with the ∥-and ⊥-absorptions.

Potassium Tetrabromo-palladate (II) Dihydrate.—The absorption curve in the region for the low value of α was determined in the present measurement (Fig. 4). A slight

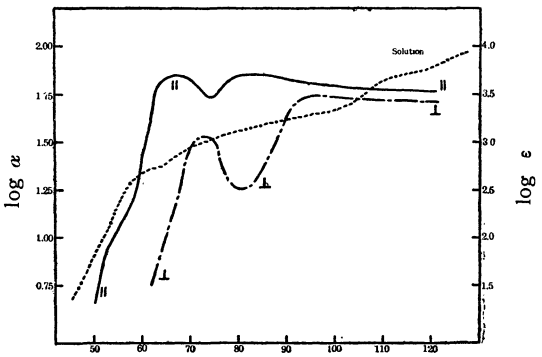

Fig. 4. Absorption spectra of $K_2PdBr_4\cdot 2H_2O$.

TABLE I
ABSORPTION BANDS OF TETRAHALOGENO-COMPLEX COMPOUNDS

Compond		1st band ν 10^{13}/sec.	1st band log α	2nd Band ν 10^{13}/sec.	2nd Band log α	3rd Band ν 10^{13}/sec.	3rd Band log α
K_2PdCl_4	∥	51	0.45	64.0	1.68	(98)	(1.54)
	⊥	51	0.45	68.9	1,49	(108)	(1.51)
$K_2PdBr_4\cdot 2H_2O$	∥	(48)	(1.0)	58.8	1.85	(75)	(1.83)
	⊥	—	—	65.0	1.52	(90)	(1.75)
K_2PdI_4	∥	—	—	—	—	48.4	1.93
	⊥	—	—	40.4	1.88	(60)	1.86
K_2PtCl_4	∥	60.6	0.9	82.6	1.50	—	—
	⊥	60.6	0.9	89.1	1.45	—	—
$K_2PtBr_4\cdot 2H_2O$	∥	54.8	1.15	74	1.48	—	—
	⊥	54.8	1.15	84	1.43	—	—

inflexion is recognized in the longer wave-length part at a low value of α and at $\nu=$ about 53. This inflexion is supposed to correspond to the first absorption band. As in the case of the tetrachloro-complex, the first absorption band is found to be much week as compared with the other bands.

Comparison of Dichroisms of Planar Tetrahalogeno-Complexes.—Numerical data of the present measurements as to the dichroisms of the tetrahalogeno-complex type are tabulated in Tables I and III along with the other available data. For the tetrahalogeno-complexes of both palladium and platinum, the following relations are found to hold for the corresponding absorption bands: (1) $\nu_{Cl} > \nu_{Br} > \nu_I$ and $k_{Cl} < k_{Br} < k_I$;[11] (2) especially for the second band, the oscillator strength increases in the order, chloride<bromide<iodide.[12]

These tendencies are in accordance with those of cobaltic and chromic complexes, and they could be explained mostly in terms of the difference between the halogen atoms in their polarizability and, therefore, in the covalent character of the metal-halogen linkage

TABLE III

SECOND ABSORPTION BANDS OF TETRAHALOGENO-COMPLEX COMPOUNDS

		ν 10^{13}/sec.	half width 10^{13}/sec.	α	k
K_2PdCl_4	∥	64	12.2	47.8	57800
	⊥	68.6	10.4	30.9	37400
$K_2PdBr_4 \cdot 2H_2O$	∥	58.8	12	70.8	
	⊥	65.0	9	33.1	
K_2PdI_4	∥	—	—	—	
	⊥	40.4	—	76	
K_2PtCl_4	∥	82.6	18	31.6	38800
	⊥	89.1	14.4	28.2	34600
$K_2PtBr_4 \cdot 2H_2O$	∥	74	—	30.2	50700
	⊥	84	—	26.9	45200

Absorption Curves of $K_2Pd(SCN)_4$ and $K_2Pt(SCN)_4$.—Absorption curves of both the compounds show similar features. It is also found from the curves that the tetrathiocyanato-complexes show their absorption bands in the longer wave-length region, as compared with complexes of the same metals with other ligands; for example, they are bathochromic to the dioxalato-complexes[13] and show absorption in the longer wave-length region, comparable even to the tetrabromo- as well as tetrachloro-complexes. A similar tendency can also be noticed between potassium hexachloroplatinate (IV) and potassium hexathiocyanato-platinate (IV),[14] the former being hopsochromic to the latter. This fact seems, at first sight, inconsistent with the spectrochemical series for cobaltic complexes. Such anomalies might be attributed to the difference in the mode of co-ordination linkage between these complexes of platinum and palladium and of cobalt, and also possibly to the difference in the atom species which is bound to the central matallic ion. It may be assumed that in cobaltic and chromic complexes the thiocyanate ions co-ordinate with the metallic ion by means of the nitrogen atoms, while in the palladium and platinum complexes they co-ordinate by the sulphur atoms, since the complex, in which a thiocyanate ion co-ordinates with the central metal by its sulphur atom and which should consequently be called thiocyanato-complex, would be bathochromic to the complex, in which a thiocyanate ion coordinates by its nitrogen atom and which should consequently be called isothiocyanato-complex.[15]

The Dichroism of the Tetrahalogeno-Complex Type.—For all the planar tetrahalogeno-and tetrathiocyanato-palladium complexes shown in the table hold the following common rules.

(1) The first band: α is much smaller than that of the second or third band. $\nu_{\parallel}$ and $\nu_{\perp}$ are not greatly different from each other.

(2) The second band: ∥-absorption is bathochromic and hyperchromic to ⊥-absorption, the oscillator strength being larger for ∥-ab-sorption than for ⊥-absorption.

(3) The third band: $\alpha_{\parallel}$ is almost equal to $\alpha_{\perp}$ ∥-absorption is bathochromic to ⊥-absorption, ν_3—ν_2 being larger for ∥-absorption than for ⊥-absorption.

For the planar platinum complexes hold similar rules to those for palladium complexes, but the former differ from the latter in the facts (1) that the second band of the ∥-absorption has almost as strong intensity as that of the ⊥-absorption, and (2) that in the ∥ absorption its third band commences in almost the same wave-length region as in the ⊥-absorption.

The fact that both ∥-and ⊥-absorptions show their first bands at almost the same wave-length suggests that the band is due to isotropic transitions. As such may be cited electronic transitions of *d*-electrons in the unsaturated shell of the central metal. The smaller value of α for the first band favours this view, suggesting that the transitions are forbidden ones. This agrees well with the idea on the origins of the bands, as advanced previously by one of the authors.[9]

The second absorption band is considered by the present authors to be originate from transitions of the electrons forming the co-ordination linkages. Therefore, in the planar

11) ν_x and k_x denotes, respectively, frequency and molecular absorption coefficient at maxima ot the absorption bands of the tetrahalogeno-complex. Although the densities of the crystals $K_2PdBr_4 \cdot 2H_2O$ and K_2PdI_4 are not available, judging from the order of their magnitude and the values of α for the compounds, it seems quite clear that the above relation should hold.

12) Judging from the magnitude of k and the shape of the absorption bands, this relation seems evident.

13) R. Tsuchida and S. Yamada, unpublished.

14) H. Kuroya, unpublished.

15) The more detailed discussion related to such discrepancies will be submitted later.

complex, the electric moment responsible for the second should be larger in the direction along the plane of the complex than in the direction perpendicular to the plane. This accords well with the above rule that the oscillator strength of the second absorption band is greater in the ∥-absorption than in the ⊥-absorption. (Table III).

Diffierences between the platinum and palladium complexes are observed with respect to the second and third bands. Thus, in the palladium complexes the second band of ∥-absorption is very hyperchromic compared to that of ⊥-absorption, whereas in the platinum complexes they have almost equal magnitudes of absorption coefficients, and the oscillator strength of ∥-absorption is not so much larger than that of ⊥-absorption in the platinum complexes as in the corresponding palladium complexes. This tendency seems related to a similar discrepancy in the birefringence between complexes of the two metals, which was observed by Mellor and Quodling,[16] who reported that planar tetraco-ordinated compounds of platinum showed smaller double refraction than the corresponding palladium compounds. A completely explanation for the above fact can not be given for the present, but this phenomenon might be ascribed principally to the difference between the two metals in their polarizing powers and also in their polarizabilities.

16) D. P. Meilor and F. M. Quodling, *J. Proc. Roy. Soc. New South Wales*, **69**, 167 (1936); ibid., **70**, 205 (1936).

Summary

(1) Dichroisms of K_2PdI_4, $K_2Pd(SCN)_4$ and $K_2Pt(SCN)_4$ have been quantitatively determined by the microscopic method, and it has been found that all of them belong to the group which exhibits the dichroism of the "tetrahalogeno-complex type."

(2) For the tetrahalogeno-complexes, the following rules have been found: $\nu_{Cl}>\nu_{Br}>\nu_I$ and $k_{Cl}<k_{Br}<k_I$ for the corresponding absorption band, and the oscillator strength of the second band is larger for ∥-absorption than for ⊥-absorption.

(3) For tetrahalogeno- and tetrathiocyanato-complexes of platinum (II) and palladium (II), common regularities have been induced on the dichroisms of the tetrahalogeno-complex type.

This work was supported in part by a grant from the Ministry of Education.

Department of Chemistry, Faculty of Science,
Osaka University, Nakanoshima,
Osaka

Studies on Unsaturated Organosilicon Compounds. I.* Syntheses of Organovinylsilanes by Wurtz-Fittig Reaction

By Motonori KANAZASHI

(Received July 2, 1953)

Vinyl silicon compounds have been prepared by the elimination of hydrogen halides from haloethylsilanes,[1,2] and by the high temperature interaction of vinyl chloride and silicon in the presence of a catalyst such as copper or tin.[2,5] Recently Wagner[6] prepared vinyltrichlorosilane from acetylene and trichlorosilane at a high temperature and under pressure with platinized asbestos as a catalyst.

In this work, vinyl chloride and organohalosilanes were allowed to react with metallic sodium (in the shape of finely divided particles) in ethyl ether, to form organovinylsilanes. Trimethylchlorosilane, dimethyldichlorosilane, triethylbromosilane, and dimethylphenylchlorosilane were used as the organohalosilane.

The infrared spectra of these vinylsilanes are given in Fig. 1. From the spectra of cyclic tri- and tetra-siloxane,[7] it was found that the characteristic absorption bands for methyl, ethyl, and phenyl linked to silicon are remarkably constant in many compounds in the wave length shorter than about 11.0μ, that is 3.38, 7.08, and 7.94 μ for the methyl group, 6.84, 7.08, 7.26, 8.05, 9.9, and 10.4 μ for

* This paper was presented in the sixth annual meeting of the Chemical Society of Japan in April, 1953, at Kyoto.

1) S. N. Uschakov and A.M. Itenberg, *J. Gen. Chem.* (*U. S.S.R.*), **7**, 2495 (1947).

2) D. T. Hurd, *J. Am. Chem. Soc.*, **67**, 1813 1945), U. S.P., 2,420,912 (1947).

3) *Brit. P.* 618,608 (1949).

4) C. D. Strother and G. H. Wagner, *U.S.P.*, 2,532,430 (1950).

5) D. T. Hurd and G. F. Roedel, *Ind. Eng. Chem.*, **40**, 2078 (1948).

6) G. H. Wagner and C. O. Strother, *Brit. P.*, 670,617 (1952).

7) C. W. Young, P. C. Servais, C. C. Currie and M. J. Hunter, *J. Am. Chem. Soc.*, **70**, 3758 (1948).

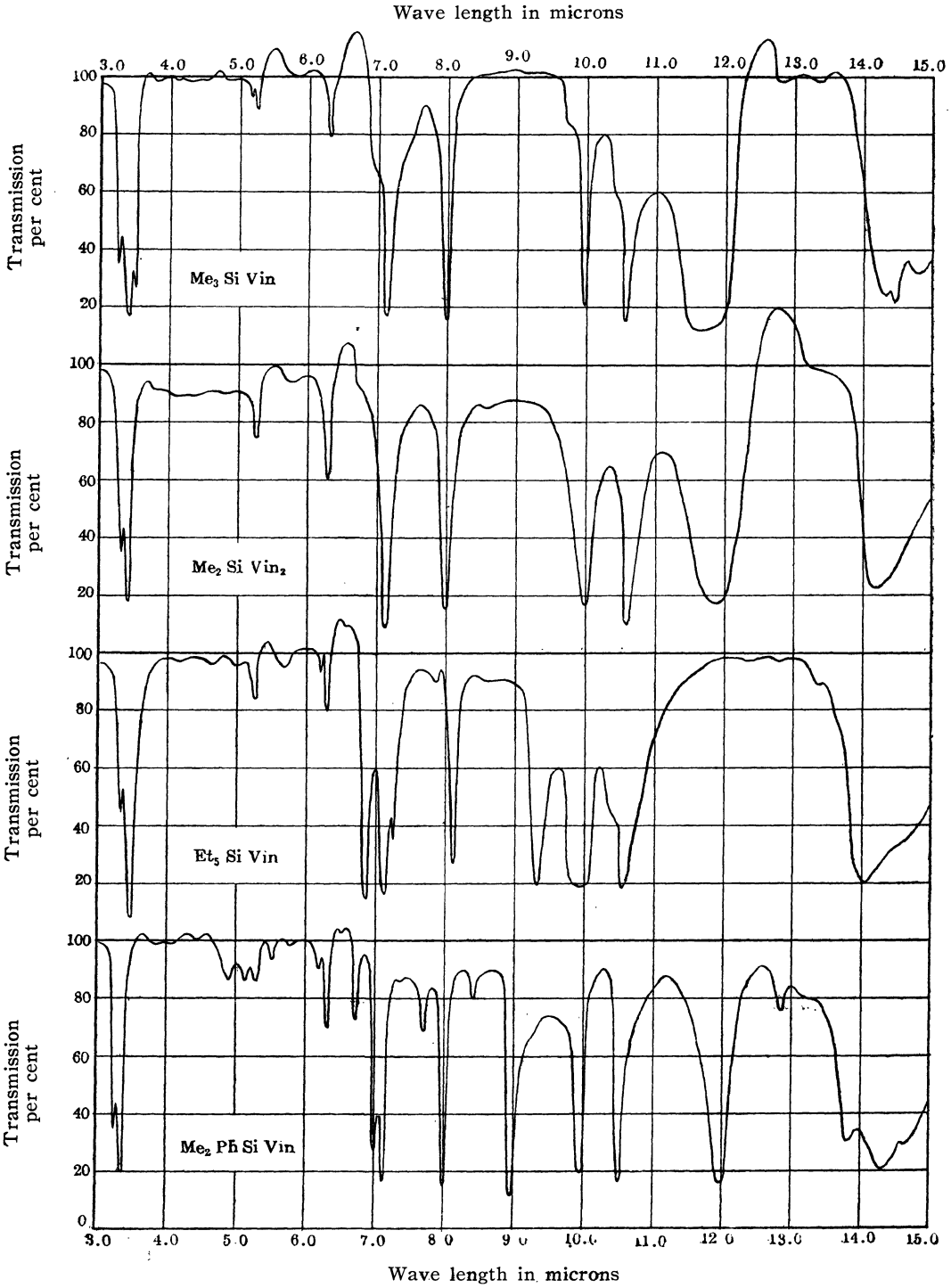

Fig. 1. The infrared spectra of organovinylsilanes

the ethyl group, and 6.28, 6.7, 6.98, 8.4, 8.9, 9.7, and 10.04 μ for the phenyl group, and allow a ready determination of the presence of these groups.

These bands are found at 3.39~3.43, 7.13~7.14, and 8.00~8.03 μ for methyl group in trimethylvinylsilane, dimethyldivinylsilane and dimethylphenylvinylsilane; 6.88, 7.12, 7.27, 8.11, 9.87 (not separated from 9.99 μ band) and 10.4 μ for ethyl group in triethylvinylsilane; and 6.21, 6.72, 7.01, 8.40, and 8.99 μ for phenyl group (9.7 and 10.04 μ bands were not found) in dimethylphenylvinylsilane.

The remaining bands common to four compounds are 5.27~5.28, 6.29~6.30. 9.94~9.99, and 10.50~10.54 μ. Of these, the bands at 6.29~6.30 and 10.50~10.54 μ were also found in vinyl siloxanediols at 6.2~6.3 and 10.3~10.4 μ and were assigned to C=C double bond and the vinyl group linked to silicon respectively, by Frisch and others.[8] The band at 5.28 μ in dimethyldivinylsilane is about twice as intense as in the other three compounds similar to the band at 6.3 μ, and it is doubtless due to the vinyl group linked to silicon. Probably the band at 9.95 μ is also believed to be assigned to the vinyl group.

Trichlorosilane was found to be added to these vinylsilanes in the presence of diacetyl peroxide like as to vinyltrichlorosilane, and the corresponding β-trichlorosilylethylsilanes were prepared.

Other reactions and properties of organovinylsilanes are under investigation in this laboratory.

Experimental

All yields reported are based on the amount of organohalosilanes or organovinylsilanes used.

Syntheses of Organovinylsilanes.

Trimethylvinylsilane I.—Ninety two grams (4.0 mole) of finely divided metallic sodium, 217 g. (2.0 mole) of trimethylchlorosilane (presented by the Shin-etsu Chem. Ind. Co.), and 250 cc. of ethyl ether were placed in a 1-l. three necked flask fitted with a mercury-sealed stirrer, a gas inlet tube and a 30 cm. Dimroth reflux condenser with a condenser sermounted with a cold finger, 4×15 cm., filled with a dry ice-aceton mixture.

Vinyl chloride gas, dried with phosphorus pentoxide, was introduced to the reaction mixture with stirring, at a rate of 10~20 l. per hour. About ten minutes after, 2 cc. of ethyl acetate was added to catalyze the reaction. When the reaction started the introduction of vinyl chloride was controlled so that a gentle reflux of ether was maintained. The reaction approached to the end in six hours then the introduction of vinyl chloride gas was stopped, and the reaction mixture was heated gently with stirring for one hour. The reaction mixture was allowed to stand overnight; then the ether layer was decanted and the residue was washed with ether and filtered. These ether solutions were mixed up and washed twice with water. After drying overnight over calcium chloride, the ether solution was fractionated through a 1-m. distillation column of about 30 theoretical plates. One hundred and fifty five grams of trimethylvinylsilane, boiling 53~56° at 767 mm. were isolated. Yield 77.5%.

The trimethylvinylsilane obtained in three runs was redistilled and the middle cut, b.p. 55.5° at 767 mm. was taken for analysis and determination of physical constants. See Table I.

Dimethyldivinylsilane II.—Ninety two grams (4 mole) of finely divided metallic sodium, 129 g. (1.0 mole) of dimethyldichlorosilane (presented by the Shin-etsu Chem. Ind. Co.), and 200 cc. of ethyl ether in a 1-l. flask reacted with vinyl chloride as indicated above, dimethyldivinylsilane were isolated, b.p., 80.8~81.6° at 760 mm., 26 g. yield 24%.

Triethylvinylsilane III.—Triethylbromosilane used in this synthesis was prepared from trichlorosilane *via* triethylsilane by the method of Whitmore and others[9] and Ladenberg,[10] and fractionated through a 30 cm. column, b.p., 78~79° at 50 mm.

Twelve grams of metallic sodium, 41 g. of triethylbromosilane and 100 cc. of ethyl ether in a 500 cc. flask reacted with vinyl chloride as outlined above, fractionation of the product through a 30 cm. column, gave triethylvinylsilane, b.p., 143.2° at 755 mm., 13.2 g., yield 45%.

8) K. C. Frisch, P. A. Goodwin and R. E. Scott, *J. Am. Chem. Soc.*, **74**, 4584 (1952).

9) F. C. Whitmore, E. W. Pietruza and L. H. Sommer, *J. Am. Chem. Soc.*, **69**, 2108 (1947).

10) Ladenberg, *Ann.*, **164**, 300 (1872).

TABLE I

THE PPOPERTIES OF ORGANOVINYLSILANES

Compound	b.p. °C	b.p. mm.	d_4^{20}	n_D^{20}	Molar ref. Calcd.	Molar ref. Obsd.	Si % Calcd.	Si % Found
I	55.5	767	0.6910	1.3914	34.44	34.50	28.02	27.8
II	80.8~81.6	760	0.7337	1.4176	38.60	38.52	25.03	24.9
III	143.2	755	0.7847	1.4330	48.33	47.47	19.60	19.6
IV	82.0	20	0.8919	1.5048	54.26	53.96	17.31	17.4

Dimethylphenylvinylsilane IV. — Dimethylphenylchlorosilane used in this synthesis was prepared from dimethyldichlorosilane and phenylmagnesium bromide in ether, and was fractionated through a 30 cm. column, b.p., 84~85° at 20 mm.

Twenty three grams (1 mole) of metallic sodium, 85 g. (0.5 mole) of dimethylphenylchlorosilane, and 100 cc. of ethyl ether in a 500 cc. flask reacted with vinyl chloride as outlined above, fractionation of the product through a 30 cm. column, gave 29.2 g. of dimethylphenylvinylsilane, b,p., 82.0° at 20 mm., yield 36%.

The physical constants and analytical data of these organovinylsilanes are given in Table I.

Addition of Trichlorosilane.

β-Trichlorosilylethyltrimethylsilane V. — A mixture of 5 g. (0.05 mole) of trimethylvinylsilane, 14 g. (0.1 mole) of trichlorosilane, and 0.25 g. (0.002 mole) of diacetyl peroxide (2.0 mole % to trichlorosilane used) in a glass sealed tube was heated for ten hours at 60° in a water bath. Then distilled in a 20 cc. Claisen flask, the excess trichlorosilane was recovered at atmospheric pressure and 10.5 g. of β-trichlorosilylethyltrimethylsilane, b.p., 94~96° at 50 mm. and 1 g. of residue was obtaind, yield 90%.

Bis(β-trichlorosilylethyl)dimethylsilane VI. —Heating a mixture of 3.5 g. (0.03 mole) of dimethyldivinylsilane, 13.6 g. (0.1 mole) of trichlorosilane, and 0.2 g of diacetyl peroxide for eleven hours in a sealed glass tube at 60°, gave 8.5 g. of bis(β-trichlorosilylethyl)dimethylsilane, b.p., 119~121° at 3 mm., yield 72%.

β-Trichlorosilylethyltriethylsilane VII.— Heating a mixture of 7.1 g. (0.05 mole) of triethylvinylsilane, 13.6 g. of trichlorosilane, and 0.2 g. of diacetyl peroxide for eight hours in a sealed glass tube at 60°, gave 6 g. of β-trichlorosilylethyltriethylsilane, b.p., 122~125° at 18 mm., yield 42%.

TABLE II

THE PROPERTIES OF β-TRICHLOROSILYLETHYLSILANES

Compound	f.p. °C	b.p. °C	b.p. mm.	d_4^{20}	n_D^{20}	Molar ref. Calcd.	Molar ref. Obsd.	Cl % Calcd.	Cl % Found
V	−18	94~96	50	1.1062	1.4473	57.32	56.96	45.13	45.0
VI	−4	119~121	3	1.2966	1.4838	84.36	84.52	55.52	55.4
VII		122~125	18	1.0713	1.4632	71.21	71.44	38.29	38.3
VIII		138~139	10	1.1553	1.5112	77.14	77.24	35.72	35.5

β-Trichlorosilylethyldimethylphenylsilane VIII.—Heating a mixture of 8.1 g. (0.05 mole) of dimethylphenylvinylsilane, 13.6 g. of trichlorosilane, and 0.2 g. of diacetyl peroxide for sixteen hours in a sealed glass tube at 60°, gave 3.5 g. of β-trichlorosilylethyldimethylphenylsilane, b.p., 138~139° at 10 mm., yield 24%.

The physical constants and analytical data of these β-trichlorosilyethylsilanes are given in Table 2.

Preparation of Spectra—The infrared spectra shown here were obtained using a Perkin-Elmer Model 12-C Spectrometer (rock salt prism) of Government Chemical Industrial Research Institute, Tokyo. All samples were run in potassium bromide cell, 0.1 mm. thick, as pure liquid.

Summary

1) Vinyl chloride and organohalosilanes were shown to react with finely divided metallic sodium in ethyl ether, and trimethyl-, dimethyldi-, triethyl- and dimethylphenyl-vinylsilanes were prepared. Of these, dimethyldi- and dimethylphenyl-vinylsilane are new compounds and their physical constants were given.

2) Infrared spectra of these four organovinylsilanes were obtained and certain characteristic absorption bands were discussed.

3) Trichlorosilane was found to add to these vinylsilanes at the presence of diacetyl peroxide and four new β-trichlorosilylethylsilanes were prepared and characterized.

The author is indebted to Mr. M. Yonemoto and Mr. S. Saeki for the spectra reported in this paper and the Shin-etsu Chem. Ind. Co. for the methylchlorosilanes used in this investigation. The author is also grateful to Dr. O. Shimamura and Dr. T. Yamada for much helpful advice in this investigation.

Electrotechnical Laboratory
Agency of Industrial Science
and Technology, Tokyo

Sterols and Other Unsaponifiable Substances in the Lipids of Shell Fishes, Crustacea and Echinoderms. XII. Occurrence of Δ^7-Cholestenol as a Major Component of the Sterol Mixture of Chiton

By Yoshiyuki TOYAMA and Tatsuo TANAKA

(Received July 11, 1953)

The first report[1] of this series recorded the results of a brief examination of the sterol mixture of chiton, *Liolophura japonica*, and several other aquatic invertebrates. In those experiments, the sterol mixture of the fatty substances extracted with ether from the chitons, caught around Sugashima Island, Mie Prefecture, and also the acetate of sterol mixture were subjected to several recrystallizations. The highest melting points of recrystallized products were 119~121°C. for the free sterol and 125~127°C. for the acetate, though neither melting points were yet constant.

In the present experiments, the chitons caught around Osaki-Shimojima Island in the Inland Sea of Seto were extracted with ether, the ether-extract was freed from the acetone-insoluble portion, and the unsaponifiable matter was separated from the acetone-soluble portion. The crystalline fraction of the unsaponifiable matter, consisting of crude sterols, was acetylated, and the acetate obtained was recrystallized from ethanol. Unlike the results described in the previous report, the acetate showed, after 4 recrystallizations, a constant melting point of 118~119°C. which was unaltered by further recrystallizations. The free sterol obtained by saponification of the acetate showed also a constant melting point of 122~122.5°C. Both free sterol and acetate were optically inactive, and a spectrophotometric examination indicated the absence of conjugated diene. They reacted very rapidly with the Liebermann-Burchard reagent and developed a blue-green color almost immediately. The acetate had a saponification value and a degree of unsaturation, determined by perbenzoic acid titration, both of which agreed closely with the calculated values for a C_{27}-stenol. These facts seem to suggest that the sterol obtained above is Δ^7-cholestenol (γ-cholestenol). In order to gain a further confirmation, the isomerization of Δ^7-cholestenol (γ-cholestenol)$\rightarrow\Delta^{8(14)}$-isomer ($\alpha$-cholestenol)$\rightarrow\Delta^{14}$-isomer ($\beta$-cholestenol) and the hydrogenation of the last named isomer to cholestanol were performed. As shown in

TABLE I

	Free sterol		Acetate		Benzoate	
	m.p., °C	$[\alpha]_D^{\circ}$	m.p., °C	$[\alpha]_D^{\circ}$	m.p., °C	$[\alpha]_D^{\circ}$
Δ^7-Cholestenol	122~122.5	0	118~119	0	158~159; 177	+6.9
„ [2]	122~123	0	118~119	0	157~158; 176	+7.14
„ [3]	125~126	+5.7	118~119	+1.5	—	—
„ [4]	122	+5.65	118	—	153~154	—
$\Delta^{8(14)}$-Cholestenol	118~120	—	77~78	+9.5	115~117; 144	—
„ [2]	119~120	+20.36	77~78	+9.46	115; 140	+8.53
Δ^{14}-Cholestenol	130~131	—	90~91	—	168~169	+31.5
„ [2]	130~131	+34	91~92	—	168	+32.54
„ [5]	131~133	+30	90~92	+22.8	172~174	+31
Cholestanol	—	—	104~105	+14.2	—	—
„ [6]	—	—	109~110	+11.5	—	—

1) Y. Toyama and F. Shibano, *J. Chem. Soc. Japan*, **64**, 323 (1943).
2) Fr. Schenck, K. Buchholz and O. Wiese, *Ber.*, **69**, 2696 (1936).
3) L. F. Fieser, *J. Am. Chem. Soc.*, **73**, 5007 (1951).
4) D. R. Idler and C. A. Baumann, *J. Biol. Chem.*, **195**, 623 (1952).
5) H. Wieland, F. Rath and W. Benend, *Ann.*, **548**, 19 (1941).
6) B. Heath-Brown, I. M. Heilbron and H. R. H. Jones, *J. Chem. Soc.*, **1940**, 1482.

Table 1, the respective products obtained in these experiments showed the same melting points and specific rotations as those recorded previously for the corresponding compounds, excepting that the hydrogenation product had a little lower melting point and higher specific rotation than cholestanol, possibly due to the contamination of unaltered Δ^{14}-cholestenol.

From sterol-free conponents of unsaponifiable matter, a small amount of saturated alcohols, possibly chimyl and batyl alcohols, was separated.

Δ^{7}-Cholestenol had been known as the reduction product of 7-dehydrocholesterol, but its occurrence among natural sterols was not known until quite recently. In 1951 Fieser[7] found this sterol, named lathosterol by him, as a companion sterol in various samples of crude cholesterol. Also Idler and Baumann[8] found a relatively large amount of this sterol in skin sterols of an albino rat, but the isolation of this sterol from skin sterols was attained by chromatography of the azoyl ester of sterol mixture, while repeated recrystallizations of the acetate of the sterol mixture were not efficient to concentrate this sterol. In contrast to these findings, it may be noted that only several recrystallizations of the acetate of sterol mixture of the chitons were sufficient to yield a pure Δ^{7}-cholestenol in the present experiments.

Since the acetate of sterol mixture of the chitons caught around Sugashima Island, as described in the previous report, did not yield an acetate of constant melting point, the authors have procured another lot of chitons caught at the same locality, and re-examined the sterol mixture from this lot of chitons. On repeatedly recrystallizing the acetate of sterol mixture, the melting point of the acetate became higher than that of Δ^{7}-cholestenyl acetate, as was the case with the previous experiments. The sterol mixture showed no ultraviolet absorption maximum, but it was positive for the Tortelli-Jaffé test, and formed a blue-green color very rapidly in the Liebermann-Burchard reaction. These facts seem to permit a presumption that the sterol mixture of the chitons caught around Sugashima Island contains Δ^{7}-cholestenol together with other sterol, and that the acetate of additional sterol is less soluble in ethanol and has a higher melting point than the acetate of Δ^{7}-cholestenol, so that repeated recrystallizations of the acetate mixture result in the concentration of the acetate of additional sterols with a higher melting point. Whether such a striking difference between the chitons from Sugashima Island and from Osaki-Shimojima Island in the content of Δ^{7}-cholestenol is a general case caused by the variation in the catching locality or a special case caused by some other factors, remains unknown.

7) l. c., (3).
8) l. c., (4).

Experimental

The chitons used in these experiments were caught around Osaki-Shimojima Island in the Inland Sea of Seto in August, 1952. Air dried chitons (4.98 kg.) were cracked to small pieces and lipid was extracted with ether, yielding 1.05% of lipid which was a dark reddish orange viscous liquid. The lipid (52.0 g.) was refluxed with 450 cc. of acetone, and the mixture was cooled and filtered, by which 42.0 g. of acetone-solubble oil with the following constants was obtained: d_4^{20} 0.9332, n_D^{20} 1.4784, acid value 110.2, saponification value 184.4, iodine value (pyridine sulfate dibromide method) 138.6, unsaponifiable matter 18.77%.

Unsaponifiable Matter—The acetone-soluble oil (36.8 g.) was saponified, and unsaponifiable matter was extracted with ether from the diluted soap solution. The unsaponifiable matter (7.2 g.) was an orange-yellow solid, and melted at 48~50°C. to a turbid liquid and at 92°C. to a clear liquid. The sterol content in the unsaponifiable matter was found to be 44.86% by the digitonide method. Recrystallization of the unsaponifiable matter from 250 cc. of methanol gave a crude sterol mixture (3.2 g.) of m.p. 113~118°C. It showed no characteristic absorption maximum in the region of 230~310 mμ. The acetate (3.1 g.), m.p. 112.5~114.5°C., prepared by refluxing the crude sterol mixture with acetic anhydride for one hour, was recrystallized from ethanol. After 4 recrystallizations, the melting point was raised to 118~119°C., which was unaltered by further recrystallizations from acetone and ether-acetone (1:2). The total yield of the acetate of m.p. 118~119°C. was 1.34 g. Further 0.94 g. of the acetate melting somewhat less sharply at 115~118.5°C. was separated from the mother liquor of recrystallizations. The remainder of the acetate recovered from the mother liquor showed a lower melting point.

The methanol filtrate from the initial recrystallization of the unsaponifiable matter was concentrated, and a solid deposit (0.67 g.) of m.p. 53~56°C. was separated and recrystallized from acetone, by which a crystalline solid (0.44 g.) of m.p. 61~63°C. was obtained. Since this solid was still contaminated with a minute amount of sterol, the latter was removed by digitonin. The sterol-free solid, after recrystallization from acetone, had m.p. 62.5~63.5°C., iodine value 0.8 and acetyl value 263.2 (calculated for chimyl alcohol 280.1; for batyl alcohol 261.8).

Acetate of m.p. 118~119°C.—This acetate showed saponification value 130.7 (calculated for $C_{29}H_{48}O_2$ 130.8) and number of ethylenic bond, determined by perbenzoic acid titration, 1.05.* It showed a positive Tortelli-Jaffé reaction, and developed a blue-green color very rapidly in the Liebermann-Burchard reaction. Free sterol obtained by saponification of the acetate showed, after recrystallization from ethanol, m.p. 122~122.5°C. and $[\alpha]_D^{12}=0$ (in chloroform). Benzoate was prepared by allowing free sterol to react with benzoyl chloride in pyridine; m.p. 158—159°C. (turbid), 176~177°C. (clear), $[\alpha]_D^{22}=+6.9°$.

$\Delta^{8(14)}$-Cholestenol—The acetate (0.65 g.) described above was dissolved in 30 cc. of acetic acid to which was added platinum black previously saturated with hydrogen. The solution was agitated in an atmosphere of hydrogen. No hydrogen absorption occured. After 3 hours, the solution was poured into 500 cc. of water, and was extracted with ether. The ether-extract, recrystallized from ethanol, gave $\Delta^{8(14)}$-cholestenyl acetate in lustrous leaflets; yield 0.56 g., m.p. 77~78°C., $[\alpha]_D^{10}=+9.5°$. Free stenol, after recrystallization from ethanol, melted at 118.5~119.5°C., and was positive for the Tortelli-Jaffé reaction. Benzoate prepared from free stenol had m.p. 115~117°C. (turbid) and 144°C. (clear).

Δ^{14}-Cholestenol — $\Delta^{8(14)}$-Cholestenyl benzoate (0.21 g.) was dissolved in 8 cc. of anhydrous chloroform, and dry hydrogen chloride was passed into the solution under cooling with ice for 2.5 hours. The solution was then washed successively with sodium bicarbonate solution and water, dried over anhydrous sodium sulfate, and the chloroform was distilled off. The residue contained no chlorine, and recrystallized from ethanol in lustrous needles; yield 0.13 g., m.p. 168~169°C., $[\alpha]_D^{22}=+31.5°$. Free stenol was obtained by saponification of the benzoate, and recrystallized from ethanol in fine needles; m.p. 130~131°C. Acetate was prepared from free stenol and recrystallized from acetone-ethanol (2:1) in fine needles; m.p. 89.5~91°C. It was negative for the Tortelli-Jaffé reaction.

Cholestanyl Acetate—Δ^{14}-Cholestenyl acetate (0.03 g.) was dissolved in 10 cc. of ether-acetic acid (1:1), and hydrogenated in the presence of platinum black as catalyst by stirring the solution in an atomosphere of hydrogen for 4 hours at room temperature. The hydrogenation product was extracted with ether from the solution diluted with water. After recrystallization from ethanol, it formed fine needles; yield 0.02 g., m.p. 104~105°C., $[\alpha]_D^{22}=+14.2°$. The final product still showed a violet color in the Liebermann-Burchard reaction.

Sterol Mixture of Chitons from Sugashima Island—Air dried material of the chitons (400 g.)* caught around Sugashima Island, Mie Prefecture, in April, 1953, yielded 7.9 g. of lipid by ether extraction, from which acetone-soluble oil was obtained in a yield of 86%; d_4^{20} 0.9356, n_D^{20} 1.4792, acid value 112.5, saponification value 185.6, iodine value 131.2, unsaponifiable matter 11.43%. Crude sterol mixture was separated by recrystallizing the unsaponifiable matter from methanol, and its acetate was repeatedly recrystallized from ethanol. The melting points of recrystallized products were121~123°C., 123.5~125.5°C. and 127~129°C., respectively, after 3, 4 and 6 recrystallizations. The final product showed a positive Tortelli-Jaffé reaction, and reacted very fast with the Liebermann-Burchard reagent. It showed no characteristic absorption maximum in the region of 230~310 mμ. The product after 3 and 4 recrystallizations showed $[\alpha]_D^{26}=+3.9°$ and $+6.5°$, respectively.

Summary

Sterol mixture of the chitons caught around Osaki-Shimojima Island in the Inland Sea of Seto contains predominantly Δ^7-cholestenol, the acetate of which is easily obtainable in a pure state by several recrystallizations of the acetate of sterol mixture. From sterol-free components of unsaponifiable matter, a saturated fraction, possibly consisting of chimyl and batyl alcohols, was separated.

The acetate of sterol mixture of another lot of chitons caught around Sugashima Island, Mie Prefecture, shows a higher melting point than Δ^7-cholestenyl acetate after several recrystallizations, as was the case with the chitons caught in the same locality which were described in the first report of this series.

Department of Applied Chemistry,
Faculty of Engineering,
Nagoya University, Nagoya

* The iodine value by the pyridine sulfate dibromide method showed an enormously high value of 232.4 against the calculated value 59.2.

* Supplied through the courtesy of Dr. E. Nakano, Biology Department, Faculty of Science, Nagoya University.

Rheology of Surface Films. I. Rheological Characteristics of Monomolecular Films of Ovalbumin and Serum Albumin*

By Kiyoshi INOKUCHI

(Received July 21, 1953)

Introduction

Recent interest in the study of surface films has been focused upon the problems of high molecular substances, such as proteins or synthetic high polymers. Since the most prominent characteristics of high polymers is their forming of viscoelastic films, excellent means for measuring the mechanical properties of surface films are now greatly needed. Although classical measurements of surface viscosity, based on the canal method[1-3] or damped oscillation method,[4-8] have shown considerable merits in the film studies of simple molecules, they were not so informative when applied to the viscoelastic films of high polymers. In view of the recent development of modern rheology with three-dimensional materials, the application of the method and concept of modern rheology to the two-dimensional systems would shed new light on the field of physical chemistry of surfaces. The aim of this series of works is to provide a set of standards of surface rheology and to achieve the analyses of mechanical properties of protein or synthetic polymer films from the modern rheological standpoint.

At the beginning of this work, the first attempt was started with protein monolayers at the air-water interface. At the present stage, it appeared necessary to make a careful preliminary study with some well-defined proteins. For this purpose, crystalline ovalbumin and serum albumin were mainly used. The present paper describes the mechanical characteristics of these protein films obtained by the method based on the analyses of deformation-time relation of the film subjected to shearing stress.

Experimental

Procedures—A static mothod was employed in this preliminary study. The apparatus is principally the same as used by Schwedoff and Hatschek[9] with three-dimensional gel. The illustration is given in Fig. 1. (A) is a platinum ring of

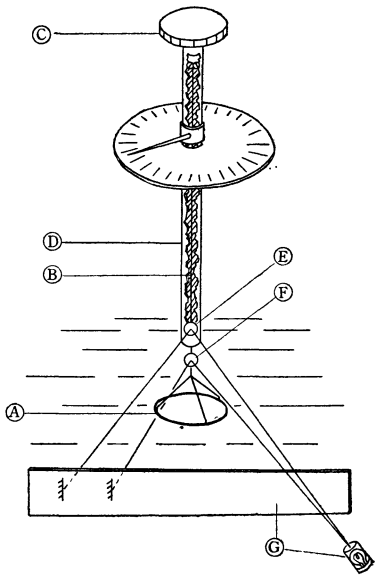

Fig. 1.—Diagrammatic illustration of the apparatus for measuring viscoelasticity of films

3.7 cm. in diameter. The suspending wire is enclosed by a protector (D) which is coaxial with the torsion head (C). The rotational angle of the torsion head and the deflection of the ring are measured by means of the mirrors (E) and (F) respectively, with lamp and scale (G). Care was taken that the experimental condition might not destroy the fine structure of films. For this purpose, both the moment of intertia of the ring

* Partly presented at the Annual Meeting of the Chemical Society of Japan, April, 1952.

1) M. Joly, *J. de phys.* **11**, 471 (1937), *Kolloid-Z*, **89**, 26 (1939).

2) E. R. Washburn and H.R.R. Wakeham, *J. Am. Chem. Soc.*, **60**, 1294 (1938).

3) R. J. Meyers and W. D. Harkins, *J. chem. phys.*, **5**, 601 (1937).

4) L. Fourt and W. D. Harkins, *J. Phys. Chem.*, **42**, 897 (1938).

5) I. Langmuir, and V. J. Schaefer, *J. Am. Chem. Soc.*, **52**, 2400 (1937).

6) L. Fourt, *J. Phys. Chem.*, **43**, 887 (1939).

7) M. Joly, "Surface Chemistry" (Supplement of Research) 157 (1949).

8) C. W. N. Gumper and A. E. Alexander, *Trans. Faraday Soc.*, **46**, 235 (1950).

9) V. E. Hatschek and R. S. Jane, *Kolloid-Z.*, **39**, 300 (1926).

and the torsion constant of a suspending wire which were chosen were sufficiently small. That is, a series of phosphor bronze wire of 25μ to 60μ in diameter and 30 cm. in length and the rotating system of moment of inertia of 0.8 g. cm^2 were used. Order of shearing stress ranged from 10^{-3} to 10^{-1} dyne per cm. The trough was 14.7 cm. wide and 60 cm. long. Wilhelmy dipping slide was applied to the one side of the trough to furnish the surface pressure-area curve (designated as F-A curve hereafter). The sensitivity of the balance was about 0.01 dyne per cm. To obtain maximum symmetry, the ring was suspended 7.3 cm. in front of the dipping slide. After the quick turn of the torsion head by a definite angle φ (less than 10 degrees), the deflection of the hanging ring ω during relaxation was measured with time t. As the surface film was distorted with the ring, ω was considered to be a strain of the film materials. When the ring was applied to a clean surface of water, the contribution of moment of intertia of the rotating system was found to be not small enough to be ignored. However, once the surface was covered by a certain amount of monolayer substance, the contribution of moment of inertia became negligible due to the increased film resistance against the motion of the ring. Under such conditions, if the film exhibits Newtonian flow, the rate of strain is given by the equation,

$$\dot{\omega} = -\frac{K}{R}(\varphi - \omega) \qquad (1)$$

In case of ideal elastic films, where only the instantaneous elastic deformation occurs, the following equation holds:

$$\omega = \frac{K}{E}(\varphi - \omega) \qquad (2)$$

In above equations, K is the torsion constant of the suspending wire, R and E, the constants related to the surface viscosity coefficient η and surface shear modulus G expressed by the following formulas, (3) and (4), respectively

$$\eta = \frac{k}{4\pi}\left(\frac{1}{r_1^2} - \frac{1}{r_2^2}\right)\left(\frac{\varphi - \omega}{\dot{\omega}}\right) \qquad (3)$$

$$G = \frac{k}{4\pi}\left(\frac{1}{r_1^2} - \frac{1}{r_2^2}\right)\left(\frac{\varphi - \omega}{\omega}\right) \qquad (4)$$

where r_1 and r_2 are the radii of the ring, and of the circular films coaxial with the ring, respectively. In the present apparatus, r_2 may be assumed to be 7.3 cm., effective radius of the trough, which is sufficiently large compared with r_1. If the film under test is perfectly elastic, the film inside the ring would not affect the motion of the ring. Therefore, so far the instaneous elasticity is concerned, the shear modulus was calculated ignoring the film formed inside the ring. This assumption was checked to be valid within the experimental error*.

As will be described later, the mechanical properties of real films were generally neither a purely viscous, nor a purely elastic, but a more complicated one, superposed by both viscositly and elasticity. The deformation-time curve of such films were found to be quite similar to that of three-dimensional materials stressed, so that the mechanical properties of films would be analyzed by the usual method in rheology[10].

Materials—Ovalbumin was prepared from a fresh hen eggs by the sodium sulfate method and successive crystalization according to Kekwick[11]. Horse serum albumin was a crystalline product prepared by the sodium sulfate method[12] and horse hemoglobin by the alcohol method.

Results

ω-t Curve of Ovalbumin Film—When the ovalbumin aqueous solution was spread on 0.1 N hydrochloric acid solution, or on 5% ammonium sulfate solution, the following ω-t curve was observed (Fig 2). When the shearing stress was imposed, an instantaneous deformation (a-b) occurred, which follows time-dependent deformation (creep, b-c-d). At a later time, if the stress was removed, the instantaneous recovery of the first deformation occurred (d-e), preceding the time-dependent recovery of the creep (e-f). Complete recovery of the overall deformation, on the removal of the stress, was not generally observed, except the case under sufficiently

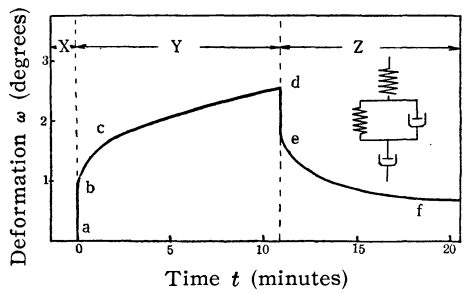

Fig. 2.—An example of ω-t curve for ovalbumin film on 0.1 N hydrochloric acid together with the illustration of the corresponding mechanical model. Range of (X) represents the dead time, (Y), the time in which the stress was imposed, and (Z), the time, the stress was removed.

* The ring, coated with paraffin, was applied to the elastic films of ovalbumin, and the shear modulus of instantaneous elasticity was obtained by equation (4). Next, after the film inside the ring was removed by being absorbed with filter paper, the same measurement was made again. Both results obtained were found to coincide each other within the experimental error.

10) T. Alfrey, "Mechanical Behaviors of High Polymers," Interscience Publishers (1948).

11) R. A. Kekwick and R. K. Cannon, *Biochem. J.*, **30**, 227 (1936).

12) R. A. Kekwick, *Biochem. J.*, **32**, 552 (1938).

small stress. Such mechanical behaviors may be approximately represented by the mechanical model of four elements with spring (elasticity) and dash pot (viscosity) as illustrated in Fig. 2. Such behavior was in common covering nearly the whole range of film areas. The instantaneous elasticity is the most definable in mechanical terms, since it mainly involves biased strain, and not any flow. So, with ovalbumin films, the main attention was directed toward the instantaneous elasticity of the film.

Relation between Stress and Instantaneous Elasticity—At a definite area, the stress-strain relation was obtained. As shown in Fig. 3, the strain was found to be proportional to the stress imposed. Such linearity holds covering almost the whole range of film areas. This means that the instantaneous elasticity obeys Hooke's law. When the shear

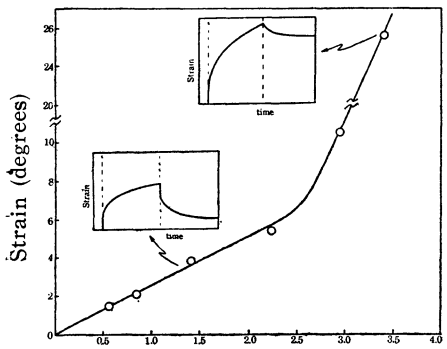

Fig. 3.—Stress-strain curve for ovalbumin films on 5% ammonium sulfate solution at 9.5 sq. m. per mg. Temperature, 10°C. Insets give the ω-t curves under the stress indicated by arrows.

stress was over a certain limit, however, the stress-strain curve became bent with the convex curvature against the stress axis. Further increase in the stress rendered the instantaneous elastic deformation obscure, causing the destruction of film structure (inset of Fig. 3). When the structure was once destroyed, reformation of the film took an appreciable time. In other words, ovalbumin film shows two-dimensional "thixotropy".

Relation between Instantaneous Elasticity and Film Area—In a sufficiently large area, ovalbumin film did not show any perceptible resistance against the motion of the ring. As the area was reduced, at a definite area, the ring suddenly received an appreciable resistance. In the case, the ω-t curve was not typical as shown in Fig. 2 and instantaneous elastic deformation was obscure. If the film was compressed a little more, however, the ω-t curve converted to give a typical instantaneous elastic response as shown in Fig. 2.

Shear modulus of instantaneous elasticity is obtained from the equation (4) at various areas, and the modulus vs. area curve (designated as G-A curve hereafter) was obtained. A typical example of the G-A curve is given in Fig. 4. The aqueous solution of 0.08 mg. per cc. was spread on 0.1 N hydrochloric acid at the initial spreading concentration of 0.2 mg. per sq. m. Twenty minutes were allowed to insure complete spreading.

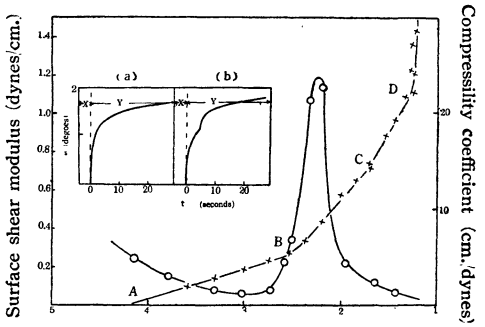

Fig. 4.—Surface shear modulus-area curve (crosses) and compressibility-area curve (circles) of ovalbumin film on 0.1 N hydrochloric acid, at 21°C. Insets give the ω-t curves. The region of (X) represents the dead time, and (Y), the time the stress is imposed.

The stepwise compression was extended to about 2 hours. Compressibility*-area curve, obtained from the F-A curve, was depicted in the same figure. It was found that the G-A curve starts at about 5 sq. m. per mg. (point A) and surface modulus increased

TABLE I

FLUCTUATION OF BOTH VALUES OF CRITICAL AREA (A) AND CRITICAL SHEAR MODULUS (G) AT BREAKS (A, B, C, D) OF SHEAR MODULUS-AREA CURVE OF OVALBUMIN FILMS ON 0.1 N HYDROCHLORIC ACID, AT 14–15°C.

	A	B	C	D
a (m^2/mg)	5.3	2.25	1.65	1.30
g ($dynes/cm$)		0.20	0.35	0.81
a (m^2/mg)	4.8	2.15	1.65	1.35
g ($dynes/cm$)		0.35	0.57	0.86
a (m^2/mg)	5.3	2.10	1.55	1.35
g ($dynes/cm$)		0.45	0.75	1.15
a (m^2/mg)	5.3	2.55		
g ($dynes/cm$)		0.37		

* Surface compressibility is defined as $-1/A(dA/dF)$, where F is the surface pressure in dynes per cm. and A, the film area in sq. m. per mg.

linearly with the decrease of the surface area, exhibiting several breaks at about 2.3 sq. m. per mg. (point B), 1.7 sq. m. per mg. (point C) and 1.3 sq. m. per mg. (point D). The extent of fluctuation of values of these breaks, obtained under the same condition, was shown in Table I. Although absolute values of shear modulus corresponding to the breaks were more or less scattered, the areas of breaking points were considerably reproducible.

It is to be noted that the minimum point of the compressibility curve appeared around the area corresponding to the breaks (point B) of the G-A curve. In addition, the particular state of the film phase in B-C range was also found from the corresponding ω-t curve. In A-B range, the ω-t curve was of such a type as in the inset (a) of Fig. 4, whereas it was converted into the type as (b) when the film was compressed to B-C range. Further compression down to C-D range made the ω-t curve into the same type as that in A-B range. From these facts it is strongly suggested that compression of the film exercises several steps of transformation of film phase which involves different modes of packing of film molecules.

In higher pressure region, the G-A curve was also obtained together with the compressibility-area curve (Fig, 5). Here, the shear modulus was found to increase steeply around the area of minimum compressibility. The type of the ω-t curve was almost similar to that of the low pressure region.

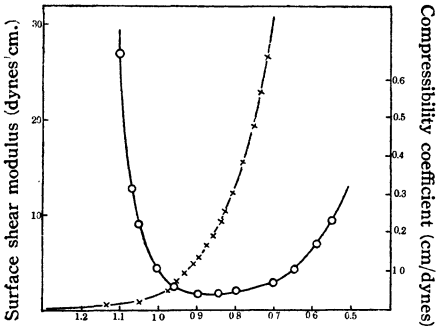

Fig. 5.—Surface shear modulus-area curve (crosses) and compressibility-area curve (circles) of ovalbumin film in high pressure region. Substrate solution, 0.1 N hydrochloric acid, and temperature, 13–14°C.

Effect of Various Experimental Conditions.—It was found that the ovalbumin film on 0.1 N hydrochloric acid, at elevated room temperature, did not exhibit an instantaneous elasticity until it was compressed down to the area of 1.7 sq.m. per mg. That is, elastic ovalbumin films at large areas underwent "melting" above certain temperature around 20°C. The film, once it was formed, showed reversible sol-gel transformation with "melting" range within 1°C, when the surface temperature was raised or lowered repeatedly by the intermittent exposure of infra-red lamp. If the film was newly formed under the same condition, however, the observed transition temperature was scattered considerably. The extent of the fluctuation was about ± 3°C. This may be due to some uncontrollable factors of the experimental conditions.

The films, when they were spread on 5% ammonium sulfate solution at pH 5.5, showed the instantaneous elasticity at the area above 15 sq.m. per mg., about three times as much area as on 0.1 N hydrochloric acid. In this case, "melting" of the film could not be observed at room temperature.

When the spreading solution of ovalbumin containing 10% formaldehyde was applied on 5% ammonium sulfate solution, at any temperature, only simple retarded elastic response was exhibited, without any instantaneous one. Although the reactions between formaldehyde and protein are complicated, in view of the fact that the amino or imino groups of protein molecules take a great part in this reaction, it seems probable that these groups are responsible for the instantaneous elasticity of the film.

Horse Serum Albumin and Hemoglobin—The proteins were spread under the same conditions with ovalbumin, but the mechanical behavior was found to be strikingly different from the case of ovalbumin. It was found that serum albumin did not exhibit any perceptible resistance against the motion of the ring, until the film was compressed to a considerably reduced area at the temperature from 5°C to 23°C. Below 1.0 sq. m. per mg., the film showed appreciable viscosity whose values increased gradually with the decrease of area, showing Newtonian flow (crosses in Fig. 6). Below 0.8 sq. m. per mg., the retarded elasticity appeared, which follows a simple viscous flow, but no sign of instantaneous elasticity was perceptible (inset of Fig. 6). This rheological behavior was referred to the compressibility-area relation obtained from the F-A curve. The compressibility curve is shown in Fig. 6 together with the illustration of the rheological behavior. It is noted that the minimum point of the compressibility curve just corresponds to the largest area

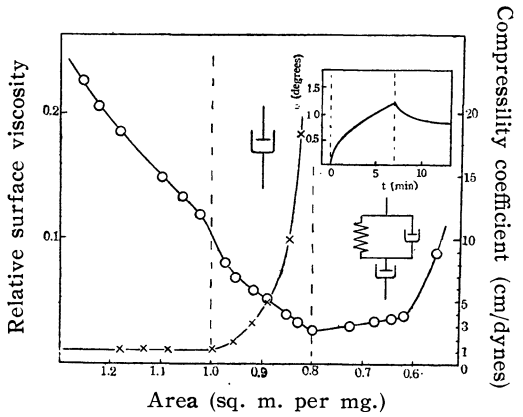

Fig. 6.—Compressibility-area curve (circles) and surface viscosity-area curve (crosses) for serum albumin film, together with the illustration of mechanical model corresponding to the film states. Relative surface viscosity is defined as the ratio of surface viscosity of the film to that of clean water. Temperature, 16°C. Inset gives the ω-t curve at the area of 0.78 sq. m. per mg. The region of (X) represents dead time, (Y), the time, stress is imposed, and (Z), the time, stress is removed.

where the film exhibited the retarded elasticity under stress, and the kink point of the compressibility at the area of 1.0 sq. m. per mg., is consistent with the largest area where the ring caught appreciable viscosity of surface film. Even though the film was extremely compressed below 0.3 sq. m. per mg., it failed to show instantaneous elasticity, exhibiting only the flow accompanied by the retarded elasticity.

Sasaki and Kimizuka[13] reported that an adsorbed layer of serum albumin aqueous solution exhibited an instantaneous elasticity, and the present author also observed this phenomenon with the solution of 10 to 50mg. per 100 cc. containing 0.1 N hydrochloric acid. It is noteworthy that the adsorbed layer exhibits an instantaneous elasticity, whereas the monolayer, as well as the polylayer made from the compression of a monolayer, fails to show any sign of instantaneous elasticity. Concerning the structural difference between a monolayer and an adsorbed layer, no work has been done, waiting for further research. Our rheological method of approach will also be promising for the solution of this problem.

The rheological behavior of horse hemoglobin was nearly similar to that of serum albumin. When hemoglobin was spread on 0.1 N hydrochloric acid solution at 14°C, it showed no elasticity at large areas, while below about 0.85 sq. m. per mg. the retarded elasticity appeared, accompanied by viscous flow. The correlation of rheological behavior with compressibility of the films was also similar to the case of serum albumin.

Discussion

The rheological method mentioned above enables the film properties to be quantitatively described in mechanical terms by the way of assigning absolute values of viscosity and elasticity to each element of corresponding mechanical model. Table II shows an example of the result obtained near the collapsing pressure of the film, i.e., at 6 dynes per cm. and 9 dynes per cm. For simplicity of computation, three element model was adopted as the mechanical model for ovalbumin film. The numbers in the table indicate the values of surface shear modulus and surface viscosity coefficient in c. g. s. unit. These values were computed approximately from the observed values corresponding to the instantaneous elastic deformation, the

TABLE II

COMPARISON OF MECHANICAL PROPERTIES OF OVALBUMIN AND HORSE SERUM ALBUMIN MONOLAYERS.

Numbers indicate the values of surface shear modulus and surface viscosity coefficient of each element of the mechanical model in c. g. s. unit. At the bottom of the table, the Joly's data of surface viscosity are given, in which R indicates the surface viscosity coefficient in c. g. s. unit at the surface pressure of 6 dynes per cm., P_n, the critical surface pressure at which the nature of flow transforms from Newtonian to non-Newtonian by compression.

		Ovalbumin	Serum albumin
Surface Pressure in dynes/cm	9	7.6, 3.6, 3030	0.1, 7.5, 22.5
	6	6.0, 2.4, 550	0.8
Jolys data	R	0.038	0.076
	P_n (dynes/cm)	4	10

13) T. Sasaki and H. Kimizuka, This Bulletin, **25**, 318 (1952).

ultimate strain at infinite time, the rate of initial flow, and the rate of the stationary flow.[14] In this table, characteristics of ovalbumin and serum albumin films are quite clear at a glance. At the bottom of this table, Joly's[7] data on surface viscosity are tabulated; these date were obtained by the method of damped oscillation of ring. It is to be noted that Joly's measurement failed to show any difference in mechanical properties of these proteins. In addition, he reported the critical pressure (P_n), at which the nature of flow is transformed from Newtonian to non-Newtonian by compression, to be 4 dynes per cm for ovalbumin, 10 dynes per cm. for serum albumin. Such values, especially for ovalbumin, are hardly expected from the present method, since the films of these proteins exhibit distinct elasticity at such high surface pressures. Such large discrepancy may presumably be due to the too large shear stress employed by the oscillation ring method. The reason becomes apparent in view of the fact that ovalbumin film shows thixotropic behavior, that is, the film structure undergoes destruction and the film shows only simple flow under too large stress. It must be emphasized that sufficiently small stress should be applied to the film if the detailed information is wanted for the film structure.

From the view point of structural theory, the occurrence of the instantaneous elasticity is to be attributed to the exsistence of intermolecular bondings. The conclusion could, therefore, be drawn that even in a large area such as 5 sq. m. per mg., ovalbumin molecules are linked together with each other, making a two dimensional network covering the whole area of spread film.* It had been suggested that the protein molecule exists on surface in an unfolded structure, probably in the form of straightened β-configuration, and at low pressure, the side chains are lying flat on the surface.[15] The calculation based on the molecular model leads to the results that the area occupied by a polypeptide chain with the side chains flat on water surface is about 1.7 sq. m. per mg. In addition, according to Bull's[16] data the area of ovalbumin film available for the close packing state is not over 2 sq. m. per mg. under the best spreading condition. Our experimental result, therefore, shows that ovalbumin film forms a two-dimensional network before its spread molecules are closely packed, i.e., spread ovalbumin molecules have a marked tendency to combine with each other.

On the other hand, with serum albumin, it is to be noted that the film did not manifest any elastic behavior until it was compressed down to the area about 0.8 sq. m. per mg., and that the critical area is just consistent with the area of minimum point of film compressibility. It is commonly said that when the compressed film exists in a close packed state of molecules, whose side chains are oriented normal to the surfacee, compressibility-area curve exhibits a minimum point. Therefore, with serum albumin, it is considered that the closest packing state of film molecules just rendered the film viscoelastic and that the looser packing no longer brings about any elastic behavior. This shows that the interaction between the film molecules is very weak. Moreover, our experiments show that no perceptible viscosity of the film was observed until it was compressed to the area about 1. sq. m. per mg. The case is similar with hemoglobin. These facts may suggest that the film molecules of serum albumin exist with the side chains oriented normal to the surface even at the uncompressed film state as well as the compressed one. In these respects, the film structure of serum albumin and hemoglobin is considered to be in striking contrast to that of ovalbumin film, whose side chains lie flat on the surface in a large area forming the interchain bonds between the film molecules.

Summary

A static method of measuring the viscoelasticity of spread monolayers is presented, and the rheological study was carried out with the monolayers of ovalbumin, horse serum albumin, and hemoglobin. The deformation-time relations, obtained under the shear stress, were found to give very detailed information about the structure of films.

With ovalbumin films spread on 0.1 N hydrochloric acid, it was found that an instantaneous elasticity, accompanying retarded elasticity, appeared in an unexpectedly large area, i.e., in the area above 5 sq. m. per mg. Surface shear modulus of instantaneous elasticity increased linearly with the decrease of surface area, exhibiting several breaks in the slope.

The films of serum albumin and hemoglobin behaved differently from ovalbumin film, as they did not exhibit any viscoelasticity until they were compressed to a considerably small area. Compression down to the area

14) cf. T. Nakagawa, "Kagaku" (Science) **21**, 138 (1951).

* Complete spreading of the film was checked by the talcum test.

15) H. Neurath and H. B. Bull, *Chem. Revs.* **23**, 391 (1938).

16) H. B. Bull, *J. Biol. Chem.*, **185**, 27 (1950).

below 1.0 sq. m. per mg., however, makes a simple viscous film and further compression down to the area below 0.8 sq. m. per mg., just rendered the film viscoelastic. Such changes of film state were found to be consistent with the breaks in the compressibility-area curve obtained from the forcearea curve. Discussions of the characterization of these protein films were briefly made in terms of molecules.

The author wishes to express his hearty thanks to Prof. Taro Tachibana for his helpful advice and encouragement in the course of this work, and to Dr. Tsurutaro Nakagawa of the Chemical Laboratory of Tokyo University for his valuable discussions of the present experimental method. The author's thanks are also due to Dr. T. Shimanouchi of the Chemical Laboratory of Tokyo University and Takeda Pharmaceutical Industries Ltd. for a gift of horse serum albumin, and to Dr. S. Nagakura of the Scientific and Technological Institute of the Tokyo University for a gift of horse hemoglobin.

Department of Chemistry, Faculty of Science, Ochanomizu University, Tokyo

Studies on Amino-hexoses. III.[1] A New Synthesis of 2-Deoxy-D-ribose

By Yoshio MATSUSHIMA and Yujiro IMANAGA

(Received August 4, 1953)

The synthesis of 2-deoxy-D-ribose, a constituent of deoxy-ribonucleic acid, has been a matter of interest from the biochemical point of view. Of several methods of synthesis which have hitherto been reported, the glycal method[2] and the more recently discovered nitro-glycitol method[3] are best in yields. Here is reported another method of synthesis which we tried recently.

D-Arabinose was isomerized in hot pyridine to ribulose which was isolated as o-nitrophenylhydrazone.[4] The ribulose-o-nitrophenyl hydrazone was reductively decomposed into o-phenylene diamine on the one hand and 2-amino-2-deoxy-pentitols on the other, using Raney nickel as catalyst. As one of the authors has demonstrated,[5] α-amino-alcohols in sugar series undergo "semi-pinacolinic deamination" when treated with nitrous acid, thus glucosamine and glucosaminol affording chitose and 2-deoxy-glucose respectively. The 2-amino-2-deoxy-pentitols, as expected, were converted by treating them with nitrous acid to 2-deoxy-ribose which was isolated as its benzylphenyl hydrazone. The reaction sequence is represented as follows:

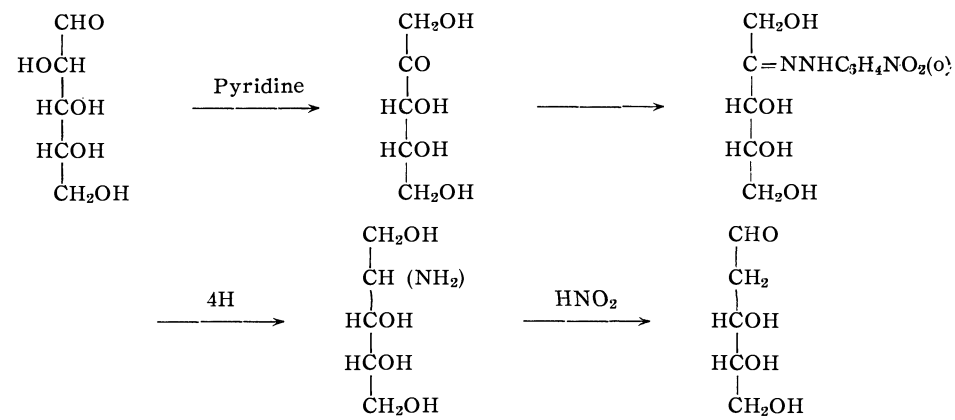

1) Previous reports of this series: This Bulletin, **24**, 17 (1951); ibid., **24**, 144 (1951); Preliminary report of this article: *Nature*, **171**, 475 (1953).

2) R. E. Deriaz, W. G. Overend, M. Stacey, E. G. Teece, L. F. Wiggins, *J. Chem. Soc.*, 1879 (1949); K. Ohta, *J. Biochem.* (Japan), **38**, 31 (1951).

3) J. C. Sowden, *J. Am. Chem. Soc.*, **71**, 1897 (1949).

4) C. Glatthaar, T. Reichstein, *Helv. Chim. Acta*, **18**, 80 (1935).

5) Y. Matsushima, This Bulletin, **24**, 144 (1951).

Experimental

Ribulose-o-nitrophenyl Hydrazone—23 g. of D-arabinose is gently boiled with 190 cc of anhydrous pyridine for 4 hours. The dark brown reaction mixture is evaporated *in vacuo*, water is added to the residue and redistilled in vacuo. After several repetitions of this operation, the syrupy material is separated with absolute alcohol from the unreacted crystalline arabinose. The alcoholic solution is seeded with arabinose and kept in an ice box in order to separate arabinose as far as possible. 17 g. of arabinose are recovered in almost pure state. After evaporation *in vacuo* of the alcoholic solution 7.25 g. of dark brown syrup is obtained.

The syrup above obtained is dissolved in 190 cc. of absolute alcohol and is boiled with 6.0 g. of o-nitrophenyl hydrazine for 10 minutes. The reaction mixture is concentrated to 75 cc. a few drops of acetic acid are added and it is placed in an ice box. The reddish yellow crystal separates and it is washed with water, absolute alcohol and then with ether-ethyl acetate (I : I). Ribulose-o-nitrophenyl hydrazone thus obtained weighs 5.2 g. and melts at 150°.

2-Amino-2-deoxy-pentitols—5.2 g of the ribulose-hydrazone above obtained is finely powdered and suspended in 70 cc. of water, 5 g. of activated Raney nickel are added, and shaken in the atmosphere of hydrogen. When the velocity of hydrogen absorption diminishes, the catalyst is added anew. 14 g. in all of the catalyst are necessary and 1970 cc. of hydrogen are absorbed in 16 hours. After the catalyst is filtered off, the solution is extracted with ether automatically for 20 hours. The ether extract, after evaporation, leaves 1.7 g. of o-phenylene-diamine. 3.2 g. of brown syrup of the 2-amino-2-deoxy-pentitols are obtained when the water solution is evaporated *in vacuo*.

2-Deoxy-D-ribose-benzylphenyl Hydrazone—3.2 g. of the syrup above obtained are dissolved in 20 cc. of 50% acetic acid and the solution of 2 g. of sodium nitrite in 5 cc. of water is dropped under ice cooling and in the atmosphere of cabon dioxide. After 20 minutes the nitrous acid is driven off by the stream of carbon dioxide and the solution is concentrated *in vacuo* to a syrup which is dissolved in 10 cc. of absolute alcohol; 2.15 g of benzylphenyl hydrazine in 2 cc. of absolute alcohol are added. The mixture is kept at 70° for 30 minutes in the atmosphere of carbon dioxide and concentrated *in vacuo*. The syrup thus obtained is extracted 3 times with each 10 cc. of benzene and the residue is once more extracted with 10 cc. of benzene after dilution with water. The benzene extract, after drying with sodium sulfate, leaves on evaporation crystalline needles mixed with syrupy matter. The crystal is separated by washing away the syrupy matter with ether and benzene. After recrystallization from benzene isopropyl alcohol and 40% ethyl alcohol, it melts at 125.5~126.5° and weighs 0.3 g. No melting point depression is observed when mixed with an authentic specimen. Colorless needle, $[\alpha]_D^{11}$ −15.25° (in pyridine).

Calculated for $C_{18}H_{22}O_3N_2$:	C, 68.79% ; H, 7.01% ; N, 8.92%
Found:	C, 68.86% ; H, 6.56% ; N, 8.98%

The authors are indebted to Prof. K. Makino and Mr. K. Ohta, of the College of Medicine, Kumamoto University, for an authentic specimen of deoxyribose, and are grateful to Prof. S. Akabori, of the College of Science, Osaka University, for his suggestions and encouragement. A part of the expenses was covered by the grant from the ministry of education in aid for fundamental scientific research.

Department of Science, Nara Women's University, Nara

Reactivity of Coke. I.
Absolute Reaction Rates of the Carbon Dioxide-Carbon Reaction

By Yoshio KAWANA

(Received August 16, 1953)

The reactivity of coke is very important in industry and so the reactions of carbon dioxide with charcoal and pure graphite have been extensively studied.[1-4] The mechanism of this reaction is at present considered as follows:

$$CO_2+C \longrightarrow CO+[CO] \quad \text{surface oxide} \quad (1)$$

$$[CO] \longrightarrow CO \quad (2)$$

The reaction (1) of the surface oxide for-

1) W. E. J. Broom and M. W. Travers, *Proc. Roy Soc.*, (London) **135A**, 512 (1932).
2) J. Gadsby, E. J. Long, P. Sleightholm and K. W. Sykes, *Proc. Roy Soc.*, (London) **A193**, 357 (1948).
3) I. Langmuir, *J. Am. Chem. Soc.*, **37**, 1154 (1915).
4) A. F. Semechkova and D. A. Frank-Kamenetzky, *Acta Physico. Chim.* (U.R.S.S.), **12**, 829 (1940).

mation is very rapid and only about 0.5 % of sites on the total carbon surface seem to take part in the reaction (1). Desorption of $\lceil CO \rceil$ is the rate-determining step.

In a recent paper, Bonner and Turkevich[5] discussed the carbon dioxide-carbon reaction using C^{14} as a tracer and supported the above mechanism.

More recently, Reif[6] discussed the mechanism of this reaction theoretically and Gulbransen and Andrew[7] questioned the surface oxide formation from their results using a sensitive microbalance. Gulbransen and Andrew, [7] Wynne-Jones and his coworkers[8] emphasized the effects of metal oxide impurities on the reaction rate of carbon dioxide with pure graphite.

In the present paper, the surface areas of eight carbons were determined by the adsorption of ammonia at 0°C by the B.E.T. method and, using these values, the absolute reaction rates of the carbon dioxide-carbon reactions were obtained and discussed from the absolute reaction rates theory.

Apparatus, Materials and Procedure

The apparatus is shown in Fig. 1. A is a reaction tube of quartz, F, a mercury reservoir, B, a gas burette and $L_1 \sim L_9$, vacuum cocks. A was kept at 0°C with the surface area determination and regulated at a constant temperature in the range from 850° to 978°C within ±1°C with the reaction rate measurement.

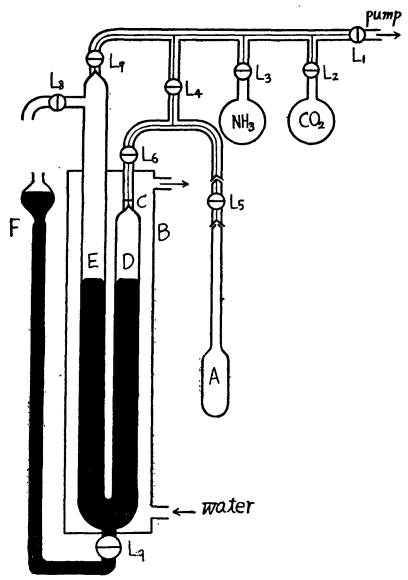

Fig. 1—Apparatus

Eight carbons as shown in Table I were used and their particle size is 10~20 mesh except for fine acetylene black and carbon for spectroscopic analysis. All carbons were previously treated with 6N-hydrochloric acid for about 40 hrs. and then washed by boiling distilled water during about 200 hrs. Analytical results and the density of all carbons using carbon tetrachloride at the end of all the experiments are shown in TABLE I.

TABLE I*

Sample	Moisture %	Ash %	Density g./cc.
Coke I	0.87	12.95	1.92
Coke II	2.03	11.18	1.79
Coke III	0.17	12.90	1.89
Pitch coke	0.30	2.32	1.90
Oil coke	0.17	0.39	2.00
Charcoal	4.82	0.70	1.27
Carbon for spectroscopic analysis	0.10	trace	2.25
Acetylene black	0.30	0.10	2.27

Ammonia was prepared by the thermal decomposition of 28% aqueous ammonia, dehydration by calcium oxide, potassium hydroxide and metallic sodium and lastly vacuum distillation at dry-ice temperature.

Carbon dioxide was prepared by the thermal decomposition of sodium bicarbonate and dehydration by both calcium chloride and phosphorus pentoxide.

Method for Determination of Surface Area.— The surface areas of carbon samples were determined using the adsorption of ammonia at 0°C following the simple B.E.T. method.[9,10]

The carbons were previously evacuated at 1100°C for 12~15 hrs. until 10^{-4} mmHg to eliminate some surface oxide and residual volatile matters. The adsorption of ammonia vapor was determined volumetrically at a series of P/Po values between 0.05 and 0.3. The B.E.T. plots of $P/v(Po-P)$ vs. P/Po were made and V_m and C in the B.E.T. equation were calculated.

$$P/v(Po-P) = \frac{1}{V_m C} + \frac{C-1}{V_m C} P/Po \qquad (3)$$

Where, V_m is the volume of monomolecular adsorption, C is a constant and approximately equal to $\exp(E_1-E_L)/RT$ where E_1 is the heat of adsorption of the first adsorption layer and E_L is the heat of liquefaction. P is the equilibrium pressure, Po, the saturation pressure, and v, the volume of gas adsorbed. From the value of V_m, the total surface area of the sample, S, can be calculated by the following equation, using the average

5) F. Bonner and J. Turkevich, *J. Am. Chem. Soc.*, **73**, 561 (1951).
6) A. E. Reif, *J. Phys. Chem.*, **56**, 785 (1952).
7) E. A. Gulbransen and K. F. Andrew, *Ind. Eng. Chem.*, **44**, 1048 (1952).
8) W. F. K. Wynne-Jones, H. E. Blayden and H. Marsh, *Brenn. Chem.*, **33**, 238 (1952).

* Samples were heated at 1100°C in vacua before surface area and reaction rates measurements and so subjected to vacuum treatment at 1100°C for about 20—60 hrs. in all.

9) S. Brunauer, P. H. Emmett and E. Teller, *J. Am Chem. Soc.*, **60**, 309 (1938).
10) S. Brunauer, L. S. Deming, W. E. Deming and E. Teller, ibid., **62**, 1723 (1940).

surface area per molecule of ammonia of 12.9×10^{-16} sq. cm. and then the specific surface area, A, of the sample can also be obtained,

$$S=(12.9\times10^{-16}\times V_m\times6.02\times10^{23})/22400\times10^4,\ m^2 \quad (4)$$

Method for Determination of Reaction Rates. After the surface area measurement, the sample was heated and the adsorbed ammonia was thoroughly desorbed. Carbon dioxide was introduced into the reaction tube A in Fig. 1 after regulating the temperature of the sample at a constant temperature in the range from 850° to 978°C and the increase of total pressure against time at constant volume was measured by cathetometer and the reaction rates of the system of carbon dioxide and carbons were determined.

After the reaction rate measurement was over and before the next surface area determination or the next reaction rate measurement, the sample was again evacuated at 1100°C for 3~15 hrs. until 10^{-4} to 10^{-5} mmHg to evaporate the surface oxide considered to be formed by the former reaction with carbon dioxide. The absolute reaction rates were obtained from the reaction rates measurement and the surface area determination.

Results and Discussion

(I) Surface Areas of Carbons. The B.E.T. plots of $P/v(Po-P)$ vs. P/Po are shown in Fig. 2 and monomolecular adsorption volume V_m, total surface area S, specific surface area A, B.E.T. constant C and the difference of the heat of adsorption of the first layer and the heat of liquefaction E_1-E_L are summarized in Table II. The surface areas and the weights of the coke I were determined before and after the reaction rate measurement with carbon dioxide as shown in No. 5-2, No. 5-3 and No. 5-4 in Table II and their differences were found to be so small that after the experiment with charcoal, No. 6 in Table II, the surface area determination was made at once and from these surface area values and kinetic data, the absolute reaction rates for various temperatures were obtained.

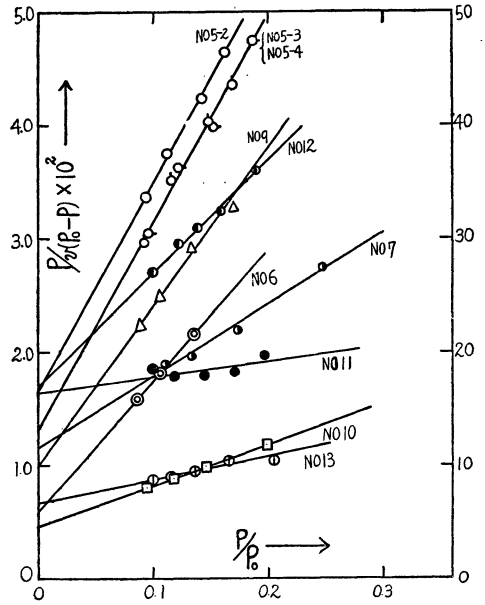

Fig. 2.—B.E.T. plots
Ordinate; left-hand, No. 5, No. 6, No. 9 and No. 12
right-hand, No. 7, No. 10, No. 11 and No. 13

The largest specific surface area of the samples investigated was 399 m^2/g of charcoal and the smallest, 0.41 m^2/g of oil coke and their ratio was about 10^3. If charcoal and acetylene black were excepted, the ratio of

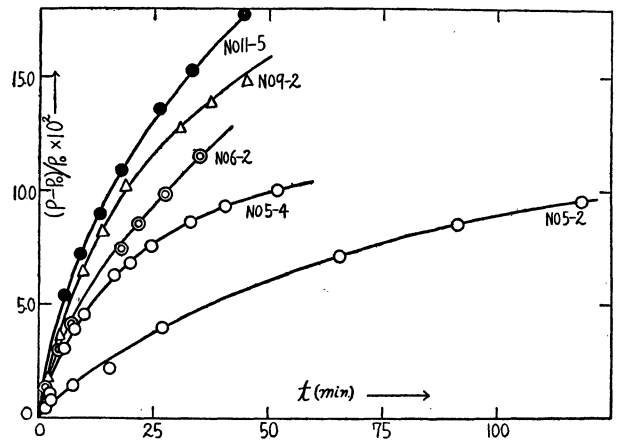

Fig. 3.—Relation between increase of total pressure and time
● acetylene black at 1230°K
△ coke II at 1173°K
◎ charcoal at 1173°K
○ coke I at 1173°K and 1223°K

TABLE II

Sample	Experimental number No.	Vacuum pretreatament at 1100°C hr.	Sample weights g	V_m cc	S m²	A m²/g	C	E_1-_1E cal/mol	Reaction temperature K	Number of moles of CO_2	Po mmHg	Slope	$1/2.303Po$	K	Ka_{obs} molecules cm^{-2} sec^{-1}	$Ka_{calc.}$ molecules cm^{-2} sec^{-1}
Coke I	5—2	15	8.0879	5.01	17.8	2.20	12.1	1360	1173	4.727×10^{-4}	784.0	5.44×10^{-4}	5.53×10^{-4}	0.0902	3.18×10^{9}	2.21×10^{9}
	5—3	15	8.0749	5.02	17.9	2.22	15.4	1490	1123	4.124 〃	665.4	6.47 〃	6.52 〃	0.00765	2.79×10^{8}	3.36×10^{8}
	5—4	15	8.0658	5.03	17.9	2.22	15.4	1490	1223	4.301 〃	719.0	5.98 〃	6.03 〃	0.298	1.08×10^{10}	1.30×10^{10}
	5—5	15	8.0590						1223	4.514 〃	752.0	5.73 〃	5.76 〃	0.311	1.11×10^{10}	1.30×10^{10}
Charcoal	6—1	15	0.0735	8.25	29.3	399.0	20.2	1640	1123	3.877 〃	573.0	7.18 〃	7.56 〃	0.0633	1.56×10^{9}	8.43×10^{8}
	6—2	3							1173	3.262 〃	495.0	8.45 〃	8.75 〃	0.342	8.19×10^{9}	5.06×10^{9}
	6—3	3							1223	4.664 〃	718.5	5.33 〃	6.04 〃	2.22	5.31×10^{10}	3.28×10^{10}
Oil coke	7—1	15	11.6119	1.34	4.76	0.41	6.43	1020	1223	4.157 〃	727.0	5.37 〃	5.97 〃	2.21	2.87×10^{11}	3.64×10^{11}
	7—2	10							1173	5.538 〃	635.0	6.65 〃	6.54 〃	0.220	4.10×10^{10}	7.32×10^{10}
	7—3	10							1123	4.493 〃	764.5	5.66 〃	5.66 〃	0.060	7.75×10^{9}	1.33×10^{10}
	7—4	10							1173	4.083 〃	700.1	6.07 〃	6.20 〃	0.393	5.04×10^{10}	7.32×10^{10}
	7—5	10							1223	3.649 〃	645.0	6.27 〃	6.72 〃	1.55	1.99×10^{11}	3.64×10^{11}
Coke II	9—2	15	6.9295	6.66	23.7	3.42	15.0	1480	1173	3.542 〃	562.0	7.55 〃	7.71 〃	0.492	1.19×10^{10}	1.30×10^{10}
	9—4	5							1223	4.415 〃	755.0	5.57 〃	5.75 〃	2.09	6.19×10^{10}	7.30×10^{10}
	9—5	5							1123	3.433 〃	535.0	8.25 〃	8.11 〃	0.0616	1.86×10^{9}	2.12×10^{9}
	9—7	5							1223	4.232 〃	703.0	5.90 〃	6.19 〃	1.94	5.70×10^{10}	7.30×10^{10}
	9—9	5							1223	4.254 〃	702.0	6.25 〃	6.18 〃	2.10	6.29×10^{10}	7.30×10^{10}
Coke III	10—1	15	10.1108	2.42	8.6	0.85	9.21	1210	1123	4.341 〃	700.0	5.95 〃	6.20 〃	0.0903	7.13×10^{9}	1.33×10^{10}
	10—2	10							1153	3.668 〃	600.0	6.80 〃	7.24 〃	0.360	2.86×10^{10}	3.70×10^{10}
	10—3	5							1183	3.946 〃	650.5	6.66 〃	6.69 〃	0.780	6.20×10^{10}	1.09×10^{11}
	10—5	5							1223	4.202 〃	713.0	5.88 〃	6.09 〃	2.23	1.76×10^{11}	3.82×10^{11}
Acetylene black	11—1	12	0.2309	3.36	12.0	52.0	1.81	326	1172	3.653 〃	552.2	7.58 〃	7.87 〃	0.089	6.07×10^{9}	5.55×10^{9}
	11—2	3							1212	4.768 〃	734.0	5.49 〃	5.91 〃	0.379	2.13×10^{10}	2.28×10^{10}
	11—3	3							1251	4.140 〃	642.0	6.60 〃	6.78 〃	1.18	6.58×10^{10}	7.46×10^{10}
	11—4	3							1193	4.148 〃	630.0	6.64 〃	6.88 〃	0.151	8.20×10^{9}	1.15×10^{10}
	11—5	3							1230	4.361 〃	675.0	6.16 〃	6.43 〃	0.870	4.85×10^{10}	3.95×10^{10}
	11—6	3							1216	4.906 〃	753.0	5.58 〃	5.76 〃	0.417	2.33×10^{10}	2.57×10^{10}
Pitch coke	12—1	15	12.2474	8.49	30.2	2.46	6.93	1055	1213	5.170 〃	681.0	6.21 〃	6.37 〃	0.366	1.00×10^{10}	0.91×10^{10}
	12—2	3							1252	3.544 〃	613.0	6.82 〃	7.07 〃	1.41	3.13×10^{10}	3.24×10^{10}
	12—3	3							1172	4.596 〃	774.0	5.58 〃	5.61 〃	0.117	2.58×10^{9}	1.97×10^{9}
	12—4	3							1143	3.839 〃	644.0	6.73 〃	6.74 〃	0.0296	6.58×10^{8}	7.30×10^{8}
Carbon for spectroscopic Analysis	13—1	12	9.0180	3.76	13.8	1.49	3.86	736	1223	3.722 〃	621.0	6.53 〃	6.99 〃	0.687	3.44×10^{10}	3.26×10^{10}
	13—2	3							1224	4.186 〃	691.0	5.86 〃	6.29 〃	1.15	5.76×10^{10}	6.62×10^{10}
	13—3	3							1192	3.930 〃	643.0	6.55 〃	6.75 〃	0.237	1.18×10^{10}	1.13×10^{10}
	13—4	3							1142	4.245 〃	680.0	6.33 〃	6.38 〃	0.0376	1.92×10^{9}	1.83×10^{9}

the largest specific surface area of cokes to the smallest was about 8.

(II) Reaction Rates of Carbons with Carbon Dioxide. Typical examples of the increase of the total pressure P against time t at constant temperature and volume are illustrated in Fig. 3. Po is the initial pressure. As time passes. the increase of the total pressure becomes smaller. It has been interpreted that this decrease was due to the retardation effect of the adsorption of carbon monoxide formed by the reaction of carbon dioxide with carbon; but more recently, Reif concluded that it was due to the reversible reaction of the reaction (1).

In the present paper, assuming that

a) the reaction (1) is rapid and always in equilibrium and the concentration of surface oxide is negligibly small compared with total active centers on the carbon surface,

b) the reaction (2) is the rate-determining step,

the following experimental equation is easily obtained,

$$dP/dt = K\ P_{co_2}/P_{co} \qquad (5)$$

where P is the total pressure, t, the time, K, a rate constant and Pco_2 and Pco denote the partial pressure of carbon dioxide and carbon monoxide respectively. From the assumption (a), there are the following approximate relations,

$$Pco_2 = 2Po - P, \qquad Pco = 2(P - Po) \qquad (6)$$

Integrating Eq. (5) under the initial condition that P is equal to Po at $t=0$ using the relation of Eq. (6), the following equation is obtained,

$$Y = K/4.606\ Po + X/2.303\ Po \qquad (7)$$

where Y is equal to $1/t \log Po/(2Po-P)$ and X equals $(P-Po)/t$. There must be a linear relation between Y and X from Eq. (7). The examples of these relations using experimental data in Fig. 3 are indicated in Fig. 4. Very good straight lines are obtained and $1/2.303Po$ must give the slope of these straight lines from Eq. (7). The comparison between the slope obtained from the figures and calculated values of $1/2.303Po$ are indicated in

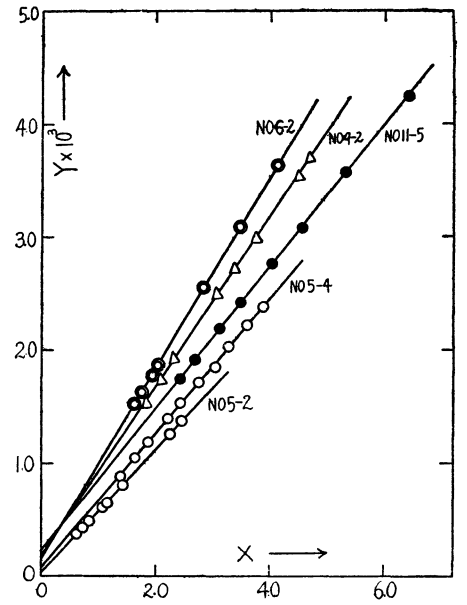

Fig. 4.—Relation between Y and X
○ coke I at 1173°K and 1223°K
● acetylene black at 1230°K
△ coke II at 1173°K
◎ charcoal at 1173°K

Table II and their differences are only a small percentage. Accordingly, Eq. (5) may satisfactorily represent the experimental data. The value of Y at $X=0$ is $K/4.606Po$ and then the rate constant, K, can be obtained. K represents the reaction rate when Pco_2/Pco equals unity. The number of molecules which react per sq. cm. per second at $Pco_2/Pco=1$, Ka, can be calculated by the following equation from K and the total surface area S,

$$Ka = a\ K \frac{273}{760}\frac{1}{60}\frac{6.02\times10^{23}}{22400}\frac{1}{S\times10^4} \qquad (8)$$

where, a *is* a constant determined by the volume of the reaction tube, the sample weight, the density of carbon and etc., and other figures are conversion factors.

K and $Ka_{obs.}$ are summarized in Table II. The plots of log Ka vs. $1/T$ are illustrated in Fig. 5 and Ka may by expressed in the form of

TABLE III

Sample	$A_{obs.}$ molecules cm^{-2} sec^{-1}	$A_{calc.}$ molecules cm^{-2} sec^{-1}	E, Kcal/mol
Oil coke	3.39×10^{27}	5.57×10^{27}	91
Coke III	〃	〃	〃
Coke II	5.12×10^{27}	〃	95
Charcoal	8.9×10^{27}	〃	97
Acetylene black	5.62×10^{27}	〃	〃
Carbon for spectroscopic analysis	〃	〃	〃
Pitch coke	5.75×10^{27}	〃	99
Coke I	〃	〃	〃

$$Ka = A\exp(-E/RT) \quad (9)$$

whe A and E are respectively the frequency factor and the observed activation energy. A and E obtained by the least squares are shown in Table III.

The values of A and E of oil coke, acetylene black and pitch coke coincide with those of coke III, carbon for spectroscopic analysis and coke I respectively.

The activation energy becomes smaller as the straight lines in Fig. 5 go upwards. It is very interesting that the line of charcoal does not deviate so much from those of coke II and carbon for spectroscopic analysis in Fig. 5 and that acetylene black and carbon for spectroscopic analysis fall exactly on the same line. Generally speaking, the ratio of the maximum value of Ka to minimum at the same temperature is about 16—20 for various carbons and is very small compared with the ratio of the largest specific surface area to the smallest, that is, 10^3, but among various cokes, except for charcoal and acetylene black, the difference of Ka is much greater than that of the speific surface area.

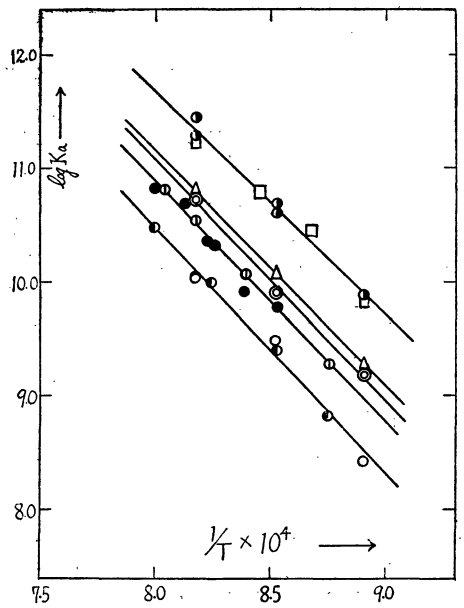

Fig. 5. Relation between log Ka and $1/T$
◑ Oil coke
□ coke III
△ coke II
◎ charcoal
● acetylene black
① Carbon for spectroscopic analysis
◐ Pitch coke
○ coke I

The systematic relations between the crystallographic structure of carbons and the values of Ka were not observed as shown in Fig. 5. This might be masked by the catalytic effects of impurities. From the above experimental results, it may be concluded that the difference of the specific reaction rates of pure amorphous carbon and pure graphite will be small and for carbons containing some impurities, the catalytic effects of the ash in carbons on the reaction rates may be much greater than that of the crystallographic structure of carbons that is, the degree of graphitization of carbons, and the difference of the observed activation energies may be due to the difference of the catalytic action of some impurities in carbons. These conclusions may be properly understood from various experimental facts that even small quantities of metallic oxide impurities usually play a very important part on the catalytic reactions. For example, Wynne-Jones and his co-workers[8] indicated that the addition of 0.1—0.02 per cent of sodium carbonates or elemental iron greatly affects the reactivity of pure graphite. In a recent paper, Parravano[11] indicated the change of the activation energies with the addition of some metallic oxide to nickel oxide in the reduction of nickel oxide by hydrogen. The activation energy of pure nickel oxide was 26.4 Kcal/mol, and with the addition of 1 mole per cent of alumina and 0.5 mole per cent of tungsten oxide, they became 35.2 Kcal/mol and 9.2 Kcal/mol respectively.

(III) A Theoretical Consideration of the Reaction Rates. The reaction mechanism of this system may be assumed as already mentioned and the absolute reaction rate theory[12] may be applied to this mechanism as follows,

$$\underset{P_{co_2}}{CO_2} + \underset{C_s}{C} \rightleftarrows \underset{P_{co}}{CO} + \underset{C_a}{[CO]} \quad \text{surface oxide} \quad (1')$$

$$\underset{C_a}{[CO]} \rightleftarrows \underset{C_a^*}{[CO]^*} \longrightarrow CO \quad (2')$$

The absolute reaction rates can be obtained from the following equation,

$$v = kT/h \cdot C_a \cdot f_a^*/f_a \exp(-E_1/RT) \quad (10)$$

where k, R, and h are universal constants, Ca, the concentration of the surface oxide, f_a^*/f_a, the ratio of the partition functions of the activated state and the surface oxide, E_1, surface activation energy and T, the temperature.

From the assumption (a) already stated, there is the following relation,

$$\frac{C_a}{C_s} = \frac{P_{co_2}}{P_{co}} \cdot \frac{f_{co}}{f_{co_2}} \cdot \frac{f_a}{f_s} \exp(-E_2/RT) \quad (11)$$

11) G. Parravano, *J. Am. Chem. Soc.*, **74**, 1194 (1952).
12) S. Glasstone, K. J. Laidler and H. Eyring: "The Theory of Rate Process," p. 369 (1941).

where, C_S is the concentration of the bare sites, P_{co_2} and P_{co}, the partial pressure of carbon dioxide and carbon monoxide, f denotes the partition functions of each species and E_2, the heat of reaction of the reaction (1'). From the assumption (a) C_s is also nearly equal to L, the concentration of the total active centers. When Eq. (11) is substituted for Ca in Eq. (10) using the relation of $C_s \fallingdotseq L$, some equations can be obtained as follows,

$$v = kT/h \cdot L \cdot P_{co_2}/P_{co} \cdot f_{co}/f_{co_2} \cdot f_a^*/f_s \exp\{-(E_1+E_2)/RT\} \equiv Ka\ P_{co_2}/P_{co} \quad (12)$$

where $$Ka = kT/h \cdot L \cdot f_{co_2}/f_{co} \cdot f_a^*/f_s \exp\{-(E_1+E_2)/RT\} \equiv A\exp(-E/RT) \quad (13)$$

here $$A = kT/h \cdot L \cdot f_{co}/f_{co_2} \cdot f_a^*/f_s \quad (14)$$

$$E = E_1 + E_2 \quad (15)$$

Eq. (12) is identical with the experimental reaction rate equation (5). A can be calculated from Eq. (14) and the calculated value using $L=10^{15}$, $f_a^*/f_s=1$ and $T=1173$°K as the mean of the experimental temperatures is 5.57×10^{27} molecules cm^{-2} sec^{-1}. The calculated value of A is in satisfactory agreement with the observed values in Table 3. Ka can also be calculated from Eq. (13) using the activation energies obtained experimentally. $Ka_{calc.}$ for each temperature are tabulated in Table 2. The agreement of the calculated values with the observed is also very excellent. Accordingly, the mechanism presented in this paper may be interpreted by the absolute reaction rate theory.

Summary

The absolute reaction rates of carbon dioxide with eight carbons have been obtained from the surface area measurement by the B.E.T. method using ammonia adsorption at 0°C and the reaction rate measurement.

The activation energies ranged from 91 Kcal/mol of oil coke and coke III to 99 Kcal/mol of coke I and pitch coke.

The reaction mechanism that the reaction of the formation of surface oxide is rapid and always in equilibrium and the concentration of the surface oxide is negligibly small compared with total active centers and the rate-determining step is the desorption of surface oxide can be interpreted by the theory of absolute reaction rates.

It may be concluded that the difference of the activation energies will be due to catalytic effects of some impurities in carbons, and that the difference of the absolute reaction rates due only to the difference of the crystallographic structure of pure carbons without the catalytic effects of impurities will be small.

The author wishes to express his earnest thanks to Mr. A. Baba, Dr. H. Honda and Mr. Y. Yoshida (this institute) for their kind advice and interest in this study.

The author's thanks are also due to Mr. R. Sato (this institute) for his helpful assistance in this experiment.

Shigen-Gijutsu-Shikenjo
(Resources Research Institute)
Saitama-Kawaguchi, Japan

Studies on the Polarographic Analysis. XVII.* Electrolytic Reduction of Cyclohexanedionedioxime and its Application to Amperometric Titrations

By Masayoshi ISHIBASHI, Taitiro FUJINAGA, and Kazuo KAWAMURA

(Received May 6, 1953)

In a previous paper[1], the behavior of electrolytic reduction of 8-hydroxyquinoline at the dropping mercury electrode and the amperometric titration using it have been described. In the present paper, polarographic and amperometric investigations of cyclohexanedionedioxime are reported. Cyclohexanedionedioxime (nioxime) was first employed by Wallach[2] as a reagent for nickel. It is very similar to dimethylglyoxime in its reac-

* Subtitle: Analytical Chemistry by Means of Organic Compounds XVII.

1) M. Ishibashi, T. Fujinaga, This Bulletin, **23**, 25, 27 (1950).

2) O. Wallach, *Ann.*, **437**, 148 (1924).

tion with nickel to form the red insoluble precipitate in an ammoniacal and weakly acid medium. However, nioxime has many advantages over dimethylglyoxime in the sensitivity of reaction, in the smaller percentage of nickel in the precipitate and in the solubility of the reagent in water (0.824 g./100 ml. at 25°C). Together with its stable property, nioxime is an ideal organic reagent for the amperometric titration of nickel.

Experimental

Chemicals Used. Nioxime.—This product was synthesized according to the method of Rauh, Smith, Banks and Diehl[3], which was modified in some respects. The crude nioxime was recrystallized several times from alcohol.

Other Reagents.—Such reagents as nickel sulfate and buffer agents were all of analytical grade. They were all examined as to their purity by the polarographic method. Buffer solutions were prepared according to Kolthoff and Vleeschhower[4].

Apparatus Used.—The potentiometric manual polarograph designed by the authors[5] is used for the polarographic study, for the amperometric titration and for the determination of pH.

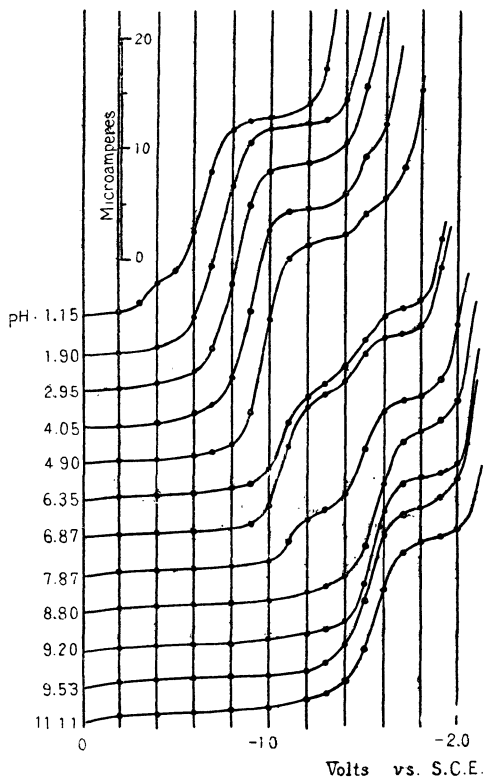

Fig. 1. Polarograms of nioxime at various pH

Polarographic Behavior of Nioxime.—Polarograms of nioxime at the dropping mercury cathode in various pH solutions are shown in Figure 1. These solutions have the composition of 10^{-3} M-nioxime, 10^{-2} M-KCl, and 0.01% gelatine except in the can of buffer agents. At a pH of 1.15, two waves appear at $E_{1/2}=-0.35$ and -0.65 volt vs. the saturated calomel electrode (S. C. E.) and in the pH range between 1.9 and 4.9, the first wave disappears and the second wave comes to predominate shifting to a more negative potential. At a pH of 4, the third wave appears at $E_{1/2}=-1.5$ volts vs. S. C. E. and above a pH of 8.8, the second wave disappears and the well-defined third wave predominates.

Amperometric Titration.—The general set-up was similar to that described in the previous paper[1]. For the performance of titration, a measured volume of the standard nickel solution in the proper medium was introduced into the cell, hydrogen was passed through for twenty minutes, the proper e.m.f. was applied to the cell and the current was measured. Successive amounts of nioxime standard solution were added from the burette. After each addition the contents of the cell were mixed by passing hydrogen through for half a minute and the current was recorded after it had become constant. In all cases the values of the current corrected for the volume change, were plotted against the amounts of reagent added.

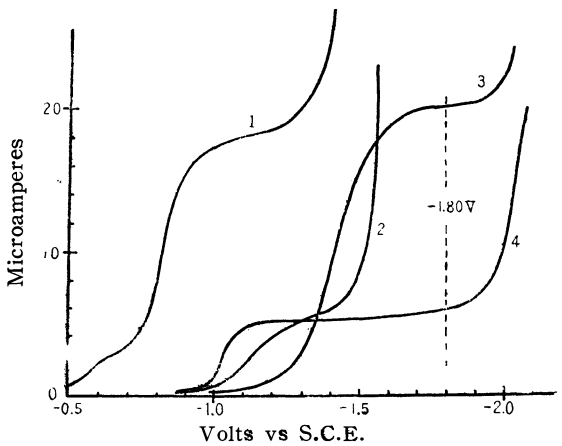

Fig. 2. Polarograms of nickel and nioxime in acetic acid medium and in ammoniacal medium
Curve 1. nioxime in 0.25M—CH_3CO_2Na, CH_3CO_2H
Curve 2. nickel in the same electrolyte
Curve 3. nioxime in 0.25M—NH_4Cl, NH_4OH
Curve 4. nickel in the same electrolyte
[nioxime]=1mM/l [Ni^{++}]=1mM/l

3) E. Rauh, G. F. Smith, C. V. Banks, H. Diehl, *J. Org. Chem.*, **10**, 197 (1945).
4) I. M. Kolthoff, "Acid-base Indicators", Macmillian Co., p. 251 (1937).
5) M. Ishibashi, T. Fujinaga, *J. Japanese Chem.* (in Japanese), **4**, 554 (1950).

The most suitable titration medium for nickel was found to be an ammoniacal solution. Consequently, current voltage curves of nickel and nioxime were determined in order to find the most suitable condition for the titration. An applied e.m.f. of 1.80 volts was found to be the most suitable for the performance of the titration. See Figure 2.

In Figure 3 are given the data obtained in the titration of 0.000033M (1.955 mg.) nickel solution

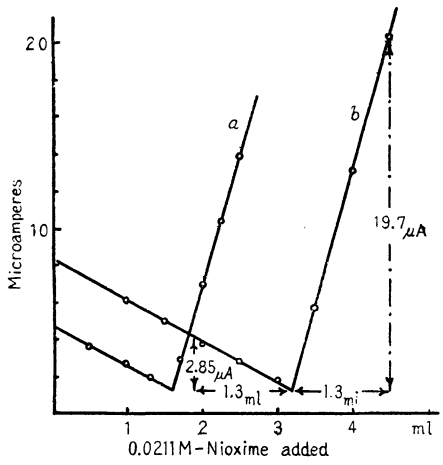

Fig. 3. Amperometric titration curves of nickel with nioxime
Curve a: 0.977 mg. of nickel in 20 ml. of 0.25M—NH_4Cl, NH_4OH.
Curve b: 1.955 mg. of nickel in the same solution

in 0.25M-ammonium chloride and ammonia with 0.0211M-nioxime at an applied e.m.f. of 1.8 v. The concentrations of ammonia and ammonium chloride could be changed within wide limits without affecting the results. In Table I is given a

TABLE I TITRATION OF NICKEL WITH NIOXIME

0.0667 N-Ni taken		0.211 N-nioxime used	Ni found	Error
0.50 ml.	(0.977 mg.)	1.59 ml.	0.987 mg.	+1.0 %
1.00	(1.955)	3.20	1.980	+1.2 %
2.00	(3.91)	6.35	3.92	+0.3 %
	„	6.36	3.93	+0.5 %
	„	6.37	3.94	+0.7 %
	„	6.39	3.96	+1.2 %
4.00	(7.82)	12.41	7.69	−1.7 %
Ni used		Nioxime taken	Ni found	Error
1.59 ml.	(3.12 mg.)	5.0 ml.	3.10 mg.	−0.7 %
3.17	(6.20)	10.0	6.19	−0.2 %
4.73	(9.27)	15.0	9.30	+0.3 %

summary of some results obtained in the titration of nickel with nioxime and in the reverse titration. In an acetic acid medium, it is difficult to select a proper e.m.f. riding over good plateaux of the diffusion currents of both nickel and nioxime. So good reproducibility in the titration curve is not expected.

Discussion

Numbers of Electrons Transferred in the Reduction of Nioxime.—The theoretical equation, derived by Ilkovic, for the diffusion current at the dropping mercury electrode is

$$i_d = 605 n D^{1/2} C m^{2/3} t^{1/6} = KC$$

where i_d is the average current in microamperes, n is the number of Faraday's transferred per mole, D is the diffusion coefficient in $cm.^2\ sec.^{-1}$, C is the concentration of reduced ion in millimoles per litre, m is the rate of flow of mercury from the dropping mercury electrode in $mg.\ sec.^{-1}$, t is the drop time in seconds, and K is the proportionality constant. Although diffusion coefficient D of nioxime is not known, by means of the Stokes-Einstein diffusion equation, it is computed to be about 5×10^{-6} $cm.^2\ sec.^{-1}$ from its molecular weight ($C_8H_{14}O_2N_2=142.16$). Substitution of experimental values to the equation (1) yields a value for n of approximately 8; e.g. in one experiment, using the mercury electrode of characteristics of m=0.641 and t=2.10, 0.9 mM/l-nioxime showed the diffusion current of 8.25 microamperes. Then

$$n = i_d/605 D^{1/2} C m^{2/3} t^{1/6}$$
$$= 8.25/605 \cdot (5\times10^{-6})^{1/2} \cdot 0.9 \cdot (0.641)^{2/3} \cdot (2.1)^{1/6}$$
$$= 7.65$$

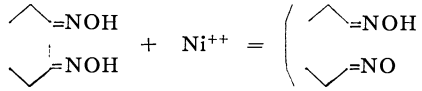

Again the number of electrons n was also calculated using the value of an amperometric titration curve of nickel with nioxime as they react according to the next formula.

At an applied e.m.f. of 1.8 volts, both nickel and nioxime are reduced at the dropping mercury electrode, thus the V shaped titration curves are obtained in the present titrations. In such a case, the normal concentration of nickel at one point before the end point of titration is equal to that of nioxime at the point symmetric for the end point, in other words, at the point where the corresponding volume of the reagent is further added after the end point of titration, provided that the volume change in titration is negligible. As the reduction current, which is proportional to its concentration, is corrected for the volume change, the ratio of two reduction currents at the two points should follow the following equation assuming that the capillary characteristics at the two points are unchanged.

$$\frac{i}{i'} = \frac{n \cdot D^{1/2} \cdot C}{n' \cdot D'^{1/2} \cdot C'}$$

Here the numerators are of nickel and the denominators are of nioxime. As nickel ions are reduced to the metallic state at the applied e.m.f., $n=2$ and $C=C'/2$. Therefore,

$$n' = \frac{D^{1/2} \cdot i'}{D'^{1/2} \cdot i}$$

From the experimental data shown in Figure 3, $i'/i = 19.7/2.85 = 6.9$ and the diffusion coefficient of nickel calculated from its equivalent conductance at infinite dilution is 7.1×10^{-6} cm^2 sec^{-1}. Using the above numerical value,

$$n' = \frac{(7.1 \times 10^{-6})^{1/2}}{(5 \times 10^{-6})^{1/2}} \times 6.9 = 8.2$$

This value for n' is also very close to 8 and shows good coincidence with the value calculated according to the equation (1). This value for the number of electrons indicates that nioxime in an alkaline medium is reduced to 1,2-diaminocyclohexane at the dropping mercury cathode.

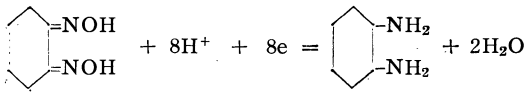

From the fact that oximes are generally reduced to the corresponding amines by metal reductants, the above inference is thought to be reasonable.

Summary

1. Cyclohexanedionedioxime (nioxime) was synthesized and its aqueous solution was used for the amperometric titration of nickel in ammoniacal medium, and the accurate results were obtained.

2. The polarographic behavior of nioxime was investigated and the reduction mechanism at the dropping mercury cathode was discussed.

Acknowledgement

It is a pleasure to these authors to express appreciation to Takeshi Kato and Manabu Matsuoka for their assistance in the measurement and also they wish to express their sincere thanks to the Ministry of Education for its financial grant.

Laboratory of Analytical Chemistry,
Faculty of Science,
University of Kyoto, Kyoto

This work was presented at the discussion on analytical chemistry held at Sendai in 1951 by the Chemical Society of Japan.

An Equation of State in Analytical Form (Continued)

By Tetsuya ISHIKAWA and Minoru IKEDA

(Received June 1, 1953)

In the previous paper[1] one of the authors (Ishikawa) proposed an equation of state slightly differed in its form from van der Waals' equation, but greatly improved in having a quantitative nature, i.e., for 1 mole of a gas the state is expressed by

$$p+\frac{a}{V^2-\varepsilon}=\frac{RT}{V-b},\quad a=3p_cV_c^2,\quad b=V_c/3,$$

in which ε is an **analytically** determinable constant at each isotherm.

As clearly understood from the derivation of the equation, a and b are not the constants which satisfy $(\partial p/\partial V)_T=0$ and $(\partial^2 p/\partial V^2)_T=0$, so that at critical isotherm, the equation

$$p+\frac{a}{V^2-\varepsilon}=\frac{RT_c}{V-b},\quad a=3p_cV_c^2,\quad b=V_c/3 \qquad (1)$$

should be combined with its critical condition:

$$p_c=\frac{3RT_c}{2V_c(1+3V_c\varepsilon)} \qquad (2)$$

where ε is not the value at the critical point, but the mean at the critical isotherm, or ε_c as denoted in the foregoing paper.

From the standpoint of the continuity of state, the unstable region of state at temperatures below the critical temperature has been supposed to consist of three portions of superheated liquid, supersaturated vapour and $\partial V/\partial p>0$, the first and second portions being realizable, but the third being never realizable. Actually in the stable state these three

1) Tetsuya Ishikawa: This Bulletin, **26**, 78 (1953).

portion coincide on a horizontal straight line corresponding to a given temperature to realize a liquid-vapour coexistence region expressed by a well known relation:

$$\log_e \frac{p}{p_c} = A - B\frac{T_c}{T} \qquad (3)$$

A and B being constants of nearly equal magnitude, so that the state may be fully expressed by this relation in combination with an equation of state in a van der Waals' form which holds true even at temperature below the critical temperature.

We are fortunate to find the recent measurements done by Oliver and his collaborators on monomer of chlorotrifluoroethylene, C_2ClF_3, having average purity of 99.84%[2].

The molecular volumes of this substance at 25.0°C under high pressure range are all less than $b_{corr.} = b.(3RT_c/8p_cV_c) = RT_c/8p_c$, hence van der Waals' equation should be rejected.

Tests for the new equation are diagrammatically shown in Fig. 1, in which the curves in full and their connecting broken lines are plotted by taking $2-\varepsilon = 1.861$, 1.879, 1.903 and 1.920 as the mean values at 25, 50, 75 and 100°C respectively, excluding the values in parentheses in Table I, which are far from

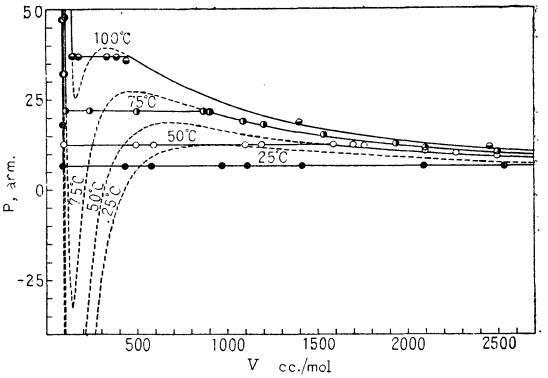

Fig. 1. Isotherms of C_2ClF_3.

TABLE I

(2—ε) Values of C_2ClF_3 (t_c=105.8°C, p_c=40.1 atm., d_c=0.55 g./cc.)

b=70.59, log a=6.732021

25.0°C			50.0°C			75.0°C			100.0°C		
p(atm.)	V(cc./mol.)	2—ε	p(atm.)	V(cc./mol.)	2—ε	p(atm.)	V(cc./mol.)	2—ε	p(atm.)	V(cc./mol.)	2—ε
47.29	89.34	1.862	47.30	95.74	1.908	47.91	105.88	1.902	37.05	142.92	1.923
32.26	89.57	1.861	12.81	99.01	1.888	32.27	108.67	1.904	37.02	150.02	1.925
18.24	89.80	1.860	12.73	99.36	1.889	22.14	111.70	1.907	36.93	179.77	1.927
6.774	90.97	1.866	12.66	497.71	1.868	22.20	112.05	1.907	36.91	335.80	1.915
6.796	91.78	1.871	12.53	594.27	1.857	22.06	241.69	1.918	36.82	389.97	1.915
6.766	94.93	1.888	12.50	1100.01	1.844	21.85	501.55	1.883	35.86	444.01	1.914
6.689	433.64	1.877	12.53	1190.04	1.848	21.74	868.57	1.900	18.80	1401.68	(1.941)
6.608	581.57	1.851	12.41	1591.31	1.882	21.61	902.00	1.904	11.91	2455.10	(1.995)
6.608	970.25	1.814	12.44	1705.22	1.904	21.58	905.03	1.904	8.629	3490.35	(2.038)
6.564	1109.56	(1.807)	12.42	1705.92	1.904	19.02	1088.82	(1.902)	6.650	4520.70	(2.015)
6.563	1418.57	(1.798)	12.16	1763.00	(1.906)	18.19	1200.76	(1.910)			
6.526	2093.09	(1.803)	10.68	2101.36	(1.913)	15.26	1535.98	(1.916)			
6.488	2537.80	(1.820)	10.05	2269.79	(1.916)	12.75	1935.38	(1.923)			
			9.311	2497.38	(1.920)	10.52	2498.66	(1.953)			
	mean	1.861		mean	1.879		mean	1.903		mean	1.920

having uniform pressures in unstable portions and those probably due to errors coming from the samples of different purity as noticed by the experimenters. These values together with the value at the critical point, 1.925, directly calculated by means of formula (2), are on a straight line as expected from the previous study. This proposition, therefore, serves as a supplemental test for estimating a probable value of (2−ε).

The fair coincidences between the observed points denoted by ●, ○, ◑ and ◒ at 25, 50, 75 and 100°C respectively and the calculated curves outside of liquid-vapour coexistence regions are quite satisfactory.

The liquid-vapour coexistence regions can be represented by the following relation with less than 1.6% error:

$$\log_e \frac{p}{p_c} = 6.743 - 6.729\frac{T_c}{T},$$

which fits better than log p_{mm}=7.75412 −1392.82/(t+319.70) proposed by the same experimenters.

Next we shall consider critical isotherms with two examples of hydrogen and carbon dioxide[3]. According to the classical theory, the critical point has been treated as a mathematical point of inflexion, e.g., applying van der Waals' equation, the condition of it is

2) G. D. Oliver, J. W. Grisard. C. W. Cuningham: *J. Am. Chem. Soc.*, 73, 5719 (1951).

3) Adopted from "International Critical Tables" III, p. 5, 12.

$(8p_cV_c-3RT_c)^3=0$, or $V_c=3RT_c/8p_c$. The actual volume range at the critical pressure, however, is always found to be appreciably longer than that in the neighbourhood of this point, or diagrammatically, the curve of the liquid portion calculated from van der Waals' equation is situated farther from p-axis than the observed points (see Fig. 2 and 3, in which dotted curves are van der Waals'

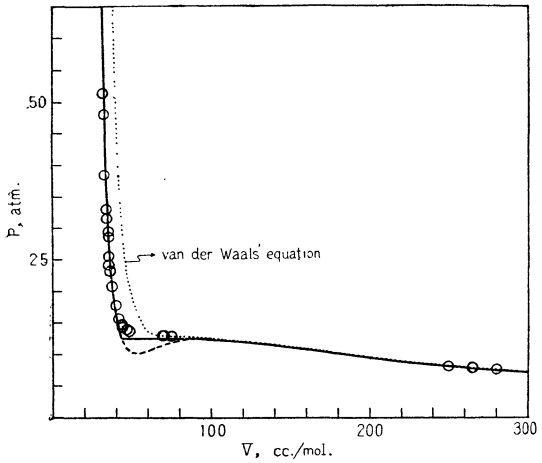

Fig. 2. Critical isotherm of H_2.

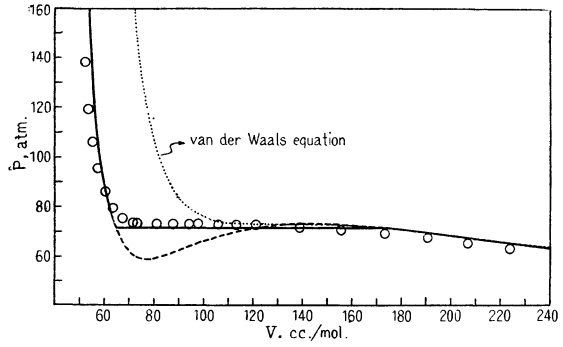

Fig. 3. Critical isotherm of CO_2.

equation and ○ are observed points). This divergency needs another reasonable explanation.

Draw a horizontal straight line passing through the critical condition, $p_c=3RT_c/2V_c(1+3V_c^{\varepsilon})$, where ε is taken to be ε_c as stated above, i.e., $2-\varepsilon=1.928$ for H_2 and 1.912 for CO_2 (compare with Table 4 in the preceding paper). We see that experimental points lie near the line, and that by so doing the portion of supersaturated vapour almost disappears but a realizable portion of superheated liquid still remains. Further tests at other temperatures show that similarity though flat in its form happens even at a few or a few tens degrees above the critical temperature.

The above elucidation is no other than an extension of the already explained liquid-vapour coexistence to a critical region where p must tend to p_c, but $\log_e p/p_c=A-BT_c/T$ fails since A is not exactly equal to B.

The indefiniteness of the critical state (which means that even after the meniscus has disappeared, the density of the system is not uniform) since 1904, has long been the subject of investigation and the present recognition is that there exists a critical region between the temperature at which the meniscus disappears and that at which liquid can no longer exist[4].

Taking this recognition into account, the conception of combination of equation (1) with p_c from formula (2) which is elongated horizontally as a limiting case of relation (3) for the volume range between two portions of liquid and vapour states may be permissible.

Trials show that the calculated curve by use of the new equation passes on or by the observed points in both portions of liquid and vapour states (full line and its connecting broken line in Fig. 2 and 3 denote the calculated curves taking the same values of $(2-\varepsilon)$ as above).

This and foregoing results lead to the conclusion that the new equation of state, which is valid for gases, is also available for liquids.

Sasebo Commercial Junior College
Sasebo, Nagasaki

4) e. g., S. Glasstone "Textbook of Physical Chemistry", p. 433 (2nd Edition).

Microscopic Studies on Fused Catalysts for Ammonia Synthesis. III. Weak Ferromagnetic Inclusions and Their Isolation for X-ray Study

By Yoshio Ōsumi

(Received September 4, 1953)

Introduction

Iron catalysts for ammonia synthesis have been studied by different workers from different view-points. For these several years in our laboratory, microstructures of the polished surfaces of these catalysts have been examined using the optical, the surface-electron and the surface-ion microscopes.

As reported in our first paper[1] the unreduced polished surfaces of usual catalysts with potash addition, when optically observed, consist of two different sorts of grains. A grains are large and each of them is filled with fine regular cleavage surfaces peculiar to magnetite. B grains, much less abundant than A grains, are found mainly along the grain bonudaries of A and are more capable of fine polishing, less markedly changed by hydrogen reduction, but more easily attacked by hydrochloric acid than A grains.

It was found that unreduced surfaces of these catalysts emit enough electrons at about 1000°C to permit observations with the surface-electron microscope. Such observations made with twelve sorts of catalysts showed that potash-promoted catalysts generally gave brightest electronic images, and in particular, those with well developed crystal grains gave almost exact patterns of B grains (Phot. 1a, 1b).

1a ×40

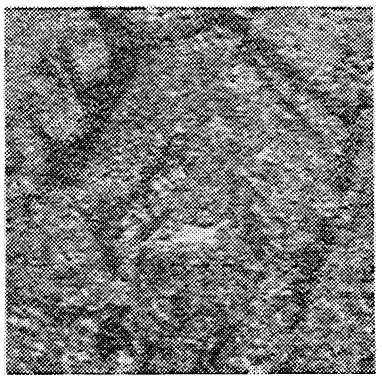

Optical image of polished surface (Cat. No. 10)

1b ×40

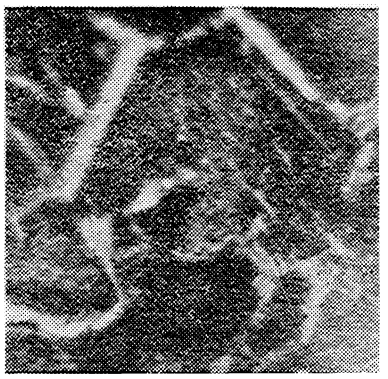

Thermo-electronic image of the same sample using a magnetic lens

The second paper contains observations with the surface-ion microscope of our own construction[2]. The catalysts, when reduced, emit positive ions mainly from B at about the same temperature as they do electrons (Phot. 2a, 2b). These ions could be identified

2a ×20

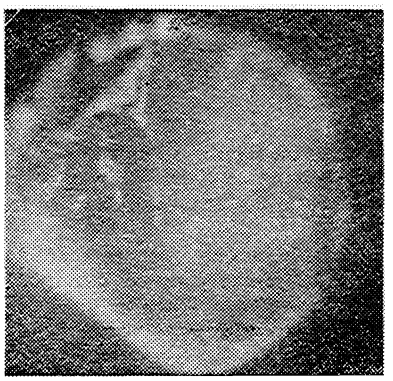

Thermo-electronic image of another sample using electrostatic lens (Cat. No. 10)

1) N. Sasaki, Y. Ōsumi, *J. Chem. Soc. of Japan*, (Pure Chemistry Section, Japanese), **73**, 808 (1952).

2) Y. Ōsumi, *J. Chem. Soc. of Japan*, (Pure Chemistry Section, Japanese), **74**, 308 (1953). More details of the results of optical-microscopy and of electron-microscopy are found in 3) and 4) respectively.

2b ×20

Thermo-ionic image of the same sample

with potassium ions, because the application of a magnetic field transversal to the ion path displaced the ionic image to the same extent as the image of a potassium ion source[6].

These potash-rich regions (B grains) seem to have become segregated from the ground magnetite mass of the potassium-promoted catalysts during its solidification.

In the present third paper[5], it will be reported that B grains have been found sufficiently less ferromagnetic than A grains to be magnetically separated from A grains and that they have been studied for their chemical and x-ray crystallographic properties in comparison with A grains.

Isolation of Weak Ferromagnetic B Grains for Surface-electron Microscopic Studies

From the polished surfaces of catalysts no. 4 and 10 (Table I) where B grains were relatively clearly observable, a small amounts of A and B were scraped off with the tip of a needle under an optical microscope. When a pole of a bar magnet whose strength was about 500 gausses was approached from above, it began to attract A powder at the distance of 2–3 cm., while B powder remained unattracted even at the distance of 2–3 mm.

TABLE I

Catalyst No.*	Promoter Added in %				Polished Surface as Observed		X-ray Diffraction Pattern of Powder	
	Al_2O_3	K_2O	CaO	MgO	Optically	Surface-Electronically	A	B**
1	—	—	—	—	no B	faint emission from whole surface	magnetite with slight α-Fe_2O_3	—
2	5	—	—	—	ditto	ditto	magnetite	—
3	—	1	—	—	B	strong emission from B	magnetite with slight FeO	FeO with slight magnetite
4	5	1	—	—	ditto (distinct)	ditto	magnetite	M
8	4	—	1	—	no B	somewhat bright emission from whole surface	ditto	—
9	4	—	—	1	ditto	faint emission from whole surface	ditto	—
10	10	1	1	—	B (distinct)	strong emission from B	ditto	M
11	4	1	1	—	ditto	ditto	ditto	M
12	4	1	—	1	ditto	ditto	ditto	M

* The catalyst numbers are the same as those used in the first report.
** In the column of X-ray diffraction pattern of B powder, blanks mean that weak ferromagnetic substance is not separable, and M indicates a peculiar diffraction pattern mentioned in the text.

A small piece of the catalyst as a whole was ground in an agate-mortar to a fine powder. It was then all attracted to the underside of a sheet of paper horizontally held, by placing the end surface of the magnet pole on the upper side of it. When the magnet was then moved about slowly along the sheet, weakly magnetic particles fell down from the paper, while the strong magnetic ones remained attached to it. From the powder made from pure magnetite no particles fell off during this treatment irrespective of the

3) Y. Osumi, "Ammonium Sulphate Engineering" (Japanese) **16**, 13 (1952).
4) Y. Osumi, ibid., **17**, 8 (1953).
5) Details about this work will soon be published in "Ammonium Sulphate Engineering" (Japanese).
6) N. Sasaki, K. Mitani, *Proc. Imp. Acad.*, (Tokyo) **17**, 36 (1941); N. Sasaki, *J. Applied Phys.*, **19**, 1050 (1948).

way and degree of pulverization. All the fallen particles must have come from B grains. Actually these were not attracted by the magnet 2-3mm from them.

One may suppose that B grains are inherently non-magnetic and the observed weak magnetism of B particles is due to the presence of a very small amount of A not separated from B particles by the process of pulverization. But the fact that even extrafine powder of B can finally be attracted to the last particle shows the magnetism is inherent in B. Incidentally the Curie point has been estimated to about 520°C for A powder and about 580°C for B powder made from catalyst no. 4.

By the magnetic separation, no. 4 and 10 catalysts respectively gave 3 and 5 per cent of B powder. These figures almost agreed with those calculated from the relative areas of A and B in the optical photographs of the polished surfaces.

A and B powders each in a small amount were kneaded with a drop of liquid paraffin, and placed side by side on a small disc cathode of nickel in our surface-electron microscope. Phot. 3a and 3b show that B powder is as good an emitter as

3a ×25

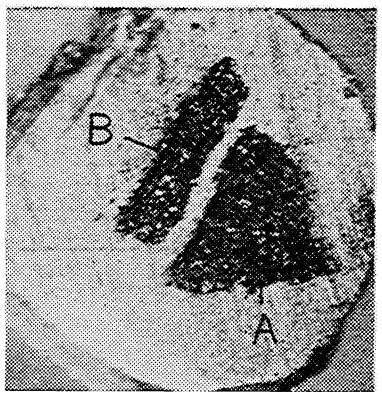

Optical image of powders on Ni-plate
(Cat. No. 4)

3b ×50

Thermo-electronic image of the same sample using a magnetic lens

B grains on the polished surface of the original catalyst.

Under the optical microscope fine particles of A powder are seen aggregated in arabesque figures, dispersed with difficulty probably due to mutual attraction between the magnetized particles (Phot. 4a), while B powder is seen as separated

4a ×50

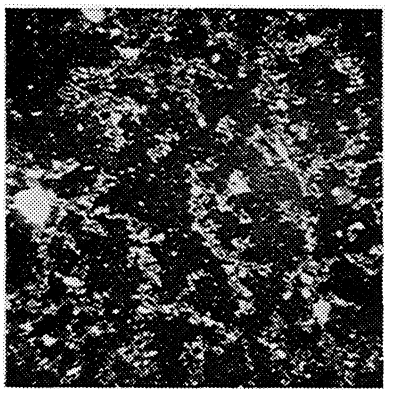

Optical image of powder A
(Cat. No. 4)

particles with rather sharp facets and edges, a fact unexpected from the mere appearance of B grains on the polished surface (Phot. 4b).

4b ×50

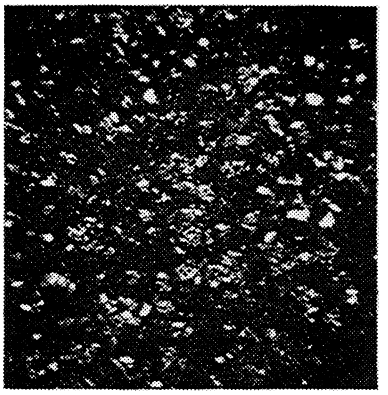

Optical image of powder B
(Cat. No. 4)

The weak ferromagnetic substances can be obtained from all potash-promoted catalysts which give distinct optical and electronic images of B grains. (Table I)

Chemical Compositions of A and B

In the foregoing reports the possible segregation of potash in B grains has merely been assumed from the study of some properties of polished surfaces. This can now be confirmed by analysing A and B powders separately. The results are given in Table II.

TABLE II

Catalyst No.		Weight Percentages of A & B	Oxide Percentages Found in Powder				
			Fe-oxides	Al_2O_3	K_2O	CaO	MgO
3	A	96.1	99.42*	—	0.58	—	—
	B	3.9	97.87*	—	2.13	—	—
4	A	96.9	92.8 (Fe_3O_4)	4.8	0.40 (0.29)**	—	—
	B	3.1	84.5 (Fe_2O_3)	6.3	4.00 (2.95)**	—	—
10	A	95.0	84.4 (Fe_3O_4)	11.3	0.52	0.46	—
	B	5.0	71.6 (Fe_2O_3)	25.0	3.49	2.41	—
12	A	92.0	68.0 (Fe_2O_3) 25.7*** (FeO)	4.9	0.34	—	0.70
	B	8.0	93.14 (Fe_2O_3)	3.4	1.98	—	0.61

* These figures were obtained not by analysis but by subtraction of the weight percentage of potash from one hundred.

** These figures were obtained by the analysis of the sample after boiling for 4 hours in water.

*** These figures obtained by analysis correspond very roughly to Fe_3O_4, so that in other samples shown qualitatively to contain both Fe^{++} and Fe^{+++}, total Fe is assumed to exist in the form of Fe_3O_4.

The alkali content of B is definitely greater than that of A for all the catalysts studied. Here we may tentatively assume that the crystal structure of A is not capable of containing more than about 0,5 per cent of potash, and in the solidifying process B crystals separate out to take over the excers of it. Calcium oxide behaves similarly (Catalyst no. 10), but magnesium oxide does differently (Catalyst no. 12).

X-ray Studies of A and B

Of all A and B specimens listed in Table I, X-ray diffraction photographs were taken using unfiltered Fe-K radiation (Camera diameter: 90 mm). Specimens A from the non-promoted iron oxide (Catalyst no. 1) and from singly promoted catalyst with potash addition (Catalyst no. 3) gave patterns characteristic of magnetite intermingled with some of the strongest lines of α-Fe_2O_3 and FeO respectively, while specimens A from catalysts with alumina addition (Catalyst no. 2, 4, 8–12) always gave the pattern of magnetite only, irrespectively whether they contained other promoters or not. Alumina addition seems to facilitate the formation of spinel lattice of magnetite[7].

Specimen B from a singly promoted catalyst with potash addition (Catalyst no. 3) gave patterns of FeO intermingled with some very strong lines of magnetite. Potash addition seems to favour the formation of FeO, for Fe_2O_3 fused with K_2CO_3 (1:1 in weight) for one hour at about 1100°C also contains FeO in an amount detectable by X-ray.

Specimens B from catalysts containing K_2O and Al_2O_3 (Catalyst no. 4, 10–12) all exhibit complicated diffraction patterns of similar type (denoted by M in Table I). The lattice spacings calculated from these lines and the relative intensities do not correspond to any compound listed in the A. S. T. M. or the Hanawalt tables.[8] However, the comparison of the lines of A and B of catalyst 4 (Phot. 5a, 5b) shows that these two crystal structures are not essentially different.

On both diagrams we notice a few lines exactly in the same positions which may be attributed to indices (044), (004) and (022), or some of the planes most densely packed with O atoms in magnetite structure. The strong lines in Phot. 5a with indices (113) and (115) seem in Phot. 5b to have split into many closely situated lines. Potash added in sufficient quantity seems to change the spinel lattice of magnetite into a slightly modified lattice with reduced degrees of symmetry

7) A possibility of solid solution formation between Fe_3O_4 and γ-Al_2O_3 has been reported by R. W. G. Wyckoff, E. D. Crittenden, *J. Am. Chem. Soc.*, **47**, 2866 (1925); R. Brill, *Z. Elektrochem.*, **38**, 669 (1932).

8) They also do not correspond to $KFeO_2$ or $KAlO_2$, T. F. W. Barth, *J. Chem. Phys.*, **3**, 323 (1935); L. T. Brownmiller, *Am. J. Sci.*, **29**, 260 (1935).

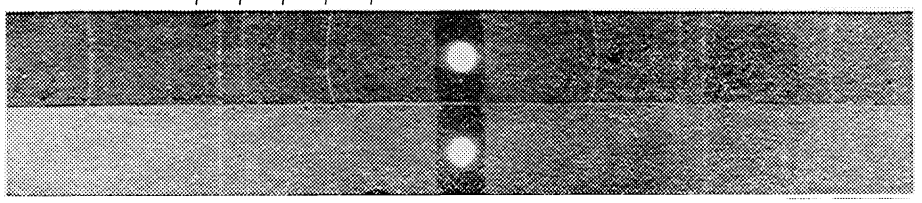

(thereby probably leaving the closely packed configuration of oxygen atoms almost intact).

Attempts were made to reproduce this interesting M type structure in specimens directly synthesized by fusing for 3 hours at about 1000°C Fe_3O_4 (Catalyst no. 1) with an equal amount of potash and 1, 5, 10, and 20 per cent of Al_2O_3. Of these only one with 5 per cent Al_2O_3 addition gave the M pattern (Phot. 5c).

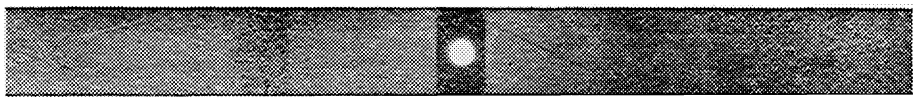

These facts make highly probable our abovementioned assumption that potash added in the course of melting to usual doubly promoted catalysts with K_2O and Al_2O_3 is retained in the spinellattice of magnetite in high dilution and in the M type lattice of B grains in much higher concentration. By the way, when boiled for 4 hours in water, B powder lost about a quarter of the total potash but still retained the M pattern unaltered.

Formerly Okamoto and Kobayashi[9] measured the activation energy for high pressure ammonia synthesis on various kinds of usual doubly promoted catalysts in relation to the amounts of K_2O retained after washing with water at room temperature for one day. They found that the activation energy was large for catalysts with K_2O content less than about 0.5 per cent, and it decreased with increase of K_2O content to a constant minimum value of about 15 Kcals for the K_2O content larger than 0.5 per cent. This fact may be explained by the assumption that the activity of catalysts is determined by A grains which constitute almost the whole mass and can contain K_2O to at most about 0.5 per cent and K_2O soluble in water at room temperature is contained not in A and B but in some other unidentified potassium compounds.

Summary

On the basis of our new finding that B grains on the polished surface (Report 1 and 2) of usual iron synthetic ammonia catalysts are less ferromagnetic than A grains, we attempted to separate magnetically B grains from A grains. The more magnetic fraction (called A powder) and the less magnetic fraction (called B powder) have the following properties:

1. B powder as observed by the surface-electron microscope is as strongly electron-emissive as B grains on the polished surface. This suggests a successful separation.
2. Chemical analysis shows that B powder is far richer in K_2O and CaO than A powder.
3. X-ray diffraction patterns of A powders separated from usual doubly or triply promoted catalysts are identified with that of magnetite, and those of B powders are all similar and complicated, whether they contain CaO or MgO or not. The product of potash fusion of Fe_3O_4 with 5 per cent Al_2O_3 gave the same diffraction pattern as B. Some relation of this new crystal structure to the spinel lattice of magnetite was discussed.

In the next paper will be reported the results of ammonia decomposition tests carried out with A and B powders under atmospheric pressure.

I should like to express my sincere thanks to Professor Nobuji Sasaki for his kind guidance throughout this work; my deep gratitude is also due to assistant R. Kiriyama and I. Taguchi of the laboratory of Professor Nitta, Osaka University, and to Professor J. Kakinoki, Osaka City University, and to Shimazu-Seisakusho Laboratory for taking X-ray diagrams, and to assistant T. Shigematsu of the laboratory of Professor Ishibashi, Kyoto University for his help in chemical analysis.

Department of Chemistry, Faculty of Science, Kyoto University, Kyoto; *Mitsubishi Kasei*

9) T. Okamoto, *J. Soc. of High Pressure Gas Industry* (Japan), **16**, 216 (1952).

Effect of Organic Molecules on the Adsorption of Hydrogen on the Electrode Surface*

By Takashi MUKAIBO and Mitsuru OIKAWA

(Received June 22, 1953)

Introduction

The effect of solvents on the hydrogen overpotential has been discussed recently by J. O'M. Bockris[1)~3)] and A. Wetterholm.[4)] They have obtained many interesting results relating to the mechanism of the hydrogen electrode reaction, and the theoretical presumption on these phenomena has been given. According to these authors,

(a) The solvent effect depends on both the cathode material and the nature of organic solute and therefore does not seem to depend principally upon solvation of the hydrogen ion, which should have some effects according to the slow discharge theories.

(b) The solute layer, held on the surface of the electrode by coulombic or van der Waals adsorption force, affects the velocity of the recombination of hydrogen atoms, which may be the rate-determining step of the electrolytic evolution of hydrogen molecules.

(c) The solvent effect on the adsorption energy of hydrogen molecules on the surface of the working electrode[5)] may change the hydrogen overpotential.

The measurement of the number of metal atoms on the electrode surface covered by organic molecules during the evolution of hydrogen being very difficult, the above theoretical presumption has only poor and indirect experimental evidence.

J.A.V. Butler [6)7)] has proposed the method of measuring the electrode potential in the initial stage of cathodic polarization with a cathode ray or an electromagnetic oscillograph and calculated the number of hydrogen atoms adsorbed on the electrode surface. By this method, we studied about the relation between the hydrogen overpotential and the effect of the adsorption of organic molecules especially in case of a smooth platinum electrode which has been assumed to obey the catalytic mechanism in the cathodic current density between 10^{-3} and 1 A./cm^2.

Under the assumption that the cathode area available for the hydrogen evolution decreases by the steric hindrance of organic molecules adsorbed on the cathode surface, we[8)] estimated the number of surface points covered by organic molecules, by analysing these polarization curves.

Experimental Procedures

The measuring cell was divided into three rooms separated from each other by diaphragms of glass filter. A platinum electrode, having an available area of approximately 3.6 cm^2, was placed between two auxiliary platinum electrodes in the middle room.

The change of the potential difference was recorded with an electromagnetic oscillograph (Yokogawa N-3, D-Type) through a suitably set 1-valve amplifier. At the same time the potential scale was given by a potentiometer through the amplifier.

During experiments air and free oxygen were removed from the apparatus by bubbling hydrogen, purified by passing through heated palladium asbestos in a silica tube. The electrode was first anodically polarized to remove adsorbed hydrogen and to give a constant electrode potential, and then a cathodic current was passed. By this procedure, we obtained curves of good reproducibility. As shown in Fig. 1 three main stages in the initial build up of cathodic polarization have been distinguished, corresponding to the ionisation of adsorbed oxygen (stage α), the charging of a double layer (stage β), and the adsorption of hydrogen at the electrode (stage γ) respectively.

The number of sites of the electrode surface covered by discharged hydrogen atoms can be calculated from the quantity of electricity consumed during the stage γ[9)]. The difference in above numbers before and after the addition of organic molecules to the solution shows the

* This paper was read at the annurl meeting of this society on April, 8. 1953.

1) J. J. O'M. Bockris: *Discuss. Farad. Soc.* No. 1. 95 (1947).

2) J. O'M, Bockris and S, Ignatowicz: *Trans, Farad,* **44**, 519 (1948).

3) J. O'M, Bockris and R, Parsons: ibid. **44**, 860 (1948).

4) Allan Wetterholm: ibid. **45**, 861 (1949).

5) R. Parsons and J.O'M. Bockris: ibid. **47**, 914 (1951).

6) R. Pearson and J. A. V. Butler: *Trans. Farad. Soc.* **34**, 1163 (1938).

7) F. P. Bowden: *Proc. Roy. Soc.* **125A**, 446 (1929).

8) M. Oikawa and T. Mukaibo: *J. Electrochem, Soc., Japan.* **20**, 568 (1952).

9) J. A. V. Butler: "Electrocapillarity." p. 178, (1940).

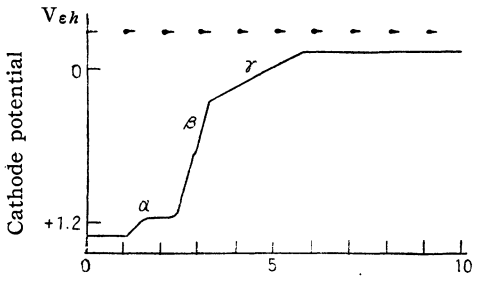

Fig. 1.
Polarization curve of platinum cathode in N. H_2SO_4

number of sites covered by organic molecules.[8] Cathodic current densities were limited between 10^{-3} & 5×10^{-1} A./cm². In this range we can assume that the mechanism of hydrogen electrode reaction belongs to that of the catalytic.[10][11] During the experiments the cell was saturated with pure hydrogen gas, the pressure of which was maintained about one atmosphere.

Results and Discussions

A. Preliminary Experiments. Table I shows the length of stage γ on the smooth platinum electrode in pure N. H_2SO_4 solution. It was found that the length of the stage was almost independent of the current density over the range of $3.0\times10^{-3}\sim1\times10^{-1}$ A./cm².

TABLE I

Cathodic Current Density D.A./cm² $\times10^{-3}$	Stage γ Coul. $\times10^{-3}$	Log D (D,A/cm²)	Electrode Potential V, ε_h
3.2	3.3	−2.49	0.000
5.0	3.3	−2.29	0.015
10.0	3.5	−2.00	0.035
32.0	3.6	−1.49	0.070
100.	3.6	−1.00	0.11

Moreover it was confirmed that the oxygen adsorbed during the anodic polarization was perfectly consumed in the stage α.[8] Though the length of stage α had a wide range of values by the time of duration of the anodic polarization or by the anodic current density, the length of stage γ was almost independent of such conditions, as shown in Table II.

TABLE II

Anodic Polarization (mA.×sec.) /3.6cm²	Cathodic Polarization (A./3.6cm²)	Stage γ (coul.) $\times10^{-3}$
5×30	36.4	3.5
5×60	36.5	3.6
2×30	36.9	3.7
10×20	36.3	3.7
2×20	11.5	3.5
3×30	18.0	3.5

Taking the diameter of a platinum atom as 2.5Å, we calculated the quantity of electricity required to deposit one hydrogen atom on each platinum atom of the electrode surface to be 2.7×10^{-4} coulombs/cm². The same quantity found experimentally by the above mentioned procedure was about 9.7×10^{-4} coulombs per sq. cm. of the apparent surface. This value agrees with the calculated one if we assume the real area of the electrode to be about 3.6 times the apparent area of it. Though there is some uncertainty as to this ratio at the smooth platinum surface, the value 3.6 obtained by us may be reasonable when compared with those estimated by many other authors which lie between 2 and 4[12]. From the values in column 3 and 4 of Table I we get Tafel's constant b of about 0.08.

Then, by adding organic compounds at various concentrations to N. H_2SO_4, we obtained the results shown in Fig. 2 and Fig. 3.

The quantity of electricity consumed in the stage γ is sharply affected by the addition of acetaldehyde; and the larger the concentration of it the smaller becomes the length of the stage.

Fig. 2 shows the relation between the concentration of acetaldehyde in the bulk of the solution and the number of adsorption points covered by molecules of acetaldehyde.

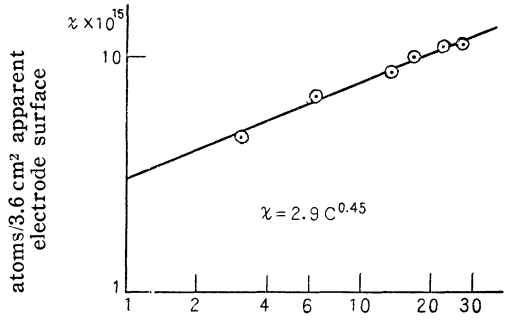

Fig. 2.
Freundlich's adsorption isotherm of the electrode surface (measured at the current density 10mA./cm², 3°C)
x: number of adsorption point covered by acetaldehyde
c: concentration of acetaldehyde (M./l. solution) x and c in log. scale

This figure shows also that the relation fits Freundlich's isotherm very well. The parameters of the equation were determined and are shown also. From Fig. 3 we can see that there exists a parallelism between the adsorption of organic molecules and the electrode potential. This fact suggests to us that the relation between these factors is very important.

10) J. O'M. Bockris and A. M. Azzam: *Trans. Farad. Soc.* **48**, 145 (1952).
11) J. O'M. Bockris: *Chem. Rev.*, **43**, 525 (1948).
12) J. A. V. Butler: "Electrocapillarity" p. 73 (1940).

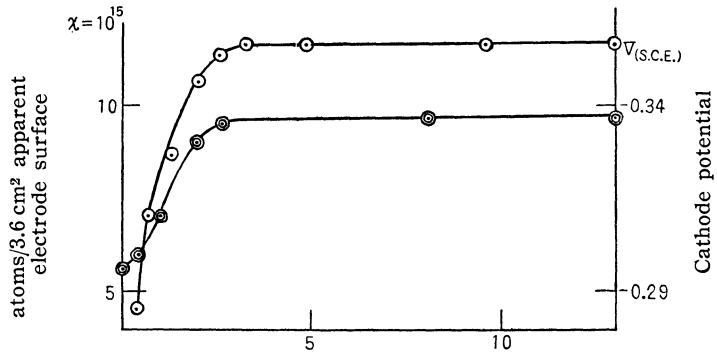

Fig. 3.
The relation between the adsorption of acetaldehyde (⊙) and the cathode potential (◎) (at 3°C)
V: potential in volts referred to the saturated calomel electrode (S.C.E.) the amount of adsorption of acetaldehyde and the electrode potential were all measured at the cathode density 10 mA./cm².

B. Case 1. According to J. O'M. Bockris, an increase of the concentration of an organic compound occurs at the metal-solution interface and this positive adsorption is influenced by several factors, such as the dipole moment of the solute and the properties of the cathode surface. So in the first place we added acetaldehyde to the electrolyte as the organic compound soluble in water and having the dipole moment larger than that of the solvent. Though we feared that acetaldehyde might be reduced at the cathode, it was confirmed by the preliminary experiments that acetaldehyde was not reducible at the platinum cathode in the N. H_2SO_4 solution.[13,14,15]

We measured the hydrogen overpotential on the platinum electrode dipped in the electrolyte containing a different amount of acetaldehyde, under several cathodic current densities.

The results are shown in Table III and Fig. 4.

TABLE III

Composition of Electrolyte	Log D* (D.A./cm²)	Available Area** cm²	Log D'*** (D',A./cm²)	Electrode**** Potential V, ε_h
0.96M. Acetaldehyde/L of N. H_2SO_4	−2.49	1.67	−2.16	0.02
	−2.29	1.94	−2.03	0.03
	−2.00	2.00	−1.70	0.05
	−1.48	2.54	−1.33	0.08
0.48M. Acetaldehyde/L of N. H_2SO_4	−2.49	1.95	−2.23	0.01
	−2.29	2.00	−2.04	0.02
	−2.00	2.25	−1.80	0.04
	−1.67	2.75	−1.56	0.06
	−1.48	3.00	−1.41	0.07

* D: Cathodic current density A./cm² apparent area.
** Cathode area for hydrogen evolution reaction corrected by taking the steric hindrance of organic molecules.
*** D': (D×3.6)/(available area), 3.6cm²: apparent area of the cathode.
**** Considering the exactness of our data, we took the numerical value of the electrode potential to the order of 10 mV when the electrolyte contained organic molecules.

In column 4, D' is the current density corrected by taking the steric hindrance of acetaldehyde into consideration, that is, it was assumed that the surface points covered by organic molecules did not take part in the discharge of hydrogen ions.

As seen in Fig. 4 and 3, the hydrogen overpotential increases with the increase of the concentration of acetaldehyde in accordance with the results of Wetterholm (10^{-5}~10^{-2}A./cm²). Tafel's

13) C. J. Brockman: "Electro Organic Chemistry" p. 287 (1926).
14) V. Stern and S. Polak: *Acta Phsicochim U. R. S. S.* **11**, 797 (1939).
15) Böttger: "Physik. Methode d. Anal. Chem" Bd. II. p. 295, (1936).

constant b changes between 0.06~0.08, but after the correction of the effective cathode area which

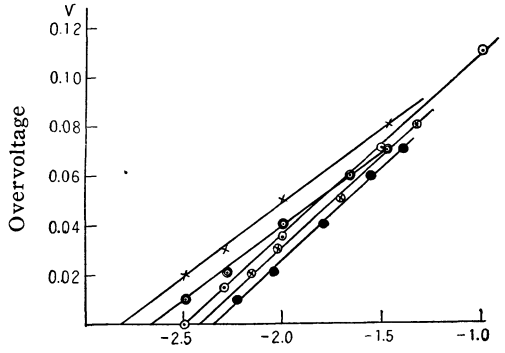

Fig. 4.
Effect of acetaldehyde on the relation between the cathodic current density and the overpotential (at 3°C)
(⊙) $N.H_2SO_4$, b=0.08
(×) 0.96M. acetaldehyde/L $N.H_2SO_4$, b=0.06
(◎) 0.48M. acetaldehyde/L $N.H_2SO_4$, b=0.06
(⊗) after the correction of the current density (0.96M. acetaldehyde/L $N.H_2SO_4$) b=0.08
(●) after the correction of the current density (0.48M. acetaldehyde/L $N.H_2SO_4$) b=0.08

we supposed would diminish by the adsorption of acetaldehyde, b becomes about 0.08, the same value as when there is no addition. Though Tafel's another constant a also changes slightly, we may attribute the main effect of acetaldehyde to the steric hindrance of it on the electrode surface.

Of course we must take account of the effect of the solute on δ, the thickness of the double layer, or the value of ΔH^{*} (the heat of activation of hydrogen evolution) as J. O'M. Bockris mentioned,[5,16] but according to our experiments the chief effect of the solute seemed to be the steric hindrance.

C. Case II. Next we examined the effect of the addition of ethyl alcohol as the solute having smaller dipole moment than that of water.

The results are shown in Fig. 5 to Fig. 7. In Fig. 5 we can see that the amount of adsorption of ethyl alcohol is very small as compared with the case of acetaldehyde even in the concentrated solution. In Fig. 6 we showed Tafel's lines in

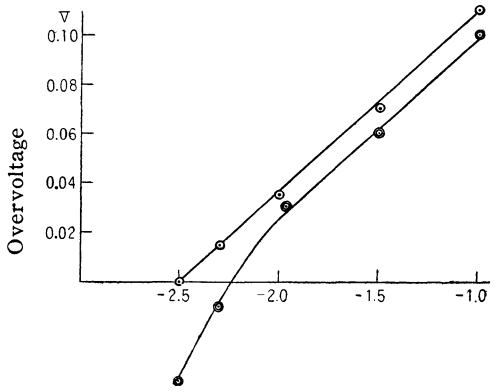

Fig. 6.
Tafel's line on $N.H_2SO_4$ and on the solution of ethyl alcohol (at 3°C)
(⊙) $N.H_2SO_4$
(◎) ethyl alcohol (1.7M./l.$N.H_2SO_4$)

$N.H_2SO_4$ and in the solution of ethyl alcohol. The relation between the electrode potential and the concentration of ethyl alcohol is shown in Fig. 7.

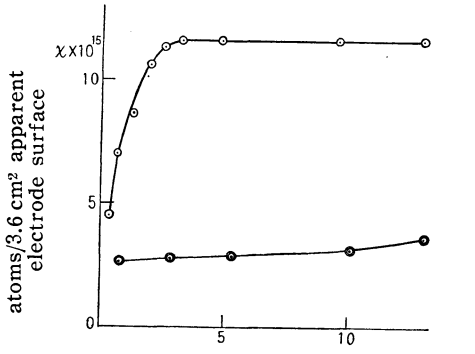

Fig. 5.
Relation between the adsorbed amount of organic compounds and their concentration (at 3°C)
(⊙) acetaldehyde M./L $N.H_2SO_4$
(◎) ethyl alcohol M./L $N.H_2SO_4$ measured at the current density 10 mA./cm²

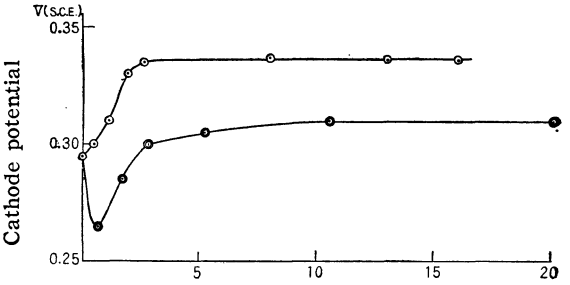

Fig. 7.
The relation between the cathode potential and the concentration of organic compound (at 3°C)
(⊙) acetaldehyde (◎) ethyl alcohol measured at the cathode density 10 mA./cm²

16) P. J. Hillson: *Trans. Farad. Soc.* **48**, 462 (1952).

The electrode potential decreases at first, but becomes high with the further increasing concentration of the alcohol. After reaching the value near that in pure $N.H_2SO_4$, it stays there over a wide range of concentration of ethyl alcohol (5~35 M. EtoH/1), then decreases slowly at higher concentrations (ca. 35M./1).

In the concentrated solution of ethyl alcohol, we found that the bending point of the polarization curve in the oscillograph showing the saturation of the adsorption of the hydrogen atom disappears. From this fact, we may attribute the reason of the lowering of the potential in the concentrated solution to the existence of some reaction other than pure hydrogen evolution on the cathode surface. From these we may conclude as follows.

The organic molecules having dipole moments smaller than that of water such as ethyl alcohol are adsorbed very poorly on platinum cathode as shown in this experiment, so the change of electrode potential by its steric hindrance may be small.

Accordingly, the change of the electrode potential in this case may be largely due to another factor such as the change of adsorption energy of discharged hydrogen by the addition of ethyl alcohol, as J. O'M. Bockris proposed.[17,18]

Conclusion

The relation between the electrode potential and the adsorption of organic molecules was studied by measuring the adsorption by the oscillograph. We can divide in two types the effects of organic molecules adsorbed to the surface of the cathode, when the evolution of hydrogen is of catalytic mechanism.

Type I. The organic molecule having the dipole moment greater than that of water is strongly adsorbed on the surface of platinum cathode and by its steric hindrance, the cathode potential becomes less noble with the increase of its addition to the solution. On such a type, by correcting current densities as to the cathode area covered by organic molecules, Tafel's constant and also the potential become almost the same as when there is no addition.

Type II. The organic molecule having the dipole moment smaller than that of water is adsorbed only a little on the electrode and the effect of it on the electrode potential seems rather due to the solvent effect than to the steric hindrance, when the size of the molecule is small.

These conclusions may be reasonable in reference to the discussion of former authors, especially to that of J.O'M. Bockris.[1)~3)]

The expenses incured for this work were met by the Grant in Aid for Fundamental Scientific Research, to which our thanks are due.

Laboratory of Applied Electrochemistry, and Photochemistry Faculty of Engineering, University of Tokyo

17) J.O'M. Bockris & R. Parsons: *Trans. Farad. Soc.*, **44**, 860 (1948).
18) R. Parsons & J.O'M. Bockris: ibid **47**, 914 (1951).

LETTER

The Phase Transitions of the Solid Cyclohexanol*)

By Sei-ichi KONDO and Kiyoshi NOZAKI

(Received June 8, 1953)

Investigations have been made of the dilatometry and the dielectric constant of the pure cyclohexanol mainly on the behavior of the phase transitions at −8.1°C and −28.6°C. These two phase transitions were well studied thermally by Kelly,[1] and Otsubo,[2] dielectrically by White and Morgan,[3] and Smyth,[4] and structurally with X-rays by Sugawara.[5]

Cyclohexanol was boiled with calcium oxide for one day, fractionally distilled, warmed again with calcium oxide for about 30 hours and evaporated in a high vacuum into a dilatometer vessel to which distilled and evacuated mercury was introduced. The melting point of this material thus purified

* This research was made in part under the support of the scientific research grant of the Education Ministry.

1) K.K. Kelly; *J. Am. Chem. Soc.*, **51**, 1400 (1929).
2) E. Kanda and Otsubo; read at the annual meeting of the *Chem. Soc. Japan.* in (1952).
3) White and Morgan; *J. Am. Chem. Soc.*, **57**, 2081 (1935).
4) C.P. Smyth and R.W. Crowe; *J. Am. Chem. Soc.*, **73**, 5409 (1951).
5) T. Sugawara; will appear in "X-Sen" Vol. 12 No. (1953).

was 24.2°C.

The results of the experiments are illustrated in Fig. 1. Cyclohexanol is supercooled very easily to the temperature of liquid air. (the full line in Fig. 1.) The volume expansion coefficient of this phase is 4.4×10^{-4} cc/degree, which is in good agreement with the value 4.4×10^{-4} calculated from the lattice constant of the room temperature α phase by Oda[6] and that of the supercooled α phase.[5] When heating it immediately after cooling to the temperature of dry-ice alcohol mixture or liquid air, the volume change at the lower transition point is small and indefinite. (the dotted line in Fig. 1.) When cooled for about one day in liquid air or dry-ice mixture, the

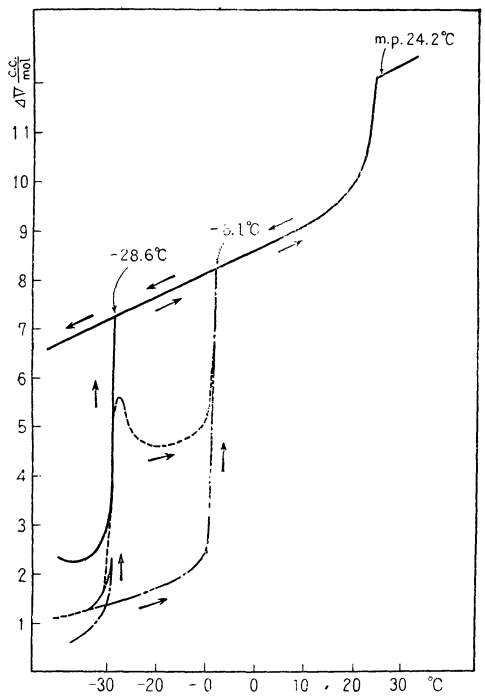

Fig. 1. The volume expansion $\triangle V$ c.c./mol. of the solid cyclohexanol. The full line shows the curve warmed after cooling for 2 hrs. and the dotted and broken lines are those warmed after cooling for 24 hrs. in dry-ice alcohol mixture in each case.

volume difference at this point between the γ phase below -28.6°C. and supercooled α phase is constant in every case, which shows that the phase transition from α to γ phase is apparently completed. The γ phase exists always in our thermal treatment, but disappears when the sample is once more cooled a little below -28.6°C. in the middle of this phase transition, and then there exists only the transition at -8.1°C., the volume change of which is about 5.8 cc/mol. (the broken line in Fig. 1.)

When cyclohexane is mixed with this sample, which is soluble with this in the solid state, the phase transition at -8.1°C. becomes smaller in proportion to the concentration of cyclohexane and disappears at about 10% cyclohexane, and there exists only the transition at -31°C., and the β phase below -8.1°C. may disappear.

The dielectric constant and loss were measured with the modified transformer method. Although the main features are the same as Smyth's experiment, the purity of the sample is better in our case, and the dielectric constant of α phase is 15.0 at 8.2°C. which is smaller than that of Smyth and that of γ phase is 2.41. The dielectric constant of the β phase is slightly less than the γ phase.

These features may probably lead us to such a conclusion that the γ phase is unstable and an intermediate one to the stable β phase, and that this β phase is characterized by an intermolecular O—H···O hydrogen-bond regularly throughout the crystal in contract to the other phases and by mixing cyclohexane the effect of this sort of hydrogen-bond becomes less and the γ phase becomes stable.

It is a pleasure to acknowledge our indebtness to Dr. T. Sugawara of Tohoku University for his kindness in showing us his unpublished data and also to Dr. T. Oda of our University and Dr. S. Seki of Osaka University for their useful discussions.

Laboratory of Physical Chemistry
Osaka Liberal Arts University

6) T. Oda; X-cap, **54**, 2 (1945).

Application of the New equation of state to the Joule-Thomson effect

By Tetsuya ISHIKAWA

(Received July 27, 1953)

In a recent paper[1] I proposed an equation of state which equally satisfies the three criteria for state equations: RT_c/p_cV_c, T_B/T_c and $T_c/p_c \cdot (dp/dT)_c$. One more criterion with technical importance is the Joule-Thomson effect which is formulated thermodynamically

1) This *Bulletin*, **26**, 78 (1953).

by the aid of van der Waals' equation of state, but results in a qualitative formula:

$$\mu=\frac{2a_{corr}/RT-b_{corr}}{C_p},\quad a_{corr}=\frac{27R^2T_c^2}{64p_c},$$

$$b_{corr}=\frac{RT_c}{8p_c} \qquad ...(1)$$

where μ is the Joule-Thomson coefficient, C_p the molecular heat, R the gas constant, and T the temperature, these together with a_{corr} and b_{corr} being expressed in liters, atmospheres, moles, deg. absolute.

I will communicate in this letter the applicability of my equation of state to this problem.

Taking my equation, $p+a/V^{2-}=RT/(V-b)$, in the deduction of the above formula, it readily follows that

$$\mu=\frac{2aV^{\varepsilon'}/RT-b}{Cp},\quad a=3p_cV_c^2,$$

$$b=V_c/3, \qquad ...(2)$$

here a, b &c. are expressed in the same units as above.

It is noticed here that ε in the preceding paper where V is expressed in cc./mole, and ε' denoted here where V is expressed in liter/mole are related by $\varepsilon=\varepsilon'\times \log V/(\log V+3)$.

From International Critical Tables III, V, and Henning's "Warmetechnische Richtwerte", five available data of H_2, CO_2, N_2, O_2 and air can be taken, among which, however, only air may serve as a test case for pressure effect.

To compare with (2—ε) directly from the equation of state, the test for its validity being the present purpose, estimate ε' from formula (2) and transform it into ε, from which (2—ε) from formula (2) is obtained.

	Hydrogen	
	0°C	100°C
(2—ε) from formula (2)	1.979	2.005
(2—ε) from equation of state	2.000	2.009
	(p=50 atm.)	(p=50 atm.)
Divergence in %	1.1	0.2

	Carbon dioxide	
	0°C	100°C
(2—ε) from formula (2)	1.890	1.910
(2—ε) from equation of state	1.900	1.930
	(extrapolated)	(p=50−1000 atm.)
Divergence in %	0.5	1.0

	Nitrogen	
	0°C	100°C
(2—ε) from formula (2)	1.944	1.965
(2—ε) from equation of state	2.007	2.039
	(p=50−1000 atm.)	(p=50−1000 atm.)
Divergence in %	3.1	3.6

	Oxygen	
	0°C	100°C
(2—ε) from formula (2)	1.941	1.959
(2—ε) from equation of state	1.967	2.026
	(p=36−62 atm.)	(p=100−1000 atm.)
Divergence in %	1.3	3.3

	Air at 0°C			
	p (atm.)			
	1	20	60	100
(2—ε) from formula (2)	1.977	1.969	1.973	1.987
(2—ε) from equation of state	1.987	1.997	2.000	2.002
Divergence in %	0.5	1.4	1.4	0.8

	Air at 100°C			
	p (atm.)			
	1	20	60	100
(2—ε) from formula (2)	1.995	1.995	2.005	2.019
(2—ε) from equation of state	1.986	2.019	2.025	2.029
Divergence in %	0.4	1.2	1.0	0.5

The agreements between these two are fairly good as seen from the above tables, and even the greatest divergence arising in the cases of N_2 and O_2 is less than 4%, where the mean values of $(2-\varepsilon)$ from the equation of state at 50 or 100—1000 atms. are presumably the same as those at 1 atm. These results lead to the conclusion that the Joule-Thomson effect is formulated with accuracy by making use of my equation of state.

Sasebo Commercial Junior College,
Sasebo, Nagasaki

Dielectric Properties of Disodium Monohydrogen Phosphate Dodecahydrate, $Na_2HPO_4 \cdot 12H_2O$

By Ryôiti KIRIYAMA and Yusiro SAITO

(Received August 25, 1953)

Using large single crystals we measured the temperature and frequency dependences of the dielectric constants and losses of several hydrated salts. The region of the temperatures measured is from −170°C to the temperature of dehydration and that of frequencies is from 0.3 kc to 3 Mc. For disodium monohydrogen phosphate dodecahydrate, $Na_2HPO_4 \cdot 12H_2O$ (crystal class, C_{2h}), no appreciable anisotropy in its dielectric behaviour is observed. At 3 Mc the dielectric constant perpendicular to (001) is 5.2, monotonously increasing with temperature coefficient 3×10^{-3}. At 0.5 kc, as temperature rises the dielectric dispersion becomes appreciable from about 10°C upward, and ε' reaches a value twice as great as that measured at 3 Mc, accompanying a large conductivity when the temperature is raised to its dehydration temperature 35°C. These are the results obtained with the tin-foiled specimen. On the other hand, in the case of the sandwiched specimen by mica-foils for avoiding the d.c. conductivity, the temperature and frequency dependences of ε' become considerably greater and at 0.5 kc ε' attains to a value of about 70 at 35°C as shown in Fig. 1. The ε' and ε'' values fit in with the Cole-Cole diagram in this dispersion region with distribution parameter α of about 10° (Fig. 2). From the relaxation time and its temperature variation, the free energy of activation is obtained to be $\Delta F = 13$ kcal/mole and the enthalpy $\Delta H = 27$ kcal/mole. For the single crystals of $Na_2SO_4 \cdot 10H_2O$ and $Na_2CO \cdot 10H_2O$, we obtained similar results and the single crystal of $Na_2S_2O_3 \cdot 5H_2O$ shows a similar behaviour but to a less extent, and that of $Na_2B_4O_7 \cdot 10H_2O$ no appreciable effects.

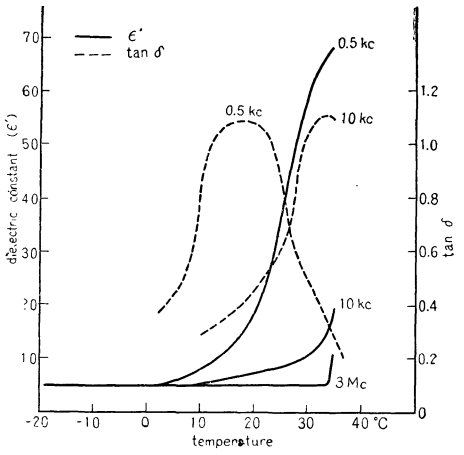

Fig. 1.
Dielectric constant-temperature and loss tangent-temperature curves for $Na_2HPO_4 \cdot 12H_2O$ (perpendicular to (001))

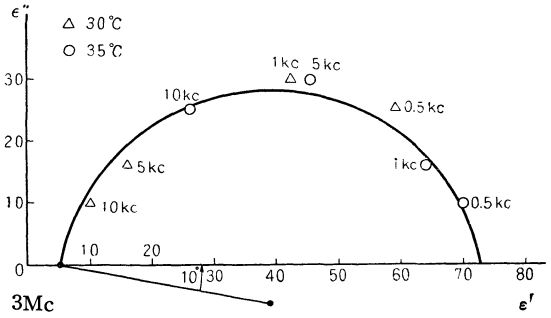

Fig. 2.
Cole-Cole diagram for $Na_2HPO_4 \cdot 12H_2O$ (perpendicular to (001))

All these crystals are very efflorescent, and the dehydrated water molecules are set free from the crystal surfaces and affect the dielectric properties considerably. In the above experiments, we have taken precaution by passing dry air through the measuring cell in order to avoid these effects of dehydrated water as far as possible.

From these measurements and our previous experiments about such behaviours of water of crystallization, it may be concluded that water molecules in these hydrated phosphate, sulphate and carbonate crystals are linked to oxygen atoms in a manner somewhat similar to the water molecules in ice and further the observed dielectric phenomena due to rotation of the water molecules may be originated at some points of lattice defects.

Detailed discussion will be published in this Bulletin.

Department of Chemistry, Faculty of Science, Osaka University, Osaka